ASSL
ASTROPHYSICS AND
SPACE SCIENCE LIBRARY

POLARIZATION IN SPECTRAL LINES

E. LANDI DEGL'INNOCENTI
M. LANDOLFI

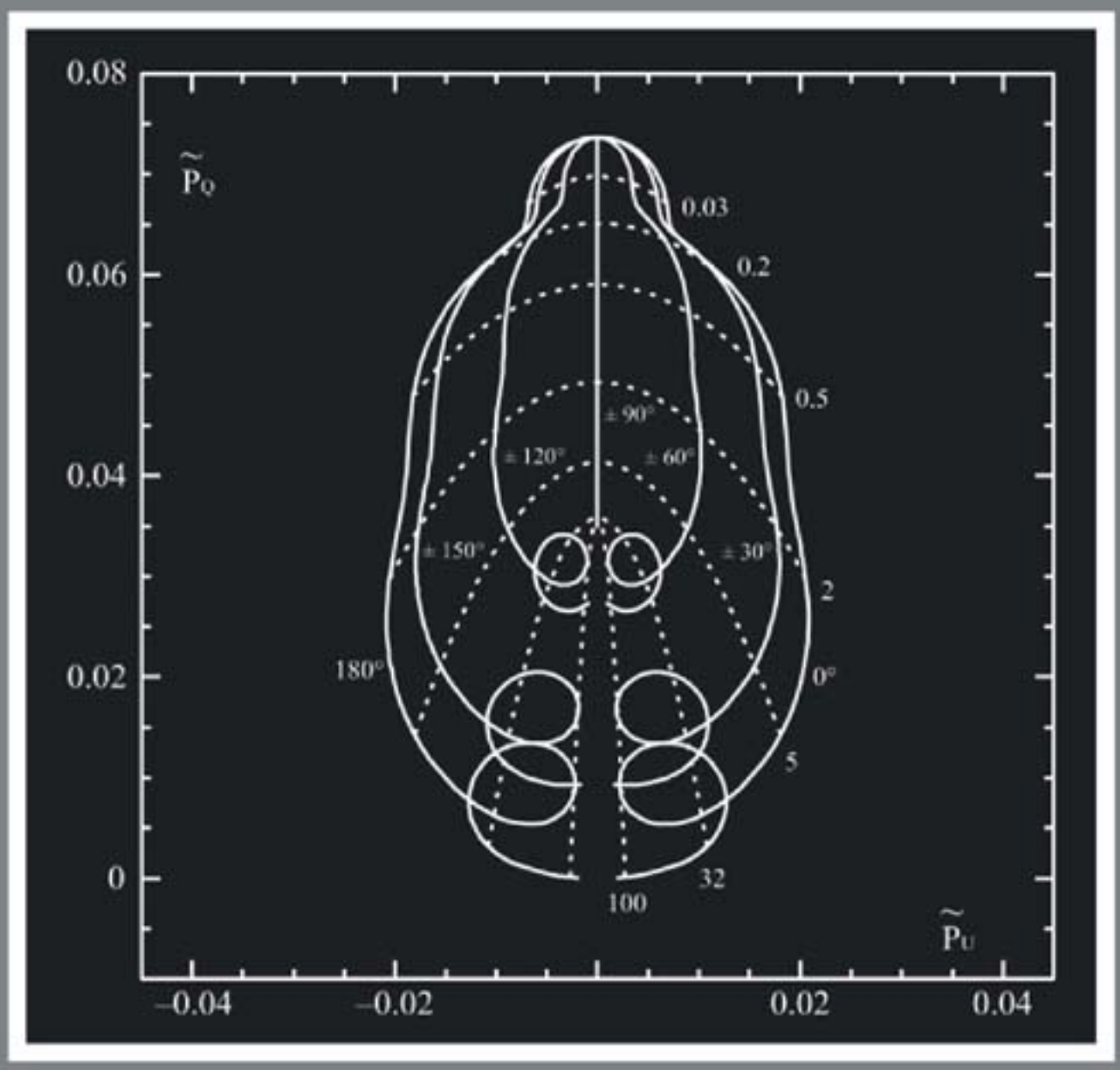

KLUWER ACADEMIC PUBLISHERS

POLARIZATION IN SPECTRAL LINES

ASTROPHYSICS AND SPACE SCIENCE LIBRARY

VOLUME 307

POLARIZATION IN SPECTRAL LINES

by

EGIDIO LANDI DEGL'INNOCENTI
University of Firenze,
Firenze, Italy

and

MARCO LANDOLFI
Arcetri Observatory,
Firenze, Italy

KLUWER ACADEMIC PUBLISHERS
NEW YORK, BOSTON, DORDRECHT, LONDON, MOSCOW

eBook ISBN: 1-4020-2415-0
Print ISBN: 1-4020-2414-2

Created in the United States of America

Visit Springer's eBookstore at: http://ebooks.springerlink.com
and the Springer Global Website Online at: http://www.springeronline.com

To Nadine and Vanessa,
and to Gianna

This page intentionally left blank

PREFACE

Quod si tam celebris est apud omnes gloria Adamantis, atque varia ista opum gaudia, gemmae unionesque, ad ostentationem tantum placent, ut digitis colloque circumferantur; non minori afficiendos speraverim gaudio eos, quibus curiositatis conscientia quam deliciarum est potior, novitate corporis alicujus, instar crystalli translucidi, quod ex Islandia nuper ad nos perlatum est; cujus tam mira est constitutio, ut haud sciam, num alias magis naturae apparuerit gratia.

Erasmus Bartholinus, Experimenta crystalli islandici disdiaclastici

Apart from a few objects of our immediate neighborhood (the solar system), all the information on the physical phenomena taking place in the Universe comes from the radiation that the astronomical objects send into space and that is finally collected on earth by telescopes or other instruments. Among the different kinds of radiation, electromagnetic waves have by far played the most important role in the history of Astronomy – probably, it is not unrealistic to say that more than 99% of our present knowledge of the Universe derives from the analysis of the electromagnetic radiation.

Such radiation contains three different kinds of information, encoded into as many physical characteristics typical of any oscillatory propagation phenomenon: the propagation direction, the frequency and amplitude of the oscillation, and the oscillation direction – or polarization.

The first one is the most direct and the easiest to measure: the human eye is itself a suitable instrument, though of limited accuracy. As time passed, positional astronomy became more and more accurate thanks to the invention of the optical telescope, the introduction of photographic and digital techniques and, more recently, the development of technologies for producing images of a given region at different wavelengths via radio, infrared, X-ray and γ-ray telescopes, often operating on board of spacecrafts. Our present knowledge of the morphology and dynamics of the Universe, and of the different objects of which it is composed (from planets to stars, from nebulae to globular clusters, from galaxies to Active Galactic Nuclei and to clusters of galaxies) is based on the huge number of such observations that have been accumulating during several centuries.

However, even if very accurate, the measurement of the propagation direction of the electromagnetic radiation is inadequate to study other fundamental aspects of the physical Universe such as the composition, structure, and evolution of the different objects. To this aim, a detailed analysis of the frequency (or wavelength) distribution of the energy carried by the electromagnetic radiation is required, which was made possible by the invention of the spectrograph. Only through the systematic use of spectroscopic methods it has been possible to obtain a direct comprehension of the physical mechanisms which govern the equilibrium of stars, their birth, evolution and death, and the complicated processes taking place in the interstellar medium and in the nuclei of galaxies. Spectroscopy, which is also

at the basis of the idea of an expanding Universe, has played such a key role in the comprehension of the physical Universe that a new name, astrophysics, was introduced in the scientific lexicon to denote the astronomical research based on this technique.

The third, and often neglected, characteristic of the electromagnetic radiation is polarization. The earliest studies on polarization were performed around 1670 by the Danish scientist Erasmus Bartholinus, who was strongly impressed by the properties of a newly discovered crystal, the Iceland spar ('... whose behavior is so surprising that, as far as I know, never the grace of nature appeared more clearly') and who immediately realized that those properties could prove useful to improve human knowledge.

Since polarization is mainly related to the geometrical aspects of the emission process (rather than to its energetics), and since polarization measurements are often difficult to perform because of the intrinsic weakness of the signals, the study of polarization found its place in the astronomical research with some difficulty. But eventually the prediction of Erasmus Bartholinus was fully confirmed: some of the most important astronomical discoveries of the 20^{th} century were made thanks to polarimetry – or, more properly, spectropolarimetry. Suffice it to quote the discovery of magnetic fields in the sun, stars, and the interstellar medium.

The first application of spectropolarimetry to the astronomical research dates back to 1908 when, using a Nicol prism as a polarizer and a Fresnel rhomb as a quarter-wave plate, George Ellery Hale succeeded in taking two spectra of the same area of a sunspot in opposite directions of circular polarization. The comparison of the spectra showed the presence of the typical signature induced by a strong magnetic field, the Zeeman effect.

Since 1908, things have considerably evolved from the technological point of view. Spectropolarimetric observations of the solar spectrum have now attained a sensitivity level which goes beyond the most optimistic expectations of only two or three decades ago. The first dedicated instrument for the measurement of Stokes parameters profiles in Fraunhofer lines, the 'mythic' Stokes-I polarimeter, developed in the mid 1970s at the High Altitude Observatory, hardly attained a sensitivity of 1%. Nowadays, sensitivity in solar spectropolarimetry has reached the level of 10^{-5} for spatially unresolved observations, and approximately one order of magnitude less for observations at high spatial and temporal resolution. It has to be expected that these limits will be rapidly overcome by the next generation polarimeters and that the same technologies will be adapted to galactic and extragalactic observations.

The dramatic increase of polarimetric sensitivity in solar observations has raised a serious challenge to the theoretical interpretation. Polarization in spectral lines is indeed a subtle phenomenon since, in astrophysical plasmas, there are several physical mechanisms that can generate polarization signatures in line profiles and many others that can modify them during the propagation. Some of these mechanisms have been known for a long time from laboratory atomic physics. They are – just to mention the most remarkable – the Zeeman effect, resonance polarization, and the Hanle effect. Other mechanisms are characteristic of optically thick plasmas, and are related to the propagation of radiation in anisotropic media.

They are known under the general names of dichroism and anomalous dispersion, though in special cases different denominations are often used (inverse Zeeman effect, magneto-optical effects, Faraday rotation, Faraday pulsation, etc.).

These processes have mostly been studied in specific physical contexts, for different purposes and at different levels of sophistication, and the scientific literature on the subject is scattered across books and journals, spanning almost a century of active research. For this reason we felt that a book capable of describing, in a unique and self-consistent formalism, all the known physical phenomena that may affect the polarization signatures of spectral lines, might be welcome to the scientific community. The diagnostic content of spectropolarimetry is high, but the correct interpretation of the observations requires a full understanding of the physics underlying the generation and transfer of polarized radiation.

The redaction of this book required several years. We might try to say, like Huygens in the preface to his *Treatise on light*, 'The reason is that I wrote it rather carelessly in the Language in which it appears, with the intention of translating it into Latin, so doing in order to obtain greater attention to the thing',[1] but we feel it would be hardly believed. The true reason is that the theory of spectropolarimetry is complicated, because it implies some knowledge of several subjects: atomic physics, quantum mechanics (with special emphasis on the theory of angular momentum and of the density matrix), quantum electrodynamics, radiative transfer (both under LTE and Non-LTE conditions).

Moreover, spectropolarimetry is full of traps: among all the disciplines in astrophysics, there can hardly be found one where more attention has to be payed to each single definition, each transformation, each physical application. Sign errors are especially insidious, as most remarkably shown by the classical example of circular polarization in a given wing of a spectral line formed in a magnetic atmosphere. There are four operations which produce a sign change in such polarization, and obviously, there are as many possibilities to make a sign error. To have a sign switch, one can: a) invert the direction of the magnetic field; b) interchange the red with the blue wing; c) use the opposite definition of positive and negative circular polarization; d) consider an emission line instead of an absorption line. This is just an example, but it shows very well the subtleties of the subject. We tried to make the exposition as clear as possible by using everywhere the same definitions and conventions, and by carefully describing all the mathematical developments.

We hope that this book may be useful to the next generations of scholars that will like to enter the field of spectropolarimetry, solar and non-solar. And we hope that it may contribute to make this research field more accessible and less hermetic, thus attracting more and more scientists to the fascinanting world of the Stokes parameters profiles and of their interpretation.

Arcetri, March 2004

Egidio Landi Degl'Innocenti
Marco Landolfi

[1] Christiaan Huygens, *Treatise on light* (1690), translated by S.P. Thompson, Dover Publications, New York, 1962.

This page intentionally left blank

CONTENTS

This page intentionally left blank

CHAPTER 1

DESCRIPTION OF POLARIZED RADIATION

According to Maxwell's equations, the electric and magnetic fields associated with a radiation beam propagating in vacuum are perpendicular to each other and to the direction of propagation. The phenomena of polarization are connected with the possibility that is left to the electric field vector (or, alternatively, to the associated magnetic field vector) of spanning the plane perpendicular to the direction of propagation.

The polarization properties of a radiation beam can be described in several different ways, each of them having its proper advantages and disadvantages. In the following we will go through some of these descriptions showing how they are interrelated and, most of all, how they can be translated into operational definitions having a direct physical meaning in terms of measured quantities.

1.1. The Polarization Ellipse

We start from the classical (non-quantum) description of the electromagnetic field and we refer to the idealized case of a pure monochromatic, plane wave propagating in vacuum along the positive z-axis of a right-handed coordinate system. A full description of the wave can be given either specifying its electric field vector or, alternatively, its magnetic field vector, as the two quantities are related by the equation

$$\vec{B}(\vec{r},t) = \vec{n} \times \vec{E}(\vec{r},t) \; , \tag{1.1}$$

where $\vec{n}$ is the unit vector in the direction of propagation, and where $\vec{E}$ and $\vec{B}$ are both measured in c.g.s. units (the Gauss-Hertz system, that will be used – with some few exceptions – throughout the whole book). As far as the cross product is concerned, we will follow the almost universally accepted convention that is referred to as the *right-hand* (or *screwdriver*) *rule*, and that is illustrated in Fig. 1.1. However, we remind the reader that the sign in Eq. (1.1) is related to the sign conventions which have been historically adopted to define the positive directions for $\vec{E}$ and $\vec{B}$. These are, in turn, connected with the historical convention of adopting the positive sign for the proton charge and, in magnetostatic experiments, the positive sign for the idealized monopole which is found at the North-end of a dipole oriented in the earth magnetic field (Maxwell, 1873). Note that, according to this definition, the earth presently shows a South magnetic pole close to the North geographic pole.

To define the polarization properties of an electromagnetic wave we choose its representation in terms of electric field vibrations. Again, there are historical rea-

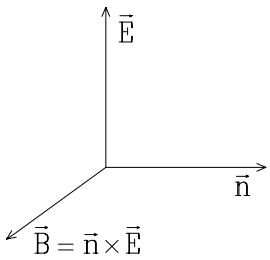

Fig.1.1. Mutual relationship among instantaneous electric field vector, instantaneous magnetic field vector and direction of propagation of an ordinary electromagnetic wave. The cross product is defined according to the right-hand convention.

sons behind this choice; the description in terms of electric vibrations is nowadays preferred because polarization measurements are mostly performed, at least in the optical spectrum, by means of materials whose interaction with the electromagnetic radiation is dominated by the electric vector. However, a description in terms of magnetic vibrations would be as appropriate as the former.

In the right-handed coordinate system introduced above, with its x-axis pointing in an arbitrary direction in the plane perpendicular to the direction of propagation, the electromagnetic wave is described by the following expressions

$$\begin{aligned} E_x(\vec{r},t) &= E_1 \cos(kz - \omega t + \phi_1) \\ E_y(\vec{r},t) &= E_2 \cos(kz - \omega t + \phi_2) \ , \end{aligned} \tag{1.2}$$

where E_1, E_2, ϕ_1, and ϕ_2 are four positive constants specifying the amplitudes and phases of the electric oscillations, and where k and ω have the usual meaning of wavenumber and angular frequency.

In a given plane that is held fixed in space, for instance in the plane $z = 0$, the electric field vector oscillates according to the equations

$$\begin{aligned} E_x(t) &= E_1 \cos(\omega t - \phi_1) \\ E_y(t) &= E_2 \cos(\omega t - \phi_2) \ . \end{aligned} \tag{1.3}$$

The tip of the electric field vector rotates in the x-y plane describing an ellipse that is called the *polarization ellipse* and whose characteristic parameters can be found with the following algebraic manipulations.

Let us consider the couple of axes $(x'y')$ that are obtained by rotating the old couple (xy) through an angle α measured positively from the x-axis to the y-axis (see Fig. 1.2). In this new system, with the position

$$C = \cos\alpha \ , \qquad S = \sin\alpha$$

we have

$$\begin{aligned} E_{x'}(t) = &(E_1 C \cos\phi_1 + E_2 S \cos\phi_2)\cos\omega t \\ &+ (E_1 C \sin\phi_1 + E_2 S \sin\phi_2)\sin\omega t \end{aligned}$$

$$\begin{aligned} E_{y'}(t) = &(-E_1 S \cos\phi_1 + E_2 C \cos\phi_2)\cos\omega t \\ &+ (-E_1 S \sin\phi_1 + E_2 C \sin\phi_2)\sin\omega t \ . \end{aligned} \tag{1.4}$$

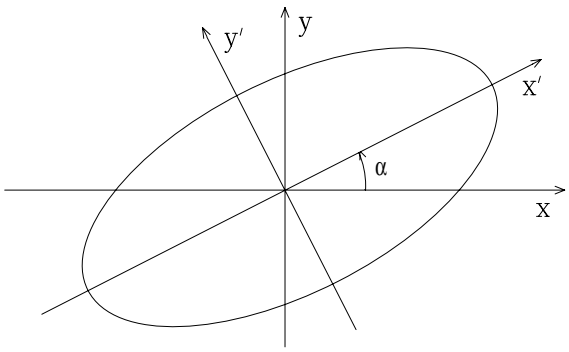

Fig.1.2. Polarization ellipse.

We now choose the angle α so as to make the x' and y' axes coincide with the proper axes of the polarization ellipse, the long axis being directed along x'. If a and b are the semi-major and semi-minor axes, respectively, we have

$$\begin{aligned} E_{x'}(t) &= a\cos(\omega t - \phi_0) \\ E_{y'}(t) &= b\sin(\omega t - \phi_0)\ , \end{aligned} \tag{1.5}$$

where the phase ϕ_0 must be determined in such a way that $a > 0$ and $a \geq |b|$. Comparing Eqs. (1.4) and (1.5) we obtain

$$\begin{aligned} a\cos\phi_0 &= E_1 C\cos\phi_1 + E_2 S\cos\phi_2 \\ a\sin\phi_0 &= E_1 C\sin\phi_1 + E_2 S\sin\phi_2 \\ b\cos\phi_0 &= -E_1 S\sin\phi_1 + E_2 C\sin\phi_2 \\ b\sin\phi_0 &= E_1 S\cos\phi_1 - E_2 C\cos\phi_2\ . \end{aligned}$$

From these equations we easily get

$$\begin{aligned} &a^2 + b^2 = E_1^2 + E_2^2 \\ &ab = -E_1 E_2\sin(\phi_1 - \phi_2) \\ &a^2 - b^2 = (E_1^2 - E_2^2)\cos 2\alpha + 2E_1 E_2\cos(\phi_1 - \phi_2)\sin 2\alpha \\ &(E_1^2 - E_2^2)\sin 2\alpha = 2E_1 E_2\cos(\phi_1 - \phi_2)\cos 2\alpha\ . \end{aligned} \tag{1.6}$$

Equations (1.6) show that the geometrical properties of the polarization ellipse depend on four bilinear combinations of the electric field components. Introducing the notations

$$\begin{aligned} P_I &= E_1^2 + E_2^2 \\ P_Q &= E_1^2 - E_2^2 \\ P_U &= 2E_1 E_2\cos(\phi_1 - \phi_2) \\ P_V &= 2E_1 E_2\sin(\phi_1 - \phi_2)\ , \end{aligned} \tag{1.7}$$

the angle α can be found from the equation

$$P_Q \sin 2\alpha = P_U \cos 2\alpha$$

added to the further constraint

$$a^2 - b^2 = P_Q \cos 2\alpha + P_U \sin 2\alpha \geq 0 \ .$$

If we choose $(0, \pi)$ as the interval of definition for α, we obtain, for $P_Q \neq 0$

$$\alpha = \frac{1}{2} \arctan\left(\frac{P_U}{P_Q}\right) + \alpha_0 \tag{1.8a}$$

where

$$\alpha_0 = \begin{cases} 0 & \text{if } P_Q > 0 \text{ and } P_U \geq 0 \\ \pi & \text{if } P_Q > 0 \text{ and } P_U < 0 \\ \pi/2 & \text{if } P_Q < 0 \ , \end{cases} \tag{1.8b}$$

and for $P_Q = 0$

$$\alpha = \begin{cases} \frac{1}{4}\pi & \text{if } P_U > 0 \\ \frac{3}{4}\pi & \text{if } P_U < 0 \ . \end{cases} \tag{1.8c}$$

Obviously, in the case $P_Q = P_U = 0$ the angle α is left undefined.

From Eqs. (1.6) we can also find the values of the semiaxes of the polarization ellipse. Since

$$(a + b)^2 = P_I - P_V \ ,$$

the values of a and b can be found as the solutions of the second degree equation

$$x^2 - \sqrt{P_I - P_V}\, x - \frac{1}{2} P_V = 0 \ ,$$

which gives

$$\begin{aligned} a &= \frac{1}{2}\left[\sqrt{P_I - P_V} + \sqrt{P_I + P_V}\right] \\ b &= \frac{1}{2}\left[\sqrt{P_I - P_V} - \sqrt{P_I + P_V}\right] \ . \end{aligned} \tag{1.9}$$

Note that the four quantities defined in Eqs. (1.7) are not independent, being related by the expression

$$P_I^2 = P_Q^2 + P_U^2 + P_V^2 \ . \tag{1.10}$$

1.2. Special Cases of the Polarization Ellipse

For some special values of the parameters E_1, E_2, and $(\phi_1 - \phi_2)$, the polarization ellipse degenerates either into a segment or into a circle. The first case takes place when $P_V = 0$, which means that either E_1 or E_2 vanish, or, alternatively, that $\phi_1 = \phi_2$ or $\phi_1 = \phi_2 \pm \pi$. From Eqs. (1.9) we get

$$a = \sqrt{P_I}\,, \qquad b = 0\,,$$

while the angle α can still be deduced from Eqs. (1.8). In this case the monochromatic wave is said to be *linearly polarized*, and its electric field oscillates in the constant plane containing the direction of propagation and the direction, in the normal plane, characterized by the angle α.

The other case corresponds to $P_Q = P_U = 0$, which means that $E_1 = E_2$ and that $(\phi_1 - \phi_2) = \pm\,\pi/2$; in other words the electric oscillations have the same amplitude along the x and y axes and are in phase quadrature. For the fourth parameter we then obtain

$$P_V = \pm\, P_I\,,$$

and correspondingly

$$a = \sqrt{P_I/2}\,, \qquad b = \mp\sqrt{P_I/2}\,.$$

In both cases the polarization ellipse degenerates into a circle. When $P_V = +P_I$, the tip of the electric field vector rotates clockwise for an observer facing the radiation source, as apparent from Eqs. (1.5) being $a > 0$, $b < 0$. Conversely, when $P_V = -P_I$ the rotation is counterclockwise as seen by the same observer. In this book we will adopt the convention of referring to the first case as *positive* (or *right-handed*) *circular polarization*, and to the second case as *negative* (or *left-handed*) *circular polarization*. In the first case a snapshot of the electromagnetic wave shows that the end point of the electric field vector draws a helix that fits the thread of a usual, right-handed screw; in the second case we have a left-handed screw.

Our convention, which is summarized in Fig. 1.3, agrees with those proposed in the classical textbooks on polarized light by Shurcliff (1962) and by Clarke and Grainger (1971). The same convention is also used, although with some few exceptions, by optical astronomers working in the field of polarimetry. Many radioastronomers, on the other hand, use the opposite convention, so that the situation in this field is still rather confusing (see for instance Clarke, 1974).

The sign of circular polarization is also connected with the helicity (or spin) of photons. This connection is discussed in some detail in the following of this book (see Sect. 4.4 and App. 3).

1.3. Polarization Tensor

In Sect. 1.1 we have described the electric vibration of a plane monochromatic wave by means of the real quantities E_1, E_2, ϕ_1, ϕ_2. Alternatively, the electric

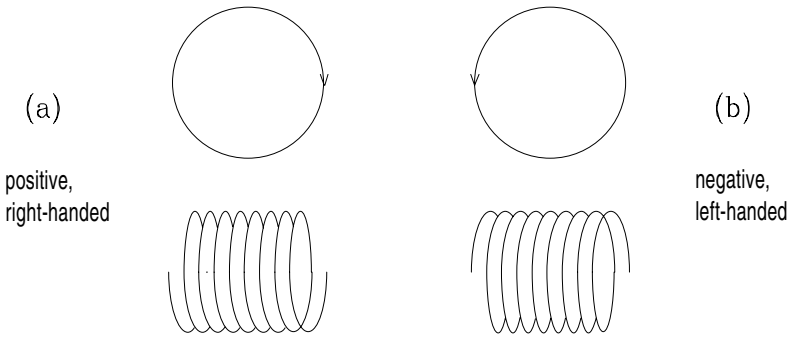

Fig.1.3. Conventions for defining the sign and handedness of circular polarization. The tip of the electric field vector rotates, as a function of time, in a fixed plane perpendicular to the direction of propagation; the observer, receiving the radiation into his/her eye, sees a clockwise (a) or counterclockwise (b) rotation. The corresponding snapshots are shown in the lower half of the figure.

vibration can be described using complex numbers, with the usual convention that the physical quantity is represented by the real part of the complex number. The first of Eqs. (1.2) can then be rewritten in either of the two equivalent forms (i is the imaginary unit)

$$E_x(\vec{r},t) = \mathrm{Re}\left[\mathcal{E}_1\,\mathrm{e}^{\,\mathrm{i}(kz-\omega t)}\right] \tag{1.11}$$

where $\mathcal{E}_1 = E_1\,\mathrm{e}^{\mathrm{i}\phi_1}$, or

$$E_x(\vec{r},t) = \mathrm{Re}\left[\mathcal{E}'_1\,\mathrm{e}^{\,\mathrm{i}(-kz+\omega t)}\right] \tag{1.12}$$

where $\mathcal{E}'_1 = E_1\,\mathrm{e}^{-\mathrm{i}\phi_1}$ is the complex conjugate of $\mathcal{E}_1$. Here and in the following we will use the further convention of describing oscillating quantities with a temporal exponential of the form $\mathrm{e}^{-\mathrm{i}\omega t}$ (rather than $\mathrm{e}^{\mathrm{i}\omega t}$), so that the expression for $E_x(\vec{r},t)$ in terms of complex notations is that of Eq. (1.11). With the same convention, we have for the electric oscillation along the y-axis

$$E_y(\vec{r},t) = \mathrm{Re}\left[\mathcal{E}_2\,\mathrm{e}^{\,\mathrm{i}(kz-\omega t)}\right] \tag{1.13}$$

with $\mathcal{E}_2 = E_2\,\mathrm{e}^{\mathrm{i}\phi_2}$.

Using the complex quantities $\mathcal{E}_1$ and $\mathcal{E}_2$ it is possible to introduce a 2×2 Hermitian matrix $\boldsymbol{J}$, called the *polarization tensor*, defined by

$$J_{ij} = \mathcal{E}_i^*\,\mathcal{E}_j \qquad (i,j=1,2)\,,$$

with

$$J_{ij}^* = J_{ji}\,. \tag{1.14}$$

The four parameters describing the geometrical properties of the polarization ellipse (Eqs. (1.7)) are related to the components of the polarization tensor by the simple

expressions

$$\begin{aligned} P_I &= \mathcal{E}_1^* \, \mathcal{E}_1 + \mathcal{E}_2^* \, \mathcal{E}_2 \\ P_Q &= \mathcal{E}_1^* \, \mathcal{E}_1 - \mathcal{E}_2^* \, \mathcal{E}_2 \\ P_U &= \mathcal{E}_1^* \, \mathcal{E}_2 + \mathcal{E}_2^* \, \mathcal{E}_1 \\ P_V &= \mathrm{i} \, (\mathcal{E}_1^* \, \mathcal{E}_2 - \mathcal{E}_2^* \, \mathcal{E}_1) \; . \end{aligned} \tag{1.15}$$

Note that a minus sign would appear in the expression for P_V if Eq. (1.12) were used.

After inversion of Eqs. (1.15) the polarization tensor can be written as

$$\boldsymbol{J} = \frac{1}{2} \begin{pmatrix} P_I + P_Q & P_U - \mathrm{i} P_V \\ P_U + \mathrm{i} P_V & P_I - P_Q \end{pmatrix} \; ,$$

which can be cast into a more synthetic form. Defining the formal vector

$$\begin{pmatrix} P_0 \\ P_1 \\ P_2 \\ P_3 \end{pmatrix} = \begin{pmatrix} P_I \\ P_Q \\ P_U \\ P_V \end{pmatrix} \; ,$$

and introducing the 2×2 identity matrix $\boldsymbol{\sigma}_0$ and the Pauli spin matrices $\boldsymbol{\sigma}_1$, $\boldsymbol{\sigma}_2$, and $\boldsymbol{\sigma}_3$, we can write[1]

$$\boldsymbol{J} = \frac{1}{2} \sum_{i=0}^{3} P_i \, \boldsymbol{\sigma}_i \; , \tag{1.16}$$

where

$$\boldsymbol{\sigma}_0 = \begin{pmatrix} 1 & 0 \\ 0 & 1 \end{pmatrix}, \quad \boldsymbol{\sigma}_1 = \begin{pmatrix} 1 & 0 \\ 0 & -1 \end{pmatrix}, \quad \boldsymbol{\sigma}_2 = \begin{pmatrix} 0 & 1 \\ 1 & 0 \end{pmatrix}, \quad \boldsymbol{\sigma}_3 = \begin{pmatrix} 0 & -\mathrm{i} \\ \mathrm{i} & 0 \end{pmatrix} \tag{1.17}$$

with

$$\boldsymbol{\sigma}_j \boldsymbol{\sigma}_k = \delta_{jk} \, \boldsymbol{\sigma}_0 + \mathrm{i} \sum_l \epsilon_{jkl} \, \boldsymbol{\sigma}_l \qquad (j,k,l = 1,2,3) \; . \tag{1.18}$$

In the last equation δ_{jk} is the *Kronecker symbol* – equal to 1 for $j = k$ and to 0 for $j \neq k$ – and ϵ_{jkl} is the *antisymmetric* (or *Levi-Civita*) *tensor* – equal to $+1$ if (j,k,l) is an even permutation of $(1,2,3)$, to -1 if (j,k,l) is an odd permutation of $(1,2,3)$, and to 0 if two (or three) indices are equal.

Multiplying Eq. (1.16) by $\boldsymbol{\sigma}_j$ and using the relation

$$\mathrm{Tr} \, (\boldsymbol{\sigma}_j \boldsymbol{\sigma}_i) = 2 \, \delta_{ji} \qquad (i,j = 0, \ldots, 3) \; , \tag{1.19}$$

[1] The representation that we have chosen here for the Pauli spin matrices differs from the standard one, initially introduced by Pauli (1927) and then followed in classical textbooks on Quantum Mechanics (Schiff, 1949; Messiah, 1961; etc.). The matrices introduced by Pauli ($\boldsymbol{\sigma}_x$, $\boldsymbol{\sigma}_y$, $\boldsymbol{\sigma}_z$) are connected with the ones defined here by the relations: $\boldsymbol{\sigma}_x = \boldsymbol{\sigma}_2$, $\boldsymbol{\sigma}_y = \boldsymbol{\sigma}_3$, $\boldsymbol{\sigma}_z = \boldsymbol{\sigma}_1$.

we can rewrite Eqs. (1.15) in the form

$$P_j = \mathrm{Tr}\,(\boldsymbol{\sigma}_j\,\boldsymbol{J}\,)\;. \tag{1.20}$$

Finally, Eq. (1.10) can be expressed in the compact form

$$\det\,\boldsymbol{J} = 0\;. \tag{1.21}$$

1.4. Quasi-monochromatic Wave

The pure monochromatic wave considered in Sect. 1.1 is nothing but a mathematical abstraction; in the physical world one always deals with radiation beams having a non-zero angular spread and a finite frequency bandwidth. Such beams can be described using wave packets of the form

$$\vec{E}(\vec{r},t) = \mathrm{Re}\left[\int \vec{\mathcal{E}}(\vec{k}')\,\mathrm{e}^{\,\mathrm{i}(\vec{k}'\cdot\vec{r}-\omega' t)}\,n(\vec{k}')\,\mathrm{d}^3\vec{k}'\right]\;,$$

where $\vec{\mathcal{E}}(\vec{k}')$ is the complex electric field amplitude of the single wave propagating with wavenumber $\vec{k}'$ and angular frequency $\omega' = c\,|\vec{k}'|$, with

$$\vec{\mathcal{E}}(\vec{k}')\cdot\vec{k}' = 0\;,$$

and where $n(\vec{k}')$ is the number density of waves in the three-dimensional wavenumber space.

We now suppose the wave packet to be confined into a small range of wavenumbers $\Delta\vec{k}$ centered around $\vec{k}$. This means that our packet has an angular spread in the solid angle $\Delta\Omega \approx |\Delta\vec{k}|/|\vec{k}|$ and a finite frequency bandwidth $\Delta\omega \approx c\,|\Delta\vec{k}|$. Writing

$$\vec{k}' = \vec{k} + \delta\vec{k}\;, \qquad \omega' = \omega + \delta\omega$$

we obtain

$$\vec{E}(\vec{r},t) = \mathrm{Re}\left[\mathrm{e}^{\,\mathrm{i}(\vec{k}\cdot\vec{r}-\omega t)}\int \vec{\mathcal{E}}(\vec{k}+\delta\vec{k})\,\mathrm{e}^{\,\mathrm{i}(\delta\vec{k}\cdot\vec{r}-\delta\omega\, t)}\,n(\delta\vec{k})\,\mathrm{d}^3(\delta\vec{k})\right]\;. \tag{1.22}$$

Let us consider a surface element Σ perpendicular to the $\vec{k}$ direction, and a coordinate system (xyz) as shown in Fig. 1.4. At any point P of the surface Σ the components of the electric field vector are given by

$$\begin{aligned} E_x(\mathrm{P},t) &= \mathrm{Re}\left[\mathcal{E}_1(\mathrm{P},t)\,\mathrm{e}^{\,-\mathrm{i}\omega t}\right] \\ E_y(\mathrm{P},t) &= \mathrm{Re}\left[\mathcal{E}_2(\mathrm{P},t)\,\mathrm{e}^{\,-\mathrm{i}\omega t}\right]\;, \end{aligned} \tag{1.23}$$

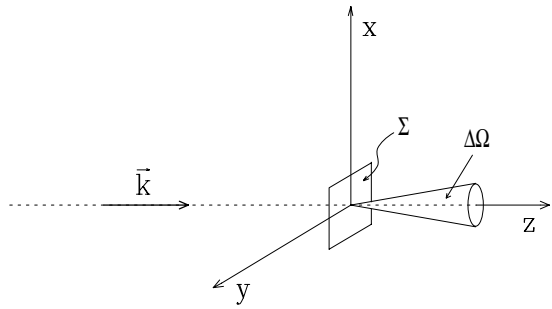

Fig.1.4. Coordinate system for defining the various components of the electric vibration of a quasi-monochromatic wave. The vector $\vec{k}$ is directed along the z-axis.

where $\mathcal{E}_1(\mathrm{P},t)$ and $\mathcal{E}_2(\mathrm{P},t)$ are the x and y components, respectively, of the vector resulting from the evaluation of the integral in Eq. (1.22). The third component $E_z(\mathrm{P},t)$ is much smaller than the x and y components (a typical ratio E_z/E_x being of order $\Delta\Omega$) and will be neglected in the following.

If the linear dimensions L of the surface Σ are such that $L|\Delta\vec{k}| \ll 1$, the quantities $\mathcal{E}_1(\mathrm{P},t)$ and $\mathcal{E}_2(\mathrm{P},t)$ are weakly varying functions of the point P. Moreover, they are slowly varying functions of time, having temporal variations on typical time-scales much larger than the period of the wave. As a result, the tip of the electric field vector at the point P describes a polarization ellipse whose characteristic parameters vary slowly with time; these parameters will also show a smooth variation from point to point on the surface Σ.

Obviously, it is impossible to define an instantaneous polarization ellipse in this situation. It is however possible to define appropriate average quantities by generalizing Eqs. (1.15) in the form

$$\begin{aligned} P_I &= \left\langle \mathcal{E}_1^*(\mathrm{P},t)\,\mathcal{E}_1(\mathrm{P},t)\right\rangle + \left\langle \mathcal{E}_2^*(\mathrm{P},t)\,\mathcal{E}_2(\mathrm{P},t)\right\rangle \\ P_Q &= \left\langle \mathcal{E}_1^*(\mathrm{P},t)\,\mathcal{E}_1(\mathrm{P},t)\right\rangle - \left\langle \mathcal{E}_2^*(\mathrm{P},t)\,\mathcal{E}_2(\mathrm{P},t)\right\rangle \\ P_U &= \left\langle \mathcal{E}_1^*(\mathrm{P},t)\,\mathcal{E}_2(\mathrm{P},t)\right\rangle + \left\langle \mathcal{E}_2^*(\mathrm{P},t)\,\mathcal{E}_1(\mathrm{P},t)\right\rangle \\ P_V &= \mathrm{i}\Big[\left\langle \mathcal{E}_1^*(\mathrm{P},t)\,\mathcal{E}_2(\mathrm{P},t)\right\rangle - \left\langle \mathcal{E}_2^*(\mathrm{P},t)\,\mathcal{E}_1(\mathrm{P},t)\right\rangle\Big]\,, \end{aligned} \tag{1.24}$$

where the symbol $\langle\cdots\rangle$ means an average over a time interval much longer than the wave period and an average over the surface Σ.

Similarly, one can generalize the definition of the polarization tensor by writing

$$J_{ij} = \left\langle \mathcal{E}_i^*(\mathrm{P},t)\,\mathcal{E}_j(\mathrm{P},t)\right\rangle\,, \tag{1.25}$$

so that Eqs. (1.16) and (1.20) are still valid.

The important difference from the case of the monochromatic wave lies in the fact that Eqs. (1.10) and (1.21) no longer are valid. To prove this statement, let us consider the complex quantity $\mathcal{A}$ defined by

$$\mathcal{A} = \mathcal{E}_2(\mathrm{P},t)\left\langle \mathcal{E}_1^*(\mathrm{P},t)\,\mathcal{E}_1(\mathrm{P},t)\right\rangle - \mathcal{E}_1(\mathrm{P},t)\left\langle \mathcal{E}_1^*(\mathrm{P},t)\,\mathcal{E}_2(\mathrm{P},t)\right\rangle\,.$$

For the average value of its square modulus we have, with easy transformations

$$\left\langle |\mathcal{A}|^2 \right\rangle = \left\langle \mathcal{E}_1^*(\mathrm{P},t)\,\mathcal{E}_1(\mathrm{P},t)\right\rangle \Big[\left\langle \mathcal{E}_1^*(\mathrm{P},t)\,\mathcal{E}_1(\mathrm{P},t)\right\rangle \left\langle \mathcal{E}_2^*(\mathrm{P},t)\,\mathcal{E}_2(\mathrm{P},t)\right\rangle - \left\langle \mathcal{E}_1^*(\mathrm{P},t)\,\mathcal{E}_2(\mathrm{P},t)\right\rangle \left\langle \mathcal{E}_2^*(\mathrm{P},t)\,\mathcal{E}_1(\mathrm{P},t)\right\rangle \Big] .$$

From this equation, excluding the trivial case $\mathcal{E}_1(\mathrm{P},t) \equiv 0$, we conclude that, being

$$\left\langle \mathcal{E}_1^*(\mathrm{P},t)\,\mathcal{E}_1(\mathrm{P},t)\right\rangle > 0 \quad \text{and} \quad \left\langle |\mathcal{A}|^2 \right\rangle \geq 0 ,$$

we must have

$$\left\langle \mathcal{E}_1^*(\mathrm{P},t)\,\mathcal{E}_1(\mathrm{P},t)\right\rangle \left\langle \mathcal{E}_2^*(\mathrm{P},t)\,\mathcal{E}_2(\mathrm{P},t)\right\rangle - \left\langle \mathcal{E}_1^*(\mathrm{P},t)\,\mathcal{E}_2(\mathrm{P},t)\right\rangle \left\langle \mathcal{E}_2^*(\mathrm{P},t)\,\mathcal{E}_1(\mathrm{P},t)\right\rangle \geq 0 ,$$

that is

$$\det \boldsymbol{J} = P_I^2 - P_Q^2 - P_U^2 - P_V^2 \geq 0 . \tag{1.26}$$

The equal sign holds only in the case $\mathcal{A} \equiv 0$, which implies

$$\frac{\mathcal{E}_2(\mathrm{P},t)}{\mathcal{E}_1(\mathrm{P},t)} = \frac{\left\langle \mathcal{E}_1^*(\mathrm{P},t)\,\mathcal{E}_2(\mathrm{P},t)\right\rangle}{\left\langle \mathcal{E}_1^*(\mathrm{P},t)\,\mathcal{E}_1(\mathrm{P},t)\right\rangle} ;$$

this means either that one of the two components is identically zero, or that the two components have, at any point P and any time t, the same amplitude ratio and phase difference. In both cases the quasi-monochromatic wave is said to be *totally polarized*. The opposite situation occurs when the two components $\mathcal{E}_1(\mathrm{P},t)$ and $\mathcal{E}_2(\mathrm{P},t)$ have the same average amplitude and random phase difference, so that

$$\left\langle \mathcal{E}_1^*(\mathrm{P},t)\,\mathcal{E}_1(\mathrm{P},t)\right\rangle = \left\langle \mathcal{E}_2^*(\mathrm{P},t)\,\mathcal{E}_2(\mathrm{P},t)\right\rangle$$
$$\left\langle \mathcal{E}_1^*(\mathrm{P},t)\,\mathcal{E}_2(\mathrm{P},t)\right\rangle = \left\langle \mathcal{E}_2^*(\mathrm{P},t)\,\mathcal{E}_1(\mathrm{P},t)\right\rangle = 0 .$$

We have in this case

$$P_Q = P_U = P_V = 0 ,$$

and the quasi-monochromatic wave is said to be *totally unpolarized* (if the frequency of the radiation beam is in the visible band of the spectrum, the beam is said to be composed of *natural light*). In intermediate cases the quasi-monochromatic wave is said to be *partially polarized* with a *polarization degree* given by

$$p = \sqrt{P_Q^2 + P_U^2 + P_V^2} \;/\; P_I ,$$

with $0 \leq p \leq 1$.

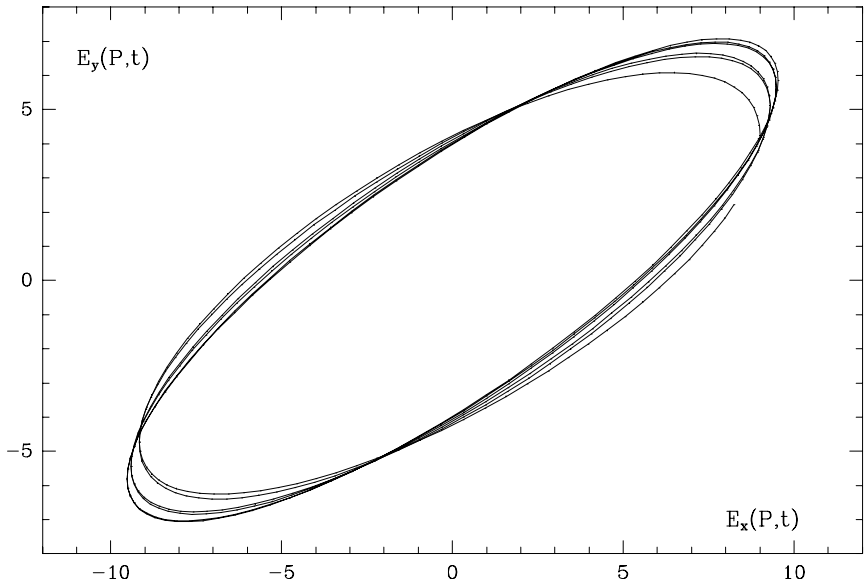

Fig.1.5. For a partially polarized quasi-monochromatic wave, the tip of the electric field vector at a given point P describes, as a function of time, the trajectory shown in this graph. Note that the characteristic shape of the polarization ellipse has a slow variation with time. The electric field is given in arbitrary units.

In Figs. 1.5 and 1.6 the trajectory of the tip of the electric field vector is plotted for two schematic situations corresponding to a partially polarized and a totally polarized quasi-monochromatic wave, respectively.

1.5. Polarizers and Retarders

In the previous sections we have described the polarization properties of a radiation beam using appropriate averages of the electric vibrations. Now we must give some operational definitions capable of relating these properties to actual measurements to be performed on the beam. For this purpose it is necessary to introduce the concept of *ideal polarizing filters*, a concept that will be used in the following to give an operational definition of the Stokes parameters.

We define an *ideal linear polarizer* (sometimes called *analyzer*) as a device that is totally transparent to the electric vibration along a given axis (called the *transmission* – or *acceptance* – axis of the polarizer) and totally opaque to the electric vibration along the axis perpendicular to the former. When such a device is introduced in the optical path of a radiation beam, the components of the electric vibration are modified inside the polarizer according to the equation

$$\begin{pmatrix} \mathcal{E}'_a \\ \mathcal{E}'_b \end{pmatrix} = \mathrm{e}^{\,\mathrm{i}\psi} \begin{pmatrix} 1 & 0 \\ 0 & 0 \end{pmatrix} \begin{pmatrix} \mathcal{E}_a \\ \mathcal{E}_b \end{pmatrix} = \mathrm{e}^{\,\mathrm{i}\psi} \begin{pmatrix} \mathcal{E}_a \\ 0 \end{pmatrix} \ ,$$

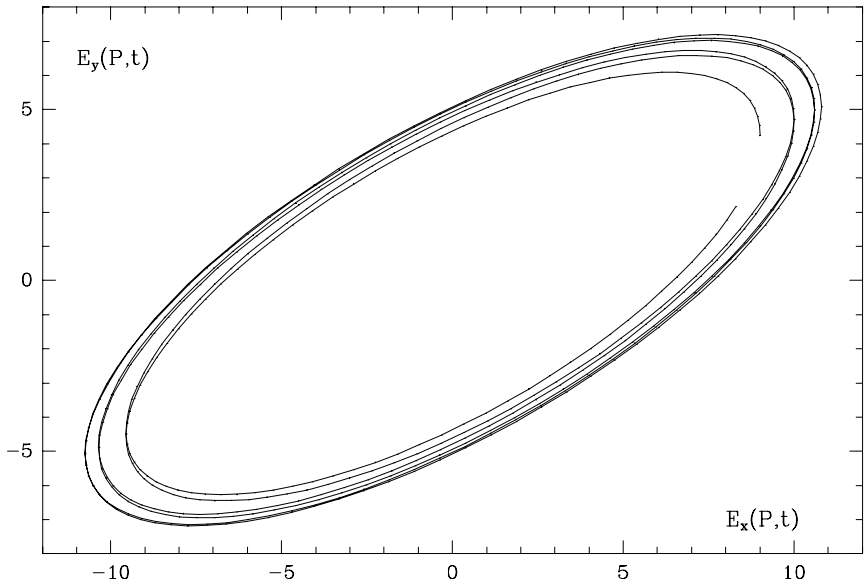

Fig.1.6. Same as Fig.1.5 for a totally polarized quasi-monochromatic wave. Although the size of the ellipse changes with time, its characteristic shape (i.e. the α angle defined in Fig.1.2 and the ratio between the axes) remains fixed.

where $\mathcal{E}_a$ and $\mathcal{E}_b$ are the components, at the entrance of the polarizer, along the transmission axis and the orthogonal axis, respectively; $\mathcal{E}'_a$ and $\mathcal{E}'_b$ are the same components at the exit of the polarizer, and ψ is a phase difference that is totally inessential in determining the polarization properties of the beam.

The simplest device whose performances approach in practice those of an ideal polarizer (in the optical range of the electromagnetic spectrum) is the well-known *Polaroid* which has been developed commercially in various forms by the Polaroid Corporation, Cambridge, Massachusetts, U.S.A. This device is based on the property shown by some organic, needle-shaped microcrystals of absorbing light preferentially along the longest axis of the crystal. Roughly speaking, a Polaroid consists of a large number of such microcrystals oriented through a procedure of unidirectional stretching. Since the basic physical phenomenon involved in the operation of a Polaroid is *dichroism* (the property of absorbing light to different extents depending on the polarization of the incident beam), the Polaroid is often referred to as a *dichroic polarizer*.

Linear polarizers of a different kind are the so-called *birefringence polarizers* which consist of one or more birefringent crystals (generally calcite) suitably prepared and arranged into a compact system. These polarizers operate according to the following scheme: the incident beam is divided in two orthogonally polarized components that propagate along different directions in the birefringent crystal; one of the two components is physically removed by absorption or lateral deflection, so that a single, linearly polarized component is transmitted through the whole system. Examples of birefringence polarizers are those bearing the names of

Ahrens, Wollaston, Rochon, Glan-Foucault, and Nicol. More details on birefringent polarizers, as well as on dichroic polarizers, can be found in Shurcliff (1962). In the same book different kinds of linear polarizers, like *reflection polarizers* and *scattering polarizers*, are also described.

Turning now our attention to retarders, we define an *ideal retarder* as a device which divides the incident beam in two orthogonally polarized components, dephases one of them relative to the other without altering their amplitudes, and, finally, reunites the two components giving rise to a beam whose polarization characteristics are, in general, completely different from those of the incident beam. An ideal retarder (sometimes called *compensator*) is characterized by the fact that the phase velocity of an electromagnetic wave propagating along the optical axis depends on the direction of the electric vibration. For an electric vibration parallel to the fast axis the retarder is characterized by the index of refraction n_f, while for an electric vibration parallel to the slow axis the index of refraction is n_s, with $n_\mathrm{s} > n_\mathrm{f}$.

Let us consider a monochromatic wave that propagates along the optical axis of a retarder of given thickness l. The electric field carried by the wave is described in complex notations by the equations

$$\begin{aligned} E_\mathrm{f}(z,t) &= \mathrm{Re}\left[\mathcal{E}_\mathrm{f}\,\mathrm{e}^{\,\mathrm{i}(n_\mathrm{f}kz-\omega t)}\right] \\ E_\mathrm{s}(z,t) &= \mathrm{Re}\left[\mathcal{E}_\mathrm{s}\,\mathrm{e}^{\,\mathrm{i}(n_\mathrm{s}kz-\omega t)}\right] , \end{aligned} \qquad (0 \le z \le l)$$

where z is the coordinate along the optical axis of the retarder with the origin ($z = 0$) at the entrance, $\mathcal{E}_\mathrm{f}$ and $\mathcal{E}_\mathrm{s}$ are the complex amplitudes of the electric vibration along the fast and slow axes, respectively, and k is the wavenumber in vacuum.

Comparing the electric vibrations at the exit of the retarder with those at the entrance, we have with obvious notations

$$\begin{pmatrix} \mathcal{E}'_\mathrm{f} \\ \mathcal{E}'_\mathrm{s} \end{pmatrix} = \mathrm{e}^{\,\mathrm{i}\psi} \begin{pmatrix} 1 & 0 \\ 0 & \mathrm{e}^{\,\mathrm{i}\delta} \end{pmatrix} \begin{pmatrix} \mathcal{E}_\mathrm{f} \\ \mathcal{E}_\mathrm{s} \end{pmatrix} = \mathrm{e}^{\,\mathrm{i}\psi} \begin{pmatrix} \mathcal{E}_\mathrm{f} \\ \mathrm{e}^{\,\mathrm{i}\delta}\,\mathcal{E}_\mathrm{s} \end{pmatrix} , \qquad (1.27)$$

where ψ is a phase that does not affect the polarization properties of the wave, while δ, the so-called *retardance* (or *retardation*), is given by

$$\delta = (n_\mathrm{s} - n_\mathrm{f})\,kl = 2\pi\,(n_\mathrm{s} - n_\mathrm{f})\,l\,/\lambda\,, \qquad (1.28)$$

λ being the wavelength in vacuum. When the thickness of the retarder is such that $\delta = \pi/2$, the retarder is called a *quarter-wave plate*, and, similarly, when $\delta = \pi$ the retarder is called a *half-wave plate*.

It is interesting to note that an ideal quarter-wave plate followed by an ideal linear polarizer whose transmission axis is directed at 45° from the fast axis in the counterclockwise direction (as seen by an observer facing the radiation source) behaves

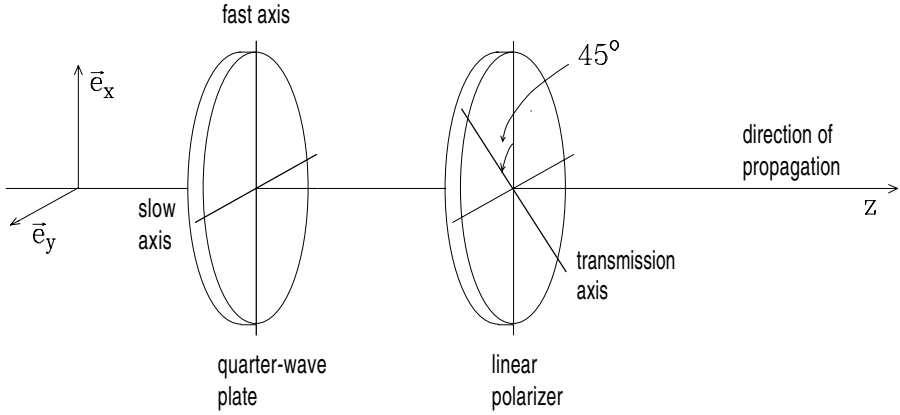

Fig.1.7. Practical realization of a filter transparent to positive circular polarization and opaque to negative circular polarization.

like an ideal filter that is totally transparent to positive (or right-handed) circular polarization and totally opaque to negative (or left-handed) circular polarization.[1]

To prove this statement, let us consider a circularly polarized monochromatic wave propagating along the direction shown in Fig. 1.7. If the wave is totally circularly polarized in the positive direction, the components of the electric field vibration along the unit vectors $\vec{e}_x$ and $\vec{e}_y$ before entering the retarder are (in complex notations)

$$\begin{aligned} E_x &= \mathrm{Re}\left[A\,\mathrm{e}^{-\mathrm{i}\omega t}\right] \\ E_y &= \mathrm{Re}\left[-\mathrm{i}A\,\mathrm{e}^{-\mathrm{i}\omega t}\right] \ , \end{aligned} \tag{1.29}$$

where A is a constant. At the exit of the retarder, we have from Eq. (1.27) (apart from an inessential phase factor)

$$E'_x = E'_y = \mathrm{Re}\left[A\,\mathrm{e}^{-\mathrm{i}\omega t}\right] \ , \tag{1.30}$$

thus the component of the electric vibration along the transmission axis of the polarizer is given by

$$E_a = \frac{1}{\sqrt{2}}\left(E'_x + E'_y\right) = \sqrt{2}\,\mathrm{Re}\left[A\,\mathrm{e}^{-\mathrm{i}\omega t}\right] \ .$$

Since this component is simply transmitted through the linear polarizer, the electric vibration at the exit is still described by Eq. (1.30). Therefore, although the

[1] Obviously, when the transmission axis is inclined at 45° in the opposite direction, the optical combination behaves in the opposite way with respect to circular polarization.

polarization has been transformed from circular to linear, the energy carried by the wave has not been changed by the system (the overbar means a time average)

$$\overline{E_x^2} + \overline{E_y^2} = \overline{E_x'^2} + \overline{E_y'^2} = |A|^2 \, .$$

It follows that the device schematized in Fig. 1.7 is totally transparent to positive circular polarization.

Applying the same argument to a monochromatic wave of negative circular polarization (E_y in Eq. (1.29) must be changed in sign) we obtain that the wave is totally absorbed inside the polarizer.

Most of the retarders that are used in practice are of the birefringent type; they often consist of a crystal, like quartz or calcite, cut parallel to the optical axis. More recently *piezo-optical birefringence modulators* have also been used. In these devices the birefringence is induced by compressing or distending a material (otherwise isotropic and uniform) along a given direction. According to Kemp (1969) a very modest force, that can even be attained by simple finger pressure, is enough to produce a quarter-wave plate by stressing a block of glass having the size of a match-box.

Other devices that have been often used to produce retarders with variable or modulated retardance are the so-called *Pockels cells*. Here the birefringence is induced by application of high electric fields (of the order of several kV/cm) in materials such as ammonium dihydrogen phosphate (ADP) or potassium dihydrogen phosphate (KDP).

1.6. Stokes Parameters

A simple operational definition of the Stokes parameters can be given in terms of a set of ideal filters and an ideal detector capable of measuring, in absolute units, the electromagnetic energy falling on its acceptance area. For this definition – or, more precisely, for the definition of the two parameters connected with linear polarization – it is also necessary to fix a particular direction in the plane perpendicular to the direction of propagation. Such direction will be referred to in the following as the *reference direction* or the *reference axis*.

Given a quasi-monochromatic radiation beam having a small aperture $\mathrm{d}\Omega$, and frequency contained in the interval $(\nu, \nu + \mathrm{d}\nu)$, we define the first Stokes parameter, I, as the energy measured by our ideal detector per unit time and per unit cross-sectional area. In formulae, if $\mathrm{d}W_0$ is the energy measured by the detector in the time interval $\mathrm{d}t$ over the surface $\mathrm{d}S$ oriented perpendicularly to the beam, we have

$$\mathrm{d}W_0 = I \, \mathrm{d}S \, \mathrm{d}t \, \mathrm{d}\Omega \, \mathrm{d}\nu \, .$$

This is just the usual definition of the radiation specific intensity, so that the first Stokes parameter is simply called the *intensity* of the beam.

Let's now insert in the beam path an ideal linear polarizer with its transmission axis directed in succession at 0°, 45°, 90°, and 135° from the reference axis, all the

angles being reckoned counterclockwise for an observer looking at the beam from the detector. If $\mathrm{d}W_1$, $\mathrm{d}W_2$, $\mathrm{d}W_3$, and $\mathrm{d}W_4$ are the corresponding energies measured by the detector in the time interval $\mathrm{d}t$ over the surface $\mathrm{d}S$, the second and third Stokes parameters, Q and U, are defined by

$$\begin{aligned} \mathrm{d}W_1 - \mathrm{d}W_3 &= Q\,\mathrm{d}S\,\mathrm{d}t\,\mathrm{d}\Omega\,\mathrm{d}\nu \\ \mathrm{d}W_2 - \mathrm{d}W_4 &= U\,\mathrm{d}S\,\mathrm{d}t\,\mathrm{d}\Omega\,\mathrm{d}\nu\ . \end{aligned}$$

Finally, for the definition of the fourth parameter we introduce two ideal filters, the first being totally opaque to negative (left-handed) circular polarization and totally transparent to positive (right-handed) circular polarization, and the second behaving in the opposite way (such filters can be realized as shown in the former section). If $\mathrm{d}W_5$ and $\mathrm{d}W_6$ are the energies measured by the detector (in the time interval $\mathrm{d}t$ over the surface $\mathrm{d}S$) with the first and second filters – respectively – interposed, the definition of the fourth parameter, V, is the following

$$\mathrm{d}W_5 - \mathrm{d}W_6 = V\,\mathrm{d}S\,\mathrm{d}t\,\mathrm{d}\Omega\,\mathrm{d}\nu\ .$$

The symbols used in this book to represent the Stokes parameters (I, Q, U, V) were introduced for the first time by Walker (1954). In his original note, Stokes (1852) used the symbols (A, B, C, D), while Jones (1941) and Perrin (1942) used the notation (I, M, C, S). Walker's notation seems nowadays to be preferred especially in the astrophysical literature.

The operational definitions given above are not universally adopted. In particular, the opposite sign is used in the definition of V by those authors who name positive circular polarization the one that we have defined as negative and vice versa (see the discussion at the end of Sect. 1.2). Less frequently a sign inversion is found in the definition of U. Figure 1.8 summarizes the conventions that are used in this book.

Now that the Stokes parameters have been defined, it is necessary to establish their connection with the description, given in the previous sections, of the polarization properties of an electromagnetic wave in terms of electric fields. Since the energy flux carried by an electromagnetic wave is given by its Poynting vector, the energy ΔW measured in the time interval Δt by an ideal detector having cross-sectional area ΔS is connected with the electric field components by the relation

$$\Delta W = \frac{c}{4\pi}\left\langle E_x^2 + E_y^2 \right\rangle \Delta S\,\Delta t\ ,$$

where E_x and E_y are the components of the electric field along two axes perpendicular to each other and to the direction of propagation, and where the brackets mean an average over the time interval Δt and over the surface ΔS of the detector. Using Eqs. (1.3), (1.11), and (1.13), we can also write

$$\Delta W = \frac{c}{8\pi}\left\langle E_1^2 + E_2^2 \right\rangle \Delta S\,\Delta t = \frac{c}{8\pi}\left\langle \mathcal{E}_1^*\,\mathcal{E}_1 + \mathcal{E}_2^*\,\mathcal{E}_2 \right\rangle \Delta S\,\Delta t\ . \tag{1.31}$$

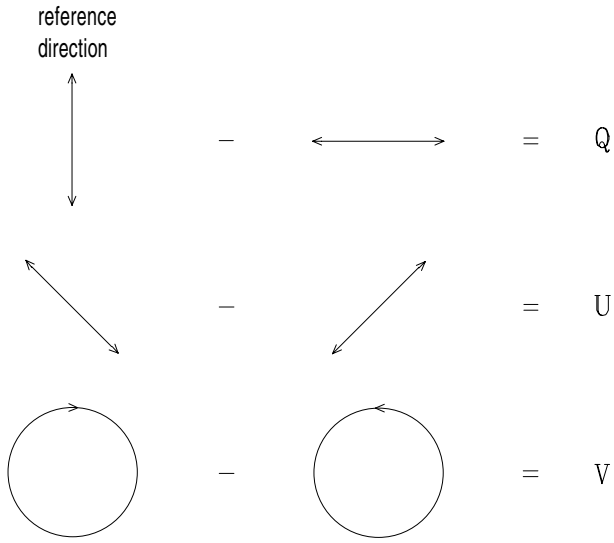

Fig.1.8. Schematic representation of the definition of the Stokes parameters. The observer is supposed to face the radiation source.

Referring to the general case of a quasi-monochromatic wave, we introduce a couple of orthogonal unit vectors $\vec{e}_a$ and $\vec{e}_b$, with $\vec{e}_a$ specifying the reference direction and $\vec{e}_b$ oriented in such a way that $\vec{e}_a$, $\vec{e}_b$, and the direction of propagation form a right-handed coordinate system.[1] If $\mathcal{E}_1(\mathrm{P},t)$ and $\mathcal{E}_2(\mathrm{P},t)$ are the complex amplitudes of the electric field along the $\vec{e}_a$ and $\vec{e}_b$ directions, the energy measured by the detector in the various configurations specified above is given by (see Eqs. (1.23)):
a) without any filter

$$\Delta W_0 = \left[\left\langle \mathcal{E}_1^*(\mathrm{P},t)\,\mathcal{E}_1(\mathrm{P},t)\right\rangle + \left\langle \mathcal{E}_2^*(\mathrm{P},t)\,\mathcal{E}_2(\mathrm{P},t)\right\rangle\right]\frac{c}{8\pi}\,\Delta S\,\Delta t\;;$$

b) with a linear polarizer interposed, having its transmission axis at 0°, 45°, 90°, and 135°, respectively

$$\begin{aligned}
\Delta W_1 &= \left\langle \mathcal{E}_1^*(\mathrm{P},t)\,\mathcal{E}_1(\mathrm{P},t)\right\rangle\frac{c}{8\pi}\,\Delta S\,\Delta t\\
\Delta W_2 &= \frac{1}{2}\Big[\left\langle \mathcal{E}_1^*(\mathrm{P},t)\,\mathcal{E}_1(\mathrm{P},t)\right\rangle + \left\langle \mathcal{E}_2^*(\mathrm{P},t)\,\mathcal{E}_2(\mathrm{P},t)\right\rangle\\
&\qquad + \left\langle \mathcal{E}_1^*(\mathrm{P},t)\,\mathcal{E}_2(\mathrm{P},t)\right\rangle + \left\langle \mathcal{E}_2^*(\mathrm{P},t)\,\mathcal{E}_1(\mathrm{P},t)\right\rangle\Big]\frac{c}{8\pi}\,\Delta S\,\Delta t\\
\Delta W_3 &= \left\langle \mathcal{E}_2^*(\mathrm{P},t)\,\mathcal{E}_2(\mathrm{P},t)\right\rangle\frac{c}{8\pi}\,\Delta S\,\Delta t
\end{aligned}$$

[1] In the following, $\vec{e}_a$ will be referred to as the *reference direction unit vector*, while $\vec{e}_b$ will be referred to as the *associated unit vector*. Note that the definition of the Stokes parameters remains the same if we replace $\vec{e}_a$ by $-\vec{e}_a$ and $\vec{e}_b$ by $-\vec{e}_b$.

$$\Delta W_4 = \frac{1}{2}\Big[\big\langle \mathcal{E}_1^*(\mathrm{P},t)\,\mathcal{E}_1(\mathrm{P},t)\big\rangle + \big\langle \mathcal{E}_2^*(\mathrm{P},t)\,\mathcal{E}_2(\mathrm{P},t)\big\rangle - \big\langle \mathcal{E}_1^*(\mathrm{P},t)\,\mathcal{E}_2(\mathrm{P},t)\big\rangle - \big\langle \mathcal{E}_2^*(\mathrm{P},t)\,\mathcal{E}_1(\mathrm{P},t)\big\rangle\Big]\frac{c}{8\pi}\,\Delta S\,\Delta t\;;$$

c) with a filter for circular polarization interposed, opaque to negative polarization (and transparent to positive), and vice versa

$$\Delta W_5 = \frac{1}{2}\Big[\big\langle \mathcal{E}_1^*(\mathrm{P},t)\,\mathcal{E}_1(\mathrm{P},t)\big\rangle + \big\langle \mathcal{E}_2^*(\mathrm{P},t)\,\mathcal{E}_2(\mathrm{P},t)\big\rangle + \mathrm{i}\big\langle \mathcal{E}_1^*(\mathrm{P},t)\,\mathcal{E}_2(\mathrm{P},t)\big\rangle - \mathrm{i}\big\langle \mathcal{E}_2^*(\mathrm{P},t)\,\mathcal{E}_1(\mathrm{P},t)\big\rangle\Big]\frac{c}{8\pi}\,\Delta S\,\Delta t$$

$$\Delta W_6 = \frac{1}{2}\Big[\big\langle \mathcal{E}_1^*(\mathrm{P},t)\,\mathcal{E}_1(\mathrm{P},t)\big\rangle + \big\langle \mathcal{E}_2^*(\mathrm{P},t)\,\mathcal{E}_2(\mathrm{P},t)\big\rangle - \mathrm{i}\big\langle \mathcal{E}_1^*(\mathrm{P},t)\,\mathcal{E}_2(\mathrm{P},t)\big\rangle + \mathrm{i}\big\langle \mathcal{E}_2^*(\mathrm{P},t)\,\mathcal{E}_1(\mathrm{P},t)\big\rangle\Big]\frac{c}{8\pi}\,\Delta S\,\Delta t\;.$$

From these expressions, taking the limit for infinitesimal values of ΔS and Δt, and bearing in mind Eqs. (1.24) and the operational definitions of the Stokes parameters, we obtain

$$\begin{aligned} I &= kP_I = k\Big[\big\langle \mathcal{E}_1^*(\mathrm{P},t)\,\mathcal{E}_1(\mathrm{P},t)\big\rangle + \big\langle \mathcal{E}_2^*(\mathrm{P},t)\,\mathcal{E}_2(\mathrm{P},t)\big\rangle\Big] \\ Q &= kP_Q = k\Big[\big\langle \mathcal{E}_1^*(\mathrm{P},t)\,\mathcal{E}_1(\mathrm{P},t)\big\rangle - \big\langle \mathcal{E}_2^*(\mathrm{P},t)\,\mathcal{E}_2(\mathrm{P},t)\big\rangle\Big] \\ U &= kP_U = k\Big[\big\langle \mathcal{E}_1^*(\mathrm{P},t)\,\mathcal{E}_2(\mathrm{P},t)\big\rangle + \big\langle \mathcal{E}_2^*(\mathrm{P},t)\,\mathcal{E}_1(\mathrm{P},t)\big\rangle\Big] \\ V &= kP_V = k\,\mathrm{i}\Big[\big\langle \mathcal{E}_1^*(\mathrm{P},t)\,\mathcal{E}_2(\mathrm{P},t)\big\rangle - \big\langle \mathcal{E}_2^*(\mathrm{P},t)\,\mathcal{E}_1(\mathrm{P},t)\big\rangle\Big]\;, \end{aligned} \tag{1.32}$$

where k is a dimensional positive constant whose actual value is important only when absolute measurements are to be performed.

It should be kept in mind that Eqs. (1.32) are valid only when the component $\mathcal{E}_1$ of the electric vibration refers to the reference axis defining the Stokes parameters, and when the conventions implicit in Eqs. (1.11) and (1.13) are used. Note also that Eqs. (1.32) give a deeper physical meaning to the quantities P_I, P_Q, P_U, P_V introduced in former sections (see Eqs. (1.7), (1.15), and (1.24)).

1.7. Measurements of the Stokes Parameters

The Stokes parameters can be measured by several different techniques, and the various instruments that have been devised for this purpose cannot be classified in a unique scheme. Following Hauge (1976) it is however possible to describe a kind of prototype instrument that summarizes the essential characteristics of most of

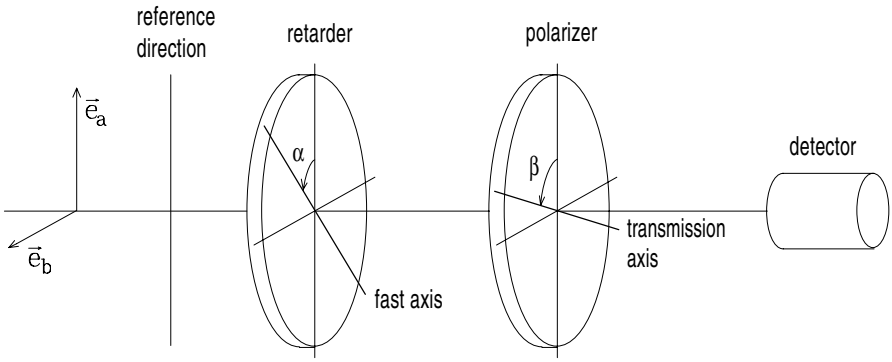

Fig.1.9. Schematic representation of a prototype instrument aimed at the measurement of the Stokes parameters.

the devices that are used in practice, especially for the measurement of the Stokes parameters in the visible or near-infrared range of the electromagnetic spectrum.

Referring to Fig. 1.9, if $\mathcal{E}_1$ and $\mathcal{E}_2$ are (in complex notations) the electric vibrations along the unit vectors $\vec{e}_a$ and $\vec{e}_b$ (where $\vec{e}_a$ is the reference direction), we have, after the beam has crossed the retarder (inessential phase factors are omitted)

$$\begin{aligned}\mathcal{E}_{\rm f} &= \mathcal{E}_1 \cos\alpha + \mathcal{E}_2 \sin\alpha \\ \mathcal{E}_{\rm s} &= {\rm e}^{{\rm i}\delta}(-\mathcal{E}_1 \sin\alpha + \mathcal{E}_2 \cos\alpha)\ ,\end{aligned}$$

where $\mathcal{E}_{\rm f}$ and $\mathcal{E}_{\rm s}$ are the components of the electric vibrations along the fast and slow axes, respectively, and δ is the retardance. The only component transmitted by the polarizer is the one parallel to the transmission axis. This component is given by

$$\mathcal{E}_{\rm p} = \cos(\beta-\alpha)\,\mathcal{E}_{\rm f} + \sin(\beta-\alpha)\,\mathcal{E}_{\rm s}\ ,$$

so that for the signal D of the detector we obtain after some algebra

$$\begin{aligned}D(\alpha,\beta,\delta) = k\left\langle \mathcal{E}_{\rm p}^*\,\mathcal{E}_{\rm p}\right\rangle = \frac{1}{2}\Big[& I + (Q\cos 2\alpha + U\sin 2\alpha)\cos 2(\beta-\alpha) \\ & - (Q\sin 2\alpha - U\cos 2\alpha)\sin 2(\beta-\alpha)\cos\delta \\ & + V\sin 2(\beta-\alpha)\sin\delta\Big]\ . \end{aligned} \tag{1.33}$$

A first method for measuring the Stokes parameters is to set the various devices at particular angles. If we are concerned with linear polarization only, the retarder can be removed ($\delta = 0°$), or, alternatively, its fast axis can be set parallel to the transmission axis of the polarizer ($\alpha = \beta$). In both cases the signal D' of the detector takes the simpler form

$$D'(\beta) = \frac{1}{2}\Big[I + Q\cos 2\beta + U\sin 2\beta\Big]\ ,$$

and the Stokes parameters I, Q, and U can be found by the combination of four measurements

$$\begin{aligned} I &= D'(0^\circ) + D'(90^\circ) \\ Q &= D'(0^\circ) - D'(90^\circ) \\ U &= D'(45^\circ) - D'(135^\circ) \,, \end{aligned}$$

or, alternatively, with only three measurements

$$\begin{aligned} I &= \frac{2}{3}\Big[D'(0^\circ) + D'(60^\circ) + D'(120^\circ)\Big] \\ Q &= \frac{2}{3}\Big[2D'(0^\circ) - D'(60^\circ) - D'(120^\circ)\Big] \\ U &= \frac{2}{\sqrt{3}}\Big[D'(60^\circ) - D'(120^\circ)\Big] \,. \end{aligned}$$

For the measurement of V the retarder is essential. Setting a quarter-wave plate ($\delta = 90^\circ$) at $\alpha = 0^\circ$ we get from Eq. (1.33)

$$D''(\beta) = \frac{1}{2}\Big[I + Q\cos 2\beta + V \sin 2\beta\Big] \,,$$

and the Stokes parameters I, Q, and V are found by

$$\begin{aligned} I &= D''(0^\circ) + D''(90^\circ) \\ Q &= D''(0^\circ) - D''(90^\circ) \\ V &= D''(45^\circ) - D''(135^\circ) \,. \end{aligned}$$

This technique, however, has the disadvantage of implying a rotation of the exit polarizer, which is often a dangerous procedure especially if the polarization analysis is to be followed by a spectral analysis (a grating spectrometer, for instance, has a response that is rather sensitive to the polarization of the incident radiation). To avoid these problems one can employ, for the measurement of linear polarization, a half-wave plate ($\delta = 180^\circ$) and keep the polarizer fixed at $\beta = 0^\circ$. The signal is now

$$D'''(\alpha) = \frac{1}{2}\Big[I + Q\cos 4\alpha + U \sin 4\alpha\Big] \,,$$

and the Stokes parameters I, Q, and U can be obtained by the relations

$$\begin{aligned} I &= D'''(0^\circ) + D'''(45^\circ) \\ Q &= D'''(0^\circ) - D'''(45^\circ) \\ U &= D'''(22.5^\circ) - D'''(67.5^\circ) \,. \end{aligned}$$

For circular polarization, keeping the polarizer fixed at $\beta = 0°$, one gets (again using a quarter-wave plate)

$$D''''(\alpha) = \frac{1}{2}\Big[I + Q\cos^2 2\alpha + U\sin 2\alpha\cos 2\alpha - V\sin 2\alpha\Big] ,$$

and the Stokes parameters I, Q, U, and V can be found by the combination of five measurements

$$\begin{aligned} I &= D''''(45°) + D''''(135°) \\ Q &= 2\,D''''(0°) - D''''(45°) - D''''(135°) \\ U &= 2\Big[D''''(22.5°) - D''''(67.5°)\Big] \\ V &= D''''(135°) - D''''(45°) \, . \end{aligned}$$

A different method for measuring the Stokes parameters is based on rotating devices. Using a quarter-wave plate rotating with angular frequency ω and setting $\beta = 0°$, we obtain for the detector signal $D(t)$ the expression

$$D(t) = \frac{1}{2}\left[\left(I + \frac{Q}{2}\right) + \frac{Q}{2}\cos 4\omega t + \frac{U}{2}\sin 4\omega t - V\sin 2\omega t\right] ,$$

and the various Stokes parameters can be measured (for a stationary source) by extracting the Fourier components of the signal $D(t)$.

A third method is to use a compensator with modulated retardance (like a Pockels cell) while keeping the optical components at fixed orientations. To maximize the modulation effect it is convenient to set $(\beta - \alpha) = \pm 45°$, and two sets of measurements are necessary to get the four Stokes parameters. For instance, setting $\alpha = 0°$ and $\beta = 45°$ we have

$$D(t) = \frac{1}{2}\Big[I + U\cos\delta(t) + V\sin\delta(t)\Big] ,$$

whereas setting $\alpha = -45°$, $\beta = 0°$ we get

$$D(t) = \frac{1}{2}\Big[I + Q\cos\delta(t) + V\sin\delta(t)\Big] ,$$

and in both cases three of the four Stokes parameters can be obtained by an analysis of the modulated signal.

We want to remark that the measurement of Stokes parameters is an art in itself that can be pushed to a very high degree of sophistication. The few words that have been spent here on this subject are not meant to be complete, but just to give the reader an intuitive grasp on how this kind of measurements are performed in practice.

1.8. Stokes Parameters and Polarization Tensor

In Sect. 1.6 we have found the relation between the Stokes parameters and the components of the electric vibration along two orthogonal unit vectors, $\vec{e}_a$ and $\vec{e}_b$, with $\vec{e}_a$ the reference direction unit vector and $\vec{e}_b$ the associated unit vector. Equations (1.32) can be rewritten in terms of the polarization tensor defined in Sects. 1.3 and 1.4. From Eq. (1.25) we have

$$\begin{aligned} I &= k\,(J_{11} + J_{22}) \\ Q &= k\,(J_{11} - J_{22}) \\ U &= k\,(J_{12} + J_{21}) \\ V &= k\,\mathrm{i}\,(J_{12} - J_{21})\ . \end{aligned} \tag{1.34}$$

Introducing the so-called *Stokes vector* S_i $(i = 0, \ldots, 3)$ via the equation

$$\begin{pmatrix} S_0 \\ S_1 \\ S_2 \\ S_3 \end{pmatrix} = \begin{pmatrix} I \\ Q \\ U \\ V \end{pmatrix}$$

we have, in strict analogy with Eqs. (1.16) and (1.20)

$$\begin{aligned} \boldsymbol{J} &= \frac{1}{2k} \sum_{j=0}^{3} S_j \boldsymbol{\sigma}_j \\ S_j &= k\ \mathrm{Tr}\big(\boldsymbol{\sigma}_j\, \boldsymbol{J}\big) \qquad (j = 0, \ldots, 3)\ , \end{aligned} \tag{1.35}$$

where $\boldsymbol{\sigma}_j$ are the matrices defined in Eqs. (1.17).

The preceding relations between the Stokes vector and the polarization tensor involve the dimensional quantity k introduced in Eqs. (1.32). This is a consequence of the fact that the Stokes parameters have the dimensions of an intensity, while the polarization tensor has the dimensions of a squared electric field. To simplify the theoretical treatment of polarized radiation it is often convenient to leave out the constant k, by defining a 'new' polarization tensor $\boldsymbol{I}$ having the dimensions of intensity

$$\boldsymbol{I} = k\,\boldsymbol{J}\ , \tag{1.36}$$

where $\boldsymbol{J}$ is the tensor introduced in Sects. 1.3-1.4 and k is the quantity appearing in Eqs. (1.32). In the following we will use the term 'polarization tensor', without distinction, for both $\boldsymbol{J}$ and $\boldsymbol{I}$. Obviously, the tensor $\boldsymbol{I}$ obeys the relations (cf. Eqs. (1.14) and (1.26))

$$I^*_{ij} = I_{ji}\ , \tag{1.37}$$

and

$$\det \boldsymbol{I} \geq 0\ . \tag{1.38}$$

In terms of $\boldsymbol{I}$, Eqs. (1.34) and (1.35) read, respectively

$$\begin{aligned} I &= I_{11} + I_{22} \\ Q &= I_{11} - I_{22} \\ U &= I_{12} + I_{21} \\ V &= \mathrm{i}\left(I_{12} - I_{21}\right) \end{aligned} \tag{1.39}$$

and

$$\begin{aligned} \boldsymbol{I} &= \frac{1}{2}\sum_{j=0}^{3} S_j \boldsymbol{\sigma}_j \\ S_j &= \mathrm{Tr}\left(\boldsymbol{\sigma}_j\, \boldsymbol{I}\right) \qquad (j = 0, \ldots, 3)\ . \end{aligned} \tag{1.40}$$

If the unit vectors chosen to define the polarization tensor differ from $(\vec{e}_a, \vec{e}_b)$, the relations between the Stokes parameters and the components I_{ij} are not as simple as in Eqs. (1.39). Let us consider, in particular, the (complex) unit vectors $\vec{e}_+$ and $\vec{e}_-$ defined by

$$\begin{aligned} \vec{e}_+ &= \cos\theta\, \vec{e}_a + \sin\theta\, \mathrm{e}^{\,\mathrm{i}\phi}\, \vec{e}_b \\ \vec{e}_- &= -\sin\theta\, \vec{e}_a + \cos\theta\, \mathrm{e}^{\,\mathrm{i}\phi}\, \vec{e}_b\ , \end{aligned} \tag{1.41}$$

with

$$\begin{aligned} \vec{e}_+^{\,*} \cdot \vec{e}_+ &= \vec{e}_-^{\,*} \cdot \vec{e}_- = 1 \\ \vec{e}_+^{\,*} \cdot \vec{e}_- &= \vec{e}_-^{\,*} \cdot \vec{e}_+ = 0\ . \end{aligned}$$

Denoting by $\mathcal{E}_+$ and $\mathcal{E}_-$ the controvariant components of the electric vibration along the unit vectors $\vec{e}_+$ and $\vec{e}_-$, defined in such a way that $\vec{\mathcal{E}} = \mathcal{E}_1 \vec{e}_a + \mathcal{E}_2 \vec{e}_b = \mathcal{E}_+ \vec{e}_+ + \mathcal{E}_- \vec{e}_-$, we have

$$\begin{aligned} \mathcal{E}_1 &= \cos\theta\, \mathcal{E}_+ - \sin\theta\, \mathcal{E}_- \\ \mathcal{E}_2 &= \mathrm{e}^{\,\mathrm{i}\phi}\left(\sin\theta\, \mathcal{E}_+ + \cos\theta\, \mathcal{E}_-\right)\ , \end{aligned}$$

and simple relations can be established between the 'old' polarization tensor $I_{ij} = k\,\langle \mathcal{E}_i^*\, \mathcal{E}_j \rangle$ $(i, j = 1, 2)$ and the 'new' polarization tensor $I_{\alpha\beta} = k\,\langle \mathcal{E}_\alpha^*\, \mathcal{E}_\beta \rangle$ $(\alpha, \beta = +, -)$

$$\begin{aligned} I_{11} &= \cos^2\theta\, I_{++} + \sin^2\theta\, I_{--} - \sin\theta\cos\theta\left(I_{+-} + I_{-+}\right) \\ I_{22} &= \sin^2\theta\, I_{++} + \cos^2\theta\, I_{--} + \sin\theta\cos\theta\left(I_{+-} + I_{-+}\right) \\ I_{12} &= I_{21}^* = \mathrm{e}^{\,\mathrm{i}\phi}\Big[\sin\theta\cos\theta\left(I_{++} - I_{--}\right) + \cos^2\theta\, I_{+-} - \sin^2\theta\, I_{-+}\Big]\ , \end{aligned}$$

and conversely

$$
\begin{aligned}
I_{++} &= \cos^2\theta\, I_{11} + \sin^2\theta\, I_{22} + \sin\theta\cos\theta\,\left(\mathrm{e}^{-\mathrm{i}\phi} I_{12} + \mathrm{e}^{\mathrm{i}\phi} I_{21}\right) \\
I_{--} &= \sin^2\theta\, I_{11} + \cos^2\theta\, I_{22} - \sin\theta\cos\theta\,\left(\mathrm{e}^{-\mathrm{i}\phi} I_{12} + \mathrm{e}^{\mathrm{i}\phi} I_{21}\right) \\
I_{+-} &= I^*_{-+} = -\sin\theta\cos\theta\,\left(I_{11} - I_{22}\right) + \cos^2\theta\,\mathrm{e}^{-\mathrm{i}\phi} I_{12} - \sin^2\theta\,\mathrm{e}^{\mathrm{i}\phi} I_{21}\ .
\end{aligned}
$$

Using these transformations we can express the Stokes parameters in the form

$$
\begin{aligned}
I &= I_{++} + I_{--} \\
Q &= \cos 2\theta\,\left(I_{++} - I_{--}\right) - \sin 2\theta\,\left(I_{+-} + I_{-+}\right) \\
U &= \sin 2\theta\cos\phi\,\left(I_{++} - I_{--}\right) + \cos 2\theta\cos\phi\,\left(I_{+-} + I_{-+}\right) \\
&\quad + \mathrm{i}\,\sin\phi\,\left(I_{+-} - I_{-+}\right) \\
V &= -\sin 2\theta\sin\phi\,\left(I_{++} - I_{--}\right) - \cos 2\theta\sin\phi\,\left(I_{+-} + I_{-+}\right) \\
&\quad + \mathrm{i}\,\cos\phi\,\left(I_{+-} - I_{-+}\right)\ ,
\end{aligned}
\tag{1.42}
$$

with the inverse relations

$$
\begin{aligned}
I_{++} + I_{--} &= I \\
I_{++} - I_{--} &= \cos 2\theta\; Q + \sin 2\theta\cos\phi\; U - \sin 2\theta\sin\phi\; V \\
I_{+-} + I_{-+} &= -\sin 2\theta\; Q + \cos 2\theta\cos\phi\; U - \cos 2\theta\sin\phi\; V \\
\mathrm{i}\big(I_{+-} - I_{-+}\big) &= \sin\phi\; U + \cos\phi\; V\ .
\end{aligned}
\tag{1.43}
$$

These formulae show that it is possible to find a particular couple of complex unit vectors of the form (1.41) such that the polarization tensor is diagonal. In fact, it can be easily shown that for ϕ and θ implicitly defined by

$$
\tan\phi = -V/U\ , \qquad \tan 2\theta = \sqrt{V^2 + U^2}\ \big/\ Q\ ,
\tag{1.44}
$$

the components of the polarization tensor satisfy the relations

$$
\begin{aligned}
I_{++} + I_{--} &= I \\
I_{++} - I_{--} &= \pm\sqrt{Q^2 + U^2 + V^2} \\
I_{+-} = I_{-+} &= 0\ ,
\end{aligned}
$$

where the sign ambiguity in the right-hand side of the middle equation is connected with the determination chosen for the ϕ and θ angles in Eqs. (1.44). On this basis of complex unit vectors the electric vibration is decomposed in two independent orthogonal components.

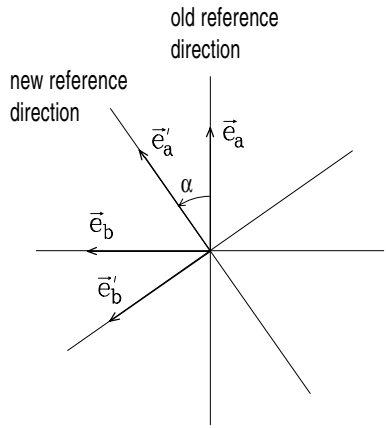

Fig.1.10. The rotation of the reference direction is specified by the angle α. The radiation beam is propagating from behind the page to the reader's eye.

1.9. Properties of the Stokes Parameters

Since the Stokes parameters are defined with respect to a given reference direction, we must establish how they are changed when a different reference direction is chosen. Referring to Fig. 1.10, and denoting by (I, Q, U, V) and (I', Q', U', V') the Stokes parameters relative to the old and new reference direction, respectively, the transformation law can be established with the help of the equations derived in the previous section. Substituting α for θ and 0 for ϕ into Eqs. (1.41), and interpreting the unit vectors $\vec{e}_+$ and $\vec{e}_-$ as $\vec{e}_a'$ and $\vec{e}_b'$, respectively, we obtain from Eqs. (1.43) and (1.39)

$$\begin{aligned} I' &= I \\ Q' &= \cos 2\alpha\, Q + \sin 2\alpha\, U \\ U' &= -\sin 2\alpha\, Q + \cos 2\alpha\, U \\ V' &= V\ . \end{aligned} \tag{1.45}$$

These transformations show that I and V are invariant under rotation of the reference direction, while the linear polarization parameters undergo a rotation through an angle 2α in the Q-U plane, which leaves unchanged the *total linear polarization* $P_{\rm L} = \sqrt{Q^2 + U^2}$. It is also apparent that the reference direction has a 180° ambiguity, an obvious consequence of the definition of the Stokes parameters.

Introducing the *position angle* α_0, defined by

$$\begin{aligned} Q &= P_{\rm L} \cos 2\alpha_0 \\ U &= P_{\rm L} \sin 2\alpha_0\ , \end{aligned} \tag{1.46}$$

the former equations for Q' and U' become

$$\begin{aligned} Q' &= P_{\rm L} \cos 2(\alpha_0 - \alpha) \\ U' &= P_{\rm L} \sin 2(\alpha_0 - \alpha)\ . \end{aligned}$$

The two quantities $P_{\rm L}$ and α_0 are often used to characterize the linear polarization in place of Q and U. In astronomical observations the reference direction is generally taken along the meridian through the observed object, and the position angle is measured counterclockwise from the same meridian. In solar observations the reference direction is sometimes chosen to represent a physical direction, like, for instance, the radial direction from the center of the sun to the observed point, or the parallel to the solar limb.

Another fundamental property of the Stokes parameters is their additivity for incoherent beams. This property can be proved quite easily from Eqs. (1.32). Indeed, if the electric vibrations of two beams are described (in complex notations) by $\mathcal{E}_i^{(1)}(\mathrm{P},t)$ and $\mathcal{E}_i^{(2)}(\mathrm{P},t)$, respectively, and if the two beams are incoherent, so that

$$\left\langle \mathcal{E}_i^{(1)}(\mathrm{P},t)^*\, \mathcal{E}_j^{(2)}(\mathrm{P},t)\right\rangle = \left\langle \mathcal{E}_i^{(2)}(\mathrm{P},t)^*\, \mathcal{E}_j^{(1)}(\mathrm{P},t)\right\rangle = 0 \qquad (i,j=1,2)\ ,$$

we obtain for the Stokes parameters of the composite beam

$$S_k = S_k^{(1)} + S_k^{(2)} \qquad (k=0,\ldots,3)\ ,$$

where $S_k^{(1)}$ and $S_k^{(2)}$ are the Stokes parameters of the separate beams. This property, which can obviously be generalized to an arbitrary number of incoherent beams, will be referred to in the following as the *addition theorem*.

As the Stokes parameters of a radiation beam satisfy the relation (see Eqs. (1.38) and (1.40))

$$I^2 \geq Q^2 + U^2 + V^2\ , \tag{1.47}$$

we can write, using the addition theorem

$$\begin{pmatrix} I \\ Q \\ U \\ V \end{pmatrix} = \begin{pmatrix} I - \sqrt{Q^2+U^2+V^2} \\ 0 \\ 0 \\ 0 \end{pmatrix} + \begin{pmatrix} \sqrt{Q^2+U^2+V^2} \\ Q \\ U \\ V \end{pmatrix}\ .$$

This means that any radiation beam can be considered as the incoherent superposition of an unpolarized beam and a totally polarized beam. The latter is characterized by a well-defined polarization ellipse, whose elements can be found from Eqs. (1.8) and (1.9). The former, on the contrary, is composed of natural radiation.

Another interesting feature of the Stokes parameters stems from the possibility of establishing a mapping between the Stokes vectors and the points of a three-dimensional space that will be referred to as the *Poincaré space*. To the Stokes vector $\boldsymbol{S} = (I,Q,U,V)^\dagger$ we associate the point P having coordinates $(Q/I, U/I, V/I)$, as shown in Fig. 1.11. When the point P lies on the surface of the sphere of unit radius (the *Poincaré sphere*), the corresponding Stokes vector represents a totally polarized radiation beam, while the center of the sphere represents a beam of natural radiation. This mapping, proposed by Poincaré (1892) in a classical monograph, is particularly suitable to visualize the effect produced on a light beam by a given

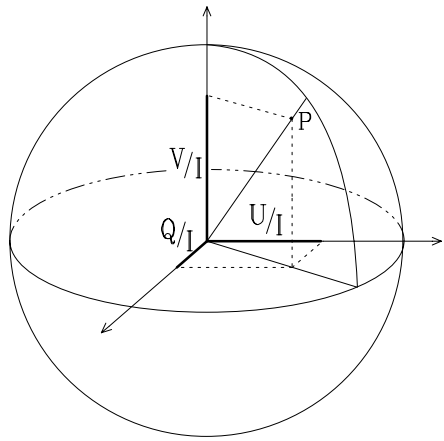

Fig.1.11. Mapping of a Stokes vector (I, Q, U, V) into the representative point P inside the Poincaré sphere of unit radius.

device (like a polarizer or a retarder) as a stepwise movement of the representative point on the sphere. In Chap. 5 we will see how it is possible to visualize the transfer of polarized radiation as a continuous movement of the representative point inside the Poincaré sphere.

1.10. Photons and Stokes Parameters

As we have seen in the former sections, the operational definition of the Stokes parameters of a radiation beam involves at least four independent measurements performed by interposing polarizers or retarders in the beam path. On the other hand, according to the principles of Quantum Mechanics, a photon which interacts with a polarizer is either absorbed or transmitted; in the latter case its state is in general modified, the photon polarization being now parallel to the transmission axis of the polarizer. All information about the original polarization state of the photon is in any case lost, so that it is impossible to perform the four independent measurements needed to determine its Stokes parameters. We conclude that to speak about the Stokes parameters of a single photon has no physical meaning.

Stokes parameters can only be measured for a *statistical ensemble* of photons. The connection between the measured Stokes parameters and the photon wavefunction can be easily established. Referring to Fig. 1.7, let us suppose that the i-th photon has a wavefunction of the form

$$|\psi^{(i)}\rangle = c_1^{(i)} |\psi_1\rangle + c_2^{(i)} |\psi_2\rangle \ ,$$

where $|\psi_1\rangle$ ($|\psi_2\rangle$) is the wavefunction in the polarization space of a photon which propagates along the z-axis and is transmitted through a polarizer having its transmission axis in the $\vec{e}_x$ ($\vec{e}_y$) direction. Applying to the photon beam the same arguments developed for wave packets in Sect. 1.6, we can express the Stokes parameters

as

$$
\begin{aligned}
I &= k' \left[\langle c_1^* c_1 \rangle + \langle c_2^* c_2 \rangle\right] \\
Q &= k' \left[\langle c_1^* c_1 \rangle - \langle c_2^* c_2 \rangle\right] \\
U &= k' \left[\langle c_1^* c_2 \rangle + \langle c_2^* c_1 \rangle\right] \\
V &= k' \mathrm{i} \left[\langle c_1^* c_2 \rangle - \langle c_2^* c_1 \rangle\right] ,
\end{aligned}
$$

where k' is a dimensional constant and where the statistical averages $\langle c_k^* c_j \rangle$ are defined by

$$
\langle c_k^* c_j \rangle = \frac{1}{N} \sum_{i=1}^{N} c_k^{(i)\,*} \, c_j^{(i)} \qquad (k, j = 1, 2) ,
$$

N being the number of photons falling on the measuring device in a given time interval Δt.

Only when all the photons are in the same state, so that the amplitudes $c_j^{(i)}$ are independent of i, it is possible to determine their wavefunction from the measured Stokes parameters.[1] This case, characterized by the equality

$$
I^2 = Q^2 + U^2 + V^2 ,
$$

is the analogue of the macroscopic case of the monochromatic wave. On the contrary, when the states of the single photons are different from each other, we have the more complicated situation described by Eq. (1.47), that has its macroscopic analogue in the quasi-monochromatic wave. From the quantum-mechanical point of view, the photons are said to be in a *pure state* in the former case and in a *mixture of states* in the latter.

[1] Apart from an inessential phase factor. According to the principles of Quantum Mechanics, absolute phases of wavefunctions are not observable quantities.

CHAPTER 2

ANGULAR MOMENTUM AND RACAH ALGEBRA

This chapter, and the two following, are devoted to establish the quantum-mechanical bases that will be needed to approach the theoretical problems involved in the generation and transfer of polarized radiation. In particular, we will recall in the present chapter some important concepts about angular momentum and Racah algebra and will introduce a set of notations and definitions that will be useful in the following.

These arguments have been treated in various classical textbooks or monographs (see e.g. Edmonds, 1957; Messiah, 1961; Brink and Satchler, 1968; Varshalovich et al., 1988). The reason why they are repeated here is to spare the reader the painful job of translating notations and conventions from one book to the other. Obviously, the reader who is already familiar with the theory of angular momentum can simply skip this chapter.

2.1. Eigenvalues and Eigenvectors of Angular Momentum

Angular momentum is defined in Quantum Mechanics as a Hermitian vector operator, $\vec{J}$, whose components along the axes (xyz) of a right-handed coordinate system satisfy the following commutation rules[1]

$$\begin{aligned} [J_x, J_y] &= \mathrm{i} J_z \\ [J_y, J_z] &= \mathrm{i} J_x \\ [J_z, J_x] &= \mathrm{i} J_y \ . \end{aligned} \tag{2.1}$$

From these equations it can be easily shown that the square of the angular momentum,

$$J^2 = J_x^2 + J_y^2 + J_z^2 \ ,$$

commutes with each of the three components

$$[J^2, J_x] = [J^2, J_y] = [J^2, J_z] = 0 \ .$$

Taking J^2 and one of the three components – say J_z – as a maximum set of commuting operators, we can look for the common eigenvectors of these two operators that we denote by the symbol $|\lambda m\rangle$

$$J^2 |\lambda m\rangle = \lambda \, |\lambda m\rangle \ , \qquad J_z |\lambda m\rangle = m \, |\lambda m\rangle \ .$$

[1] The operator $\vec{J}$ considered here is the angular momentum expressed in units of the reduced Planck constant $\hbar = h/(2\pi)$.

The Hermitian character of the operators J_x, J_y, and J_z, together with the commutation rules (2.1), are sufficient to deduce the eigenvalue spectrum or, in other words, the allowed values for λ and m.

Let us introduce the operators J_+ and J_-, usually called the *shift operators*, defined by

$$J_\pm = J_x \pm \mathrm{i} J_y \ .$$

Directly from the definition it is possible to prove the following relations

$$(J_\pm)^\dagger = J_\mp \tag{2.2a}$$

$$[J^2, J_\pm] = 0 \tag{2.2b}$$

$$[J_z, J_\pm] = \pm J_\pm \tag{2.2c}$$

$$[J_+, J_-] = 2J_z \tag{2.2d}$$

$$J_+ J_- = J^2 - J_z^2 + J_z \tag{2.2e}$$

$$J_- J_+ = J^2 - J_z^2 - J_z \ . \tag{2.2f}$$

Using these relations it can be proved that the vectors $J_\pm|\lambda m\rangle$ are still eigenvectors of J^2 and J_z, corresponding to the eigenvalues λ and $(m \pm 1)$, respectively. From Eqs. (2.2b) and (2.2c) we have

$$\begin{aligned} J^2 \left[J_\pm|\lambda m\rangle\right] &= J_\pm J^2 \left|\lambda m\right\rangle = \lambda \left[J_\pm|\lambda m\rangle\right] \\ J_z \left[J_\pm|\lambda m\rangle\right] &= \left[J_\pm J_z \pm J_\pm\right]|\lambda m\rangle = (m \pm 1)\left[J_\pm|\lambda m\rangle\right] \ . \end{aligned} \tag{2.3}$$

On the other hand, if we consider the norms of the vectors $J_+|\lambda m\rangle$ and $J_-|\lambda m\rangle$ (that cannot be negative numbers), and take into account Eqs. (2.2a), (2.2e), and (2.2f), we have

$$\begin{aligned} \langle\lambda m|J_+^\dagger J_+|\lambda m\rangle &= \langle\lambda m|J_- J_+|\lambda m\rangle = (\lambda - m^2 - m)\langle\lambda m|\lambda m\rangle \geq 0 \\ \langle\lambda m|J_-^\dagger J_-|\lambda m\rangle &= \langle\lambda m|J_+ J_-|\lambda m\rangle = (\lambda - m^2 + m)\langle\lambda m|\lambda m\rangle \geq 0 \ , \end{aligned} \tag{2.4}$$

so that

$$\lambda - m^2 - m \geq 0 \ , \qquad \lambda - m^2 + m \geq 0 \ .$$

Since λ and m are real numbers (being eigenvalues of Hermitian operators), these two inequalities give

$$\lambda \geq 0 \ , \qquad |m| \leq \lambda \ . \tag{2.5}$$

Therefore, once we fix a particular eigenvalue λ for J^2, the eigenvalues of J_z must be confined within a limited interval.

Starting now from a given eigenvector $|\lambda m\rangle$ and applying repeatedly the shift operator J_+ (or J_-, respectively), we obtain two distinct chains of eigenvectors corresponding to eigenvalues of J_z increasing (or decreasing) by unity as shown in Eq. (2.3). These two chains have to stop at a certain point so that the second

inequality in Eq. (2.5) can be satisfied. Thus there must be a maximum eigenvalue for J_z – say j – such that

$$J_+|\lambda j\rangle = 0 \ .$$

Equations (2.4) give for this eigenvector

$$\lambda - j^2 - j = 0 \ , \tag{2.6}$$

so that

$$\lambda = j(j+1) \ .$$

Similarly, there must be a minimum eigenvalue for J_z – say j' – such that

$$J_-|\lambda j'\rangle = 0 \ .$$

From Eqs. (2.4) we obtain for this eigenvector

$$\lambda - j'^2 + j' = 0 \ ,$$

and comparing this equation with Eq. (2.6) we get the following relation between j and j'

$$j(j+1) = j'(j'-1) \ .$$

This is a second degree equation whose solutions are

$$\begin{cases} j' = -j \\ j' = j+1 \ . \end{cases}$$

The second solution must be rejected as it leads to $j' > j$. We are then left with the first solution which implies that the minimum eigenvalue of J_z is just the opposite of the maximum eigenvalue.

On the other hand, we can obtain the eigenvector $|\lambda \ -j\rangle$ from the eigenvector $|\lambda\, j\rangle$ by applying to the latter a finite number of times the operator J_-; this implies that the number $[j-(-j)] = 2j$ is an integer, so that the only allowed values for j are integers or half-integers; moreover, the number of eigenvectors associated with a given eigenvalue of J^2 is $(2j+1)$.

From now on, the eigenvectors of J^2 and J_z will be denoted by the symbol $|jm\rangle$; they are supposed to be normalized to unity and to satisfy the eigenvalue equations

$$\begin{aligned} &J^2|jm\rangle = j(j+1)\,|jm\rangle \\ &J_z|jm\rangle = m\,|jm\rangle \qquad (m = -j, -j+1, \ldots, j) \ . \end{aligned} \tag{2.7}$$

Note also that the eigenvectors $|jm\rangle$ obey the orthogonality relation

$$\langle jm|j'm'\rangle = \delta_{jj'}\,\delta_{mm'} \ , \tag{2.8}$$

since J^2 and J_z are Hermitian operators.

The phase relations among the various eigenvectors characterized by the same j-value and different m-values must be established using suitable conventions. From the properties of the shift operators we have

$$J_+|jm\rangle = \alpha\,|j\ \ m{+}1\rangle\ ,$$

where

$$|\alpha|^2 = j(j+1) - m(m+1)\ .$$

The phase of the α constant is conventionally set equal to zero, so that

$$\begin{aligned} J_+|jm\rangle &= \sqrt{j(j+1)-m(m+1)}\,|j\ \ m{+}1\rangle \\ &= \sqrt{(j+m+1)(j-m)}\,|j\ \ m{+}1\rangle\ , \end{aligned} \tag{2.9}$$

and, similarly

$$\begin{aligned} J_-|jm\rangle &= \sqrt{j(j+1)-m(m-1)}\,|j\ \ m{-}1\rangle \\ &= \sqrt{(j-m+1)(j+m)}\,|j\ \ m{-}1\rangle\ . \end{aligned} \tag{2.10}$$

With these phase convention, it is easily found from Eq. (2.10) that any eigenvector $|jm\rangle$ is related to the 'parent' eigenvector $|jj\rangle$ by the equation

$$|jm\rangle = \sqrt{\frac{(j+m)!}{(2j)!\,(j-m)!}}\ J_-^{j-m}\,|jj\rangle\ . \tag{2.11}$$

2.2. Coupling of Two Angular Momenta: Vector-Coupling Coefficients and 3-j Symbols

A fundamental problem encountered in Quantum Mechanics is the addition of the angular momenta relative to two independent particles, or to two different degrees of freedom (like orbital motion and spin) of the same particle. If $\vec{J}_1$ and $\vec{J}_2$ are the angular momenta of the two separate systems, with

$$[J_{1i}, J_{2j}] = 0 \qquad (i,j = x,y,z)\ ,$$

the angular momentum eigenvectors (normalized to unity) of the total system can be written as

$$|j_1 j_2 m_1 m_2\rangle\ ,$$

each eigenvector being a dyadic product of the form $|j_1 m_1\rangle|j_2 m_2\rangle$ that satisfies the eigenvalue equations

$$\begin{aligned} J_1^2|j_1 j_2 m_1 m_2\rangle &= j_1(j_1+1)\,|j_1 j_2 m_1 m_2\rangle \\ J_{1z}|j_1 j_2 m_1 m_2\rangle &= m_1\,|j_1 j_2 m_1 m_1\rangle \\ J_2^2|j_1 j_2 m_1 m_2\rangle &= j_2(j_2+1)\,|j_1 j_2 m_1 m_2\rangle \\ J_{2z}|j_1 j_2 m_1 m_2\rangle &= m_2\,|j_1 j_2 m_1 m_2\rangle\ . \end{aligned}$$

On the other hand, the total system can also be described, from the point of view of its angular momentum properties, in terms of a different set of operators, namely J_1^2, J_2^2, J^2, J_z, where

$$\vec{J} = \vec{J}_1 + \vec{J}_2 \ .$$

It is easily seen that these four operators commute among each other; as a consequence, we can introduce a new set of normalized eigenvectors of the form $|j_1 j_2 JM\rangle$ such that

$$\begin{aligned} J_1^2 |j_1 j_2 JM\rangle &= j_1(j_1+1)\, |j_1 j_2 JM\rangle \\ J_2^2 |j_1 j_2 JM\rangle &= j_2(j_2+1)\, |j_1 j_2 JM\rangle \\ J^2 |j_1 j_2 JM\rangle &= J(J+1)\, |j_1 j_2 JM\rangle \\ J_z |j_1 j_2 JM\rangle &= M\, |j_1 j_2 JM\rangle \ . \end{aligned}$$

Since the two different sets of eigenvectors span the same Hilbert space, they must be connected by a unitary similarity transformation of the form

$$\begin{aligned} |j_1 j_2 JM\rangle &= \sum_{m_1 m_2} |j_1 j_2 m_1 m_2\rangle \langle j_1 j_2 m_1 m_2 | j_1 j_2 JM\rangle \\ |j_1 j_2 m_1 m_2\rangle &= \sum_{JM} |j_1 j_2 JM\rangle \langle j_1 j_2 JM | j_1 j_2 m_1 m_2\rangle \ . \end{aligned} \tag{2.12}$$

The coefficients appearing in these expressions are called *vector-coupling coefficients*, or *Wigner coefficients*, or *Clebsh-Gordan coefficients*. In shorthand notations they are often denoted by the symbol $\langle j_1 j_2 m_1 m_2 | JM\rangle$, as the repetition of the arguments j_1 and j_2 in the ket is unnecessary.

To deduce the expression for these coefficients we must first of all establish suitable phase conventions. The phase relations among the eigenvectors of the form $|j_1 j_2 m_1 m_2\rangle$ are the same as those of the former section, so that we can write (see Eq. (2.11))

$$|j_1 j_2 m_1 m_2\rangle = \sqrt{\frac{(j_1+m_1)!\,(j_2+m_2)!}{(2j_1)!\,(2j_2)!\,(j_1-m_1)!\,(j_2-m_2)!}}\ J_{1-}^{j_1-m_1}\, J_{2-}^{j_2-m_2}\, |j_1 j_2 j_1 j_2\rangle \ ,$$

and the same convention of the former section applies also to the phase relations among the eigenvectors of the form $|JM\rangle$ corresponding to a fixed J-value. The remaining phase conventions will be established in the following.

Let us consider the eigenvector of the form $|j_1 j_2 m_1 m_2\rangle$ corresponding to the maximum m-values ($m_1 = j_1$, $m_2 = j_2$). We have

$$\begin{aligned} J_z |j_1 j_2 j_1 j_2\rangle &= [J_{1z} + J_{2z}]\, |j_1 j_2 j_1 j_2\rangle = (j_1 + j_2) |j_1 j_2 j_1 j_2\rangle \\ J^2 |j_1 j_2 j_1 j_2\rangle &= [J_1^2 + J_2^2 + 2J_{1z}J_{2z} + J_{1+}J_{2-} + J_{1-}J_{2+}]\, |j_1 j_2 j_1 j_2\rangle \\ &= [j_1(j_1+1) + j_2(j_2+1) + 2j_1 j_2]\, |j_1 j_2 j_1 j_2\rangle \\ &= (j_1+j_2)(j_1+j_2+1)\, |j_1 j_2 j_1 j_2\rangle \ . \end{aligned}$$

These equations show that the eigenvector $|j_1 j_2 j_1 j_2\rangle$ is also an eigenvector of the form $|JM\rangle$, with $J = M = (j_1 + j_2)$. By convention we take the same phase for the two eigenvectors, so that

$$|j_1{+}j_2 \;\; j_1{+}j_2\rangle = |j_1 j_2 j_1 j_2\rangle \; .$$

The above value of J is the maximum of the possible J-values, as it can be argued from the fact that the maximum eigenvalue of J_z is $(j_1 + j_2)$. The eigenvectors with the same J-value and lower M-values can be found by repeated application of the operator J_-, so that (see Eq. (2.11))

$$|j_1{+}j_2 \;\; M\rangle = \sqrt{\frac{(j_1 + j_2 + M)!}{(2j_1 + 2j_2)!\,(j_1 + j_2 - M)!}}\; [J_{1-} + J_{2-}]^{j_1+j_2-M}\, |j_1 j_2 j_1 j_2\rangle \; .$$

The eigenvectors of the form $|JM\rangle$ with $J < (j_1 + j_2)$ can be found using a set of operators, O_n, that will be called the *supershift operators*, defined by

$$O_n = \sum_{r=0}^{n} (-1)^{n-r}\; J_{1+}^{r}\, J_{2+}^{n-r}\, J_{1-}^{n}\, J_{2-}^{n} \; .$$

Let us consider the application of the operator O_n to the vector $|j_1 j_2 j_1 j_2\rangle$. Using Eqs. (2.9) and (2.10) we have, after some algebra

$$O_n\, |j_1 j_2 j_1 j_2\rangle = \frac{(n!\,)^2 \sqrt{(2j_1)!\,(2j_2)!}}{(2j_1 - n)!\,(2j_2 - n)!}$$
$$\times \sum_{r=0}^{n} (-1)^{n-r} \sqrt{\frac{(2j_1 - n + r)!\,(2j_2 - r)!}{r!\,(n - r)!}}\;\; |j_1 j_2 \;\; j_1{-}n{+}r \;\; j_2{-}r\rangle \; . \tag{2.13}$$

Applying to this vector the operator J_z we have

$$J_z\big[O_n |j_1 j_2 j_1 j_2\rangle\big] = (j_1 + j_2 - n)\big[O_n |j_1 j_2 j_1 j_2\rangle\big] \; , \tag{2.14}$$

and applying the operator J^2, after some heavy algebra that is left to the reader as an exercise, we have

$$J^2\big[O_n |j_1 j_2 j_1 j_2\rangle\big] = (j_1 + j_2 - n)(j_1 + j_2 - n + 1)\big[O_n |j_1 j_2 j_1 j_2\rangle\big] \; . \tag{2.15}$$

Equations (2.14) and (2.15) show that the vector $O_n |j_1 j_2 j_1 j_2\rangle$ is, apart from a normalization factor and a phase factor, a vector of the form $|JJ\rangle$ with $J = (j_1 + j_2 - n)$. Note that n cannot be larger than the smaller of the values $2j_1$ and $2j_2$ (otherwise $O_n |j_1 j_2 j_1 j_2\rangle = 0$), so that the allowed values for J must satisfy the triangular condition

$$|j_1 - j_2| \le J \le j_1 + j_2 \; .$$

The norm N_n of the vector $O_n|j_1j_2j_1j_2\rangle$ can be easily obtained from Eq. (2.13)

$$N_n = \frac{(n!)^4\,(2j_1)!\,(2j_2)!}{[(2j_1-n)!\,(2j_2-n)!]^2}\sum_{r=0}^{n}\frac{(2j_1-n+r)!\,(2j_2-r)!}{r!\,(n-r)!}\ .$$

The summation above can be evaluated using some properties of the binomial coefficients (see App. 1 of Edmonds, 1957, for a formal proof)

$$\sum_{r=0}^{n}\frac{(2j_1-n+r)!\,(2j_2-r)!}{r!\,(n-r)!} = \frac{(2j_1-n)!\,(2j_2-n)!\,(2j_1+2j_2-n+1)!}{n!\,(2j_1+2j_2-2n+1)!}\ ,$$

and hence

$$N_n = \frac{(n!)^3\,(2j_1)!\,(2j_2)!\,(2j_1+2j_2-n+1)!}{(2j_1-n)!\,(2j_2-n)!\,(2j_1+2j_2-2n+1)!}\ . \tag{2.16}$$

From Eqs. (2.13) and (2.16) we can express any vector $|JJ\rangle$ (normalized to unity) as a function of the vectors of the form $|j_1j_2m_1m_2\rangle$. Apart from a phase factor we have

$$\begin{aligned}|JJ\rangle =& \sqrt{\frac{(j_1+j_2-J)!\,(2J+1)!}{(j_1-j_2+J)!\,(j_2-j_1+J)!\,(j_1+j_2+J+1)!}}\\ &\times\sum_{r=0}^{j_1+j_2-J}(-1)^{j_1+j_2-J-r}\sqrt{\frac{(j_1-j_2+J+r)!\,(2j_2-r)!}{r!\,(j_1+j_2-J-r)!}}\\ &\qquad\times|j_1j_2\ \ J-j_2+r\ \ j_2-r\rangle\ .\end{aligned} \tag{2.17}$$

The phase convention that will be used in this book is that of assuming Eq. (2.17) (with no phase factor in front) valid for any value of J. This convention agrees with those given by Racah (1942), Edmonds (1957), Messiah (1961), Brink and Satchler (1968), Varshalovich et al. (1988), and, together with the other conventions established previously, leads to vector-coupling coefficients that are all *real*.

Now that the phase conventions have been fully established, we can turn to the evaluation of the vector-coupling coefficients. From Eq. (2.11) we have

$$|JM\rangle = \sqrt{\frac{(J+M)!}{(2J)!\,(J-M)!}}\,J_-^{J-M}|JJ\rangle\ . \tag{2.18}$$

Writing

$$J_-^{J-M} = [J_{1-}+J_{2-}]^{J-M} = \sum_{k=0}^{J-M}\frac{(J-M)!}{k!\,(J-M-k)!}\,J_{1-}^{k}\,J_{2-}^{J-M-k}$$

and introducing Eq. (2.17) into (2.18) we obtain

$$
\begin{aligned}
|JM\rangle =& \sqrt{\frac{(j_1+j_2-J)!\,(J+M)!\,(J-M)!\,(2J+1)}{(j_1-j_2+J)!\,(j_2-j_1+J)!\,(j_1+j_2+J+1)!}} \\
&\times \sum_{k=0}^{J-M} \sum_{r=0}^{j_1+j_2-J} (-1)^{j_1+j_2-J-r} \frac{(j_1-j_2+J+r)!\,(2j_2-r)!}{k!\,(J-M-k)!\,r!\,(j_1+j_2-J-r)!} \\
&\times \sqrt{\frac{(j_1+j_2-J+k-r)!\,(J-M-k+r)!}{(j_1-j_2+J-k+r)!\,(2j_2-J+M+k-r)!}} \\
&\times |j_1 j_2 \;\; J-j_2-k+r \;\; j_2-J+M+k-r\rangle \; .
\end{aligned}
$$

From this expression the vector-coupling coefficients are easily calculated. Taking the scalar product with $\langle j_1 j_2 m_1 m_2|$, all the terms in the right-hand side are zero except those satisfying the conditions

$$
\begin{aligned}
J - j_2 - k + r &= m_1 \\
j_2 - J + M + k - r &= m_2 \; .
\end{aligned}
$$

Adding these two equations we find

$$M = m_1 + m_2 \; ,$$

and we can eliminate the sum over k by substituting

$$k = J - j_2 - m_1 + r = J - j_2 - M + m_2 + r \; .$$

Thus we obtain

$$
\begin{aligned}
&\langle j_1 j_2 m_1 m_2 | JM\rangle = \delta_{m_1+m_2,M} \\
&\times \sqrt{\frac{(2J+1)\,(j_1+j_2-J)!\,(J+M)!\,(J-M)!\,(j_1-m_1)!\,(j_2-m_2)!}{(j_1-j_2+J)!\,(j_2-j_1+J)!\,(j_1+j_2+J+1)!\,(j_1+m_1)!\,(j_2+m_2)!}} \\
&\times \sum_{r=0}^{j_1+j_2-J} (-1)^{j_1+j_2-J-r} \frac{(j_1-j_2+J+r)!\,(2j_2-r)!}{(J-j_2-m_1+r)!\,(j_2-m_2-r)!\,(j_1+j_2-J-r)!\,r!} \; .
\end{aligned}
$$

This expression can be transformed into a more symmetrical one (Racah, 1942)

$$
\begin{aligned}
&\langle j_1 j_2 m_1 m_2 | JM\rangle = \delta_{m_1+m_2,M} \\
&\times \sqrt{\frac{(2J+1)(j_1+j_2-J)!\,(j_1-j_2+J)!\,(-j_1+j_2+J)!}{(j_1+j_2+J+1)!}} \\
&\times \sqrt{(j_1+m_1)!\,(j_1-m_1)!\,(j_2+m_2)!\,(j_2-m_2)!\,(J+M)!\,(J-M)!} \\
&\times \sum_t (-1)^t \left[t!\,(j_1+j_2-J-t)!\,(j_1-m_1-t)!\,(j_2+m_2-t)! \right. \\
&\qquad \left. \times (J-j_2+m_1+t)!\,(J-j_1-m_2+t)! \right]^{-1} \; , \qquad (2.19)
\end{aligned}
$$

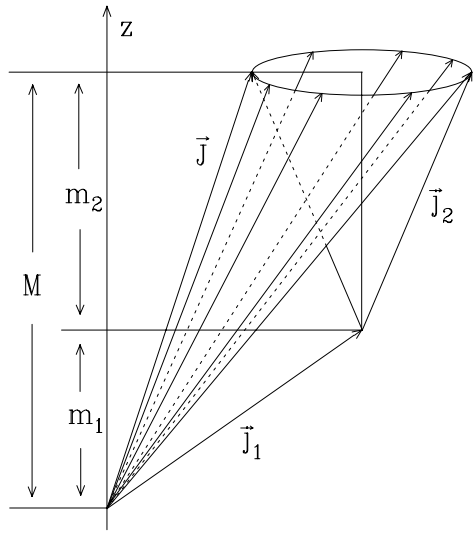

Fig.2.1. The addition of two vectors having fixed projections on a given axis leads, in classical physics, to a continuous distribution for the modulus of the resultant vector.

where the sum over t runs over all the values leading to non-negative factorials.

The vector-coupling coefficients have a very simple physical meaning. Given two independent systems of angular momenta j_1 and j_2, suppose that the z-axis projections of these momenta have been measured and found equal to m_1 and m_2, respectively. The square modulus $|\langle j_1 j_2 m_1 m_2 | JM \rangle|^2$ represents the probability of finding the values J and M, respectively, when measuring the angular momentum of the total system and its z-projection. The Kronecker symbol in Eq. (2.19) implies that the measured M-value must be equal to $(m_1 + m_2)$, which is the same result found for classical (non quantum-mechanical) angular momenta. In the classical case, however, the total angular momentum J has a *continuous* distribution of values that depend on the relative orientation of the vectors $\vec{j}_1$ and $\vec{j}_2$ (see Fig. 2.1). The vector-coupling coefficients can be regarded as the quantum-mechanical analogue of this distribution; but the distribution is now *discrete*, which reflects the quantum nature of the angular momenta.

The vector-coupling coefficients satisfy a large number of properties. Multiplying Eqs. (2.12) by $\langle j_1 j_2 J' M' |$ and $\langle j_1 j_2 m_1' m_2' |$, respectively, taking Eq. (2.8) into account, and recalling that the vector-coupling coefficients are real, one gets the orthogonality relations

$$\sum_{m_1 m_2} \langle j_1 j_2 m_1 m_2 | JM \rangle \langle j_1 j_2 m_1 m_2 | J' M' \rangle = \delta_{JJ'}\, \delta_{MM'} \tag{2.20a}$$

$$\sum_{JM} \langle j_1 j_2 m_1 m_2 | JM \rangle \langle j_1 j_2 m_1' m_2' | JM \rangle = \delta_{m_1 m_1'}\, \delta_{m_2 m_2'}\,. \tag{2.20b}$$

The identity $\langle j_1 j_2 m_1 m_2 | J_+ | JM \rangle = \langle j_1 j_2 m_1 m_2 | J_{1-}^\dagger + J_{2-}^\dagger | JM \rangle$ leads to the re-

cursion relation

$$\sqrt{J(J+1)-M(M+1)}\,\langle j_1 j_2 m_1 m_2|J\ \ M{+}1\rangle = \\ = \sqrt{j_1(j_1+1)-m_1(m_1-1)}\,\langle j_1 j_2\ \ m_1{-}1\ \ m_2|JM\rangle \\ + \sqrt{j_2(j_2+1)-m_2(m_2-1)}\,\langle j_1 j_2 m_1\ \ m_2{-}1|JM\rangle\ . \tag{2.21}$$

The other properties of the vector-coupling coefficients are more easily expressed in terms of the *3-j symbols*, which are defined by

$$\langle j_1 j_2 m_1 m_2|J\ \ -M\rangle = (-1)^{j_1-j_2-M}\sqrt{2J+1}\begin{pmatrix} j_1 & j_2 & J \\ m_1 & m_2 & M\end{pmatrix}\ . \tag{2.22}$$

Nowadays the 3-j coefficients are employed more often than the vector-coupling coefficients. We just summarize below a set of relations that will be needed later. Formal proofs can be easily obtained with the help of Eqs. (2.19), (2.20), and (2.22).
a) Orthogonality relations

$$\sum_{\alpha\beta}(2c+1)\begin{pmatrix} a & b & c \\ \alpha & \beta & \gamma\end{pmatrix}\begin{pmatrix} a & b & c' \\ \alpha & \beta & \gamma'\end{pmatrix} = \delta_{cc'}\,\delta_{\gamma\gamma'} \tag{2.23a}$$

$$\sum_{c\gamma}(2c+1)\begin{pmatrix} a & b & c \\ \alpha & \beta & \gamma\end{pmatrix}\begin{pmatrix} a & b & c \\ \alpha' & \beta' & \gamma\end{pmatrix} = \delta_{\alpha\alpha'}\,\delta_{\beta\beta'}\ . \tag{2.23b}$$

b) The 3-j symbols are invariant under cyclic permutations of their columns and are multiplied by $(-1)^{a+b+c}$ under non-cyclic ones

$$\begin{pmatrix} a & b & c \\ \alpha & \beta & \gamma\end{pmatrix} = \begin{pmatrix} b & c & a \\ \beta & \gamma & \alpha\end{pmatrix} = (-1)^{a+b+c}\begin{pmatrix} c & b & a \\ \gamma & \beta & \alpha\end{pmatrix}\ ,\text{etc.} \tag{2.24}$$

c) They are multiplied by $(-1)^{a+b+c}$ under sign inversion of the second row

$$\begin{pmatrix} a & b & c \\ \alpha & \beta & \gamma\end{pmatrix} = (-1)^{a+b+c}\begin{pmatrix} a & b & c \\ -\alpha & -\beta & -\gamma\end{pmatrix}\ . \tag{2.25}$$

d) By assigning particular values to some of the arguments, compact analytical expressions can be easily obtained; we have for instance

$$\begin{pmatrix} a & b & 0 \\ \alpha & \beta & 0\end{pmatrix} = (-1)^{a-\alpha}\,\delta_{ab}\,\delta_{\alpha,-\beta}\,\frac{1}{\sqrt{2a+1}} \tag{2.26a}$$

$$\begin{pmatrix} a & a+\frac{1}{2} & \frac{1}{2} \\ \alpha & -\alpha-\frac{1}{2} & \frac{1}{2}\end{pmatrix} = (-1)^{1-a+\alpha}\sqrt{\frac{a+\alpha+1}{(2a+2)(2a+1)}} \tag{2.26b}$$

$$\begin{pmatrix} a & a & 1 \\ \alpha & -\alpha-1 & 1\end{pmatrix} = (-1)^{a-\alpha}\sqrt{\frac{(a-\alpha)(a+\alpha+1)}{2a(a+1)(2a+1)}} \tag{2.26c}$$

$$\begin{pmatrix} a & a & 1 \\ \alpha & -\alpha & 0 \end{pmatrix} = (-1)^{a-\alpha} \frac{\alpha}{\sqrt{a(a+1)(2a+1)}} \tag{2.26d}$$

$$\begin{pmatrix} a & a+1 & 1 \\ \alpha & -\alpha-1 & 1 \end{pmatrix} = (-1)^{a-\alpha} \sqrt{\frac{(a+\alpha+1)(a+\alpha+2)}{(2a+1)(2a+2)(2a+3)}} \tag{2.26e}$$

$$\begin{pmatrix} a & a+1 & 1 \\ \alpha & -\alpha & 0 \end{pmatrix} = (-1)^{a-\alpha-1} \sqrt{\frac{(a-\alpha+1)(a+\alpha+1)}{(a+1)(2a+1)(2a+3)}} \,. \tag{2.26f}$$

Analytical expressions for the 3-j coefficients with one of the three elements of the first row set at 3/2 or 2 can be found in Brink and Satchler (1968); analogous formulae with one j-value equal to 5/2 are given by Saito and Morita (1955), and with one j-value equal to 3 by Falkoff et al. (1952). These analytical expressions, together with the various numerical tables of 3-j symbols (or vector-coupling coefficients) prepared by several authors (Alder, 1952; Simon, 1954; Simon et al., 1954; Rotenberg et al., 1959; Varshalovich et al., 1988) have nowadays lost some of their interest due to the fact that, with modern computers, the direct computation of 3-j symbols via Eqs. (2.19) and (2.22) can be easily performed. A sample Fortran code is given in App. 1.

2.3. Coupling of Three Angular Momenta: Racah Coefficients and 6-j Symbols

In the previous section we have shown how it is possible to couple two angular momenta $\vec{J}_1$ and $\vec{J}_2$ to get the resultant vector $\vec{J}$. When three angular momenta are present, say $\vec{J}_1$, $\vec{J}_2$, and $\vec{J}_3$, one can follow the same line of reasoning, by first adding two angular momenta and then adding the third one to the sum of the first two to obtain, as a final result, the total angular momentum $\vec{J}$.

In this procedure we are however faced with some ambiguity. In fact, we could start from the couple $(\vec{J}_1, \vec{J}_2)$ to obtain $\vec{J}_{12} = \vec{J}_1 + \vec{J}_2$, and then add $\vec{J}_{12}$ to $\vec{J}_3$ to obtain $\vec{J}$. Alternatively, we could start from the couple $(\vec{J}_2, \vec{J}_3)$ to obtain $\vec{J}_{23} = \vec{J}_2 + \vec{J}_3$, and then add $\vec{J}_{23}$ to $\vec{J}_1$ to obtain again the resultant $\vec{J}$. Finally, we could introduce the intermediate vector $\vec{J}_{13} = \vec{J}_1 + \vec{J}_3$ and then add $\vec{J}_{13}$ to $\vec{J}_2$.

These different coupling schemes are related to the fact that, given three commuting angular momentum operators $\vec{J}_1$, $\vec{J}_2$, and $\vec{J}_3$, three different sets of six commuting operators can be considered, namely

$$\text{I)} \quad J_1^2,\, J_2^2,\, J_3^2,\, J_{12}^2,\, J^2,\, J_z$$

$$\text{II)} \quad J_1^2,\, J_2^2,\, J_3^2,\, J_{23}^2,\, J^2,\, J_z$$

$$\text{III)} \quad J_1^2,\, J_2^2,\, J_3^2,\, J_{13}^2,\, J^2,\, J_z \,,$$

besides the standard set

$$\text{IV)} \quad J_1^2,\, J_2^2,\, J_3^2,\, J_{1z},\, J_{2z},\, J_{3z} \,.$$

Expressing the eigenvectors of sets I, II, and III in terms of the eigenvectors of set IV, it is possible to find the transformations connecting the different bases. The coefficients entering these transformations are called the *recoupling coefficients* and can be derived as follows.

Denoting the eigenvectors of set I by the symbol

$$|(j_1 j_2) j_{12}, j_3, JM\rangle \,, \tag{2.27}$$

we apply twice the first of Eqs. (2.12) to obtain

$$\begin{aligned} |(j_1 j_2) j_{12}, j_3, JM\rangle &= \sum_{m_{12} m_3} |j_{12} j_3 m_{12} m_3\rangle \langle j_{12} j_3 m_{12} m_3 | j_{12} j_3 JM\rangle \\ &= \sum_{m_1 m_2 m_3 m_{12}} |j_1 j_2 j_3 m_1 m_2 m_3\rangle \\ &\qquad \times \langle j_1 j_2 m_1 m_2 | j_1 j_2 j_{12} m_{12}\rangle \langle j_{12} j_3 m_{12} m_3 | j_{12} j_3 JM\rangle \,, \end{aligned} \tag{2.28}$$

where we have used the symbol

$$|j_1 j_2 j_3 m_1 m_2 m_3\rangle = |j_1 m_1\rangle |j_2 m_2\rangle |j_3 m_3\rangle$$

to represent the eigenvectors of set IV.

Similarly, for a given eigenvector of set II of the form $|j_1, (j_2 j_3) j_{23}, J'M'\rangle$ we obtain

$$\begin{aligned} |j_1, (j_2 j_3) j_{23}, J'M'\rangle &= \\ &= \sum_{m_1 m_2 m_3 m_{23}} |j_1 j_2 j_3 m_1 m_2 m_3\rangle \\ &\qquad \times \langle j_2 j_3 m_2 m_3 | j_2 j_3 j_{23} m_{23}\rangle \langle j_1 j_{23} m_1 m_{23} | j_1 j_{23} J'M'\rangle \,. \end{aligned} \tag{2.29}$$

If we now take the scalar product of the two vectors in Eqs. (2.28) and (2.29) we obtain, using the shorthand notation of the vector-coupling coefficients

$$\begin{aligned} \langle (j_1 j_2) j_{12}, j_3, JM | j_1, (j_2 j_3) j_{23}, J'M'\rangle &= \\ &= \sum_{m_1 m_2 m_3 m_{12} m_{23}} \langle j_1 j_2 m_1 m_2 | j_{12} m_{12}\rangle \langle j_{12} j_3 m_{12} m_3 | JM\rangle \\ &\qquad \times \langle j_2 j_3 m_2 m_3 | j_{23} m_{23}\rangle \langle j_1 j_{23} m_1 m_{23} | J'M'\rangle \, \delta_{JJ'} \, \delta_{MM'} \,. \end{aligned} \tag{2.30}$$

The scalar product in the left-hand side is independent of the M-value, as it can be easily proved by evaluation of the matrix element

$$\langle (j_1 j_2) j_{12}, j_3, JM | J_- J_+ | j_1, (j_2 j_3) j_{23}, JM\rangle$$

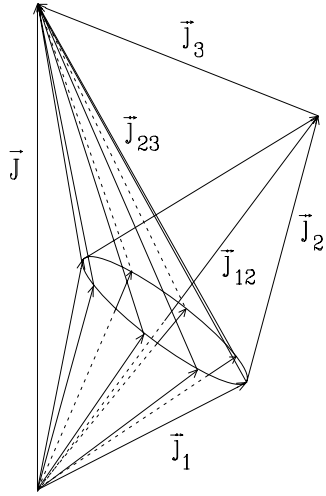

Fig.2.2. When adding in classical physics three angular momenta $\vec{j}_1, \vec{j}_2, \vec{j}_3$ to give the resultant $\vec{J}$, once the sum of two of them ($\vec{j}_1$ and $\vec{j}_2$) is specified, the modulus of $(\vec{j}_2 + \vec{j}_3)$ shows a continuous distribution.

via Eqs. (2.9), (2.2a), and (2.2f). On the other hand, owing to the properties of the vector-coupling coefficients, the summation in the right-hand side can be restricted to m_1, m_2, and m_3, with the condition $(m_1 + m_2 + m_3) = M$.

The scalar product now derived is called the recoupling coefficient and has a simple physical meaning. Given three vectors $\vec{j}_1$, $\vec{j}_2$, and $\vec{j}_3$, that combine to give the resultant $\vec{J}$, the square modulus of the recoupling coefficient is the probability that, if by measuring $(\vec{j}_1+\vec{j}_2)^2$ we found the value $j_{12}(j_{12}+1)$, then, when measuring $(\vec{j}_2+\vec{j}_3)^2$, we find the value $j_{23}(j_{23}+1)$. As illustrated in Fig. 2.2, the modulus of the vector $\vec{j}_{23}$ is undetermined in classical physics too; it has a continuous distribution of probabilities which originates from purely geometrical reasons. The quantum nature of the angular momenta adds to this 'geometrical indetermination' to give a discrete distribution for the probabilities.

Dropping the inessential parameter M, the recoupling coefficients can be used to express the transformations between different bases in the form

$$|j_1,(j_2j_3)j_{23},JM\rangle = \sum_{j_{12}} |(j_1j_2)j_{12},j_3,JM\rangle \times \langle (j_1j_2)j_{12},j_3,J|j_1,(j_2j_3)j_{23},J\rangle \,. \qquad (2.31)$$

In place of the recoupling coefficients it is customary to introduce different symbols like the *Racah coefficients* (or *Racah functions*) defined by

$$W(j_1j_2Jj_3;j_{12}j_{23}) = \\ = \frac{1}{\sqrt{(2j_{12}+1)(2j_{23}+1)}} \langle (j_1j_2)j_{12},j_3,J|j_1,(j_2j_3)j_{23},J\rangle \,, \qquad (2.32)$$

or the more symmetrical *6-j symbols*

$$\left\{ \begin{matrix} j_1 & j_2 & j_{12} \\ j_3 & J & j_{23} \end{matrix} \right\} = (-1)^{j_1+j_2+j_3+J}\, W(j_1 j_2 J j_3; j_{12} j_{23}) \,. \tag{2.33}$$

Starting from Eq. (2.30), and using Eqs. (2.22), (2.32), and (2.33), it is possible to express the 6-j symbol as a sum of products of four 3-j symbols

$$\delta_{ee'}\,\delta_{\epsilon\epsilon'} \left\{ \begin{matrix} a & b & c \\ d & e & f \end{matrix} \right\} = \sum_{\alpha\beta\gamma\delta\phi} (-1)^{b+c+d+\beta+\gamma+\delta}\,(2e+1)$$
$$\times \begin{pmatrix} c & d & e \\ \gamma & -\delta & \epsilon \end{pmatrix} \begin{pmatrix} d & b & f \\ \delta & -\beta & \phi \end{pmatrix} \begin{pmatrix} b & c & a \\ \beta & -\gamma & \alpha \end{pmatrix} \begin{pmatrix} f & a & e' \\ \phi & \alpha & \epsilon' \end{pmatrix} . \tag{2.34}$$

It should be remarked that, owing to the symmetry properties (2.24) and (2.25), the right-hand side can be written in several equivalent ways, obtained by column permutations or by sign change of the second row of each 3-j symbol. Since for each 3-j symbol there are six permutations of the columns and two determinations for the sign of the second row, 12^4 different realizations exist for the right-hand side of Eq. (2.34), apart from the ordering of the 3-j coefficients. All these realizations have however the same 'topological invariant' which can be visualized by graphical methods. The theory of graphical methods for angular momentum problems can be found in Edmonds (1957) or in Brink and Satchler (1968).

The 6-j symbol has several important properties. First of all, it is zero unless four triangular conditions are satisfied. These conditions can be illustrated as follows

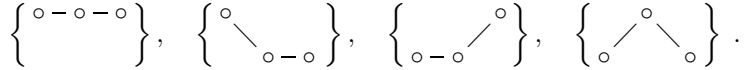

Another remarkable property is the invariance of the 6-j symbol both under interchange of any two columns and under interchange of the upper and lower arguments in any two columns.

An analytical expression for the 6-j symbol can be obtained from Eq. (2.30) by substituting the series expansion (2.19) of the vector-coupling coefficients. After a long calculation, Racah (1942) gives the following expression

$$\left\{ \begin{matrix} a & b & c \\ d & e & f \end{matrix} \right\} = \Delta(abc)\,\Delta(aef)\,\Delta(dbf)\,\Delta(dec) \sum_z (-1)^z (z+1)!$$
$$\times \big[(z-a-b-c)!\,(z-a-e-f)!\,(z-d-b-f)!\,(z-d-e-c)!$$
$$\times (a+b+d+e-z)!\,(b+c+e+f-z)!\,(a+c+d+f-z)! \big]^{-1} , \tag{2.35}$$

where

$$\Delta(abc) = \sqrt{\frac{(a+b-c)!\,(a-b+c)!\,(-a+b+c)!}{(a+b+c+1)!}}$$

and where the sum is extended to all the values of z leading to non-negative factorials.

By specifying the value of one of the arguments, simple analytical formulae can be obtained, e.g.:

$$\left\{ \begin{matrix} a & b & 0 \\ d & e & f \end{matrix} \right\} = \delta_{ab}\, \delta_{ed}\, (-1)^{a+e+f}\, \frac{1}{\sqrt{(2a+1)(2d+1)}} \tag{2.36a}$$

$$\left\{ \begin{matrix} a & a+\frac{1}{2} & \frac{1}{2} \\ b+\frac{1}{2} & b & c \end{matrix} \right\} = (-1)^{a+b+c+1}\, \frac{1}{2} \sqrt{\frac{(a+b+c+2)(a+b-c+1)}{(a+1)(2a+1)(b+1)(2b+1)}} \tag{2.36b}$$

$$\left\{ \begin{matrix} a & a+\frac{1}{2} & \frac{1}{2} \\ b-\frac{1}{2} & b & c \end{matrix} \right\} = (-1)^{a+b+c}\, \frac{1}{2} \sqrt{\frac{(a-b+c+1)(c-a+b)}{(a+1)(2a+1)b(2b+1)}} \tag{2.36c}$$

$$\left\{ \begin{matrix} a & a & 1 \\ b & b & c \end{matrix} \right\} = (-1)^{a+b+c+1}\, \frac{1}{2}\, \frac{a(a+1)+b(b+1)-c(c+1)}{\sqrt{a(a+1)(2a+1)b(b+1)(2b+1)}} \tag{2.36d}$$

$$\left\{ \begin{matrix} a & a+1 & 1 \\ b+1 & b & c \end{matrix} \right\} = (-1)^{a+b+c} \times \frac{1}{2} \sqrt{\frac{(a+b+c+3)(a+b+c+2)(a+b-c+2)(a+b-c+1)}{(a+1)(2a+1)(2a+3)(b+1)(2b+1)(2b+3)}} \tag{2.36e}$$

$$\left\{ \begin{matrix} a & a+1 & 1 \\ b & b & c \end{matrix} \right\} = (-1)^{a+b+c+1} \times \frac{1}{2} \sqrt{\frac{(a+b+c+2)(a-b+c+1)(a+b-c+1)(c-a+b)}{(a+1)(2a+1)(2a+3)b(b+1)(2b+1)}} \tag{2.36f}$$

$$\left\{ \begin{matrix} a & a+1 & 1 \\ b-1 & b & c \end{matrix} \right\} = (-1)^{a+b+c} \times \frac{1}{2} \sqrt{\frac{(c-a+b)(c-a+b-1)(a-b+c+2)(a-b+c+1)}{(a+1)(2a+1)(2a+3)(2b-1)b(2b+1)}} \tag{2.36g}$$

$$\left\{ \begin{matrix} a & a & 2 \\ b & b & c \end{matrix} \right\} = (-1)^{a+b+c} \times \frac{3}{2}\, \frac{s(s+1) - \frac{4}{3}a(a+1)b(b+1)}{\sqrt{(2a-1)a(a+1)(2a+1)(2a+3)(2b-1)b(b+1)(2b+1)(2b+3)}} \tag{2.36h}$$

where

$$s = c(c+1) - a(a+1) - b(b+1)\ .$$

Further analytical formulae have been given by Biedenharn et al. (1952), while numerical tables have been prepared by Biedenharn (1952), Sharp et al. (1954), Simon et al. (1954), Rotenberg et al. (1959), and Varshalovich et al. (1988). As noted in the previous section, these tabulations have nowadays lost much of their interest since modern computers provide the possibility of computing 6-j symbols with simple numerical codes like that in App. 1.

Other important properties of the 6-j symbols, that can be proved either from the analytical expression (2.35) or directly from their definition, are given below.

Sum rules:

$$\sum_c (-1)^{2c}\,(2c+1) \begin{Bmatrix} a & b & c \\ a & b & f \end{Bmatrix} = 1 \tag{2.37}$$

$$\sum_c (-1)^{a+b+c}\,(2c+1) \begin{Bmatrix} a & b & c \\ b & a & f \end{Bmatrix} = \delta_{f0}\,\sqrt{(2a+1)(2b+1)} \tag{2.38}$$

$$\sum_c (2c+1)(2f+1) \begin{Bmatrix} a & b & c \\ d & e & f \end{Bmatrix} \begin{Bmatrix} a & b & c \\ d & e & g \end{Bmatrix} = \delta_{fg} \tag{2.39}$$

$$\sum_c (-1)^{f+g+c}\,(2c+1) \begin{Bmatrix} a & b & c \\ d & e & f \end{Bmatrix} \begin{Bmatrix} a & b & c \\ e & d & g \end{Bmatrix} = \begin{Bmatrix} a & e & f \\ b & d & g \end{Bmatrix} \tag{2.40}$$

$$\sum_c (-1)^{a+b+c+d+e+f+g+h+i+j}\,(2c+1) \begin{Bmatrix} a & b & c \\ d & e & f \end{Bmatrix} \begin{Bmatrix} a & b & c \\ g & h & i \end{Bmatrix} \begin{Bmatrix} g & h & c \\ e & d & j \end{Bmatrix} = \\ = \begin{Bmatrix} f & i & j \\ g & d & b \end{Bmatrix} \begin{Bmatrix} f & i & j \\ h & e & a \end{Bmatrix} \tag{2.41}$$

Contraction of 3-j symbols:

$$\sum_{\beta\gamma\delta} (-1)^{b+c+d+\beta+\gamma+\delta} \begin{pmatrix} c & d & e \\ \gamma & -\delta & \epsilon \end{pmatrix} \begin{pmatrix} d & b & f \\ \delta & -\beta & \phi \end{pmatrix} \begin{pmatrix} b & c & a \\ \beta & -\gamma & \alpha \end{pmatrix} = \\ = \begin{pmatrix} f & a & e \\ \phi & \alpha & \epsilon \end{pmatrix} \begin{Bmatrix} f & a & e \\ c & d & b \end{Bmatrix} \tag{2.42}$$

$$\sum_f (-1)^{a+b+c+d-e+f-\alpha-\delta}\,(2f+1) \begin{Bmatrix} a & b & e \\ d & c & f \end{Bmatrix} \begin{pmatrix} c & a & f \\ \gamma & \alpha & \phi \end{pmatrix} \begin{pmatrix} b & d & f \\ \beta & \delta & -\phi \end{pmatrix} = \\ = \begin{pmatrix} a & b & e \\ \alpha & \beta & -\epsilon \end{pmatrix} \begin{pmatrix} d & c & e \\ \delta & \gamma & \epsilon \end{pmatrix} . \tag{2.43}$$

2.4. Coupling of Four Angular Momenta: 9-j Symbols

When four angular momenta are present, say $\vec{J}_1$, $\vec{J}_2$, $\vec{J}_3$, and $\vec{J}_4$, different coupling schemes can be followed, as in the case of three angular momenta discussed in the previous section. For instance, one can start from the couples $(\vec{J}_1, \vec{J}_2)$ and $(\vec{J}_3, \vec{J}_4)$ to obtain the intermediate vectors $\vec{J}_{12} = \vec{J}_1 + \vec{J}_2$ and $\vec{J}_{34} = \vec{J}_3 + \vec{J}_4$, and then add $\vec{J}_{12}$ to $\vec{J}_{34}$ to obtain the resultant $\vec{J}$. Alternatively, one can start from the couples $(\vec{J}_1, \vec{J}_3)$ and $(\vec{J}_2, \vec{J}_4)$ to get the intermediate vectors $\vec{J}_{13} = \vec{J}_1 + \vec{J}_3$ and $\vec{J}_{24} = \vec{J}_2 + \vec{J}_4$, and then add $\vec{J}_{13}$ to $\vec{J}_{24}$ to obtain again the resultant $\vec{J}$. A third possibility would be to introduce the intermediate vectors $\vec{J}_{14} = \vec{J}_1 + \vec{J}_4$ and $\vec{J}_{23} = \vec{J}_2 + \vec{J}_3$.

These different coupling schemes are related to the fact that, given four independent angular momenta, three different sets of eight commuting operators can be constructed, namely

$$\begin{aligned}
&\text{I)} \quad J_1^2,\ J_2^2,\ J_3^2,\ J_4^2,\ J_{12}^2,\ J_{34}^2,\ J^2,\ J_z \\
&\text{II)} \quad J_1^2,\ J_2^2,\ J_3^2,\ J_4^2,\ J_{13}^2,\ J_{24}^2,\ J^2,\ J_z \\
&\text{III)} \quad J_1^2,\ J_2^2,\ J_3^2,\ J_4^2,\ J_{14}^2,\ J_{23}^2,\ J^2,\ J_z\ ,
\end{aligned}$$

besides the standard set

$$\text{IV)} \quad J_1^2,\ J_2^2,\ J_3^2,\ J_4^2,\ J_{1z},\ J_{2z},\ J_{3z},\ J_{4z}\ .$$

Denoting the eigenvectors of set I by the symbol

$$|(j_1 j_2) j_{12}, (j_3 j_4) j_{34}, JM\rangle$$

and those of set II by the symbol

$$|(j_1 j_3) j_{13}, (j_2 j_4) j_{24}, JM\rangle\ ,$$

the two bases are connected by the transformation

$$\begin{aligned}
|(j_1 j_2) j_{12}, (j_3 j_4) j_{34}, JM\rangle &= \sum_{j_{13}\, j_{24}} |(j_1 j_3) j_{13}, (j_2 j_4) j_{24}, JM\rangle \\
&\times \langle (j_1 j_3) j_{13}, (j_2 j_4) j_{24}, JM | (j_1 j_2) j_{12}, (j_3 j_4) j_{34}, JM\rangle\ .
\end{aligned}$$

The recoupling coefficients defined in this equation are independent of M (see the comments about Eq. (2.30)). In their place different symbols are usually introduced, like the *9-j symbols* defined by

$$\begin{aligned}
&\langle (j_1 j_3) j_{13}, (j_2 j_4) j_{24}, J | (j_1 j_2) j_{12}, (j_3 j_4) j_{34}, J\rangle = \\
&= \sqrt{(2j_{12}+1)(2j_{34}+1)(2j_{13}+1)(2j_{24}+1)} \begin{Bmatrix} j_1 & j_3 & j_{13} \\ j_2 & j_4 & j_{24} \\ j_{12} & j_{34} & J \end{Bmatrix}\ . \qquad (2.44)
\end{aligned}$$

The 9-j symbol can be easily expressed in terms of 3-j coefficients by means of a procedure similar to that of the previous section for the 6-j coefficients (Eqs. (2.27)-(2.30)). The final result is the compact formula

$$\begin{Bmatrix} a & b & c \\ d & e & f \\ g & h & i \end{Bmatrix} = (2a+1) \sum \begin{pmatrix} a & b & c \\ \alpha & \beta & \gamma \end{pmatrix} \begin{pmatrix} d & e & f \\ \delta & \epsilon & \phi \end{pmatrix} \begin{pmatrix} g & h & i \\ \chi & \eta & \xi \end{pmatrix} \times \begin{pmatrix} a & d & g \\ \alpha & \delta & \chi \end{pmatrix} \begin{pmatrix} b & e & h \\ \beta & \epsilon & \eta \end{pmatrix} \begin{pmatrix} c & f & i \\ \gamma & \phi & \xi \end{pmatrix},$$

where the sum runs over all the Greek symbols except α, namely over β, γ, δ, ϵ, ϕ, χ, η, ξ.

The 9-j symbol can be also expressed in terms of 6-j symbols. We start from the vector $|(ad)g,(be)h,i\rangle$ and neglect the fact that the vector h is obtained by combining b with e. From Eq. (2.31) we have

$$|(ad)g,(be)h,i\rangle = \sum_k \langle a,(dh)k,i|(ad)g,h,i\rangle \, |a,(dh)k,i\rangle \, . \tag{2.45}$$

Recalling that h is the resultant of b and e, we recouple the three angular momenta d, b, e to obtain

$$|a,(dh)k,i\rangle = \sum_f \langle b,(de)f,k|d,(be)h,k\rangle \, |a,(bf)k,i\rangle \, . \tag{2.46}$$

Finally we recouple the three vectors a, b, f to get

$$|a,(bf)k,i\rangle = \sum_c \langle (ab)c,f,i|a,(bf)k,i\rangle \, |(ab)c,f,i\rangle \, . \tag{2.47}$$

Substituting Eq. (2.47) into Eq. (2.46) and then into Eq. (2.45), and recalling that the vector f is the combination of d and e, we obtain

$$|(ad)g,(be)h,i\rangle = \sum_{kfc} \langle a,(dh)k,i|(ad)g,h,i\rangle \langle b,(de)f,k|d,(be)h,k\rangle \times \langle (ab)c,f,i|a,(bf)k,i\rangle |(ab)c,(de)f,i\rangle \, .$$

The three recoupling coefficients can be expressed in terms of 6-j symbols. For this purpose it is necessary to recall the definitions (2.32)-(2.33) and to observe that, owing to the properties of the vector-coupling coefficients, the order of the various angular momenta can be changed according to the following rules

$$|a,(bc)d,e\rangle = (-1)^{d-b-c} \, |a,(cb)d,e\rangle$$
$$|a,(bc)d,e\rangle = (-1)^{e-a-d} \, |(bc)d,a,e\rangle \, .$$

Using these properties and the definition of the 9-j symbol given in Eq. (2.44), we obtain the remarkable expression

$$\begin{Bmatrix} a & b & c \\ d & e & f \\ g & h & i \end{Bmatrix} = \sum_k (-1)^{2k}(2k+1) \begin{Bmatrix} a & i & k \\ h & d & g \end{Bmatrix} \begin{Bmatrix} b & f & k \\ d & h & e \end{Bmatrix} \begin{Bmatrix} a & i & k \\ f & b & c \end{Bmatrix} . \quad (2.48)$$

The 9-j symbol satisfies several important properties. First of all, the symbol is zero unless the six triangular conditions illustrated below are satisfied

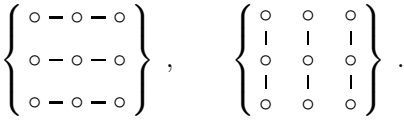

Moreover, it is invariant under reflection about either diagonal, and is multiplied by $(-1)^t$, t being the sum of its nine arguments, under interchange of two adjacent rows or columns.

If one of the arguments is zero, the 9-j symbol reduces to a 6-j symbol times a constant. This can be proved directly from Eq. (2.48), which gives

$$\begin{Bmatrix} a & b & c \\ d & e & f \\ g & h & 0 \end{Bmatrix} = \delta_{cf}\, \delta_{gh}\, (-1)^{b+c+d+g} \frac{1}{\sqrt{(2c+1)(2g+1)}} \begin{Bmatrix} a & b & c \\ e & d & g \end{Bmatrix} . \quad (2.49)$$

For the numerical evaluation of 9-j symbols Eq. (2.48) can be conveniently used, and numerical tables are also available (Smith and Stevenson, 1957; Smith, 1958; Varshalovich et al., 1988). However, as already mentioned about 3-j and 6-j symbols, simple computer codes like that in App. 1 are nowadays generally preferred.

Other important properties of the 9-j symbols are given below.

Orthogonality:

$$\sum_{cf} (2c+1)(2f+1)(2g+1)(2h+1) \begin{Bmatrix} a & b & c \\ d & e & f \\ g & h & i \end{Bmatrix} \begin{Bmatrix} a & b & c \\ d & e & f \\ g' & h' & i \end{Bmatrix} = \delta_{gg'}\, \delta_{hh'} \quad (2.50)$$

Sum rule:

$$\sum_{gh} (-1)^{2b+h+k-f}\, (2g+1)(2h+1) \begin{Bmatrix} a & b & c \\ d & e & f \\ g & h & i \end{Bmatrix} \begin{Bmatrix} a & d & g \\ e & b & h \\ j & k & i \end{Bmatrix} = \begin{Bmatrix} a & b & c \\ e & d & f \\ j & k & i \end{Bmatrix} \quad (2.51)$$

Contraction of 3-j symbols:

$$\begin{pmatrix} a & b & c \\ \alpha & \beta & \gamma \end{pmatrix} \begin{Bmatrix} a & b & c \\ d & e & f \\ g & h & i \end{Bmatrix} =$$

$$= \sum_{\epsilon\eta\phi\xi\delta\chi} \begin{pmatrix} b & e & h \\ \beta & \epsilon & \eta \end{pmatrix} \begin{pmatrix} c & f & i \\ \gamma & \phi & \xi \end{pmatrix} \begin{pmatrix} a & d & g \\ \alpha & \delta & \chi \end{pmatrix} \begin{pmatrix} d & e & f \\ \delta & \epsilon & \phi \end{pmatrix} \begin{pmatrix} g & h & i \\ \chi & \eta & \xi \end{pmatrix} \tag{2.52}$$

$$\sum_b (2b+1) \begin{pmatrix} a & b & c \\ \alpha & \beta & \gamma \end{pmatrix} \begin{pmatrix} b & e & h \\ \beta & \epsilon & \eta \end{pmatrix} \begin{Bmatrix} a & b & c \\ d & e & f \\ g & h & i \end{Bmatrix} =$$

$$= \sum_{\phi\xi\delta\chi} \begin{pmatrix} c & f & i \\ \gamma & \phi & \xi \end{pmatrix} \begin{pmatrix} a & d & g \\ \alpha & \delta & \chi \end{pmatrix} \begin{pmatrix} d & e & f \\ \delta & \epsilon & \phi \end{pmatrix} \begin{pmatrix} g & h & i \\ \chi & \eta & \xi \end{pmatrix} \tag{2.53}$$

$$\sum_{bc} (2b+1)(2c+1) \begin{pmatrix} a & b & c \\ \alpha & \beta & \gamma \end{pmatrix} \begin{pmatrix} b & e & h \\ \beta & \epsilon & \eta \end{pmatrix} \begin{pmatrix} c & f & i \\ \gamma & \phi & \xi \end{pmatrix} \begin{Bmatrix} a & b & c \\ d & e & f \\ g & h & i \end{Bmatrix} =$$

$$= \begin{pmatrix} a & d & g \\ \alpha & \delta & \chi \end{pmatrix} \begin{pmatrix} d & e & f \\ \delta & \epsilon & \phi \end{pmatrix} \begin{pmatrix} g & h & i \\ \chi & \eta & \xi \end{pmatrix} \tag{2.54}$$

Contraction of 6-j and 9-j symbols:

$$\sum_c (2c+1) \begin{Bmatrix} a & b & c \\ d & e & f \\ g & h & i \end{Bmatrix} \begin{Bmatrix} a & b & c \\ f & i & k \end{Bmatrix} = (-1)^{2k} \begin{Bmatrix} a & i & k \\ h & d & g \end{Bmatrix} \begin{Bmatrix} b & f & k \\ d & h & e \end{Bmatrix} \tag{2.55}$$

$$\sum_{st} (-1)^{s+c+d+f-b-g-h-l} (2s+1)(2t+1)$$

$$\times \begin{Bmatrix} a & b & c \\ d & t & s \\ g & l & k \end{Bmatrix} \begin{Bmatrix} c & f & i \\ j & k & s \end{Bmatrix} \begin{Bmatrix} d & e & f \\ j & s & t \end{Bmatrix} \begin{Bmatrix} b & e & h \\ j & l & t \end{Bmatrix} =$$

$$= \begin{Bmatrix} a & b & c \\ d & e & f \\ g & h & i \end{Bmatrix} \begin{Bmatrix} g & h & i \\ j & k & l \end{Bmatrix} . \tag{2.56}$$

Finally, we want to remark that the methods illustrated so far for the coupling of 2, 3, and 4 angular momentum operators can be directly generalized to any number of operators. The addition of n angular momenta will involve recoupling

coefficients depending on $3(n-1)$ parameters. For $n = 5$ two different types of 12-j symbols have been introduced (Jahn and Hope, 1954; Ord-Smith, 1954; Elliott and Flowers, 1955). Fortunately we will not need such symbols in this book.

2.5. Rotations and Euler Angles

It is well-known that in Quantum Mechanics the state of a physical system is described by a vector in the Hilbert space, while the dynamical variables of the system are described by linear Hermitian operators. According to the postulates of Quantum Mechanics, the result of any given measurement accomplished on the system is expressed in terms of probabilities, which are calculated by taking the square modulus of scalar products between appropriate vectors of the Hilbert space. Similarly, the mean value of any given observable (its expectation value) is given by the diagonal matrix element $\langle\psi|O|\psi\rangle$, where $|\psi\rangle$ is the state vector of the system and O is the Hermitian operator associated with the measured observable.

When a rotation is performed in the ordinary three-dimensional space, two different points of view can be followed: either a *passive* point of view which consists in rotating the observer's coordinate system leaving the physical system unchanged, or an *active* point of view which consists in rotating the physical system leaving the coordinate system unchanged.

Adopting the first point of view, the state vector $|\psi\rangle$ of the physical system remains unchanged, while the Hermitian operator O corresponding to a classical observable changes into a different operator, O', connected with O by the same transformation that holds for the corresponding classical observable (Correspondence Principle). This can be performed by introducing a unitary similarity transformation on the operators,

$$O' = D(R)\, O D^{\dagger}(R)\ , \tag{2.57}$$

where $D(R)$ is an appropriate linear operator such that $D^{\dagger}(R) = D^{-1}(R)$ and $D(R^{-1}) = D^{-1}(R)$, where R^{-1} is the inverse rotation of R.

On the contrary, adopting the active point of view, the operators remain unchanged, while the state vector $|\psi\rangle$ changes into the new state vector $|\psi'\rangle$ given by

$$|\psi'\rangle = D(R)|\psi\rangle\ .$$

Obviously these transformations satisfy the property

$$\langle\psi'|O'|\psi'\rangle = \langle\psi|O|\psi\rangle\ ,$$

which means that if the *same* rotation is performed both on the coordinate system and on the physical system, the expectation value of any observable remains the same.

Note that the formalism here introduced is consistent with the intuitive fact that an arbitrary rotation R performed on the coordinate system is equivalent to

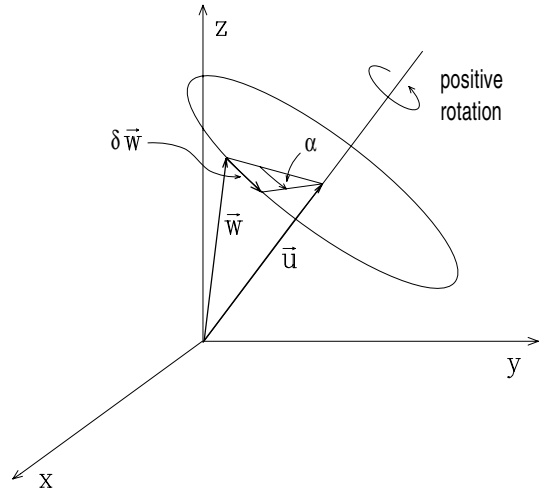

Fig.2.3. To find the variation $\delta\vec{v}$ of the components of the vector $\vec{v}$ under a positive rotation of the coordinate system through an angle ϕ about the $\vec{u}$-axis, we observe that this variation is the same as that obtained by rotating the vector $\vec{v}$ through an angle $-\phi$ about the same axis. The figure shows that for an infinitesimal rotation of the arbitrary vector $\vec{w}$ through an infinitesimal angle α we have $\delta\vec{w} = \alpha\,\vec{u}\times\vec{w}$, so that $\delta\vec{v} = -\,\phi\,\vec{u}\times\vec{v}$.

the inverse rotation R^{-1} performed on the physical system. This can be formally proved by considering the quantity

$$\langle\psi|D(R)\,OD^{\dagger}(R)|\psi\rangle\ .$$

On one hand, this expression can be regarded as

$$\langle\psi|\Big[D(R)\,OD^{\dagger}(R)\Big]|\psi\rangle = \langle\psi|O'|\psi\rangle\ ,$$

which represents the expectation value of the operator O after a rotation of the coordinate system (passive point of view). On the other hand, the same expression can be considered as

$$\Big[\langle\psi|D(R)\Big]O\Big[D^{\dagger}(R)|\psi\rangle\Big] = \Big[\langle\psi|D^{\dagger}(R^{-1})\Big]O\Big[D(R^{-1})|\psi\rangle\Big]\ ,$$

which represents the expectation value of the same operator after the inverse rotation of the physical system (active point of view).

The expression for the operator $D(R)$ can be easily found in the following way. We consider a physical system referred to a given coordinate system, and fix our attention on a particular observable like the vector $\vec{v}$ (representing for instance the position or the velocity or the angular momentum of a particle, etc.). We now perform a positive rotation of the coordinate system through an infinitesimal angle ϕ about the unit vector $\vec{u}$, where by positive rotation we mean, here and in the following, the one that makes a right-handed screw advance along the direction of $\vec{u}$. The vector $\vec{v}$ will be changed by the quantity (see Fig. 2.3)

$$\delta\vec{v} = -\,\phi\,\vec{u}\times\vec{v}\ . \tag{2.58}$$

According to Eq. (2.57) the operator $D_u(\phi)$ corresponding to this infinitesimal rotation must therefore satisfy the relation

$$\vec{v}\,' = \vec{v} + \delta\vec{v} = D_u(\phi)\,\vec{v}\,D_u^\dagger(\phi)\ , \tag{2.59}$$

with $\delta\vec{v}$ given by Eq. (2.58).

Let's now recall that the commutation relations between any dynamical variable of vectorial character and the total angular momentum $\vec{J}$ are of the form[1]

$$[J_k, v_l] = \mathrm{i}\sum_m \epsilon_{klm} v_m \qquad (k,l,m = x,y,z)\ . \tag{2.60}$$

From Eqs. (2.59) and (2.60) it can be easily proved that

$$D_u(\phi) = 1 - \mathrm{i}\,\phi J_u\ , \tag{2.61}$$

where $J_u = \vec{J}\cdot\vec{u}$ is the projection of the total angular momentum on the $\vec{u}$-direction (note that $D_u^\dagger(\phi) = D_u^{-1}(\phi) = D_u(-\phi)$).

From Eq. (2.61) we can find the expression for the operator corresponding to the rotation through a finite angle Ω. To this aim, we divide the angle Ω into a large number n of equal parts, and perform the finite rotation as the succession of n infinitesimal rotations of amplitude Ω/n. We have

$$\begin{aligned} D_u(\Omega) &= \lim_{n\to\infty}\left[1 - \mathrm{i}\frac{\Omega}{n}J_u\right]^n = \lim_{n\to\infty}\sum_{r=0}^{n}\frac{n!}{r!\,(n-r)!}\,\frac{(-\mathrm{i}\Omega J_u)^r}{n^r} \\ &= \sum_{r=0}^{\infty}\frac{(-\mathrm{i}\Omega J_u)^r}{r!}\lim_{n\to\infty}\frac{n!}{(n-r)!\,n^r}\ , \end{aligned}$$

and since the limit gives 1, we obtain

$$D_u(\Omega) = \sum_{r=0}^{\infty}\frac{(-\mathrm{i}\Omega J_u)^r}{r!} = \mathrm{e}^{-\mathrm{i}\Omega J_u}\ , \tag{2.62}$$

where, by definition, the exponential of an operator has the usual meaning given by its Taylor expansion.

Having established the expression for the operator D corresponding to a finite rotation about an arbitrary axis, we can easily find its expression for the most

[1] For a system consisting of one particle, if $\vec{r}$, $\vec{p}$, $\vec{l} = \frac{1}{\hbar}\,\vec{r}\times\vec{p}$, $\vec{s}$, and $\vec{J} = \vec{l} + \vec{s}$ are the position, momentum, orbital angular momentum, spin, and total angular momentum operators, respectively, Eq. (2.60), with $\vec{v}$ denoting any of these vectors as well as any linear combination of them, can be easily deduced from the fundamental commutation rules

$$[r_i, r_j] = [p_i, p_j] = 0\ , \qquad [r_i, p_j] = \mathrm{i}\hbar\,\delta_{ij}\ , \qquad [s_i, s_j] = \mathrm{i}\sum_k \epsilon_{ijk}\,s_k\ .$$

The generalization to the case of many-particle systems is straightforward.

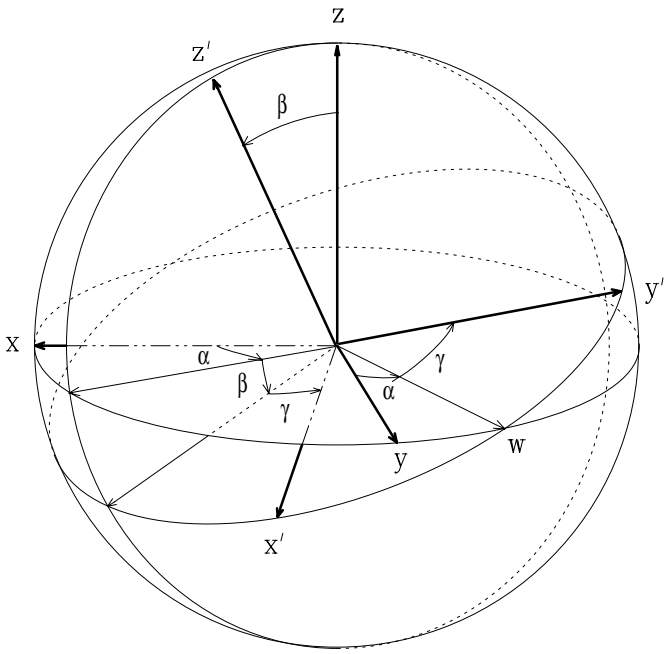

Fig.2.4. Definition of the Euler angles.

general rotation of the reference system. But we must first introduce the *Euler angles*, which are defined as follows.

Referring to Fig. 2.4, we first perform a rotation through an angle α $(0 \leq \alpha < 2\pi)$ about the z-axis of the original reference system. This rotation brings the y-axis into a new axis, called the *line of nodes*, or w-axis. Next we perform a rotation through an angle β $(0 \leq \beta < \pi)$ about the line of nodes. This rotation brings the z-axis of the original system into a new axis, called the *figure-axis*, or z'-axis. Finally we perform a rotation through an angle γ $(0 \leq \gamma < 2\pi)$ about the figure-axis to get the new system $(x'y'z')$.

For the general rotation specified by the three Euler angles (α, β, γ) we have

$$D(\alpha, \beta, \gamma) = D_{z'}(\gamma)\, D_{w}(\beta)\, D_{z}(\alpha)\ , \tag{2.63}$$

an expression which has the disadvantage that the rotations β and γ are relative to axes that have been carried over by previous rotations. To overcome this drawback we observe that[1]

$$D_{w}(\beta) = D_{z}(\alpha)\, D_{y}(\beta)\, D_{z}(-\alpha) \tag{2.64}$$

[1] Equation (2.64) is self-evident from geometrical considerations, since

$$D_{w}(\beta)\, D_{z}(\alpha) = D_{z}(\alpha)\, D_{y}(\beta)\ ;$$

however, it can also be proved analytically. From Eq. (2.62) we have

$$D_{w}(\beta) = \mathrm{e}^{-\mathrm{i}\beta J_{w}}\ ,$$

and that

$$D_{z'}(\gamma) = D_w(\beta)\, D_z(\gamma)\, D_w(-\beta)\ . \tag{2.65}$$

Substituting Eqs. (2.65) and (2.64) into Eq. (2.63), and noting that two rotations about the same axis commute, we obtain

$$D(\alpha,\beta,\gamma) = D_z(\alpha)\, D_y(\beta)\, D_z(\gamma) = \mathrm{e}^{-\mathrm{i}\alpha J_z}\ \mathrm{e}^{-\mathrm{i}\beta J_y}\ \mathrm{e}^{-\mathrm{i}\gamma J_z}\ . \tag{2.66}$$

This expression shows that the rotation described by Eq. (2.63) can also be achieved by performing three successive rotations about the axes of the *old* reference system in the following order: first a rotation through an angle γ about the z-axis, then a rotation through an angle β about the y-axis, and finally a rotation through an angle α about the z-axis. The former realization of the rotation, involving the line of nodes and the figure-axis, is easier to visualize; the latter is more useful in practice, since it involves rotation operators depending on the projections of the angular momentum along the axes of a unique coordinate system.

2.6. Rotation Matrices

The matrix elements of the rotation operator $D(\alpha,\beta,\gamma)$ between eigenstates of the total angular momentum are called *rotation matrices*. These quantities, which are explicitly defined by the relation[1]

$$\mathcal{D}^J_{MN}(R) = \langle JM|D(R)|JN\rangle \tag{2.67}$$

with the symbol R representing the triad (α,β,γ), are of fundamental importance in angular momentum theory. Their physical meaning descends directly from that of the rotation operator $D(R)$ defined in the previous section. Given a physical system of angular momentum J, the square modulus

$$|\mathcal{D}^J_{MN}(R)|^2$$

represents the probability of finding the value N for the z'-axis projection of the momentum after its z-axis projection has been measured and found equal to M, the system $(x'y'z')$ being obtained from (xyz) through the rotation R. Note that

---

where J_w is the operator obtained from J_y by a rotation through an angle α about the z-axis,

$$J_w = D_z(\alpha)\, J_y\, D_z^{-1}(\alpha) = D_z(\alpha)\, J_y\, D_z(-\alpha)\ .$$

Taking this expression into account we obtain, by a power series expansion of the exponential

$$D_w(\beta) = D_z(\alpha)\, \mathrm{e}^{-\mathrm{i}\beta J_y}\, D_z(-\alpha) = D_z(\alpha)\, D_y(\beta)\, D_z(-\alpha)\ .$$

The same argument can be applied to deduce Eq. (2.65).

[1] Note that the matrix elements $\langle JM|D(R)|J'M'\rangle$, with $J' \neq J$, identically vanish. This is a consequence of the fact that the operator $D(R)$ commutes with J^2.

if $|JM\rangle$ is the eigenvector corresponding to the projection M of the angular momentum along the z-axis of the old reference system, the vector $D(R)|JM\rangle$ is the eigenvector corresponding to the same projection along the axis z' of the new reference system.

To find an explicit expression for the rotation matrices, we first define the *reduced rotation matrices* d^J_{MN}. From Eq. (2.66) we have

$$\mathcal{D}^J_{MN}(\alpha\beta\gamma) = \langle JM|\mathrm{e}^{-\mathrm{i}\alpha J_z}\,\mathrm{e}^{-\mathrm{i}\beta J_y}\,\mathrm{e}^{-\mathrm{i}\gamma J_z}|JN\rangle = \mathrm{e}^{-\mathrm{i}(\alpha M+\gamma N)}d^J_{MN}(\beta)\ , \qquad (2.68)$$

where

$$d^J_{MN}(\beta) = \langle JM|\mathrm{e}^{-\mathrm{i}\beta J_y}|JN\rangle\ .$$

The reduced rotation matrices can be easily calculated in the case $J = 1/2$. Introducing the spinors $|+\rangle$ and $|-\rangle$ to represent the eigenstates $|JM\rangle$ having $J = 1/2$ and M equal to $+1/2$ and $-1/2$, respectively, we have from Eqs. (2.9) and (2.10), taking into account that $J_y = -\mathrm{i}\,(J_+ - J_-)/2$

$$J_y|+\rangle = \frac{\mathrm{i}}{2}\,|-\rangle\ , \qquad J_y|-\rangle = -\frac{\mathrm{i}}{2}\,|+\rangle\ ,$$

so that, with easy transformations

$$\mathrm{e}^{-\mathrm{i}\beta J_y}|+\rangle = \sum_{n=0}^{\infty}\frac{(-\mathrm{i}\beta)^n}{n!}J_y^n|+\rangle = \cos\frac{\beta}{2}\,|+\rangle + \sin\frac{\beta}{2}\,|-\rangle\ ,$$

and similarly

$$\mathrm{e}^{-\mathrm{i}\beta J_y}|-\rangle = \cos\frac{\beta}{2}\,|-\rangle - \sin\frac{\beta}{2}\,|+\rangle\ .$$

Thus the reduced rotation matrices for $J = 1/2$ are the following

$$d^{\frac{1}{2}}_{\frac{1}{2}\frac{1}{2}}(\beta) = d^{\frac{1}{2}}_{-\frac{1}{2}-\frac{1}{2}}(\beta) = \cos\frac{\beta}{2}$$

$$d^{\frac{1}{2}}_{-\frac{1}{2}\frac{1}{2}}(\beta) = -d^{\frac{1}{2}}_{\frac{1}{2}-\frac{1}{2}}(\beta) = \sin\frac{\beta}{2}\ .$$

Turning to the general case, let us consider an angular momentum eigenstate of the form $|JJ\rangle$. This eigenstate can be expressed in terms of spinors by regarding the angular momentum $\vec{J}$ as the result of the addition of $2J$ momenta $\vec{J}_1, \vec{J}_2, \ldots, \vec{J}_{2J}$ each equal to $1/2$. In this representation we have, with obvious notations

$$|JJ\rangle = |+\rangle_1|+\rangle_2\cdots|+\rangle_{2J}\ ,$$

where $|+\rangle_i$ is the normalized eigenvector of the operator J_{iz} corresponding to the eigenvalue $+1/2$.

In the same representation, the eigenvector $|JM\rangle$ can be obtained by repeated application of the operator

$$J_- = J_{1-} + J_{2-} + \cdots + J_{2J-}\ .$$

Starting from the eigenvector $|JJ\rangle$ we have from Eq. (2.11)

$$|J\ J-1\rangle = \frac{1}{\sqrt{2J}} J_- |JJ\rangle = \frac{1}{\sqrt{2J}} \Big[J_{1-} + J_{2-} + \cdots + J_{2J-} \Big] |+\rangle_1 |+\rangle_2 \cdots |+\rangle_{2J}$$

$$= \frac{1}{\sqrt{2J}} \Big\{ |-\rangle_1 |+\rangle_2 \cdots |+\rangle_{2J} + |+\rangle_1 |-\rangle_2 \cdots |+\rangle_{2J} + \cdots$$

$$+ |+\rangle_1 |+\rangle_2 \cdots |-\rangle_{2J} \Big\} ,$$

and expressing in succession the eigenvectors $|J\ J-2\rangle$, $|J\ J-3\rangle$, ... we finally obtain

$$|JM\rangle = \sqrt{\frac{(J+M)!\,(J-M)!}{(2J)!}} \sum_p \Big\{ \underbrace{|-\rangle|-\rangle\cdots|-\rangle}_{(J-M)\text{terms}} \underbrace{|+\rangle|+\rangle\cdots|+\rangle}_{(J+M)\text{terms}} \Big\} ,$$

with the sum extended to all the permutations having $(J-M)$ spinors of the form $|-\rangle$ and $(J+M)$ spinors of the form $|+\rangle$.

Thus we can write

$$d^J_{MN}(\beta) = \langle JM | \mathrm{e}^{-\mathrm{i}\beta J_y} | JN \rangle = \frac{\sqrt{(J+M)!\,(J-M)!\,(J+N)!\,(J-N)!}}{(2J)!}$$

$$\times \sum_p \Big\{ \underbrace{\langle -|\langle -|\cdots\langle -|}_{(J-M)\text{terms}} \underbrace{\langle +|\langle +|\cdots\langle +|}_{(J+M)\text{terms}} \Big\} \mathrm{e}^{-\mathrm{i}\beta(J_{1y}+J_{2y}+\cdots+J_{2Jy})}$$

$$\times \sum_q \Big\{ \underbrace{|-\rangle|-\rangle\cdots|-\rangle}_{(J-N)\text{terms}} \underbrace{|+\rangle|+\rangle\cdots|+\rangle}_{(J+N)\text{terms}} \Big\} .$$

Let us consider a single term in the sum over q; the operator $\mathrm{e}^{-\mathrm{i}\beta J_y}$, acting on it, will produce, apart from the ordering of the single vectors $|+\rangle$ and $|-\rangle$, a state vector of the form

$$\left(\cos\frac{\beta}{2} |-\rangle - \sin\frac{\beta}{2} |+\rangle \right)^{J-N} \left(\cos\frac{\beta}{2} |+\rangle + \sin\frac{\beta}{2} |-\rangle \right)^{J+N} =$$

$$= \sum_{t=0}^{J-N} \sum_{r=0}^{J+N} \binom{J-N}{t} \binom{J+N}{r} (-1)^t \left(\cos\frac{\beta}{2} \right)^{J-N-t+J+N-r} \left(\sin\frac{\beta}{2} \right)^{t+r}$$

$$\times \underbrace{|-\rangle|-\rangle\cdots|-\rangle}_{(J-N-t+r)\text{terms}} \underbrace{|+\rangle|+\rangle\cdots|+\rangle}_{(J+N-r+t)\text{terms}} .$$

Whatever the ordering of the various indices, this state vector gives a non-zero scalar product with one and only one of the terms in the sum over p, provided that

$$J - M = J - N - t + r$$
$$J + M = J + N - r + t .$$

These equalities are both satisfied if $r = N - M + t$, and since the sum over q gives $(2J)!\,[(J+N)!\,(J-N)!\,]^{-1}$ terms of the same kind

$$d^J_{MN}(\beta) = \sqrt{(J+M)!\,(J-M)!\,(J+N)!\,(J-N)!} \times \sum_t (-1)^t \frac{\left(\cos\frac{\beta}{2}\right)^{2J+M-N-2t} \left(\sin\frac{\beta}{2}\right)^{2t-M+N}}{(J+M-t)!\,(J-N-t)!\,t!\,(t+N-M)!}\,, \tag{2.69}$$

where the sum runs over all the t values which lead to non-negative factorials.

The reduced rotation matrices have several important properties that can be easily deduced either from their definition or from their analytical expression.

Reality:

$$d^J_{MN}(\beta)^* = d^J_{MN}(\beta)$$

Closure:

$$\sum_N d^J_{MN}(\beta_1)\, d^J_{NP}(\beta_2) = d^J_{MP}(\beta_1 + \beta_2)$$

Symmetry:

$$\begin{aligned} d^J_{MN}(\beta) &= (-1)^{M-N}\, d^J_{-M-N}(\beta) \\ &= (-1)^{M-N}\, d^J_{NM}(\beta) \\ &= (-1)^{M-N}\, d^J_{MN}(-\beta) \\ &= (-1)^{J+M}\, d^J_{M-N}(\pi - \beta) \\ &= (-1)^{J+N}\, d^J_{M-N}(\pi + \beta)\,. \end{aligned} \tag{2.70}$$

Explicit analytical formulae for $J = 1$ and 2 are given in Table 2.1. Additional formulae for $J = 3$ to 6 can be found in Buckmaster (1964, 1966). An interesting connection between reduced rotation matrices and Jacobi polynomials can be found in Edmonds (1957).

Going back to the rotation matrices defined in Eq. (2.67), it is possible to establish for them a number of important properties. First of all, as the rotation operator $D(R)$ is a unitary operator ($D^\dagger(R) = D^{-1}(R)$), we have

$$\mathcal{D}^J_{MN}(\alpha\beta\gamma)^* = \mathcal{D}^J_{NM}(-\gamma - \beta - \alpha)\,, \tag{2.71}$$

where $(-\gamma - \beta - \alpha)$ are the Euler angles characterizing the inverse rotation of $(\alpha\beta\gamma)$.

From the unitary character of the operator $D(R)$ one gets the orthogonality relations

$$\begin{aligned} \sum_P \mathcal{D}^J_{PN}(R)^*\, \mathcal{D}^J_{PM}(R) &= \delta_{MN} \\ \sum_P \mathcal{D}^J_{MP}(R)\, \mathcal{D}^J_{NP}(R)^* &= \delta_{MN}\,. \end{aligned} \tag{2.72}$$

TABLE 2.1

Algebraic formulae for $d^1_{MN}(\beta)$ (top) and $d^2_{MN}(\beta)$ (bottom). C and S stand for $\cos\beta$ and $\sin\beta$, respectively.

	$N=-1$	$N=0$	$N=+1$
$M=-1$	$\frac{1}{2}(1+C)$	$\frac{1}{\sqrt{2}}S$	$\frac{1}{2}(1-C)$
$M=0$	$-\frac{1}{\sqrt{2}}S$	C	$\frac{1}{\sqrt{2}}S$
$M=+1$	$\frac{1}{2}(1-C)$	$-\frac{1}{\sqrt{2}}S$	$\frac{1}{2}(1+C)$

	$N=-2$	$N=-1$	$N=0$	$N=+1$	$N=+2$
$M=-2$	$\frac{1}{4}(1+C)^2$	$\frac{1}{2}S(1+C)$	$\sqrt{\frac{3}{8}}S^2$	$\frac{1}{2}S(1-C)$	$\frac{1}{4}(1-C)^2$
$M=-1$	$-\frac{1}{2}S(1+C)$	$(C-\frac{1}{2})(C+1)$	$\sqrt{\frac{3}{2}}SC$	$(C+\frac{1}{2})(1-C)$	$\frac{1}{2}S(1-C)$
$M=0$	$\sqrt{\frac{3}{8}}S^2$	$-\sqrt{\frac{3}{2}}SC$	$\frac{1}{2}(3C^2-1)$	$\sqrt{\frac{3}{2}}SC$	$\sqrt{\frac{3}{8}}S^2$
$M=+1$	$-\frac{1}{2}S(1-C)$	$(C+\frac{1}{2})(1-C)$	$-\sqrt{\frac{3}{2}}SC$	$(C-\frac{1}{2})(C+1)$	$\frac{1}{2}S(1+C)$
$M=+2$	$\frac{1}{4}(1-C)^2$	$-\frac{1}{2}S(1-C)$	$\sqrt{\frac{3}{8}}S^2$	$-\frac{1}{2}S(1+C)$	$\frac{1}{4}(1+C)^2$

From Eq. (2.68), using the symmetry properties (2.70), it can be easily shown that

$$\mathcal{D}^J_{MN}(\alpha\beta\gamma)^* = (-1)^{M-N}\,\mathcal{D}^J_{-M-N}(\alpha\beta\gamma)\ . \tag{2.73}$$

If R is a rotation composed of two consecutive rotations R_1 and R_2, the operator $D(R)$ can be written as the product $D(R_1)\,D(R_2)$.[1] For the rotation matrices we thus have, directly from their definition

$$\mathcal{D}^J_{MN}(R) = \langle JM|D(R_1)D(R_2)|JN\rangle = \sum_P \mathcal{D}^J_{MP}(R_1)\,\mathcal{D}^J_{PN}(R_2)\ , \tag{2.74}$$

[1] This statement is not trivial. Indeed the operator $D(R)$ should be written

$$D(R) = D'(R_2)\,D(R_1)\ ,$$

where

$$D'(R_2) = \mathrm{e}^{-\mathrm{i}\alpha_2 J_{z'}}\ \mathrm{e}^{-\mathrm{i}\beta_2 J_{y'}}\ \mathrm{e}^{-\mathrm{i}\gamma_2 J_{z'}}\ ,$$

with $J_{y'}$, $J_{z'}$ the components of $\vec{J}$ on the axes y', z' obtained from y, z through the rotation R_1. Since

$$J_{y'} = D(R_1)\,J_y\,D^{-1}(R_1)\ , \qquad J_{z'} = D(R_1)\,J_z\,D^{-1}(R_1)\ ,$$

we have, by series expansion of the exponentials

$$D'(R_2) = \left[D(R_1)\,\mathrm{e}^{-\mathrm{i}\alpha_2 J_z}\,D^{-1}(R_1)\right]\left[D(R_1)\,\mathrm{e}^{-\mathrm{i}\beta_2 J_y}\,D^{-1}(R_1)\right]\left[D(R_1)\,\mathrm{e}^{-\mathrm{i}\gamma_2 J_z}\,D^{-1}(R_1)\right]\ ,$$

so that

$$D(R) = D(R_1)\,D(R_2)\ .$$

the so-called *closure property* of the rotation matrices.

Another important property follows from the addition rules of two angular momenta. Let us consider the product

$$\mathcal{D}^{J}_{MN}(\alpha\beta\gamma)\,\mathcal{D}^{J'}_{M'N'}(\alpha\beta\gamma)\;;$$

according to the definition of rotation matrices, this product can be written in the form

$$\langle JM|\mathrm{e}^{-\mathrm{i}\alpha J_z}\,\mathrm{e}^{-\mathrm{i}\beta J_y}\,\mathrm{e}^{-\mathrm{i}\gamma J_z}|JN\rangle\langle J'M'|\mathrm{e}^{-\mathrm{i}\alpha J_z}\,\mathrm{e}^{-\mathrm{i}\beta J_y}\,\mathrm{e}^{-\mathrm{i}\gamma J_z}|J'N'\rangle\;.$$

If we now consider the angular momentum operators appearing in the two matrix elements as referring to two different systems, we can write

$$\mathcal{D}^{J}_{MN}(\alpha\beta\gamma)\,\mathcal{D}^{J'}_{M'N'}(\alpha\beta\gamma)=\langle JJ'MM'|\mathrm{e}^{-\mathrm{i}\alpha J_z}\,\mathrm{e}^{-\mathrm{i}\beta J_y}\,\mathrm{e}^{-\mathrm{i}\gamma J_z}|JJ'NN'\rangle\;,$$

where the J-operator is the resultant of the angular momenta of the two systems. On the other hand, bearing in mind the coupling rules of two angular momenta and the definition of 3-j symbols (Eqs. (2.12) and (2.22)), one obtains with easy transformations[1]

$$\begin{aligned}&\mathcal{D}^{J}_{MN}(\alpha\beta\gamma)\,\mathcal{D}^{J'}_{M'N'}(\alpha\beta\gamma)=\\&=\sum_{K}(2K+1)\begin{pmatrix}J & J' & K\\ M & M' & Q\end{pmatrix}\begin{pmatrix}J & J' & K\\ N & N' & Q'\end{pmatrix}\mathcal{D}^{K}_{QQ'}(\alpha\beta\gamma)^{*}\;,\end{aligned}\tag{2.75}$$

a formula that shows how the product of two rotation matrices of rank J and J' can be reduced to the linear combination of rotation matrices having rank K such that $|J-J'|\le K\le(J+J')$.

From Eq. (2.75), using the orthogonality relation (2.23a) of the 3-j symbols, the following expressions are also obtained

$$\begin{aligned}&\mathcal{D}^{K}_{QQ'}(\alpha\beta\gamma)^{*}=\\&=\sum_{MM'NN'}(2K+1)\begin{pmatrix}J & J' & K\\ M & M' & Q\end{pmatrix}\begin{pmatrix}J & J' & K\\ N & N' & Q'\end{pmatrix}\mathcal{D}^{J}_{MN}(\alpha\beta\gamma)\,\mathcal{D}^{J'}_{M'N'}(\alpha\beta\gamma)\;;\end{aligned}$$

$$\begin{aligned}&\sum_{MM'M''}\mathcal{D}^{J}_{MN}(\alpha\beta\gamma)\,\mathcal{D}^{J'}_{M'N'}(\alpha\beta\gamma)\,\mathcal{D}^{J''}_{M''N''}(\alpha\beta\gamma)\begin{pmatrix}J & J' & J''\\ M & M' & M''\end{pmatrix}=\\&\qquad=\begin{pmatrix}J & J' & J''\\ N & N' & N''\end{pmatrix}\;.\end{aligned}$$

[1] Note that a formal summation over Q and Q' might be added in the right-hand side of Eq. (2.75).

Another important property of the rotation matrices is the so-called *Weyl theorem*

$$\int_0^{2\pi} \mathrm{d}\alpha \int_0^{2\pi} \mathrm{d}\gamma \int_0^{\pi} \mathrm{d}\beta \, \sin\beta \, \mathcal{D}^{J}_{MN}(\alpha\beta\gamma) \, \mathcal{D}^{J'}_{M'N'}(\alpha\beta\gamma)^* =$$

$$= \frac{8\pi^2}{2J+1} \, \delta_{JJ'} \, \delta_{MM'} \, \delta_{NN'} \, , \tag{2.76}$$

which is indeed valid only when J and J' are both integers or both half-integers.

To prove the theorem, we note that Eqs. (2.73) and (2.75) give

$$\mathcal{D}^{J}_{MN}(\alpha\beta\gamma) \, \mathcal{D}^{J'}_{M'N'}(\alpha\beta\gamma)^* = (-1)^{M'-N'}$$

$$\times \sum_K (2K+1) \begin{pmatrix} J & J' & K \\ M & -M' & Q \end{pmatrix} \begin{pmatrix} J & J' & K \\ N & -N' & Q' \end{pmatrix} \mathcal{D}^{K}_{QQ'}(\alpha\beta\gamma)^* \, , \tag{2.77}$$

where, if we confine ourselves to one of the two cases specified above, the sum over K runs only over integral values. The integral in Eq. (2.76) is therefore reduced to the sum of various integrals of the form

$$\int_0^{2\pi} \mathrm{d}\alpha \int_0^{2\pi} \mathrm{d}\gamma \int_0^{\pi} \mathrm{d}\beta \, \sin\beta \, \mathcal{D}^{K}_{QQ'}(\alpha\beta\gamma)^* \, ,$$

with K, Q, and Q' integers. The integrals over α and γ can be easily performed (see Eq. (2.68)) and give the value $4\pi^2 \delta_{Q0} \, \delta_{Q'0}$. On the other hand, Eq. (2.69) yields

$$d^{K}_{00}(\beta) = (K!\,)^2 \sum_t (-1)^t \, \frac{\left(\cos\frac{\beta}{2}\right)^{2K-2t} \left(\sin\frac{\beta}{2}\right)^{2t}}{[(K-t)!\,t!\,]^2} \, ,$$

and since

$$\int_0^{\pi/2} (\sin x)^{2a+1} (\cos x)^{2b+1} \, \mathrm{d}x = \frac{a!\,b!}{2\,(a+b+1)!} \, ,$$

we have

$$\int_0^{\pi} d^{K}_{00}(\beta) \sin\beta \, \mathrm{d}\beta = \frac{2}{K+1} \sum_t (-1)^t \frac{K!}{(K-t)!\,t!} = 2\,\delta_{K0} \, .$$

Thus the integral in Eq. (2.76) reduces to

$$8\pi^2 \, (-1)^{M'-N'} \begin{pmatrix} J & J' & 0 \\ M & -M' & 0 \end{pmatrix} \begin{pmatrix} J & J' & 0 \\ N & -N' & 0 \end{pmatrix}$$

or, using Eq. (2.26a), to

$$\frac{8\pi^2}{2J+1}\,\delta_{JJ'}\,\delta_{MM'}\,\delta_{NN'}\ ,$$

which proves the Weyl theorem.

This theorem can be generalized to the case where one of the angular momenta J and J' appearing in the rotation matrices of Eq. (2.76) is a half-integer while the other is an integer. In this case, however, the integrals over α and γ must be extended to the interval $(0, 4\pi)$ instead of $(0, 2\pi)$, and the result is zero. Therefore the general form of the Weyl theorem, valid for any value of J and J', is the following

$$\int_0^{4\pi} \mathrm{d}\alpha \int_0^{4\pi} \mathrm{d}\gamma \int_0^{\pi} \mathrm{d}\beta\, \sin\beta\, \mathcal{D}^{J}_{MN}(\alpha\beta\gamma)\, \mathcal{D}^{J'}_{M'N'}(\alpha\beta\gamma)^* = \frac{32\pi^2}{2J+1}\,\delta_{JJ'}\,\delta_{MM'}\,\delta_{NN'}\ .$$

From the Weyl theorem in the form of Eq. (2.76) it is possible to find a highly symmetrical expression for the integral of the product of three rotation matrices

$$\int_0^{2\pi} \mathrm{d}\alpha \int_0^{2\pi} \mathrm{d}\gamma \int_0^{\pi} \mathrm{d}\beta\, \sin\beta\, \mathcal{D}^{J_1}_{M_1N_1}(\alpha\beta\gamma)\, \mathcal{D}^{J_2}_{M_2N_2}(\alpha\beta\gamma)\, \mathcal{D}^{J_3}_{M_3N_3}(\alpha\beta\gamma) =$$

$$= 8\pi^2 \begin{pmatrix} J_1 & J_2 & J_3 \\ M_1 & M_2 & M_3 \end{pmatrix} \begin{pmatrix} J_1 & J_2 & J_3 \\ N_1 & N_2 & N_3 \end{pmatrix}\ .$$

It should be remarked, however, that this expression is valid only when the three J's are integers or when two of them are half-integers and the third is an integer. In different cases the expression in the right-hand side is meaningless.

2.7. Irreducible Spherical Tensors

In the ordinary three-dimensional space referred to a right-handed coordinate system, a *Cartesian tensor* of rank k is defined as a set of 3^k quantities (called the components of the tensor) which, under rotation of the coordinate system, change according to the linear relationship

$$T'(i_1, i_2, \ldots, i_k) = \sum_{j_1 j_2 \cdots j_k} a(i_1, j_1)\, a(i_2, j_2) \ldots a(i_k, j_k)\, T(j_1, j_2, \ldots, j_k)$$

$$(i_1, i_2, \ldots i_k, j_1, j_2, \ldots, j_k = 1, 2, 3)\ ,$$

where $T(j_1, j_2, \ldots, j_k)$ and $T'(i_1, i_2, \ldots, i_k)$ are the tensor components in the old and new reference system, respectively, and where the coefficients $a(i_l, j_l)$ are the direction cosines of the new axes relative to the old axes.

For instance, the Cartesian components of a usual vector $\vec{A}$ satisfy a transformation of the form

$$A'_i = \sum_j a(i,j)\, A_j \ ,$$

thus a vector is a Cartesian tensor of rank 1. If $\vec{A}$ and $\vec{B}$ are two arbitrary vectors, defining

$$C_{ij} = A_i B_j$$

we have

$$C'_{ij} = \sum_{kl} a(i,k)\, a(j,l)\, C_{kl} \ ,$$

which shows that the dyadic product of two vectors forms a Cartesian tensor of rank 2.

An *irreducible spherical tensor* of rank k is defined as a set of $(2k+1)$ quantities (called the components of the spherical tensor) which, under rotation of the coordinate system, change according to the linear relation

$$T'^k_q = \sum_p T^k_p\, \mathcal{D}^k_{pq}(R) \qquad (q,p = -k, -k+1, \ldots, k) \ , \tag{2.78}$$

where T'^k_q and T^k_p are the tensor components in the new and old reference system, respectively, and where R is the rotation that brings the old system into the new one.

Contrary to the case of Cartesian tensors, the dyadic product of two irreducible spherical tensors no longer is an irreducible spherical tensor. In fact, if R^k_q and $S^{k'}_{q'}$ are two irreducible tensors, the $(2k+1)(2k'+1)$ components of the form $R^k_q S^{k'}_{q'}$ change, under the rotation R, into

$$(R^k_q S^{k'}_{q'})' = \sum_{pp'} (R^k_p S^{k'}_{p'})\, \mathcal{D}^k_{pq}(R)\, \mathcal{D}^{k'}_{p'q'}(R) \ .$$

On the other hand, using Eq. (2.75) we can write

$$(R^k_q S^{k'}_{q'})' = \sum_{pp'} (R^k_p S^{k'}_{p'}) \sum_{K'} (2K'+1) \begin{pmatrix} k & k' & K' \\ p & p' & Q' \end{pmatrix} \begin{pmatrix} k & k' & K' \\ q & q' & P' \end{pmatrix} \mathcal{D}^{K'}_{Q'P'}(R)^* \ .$$

Multiplying both sides by

$$(-1)^{k-k'+Q} \begin{pmatrix} k & k' & K \\ q & q' & -Q \end{pmatrix} \ ,$$

summing over q and q', and defining

$$T^K_Q = \sum_{qq'} (-1)^{k-k'+Q} \begin{pmatrix} k & k' & K \\ q & q' & -Q \end{pmatrix} (R^k_q S^{k'}_{q'}) \ , \tag{2.79}$$

we obtain, with the help of Eq. (2.23a)

$$T'^{K}_{Q} = \sum_{pp'} (R^{k}_{p} S^{k'}_{p'}) \, (-1)^{k-k'+Q} \begin{pmatrix} k & k' & K \\ p & p' & Q' \end{pmatrix} \mathcal{D}^{K}_{Q'-Q}(R)^{*}$$
$$= \sum_{Q'} T^{K}_{-Q'} \, (-1)^{Q+Q'} \, \mathcal{D}^{K}_{Q'-Q}(R)^{*} \, .$$

Recalling the conjugation property of the rotation matrices (Eq. (2.73)) and changing the dummy index Q' in $-P$, we obtain for T^{K}_{Q} the typical transformation law for spherical tensors,

$$T'^{K}_{Q} = \sum_{P} T^{K}_{P} \, \mathcal{D}^{K}_{PQ}(R) \, .$$

Equation (2.79) can thus be regarded as a kind of recipe to obtain a spherical tensor of rank K from the dyadic product of two spherical tensors of rank k and k'. It should be noted, however, that definition (2.79) is by no means unique, as the multiplication of the right-hand side by a factor of the form $f(K)$, with f an arbitrary function, does not affect the transformation law of the tensor T^{K}_{Q} under rotations.

The concept of spherical tensor can be easily extended to quantum-mechanical operators. A *spherical tensor operator* of rank k is defined as a set of $(2k+1)$ operators (called the components of the tensor) which, under rotation of the coordinate system, change according to the linear relation (2.78). Since, on the other hand, quantum-mechanical operators are transformed according to Eq. (2.57), the components of a spherical tensor operator must satisfy the relation

$$D(R) \, T^{k}_{q} \, D^{\dagger}(R) = \sum_{p} T^{k}_{p} \, \mathcal{D}^{k}_{pq}(R) \, . \tag{2.80}$$

From this equation it is possible to deduce the commutation rules of a spherical tensor operator with angular momentum. Let us consider an infinitesimal rotation of the coordinate system through an angle ϕ about the unit vector $\vec{u}$. We have (see Eq. (2.61))

$$D(R) = 1 - \mathrm{i}\phi J_{u}$$
$$D^{\dagger}(R) = 1 + \mathrm{i}\phi J_{u}$$
$$\mathcal{D}^{k}_{pq}(R) = \langle kp|1 - \mathrm{i}\phi J_{u}|kq\rangle = \delta_{pq} - \mathrm{i}\phi \langle kp|J_{u}|kq\rangle \, .$$

Substitution into Eq. (2.80) yields

$$[J_{u}, T^{k}_{q}] = \sum_{p} T^{k}_{p} \, \langle kp|J_{u}|kq\rangle \, ,$$

and equating J_{u} with J_{x}, J_{y}, and J_{z} one gets (see Eqs. (2.7), (2.9), and (2.10))

$$[J_{z}, T^{k}_{q}] = q \, T^{k}_{q}$$
$$[J_{\pm}, T^{k}_{q}] = \sqrt{(k \pm q + 1)(k \mp q)} \, T^{k}_{q\pm 1} \, . \tag{2.81}$$

Conversely,these commutation rules could be taken as basic definitions of a spherical tensor operator. It can indeed be proved that from these equations one easily gets back transformation (2.78).

From Eqs. (2.81) it is possible to find the spherical components, A^1_q, of a vector operator $\vec{A}$. Equation (2.60) gives

$$[J_z, A_z] = 0 \,,$$

hence we can write

$$A^1_0 = A_z \,.$$

Setting $k = 1$ and $q = 0$ in the second of Eqs. (2.81) we further obtain

$$[J_\pm, A^1_0] = \sqrt{2}\, A^1_{\pm 1} \,,$$

so that, summarizing

$$\begin{aligned} A^1_{-1} &= \frac{1}{\sqrt{2}} \left(A_x - \mathrm{i} A_y\right) \\ A^1_0 &= A_z \\ A^1_1 &= -\frac{1}{\sqrt{2}} \left(A_x + \mathrm{i} A_y\right) . \end{aligned} \tag{2.82}$$

Given two tensor operators of rank 1, it is possible to construct three tensor operators of rank 0, 1, and 2, respectively, by considering the linear combinations (2.79). For the 0-rank tensor one gets, using Eq. (2.26a)

$$\begin{aligned} T^0_0 &= \frac{1}{\sqrt{3}} \sum_q (-1)^{1-q} R^1_q S^1_{-q} = \frac{1}{\sqrt{3}} \left(R^1_1 S^1_{-1} - R^1_0 S^1_0 + R^1_{-1} S^1_1\right) \\ &= -\frac{1}{\sqrt{3}}\, \vec{R} \cdot \vec{S} \,, \end{aligned} \tag{2.83}$$

which shows that, apart from a numerical factor $(-1/\sqrt{3})$, the 0-rank tensor is simply the scalar product of the two vectors.

For the tensor of rank 1, a direct application of Eq. (2.79), with the 3-j symbols computed from Eqs. (2.26c,d), gives

$$\begin{aligned} T^1_{-1} &= \frac{1}{\sqrt{6}} \left(R^1_0 S^1_{-1} - R^1_{-1} S^1_0\right) \\ T^1_0 &= \frac{1}{\sqrt{6}} \left(R^1_1 S^1_{-1} - R^1_{-1} S^1_1\right) \\ T^1_1 &= \frac{1}{\sqrt{6}} \left(R^1_1 S^1_0 - R^1_0 S^1_1\right) , \end{aligned}$$

or, in terms of Cartesian components (see Eqs. (2.82) and their inverse)

$$T_x = \frac{\mathrm{i}}{\sqrt{6}}\,(R_y S_z - R_z S_y)$$
$$T_y = \frac{\mathrm{i}}{\sqrt{6}}\,(R_z S_x - R_x S_z)$$
$$T_z = \frac{\mathrm{i}}{\sqrt{6}}\,(R_x S_y - R_y S_x)\,.$$

Therefore the spherical components of the tensor of rank 1 determine a vector $\vec{T}$ which, apart from a numerical factor, is simply the cross product of the vectors $\vec{R}$ and $\vec{S}$,

$$\vec{T} = \frac{\mathrm{i}}{\sqrt{6}}\,\vec{R}\times\vec{S}\,.$$

Finally, the components of the tensor of rank 2 are given by

$$T^2_{-2} = \frac{1}{\sqrt{5}}\,R^1_{-1}S^1_{-1}$$
$$T^2_{-1} = \frac{1}{\sqrt{10}}\,(R^1_0 S^1_{-1} + R^1_{-1}S^1_0)$$
$$T^2_0 = \frac{1}{\sqrt{30}}\,(R^1_{-1}S^1_1 + 2R^1_0 S^1_0 + R^1_1 S^1_{-1})$$
$$T^2_1 = \frac{1}{\sqrt{10}}\,(R^1_0 S^1_1 + R^1_1 S^1_0)$$
$$T^2_2 = \frac{1}{\sqrt{5}}\,R^1_1 S^1_1\,. \tag{2.84}$$

It should be remarked that the adjoint (or Hermitian conjugate) of a spherical tensor operator T^k_q no longer is a spherical tensor operator. This can be easily proved by taking the Hermitian conjugates of Eqs. (2.81), recalling that

$$[A,B]^\dagger = -[A^\dagger, B^\dagger]\,, \qquad (J_\pm)^\dagger = J_\mp\,;$$

we have

$$[J_z, (T^k_q)^\dagger] = -q\,(T^k_q)^\dagger$$
$$[J_\pm, (T^k_q)^\dagger] = -\sqrt{(k\mp q+1)(k\pm q)}\,(T^k_{q\mp1})^\dagger\,.$$

However, the operator

$$O^k_q = (-1)^{r-q}\,(T^k_{-q})^\dagger\,,$$

where r is zero for k integer and $1/2$ for k half-integer, is indeed a spherical tensor operator. In fact

$$[J_z, O^k_q] = -(-1)^{r-q}\,[J_z, T^k_{-q}]^\dagger = (-1)^{r-q}\,q\,(T^k_{-q})^\dagger = q\,O^k_q$$
$$[J_\pm, O^k_q] = -(-1)^{r-q}\,[J_\mp, T^k_{-q}]^\dagger = (-1)^{r-q\mp1}\sqrt{(k\pm q+1)(k\mp q)}\,(T^k_{-q\mp1})^\dagger$$
$$= \sqrt{(k\pm q+1)(k\mp q)}\,O^k_{q\pm1}\,.$$

The spherical tensor operator O^k_q can be considered as the Hermitian conjugate of the tensor T^k_q; employing for this tensor the notation $T^\dagger$ we have

$$(T^\dagger)^k_q = (-1)^{r-q}\,(T^k_{-q})^\dagger\ . \tag{2.85}$$

A *Hermitian spherical tensor operator* is defined as an operator such that

$$(T^\dagger)^k_q = T^k_q\ ;$$

as a consequence, the components of such operators satisfy the relation

$$T^k_q = (-1)^{r-q}\,(T^k_{-q})^\dagger\ . \tag{2.86}$$

It is seen at once that the spherical components A^1_q of a Hermitian vector $\vec{A}$ form a Hermitian spherical tensor operator. From Eqs. (2.82) we have

$$\begin{aligned}
(A^1_{-1})^\dagger &= \frac{1}{\sqrt{2}}\,(A_x + \mathrm{i}A_y) = -A^1_1\\
(A^1_0)^\dagger &= A_z = A^1_0\\
(A^1_1)^\dagger &= -\frac{1}{\sqrt{2}}\,(A_x - \mathrm{i}A_y) = -A^1_{-1}\ ,
\end{aligned}$$

so that Eq. (2.86) is satisfied.

2.8. The Wigner-Eckart Theorem and its Consequences

The Wigner-Eckart theorem has a fundamental importance in angular momentum theory, as it allows the matrix elements of spherical tensor operators to be reduced to simple mathematical expressions.

For the evaluation of the matrix element

$$\langle \alpha JM|T^k_q|\alpha' J'M'\rangle\ , \tag{2.87}$$

where T^k_q is the q-component of a spherical tensor operator of rank k, and where α and α' are supplementary quantum numbers (relative to Hermitian operators commuting with J^2 and J_z), we first consider the $(2k+1)(2J'+1)$ vectors

$$T^k_q\,|\alpha' J'M'\rangle\ ,$$

or, more precisely, their linear combinations

$$\sum_{M'q} T^k_q\,|\alpha' J'M'\rangle\langle J'kM'q|J''M''\rangle\ , \tag{2.88}$$

where J'' is a given angular momentum eigenvalue having the same character (integer or half-integer) of $(J'+k)$, and limited between $|J'-k|$ and $(J'+k)$. We will now show that the $(2J''+1)$ vectors obtained by varying M'' in the linear combinations (2.88) are eigenvectors of J^2 and J_z corresponding to the eigenvalues $J''(J''+1)$ and M'', respectively.

Denoting by $|v(J'',M'')\rangle$ the linear combination (2.88), we have

$$J_z|v(J'',M'')\rangle = \sum_{M'q} J_z T^k_q \,|\alpha' J' M'\rangle\langle J' k M' q|J'' M''\rangle \;,$$

and using the commutation rules of spherical tensors (Eqs. (2.81)) we obtain

$$\begin{aligned} J_z|v(J'',M'')\rangle &= \sum_{M'q} (M'+q)\, T^k_q \,|\alpha' J' M'\rangle\langle J' k M' q|J'' M''\rangle \\ &= M''\,|v(J'',M'')\rangle \;. \end{aligned} \tag{2.89}$$

Similarly, one gets from Eqs. (2.81) and (2.9)

$$\begin{aligned} &J_+|v(J'',M'')\rangle = \\ &= \sum_{M'q} \sqrt{J'(J'+1)-M'(M'+1)}\, T^k_q \,|\alpha' J' \;\; M'+1\rangle\langle J' k M' q|J'' M''\rangle \\ &\quad + \sum_{M'q} \sqrt{k(k+1)-q(q+1)}\, T^k_{q+1} \,|\alpha' J' M'\rangle\langle J' k M' q|J'' M''\rangle \;, \end{aligned}$$

and renaming the summation indices

$$\begin{aligned} &J_+|v(J'',M'')\rangle = \\ &= \sum_{M'q} T^k_q \,|\alpha' J' M'\rangle \Big[\sqrt{J'(J'+1)-M'(M'-1)}\,\langle J' k \;\; M'-1 \;\; q|J'' M''\rangle \\ &\qquad\qquad + \sqrt{k(k+1)-q(q-1)}\,\langle J' k M' \;\; q-1|J'' M''\rangle \Big] \;, \end{aligned}$$

which can be rewritten, with the help of the recursion relation (2.21), in the form

$$J_+|v(J'',M'')\rangle = \sqrt{J''(J''+1)-M''(M''+1)}\,|v(J'',M''+1)\rangle \;. \tag{2.90}$$

In a similar way one can prove that

$$J_-|v(J'',M'')\rangle = \sqrt{J''(J''+1)-M''(M''-1)}\,|v(J'',M''-1)\rangle \;, \tag{2.91}$$

so that, from Eqs. (2.89), (2.90), and (2.91)

$$\begin{aligned} J^2\,|v(J'',M'')\rangle &= \left[J_z^2 + \frac{1}{2}(J_+J_- + J_-J_+) \right] |v(J'',M'')\rangle \\ &= J''(J''+1)\,|v(J'',M'')\rangle \;. \end{aligned} \tag{2.92}$$

Equations (2.89) and (2.92) show that the $(2J'' + 1)$ vectors of the form $|v(J'', M'')\rangle$ are angular momentum eigenvectors (in general not normalized) corresponding to the eigenvalues J'' and M''.

Recalling the definition of $|v(J'', M'')\rangle$ we have, after inversion of Eq. (2.88) via the orthogonality relations of the vector-coupling coefficients (Eq. (2.20b))

$$T_q^k \, |\alpha' J' M'\rangle = \sum_{J''} \langle J' k M' q | J'' M''\rangle \, |v(J'', M'')\rangle \ ,$$

and hence the scalar products (2.87) can be written in the form

$$\langle \alpha J M | T_q^k | \alpha' J' M'\rangle = \sum_{J''} \langle J' k M' q | J'' M''\rangle \langle \alpha J M | v(J'', M'')\rangle \ . \tag{2.93}$$

On the other hand, the scalar product $\langle \alpha J M | v(J'', M'')\rangle$ is zero unless $J = J''$ and $M = M''$. Moreover, it is independent of M (see the comments after Eq. (2.30)) so that we can write

$$\langle \alpha J M | v(J'', M'')\rangle = \delta_{JJ''} \, \delta_{MM''} \, (-1)^{2k} \langle \alpha J \| \boldsymbol{T}^k \| \alpha' J'\rangle \ , \tag{2.94}$$

where the quantity $\langle \alpha J \| \boldsymbol{T}^k \| \alpha' J'\rangle$ is the so-called *reduced matrix element*[1] of the operator T_q^k. Substitution of Eq. (2.94) into Eq. (2.93) leads to the final expression of the Wigner-Eckart theorem

$$\langle \alpha J M | T_q^k | \alpha' J' M'\rangle = (-1)^{2k} \langle \alpha J \| \boldsymbol{T}^k \| \alpha' J'\rangle \langle J' k M' q | J M\rangle \ , \tag{2.95}$$

or, in terms of 3-j symbols

$$\begin{aligned} &\langle \alpha J M | T_q^k | \alpha' J' M'\rangle = \\ &= (-1)^{J'+k+M} \sqrt{2J+1} \begin{pmatrix} J & J' & k \\ -M & M' & q \end{pmatrix} \langle \alpha J \| \boldsymbol{T}^k \| \alpha' J'\rangle \ . \end{aligned} \tag{2.96}$$

The reduced matrix element can be expressed in terms of ordinary matrix elements by inversion of Eq. (2.96). From the orthogonality relation of the vector-coupling coefficients (Eq. (2.20a)) we have

$$\langle \alpha J \| \boldsymbol{T}^k \| \alpha' J'\rangle = (-1)^{2k} \sum_{M' q} \langle J' k M' q | J M\rangle \langle \alpha J M | T_q^k | \alpha' J' M'\rangle \ .$$

A different way for calculating the reduced matrix element is to substitute some special values of M and M' into Eq. (2.95). For the reduced matrix element of the angular momentum operator $\vec{J}$ we have for instance (denoting $\boldsymbol{J}^1$ by $\vec{J}$)

$$\langle \alpha J M | J_0^1 | \alpha' J' M'\rangle = M \, \delta_{\alpha\alpha'} \, \delta_{JJ'} \, \delta_{MM'} = \langle \alpha J \| \vec{J} \| \alpha' J'\rangle \langle J' 1 M' 0 | J M\rangle \ ,$$

[1] The definition given here for the reduced matrix element agrees with that given by Brink and Satchler (1968), while it differs by a factor $\sqrt{2J+1}$ from those given by Racah (1942) and Edmonds (1957).

and being

$$\langle J1M0|JM\rangle = \frac{M}{\sqrt{J(J+1)}}$$

one obtains

$$\langle \alpha J\|\vec{J}\|\alpha' J'\rangle = \delta_{\alpha\alpha'}\,\delta_{JJ'}\,\sqrt{J(J+1)}\,. \tag{2.97}$$

An important property of the reduced matrix element can be easily deduced from the orthogonality relation of the vector-coupling coefficients

$$\sum_{M'q} |\langle \alpha JM|T^k_q|\alpha' J'M'\rangle|^2 = |\langle \alpha J\|\boldsymbol{T}^k\|\alpha' J'\rangle|^2\,.$$

The most striking consequence of the Wigner-Eckart theorem is the direct appearance of *selection rules* for the matrix elements of the components of spherical tensor operators. Indeed, because of the presence of the 3-j symbol in Eq. (2.96), the matrix element $\langle \alpha JM|T^k_q|\alpha' J'M'\rangle$ is identically zero unless

$$|J-k| \le J' \le J+k\,, \qquad M' = M-q\,.$$

In particular, we obtain from Eq. (2.26a) that the matrix elements of a zero-rank spherical tensor operator are diagonal with respect to J and M, and are independent of M.

2.9. Properties of Reduced Matrix Elements

From the Wigner-Eckart theorem an important relation can be deduced for the reduced matrix elements of a Hermitian spherical tensor operator H^k_q. Taking the complex conjugate of Eq. (2.95) we have

$$\langle \alpha JM|H^k_q|\alpha' J'M'\rangle^* = (-1)^{2k}\,\langle \alpha J\|\boldsymbol{H}^k\|\alpha' J'\rangle^*\,\langle J'kM'q|JM\rangle\,. \tag{2.98}$$

On the other hand, being H^k_q Hermitian, from Eq. (2.86) we deduce

$$\begin{aligned}\langle \alpha JM|H^k_q|\alpha' J'M'\rangle^* &= \langle \alpha' J'M'|(H^k_q)^\dagger|\alpha JM\rangle \\ &= (-1)^{r+q}\,\langle \alpha' J'M'|H^k_{-q}|\alpha JM\rangle\,.\end{aligned}$$

Applying again the Wigner-Eckart theorem to the last matrix element we get

$$\langle \alpha JM|H^k_q|\alpha' J'M'\rangle^* = (-1)^{r+q+2k}\,\langle \alpha' J'\|\boldsymbol{H}^k\|\alpha J\rangle\langle JkM\ -q|J'M'\rangle\,. \tag{2.99}$$

From the symmetry properties of the vector-coupling coefficients (Eqs. (2.22), (2.24), (2.25)) we have

$$\langle JkM\ -q|J'M'\rangle = (-1)^{J-J'-M+M'}\sqrt{\frac{2J'+1}{2J+1}}\,\langle J'kM'q|JM\rangle\,, \tag{2.100}$$

and, finally, from Eqs. (2.98), (2.99), and (2.100) we get

$$\sqrt{2J+1}\,\langle \alpha J \| \boldsymbol{H}^k \| \alpha' J' \rangle^* = (-1)^{J-J'+r}\,\sqrt{2J'+1}\,\langle \alpha' J' \| \boldsymbol{H}^k \| \alpha J \rangle\ , \qquad (2.101)$$

which is the relation, valid for Hermitian spherical tensor operators only, between reduced matrix elements of the form $\langle \alpha J \| \boldsymbol{H}^k \| \alpha' J' \rangle$ and $\langle \alpha' J' \| \boldsymbol{H}^k \| \alpha J \rangle$.

In Sect. 2.7 we have shown how it is possible to construct an irreducible spherical tensor T^K_Q from the product of two irreducible tensors R^k_q and $S^{k'}_{q'}$. We want here to show how the reduced matrix elements of these tensors are related among each other. The Wigner-Eckart theorem, applied to the tensor T^K_Q, gives

$$\langle \alpha J M | T^K_Q | \alpha' J' M' \rangle = (-1)^{J'+K+M}\sqrt{2J+1}\begin{pmatrix} J & J' & K \\ -M & M' & Q \end{pmatrix}\langle \alpha J \| \boldsymbol{T}^K \| \alpha' J' \rangle\ .$$

From Eq. (2.79), introducing intermediate states between the tensors R^k_q and $S^{k'}_{q'}$ and applying again the Wigner-Eckart theorem, one obtains

$$\begin{aligned}\sum_{qq'}\sum_{\alpha'' J'' M''} & (-1)^{J''+M''+2k-K+Q}\sqrt{2J''+1} \\ & \times \begin{pmatrix} J & J'' & k \\ -M & M'' & q \end{pmatrix}\begin{pmatrix} J'' & J' & k' \\ -M'' & M' & q' \end{pmatrix}\begin{pmatrix} k & k' & K \\ q & q' & -Q \end{pmatrix} \\ & \times \langle \alpha J \| \boldsymbol{R}^k \| \alpha'' J'' \rangle \langle \alpha'' J'' \| \boldsymbol{S}^{k'} \| \alpha' J' \rangle = \\ & = \begin{pmatrix} J & J' & K \\ -M & M' & Q \end{pmatrix}\langle \alpha J \| \boldsymbol{T}^K \| \alpha' J' \rangle\ .\end{aligned}$$

Multiplication of both sides by

$$\begin{pmatrix} J & J' & K \\ -M & M' & Q \end{pmatrix}$$

followed by summation over M and M' gives, using Eqs. (2.23a) and (2.34)[1]

$$\begin{aligned}\langle \alpha J \| \boldsymbol{T}^K \| \alpha' J' \rangle = & (-1)^{J+J'+K}\sum_{\alpha'' J''}\sqrt{2J''+1}\begin{Bmatrix} J & J' & K \\ k' & k & J'' \end{Bmatrix} \\ & \times \langle \alpha J \| \boldsymbol{R}^k \| \alpha'' J'' \rangle \langle \alpha'' J'' \| \boldsymbol{S}^{k'} \| \alpha' J' \rangle\ , \qquad (2.102)\end{aligned}$$

which shows how the reduced matrix element of a 'composite' spherical tensor is related to the reduced matrix elements of the constituent tensors.

[1] The deduction of Eq. (2.102) is not trivial, as it involves the contraction of four 3-j symbols which must be suitably manipulated to obtain the formula (Eq. (2.34)) leading to the final result. In App. 2 we give, for the unexperienced reader, an example of how the various manipulations can be performed.

A direct application of this formula to the 0-rank tensor $\boldsymbol{T}^0$ obtained from the scalar product of an arbitrary vector $\vec{v}$ with the angular momentum $\vec{J}$ gives (see Eq. (2.83))

$$\begin{aligned}\langle \alpha J \| \boldsymbol{T}^0 \| \alpha' J' \rangle &= -\frac{1}{\sqrt{3}} \langle \alpha J \| \vec{v} \cdot \vec{J} \| \alpha' J' \rangle \\ &= (-1)^{J+J'} \sum_{\alpha'' J''} \sqrt{2J''+1} \begin{Bmatrix} J & J' & 0 \\ 1 & 1 & J'' \end{Bmatrix} \langle \alpha J \| \vec{v} \| \alpha'' J'' \rangle \langle \alpha'' J'' \| \vec{J} \| \alpha' J' \rangle ,\end{aligned}$$

which, using Eqs. (2.36a) and (2.97), can be written in the form

$$\langle \alpha J \| \vec{v} \cdot \vec{J} \| \alpha' J' \rangle = \delta_{JJ'} \sqrt{J(J+1)} \langle \alpha J \| \vec{v} \| \alpha' J \rangle .$$

From this equation a remarkable relation, often referred to as the *projection theorem*, can be easily proved by a double application of the Wigner-Eckart theorem,

$$[J(J+1)] \langle \alpha JM | \vec{v} | \alpha' JM' \rangle = \langle \alpha JM | (\vec{v} \cdot \vec{J}) \vec{J} | \alpha' JM' \rangle . \tag{2.103}$$

We have indeed for the spherical components of the operator $\vec{J}$

$$\begin{aligned}&\langle \alpha JM | (\vec{v} \cdot \vec{J}) J^1_q | \alpha' JM' \rangle = \\ &= \sum_{\alpha'' J'' M''} \langle \alpha JM | \vec{v} \cdot \vec{J} | \alpha'' J'' M'' \rangle \langle \alpha'' J'' M'' | J^1_q | \alpha' JM' \rangle \\ &= \sum_{M''} \langle \alpha J \| \vec{v} \cdot \vec{J} \| \alpha' J \rangle \langle J 0 M'' 0 | JM \rangle \langle \alpha' J \| \vec{J} \| \alpha' J \rangle \langle J 1 M' q | JM'' \rangle \\ &= J(J+1) \langle \alpha J \| \vec{v} \| \alpha' J \rangle \langle J 1 M' q | JM \rangle \\ &= J(J+1) \langle \alpha JM | v^1_q | \alpha' JM' \rangle ,\end{aligned} \tag{2.104}$$

which proves Eq. (2.103).

The projection theorem has a very simple physical meaning that is depicted in Fig. 2.5. According to the vectorial model, the vector $\vec{v}$ rotates rapidly about $\vec{J}$, so that its only effective component, $\vec{v}_{\text{eff}}$, points in the $\vec{J}$-direction. On the other hand, $\vec{v}_{\text{eff}}$ can be written in the form

$$\vec{v}_{\text{eff}} = \frac{(\vec{v} \cdot \vec{J}) \vec{J}}{J^2} ,$$

thus the projection theorem can be considered as the direct generalization to Quantum Mechanics of this simple geometrical expression.

The projection theorem can be expressed in the equivalent form (see Eq. (2.104))

$$\langle \alpha JM | \vec{v} | \alpha' JM' \rangle = g_{\alpha \alpha' J}(\vec{v}) \langle \alpha' JM | \vec{J} | \alpha' JM' \rangle ,$$

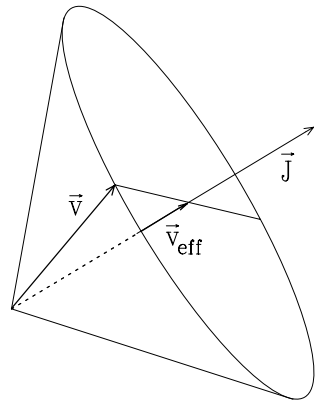

Fig.2.5. The vector $\vec{v}$ is rapidly spinning about $\vec{J}$, so that its only effective component, $\vec{v}_{\rm eff}$, is in the $\vec{J}$-direction.

where

$$g_{\alpha\alpha' J}(\vec{v}) = \frac{\langle \alpha JM | \, \vec{v} \cdot \vec{J} \, | \alpha' JM \rangle}{J(J+1)} = \frac{\langle \alpha J \| \, \vec{v} \, \| \alpha' J \rangle}{\sqrt{J(J+1)}} \tag{2.105}$$

is the generalization of the Landé factor that will be encountered in the next chapter.

A final application of the Wigner-Eckart theorem concerns the matrix elements of a spherical tensor operator acting on the dynamical variables of a single component of a composite system.

Let us consider a system composed of two parts of angular momenta $\vec{J}_1$ and $\vec{J}_2$, respectively, having total angular momentum $\vec{J} = \vec{J}_1 + \vec{J}_2$. If $T^k_q(1)$ is a spherical tensor operator (the argument (1) means that it is acting only on the first component of the system), we have for its matrix elements

$$\begin{aligned} &\langle \alpha j_1 j_2 JM | \, T^k_q(1) \, | \alpha' j'_1 j'_2 J' M' \rangle = \\ &= (-1)^{2k} \, \langle J' k M' q | JM \rangle \langle \alpha j_1 j_2 J \| \, \boldsymbol{T}^k(1) \, \| \alpha' j'_1 j'_2 J' \rangle \, . \end{aligned} \tag{2.106}$$

On the other hand, if we change the coupling scheme using the vector-coupling coefficients, we can write

$$\begin{aligned} &\langle \alpha j_1 j_2 JM | \, T^k_q(1) \, | \alpha' j'_1 j'_2 J' M' \rangle = \\ &= \sum_{m_1 m_2 m'_1 m'_2} \langle j_1 j_2 m_1 m_2 | JM \rangle \langle j'_1 j'_2 m'_1 m'_2 | J' M' \rangle \\ &\qquad \times \langle \alpha j_1 j_2 m_1 m_2 | \, T^k_q(1) \, | \alpha' j'_1 j'_2 m'_1 m'_2 \rangle \, . \end{aligned}$$

Since $T^k_q(1)$ acts only on the first component of the system, applying again the Wigner-Eckart theorem we obtain

$$\begin{aligned} &\langle \alpha j_1 j_2 m_1 m_2 | \, T^k_q(1) \, | \alpha' j'_1 j'_2 m'_1 m'_2 \rangle = \\ &= (-1)^{2k} \, \langle j'_1 k \, m'_1 q | j_1 m_1 \rangle \langle \alpha j_1 \| \, \boldsymbol{T}^k(1) \, \| \alpha' j'_1 \rangle \, \delta_{j_2 j'_2} \, \delta_{m_2 m'_2} \, . \end{aligned} \tag{2.107}$$

Comparison of Eqs. (2.106) and (2.107) gives the following relation between reduced matrix elements

$$\begin{aligned}
&\langle J'kM'q|JM\rangle \langle \alpha j_1 j_2 J\| \boldsymbol{T}^k(1) \|\alpha' j_1' j_2' J'\rangle = \\
&= \sum_{m_1 m_2 m_1'} \langle j_1 j_2 m_1 m_2|JM\rangle \langle j_1' j_2 m_1' m_2|J'M'\rangle \langle j_1' k\, m_1' q|j_1 m_1\rangle \\
&\qquad \times \langle \alpha j_1\| \boldsymbol{T}^k(1) \|\alpha' j_1'\rangle \, \delta_{j_2 j_2'} \, .
\end{aligned}$$

This relation can be expressed in a more compact form by a calculation similar to that in App. 2. This calculation, which is left as an exercise to the reader, leads to the following expression

$$\begin{aligned}
&\langle \alpha j_1 j_2 J\| \boldsymbol{T}^k(1) \|\alpha' j_1' j_2' J'\rangle = \\
&= (-1)^{j_1+j_2+J'+k} \sqrt{(2J'+1)(2j_1+1)} \begin{Bmatrix} j_1 & j_1' & k \\ J' & J & j_2 \end{Bmatrix} \\
&\qquad \times \langle \alpha j_1\| \boldsymbol{T}^k(1) \|\alpha' j_1'\rangle \, \delta_{j_2 j_2'} \, .
\end{aligned} \tag{2.108}$$

Similarly, if $T_q^k(2)$ is a spherical tensor operator acting only on the second part of the composite system, we obtain

$$\begin{aligned}
&\langle \alpha j_1 j_2 J\| \boldsymbol{T}^k(2) \|\alpha' j_1' j_2' J'\rangle = \\
&= (-1)^{j_1+j_2'+J+k} \sqrt{(2J'+1)(2j_2+1)} \begin{Bmatrix} j_2 & j_2' & k \\ J' & J & j_1 \end{Bmatrix} \\
&\qquad \times \langle \alpha j_2\| \boldsymbol{T}^k(2) \|\alpha' j_2'\rangle \, \delta_{j_1 j_1'} \, .
\end{aligned} \tag{2.109}$$

More generally, if $R_{q_1}^{k_1}(1)$ and $S_{q_2}^{k_2}(2)$ are two spherical tensor operators acting on the first and second part of the composite system, respectively, and if T_Q^K is the spherical tensor operator constructed according to Eq. (2.79), the reduced matrix elements are connected by the following relation

$$\begin{aligned}
&\langle \alpha j_1 j_2 J\| \boldsymbol{T}^K \|\alpha' j_1' j_2' J'\rangle = \\
&= \sqrt{(2j_1+1)(2j_2+1)(2J'+1)} \begin{Bmatrix} J & J' & K \\ j_1 & j_1' & k_1 \\ j_2 & j_2' & k_2 \end{Bmatrix} \\
&\qquad \times \sum_{\alpha''} \langle \alpha j_1\| \boldsymbol{R}^{k_1}(1) \|\alpha'' j_1'\rangle \langle \alpha'' j_2\| \boldsymbol{S}^{k_2}(2) \|\alpha' j_2'\rangle \, .
\end{aligned}$$

The proof of this relation, that follows from Eqs. (2.34) and (2.48), is left as an exercise to the reader.

CHAPTER 3

ATOMIC SPECTROSCOPY

Polarization can be introduced in spectral lines by several different mechanisms, that are connected either with the presence of an external field (like for instance a magnetic or an electric field) or with the existence of some kind of anisotropy in the excitation of the atomic system (optical pumping, impact polarization, etc.).

While the detailed theory describing the interplay of the various mechanisms will be tackled in the following chapters, it is first necessary to state some specific spectroscopic notations, and to give a number of basic results concerning the interaction of an atomic system with an external field, in order to establish an adequate physical background. In particular, we will review in this chapter the theory of the Zeeman and Paschen-Back effects, including the case of hyperfine structure, and we will give a description of atomic polarization in terms of the density (or statistical) operator and of statistical tensors.

3.1. Zeeman Effect

According to the theory of atomic structure (see for instance Condon and Shortley, 1935; Condon and Odabaşi, 1980), the modifications produced in atomic spectra by an external, uniform magnetic field can be described by adding to the unperturbed Hamiltonian H_0 of the atomic system an additional term H_B, called the *magnetic Hamiltonian*, given by

$$H_B = \frac{e_0 h}{4\pi mc} (\vec{L} + 2\vec{S}) \cdot \vec{B} + \frac{e_0^2}{8mc^2} (\vec{B} \times \vec{r})^2 , \tag{3.1}$$

where e_0 is the absolute value of the electron charge, m is the electron mass, h and c have their usual meaning of Planck constant and speed of light, $\vec{L}$ and $\vec{S}$ are the (dimensionless) total orbital angular momentum and total spin of the electronic cloud, $\vec{B}$ is the magnetic field vector, and $\vec{r}$ is the position operator defined by

$$\vec{r} = \sum_i \vec{r}_i ,$$

where $\vec{r}_i$ is the position of the i-th optical electron relative to the nucleus. For one-electron atoms, Eq. (3.1) can be derived by taking the lowest-order, non relativistic limit of Dirac's equation describing the motion of a particle in an electromagnetic field (see for instance Schiff, 1949).

The second term in Eq. (3.1) is the so-called *diamagnetic term*. Its importance is very limited in practice, at least for the magnetic fields that are usually found

in laboratory or astrophysical plasmas. Indeed, comparing the two terms in the right-hand side of Eq. (3.1) and taking, as an order of magnitude, the radius of the first Bohr's orbit for the expectation value of r, we obtain for their ratio

$$\frac{\text{second term}}{\text{first term}} \approx \frac{1}{32\pi^3}\frac{h^3}{m^2 c\, e_0^3} B = 1.06 \times 10^{-10} B \,, \tag{3.2}$$

where B is expressed in G. If we exclude the extremely large fields that are found in magnetic white dwarfs (see e.g. Angel et al., 1981, or Schmidt, 1987, for a review on the subject) or are supposed to exist in neutron stars, the diamagnetic term can be safely neglected in Eq. (3.1), so that we can write

$$H_B = \frac{e_0 h}{4\pi mc} (\vec{L} + 2\vec{S}) \cdot \vec{B} = \mu_0 (\vec{L} + 2\vec{S}) \cdot \vec{B} \,, \tag{3.3}$$

where μ_0 is the so-called *Bohr magneton* ($\mu_0 = 9.27 \times 10^{-21}$ erg G^{-1}).

If the magnetic field is so weak as to keep the magnetic energy much smaller than the energy intervals relative to the unperturbed Hamiltonian H_0, the effect of H_B can be computed by perturbation theory (see Messiah, 1961, for an introduction to the argument). According to this theory, the shifts of an N-fold degenerate energy level of H_0 are obtained by diagonalization of the matrix

$$(H_B)_{ij} = \langle u_i^{(\alpha)} | H_B | u_j^{(\alpha)} \rangle \qquad (i, j = 1, \ldots, N) \,,$$

where $|u_k^{(\alpha)}\rangle$ $(k = 1, \ldots, N)$ are the degenerate eigenvectors of H_0 corresponding to the eigenvalue E_α.

In our case, since the Hamiltonian H_0 is invariant under rotations, the total angular momentum J and its projection M along an arbitrary z-axis are good quantum numbers, so that the eigenvectors can be written in the form $|\alpha JM\rangle$ (where α is a collection of inner quantum numbers of H_0), with

$$\begin{aligned} H_0 |\alpha JM\rangle &= E_{\alpha J} |\alpha JM\rangle \\ J^2 |\alpha JM\rangle &= J(J+1) |\alpha JM\rangle \\ J_z |\alpha JM\rangle &= M |\alpha JM\rangle \,. \end{aligned} \tag{3.4}$$

When we add to H_0 the magnetic Hamiltonian H_B, the corrections to the degenerate energy $E_{\alpha J}$ are found by diagonalization of the matrix

$$\langle \alpha JM | H_B | \alpha JM' \rangle = \mu_0 \langle \alpha JM | (\vec{L} + 2\vec{S}) \cdot \vec{B} \, | \alpha JM' \rangle \,.$$

The matrix elements can be evaluated for any direction of the magnetic field in the reference system (xyz) chosen to describe the atomic system. Writing $\vec{B}$ in the form $\vec{B} = B\vec{b}$, where $\vec{b}$ is a unit vector in the magnetic field direction, and writing $(\vec{L} + 2\vec{S})$ in the form $(\vec{J} + \vec{S})$, where $\vec{J}$ is the total angular momentum of the atomic system, we have

$$\langle \alpha JM | H_B | \alpha JM' \rangle = \mu_0 B \langle \alpha JM | (\vec{J} + \vec{S}) \cdot \vec{b} \, | \alpha JM' \rangle \,.$$

Introducing the spherical components of the three vectors, the scalar product can be written in the form (see Eq. (2.83))

$$(\vec{J}+\vec{S})\cdot\vec{b}=\sum_q(-1)^q\,(J_q+S_q)\,b_{-q}\,,$$

so that, applying the Wigner-Eckart theorem in the form of Eq. (2.96), and using Eq. (2.97), one obtains

$$\langle\alpha JM|H_B|\alpha JM'\rangle=\mu_0 B\sum_q(-1)^{J+M+q+1}\sqrt{2J+1}\begin{pmatrix}J & J & 1\\ -M & M' & q\end{pmatrix}\times\Big(\sqrt{J(J+1)}+\langle\alpha J\|\vec{S}\,\|\alpha J\rangle\Big)b_{-q}\,. \tag{3.5}$$

Owing to the selection rules of the 3-j symbol, these matrix elements are zero unless $(M'-M)=0$, or ±1. We have therefore a tridiagonal matrix that might in principle be diagonalized by standard methods.

The diagonalization can however be avoided by aligning the z-axis of the reference system with the direction of the magnetic field. In this case, in fact, the only non-zero component of the unit vector $\vec{b}$ is $b_0=1$, and we easily obtain, substituting the value of the 3-j symbol given by Eq. (2.26d)

$$\langle\alpha JM|H_B|\alpha JM'\rangle=\mu_0 B\,g\,M\,\delta_{MM'}\,, \tag{3.6}$$

where g, the so-called *Landé factor*, can be written in the form[1]

$$g=1+\frac{\langle\alpha J\|\vec{S}\,\|\alpha J\rangle}{\sqrt{J(J+1)}}\qquad(J\neq0). \tag{3.7}$$

Equation (3.6) shows that the magnetic Hamiltonian is now represented by a diagonal matrix. This means that, to the first order of perturbation theory, the eigenstates of the total Hamiltonian (H_0+H_B) are of the form $|\alpha JM\rangle$, while the eigenvalues are given by

$$E_{\alpha J}+\mu_0\,gBM\qquad(M=-J,-J+1,\ldots,J).$$

Thus the Hamiltonian H_B removes the degeneracy, and any level characterized by the quantum number J is split into $(2J+1)$ equally spaced sublevels, the splitting being proportional to the Landé factor g and to the magnetic field.

We want to remark, however, that the states $|\alpha JM\rangle$ are eigenvectors of the total Hamiltonian *only* when the z-axis of the reference system points in the magnetic

[1] As apparent from the 3-j symbol in Eq. (3.5), the matrix elements of H_B identically vanish if $J=0$. This simply means that the magnetic field does not affect, to the first order, the energy of the atomic levels characterized by $J=0$. Consequently, one can formally put $g=0$ for such levels.

field direction. This means that a state having a definite value for the projection of the total angular momentum *along the direction of the magnetic field* has a well-defined energy value. When the z-axis of the reference system is *not* in the direction of the magnetic field, a state of the form $|\alpha JM\rangle$ is an eigenvector of H_0, but not of $(H_0 + H_B)$.

The general expression for the Landé factor, given in Eq. (3.7), involves the evaluation of the reduced matrix element of $\vec{S}$. This can be easily done when the levels are described by the *Russel-Saunders* (or *L-S*) *coupling scheme* (see e.g. Condon and Shortley, 1935). In this scheme the quantum numbers L and S corresponding to the total orbital angular momentum and to the total spin, respectively, are good quantum numbers, so that an eigenvector of the Hamiltonian H_0 can be written in the form

$$|\beta LSJM\rangle \ ,$$

where β is a collection of quantum numbers representing the electronic configuration. The reduced matrix element is then

$$\langle \beta LSJ \| \vec{S} \| \beta LSJ \rangle \ ,$$

and it can be evaluated in the easiest way with the help of the projection theorem. From Eq. (2.105) we have

$$\langle \beta LSJ \| \vec{S} \| \beta LSJ \rangle = \frac{\langle \beta LSJM | \vec{S} \cdot \vec{J} | \beta LSJM \rangle}{\sqrt{J(J+1)}} \ ,$$

and writing $\vec{S} \cdot \vec{J}$ in the form

$$\vec{S} \cdot \vec{J} = \frac{1}{2} \left[J^2 + S^2 - L^2 \right]$$

we obtain for the Landé factor

$$g_{LS} = 1 + \frac{1}{2} \, \frac{J(J+1) + S(S+1) - L(L+1)}{J(J+1)} \ . \tag{3.8}$$

This formula can be rewritten in the form

$$g_{LS} = 1 + \gamma(J, S, L) \ ,$$

where we have used the compact notation

$$\gamma(A, B, C) = \frac{A(A+1) + B(B+1) - C(C+1)}{2A(A+1)} \ .$$

In the *j-j coupling scheme* (see e.g. Condon and Shortley, 1935) a simple expression for the Landé factor can be obtained for levels originating from two optical

electrons of orbital angular momentum l_1 and l_2, respectively. In this case the reduced matrix element to be evaluated is the following

$$\left\langle \beta\,(l_1 s_1)j_1, (l_2 s_2)j_2, J \| \vec{S} \| \beta\,(l_1 s_1)j_1, (l_2 s_2)j_2, J \right\rangle ,$$

where $s_1 = s_2 = 1/2$. Writing $\vec{S}$ in terms of the spins of the single electrons ($\vec{S} = \vec{s}_1 + \vec{s}_2$) and applying Eqs. (2.108), (2.109), and (2.36d), one obtains after some calculations

$$g_{jj} = 1 + \gamma(J, j_1, j_2)\,\gamma(j_1, 1/2, l_1) + \gamma(J, j_2, j_1)\,\gamma(j_2, 1/2, l_2) .$$

Another case where it is possible to find an analytical expression for the Landé factor is the case of the so-called J_1-l *coupling*. In this coupling scheme a 'parent' level of orbital angular momentum L_1 and spin S_1 couples its total angular momentum J_1 with the orbital angular momentum l of a further electron, to give an angular momentum K which in its turn couples with the electron spin to give the total angular momentum J. Thus the reduced matrix element to be evaluated is the following

$$\left\langle \beta\left((L_1 S_1)J_1, l\right)K, s, J \| \vec{S} \| \beta\left((L_1 S_1)J_1, l\right)K, s, J \right\rangle ,$$

where $s = 1/2$. After some tedious algebra, that is left as an exercise to the reader, one gets the formula

$$g_{J_1 l} = 1 + \gamma(J, 1/2, K) + \gamma(J, K, 1/2)\,\gamma(K, J_1, l)\,\gamma(J_1, S_1, L_1) .$$

In more complicated coupling schemes, or in *intermediate coupling*, no simple analytical expression can be found for the Landé factor unless the eigenfunction of the level is known in full detail. If we know, for instance, how to express the eigenvector $|\alpha JM\rangle$ of a given level in terms of the L-S coupling eigenvectors (see Condon and Shortley, 1935, for further details),

$$|\alpha JM\rangle = \sum_{\beta LS} c(\beta, L, S)\,|\beta LSJM\rangle ,$$

it can be shown by some Racah algebra that

$$g_{\mathrm{ic}} = \sum_{\beta LS} |c(\beta, L, S)|^2 g_{LS} ,$$

where g_{LS} are the Landé factors computed from Eq. (3.8). This formula is however of little use, because the coefficients are seldom known with a sufficient degree of accuracy.

It should be remarked, however, that in many cases the Landé factors are known from experimental work carried out in spectroscopy laboratories. A systematic (but incomplete and non-updated) list of experimental g-values can be found in

Moore (1949, 1952, 1958). For the FeI and FeII spectra, further g-values can be found in Reader and Sugar (1975) and in Corliss and Sugar (1982).

For an atom in L-S coupling, the Landé factor is equal to 1 for a level having $S = 0$, while it is equal to 2 for a level having $L = 0$. When both L and S are non-zero, g is generally bounded between 1 and 2, although many exceptions are found to this simple rule, especially for low J-values. In rare cases, the combination of the quantum numbers may give a negative or vanishing value for g. L-S levels having $g = 0$ are ${}^4\mathrm{D}_{1/2}$, ${}^5\mathrm{F}_1$, ${}^6\mathrm{G}_{3/2}$, ${}^7\mathrm{H}_2$, ${}^8\mathrm{I}_{5/2}$, etc., while L-S levels having $g < 0$ are ${}^6\mathrm{F}_{1/2}$, ${}^7\mathrm{G}_1$, ${}^8\mathrm{G}_{1/2}$, ${}^8\mathrm{H}_{3/2}$, etc. In other cases, large values of g can result; for instance, L-S levels having $g \geq 2.5$ are ${}^4\mathrm{P}_{1/2}$ ($g = 2.667$), ${}^5\mathrm{P}_1$ ($g = 2.5$), ${}^6\mathrm{D}_{1/2}$ ($g = 3.333$), ${}^7\mathrm{D}_1$ ($g = 3$), ${}^8\mathrm{D}_{3/2}$ ($g = 2.8$), ${}^8\mathrm{F}_{1/2}$ ($g = 4$), etc.

Let's now consider the Zeeman pattern to be expected in the transition between two atomic levels, both split by the presence of a magnetic field. If J and J' are the angular momentum quantum numbers of the lower and upper level, respectively, and if g and g' are the corresponding Landé factors, the spectral line originating from the transition between the two levels splits, owing to the magnetic field, into a collection of components whose frequencies are given by

$$\nu_{MM'}^{JJ'} = \nu_0 + \frac{\mu_0 B}{h} \left(g' M' - g M\right) , \tag{3.9}$$

where ν_0 is the frequency of the unperturbed line and where M and M' are the magnetic quantum numbers of the lower and upper sublevels, respectively. Formula (3.9) is often written in the form

$$\nu_{MM'}^{JJ'} = \nu_0 + \nu_{\mathrm{L}} \left(g' M' - g M\right) ,$$

where

$$\nu_{\mathrm{L}} = \frac{\mu_0 B}{h} = \frac{e_0 B}{4\pi m c} \tag{3.10}$$

is the so-called *Larmor frequency*; numerically we have

$$\nu_{\mathrm{L}} = 1.3996 \times 10^6 \, B , \tag{3.11}$$

with B expressed in G and ν_{L} in s^{-1}.

The wavelengths of the transitions can be easily evaluated in the visible and infrared, since in these cases the Larmor frequency is much smaller than ν_0 (for instance, for a line at $1.2\,\mu$m and for $B = 10^4$G, the ratio ν_{L}/ν_0 is of order 6×10^{-5}), so that we can write

$$\lambda_{MM'}^{JJ'} = \lambda_0 - \Delta\lambda_B \left(g' M' - g M\right) , \tag{3.12}$$

where $\lambda_0 = c/\nu_0$ is the wavelength of the unperturbed line, and where

$$\Delta\lambda_B = \lambda_0^2 \, \frac{\nu_{\mathrm{L}}}{c} = \frac{\lambda_0^2 \, e_0 \, B}{4\pi m c^2} . \tag{3.13}$$

Numerically we have

$$\Delta\lambda_B = 4.6686 \times 10^{-10}\, \lambda_0^2\, B\ , \tag{3.14}$$

where $\Delta\lambda_B$ is in mÅ, λ_0 in Å, and B in G.

It is important to note that, of the various Zeeman components (whose wavelengths are given by Eq. (3.12)) arising in a given transition, only a limited number is actually observed: this is due to selection rules that depend on the interaction between atoms and radiation field. The general properties of Zeeman patterns (namely the number of observed lines, their wavelength position, their relative strength and polarization features) depend on the kind of interaction (electric-dipole, magnetic-dipole, electric-quadrupole, etc.). In the rest of this section we summarize the main properties of the Zeeman patterns resulting from the electric-dipole interaction, which is the simplest one and the most important in practice. The reader is referred to Sect. 9.1 for a formal derivation of what is anticipated here.

The selection rule for electric-dipole transitions is

$$\Delta M = M' - M = 0, \pm 1\ , \tag{3.15}$$

from which three distinct groups of Zeeman components arise.

The components having $\Delta M = -1$, that will be called in the following the $\sigma_{\rm r}$ components, are generally displaced to longer wavelengths (or towards the *red* side of the spectrum) from the unperturbed line. In emission, they give rise in general to elliptically polarized radiation, which degenerates into circularly polarized radiation when observed along the direction of the magnetic field, and into linearly polarized radiation when observed in the plane perpendicular to the magnetic field. In particular, referring to Fig. 3.1, any $\sigma_{\rm r}$ component produces in emission: right-handed (or positive) circular polarization along the positive z-axis, left-handed (or negative) circular polarization along the negative z-axis, and linear polarization, perpendicular to the z-axis, along any direction in the x-y plane.[1]

The components having $\Delta M = +1$ ($\sigma_{\rm b}$ components) are generally displaced to shorter wavelengths (or towards the *blue* side of the spectrum) from the unperturbed line. Their behavior is similar to that of the $\sigma_{\rm r}$ components except for the handedness of circular polarization. Referring again to Fig. 3.1, any $\sigma_{\rm b}$ component produces in emission: left-handed (or negative) circular polarization along the positive z-axis, and right-handed (or positive) circular polarization along the negative z-axis. In the x-y plane the $\sigma_{\rm b}$ components have the same properties as the $\sigma_{\rm r}$ components.

Finally, the wavelengths of the components having $\Delta M = 0$ (the so-called π components) fall in between those of the $\sigma_{\rm r}$ and $\sigma_{\rm b}$ components. In emission, the

[1] In absorption, the situation is more complicated because the polarization of the radiation absorbed by the $\sigma_{\rm r}$ components depends also on the polarization of the incident radiation. For the special case of an unpolarized incident beam, the absorbed radiation has the same polarization characteristics as the radiation that would be emitted in the direction of the beam. As a consequence, the *opposite* polarization will be present in the beam after absorption.

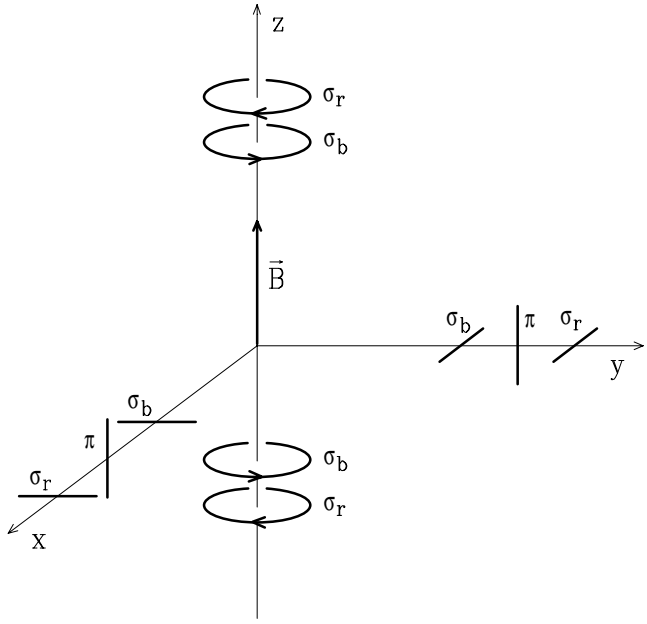

Fig.3.1. The polarization properties of the radiation emitted by different Zeeman components depend on the type of component and on the angle between the observing direction and the magnetic field vector. For the radiation emitted along the x, y, and z-axes, the tip of the wave electric field vector draws, in a fixed point, the figures here shown.

π components give rise to linear polarization whose direction is always parallel to the magnetic field, as represented schematically in Fig. 3.1.

In particular, for an observer located in the x-y plane, all the components produce linear polarization that is parallel (for the π components) or perpendicular (for the σ components) to the direction of the magnetic field. This explains the denominations π and σ, which follow from the German words *parallel* and *senkrecht* (perpendicular).

As far as the number of Zeeman components is concerned, the simplest case (often referred to as *normal Zeeman effect*) occurs when the angular momentum of any of the two levels involved in the transition is zero ($J = 0$ or $J' = 0$), or when both levels have the same Landé factor ($g = g'$).[1] In both cases only three components are left: one $\sigma_{\rm r}$ component at the wavelength ($\lambda_0 + g\Delta\lambda_B$), one $\sigma_{\rm b}$ component at the wavelength ($\lambda_0 - g\Delta\lambda_B$), and one π component at the wavelength λ_0, where the g-factor is either the Landé factor of the level having $J \neq 0$, or the Landé factor common to the two levels.[2]

[1] The two cases will be referred to in this book as *normal Zeeman triplet* and *anomalous Zeeman triplet*, respectively. Other authors reserve both names for the case ($J = 0$ or $J' = 0$), and use *normal* or *anomalous* according as the Landé factor is unity or not.

[2] The normal Zeeman effect (or, more properly, the normal Zeeman triplet case) can also be treated by a classical (non quantum-mechanical) approach, that will be presented in the next section.

TABLE 3.1

Analytical expressions for the strengths of Zeeman components. J and M are the quantum numbers of the lower sublevels, J' and M' the quantum numbers of the upper sublevels.

		$J' = J+1$	$J' = J$	$J' = J-1$
σ_b	$M' = M+1$	$\frac{3(J+M+1)(J+M+2)}{2(J+1)(2J+1)(2J+3)}$	$\frac{3(J-M)(J+M+1)}{2J(J+1)(2J+1)}$	$\frac{3(J-M)(J-M-1)}{2J(2J-1)(2J+1)}$
π	$M' = M$	$\frac{3(J-M+1)(J+M+1)}{(J+1)(2J+1)(2J+3)}$	$\frac{3M^2}{J(J+1)(2J+1)}$	$\frac{3(J-M)(J+M)}{J(2J-1)(2J+1)}$
σ_r	$M' = M-1$	$\frac{3(J-M+1)(J-M+2)}{2(J+1)(2J+1)(2J+3)}$	$\frac{3(J+M)(J-M+1)}{2J(J+1)(2J+1)}$	$\frac{3(J+M)(J+M-1)}{2J(2J-1)(2J+1)}$

In the other cases (referred to as *anomalous Zeeman effect*), more complicated patterns occur. It will be proved later (see Sect. 9.1) that the relative strengths of the various components are given by the expression

$$S_q^{JJ'}(M,M') = 3\begin{pmatrix} J' & J & 1 \\ -M' & M & -q \end{pmatrix}^2 \qquad (q=-1,0,+1)\,, \tag{3.16}$$

where the index $q = -(M'-M) = -\Delta M$ is equal to -1, 0, $+1$ for the σ_b, π, and σ_r components, respectively. It can be easily seen that the relative strengths, as defined by Eq. (3.16), are normalized to unity; from Eq. (2.23a) we have in fact

$$\sum_{MM'} S_q^{JJ'}(M,M') = \sum_{MM'} 3\begin{pmatrix} J' & J & 1 \\ -M' & M & -q \end{pmatrix}^2 = 1 \qquad (q=-1,0,+1)\,. \tag{3.17}$$

Using the analytical expressions of the 3-j symbols (Eqs. (2.26)), the strengths of the various components can be written as algebraic functions of M and M'. The results are summarized in Table 3.1.

From Eq. (3.16) one can prove some symmetry properties for the strengths. Equations (2.24) and (2.25) give

$$S_q^{JJ'}(M,M') = S_{-q}^{JJ'}(-M,-M') \tag{3.18}$$

$$S_q^{JJ'}(M,M') = S_q^{J'J}(-M',-M)\,. \tag{3.19}$$

On the other hand, defining the wavelength displacement from line center via Eq. (3.12),

$$\Delta\lambda_{MM'}^{JJ'} = -\Delta\lambda_B\,(g'M' - gM)\,, \tag{3.20}$$

we also have

$$\Delta\lambda_{MM'}^{JJ'} = -\Delta\lambda_{-M-M'}^{JJ'} \tag{3.21}$$

$$\Delta\lambda_{MM'}^{JJ'} = \Delta\lambda_{-M'-M}^{J'J}\,. \tag{3.22}$$

Equations (3.18) and (3.21) show that for any σ_r (σ_b) component there is a σ_b (σ_r) component of the same strength symmetrical about line center, and for any

π component (except the one corresponding to $M = M' = 0$, if it exists) there is another π component of the same strength symmetrical about line center. From Eqs. (3.19) and (3.22) we further deduce that the inversion of the upper and lower level in a given transition yields the same combination of strengths and splittings of the various components, or, in other words, the same Zeeman pattern; the component connecting, in the original pattern, the lower sublevel (J, M) with the upper sublevel (J', M') corresponds in the 'inverted' pattern to the component connecting the lower sublevel $(J', -M')$ with the upper sublevel $(J, -M)$.

Some representative Zeeman patterns are shown in Fig. 3.2. An extensive numerical table of Zeeman patterns for a large number of electric-dipole atomic transitions has been given by Beckers (1969b).[1]

3.2. Classical Theory of the Zeeman Effect

According to the classical theory of the electron, as developed by Lorentz in the early years of this century, we schematize the emitting atom as a negative electric charge (-e_0) oscillating, at the frequency ν_0, around a point P under the action of an elastic, restoring force. In the presence of a magnetic field $\vec{B}$, the motion of the electron is described by the equation

$$\frac{\mathrm{d}^2\vec{x}}{\mathrm{d}t^2} = -4\pi^2\nu_0^2\,\vec{x} - \frac{e_0}{mc}\,\frac{\mathrm{d}\vec{x}}{\mathrm{d}t} \times \vec{B} - \gamma\,\frac{\mathrm{d}\vec{x}}{\mathrm{d}t}\,, \tag{3.23}$$

where γ is a constant which accounts for the damping of the electron due to its energy loss by radiation.

The actual value of this constant, that is introduced here in a purely phenomenological way, can be deduced by equating the work per unit time done on the electron by the friction force

$$\frac{\mathrm{d}L}{\mathrm{d}t} = m\gamma\left(\frac{\mathrm{d}\vec{x}}{\mathrm{d}t}\right)^2$$

with the energy loss by radiation per unit time

$$W = \frac{2e_0^2}{3c^3}\left(\frac{\mathrm{d}^2\vec{x}}{\mathrm{d}t^2}\right)^2\,.$$

By averaging these quantities over an oscillation period, and disregarding the slight difference – due to the magnetic field – between the actual oscillation frequency and ν_0, we have

$$\gamma = \frac{8\pi^2}{3}\frac{e_0^2}{mc^3}\,\nu_0^2 = \frac{8\pi}{3}\left(\frac{\pi e_0^2}{mc}\right)\frac{1}{\lambda_0^2}\,. \tag{3.24}$$

[1] In Beckers' table the Landé factors of the levels involved in the transitions are calculated according to the L-S coupling scheme (Eq. (3.8)).

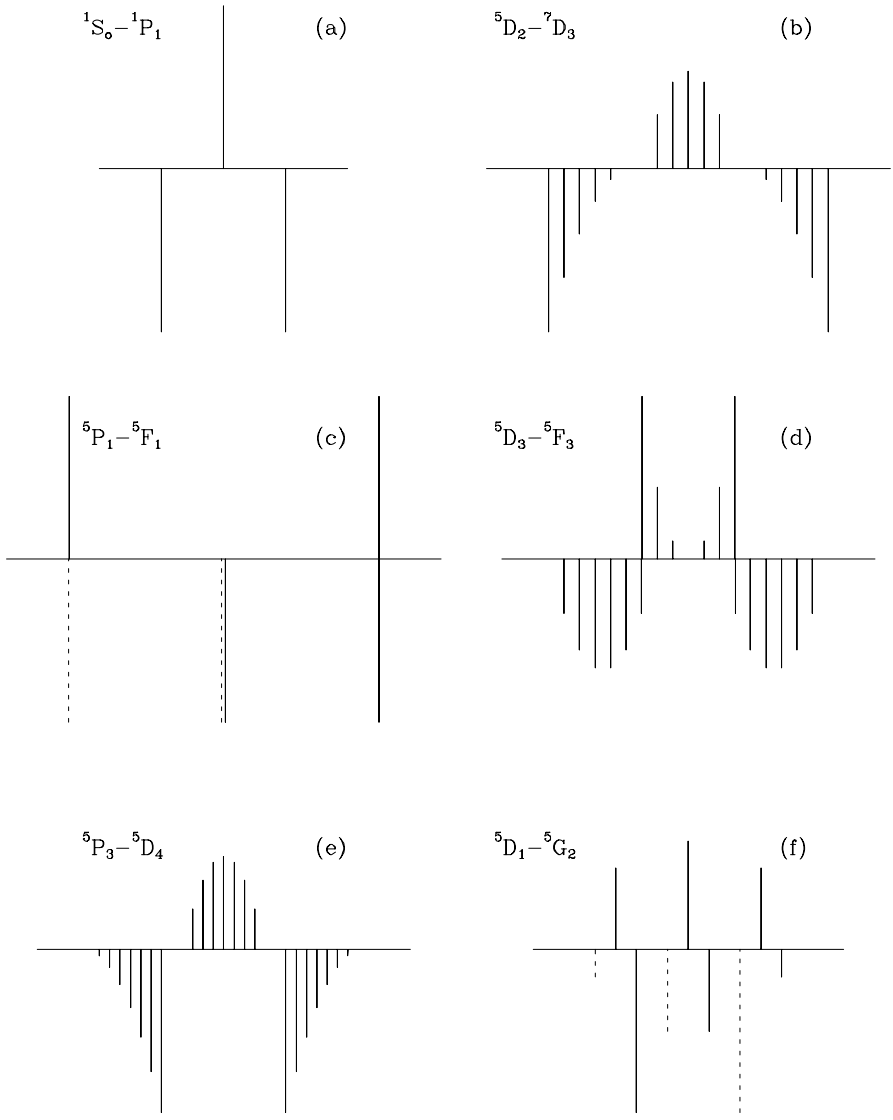

Fig.3.2. Characteristic Zeeman patterns for different transitions. The Landé factors are computed according to the L-S coupling scheme. Following the usual convention, the π components are drawn upward and the σ components downward. The σ_b components in panels (c) and (f) are dashed for clarity; the σ_r and σ_b components at line center in panel (c) are drawn somewhat apart but they actually coincide. From left to right, top to bottom, we have patterns of Type 0 (a), Type II (b), Type III (c,d), and Type I (e,f) (see Sect. 3.3 for the definition of Type).

To find the solution to Eq. (3.23) we introduce a real unit vector $\vec{u}_0$ parallel to $\vec{B}$ and two real unit vectors $\vec{u}_r$ and $\vec{u}_s$ in the plane perpendicular to $\vec{B}$, in such a way that $(\vec{u}_r, \vec{u}_s, \vec{u}_0)$ form, in this order, a right-handed coordinate system. From $\vec{u}_r$ and $\vec{u}_s$ we next define two complex unit vectors $\vec{u}_{\pm 1}$ by the equation

$$\vec{u}_{\pm 1} = \frac{1}{\sqrt{2}} \left(\mp \vec{u}_r + \mathrm{i}\, \vec{u}_s \right) . \tag{3.25}$$

Expanding $\vec{x}$ on the basis $\vec{u}_\alpha$ $(\alpha = 0, \pm 1)$,

$$\vec{x} = \sum_\alpha x_\alpha \, \vec{u}_\alpha \ ,$$

and noting that

$$\vec{u}_\alpha \times \vec{u}_0 = -\mathrm{i}\, \alpha \, \vec{u}_\alpha \ , \tag{3.26}$$

we obtain for x_α the following decoupled equations

$$\frac{\mathrm{d}^2 x_\alpha}{\mathrm{d}t^2} = -4\pi^2 \nu_0^2 \, x_\alpha + 4\pi \mathrm{i}\, \alpha \, \nu_\mathrm{L} \frac{\mathrm{d}x_\alpha}{\mathrm{d}t} - \gamma \frac{\mathrm{d}x_\alpha}{\mathrm{d}t} \qquad (\alpha = 0, \pm 1) \ , \tag{3.27}$$

where ν_L is the Larmor frequency defined in Eq. (3.10). If we now look for a solution of the form

$$x_\alpha = A_\alpha \, \mathrm{e}^{-2\pi \mathrm{i}\, \nu_\alpha t} \ ,$$

and observe that the quantities ν_L and γ are generally much smaller than the frequency ν_0,[1] we obtain

$$x_\alpha = A_\alpha \, \mathrm{e}^{-2\pi \mathrm{i}\, (\nu_0 - \alpha \nu_\mathrm{L})\, t} \, \mathrm{e}^{-\frac{\gamma}{2} t} \ , \tag{3.28}$$

where the constants A_α are to be determined from the initial conditions and depend on the excitation mechanism of the classical dipole.

To determine the radiation emitted by our classical model atom we have just to recall some important results from classical electrodynamics. It is well-known (see e.g. Jackson, 1962) that an oscillating, monochromatic dipole $\vec{p}\,(t)$ produces in the radiation zone an electromagnetic wave whose frequency is the same as that of the dipole, and whose electric field is described by the equation

$$\vec{\mathcal{E}}\,(r, \vec{\Omega}, t) = k^2 \, \frac{\mathrm{e}^{\mathrm{i}kr}}{r} \left(\vec{\Omega} \times \vec{p}\,(t) \right) \times \vec{\Omega} = \frac{k^2 \, \mathrm{e}^{\mathrm{i}kr}}{r} \, \vec{p}_\perp(t) \ , \tag{3.29}$$

where k is the wavenumber, r is the distance from the dipole, $\vec{\Omega}$ is a unit vector in the direction of propagation, and $\vec{p}_\perp = \vec{p} - \vec{\Omega}\,(\vec{\Omega} \cdot \vec{p})$ is the component of the dipole

[1] For instance, for a spectral line at 5000 Å and a magnetic field of 10^3G, we have (see Eqs. (3.11) and (3.24))

$$\nu_\mathrm{L} \simeq 1.4 \times 10^9 \, \mathrm{s}^{-1} \ , \qquad \gamma \simeq 8.9 \times 10^7 \, \mathrm{s}^{-1} \ , \qquad \nu_0 \simeq 6.0 \times 10^{14} \, \mathrm{s}^{-1} \ .$$

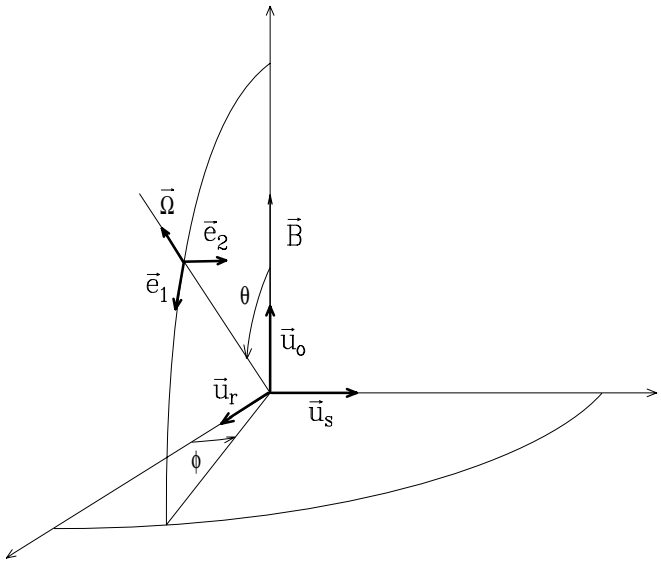

Fig.3.3. Geometry for calculating the polarization properties of the radiation emitted by a classical dipole in a magnetic field $\vec{B}$. The unit vector $\vec{e}_1$ is the reference direction for defining the Stokes parameters.

in the plane perpendicular to $\vec{\Omega}$. From this equation it is possible to determine the polarization of the electromagnetic wave emitted by a classical dipole in any direction.

To define the Stokes parameters (see Sect. 1.6) we choose, in the plane perpendicular to $\vec{\Omega}$, the reference direction unit vector $\vec{e}_1$ and the associated unit vector $\vec{e}_2$, oriented as shown in Fig. 3.3. Since the oscillating dipole is $\vec{p} = -e_0\,\vec{x}$, the components of the vector $\vec{p}_\perp$ along the directions $\vec{e}_1$ and $\vec{e}_2$ can be easily obtained

$$p_{\perp i}(t) = p_i(t) = -e_0 \sum_\alpha C_{\alpha i}\, A_\alpha\, \mathrm{e}^{-2\pi \mathrm{i}\,(\nu_0 - \alpha\nu_\mathrm{L})\,t}\, \mathrm{e}^{-\frac{\gamma}{2}t} \qquad (i = 1, 2)\,, \tag{3.30}$$

where the direction cosines $C_{\alpha i}$ are defined by[1]

$$C_{\alpha i} = \vec{u}_\alpha \cdot \vec{e}_i^{\,*}\,. \tag{3.31}$$

We must consider, however, that the dipole oscillation is not monochromatic. By Fourier series expansion we get

$$p_i(t) = -e_0 \sum_\alpha C_{\alpha i}\, A_\alpha \int_{-\infty}^{\infty} F_\alpha(\nu)\, \mathrm{e}^{-2\pi \mathrm{i}\nu t}\, \mathrm{d}\nu\,, \tag{3.32}$$

[1] Indeed, in this formula, the direction cosines could be just defined as $C_{\alpha i} = \vec{u}_\alpha \cdot \vec{e}_i$, since the unit vectors $\vec{e}_1$ and $\vec{e}_2$ are real. However, Eq. (3.30) and the following ones up to Eq. (3.37) are valid also when the unit vectors $\vec{e}_1$, $\vec{e}_2$ are of the more general form of Eqs. (1.41).

where

$$F_\alpha(\nu) = \int_0^\infty \mathrm{e}^{-2\pi\mathrm{i}\,(\nu_0-\alpha\nu_{\mathrm{L}}-\nu)\,t}\;\mathrm{e}^{-\frac{\gamma}{2}t}\,\mathrm{d}t = -\frac{\mathrm{i}}{2\pi}\,\frac{1}{(\nu_0-\alpha\nu_{\mathrm{L}}-\nu)-\mathrm{i}\Gamma} \tag{3.33}$$

with $\Gamma = \gamma/4\pi$. Thus the component of the electric field along the unit vector $\vec{e}_i$ can be written in the form (as $k = 2\pi\nu/c$)

$$\mathcal{E}_i(r,\vec{\Omega},t) = -\frac{4\pi^2 e_0}{rc^2}\sum_\alpha C_{\alpha i}\,A_\alpha \int_{-\infty}^{\infty} F_\alpha(\nu)\,\nu^2\,\mathrm{e}^{\mathrm{i}(kr-2\pi\nu t)}\,\mathrm{d}\nu\;,$$

and hence

$$\mathcal{E}_i^*\mathcal{E}_j = \frac{16\pi^4 e_0^2}{r^2c^4}\sum_{\alpha\beta} C_{\alpha i}^*\,C_{\beta j}\,A_\alpha^*\,A_\beta \times \int_{-\infty}^{\infty}\mathrm{d}\nu \int_{-\infty}^{\infty}\mathrm{d}\nu'\,F_\alpha(\nu)^*\,F_\beta(\nu')\,\nu^2\,\nu'^2\,\mathrm{e}^{\mathrm{i}(k'-k)r}\,\mathrm{e}^{-2\pi\mathrm{i}(\nu'-\nu)t}\;.$$

To obtain the polarization tensor we must take the average of this quantity over a time interval τ sufficiently long as specified in Sect. 1.4. This leads to

$$\left\langle \mathrm{e}^{-2\pi\mathrm{i}(\nu'-\nu)t}\right\rangle = \frac{1}{\tau}\lim_{\tau\to\infty}\int_{-\tau/2}^{\tau/2}\mathrm{e}^{-2\pi\mathrm{i}(\nu'-\nu)t}\,\mathrm{d}t = \frac{1}{\tau}\,\delta(\nu-\nu')\;,$$

with $\delta(x)$ the Dirac delta-function, so that (see Eq. (1.25))[1]

$$J_{ij}(r) = \frac{16\pi^4 e_0^2}{r^2c^4}\sum_{\alpha\beta} C_{\alpha i}^*\,C_{\beta j}\,\frac{A_\alpha^* A_\beta}{\tau}\int_{-\infty}^{\infty}\nu^4 F_\alpha(\nu)^*\,F_\beta(\nu)\,\mathrm{d}\nu\;. \tag{3.34}$$

The quantities A_α depend on the initial conditions for the motion of the oscillator. For random initial conditions (as one would have, for instance, if the oscillator were collisionally excited by a population of perturbing particles with isotropically distributed velocities), these quantities are uncorrelated with each other, so that, performing a statistical average over the initial conditions, we can replace $A_\alpha^* A_\beta$ by $\overline{|A|^2}\,\delta_{\alpha\beta}$. On the other hand, the quantity $\overline{|A|^2}$ is related to the average energy $\bar{E}$ contained in each of the three degrees of freedom of the oscillator. In fact, since

[1] Note that this formula contains the normalization time τ which is not related to any physical quantity. We will see shortly (Eq. (3.35)) how this quantity disappears from the final results.

for a classical oscillator the average kinetic energy is equal to the average potential energy, writing $A_\alpha = |A|\,\mathrm{e}^{\mathrm{i}\phi}$ we have from Eq. (3.28)

$$\bar{E} = 4\pi^2\nu_0^2\, m\, \overline{\left[\mathrm{Re}(x_\alpha)\right]^2} = 4\pi^2\nu_0^2\, m\, \overline{|A|^2 \cos^2[2\pi(\nu_0 - \alpha\nu_\mathrm{L})t - \phi]\,\mathrm{e}^{-\gamma t}}\ ,$$

and being the time interval τ much larger than the decay time γ^{-1} of the oscillator, we can write

$$\bar{E} = 4\pi^2\nu_0^2\, m\, \frac{1}{2}\,\overline{|A|^2}\,\frac{1}{\tau}\lim_{\tau\to\infty}\int_0^\tau \mathrm{e}^{-\gamma t}\,\mathrm{d}t = \frac{2\pi^2\nu_0^2\, m}{\gamma\tau}\,\overline{|A|^2}\ . \tag{3.35}$$

Let us now introduce the emission coefficient in tensorial form, $\varepsilon_{ij}(\nu, \vec{\Omega})$. Assuming N oscillators per unit volume, we have (see the analogous Eq. (1.31))

$$\Big[\int_{-\infty}^{\infty} \varepsilon_{ij}(\nu, \vec{\Omega})\,\mathrm{d}\nu\Big]\mathrm{d}t\,\mathrm{d}\Omega = \frac{c}{8\pi}\, J_{ij}(r)\, N\,\mathrm{d}t\, r^2\,\mathrm{d}\Omega\ , \tag{3.36}$$

and using Eqs. (3.34) and (3.35) we get

$$\varepsilon_{ij}(\nu, \vec{\Omega}) = \frac{\pi e_0^2}{mc^3}\,\nu_0^2\,\gamma\, N\bar{E}\sum_\alpha C^*_{\alpha i}\, C_{\alpha j}\,|F_\alpha(\nu)|^2\ ,$$

which via Eq. (3.33) can be written in the form

$$\varepsilon_{ij}(\nu, \vec{\Omega}) = \frac{\pi e_0^2}{mc}\, N\,\frac{\nu_0^2}{c^2}\,\bar{E}\sum_\alpha C^*_{\alpha i}\, C_{\alpha j}\,\frac{1}{\pi}\,\frac{\Gamma}{(\nu_0 - \alpha\nu_\mathrm{L} - \nu)^2 + \Gamma^2}\ . \tag{3.37}$$

From Eqs. (1.39), defining the profiles ϕ_b, ϕ_p, ϕ_r (normalized to 1 in frequency) as

$$\begin{aligned}
\phi_\mathrm{b} &= \frac{1}{\pi}\,\frac{\Gamma}{(\nu_0 + \nu_\mathrm{L} - \nu)^2 + \Gamma^2}\\
\phi_\mathrm{p} &= \frac{1}{\pi}\,\frac{\Gamma}{(\nu_0 - \nu)^2 + \Gamma^2}\\
\phi_\mathrm{r} &= \frac{1}{\pi}\,\frac{\Gamma}{(\nu_0 - \nu_\mathrm{L} - \nu)^2 + \Gamma^2}\ ,
\end{aligned} \tag{3.38}$$

and expressing the direction cosines for the geometry specified in Fig. 3.3,

$$\begin{aligned}
C_{\pm 1\,1} &= \frac{1}{\sqrt{2}}\,(\mp\cos\theta\,\cos\phi + \mathrm{i}\sin\theta\,\sin\phi)\\
C_{0\,1} &= -\sin\theta\\
C_{\pm 1\,2} &= \frac{1}{\sqrt{2}}\,(\pm\sin\phi + \mathrm{i}\cos\phi)\\
C_{0\,2} &= 0\ ,
\end{aligned} \tag{3.39}$$

we finally obtain the emission coefficient in the four Stokes parameters

$$\begin{aligned}
\varepsilon_I(\nu,\vec{\Omega}) &= \varepsilon_{11}(\nu,\vec{\Omega}) + \varepsilon_{22}(\nu,\vec{\Omega}) = k\,\frac{1}{2}\left[\phi_{\rm p}\sin^2\theta + \frac{\phi_{\rm b}+\phi_{\rm r}}{2}\,(1+\cos^2\theta)\right] \\
\varepsilon_Q(\nu,\vec{\Omega}) &= \varepsilon_{11}(\nu,\vec{\Omega}) - \varepsilon_{22}(\nu,\vec{\Omega}) = k\,\frac{1}{2}\left[\phi_{\rm p} - \frac{\phi_{\rm b}+\phi_{\rm r}}{2}\right]\sin^2\theta \\
\varepsilon_U(\nu,\vec{\Omega}) &= \varepsilon_{12}(\nu,\vec{\Omega}) + \varepsilon_{21}(\nu,\vec{\Omega}) = 0 \\
\varepsilon_V(\nu,\vec{\Omega}) &= {\rm i}\Big(\varepsilon_{12}(\nu,\vec{\Omega}) - \varepsilon_{21}(\nu,\vec{\Omega})\Big) = k\,\frac{1}{2}\left[\phi_{\rm r} - \phi_{\rm b}\right]\cos\theta\,,
\end{aligned} \tag{3.40}$$

where

$$k = \frac{\pi e_0^2}{mc}\,N\,\frac{2\nu_0^2}{c^2}\,\bar{E}\,.$$

These formulae show that our collection of randomly excited classical model atoms emits along $\vec{B}$ ($\theta = 0$) a radiation that is right-handed (or positively) circularly polarized around $\nu = (\nu_0 - \nu_{\rm L})$ (in the 'red' component $\sigma_{\rm r}$) and left-handed (or negatively) circularly polarized around $\nu = (\nu_0 + \nu_{\rm L})$ (in the 'blue' component $\sigma_{\rm b}$). Obviously, the handedness of circular polarization changes when the direction is reversed ($\theta = \pi$). For $\theta = \pi/2$, on the contrary, the emitted radiation is linearly polarized. The direction of linear polarization is parallel to the magnetic field in the π component and perpendicular to the magnetic field in the $\sigma_{\rm b}$ and $\sigma_{\rm r}$ components.

To sum up, we see that the classical theory provides a satisfactory explanation for the normal Zeeman effect with respect both to the wavelength separation of the Zeeman components and to their polarization characteristics. In the classical theory the frequency separation of the components is found to be $\nu_{\rm L}$, which corresponds to a Landé factor $g = 1$. This is quite obvious since g-values other than 1 are produced by the spin (see Eq. (3.7)), that cannot be accounted for by a classical theory.

We also want to remark that the results obtained for the polarization of the various components depend on the negative sign that we have assumed for the electric charge (see Eq. (3.23)). Assuming a positive charge for the electron, $\nu_{\rm L}$ has to be replaced by -$\nu_{\rm L}$ in Eqs. (3.27) and following, and a further sign change must be performed in Eq. (3.30). This last change is irrelevant, as the Stokes parameters are quadratic functions of the dipole components, so that the net result is the exchange of $\phi_{\rm r}$ and $\phi_{\rm b}$ in Eqs. (3.40), which leads to the opposite sign for $\varepsilon_V(\nu,\vec{\Omega})$. In other words, a sign inversion in the electron charge produces a sign inversion of circular polarization. This also means that by measuring the handedness of circular polarization in the various Zeeman components it is possible to determine the sign of the electron charge.

This was just the procedure followed by Lorentz and Zeeman to give, for the first time, the correct negative sign for the electron charge. It is curious to note, however, that at first they deduced the wrong sign: hence the witty remark by Segrè (1976) that 'when signs are involved, even two Dutch physicists as scrupulous as Lorentz and Zeeman may make errors'.

3.3. Classification of Zeeman Patterns

The first parameter that can be used to characterize Zeeman patterns is the so-called *effective Landé factor* $\bar{g}$,[1] which represents the wavelength shift from line center of the 'center of gravity' of the $\sigma_{\rm r}$ components in units of $\Delta\lambda_B$ (sometimes also called *Lorentz units*). For an electric-dipole transition connecting a given level, having angular momentum J_1 and Landé factor g_1, with another level of angular momentum J_2 and Landé factor g_2, the value of $\bar{g}$ can be easily derived from Eqs. (3.12) and (3.16)

$$\begin{aligned}\bar{g} &= \sum_{M_1 M_2} S_1^{J_1 J_2}(M_1, M_2)\left[\frac{\lambda_{M_1 M_2}^{J_1 J_2} - \lambda_0}{\Delta\lambda_B}\right] \\ &= \sum_{M_1 M_2} 3\begin{pmatrix} J_2 & J_1 & 1 \\ -M_2 & M_1 & -1 \end{pmatrix}^2 (g_1 M_1 - g_2 M_2)\,. \end{aligned} \tag{3.41}$$

This expression is valid both when the index 1 refers to the lower level and the index 2 to the upper level, and in the opposite case. This is a consequence of the symmetry properties discussed at the end of Sect. 3.1, and reflects the fact that Zeeman patterns depend only on the quantum numbers of the levels involved in the transition, and not on which of them is the lower or the upper.

Obviously, because of the symmetry properties just mentioned (Eqs. (3.18)-(3.22)), the center of gravity of the $\sigma_{\rm b}$ components is -$\bar{g}$, while the center of gravity of the π components is 0.

Equation (3.41) can be transformed into a simpler expression by means of some Racah algebra. First we note that, with the help of Eq. (2.26d), we can write for M_1 and M_2

$$M_1 = \sqrt{J_1(J_1+1)(2J_1+1)}\,(-1)^{J_1 - M_1}\begin{pmatrix} J_1 & J_1 & 1 \\ M_1 & -M_1 & 0 \end{pmatrix} \tag{3.42a}$$

$$M_2 = \sqrt{J_2(J_2+1)(2J_2+1)}\,(-1)^{J_2 - M_2}\begin{pmatrix} J_2 & J_2 & 1 \\ M_2 & -M_2 & 0 \end{pmatrix}\,. \tag{3.42b}$$

Next we observe that the term originating from M_1 in Eq. (3.41) can be written, using Eq. (2.42), in the form

$$\begin{aligned}&\sum_{M_1 M_2}\begin{pmatrix} J_2 & J_1 & 1 \\ -M_2 & M_1 & -1 \end{pmatrix}^2 (-1)^{J_1 - M_1}\begin{pmatrix} J_1 & J_1 & 1 \\ M_1 & -M_1 & 0 \end{pmatrix} = \\ &= \sum_{M_1 M_1' M_2} (-1)^{J_1 - M_1}\begin{pmatrix} J_1 & J_1 & 1 \\ M_1 & -M_1' & 0 \end{pmatrix}\begin{pmatrix} J_2 & J_1 & 1 \\ -M_2 & M_1 & -1 \end{pmatrix} \\ &\qquad \times \begin{pmatrix} J_2 & J_1 & 1 \\ -M_2 & M_1' & -1 \end{pmatrix} = \end{aligned}$$

[1] The quantity $\bar{g}$ is often denoted by the symbol z in the literature concerning magnetic stars.

$$= (-1)^{1+J_1+J_2} \begin{pmatrix} 1 & 1 & 1 \\ -1 & 1 & 0 \end{pmatrix} \begin{Bmatrix} 1 & 1 & 1 \\ J_1 & J_1 & J_2 \end{Bmatrix} . \tag{3.43}$$

Performing the same transformation on the other term of Eq. (3.41), and taking into account the analytical expressions of the 3-j and 6-j symbols (Eqs. (2.26d) and (2.36d)), we obtain

$$\bar{g} = \frac{1}{2}(g_1 + g_2) + \frac{1}{4}(g_1 - g_2)\, d , \tag{3.44}$$

where

$$d = J_1(J_1 + 1) - J_2(J_2 + 1) .$$

Note that this formula, originally due to Shenstone and Blair (1929), is invariant under interchange of the indices 1 and 2. In most cases, Eq. (3.44) is employed together with the Landé factors obtained from the L-S coupling scheme (Eq. (3.8)). The resulting $\bar{g}$-value, that will be denoted in the following by $\bar{g}_{LS}$, can be easily calculated for any given electric-dipole transition (see e.g. Beckers, 1969b). A more appropriate value for $\bar{g}$ can be obtained by substituting in Eq. (3.44) the values g_1 and g_2 deduced by spectroscopic measurements. In some cases, and especially for lines belonging to complex spectra and involving levels of high excitation potential, the L-S coupling scheme fails, so that the value $\bar{g}_{LS}$ may be very different from $\bar{g}$. Comparisons between $\bar{g}$ and $\bar{g}_{LS}$ values for several lines of the FeI and FeII spectra have been published by Landi Degl'Innocenti (1982a) and by Solanki and Stenflo (1985).

Typical $\bar{g}$ values range from 0.5 to 2.5, but, for some transitions, $\bar{g}$ can attain null or even negative values, while for other transitions it can be larger than 2.5. A list of transitions characterized by such 'anomalous' values of the effective Landé factor is presented in Table 3.2. The list includes all the transitions between L-S levels having $S \leq 7/2$ and $L \leq 5$, and subjected to the following limitations

$$\Delta J = 0, \pm 1 , \qquad \Delta S = 0, \pm 1 , \qquad \Delta L = 0, \pm 1, \pm 2 .$$

Lines having either exceptionally large values or null values for their effective Landé factor are of great importance for the study of solar (and stellar) magnetism. Obviously, lines with large $\bar{g}$ values produce strong polarization signals, and are particularly useful for the detection and measurement of magnetic fields. On the other hand, lines with $\bar{g} = 0$ are especially useful for velocity measurements and for calibration. A reduced list of lines with large $\bar{g}$-values has been given by Harvey (1973), while Sistla and Harvey (1970) have presented a list of $\bar{g} = 0$ lines. A table of close line pairs (less than 100 Å apart), with one line having a large $\bar{g}$ value and the other a small (or null) $\bar{g}$ value, has been presented by Robinson (1980).

In some studies of stellar magnetism, it can be useful to compute an average value for the effective Landé factor over the lines contained in a given statistical sample or in an assigned spectral interval. For instance, considering the sample of approximately 400 unblended lines of the FeI solar spectrum given by Stenflo and Lindegren (1977), if the effective Landé factor of each line is weighted by the

TABLE 3.2

Transitions having 'anomalous' values for the effective Landé factor $\bar{g}_{LS}$. The transitions listed are those obeying the restrictions specified in the text.

Transition	$\bar{g}_{LS}$	Transition	$\bar{g}_{LS}$	Transition	$\bar{g}_{LS}$
		$\bar{g}_{LS} < 0$			
$^4P_{\frac{1}{2}} - {}^4F_{\frac{3}{2}}$	−0.167	$^8D_{\frac{3}{2}} - {}^6G_{\frac{5}{2}}$	−0.6	$^8F_{\frac{1}{2}} - {}^6G_{\frac{3}{2}}$	−1.
$^5P_1 - {}^3F_2$	−0.25	$^5F_1 - {}^7G_1$	−0.25	$^8F_{\frac{1}{2}} - {}^8H_{\frac{3}{2}}$	−1.5
$^4D_{\frac{1}{2}} - {}^6F_{\frac{1}{2}}$	−0.333	$^6F_{\frac{1}{2}} - {}^6F_{\frac{1}{2}}$	−0.667	$^8F_{\frac{3}{2}} - {}^6H_{\frac{5}{2}}$	−1.
$^5D_0 - {}^7G_1$	−0.5	$^6F_{\frac{1}{2}} - {}^8G_{\frac{1}{2}}$	−1.	$^8F_{\frac{3}{2}} - {}^8H_{\frac{5}{2}}$	−0.3
$^5D_1 - {}^5G_2$	−0.25	$^6F_{\frac{1}{2}} - {}^8H_{\frac{3}{2}}$	−0.333	$^8F_{\frac{5}{2}} - {}^6H_{\frac{7}{2}}$	−0.286
$^6D_{\frac{1}{2}} - {}^4F_{\frac{3}{2}}$	−0.333	$^6F_{\frac{3}{2}} - {}^6H_{\frac{5}{2}}$	−0.3	$^6G_{\frac{3}{2}} - {}^8H_{\frac{3}{2}}$	−0.2
$^6D_{\frac{1}{2}} - {}^6G_{\frac{3}{2}}$	−0.833	$^6F_{\frac{5}{2}} - {}^4H_{\frac{7}{2}}$	−0.143	$^7G_1 - {}^7G_1$	−0.5
$^6D_{\frac{3}{2}} - {}^4G_{\frac{5}{2}}$	−0.4	$^7F_0 - {}^7G_1$	−0.5	$^8G_{\frac{1}{2}} - {}^8G_{\frac{1}{2}}$	−1.333
$^7D_1 - {}^5G_2$	−1.	$^7F_1 - {}^5G_2$	−0.25	$^8G_{\frac{1}{2}} - {}^8H_{\frac{3}{2}}$	−0.167
$^7D_1 - {}^7G_2$	−0.25	$^7F_1 - {}^7H_2$	−0.75	$^8G_{\frac{3}{2}} - {}^6H_{\frac{5}{2}}$	−0.2
$^7D_2 - {}^5G_3$	−0.167	$^7F_2 - {}^5H_3$	−0.5	$^8H_{\frac{3}{2}} - {}^8H_{\frac{3}{2}}$	−0.4
		$\bar{g}_{LS} = 0$			
$^3P_0 - {}^5F_1$		$^7D_1 - {}^5F_2$		$^7F_2 - {}^7H_3$	
$^6P_{\frac{3}{2}} - {}^4F_{\frac{5}{2}}$		$^8D_{\frac{5}{2}} - {}^6G_{\frac{7}{2}}$		$^7F_3 - {}^5H_4$	
$^4D_{\frac{1}{2}} - {}^4D_{\frac{1}{2}}$		$^5F_1 - {}^5F_1$		$^8F_{\frac{3}{2}} - {}^6G_{\frac{5}{2}}$	
$^4D_{\frac{1}{2}} - {}^6G_{\frac{3}{2}}$		$^5F_1 - {}^7F_0$		$^6G_{\frac{3}{2}} - {}^6G_{\frac{3}{2}}$	
$^5D_0 - {}^5F_1$		$^5F_1 - {}^7H_2$		$^7H_2 - {}^7H_2$	
$^5D_2 - {}^3G_3$		$^5F_2 - {}^5H_3$			
		$\bar{g}_{LS} \geq 3$			
$^4P_{\frac{1}{2}} - {}^6D_{\frac{1}{2}}$	3.	$^6D_{\frac{1}{2}} - {}^8F_{\frac{1}{2}}$	3.667	$^8D_{\frac{5}{2}} - {}^6G_{\frac{3}{2}}$	3.6
$^6P_{\frac{3}{2}} - {}^4D_{\frac{1}{2}}$	3.	$^7D_1 - {}^7D_1$	3.	$^8D_{\frac{7}{2}} - {}^6G_{\frac{5}{2}}$	3.
$^6P_{\frac{3}{2}} - {}^6F_{\frac{1}{2}}$	3.167	$^7D_1 - {}^7F_0$	3.	$^7F_3 - {}^7H_2$	3.
$^6P_{\frac{5}{2}} - {}^4F_{\frac{3}{2}}$	3.	$^7D_2 - {}^5F_1$	3.	$^7F_4 - {}^5H_3$	3.
$^7P_2 - {}^5F_1$	3.5	$^7D_2 - {}^7G_1$	3.25	$^8F_{\frac{1}{2}} - {}^8F_{\frac{1}{2}}$	4.
$^8P_{\frac{5}{2}} - {}^6F_{\frac{3}{2}}$	3.2	$^7D_3 - {}^5G_2$	3.167	$^8F_{\frac{5}{2}} - {}^6G_{\frac{3}{2}}$	3.
$^5D_0 - {}^7D_1$	3.	$^8D_{\frac{3}{2}} - {}^6F_{\frac{1}{2}}$	3.667	$^8F_{\frac{5}{2}} - {}^8H_{\frac{3}{2}}$	3.3
$^6D_{\frac{1}{2}} - {}^6D_{\frac{1}{2}}$	3.333	$^8D_{\frac{3}{2}} - {}^8G_{\frac{1}{2}}$	3.833	$^8F_{\frac{7}{2}} - {}^6H_{\frac{5}{2}}$	3.286

central depression observed for the same line, one finds the value $\langle \bar{g}_{LS} \rangle = 1.22$ (Landi Degl'Innocenti, 1985a).[1]

Besides the effective Landé factor, higher order moments can be introduced to characterize Zeeman patterns. For each type of component we define the *barycentric n-th order moment* $v_q^{(n)}$ to be

$$v_q^{(n)}(J_1, J_2) = \sum_{M_1 M_2} S_q^{J_1 J_2}(M_1, M_2) \left[\Delta\lambda_{M_1 M_2}^{J_1 J_2} - q\, \bar{g}\, \Delta\lambda_B \right]^n , \tag{3.45}$$

where $\Delta\lambda_{M_1 M_2}^{J_1 J_2}$ and $S_q^{J_1 J_2}(M_1, M_2)$ are defined in Eqs. (3.20) and (3.16), and where $q = -1, 0, +1$ for the $\sigma_{\rm b}$, π, and $\sigma_{\rm r}$ components, respectively.

Using the symmetry properties derived in Sect. 3.1 (Eqs. (3.18)-(3.22)), and recalling that $\bar{g}$ is invariant under interchange of J_1 and J_2, one easily gets

$$v_q^{(n)}(J_2, J_1) = v_q^{(n)}(J_1, J_2) \tag{3.46}$$

$$v_{-q}^{(n)}(J_1, J_2) = (-1)^n\, v_q^{(n)}(J_1, J_2) . \tag{3.47}$$

Equation (3.46) shows that the various moments are not altered by the interchange of the lower and the upper level – an obvious consequence of the same property holding for the Zeeman patterns. Equation (3.47) shows that the odd-order moments of the π components identically vanish, while, for the σ components, the even-order moments of the $\sigma_{\rm b}$ and $\sigma_{\rm r}$ components are the same, and the odd-order moments have opposite sign. Obviously, all the even-order moments are positive quantities.

We will now show that the barycentric moments defined in Eq. (3.45) can be reduced to a simple form which contains 3-j and 6-j symbols only. Substitution of Eqs. (3.20) and (3.44) into Eq. (3.45) leads after some algebra to the expression

$$v_q^{(n)}(J_1, J_2) = \Delta\lambda_B^n\, (g_1 - g_2)^n\, X_q^{(n)}(J_1, J_2) , \tag{3.48}$$

with

$$\begin{aligned} X_q^{(n)}(J_1, J_2) &= \sum_{M_1 M_2} \left[M_1 - \frac{d+2}{4}\, q \right]^n S_q^{J_1 J_2}(M_1, M_2) \\ &= \sum_{i=0}^{n} (-1)^{n-i} \binom{n}{i} \left(\frac{d+2}{4}\, q \right)^{n-i} Z_q^{(i)}(J_1, J_2) , \end{aligned} \tag{3.49}$$

where $Z_q^{(i)}(J_1, J_2)$ is the i-th moment of M_1 weighted by the strength of the q-transition originating from M_1,

$$Z_q^{(i)}(J_1, J_2) = \sum_{M_1 M_2} M_1^i\, S_q^{J_1 J_2}(M_1, M_2) . \tag{3.50}$$

[1] Owing both to the L-S assumption and to the procedure itself by which it is obtained, this value has only an approximate and statistical meaning.

The quantities $Z_q^{(i)}(J_1, J_2)$ can be evaluated by some Racah algebra. For this purpose we note that the α-component of an angular momentum a can be written in the form (see Eqs. (3.42))

$$\alpha = (-1)^{a-\alpha}\sqrt{a(a+1)(2a+1)}\begin{pmatrix} a & a & 1 \\ \alpha & -\alpha & 0 \end{pmatrix} . \tag{3.51}$$

Squaring this equation we get

$$\alpha^2 = \big[a(a+1)(2a+1)\big]\begin{pmatrix} a & a & 1 \\ \alpha & -\alpha & 0 \end{pmatrix}\begin{pmatrix} a & a & 1 \\ \alpha & -\alpha & 0 \end{pmatrix} ,$$

or, with the help of Eq. (2.43)

$$\alpha^2 = (-1)^{a+\alpha}\big[a(a+1)(2a+1)\big] \times \sum_f (2f+1)\begin{Bmatrix} 1 & 1 & f \\ a & a & a \end{Bmatrix}\begin{pmatrix} 1 & 1 & f \\ 0 & 0 & 0 \end{pmatrix}\begin{pmatrix} a & a & f \\ \alpha & -\alpha & 0 \end{pmatrix} , \tag{3.52}$$

where the sum over f runs over the values 0 and 2 only (for $f = 1$ the first 3-j symbol in the right-hand side is zero).

Repeated application of the same procedure gives the following remarkable formula

$$\begin{aligned}\alpha^n = (-1)^{(2n-3)a+\alpha}\ &\big[a(a+1)(2a+1)\big]^{n/2} \\ &\times \sum_{f_1 f_2 \cdots f_{n-1}} (2f_1+1)(2f_2+1)\cdots(2f_{n-1}+1) \\ &\times \begin{Bmatrix} 1 & 1 & f_1 \\ a & a & a \end{Bmatrix}\begin{Bmatrix} 1 & f_1 & f_2 \\ a & a & a \end{Bmatrix}\cdots\begin{Bmatrix} 1 & f_{n-2} & f_{n-1} \\ a & a & a \end{Bmatrix} \\ &\times \begin{pmatrix} 1 & 1 & f_1 \\ 0 & 0 & 0 \end{pmatrix}\begin{pmatrix} 1 & f_1 & f_2 \\ 0 & 0 & 0 \end{pmatrix}\cdots\begin{pmatrix} 1 & f_{n-2} & f_{n-1} \\ 0 & 0 & 0 \end{pmatrix} \\ &\times \begin{pmatrix} a & a & f_{n-1} \\ \alpha & -\alpha & 0 \end{pmatrix} \qquad (n = 2, 3, \ldots) .\end{aligned}$$

Owing to the property (2.24) of the 3-j symbols, the indices f_1, f_2,... are alternately even and odd numbers. Moreover, they are chained in such a way that the allowed values for f_{i+1} are $(f_i \pm 1)$, starting from $f_1 = 0$ and $f_1 = 2$. For example, if $n = 4$ the chains of allowed values for f_1, f_2, and f_3 are: (0,1,0), (0,1,2), (2,1,0), (2,1,2), (2,3,2), $(2, 3, 4)$.

We now use the above expansion to express the quantity M_1^i in Eq. (3.50), and substitute the explicit expression for the strengths given by Eq. (3.16). Performing

the sum over M_1 and M_2 by the same method that leads to Eq. (3.43), we obtain, for $i \geq 2$

$$
\begin{aligned}
&Z_q^{(i)}(J_1, J_2) = \\
&= (-1)^{(2i-3)J_1 - J_2 + q}\, 3\big[J_1(J_1+1)(2J_1+1)\big]^{i/2} \\
&\quad \times \sum_{f_1 f_2 \cdots f_{i-1}} (2f_1+1)(2f_2+1)\cdots(2f_{i-1}+1) \\
&\qquad \times \begin{Bmatrix} 1 & 1 & f_1 \\ J_1 & J_1 & J_1 \end{Bmatrix} \begin{Bmatrix} 1 & f_1 & f_2 \\ J_1 & J_1 & J_1 \end{Bmatrix} \cdots \begin{Bmatrix} 1 & f_{i-2} & f_{i-1} \\ J_1 & J_1 & J_1 \end{Bmatrix} \\
&\qquad \times \begin{pmatrix} 1 & 1 & f_1 \\ 0 & 0 & 0 \end{pmatrix} \begin{pmatrix} 1 & f_1 & f_2 \\ 0 & 0 & 0 \end{pmatrix} \cdots \begin{pmatrix} 1 & f_{i-2} & f_{i-1} \\ 0 & 0 & 0 \end{pmatrix} \\
&\qquad \times \begin{pmatrix} 1 & 1 & f_{i-1} \\ -q & q & 0 \end{pmatrix} \begin{Bmatrix} 1 & 1 & f_{i-1} \\ J_1 & J_1 & J_2 \end{Bmatrix} ,
\end{aligned}
$$

while for $i = 0$ and $i = 1$ we have

$$
\begin{aligned}
Z_q^{(0)}(J_1, J_2) &= 1 \\
Z_q^{(1)}(J_1, J_2) &= (-1)^{J_1 + J_2 + q}\, 3\sqrt{J_1(J_1+1)(2J_1+1)} \\
&\qquad \times \begin{pmatrix} 1 & 1 & 1 \\ -q & q & 0 \end{pmatrix} \begin{Bmatrix} 1 & 1 & 1 \\ J_1 & J_1 & J_2 \end{Bmatrix} .
\end{aligned}
$$

These formulae, together with Eqs. (3.49) and (3.48), give the required expressions for the barycentric moments. Using Eqs. (2.26) and (2.36) one can indeed obtain simple analytical formulae for the low-order moments. The results, that are contained in Table 3.3, show the characteristic symmetrical behavior of the quantities $X_q^{(n)}(J_1, J_2)$ under interchange of J_1 with J_2 and of q with $-q$.

Besides the barycentric moments of the components, it is also convenient to introduce the *moments* tout court. These moments are defined by

$$
w_q^{(n)}(J_1, J_2) = \sum_{M_1 M_2} S_q^{J_1 J_2}(M_1, M_2) \left[\Delta\lambda_{M_1 M_2}^{J_1 J_2}\right]^n , \tag{3.53}
$$

and it can be easily seen that they satisfy the same symmetry properties found for the barycentric moments (Eqs. (3.46) and (3.47)).

The relations between the two types of moments are the following

$$
\begin{aligned}
v_q^{(n)}(J_1, J_2) &= \sum_{i=0}^{n} (-1)^{n-i} \binom{n}{i} w_q^{(i)}(J_1, J_2) \left[q\, \bar{g}\, \Delta\lambda_B\right]^{n-i} \\
w_q^{(n)}(J_1, J_2) &= \sum_{i=0}^{n} \binom{n}{i} v_q^{(i)}(J_1, J_2) \left[q\, \bar{g}\, \Delta\lambda_B\right]^{n-i} .
\end{aligned}
$$

TABLE 3.3

Analytical expressions for the low-order barycentric moments of Zeeman components.(*) The expressions have been simplified taking into account that, for electric dipole transitions, the quantity $[d(2s - d^2)]$ is identically zero.

$Z_q^{(0)} = 1$	$X_q^{(0)} = 1$
$Z_0^{(1)} = 0$	$X_0^{(1)} = 0$
$Z_{\pm1}^{(1)} = \pm\,\frac{1}{4}\,(d+2)$	$X_{\pm1}^{(1)} = 0$
$Z_0^{(2)} = \frac{1}{10}\,(-d^2+3s-2)$	$X_0^{(2)} = \frac{1}{10}\,(-d^2+3s-2)$
$Z_{\pm1}^{(2)} = \frac{1}{20}\,(d^2+5d+2s+2)$	$X_{\pm1}^{(2)} = \frac{1}{80}\,(-d^2+8s-12)$
$Z_0^{(3)} = 0$	$X_0^{(3)} = 0$
$Z_{\pm1}^{(3)} = \pm\,\frac{1}{80}\,(3d^3+6d^2+12s+8d-8)$	$X_{\pm1}^{(3)} = \pm\,\frac{1}{160}\,d(4-d^2)$
$Z_0^{(4)} = \frac{1}{140}\,(-3d^4+7d^2+15s^2-30s+20)$	$X_0^{(4)} = \frac{1}{140}\,(-3d^4+7d^2+15s^2-30s+20)$
$Z_{\pm1}^{(4)} = \frac{1}{280}\,(3d^4+21d^3+14d^2+6s^2+16s$ $-14d-20)$	$X_{\pm1}^{(4)} = \frac{1}{8960}\,(-9d^4+56d^2+192s^2-832s$ $+816)$

(*) $s = [J_1(J_1+1) + J_2(J_2+1)]\,,\; d = [J_1(J_1+1) - J_2(J_2+1)]$

After some algebraic manipulations, $w_q^{(n)}$ can be expressed in the form

$$w_q^{(n)}(J_1, J_2) = \Delta\lambda_B^n\, G_q^{(n)}(J_1, J_2)\;, \tag{3.54}$$

where

$$G_q^{(n)}(J_1, J_2) = \sum_{i=0}^{n} \binom{n}{i} (g_1 - g_2)^i\, (g_2\, q)^{n-i}\, Z_q^{(i)}(J_1, J_2)\;. \tag{3.55}$$

Analytical formulae for the quantities $G_q^{(n)}(J_1, J_2)$ up to $n = 4$ are contained in Table 3.4.

An alternative derivation of the quantities $v_q^{(n)}$ and $w_q^{(n)}$ in terms of Bernoulli polynomials has been given by Mathys and Stenflo (1987a,b), who employ the notations $\mu_q^{(n)}$ and $n!\,(-\Delta\lambda_B)^n C_n^{(q)}$, respectively. In their second paper (1987b), these authors give also extensive numerical tables for $\mu_q^{(n)}$ and $C_n^{(q)}$; these last quantities are however evaluated, for any given transition, by assuming for the Landé factors the values deduced from the L-S coupling scheme.

Zeeman patterns can be classified into four different types according to the value of their barycentric moments, with particular emphasis on the third-order moment $v_1^{(3)}$.

First of all, we will call *Type 0* the normal and anomalous Zeeman triplets (see Sect. 3.1): obviously, these patterns are characterized by $v_q^{(n)} = 0$ for $n \geq 1$. A complete list of transitions giving rise to Type 0 patterns has been published by Mathys and Stenflo (1987b).

TABLE 3.4

Analytical expressions for the low-order moments of Zeeman components [*]

$$G_q^{(0)} = 1$$

$$G_0^{(1)} = 0$$

$$G_{\pm 1}^{(1)} = \pm\,(\tfrac{1}{2} g_s + \tfrac{1}{4} d g_d) = \pm\,\bar{g}$$

$$G_0^{(2)} = \tfrac{1}{10}\,(3s - d^2 - 2) g_d^2$$

$$G_{\pm 1}^{(2)} = \tfrac{1}{20}\left[(d^2 + 2s - 3) g_d^2 + 5 d g_s g_d + 5 g_s^2\right]$$

$$G_0^{(3)} = 0$$

$$G_{\pm 1}^{(3)} = \pm\,\tfrac{1}{80}\left[(3d^2 - 7) d g_d^3 + 6(d^2 + 2s - 3) g_d^2 g_s + 15 d g_d g_s^2 + 10 g_s^3\right]$$

$$G_0^{(4)} = \tfrac{1}{140}\,(-3d^4 + 7d^2 + 15 s^2 - 30 s + 20) g_d^4$$

$$G_{\pm 1}^{(4)} = \tfrac{1}{560}\left[(6d^4 - 14 d^2 + 12 s^2 - 52 s + 51) g_d^4 + 14(3d^2 - 7) d g_d^3 g_s + 42(d^2 + 2s - 3) g_d^2 g_s^2 + 70 d g_d g_s^3 + 35 g_s^4\right]$$

[*] $s = [J_1(J_1+1) + J_2(J_2+1)]$, $d = [J_1(J_1+1) - J_2(J_2+1)]$, $g_s = (g_1 + g_2)$, $g_d = (g_1 - g_2)$

For anomalous Zeeman patterns, we will call, following Back and Landé (1925), *Type I* those having $v_1^{(3)} > 0$, *Type II* those having $v_1^{(3)} < 0$, and *Type III* those with $v_1^{(3)} = 0$. As it can be argued from the definition of the barycentric moments (Eq. (3.45)), patterns of Type I have their strongest $\sigma_{\rm r}$ component toward the blue side of the spectrum, while patterns of Type II have their strongest $\sigma_{\rm r}$ component toward the red side of the spectrum. Finally, Type III patterns have σ components symmetrical about their center of gravity. Some examples of Zeeman patterns of different types are shown in Fig. 3.2.

From the analytical expressions given in Table 3.3 and from Eq. (3.48) we have

$$v_1^{(3)} = \frac{1}{160}\,\Delta\lambda_B^3\,(g_1 - g_2)^3\,d\,(4 - d^2)\,.$$

This formula shows that Type III patterns can only originate when $d = 0$, or, in other words, when $J_1 = J_2$. By contrast, Type I and Type II patterns correspond to transitions having $\Delta J = \pm 1$. In particular, Type I patterns arise when the Landé factor of the level having the smaller J is larger than the Landé factor of the level having the larger J, while the opposite situation leads to Type II patterns.

It should be remarked that the classification of Zeeman patterns, although based on the σ components, characterizes at the same time the behavior of the π components. Indeed, with increasing distance from line center the strengths of the π components decrease (quadratically) for Type I and Type II patterns, while they increase (also quadratically) for Type III patterns. This is apparent from Table 3.1 and Eq. (3.20).

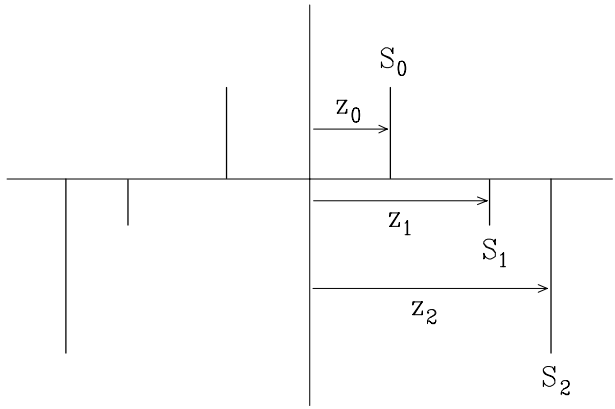

Fig.3.4. Definition of the minimal equivalent Zeeman pattern.

It should also be mentioned that a useful concept for certain applications is that of *minimal equivalent Zeeman pattern*. Given an arbitrary Zeeman pattern, we define its minimal equivalent as the pattern having only two π components and two σ components (both for the blue and the red wing) with such splittings and strengths that the barycentric moments up to $n = 3$ of the original pattern are reproduced. The minimal equivalent Zeeman pattern is sketched in Fig. 3.4. It can be shown that the strengths S_i and the splittings z_i (expressed in units of $\Delta\lambda_B$, and satisfying the condition $z_2 > z_1$) are given by

$$
\begin{aligned}
z_0 &= |g_d| \sqrt{X_0^{(2)}} & S_0 &= \frac{1}{2} \\
z_1 &= \bar{g} - \frac{1}{2} |g_d| \sqrt{X_1^{(2)}} \left[\sqrt{4 + z^2} - z \right] & S_1 &= \frac{1}{2} \left[1 + \frac{z}{\sqrt{4 + z^2}} \right] \\
z_2 &= \bar{g} + \frac{1}{2} |g_d| \sqrt{X_1^{(2)}} \left[\sqrt{4 + z^2} + z \right] & S_2 &= \frac{1}{2} \left[1 - \frac{z}{\sqrt{4 + z^2}} \right] ,
\end{aligned}
$$

where

$$
z = \frac{g_d}{|g_d|} \frac{X_1^{(3)}}{\left[X_1^{(2)} \right]^{3/2}} .
$$

Note that the value of z remains undefined when $X_1^{(2)} = 0$; this is a degenerate case corresponding either to a Zeeman triplet (Type 0 pattern) or to the transition $1/2 \rightarrow 1/2$. In both cases the two σ components merge into a single one with $z_1 = z_2 = \bar{g}$, $(S_1 + S_2) = 1$.

3.4. The Paschen-Back Effect

As already stated in Sect. 3.1, when the magnetic field is so strong as to produce on a J-level a splitting comparable with the energy separation between different

J-levels, the perturbation theory presented for the Zeeman effect cannot be applied any longer. In this regime, that is called the *Paschen-Back effect regime*, the energy levels have to be found by diagonalization of the total Hamiltonian H given by

$$H = H_0 + H_B \ ,$$

where H_0 and H_B are the unperturbed and magnetic Hamiltonians, respectively, with H_B given by Eq. (3.3).

The diagonalization of the Hamiltonian H can be performed on the basis of the eigenvectors $|\alpha JM\rangle$ of H_0 (see Eqs. (3.4)). This implies the evaluation of matrix elements of the form

$$\langle \alpha JM|H_B|\alpha' J'M'\rangle = \mu_0 \langle \alpha JM|(\vec{L} + 2\vec{S}\,) \cdot \vec{B}\,|\alpha' J'M'\rangle \ .$$

A calculation similar to that of Sect. 3.1 leads to the expression

$$\begin{aligned}\langle \alpha JM|H_B|\alpha' J'M'\rangle = \mu_0 B \sum_q (-1)^{J'+M+q+1}\sqrt{2J+1}\begin{pmatrix} J & J' & 1 \\ -M & M' & q \end{pmatrix} \\ \times \left[\sqrt{J(J+1)}\,\delta_{\alpha\alpha'}\,\delta_{JJ'} + \langle \alpha J\|\vec{S}\,\|\alpha' J'\rangle\right] b_{-q} \ ,\end{aligned}$$

and, in particular, when the quantization axis for $\vec{J}$ is in the magnetic field direction

$$\begin{aligned}&\langle \alpha JM|H_B|\alpha' J'M'\rangle = \\ &= \mu_0 B\Big[M\,\delta_{\alpha\alpha'}\,\delta_{JJ'} \\ &\qquad + (-1)^{J'+M+1}\sqrt{2J+1}\begin{pmatrix} J & J' & 1 \\ -M & M & 0 \end{pmatrix}\langle \alpha J\|\vec{S}\,\|\alpha' J'\rangle\Big]\,\delta_{MM'} \ . \qquad (3.56)\end{aligned}$$

Equation (3.56) shows that the magnetic Hamiltonian H_B connects only eigenstates having the same value of the magnetic quantum number M: in other words, it is block-diagonal, each block being characterized by an assigned M-value.

The general problem of finding the eigenvalues and the eigenvectors of the matrix H can be solved only by numerical methods. There are, however, some special cases where the analytical calculations can be pushed somewhat further. If we suppose, for instance, that the atomic system is exactly described by the L-S coupling scheme, the eigenstates of H_0 are of the form $|\beta LSJM\rangle$ (where β summarizes the electronic configuration quantum numbers), so that Eq. (3.56) becomes

$$\begin{aligned}&\langle \beta LSJM|H_B|\beta' L'S'J'M'\rangle = \\ &= \mu_0 B\Big[M\,\delta_{\beta\beta'}\,\delta_{LL'}\,\delta_{SS'}\,\delta_{JJ'} \\ &\qquad + (-1)^{J'+M+1}\sqrt{2J+1}\begin{pmatrix} J & J' & 1 \\ -M & M & 0 \end{pmatrix}\langle \beta LSJ\|\vec{S}\,\|\beta' L'S'J'\rangle\Big]\,\delta_{MM'} \ ,\end{aligned}$$

and using Eqs. (2.109) and (2.97)

$$\langle \beta LSJM|H_B|\beta' L'S'J'M'\rangle = \mu_0 B\, \delta_{\beta\beta'}\, \delta_{LL'}\, \delta_{SS'}\, \delta_{MM'}$$
$$\times \Bigg[M\, \delta_{JJ'} + (-1)^{J+J'+L+S+M} \sqrt{(2J+1)(2J'+1)S(S+1)(2S+1)}$$
$$\times \begin{pmatrix} J & J' & 1 \\ -M & M & 0 \end{pmatrix} \begin{Bmatrix} J & J' & 1 \\ S & S & L \end{Bmatrix} \Bigg] . \tag{3.57}$$

From this expression we obtain the important result that in the L-S coupling scheme the magnetic Hamiltonian is block-diagonal, each block being now characterized by the magnetic quantum number M *and* by the quantum numbers (β, L, S) specifying the term. In other words, the magnetic field produces a J-mixing of the various levels belonging to a particular term, so that the eigenvectors of the total Hamiltonian will be of the form

$$|\beta LSjM\rangle = \sum_J C_J^j(\beta LS, M)\, |\beta LSJM\rangle \ , \tag{3.58}$$

where the index j labels the different states of the N-fold degenerate subspace corresponding to assigned values of (β, L, S, M); N is given by

$$N = 1 + L + S - \max(|M|, |L - S|) \ .$$

Of course, in contrast with the Zeeman effect regime, J is not a good quantum number.

We now recall that in the L-S coupling scheme the energies $E_{\beta LS}(J)$ of the different J-levels originating from a given term (β, L, S) are determined by the spin-orbit Hamiltonian $H_{\rm so}$ (included in H_0), which in most cases can be written in the form (see Condon and Shortley, 1935)

$$H_{\rm so} = \zeta(\beta LS)\, \vec{L} \cdot \vec{S} \ , \tag{3.59}$$

where ζ is a constant having the dimensions of energy. Writing $\vec{L} \cdot \vec{S}$ in the form

$$\vec{L} \cdot \vec{S} = \frac{1}{2} \left[J^2 - L^2 - S^2 \right] \ ,$$

we have[1]

$$E_{\beta LS}(J) = \langle \beta LSJM|H_{\rm so}|\beta LSJM\rangle$$
$$= \frac{1}{2}\, \zeta(\beta LS) \left[J(J+1) - L(L+1) - S(S+1) \right] . \tag{3.60}$$

[1] Note in passing that the energy difference between two adjacent J-levels is given by

$$E_{\beta LS}(J) - E_{\beta LS}(J-1) = \zeta(\beta LS)\, J \ ,$$

which is the well-known *Landé interval rule*.

Thus the whole problem of finding the energy levels of an atom described by the L-S coupling scheme, embedded in a magnetic field, reduces to the diagonalization of a set of matrices of the form

$$\langle \beta LSJM | H_{\rm so} + H_B | \beta LSJ'M \rangle \ .$$

From Eq. (3.57), using the analytical expressions of the 3-j and 6-j symbols (Eqs. (2.26) and (2.36)), we have that the only non-zero matrix elements are those of the form

$$\langle \beta LSJM | H_{\rm so} + H_B | \beta LSJM \rangle = E_{\beta LS}(J) + \mu_0 B \, g_{LS}(J) \, M \tag{3.61a}$$

$$\langle \beta LS\ J{-}1\ M | H_{\rm so} + H_B | \beta LSJM \rangle = \langle \beta LSJM | H_{\rm so} + H_B | \beta LS\ J{-}1\ M \rangle$$

$$= -\frac{\mu_0 B}{2J} \sqrt{\frac{(J{+}S{+}L{+}1)(J{-}S{+}L)(J{+}S{-}L)(-J{+}S{+}L{+}1)(J^2{-}M^2)}{(2J{+}1)(2J{-}1)}} \ , \tag{3.61b}$$

where $g_{LS}(J)$ is the Landé factor defined in Eq. (3.8).

Diagonalization of the matrix (3.61) (which is seen to be tridiagonal, real, and symmetric) gives the energy eigenvalues $\lambda_j(\beta LS, M)$ and the corresponding eigenvectors expressed in terms of the coefficients $C_J^j(\beta LS, M)$ of Eq. (3.58). Since the matrix is real and symmetric, the coefficients C_J^j can be chosen to be real. Moreover, from general theorems concerning the diagonalization of matrices one can prove the relations

$$\sum_J C_J^j(\beta LS, M) \, C_J^{j'}(\beta LS, M) = \delta_{jj'} \tag{3.62a}$$

$$\sum_j C_J^j(\beta LS, M) \, C_{J'}^j(\beta LS, M) = \delta_{JJ'} \tag{3.62b}$$

$$\sum_j C_J^j(\beta LS, M) \, C_{J'}^j(\beta LS, M) \lambda_j(\beta LS, M) =$$

$$= \langle \beta LSJM | H_{\rm so} + H_B | \beta LSJ'M \rangle \ . \tag{3.62c}$$

The diagonalization of matrix (3.61) can be performed analytically for doublet terms only ($S = 1/2$). The energy eigenvalues are found to be

$$\lambda_1 = \frac{1}{2} L \, \zeta + \mu_0 B \, \frac{L+1}{L+\frac{1}{2}} \, M$$

for $M = \pm(L + 1/2)$, and

$$\lambda_{1,2} = -\frac{1}{4} \zeta + \mu_0 B \, M \pm \frac{1}{2} \sqrt{\zeta^2 \left(L + \frac{1}{2} \right)^2 + 2\zeta \mu_0 B M + (\mu_0 B)^2}$$

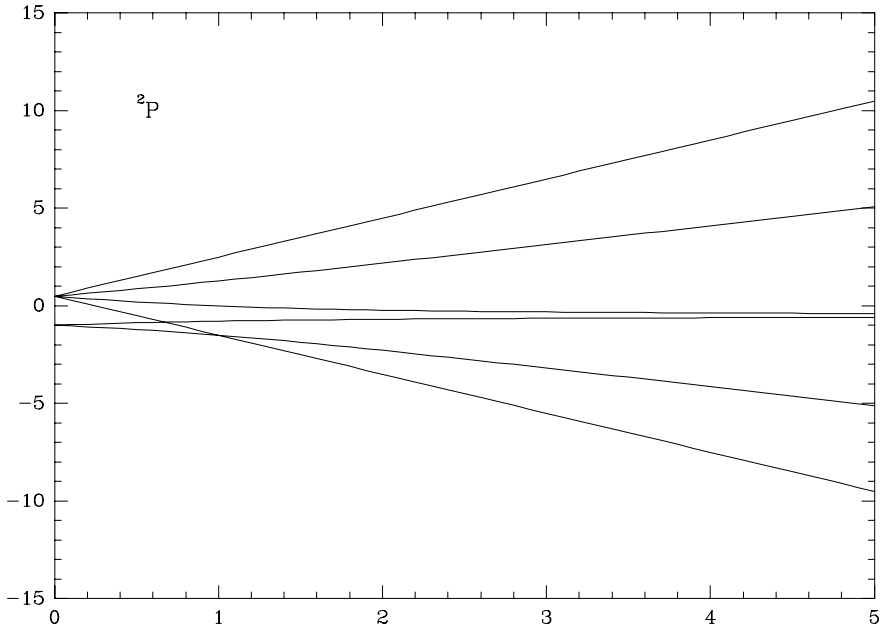

Fig.3.5. The energy levels of the term ^{2}P plotted as functions of the magnetic field strength. The energy E (vertical scale) and the magnetic energy $\mu_0 B$ (horizontal scale) are both normalized to the fine-structure energy ζ (supposed positive). For an inverted multiplet ($\zeta < 0$) the graph is simply reversed about the $E = 0$ axis.

for $M \neq \pm(L + 1/2)$. In all the other cases, the diagonalization can be performed only by numerical methods.

Figures 3.5 to 3.9 illustrate the behavior of the energy eigenvalues of the most common L-S terms as a function of the magnetic field strength, parameterized through the quantity γ defined by

$$\gamma = \frac{\mu_0 B}{\zeta} \,. \tag{3.63}$$

For $\gamma \ll 1$ the eigenvalues spread out linearly from their degenerate, zero-magnetic field value (Zeeman effect regime). For intermediate values of γ, the eigenvalues start crossing each other and the linearity with the magnetic field is, in general, lost (*incomplete Paschen-Back effect regime*); finally, for large values of γ ($\gamma \gg 1$), the eigenvalues behave again linearly with γ, as shown in Fig. 3.10 (*complete Paschen-Back effect regime*).

In this last regime, the spin-orbit interaction can be considered as a perturbation in comparison with the magnetic interaction. On the other hand, the magnetic Hamiltonian is diagonal on the basis $|\beta LSM_L M_S\rangle$, and the eigenvalues are given by

$$\langle \beta LSM_L M_S | H_B | \beta LSM_L M_S \rangle = \mu_0 B \, (M_L + 2M_S) \,,$$

which explains their linear behavior with B for $\gamma \gg 1$. As the magnetic field increases from $\gamma \ll 1$ to $\gamma \gg 1$, the energy eigenvectors gradually evolve from

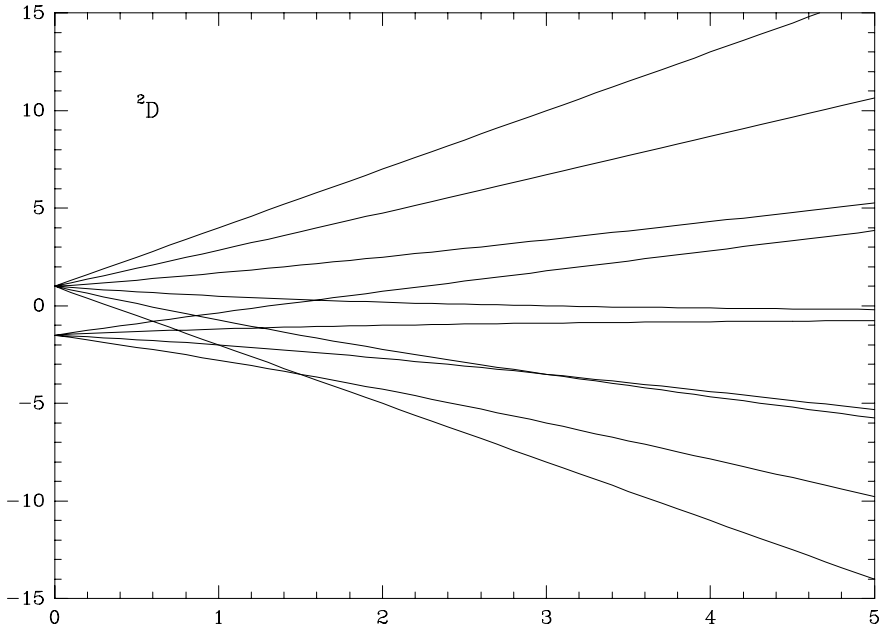

Fig.3.6. Same as Fig.3.5 for the term ^{2}D.

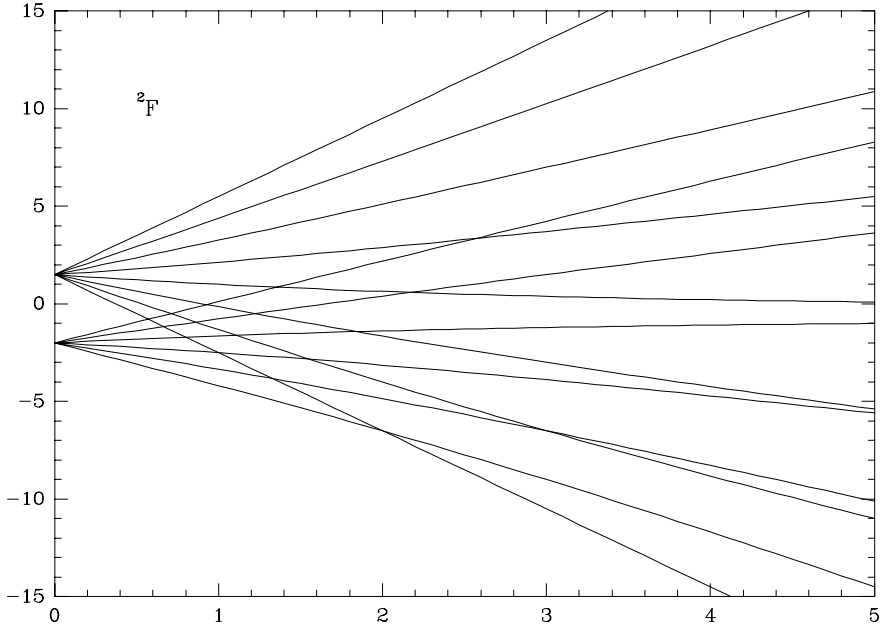

Fig.3.7. Same as Fig.3.5 for the term ^{2}F.

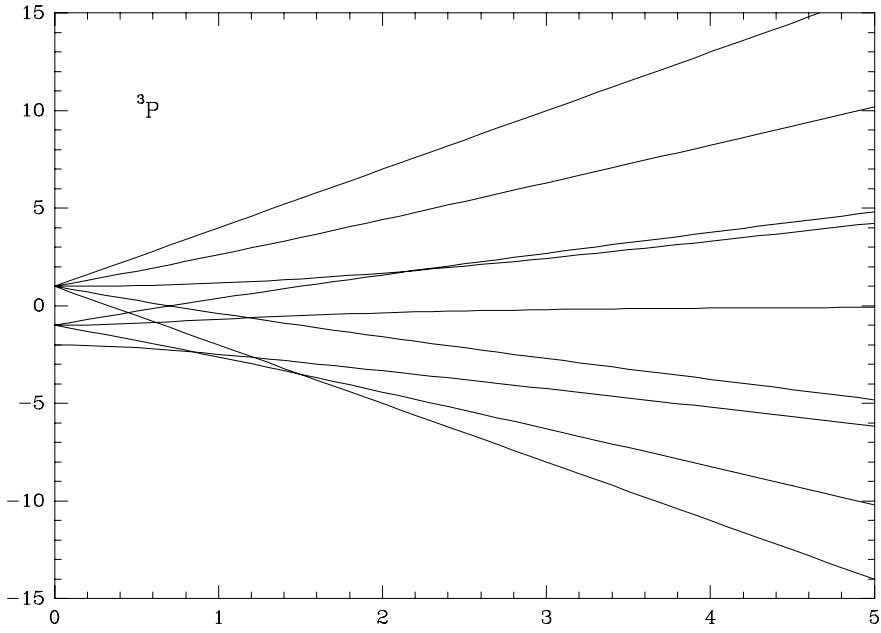

Fig.3.8. Same as Fig.3.5 for the term ^{3}P.

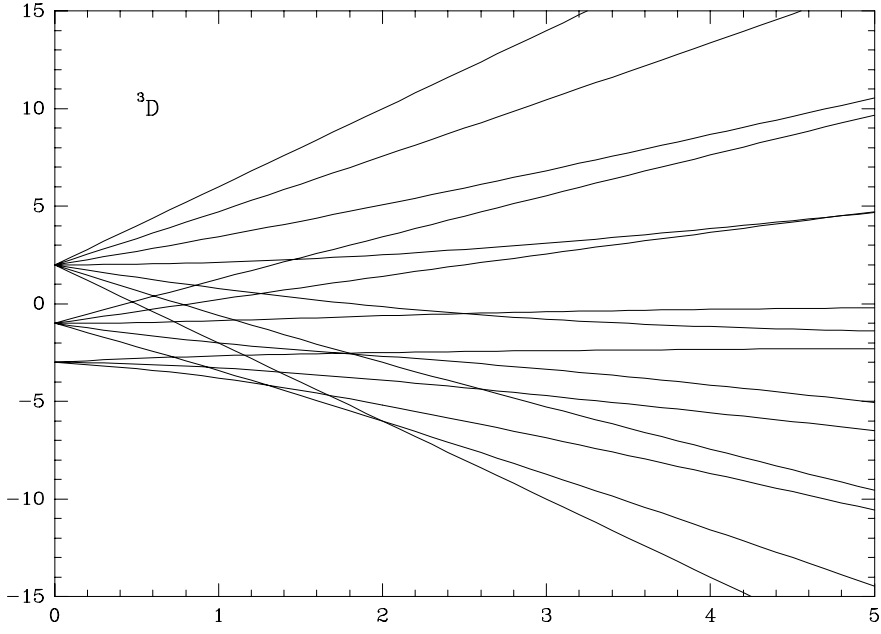

Fig.3.9. Same as Fig.3.5 for the term ^{3}D.

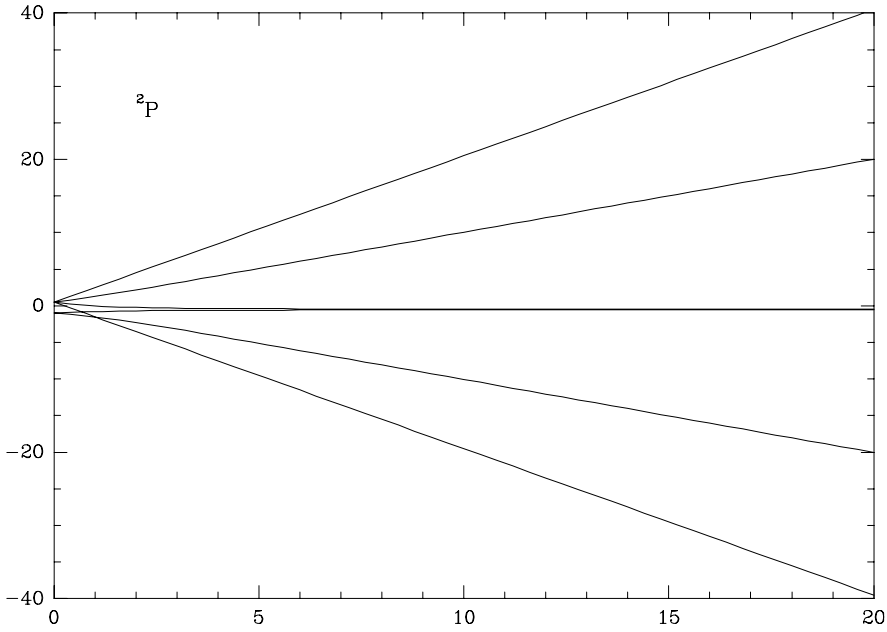

Fig.3.10. For large values of the magnetic field, the energy eigenvalues spread out linearly. This figure is just an enlargement of Fig.3.5 and is intended to show the behavior of the eigenvalues for $\gamma \gg 1$.

the form $|\beta LSJM\rangle$ to the form $|\beta LSM_L M_S\rangle$. In other words, the magnetic field induces a gradual basis-transformation on the energy eigenstates.

As apparent from Figs. 3.5-3.9, the incomplete Paschen-Back effect regime is characterized by several 'crossings' of the energy eigenvalues, each corresponding to a well-defined value of the γ parameter. It will be shown in Sect. 10.18 that such level-crossings induce important phenomena in resonance scattering. Table 3.5 gives, for the most common L-S terms, the values of γ relative to each level-crossing, and the corresponding M-values of the levels involved. To illustrate how this table should be used, consider the $3p\,^2$P term of NaI: from the tables of Moore (1949) we get a value for the constant ζ equal to 11.4642 cm^{-1}, whence we deduce that level-crossing takes place for $B = 1.64 \times 10^5$ G and for $B = 2.46 \times 10^5$ G.

In some cases, and particularly for light atoms such as He, the spin-orbit interaction cannot be described by the simple expression given in Eq. (3.59). In these cases the energy levels in the presence of a magnetic field can still be obtained by diagonalizing the matrix given in Eqs. (3.61), but the actual values $E_{\beta LS}(J)$ are now to be found in tables of atomic energy levels (see e.g. Moore, 1949, 1952, 1958) or in the specialized literature.

Let's now consider how the splitting of the energy levels due to the magnetic field affects, in the general case of the Paschen-Back regime, the spectral lines originating in the transition between two given terms. The main properties of the Paschen-Back patterns resulting from the electric-dipole interaction are described

TABLE 3.5

Level-crossings for the most common L-S terms. The magnetic field is expressed through the parameter γ defined in the text. The M-values refer to a normal multiplet ($\zeta > 0$). For inverted multiplets they must be changed in sign.

Term	γ	M	M'	Term	γ	M	M'
^{2}P	0.667	$-\frac{3}{2}$	$\frac{1}{2}$	^{3}P	0.45	-2	1
	1.	$-\frac{3}{2}$	$-\frac{1}{2}$		0.616	-2	0
^{2}D	0.6	$-\frac{5}{2}$	$\frac{3}{2}$		0.707	-1	1
	0.75	$-\frac{5}{2}$	$\frac{1}{2}$		0.859	-1	0
	0.866	$-\frac{3}{2}$	$\frac{3}{2}$		1.185	-1	0
	1.	$-\frac{5}{2}$	$-\frac{1}{2}$		1.217	-2	0
	1.257	$-\frac{3}{2}$	$\frac{1}{2}$		1.5	-2	-1
	1.5	$-\frac{5}{2}$	$-\frac{3}{2}$		2.210	0	1
	1.591	$-\frac{1}{2}$	$\frac{3}{2}$	^{3}D	0.476	-3	2
	3.	$-\frac{3}{2}$	$-\frac{1}{2}$		0.576	-3	1
^{2}F	0.571	$-\frac{7}{2}$	$\frac{5}{2}$		0.611	-1	2
	0.667	$-\frac{7}{2}$	$\frac{3}{2}$		0.724	-2	1
	0.707	$-\frac{5}{2}$	$\frac{5}{2}$		0.730	-3	0
	0.8	$-\frac{7}{2}$	$\frac{1}{2}$		0.786	-2	1
	0.862	$-\frac{5}{2}$	$\frac{3}{2}$		0.856	-1	2
	0.928	$-\frac{3}{2}$	$\frac{5}{2}$		0.930	-2	0
	1.	$-\frac{7}{2}$	$-\frac{1}{2}$		1.	-3	-1
	1.106	$-\frac{5}{2}$	$\frac{1}{2}$		1.100	-2	0
	1.225	$-\frac{3}{2}$	$\frac{3}{2}$		1.157	-3	1
	1.333	$-\frac{7}{2}$	$-\frac{3}{2}$		1.253	-1	1
	1.356	$-\frac{1}{2}$	$\frac{5}{2}$		1.287	-2	-1
	1.562	$-\frac{5}{2}$	$-\frac{1}{2}$		1.370	-3	0
	1.840	$-\frac{3}{2}$	$\frac{1}{2}$		1.463	0	2
	2.	$-\frac{7}{2}$	$-\frac{5}{2}$		1.667	-3	-1
	2.174	$-\frac{1}{2}$	$\frac{3}{2}$		1.760	-1	1
	2.562	$\frac{1}{2}$	$\frac{5}{2}$		1.797	-2	1
	3.	$-\frac{5}{2}$	$-\frac{3}{2}$		1.813	-2	-1
	6.	$-\frac{3}{2}$	$-\frac{1}{2}$		2.	-3	-2
					2.5	-1	0
					2.600	-2	0
					4.773	0	1

below.

First of all, since the projection M of the total angular momentum on the magnetic field direction is a good quantum number, the individual components can be characterized by the value $\Delta M = (M' - M)$, where M refers to the lower level and M' to the upper one. Owing to the selection rule (3.15) we thus obtain that – in strict analogy with the Zeeman effect – the components can be divided into three distinct groups: $\sigma_{\rm r}$ ($\Delta M = -1$), π ($\Delta M = 0$), and $\sigma_{\rm b}$ ($\Delta M = +1$).

As far as the strengths of the components are concerned, it can be shown that they are proportional to the quantities

$$\mathcal{S}_q^{jM,j'M'} = |\langle \beta LSjM|r_q|\beta' L'S'j'M'\rangle|^2 \qquad (q = -1, 0, +1)\,,$$

where the unprimed quantum numbers refer to the lower level, the primed ones to the upper level, and where r_q are the spherical components of the position operator of the optical electrons.

Expanding the eigenvectors as in Eq. (3.58), and taking into account that the coefficients C_J^j are real, one obtains

$$\begin{aligned}\mathcal{S}_q^{jM,j'M'} = \sum_{JJ'J''J'''} & C_J^j(\beta LS, M)\, C_{J''}^j(\beta LS, M)\, C_{J'}^{j'}(\beta' L'S', M')\, C_{J'''}^{j'}(\beta' L'S', M') \\ & \times \langle \beta LSJM|r_q|\beta' L'S'J'M'\rangle \langle \beta LSJ''M|r_q|\beta' L'S'J'''M'\rangle^* \,.\end{aligned}$$

Evaluating the matrix elements through the Wigner-Eckart theorem (Eq. (2.96)), and noting that r_q is an operator which acts only on the orbital part of the eigenvector, one gets from Eq. (2.108)

$$\begin{aligned}&\mathcal{S}_q^{jM,j'M'} = \\ &= \sum_{JJ'J''J'''} C_J^j(\beta LS, M)\, C_{J''}^j(\beta LS, M)\, C_{J'}^{j'}(\beta' L'S, M')\, C_{J'''}^{j'}(\beta' L'S, M') \\ &\qquad \times (2L+1)\sqrt{(2J+1)(2J'+1)(2J''+1)(2J'''+1)} \\ &\qquad \times \begin{Bmatrix} L & L' & 1 \\ J' & J & S \end{Bmatrix} \begin{Bmatrix} L & L' & 1 \\ J''' & J'' & S \end{Bmatrix} \\ &\qquad \times \begin{pmatrix} J' & J & 1 \\ -M' & M & -q \end{pmatrix} \begin{pmatrix} J''' & J'' & 1 \\ -M' & M & -q \end{pmatrix} |\langle \beta L\|\vec{r}\,\|\beta' L'\rangle|^2\, \delta_{SS'}\,,\end{aligned}$$

a formula that contains all the relevant selection rules, namely

$$\begin{aligned}&\Delta L = 0, \pm 1 \qquad L = 0 \nrightarrow L' = 0 \\ &\Delta S = 0 \\ &\Delta M = 0, \pm 1\,.\end{aligned}$$

Summation over all the possible transitions gives (see Eq. (3.62b))

$$\sum_{jj'MM'} \mathcal{S}_q^{jM,j'M'} = \sum_{JJ'MM'} (2L+1)(2J+1)(2J'+1) \begin{Bmatrix} L & L' & 1 \\ J' & J & S \end{Bmatrix}^2 \times \begin{pmatrix} J' & J & 1 \\ -M' & M & -q \end{pmatrix}^2 |\langle \beta L \| \vec{r} \| \beta' L' \rangle|^2 ,$$

which can be reduced, using Eqs. (2.23a) and (2.39), to

$$\sum_{jj'MM'} \mathcal{S}_q^{jM,j'M'} = \frac{1}{3} (2L+1)(2S+1) |\langle \beta L \| \vec{r} \| \beta' L' \rangle|^2 .$$

This property makes it possible to define the *normalized* strengths in the form

$$\begin{aligned} S_q^{jM,j'M'} &= \\ &= \sum_{JJ'J''J'''} \frac{3}{2S+1} C_J^j(\beta LS, M)\, C_{J''}^j(\beta LS, M)\, C_{J'}^{j'}(\beta' L'S, M')\, C_{J'''}^{j'}(\beta' L'S, M') \\ &\quad \times \sqrt{(2J+1)(2J'+1)(2J''+1)(2J'''+1)} \\ &\quad \times \begin{Bmatrix} L & L' & 1 \\ J' & J & S \end{Bmatrix} \begin{Bmatrix} L & L' & 1 \\ J''' & J'' & S \end{Bmatrix} \\ &\quad \times \begin{pmatrix} J' & J & 1 \\ -M' & M & -q \end{pmatrix} \begin{pmatrix} J''' & J'' & 1 \\ -M' & M & -q \end{pmatrix} , \end{aligned} \tag{3.64}$$

with

$$\sum_{jj'MM'} S_q^{jM,j'M'} = 1 \qquad (q = -1, 0, +1) .$$

The strengths as defined by Eq. (3.64) have some important properties:

a) In the absence of magnetic fields, J is a good quantum number, and the eigenvectors $|\beta LSjM\rangle$ converge towards the states $|\beta LSJM\rangle$ which are degenerate with respect to M. For the coefficients C_J^j we have

$$C_J^j(\beta LS, M) = \delta_{jJ} ,$$

so that

$$S_q^{JM,J'M'} = \frac{3}{2S+1} (2J+1)(2J'+1) \begin{Bmatrix} L & L' & 1 \\ J' & J & S \end{Bmatrix}^2 \begin{pmatrix} J' & J & 1 \\ -M' & M & -q \end{pmatrix}^2 ,$$

and summing over the degeneracy parameters M and M' we obtain the usual expression for the relative strengths of a fine-structure multiplet

$$S^{J,J'} = \sum_{MM'} S_q^{JM,J'M'} = \frac{(2J+1)(2J'+1)}{2S+1} \begin{Bmatrix} L & L' & 1 \\ J' & J & S \end{Bmatrix}^2 . \tag{3.65}$$

b) The centers of gravity in frequency of the π, $\sigma_{\rm r}$, and $\sigma_{\rm b}$ components ($q = 0$, $+1$, and -1, respectively) are linear functions of the magnetic field

$$\Delta\nu_q = -q\,\nu_{\rm L}\ , \tag{3.66}$$

where $\nu_{\rm L}$ is the Larmor frequency and $\Delta\nu_q$ is defined by

$$\Delta\nu_q = \sum_{jj'MM'} S_q^{jM,j'M'}\,\Delta\nu_{MM'}^{jj'}\ , \tag{3.67}$$

with $\Delta\nu_{MM'}^{jj'}$ the frequency shift of the component corresponding to the transition between the lower state $|\beta LSjM\rangle$ and the upper state $|\beta' L'Sj'M'\rangle$ from the unperturbed frequency of the transition between the two terms (βLS) and $(\beta' L'S)$.

To prove Eq. (3.66) we substitute into Eq. (3.67) the strengths of Eq. (3.64) and the frequency shifts

$$\Delta\nu_{MM'}^{jj'} = \frac{\lambda_{j'}(\beta' L'S, M') - \lambda_j(\beta LS, M)}{h}\ , \tag{3.68}$$

where λ_j, $\lambda_{j'}$ are the eigenvalues of the matrix (3.61) for the lower and the upper term, respectively. We then perform the sums over j and j' using Eqs. (3.62b) and (3.62c), to obtain

$$\begin{aligned}\Delta\nu_q = \frac{1}{h}\sum_{MM'}\sum_{JJ'J''J'''}\ &\frac{3}{2S+1}\sqrt{(2J+1)(2J'+1)(2J''+1)(2J'''+1)}\\ &\times\begin{Bmatrix} L & L' & 1\\ J' & J & S\end{Bmatrix}\begin{Bmatrix} L & L' & 1\\ J''' & J'' & S\end{Bmatrix}\\ &\times\begin{pmatrix} J' & J & 1\\ -M' & M & -q\end{pmatrix}\begin{pmatrix} J''' & J'' & 1\\ -M' & M & -q\end{pmatrix}\\ &\times\Big[\delta_{JJ''}\,\langle\beta' L'SJ'M'|H_{\rm so}+H_B|\beta' L'SJ'''M'\rangle\\ &\qquad-\delta_{J'J'''}\,\langle\beta LSJM|H_{\rm so}+H_B|\beta LSJ''M\rangle\Big]\ .\end{aligned} \tag{3.69}$$

It is easy to prove that the spin-orbit Hamiltonian gives zero contribution. Indeed, noting that this Hamiltonian is diagonal with respect to the quantum numbers J and M, and that its matrix elements are independent of M, and performing the sums over M and M' via Eq. (2.23a), we have for this contribution

$$\begin{aligned}\left(\Delta\nu_q\right)_{\rm so} = \frac{1}{h}\sum_{JJ'}\ &\frac{(2J+1)(2J'+1)}{(2S+1)}\begin{Bmatrix} L & L' & 1\\ J' & J & S\end{Bmatrix}^2\\ &\times\Big[\langle\beta' L'SJ'M'|H_{\rm so}|\beta' L'SJ'M'\rangle-\langle\beta LSJM|H_{\rm so}|\beta LSJM\rangle\Big]\ .\end{aligned}$$

Summation over J for the first term, and over J' for the second term gives, with the use of Eq. (2.39)

$$\left(\Delta\nu_q\right)_{\rm so} = \frac{1}{h}\left[\sum_{J'} \frac{2J'+1}{(2L'+1)(2S+1)} \left\langle \beta' L' S J' M' | H_{\rm so} | \beta' L' S J' M' \right\rangle \right.$$
$$\left. - \sum_{J} \frac{2J+1}{(2L+1)(2S+1)} \left\langle \beta L S J M | H_{\rm so} | \beta L S J M \right\rangle \right].$$

The first sum is simply the average energy of the fine-structure levels of the upper term, while the second sum is the same quantity for the lower term. It can be easily proved that both these quantities are identically zero when the spin-orbit Hamiltonian is described by Eq. (3.59).[1]

The only non-vanishing contribution to Eq. (3.69) is due to the magnetic field. To evaluate this contribution, we substitute the matrix elements given by Eq. (3.57) and perform the sums over M and M' by means of Eq. (2.42). After some tedious Racah-algebra calculations which involve the use of Eqs. (2.38), (2.48), (2.55), and (3.51), we obtain that only the first term in the square bracket of the matrix element (3.57) gives a non-zero contribution, and we get the expression

$$\Delta\nu_q = \frac{3\,\nu_{\rm L}}{2S+1} \sum_{JJ'} (-1)^{J+J'+q} (2J+1)(2J'+1) \begin{Bmatrix} L & L' & 1 \\ J' & J & S \end{Bmatrix}^2 \begin{pmatrix} 1 & 1 & 1 \\ q & -q & 0 \end{pmatrix}$$
$$\times \left[\sqrt{J'(J'+1)(2J'+1)} \begin{Bmatrix} 1 & 1 & 1 \\ J' & J' & J \end{Bmatrix} \right.$$
$$\left. + \sqrt{J(J+1)(2J+1)} \begin{Bmatrix} 1 & 1 & 1 \\ J & J & J' \end{Bmatrix} \right].$$

Evaluating the 6-j symbols in the square bracket by Eq. (2.36d) and the 3-j symbol by Eq. (2.26d), and performing the sums over J and J' via Eq. (2.39), we finally obtain Eq. (3.66).

The theorem just proved shows an interesting property of the Paschen-Back effect which can be summarized by the following statement: *The frequency shifts of the centers of gravity of the $\sigma_{\rm r}$, $\sigma_{\rm b}$, and π components in the Paschen-Back effect regime are those typical of the normal Zeeman effect between two spinless levels*. In other words, given a fine-structured lower term (βLS) and a fine-structured upper term

[1] To prove this statement, one has just to recall the sum rules for integers

$$\sum_{k=1}^{n} k = \tfrac{1}{2}\, n\,(n+1), \qquad \sum_{k=1}^{n} k^2 = \tfrac{1}{6}\, n\,(n+1)(2n+1), \qquad \sum_{k=1}^{n} k^3 = \tfrac{1}{4}\, n^2 (n+1)^2.$$

If, on the other hand, the spin-orbit Hamiltonian cannot be written in the form (3.59), the quantity $\left(\Delta\nu_q\right)_{\rm so}$ may indeed differ from zero. In such cases, it represents a constant shift (independent of q) that affects the unperturbed frequency of the transition. In other words, Eq. (3.66) still holds provided Eq. (3.68) is replaced by

$$\Delta\nu^{jj'}_{MM'} = \frac{1}{h}\left[\lambda_{j'}(\beta' L' S, M') - \lambda_j(\beta L S, M)\right] - \left(\Delta\nu_q\right)_{\rm so}.$$

$(\beta' L' S)$, the centers of gravity of the $\sigma_{\rm r}$, $\sigma_{\rm b}$, and π components have the same frequencies as the individual components that would originate from the transition between a spinless lower level (βL) and a spinless upper level $(\beta' L')$, both split according to the normal Zeeman effect. This result is what should be expected from the *principle of spectroscopic stability*,[1] as it can be inferred from considering the limit of negligible fine structure.

3.5. Magnetic Field and Hyperfine Structure

It is well-known that hyperfine structure results from the interaction of the electronic cloud with the atomic nucleus. The energy involved in this interaction is approximately one thousand times smaller than the energy relative to the spin-orbit interaction, so that the hyperfine-structure components of a spectral line have typical wavelength separations of a few mÅ.

In most cases (and particularly for lines originating from astrophysical plasmas), these components remain unresolved, because their separation is much smaller than the line width due to different broadening mechanisms. For this reason the hyperfine structure of spectral lines is often neglected, especially in usual astrophysical applications.

However, when polarization phenomena are involved, the situation is substantially different, and hyperfine structure generally plays an important role (see Sect. 9.23). We describe here the effect of a magnetic field on a hyperfine-structured line, in order to state some basic properties of the resulting pattern.

We consider a particular isotope having nuclear spin I, and introduce the representation $|\alpha JIFf\rangle$ to describe its energy eigenvectors. In this notation, apart from the symbols already used, F is the total angular momentum (electronic plus nuclear: $\vec{F} = \vec{J} + \vec{I}$) quantum number, while f represents its projection on the z-axis of the coordinate system ($f = -F, -F+1, \ldots, F$).

The hyperfine-structure interaction energy can be expressed as an infinite series of electric and magnetic multipoles (see for instance Kopfermann, 1958). In most cases, a very good approximation to the observed energy intervals is obtained by retaining only the first two terms in the multipole series; these are the magnetic-dipole and electric-quadrupole terms, which are given by

$$\begin{aligned}
\langle \alpha JIFf | H^{(1)}_{\rm hfs} | \alpha JIF'f' \rangle &= \delta_{FF'}\, \delta_{ff'}\, \frac{\mathcal{A}(\alpha, J, I)}{2}\, K \\
\langle \alpha JIFf | H^{(2)}_{\rm hfs} | \alpha JIF'f' \rangle &= \delta_{FF'}\, \delta_{ff'}\, \mathcal{B}(\alpha, J, I) \\
&\quad \times \left[K(K+1) - \frac{4}{3} J(J+1) I(I+1) \right], \qquad (3.70)
\end{aligned}$$

where $\mathcal{A}(\alpha, J, I)$ and $\mathcal{B}(\alpha, J, I)$ are the *magnetic-dipole* and *electric-quadrupole hyperfine structure constants* relative to a given atomic level of a given isotope, while

[1] A formulation of this principle is given in Sect. 7.10.

K is defined by

$$K = F(F+1) - J(J+1) - I(I+1) \; . \tag{3.71}$$

An extensive table of experimental $\mathcal{A}$ and $\mathcal{B}$ values can be found in Brix and Kopfermann (1952). From such values, and from Eqs. (3.70), the energy of the various hyperfine-structure sublevels can be easily computed. The sublevels are characterized by the total angular momentum F and are degenerate with respect to f.

If a magnetic field is present, so weak as to produce a splitting much smaller than the energy differences between the various hyperfine-structure sublevels, its effect can be deduced from perturbation theory, by diagonalizing the magnetic Hamiltonian H_B of Eq. (3.3) on the degenerate basis $|\alpha JIFf\rangle$.[1] Aligning the z-axis of the reference system with the direction of the magnetic field, the matrix elements to be evaluated are of the form

$$\langle \alpha JIFf | \mu_0 B (L_z + 2S_z) | \alpha JIFf' \rangle \; .$$

Let us evaluate the more general matrix element (that will be needed later) between two states having different F-values. Writing $(L_z + 2S_z)$ in the form $(J_z + S_z)$ and bearing in mind the definition of the Landé factor (Eq. (3.7)), we obtain from Eqs. (2.96) (Wigner-Eckart theorem) and (2.108)

$$\begin{aligned} &\langle \alpha JIFf | \mu_0 B (J_z + S_z) | \alpha JIF'f' \rangle = \\ &= \mu_0 B \, g_{\alpha J} \, \delta_{ff'} \, (-1)^{J+I-f} \sqrt{J(J+1)(2J+1)(2F+1)(2F'+1)} \\ &\quad \times \begin{Bmatrix} F' & F & 1 \\ J & J & I \end{Bmatrix} \begin{pmatrix} F & F' & 1 \\ -f & f & 0 \end{pmatrix} . \end{aligned} \tag{3.72}$$

In particular, for $F = F'$ we have

$$\langle \alpha JIFf | \mu_0 B (J_z + S_z) | \alpha JIFf' \rangle = \mu_0 B \, g_{\alpha J} \, g_{\mathrm{hfs}}(F) \, f \, \delta_{ff'} \; ,$$

where the hyperfine-structure Landé factor, $g_{\mathrm{hfs}}(F)$, is given by

$$g_{\mathrm{hfs}}(F) = \frac{1}{2} \, \frac{F(F+1) + J(J+1) - I(I+1)}{F(F+1)} \qquad (F \neq 0) \; . \tag{3.73}$$

Thus for weak magnetic fields any hyperfine level of total angular momentum F splits up into $(2F+1)$ magnetic sublevels, each characterized by its own f-value. The splitting is proportional to the magnetic field and to the product of the usual Landé factor $g_{\alpha J}$ times a Landé factor $g_{\mathrm{hfs}}(F)$ which depends on the particular hyperfine level. This is the *Zeeman effect for hyperfine structure*.

[1] The Hamiltonian describing the direct interaction between the magnetic field and the nuclear spin can be safely neglected, since the corresponding energy is about 10^3 times smaller than the energy involved in the interaction between the magnetic field and the electronic cloud.

If the magnetic field is so strong that the Zeeman splitting is of the same order as the energy difference between different hyperfine levels, perturbation theory cannot be applied any longer, and one has to go back to the simultaneous diagonalization of the hyperfine-structure and magnetic Hamiltonians, whose matrix elements are given in Eqs. (3.70) and (3.72). The situation here is quite similar to that of the Paschen-Back effect (Sect. 3.4): since the matrix elements are diagonal with respect to f, the overall Hamiltonian can be factored into $[2(I+J)+1]$ submatrices, each characterized by a particular f-value.[1] Thus the eigenvalues and eigenvectors are of the form

$$\begin{aligned} &\lambda_i(\alpha JI, f) \\ &|\alpha JIif\rangle = \sum_F C_F^i(\alpha JI, f)\,|\alpha JIFf\rangle \end{aligned} \tag{3.74}$$

(where the C_F^i coefficients can be chosen real) and can be found, in general, by numerical diagonalization of the total Hamiltonian. Figure 3.11 illustrates the behavior of the energy eigenvalues for the hyperfine-structure components of the level 3 $^2\mathrm{P}_{3/2}$ of NaI as a function of the magnetic field (the values of the hyperfine-structure constants are from Figger and Walther, 1974). As in the case of the Paschen-Back effect, there are several level-crossings between the hyperfine-structure magnetic sublevels. Such level-crossings induce important phenomena in resonance scattering (see Sect. 10.22).

The strengths and the splittings of the various hyperfine-structure components can be computed in strict analogy with the case of the Paschen-Back effect. For the normalized strengths of the hyperfine components of the transition connecting a lower level (αJ) with an upper level $(\alpha' J')$ one obtains

$$\begin{aligned} S_q^{if,i'f'} = \sum_{FF'F''F'''} &\frac{3}{2I+1}\, C_F^i(\alpha JI, f)\, C_{F''}^i(\alpha JI, f)\, C_{F'}^{i'}(\alpha' J'I, f')\, C_{F'''}^{i'}(\alpha' J'I, f') \\ &\times \sqrt{(2F+1)(2F'+1)(2F''+1)(2F'''+1)} \\ &\times \begin{Bmatrix} J & J' & 1 \\ F' & F & I \end{Bmatrix} \begin{Bmatrix} J & J' & 1 \\ F''' & F'' & I \end{Bmatrix} \\ &\times \begin{pmatrix} F' & F & 1 \\ -f' & f & -q \end{pmatrix} \begin{pmatrix} F''' & F'' & 1 \\ -f' & f & -q \end{pmatrix}, \end{aligned} \tag{3.75}$$

with

$$\sum_{ii'ff'} S_q^{if,i'f'} = 1 \qquad (q = -1, 0, +1)\,.$$

The relevant selection rules are

$$\begin{aligned} &\Delta J = 0, \pm 1 \qquad J = 0 \nrightarrow J' = 0 \\ &\Delta f = 0, \pm 1\,. \end{aligned}$$

[1] It is assumed here that the magnetic splitting is much smaller than the energy differences among the various J-levels. The opposite case will not be considered in this book.

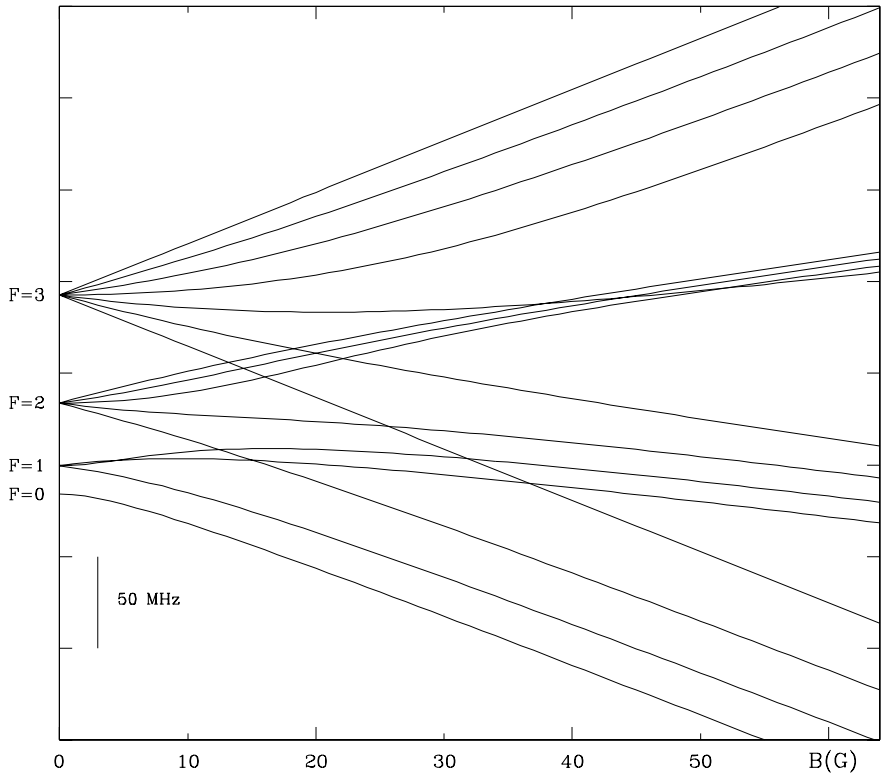

Fig.3.11. Energies of the hyperfine sublevels of the level $3\,^2\mathrm{P}_{3/2}$ of NaI as functions of the magnetic field strength.

Similarly to the Paschen-Back effect, the strengths defined in Eq. (3.75) have some important properties, which can be proved by observing that the coefficients $C^i_F(\alpha JI, f)$ satisfy the following relations, similar to Eqs. (3.62)

$$\sum_F C^i_F(\alpha JI, f)\, C^{i'}_F(\alpha JI, f) = \delta_{ii'} \tag{3.76a}$$

$$\sum_i C^i_F(\alpha JI, f)\, C^i_{F'}(\alpha JI, f) = \delta_{FF'} \tag{3.76b}$$

$$\sum_i C^i_F(\alpha JI, f)\, C^i_{F'}(\alpha JI, f)\, \lambda_i(\alpha JI, f) = \\ = \langle \alpha JIFf | H^{(1)}_{\mathrm{hfs}} + H^{(2)}_{\mathrm{hfs}} + H_B | \alpha JIF'f \rangle \ . \tag{3.76c}$$

The properties of the strengths are the following:

a) In the absence of magnetic fields, F is a good quantum number, and the eigenvectors $|\alpha JIif\rangle$ converge towards the states $|\alpha JIFf\rangle$ that are degenerate with respect to f; the coefficients C^i_F are given by

$$C^i_F(\alpha JI, f) = \delta_{iF} \ ,$$

so that we obtain

$$S_q^{Ff,F'f'} = \frac{3}{2I+1}\,(2F+1)(2F'+1)\begin{Bmatrix} J & J' & 1 \\ F' & F & I \end{Bmatrix}^2 \begin{pmatrix} F' & F & 1 \\ -f' & f & -q \end{pmatrix}^2 ,$$

and summing over the degeneracy parameters f and f' one gets the usual expression for the relative strengths of hyperfine-structure multiplets

$$S^{F,F'} = \sum_{ff'} S_q^{Ff,F'f'} = \frac{(2F+1)(2F'+1)}{(2I+1)}\begin{Bmatrix} J & J' & 1 \\ F' & F & I \end{Bmatrix}^2 .$$

b) The centers of gravity in frequency of the π, $\sigma_{\rm r}$, and $\sigma_{\rm b}$ components ($q = 0$, $+1$, and -1, respectively) are linear functions of the magnetic field

$$\Delta\nu_q = \sum_{ii'ff'} S_q^{if,i'f'}\,\Delta\nu_{ff'}^{ii'} = -q\,\bar{g}\,\nu_{\rm L} , \tag{3.77}$$

where $\nu_{\rm L}$ is the Larmor frequency, $\Delta\nu_{ff'}^{ii'}$ is the frequency shift of the component corresponding to the transition between the lower state $|\alpha JIif\rangle$ and the upper state $|\alpha' J' I i' f'\rangle$ from the unperturbed frequency of the transition between the two levels (αJI) and $(\alpha' J' I)$,

$$\Delta\nu_{ff'}^{ii'} = \frac{\lambda_{i'}(\alpha' J' I, f') - \lambda_i(\alpha JI, f)}{h} , \tag{3.78}$$

and where $\bar{g}$ is given in terms of the Landé factors of the lower and upper level

$$\bar{g} = \frac{1}{2}\,(g_{\alpha J} + g_{\alpha' J'}) + \frac{1}{4}\,(g_{\alpha J} - g_{\alpha' J'})\,[J(J+1) - J'(J'+1)] .$$

Comparison with Eq. (3.44) shows that the factor $\bar{g}$ is just the effective Landé factor that one would obtain for the transition between the levels (αJ), $(\alpha' J')$ if hyperfine structure were not present.

The proof of Eq. (3.77) is rather tedious and quite similar to the proof of the analogous equation for the Paschen-Back effect. For this reason it will not be given here and is left as an exercise to the reader.[1] Equation (3.77) is particularly important, and it can be expressed by the following statement: *The frequency shifts of the centers of gravity of the $\sigma_{\rm r}$, $\sigma_{\rm b}$, and π components of a hyperfine-structured line are the same as those resulting from the same line without hyperfine structure.* This result is what should be expected from the principle of spectroscopic stability.

[1] To prove that the hyperfine-structure Hamiltonian (Eqs. (3.70)) gives no contribution to the quantity $\Delta\nu_q$, one needs the sum rules

$$\sum_{k=1}^{n} k^4 = \tfrac{1}{30}\,n(n+1)(2n+1)(3n^2+3n-1), \qquad \sum_{k=1}^{n} k^5 = \tfrac{1}{12}\,n^2(n+1)^2(2n^2+2n-1).$$

To evaluate the contribution of the magnetic Hamiltonian (Eq. (3.72)), the sum rule (2.41) must be used (instead of (2.48), employed for the Paschen-Back calculation).

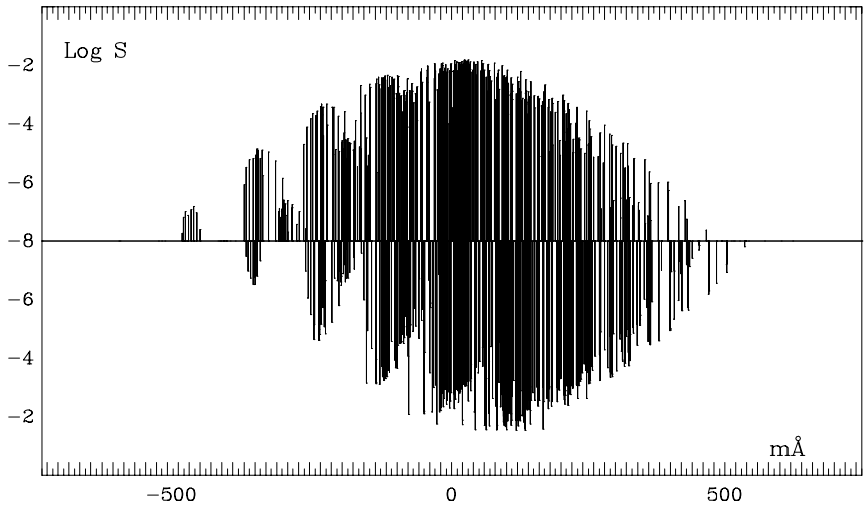

Fig.3.12. Logarithm of the strengths of π (upper) and σ_r (lower) components against wavelength for the line EuII λ 4205. The value of the magnetic field is 6 kG. Only the components having strength larger than 10^{-8} are shown. The number of components of each type is approximately 400.

The numerical calculation of the strengths and splittings of the various hyperfine-structure components of a spectral line requires the diagonalization of the total Hamiltonian for the lower and for the upper level followed by the evaluation of expressions (3.75). If the element has more than one isotope, the calculations must be repeated for each of them and the splittings must be adjusted to allow for isotope shift.

Landi Degl'Innocenti (1978a) has presented a computer program to perform such calculations. The program has then been applied to the line EuII λ 4205 using the data for the hyperfine-structure constants given by Krebs and Winckler (1960). The result is shown in Fig. 3.12 for a magnetic field of 6 kG. The number of components is indeed striking, with an intricate pattern recalling a 'wild forest'. The implications of such a pattern on the determination of the europium abundance in magnetic stars have been discussed by Landi Degl'Innocenti (1975).

3.6. Atomic Level Polarization and Density Matrix

When an atomic system is excited through a physical process which, for any reason, is not spatially isotropic, the various magnetic sublevels of the system, degenerate or quasi-degenerate with respect to energy, are, in general, not evenly populated; moreover, they are characterized by definite phase relations, and the atomic system is said to be *polarized*. A typical example occurs when the atomic system is excited by a unidirectional (or polarized) radiation beam, or by collisions with a collimated beam of fast particles.

In such situations, the description of the atomic excitation in terms of the usual concept of populations of the atomic levels (or sublevels) is no longer adequate, and one must resort to the more sophisticated concept of atomic *density operator*.

The density operator can be defined for any assigned quantum system. If p_α ($p_\alpha \geq 0$) is the probability of finding the system in the pure state $|\psi^{(\alpha)}\rangle$ (normalized to 1), the density operator ρ is defined by

$$\rho = \sum_\alpha p_\alpha \, |\psi^{(\alpha)}\rangle \langle \psi^{(\alpha)}| \, . \tag{3.79}$$

Introducing a complete and orthogonal basis of unit vectors $\{|u_k\rangle\}$ for the Hilbert space spanned by the vectors $|\psi^{(\alpha)}\rangle$, one has

$$\langle u_m| \, \rho \, |u_n\rangle = \rho_{mn} = \sum_\alpha p_\alpha \langle u_m|\psi^{(\alpha)}\rangle \langle \psi^{(\alpha)}|u_n\rangle \, ,$$

where ρ_{mn} are the matrix elements of the density operator, also called *density-matrix elements*.

Some important properties of the density operator follow directly from its definition:

a) The density operator is Hermitian,

$$\rho = \rho^\dagger \, ,$$

which leads to the remarkable symmetry property of the density matrix

$$\rho_{mn} = \rho^*_{nm} \, . \tag{3.80}$$

b) The density operator is positive definite. In fact, for an arbitrary state vector $|\phi\rangle$ we have

$$\langle \phi| \, \rho \, |\phi\rangle = \sum_\alpha p_\alpha \, |\langle \psi^{(\alpha)}|\phi\rangle|^2 \geq 0 \, ;$$

in particular, for $|\phi\rangle = |u_n\rangle$

$$\rho_{nn} \geq 0 \, , \tag{3.81}$$

and hence the diagonal matrix elements are real and non-negative.

c) The trace of the density matrix is independent of the basis chosen to define its matrix elements. In fact, since a complete, orthonormal basis satisfies the relation

$$\sum_n |u_n\rangle \langle u_n| = 1 \, , \tag{3.82}$$

we obtain from Eq. (3.79)

$$\begin{aligned} \mathrm{Tr}\,(\rho) = \sum_n \rho_{nn} &= \sum_n \sum_\alpha p_\alpha \, \langle u_n|\psi^{(\alpha)}\rangle \langle \psi^{(\alpha)}|u_n\rangle \\ &= \sum_\alpha p_\alpha \, \langle \psi^{(\alpha)}| \Big[\sum_n |u_n\rangle \langle u_n| \Big] |\psi^{(\alpha)}\rangle = \sum_\alpha p_\alpha \, . \end{aligned} \tag{3.83}$$

In particular, if the probabilities p_α are normalized to unity one gets

$$\mathrm{Tr}\,(\rho) = 1\ . \tag{3.84}$$

d) The density-matrix elements satisfy the following *Schwarz inequality*

$$|\rho_{nm}|^2 \leq \rho_{nn}\,\rho_{mm}\ . \tag{3.85}$$

To prove this relation, let us consider the state vector

$$|\phi\rangle = \rho_{nm}\,|u_n\rangle - \rho_{nn}\,|u_m\rangle\ ;$$

for the diagonal matrix element $\langle\phi|\,\rho\,|\phi\rangle$ one gets

$$\langle\phi|\,\rho\,|\phi\rangle = \rho_{nn}\Big(\rho_{nn}\,\rho_{mm} - |\rho_{nm}|^2\Big)\ ,$$

which proves Eq. (3.85) since $\langle\phi|\,\rho\,|\phi\rangle \geq 0$ and $\rho_{nn} \geq 0$.

e) If the quantum system is in a pure state rather than a statistical mixture of states, or, in other words, if the sum in Eq. (3.79) is restricted to only one state $|\psi^{(0)}\rangle$, the above inequality reduces to an equality

$$|\rho_{nm}|^2 = |\langle u_n|\psi^{(0)}\rangle|^2\,|\langle u_m|\psi^{(0)}\rangle|^2 = \rho_{nn}\,\rho_{mm}\ .$$

f) The expectation value of any dynamical variable is equal to the trace of the product of the density operator times the operator associated to the variable

$$\langle A\rangle = \sum_\alpha p_\alpha\,\langle\psi^{(\alpha)}|A|\psi^{(\alpha)}\rangle = \mathrm{Tr}\,(\rho A)\ . \tag{3.86}$$

Indeed, using Eq. (3.82) one obtains

$$\begin{aligned}
\mathrm{Tr}\,(\rho A) &= \sum_n \langle u_n|\rho A|u_n\rangle \\
&= \sum_n \langle u_n|\sum_\alpha p_\alpha|\psi^{(\alpha)}\rangle\langle\psi^{(\alpha)}|A|u_n\rangle \\
&= \sum_n\sum_\alpha p_\alpha\langle\psi^{(\alpha)}|A|u_n\rangle\langle u_n|\psi^{(\alpha)}\rangle \\
&= \sum_\alpha p_\alpha\langle\psi^{(\alpha)}|A|\psi^{(\alpha)}\rangle = \langle A\rangle\ .
\end{aligned}$$

g) If a system consists of two subsystems a and b, the trace of the density operator of the system over the states of one subsystem is the density operator of the other one. Indeed, let $\{|\,a_n\rangle\}$ and $\{|\,b_m\rangle\}$ be two complete bases for the Hilbert spaces

of subsystems a and b, respectively, and ρ the density operator of the compound system. If $O^{(a)}$ is an operator acting on subsystem a only, we have

$$\begin{aligned}\left\langle O^{(a)}\right\rangle = \mathrm{Tr}\left(\rho\, O^{(a)}\right) &= \sum_{nm} \langle a_n \,|\, \langle b_m \,|\, \rho\, O^{(a)} \,|\, b_m\rangle \,|\, a_n\rangle \\ &= \sum_{n} \langle a_n \,|\, \Big\{\sum_{m} \langle b_m \,|\, \rho \,|\, b_m\rangle\Big\}\, O^{(a)} \,|\, a_n\rangle \\ &= \sum_{n} \langle a_n \,|\, \mathrm{Tr}^{(b)}(\rho)\; O^{(a)} \,|\, a_n\rangle \;.\end{aligned}$$

On the other hand, if $\rho^{(a)}$ is the density operator of subsystem a, we also have

$$\left\langle O^{(a)}\right\rangle = \mathrm{Tr}^{(a)}\big(\rho^{(a)}\, O^{(a)}\big) = \sum_{n} \langle a_n \,|\, \rho^{(a)}\, O^{(a)} \,|\, a_n\rangle \;.$$

Comparison of these two relations shows that

$$\mathrm{Tr}^{(b)}(\rho) = \rho^{(a)} \;. \tag{3.87}$$

h) The time evolution of the density operator in the Schrödinger representation is described by the equation

$$\frac{\mathrm{d}}{\mathrm{d}t}\,\rho = \frac{2\pi}{\mathrm{i}h}\,[H,\rho] \;, \tag{3.88}$$

where the symbol $[A,B]$ denotes the commutator of the two operators A and B, and where H is the Hamiltonian of the system.

This equation follows directly from the Schrödinger equation applied to the state vectors $|\psi^{(\alpha)}\rangle$ entering the definition of ρ. In fact, we have from Eq. (3.79)

$$\begin{aligned}\frac{\mathrm{d}}{\mathrm{d}t}\,\rho &= \sum_{\alpha} p_\alpha \left[\left(\frac{\mathrm{d}}{\mathrm{d}t}|\psi^{(\alpha)}\rangle\right)\langle\psi^{(\alpha)}| + |\psi^{(\alpha)}\rangle\left(\frac{\mathrm{d}}{\mathrm{d}t}\langle\psi^{(\alpha)}|\right)\right] \\ &= \sum_{\alpha} p_\alpha\, \frac{2\pi}{\mathrm{i}h}\, H|\psi^{(\alpha)}\rangle\langle\psi^{(\alpha)}| - \sum_{\alpha} p_\alpha\, \frac{2\pi}{\mathrm{i}h}\, |\psi^{(\alpha)}\rangle\langle\psi^{(\alpha)}|H \;,\end{aligned}$$

which proves Eq. (3.88).

As far as the density-matrix elements are concerned, their time evolution depends on the particular basis $\{|u_n\rangle\}$. If we choose the basis of the energy eigenvectors, or, in other words, if the vectors $|u_n\rangle$ are such that

$$H|u_n\rangle = E_n|u_n\rangle \;,$$

we have from Eq. (3.88)

$$\frac{\mathrm{d}}{\mathrm{d}t}\,\rho_{mn} = \frac{\mathrm{d}}{\mathrm{d}t}\,\langle u_m|\,\rho\,|u_n\rangle = \frac{2\pi}{\mathrm{i}h}\,\langle u_m|\,[H,\rho]\,|u_n\rangle = -2\pi\mathrm{i}\,\nu_{mn}\,\rho_{mn} \;,$$

where the *Bohr frequency* ν_{mn} is defined by

$$\nu_{mn} = \frac{E_m - E_n}{h} \ .$$

On the other hand, for a different basis one gets

$$\frac{\mathrm{d}}{\mathrm{d}t}\,\rho_{mn} = -\frac{2\pi\mathrm{i}}{h}\,\sum_p \Big(H_{mp}\,\rho_{pn} - H_{pn}\,\rho_{mp}\Big) \ ,$$

where

$$H_{ij} = \langle u_i|H|u_j\rangle \ .$$

For an atomic system, the most natural basis for defining the matrix elements of the density operator is the basis of the eigenvectors of the angular momentum, although in some cases this is not the basis of the energy eigenvectors (see for instance the discussion of the Paschen-Back effect in Sect. 3.4). On this basis, the elements of the density matrix are

$$\rho\,(\alpha JM, \alpha' J' M') = \langle \alpha JM|\,\rho\,|\alpha' J' M'\rangle \ .$$

In this representation – usually referred to as the *standard representation* of the atomic density operator – the diagonal terms, $\rho\,(\alpha JM, \alpha JM)$, represent the populations of the various magnetic sublevels, with the overall population n_J of an assigned J-level given by

$$n_J = \sum_M \rho\,(\alpha JM, \alpha JM) \ . \tag{3.89}$$

Conversely, the off-diagonal terms $\rho\,(\alpha JM, \alpha' J' M')$ represent the so-called *coherences* or *phase-interferences* between different magnetic sublevels. Their physical meaning is illustrated, in a qualitative way, by the following example.

Suppose that a simple atomic system, namely a two-level atom with a lower level having $J = 0$ and an upper level having $J = 1$, is excited by a stationary radiation field tuned at the frequency of the atomic transition. If we choose a quantization direction for the atomic system, and take a reference system (xyz) with the z-axis in the quantization direction, the eigenvectors $|\alpha JM\rangle$ are of the form $|1\ -1\rangle$, $|1\ 0\rangle$, $|1\ 1\rangle$ for the upper level, and $|0\ 0\rangle$ for the lower level.

It will be proved later (see Sect. 7.1) that if the atom absorbs a photon propagating along any direction in the x-y plane and linearly polarized in the z-direction, it is excited from the level $|0\ 0\rangle$ to the level $|1\ 0\rangle$. Similarly, if the atom absorbs a circularly polarized photon propagating along the z-direction, it is excited to the level $|1\ 1\rangle$, or $|1\ -1\rangle$, according to the handedness of circular polarization. In all these cases, the diagonal matrix elements $\langle 1M|\,\rho\,|1M\rangle$ for the upper level attain a definite value, but the coherences remain zero.

For any other incidence direction, or any other polarization of the absorbed photon, the atom is excited to an upper level which is a linear combination of the form

$$c_{-1}\,|1\ -1\rangle + c_0\,|1\ 0\rangle + c_1\,|1\ 1\rangle = \sum_M c_M\,|1M\rangle\ ,$$

where the three coefficients c_M depend on the direction and polarization of the absorbed photon. In this case the coherences are non-zero and take the simple form

$$\langle 1M|\,\rho\,|1M'\rangle = c_M\,c^*_{M'}\ .$$

The physical meaning of coherences is just contained in this simple example. We will see in Sect. 5.13 how a qualitative analogy can be drawn between atomic coherences and interferences in classical oscillators.

Although coherences can be defined for any pair of magnetic sublevels, no matter how large is the energy difference between them, the most important are those between degenerate or quasi-degenerate sublevels. For such coherences one can introduce more compact symbols to simplify the notations; for instance, for the magnetic sublevels pertaining to an assigned term α one can write

$$\langle \alpha JM|\,\rho\,|\alpha J'M'\rangle = \rho_\alpha(JM, J'M')\ ,$$

and if the term is described by the L-S coupling scheme

$$\langle \beta LSJM|\,\rho\,|\beta LSJ'M'\rangle = \rho_{\beta LS}(JM, J'M')\ . \tag{3.90}$$

For the coherences between magnetic sublevels of the same J-level the following notation can be used

$$\langle \alpha JM|\,\rho\,|\alpha JM'\rangle = \rho_{\alpha J}(M, M')\ , \tag{3.91a}$$

and for the diagonal elements[1]

$$\langle \alpha JM|\,\rho\,|\alpha JM\rangle = \rho_{\alpha J}(M, M) = \rho_{\alpha J}(M)\ . \tag{3.91b}$$

The atomic density matrix can be defined in the presence of hyperfine structure as well. With obvious notations, for the matrix elements between different hyperfine-structure magnetic sublevels one can write in general

$$\langle \alpha JIFf|\,\rho\,|\alpha' J'IF'f'\rangle = \rho\,(\alpha JIFf, \alpha' J'IF'f')\ ,$$

and for the coherences between hyperfine-structure sublevels belonging to the same J-level

$$\langle \alpha JIFf|\,\rho\,|\alpha JIF'f'\rangle = \rho_{\alpha JI}(Ff, F'f')\ . \tag{3.92}$$

[1] The more compact notation $\rho_{\alpha J}(M)$ can be conveniently used in the physical situations where all the off-diagonal elements vanish.

Important relations can be established between the different quantities here introduced, like for instance between those defined in Eqs. (3.91) and those defined in Eq. (3.92). We can consider an atom with hyperfine structure as consisting of two separate parts, characterized by the eigenstates $|\alpha JM\rangle$ and $|IM_I\rangle$ (where M_I is the projection of the nuclear spin along the z-axis) and by the density operators $\rho^{(J)}$ and $\rho^{(I)}$, respectively. Since the quantum number I of the atomic system is fixed, we have from Eq. (3.87)

$$\sum_{M_I} \langle IM_I|\,\rho\,|IM_I\rangle = \rho^{(J)} ,$$

where ρ is the density operator of the whole system. Taking the matrix element of these operators between the eigenstates $|\alpha JM\rangle$ and $|\alpha JM'\rangle$ we get

$$\langle \alpha JM|\,\rho^{(J)}\,|\alpha JM'\rangle = \sum_{M_I} \langle \alpha JIMM_I|\,\rho\,|\alpha JIM'M_I\rangle ,$$

which relates the density-matrix elements in Eqs. (3.91) to those in Eq. (3.92). In the following we will use this kind of relations by dropping the apex (J), and we will simply write

$$\rho_{\alpha J}(M,M') = \sum_{M_I} \langle \alpha JIMM_I|\,\rho\,|\alpha JIM'M_I\rangle .$$

Changing the coupling scheme via Eq. (2.12) we have

$$\rho_{\alpha J}(M,M') = \sum_{FF'ff'M_I} \langle JIMM_I|JIFf\rangle\langle JIM'M_I|JIF'f'\rangle \times \langle \alpha JIFf|\,\rho\,|\alpha JIF'f'\rangle ,$$

or, in terms of 3-j symbols

$$\rho_{\alpha J}(M,M') = \sum_{FF'ff'M_I} (-1)^{f-f'}\sqrt{(2F+1)(2F'+1)} \times \begin{pmatrix} J & I & F \\ M & M_I & -f \end{pmatrix}\begin{pmatrix} J & I & F' \\ M' & M_I & -f' \end{pmatrix} \times \rho_{\alpha JI}(Ff,F'f') . \tag{3.93}$$

A similar relation can be established between the density-matrix elements relative to different J-levels of a term (Eq. (3.90)) and the density-matrix elements that one can define for the same term by neglecting its fine structure. Setting first

$$\langle \beta LM_L|\,\rho\,|\beta LM'_L\rangle = \rho_{\beta L}(M_L,M'_L) ,$$

where M_L is the projection of the orbital angular momentum on the z-axis, and then introducing the inner structure due to the spin, one obtains

$$\rho_{\beta L}(M_L, M'_L) = \sum_{JJ'MM'M_S} (-1)^{M-M'} \sqrt{(2J+1)(2J'+1)} \times \begin{pmatrix} L & S & J \\ M_L & M_S & -M \end{pmatrix} \begin{pmatrix} L & S & J' \\ M'_L & M_S & -M' \end{pmatrix} \times \rho_{\beta LS}(JM, J'M') \, . \tag{3.94}$$

We want to remark that the density-matrix elements on the basis of the eigenvectors of the angular momentum depend on the reference system chosen to define such eigenvectors. If R is the rotation that brings a reference system (the 'old' one) into another reference system (the 'new' one), the eigenvectors of the angular momentum in the new system are connected with those in the old system by the relation

$$|JM\rangle_{\text{new}} = D(R) \, |JM\rangle_{\text{old}} \, ,$$

so that the transformation law for the density-matrix elements is the following

$$\begin{aligned} &\Big[\rho\,(\alpha JM, \alpha' J'M')\Big]_{\text{new}} = \\ &= {}_{\text{new}}\langle \alpha JM| \, \rho \, |\alpha' J'M'\rangle_{\text{new}} = {}_{\text{old}}\langle \alpha JM| \, D^\dagger \rho D \, |\alpha' J'M'\rangle_{\text{old}} \\ &= \sum_{NN'} \mathcal{D}^J_{NM}(R)^* \, \mathcal{D}^{J'}_{N'M'}(R) \Big[\rho\,(\alpha JN, \alpha' J'N')\Big]_{\text{old}} \, . \end{aligned} \tag{3.95}$$

In particular, for the matrix elements diagonal with respect to α and J

$$\Big[\rho_{\alpha J}(M, M')\Big]_{\text{new}} = \sum_{NN'} \mathcal{D}^J_{NM}(R)^* \, \mathcal{D}^J_{N'M'}(R) \Big[\rho_{\alpha J}(N, N')\Big]_{\text{old}} \, . \tag{3.96}$$

3.7. Multipole Moments of the Density Matrix

As shown by Eq. (3.95), the transformation law for the density-matrix elements on the basis of the eigenvectors of the angular momentum involves the product of two rotation matrices. We can however construct – similarly to Sect. 2.7 – linear combinations of these matrix elements whose transformation law involves just one rotation matrix. By so doing we obtain the irreducible spherical components of the density matrix, which are often referred to as the *multipole moments of the density matrix* or the *spherical statistical tensors*.

Defining the multipole moments of the density matrix by the expression[1]

$$\rho^K_Q(\alpha J, \alpha' J') = \sum_{MM'} (-1)^{J-M} \sqrt{2K+1} \times \begin{pmatrix} J & J' & K \\ M & -M' & -Q \end{pmatrix} \rho\,(\alpha JM, \alpha' J' M') \,, \qquad (3.97)$$

it is easy to prove that, under the rotation R of the reference system, the multipole moments change according to the law

$$\left[\rho^K_Q(\alpha J, \alpha' J')\right]_{\text{new}} = \sum_{Q'} \left[\rho^K_{Q'}(\alpha J, \alpha' J')\right]_{\text{old}} \mathcal{D}^K_{Q'Q}(R)^* \,. \qquad (3.98)$$

The proof of Eq. (3.98) will not be given here, being quite similar to an analogous proof given in Sect. 2.7. We just want to remark that the factor $\sqrt{2K+1}$ in Eq. (3.97) is inessential: in fact, if this factor is replaced by an arbitrary function of K, Eq. (3.98) is still satisfied. The definition given in Eq. (3.97) is the same as Omont's (1977), but different authors give different definitions for the multipole moments, and no definition has a special advantage.

Comparison of Eqs. (3.98) and (2.78) shows that the transformation law for the multipole moments involves the complex conjugate of the rotation matrix, whereas the transformation law for irreducible spherical tensors involves the rotation matrix itself. Thus the multipole moments – as defined in Eq. (3.97) – are not, strictly speaking, irreducible spherical tensors. A different definition could be given by substituting $\rho\,(\alpha' J' M', \alpha J M)$ for $\rho\,(\alpha JM, \alpha' J' M')$ in Eq. (3.97), and the multipole moments so defined would indeed satisfy the transformation law for irreducible spherical tensors. However, this alternative definition has no advantages over ours.

Equation (3.97) can be easily inverted using the orthogonality relations of the 3-j symbols. From Eq. (2.23b) one obtains

$$\rho\,(\alpha JM, \alpha' J' M') = \sum_{KQ} (-1)^{J-M} \sqrt{2K+1} \times \begin{pmatrix} J & J' & K \\ M & -M' & -Q \end{pmatrix} \rho^K_Q(\alpha J, \alpha' J') \,. \qquad (3.99)$$

The conjugation property of the multipole moments follows from Eq. (3.97) and from the Hermitian character of the density operator

$$\rho^K_Q(\alpha J, \alpha' J')^* = (-1)^{J-J'-Q}\, \rho^K_{-Q}(\alpha' J', \alpha J) \,. \qquad (3.100)$$

Similarly to Sect. 3.6, one can introduce shorthand notations for the multipole moments when dealing with restricted subspaces. For instance, for the multipole moments relative to the magnetic sublevels of a term one can write

$$\rho^K_Q(\alpha J, \alpha J') = {}^{\alpha}\rho^K_Q(J, J') \,,$$

[1] Note that for any atom (or ion) the quantum numbers J and J' are both integers or both half-integers, thus the rank K of the multipole moments is always an integer.

and for the magnetic sublevels of a given J-level

$$\rho^K_Q(\alpha J, \alpha J) = \rho^K_Q(\alpha J)$$
$$= \sum_{MM'} (-1)^{J-M} \sqrt{2K+1} \begin{pmatrix} J & J & K \\ M & -M' & -Q \end{pmatrix} \rho_{\alpha J}(M, M') \,, \qquad (3.101)$$

with the conjugation property

$$\rho^K_Q(\alpha J)^* = (-1)^Q \, \rho^K_{-Q}(\alpha J) \,. \qquad (3.102)$$

The analytical expressions for the most common multipole moments, as functions of the ordinary density-matrix elements, are given in Tables 3.6 and 3.7.

The multipole moments can be also defined for a J-level having hyperfine structure. With self-evident notations, we have

$$^{\alpha JI}\rho^K_Q(F, F') = \sum_{ff'} (-1)^{F-f} \sqrt{2K+1}$$
$$\times \begin{pmatrix} F & F' & K \\ f & -f' & -Q \end{pmatrix} \rho_{\alpha JI}(Ff, F'f') \,. \qquad (3.103)$$

Relations similar to those in Eqs. (3.93) and (3.94) can be easily established for the multipole moments. From Eq. (3.93), after some Racah algebra involving the contraction of 3-j symbols (Eq. (2.42)), one obtains

$$\rho^K_Q(\alpha J) = \sum_{FF'} (-1)^{J+I+F'+K} \sqrt{(2F+1)(2F'+1)}$$
$$\times \begin{Bmatrix} F & F' & K \\ J & J & I \end{Bmatrix} {}^{\alpha JI}\rho^K_Q(F, F') \,. \qquad (3.104)$$

In a similar way, from Eq. (3.94) the following relation can be proved

$$\rho^K_Q(\beta L) = \sum_{JJ'} (-1)^{L+S+J'+K} \sqrt{(2J+1)(2J'+1)}$$
$$\times \begin{Bmatrix} J & J' & K \\ L & L & S \end{Bmatrix} {}^{\beta LS}\rho^K_Q(J, J') \,, \qquad (3.105)$$

where $\rho^K_Q(\beta L)$, the multipole moment for a spinless L-term, is defined by

$$\rho^K_Q(\beta L) = \sum_{M_L M'_L} (-1)^{L-M_L} \sqrt{2K+1} \begin{pmatrix} L & L & K \\ M_L & -M'_L & -Q \end{pmatrix} \rho_{\beta L}(M_L, M'_L) \,.$$

An important property of the multipole moments follows from the evaluation of the expectation value of an arbitrary spherical tensor operator T^K_Q. Denoting

TABLE 3.6

Analytical expressions for the multipole moments $\rho^K_Q(\alpha J)$ as functions of the matrix elements $\rho_{\alpha J}(M, M')$. The index (αJ) is suppressed for conciseness. The multipole moments for negative values of Q can be obtained through the relation $\rho^K_{-Q}(\alpha J) = (-1)^Q\, \rho^K_Q(\alpha J)^*$.

$J = 0$	$\rho^0_0 = \rho(0,0)$
$J = \frac{1}{2}$	$\rho^0_0 = \frac{1}{\sqrt{2}}\left[\rho(\frac{1}{2},\frac{1}{2}) + \rho(-\frac{1}{2},-\frac{1}{2})\right]$ $\rho^1_0 = \frac{1}{\sqrt{2}}\left[\rho(\frac{1}{2},\frac{1}{2}) - \rho(-\frac{1}{2},-\frac{1}{2})\right]$ $\rho^1_1 = -\rho(\frac{1}{2},-\frac{1}{2})$
$J = 1$	$\rho^0_0 = \frac{1}{\sqrt{3}}\left[\rho(1,1) + \rho(0,0) + \rho(-1,-1)\right]$ $\rho^1_0 = \frac{1}{\sqrt{2}}\left[\rho(1,1) - \rho(-1,-1)\right]$ $\rho^1_1 = -\frac{1}{\sqrt{2}}\left[\rho(1,0) + \rho(0,-1)\right]$ $\rho^2_0 = \frac{1}{\sqrt{6}}\left[\rho(1,1) - 2\,\rho(0,0) + \rho(-1,-1)\right]$ $\rho^2_1 = -\frac{1}{\sqrt{2}}\left[\rho(1,0) - \rho(0,-1)\right]$ $\rho^2_2 = \rho(1,-1)$
$J = \frac{3}{2}$	$\rho^0_0 = \frac{1}{2}\left[\rho(\frac{3}{2},\frac{3}{2}) + \rho(\frac{1}{2},\frac{1}{2}) + \rho(-\frac{1}{2},-\frac{1}{2}) + \rho(-\frac{3}{2},-\frac{3}{2})\right]$ $\rho^1_0 = \frac{1}{2\sqrt{5}}\left[3\,\rho(\frac{3}{2},\frac{3}{2}) + \rho(\frac{1}{2},\frac{1}{2}) - \rho(-\frac{1}{2},-\frac{1}{2}) - 3\,\rho(-\frac{3}{2},-\frac{3}{2})\right]$ $\rho^1_1 = -\frac{1}{\sqrt{10}}\left[\sqrt{3}\,\rho(\frac{3}{2},\frac{1}{2}) + 2\,\rho(\frac{1}{2},-\frac{1}{2}) + \sqrt{3}\,\rho(-\frac{1}{2},-\frac{3}{2})\right]$ $\rho^2_0 = \frac{1}{2}\left[\rho(\frac{3}{2},\frac{3}{2}) - \rho(\frac{1}{2},\frac{1}{2}) - \rho(-\frac{1}{2},-\frac{1}{2}) + \rho(-\frac{3}{2},-\frac{3}{2})\right]$ $\rho^2_1 = -\frac{1}{\sqrt{2}}\left[\rho(\frac{3}{2},\frac{1}{2}) - \rho(-\frac{1}{2},-\frac{3}{2})\right]$ $\rho^2_2 = \frac{1}{\sqrt{2}}\left[\rho(\frac{3}{2},-\frac{1}{2}) + \rho(\frac{1}{2},-\frac{3}{2})\right]$ $\rho^3_0 = \frac{1}{2\sqrt{5}}\left[\rho(\frac{3}{2},\frac{3}{2}) - 3\,\rho(\frac{1}{2},\frac{1}{2}) + 3\,\rho(-\frac{1}{2},-\frac{1}{2}) - \rho(-\frac{3}{2},-\frac{3}{2})\right]$ $\rho^3_1 = -\frac{1}{\sqrt{5}}\left[\rho(\frac{3}{2},\frac{1}{2}) - \sqrt{3}\,\rho(\frac{1}{2},-\frac{1}{2}) + \rho(-\frac{1}{2},-\frac{3}{2})\right]$ $\rho^3_2 = \frac{1}{\sqrt{2}}\left[\rho(\frac{3}{2},-\frac{1}{2}) - \rho(\frac{1}{2},-\frac{3}{2})\right]$ $\rho^3_3 = -\rho(\frac{3}{2},-\frac{3}{2})$
$J = 2$	$\rho^0_0 = \frac{1}{\sqrt{5}}\left[\rho(2,2) + \rho(1,1) + \rho(0,0) + \rho(-1,-1) + \rho(-2,-2)\right]$ $\rho^1_0 = \frac{1}{\sqrt{10}}\left[2\,\rho(2,2) + \rho(1,1) - \rho(-1,-1) - 2\,\rho(-2,-2)\right]$ $\rho^1_1 = -\frac{1}{\sqrt{10}}\left[\sqrt{2}\,\rho(2,1) + \sqrt{3}\,\rho(1,0) + \sqrt{3}\,\rho(0,-1) + \sqrt{2}\,\rho(-1,-2)\right]$ $\rho^2_0 = \frac{1}{\sqrt{14}}\left[2\,\rho(2,2) - \rho(1,1) - 2\,\rho(0,0) - \rho(-1,-1) + 2\,\rho(-2,-2)\right]$ $\rho^2_1 = -\frac{1}{\sqrt{14}}\left[\sqrt{6}\,\rho(2,1) + \rho(1,0) - \rho(0,-1) - \sqrt{6}\,\rho(-1,-2)\right]$ $\rho^2_2 = \frac{1}{\sqrt{7}}\left[\sqrt{2}\,\rho(2,0) + \sqrt{3}\,\rho(1,-1) + \sqrt{2}\,\rho(0,-2)\right]$

TABLE 3.6

(continued)

$J=2$	$\rho_0^3 = \frac{1}{\sqrt{10}}\left[\rho(2,2) - 2\,\rho(1,1) + 2\,\rho(-1,-1) - \rho(-2,-2)\right]$
	$\rho_1^3 = -\frac{1}{\sqrt{10}}\left[\sqrt{3}\,\rho(2,1) - \sqrt{2}\,\rho(1,0) - \sqrt{2}\,\rho(0,-1) + \sqrt{3}\,\rho(-1,-2)\right]$
	$\rho_2^3 = \frac{1}{\sqrt{2}}\left[\rho(2,0) - \rho(0,-2)\right]$
	$\rho_3^3 = -\frac{1}{\sqrt{2}}\left[\rho(2,-1) + \rho(1,-2)\right]$
	$\rho_0^4 = \frac{1}{\sqrt{70}}\left[\rho(2,2) - 4\,\rho(1,1) + 6\,\rho(0,0) - 4\,\rho(-1,-1) + \rho(-2,-2)\right]$
	$\rho_1^4 = -\frac{1}{\sqrt{14}}\left[\rho(2,1) - \sqrt{6}\,\rho(1,0) + \sqrt{6}\,\rho(0,-1) - \rho(-1,-2)\right]$
	$\rho_2^4 = \frac{1}{\sqrt{14}}\left[\sqrt{3}\,\rho(2,0) - 2\sqrt{2}\,\rho(1,-1) + \sqrt{3}\,\rho(0,-2)\right]$
	$\rho_3^4 = -\frac{1}{\sqrt{2}}\left[\rho(2,-1) - \rho(1,-2)\right]$
	$\rho_4^4 = \rho(2,-2)$

by $\langle T_Q^K \rangle$ its expectation value, and referring, for simplicity, to an atom devoid of hyperfine structure, we have

$$\langle T_Q^K \rangle = \mathrm{Tr}\left(\rho\, T_Q^K\right) = \sum_{\alpha' J' M'} \langle \alpha' J' M' |\, \rho\, T_Q^K | \alpha' J' M' \rangle \ .$$

Introducing between ρ and T_Q^K the completeness relation

$$1 = \sum_{\alpha J M} |\alpha J M\rangle \langle \alpha J M| \ ,$$

and applying the Wigner-Eckart theorem (Eq. (2.96)) and Eq. (3.99), one obtains

$$\langle T_Q^K \rangle = \sum_{\alpha \alpha' J J'} \sqrt{\frac{2J+1}{2K+1}}\, \langle \alpha J \| \boldsymbol{T}^K \| \alpha' J' \rangle\, \rho_Q^K(\alpha J, \alpha' J')^* \ , \tag{3.106}$$

which shows that the expectation value of a spherical tensor operator is strictly connected with the multipole moments of the same rank.

Let's now consider the physical meaning of the multipole moments. For the 0-rank moment, we have from Eq. (3.101)

$$\rho_0^0(\alpha J) = \frac{1}{\sqrt{2J+1}} \sum_M \rho_{\alpha J}(M,M) \ , \tag{3.107}$$

so that the overall population $n_{\alpha J}$ of the (αJ)-level is given by

$$n_{\alpha J} = \sqrt{2J+1}\, \rho_0^0(\alpha J) \ . \tag{3.108}$$

TABLE 3.7

Analytical expressions for the multipole moments ${}^{\alpha}\rho^K_Q(J,J')$ as functions of the matrix elements $\rho_\alpha(JM,J'M')$. The index α is suppressed for conciseness. The multipole moments ${}^{\alpha}\rho^K_Q(J',J)$ can be obtained through the relation ${}^{\alpha}\rho^K_Q(J',J) = (-1)^{J-J'+Q}\ {}^{\alpha}\rho^K_{-Q}(J,J')^*$.

$J=0$	$\rho^1_1(0,1) = \rho(0\,0,1\,-1)$
$J'=1$	$\rho^1_0(0,1) = -\rho(0\,0,1\,0)$
	$\rho^1_{-1}(0,1) = \rho(0\,0,1\,1)$
$J=\frac{1}{2}$	$\rho^1_1(\frac{1}{2},\frac{3}{2}) = \frac{1}{2}\left[\rho(\frac{1}{2}\,\frac{1}{2},\frac{3}{2}\,-\frac{1}{2}) + \sqrt{3}\,\rho(\frac{1}{2}\,-\frac{1}{2},\frac{3}{2}\,-\frac{3}{2})\right]$
$J'=\frac{3}{2}$	$\rho^1_0(\frac{1}{2},\frac{3}{2}) = -\frac{1}{\sqrt{2}}\left[\rho(\frac{1}{2}\,\frac{1}{2},\frac{3}{2}\,\frac{1}{2}) + \rho(\frac{1}{2}\,-\frac{1}{2},\frac{3}{2}\,-\frac{1}{2})\right]$
	$\rho^1_{-1}(\frac{1}{2},\frac{3}{2}) = \frac{1}{2}\left[\sqrt{3}\,\rho(\frac{1}{2}\,\frac{1}{2},\frac{3}{2}\,\frac{3}{2}) + \rho(\frac{1}{2}\,-\frac{1}{2},\frac{3}{2}\,\frac{1}{2})\right]$
	$\rho^2_2(\frac{1}{2},\frac{3}{2}) = -\rho(\frac{1}{2}\,\frac{1}{2},\frac{3}{2}\,-\frac{3}{2})$
	$\rho^2_1(\frac{1}{2},\frac{3}{2}) = \frac{1}{2}\left[\sqrt{3}\,\rho(\frac{1}{2}\,\frac{1}{2},\frac{3}{2}\,-\frac{1}{2}) - \rho(\frac{1}{2}\,-\frac{1}{2},\frac{3}{2}\,-\frac{3}{2})\right]$
	$\rho^2_0(\frac{1}{2},\frac{3}{2}) = -\frac{1}{\sqrt{2}}\left[\rho(\frac{1}{2}\,\frac{1}{2},\frac{3}{2}\,\frac{1}{2}) - \rho(\frac{1}{2}\,-\frac{1}{2},\frac{3}{2}\,-\frac{1}{2})\right]$
	$\rho^2_{-1}(\frac{1}{2},\frac{3}{2}) = \frac{1}{2}\left[\rho(\frac{1}{2}\,\frac{1}{2},\frac{3}{2}\,\frac{3}{2}) - \sqrt{3}\,\rho(\frac{1}{2}\,-\frac{1}{2},\frac{3}{2}\,\frac{1}{2})\right]$
	$\rho^2_{-2}(\frac{1}{2},\frac{3}{2}) = \rho(\frac{1}{2}\,-\frac{1}{2},\frac{3}{2}\,\frac{3}{2})$
$J=1$	$\rho^1_1(1,2) = \frac{1}{\sqrt{10}}\left[\rho(1\,1,2\,0) + \sqrt{3}\,\rho(1\,0,2\,-1) + \sqrt{6}\,\rho(1\,-1,2\,-2)\right]$
$J'=2$	$\rho^1_0(1,2) = -\frac{1}{\sqrt{10}}\left[\sqrt{3}\,\rho(1\,1,2\,1) + 2\,\rho(1\,0,2\,0) + \sqrt{3}\,\rho(1\,-1,2\,-1)\right]$
	$\rho^1_{-1}(1,2) = \frac{1}{\sqrt{10}}\left[\sqrt{6}\,\rho(1\,1,2\,2) + \sqrt{3}\,\rho(1\,0,2\,1) + \rho(1\,-1,2\,0)\right]$
	$\rho^2_2(1,2) = -\frac{1}{\sqrt{3}}\left[\rho(1\,1,2\,-1) + \sqrt{2}\,\rho(1\,0,2\,-2)\right]$
	$\rho^2_1(1,2) = \frac{1}{\sqrt{6}}\left[\sqrt{3}\,\rho(1\,1,2\,0) + \rho(1\,0,2\,-1) - \sqrt{2}\,\rho(1\,-1,2\,-2)\right]$
	$\rho^2_0(1,2) = -\frac{1}{\sqrt{2}}\left[\rho(1\,1,2\,1) - \rho(1\,-1,2\,-1)\right]$
	$\rho^2_{-1}(1,2) = \frac{1}{\sqrt{6}}\left[\sqrt{2}\,\rho(1\,1,2\,2) - \rho(1\,0,2\,1) - \sqrt{3}\,\rho(1\,-1,2\,0)\right]$
	$\rho^2_{-2}(1,2) = \frac{1}{\sqrt{3}}\left[\sqrt{2}\,\rho(1\,0,2\,2) + \rho(1\,-1,2\,1)\right]$
	$\rho^3_3(1,2) = \rho(1\,1,2\,-2)$
	$\rho^3_2(1,2) = -\frac{1}{\sqrt{3}}\left[\sqrt{2}\,\rho(1\,1,2\,-1) - \rho(1\,0,2\,-2)\right]$
	$\rho^3_1(1,2) = \frac{1}{\sqrt{15}}\left[\sqrt{6}\,\rho(1\,1,2\,0) - 2\sqrt{2}\,\rho(1\,0,2\,-1) + \rho(1\,-1,2\,-2)\right]$
	$\rho^3_0(1,2) = -\frac{1}{\sqrt{5}}\left[\rho(1\,1,2\,1) - \sqrt{3}\,\rho(1\,0,2\,0) + \rho(1\,-1,2\,-1)\right]$
	$\rho^3_{-1}(1,2) = \frac{1}{\sqrt{15}}\left[\rho(1\,1,2\,2) - 2\sqrt{2}\,\rho(1\,0,2\,1) + \sqrt{6}\,\rho(1\,-1,2\,0)\right]$
	$\rho^3_{-2}(1,2) = \frac{1}{\sqrt{3}}\left[\rho(1\,0,2\,2) - \sqrt{2}\,\rho(1\,-1,2\,1)\right]$
	$\rho^3_{-3}(1,2) = \rho(1\,-1,2\,2)$

To give a physical interpretation to the other multipole moments, let us consider the spherical tensor operators J^K_Q that can be constructed with the rectangular components J_x, J_y, and J_z of the angular momentum according to Eqs. (2.82) and (2.84). Assuming for simplicity the density-matrix elements to be non-zero for just one (αJ)-level, from Eqs. (3.106) and (2.97) we obtain

$$\langle J^1_0 \rangle = \langle J_z \rangle = \sqrt{\frac{J(J+1)(2J+1)}{3}}\, \rho^1_0(\alpha J)$$

$$\langle J^1_1 \rangle = \Big\langle -\frac{1}{\sqrt{2}}\,(J_x + \mathrm{i}\, J_y) \Big\rangle = \sqrt{\frac{J(J+1)(2J+1)}{3}}\, \rho^1_1(\alpha J)^* \ ,$$

which give after inversion[1]

$$\rho^1_0(\alpha J) = \sqrt{3}\, \frac{1}{\sqrt{J(J+1)(2J+1)}}\, \langle J_z \rangle$$

$$\mathrm{Re}\Big[\rho^1_1(\alpha J)\Big] = -\sqrt{\frac{3}{2}}\, \frac{1}{\sqrt{J(J+1)(2J+1)}} \langle J_x \rangle$$

$$\mathrm{Im}\Big[\rho^1_1(\alpha J)\Big] = \sqrt{\frac{3}{2}}\, \frac{1}{\sqrt{J(J+1)(2J+1)}} \langle J_y \rangle \ . \tag{3.109}$$

These formulae show that the multipole moments of rank 1 are connected with the average value of the angular momentum components on the axes x, y, and z. When such values are non-zero, there is a preferred direction in space, identified by the vector $\langle \vec{J} \rangle$, along which the atom may be thought to be oriented. For this reason the multipole moments of rank 1 are called the *orientation* components of the density matrix.

For the tensors of rank 2 one obtains, again from Eq. (3.106)[2]

$$\rho^2_0(\alpha J) = \sqrt{5}\, f(J)\, \langle 2J_z^2 - J_x^2 - J_y^2 \rangle \tag{3.110a}$$

$$\mathrm{Re}\Big[\rho^2_1(\alpha J)\Big] = -\sqrt{\frac{15}{2}}\, f(J)\, \langle J_z J_x + J_x J_z \rangle \tag{3.110b}$$

$$\mathrm{Im}\Big[\rho^2_1(\alpha J)\Big] = \sqrt{\frac{15}{2}}\, f(J)\, \langle J_y J_z + J_z J_y \rangle \tag{3.110c}$$

$$\mathrm{Re}\Big[\rho^2_2(\alpha J)\Big] = \sqrt{\frac{15}{2}}\, f(J)\, \langle J_x^2 - J_y^2 \rangle \tag{3.110d}$$

$$\mathrm{Im}\Big[\rho^2_2(\alpha J)\Big] = -\sqrt{\frac{15}{2}}\, f(J)\, \langle J_x J_y + J_y J_x \rangle \tag{3.110e}$$

[1] Note that, for $J = 0$, the quantities ρ^1_Q are identically zero as it follows directly from Eq. (3.101). Equations (3.109) are valid for $J \neq 0$ only. For the same reason Eqs. (3.110) are valid for $J \geq 1$ only.

[2] Note that the operators $(J_i J_k + J_k J_i)$, $(i, k = x, y, z)$ are Hermitian, so that their expectation values are real.

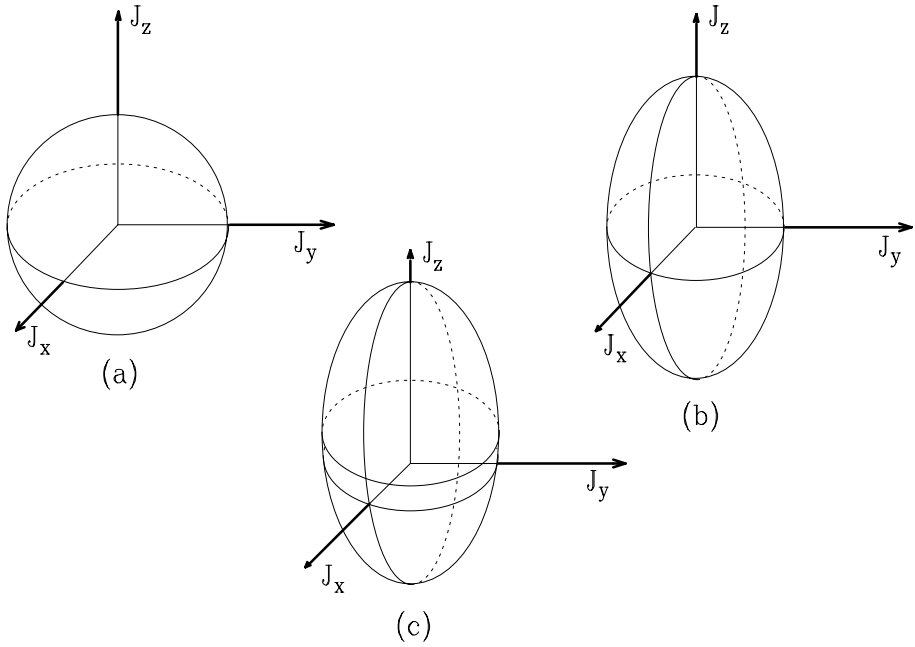

Fig.3.13. To get an intuitive grasp of the meaning of the orientation and alignment components of the density matrix, we can regard the atomic angular momentum as having a uniform probability of being found on the surface of the figures drawn above. For the sphere in panel (a), the atom is neither oriented nor aligned; for the ellipsoid in panel (b) the atom is aligned but not oriented; finally, for the ellipsoid in panel (c) the atom is both oriented and aligned. To have an example of an atom oriented but not aligned we can go back to panel (a) and regard the angular momentum as having more probability of being found on the upper hemisphere than on the lower one.

with

$$f(J) = \frac{1}{\sqrt{J(J+1)(2J-1)(2J+1)(2J+3)}} \,,$$

the reduced matrix element $\langle \alpha J \| \boldsymbol{J}^2 \| \alpha J \rangle$ having been evaluated via Eqs. (2.102) and (2.36h).

The formulae now deduced show that the multipole moments of rank 2 are connected with the average value of bilinear combinations of the angular momentum components J_x, J_y, and J_z. These multipole moments are called the *alignment* components of the density matrix. The word 'alignment', as opposed to 'orientation', is used in this context to mean that the atom may be regarded as aligned with a particular straight line in space, irrespective, however, of which direction is chosen on the line. In Fig. 3.13 we give an intuitive illustration of the meaning of the multipole moments of rank 1 and 2.

Turning to multipole moments of higher rank, it is possible to show that those of rank n are connected with the average values of polynomials of degree n in the angular momentum components J_x, J_y, and J_z. No particular name has been assigned to these moments.

Another general property of multipole moments, which follows directly from the definition (3.97), should be remarked: a moment of the form ρ^K_Q ($Q \neq 0$) is a linear combination of coherences between states characterized by projections of the angular momentum differing by Q; a moment of the form ρ^K_0 is a linear combination of populations.

Finally, some inequalities can be established for the multipole moments as a consequence of Eq. (3.85). Taking the square modulus of Eq. (3.101) and summing over K and Q we obtain

$$\sum_{KQ} |\rho^K_Q(\alpha J)|^2 = \sum_{MM'} |\rho_{\alpha J}(M, M')|^2 \; ;$$

on the other hand, from Eqs. (3.107) and (3.85) we have

$$\begin{aligned} \Big[\rho^0_0(\alpha J)\Big]^2 &= \frac{1}{2J+1} \sum_{MM'} \rho_{\alpha J}(M, M)\, \rho_{\alpha J}(M', M') \\ &\geq \frac{1}{2J+1} \sum_{MM'} |\rho_{\alpha J}(M, M')|^2 \; , \end{aligned}$$

and from these two relations we get

$$\sum_{K\neq 0} \sum_{Q} |\rho^K_Q(\alpha J)|^2 \leq 2J \Big[\rho^0_0(\alpha J)\Big]^2 \; .$$

Similarly, for the multipole moments connecting two levels (αJ), $(\alpha' J')$ one obtains, starting from Eq. (3.97)

$$\sum_{KQ} |\rho^K_Q(\alpha J, \alpha' J')|^2 \leq \sqrt{(2J+1)(2J'+1)}\; \rho^0_0(\alpha J)\, \rho^0_0(\alpha' J') \; .$$

Another important inequality can be established for the quantities $\rho^K_0(\alpha J)$. From Eq. (3.101) we have

$$\rho^K_0(\alpha J) = \sqrt{2K+1} \sum_M (-1)^{J-M} \begin{pmatrix} J & J & K \\ M & -M & 0 \end{pmatrix} \rho_{\alpha J}(M, M) \; .$$

On the other hand, all the quantities $\rho_{\alpha J}(M, M)$ are non-negative (see Eq. (3.81)); since their sum equals $[2J+1]^{1/2}\, \rho^0_0(\alpha J)$, we can write

$$|\rho^K_0(\alpha J)| \leq \sqrt{(2K+1)(2J+1)} \left| \begin{pmatrix} J & J & K \\ \tilde{M} & -\tilde{M} & 0 \end{pmatrix} \right| \rho^0_0(\alpha J) \; ,$$

where $\tilde{M}$ is the M-value giving the largest absolute value for the 3-j symbol.

CHAPTER 4

QUANTIZATION OF THE ELECTROMAGNETIC FIELD (NON-RELATIVISTIC THEORY)

Many of the physical phenomena involved in the generation and the transfer of polarized radiation in spectral lines can indeed be described by means of the classical theories of the electron and of the radiation field. In Chap. 5 we will apply these theories to obtain a simple derivation of the radiative transfer equations for polarized radiation and of the law of resonance scattering in the presence of a magnetic field.

However, only the most simplified cases are accurately described by the classical theory. As far as the atomic system is concerned, the classical theory of the electron gives an appropriate representation only of a two-level atom with a normal Zeeman triplet and an unpolarized ground level, so that its applicability is very limited. Similarly, the classical description of the radiation field prevents the correct treatment of important phenomena such as, for instance, stimulated emission.

In the main body of this book the interaction between atomic systems and the electromagnetic field will be described through a full quantum-mechanical formalism: this will allow us to handle even the most complicated physical situations without being obliged to introduce additional terms into the relevant equations by using phenomenological or heuristic arguments. To this aim, we need however the formalism of *second quantization* for the electromagnetic field, a formalism that we are going to develop in this chapter.

We also want to remark that the formalism of second quantization for the radiation field is a classical subsection of quantum field theory and has been fully treated in excellent monographs (see for instance Dirac, 1935; Heitler, 1954; Akhiezer and Berestetskii, 1965). The reason why these concepts are again developed in this book is to establish on a firm basis a set of notations that will be employed in the following. On the other hand, in view of the physical applications that will be presented later, the formalism of second quantization needs not to be developed in its general, relativistically invariant form. We will thus restrict attention to the simpler non-relativistic formulation, while we refer the reader to the textbooks quoted above for an introduction to invariant formalisms.

4.1. Quantization of the Harmonic Oscillator

The quantization of the harmonic oscillator is at the basis of the formalism of second quantization, because, as it will be shown in the following, the Hamiltonian of the electromagnetic field reduces to the sum of an infinite number of independent Hamiltonians each formally equal to that of the harmonic oscillator.

The classical Hamiltonian of a one-dimensional harmonic oscillator, expressed as a function of the canonical variables q and p, is given by

$$H(q,p) = \frac{p^2}{2m} + \frac{m\omega^2}{2}\, q^2 \ , \tag{4.1}$$

where m and ω are the mass and the angular frequency of the oscillating particle, respectively. The Hamilton equations give for the particle motion

$$\frac{\mathrm{d}q}{\mathrm{d}t} = \frac{\partial H(q,p)}{\partial p} = \frac{p}{m}$$
$$\frac{\mathrm{d}p}{\mathrm{d}t} = -\frac{\partial H(q,p)}{\partial q} = -m\omega^2 q.$$

To solve these coupled equations we introduce, following Dirac (1935), two linear combinations of the variables q and p of the form

$$a = A\,(p - \mathrm{i}\, m\omega q) \ , \qquad a^* = A\,(p + \mathrm{i}\, m\omega q) \ , \tag{4.2}$$

where A is a real constant which, for the moment, does not need to be specified. Taking the time derivative of these quantities we get the equations

$$\frac{\mathrm{d}a}{\mathrm{d}t} = -\mathrm{i}\,\omega a \ , \qquad \frac{\mathrm{d}a^*}{\mathrm{d}t} = \mathrm{i}\,\omega a^* \ ,$$

which have the obvious solution

$$a = a_0\, \mathrm{e}^{-\mathrm{i}\omega t} \ , \qquad a^* = a_0^*\, \mathrm{e}^{\mathrm{i}\omega t} \ , \tag{4.3}$$

with a_0 to be determined from the initial conditions. Inversion of Eqs. (4.2) yields the solution to the classical problem

$$q = \frac{\mathrm{i}}{2m\omega A}\,(a - a^*) \ , \qquad p = \frac{1}{2A}\,(a + a^*) \ ,$$

with a and a^* given by Eqs. (4.3).

The corresponding quantum-mechanical problem can be treated along the lines of the Correspondence Principle. The Hamiltonian is still given by Eq. (4.1), but q and p are now Hermitian operators obeying the commutation rule

$$[q,p] = \mathrm{i}\hbar \ .$$

To solve the quantum-mechanical problem we introduce the operator a defined as in Eqs. (4.2) and its Hermitian conjugate $a^\dagger$ defined as a^* in Eqs. (4.2). Expressing the Hamiltonian in terms of a and $a^\dagger$ we obtain

$$H = \frac{1}{4mA^2}\,(a\,a^\dagger + a^\dagger a) \ ,$$

and evaluating the commutator of a and $a^\dagger$ we get

$$[a, a^\dagger] = 2A^2 m\hbar\omega \; .$$

We now choose the constant A in such a way as to make this commutator equal to unity; expressing $a\,a^\dagger$ in terms of $a^\dagger a$ we get

$$H = \hbar\omega \left(a^\dagger a + \frac{1}{2} \right)$$

with

$$[a, a^\dagger] = 1 \; . \tag{4.4}$$

To find the eigenvalues and the eigenvectors of H, first of all we observe that if $|v\rangle$ is an eigenvector of H corresponding to the eigenvalue v,

$$H|v\rangle = v\,|v\rangle \; ,$$

we have

$$\langle v|a^\dagger a|v\rangle = \langle v| \frac{H}{\hbar\omega} - \frac{1}{2}\,|v\rangle = \left(\frac{v}{\hbar\omega} - \frac{1}{2} \right) \langle v|v\rangle \; .$$

Since the left-hand side of this equality is the square modulus of the vector $a\,|v\rangle$, it must be non-negative, so that we obtain

$$v \geq \frac{1}{2}\,\hbar\omega \; , \tag{4.5}$$

which means that all the eigenvalues are larger than $\hbar\omega/2$.

Next we observe that, owing to the commutation relations

$$[H, a] = -\hbar\omega a \; , \qquad [H, a^\dagger] = \hbar\omega a^\dagger \; , \tag{4.6}$$

we have

$$Ha\,|v\rangle = (aH - \hbar\omega\, a)|v\rangle = (v - \hbar\omega)\, a\,|v\rangle \; ,$$

which means that the vector $a\,|v\rangle$ is an eigenvector of the Hamiltonian H corresponding to the eigenvalue $(v - \hbar\omega)$.

Similarly, it can be easily shown that the vector $a^2|v\rangle$ is an eigenvector of H corresponding to the eigenvalue $(v - 2\hbar\omega)$, and, in general, that the vector $a^n|v\rangle$ is an eigenvector corresponding to the eigenvalue $(v - n\hbar\omega)$. The chain of eigenvectors $a\,|v\rangle$, $a^2|v\rangle, \ldots, a^n|v\rangle, \ldots$, corresponding to smaller and smaller eigenvalues, must however be limited, because otherwise property (4.5) would be violated. This means that it must exist an eigenvector, which we denote by the symbol $|0\rangle$, such that

$$a\,|0\rangle = 0 \; . \tag{4.7}$$

For this eigenvector we have

$$H\,|0\rangle = \hbar\omega \left(a^\dagger a + \frac{1}{2} \right) |0\rangle = \frac{1}{2}\,\hbar\omega\,|0\rangle \; .$$

Conversely, from the eigenvector $|0\rangle$ one can construct different eigenvectors corresponding to larger and larger eigenvalues. In fact, from Eq. (4.6) we obtain

$$H a^\dagger |0\rangle = \left(a^\dagger H + \hbar\omega\, a^\dagger\right)|0\rangle = \frac{3}{2}\,\hbar\omega\, a^\dagger |0\rangle \ ,$$

and, in general

$$H a^{\dagger n} |0\rangle = \left(n + \frac{1}{2}\right)\hbar\omega\, a^{\dagger n} |0\rangle \ .$$

The eigenvector $a^{\dagger n}|0\rangle$, however, needs to be normalized. Assuming the eigenvector $|0\rangle$ to be normalized,

$$\langle 0|0\rangle = 1 \ ,$$

it is easy to prove via Eqs. (4.4) and (4.7) that

$$\langle 0|a^n a^{\dagger n}|0\rangle = n! \ .$$

The normalized eigenvectors of the Hamiltonian H, which we denote by the symbol $|n\rangle$, are therefore defined by

$$|n\rangle = \frac{1}{\sqrt{n!}}\, a^{\dagger n}|0\rangle \ ,$$

and are such that

$$\begin{aligned} H\,|n\rangle &= \left(n + \frac{1}{2}\right)\hbar\omega\,|n\rangle \\ a\,|n\rangle &= \sqrt{n}\;|n-1\rangle \\ a^\dagger|n\rangle &= \sqrt{n+1}\;|n+1\rangle \ . \end{aligned} \tag{4.8}$$

To conclude, the energy spectrum of the Hamiltonian of the harmonic oscillator consists of a series of equispaced energy levels of the form $(n+1/2)\,\hbar\omega$. The integer n can be regarded as the number of a sort of particles, or discrete quanta, of energy $\hbar\omega$ that can be created or destroyed and whose presence contributes to the total energy of the harmonic oscillator. Formulae (4.8) show that the operator a, when acting on an eigenvector, has the effect of decreasing the number of particles, while the operator $a^\dagger$ has the opposite effect of increasing it. For this reason the operators $a^\dagger$ and a are called the *creation* and the *destruction* (or *annihilation*) operators, respectively.

4.2. The Electromagnetic Field as a Superposition of Plane Waves

Consider the electromagnetic field enclosed in a cubic cavity having its sides equal to L. In the absence of charges and currents, one can choose a special case of the

Lorentz gauge where the scalar potential $\phi(\vec{r},t)$ is identically zero, so that the field is described only by the vector potential $\vec{A}(\vec{r},t)$ which obeys the wave equation

$$\nabla^2\vec{A}(\vec{r},t) - \frac{1}{c^2}\frac{\partial^2}{\partial t^2}\vec{A}(\vec{r},t) = 0\ . \tag{4.9}$$

The Lorentz gauge is now expressed by[1]

$$\operatorname{div}\vec{A}(\vec{r},t) = 0\ . \tag{4.10}$$

The electric and magnetic fields are connected with $\vec{A}(\vec{r},t)$ by the relations

$$\begin{aligned}\vec{E}(\vec{r},t) &= -\frac{1}{c}\frac{\partial}{\partial t}\vec{A}(\vec{r},t)\\ \vec{B}(\vec{r},t) &= \operatorname{curl}\vec{A}(\vec{r},t)\ .\end{aligned} \tag{4.11}$$

At any given time t the vector potential, as well as any other physical function of $\vec{r}$, can be expanded in Fourier series. If we require that the vector potential obey the so-called *periodicity conditions*

$$\vec{A}(x,y,z,t) = \vec{A}(x+m_xL, y+m_yL, z+m_zL, t)$$

with m_x, m_y, m_z arbitrary integers, we obtain

$$\vec{A}(\vec{r},t) = \sum_{\vec{k}}\vec{C}_{\vec{k}}(t)\ \mathrm{e}^{\mathrm{i}\vec{k}\cdot\vec{r}}\ , \tag{4.12}$$

where the summation is extended to all the values of $\vec{k}$ satisfying the periodicity conditions

$$\vec{k} = \left(n_x\frac{2\pi}{L}, n_y\frac{2\pi}{L}, n_z\frac{2\pi}{L}\right)\ , \tag{4.13}$$

with n_x, n_y, n_z arbitrary integers. Because of the real character of the function $\vec{A}(\vec{r},t)$, the complex vector $\vec{C}_{\vec{k}}(t)$ satisfies the conjugation property

$$\vec{C}_{\vec{k}}(t)^* = \vec{C}_{-\vec{k}}(t)\ .$$

We now require that the vector potential $\vec{A}$ obey the wave equation (4.9). This means

$$\frac{\mathrm{d}^2\vec{C}_{\vec{k}}(t)}{\mathrm{d}t^2} = -\omega_{\vec{k}}^2\,\vec{C}_{\vec{k}}(t)\ , \tag{4.14}$$

where

$$\omega_{\vec{k}} = c\,|\vec{k}|\ . \tag{4.15}$$

[1] Note that Eq. (4.10) is not relativistically invariant.

Equation (4.14) can be easily solved to give

$$\vec{C}_{\vec{k}}(t) = \vec{C}^{(-)}_{\vec{k}}\, \mathrm{e}^{-\mathrm{i}\omega_{\vec{k}}t} + \vec{C}^{(+)}_{\vec{k}}\, \mathrm{e}^{\mathrm{i}\omega_{\vec{k}}t} \,,$$

where $\vec{C}^{(-)}_{\vec{k}}$ and $\vec{C}^{(+)}_{\vec{k}}$ are constants. Substituting into Eq. (4.12) we obtain

$$\vec{A}(\vec{r},t) = \sum_{\vec{k}} \vec{C}^{(-)}_{\vec{k}}\, \mathrm{e}^{\mathrm{i}(\vec{k}\cdot\vec{r}-\omega_{\vec{k}}t)} + \sum_{\vec{k}} \vec{C}^{(+)}_{\vec{k}}\, \mathrm{e}^{\mathrm{i}(\vec{k}\cdot\vec{r}+\omega_{\vec{k}}t)} \tag{4.16}$$

with

$$\vec{C}^{(-)*}_{\vec{k}} = \vec{C}^{(+)}_{-\vec{k}} \,.$$

The vector potential in Eq. (4.16) is decomposed into progressive and regressive waves. Taking into account that $\omega_{\vec{k}} = \omega_{-\vec{k}}$, we write the exponential of the regressive wave term in the form

$$\mathrm{e}^{\mathrm{i}(\vec{k}\cdot\vec{r}+\omega_{\vec{k}}t)} = \mathrm{e}^{-\mathrm{i}(-\vec{k}\cdot\vec{r}-\omega_{-\vec{k}}t)}$$

and then we change the summation index of this term from $\vec{k}$ to -$\vec{k}$ to obtain

$$\vec{A}(\vec{r},t) = \sum_{\vec{k}} \left[\vec{C}^{(-)}_{\vec{k}}\, \mathrm{e}^{\mathrm{i}(\vec{k}\cdot\vec{r}-\omega_{\vec{k}}t)} + \vec{C}^{(-)*}_{\vec{k}}\, \mathrm{e}^{-\mathrm{i}(\vec{k}\cdot\vec{r}-\omega_{\vec{k}}t)} \right] .$$

The supplementary condition (4.10) implies, for any $\vec{k}$,

$$\vec{k}\cdot\vec{C}^{(-)}_{\vec{k}} = 0 \,,$$

which is a transversality condition holding for any Fourier component of the vector potential. This relation can be satisfied in the following way. For any wavevector $\vec{k}$ we define two complex unit vectors $\vec{e}_{\vec{k}\lambda}$ $(\lambda = 1, 2)$ both perpendicular to $\vec{k}$ and perpendicular to each other,

$$\vec{e}_{\vec{k}\lambda}\cdot\vec{k} = 0 \,, \qquad \vec{e}_{\vec{k}\lambda}\cdot\vec{e}^{\,*}_{\vec{k}\lambda'} = \delta_{\lambda\lambda'} \,. \tag{4.17}$$

Next we write

$$\vec{C}^{(-)}_{\vec{k}}\, \mathrm{e}^{-\mathrm{i}\omega_{\vec{k}}t} = \sum_{\lambda=1,2} c_{\vec{k}\lambda}(t)\, \vec{e}_{\vec{k}\lambda} \,,$$

where $c_{\vec{k}\lambda}(t)$ are oscillatory functions satisfying the differential equation

$$\frac{\mathrm{d}}{\mathrm{d}t}\, c_{\vec{k}\lambda}(t) = -\mathrm{i}\,\omega_{\vec{k}}\, c_{\vec{k}\lambda}(t) \,, \tag{4.18}$$

and we finally obtain

$$\vec{A}(\vec{r},t) = \sum_{\vec{k}\lambda} \left[c_{\vec{k}\lambda}(t)\, \vec{e}_{\vec{k}\lambda}\, \mathrm{e}^{\mathrm{i}\vec{k}\cdot\vec{r}} + c_{\vec{k}\lambda}(t)^*\, \vec{e}^{\,*}_{\vec{k}\lambda}\, \mathrm{e}^{-\mathrm{i}\vec{k}\cdot\vec{r}} \right] , \tag{4.19}$$

from which the electric and magnetic fields can be obtained via Eqs. (4.11)

$$\vec{E}(\vec{r},t) = \frac{\mathrm{i}}{c}\sum_{\vec{k}\lambda}\omega_{\vec{k}}\left[c_{\vec{k}\lambda}(t)\;\vec{e}_{\vec{k}\lambda}\;\mathrm{e}^{\,\mathrm{i}\vec{k}\cdot\vec{r}} - c_{\vec{k}\lambda}(t)^*\;\vec{e}^{\,*}_{\vec{k}\lambda}\;\mathrm{e}^{\,-\mathrm{i}\vec{k}\cdot\vec{r}}\right]$$

$$\vec{B}(\vec{r},t) = \mathrm{i}\sum_{\vec{k}\lambda}\vec{k}\times\left[c_{\vec{k}\lambda}(t)\;\vec{e}_{\vec{k}\lambda}\;\mathrm{e}^{\,\mathrm{i}\vec{k}\cdot\vec{r}} - c_{\vec{k}\lambda}(t)^*\;\vec{e}^{\,*}_{\vec{k}\lambda}\;\mathrm{e}^{\,-\mathrm{i}\vec{k}\cdot\vec{r}}\right]. \tag{4.20}$$

The summations are extended to all the wavenumbers satisfying Eq. (4.13) and, for each wavenumber, to the two possible polarization states. Each set of values $(\vec{k},\lambda)$ defines a *mode* of the radiation field inside the cavity. The number of modes for which the modulus of $\vec{k}$ is contained within k and $k+\mathrm{d}k$ and its direction is contained in the solid angle $\mathrm{d}\Omega$ is given by

$$N(k)\,\mathrm{d}k\,\mathrm{d}\Omega = 2\,k^2\,\mathrm{d}k\,\mathrm{d}\Omega\left(\frac{L}{2\pi}\right)^3 = \frac{1}{4\pi^3}\,\mathcal{V}\,k^2\,\mathrm{d}k\,\mathrm{d}\Omega\,, \tag{4.21}$$

where $\mathcal{V}=L^3$ is the cavity volume.

4.3. Quantization of the Electromagnetic Field

We can now introduce the formalism of second quantization by interpreting the coefficients $c_{\vec{k}\lambda}(t)$ and $c_{\vec{k}\lambda}(t)^*$ in Eqs. (4.19) and (4.20) as two operators $c_{\vec{k}\lambda}$ and $c^\dagger_{\vec{k}\lambda}$ acting on a suitable Hilbert space. By so doing, the vector potential and the electric and magnetic fields become quantum operators acting on the same Hilbert space.

The Hamiltonian of the electromagnetic field can be found with the help of the Correspondence Principle, starting from the classical expression

$$H = \frac{1}{8\pi}\int_{\mathcal{V}}(E^2+B^2)\,\mathrm{d}V \tag{4.22}$$

which gives the energy of the field contained in the volume $\mathcal{V}$. Substituting for $\vec{E}$ and $\vec{B}$ their expressions given in Eqs. (4.20) (with the coefficients $c_{\vec{k}\lambda}(t)$ and $c_{\vec{k}\lambda}(t)^*$ replaced by the operators $c_{\vec{k}\lambda}$ and $c^\dagger_{\vec{k}\lambda}$, respectively) the integral in Eq. (4.22) reduces to the sum of integrals of the form

$$\int_{\mathcal{V}}\mathrm{e}^{\,\mathrm{i}(\vec{k}+\vec{k}')\cdot\vec{r}}\,\mathrm{d}V\,,$$

which can be easily evaluated to give, owing to the periodicity conditions (4.13),

$$\mathcal{V}\,\delta_{\vec{k},-\vec{k}'}\,.$$

We thus obtain

$$H = -\frac{\mathcal{V}}{8\pi} \sum_{\vec{k}\lambda\lambda'} \Bigg\{ \; c_{\vec{k}\lambda}\, c_{-\vec{k}\lambda'} \left[\frac{\omega_{\vec{k}}^2}{c^2} \left(\vec{e}_{\vec{k}\lambda} \cdot \vec{e}_{-\vec{k}\lambda'} \right) - \left(\vec{k} \times \vec{e}_{\vec{k}\lambda} \right) \cdot \left(\vec{k} \times \vec{e}_{-\vec{k}\lambda'} \right) \right]$$
$$+ c_{\vec{k}\lambda}^{\dagger}\, c_{-\vec{k}\lambda'}^{\dagger} \left[\frac{\omega_{\vec{k}}^2}{c^2} \left(\vec{e}_{\vec{k}\lambda}^{\,*} \cdot \vec{e}_{-\vec{k}\lambda'}^{\,*} \right) - \left(\vec{k} \times \vec{e}_{\vec{k}\lambda}^{\,*} \right) \cdot \left(\vec{k} \times \vec{e}_{-\vec{k}\lambda'}^{\,*} \right) \right]$$
$$- c_{\vec{k}\lambda}\, c_{\vec{k}\lambda'}^{\dagger} \left[\frac{\omega_{\vec{k}}^2}{c^2} \left(\vec{e}_{\vec{k}\lambda} \cdot \vec{e}_{\vec{k}\lambda'}^{\,*} \right) + \left(\vec{k} \times \vec{e}_{\vec{k}\lambda} \right) \cdot \left(\vec{k} \times \vec{e}_{\vec{k}\lambda'}^{\,*} \right) \right]$$
$$- c_{\vec{k}\lambda}^{\dagger}\, c_{\vec{k}\lambda'} \left[\frac{\omega_{\vec{k}}^2}{c^2} \left(\vec{e}_{\vec{k}\lambda}^{\,*} \cdot \vec{e}_{\vec{k}\lambda'} \right) + \left(\vec{k} \times \vec{e}_{\vec{k}\lambda}^{\,*} \right) \cdot \left(\vec{k} \times \vec{e}_{\vec{k}\lambda'} \right) \right] \Bigg\} . \qquad (4.23)$$

Using Eqs. (4.15) and (4.17) we have that the first two terms in the right-hand side identically vanish, while the last two terms give[1]

$$H = \frac{\mathcal{V}}{4\pi c^2} \sum_{\vec{k}\lambda} \omega_{\vec{k}}^2 \left[c_{\vec{k}\lambda}\, c_{\vec{k}\lambda}^{\dagger} + c_{\vec{k}\lambda}^{\dagger} c_{\vec{k}\lambda} \right] . \qquad (4.24)$$

Finally, performing the substitutions

$$a_{\vec{k}\lambda} = \frac{1}{c} \sqrt{\frac{\omega_{\vec{k}} \mathcal{V}}{2\pi\hbar}}\; c_{\vec{k}\lambda} \; , \qquad a_{\vec{k}\lambda}^{\dagger} = \frac{1}{c} \sqrt{\frac{\omega_{\vec{k}} \mathcal{V}}{2\pi\hbar}}\; c_{\vec{k}\lambda}^{\dagger} \; , \qquad (4.25)$$

we can express the Hamiltonian of the electromagnetic field as the sum of an infinite number of Hamiltonians (one for each mode) formally identical to the Hamiltonian of the harmonic oscillator,

$$H = \sum_{\vec{k}\lambda} \frac{1}{2}\, \hbar\omega_{\vec{k}} \left[a_{\vec{k}\lambda}\, a_{\vec{k}\lambda}^{\dagger} + a_{\vec{k}\lambda}^{\dagger} a_{\vec{k}\lambda} \right] .$$

The commutation properties of the operators $a_{\vec{k}\lambda}$ and $a_{\vec{k}\lambda}^{\dagger}$ can be derived from the Correspondence Principle. Since these operators are, apart from a factor, the quantum equivalent of the coefficients $c_{\vec{k}\lambda}(t)$ which obey the differential equation (4.18), we require that the same differential equation hold for the expectation value of the operator $a_{\vec{k}\lambda}$ on an arbitrary state vector $|\phi\rangle$ of the Hilbert space,

$$\frac{\mathrm{d}}{\mathrm{d}t} \langle \phi | a_{\vec{k}\lambda} | \phi \rangle = -\mathrm{i}\, \omega_{\vec{k}} \, \langle \phi | a_{\vec{k}\lambda} | \phi \rangle \; .$$

[1] The cross products in Eq. (4.23) can be easily evaluated using the relations

$$\left(\vec{a} \times \vec{b} \right)_i = \textstyle\sum_{jk} \epsilon_{ijk}\, a_j b_k \; , \qquad \sum_k \epsilon_{ijk}\, \epsilon_{lmk} = \delta_{il}\, \delta_{jm} - \delta_{im}\, \delta_{jl} \; ,$$

where the antisymmetrical tensor ϵ_{ijk} is defined on p.7.

Since the state vector $|\phi\rangle$ evolves according to the Schrödinger equation

$$\mathrm{i}\hbar \frac{\mathrm{d}}{\mathrm{d}t} |\phi\rangle = H |\phi\rangle \ ,$$

we obtain

$$\langle\phi| [a_{\vec{k}\lambda}, H] |\phi\rangle = \hbar\omega_{\vec{k}} \langle\phi| a_{\vec{k}\lambda} |\phi\rangle \ ,$$

or

$$\sum_{\vec{k}'\lambda'} \frac{1}{2} \omega_{\vec{k}'} \langle\phi| [a_{\vec{k}\lambda}, a_{\vec{k}'\lambda'} a^{\dagger}_{\vec{k}'\lambda'} + a^{\dagger}_{\vec{k}'\lambda'} a_{\vec{k}'\lambda'}] |\phi\rangle = \omega_{\vec{k}} \langle\phi| a_{\vec{k}\lambda} |\phi\rangle \ .$$

Being $|\phi\rangle$ an arbitrary state vector, it can be proved that this equation is satisfied if

$$[a_{\vec{k}\lambda}, a_{\vec{k}'\lambda'}] = [a_{\vec{k}\lambda}, a^{\dagger}_{\vec{k}'\lambda'}] = 0 \tag{4.26}$$

when the operators refer to different modes ($\vec{k} \neq \vec{k}'$ or $\lambda \neq \lambda'$), and if

$$[a_{\vec{k}\lambda}, a^{\dagger}_{\vec{k}\lambda}] = 1 \ . \tag{4.27}$$

The Hamiltonian H can then be expressed in its final form

$$H = \sum_{\vec{k}\lambda} \hbar\omega_{\vec{k}} \left(a^{\dagger}_{\vec{k}\lambda} a_{\vec{k}\lambda} + \frac{1}{2} \right) \ . \tag{4.28}$$

Equation (4.28), together with the commutation rules (4.26) and (4.27), proves that the Hamiltonian of the electromagnetic field is the sum of an infinite number of *independent* Hamiltonians, each formally identical to the Hamiltonian of the harmonic oscillator.

If we now arrange the different modes of the electromagnetic field in some definite order, and recall the results obtained in Sect. 4.1 for the harmonic oscillator, we have that the eigenvectors of the Hamiltonian H can be described by a state vector of the form

$$|n_1, n_2, \ldots, n_i, \ldots\rangle = \frac{1}{\sqrt{n_1!\, n_2! \cdots n_i! \cdots}} (a^{\dagger}_1)^{n_1} (a^{\dagger}_2)^{n_2} \cdots (a^{\dagger}_i)^{n_i} \cdots |\phi_0\rangle \ , \tag{4.29}$$

where $(n_1, n_2, \ldots, n_i, \ldots)$ are the *occupation numbers* and

$$|\phi_0\rangle = |0, 0, \ldots, 0, \ldots\rangle$$

is the so-called *vacuum state*.

The corresponding energy eigenvalues are given by

$$H |n_1, n_2, \ldots, n_i, \ldots\rangle = \left\{ \sum_j \hbar\omega_j \left(n_j + \frac{1}{2} \right) \right\} |n_1, n_2, \ldots, n_i, \ldots\rangle \ .$$

Note that the presence of the term $1/2$ in this expression leads to a non-zero (and indeed infinite) energy eigenvalue even when all the occupation numbers are zero. This represents a zero-point energy that can be eliminated from the theory by simply shifting the scale on which energy is measured. By so doing we can write

$$H\,|n_1, n_2, \ldots, n_i, \ldots\rangle = \left\{\sum_j \hbar\omega_j n_j\right\} |n_1, n_2, \ldots, n_i, \ldots\rangle\ .$$

The physical interpretation of the formalism introduced above is the following. The occupation number n_i is the number of photons in the i-th mode, thus the state vector in Eq. (4.29) represents the physical state where n_1 photons are present in mode 1, n_2 photons in mode 2, and so on. Since the occupation number n_i relative to the i-th mode can take all the values $0, 1, 2, \ldots$, and since, moreover, this number is independent of the occupation numbers relative to all the other modes, it follows that photons obey the Bose-Einstein statistics. This allows a direct deduction of Planck's law. In thermodynamic equilibrium at temperature T, the probability P_n (normalized to unity) of having n photons in a given mode of angular frequency ω is given by

$$P_n = \frac{\mathrm{e}^{-n\frac{\hbar\omega}{k_{\mathrm{B}}T}}}{\sum\limits_{m=0}^{\infty} \mathrm{e}^{-m\frac{\hbar\omega}{k_{\mathrm{B}}T}}}\ ,$$

where k_{B} is the Boltzmann constant, so that the mean number of photons in the mode is

$$\bar{n} = \sum_{n=0}^{\infty} n\,P_n = \frac{1}{\mathrm{e}^{\frac{\hbar\omega}{k_{\mathrm{B}}T}} - 1}\ .$$

Recalling Eq. (4.21), one obtains that the energy per unit volume with angular frequency between ω and $\omega + \mathrm{d}\omega$ is given by

$$u(\omega) = \oint \hbar\omega\,\bar{n}\,N(k)\,\frac{\mathrm{d}k}{\mathrm{d}\omega}\,\frac{1}{\mathcal{V}}\,\mathrm{d}\Omega = \frac{\hbar\omega^3}{\pi^2 c^3}\,\frac{1}{\mathrm{e}^{\frac{\hbar\omega}{k_{\mathrm{B}}T}} - 1}\ ,$$

and that the energy density with frequency between ν and $\nu + \mathrm{d}\nu$ is

$$u(\nu) = u(\omega)\,\frac{\mathrm{d}\omega}{\mathrm{d}\nu} = 8\pi\,\frac{h\nu^3}{c^3}\,\frac{1}{\mathrm{e}^{\frac{h\nu}{k_{\mathrm{B}}T}} - 1}\ ,$$

which is the classical *Planck's law*.

The action of the operators a_i and $a_i^\dagger$ on a given state vector can be deduced from Eqs. (4.8)

$$\begin{aligned}
a_i\,|n_1, n_2, \ldots, n_i, \ldots\rangle &= \sqrt{n_i}\,|n_1, n_2, \ldots, n_i - 1, \ldots\rangle \\
a_i^\dagger\,|n_1, n_2, \ldots, n_i, \ldots\rangle &= \sqrt{n_i + 1}\,|n_1, n_2, \ldots, n_i + 1, \ldots\rangle \\
a_i^\dagger a_i\,|n_1, n_2, \ldots, n_i, \ldots\rangle &= n_i\,|n_1, n_2, \ldots, n_i, \ldots\rangle\ .
\end{aligned}$$

These equations fully justify the denomination of destruction and creation operators for a_i and $a_i^\dagger$, respectively. The last equation shows that $a_i^\dagger a_i$ is a positive definite Hermitian operator whose eigenvalues are the occupation numbers n_i. For this reason it is named the *occupation number operator* relative to the i-th mode.

4.4. The Stokes Parameters in the Formalism of Second Quantization

The formalism introduced in the previous sections can be slightly modified to make it more suitable for the physical applications that will be presented in Chap. 6. Instead of labelling the modes with the wavenumber $\vec{k}$ we characterize them by the frequency ν and the direction $\vec{\Omega}$. Thus we replace the operators $a_{\vec{k}\lambda}$ and $a_{\vec{k}\lambda}^\dagger$ by the operators $a(\nu, \vec{\Omega}, \lambda)$ and $a^\dagger(\nu, \vec{\Omega}, \lambda)$, respectively. Moreover, instead of the unit vectors $\vec{e}_{\vec{k}\lambda}$ we will use the unit vectors $\vec{e}_\lambda(\vec{\Omega})$ which still depend on the direction $\vec{\Omega}$ but not any longer on the radiation frequency. With these notations, and taking into account Eqs. (4.25) and (4.15), we can write for the operator $\hat{\vec{A}}(\vec{r})$ defined in its classical form in Eq. (4.19)[1]

$$\hat{\vec{A}}(\vec{r}) = \sum_{\nu\vec{\Omega}\lambda} c\sqrt{\frac{h}{2\pi\nu\mathcal{V}}}\left\{a(\nu,\vec{\Omega},\lambda)\,\vec{e}_\lambda(\vec{\Omega})\,\mathrm{e}^{\mathrm{i}\vec{k}\cdot\vec{r}} + a^\dagger(\nu,\vec{\Omega},\lambda)\,\vec{e}_\lambda(\vec{\Omega})^*\,\mathrm{e}^{-\mathrm{i}\vec{k}\cdot\vec{r}}\right\}, \quad (4.30)$$

where

$$\vec{k} = \frac{2\pi\nu}{c}\,\vec{\Omega}$$

$$\vec{e}_\lambda(\vec{\Omega})\cdot\vec{\Omega} = 0\,, \qquad \vec{e}_\lambda(\vec{\Omega})\cdot\vec{e}_{\lambda'}(\vec{\Omega})^* = \delta_{\lambda\lambda'} \qquad (\lambda,\lambda' = 1,2)\,, \qquad (4.31)$$

and

$$\left[a(\nu,\vec{\Omega},\lambda), a(\nu',\vec{\Omega}',\lambda')\right] = \left[a^\dagger(\nu,\vec{\Omega},\lambda), a^\dagger(\nu',\vec{\Omega}',\lambda')\right] = 0$$

$$\left[a(\nu,\vec{\Omega},\lambda), a^\dagger(\nu',\vec{\Omega}',\lambda')\right] = \delta_{\nu\nu'}\,\delta_{\vec{\Omega}\vec{\Omega}'}\,\delta_{\lambda\lambda'}\,. \qquad (4.32)$$

Similarly, for the electric and magnetic field operators we have

$$\hat{\vec{E}}(\vec{r}) = \mathrm{i}\sum_{\nu\vec{\Omega}\lambda}\sqrt{\frac{2\pi\nu h}{\mathcal{V}}}\left\{a(\nu,\vec{\Omega},\lambda)\,\vec{e}_\lambda(\vec{\Omega})\,\mathrm{e}^{\mathrm{i}\vec{k}\cdot\vec{r}} - a^\dagger(\nu,\vec{\Omega},\lambda)\,\vec{e}_\lambda(\vec{\Omega})^*\,\mathrm{e}^{-\mathrm{i}\vec{k}\cdot\vec{r}}\right\}$$

$$\hat{\vec{B}}(\vec{r}) = \mathrm{i}\sum_{\nu\vec{\Omega}\lambda}\sqrt{\frac{2\pi\nu h}{\mathcal{V}}}\left\{a(\nu,\vec{\Omega},\lambda)\left[\vec{\Omega}\times\vec{e}_\lambda(\vec{\Omega})\right]\mathrm{e}^{\mathrm{i}\vec{k}\cdot\vec{r}} - a^\dagger(\nu,\vec{\Omega},\lambda)\left[\vec{\Omega}\times\vec{e}_\lambda(\vec{\Omega})^*\right]\mathrm{e}^{-\mathrm{i}\vec{k}\cdot\vec{r}}\right\}, \qquad (4.33)$$

[1] To avoid any possible confusion, we use in this section the symbol ˆ to distinguish the operators from the corresponding classical quantities.

and for the Hamiltonian (with the vacuum energy removed)

$$\hat{H} = \sum_{\nu\vec{\Omega}\lambda} h\nu \, a^\dagger(\nu, \vec{\Omega}, \lambda) \, a(\nu, \vec{\Omega}, \lambda) \; . \tag{4.34}$$

From these expressions it is possible to derive, according to the Correspondence Principle, the quantum-mechanical operators corresponding to a number of classical dynamical variables. In App. 3 we present such derivations for the momentum and for the angular momentum of the electromagnetic field.

Let us now consider the classical definition of the intensity of a radiation beam,

$$I(\nu, \vec{\Omega}) = \frac{\mathrm{d}E}{\mathrm{d}S \, \mathrm{d}t \, \mathrm{d}\nu \, \mathrm{d}\Omega} \; ,$$

where $\mathrm{d}E$ is the energy crossing the surface $\mathrm{d}S$ (perpendicular to the beam) in the time interval $\mathrm{d}t$, with frequency between ν and $\nu + \mathrm{d}\nu$ and direction contained in the solid angle $\mathrm{d}\Omega$ around the direction $\vec{\Omega}$. The corresponding quantum operator can be derived by the following arguments. The number of modes having frequency contained in the interval $(\nu, \nu + \mathrm{d}\nu)$ and direction in the solid angle $\mathrm{d}\Omega$ is given, for each polarization state, by (see Eq. (4.21))

$$N(\nu) \, \mathrm{d}\nu \, \mathrm{d}\Omega = \mathcal{V} \frac{\nu^2}{c^3} \, \mathrm{d}\nu \, \mathrm{d}\Omega \; . \tag{4.35}$$

If $n(\nu, \vec{\Omega}, \lambda)$ is the number of photons belonging to a particular mode, the number of such photons crossing the surface $\mathrm{d}S$ in the time interval $\mathrm{d}t$ is

$$n(\nu, \vec{\Omega}, \lambda) \, \frac{c \, \mathrm{d}t \, \mathrm{d}S}{\mathcal{V}} \; ,$$

and since each photon carries the energy $h\nu$ one obtains

$$I(\nu, \vec{\Omega}) = \frac{h\nu^3}{c^2} \sum_{\lambda=1,2} n(\nu, \vec{\Omega}, \lambda) \; . \tag{4.36}$$

This expression immediately suggests the form of the corresponding quantum-mechanical operator

$$\hat{I}(\nu, \vec{\Omega}) = \frac{h\nu^3}{c^2} \sum_{\lambda=1,2} a^\dagger(\nu, \vec{\Omega}, \lambda) \, a(\nu, \vec{\Omega}, \lambda) \; ,$$

and the generalization to the polarization tensor defined in Eq. (1.36) is quite obvious

$$\hat{I}_{\alpha\beta}(\nu, \vec{\Omega}) = \frac{h\nu^3}{c^2} \, a^\dagger(\nu, \vec{\Omega}, \alpha) \, a(\nu, \vec{\Omega}, \beta) \; . \tag{4.37}$$

The relations connecting the Stokes parameters with the components of the polarization tensor depend on the reference direction chosen to define the Stokes

parameters (see Sect. 1.6) and on the specific unit vectors $\vec{e}_\lambda(\vec{\Omega})$ chosen to expand the vector potential $\hat{\vec{A}}(\vec{r})$ (see Eq. (4.30)). Obviously, both choices are completely arbitrary, and the relation between the Stokes parameters and the polarization tensor is in general rather involved (see Eqs. (1.42)). It is however convenient, for future applications, to define the unit vectors $\vec{e}_\lambda(\vec{\Omega})$ in the following way

$$\begin{aligned}\vec{e}_{+1}(\vec{\Omega}) &= \frac{1}{\sqrt{2}}\left[-\vec{e}_a(\vec{\Omega}) + \mathrm{i}\,\vec{e}_b(\vec{\Omega})\right] \\ \vec{e}_{-1}(\vec{\Omega}) &= \frac{1}{\sqrt{2}}\left[\vec{e}_a(\vec{\Omega}) + \mathrm{i}\,\vec{e}_b(\vec{\Omega})\right] ,\end{aligned} \tag{4.38}$$

where $\vec{e}_a(\vec{\Omega})$ and $\vec{e}_b(\vec{\Omega})$ are the reference direction unit vector and the associated unit vector, respectively (see Sect. 1.6). It can be easily shown that these vectors satisfy Eqs. (4.17), namely

$$\begin{aligned}&\vec{e}_{\pm1}(\vec{\Omega}) \cdot \vec{\Omega} = 0 \\ &\vec{e}_{+1}(\vec{\Omega}) \cdot \vec{e}_{+1}(\vec{\Omega})^* = \vec{e}_{-1}(\vec{\Omega}) \cdot \vec{e}_{-1}(\vec{\Omega})^* = 1 \\ &\vec{e}_{+1}(\vec{\Omega}) \cdot \vec{e}_{-1}(\vec{\Omega})^* = \vec{e}_{-1}(\vec{\Omega}) \cdot \vec{e}_{+1}(\vec{\Omega})^* = 0 .\end{aligned}$$

Moreover, they satisfy the relation

$$\vec{e}_{\pm1}(\vec{\Omega})^* = -\,\vec{e}_{\mp1}(\vec{\Omega}) .$$

With this choice for the unit vectors $\vec{e}_\lambda(\vec{\Omega})$ – a choice that will appear clearer in the following, see Sect. 5.10 – the relation between the Stokes parameters and the polarization tensor can be derived from Eqs. (1.42) substituting $\theta = 5\pi/4$, $\phi = -\pi/2$ (which makes Eqs. (1.41) coincident with Eqs. (4.38)). We have

$$\begin{aligned}\hat{I}(\nu,\vec{\Omega}) &= \hat{I}_{++}(\nu,\vec{\Omega}) + \hat{I}_{--}(\nu,\vec{\Omega}) \\ \hat{Q}\,(\nu,\vec{\Omega}) &= -\hat{I}_{+-}(\nu,\vec{\Omega}) - \hat{I}_{-+}(\nu,\vec{\Omega}) \\ \hat{U}(\nu,\vec{\Omega}) &= -\mathrm{i}\,\hat{I}_{+-}(\nu,\vec{\Omega}) + \mathrm{i}\,\hat{I}_{-+}(\nu,\vec{\Omega}) \\ \hat{V}(\nu,\vec{\Omega}) &= \hat{I}_{++}(\nu,\vec{\Omega}) - \hat{I}_{--}(\nu,\vec{\Omega}) ,\end{aligned} \tag{4.39}$$

where we have shortened the notations writing $\hat{I}_{++}$ instead of $\hat{I}_{+1\,+1}$, and so on. Finally, substituting Eq. (4.37) we obtain

$$\begin{aligned}\hat{I}(\nu,\vec{\Omega}) &= \frac{h\nu^3}{c^2}\left[a^\dagger(\nu,\vec{\Omega},+1)\,a(\nu,\vec{\Omega},+1) + a^\dagger(\nu,\vec{\Omega},-1)\,a(\nu,\vec{\Omega},-1)\right] \\ \hat{Q}\,(\nu,\vec{\Omega}) &= -\frac{h\nu^3}{c^2}\left[a^\dagger(\nu,\vec{\Omega},+1)\,a(\nu,\vec{\Omega},-1) + a^\dagger(\nu,\vec{\Omega},-1)\,a(\nu,\vec{\Omega},+1)\right] \\ \hat{U}(\nu,\vec{\Omega}) &= -\mathrm{i}\,\frac{h\nu^3}{c^2}\left[a^\dagger(\nu,\vec{\Omega},+1)\,a(\nu,\vec{\Omega},-1) - a^\dagger(\nu,\vec{\Omega},-1)\,a(\nu,\vec{\Omega},+1)\right] \\ \hat{V}(\nu,\vec{\Omega}) &= \frac{h\nu^3}{c^2}\left[a^\dagger(\nu,\vec{\Omega},+1)\,a(\nu,\vec{\Omega},+1) - a^\dagger(\nu,\vec{\Omega},-1)\,a(\nu,\vec{\Omega},-1)\right] ,\end{aligned}$$

which give the Stokes parameters of the radiation field in terms of creation and destruction operators. The connection between the operator $\hat{V}(\nu, \vec{\Omega})$ and the angular momentum operator of the electromagnetic field is discussed in App. 3.

4.5. The Density Operator of the Radiation Field

The density operator $\rho^{(\mathrm{R})}$ of the radiation field can be introduced using the same general formalism presented at the beginning of Sect. 3.6. The definition of $\rho^{(\mathrm{R})}$ is indeed the same as that of Eq. (3.79),

$$\rho^{(\mathrm{R})} = \sum_{\alpha} p_{\alpha} \, |\psi_{\mathrm{R}}^{(\alpha)}\rangle\langle\psi_{\mathrm{R}}^{(\alpha)}| \, ,$$

where $|\psi_{\mathrm{R}}^{(\alpha)}\rangle$ is now a state vector of the Hilbert space considered in Sect. 4.3.

A complete basis of this Hilbert space is that of the energy eigenvectors given in Eq. (4.29),

$$\left\{ \, |n_1, n_2, \ldots, n_i, \ldots\rangle \, \right\} ,$$

so that the matrix elements of the operator $\rho^{(\mathrm{R})}$ have the form

$$\rho^{(\mathrm{R})}_{(n_1,n_2,\ldots,n_i,\ldots)\,(n'_1,n'_2,\ldots,n'_i,\ldots)} = \langle n_1, n_2, \ldots, n_i, \ldots | \, \rho^{(\mathrm{R})} \, |n'_1, n'_2, \ldots, n'_i, \ldots\rangle \, .$$

The expectation value of any dynamical variable can be expressed in terms of the density operator $\rho^{(\mathrm{R})}$. For instance, the expectation value of the electric field in a given point is expressed by

$$\vec{E}(\vec{r}) = \mathrm{Tr}\left(\hat{\vec{E}}(\vec{r}) \, \rho^{(\mathrm{R})}\right) ,$$

and analogous formulae can be written for the other physical variables associated with the electromagnetic radiation field.

In some special cases, the density operator of the radiation field can be written as the direct product of an infinite number of operators each spanning one mode of the radiation field characterized by the frequency ν and the direction $\vec{\Omega}$.[1] In these cases we have

$$\rho^{(\mathrm{R})} = \rho^{(\mathrm{R})}(\nu_1, \vec{\Omega}_1) \otimes \rho^{(\mathrm{R})}(\nu_2, \vec{\Omega}_2) \cdots \otimes \rho^{(\mathrm{R})}(\nu_i, \vec{\Omega}_i) \cdots \, .$$

The expectation values of the polarization tensor components relative to the mode $(\nu_0, \vec{\Omega}_0)$ are then given by

$$I_{\alpha\beta}(\nu_0, \vec{\Omega}_0) = \mathrm{Tr}\left(\hat{I}_{\alpha\beta}(\nu_0, \vec{\Omega}_0) \, \rho^{(\mathrm{R})}\right) = \mathrm{Tr}\left(\hat{I}_{\alpha\beta}(\nu_0, \vec{\Omega}_0) \, \rho^{(\mathrm{R})}(\nu_0, \vec{\Omega}_0)\right) ,$$

[1] The concept of mode is used here in a broader sense than in previous sections. Modes are defined here irrespective of the photon polarization, so that, more precisely, they are double-modes.

or, with shorthand notations,

$$I_{\alpha\beta} = \mathrm{Tr}\left(\hat{I}_{\alpha\beta}\,\rho_0^{(\mathrm{R})}\right) = \frac{h\nu^3}{c^2}\,\mathrm{Tr}\left(a_\alpha^\dagger a_\beta\,\rho_0^{(\mathrm{R})}\right),$$

where $\rho_0^{(\mathrm{R})}$ is the 'reduced' density operator acting on the mode $(\nu_0, \vec{\Omega}_0)$ and where $a_\alpha^\dagger$ and a_β are the operators $a^\dagger(\nu_0, \vec{\Omega}_0, \alpha)$ and $a(\nu_0, \vec{\Omega}_0, \beta)$, respectively.

It should be remarked that the density operator described above is an operator acting on the Hilbert space of the occupation numbers. Sometimes, a different density operator is introduced, acting on the wavefunction space of the photons (Fano, 1949; Blum, 1981). This latter operator will not be used in this book.

This page intentionally left blank

CHAPTER 5

INTERACTION OF MATERIAL SYSTEMS WITH POLARIZED RADIATION (THE CLASSICAL APPROACH)

In this chapter we will discuss the physical mechanisms involved in the generation and transfer of polarized radiation in spectral lines within the framework of classical physics. In particular, the classical theory of the electron (already introduced in Sect. 3.2) will be used to describe the atomic system interacting with polarized radiation, and the electromagnetic radiation field will be described in terms of classical electrodynamics.

The results that will be derived are of limited validity as, in most cases, the correct results can only be obtained by a quantum-mechanical treatment. The formalism of classical physics is, however, simpler and more transparent than the quantum-mechanical one. Thus it is suited to give the reader a plain introduction and an intuitive approach to the physical processes that will be treated in full generality in the following chapters. Moreover, some of the results obtained from classical physics coincide with special cases of the corresponding quantum results. And it is indeed illuminating and encouraging to find, as a limiting case of an involved quantum-mechanical calculation, the same result deduced from the simpler, classical formalism.

This chapter is also intended to show the strict connection between some classical and quantum concepts. This subject – generally overlooked in textbooks on Quantum Mechanics – can be conveniently illustrated by the physical processes described here, such as resonance scattering and the Hanle effect. Although the connection can be established only in a qualitative way, it is nevertheless important for the correct understanding of polarization phenomena.

5.1. Propagation of Electromagnetic Waves in Anisotropic Media

The propagation properties of electromagnetic waves in a material medium can be derived, in classical physics, from the Maxwell equations. In the following we will restrict attention to a homogeneous medium having magnetic permeability $\mu = 1$, so that it is not necessary to distinguish between the two vectors $\vec{B}$ (magnetic induction) and $\vec{H}$ (magnetic field).

In such a medium, with no free charges, the Maxwell equations take the form (in the Gauss-Hertz system of units)

$$\mathrm{div}\vec{D} = 0 \tag{5.1a}$$

$$\mathrm{div}\vec{B} = 0 \tag{5.1b}$$

$$\operatorname{curl} \vec{B} = \frac{1}{c} \frac{\partial \vec{D}}{\partial t} \tag{5.1c}$$

$$\operatorname{curl} \vec{E} = -\frac{1}{c} \frac{\partial \vec{B}}{\partial t} \ , \tag{5.1d}$$

where c is the velocity of light and where the electric displacement $\vec{D}$ is connected with $\vec{E}$ by the equation

$$\vec{D} = \vec{E} + 4\pi \vec{P} \ ,$$

$\vec{P}$ being the electric polarization. From Eqs. (5.1c) and (5.1d) it easily follows that

$$\nabla^2 \vec{E} - \operatorname{grad} \operatorname{div} \vec{E} = \frac{1}{c^2} \frac{\partial^2 \vec{D}}{\partial t^2} \ . \tag{5.2}$$

For an isotropic medium, $\vec{D}$ is related to $\vec{E}$ by the simple equation

$$\vec{D} = \epsilon \, \vec{E} \ ,$$

where ϵ is the dielectric constant of the medium. Substitution into Eqs. (5.2) and (5.1a) leads to the wave equation for the electric field

$$\nabla^2 \vec{E} = \frac{\epsilon}{c^2} \frac{\partial^2 \vec{E}}{\partial t^2}$$

and to the transversality condition

$$\operatorname{div} \vec{E} = 0 \ .$$

A particular solution to these equations is the well-known plane wave of frequency ν propagating along the direction $\vec{\Omega}$

$$\vec{E} = \vec{E}_0 \, \mathrm{e}^{2\pi \mathrm{i} \frac{\nu}{c} (n \, \vec{r} \cdot \vec{\Omega} - ct)} \ , \tag{5.3}$$

where $n = \sqrt{\epsilon}$ is the *index of refraction* of the medium and $\vec{E}_0$ is a constant such that

$$\vec{E}_0 \cdot \vec{\Omega} = 0 \ .$$

Note that Eq. (5.3) gives for the spatial evolution of the electric field components

$$\frac{\partial \mathcal{E}_j}{\partial s} = 2\pi \mathrm{i} \frac{\nu}{c} \, n \, \mathcal{E}_j \ ,$$

where $\mathcal{E}_j$ is the component of $\vec{E}$ along any direction perpendicular to $\vec{\Omega}$ and $s = \vec{r} \cdot \vec{\Omega}$ is the coordinate measured along the ray path.

For an anisotropic medium, like for instance a birefringent crystal, or a vapor permeated by a magnetic and/or electric field, the relation between $\vec{D}$ and $\vec{E}$ becomes of tensorial form,

$$\mathcal{D}_i = \sum_j \epsilon_{ij}\, \mathcal{E}_j \ ,$$

where $\mathcal{D}_i$ $(i = 1, 2, 3)$ and $\mathcal{E}_j$ $(j = 1, 2, 3)$ are the Cartesian components of the vectors $\vec{D}$ and $\vec{E}$, respectively, and where ϵ_{ij} is the dielectric tensor.

From general theorems on matrices it follows that the dielectric tensor can always be diagonalized through a suitable similarity transformation. This means that any medium is characterized by a triplet of axes $\vec{u}_\alpha$ $(\alpha = 1, 2, 3)$, called the *principal dielectric axes*, such that when the vectors $\vec{D}$ and $\vec{E}$ are expanded on this basis,

$$\vec{D} = \sum_\alpha \mathcal{D}_\alpha\, \vec{u}_\alpha \ , \qquad \vec{E} = \sum_\alpha \mathcal{E}_\alpha\, \vec{u}_\alpha \ , \tag{5.4}$$

one simply has

$$\mathcal{D}_\alpha = \epsilon_\alpha\, \mathcal{E}_\alpha \ . \tag{5.5}$$

The quantities ϵ_α are called the *principal dielectric constants*. In the special case where the medium is a crystal, the dielectric tensor is real and symmetric (Born and Wolf, 1964). In this case the principal dielectric constants are real, and the three unit vectors $\vec{u}_\alpha$ are also real and form an orthogonal triplet.

By contrast, these properties break down for *absorbing* anisotropic media. In this case the principal dielectric constants are generally complex and the same holds for the unit vectors $\vec{u}_\alpha$, which no longer are orthogonal. It follows that if we expand any vector $\vec{v}$ on the basis $\vec{u}_\alpha$,

$$\vec{v} = \sum_\alpha v_\alpha\, \vec{u}_\alpha \ , \tag{5.6}$$

the components v_α are given by

$$v_\alpha = \vec{u}'_\alpha \cdot \vec{v} \ , \tag{5.7}$$

where the unit vectors $\vec{u}'_\alpha$ $(\alpha = 1, 2, 3)$ are such that

$$\vec{u}'_\alpha \cdot \vec{u}_\beta = \delta_{\alpha\beta} \ .$$

These vectors can be explicitly written in the form[1]

$$\vec{u}'_1 = \frac{1}{g}\, \vec{u}_2 \times \vec{u}_3 \ , \qquad \vec{u}'_2 = \frac{1}{g}\, \vec{u}_3 \times \vec{u}_1 \ , \qquad \vec{u}'_3 = \frac{1}{g}\, \vec{u}_1 \times \vec{u}_2 \ , \tag{5.8}$$

[1] For a dielectric crystal we simply have $\vec{u}'_\alpha = \vec{u}_\alpha$. In the case of a vapor permeated by a magnetic field, it will be shown in Sect. 5.3 that $\vec{u}'_\alpha = \vec{u}^{\,*}_\alpha$.

where $g = \vec{u}_1 \cdot (\vec{u}_2 \times \vec{u}_3)$.

The general solution to Eqs. (5.2) and (5.1a) in an anisotropic absorbing medium is quite complicated, except for some particular directions of propagation and polarization. For instance, if we consider the wave

$$\vec{E} = E_\alpha \, \vec{u}_\alpha \, \mathrm{e}^{2\pi \mathrm{i} \frac{\nu}{c} (n_\alpha \, \vec{r} \cdot \vec{\Omega} - ct)}$$

with

$$n_\alpha^2 = \epsilon_\alpha \tag{5.9}$$

and

$$\vec{u}_\alpha \cdot \vec{\Omega} = 0 \, ,$$

we easily see that Eqs. (5.2) and (5.1a) are satisfied. Obviously this is a very special case because the wave is polarized along one of the principal dielectric axes and it propagates along a direction perpendicular to the same axis.

Instead of looking for a general solution to the problem of wave propagation within the medium,[1] we will confine ourselves to establishing an evolution equation for the components of the electric field. Our derivation will be further restricted to media having principal dielectric constants very close to unity. In other words, defining

$$\epsilon_\alpha = 1 + \xi_\alpha \qquad (\alpha = 1, 2, 3) \, , \tag{5.10}$$

we suppose that $|\xi_\alpha| \ll 1$.

Let us now consider a stationary plane wave of frequency ν propagating along an arbitrary direction $\vec{\Omega}$. The vectors $\vec{E}$ and $\vec{D}$ associated with the wave depend only on s (the spatial coordinate measured along $\vec{\Omega}$) and on time t, thus Eq. (5.2) can be written in the form

$$\frac{\partial^2 \vec{E}}{\partial s^2} - \vec{\Omega} \, \frac{\partial^2}{\partial s^2} (\vec{E} \cdot \vec{\Omega}) = -\frac{4\pi^2 \nu^2}{c^2} \, \vec{D} \, . \tag{5.11}$$

Scalar multiplication by $\vec{\Omega}$ gives

$$\vec{D} \cdot \vec{\Omega} = 0 \, , \tag{5.12}$$

so that the transversality condition (5.1a) is satisfied. These equations show that $\vec{D}$ is perpendicular to $\vec{\Omega}$ while $\vec{E}$ has, in general, a non-zero component along the direction of propagation.

Let's now introduce two mutually orthogonal unit vectors $\vec{e}_j$ perpendicular to the direction of propagation,

$$\vec{e}_j^{\,*} \cdot \vec{e}_k = \delta_{jk} \, , \qquad \vec{e}_j \cdot \vec{\Omega} = 0 \qquad (j, k = 1, 2) \, . \tag{5.13}$$

[1] This is a classical problem in crystal optics and leads to the so-called *Fresnel equation of wave normals* (see Born and Wolf, 1964).

These vectors can be, for instance, the reference direction unit vector $\vec{e}_a$ and the associated unit vector $\vec{e}_b$ defined in Sect. 1.6 or, more generally, the complex unit vectors $\vec{e}_+$ and $\vec{e}_-$ defined in Eqs. (1.41). Defining also

$$\vec{e}_3 = \vec{e}_3^{\,*} = \vec{\Omega} \,, \tag{5.14}$$

we can expand the vectors $\vec{E}$ and $\vec{D}$ on the basis $(\vec{e}_1, \vec{e}_2, \vec{e}_3)$,

$$\vec{E} = \sum_i \mathcal{E}_i \, \vec{e}_i \,, \qquad \vec{D} = \sum_i \mathcal{D}_i \, \vec{e}_i \,,$$

where

$$\mathcal{E}_i = \vec{e}_i^{\,*} \cdot \vec{E} \,, \qquad \mathcal{D}_i = \vec{e}_i^{\,*} \cdot \vec{D} \,.$$

The relation between the components $\mathcal{E}_i$ of the electric field in the reference system $(\vec{e}_1, \vec{e}_2, \vec{e}_3)$ and the components $\mathcal{E}_\alpha$ along the triplet $(\vec{u}_1, \vec{u}_2, \vec{u}_3)$ is the following

$$\mathcal{E}_i = \sum_\alpha (\vec{e}_i^{\,*} \cdot \vec{u}_\alpha) \, \mathcal{E}_\alpha \,, \qquad \mathcal{E}_\alpha = \sum_i (\vec{u}'_\alpha \cdot \vec{e}_i) \, \mathcal{E}_i \,. \tag{5.15}$$

Analogous equations obviously hold for the components of the electric displacement.

From the transversality condition (5.12) one obtains, using Eqs. (5.4), (5.5), (5.15), (5.14), and (5.10)

$$\sum_j \Big[\sum_\alpha (\vec{e}_3^{\,*} \cdot \vec{u}_\alpha) \, (\vec{u}'_\alpha \cdot \vec{e}_j) \, (1 + \xi_\alpha) \Big] \mathcal{E}_j = 0 \,. \tag{5.16}$$

On the other hand, if we expand any vector $\vec{e}_j$ on the basis $\vec{u}_\alpha$ via Eqs. (5.6) and (5.7),

$$\vec{e}_j = \sum_\alpha (\vec{u}'_\alpha \cdot \vec{e}_j) \, \vec{u}_\alpha \,,$$

we obtain from Eqs. (5.13) and (5.14)

$$\sum_\alpha (\vec{e}_i^{\,*} \cdot \vec{u}_\alpha) \, (\vec{u}'_\alpha \cdot \vec{e}_j) = \delta_{ij} \,, \tag{5.17}$$

therefore Eq. (5.16) can be written in the form

$$\begin{aligned} &\Big[1 + \sum_\alpha (\vec{e}_3^{\,*} \cdot \vec{u}_\alpha) \, (\vec{u}'_\alpha \cdot \vec{e}_3) \, \xi_\alpha \Big] \mathcal{E}_3 = \\ &= - \Big[\sum_\alpha (\vec{e}_3^{\,*} \cdot \vec{u}_\alpha) \, (\vec{u}'_\alpha \cdot \vec{e}_1) \, \xi_\alpha \Big] \mathcal{E}_1 - \Big[\sum_\alpha (\vec{e}_3^{\,*} \cdot \vec{u}_\alpha) \, (\vec{u}'_\alpha \cdot \vec{e}_2) \, \xi_\alpha \Big] \mathcal{E}_2 \,. \end{aligned}$$

This formula shows that the ratio of the longitudinal component $\mathcal{E}_3$ of the electric field to the transverse components is of order ξ_α. Since we have supposed $|\xi_\alpha| \ll 1$, we have

$$| \, \mathcal{E}_3 \, | \ll | \, \mathcal{E}_i \, | \qquad (i = 1, 2) \,.$$

Consider now Eq. (5.11). Performing the scalar product by $\vec{e}_j^{\,*}$ $(j = 1, 2)$ and using Eqs. (5.4), (5.5), (5.10), and (5.15), we get[1]

$$\frac{\partial^2 \mathcal{E}_j}{\partial s^2} = -\frac{4\pi^2\nu^2}{c^2}\,\mathcal{D}_j$$
$$= -\frac{4\pi^2\nu^2}{c^2}\sum_{k=1}^{3}\Big[\sum_{\alpha}(\vec{e}_j^{\,*}\cdot\vec{u}_\alpha)\,(\vec{u}'_\alpha\cdot\vec{e}_k)\,(1+\xi_\alpha)\Big]\,\mathcal{E}_k \qquad (j=1,2)\,.$$

The contribution from $k = 3$ has the form

$$-\frac{4\pi^2\nu^2}{c^2}\sum_{\alpha}(\vec{e}_j^{\,*}\cdot\vec{u}_\alpha)\,(\vec{u}'_\alpha\cdot\vec{e}_3)\,\xi_\alpha\,\mathcal{E}_3\,,$$

and since $\mathcal{E}_3$ is itself of order ξ_α, this contribution can be neglected according to the assumption $|\,\xi_\alpha\,| \ll 1$. Up to first-order terms in ξ_α we thus have

$$\frac{\partial^2 \mathcal{E}_j}{\partial s^2} = -\frac{4\pi^2\nu^2}{c^2}\sum_{k=1}^{2}\Big[\sum_{\alpha}(\vec{e}_j^{\,*}\cdot\vec{u}_\alpha)\,(\vec{u}'_\alpha\cdot\vec{e}_k)\,(1+\xi_\alpha)\Big]\,\mathcal{E}_k\,.$$

To the same order of approximation it can be easily shown, with the help of Eq. (5.17), that this equation is equivalent to the following

$$\frac{\partial \mathcal{E}_j}{\partial s} = \pm\,2\pi\mathrm{i}\,\frac{\nu}{c}\sum_{k=1}^{2}\Big[\sum_{\alpha}(\vec{e}_j^{\,*}\cdot\vec{u}_\alpha)\,(\vec{u}'_\alpha\cdot\vec{e}_k)\Big(1+\frac{1}{2}\,\xi_\alpha\Big)\Big]\,\mathcal{E}_k\,. \tag{5.18}$$

The $\pm$ sign appearing in this equation is a consequence of the existence of progressive and regressive waves. If we choose to describe the temporal oscillation of the wave through an exponential of the form $\mathrm{e}^{-2\pi\mathrm{i}\nu t}$ (consistently with the convention of Sect. 1.3), we must take the positive sign. Since from Eqs. (5.9) and (5.10) we also have

$$1+\frac{1}{2}\,\xi_\alpha = n_\alpha\,, \tag{5.19}$$

Eq. (5.18) can be finally written in the form

$$\frac{\partial \mathcal{E}_j}{\partial s} = 2\pi\mathrm{i}\,\frac{\nu}{c}\sum_{k=1}^{2}\Big[\sum_{\alpha}(\vec{e}_j^{\,*}\cdot\vec{u}_\alpha)\,(\vec{u}'_\alpha\cdot\vec{e}_k)\,n_\alpha\Big]\,\mathcal{E}_k \qquad (j=1,2)\,. \tag{5.20}$$

This equation expresses the variation along the propagation direction of the transverse components of the electric field. Its validity is limited to media whose principal dielectric constants differ slightly from unity and it cannot be applied, in general, to crystals. The same equation has been used (although without physical explanation) by Jefferies et al. (1989) in their derivation of the transfer equations

[1] The scalar product by $\vec{e}_3^{\,*}$ leads to the trivial identity $0 = 0$.

for polarized radiation from classical physics. A simpler, heuristic derivation, that is however basically inconsistent, has been given by Landi Degl'Innocenti (1992).

5.2. Transfer Equations for Polarized Radiation

Equation (5.20) describes the spatial evolution, along the ray path, of the transverse components of the electric field associated with a stationary plane wave of frequency ν. This equation can be rewritten in the form

$$\frac{\partial}{\partial s}\,\mathcal{E}_j(s,t) = -\sum_k G_{jk}\,\mathcal{E}_k(s,t) \qquad (j,k=1,2)\;, \tag{5.21}$$

where

$$G_{jk} = -2\pi\mathrm{i}\,\frac{\nu}{c}\sum_\alpha (\vec{u}_\alpha\cdot\vec{e}_j^{\,*})\,(\vec{u}'_\alpha\cdot\vec{e}_k)\,n_\alpha\;. \tag{5.22}$$

The tensor $\boldsymbol{G}$, which will be referred to in the following as the *propagation tensor* of the electric field, depends both on the physical nature of the medium, specified by the (complex) refractive indices n_α, and on the geometry of the propagation specified by the two scalar products. It is worth noticing that in an isotropic medium, where $n_\alpha = n$, we get from Eq. (5.17)

$$G_{jk} = -2\pi\mathrm{i}\,\frac{\nu}{c}\,n\,\delta_{jk}\;. \tag{5.23}$$

From Eq. (5.21) the transfer equation for the polarization tensor can be easily derived. Recalling the definition of polarization tensor given in Chap. 1 (see Eq. (1.25) and its generalization in Sect. 1.8) we have

$$\begin{aligned}\frac{\mathrm{d}}{\mathrm{d}s}\,J_{jk} &= \lim_{\Delta s\to 0}\frac{J_{jk}(s+\Delta s)-J_{jk}(s)}{\Delta s}\\ &= \lim_{\Delta s\to 0}\frac{\big\langle\mathcal{E}_j^*(s+\Delta s,t)\,\mathcal{E}_k(s+\Delta s,t)\big\rangle-\big\langle\mathcal{E}_j^*(s,t)\,\mathcal{E}_k(s,t)\big\rangle}{\Delta s}\\ &= \left\langle\frac{\partial\mathcal{E}_j^*(s,t)}{\partial s}\,\mathcal{E}_k(s,t)\right\rangle+\left\langle\mathcal{E}_j^*(s,t)\,\frac{\partial\mathcal{E}_k(s,t)}{\partial s}\right\rangle\;,\end{aligned}$$

and since the propagation tensor can be extracted from the statistical average implied by the symbol $\langle\cdots\rangle$, we obtain

$$\frac{\mathrm{d}}{\mathrm{d}s}\,J_{jk} = -\sum_{l=1}^{2}\left(G_{jl}^*\,J_{lk}+G_{kl}\,J_{jl}\right) \qquad (j,k=1,2)\;. \tag{5.24}$$

To derive the transfer equations for the Stokes parameters we need the relation between these quantities and the components of the polarization tensor. We recall

that this relation depends on the choice of the unit vectors $\vec{e}_1$ and $\vec{e}_2$ defined in Eq. (5.13). The easiest choice is

$$\vec{e}_1 = \vec{e}_a \,, \qquad \vec{e}_2 = \vec{e}_b \,,$$

where $\vec{e}_a$ is the reference direction unit vector and $\vec{e}_b$ the associated unit vector (see Sect. 1.6). With this definition the relation between the Stokes parameters and the components of the polarization tensor is given by Eqs. (1.34), which can be inverted to give

$$\begin{aligned} J_{11} &= \frac{1}{2k}\left(I+Q\right) & J_{12} &= \frac{1}{2k}\left(U-\mathrm{i}\,V\right) \\ J_{22} &= \frac{1}{2k}\left(I-Q\right) & J_{21} &= \frac{1}{2k}\left(U+\mathrm{i}\,V\right) . \end{aligned}$$

Substitution into Eqs. (5.24) leads to the following propagation equation for the Stokes parameters

$$\frac{\mathrm{d}}{\mathrm{d}s}\begin{pmatrix} I \\ Q \\ U \\ V \end{pmatrix} = -\begin{pmatrix} \eta_I & \eta_Q & \eta_U & \eta_V \\ \eta_Q & \eta_I & \rho_V & -\rho_U \\ \eta_U & -\rho_V & \eta_I & \rho_Q \\ \eta_V & \rho_U & -\rho_Q & \eta_I \end{pmatrix}\begin{pmatrix} I \\ Q \\ U \\ V \end{pmatrix} , \tag{5.25}$$

where the seven independent quantities appearing in the *propagation matrix* are given by

$$\begin{aligned} \eta_I &= \mathrm{Re}\,(G_{11}+G_{22}) & & \\ \eta_Q &= \mathrm{Re}\,(G_{11}-G_{22}) & \rho_Q &= -\mathrm{Im}\,(G_{11}-G_{22}) \\ \eta_U &= \mathrm{Re}\,(G_{12}+G_{21}) & \rho_U &= -\mathrm{Im}\,(G_{12}+G_{21}) \\ \eta_V &= \mathrm{Im}\,(G_{12}-G_{21}) & \rho_V &= \mathrm{Re}\,(G_{12}-G_{21}) \,. \end{aligned} \tag{5.26}$$

Equations (5.25) and (5.26) are at the basis of radiative transfer for polarized radiation and deserve some discussion. First of all it should be emphasized the remarkable symmetry property of the 4×4 propagation matrix. This matrix is constructed with only seven independent quantities and can be decomposed into a diagonal matrix, proportional to η_I, and two off-diagonal matrices, one symmetric and the other antisymmetric about the main diagonal.

Denoting the propagation matrix by $\boldsymbol{K}$, we have

$$\begin{aligned} \boldsymbol{K} = &\begin{pmatrix} \eta_I & 0 & 0 & 0 \\ 0 & \eta_I & 0 & 0 \\ 0 & 0 & \eta_I & 0 \\ 0 & 0 & 0 & \eta_I \end{pmatrix} + \\ &+\begin{pmatrix} 0 & \eta_Q & \eta_U & \eta_V \\ \eta_Q & 0 & 0 & 0 \\ \eta_U & 0 & 0 & 0 \\ \eta_V & 0 & 0 & 0 \end{pmatrix} + \begin{pmatrix} 0 & 0 & 0 & 0 \\ 0 & 0 & \rho_V & -\rho_U \\ 0 & -\rho_V & 0 & \rho_Q \\ 0 & \rho_U & -\rho_Q & 0 \end{pmatrix} . \end{aligned} \tag{5.27}$$

The first matrix is responsible for the absorption of the energy of the electromagnetic wave irrespective of its polarization state. This matrix would produce by itself an exponential decrease of the whole Stokes vector, so that the quantity η_I can be regarded as the generalization to the polarized case of the absorption coefficient encountered in the standard theory of radiative transfer. In this respect it is worth noticing that for an isotropic medium we simply have from Eq. (5.23)

$$\eta_I = 4\pi \frac{\nu}{c} k \, ,$$

k being the imaginary part of the refractive index which is connected with the standard absorption coefficient. This first matrix will be referred to in the following as the *absorption matrix*.

As apparent from Eq. (5.23), both the second and the third matrix are zero for an isotropic medium. For reasons that will be clarified in the next section, these matrices will be referred to in the following as *dichroism matrix* and *dispersion matrix*, respectively.

The expression that we have obtained for the propagation matrix $\boldsymbol{K}$, and in particular its symmetry properties, descend directly from the physical approximations adopted. First of all we have assumed the principal dielectric constants ϵ_α – which describe the dielectric properties of the medium – to be independent of the amplitude of the propagating electric field. This means that the polarization $\vec{P}$ induced in the medium is linearly related to the electric field itself. The present theory is therefore inadequate to treat the physical phenomena connected with non-linear optics. Moreover, we have assumed the principal dielectric constants of the medium to differ slightly from unity, so that the applicability of Eqs. (5.25)-(5.26) is limited to such media. Finally, we have supposed the electromagnetic wave to propagate in a homogeneous medium, whose properties do not depend on the spatial coordinate $\vec{r}$. It can however be shown that for non-homogeneous media the equations now derived can still be applied provided that

$$\left| \operatorname{grad} n_\alpha \right| \ll \left| n_\alpha \frac{2\pi}{\lambda} \right| \, ,$$

a condition which is generally well-satisfied for optical radiation propagating in astrophysical or laboratory plasmas.

5.3. Application to Magnetic Lines

We now apply the results of the previous section to the case of an atomic vapor in the presence of a magnetic field. We describe the atom by the classical theory of the electron, going back to the oscillator model already used in Sect. 3.2. In the presence of a constant magnetic field $\vec{B}$ and of an oscillating electric field of the form

$$\vec{E} \, \mathrm{e}^{-2\pi \mathrm{i} \nu t} \, ,$$

the motion of the electron is described by the equation

$$\frac{\mathrm{d}^2\vec{x}}{\mathrm{d}t^2} = -4\pi^2\nu_0^2\,\vec{x} - \frac{e_0}{mc}\,\frac{\mathrm{d}\vec{x}}{\mathrm{d}t}\times\vec{B} - \gamma\,\frac{\mathrm{d}\vec{x}}{\mathrm{d}t} - \frac{e_0}{m}\,\vec{E}\,\mathrm{e}^{-2\pi\mathrm{i}\nu t}\,, \tag{5.28}$$

where ν_0 is the frequency of the oscillator and γ is the damping constant.

To find the dipole induced by the oscillating electric field associated with the incident electromagnetic wave we disregard the transient solution depending on the initial conditions and we look for a solution of the form

$$\vec{x} = \vec{a}\;\mathrm{e}^{-2\pi\mathrm{i}\nu t}\,.$$

Substitution into Eq. (5.28) gives

$$\left[4\pi^2(\nu_0^2-\nu^2) - 2\pi\mathrm{i}\,\nu\gamma\right]\vec{a} - 8\pi^2\mathrm{i}\,\nu\nu_{\mathrm{L}}\,\vec{a}\times\vec{u}_0 = -\frac{e_0}{m}\,\vec{E}\,,$$

where ν_{L} is the Larmor frequency defined in Eq. (3.10) and $\vec{u}_0$ is a real unit vector directed along the magnetic field.

Similarly to Sect. 3.2, we introduce the real orthogonal unit vectors $\vec{u}_r$, $\vec{u}_s$ (such that $(\vec{u}_r, \vec{u}_s, \vec{u}_0)$ is a right-handed coordinate system), and their linear combinations $\vec{u}_{\pm1}$ defined in Eqs. (3.25). Expanding the vectors $\vec{a}$ and $\vec{E}$ on the basis $\vec{u}_\alpha$ ($\alpha = 0, \pm1$),

$$\vec{a} = \sum_\alpha a_\alpha\,\vec{u}_\alpha\,, \qquad \vec{E} = \sum_\alpha E_\alpha\,\vec{u}_\alpha\,,$$

one easily obtains, with the help of Eq. (3.26)

$$a_\alpha = \chi_\alpha\,E_\alpha\,, \tag{5.29}$$

where χ_α is the electric susceptibility

$$\chi_\alpha = -\frac{e_0}{4\pi^2 m}\,\frac{1}{(\nu_0^2-\nu^2) - 2\mathrm{i}\nu\Gamma - 2\alpha\nu\nu_{\mathrm{L}}} \qquad (\alpha = 0, \pm1) \tag{5.30}$$

with $\Gamma = \gamma/4\pi$.

If there are N oscillators per unit volume, the electric polarization is

$$\vec{P} = -N\,e_0\,\vec{a}$$

and the electric displacement is

$$\vec{D} = \vec{E} + 4\pi\vec{P} = \vec{E} - 4\pi N e_0\,\vec{a}\,.$$

Therefore the principal dielectric constants ϵ_α defined in Eq. (5.5) are given by

$$\epsilon_\alpha = 1 + \frac{Ne_0^2}{\pi m}\,\frac{1}{(\nu_0^2-\nu^2) - 2\alpha\nu\nu_{\mathrm{L}} - 2\mathrm{i}\nu\Gamma} \qquad (\alpha = 0, \pm1)\,.$$

Since both $\nu_{\rm L}$ and Γ are usually much smaller than ν_0 (see Sect. 3.2), the principal dielectric constants are sharp functions of the frequency ν peaked at ν_0, so that we can replace $(\nu_0^2 - \nu^2)$ by $2\nu\,(\nu_0 - \nu)$.

If we now assume – consistently with the treatment of Sect. 5.2 – the principal dielectric constants to be close to unity, and separate the refractive indices n_α in their real and imaginary parts,

$$n_\alpha = (1 + \delta_\alpha) + \mathrm{i}\, k_\alpha \tag{5.31}$$

with δ_α and k_α real, we obtain from Eqs. (5.9) and (5.19)

$$\begin{aligned} k_\alpha &= \frac{N e_0^2}{4\pi m \nu}\, \frac{\Gamma}{(\nu_0 - \alpha\nu_{\rm L} - \nu)^2 + \Gamma^2} \\ \delta_\alpha &= \frac{N e_0^2}{4\pi m \nu}\, \frac{\nu_0 - \alpha\nu_{\rm L} - \nu}{(\nu_0 - \alpha\nu_{\rm L} - \nu)^2 + \Gamma^2}\ . \end{aligned} \tag{5.32}$$

It should be emphasized that the basis $\vec{u}_\alpha$ $(\alpha = 0, \pm 1)$ introduced above is such that the unit vectors $\vec{u}'_\alpha$ appearing in the expression of the propagation tensor $\boldsymbol{G}$ (Eq. (5.22)) are given by

$$\vec{u}'_\alpha = \vec{u}^{\,*}_\alpha\ ,$$

as it can be proved directly from Eqs. (5.8). As a consequence, the propagation tensor reduces to

$$G_{jk} = -2\pi\mathrm{i}\,\frac{\nu}{c} \sum_\alpha C_{\alpha j}\, C^*_{\alpha k}\, n_\alpha\ , \tag{5.33}$$

where $C_{\alpha j}$ are the direction cosines defined in Eq. (3.31), and the completeness relation (5.17) becomes

$$\sum_\alpha C_{\alpha i}\, C^*_{\alpha j} = \delta_{ij}\ . \tag{5.34}$$

Equations (5.33), (5.34), and (5.31) allow the coefficients of the propagation matrix $\boldsymbol{K}$ given in Eq. (5.26) to be written in the form[1]

$$\begin{aligned} \eta_I &= 2\pi\,\frac{\nu}{c} \sum_\alpha k_\alpha \left(|C_{\alpha 1}|^2 + |C_{\alpha 2}|^2\right) \\ \eta_Q &= 2\pi\,\frac{\nu}{c} \sum_\alpha k_\alpha \left(|C_{\alpha 1}|^2 - |C_{\alpha 2}|^2\right) \\ \eta_U &= 2\pi\,\frac{\nu}{c} \sum_\alpha k_\alpha\, 2\,\mathrm{Re}\left(C_{\alpha 1}\, C^*_{\alpha 2}\right) \\ \eta_V &= 2\pi\,\frac{\nu}{c} \sum_\alpha k_\alpha\, 2\,\mathrm{Im}\left(C_{\alpha 1}\, C^*_{\alpha 2}\right) \end{aligned}$$

[1] Note that these expressions hold provided the unit vectors $\vec{e}_i$ appearing in the direction cosines $C_{\alpha i}$ are the reference direction unit vector $\vec{e}_a$ and the associated unit vector $\vec{e}_b$ (see Sect. 5.2).

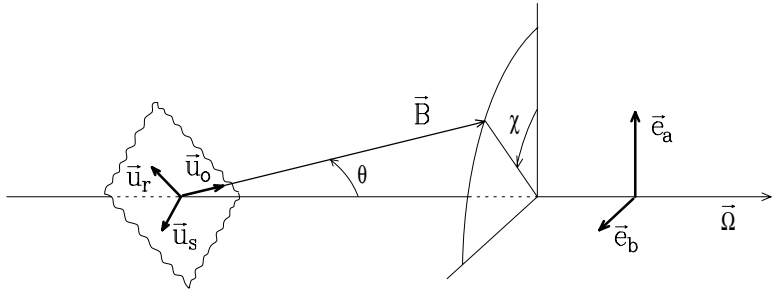

Fig.5.1. The direction of the magnetic field $\vec{B}$ is specified by the polar angle θ and the azimuth angle χ, reckoned from the reference direction $\vec{e}_a$. In the plane perpendicular to $\vec{B}$, the unit vector $\vec{u}_r$ lies in the plane containing $\vec{B}$ and $\vec{\Omega}$; $\vec{u}_s$ is defined accordingly.

$$\rho_Q = 2\pi \frac{\nu}{c} \sum_\alpha \delta_\alpha \left(|C_{\alpha 1}|^2 - |C_{\alpha 2}|^2 \right)$$
$$\rho_U = 2\pi \frac{\nu}{c} \sum_\alpha \delta_\alpha \, 2\,\mathrm{Re}\left(C_{\alpha 1}\, C^*_{\alpha 2} \right)$$
$$\rho_V = 2\pi \frac{\nu}{c} \sum_\alpha \delta_\alpha \, 2\,\mathrm{Im}\left(C_{\alpha 1}\, C^*_{\alpha 2} \right) . \qquad (5.35)$$

Thus in the case considered in this section (propagation of electromagnetic waves through an atomic vapor permeated by a magnetic field), the quantities η_I, η_Q, η_U, η_V depend only on the imaginary parts k_α of the refractive indices, while ρ_Q, ρ_U, ρ_V depend only on the real parts δ_α. More precisely, η_Q, η_U, η_V depend upon *differences* between the imaginary parts, as apparent from the fact that these quantities vanish when the three k_α are equal (isotropic case). Therefore the phenomena described by the second matrix in the expansion (5.27) consist in a differential absorption of the different polarization states: hence the denomination of 'dichroism matrix' introduced in Sect. 5.2. By contrast, the third matrix in Eq. (5.27) is connected with differences between the real parts of the refractive indices, thus it describes phenomena associated with the dephasing of the different polarization states in the propagation through the medium (hence the denomination of 'dispersion matrix').

The direction cosines $C_{\alpha i}$ can be explicitly evaluated once the geometry of the magnetic field is specified. From Fig. 5.1 we easily obtain

$$\vec{u}_r = \cos\theta \cos\chi \, \vec{e}_a + \cos\theta \sin\chi \, \vec{e}_b - \sin\theta \, \vec{\Omega}$$
$$\vec{u}_s = -\sin\chi \, \vec{e}_a + \cos\chi \, \vec{e}_b$$
$$\vec{u}_0 = \sin\theta \cos\chi \, \vec{e}_a + \sin\theta \sin\chi \, \vec{e}_b + \cos\theta \, \vec{\Omega} \, ,$$

so that

$$\vec{u}_{\pm 1} = \frac{1}{\sqrt{2}} \Big[(\mp \cos\theta \cos\chi - \mathrm{i} \, \sin\chi) \, \vec{e}_a + (\mp \cos\theta \sin\chi + \mathrm{i} \, \cos\chi) \, \vec{e}_b \pm \sin\theta \, \vec{\Omega} \Big] \, .$$

TABLE 5.1

Expressions for the bilinear combinations of the quantities $C_{\alpha i}$

	$\alpha = -1$	$\alpha = 0$	$\alpha = +1$
$\lvert C_{\alpha 1}\rvert^2 + \lvert C_{\alpha 2}\rvert^2$	$\frac{1}{2}\,(1+\cos^2\theta)$	$\sin^2\theta$	$\frac{1}{2}\,(1+\cos^2\theta)$
$\lvert C_{\alpha 1}\rvert^2 - \lvert C_{\alpha 2}\rvert^2$	$-\frac{1}{2}\,\sin^2\theta\,\cos 2\chi$	$\sin^2\theta\,\cos 2\chi$	$-\frac{1}{2}\,\sin^2\theta\,\cos 2\chi$
$2\,\mathrm{Re}\left(C_{\alpha 1} C^*_{\alpha 2}\right)$	$-\frac{1}{2}\,\sin^2\theta\,\sin 2\chi$	$\sin^2\theta\,\sin 2\chi$	$-\frac{1}{2}\,\sin^2\theta\,\sin 2\chi$
$2\,\mathrm{Im}\left(C_{\alpha 1} C^*_{\alpha 2}\right)$	$-\cos\theta$	0	$\cos\theta$

The $C_{\alpha i}$ combinations appearing in Eqs. (5.35) are summarized in Table 5.1. Using Eqs. (5.32) one finally obtains the following expressions for the elements of the propagation matrix

$$
\begin{aligned}
\eta_I &= \frac{\pi e_0^2}{mc}\,N\,\frac{1}{2}\left[\phi_{\mathrm{p}}\sin^2\theta + \frac{\phi_{\mathrm{b}}+\phi_{\mathrm{r}}}{2}\,(1+\cos^2\theta)\right] \\
\eta_Q &= \frac{\pi e_0^2}{mc}\,N\,\frac{1}{2}\left[\phi_{\mathrm{p}} - \frac{\phi_{\mathrm{b}}+\phi_{\mathrm{r}}}{2}\right]\sin^2\theta\,\cos 2\chi \\
\eta_U &= \frac{\pi e_0^2}{mc}\,N\,\frac{1}{2}\left[\phi_{\mathrm{p}} - \frac{\phi_{\mathrm{b}}+\phi_{\mathrm{r}}}{2}\right]\sin^2\theta\,\sin 2\chi \\
\eta_V &= \frac{\pi e_0^2}{mc}\,N\,\frac{1}{2}\left[\phi_{\mathrm{r}} - \phi_{\mathrm{b}}\right]\cos\theta \\
\rho_Q &= \frac{\pi e_0^2}{mc}\,N\,\frac{1}{2}\left[\psi_{\mathrm{p}} - \frac{\psi_{\mathrm{b}}+\psi_{\mathrm{r}}}{2}\right]\sin^2\theta\,\cos 2\chi \\
\rho_U &= \frac{\pi e_0^2}{mc}\,N\,\frac{1}{2}\left[\psi_{\mathrm{p}} - \frac{\psi_{\mathrm{b}}+\psi_{\mathrm{r}}}{2}\right]\sin^2\theta\,\sin 2\chi \\
\rho_V &= \frac{\pi e_0^2}{mc}\,N\,\frac{1}{2}\left[\psi_{\mathrm{r}} - \psi_{\mathrm{b}}\right]\cos\theta\,,
\end{aligned}
\tag{5.36}
$$

where

$$
\begin{aligned}
\phi_{\mathrm{b}} &= \frac{1}{\pi}\,\frac{\Gamma}{(\nu_0+\nu_{\mathrm{L}}-\nu)^2+\Gamma^2} & \psi_{\mathrm{b}} &= \frac{1}{\pi}\,\frac{\nu_0+\nu_{\mathrm{L}}-\nu}{(\nu_0+\nu_{\mathrm{L}}-\nu)^2+\Gamma^2} \\
\phi_{\mathrm{p}} &= \frac{1}{\pi}\,\frac{\Gamma}{(\nu_0-\nu)^2+\Gamma^2} & \psi_{\mathrm{p}} &= \frac{1}{\pi}\,\frac{\nu_0-\nu}{(\nu_0-\nu)^2+\Gamma^2} \\
\phi_{\mathrm{r}} &= \frac{1}{\pi}\,\frac{\Gamma}{(\nu_0-\nu_{\mathrm{L}}-\nu)^2+\Gamma^2} & \psi_{\mathrm{r}} &= \frac{1}{\pi}\,\frac{\nu_0-\nu_{\mathrm{L}}-\nu}{(\nu_0-\nu_{\mathrm{L}}-\nu)^2+\Gamma^2}\,.
\end{aligned}
\tag{5.37}
$$

The functions ϕ_{b}, ϕ_{p}, ϕ_{r} – where the subscripts stand for 'blue', 'parallel', and 'red', respectively – have already been encountered in Sect. 3.2 (see Eqs. (3.38)). They are Lorentzian profiles centered at the frequencies $(\nu_0+\nu_{\mathrm{L}})$, ν_0, and $(\nu_0-\nu_{\mathrm{L}})$,

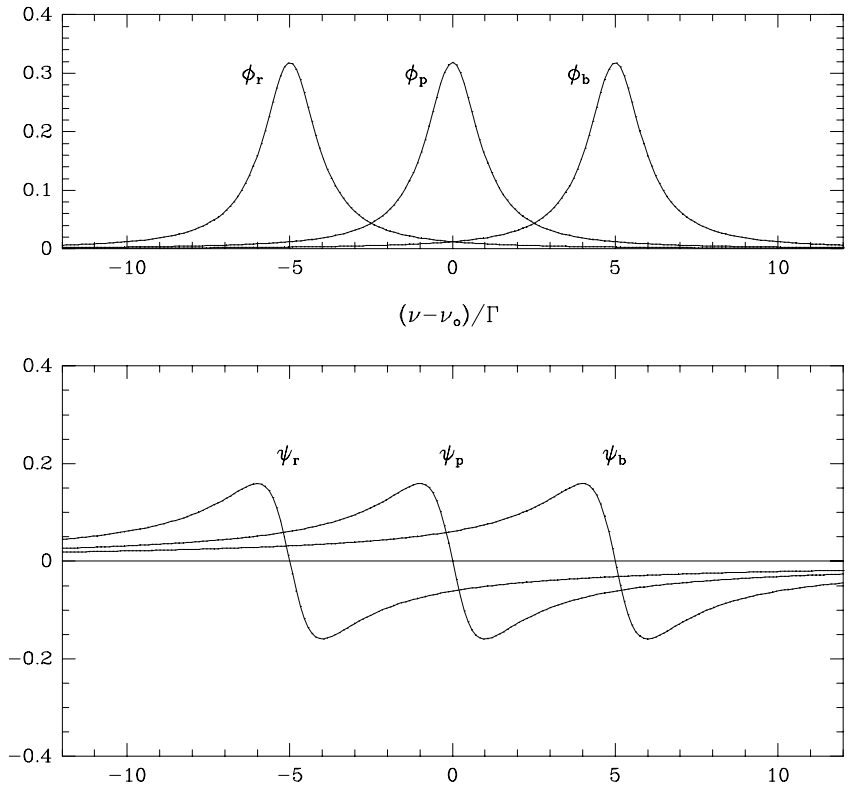

Fig.5.2. Absorption profiles ϕ and dispersion profiles ψ in units of Γ^{-1}, for $\nu_L/\Gamma = 5$.

respectively, and normalized to unity in frequency,

$$\int_{-\infty}^{\infty} \phi_{b,p,r}\, d\nu = 1 \, .$$

The functions ψ_b, ψ_p, ψ_r are the corresponding dispersion profiles. An illustrative example of such profiles is shown in Fig. 5.2. These profiles can be easily generalized to include the effect of microscopic velocity fields that may be present in the medium (see Sect. 5.4).

An important extension of the theory presented in this section concerns the inclusion of the emission term into the propagation equation. This term has already been derived in Sect. 3.2, although in a slightly different geometry (see Fig. 3.3). For the geometrical configuration of Fig. 5.1 the expressions (3.39) for the direction cosines must be replaced by corresponding expressions which lead to the bilinear combinations of Table 5.1. The emission coefficient becomes accordingly

$$\varepsilon_I = k\,\frac{1}{2}\left[\phi_p \sin^2\theta + \frac{\phi_b + \phi_r}{2}\,(1+\cos^2\theta)\right]$$

$$\varepsilon_Q = k\,\frac{1}{2}\left[\phi_{\rm p} - \frac{\phi_{\rm b}+\phi_{\rm r}}{2}\right]\sin^2\theta\cos 2\chi$$
$$\varepsilon_U = k\,\frac{1}{2}\left[\phi_{\rm p} - \frac{\phi_{\rm b}+\phi_{\rm r}}{2}\right]\sin^2\theta\sin 2\chi$$
$$\varepsilon_V = k\,\frac{1}{2}\left[\phi_{\rm r} - \phi_{\rm b}\right]\cos\theta\ , \tag{5.38}$$

where

$$k = \frac{\pi e_0^2}{mc}\,N\,\frac{2\nu_0^2}{c^2}\,\bar{E}\ ,$$

$\bar{E}$ being the mean energy contained into each degree of freedom of the classical oscillator.

Adding to Eq. (5.25) the contribution due to emission, we obtain the radiative transfer equations for polarized radiation in the form

$$\frac{\mathrm{d}}{\mathrm{d}s}\begin{pmatrix} I \\ Q \\ U \\ V \end{pmatrix} = -\begin{pmatrix} \eta_I & \eta_Q & \eta_U & \eta_V \\ \eta_Q & \eta_I & \rho_V & -\rho_U \\ \eta_U & -\rho_V & \eta_I & \rho_Q \\ \eta_V & \rho_U & -\rho_Q & \eta_I \end{pmatrix}\begin{pmatrix} I-S \\ Q \\ U \\ V \end{pmatrix}\ , \tag{5.39}$$

where the scalar source function S is given by

$$S = \frac{2\nu_0^2}{c^2}\,\bar{E}\ . \tag{5.40}$$

In particular, under the hypothesis of *Local Thermodynamic Equilibrium* (LTE) the mean energy $\bar{E}$ is given by $k_{\rm B}T$, where $k_{\rm B}$ is the Boltzmann constant and T the absolute temperature, so that

$$S_{\rm LTE} = \frac{2\nu_0^2}{c^2}\,k_{\rm B}\,T\ ,$$

which is the classical expression for the Planck function $B_{\rm P}$ in the limit $h \to 0$ (*approximation of Rayleigh and Jeans*).

Obviously, we cannot expect to find by a classical theory the exact expression for the Planck function, which is intimately connected with quantum concepts. However, using a semiclassical approach, we can go back to the quantization of the harmonic oscillator (see Sect. 4.1) and write

$$\bar{E} = h\nu_0\,\frac{\sum\limits_{n=0}^{\infty} n\,\mathrm{e}^{-nx}}{\sum\limits_{n=0}^{\infty}\mathrm{e}^{-nx}} = h\nu_0\,\frac{1}{\mathrm{e}^{x}-1}$$

where $x = h\nu_0/k_{\rm B}T$, and substituting this result into Eq. (5.40) we obtain

$$S_{\rm LTE} = \frac{2h\nu_0^3}{c^2}\,\frac{1}{\mathrm{e}^{\frac{h\nu_0}{k_{\rm B}T}}-1} = B_{\rm P}(\nu_0)\ ,$$

an expression that could also be obtained by invoking the Kirchhoff law for the emission of a source in LTE.

Equation (5.39), with the matrix coefficients given by Eqs. (5.36) and with the Planck function in the place of the source function, was first obtained by Unno (1956) by a heuristic approach which neglected anomalous dispersion effects ($\rho_Q = \rho_U = \rho_V = 0$). These effects were subsequently introduced by Rachkovsky (1962a) through classical considerations, similar to those presented in this section, based on the refractive index. Another derivation has been recently presented by Jefferies et al. (1989). In the meantime a quantum derivation of the same equation was given by Landi Degl'Innocenti and Landi Degl'Innocenti (1972), who pointed out some minor errors or ambiguities (mainly connected with sign conventions) appearing both in the original papers and in subsequent papers based on those (like for instance in Beckers, 1969a). The reader is referred to Rees (1987) for a clear presentation of the possible errors that may arise in the derivation of Eq. (5.39).

5.4. The Voigt Function and the Associated Dispersion Profile

In the previous section we have derived the absorption profiles $\phi_{\rm b}$, $\phi_{\rm p}$, $\phi_{\rm r}$ and the corresponding dispersion profiles $\psi_{\rm b}$, $\psi_{\rm p}$, $\psi_{\rm r}$ for a collection of atoms supposed at rest in the laboratory frame (the frame where the Stokes parameters are defined). These profiles are of the form $p\,(\nu_0 - \nu)$, where ν_0 is the frequency of the classical oscillator.

Actually, however, the atoms will always be in motion. In order to realize how the profiles are affected by these motions, let us consider a radiation beam of frequency ν propagating along a given direction, which we identify with the line of sight. If w is the velocity component of the atom along the line of sight, the atomic frequency ν_0 is shifted, according to the classical formula of the Doppler effect, to the new value

$$\nu_0' = \nu_0 \left(1 - \frac{w}{c}\right) ,$$

where we have assumed $w \ll c$ (non-relativistic approximation) and where we have adopted the sign astrophysical convention according to which $w > 0$ when the atom is receding from the observer.

Therefore, for a collection of atoms having a normalized distribution of velocity components $f(w)$, the profile $p\,(\nu_0 - \nu)$ must be replaced by the expression

$$\int_{-\infty}^{\infty} p\left(\nu_0 - \nu_0 \frac{w}{c} - \nu\right) f(w)\,{\rm d}w \ . \tag{5.41}$$

In many cases of astrophysical interest the velocity w can be decomposed in two parts: the bulk (or macroscopic) velocity $w_{\rm A}$ of the ambient medium, plus a random velocity due to thermal or microturbulent motions, usually distributed according

to the Maxwellian law and characterized by the velocity w_{T}. We thus assume for $f(w)$ the following expression

$$f(w) = \frac{1}{\sqrt{\pi}\, w_{\mathrm{T}}}\, \mathrm{e}^{-\left(\frac{w-w_{\mathrm{A}}}{w_{\mathrm{T}}}\right)^2} \,. \tag{5.42}$$

Substituting Eq. (5.42) into Eq. (5.41), and introducing the reduced variables

$$\begin{aligned} &\Delta\nu_{\mathrm{D}} = \nu_0\, \frac{w_{\mathrm{T}}}{c}\,, \qquad a = \frac{\Gamma}{\Delta\nu_{\mathrm{D}}} \\ &v_B = \frac{\nu_{\mathrm{L}}}{\Delta\nu_{\mathrm{D}}}\,, \qquad v_{\mathrm{A}} = \frac{w_{\mathrm{A}}}{w_{\mathrm{T}}} = \frac{\nu_0\, w_{\mathrm{A}}}{c\, \Delta\nu_{\mathrm{D}}}\,, \qquad v = \frac{\nu_0 - \nu}{\Delta\nu_{\mathrm{D}}} \end{aligned} \tag{5.43}$$

one obtains with easy transformations

$$\begin{aligned} \phi_\alpha &= \frac{1}{\sqrt{\pi}\, \Delta\nu_{\mathrm{D}}}\, H(v - v_{\mathrm{A}} + \alpha\, v_B,\, a) \\ \psi_\alpha &= \frac{1}{\sqrt{\pi}\, \Delta\nu_{\mathrm{D}}}\, L(v - v_{\mathrm{A}} + \alpha\, v_B,\, a)\,, \end{aligned} \tag{5.44}$$

where $\alpha = -1, 0, +1$ for the 'red', 'parallel', and 'blue' component, respectively, and where we have defined the functions

$$\begin{aligned} H(v,a) &= \frac{a}{\pi} \int_{-\infty}^{\infty} \mathrm{e}^{-y^2}\, \frac{1}{(v-y)^2 + a^2}\, \mathrm{d}y \\ L(v,a) &= \frac{1}{\pi} \int_{-\infty}^{\infty} \mathrm{e}^{-y^2}\, \frac{v-y}{(v-y)^2 + a^2}\, \mathrm{d}y\,. \end{aligned} \tag{5.45}$$

In the above expressions $\Delta\nu_{\mathrm{D}}$ represents the Doppler width in frequency units, and it is used to normalize all the other quantities: v is the so-called *reduced frequency*, v_B the normalized Zeeman splitting, v_{A} the normalized shift due to the bulk motion, and a the *damping constant*. Figure 5.3 shows the two sets of profiles ϕ and ψ.

The functions defined in Eqs. (5.45) are the so-called *Voigt function* $H(v,a)$ and the *associated dispersion profile* $L(v,a)$. In previous works on this subject the function $L(v,a)$ has been usually written in the form

$$L(v,a) = 2F(v,a)\,,$$

and the name of *Faraday-Voigt function* has sometimes been employed for $F(v,a)$.

It should be remarked that the quantities defined in Eqs. (5.43) can be expressed in terms of wavelength (instead of frequency) displacements and broadenings. Introducing the Doppler width in wavelength units,

$$\Delta\lambda_{\mathrm{D}} = \frac{\lambda_0^2}{c}\, \Delta\nu_{\mathrm{D}} = \lambda_0\, \frac{w_{\mathrm{T}}}{c}\,, \tag{5.46}$$

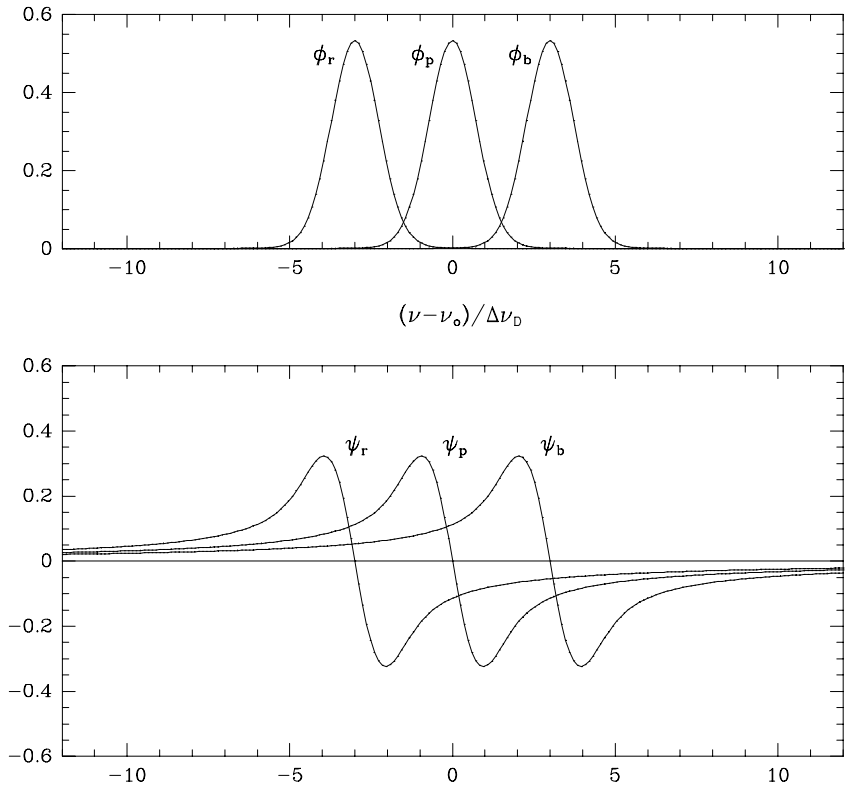

Fig.5.3. Absorption profiles ϕ and dispersion profiles ψ in units of $\Delta\nu_{\rm D}^{-1}$, corresponding to $v_B = 3$, $v_{\rm A} = 0$, and $a = 0.05$. Note that the magnetic field is 12 times stronger than in Fig.5.2.

Eqs. (5.43) can be written in the form

$$v = \frac{\lambda - \lambda_0}{\Delta\lambda_{\rm D}} , \qquad a = \frac{\lambda_0^2\,\Gamma}{c\,\Delta\lambda_{\rm D}} , \qquad v_{\rm A} = \frac{\lambda_0\, w_{\rm A}}{c\,\Delta\lambda_{\rm D}}$$

$$v_B = \frac{\lambda_0^2\,\nu_{\rm L}}{c\,\Delta\lambda_{\rm D}} = \frac{\lambda_0^2\, e_0\, B}{4\pi m c^2\,\Delta\lambda_{\rm D}} = \frac{\Delta\lambda_B}{\Delta\lambda_{\rm D}} , \tag{5.47}$$

where $\Delta\lambda_B$ is defined in Eq. (3.13). With these positions Eqs. (5.44) are still valid.[1]

The *thermal velocity* $w_{\rm T}$ in the above equations can be related to the kinetic temperature T and to the microturbulent velocity ξ by the expression

$$w_{\rm T} = \sqrt{\frac{2k_{\rm B}T}{\mu M} + \xi^2} , \tag{5.48}$$

[1] Note, however, that the profiles ϕ_α defined in Eqs. (5.44) are normalized to unity in frequency. The corresponding profiles, normalized to unity in wavelength, are obtained by substituting $\Delta\lambda_{\rm D}$ for $\Delta\nu_{\rm D}$ in the same equations.

where μ is the atomic weight of the atom which originates the spectral line and M is the mass of unit atomic weight. Therefore, the normalized Zeeman splitting v_B can be expressed in the form

$$v_B = \frac{\lambda_0 e_0 B}{4\pi mc} \frac{1}{\sqrt{\frac{2k_B T}{\mu M} + \xi^2}}$$

or, numerically

$$v_B = 1.400 \times 10^{-7} \lambda_0 B \frac{1}{\sqrt{1.663 \times 10^{-2} \frac{T}{\mu} + \xi^2}} , \tag{5.49}$$

where λ_0 is in Å, B in G, T in K and ξ in km s^{-1}.

In the following of this section we discuss the main mathematical properties of the functions $H(v, a)$ and $L(v, a)$ defined in Eqs. (5.45). These properties are easily obtained by considering, rather than the separate functions, their complex linear combination

$$W(v, a) = H(v, a) + \mathrm{i}\, L(v, a) . \tag{5.50}$$

Introducing the complex variable z defined as

$$z = v + \mathrm{i}\, a , \tag{5.51}$$

we obtain with easy transformations

$$W(z) = \frac{\mathrm{i}}{\pi} \int_{-\infty}^{\infty} \frac{\mathrm{e}^{-y^2}}{z - y} \, \mathrm{d}y , \tag{5.52}$$

where, being $a > 0$, we have $\operatorname{Im} z > 0$. The function $W(z)$ is an analytical function of the complex variable z that can be related to the *complementary error function* (see Abramowitz and Stegun, 1965).

By the substitution $(z - y) = u$ we first transform the integral in Eq. (5.52) into the following

$$W(z) = \frac{\mathrm{i}}{\pi} \mathrm{e}^{-z^2} \int_L \frac{\mathrm{e}^{-u^2+2uz}}{u} \, \mathrm{d}u ,$$

where L is a straight line parallel to the real axis in the half plane $\operatorname{Im} u > 0$ (see Fig. 5.4).

Next we observe that

$$\frac{\mathrm{d}}{\mathrm{d}z} \int_L \frac{\mathrm{e}^{-u^2+2uz}}{u} \, \mathrm{d}u = 2 \int_L \mathrm{e}^{-u^2+2uz} \, \mathrm{d}u = 2\, \mathrm{e}^{z^2} \int_L \mathrm{e}^{-(u-z)^2} \, \mathrm{d}u = 2\sqrt{\pi}\, \mathrm{e}^{z^2} ,$$

whence we obtain by integration

$$\int_L \frac{\mathrm{e}^{-u^2+2uz}}{u} \, \mathrm{d}u = C + 2\sqrt{\pi} \int_0^z \mathrm{e}^{t^2} \, \mathrm{d}t , \tag{5.53}$$

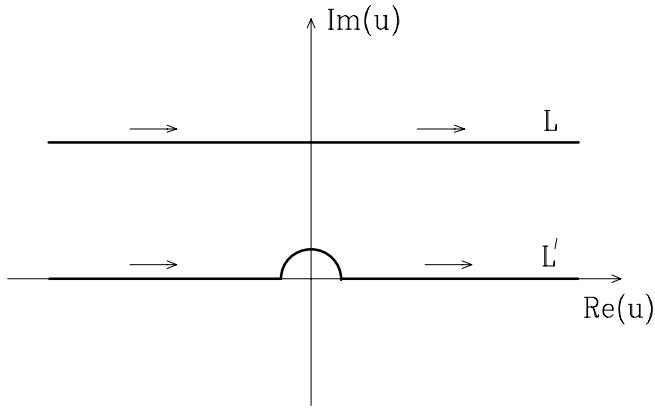

Fig.5.4. Integration paths L and L' in the plane of the complex variable u.

where C is a constant that can be determined by taking the limit $z \to 0$ of Eq. (5.53)

$$C = \lim_{z\to 0} \int_L \frac{\mathrm{e}^{-u^2+2uz}}{u}\,\mathrm{d}u = \int_L \frac{\mathrm{e}^{-u^2}}{u}\,\mathrm{d}u\ .$$

The last integral can be evaluated by observing that the integration variable u has a pole at the origin. Deforming the integration path L into the path L' shown in Fig. 5.4, the contributions arising from the integration along the real axis cancel out, while the contribution from the semicircle around the origin simply gives $-\mathrm{i}\pi$.

To conclude, we have obtained that the function $W(z)$ can be written in the form

$$W(z) = \mathrm{e}^{-z^2}\left[1 + \frac{2\mathrm{i}}{\sqrt{\pi}}\int_0^z \mathrm{e}^{t^2}\,\mathrm{d}t\right] = \mathrm{e}^{-z^2}\,\mathrm{erfc}\,(-\mathrm{i}z)\ , \tag{5.54}$$

where $\mathrm{erfc}\,(x)$ is the complementary error function defined as in Abramowitz and Stegun (1965).

From Eqs. (5.52) and (5.54) some important properties of the functions $H(v,a)$ and $L(v,a)$ can be easily derived:

i) *Limiting case* $a = 0$.

For $a = 0$, being $z = v$, Eq. (5.54) gives

$$W(z) = \mathrm{e}^{-v^2} + \frac{2\mathrm{i}}{\sqrt{\pi}}\,\mathrm{e}^{-v^2}\int_0^v \mathrm{e}^{t^2}\,\mathrm{d}t\ ,$$

thus from Eq. (5.50) one gets

$$H(v,0) = \mathrm{e}^{-v^2}\ , \qquad L(v,0) = \frac{2}{\sqrt{\pi}}\,D(v)\ , \tag{5.55}$$

where $D(v)$ is the so-called *Dawson integral*

$$D(v) = \mathrm{e}^{-v^2} \int_0^v \mathrm{e}^{t^2}\, \mathrm{d}t \,. \tag{5.56}$$

ii) *Limiting case* $v = 0$.
Being now $z = \mathrm{i}a$ we get

$$W(z) = \mathrm{e}^{a^2} \left[1 + \frac{2\mathrm{i}}{\sqrt{\pi}} \int_0^{\mathrm{i}a} \mathrm{e}^{t^2}\, \mathrm{d}t\right] ,$$

so that

$$H(0,a) = \mathrm{e}^{a^2} \left[1 - \frac{2}{\sqrt{\pi}} \int_0^a \mathrm{e}^{-t^2}\, \mathrm{d}t\right] = \mathrm{e}^{a^2}\, \mathrm{erfc}\,(a)$$
$$L(0,a) = 0 \,.$$

iii) *Asymptotic expansion for large values of the argument:* $(v^2 + a^2) \gg 1$.
In Eq. (5.52) one can write

$$\frac{1}{z-y} = \frac{1}{z}\, \left[1 - \frac{y}{z}\right]^{-1} = \sum_{k=0}^{\infty} \frac{y^k}{z^{k+1}} \,,$$

therefore

$$W(z) = \frac{\mathrm{i}}{\pi} \sum_{k=0}^{\infty} \int_{-\infty}^{\infty} \frac{y^k}{z^{k+1}}\, \mathrm{e}^{-y^2}\, \mathrm{d}y = \frac{\mathrm{i}}{\pi} \sum_{n=0}^{\infty} \frac{\Gamma(n+1/2)}{z^{2n+1}} \,,$$

where $\Gamma(x)$ is the Euler Gamma function. By taking the leading terms of the expansion in inverse powers of z one easily obtains the asymptotic behavior

$$H(v,a) \sim \frac{1}{\sqrt{\pi}}\, \frac{a}{a^2+v^2} \left[1 + \frac{1}{2}\, \frac{3v^2 - a^2}{(a^2+v^2)^2} + \cdots\right]$$
$$L(v,a) \sim \frac{1}{\sqrt{\pi}}\, \frac{v}{a^2+v^2} \left[1 + \frac{1}{2}\, \frac{v^2 - 3a^2}{(a^2+v^2)^2} + \cdots\right] . \tag{5.57}$$

iv) *Derivatives*.
From Eq. (5.54) we have

$$\frac{\mathrm{d}W(z)}{\mathrm{d}z} = -2z\, W(z) + \frac{2\mathrm{i}}{\sqrt{\pi}} \,,$$

from which we deduce

$$\frac{\partial}{\partial v}(H + \mathrm{i}\, L) = -\mathrm{i}\, \frac{\partial}{\partial a}(H + \mathrm{i}\, L) = -2\,(v + \mathrm{i}\, a)\,(H + \mathrm{i}\, L) + \frac{2\mathrm{i}}{\sqrt{\pi}}\ ,$$

whence

$$\begin{aligned} \frac{\partial H(v,a)}{\partial v} &= \frac{\partial L(v,a)}{\partial a} = 2\Big[-vH(v,a) + aL(v,a)\Big] \\ \frac{\partial H(v,a)}{\partial a} &= -\frac{\partial L(v,a)}{\partial v} = 2\Big[-\frac{1}{\sqrt{\pi}} + aH(v,a) + vL(v,a)\Big]\ , \end{aligned} \tag{5.58}$$

a set of formulae which allows to express the derivatives of $H(v,a)$ and $L(v,a)$ in terms of the functions themselves.

v) *Power series expansion.*

For $a \ll 1$, a useful series expansion can be easily derived from Eqs. (5.58). We give here the expansion up to the fourth order in powers of a

$$\begin{aligned} H(v,a) &= \mathrm{e}^{-v^2} + \frac{2a}{\sqrt{\pi}}\Big(2vD(v) - 1\Big) + a^2\Big(1 - 2v^2\Big)\,\mathrm{e}^{-v^2} \\ &\quad + \frac{4a^3}{3\sqrt{\pi}}\Big[v^2 - 1 + v(3 - 2v^2)D(v)\Big] + \frac{a^4}{6}\Big(3 - 12v^2 + 4v^4\Big)\,\mathrm{e}^{-v^2} + \cdots \\ L(v,a) &= \frac{2}{\sqrt{\pi}}\,D(v) - 2av\,\mathrm{e}^{-v^2} + \frac{2}{\sqrt{\pi}}a^2\Big[v + (1 - 2v^2)D(v)\Big] - \frac{2}{3}a^3 v(3 - 2v^2)\,\mathrm{e}^{-v^2} \\ &\quad + \frac{1}{3\sqrt{\pi}}a^4\Big[v(5 - 2v^2) + (3 - 12v^2 + 4v^4)D(v)\Big] + \cdots \end{aligned}$$

vi) *Symmetry properties.*

From Eqs. (5.45) the following symmetry properties are easily derived

$$H(-v,a) = H(v,a)\ , \qquad L(-v,a) = -L(v,a)\ , \tag{5.59}$$

which means that H is symmetrical in v, while L is antisymmetrical.

vii) *Integral properties.*

From Eq. (5.52), integrating in the complex plane z along the real axis R, and using the residue theorem, we obtain

$$\int_R W(z)\,\mathrm{d}z = \frac{\mathrm{i}}{\pi}\int_{-\infty}^{\infty}\mathrm{d}y\ \ \mathrm{e}^{-y^2}\int_R \frac{1}{z - y}\,\mathrm{d}z = \int_{-\infty}^{\infty}\mathrm{e}^{-y^2}\,\mathrm{d}y = \sqrt{\pi}\ ,$$

whence

$$\int_{-\infty}^{\infty} H(v,a)\,\mathrm{d}v = \sqrt{\pi}\ , \qquad \int_{-\infty}^{\infty} L(v,a)\,\mathrm{d}v = 0\ . \tag{5.60}$$

This formula proves that the profiles ϕ_α in Eqs. (5.44) are normalized to unity in frequency.

viii) *Convolutions*.
Consider the integral

$$\int_{-\infty}^{\infty} W(v - v_0\,, a)\, W(v - v_0'\,, a')\, \mathrm{d}v\ .$$

Using Eqs. (5.51)-(5.52) and inverting the order of the integrals one gets

$$\int_{-\infty}^{\infty} W(v - v_0\,, a)\, W(v - v_0'\,, a')\, \mathrm{d}v =$$

$$= -\frac{1}{\pi^2} \int_{-\infty}^{\infty} \mathrm{d}y\ \mathrm{e}^{-y^2} \int_{-\infty}^{\infty} \mathrm{d}y'\ \mathrm{e}^{-y'^2} \int_{-\infty}^{\infty} \frac{1}{(v - v_0 - y + \mathrm{i}\, a)\,(v - v_0' - y' + \mathrm{i}\, a')}\ \mathrm{d}v\ .$$

The last integral can be performed via the residue theorem. Since both poles lie in the half plane $\mathrm{Im}\ v < 0$, one obtains

$$\int_{-\infty}^{\infty} W(v - v_0\,, a)\, W(v - v_0'\,, a')\, \mathrm{d}v = 0\ . \tag{5.61}$$

Similarly,

$$\int_{-\infty}^{\infty} W(v - v_0\,, a)\, W(v - v_0'\,, a')^*\, \mathrm{d}v =$$

$$= \frac{1}{\pi^2} \int_{-\infty}^{\infty} \mathrm{d}y\ \mathrm{e}^{-y^2} \int_{-\infty}^{\infty} \mathrm{d}y'\ \mathrm{e}^{-y'^2} \int_{-\infty}^{\infty} \frac{1}{(v - v_0 - y + \mathrm{i}\, a)\,(v - v_0' - y' - \mathrm{i}\, a')}\ \mathrm{d}v\ ,$$

and using again the residue theorem we obtain

$$\int_{-\infty}^{\infty} W(v - v_0\,, a)\, W(v - v_0'\,, a')^*\, \mathrm{d}v =$$

$$= \frac{2\,\mathrm{i}}{\pi} \int_{-\infty}^{\infty} \mathrm{d}y\ \mathrm{e}^{-y^2} \int_{-\infty}^{\infty} \mathrm{d}y'\ \mathrm{e}^{-y'^2}\ \frac{1}{v_0' - v_0 + y' - y + \mathrm{i}\,(a' + a)}\ .$$

The double integral can be evaluated by the substitution

$$x = \frac{1}{\sqrt{2}} \left(y - y'\right) , \qquad x' = \frac{1}{\sqrt{2}} \left(y + y'\right) , \tag{5.62}$$

which leads to

$$\int_{-\infty}^{\infty} W(v - v_0 , a)\, W(v - v_0' , a')^* \, \mathrm{d}v =$$

$$= \frac{2\,\mathrm{i}}{\pi} \int_{-\infty}^{\infty} \mathrm{e}^{-x'^2} \, \mathrm{d}x' \int_{-\infty}^{\infty} \frac{\mathrm{e}^{-x^2}}{v_0' - v_0 - \sqrt{2}\, x + \mathrm{i}\,(a' + a)} \, \mathrm{d}x \, .$$

Performing the integral in $\mathrm{d}x'$ and recalling Eq. (5.52), one finally obtains

$$\int_{-\infty}^{\infty} W(v - v_0 , a)\, W(v - v_0' , a')^* \, \mathrm{d}v = \sqrt{2\pi} \;\; W\!\left(\frac{v_0' - v_0}{\sqrt{2}} , \frac{a' + a}{\sqrt{2}} \right) . \tag{5.63}$$

Substitution of Eq. (5.50) into Eqs. (5.61) and (5.63) yields

$$\begin{aligned}
\int_{-\infty}^{\infty} H(v - v_0 , a)\, H(v - v_0' , a') \, \mathrm{d}v &= \sqrt{\frac{\pi}{2}} \;\; H\!\left(\frac{v_0' - v_0}{\sqrt{2}} , \frac{a' + a}{\sqrt{2}} \right) \\
\int_{-\infty}^{\infty} L(v - v_0 , a)\, L(v - v_0' , a') \, \mathrm{d}v &= \sqrt{\frac{\pi}{2}} \;\; H\!\left(\frac{v_0' - v_0}{\sqrt{2}} , \frac{a' + a}{\sqrt{2}} \right) \\
\int_{-\infty}^{\infty} L(v - v_0 , a)\, H(v - v_0' , a') \, \mathrm{d}v &= \sqrt{\frac{\pi}{2}} \;\; L\!\left(\frac{v_0' - v_0}{\sqrt{2}} , \frac{a' + a}{\sqrt{2}} \right) .
\end{aligned} \tag{5.64}$$

These formulae can be easily generalized to more complicated convolutions. Considering the integrals

$$\int_{-\infty}^{\infty} W\!\left(\frac{v - v_0}{b} , a \right) W\!\left(\frac{v - v_0'}{b'} , a' \right) \mathrm{d}v$$

and

$$\int_{-\infty}^{\infty} W\!\left(\frac{v - v_0}{b} , a \right) W\!\left(\frac{v - v_0'}{b'} , a' \right)^* \mathrm{d}v \, ,$$

we obtain with similar manipulations[1]

$$\int_{-\infty}^{\infty} H\left(\frac{v - v_0}{b}, a\right) H\left(\frac{v - v_0'}{b'}, a'\right) \mathrm{d}v =$$

$$= \frac{b\, b' \sqrt{\pi}}{\sqrt{b^2 + b'^2}} H\left(\frac{v_0' - v_0}{\sqrt{b^2 + b'^2}}, \frac{a' b' + ab}{\sqrt{b^2 + b'^2}}\right)$$

$$\int_{-\infty}^{\infty} L\left(\frac{v - v_0}{b}, a\right) L\left(\frac{v - v_0'}{b'}, a'\right) \mathrm{d}v =$$

$$= \frac{b\, b' \sqrt{\pi}}{\sqrt{b^2 + b'^2}} H\left(\frac{v_0' - v_0}{\sqrt{b^2 + b'^2}}, \frac{a' b' + ab}{\sqrt{b^2 + b'^2}}\right)$$

$$\int_{-\infty}^{\infty} L\left(\frac{v - v_0}{b}, a\right) H\left(\frac{v - v_0'}{b'}, a'\right) \mathrm{d}v =$$

$$= \frac{b\, b' \sqrt{\pi}}{\sqrt{b^2 + b'^2}} L\left(\frac{v_0' - v_0}{\sqrt{b^2 + b'^2}}, \frac{a' b' + ab}{\sqrt{b^2 + b'^2}}\right). \tag{5.65}$$

ix) *Maxima and minima.*

The function $H(v, a)$, considered as a function of v, has a single maximum at $v = 0$. The maxima and minima of the function $L(v, a)$ with respect to v can be found by solving the implicit equation (see Eqs. (5.58))

$$a\, H(v_0, a) + v_0\, L(v_0, a) = \frac{1}{\sqrt{\pi}}\,.$$

Using numerical methods, the value of v_0 is found to be 0.9241 for $a = 0$, and to increase almost linearly to 1.5372 for $a = 1$. For larger values of a, v_0 converges asymptotically towards a as it can be deduced from Eq. (5.57). Obviously, there is a corresponding minimum at $v = -v_0$.

x) *Numerical methods.*

Several algorithms have been proposed for the numerical computation of the functions $H(v, a)$ and $L(v, a)$. The most extensively used for astrophysical applications are those by Reichel (1968), Hui et al. (1978), and Humlicek (1982). The values obtained using these algorithms can be checked against the tabulated values of the complex function $W(z)$ given by Faddeeva and Terent'ev (1961).

---

[1] Transformation (5.62) should be replaced by the following

$$x = \frac{by - b'y'}{\sqrt{b^2 + b'^2}}\,, \qquad x' = \frac{b'y + by'}{\sqrt{b^2 + b'^2}}\,.$$

5.5. Symmetry Properties of the Transfer Equations for Polarized Radiation

In Sect. 5.2 we have derived, in the framework of classical electrodynamics, a compact expression for the propagation matrix $\boldsymbol{K}$ which describes the transfer of polarized radiation, and we have seen that this matrix satisfies the remarkable symmetry properties summarized in Eq. (5.27). It will be shown in Sect. 6.7 that the quantum-mechanical treatment leads to the same symmetry properties, so that it seems natural to ascribe them to general physical principles. Following Landi Degl'Innocenti and Landi Degl'Innocenti (1981) we present here a series of arguments leading to an alternative proof of Eq. (5.27).

Consider a radiation beam of frequency ν, characterized by the Stokes parameters I, Q, U, and V, propagating through an arbitrary medium within the solid angle $\mathrm{d}\Omega$ in the direction $\vec{\Omega}$. By analogy with the usual transfer equation for unpolarized radiation we can write for the Stokes parameters a transfer equation of the form

$$\frac{\mathrm{d}}{\mathrm{d}s} S_i = -\sum_{j=0}^{3} K_{ij} S_j + \varepsilon_i \qquad (i = 0, \ldots, 3) \,, \tag{5.66}$$

where $\boldsymbol{S}$ is the Stokes vector defined by

$$\boldsymbol{S}^\dagger \equiv (S_0, S_1, S_2, S_3) = (I, Q, U, V) \,,$$

$\boldsymbol{K}$ is a 4×4 matrix which is composed in principle of 16 independent quantities, and $\boldsymbol{\varepsilon}$ is the emission vector

$$\boldsymbol{\varepsilon}^\dagger \equiv (\varepsilon_0, \varepsilon_1, \varepsilon_2, \varepsilon_3) = (\varepsilon_I, \varepsilon_Q, \varepsilon_U, \varepsilon_V) \,.$$

We assume here that both $\boldsymbol{K}$ and $\boldsymbol{\varepsilon}$ do not depend on the Stokes vector $\boldsymbol{S}$. This may indeed appear as a rather restrictive assumption, because there are many physical situations, mainly of astrophysical interest, where the properties of the medium at any given point depend in fact upon the local radiation field. It should be remarked, however, that the angular spread of the radiation beam that we are considering can always be made sufficiently small for the properties of the medium to be not affected by the beam itself. Keeping this argument in mind, we can derive some important properties of $\boldsymbol{K}$ and $\boldsymbol{\varepsilon}$ by varying arbitrarily – in a sort of *Gedankenexperiment* – the value of the Stokes vector $\boldsymbol{S}$ appearing in Eq. (5.66).

If we start by considering the limiting case of very intense radiation beams, the contribution of the emission vector in Eq. (5.66) can be simply neglected and the transfer equations reduce to

$$\frac{\mathrm{d}}{\mathrm{d}s} S_i = -\sum_{j=0}^{3} K_{ij} S_j \qquad (i = 0, \ldots, 3) \,, \tag{5.67}$$

from which we deduce

$$\begin{aligned}\frac{1}{2}\frac{\mathrm{d}}{\mathrm{d}s}\left(I^2-Q^2-U^2-V^2\right) &= \\ &= -K_{00}I^2+K_{11}Q^2+K_{22}U^2+K_{33}V^2 \\ &\quad +(K_{10}-K_{01})IQ+(K_{20}-K_{02})IU+(K_{30}-K_{03})IV \\ &\quad +(K_{12}+K_{21})QU+(K_{13}+K_{31})QV+(K_{23}+K_{32})UV\ . \end{aligned} \tag{5.68}$$

As proved in Chap. 1 (see Eq. (1.47)), the quantity $(I^2-Q^2-U^2-V^2)$ is always positive, except for the case of a totally polarized radiation beam when it reduces to zero. Therefore, if we consider a totally polarized radiation beam,

$$\boldsymbol{S}_0^{\dagger}=(I_0,Q_0,U_0,V_0) \qquad \text{with} \qquad I_0^2=Q_0^2+U_0^2+V_0^2\ ,$$

the right-hand side of Eq. (5.68) must be ≥ 0,

$$\begin{aligned}&(K_{11}-K_{00})Q_0^2+(K_{22}-K_{00})U_0^2+(K_{33}-K_{00})V_0^2 \\ &+(K_{10}-K_{01})I_0Q_0+(K_{20}-K_{02})I_0U_0+(K_{30}-K_{03})I_0V_0 \\ &+(K_{12}+K_{21})Q_0U_0+(K_{13}+K_{31})Q_0V_0+(K_{23}+K_{32})U_0V_0\geq 0\ . \end{aligned} \tag{5.69}$$

At this point we make a distinction between *depolarizing* and *non-depolarizing* media according to whether the greater-than or the equal sign holds in Eq. (5.69). In a non-depolarizing medium, by definition, a beam which is totally polarized remains so in the process of propagation (provided that no other terms are added to the right-hand side of Eq. (5.67)), while in a depolarizing medium this feature is lost and the propagation shows a typical irreversible character.

For non-depolarizing media – the only case that will be considered here – equality (5.69) must hold for whatever realization of the Stokes vector $\boldsymbol{S}_0$, or, in other words, for any values assigned to Q_0, U_0, V_0 satisfying the condition $I_0^2=(Q_0^2+U_0^2+V_0^2)$. Therefore all the brackets in the left-hand side of Eq. (5.69) must vanish, which implies

$$\begin{aligned}&K_{00}=K_{11}=K_{22}=K_{33} \\ &K_{01}=K_{10}\ ,\quad K_{02}=K_{20}\ ,\quad K_{03}=K_{30} \\ &K_{12}=-K_{21}\ ,\quad K_{13}=-K_{31}\ ,\quad K_{23}=-K_{32}\ .\end{aligned}$$

These are just the symmetry relations contained in Eq. (5.27). In the light of the arguments presented above we see that these relations are a direct consequence of: a) the definition of the Stokes parameters (which implies the inequality $I^2\geq Q^2+U^2+V^2$); b) the linear character of Eq. (5.67) (which is equivalent to the assumption $\boldsymbol{K}$ independent of $\boldsymbol{S}$); c) the reversible character of the interaction of radiation with the ambient medium (which implies the equal sign in Eq. (5.69)).

When conditions b) and c) are fulfilled the propagation matrix $\boldsymbol{K}$ can be written in the form

$$\boldsymbol{K} = \begin{pmatrix} \eta_I & \eta_Q & \eta_U & \eta_V \\ \eta_Q & \eta_I & \rho_V & -\rho_U \\ \eta_U & -\rho_V & \eta_I & \rho_Q \\ \eta_V & \rho_U & -\rho_Q & \eta_I \end{pmatrix} .$$

We will now prove that one, or even two, of the seven independent coefficients appearing in the expression of $\boldsymbol{K}$ can be set equal to zero by an appropriate choice of the reference direction which defines the Stokes parameters. Recalling the results derived in Sect. 1.9 (see Eq. (1.45) and Fig. 1.10), the Stokes vector $\boldsymbol{S'}$ relative to the 'new' reference direction characterized by the angle α can be written in the form

$$\boldsymbol{S'} = \boldsymbol{R}(\alpha)\, \boldsymbol{S} ,$$

where

$$\boldsymbol{R}(\alpha) = \begin{pmatrix} 1 & 0 & 0 & 0 \\ 0 & \cos 2\alpha & \sin 2\alpha & 0 \\ 0 & -\sin 2\alpha & \cos 2\alpha & 0 \\ 0 & 0 & 0 & 1 \end{pmatrix} .$$

Thus in the new reference frame the expression for the propagation matrix is

$$\boldsymbol{K'} = \boldsymbol{R}(\alpha)\, \boldsymbol{K}\, \boldsymbol{R}^{-1}(\alpha) ,$$

whence we deduce after some easy algebra

$$\eta'_I = \eta_I , \qquad \eta'_V = \eta_V , \qquad \rho'_V = \rho_V$$

$$\eta'_Q = \cos 2\alpha\, \eta_Q + \sin 2\alpha\, \eta_U , \qquad \rho'_Q = \cos 2\alpha\, \rho_Q + \sin 2\alpha\, \rho_U$$

$$\eta'_U = -\sin 2\alpha\, \eta_Q + \cos 2\alpha\, \eta_U , \qquad \rho'_U = -\sin 2\alpha\, \rho_Q + \cos 2\alpha\, \rho_U . \tag{5.70}$$

These formulae show that while the quantities η_I, η_V, and ρ_V are invariant with respect to the choice of the reference direction, η_Q and η_U change into each other according to a rotation through an angle 2α in the η_Q-η_U plane, and the same happens for ρ_Q and ρ_U. It follows that the two quantities η_{L} and ρ_{L} defined by

$$\eta_{\mathrm{L}}^2 = \eta_Q^2 + \eta_U^2 , \qquad \rho_{\mathrm{L}}^2 = \rho_Q^2 + \rho_U^2$$

are invariant. Moreover, it is possible to choose a particular reference direction, specified by the angle α_1, such that η'_U is zero, and another reference direction, specified by the angle α_2, such that ρ'_U is zero. The angles α_1 and α_2 may be different in principle, but in most cases of interest they are found to be equal. When this happens we will call *preferred reference direction* the one for which η'_U and ρ'_U are both zero.

Obviously, the expressions derived in Sect. 5.2 for the elements of the propagation matrix $\boldsymbol{K}$ are consistent with the transformation law given in Eqs. (5.70). This can be proved directly from the general equations (5.26) by taking into account

the transformation properties of the unit vectors $\vec{e}_a$, $\vec{e}_b$ under rotation of the reference direction. The proof is straightforward and will not be given here. In the special case of the propagation of radiation in a magnetized medium (Sect. 5.3) one can easily see from Eqs. (5.36) that the preferred reference direction lies (independently of frequency) in the plane containing the magnetic field and the direction of propagation.[1]

The above remarks show that when a preferred reference direction can be defined the propagation matrix $\boldsymbol{K}$ can be cast into the simpler form

$$\boldsymbol{K} = \begin{pmatrix} \eta_I & \eta_Q & 0 & \eta_V \\ \eta_Q & \eta_I & \rho_V & 0 \\ 0 & -\rho_V & \eta_I & \rho_Q \\ \eta_V & 0 & -\rho_Q & \eta_I \end{pmatrix} .$$

Going back to Eq. (5.66), we can also deduce some interesting properties of the emission vector $\boldsymbol{\varepsilon}$ by considering the limiting case of very weak intensity of the radiation beam. Under this limit the transfer equations reduce to

$$\frac{\mathrm{d}S_i}{\mathrm{d}s} = \varepsilon_i \qquad (i = 0, \ldots, 3) ,$$

and by integration over the interval Δs one gets

$$S_i(s + \Delta s) = S_i(s) + \varepsilon_i \, \Delta s .$$

Therefore, if we suppose $S_i(s) = 0$ we obtain that the following inequality must be satisfied

$$\varepsilon_I \geq \sqrt{\varepsilon_Q^2 + \varepsilon_U^2 + \varepsilon_V^2} . \tag{5.71}$$

In the case of the propagation of radiation through a magnetized medium this relation can be proved directly from Eqs. (5.38).

It should be noticed that the corresponding inequality for the components of the dichroism matrix, namely

$$\eta_I \geq \sqrt{\eta_Q^2 + \eta_U^2 + \eta_V^2} , \tag{5.72}$$

does not hold in general. However, under Local Thermodynamic Equilibrium or, more generally, when one can write

$$\begin{pmatrix} \varepsilon_I \\ \varepsilon_Q \\ \varepsilon_U \\ \varepsilon_V \end{pmatrix} = S \begin{pmatrix} \eta_I \\ \eta_Q \\ \eta_U \\ \eta_V \end{pmatrix} , \tag{5.73}$$

inequality (5.72) follows directly from (5.71).

[1] Indeed, there is another preferred reference direction at 90° from the former.

Another property of the emission vector concerns its transformation under a rotation of the reference direction. It is easy to prove that the rotation leading to Eqs. (5.70) induces the following transformation on the components of the emission vector

$$\begin{aligned}
\varepsilon'_I &= \varepsilon_I \\
\varepsilon'_Q &= \cos 2\alpha\, \varepsilon_Q + \sin 2\alpha\, \varepsilon_U \\
\varepsilon'_U &= -\sin 2\alpha\, \varepsilon_Q + \cos 2\alpha\, \varepsilon_U \\
\varepsilon'_V &= \varepsilon_V\ .
\end{aligned}$$

These formulae show that the quantity ε_{L} defined by

$$\varepsilon_{\mathrm{L}}^2 = \varepsilon_Q^2 + \varepsilon_U^2$$

is invariant, and that it is possible to choose a particular reference direction, characterized by the angle α_3, such that ε'_U is zero. When a preferred reference direction can be defined ($\eta'_U = \rho'_U = 0$) it often happens that ε'_U is zero as well.

5.6. Geometrical Interpretation of the Transfer Equations for Polarized Radiation

In Sect. 1.9 we have introduced the concept of Poincaré sphere as a mapping between Stokes vectors and points within a sphere of unit radius (see Fig. 1.11). Thus it is quite natural to give a geometrical interpretation to the radiative transfer equations for polarized radiation in terms of the motion of the representative point within the Poincaré sphere. This is schematically illustrated in Fig. 5.5.

In a right-handed orthogonal system (xyz) we consider the formal vectors $\vec{p}$, $\vec{\eta}$, $\vec{\rho}$, $\vec{\epsilon}$ defined by

$$\begin{aligned}
\vec{p} &= \left(\frac{Q}{I}, \frac{U}{I}, \frac{V}{I}\right) \\
\vec{\eta} &= \left(\eta_Q, \eta_U, \eta_V\right) \\
\vec{\rho} &= \left(\rho_Q, \rho_U, \rho_V\right) \\
\vec{\epsilon} &= \frac{\vec{\varepsilon}}{I} = \left(\frac{\varepsilon_Q}{I}, \frac{\varepsilon_U}{I}, \frac{\varepsilon_V}{I}\right)\ ,
\end{aligned}$$

and the scalar quantity

$$\epsilon_I = \frac{\varepsilon_I}{I}\ .$$

With these positions the transfer equations for polarized radiation can be transformed into the following

$$\frac{\mathrm{d}I}{\mathrm{d}s} = -(\eta_I + \vec{\eta}\cdot\vec{p} - \epsilon_I)\, I \tag{5.74a}$$

$$\frac{\mathrm{d}\vec{p}}{\mathrm{d}s} = -\vec{\eta} + (\vec{\eta}\cdot\vec{p})\,\vec{p} + \vec{\rho}\times\vec{p} + \vec{\epsilon} - \epsilon_I\,\vec{p}\,. \tag{5.74b}$$

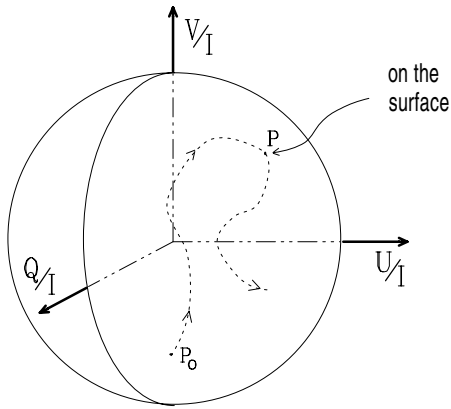

Fig.5.5. The transfer of polarized radiation in an arbitrary medium can be described in terms of the motion of the representative point inside the Poincaré sphere. The point cannot pierce the surface of the sphere but may describe a curve that is tangent to it, like in the point P. The starting point P_0 represents the radiation entering the medium.

The scalar equation describes the transfer of the beam intensity and it can be considered as the equation which controls the scaling factor connecting the Stokes parameters with their fractional value given by the vector $\vec{p}$. It is interesting to note that this equation differs from the standard equation for unpolarized radiation only for the presence of the term $(\vec{\eta} \cdot \vec{p})$ which adds to the (generalized) absorption coefficient η_I. Note also that the dispersion term, $\vec{\rho}$, does not appear directly in this equation, nevertheless it affects the intensity via the term $(\vec{\eta} \cdot \vec{p})$ (since $\vec{p}$ depends on $\vec{\rho}$).

The vector equation describes the motion of the representative point inside the Poincaré sphere. The first term in the right-hand side tends to align the fractional polarization $\vec{p}$ with the vector $-\vec{\eta}$. If we consider for instance the simple case where $\vec{\eta}$ does not depend on s, and if we take $\vec{p} = 0$ (unpolarized radiation) as the boundary condition at $s = s_0$, when the ray has traveled a distance Δs from s_0 we obtain from this term

$$\vec{p}(\Delta s) = -\vec{\eta}\, \Delta s \ ,$$

and, as Δs grows, the representative point might pierce the Poincaré sphere. This is however prevented by the second term, which is opposed to the first one and whose relative importance grows as the point approaches the surface of the sphere. Clearly this term describes a phenomenon of saturation for the fractional linear polarization.

In this respect it is also interesting to consider the effect of the term $(\vec{\eta} \cdot \vec{p})$ in the scalar equation for the intensity. In the simple situation discussed above ($\vec{\eta} = $ const., $\vec{p} = 0$ at $s = s_0$) this term brings a negative contribution to the absorption coefficient, since $\vec{p}$ is directed along $-\vec{\eta}$. Therefore, as the radiation beam propagates through the medium, the polarization grows and the medium becomes more and more transparent. We are facing again a saturation phenomenon which is strictly connected with the former.

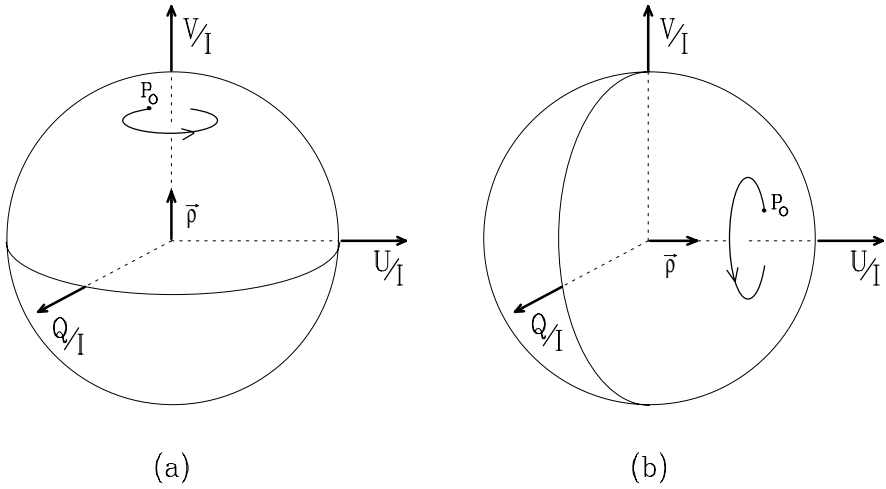

Fig.5.6. Geometrical interpretation of Faraday rotation (a) and Faraday pulsation (b). In case (a) only the component ρ_V is non-zero and we have a transformation from Q to U, and vice versa. In case (b) the component ρ_U induces a transformation from Q to V, and vice versa.

As an illustrative example, let us consider a low-temperature medium (i.e. a medium with negligible emission) which is opaque to left-handed circular polarization, and suppose that an unpolarized radiation beam is entering the medium at $s = s_0$. During the propagation, the left-handed circular polarization will decrease exponentially, so that right-handed circular polarization only will remain in the beam and the medium will be totally transparent.

Let's now consider the third term in the right-hand side of Eq. (5.74b). This term causes a precession of the vector $\vec{p}$ about the vector $\vec{\rho}$; in this motion the absolute value of the fractional polarization is unchanged, while the type of polarization changes. In particular, the z-component of the vector $\vec{\rho}$, ρ_V, induces a rotation of the representative point about the z-axis, which implies a rotation of the direction of maximum linear polarization. The x and y components (ρ_Q and ρ_U) give rise to a rotation about an axis belonging to the x-y plane, which implies a transformation from linear to circular polarization and vice versa. These two phenomena, which are illustrated in Fig. 5.6, will be referred to in the following as *Faraday rotation* and *Faraday pulsation*, respectively, although these names should more properly be employed when dealing with the propagation of polarized radiation in a magnetized medium far from resonances.

An important property of the term $(\vec{\rho} \times \vec{p})$ is that it can be efficient in removing the alignment between the vectors $\vec{p}$ and $-\vec{\eta}$ that tends to arise in the schematic situation discussed previously. Thus the presence of dispersion reduces the importance of the saturation mechanisms that we have just pointed out. The only case where the effects of dispersion can be neglected is when the three formal vectors $\vec{\eta}$, $\vec{\rho}$, and $\vec{\epsilon}$ point in the same direction. In this case, if we add the further condition that the radiation beam is unpolarized when entering the medium, the vector $\vec{p}$ will also be aligned with the same direction, and the term $(\vec{\rho} \times \vec{p})$ vanishes.

Comments similar to those on the terms $-\vec{\eta}$ and $(\vec{\eta}\cdot\vec{p})\vec{p}$ can be made for the last two terms in Eq. (5.74b), $\vec{\epsilon}$ and $-\epsilon_I\vec{p}$. The fourth term tends to align the polarization $\vec{p}$ with $\vec{\epsilon}$, but when $\vec{p}$ starts growing the other term comes in and prevents, through a saturation mechanism, the possibility of piercing the surface of the Poincaré sphere.

Finally, let us consider the special case described by Eq. (5.73) (which includes the LTE case). Defining the reduced scalar source function $\tilde{s}$ as

$$\tilde{s} = \frac{S}{I} ,$$

we have from Eq. (5.74b)

$$\frac{\mathrm{d}\vec{p}}{\mathrm{d}s} = -(1-\tilde{s})\,\vec{\eta} + (\vec{\eta}\cdot\vec{p} - \tilde{s}\,\eta_I)\,\vec{p} + \vec{\rho}\times\vec{p} ,$$

an equation containing the driving term, the saturation term, and the dispersion term.

5.7. Resonance Scattering and the Hanle Effect

We have seen in Sects. 5.1-5.2 how it is possible to deduce the transfer equations for polarized radiation using the concepts of classical electrodynamics. The general equations (5.25)-(5.26) have then been applied to the case of an atomic vapor embedded in a magnetic field. By schematizing the atomic system as a negative charge oscillating under the action of an elastic, restoring force, we have derived Eqs. (5.36) which give the basic quantities describing the transfer of polarized radiation in a magnetic field.

In this section we will use the same atomic model to deduce the laws of resonance scattering and of the Hanle effect. Starting from Eq. (3.34), we can write for the frequency-integrated radiation emitted per unit time in the solid angle $\mathrm{d}\Omega$ by an atomic oscillator embedded in a magnetic field

$$\begin{aligned}\mathrm{d}\tilde{I}_{ij}(\vec{\Omega}) &= \frac{c}{8\pi}\,J_{ij}(r)\,r^2\,\mathrm{d}\Omega \\ &= \frac{2\pi^3 e_0^2}{c^3}\,\mathrm{d}\Omega \sum_{\alpha\beta} C^*_{\alpha i} C_{\beta j}\,\frac{A^*_\alpha A_\beta}{\tau}\int_{-\infty}^{\infty} \nu^4 F_\alpha(\nu)^*\,F_\beta(\nu)\,\mathrm{d}\nu ,\end{aligned} \tag{5.75}$$

where the symbols have the same meaning as in Sect. 3.2.

To describe a scattering experiment we will now assume the initial values of the amplitudes, A_α, to be proportional to the corresponding components $\mathcal{E}'_\alpha$ of the resonant electric field impinging on the oscillator from the direction $\vec{\Omega}'$ (see Fig. 5.7). Note that the only difference between the present case and the case considered in Sect. 3.2 lies in the assumption on the amplitudes A_α. To obtain

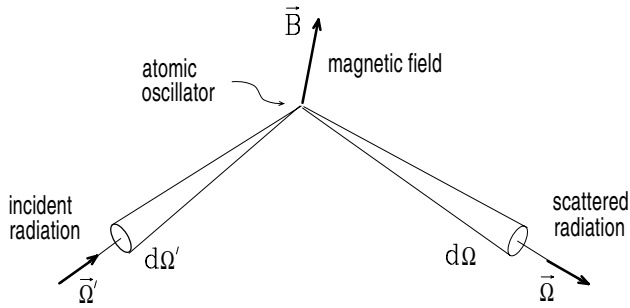

Fig.5.7. A radiation beam is scattered from the direction $\vec{\Omega}'$ to the direction $\vec{\Omega}$ in the presence of a magnetic field.

the emission in the Zeeman effect we assumed the amplitudes to be completely uncorrelated,

$$A_\alpha^* A_\beta = \overline{|A|^2}\, \delta_{\alpha\beta} \; ;$$

by contrast, we now assume

$$A_\alpha^* A_\beta = K\, \mathcal{E}_\alpha'^* \mathcal{E}_\beta'\, \mathrm{d}\Omega' \; , \tag{5.76}$$

where $\mathrm{d}\Omega'$ is an infinitesimal solid angle around the direction $\vec{\Omega}'$. Note that the frequency dependence of the components $\mathcal{E}_\alpha'$ in the above equation is not specified: they are supposed to be constant over a spectral interval centered at the resonance frequency ν_0 and much larger than the Larmor frequency ν_L (flat spectrum approximation).

If we now introduce two mutually orthogonal unit vectors perpendicular to the direction $\vec{\Omega}'$,

$$\vec{e}_i'^* \cdot \vec{e}_j' = \delta_{ij} \; , \qquad \vec{e}_i' \cdot \vec{\Omega}' = 0 \qquad (i,j = 1,2) \; ,$$

we can write

$$\mathcal{E}_\gamma' = \sum_i C_{\gamma i}'^*\, \mathcal{E}_i' \; , \tag{5.77}$$

where the direction cosines $C_{\gamma i}'$ are given by

$$C_{\gamma i}' = \vec{u}_\gamma \cdot \vec{e}_i'^* \; .$$

Substituting Eq. (5.77) into Eq. (5.76), and averaging over all the possible realizations of the incident electric field, we have

$$A_\alpha^* A_\beta = \frac{K}{k} \sum_{ij} C_{\alpha i}' C_{\beta j}'^*\, I_{ij}'(\vec{\Omega}')\, \mathrm{d}\Omega' \; , \tag{5.78}$$

where k is the constant appearing in Eqs. (1.34) and $I_{ij}'(\vec{\Omega}')$ is the polarization tensor of the incident radiation.

The dimensional constant K can be determined by considering the special case of thermodynamic equilibrium. In this case the incident radiation (isotropic and unpolarized) at the resonant frequency ν_0 is characterized by the polarization tensor

$$I'_{ij} = \frac{\nu_0^2\, k_{\mathrm{B}} T}{c^2}\, \delta_{ij} \ ,$$

where we have used the classical expression for the Planck function. Substitution into Eq. (5.78) gives

$$\begin{aligned} A^*_\alpha A_\beta &= \frac{K}{k}\, \frac{\nu_0^2\, k_{\mathrm{B}} T}{c^2} \oint \sum_i C'_{\alpha i} C'^*_{\beta i}\, \mathrm{d}\Omega' \\ &= \frac{K}{k}\, \frac{\nu_0^2\, k_{\mathrm{B}} T}{c^2} \oint \left[\delta_{\alpha\beta} - (\vec{\Omega}' \cdot \vec{u}_\alpha)(\vec{\Omega}' \cdot \vec{u}^{\,*}_\beta)\right] \mathrm{d}\Omega' \\ &= \frac{8\pi}{3}\, \frac{K}{k}\, \frac{\nu_0^2\, k_{\mathrm{B}} T}{c^2}\, \delta_{\alpha\beta} \ . \end{aligned} \tag{5.79}$$

On the other hand, the amplitudes of the atomic oscillations in thermodynamic equilibrium are given by (see Eq. (3.35) for a similar derivation)

$$A^*_\alpha A_\beta = \frac{\gamma\tau\, k_{\mathrm{B}} T}{2\pi^2 \nu_0^2 m}\, \delta_{\alpha\beta} \ . \tag{5.80}$$

Comparison of expressions (5.79) and (5.80) leads to

$$\frac{K}{k} = \frac{3}{16\pi^3}\, \frac{\gamma\tau c^2}{\nu_0^4 m} \ . \tag{5.81}$$

Using Eqs. (5.78) and (5.81), Eq. (5.75) becomes

$$\begin{aligned} &\mathrm{d}\tilde{I}_{ij}(\vec{\Omega}) = \\ &= \frac{3}{2}\, \frac{\pi e_0^2}{mc}\, \gamma \sum_{\alpha\beta} C^*_{\alpha i} C_{\beta j} \sum_{kl} C'_{\alpha k} C'^*_{\beta l}\, I'_{kl}(\vec{\Omega}')\, \frac{\mathrm{d}\Omega'}{4\pi}\, \mathrm{d}\Omega \int_{-\infty}^{\infty} F_\alpha(\nu)^*\, F_\beta(\nu)\, \mathrm{d}\nu \ , \end{aligned} \tag{5.82}$$

where we have extracted the factor ν_0^4 from the integral since the Fourier transforms $F_\alpha(\nu)$ are substantially non-zero only for $\nu \simeq \nu_0$ (see Eq. (3.33)).

The frequency integral can be easily evaluated with the help of the residue theorem

$$\int_{-\infty}^{\infty} F_\alpha(\nu)^*\, F_\beta(\nu)\, \mathrm{d}\nu = \frac{1}{\gamma}\, \frac{1}{1 + \mathrm{i}\,(\alpha - \beta) H} \ , \tag{5.83}$$

where

$$H = \frac{2\pi\nu_{\mathrm{L}}}{\gamma} = \frac{e_0 B}{2mc\gamma} \ . \tag{5.84}$$

The quantity H is proportional to the magnetic field intensity; numerically we have

$$H = 0.879\ B/\gamma\ , \tag{5.85}$$

with B in G and γ in $10^7\,\mathrm{s}^{-1}$.

Substitution of Eq. (5.83) into Eq. (5.82) leads to

$$\mathrm{d}\tilde{I}_{ij}(\vec{\Omega}) = \sigma_{\mathrm{cl}} \sum_{kl} T_{ij,kl}(\vec{\Omega},\vec{\Omega}';\vec{B}\,)\, I'_{kl}(\vec{\Omega}')\, \frac{\mathrm{d}\Omega'}{4\pi}\, \mathrm{d}\Omega\ , \tag{5.86}$$

where

$$\sigma_{\mathrm{cl}} = \frac{\pi e_0^2}{mc}$$

is the classical (frequency-integrated) cross section of the atomic oscillator, and $\boldsymbol{T}$ – the so-called scattering phase matrix for the polarization tensor – is defined by

$$T_{ij,kl}(\vec{\Omega},\vec{\Omega}';\vec{B}\,) = \frac{3}{2} \sum_{\alpha\beta} C^*_{\alpha i} C_{\beta j} C'_{\alpha k} C'^*_{\beta l}\, \frac{1}{1+\mathrm{i}\,(\alpha-\beta)H}\ . \tag{5.87}$$

This matrix depends on the geometry of the scattering event and on the magnitude and direction of the magnetic field vector; moreover, it depends on the choice of the unit vectors $(\vec{e}_1,\vec{e}_2)$ and $(\vec{e}'_1,\vec{e}'_2)$. Note that expression (5.87) is valid both for real unit vectors and, more generally, for complex unit vectors of the form of Eqs. (1.41).

The following symmetry property can be proved directly from Eq. (5.87)

$$T_{ij,kl}(\vec{\Omega},\vec{\Omega}';\vec{B}\,)^* = T_{ji,lk}(\vec{\Omega},\vec{\Omega}';\vec{B}\,)\ . \tag{5.88}$$

If the direction of the magnetic field vector is reversed, one gets a sign inversion of the term in H in Eq. (5.87) (see Eqs. (3.23), (3.27), and (3.33)). This leads to the further property

$$T_{ij,kl}(\vec{\Omega},\vec{\Omega}';-\vec{B}\,) = T_{lk,ji}(\vec{\Omega}',\vec{\Omega};\vec{B}\,)\ . \tag{5.89}$$

In the case of zero magnetic field the expression for the matrix $\boldsymbol{T}$ reduces to a much simpler form. Summation over the indices α and β yields

$$T_{ij,kl}(\vec{\Omega},\vec{\Omega}';0) \equiv T_{ij,kl}(\vec{\Omega},\vec{\Omega}') = \frac{3}{2}\, D_{ik} D^*_{jl}\ ,$$

where the direction cosines D_{ik} are given by

$$D_{ik} = \vec{e}_i \cdot \vec{e}'^*_k\ . \tag{5.90}$$

Equation (5.86) can be transformed into an equivalent equation relating the Stokes parameters of the incident and scattered radiation. As noticed several times, the relation between Stokes parameters and polarization tensor depends on the choice of the unit vectors $\vec{e}_i$ and $\vec{e}'_i$. The most natural choice is to take,

both for the incident and for the scattered radiation, the reference direction unit vector and the associated unit vector defined in Sect. 1.6. In other words, we take

$$\vec{e}_1 = \vec{e}_a(\vec{\Omega}) \qquad \vec{e}'_1 = \vec{e}'_a(\vec{\Omega}')$$
$$\vec{e}_2 = \vec{e}_b(\vec{\Omega}) \qquad \vec{e}'_2 = \vec{e}'_b(\vec{\Omega}') \ .$$

In this case the required relation is given by Eqs. (1.40), which imply that the frequency-integrated Stokes parameters $\mathrm{d}\tilde{S}_i(\vec{\Omega})$ scattered in the solid angle $\mathrm{d}\Omega$ by an atomic oscillator are given by

$$\mathrm{d}\tilde{S}_i(\vec{\Omega}) = \sum_{nm} (\sigma_i)_{nm} \, \mathrm{d}\tilde{I}_{mn}(\vec{\Omega}) \ ,$$

with $\boldsymbol{\sigma}_i$ the Pauli spin matrices defined in Eq. (1.17). Using again Eqs. (1.40), we obtain

$$\mathrm{d}\tilde{S}_i(\vec{\Omega}) = \sigma_{\mathrm{cl}} \sum_j R_{ij}(\vec{\Omega}, \vec{\Omega}'; \vec{B}\,) \; S'_j(\vec{\Omega}') \, \frac{\mathrm{d}\Omega'}{4\pi} \, \mathrm{d}\Omega \qquad (i, j = 0, \ldots, 3) \ , \tag{5.91}$$

where the scattering matrix $\boldsymbol{R}$ for the Stokes parameters, sometimes called the *phase matrix*, is given by

$$\begin{aligned} & R_{ij}(\vec{\Omega}, \vec{\Omega}'; \vec{B}\,) = \\ & = \frac{1}{2} \sum_{klmn} (\sigma_i)_{lk} (\sigma_j)_{mn} \, T_{kl,mn}(\vec{\Omega}, \vec{\Omega}'; \vec{B}\,) \\ & = \frac{3}{4} \sum_{klmn} (\sigma_i)_{lk} (\sigma_j)_{mn} \sum_{\alpha\beta} C^*_{\alpha k} C_{\beta l} C'_{\alpha m} C'^*_{\beta n} \, \frac{1}{1 + \mathrm{i}\,(\alpha - \beta) H} \ . \end{aligned} \tag{5.92}$$

In the case of zero magnetic field the matrix $\boldsymbol{R}$ reduces to the so-called *Rayleigh phase matrix*

$$R_{ij}(\vec{\Omega}, \vec{\Omega}'; 0) \equiv R_{ij}(\vec{\Omega}, \vec{\Omega}') = \frac{3}{4} \sum_{klmn} (\sigma_i)_{lk} (\sigma_j)_{mn} \, D_{km} D^*_{ln} \ ,$$

where the direction cosines D_{ij} are defined in Eq. (5.90).

Since the Stokes parameters are real, the scattering matrix must be real as well,

$$R_{ij}(\vec{\Omega}, \vec{\Omega}'; \vec{B}\,)^* = R_{ij}(\vec{\Omega}, \vec{\Omega}'; \vec{B}\,) \ ; \tag{5.93}$$

this can be checked directly from Eq. (5.92) recalling that

$$(\sigma_i)^*_{nm} = (\sigma_i)_{mn} \ .$$

Moreover, from Eq. (5.89) one gets

$$R_{ij}(\vec{\Omega}, \vec{\Omega}'; -\vec{B}\,) = R_{ji}(\vec{\Omega}', \vec{\Omega}; \vec{B}\,) \ . \tag{5.94}$$

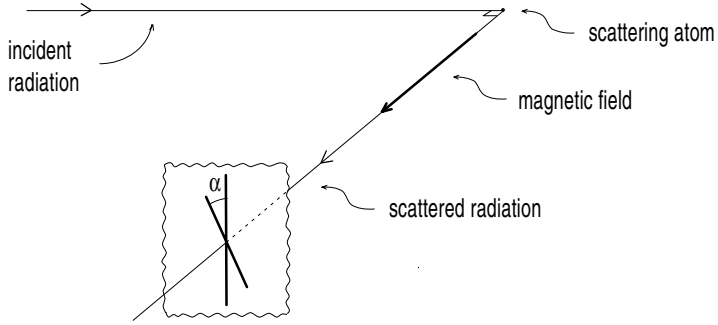

Fig.5.8. The Hanle effect is illustrated by this simple scattering experiment. For zero magnetic field the polarization of the scattered beam is perpendicular to the plane of scattering; when a magnetic field is present, the polarization is reduced and its direction is rotated through an angle α.

In the particular case of zero magnetic field this equation becomes

$$R_{ij}(\vec{\Omega},\vec{\Omega}') = R_{ji}(\vec{\Omega}',\vec{\Omega}) \ , \tag{5.95}$$

which is known as the *Helmoltz principle of reciprocity* for a scattering event. Thus Eq. (5.94) represents the generalization of this principle to the case where a magnetic field is present.

The equations that we have derived in this section describe the scattering of polarized radiation by an atomic system, schematized as a harmonic oscillator, in the presence of a magnetic field. In the limiting case of zero magnetic field the results here obtained reduce to the classical results of Rayleigh for the scattering of polarized radiation.[1]

In the presence of a magnetic field the laws of scattering are deeply modified and a new phenomenon – known as *Hanle effect* – appears. Discovered in the laboratory in the early years of this century (Hanle, 1924), this effect usually produces a depolarization of the scattered radiation and a rotation of its plane of polarization (see Fig. 5.8). However, this holds only for particular geometries of the scattering event – probably the most used in laboratory experiments and the most important for astrophysical applications. For different geometries the effect of the magnetic field can be very different, and in fact the polarization of the scattered radiation can even be increased relative to the non-magnetic situation. Thus, in general terms, one can only state that the Hanle effect consists in a *modification of the scattered radiation due to the presence of a magnetic field*. These points will be further clarified in Sect. 5.9.

[1] It should be remarked that Rayleigh's law of scattering can be applied to a broader class of phenomena and not only to the scattering by a harmonic oscillator – the simple case on which we have based our deduction. Thomson scattering by free electrons, or scattering by a dielectric sphere having a radius much smaller than the wavelength of the radiation, are just two examples where Rayleigh's law can still be applied in full generality. The only difference with the case considered here is in the cross section $\sigma_{\rm cl}$ appearing in Eqs. (5.86) and (5.91).

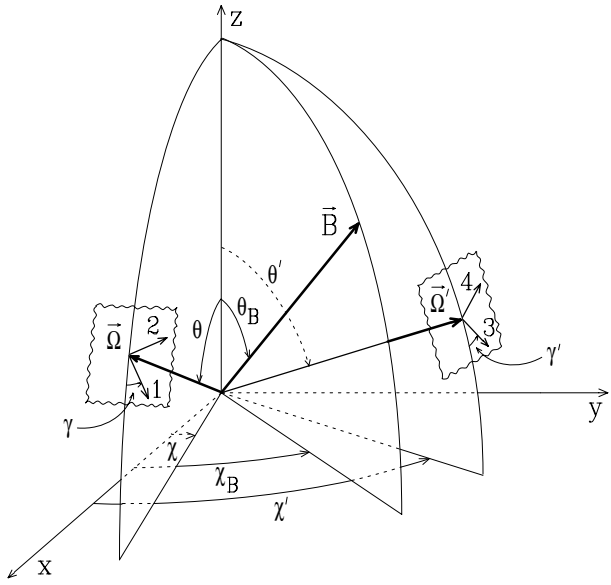

Fig.5.9. The most general geometry for the scattering event. The unit vector 1, lying in the plane perpendicular to $\vec{\Omega}$, is the reference direction unit vector $\vec{e}_a(\vec{\Omega})$, while 2 is the associated unit vector $\vec{e}_b(\vec{\Omega})$. The unit vectors 3 and 4 are $\vec{e}'_a(\vec{\Omega}')$ and $\vec{e}'_b(\vec{\Omega}')$, respectively.

Equation (5.92) describes the Hanle effect from the classical point of view; we will see in Chap. 10 how this equation is generalized in the quantum theory.

5.8. The Scattering Phase Matrix in a Particular Case

In the previous section we have obtained a general expression for the scattering phase matrix that can be applied to any geometrical configuration of the scattering event and of the magnetic field and to any choice of the reference directions for the Stokes parameters. For practical applications it is however useful to have explicit analytical expressions for the scattering phase matrix in particular geometrical situations.

The most general geometry is illustrated in Fig. 5.9, where the three directions $\vec{\Omega}$, $\vec{\Omega}'$, and $\vec{B}$ are specified by their polar angles and where the reference directions are defined by the angles γ and γ'. In this geometry the scattering phase matrix will depend on 8 parameters, namely θ, θ', θ_B, $(\chi - \chi_B)$, $(\chi' - \chi_B)$, γ, γ', and H, and the calculation of one element R_{ij} will require the sum of 144 $(= 3^2 \times 2^4)$ terms. It is not worth here to develop in detail these calculations; the interested reader is referred to Landi Degl'Innocenti and Landi Degl'Innocenti (1988), where an analytical expression for the phase matrix is derived under the assumption $\gamma = \gamma' = 0$ (which means that the positive Q-directions for the incident and scattered beams lie in the meridian planes of Fig. 5.9). Being deduced from the quantum theory,

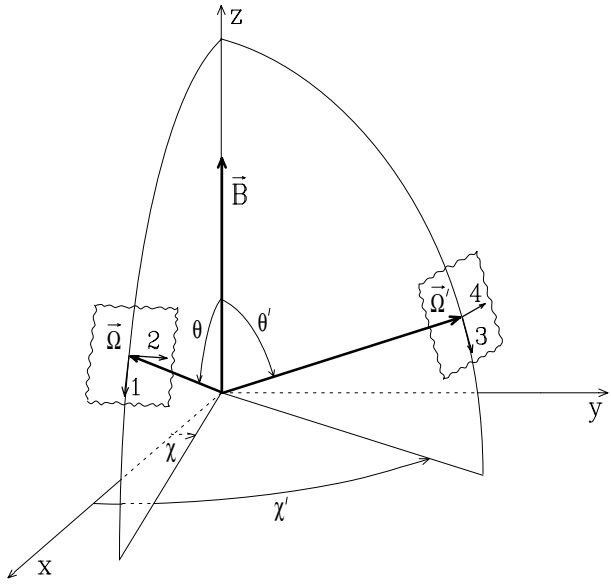

Fig.5.10. A particular geometry for the calculation of the scattering phase matrix. The polar angles of the directions $\vec{\Omega}$ and $\vec{\Omega}'$ are reckoned from the magnetic field direction. The meaning of the unit vectors 1, 2, 3, 4 is the same as in Fig.5.9.

the expressions presented in the paper just quoted are in fact more general than those obtainable from Eq. (5.92); however, they reduce to the classical results with easy transformations.

Some general properties of the scattering phase matrix relative to the geometrical configuration of Fig. 5.9 will be given in Sect. 5.12. Here we want to derive the explicit expression of this matrix for the much simpler geometry illustrated in Fig. 5.10.

Now the magnetic field vector is parallel to the z-axis and the reference direction for the Stokes parameters lies in the meridian plane containing the magnetic field and the propagation direction. The various unit vectors are given by

$$\vec{e}_a(\vec{\Omega}) = \vec{e}_1 = \cos\theta\cos\chi\ \vec{\imath} + \cos\theta\sin\chi\ \vec{\jmath} - \sin\theta\ \vec{k}$$

$$\vec{e}_b(\vec{\Omega}) = \vec{e}_2 = -\sin\chi\ \vec{\imath} + \cos\chi\ \vec{\jmath}$$

$$\vec{e}'_a(\vec{\Omega}') = \vec{e}'_1 = \cos\theta'\cos\chi'\ \vec{\imath} + \cos\theta'\sin\chi'\ \vec{\jmath} - \sin\theta'\ \vec{k}$$

$$\vec{e}'_b(\vec{\Omega}') = \vec{e}'_2 = -\sin\chi'\ \vec{\imath} + \cos\chi'\ \vec{\jmath}$$

$$\vec{u}_0 = \vec{k}$$

$$\vec{u}_{\pm 1} = \frac{1}{\sqrt{2}}\left(\mp\,\vec{\imath} + \mathrm{i}\,\vec{\jmath}\right),$$

and the direction cosines can be easily evaluated

$$
\begin{aligned}
C_{1\,1} &= -\frac{1}{\sqrt{2}}\,\cos\theta\;\mathrm{e}^{-\mathrm{i}\chi} & C_{1\,2} &= \frac{\mathrm{i}}{\sqrt{2}}\;\mathrm{e}^{-\mathrm{i}\chi} \\
C_{0\,1} &= -\sin\theta & C_{0\,2} &= 0 \\
C_{-1\,1} &= \frac{1}{\sqrt{2}}\,\cos\theta\;\mathrm{e}^{\mathrm{i}\chi} & C_{-1\,2} &= \frac{\mathrm{i}}{\sqrt{2}}\;\mathrm{e}^{\mathrm{i}\chi}\,,
\end{aligned}
$$

with analogous expressions for $C'_{\alpha i}$.

From these expressions the elements of the scattering phase matrix for the polarization tensor, given by Eq. (5.87), can be evaluated via some heavy algebra that is left to the reader as an exercise. The results are the following

$$
\begin{aligned}
T_{11,11} &= \frac{3}{2}\left[1-\mu^2-\mu'^2+\frac{3}{2}\,\mu^2\mu'^2+2\mu\mu'\sqrt{1-\mu^2}\,\sqrt{1-\mu'^2}\,C_1+\frac{1}{2}\,\mu^2\mu'^2\,C_2\right] \\
T_{11,12} &= T_{11,21} = \frac{3}{2}\left[-\mu\sqrt{1-\mu^2}\,\sqrt{1-\mu'^2}\,S_1-\frac{1}{2}\,\mu^2\mu'\,S_2\right] \\
T_{12,11} &= T_{21,11} = \frac{3}{2}\left[\mu'\sqrt{1-\mu^2}\,\sqrt{1-\mu'^2}\,S_1+\frac{1}{2}\,\mu\mu'^2\,S_2\right] \\
T_{11,22} &= \frac{3}{2}\left[\frac{1}{2}\,\mu^2-\frac{1}{2}\,\mu^2\,C_2\right] \\
T_{22,11} &= \frac{3}{2}\left[\frac{1}{2}\,\mu'^2-\frac{1}{2}\,\mu'^2\,C_2\right] \\
T_{12,12} &= T_{21,21} = \frac{3}{2}\left[\frac{1}{2}\,\mu\mu'+\sqrt{1-\mu^2}\,\sqrt{1-\mu'^2}\,C_1+\frac{1}{2}\,\mu\mu'\,C_2\right] \\
T_{12,21} &= T_{21,12} = \frac{3}{2}\left[-\frac{1}{2}\,\mu\mu'+\frac{1}{2}\,\mu\mu'\,C_2\right] \\
T_{12,22} &= T_{21,22} = \frac{3}{2}\left[-\frac{1}{2}\,\mu\,S_2\right] \\
T_{22,21} &= T_{22,12} = \frac{3}{2}\left[\frac{1}{2}\,\mu'\,S_2\right] \\
T_{22,22} &= \frac{3}{2}\left[\frac{1}{2}+\frac{1}{2}\,C_2\right]\,,
\end{aligned}
\tag{5.96}
$$

where

$$
\begin{aligned}
\mu &= \cos\theta & \mu' &= \cos\theta' \\
C_1 &= \cos\alpha_1\cos\bigl(\alpha_1+\chi'-\chi\bigr) & S_1 &= \cos\alpha_1\sin\bigl(\alpha_1+\chi'-\chi\bigr) \\
C_2 &= \cos\alpha_2\cos\bigl(\alpha_2+2\,(\chi'-\chi)\bigr) & S_2 &= \cos\alpha_2\sin\bigl(\alpha_2+2\,(\chi'-\chi)\bigr)
\end{aligned}
\tag{5.97}
$$

and where the angles α_1 and α_2, implicitly defined by

$$
\tan\alpha_1 = H\,, \qquad \tan\alpha_2 = 2H\,,
\tag{5.98}
$$

are particularly useful to express the quantities $(1 \pm \mathrm{i}H)^{-1}$ and $(1 \pm 2\mathrm{i}H)^{-1}$ in the form

$$(1 \pm \mathrm{i}H)^{-1} = \cos\alpha_1 \, \mathrm{e}^{\mp \mathrm{i}\alpha_1} = \cos^2\alpha_1 \mp \mathrm{i} \, \sin\alpha_1 \cos\alpha_1$$
$$(1 \pm 2\mathrm{i}H)^{-1} = \cos\alpha_2 \, \mathrm{e}^{\mp \mathrm{i}\alpha_2} = \cos^2\alpha_2 \mp \mathrm{i} \, \sin\alpha_2 \cos\alpha_2 \; .$$

Note that the intensity of the magnetic field is contained only in the quantities C_1, C_2, S_1, S_2. In particular, for zero magnetic field one gets

$$C_1 = \cos(\chi' - \chi) \qquad S_1 = \sin(\chi' - \chi)$$
$$C_2 = \cos 2(\chi' - \chi) \qquad S_2 = \sin 2(\chi' - \chi) \; ,$$

and for strong magnetic field ($H \gg 1$)

$$C_1 = S_1 = C_2 = S_2 = 0 \; ,$$

so that the expressions of the matrix elements are considerably simplified.

Finally, substituting Eqs. (5.96) into Eq. (5.92) and using the explicit expressions of the Pauli spin matrices (Eqs. (1.17)), one obtains for the scattering phase matrix of the Stokes parameters the following expressions

$$\begin{aligned}
R_{00}(\vec{\Omega}, \vec{\Omega}'; \vec{B}\,) &= \frac{3}{8}\left(3 - \mu^2 - \mu'^2 + 3\mu^2\mu'^2\right) + \frac{3}{2}\,\mu\mu'\sqrt{1-\mu^2}\,\sqrt{1-\mu'^2}\,C_1 \\
&\quad + \frac{3}{8}\left(1-\mu^2\right)\left(1-\mu'^2\right)C_2 \\
R_{01}(\vec{\Omega}, \vec{\Omega}'; \vec{B}\,) &= \frac{3}{8}\left(1 - 3\mu^2\right)\left(1-\mu'^2\right) + \frac{3}{2}\,\mu\mu'\sqrt{1-\mu^2}\,\sqrt{1-\mu'^2}\,C_1 \\
&\quad - \frac{3}{8}\left(1-\mu^2\right)\left(1+\mu'^2\right)C_2 \\
R_{02}(\vec{\Omega}, \vec{\Omega}'; \vec{B}\,) &= -\frac{3}{2}\,\mu\sqrt{1-\mu^2}\,\sqrt{1-\mu'^2}\,S_1 + \frac{3}{4}\left(1-\mu^2\right)\mu'\,S_2 \\
R_{03}(\vec{\Omega}, \vec{\Omega}'; \vec{B}\,) &= 0 \\
R_{10}(\vec{\Omega}, \vec{\Omega}'; \vec{B}\,) &= \frac{3}{8}\left(1-\mu^2\right)\left(1 - 3\mu'^2\right) + \frac{3}{2}\,\mu\mu'\sqrt{1-\mu^2}\,\sqrt{1-\mu'^2}\,C_1 \\
&\quad - \frac{3}{8}\left(1+\mu^2\right)\left(1-\mu'^2\right)C_2 \\
R_{11}(\vec{\Omega}, \vec{\Omega}'; \vec{B}\,) &= \frac{9}{8}\left(1-\mu^2\right)\left(1-\mu'^2\right) + \frac{3}{2}\,\mu\mu'\sqrt{1-\mu^2}\,\sqrt{1-\mu'^2}\,C_1 \\
&\quad + \frac{3}{8}\left(1+\mu^2\right)\left(1+\mu'^2\right)C_2 \\
R_{12}(\vec{\Omega}, \vec{\Omega}'; \vec{B}\,) &= -\frac{3}{2}\,\mu\sqrt{1-\mu^2}\,\sqrt{1-\mu'^2}\,S_1 - \frac{3}{4}\left(1+\mu^2\right)\mu'\,S_2 \\
R_{13}(\vec{\Omega}, \vec{\Omega}'; \vec{B}\,) &= 0
\end{aligned}$$

$$R_{20}(\vec{\Omega},\vec{\Omega}';\vec{B}\,) = \frac{3}{2}\,\mu'\sqrt{1-\mu^2}\,\sqrt{1-\mu'^2}\,S_1 - \frac{3}{4}\,\mu\big(1-\mu'^2\big)\,S_2$$

$$R_{21}(\vec{\Omega},\vec{\Omega}';\vec{B}\,) = \frac{3}{2}\,\mu'\sqrt{1-\mu^2}\,\sqrt{1-\mu'^2}\,S_1 + \frac{3}{4}\,\mu\big(1+\mu'^2\big)\,S_2$$

$$R_{22}(\vec{\Omega},\vec{\Omega}';\vec{B}\,) = \frac{3}{2}\,\sqrt{1-\mu^2}\,\sqrt{1-\mu'^2}\,C_1 + \frac{3}{2}\,\mu\mu'\,C_2$$

$$R_{23}(\vec{\Omega},\vec{\Omega}';\vec{B}\,) = 0$$

$$R_{30}(\vec{\Omega},\vec{\Omega}';\vec{B}\,) = 0$$

$$R_{31}(\vec{\Omega},\vec{\Omega}';\vec{B}\,) = 0$$

$$R_{32}(\vec{\Omega},\vec{\Omega}';\vec{B}\,) = 0$$

$$R_{33}(\vec{\Omega},\vec{\Omega}';\vec{B}\,) = \frac{3}{2}\,\mu\mu' + \frac{3}{2}\,\sqrt{1-\mu^2}\,\sqrt{1-\mu'^2}\,C_1\,. \tag{5.99}$$

These formulae show that the V Stokes parameter (S_3) is totally decoupled from the other Stokes parameters in a scattering event.

In the limiting case of strong magnetic field one gets

$$\boldsymbol{R}(\vec{\Omega},\vec{\Omega}';\vec{B}\to\infty) = \frac{3}{8}\begin{pmatrix} \frac{8}{3}+\frac{1}{3}\,(1-3\mu^2)(1-3\mu'^2) & (1-3\mu^2)(1-\mu'^2) & 0 & 0 \\ (1-\mu^2)(1-3\mu'^2) & 3(1-\mu^2)(1-\mu'^2) & 0 & 0 \\ 0 & 0 & 0 & 0 \\ 0 & 0 & 0 & 4\mu\mu' \end{pmatrix}$$

which shows that the U Stokes parameter of the scattered radiation is zero irrespective of the direction and polarization of the incoming beam. If, in addition, the incoming beam is unpolarized, the fractional polarization of the scattered radiation is found to be

$$\frac{Q}{I} = \frac{(1-\mu^2)(1-3\mu'^2)}{3-\mu^2-\mu'^2+3\mu^2\mu'^2}\,,$$

thus it is positive, negative, or zero according as $(\mu'^2-1/3)$ is negative, positive, or zero. Defining the *Van Vleck angle* $\theta_{\rm V}$ according to the formula

$$\cos\theta_{\rm V} = 1/\sqrt{3}\,, \tag{5.100}$$

which implies

$$\theta_{\rm V} = 54^\circ.74\,, \tag{5.101}$$

one obtains

$$\frac{Q}{I} > 0 \quad \text{(linear polarization parallel to } \vec{B}\,) \qquad \text{for} \quad \theta_{\rm V} < \theta' < \pi - \theta_{\rm V}$$

$$\frac{Q}{I} < 0 \quad \text{(linear polarization perpendicular to } \vec{B}\,) \quad \text{for} \quad 0 < \theta' < \theta_{\rm V}$$

$$\text{or} \quad \pi - \theta_{\rm V} < \theta' < \pi\,.$$

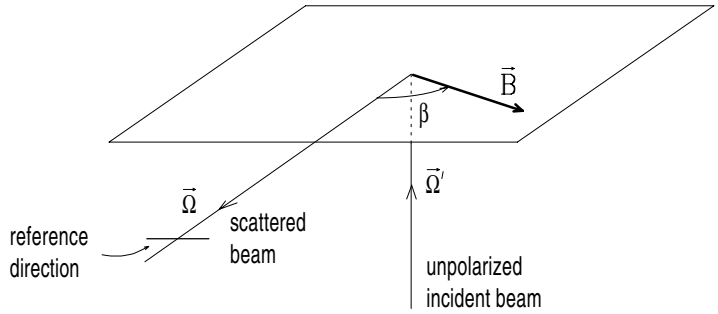

Fig.5.11. Geometry for a 90° scattering. The magnetic field lies in the plane perpendicular to the incident beam and makes an angle β with the direction of the scattered beam. The reference direction for the Stokes parameters of the scattered radiation is perpendicular to the scattering plane.

In other words, for an unpolarized incoming beam and in the limit of large magnetic field ($H \gg 1$), the linear polarization of the scattered beam is either parallel or perpendicular to the magnetic field according to the direction of the incident radiation.

Another consequence that can be easily deduced from Eqs. (5.99) concerns the particular case of an incident beam parallel (or antiparallel) to the magnetic field vector. Setting $\mu' = \pm 1$ in Eqs. (5.99) we see that the matrix elements of the form R_{i0} ($i = 0, \ldots, 3$) are independent of the magnetic field. Therefore, if the incident beam is unpolarized the scattered radiation is completely insensitive to the magnetic field.

5.9. Some Illustrations of the Hanle Effect

To understand in further detail the role of the magnetic field in resonance scattering, it is convenient to apply the results obtained in the previous section to some specific geometrical configurations of the scattering process.

Consider first the configuration of Fig. 5.11, where we want to investigate the polarization of the radiation scattered at 90° from an unpolarized incident beam. The scattering event takes place in the presence of a magnetic field which lies in the plane perpendicular to the incident beam.

Since the incident beam is unpolarized, the only elements of the scattering phase matrix that must be computed are those of the form R_{i0} ($i = 0, \ldots, 3$). Taking as reference direction the perpendicular to the scattering plane (see Fig. 5.11), these matrix elements can be deduced from Eqs. (5.99) by the substitutions

$$\mu = \cos\beta\ , \qquad \mu' = 0\ , \qquad \chi - \chi' = \frac{\pi}{2}\ .$$

This leads to the expressions

$$R_{00} = \frac{3}{8}\left(3 - \cos^2\beta - \sin^2\beta\,\cos^2\alpha_2\right)$$

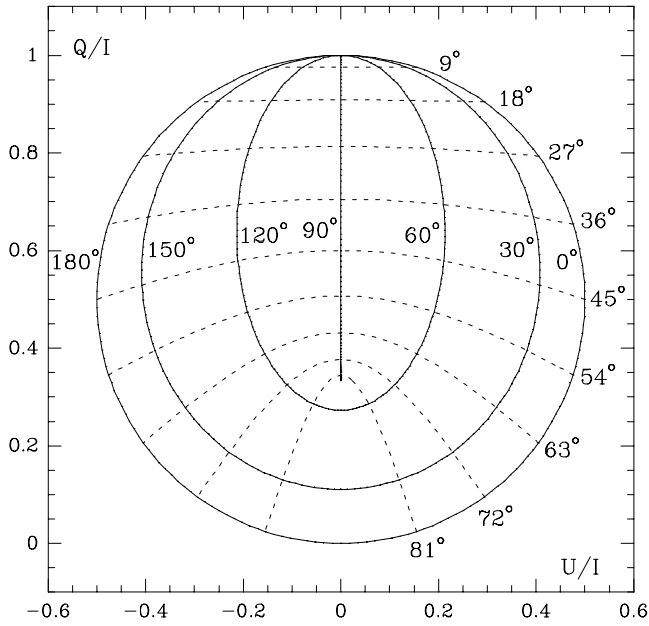

Fig.5.12. Polarization diagram (or Hanle diagram) relative to the scattering process illustrated in Fig.5.11. Full lines correspond to $\beta = \text{const.}$, while broken lines correspond to constant magnetic field strength, parameterized through the quantity α_2 (see Eqs.(5.84) and (5.98)).

$$R_{10} = \frac{3}{8}\left(\sin^2\beta + (1+\cos^2\beta)\cos^2\alpha_2\right)$$
$$R_{20} = \frac{3}{4}\cos\beta\sin\alpha_2\cos\alpha_2$$
$$R_{30} = 0\ ,$$

so that the fractional linear polarization of the scattered beam is given by

$$\frac{Q}{I} = \frac{\sin^2\beta + (1+\cos^2\beta)\cos^2\alpha_2}{3 - \cos^2\beta - \sin^2\beta\,\cos^2\alpha_2}$$
$$\frac{U}{I} = \frac{2\cos\beta\sin\alpha_2\cos\alpha_2}{3 - \cos^2\beta - \sin^2\beta\,\cos^2\alpha_2}\ . \tag{5.102}$$

The results now deduced can be conveniently plotted in the *polarization diagram* (or *Hanle diagram*) shown in Fig. 5.12. The solid lines are isoazimuth curves ($\beta = \text{const.}$), while the broken lines are isostrength curves ($\alpha_2 = \text{const.}$). For any assigned couple (β, α_2) the diagram gives the polarization Q/I, U/I of the scattered beam. Note that the values of β can be confined in the range $[0, \pi]$ since Eqs. (5.102) are invariant under the substitution $\beta \to -\beta$.

There are several characteristics of Eqs. (5.102) that it is worthwhile to discuss in some detail. First of all, in the case of zero magnetic field ($\alpha_2 = 0$) one gets

$$\frac{Q}{I} = 1\ , \qquad \frac{U}{I} = 0\ , \tag{5.103}$$

thus the scattered beam is totally polarized perpendicularly to the scattering plane. On the other hand, for very strong magnetic field ($\alpha_2 = \pi/2$) one obtains

$$\frac{Q}{I} = \frac{\sin^2\beta}{3 - \cos^2\beta} , \qquad \frac{U}{I} = 0 ,$$

so that the scattered beam is again polarized perpendicularly to the scattering plane (consistently with our former discussion on the Van Vleck angle); however, the fractional linear polarization varies now between 0 and 1/3 according to the value of β.

For intermediate values of the magnetic field, the U Stokes parameter is in general non-zero, which means that the direction of linear polarization is rotated from the zero-field direction. The maximum rotation for a given magnetic field strength occurs for $\beta = 0$ or π. In these cases we have

$$\frac{Q}{I} = \cos^2\alpha_2 , \qquad \frac{U}{I} = \pm \sin\alpha_2 \cos\alpha_2 ,$$

where the plus sign for U/I corresponds to $\beta = 0$ and the minus sign to $\beta = \pi$. In both cases the total linear polarization is given by

$$p_{\rm L} = \sqrt{\left(\frac{Q}{I}\right)^2 + \left(\frac{U}{I}\right)^2} = \cos\alpha_2 = \frac{1}{\sqrt{1 + 4H^2}} , \tag{5.104}$$

while the position angle α_0 (see Eqs. (1.46)) is

$$\alpha_0 = \pm \frac{1}{2}\, \alpha_2 = \pm \frac{1}{2} \arctan 2H \tag{5.105}$$

with the plus sign for $\beta = 0$ and the minus sign for $\beta = \pi$. This formula shows that a magnetic field with the same direction as the scattered radiation produces a counterclockwise rotation (for an observer looking at the scattering point) of the plane of linear polarization; conversely, the rotation is clockwise if the magnetic field is in the opposite direction.

Equations (5.104) and (5.105) are often used to discuss the role of the Hanle effect in scattering polarization (see e.g. Mitchell and Zemansky, 1934). They are however of limited use because they refer to an extremely particular case.

In the scattering configuration just considered the magnetic field produces, besides a rotation of the polarization direction, a decrease of the polarization degree (depolarization); but this is not always the case. A counter example is provided, for instance, by forward scattering.

The relevant geometry is now illustrated in Fig. 5.13, where we consider the effect of a magnetic field on the forward scattering of an unpolarized radiation beam. The polarization of the scattered beam can again be deduced from Eqs. (5.99) by the substitutions

$$\mu = \mu' = \cos\beta , \qquad \chi = \chi' .$$

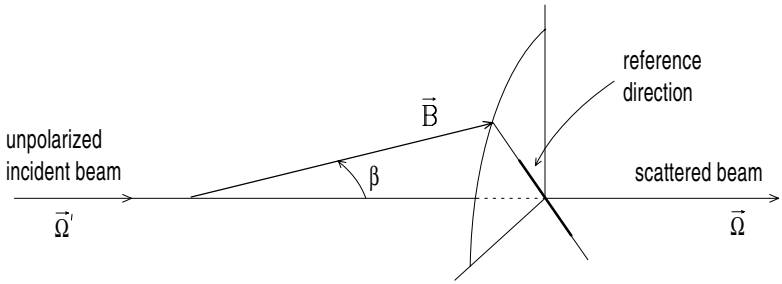

Fig.5.13. Forward scattering. The reference direction for the Stokes parameters lies in the plane containing the magnetic field and the direction $\vec{\Omega}$.

We obtain

$$
\begin{aligned}
R_{00} &= 1 + \frac{1}{8}\left(3\cos^2\beta - 1\right)^2 + \frac{3}{2}\sin^2\beta\,\cos^2\beta\,\cos^2\alpha_1 + \frac{3}{8}\sin^4\beta\,\cos^2\alpha_2 \\
R_{10} &= \frac{3}{8}\sin^2\beta\left[1 - 3\cos^2\beta + 4\cos^2\beta\,\cos^2\alpha_1 - (1+\cos^2\beta)\cos^2\alpha_2\right] \\
R_{20} &= \frac{3}{4}\sin^2\beta\,\cos\beta\left[2\sin\alpha_1\cos\alpha_1 - \sin\alpha_2\cos\alpha_2\right] \\
R_{30} &= 0\,. \qquad (5.106)
\end{aligned}
$$

For zero magnetic field ($\alpha_1 = \alpha_2 = 0$) one gets

$$\frac{Q}{I} = \frac{U}{I} = 0\,,$$

so that the scattered beam is unpolarized as the incident beam. For strong magnetic field ($\alpha_1 = \alpha_2 = \pi/2$) one obtains

$$\frac{Q}{I} = \frac{(1-\cos^2\beta)(1-3\cos^2\beta)}{3 - 2\cos^2\beta + 3\cos^4\beta}\,, \qquad \frac{U}{I} = 0$$

or, in other words, a linear polarization which is parallel or perpendicular – according to the sign of the quantity $(1 - 3\cos^2\beta)$ – to the plane containing the magnetic field and the propagation direction. For intermediate values of the magnetic field the U Stokes parameter is non-zero, which means a rotation of the plane of linear polarization. The rotation angle is a complicated function of β and H, as apparent from Eqs. (5.106).

This example shows that in some scattering configurations the magnetic field is able to produce a definite amount of linear polarization in a radiation beam which would be unpolarized if the magnetic field were not present.

5.10. The Scattering Phase Matrix Expressed in Terms of Rotation Matrices

The equations that we have derived in the preceding sections involve the evaluation of several direction cosines relating the unit vectors $\vec{u}_\alpha$, relative to the magnetic field, to the unit vectors $\vec{e}_i(\vec{\Omega})$ needed for the definition of the Stokes parameters. These direction cosines and, in particular, their bilinear combinations can be conveniently expressed in terms of ordinary rotation matrices. This leads, in most cases, to much more compact and handy expressions for the relevant physical quantities, like the scattering phase matrix derived in Sect. 5.7.

The introduction of rotation matrices requires, however, some remarks about the spherical components of ordinary vectors, an argument that we have already treated in Sect. 2.7 and that we are going to develop in further detail here.

Given an arbitrary vector $\vec{v}$, its spherical components v_q are defined by (see Eqs. (2.82))

$$\begin{aligned} v_{-1} &= \frac{1}{\sqrt{2}}\,(v_x - \mathrm{i}\,v_y) \\ v_0 &= v_z \\ v_1 &= -\frac{1}{\sqrt{2}}\,(v_x + \mathrm{i}\,v_y)\ , \end{aligned} \tag{5.107}$$

where v_x, v_y, v_z are the Cartesian components in a right-handed coordinate system. Since in the following we will often deal with vectors of the form

$$\vec{v} = \vec{a} + \mathrm{i}\,\vec{b} \tag{5.108}$$

with $\vec{a}$ and $\vec{b}$ real, we want to establish some properties of the spherical components of such vectors.

Taking the complex conjugate of Eqs. (5.107), with $\vec{v}$ given by Eq. (5.108), we have

$$\begin{aligned} (v_{-1})^* &= \frac{1}{\sqrt{2}}\left[(a_x + b_y) - \mathrm{i}\,(b_x - a_y)\right] \\ (v_0)^* &= a_z - \mathrm{i}\,b_z \\ (v_1)^* &= -\frac{1}{\sqrt{2}}\left[(a_x - b_y) - \mathrm{i}\,(b_x + a_y)\right]\ . \end{aligned} \tag{5.109}$$

On the other hand, taking the complex conjugate of Eq. (5.108),

$$\vec{v}^{\,*} = \vec{a} - \mathrm{i}\,\vec{b}\ ,$$

we have for the spherical components of the vector $\vec{v}^{\,*}$

$$\begin{aligned} (v^*)_{-1} &= \frac{1}{\sqrt{2}}\left[(a_x - b_y) - \mathrm{i}\,(b_x + a_y)\right] \\ (v^*)_0 &= a_z - \mathrm{i}\,b_z \\ (v^*)_1 &= -\frac{1}{\sqrt{2}}\left[(a_x + b_y) - \mathrm{i}\,(b_x - a_y)\right]\ . \end{aligned} \tag{5.110}$$

Comparison of Eqs. (5.110) and (5.109) shows that

$$(v^*)_q = (-1)^q \, (v_{-q})^* \, , \tag{5.111}$$

a formula that could also be deduced by application of Eq. (2.85) to ordinary vectors (tensors of rank 1). Thus the complex conjugates of the spherical components of the vector $\vec{v}$ do *not* form an irreducible spherical tensor; nevertheless they are connected with the spherical components of the vector $\vec{v}^{\,*}$ by the simple relations (5.111).

From now on we will use for simplicity the symbol v_q^* (without parentheses) to denote the complex conjugate of the spherical component of the vector $\vec{v}$,

$$v_q^* \equiv (v_q)^* \, .$$

Consider now the direction cosines $C_{\alpha i}$ defined in the former sections. Since the scalar product of two vectors $\vec{v}$ and $\vec{w}$ can be written in the form (see Eqs. (2.83))

$$\vec{v} \cdot \vec{w} = \sum_q (-1)^q \, v_q w_{-q} \, , \tag{5.112}$$

we have

$$C_{\alpha i} = \vec{u}_\alpha \cdot \vec{e}_i^{\,*} = \sum_q (-1)^q \, (u_\alpha)_q \, (e_i^*)_{-q} = \sum_q (u_\alpha)_q \, (e_i)_q^* \, , \tag{5.113}$$

and for a bilinear product of two direction cosines

$$C_{\alpha i} C_{\beta j}^* = \sum_{qq'} (u_\alpha)_q \, (u_\beta)_{q'}^* \, (e_i)_q^* \, (e_j)_{q'} \, .$$

This expression suggests the introduction of a tensor – the dyadic product of two irreducible spherical tensors of rank 1 – which plays a very important role in the description of polarization phenomena. Indeed, as we will see in the following, this tensor – and the analogous ones that will be derived from it – appears as a natural ingredient of almost any mathematical expression relevant to polarized radiation. For this reason it deserves a careful definition.

In the right-handed reference system (xyz) of Fig. 5.14 we consider a particular direction characterized by the real unit vector $\vec{c}$. In the plane perpendicular to $\vec{c}$ we introduce two real unit vectors, $\vec{a}$ and $\vec{b}$, such that $\vec{a}$, $\vec{b}$, and $\vec{c}$ form, in this order, a right-handed coordinate system. The orientation of $(\vec{a}, \vec{b}, \vec{c})$ relative to (xyz) is specified by the angles θ, χ, and γ defined in Fig. 5.14, with

$$0 \le \theta \le \pi \, , \qquad 0 \le \chi < 2\pi \, , \qquad 0 \le \gamma < 2\pi \, .$$

From the unit vectors $\vec{a}$, $\vec{b}$, $\vec{c}$ we then define the unit vectors $\vec{c}_{-1}$, $\vec{c}_0$, $\vec{c}_{+1}$ via the equations

$$\begin{aligned} \vec{c}_{-1} &= \frac{1}{\sqrt{2}} \, (\vec{a} + \mathrm{i} \, \vec{b}\,) \\ \vec{c}_0 &= \vec{c} \\ \vec{c}_{+1} &= \frac{1}{\sqrt{2}} \, (-\vec{a} + \mathrm{i} \, \vec{b}\,) \, , \end{aligned} \tag{5.114}$$

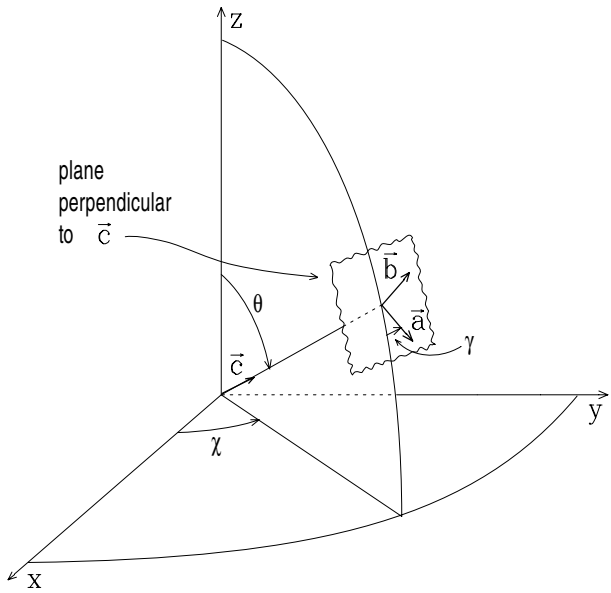

Fig.5.14. Geometry for the definition of the tensor $\mathcal{E}_{qq'}(\alpha,\beta,\vec{c})$.

and, finally, we define the reducible spherical tensor $\mathcal{E}_{qq'}$ relative to the triplet $(\vec{a},\vec{b},\vec{c})$ as[1]

$$\mathcal{E}_{qq'}(\alpha,\beta,\vec{c}) = (c_\alpha)_q\,(c_\beta)^*_{q'} \qquad (\alpha,\beta=\pm1;\;\; q,q'=0,\pm1)\;. \tag{5.115}$$

The explicit expression for $\mathcal{E}_{qq'}(\alpha,\beta,\vec{c})$ can be found by the following argument. In the reference system $(\vec{a},\vec{b},\vec{c})$ we have, from Eqs. (5.107) applied to the unit vectors defined in Eqs. (5.114)

$$(c_\alpha)_q = \delta_{\alpha q}\;, \qquad (c_\beta)_{q'} = \delta_{\beta q'}\;.$$

Since $(c_\alpha)_q$ is an irreducible spherical tensor of rank 1, its expression in the reference system (xyz) of Fig. 5.14 can be obtained by application of the transformation law of irreducible spherical tensors under rotations. From Eq. (2.78) we get

$$(c_\alpha)_q = \sum_p \delta_{\alpha p}\,\mathcal{D}^1_{pq}(R) = \mathcal{D}^1_{\alpha q}(R) \tag{5.116}$$

and, similarly

$$(c_\beta)^*_{q'} = \mathcal{D}^1_{\beta q'}(R)^*\;,$$

[1] The quantity $\mathcal{E}_{qq'}$ is neither an irreducible spherical tensor nor the dyadic product of two irreducible spherical tensors. The denomination 'reducible spherical tensor' is due to the fact that it can be *reduced* to the linear combination of irreducible spherical tensors (see Eq. (5.125)). Note also that $\mathcal{E}_{qq'}$ depends not only on the direction of the unit vector $\vec{c}$ (specified by the angles θ and χ), but also on the direction (specified by the angle γ) of the unit vector $\vec{a}$ in the plane perpendicular to $\vec{c}$. To shorten notations, we keep only $\vec{c}$ as an explicit argument of the tensor.

where $R \equiv (-\gamma, -\theta, -\chi)$ is the rotation bringing the system $(\vec{a}, \vec{b}, \vec{c})$ into the system (xyz). Thus the expression for $\mathcal{E}_{qq'}(\alpha, \beta, \vec{c})$ in the reference system (xyz) is

$$\mathcal{E}_{qq'}(\alpha, \beta, \vec{c}) = \mathcal{D}^1_{\alpha q}(R)\ \mathcal{D}^1_{\beta q'}(R)^* \ . \tag{5.117}$$

Let's now go back to the scattering phase matrix $\boldsymbol{T}$ appearing in Eqs. (5.86) and (5.87), and consider the case where the polarization unit vectors $(\vec{e}_1, \vec{e}_2)$ relative to the scattered radiation and the analogous vectors $(\vec{e}'_1, \vec{e}'_2)$ relative to the incident radiation are defined by the expressions (note the similarity with Eqs. (5.114))

$$\begin{aligned}
\vec{e}_1 &= \frac{1}{\sqrt{2}} \left[\vec{e}_a(\vec{\Omega}) + \mathrm{i}\, \vec{e}_b(\vec{\Omega}) \right] \equiv \vec{e}_{-1}(\vec{\Omega}) \\
\vec{e}_2 &= \frac{1}{\sqrt{2}} \left[-\vec{e}_a(\vec{\Omega}) + \mathrm{i}\, \vec{e}_b(\vec{\Omega}) \right] \equiv \vec{e}_{+1}(\vec{\Omega}) \\
\vec{e}'_1 &= \frac{1}{\sqrt{2}} \left[\vec{e}'_a(\vec{\Omega}') + \mathrm{i}\, \vec{e}'_b(\vec{\Omega}') \right] \equiv \vec{e}'_{-1}(\vec{\Omega}') \\
\vec{e}'_2 &= \frac{1}{\sqrt{2}} \left[-\vec{e}'_a(\vec{\Omega}') + \mathrm{i}\, \vec{e}'_b(\vec{\Omega}') \right] \equiv \vec{e}'_{+1}(\vec{\Omega}') \ ,
\end{aligned} \tag{5.118}$$

where $\vec{e}_a(\vec{\Omega})$, $\vec{e}_b(\vec{\Omega})$, $\vec{e}'_a(\vec{\Omega}')$, $\vec{e}'_b(\vec{\Omega}')$ are the reference direction unit vectors and the associated unit vectors defined as in Fig. 5.9.

With this choice Eq. (5.86) can be rewritten as

$$\mathrm{d}\tilde{I}_{\mu\nu}(\vec{\Omega}) = \sigma_{\mathrm{cl}} \sum_{\rho\sigma} T_{\mu\nu,\rho\sigma}(\vec{\Omega}, \vec{\Omega}'; \vec{B}\,)\ I'_{\rho\sigma}(\vec{\Omega}')\ \frac{\mathrm{d}\Omega'}{4\pi}\, \mathrm{d}\Omega$$

where $\mu, \nu, \rho, \sigma = \pm 1$, with the elements of the matrix $\boldsymbol{T}$ given by (see Eq. (5.113))

$$\begin{aligned}
&T_{\mu\nu,\rho\sigma}(\vec{\Omega}, \vec{\Omega}'; \vec{B}\,) = \\
&= \frac{3}{2} \sum_{\alpha\beta} \sum_{qq'q''q'''} (u_\alpha)^*_q\, (e_\mu(\vec{\Omega}))_q\, (u_\beta)_{q'}\, (e_\nu(\vec{\Omega}))^*_{q'}\, (u_\alpha)_{q''}\, (e'_\rho(\vec{\Omega}'))^*_{q''}\, (u_\beta)^*_{q'''}\, (e'_\sigma(\vec{\Omega}'))_{q'''} \\
&\qquad \times \frac{1}{1 + \mathrm{i}\,(\alpha - \beta)H} \qquad\qquad (\alpha, \beta = 0, \pm 1) \ .
\end{aligned} \tag{5.119}$$

This formula can be evaluated in any reference system. If we choose the reference system $(\vec{u}_r, \vec{u}_s, \vec{u}_0)$ used in Sects. 3.2 and 5.3 we simply have

$$(u_\alpha)_q = \delta_{\alpha q} \ , \qquad (u_\beta)_{q'} = \delta_{\beta q'} \ . \tag{5.120}$$

Thus Eq. (5.119) can be written, with the help of Eqs. (5.115) and (5.117), in the form

$$\begin{aligned}
T_{\mu\nu,\rho\sigma}(\vec{\Omega}, \vec{\Omega}'; \vec{B}\,) &= \frac{3}{2} \sum_{qq'} \frac{\mathcal{E}_{qq'}(\mu, \nu, \vec{\Omega})\ \mathcal{E}_{q'q}(\sigma, \rho, \vec{\Omega}')}{1 + \mathrm{i}\,(q - q')H} \\
&= \frac{3}{2} \sum_{qq'} \frac{\mathcal{D}^1_{\mu q}(R)\ \mathcal{D}^1_{\nu q'}(R)^*\ \mathcal{D}^1_{\rho q}(R')^*\ \mathcal{D}^1_{\sigma q'}(R')}{1 + \mathrm{i}\,(q - q')H} \ ,
\end{aligned} \tag{5.121}$$

where R is the rotation bringing the system $(\vec{e}_a(\vec{\Omega}), \vec{e}_b(\vec{\Omega}), \vec{\Omega})$ into the system $(\vec{u}_r, \vec{u}_s, \vec{u}_0)$ and, similarly, R' is the rotation bringing the system $(\vec{e}'_a(\vec{\Omega}'), \vec{e}'_b(\vec{\Omega}'), \vec{\Omega}')$ into the system $(\vec{u}_r, \vec{u}_s, \vec{u}_0)$.

In the general geometrical configuration of Fig. 5.9, R and R' can be expressed in the most convenient way as the result of two consecutive rotations,

$$\begin{aligned} R &\equiv (-\gamma, -\theta, -\chi) \times (\chi_B, \theta_B, \alpha) \\ R' &\equiv (-\gamma', -\theta', -\chi') \times (\chi_B, \theta_B, \alpha) \ , \end{aligned} \tag{5.122}$$

where α is an arbitrary angle whose actual value is unimportant for the evaluation of the quantity $T_{\mu\nu,\rho\sigma}$ and that can be set equal to zero. In the geometrical configuration of Fig. 5.10, R and R' are simply given by

$$R \equiv (0, -\theta, -\chi) \ , \qquad R' \equiv (0, -\theta', -\chi') \ . \tag{5.123}$$

As shown in Sect. 2.7, the dyadic product of two irreducible spherical tensors of rank k and k' can be used to construct an irreducible spherical tensor of rank K. Therefore, recalling Eq. (5.111), one can obtain an irreducible spherical tensor by taking appropriate linear combinations of the quantities $\mathcal{E}_{qq'}(\alpha, \beta, \vec{c})$ defined in Eq. (5.115). According to Eq. (2.79) such combinations are given by[1]

$$\mathcal{E}^K_Q(\alpha, \beta, \vec{c}) = \sum_{qq'} (-1)^{1+q} \sqrt{3(2K+1)} \begin{pmatrix} 1 & 1 & K \\ q & -q' & -Q \end{pmatrix} \mathcal{E}_{qq'}(\alpha, \beta, \vec{c}) \ , \tag{5.124}$$

with the inverse transformation

$$\mathcal{E}_{qq'}(\alpha, \beta, \vec{c}) = \sum_{KQ} (-1)^{1+q} \sqrt{\frac{2K+1}{3}} \begin{pmatrix} 1 & 1 & K \\ q & -q' & -Q \end{pmatrix} \mathcal{E}^K_Q(\alpha, \beta, \vec{c}) \ . \tag{5.125}$$

In terms of rotation matrices, one gets from Eq. (5.117)

$$\mathcal{E}^K_Q(\alpha, \beta, \vec{c}) = \sum_{qq'} (-1)^{1+q} \sqrt{3(2K+1)} \begin{pmatrix} 1 & 1 & K \\ q & -q' & -Q \end{pmatrix} \mathcal{D}^1_{\alpha q}(R) \, \mathcal{D}^1_{\beta q'}(R)^* \ ,$$

which, using Eqs. (2.77), (2.23a), (2.73) and the fact that α and β can only take the values ± 1, can be written in the form

$$\mathcal{E}^K_Q(\alpha, \beta, \vec{c}) = \sqrt{3(2K+1)} \begin{pmatrix} 1 & 1 & K \\ \alpha & -\beta & -Q' \end{pmatrix} \mathcal{D}^K_{Q'Q}(R) \qquad (\alpha, \beta = \pm 1) \ . \tag{5.126}$$

[1] The linear combinations of Eq. (2.79) have been multiplied by the factor $f(K) = -\sqrt{3(2K+1)}$. This slightly simplifies some expressions that will be deduced in the following.

Substitution of Eq. (5.125) into Eq. (5.121) leads to the expression of the scattering phase matrix $\boldsymbol{T}$ in terms of irreducible spherical tensors

$$\begin{aligned} & T_{\mu\nu,\rho\sigma}(\vec{\Omega},\vec{\Omega}';\vec{B}\,) = \\ & = \frac{1}{2}\sum_{KQ}(-1)^Q\,\mathcal{E}^K_Q(\mu,\nu,\vec{\Omega})\,\mathcal{E}^K_{-Q}(\sigma,\rho,\vec{\Omega}')\,\frac{1}{1+\mathrm{i}\,QH} \\ & = \frac{3}{2}\sum_{KQ}(-1)^Q\,(2K+1)\begin{pmatrix}1 & 1 & K\\ \mu & -\nu & -Q'\end{pmatrix}\begin{pmatrix}1 & 1 & K\\ \sigma & -\rho & -Q''\end{pmatrix} \\ & \qquad \times \mathcal{D}^K_{Q'Q}(R)\,\mathcal{D}^K_{Q''-Q}(R')\,\frac{1}{1+\mathrm{i}\,QH}\,, \end{aligned} \tag{5.127}$$

where R and R' are the rotations given in Eqs. (5.122) or (5.123).

To deduce the scattering phase matrix $\boldsymbol{R}$ for the Stokes parameters we need the relation between the Stokes parameters and the polarization tensor corresponding to the basis of unit vectors (5.118). This relation can be obtained from Eqs. (1.42) by the substitution $\theta = 5\pi/4$, $\phi = -\pi/2$. We have

$$\begin{aligned} I &= I_{++} + I_{--} & Q &= -\left(I_{+-} + I_{-+}\right) \\ V &= I_{++} - I_{--} & U &= -\,\mathrm{i}\left(I_{+-} - I_{-+}\right), \end{aligned}$$

where we have shortened the notations writing I_{++} instead of I_{+1+1} and so on. The inverse transformations are

$$\begin{aligned} I_{++} &= \frac{1}{2}\left(I+V\right) & I_{+-} &= \frac{1}{2}\left(-Q+\mathrm{i}\,U\right) \\ I_{--} &= \frac{1}{2}\left(I-V\right) & I_{-+} &= \frac{1}{2}\left(-Q-\mathrm{i}\,U\right). \end{aligned}$$

If we take an appropriate representation for the Pauli spin matrices (which differs from that of Eqs. (1.17)) we can write these transformations in a more compact form. Defining

$$\hat{\boldsymbol{\sigma}}_0 = \begin{pmatrix}1 & 0\\ 0 & 1\end{pmatrix}, \quad \hat{\boldsymbol{\sigma}}_1 = \begin{pmatrix}0 & -1\\ -1 & 0\end{pmatrix}, \quad \hat{\boldsymbol{\sigma}}_2 = \begin{pmatrix}0 & -\mathrm{i}\\ \mathrm{i} & 0\end{pmatrix}, \quad \hat{\boldsymbol{\sigma}}_3 = \begin{pmatrix}-1 & 0\\ 0 & 1\end{pmatrix} \tag{5.128}$$

with

$$\hat{\boldsymbol{\sigma}}_i\hat{\boldsymbol{\sigma}}_j = \delta_{ij}\,\hat{\boldsymbol{\sigma}}_0 + \mathrm{i}\sum_k \epsilon_{ijk}\,\hat{\boldsymbol{\sigma}}_k \qquad (i,j,k=1,2,3)$$

and

$$\mathrm{Tr}\,(\hat{\boldsymbol{\sigma}}_k\hat{\boldsymbol{\sigma}}_l) = 2\,\delta_{kl} \qquad (k,l=0,1,2,3)\,,$$

and labelling the rows and columns of the matrices in the order $(-,+)$ (so that,for instance, $(\hat{\sigma}_i)_{+-} = (\hat{\sigma}_i)_{21}$), we have[1]

$$I_{\alpha\beta} = \frac{1}{2}\sum_{j=0}^{3} S_j\,(\hat{\sigma}_j)_{\alpha\beta} \qquad (\alpha,\beta = \pm 1)$$
$$S_j = \sum_{\alpha\beta} (\hat{\sigma}_j)_{\alpha\beta}\, I_{\beta\alpha} \qquad (j = 0,1,2,3)\,. \tag{5.129}$$

Since these transformations are identical to (1.40) provided the matrices $\boldsymbol{\sigma}_i$ are exchanged with $\hat{\boldsymbol{\sigma}}_i$, the scattering phase matrix for the Stokes parameters can be easily obtained along the same lines of Sect. 5.7. The result is

$$R_{ij}(\vec{\Omega},\vec{\Omega}';\vec{B}\,) = \frac{1}{2}\sum_{\mu\nu\rho\sigma=\pm 1} (\hat{\sigma}_i)_{\nu\mu}\,(\hat{\sigma}_j)_{\rho\sigma}\; T_{\mu\nu,\rho\sigma}(\vec{\Omega},\vec{\Omega}';\vec{B}\,)$$

or, using Eq. (5.121)

$$R_{ij}(\vec{\Omega},\vec{\Omega}';\vec{B}\,) = 3\sum_{qq'} \frac{\mathcal{T}_{qq'}(i,\vec{\Omega})\;\mathcal{T}_{q'q}(j,\vec{\Omega}')}{1+\mathrm{i}\,(q-q')H}\,, \tag{5.130}$$

where we have defined the tensor $\mathcal{T}_{qq'}(i,\vec{\Omega})$ as

$$\mathcal{T}_{qq'}(i,\vec{\Omega}) = \sum_{\alpha\beta=\pm 1} \frac{1}{2}\,(\hat{\sigma}_i)_{\alpha\beta}\,\mathcal{E}_{qq'}(\beta,\alpha,\vec{\Omega})\,. \tag{5.131}$$

From the tensor $\mathcal{T}_{qq'}$ it is possible to construct – similarly to what done for $\mathcal{E}_{qq'}$ – an irreducible spherical tensor, $\mathcal{T}^K_Q$, that will play an important role in the continuation of this book

$$\begin{aligned}\mathcal{T}^K_Q(i,\vec{\Omega}) &= \sum_{qq'} (-1)^{1+q}\sqrt{3(2K+1)}\begin{pmatrix} 1 & 1 & K \\ q & -q' & -Q\end{pmatrix}\mathcal{T}_{qq'}(i,\vec{\Omega}) \\ &= \sum_{qq'}\sum_{\alpha\beta=\pm 1} (-1)^{1+q}\sqrt{3(2K+1)}\begin{pmatrix} 1 & 1 & K \\ q & -q' & -Q\end{pmatrix} \\ &\qquad\qquad \times \frac{1}{2}\,(\hat{\sigma}_i)_{\alpha\beta}\,\mathcal{E}_{qq'}(\beta,\alpha,\vec{\Omega}) \\ &= \sum_{\alpha\beta=\pm 1} \frac{1}{2}\,(\hat{\sigma}_i)_{\alpha\beta}\,\mathcal{E}^K_Q(\beta,\alpha,\vec{\Omega})\,.\end{aligned} \tag{5.132}$$

[1] Equations (5.129) have the same form as Eqs. (1.40). Note, however, that they involve the polarization tensor defined on the basis of the unit vectors (5.118), while the polarization tensor in Eqs. (1.40) is defined on the basis of the reference direction unit vector and the associated unit vector.

Inversion of the first line of Eq. (5.132) gives

$$\mathcal{T}_{qq'}(i,\vec{\Omega}) = \sum_{KQ} (-1)^{1+q} \sqrt{\frac{2K+1}{3}} \begin{pmatrix} 1 & 1 & K \\ q & -q' & -Q \end{pmatrix} \mathcal{T}^K_Q(i,\vec{\Omega}) \,,$$

which can be substituted into Eq. (5.130) to obtain the expression of the phase matrix $\boldsymbol{R}$ in terms of the irreducible spherical tensor $\mathcal{T}^K_Q$

$$R_{ij}(\vec{\Omega},\vec{\Omega}';\vec{B}\,) = \sum_{KQ} (-1)^Q \, \mathcal{T}^K_Q(i,\vec{\Omega}) \, \mathcal{T}^K_{-Q}(j,\vec{\Omega}') \, \frac{1}{1+\mathrm{i}\,QH} \,. \tag{5.133}$$

Using Eq. (5.126) the tensor $\mathcal{T}^K_Q$ can be explicitly written in terms of rotation matrices

$$\mathcal{T}^K_Q(i,\vec{\Omega}) = \sum_P t^K_P(i) \, \mathcal{D}^K_{PQ}(R) \,, \tag{5.134}$$

where

$$t^K_P(i) = \sum_{\alpha\beta=\pm 1} \frac{1}{2} \, (\hat{\sigma}_i)_{\alpha\beta} \sqrt{3(2K+1)} \begin{pmatrix} 1 & 1 & K \\ \beta & -\alpha & -P \end{pmatrix} \,. \tag{5.135}$$

From this equation, using some properties of the rotation matrices (Eqs. (2.71) and (2.73)) and noticing that $t^K_P(i)^* = t^K_{-P}(i)$, Eq. (5.133) can be rewritten in the form

$$R_{ij}(\vec{\Omega},\vec{\Omega}';\vec{B}\,) = \sum_{KPP'} t^K_P(i) \, t^K_{P'}(j)^* \sum_Q \mathcal{D}^K_{PQ}(R) \, \mathcal{D}^K_{QP'}(R'^{-1}) \, \frac{1}{1+\mathrm{i}\,QH} \,, \tag{5.136}$$

which is our final equation expressing the phase matrix $\boldsymbol{R}$ in terms of rotation matrices. In this equation we can isolate the contributions of the various K-values (sometimes referred to as the *multipole components* of the phase matrix)

$$R_{ij}(\vec{\Omega},\vec{\Omega}';\vec{B}\,) = \sum_K R^{(K)}_{ij}(\vec{\Omega},\vec{\Omega}';\vec{B}\,) \tag{5.137}$$

with

$$\begin{aligned} R^{(K)}_{ij}(\vec{\Omega},\vec{\Omega}';\vec{B}\,) &= \sum_Q (-1)^Q \, \mathcal{T}^K_Q(i,\vec{\Omega}) \, \mathcal{T}^K_{-Q}(j,\vec{\Omega}') \, \frac{1}{1+\mathrm{i}\,QH} \\ &= \sum_{PP'} t^K_P(i) \, t^K_{P'}(j)^* \sum_Q \mathcal{D}^K_{PQ}(R) \, \mathcal{D}^K_{QP'}(R'^{-1}) \, \frac{1}{1+\mathrm{i}\,QH} \,. \end{aligned} \tag{5.138}$$

The tensors introduced in this section satisfy several properties, which are collected in the following section together with a number of tables that are particularly useful for applications. With the help of such tables we can easily get back expressions (5.99) which give the scattering phase matrix in the reference system with

the z-axis parallel to the magnetic field (see Fig. 5.10). In terms of multipole components we get

$$\boldsymbol{R}^{(0)}(\vec{\Omega},\vec{\Omega}';\vec{B}\,) = \begin{pmatrix} 1 & 0 & 0 & 0 \\ 0 & 0 & 0 & 0 \\ 0 & 0 & 0 & 0 \\ 0 & 0 & 0 & 0 \end{pmatrix} ,$$

$$\boldsymbol{R}^{(1)}(\vec{\Omega},\vec{\Omega}';\vec{B}\,) = \frac{3}{2}\big(\mu\mu' + \sqrt{1-\mu^2}\,\sqrt{1-\mu'^2}\,C_1\big) \begin{pmatrix} 0 & 0 & 0 & 0 \\ 0 & 0 & 0 & 0 \\ 0 & 0 & 0 & 0 \\ 0 & 0 & 0 & 1 \end{pmatrix} ,$$

$$\begin{aligned} \boldsymbol{R}^{(2)}(\vec{\Omega},\vec{\Omega}';\vec{B}\,) = {} & \frac{1}{8} \begin{pmatrix} (1-3\mu^2)(1-3\mu'^2) & (1-3\mu^2)(3-3\mu'^2) & 0 & 0 \\ (3-3\mu^2)(1-3\mu'^2) & (3-3\mu^2)(3-3\mu'^2) & 0 & 0 \\ 0 & 0 & 0 & 0 \\ 0 & 0 & 0 & 0 \end{pmatrix} \\ & + \frac{3}{2}\,\sqrt{1-\mu^2}\,\sqrt{1-\mu'^2} \begin{pmatrix} \mu\mu'\,C_1 & \mu\mu'\,C_1 & -\mu\,S_1 & 0 \\ \mu\mu'\,C_1 & \mu\mu'\,C_1 & -\mu\,S_1 & 0 \\ \mu'\,S_1 & \mu'\,S_1 & C_1 & 0 \\ 0 & 0 & 0 & 0 \end{pmatrix} \\ & + \frac{3}{8} \begin{pmatrix} (1-\mu^2)(1-\mu'^2)C_2 & -(1-\mu^2)(1+\mu'^2)C_2 & 2(1-\mu^2)\mu' S_2 & 0 \\ -(1+\mu^2)(1-\mu'^2)C_2 & (1+\mu^2)(1+\mu'^2)C_2 & -2(1+\mu^2)\mu' S_2 & 0 \\ -2\mu(1-\mu'^2)S_2 & 2\mu(1+\mu'^2)S_2 & 4\mu\mu' C_2 & 0 \\ 0 & 0 & 0 & 0 \end{pmatrix} , \end{aligned} \tag{5.139}$$

where the notations are the same as in Eqs. (5.97). Adding the contributions of the three matrices $\boldsymbol{R}^{(0)}$, $\boldsymbol{R}^{(1)}$, and $\boldsymbol{R}^{(2)}$, Eqs. (5.99) are easily obtained.

5.11. Spherical Tensors for Polarimetry

The various tensors defined in the former section are particularly suitable for the description of polarization phenomena in spectral lines. As they will be heavily used in the following of this book, their properties deserve a thorough discussion. At the same time, we will take the opportunity of introducing some new tensors that will also be useful later.

Starting with the reducible tensors, we have defined

$$\mathcal{E}_{qq'}(\alpha,\beta,\vec{\Omega}) = \big(e_\alpha(\vec{\Omega})\big)_q \big(e_\beta(\vec{\Omega})\big)^*_{q'} \qquad (q,q'=0,\pm1; \quad \alpha,\beta=\pm1) \tag{5.140}$$

with

$$\vec{e}_{\pm1}(\vec{\Omega}) = \frac{1}{\sqrt{2}}\Big[\mp\,\vec{e}_a(\vec{\Omega}) + \mathrm{i}\,\vec{e}_b(\vec{\Omega})\Big] , \tag{5.141}$$

and we have obtained, in terms of rotation matrices (see Eq. (5.117))

$$\mathcal{E}_{qq'}(\alpha,\beta,\vec{\Omega}) = \mathcal{D}^1_{\alpha q}(R)\ \mathcal{D}^1_{\beta q'}(R)^* \ , \tag{5.142}$$

where

$$R \equiv (-\gamma, -\theta, -\chi)$$

is the rotation bringing the coordinate system $(\vec{e}_a(\vec{\Omega}), \vec{e}_b(\vec{\Omega}), \vec{\Omega})$ into the system (xyz) (refer to Fig. 5.14 with $(\vec{a},\vec{b},\vec{c})$ replaced by $(\vec{e}_a(\vec{\Omega}), \vec{e}_b(\vec{\Omega}), \vec{\Omega})$).

In terms of reduced rotation matrices (see Eq. (2.68)) one gets, with the help of Eqs. (2.70)

$$\mathcal{E}_{qq'}(\alpha,\beta,\vec{\Omega}) = \mathrm{e}^{\,\mathrm{i}\,[(q-q')\chi\,+\,(\alpha-\beta)\gamma]}\ d^1_{q\alpha}(\theta)\, d^1_{q'\beta}(\theta) \ .$$

From Eq. (5.142), using Eqs. (2.72), one obtains

$$\sum_{\alpha=\pm1} \mathcal{E}_{qq'}(\alpha,\alpha,\vec{\Omega}) = \delta_{qq'} - \mathcal{D}^1_{0q}(R)\ \mathcal{D}^1_{0q'}(R)^* \ ,$$

and by application of the Weyl theorem (Eq. (2.76))

$$\sum_{\alpha=\pm1} \oint \frac{\mathrm{d}\Omega}{4\pi}\ \mathcal{E}_{qq'}(\alpha,\alpha,\vec{\Omega}) = \frac{2}{3}\ \delta_{qq'} \ . \tag{5.143}$$

Again from Eqs. (2.72) one gets the relation

$$\sum_q \mathcal{E}_{qq}(\alpha,\beta,\vec{\Omega}) = \delta_{\alpha\beta} \ , \tag{5.144}$$

and directly from the definition (5.140)

$$\mathcal{E}_{qq'}(\alpha,\beta,\vec{\Omega})^* = \mathcal{E}_{q'q}(\beta,\alpha,\vec{\Omega}) \ . \tag{5.145}$$

The explicit expression for the tensor $\mathcal{E}_{qq'}(\alpha,\beta,\vec{\Omega})$ as a function of χ, θ, and γ is given in Table 5.2.

The other reducible tensor that we have introduced is $\mathcal{T}_{qq'}(i,\vec{\Omega})$, defined by (see Eq. (5.131))

$$\mathcal{T}_{qq'}(i,\vec{\Omega}) = \sum_{\alpha\beta=\pm1} \frac{1}{2}\ (\hat{\sigma}_i)_{\alpha\beta}\ \mathcal{E}_{qq'}(\beta,\alpha,\vec{\Omega}) \qquad \begin{matrix}(q,q'=0,\pm1)\\(i=0,\ldots,3)\ .\end{matrix} \tag{5.146}$$

Taking the complex conjugate, we have from Eq. (5.145)

$$\mathcal{T}_{qq'}(i,\vec{\Omega})^* = \sum_{\alpha\beta=\pm1} \frac{1}{2}\ (\hat{\sigma}_i)^*_{\alpha\beta}\ \mathcal{E}_{q'q}(\alpha,\beta,\vec{\Omega}) \ ,$$

TABLE 5.2

Explicit expression for the tensor $\mathcal{E}_{qq'}(\alpha,\beta,\vec{\Omega})$. The remaining components can be obtained from the relation $\mathcal{E}_{q'q}(\alpha,\beta,\vec{\Omega}) = \mathcal{E}_{qq'}(\beta,\alpha,\vec{\Omega})^*$.

$$
\begin{aligned}
\mathcal{E}_{-1\,-1}(-,-,\vec{\Omega}) &= \tfrac{1}{4}\,(1+\cos\theta)^2 \\
\mathcal{E}_{0\,0}(-,-,\vec{\Omega}) &= \tfrac{1}{2}\,\sin^2\theta \\
\mathcal{E}_{1\,1}(-,-,\vec{\Omega}) &= \tfrac{1}{4}\,(1-\cos\theta)^2 \\
\mathcal{E}_{-1\,0}(-,-,\vec{\Omega}) &= -\tfrac{1}{2\sqrt{2}}\,\sin\theta\,(1+\cos\theta)\,\mathrm{e}^{-\mathrm{i}\chi} \\
\mathcal{E}_{-1\,1}(-,-,\vec{\Omega}) &= \tfrac{1}{4}\,\sin^2\theta\,\mathrm{e}^{-2\mathrm{i}\chi} \\
\mathcal{E}_{0\,1}(-,-,\vec{\Omega}) &= -\tfrac{1}{2\sqrt{2}}\,\sin\theta\,(1-\cos\theta)\,\mathrm{e}^{-\mathrm{i}\chi}
\end{aligned}
$$

$$
\begin{aligned}
\mathcal{E}_{-1\,-1}(-,+,\vec{\Omega}) &= \tfrac{1}{4}\,\mathrm{e}^{-2\mathrm{i}\gamma}\,\sin^2\theta \\
\mathcal{E}_{0\,0}(-,+,\vec{\Omega}) &= -\tfrac{1}{2}\,\mathrm{e}^{-2\mathrm{i}\gamma}\,\sin^2\theta \\
\mathcal{E}_{1\,1}(-,+,\vec{\Omega}) &= \tfrac{1}{4}\,\mathrm{e}^{-2\mathrm{i}\gamma}\,\sin^2\theta \\
\mathcal{E}_{-1\,0}(-,+,\vec{\Omega}) &= \tfrac{1}{2\sqrt{2}}\,\mathrm{e}^{-2\mathrm{i}\gamma}\,\sin\theta\,(1+\cos\theta)\,\mathrm{e}^{-\mathrm{i}\chi} \\
\mathcal{E}_{-1\,1}(-,+,\vec{\Omega}) &= \tfrac{1}{4}\,\mathrm{e}^{-2\mathrm{i}\gamma}\,(1+\cos\theta)^2\,\mathrm{e}^{-2\mathrm{i}\chi} \\
\mathcal{E}_{0\,1}(-,+,\vec{\Omega}) &= -\tfrac{1}{2\sqrt{2}}\,\mathrm{e}^{-2\mathrm{i}\gamma}\,\sin\theta\,(1+\cos\theta)\,\mathrm{e}^{-\mathrm{i}\chi}
\end{aligned}
$$

$$
\begin{aligned}
\mathcal{E}_{-1\,-1}(+,-,\vec{\Omega}) &= \tfrac{1}{4}\,\mathrm{e}^{2\mathrm{i}\gamma}\,\sin^2\theta \\
\mathcal{E}_{0\,0}(+,-,\vec{\Omega}) &= -\tfrac{1}{2}\,\mathrm{e}^{2\mathrm{i}\gamma}\,\sin^2\theta \\
\mathcal{E}_{1\,1}(+,-,\vec{\Omega}) &= \tfrac{1}{4}\,\mathrm{e}^{2\mathrm{i}\gamma}\,\sin^2\theta \\
\mathcal{E}_{-1\,0}(+,-,\vec{\Omega}) &= -\tfrac{1}{2\sqrt{2}}\,\mathrm{e}^{2\mathrm{i}\gamma}\,\sin\theta\,(1-\cos\theta)\,\mathrm{e}^{-\mathrm{i}\chi} \\
\mathcal{E}_{-1\,1}(+,-,\vec{\Omega}) &= \tfrac{1}{4}\,\mathrm{e}^{2\mathrm{i}\gamma}\,(1-\cos\theta)^2\,\mathrm{e}^{-2\mathrm{i}\chi} \\
\mathcal{E}_{0\,1}(+,-,\vec{\Omega}) &= \tfrac{1}{2\sqrt{2}}\,\mathrm{e}^{2\mathrm{i}\gamma}\,\sin\theta\,(1-\cos\theta)\,\mathrm{e}^{-\mathrm{i}\chi}
\end{aligned}
$$

$$
\begin{aligned}
\mathcal{E}_{-1\,-1}(+,+,\vec{\Omega}) &= \tfrac{1}{4}\,(1-\cos\theta)^2 \\
\mathcal{E}_{0\,0}(+,+,\vec{\Omega}) &= \tfrac{1}{2}\,\sin^2\theta \\
\mathcal{E}_{1\,1}(+,+,\vec{\Omega}) &= \tfrac{1}{4}\,(1+\cos\theta)^2 \\
\mathcal{E}_{-1\,0}(+,+,\vec{\Omega}) &= \tfrac{1}{2\sqrt{2}}\,\sin\theta\,(1-\cos\theta)\,\mathrm{e}^{-\mathrm{i}\chi} \\
\mathcal{E}_{-1\,1}(+,+,\vec{\Omega}) &= \tfrac{1}{4}\,\sin^2\theta\,\mathrm{e}^{-2\mathrm{i}\chi} \\
\mathcal{E}_{0\,1}(+,+,\vec{\Omega}) &= \tfrac{1}{2\sqrt{2}}\,\sin\theta\,(1+\cos\theta)\,\mathrm{e}^{-\mathrm{i}\chi}
\end{aligned}
$$

and since the matrices $\hat{\boldsymbol{\sigma}}_i$ obey the conjugation property

$$(\hat{\sigma}_i)^*_{\alpha\beta} = (\hat{\sigma}_i)_{\beta\alpha} \ , \tag{5.147}$$

we get

$$\mathcal{T}_{qq'}(i,\vec{\Omega})^* = \mathcal{T}_{q'q}(i,\vec{\Omega}) \ . \tag{5.148}$$

Another property can be obtained from Eq. (5.144) using the trace properties of the matrices $\hat{\boldsymbol{\sigma}}_i$

$$\sum_q \mathcal{T}_{qq}(i,\vec{\Omega}) = \sum_{\alpha=\pm1} \frac{1}{2} \, (\hat{\sigma}_i)_{\alpha\alpha} = \frac{1}{2} \, \mathrm{Tr} \, (\hat{\boldsymbol{\sigma}}_i) = \delta_{i0} \ . \tag{5.149}$$

The explicit expression for the tensor $\mathcal{T}_{qq'}(i,\vec{\Omega})$ is given in Table 5.3.

Using the tensors $\mathcal{E}_{qq'}(\alpha,\beta,\vec{\Omega})$ and $\mathcal{T}_{qq'}(i,\vec{\Omega})$ we can construct a further reducible tensor, $\mathcal{I}_{qq'}(\nu,\vec{\Omega})$, which describes the polarization properties of the radiation field propagating along the direction $\vec{\Omega}$. If $I_{\alpha\beta}(\nu,\vec{\Omega})$ is the polarization tensor (defined on the basis of the unit vectors $\vec{e}_{\pm1}(\vec{\Omega})$ of Eq. (5.141)) and $S_i(\nu,\vec{\Omega})$ is the Stokes vector, both relative to the frequency ν and the direction $\vec{\Omega}$, we define the tensor $\mathcal{I}_{qq'}(\nu,\vec{\Omega})$ according to either of the equivalent relations (see Eqs. (5.129) and (5.146))

$$\begin{aligned} \mathcal{I}_{qq'}(\nu,\vec{\Omega}) &= \sum_{\alpha\beta=\pm1} \mathcal{E}_{qq'}(\alpha,\beta,\vec{\Omega}) \, I_{\beta\alpha}(\nu,\vec{\Omega}) \\ &= \sum_{i=0}^{3} \mathcal{T}_{qq'}(i,\vec{\Omega}) \, S_i(\nu,\vec{\Omega}) \ . \end{aligned} \tag{5.150}$$

This tensor satisfies the conjugation property (easily deduced from Eq. (5.148))

$$\mathcal{I}_{qq'}(\nu,\vec{\Omega})^* = \mathcal{I}_{q'q}(\nu,\vec{\Omega}) \ , \tag{5.151}$$

and the trace property (consequence of Eq. (5.149))

$$\sum_q \mathcal{I}_{qq}(\nu,\vec{\Omega}) = S_0(\nu,\vec{\Omega}) = I(\nu,\vec{\Omega}) \ . \tag{5.152}$$

The explicit expression for the tensor $\mathcal{I}_{qq'}(\nu,\vec{\Omega})$ is given in Table 5.4. It is important to remark that the linear polarization Stokes parameters, Q and U, enter the expressions of Table 5.4 only via the linear combinations

$$\tilde{Q} = \cos 2\gamma \, Q - \sin 2\gamma \, U \ , \qquad \tilde{U} = \cos 2\gamma \, U + \sin 2\gamma \, Q \ .$$

These combinations are independent of the angle γ which defines the reference direction for the Stokes parameters Q and U.

TABLE 5.3

Explicit expression for the tensor $\mathcal{T}_{qq'}(i,\vec{\Omega})$. The remaining components can be obtained from the relation $\mathcal{T}_{q'q}(i,\vec{\Omega}) = \mathcal{T}_{qq'}(i,\vec{\Omega})^*$.

$$\mathcal{T}_{-1\,-1}(0,\vec{\Omega}) = \tfrac{1}{4}\,(1+\cos^2\theta)$$

$$\mathcal{T}_{0\,0}(0,\vec{\Omega}) = \tfrac{1}{2}\,\sin^2\theta$$

$$\mathcal{T}_{1\,1}(0,\vec{\Omega}) = \tfrac{1}{4}\,(1+\cos^2\theta)$$

$$\mathcal{T}_{-1\,0}(0,\vec{\Omega}) = -\tfrac{1}{2\sqrt{2}}\,\sin\theta\cos\theta\,\mathrm{e}^{-\mathrm{i}\chi}$$

$$\mathcal{T}_{-1\,1}(0,\vec{\Omega}) = \tfrac{1}{4}\,\sin^2\theta\,\mathrm{e}^{-2\mathrm{i}\chi}$$

$$\mathcal{T}_{0\,1}(0,\vec{\Omega}) = \tfrac{1}{2\sqrt{2}}\,\sin\theta\cos\theta\,\mathrm{e}^{-\mathrm{i}\chi}$$

$$\mathcal{T}_{-1\,-1}(1,\vec{\Omega}) = -\tfrac{1}{4}\,\cos 2\gamma\,\sin^2\theta$$

$$\mathcal{T}_{0\,0}(1,\vec{\Omega}) = \tfrac{1}{2}\,\cos 2\gamma\,\sin^2\theta$$

$$\mathcal{T}_{1\,1}(1,\vec{\Omega}) = -\tfrac{1}{4}\,\cos 2\gamma\,\sin^2\theta$$

$$\mathcal{T}_{-1\,0}(1,\vec{\Omega}) = -\tfrac{1}{2\sqrt{2}}\,(\cos 2\gamma\,\cos\theta - \mathrm{i}\,\sin 2\gamma)\sin\theta\,\mathrm{e}^{-\mathrm{i}\chi}$$

$$\mathcal{T}_{-1\,1}(1,\vec{\Omega}) = -\tfrac{1}{4}\left[\cos 2\gamma\,(1+\cos^2\theta) - 2\mathrm{i}\,\sin 2\gamma\,\cos\theta\right]\mathrm{e}^{-2\mathrm{i}\chi}$$

$$\mathcal{T}_{0\,1}(1,\vec{\Omega}) = \tfrac{1}{2\sqrt{2}}\,(\cos 2\gamma\,\cos\theta - \mathrm{i}\,\sin 2\gamma)\sin\theta\,\mathrm{e}^{-\mathrm{i}\chi}$$

$$\mathcal{T}_{-1\,-1}(2,\vec{\Omega}) = \tfrac{1}{4}\,\sin 2\gamma\,\sin^2\theta$$

$$\mathcal{T}_{0\,0}(2,\vec{\Omega}) = -\tfrac{1}{2}\,\sin 2\gamma\,\sin^2\theta$$

$$\mathcal{T}_{1\,1}(2,\vec{\Omega}) = \tfrac{1}{4}\,\sin 2\gamma\,\sin^2\theta$$

$$\mathcal{T}_{-1\,0}(2,\vec{\Omega}) = \tfrac{1}{2\sqrt{2}}\,(\sin 2\gamma\,\cos\theta + \mathrm{i}\,\cos 2\gamma)\sin\theta\,\mathrm{e}^{-\mathrm{i}\chi}$$

$$\mathcal{T}_{-1\,1}(2,\vec{\Omega}) = \tfrac{1}{4}\left[\sin 2\gamma\,(1+\cos^2\theta) + 2\mathrm{i}\,\cos 2\gamma\,\cos\theta\right]\mathrm{e}^{-2\mathrm{i}\chi}$$

$$\mathcal{T}_{0\,1}(2,\vec{\Omega}) = -\tfrac{1}{2\sqrt{2}}\,(\sin 2\gamma\,\cos\theta + \mathrm{i}\,\cos 2\gamma)\sin\theta\,\mathrm{e}^{-\mathrm{i}\chi}$$

$$\mathcal{T}_{-1\,-1}(3,\vec{\Omega}) = -\tfrac{1}{2}\,\cos\theta$$

$$\mathcal{T}_{0\,0}(3,\vec{\Omega}) = 0$$

$$\mathcal{T}_{1\,1}(3,\vec{\Omega}) = \tfrac{1}{2}\,\cos\theta$$

$$\mathcal{T}_{-1\,0}(3,\vec{\Omega}) = \tfrac{1}{2\sqrt{2}}\,\sin\theta\,\mathrm{e}^{-\mathrm{i}\chi}$$

$$\mathcal{T}_{-1\,1}(3,\vec{\Omega}) = 0$$

$$\mathcal{T}_{0\,1}(3,\vec{\Omega}) = \tfrac{1}{2\sqrt{2}}\,\sin\theta\,\mathrm{e}^{-\mathrm{i}\chi}$$

TABLE 5.4

Explicit expression for the tensor $\mathcal{I}_{qq'}(\nu,\vec{\Omega})$. The remaining components can be obtained from the relation $\mathcal{I}_{q'q}(\nu,\vec{\Omega}) = \mathcal{I}_{qq'}(\nu,\vec{\Omega})^*$.

$$
\begin{aligned}
\mathcal{I}_{-1\,-1}(\nu,\vec{\Omega}) &= \tfrac{1}{4}\left[(1+\cos^2\theta)\, I(\nu,\vec{\Omega}) - \sin^2\theta\, \tilde{Q}(\nu,\vec{\Omega}) - 2\cos\theta\, V(\nu,\vec{\Omega})\right] \\
\mathcal{I}_{0\,0}(\nu,\vec{\Omega}) &= \tfrac{1}{2}\,\sin^2\theta\left[I(\nu,\vec{\Omega}) + \tilde{Q}(\nu,\vec{\Omega})\right] \\
\mathcal{I}_{1\,1}(\nu,\vec{\Omega}) &= \tfrac{1}{4}\left[(1+\cos^2\theta)\, I(\nu,\vec{\Omega}) - \sin^2\theta\, \tilde{Q}(\nu,\vec{\Omega}) + 2\cos\theta\, V(\nu,\vec{\Omega})\right] \\
\mathcal{I}_{-1\,0}(\nu,\vec{\Omega}) &= \tfrac{1}{2\sqrt{2}}\,\sin\theta\left[-\cos\theta\, I(\nu,\vec{\Omega}) - \cos\theta\, \tilde{Q}(\nu,\vec{\Omega}) + \mathrm{i}\,\tilde{U}(\nu,\vec{\Omega}) + V(\nu,\vec{\Omega})\right] \mathrm{e}^{-\mathrm{i}\chi} \\
\mathcal{I}_{-1\,1}(\nu,\vec{\Omega}) &= \tfrac{1}{4}\left[\sin^2\theta\, I(\nu,\vec{\Omega}) - (1+\cos^2\theta)\, \tilde{Q}(\nu,\vec{\Omega}) + 2\mathrm{i}\,\cos\theta\, \tilde{U}(\nu,\vec{\Omega})\right] \mathrm{e}^{-2\mathrm{i}\chi} \\
\mathcal{I}_{0\,1}(\nu,\vec{\Omega}) &= \tfrac{1}{2\sqrt{2}}\,\sin\theta\left[\cos\theta\, I(\nu,\vec{\Omega}) + \cos\theta\, \tilde{Q}(\nu,\vec{\Omega}) - \mathrm{i}\,\tilde{U}(\nu,\vec{\Omega}) + V(\nu,\vec{\Omega})\right] \mathrm{e}^{-\mathrm{i}\chi}
\end{aligned}
$$

where
$$
\begin{aligned}
\tilde{Q}(\nu,\vec{\Omega}) &= \cos 2\gamma\, Q(\nu,\vec{\Omega}) - \sin 2\gamma\, U(\nu,\vec{\Omega}) \\
\tilde{U}(\nu,\vec{\Omega}) &= \cos 2\gamma\, U(\nu,\vec{\Omega}) + \sin 2\gamma\, Q(\nu,\vec{\Omega})
\end{aligned}
$$

Finally, from the tensor $\mathcal{I}_{qq'}(\nu,\vec{\Omega})$ one can define the tensor $J_{qq'}(\nu)$ by averaging over the whole solid angle

$$
J_{qq'}(\nu) = \oint \frac{\mathrm{d}\Omega}{4\pi}\, \mathcal{I}_{qq'}(\nu,\vec{\Omega}) = \oint \frac{\mathrm{d}\Omega}{4\pi} \sum_{i=0}^{3} \mathcal{T}_{qq'}(i,\vec{\Omega})\, S_i(\nu,\vec{\Omega}) \; . \tag{5.153}
$$

This tensor depends on the polarized radiation field propagating in all directions, and will be called the (*reducible*) *radiation field tensor*. Its trace is given by (see Eq. (5.152))

$$
\sum_q J_{qq}(\nu) = \oint \frac{\mathrm{d}\Omega}{4\pi}\, I(\nu,\vec{\Omega}) = J(\nu) \; ,
$$

which is the usual definition of the mean intensity of the radiation field over the solid angle. From Eq. (5.151) it follows the conjugation property

$$
J_{qq'}(\nu)^* = J_{q'q}(\nu) \; . \tag{5.154}
$$

All the tensors defined so far are reducible tensors. Under rotation of the coordinate system the new components, $T'_{qq'}$, are obtained from the old ones, $T_{pp'}$, by the transformation (see the derivation of Eq. (5.117))

$$
T'_{qq'} = \sum_{pp'} \mathcal{D}^1_{pq}(\alpha\beta\gamma)\, \mathcal{D}^1_{p'q'}(\alpha\beta\gamma)^*\, T_{pp'} \; ,
$$

where α, β, γ are the Euler angles of the rotation which brings the old reference system into the new one.

We can easily construct the associated irreducible tensors through the standard procedure (see Eq. (5.124)). By so doing, the following irreducible tensors are obtained

$$\mathcal{E}^K_Q(\alpha,\beta,\vec{\Omega}), \quad \mathcal{T}^K_Q(i,\vec{\Omega}), \quad \mathcal{I}^K_Q(\nu,\vec{\Omega}), \quad J^K_Q(\nu)$$

corresponding to

$$\mathcal{E}_{qq'}(\alpha,\beta,\vec{\Omega}), \quad \mathcal{T}_{qq'}(i,\vec{\Omega}), \quad \mathcal{I}_{qq'}(\nu,\vec{\Omega}), \quad J_{qq'}(\nu)\ ,$$

respectively. The relations between the irreducible tensors and the corresponding reducible ones are repeated here for the sake of completeness

$$T^K_Q = \sum_{qq'} (-1)^{1+q} \sqrt{3(2K+1)} \begin{pmatrix} 1 & 1 & K \\ q & -q' & -Q \end{pmatrix} T_{qq'}\ , \tag{5.155}$$

with the inverse transformation

$$T_{qq'} = \sum_{KQ} (-1)^{1+q} \sqrt{\frac{2K+1}{3}} \begin{pmatrix} 1 & 1 & K \\ q & -q' & -Q \end{pmatrix} T^K_Q\ . \tag{5.156}$$

Obviously, the various irreducible tensors are connected with each other by the same relations which connect the corresponding reducible tensors, namely (cf. Eqs. (5.131), (5.150), and (5.153))

$$\begin{aligned}
\mathcal{T}^K_Q(i,\vec{\Omega}) &= \sum_{\alpha\beta=\pm1} \frac{1}{2}\, (\hat{\sigma}_i)_{\alpha\beta}\, \mathcal{E}^K_Q(\beta,\alpha,\vec{\Omega}) \\
\mathcal{I}^K_Q(\nu,\vec{\Omega}) &= \sum_{\alpha\beta=\pm1} \mathcal{E}^K_Q(\alpha,\beta,\vec{\Omega})\, I_{\beta\alpha}(\nu,\vec{\Omega}) = \sum_{i=0}^{3} \mathcal{T}^K_Q(i,\vec{\Omega})\, S_i(\nu,\vec{\Omega}) \\
J^K_Q(\nu) &= \oint \frac{\mathrm{d}\Omega}{4\pi}\, \mathcal{I}^K_Q(\nu,\vec{\Omega}) = \oint \frac{\mathrm{d}\Omega}{4\pi} \sum_{i=0}^{3} \mathcal{T}^K_Q(i,\vec{\Omega})\, S_i(\nu,\vec{\Omega})\ .
\end{aligned} \tag{5.157}$$

Their conjugation properties can be deduced from the corresponding properties of the reducible tensors, and are found to be

$$\begin{aligned}
\mathcal{E}^K_Q(\alpha,\beta,\vec{\Omega})^* &= (-1)^Q\, \mathcal{E}^K_{-Q}(\beta,\alpha,\vec{\Omega}) \\
\mathcal{T}^K_Q(i,\vec{\Omega})^* &= (-1)^Q\, \mathcal{T}^K_{-Q}(i,\vec{\Omega}) \\
\mathcal{I}^K_Q(\nu,\vec{\Omega})^* &= (-1)^Q\, \mathcal{I}^K_{-Q}(\nu,\vec{\Omega}) \\
J^K_Q(\nu)^* &= (-1)^Q\, J^K_{-Q}(\nu)\ .
\end{aligned} \tag{5.158}$$

We rewrite here, for the sake of clarity, the expressions of the tensors $\mathcal{E}^K_Q(\alpha,\beta,\vec{\Omega})$ and $\mathcal{T}^K_Q(i,\vec{\Omega})$ in terms of rotation matrices (see Eqs. (5.126), (5.134), and (5.135))

$$\mathcal{E}^K_Q(\alpha,\beta,\vec{\Omega}) = \sqrt{3(2K+1)} \begin{pmatrix} 1 & 1 & K \\ \alpha & -\beta & -Q' \end{pmatrix} \mathcal{D}^K_{Q'Q}(R) \qquad (\alpha,\beta=\pm1)\ ;$$

$$\mathcal{T}^K_Q(i,\vec{\Omega}) = \sum_P t^K_P(i)\, \mathcal{D}^K_{PQ}(R) \tag{5.159}$$

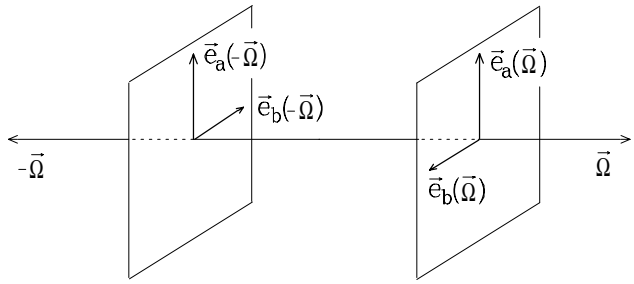

Fig.5.15. Reference direction unit vector ($\vec{e}_a$) and associated unit vector ($\vec{e}_b$) relative to the directions $\vec{\Omega}$ and $-\vec{\Omega}$. $\vec{e}_a(\vec{\Omega})$ is parallel to $\vec{e}_a(-\vec{\Omega})$.

with

$$t^K_P(i) = \sum_{\alpha\beta=\pm1} \frac{1}{2}\,(\hat{\sigma}_i)_{\alpha\beta}\,\sqrt{3(2K+1)} \begin{pmatrix} 1 & 1 & K \\ \beta & -\alpha & -P \end{pmatrix} , \tag{5.160}$$

where R is the rotation bringing the reference system $(\vec{e}_a(\vec{\Omega}), \vec{e}_b(\vec{\Omega}), \vec{\Omega})$ into the system (xyz).

One can easily deduce some remarkable properties of the coefficients $t^K_P(i)$:

a) The only non-zero components of $t^K_P(i)$ are those with $P = 0, \pm 2$, as the indices α and β can only take the values ± 1.

b) From Eq. (5.147) and from the properties of the 3-j symbols it follows the conjugation relation

$$t^K_P(i)^* = t^K_{-P}(i) \,.$$

c) Defining the quantities

$$\begin{aligned} \xi_i &= (1,1,1,-1) \\ \tau_i &= (1,1,-1,1) \\ \zeta_i &= (1,1,-1,-1) = \xi_i\,\tau_i \end{aligned} \tag{5.161}$$

with $i = 0, \ldots, 3$, one gets

$$(\hat{\sigma}_i)_{-\alpha-\beta} = \xi_i\,(\hat{\sigma}_i)_{\beta\alpha} \,, \qquad (\hat{\sigma}_i)_{\alpha\beta} = \tau_i\,(\hat{\sigma}_i)_{\beta\alpha} \,, \qquad (\hat{\sigma}_i)_{-\alpha-\beta} = \zeta_i\,(\hat{\sigma}_i)_{\alpha\beta} \,,$$

and hence

$$\begin{aligned} t^K_P(i) &= \xi_i\,(-1)^K\,t^K_P(i) \\ t^K_P(i) &= \tau_i\,t^K_{-P}(i) \\ t^K_P(i) &= \zeta_i\,(-1)^K\,t^K_{-P}(i) \,. \end{aligned} \tag{5.162}$$

These properties allow a simple derivation of the relation between the tensors $\mathcal{T}^K_Q(i,\vec{\Omega})$ and $\mathcal{T}^K_Q(i,-\vec{\Omega})$, which will be needed in the following.

Let us consider two opposite directions, $\vec{\Omega}$ and $-\vec{\Omega}$, and the corresponding reference direction unit vectors $\vec{e}_a(\vec{\Omega})$, $\vec{e}_a(-\vec{\Omega})$. We assume for simplicity that the directions $\vec{e}_a(\vec{\Omega})$ and $\vec{e}_a(-\vec{\Omega})$ coincide (see Fig. 5.15). From the definition (5.159) we have

TABLE 5.5

Values of the symbol $t_P^K(i)$

i	$K=0$	$K=1$	$K=2$
0	$\delta_{P,0}$	0	$\frac{1}{\sqrt{2}}\,\delta_{P,0}$
1	0	0	$-\frac{\sqrt{3}}{2}\left(\delta_{P,-2}+\delta_{P,2}\right)$
2	0	0	$\mathrm{i}\,\frac{\sqrt{3}}{2}\left(\delta_{P,-2}-\delta_{P,2}\right)$
3	0	$\sqrt{\frac{3}{2}}\,\delta_{P,0}$	0

$$\mathcal{T}_Q^K(i,-\vec{\Omega}) = \sum_P t_P^K(i)\;\mathcal{D}_{PQ}^K(R')\;,$$

where R' is the rotation bringing the system $(\vec{e}_a(-\vec{\Omega}),\vec{e}_b(-\vec{\Omega}),-\vec{\Omega})$ into the system (xyz). The rotation R' can be executed in two steps: first a rotation R_0 which brings the system $(\vec{e}_a(-\vec{\Omega}),\vec{e}_b(-\vec{\Omega}),-\vec{\Omega})$ into the system $(\vec{e}_a(\vec{\Omega}),\vec{e}_b(\vec{\Omega}),\vec{\Omega})$, and then a rotation R which brings this last system into (xyz). Thus from the closure property of the rotation matrices (Eq. (2.74)) we have

$$\mathcal{T}_Q^K(i,-\vec{\Omega}) = \sum_P t_P^K(i)\sum_{Q'}\mathcal{D}_{PQ'}^K(R_0)\;\mathcal{D}_{Q'Q}^K(R)\;.$$

On the other hand, the rotation R_0 is given by

$$R_0 \equiv (\pi,\pi,0)\;,$$

and since (see Eq. (2.70))

$$\mathcal{D}_{PQ'}^K(\pi\,\pi\,0) = \mathrm{e}^{-\mathrm{i}\pi P}\;d_{PQ'}^K(\pi) = \mathrm{e}^{-\mathrm{i}\pi P}\;(-1)^{K+P}\;\delta_{P,-Q'}\;,$$

we obtain

$$\mathcal{T}_Q^K(i,-\vec{\Omega}) = \sum_P t_P^K(i)\,\mathrm{e}^{-\mathrm{i}\pi P}\,(-1)^{K+P}\,\mathcal{D}_{-PQ}^K(R)\;.$$

Using property a) of the coefficients $t_P^K(i)$ (see above) and the last of Eqs. (5.162) we finally get

$$\mathcal{T}_Q^K(i,-\vec{\Omega}) = \zeta_i\,\mathcal{T}_Q^K(i,\vec{\Omega})\;. \tag{5.163}$$

It should be remarked that this relation is valid only when the directions $\vec{e}_a(\vec{\Omega})$ and $\vec{e}_a(-\vec{\Omega})$ coincide.

Let us turn to the evaluation of the irreducible tensor $\mathcal{T}_Q^K(i,\vec{\Omega})$. From Eqs. (5.160), (5.128), and (2.26) we can easily obtain the values of the coefficients $t_P^K(i)$, which are collected in Table 5.5. The explicit expressions for $\mathcal{T}_Q^K(i,\vec{\Omega})$ can then be derived from the definition (5.159) by direct evaluation of the rotation matrices (Eq. (2.68) and Table 2.1). The results are contained in Table 5.6.

TABLE 5.6

Explicit expression for the tensor $\mathcal{T}^K_Q(i,\vec{\Omega})$. The components with negative Q-value can be obtained from the relation $\mathcal{T}^K_{-Q}(i,\vec{\Omega}) = (-1)^Q\,\mathcal{T}^K_Q(i,\vec{\Omega})^*$. The angles χ, θ, γ are shown in Fig.5.14. Note that the rotation carrying the reference system $(\vec{a},\vec{b},\vec{c})$ into (xyz) is $R \equiv (-\gamma,-\theta,-\chi)$.

$$\mathcal{T}^0_0(0,\vec{\Omega}) = 1$$

$$\mathcal{T}^1_0(0,\vec{\Omega}) = 0$$

$$\mathcal{T}^1_1(0,\vec{\Omega}) = 0$$

$$\mathcal{T}^2_0(0,\vec{\Omega}) = \tfrac{1}{2\sqrt{2}}\,(3\cos^2\theta - 1)$$

$$\mathcal{T}^2_1(0,\vec{\Omega}) = -\tfrac{\sqrt{3}}{2}\,\sin\theta\cos\theta\,\mathrm{e}^{\mathrm{i}\chi}$$

$$\mathcal{T}^2_2(0,\vec{\Omega}) = \tfrac{\sqrt{3}}{4}\,\sin^2\theta\,\mathrm{e}^{2\mathrm{i}\chi}$$

$$\mathcal{T}^0_0(1,\vec{\Omega}) = 0$$

$$\mathcal{T}^1_0(1,\vec{\Omega}) = 0$$

$$\mathcal{T}^1_1(1,\vec{\Omega}) = 0$$

$$\mathcal{T}^2_0(1,\vec{\Omega}) = -\tfrac{3}{2\sqrt{2}}\,\cos 2\gamma\,\sin^2\theta$$

$$\mathcal{T}^2_1(1,\vec{\Omega}) = -\tfrac{\sqrt{3}}{2}\,(\cos 2\gamma\,\cos\theta + \mathrm{i}\,\sin 2\gamma)\sin\theta\,\mathrm{e}^{\mathrm{i}\chi}$$

$$\mathcal{T}^2_2(1,\vec{\Omega}) = -\tfrac{\sqrt{3}}{4}\,\left[\cos 2\gamma\,(1+\cos^2\theta) + 2\mathrm{i}\,\sin 2\gamma\,\cos\theta\right]\mathrm{e}^{2\mathrm{i}\chi}$$

$$\mathcal{T}^0_0(2,\vec{\Omega}) = 0$$

$$\mathcal{T}^1_0(2,\vec{\Omega}) = 0$$

$$\mathcal{T}^1_1(2,\vec{\Omega}) = 0$$

$$\mathcal{T}^2_0(2,\vec{\Omega}) = \tfrac{3}{2\sqrt{2}}\,\sin 2\gamma\,\sin^2\theta$$

$$\mathcal{T}^2_1(2,\vec{\Omega}) = \tfrac{\sqrt{3}}{2}\,(\sin 2\gamma\,\cos\theta - \mathrm{i}\,\cos 2\gamma)\sin\theta\,\mathrm{e}^{\mathrm{i}\chi}$$

$$\mathcal{T}^2_2(2,\vec{\Omega}) = \tfrac{\sqrt{3}}{4}\,\left[\sin 2\gamma(1+\cos^2\theta) - 2\mathrm{i}\,\cos 2\gamma\,\cos\theta\right]\mathrm{e}^{2\mathrm{i}\chi}$$

$$\mathcal{T}^0_0(3,\vec{\Omega}) = 0$$

$$\mathcal{T}^1_0(3,\vec{\Omega}) = \sqrt{\tfrac{3}{2}}\,\cos\theta$$

$$\mathcal{T}^1_1(3,\vec{\Omega}) = -\tfrac{\sqrt{3}}{2}\,\sin\theta\,\mathrm{e}^{\mathrm{i}\chi}$$

$$\mathcal{T}^2_0(3,\vec{\Omega}) = 0$$

$$\mathcal{T}^2_1(3,\vec{\Omega}) = 0$$

$$\mathcal{T}^2_2(3,\vec{\Omega}) = 0$$

TABLE 5.7

Explicit expression for the tensor $\mathcal{I}^K_Q(\nu,\vec{\Omega})$. The components with negative Q-value can be obtained from the relation $\mathcal{I}^K_{-Q}(\nu,\vec{\Omega}) = (-1)^Q\, \mathcal{I}^K_Q(\nu,\vec{\Omega})^*$.

$$
\begin{aligned}
\mathcal{I}^0_0(\nu,\vec{\Omega}) &= I(\nu,\vec{\Omega}) \\
\mathcal{I}^1_0(\nu,\vec{\Omega}) &= \sqrt{\tfrac{3}{2}}\,\cos\theta\; V(\nu,\vec{\Omega}) \\
\mathcal{I}^1_1(\nu,\vec{\Omega}) &= -\tfrac{\sqrt{3}}{2}\,\sin\theta\; V(\nu,\vec{\Omega})\;\mathrm{e}^{\mathrm{i}\chi} \\
\mathcal{I}^2_0(\nu,\vec{\Omega}) &= \tfrac{1}{2\sqrt{2}}\Big[(3\cos^2\theta-1)\,I(\nu,\vec{\Omega}) - 3\sin^2\theta\;\tilde{Q}(\nu,\vec{\Omega})\Big] \\
\mathcal{I}^2_1(\nu,\vec{\Omega}) &= -\tfrac{\sqrt{3}}{2}\,\sin\theta\Big[\cos\theta\, I(\nu,\vec{\Omega}) + \cos\theta\;\tilde{Q}(\nu,\vec{\Omega}) + \mathrm{i}\,\tilde{U}(\nu,\vec{\Omega})\Big]\,\mathrm{e}^{\mathrm{i}\chi} \\
\mathcal{I}^2_2(\nu,\vec{\Omega}) &= \tfrac{\sqrt{3}}{4}\Big[\sin^2\theta\, I(\nu,\vec{\Omega}) - (1+\cos^2\theta)\,\tilde{Q}(\nu,\vec{\Omega}) - 2\mathrm{i}\,\cos\theta\;\tilde{U}(\nu,\vec{\Omega})\Big]\,\mathrm{e}^{2\mathrm{i}\chi}
\end{aligned}
$$

where $\quad \tilde{Q}(\nu,\vec{\Omega}) = \cos 2\gamma\; Q(\nu,\vec{\Omega}) - \sin 2\gamma\; U(\nu,\vec{\Omega})$

$\qquad\quad\;\; \tilde{U}(\nu,\vec{\Omega}) = \cos 2\gamma\; U(\nu,\vec{\Omega}) + \sin 2\gamma\; Q(\nu,\vec{\Omega})$

The derivation of the explicit expression for the tensor $\mathcal{I}^K_Q(\nu,\vec{\Omega})$ defined in Eq. (5.157) is straightforward (see Table 5.7). Note that the expressions in Table 5.7 – like those of Table 5.4 – contain only the linear combinations $\tilde{Q}$ and $\tilde{U}$, which are independent of the reference direction chosen to define the Stokes parameters Q and U.

Finally, the irreducible tensor of the radiation field $J^K_Q(\nu)$ is obtained by averaging $\mathcal{I}^K_Q(\nu,\vec{\Omega})$ over the solid angle. In the particular case of an unpolarized radiation field having cylindrical symmetry about the z-axis only two components are not zero, namely

$$
\begin{aligned}
J^0_0(\nu) &= \oint \frac{\mathrm{d}\Omega}{4\pi}\, I(\nu,\theta) \\
J^2_0(\nu) &= \frac{1}{2\sqrt{2}} \oint \frac{\mathrm{d}\Omega}{4\pi}\,(3\cos^2\theta - 1)\, I(\nu,\theta)\;. \qquad (5.164)
\end{aligned}
$$

Obviously, the component $J^2_0(\nu)$ is also zero if the radiation field is isotropic.

5.12. Further Properties of the Scattering Phase Matrix

The expression given in Sect. 5.10 for the scattering phase matrix and the various relations proved in Sect. 5.11 allow a further extension of the remarkable properties of this matrix.

Starting from Eq. (5.133) and using Eq. (5.163) one can directly prove the following relations (which are however valid only when the same reference directions

are chosen for $\vec{\Omega}$ and $-\vec{\Omega}$, and for $\vec{\Omega}'$ and $-\vec{\Omega}'$)

$$R_{ij}(-\vec{\Omega},\vec{\Omega}';\vec{B}\,) = \zeta_i\; R_{ij}(\vec{\Omega},\vec{\Omega}';\vec{B}\,)$$
$$R_{ij}(\vec{\Omega},-\vec{\Omega}';\vec{B}\,) = \zeta_j\; R_{ij}(\vec{\Omega},\vec{\Omega}';\vec{B}\,)$$
$$R_{ij}(-\vec{\Omega},-\vec{\Omega}';\vec{B}\,) = \zeta_i\,\zeta_j\; R_{ij}(\vec{\Omega},\vec{\Omega}';\vec{B}\,)\;.$$

The first relation means that if (I,Q,U,V) is the Stokes vector scattered along the direction $\vec{\Omega}$, then, irrespective of the polarization of the incident beam and of the intensity and direction of the magnetic field, the Stokes vector scattered along the direction $-\vec{\Omega}$ is $(I,Q,-U,-V)$. The two other relations have analogous meanings.

Considering next Eq. (5.136), we can write the expression of the scattering phase matrix for the most general geometry of Fig. 5.9. The two relevant rotations are (see Eq. (5.122))

$$R \equiv (-\gamma,-\theta,-\chi)\times(\chi_B,\theta_B,\gamma_B)$$
$$R' \equiv (-\gamma',-\theta',-\chi')\times(\chi_B,\theta_B,\gamma_B)$$

where γ_B is an arbitrary angle, and hence from Eq. (2.74) we obtain

$$R_{ij}(\vec{\Omega},\vec{\Omega}';\vec{B}\,) =$$
$$= \sum_{KPP'} t_P^K(i)\; t_{P'}^K(j)^* \sum_{QQ'} \mathcal{D}_{PQ}^K(-\gamma\;\;-\theta\;\;-\chi)\;\mathcal{M}_{QQ'}^K(\vec{B}\,)\;\mathcal{D}_{Q'P'}^K(\chi'\;\theta'\;\gamma')\;, \quad (5.165)$$

where we have introduced the *magnetic kernel* defined by

$$\mathcal{M}_{QQ'}^K(\vec{B}\,) = \sum_{Q''} \mathcal{D}_{QQ''}^K(\chi_B\;\theta_B\;\gamma_B)\;\mathcal{D}_{Q''Q'}^K(-\gamma_B\;\;-\theta_B\;\;-\chi_B)\,\frac{1}{1+\mathrm{i}\,Q''H}\;. \quad (5.166)$$

In terms of reduced rotation matrices (Eq. (2.68)) we have

$$\mathcal{M}_{QQ'}^K(\vec{B}\,) = \mathrm{e}^{\,\mathrm{i}(Q'-Q)\chi_B} \sum_{Q''} d_{QQ''}^K(\theta_B)\; d_{Q''Q'}^K(-\theta_B)\,\frac{1}{1+\mathrm{i}\,Q''H}\;, \quad (5.167)$$

which shows explicitly that the magnetic kernel is independent of the angle γ_B, that can be set equal to zero.

The magnetic kernel satisfies several important properties which can be easily derived from Eqs. (5.166) and (5.167) using some properties of the rotation matrices:

i) *Limiting case of zero magnetic field*

Recalling Eqs. (5.84) and (2.74) we have

$$\lim_{B\to 0} \mathcal{M}_{QQ'}^K(\vec{B}\,) = \sum_{Q''} \mathcal{D}_{QQ''}^K(\chi_B\;\theta_B\;0)\;\mathcal{D}_{Q''Q'}^K(0\;\;-\theta_B\;\;-\chi_B)$$
$$= \mathcal{D}_{QQ'}^K(0\,0\,0) = \delta_{QQ'}\;,$$

and hence

$$R_{ij}(\vec{\Omega},\vec{\Omega}';0) = \sum_{KPP'} t_P^K(i)\; t_{P'}^K(j)^*\; \mathcal{D}_{PP'}^K(R)\;, \tag{5.168}$$

where R is the rotation bringing the reference system $(\vec{e}_a(\vec{\Omega}),\vec{e}_b(\vec{\Omega}),\vec{\Omega})$ into the system $(\vec{e}\,'_a(\vec{\Omega}'),\vec{e}\,'_b(\vec{\Omega}'),\vec{\Omega}')$.

ii) *Limiting case of strong field*

$$\lim_{B\to\infty} \mathcal{M}_{QQ'}^K(\vec{B}\,) = \mathcal{D}_{Q0}^K(\chi_B\;\theta_B\;0)\;\mathcal{D}_{0Q'}^K(0\;\;-\theta_B\;\;-\chi_B)\;.$$

iii) *Conjugation property*

$$\mathcal{M}_{QQ'}^K(\vec{B}\,)^* = (-1)^{Q-Q'}\;\mathcal{M}_{-Q-Q'}^K(\vec{B}\,)\;.$$

iv) *Magnetic field symmetries*

$$\begin{aligned}
&\mathcal{M}_{QQ'}^K(B,\pi-\theta_B,-\chi_B) = \mathcal{M}_{-Q-Q'}^K(B,\theta_B,\chi_B)\\
&\mathcal{M}_{QQ'}^K(B,\pi-\theta_B,\pi-\chi_B) = (-1)^{Q-Q'}\;\mathcal{M}_{-Q-Q'}^K(B,\theta_B,\chi_B)\\
&\mathcal{M}_{QQ'}^K(B,\theta_B,\pi+\chi_B) = (-1)^{Q-Q'}\;\mathcal{M}_{QQ'}^K(B,\theta_B,\chi_B)\;,
\end{aligned}$$

a set of formulae giving the transformation of the magnetic kernel under a 180° rotation of the magnetic field vector about the axes x, y, and z of Fig. 5.9, respectively.

v) *Magnetic field reversal*

$$\begin{aligned}
&\mathcal{M}_{QQ'}^K(-\vec{B}\,) =\\
&= \sum_{Q''} \mathcal{D}_{QQ''}^K(\pi+\chi_B\;\pi-\theta_B\;0)\;\mathcal{D}_{Q''Q'}^K(0\;\;-\pi+\theta_B\;\;-\pi-\chi_B)\,\frac{1}{1+\mathrm{i}\,Q''H}\\
&= \sum_{Q''} \mathcal{D}_{QQ''}^K(\chi_B\;\theta_B\;0)\;\mathcal{D}_{Q''Q'}^K(0\;\;-\theta_B\;\;-\chi_B)\,\frac{1}{1-\mathrm{i}\,Q''H}\;,
\end{aligned} \tag{5.169}$$

which shows that the reversal of the magnetic field can also be obtained by the formal substitution $H \to -H$.

vi) *Average over an isotropic distribution of magnetic fields*

For an isotropic distribution of magnetic field vectors we can find the average value of the magnetic kernel. Defining

$$\langle \mathcal{M}_{QQ'}^K(\vec{B}\,)\rangle = \frac{1}{4\pi}\int_0^{2\pi}\mathrm{d}\chi_B \int_0^{\pi}\sin\theta_B\;\mathcal{M}_{QQ'}^K(\vec{B}\,)\,\mathrm{d}\theta_B \tag{5.170}$$

we easily obtain, with the help of Eqs. (2.71) and (2.76)

$$\left\langle \mathcal{M}^K_{QQ'}(\vec{B}\,)\right\rangle = \mu_K\ \delta_{QQ'}\ , \tag{5.171}$$

where the quantities μ_K are given by

$$\mu_K = \frac{1}{2K+1}\sum_{Q''}\frac{1}{1+\mathrm{i}\,Q''H} \tag{5.172}$$

or, explicitly

$$\begin{aligned}
&\mu_0 = 1\\
&\mu_1 = \frac{1}{3}\left(1+2\cos^2\alpha_1\right) = \frac{1}{3}\left[1+\frac{2}{1+H^2}\right]\\
&\mu_2 = \frac{1}{5}\left(1+2\cos^2\alpha_1+2\cos^2\alpha_2\right) = \frac{1}{5}\left[1+\frac{2}{1+H^2}+\frac{2}{1+4H^2}\right],
\end{aligned} \tag{5.173}$$

the angles α_1 and α_2 being defined in Eq. (5.98).

This result shows that the average of the scattering phase matrix in an isotropically distributed magnetic field can be obtained directly from the scattering phase matrix of the non-magnetic case by multiplication of the various multipole components by the quantities μ_K,

$$\left\langle R_{ij}(\vec{\Omega},\vec{\Omega}';\vec{B}\,)\right\rangle = \sum_K \mu_K\, R^{(K)}_{ij}(\vec{\Omega},\vec{\Omega}';0)\ . \tag{5.174}$$

In particular, in the limiting case of strong magnetic fields the matrix $\boldsymbol{R}^{(1)}$ is reduced by a factor 3, while the matrix $\boldsymbol{R}^{(2)}$ is reduced by a factor 5.

5.13. Understanding Scattering Experiments through Oscillator Models

In the previous sections we have derived the expression for the scattering phase matrix in the presence of a magnetic field both in terms of direction cosines and in terms of rotation matrices. However, these derivations are rather involved and there is a danger that the physical meaning of the various results may be hidden by the mathematical formalism. Thus we think it is worthwhile to present some qualitative arguments – based on the atomic oscillator model – aimed at clarifying the underlying physics. At the same time we will draw some interesting analogies between the classical and quantum-mechanical descriptions of scattering phenomena.

Let us consider a simple scattering event like that illustrated in Fig. 5.16a, left. The incident radiation beam is unpolarized (conventionally, this is represented by

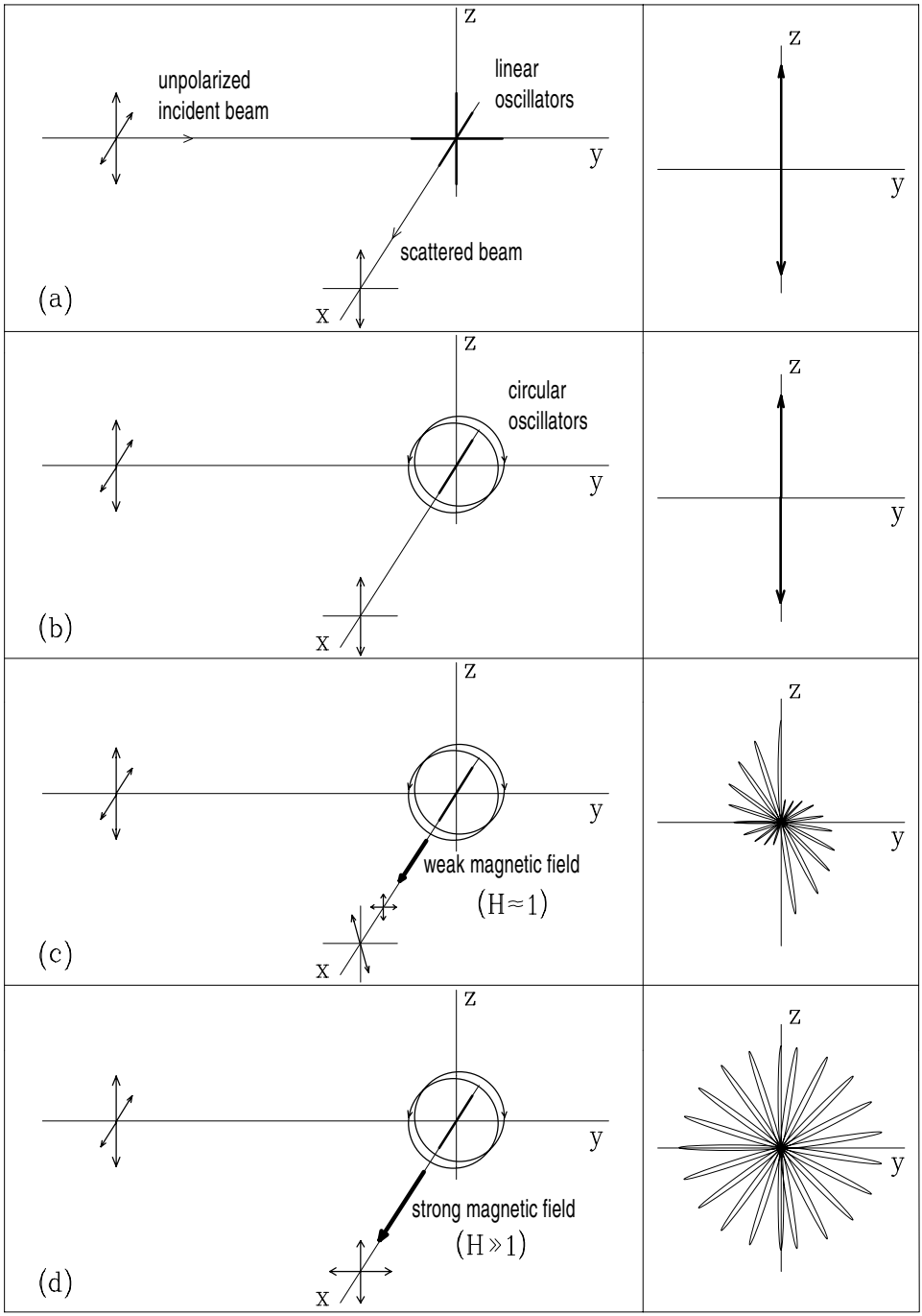

Fig.5.16. Qualitative description of a 90° scattering event in the absence of magnetic fields and in the presence of a magnetic field parallel to the line of sight. See text for explanation.

two double-ended, perpendicular arrows which should be regarded as incoherent electric field oscillations), and there is no magnetic field. We schematize the scattering atom as a collection of three linear oscillators of frequency ν_0 that will be called the x, y, and z-oscillator, respectively. The scattering experiment can be described in the following way.

i) The electric field of the incident radiation can be decomposed into its x and z components; owing to the unpolarized character of the radiation, the two components are incoherent, or, in other words, there are no phase relations between them.

ii) The x component of the electric field excites the x-oscillator, while the z component excites the z-oscillator (the latter is represented by a double-ended arrow in the right part of the figure). The incoherent character of the electric field is simply transferred to the oscillators.

iii) The oscillators decay with a damped motion and each of them emits, in any given direction, a radiation beam polarized according to the well-known laws of classical electrodynamics (see Eq. (3.29)). If we consider the beam scattered in the x direction, it is easily seen that the x-oscillator is ineffective (being pole-on), while the z-oscillator produces a radiation beam that is linearly polarized along the z direction. As a consequence, the radiation scattered in the x direction is 100% linearly polarized perpendicularly to the scattering plane, which is consistent with the results derived in Sect. 5.9 (see Eq. (5.103)).

To investigate the effect of the magnetic field it is convenient to describe the model atom by a different set of oscillators, namely the linear x-oscillator plus two circular oscillators with opposite directions (called σ_+ and σ_-) laying in the y-z plane as shown in Fig. 5.16b, left. If the magnetic field is zero, the frequency of the three oscillators is still ν_0, and we must find the same results as above.

Following the same line of reasoning, we see at step ii) that while the x component of the electric field still excites the x-oscillator, the z component excites the σ_+ and σ_- oscillators in such a way as to produce a *well-defined phase relation between them*, because the resulting motion of the electric charge takes place along the z direction (Fig. 5.16b, right). For the scattered radiation we obviously have the same result as before, but we must bear in mind that this new description of the atomic system has forced us to introduce the concept of phase relation (or coherence) between the two circular oscillators.

In the presence of a magnetic field directed along the x-axis (see Fig. 5.16c) the circular oscillators vibrate at different frequencies ($(\nu_0 + \nu_\mathrm{L})$ and $(\nu_0 - \nu_\mathrm{L})$, respectively, with ν_L the Larmor frequency). Thus the phase relation produced by the exciting electric field is lost little by little during the damped decay process. The electric charge describes in the y-z plane a complicated pattern (sometimes called a 'rosette' – Fig. 5.16c, right), and thus the polarization of the scattered radiation – which reflects the weighted average of the pattern – is decreased and rotated from the direction of the non-magnetic regime: in Fig. 5.16c (left) the scattered beam is the superposition of a linearly polarized beam plus an unpolarized beam. The shape of the rosette is controlled by the parameter $H = 2\pi\nu_\mathrm{L}/\gamma$ defined in Eq. (5.84). When the value of H is very large ($H \gg 1$) the rosette degenerates

into a different curve (that we will rather call a 'daisy', see Fig. 5.16d right) and the scattered radiation is totally unpolarized.

This simple example shows that the effect of the magnetic field is to cause a relaxation of the phase relations (or coherences) between the different oscillators: the coherence between the σ_+ and σ_- oscillators is maximum for zero magnetic field (Fig. 5.16b) and gradually decreases with increasing field strength (Fig. 5.16c,d). The Hanle effect is just the consequence of this relaxation process in resonance scattering.

Different geometrical configurations can be envisaged to get a deeper insight into the phenomena of resonance polarization and the Hanle effect. Figure 5.17 presents an example of forward scattering; here the scattered beam is unpolarized for zero magnetic field and partially linearly polarized along the field's direction when the magnetic field is present. The discussion of this case, that can be carried out along the same lines as before, is left to the reader as an exercise (cf. Eqs. (5.106)).

The classical model that represents the atom as a collection of one linear oscillator and two circular oscillators of opposite directions has a simple quantum analogue. This is the two-level atom having a lower level of angular momentum $J = 0$ and an upper level of angular momentum $J' = 1$. The excitation of one of the classical oscillators induced by the electric field of the incident beam has its quantum equivalent in the excitation of one of the Zeeman sublevels of the upper level. In this analogy, the linear oscillator corresponds to the sublevel $M' = 0$, while the circular oscillators of frequency $(\nu_0 \pm \nu_{\rm L})$ correspond to the sublevels $M' = \pm 1$, respectively.

In scattering experiments, apart from special geometrical configurations, the various oscillators are excited unevenly by the electric field of the incident beam, and well-defined phase relations arise between different oscillators. This means – in the language of Quantum Mechanics – that the upper level of the atom is polarized (see Sect. 3.6); in other words, the diagonal density-matrix elements $\rho_{J'}(M', M')$ are different from each other and the off-diagonal elements $\rho_{J'}(M', M'')$ are non-zero. In particular, the amount of excitation present in a given oscillator has its quantum analogue in the corresponding diagonal element of the density matrix, while the combined excitation of two different oscillators with a well-defined phase relation has its analogue in the off-diagonal element of the density matrix between the two corresponding sublevels. For example, in the case of panel (b) of Fig. 5.16, the non-zero density-matrix elements are $\rho\,(0,0)$, $\rho\,(1,1)$, $\rho\,(-1,-1)$, $\rho\,(1,-1)$, and $\rho\,(-1,1)$, the last two elements being related to the coherence between the circular oscillators. Passing to panels (c) and (d) of the same Figure, the diagonal elements remain unchanged, while the off-diagonal ones are reduced by the presence of the magnetic field. In the following of this book we will see that these qualitative concepts are fully confirmed by a more rigorous treatment based on Quantum Mechanics.

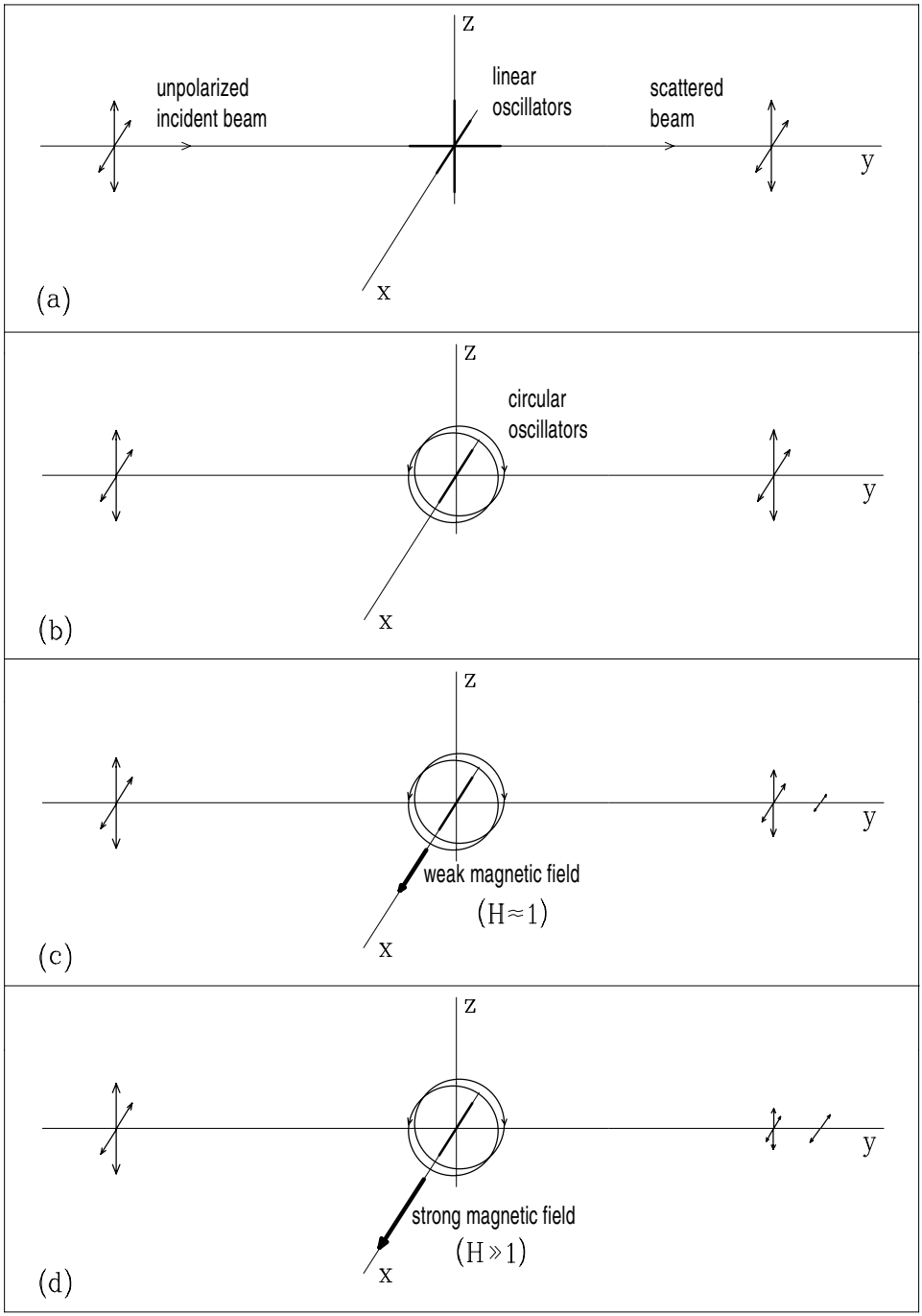

Fig.5.17. Same as Fig.5.16 for a forward scattering event. The trajectories of the oscillating electron in the y-z plane are the same as in Fig.5.16 right.

5.14. The Role of Collisions

We present in this section a simple theory to describe the effect of collisions on polarization phenomena. Both the atom and the colliding particles will be described in terms of classical physics; in particular, the atom will be schematized as a three-dimensional oscillator, like in the previous sections of this chapter.

Our first assumption is that the interactions with the closest perturbing particle (binary interactions) play the principal role. In other words, we assume that triple and multi-particle interactions can be neglected, which implies a limitation on the density n of perturbing particles in the medium,

$$\sigma^{\frac{3}{2}}\, n \ll 1$$

where σ is the typical collisional cross-section. This inequality is always well-satisfied both in laboratory plasmas and in stellar atmospheres.

Next we distinguish between two different kinds of collisions, *exciting* collisions and *perturbing* collisions, defined according to the following simple model.

a) Exciting collisions are inelastic, which implies an energy transfer from the colliding particle to the atom. When an exciting collision takes place, the oscillator is abruptly forced to interrupt its previous motion, described by Eq. (3.23), and starts oscillating again with a new set of initial conditions. These initial conditions depend on the efficiency of the collision (which sets the amplitude of the oscillation), and on the geometry of the impact event (which sets the polarization characteristics of the oscillation). The geometry of the event is specified by the direction of the colliding particle, the direction of the vector joining the center of the oscillator with the center of the colliding particle at the moment of closest approach, and on the orientation of the colliding particle if this is not spherically symmetrical.

If the colliding particles have an isotropic distribution of velocities, and – in the case of oriented particles – if they have random orientations, the initial conditions set up in the oscillator will be isotropic as well. Employing the same notations as in Sect. 3.2, the initial values of the amplitudes of the oscillations will be given by

$$\left\langle A^*_\alpha A_\beta \right\rangle = \delta_{\alpha\beta}\, \overline{|A|^2}\,, \tag{5.175}$$

where the symbol $\langle \ldots \rangle$ means a statistical average over all the possible collisions. This is just the physical situation described in Sect. 3.2. We remind the reader that exciting collisions, as defined here, have their quantum counterpart in collisions able to induce transitions between atomic levels.

In different cases, like for instance when the atom is bombarded by a collimated and/or oriented beam of particles, Eq. (5.175) does not hold and, as a result, the atom emits polarized radiation in the decay process. This phenomenon is known under the name of *impact polarization*, a subject that will not be deepened here.

b) Perturbing collisions, on the contrary, are elastic collisions which are not able to interrupt the oscillatory motion of the atom and to make it restart from scratch,

but are effective in *shifting the phase of the oscillation* during a time interval t_c that is called the *collision time*.

Following a model that was proposed by Lorentz (1915) and refined by Weisskopf (1932) and Lenz (1933), we suppose that the collision time t_c is much smaller than the other typical times involved in the physical process, namely the decay time of the oscillator $1/\gamma$ and the mean time between collisions $1/f$, where f is the frequency of perturbing collisions[1]

$$t_c \ll \frac{1}{\gamma} , \qquad t_c \ll \frac{1}{f} . \tag{5.176}$$

This hypothesis allows to treat the collisions as instantaneous (*impact approximation*). We further assume that each perturbing collision produces a large phase shift in the atomic oscillation, so that the oscillations before and after the collision are totally uncorrelated (*strong collision hypothesis*). These two assumptions are at the basis of the usual treatment of collisional broadening in spectral lines (see e.g. Sobel'man, 1972) and can also be used to derive the effect of collisions on polarization phenomena.

To this aim, however, the second assumption must be suitably specified to describe with greater accuracy the geometrical details of the collisional event. We suppose that each collision, characterized by its own geometry, induces an independent phase shift in each of the three components of the oscillatory motion along a triplet of real, orthogonal unit vectors whose orientation is fixed by the direction of the velocity of the colliding particle (and by its orientation, in case of an oriented particle). These unit vectors will be denoted in the following by the symbol $\vec{t}_i$ $(i = 1, 2, 3)$, and the corresponding phase shifts by ϕ_i. Now we are going to derive the consequences of this simplified model on the results obtained in the previous sections of this chapter.

i) *Radiative Transfer Equations.*
In the derivation of the radiative transfer equations for polarized radiation in the presence of a magnetic field (Sect. 5.3) we found in Eqs. (5.29) and (5.30) the relation between the amplitude of the oscillation and the corresponding component of the forcing electric field. This relation is based on a particular solution of the non-homogeneous equation (5.28) which disregards the transient solution depending on the initial conditions. In the presence of collisions the transient solution is important, and we take it into account in the following way.

[1] Obviously the frequency f can be written in the form

$$f = N_p \, \bar{v}_r \, \sigma ,$$

where N_p is the number density of perturbers, $\bar{v}_r$ is the average velocity of the perturbers relative to atoms, and σ is the cross-section. Expressing N_p in cm^{-3}, $\bar{v}_r$ in $\mathrm{km\ s}^{-1}$, and σ in units of a_0^2 (a_0 being the Bohr radius), we have

$$f = 2.80 \times 10^{-12} \, N_p \, \bar{v}_r \, \sigma \quad \mathrm{s}^{-1} .$$

Let $t = 0$ indicate the time at which the first collision takes place and suppose the previous collision was sufficiently far in time for its transient to be already damped (statistically, there will always be such a collision and nothing prevents us from calling it the 'first' collision). Employing the same notations as in Sect. 5.3, and making the same approximation $(\nu_0^2 - \nu^2) \approx 2\nu\,(\nu_0 - \nu)$, we can write

$$\vec{x}\,(t = 0_{-}) = -\frac{e_0}{8\pi^2 m\nu} \sum_{\alpha} \frac{1}{(\nu_0 - \alpha\nu_{\mathrm{L}} - \nu) - \mathrm{i}\Gamma}\; E_\alpha\, \vec{u}_\alpha\;. \tag{5.177}$$

Expansion on the unit vectors $\vec{t}_i$ gives

$$\vec{x}\,(t = 0_{-}) = -\frac{e_0}{8\pi^2 m\nu} \sum_{\alpha i} \frac{1}{(\nu_0 - \alpha\nu_{\mathrm{L}} - \nu) - \mathrm{i}\Gamma}\; E_\alpha\, D_{\alpha i}\, \vec{t}_i\;,$$

where the direction cosines $D_{\alpha i}$ are defined by[1]

$$D_{\alpha i} = \vec{u}_\alpha \cdot \vec{t}_i^{\,*}\;. \tag{5.178}$$

According to the above assumptions, the effect of the collision is such that

$$\vec{x}\,(t = 0_{+}) = -\frac{e_0}{8\pi^2 m\nu} \sum_{\alpha i} \frac{1}{(\nu_0 - \alpha\nu_{\mathrm{L}} - \nu) - \mathrm{i}\Gamma}\; E_\alpha\, D_{\alpha i}\; \mathrm{e}^{\,\mathrm{i}\phi_i}\; \vec{t}_i\;,$$

and returning to the basis $\vec{u}_\alpha$

$$\vec{x}\,(t = 0_{+}) = -\frac{e_0}{8\pi^2 m\nu} \sum_{\alpha\beta} \frac{1}{(\nu_0 - \alpha\nu_{\mathrm{L}} - \nu) - \mathrm{i}\Gamma}\, E_\alpha \Big[\sum_i D_{\alpha i}\; \mathrm{e}^{\,\mathrm{i}\phi_i}\; D^*_{\beta i}\Big]\, \vec{u}_\beta\,. \tag{5.179}$$

To obtain the motion of the electron after the collision we must solve Eq. (5.28). Its general solution is the following

$$\begin{aligned}\vec{x}\,(t) = &-\frac{e_0}{8\pi^2 m\nu} \sum_{\beta} \frac{1}{(\nu_0 - \beta\nu_{\mathrm{L}} - \nu) - \mathrm{i}\Gamma}\; E_\beta\; \mathrm{e}^{\,-2\pi\mathrm{i}\nu t}\; \vec{u}_\beta \\ &+ \sum_{\beta} C_\beta\; \mathrm{e}^{\,-2\pi\mathrm{i}\,(\nu_0 - \beta\nu_{\mathrm{L}})\,t}\; \mathrm{e}^{\,-\frac{\gamma}{2}t}\; \vec{u}_\beta\;,\end{aligned}$$

where the constants C_β must be determined in such a way as to satisfy the boundary condition (5.179). Hence we obtain

$$\begin{aligned}C_\beta = -\frac{e_0}{8\pi^2 m\nu} \Bigg\{ &\sum_{\alpha} \frac{E_\alpha}{(\nu_0 - \alpha\nu_{\mathrm{L}} - \nu) - \mathrm{i}\Gamma} \Big[\sum_i D_{\alpha i}\; \mathrm{e}^{\,\mathrm{i}\phi_i}\; D^*_{\beta i}\Big] \\ &- \frac{E_\beta}{(\nu_0 - \beta\nu_{\mathrm{L}} - \nu) - \mathrm{i}\Gamma} \Bigg\}\;.\end{aligned}$$

[1] The quantity $D_{\alpha i}$ could also be written as $\vec{u}_\alpha \cdot \vec{t}_i$ as we have supposed the unit vectors $\vec{t}_i$ to be real. However, we adopt the definition (5.178) to make easier a possible generalization of our hypotheses on the effects of collisions.

Now we perform a statistical average over collisions. Since the phases ϕ_i are arbitrary large numbers (strong collision hypothesis), we have

$$\left\langle \mathrm{e}^{\mathrm{i}\phi_i} \right\rangle = 0 \qquad (i = 1, 2, 3) \, .$$

The first term in curly brackets vanishes and we obtain

$$\vec{x}\,(t) = -\frac{e_0}{8\pi^2 m\nu} \sum_\beta \Big[1 - \mathrm{e}^{-2\pi\mathrm{i}\,(\nu_0 - \beta\nu_\mathrm{L} - \nu)\,t} \; \mathrm{e}^{-\frac{\gamma}{2}t} \Big] \frac{E_\beta \; \mathrm{e}^{-2\pi\mathrm{i}\nu t}}{(\nu_0 - \beta\nu_\mathrm{L} - \nu) - \mathrm{i}\Gamma} \; \vec{u}_\beta \, ,$$

so that (cf. Eq. (5.30))

$$\chi_\beta(t) = -\frac{e_0}{8\pi^2 m\nu} \, \frac{1 - \mathrm{e}^{-2\pi\mathrm{i}\,(\nu_0 - \beta\nu_\mathrm{L} - \nu)\,t} \; \mathrm{e}^{-\frac{\gamma}{2}t}}{(\nu_0 - \beta\nu_\mathrm{L} - \nu) - \mathrm{i}\Gamma}$$

or, in other words, an electric susceptibility variable with time. The average value of the electric susceptibility can then be obtained by multiplying its value at time t by the probability that no collision occurred in the interval $(0, t)$. If f is the frequency of collisions, we have[1]

$$\left\langle \chi_\beta(t) \right\rangle = f \int_0^\infty \mathrm{e}^{-ft} \, \chi_\beta(t) \, \mathrm{d}t = -\frac{e_0}{8\pi^2 m\nu} \, \frac{1}{(\nu_0 - \beta\nu_\mathrm{L} - \nu) - \mathrm{i}\Gamma'} \, ,$$

where

$$\Gamma' = \Gamma + 2\Gamma_\mathrm{c} = \frac{\gamma}{4\pi} + \frac{f}{2\pi} \, , \tag{5.180}$$

with[2]

$$\Gamma_\mathrm{c} = \frac{f}{4\pi} \, . \tag{5.181}$$

Comparison with Eq. (5.30) shows that the effect of perturbing collisions consists in a broadening of both the absorption profile and the associated dispersion profile. The same result could be formally obtained by the addition of a supplementary friction force in the equation of motion of the oscillator.

---

[1] The probability that a collision occurs in the interval $(t, t + \mathrm{d}t)$ is given by

$$\mathrm{d}p = f \, \mathrm{d}t \, .$$

Dividing the interval $(0, t)$ into a large number N of equal parts, the probability that the *first* collision occurs in the interval $(t, t + \mathrm{d}t)$ is given by (see Eq. (2.62) for a similar derivation)

$$\mathrm{d}P = \lim_{N\to\infty} \Big(1 - f \, \frac{t}{N}\Big)^N f \, \mathrm{d}t = f \, \mathrm{e}^{-ft} \, \mathrm{d}t \, .$$

[2] The definition $\Gamma_\mathrm{c} = f/4\pi$ (instead of $f/2\pi$) leads to simpler forms for the expressions that will be encountered in the following.

ii) *Zeeman Effect, Resonance Polarization and Hanle Effect.*
By a similar reasoning we can find the effect of perturbing collisions on the polarization of the radiation emitted by an atom in a decay process.

We suppose that our model oscillator is excited at time $t = t_0 = 0$ either by an exciting collision or by the radiation field, and we suppose that the first collision takes place at time t_1, the second at time t_2, and so on. In the interval (t_0, t_1) the motion of the oscillator is described by Eq. (3.23), which has the solution

$$x_\alpha(t) = A_\alpha \, \mathrm{e}^{-2\pi \mathrm{i}\,(\nu_0 - \alpha\nu_{\mathrm{L}})\,t} \; \mathrm{e}^{-\frac{\gamma}{2}t} \qquad (0 = t_0 < t < t_1) \,, \tag{5.182}$$

where A_α are the initial amplitudes set up by the exciting mechanism. At time t_1 the oscillator undergoes the first collision, which is characterized by its particular geometry (specified by the three unit vectors $\vec{t}_i^{\,(1)}$ and by the corresponding phase shifts $\phi_i^{(1)}$). Along the same lines leading from Eq. (5.177) to Eq. (5.179) one can write for the time interval (t_1, t_2)

$$x_\alpha(t) = \sum_\delta A_\delta \, K_{\delta\alpha}^{(1)} \, \mathrm{e}^{-2\pi \mathrm{i}\,(\nu_0 - \alpha\nu_{\mathrm{L}})\,t} \; \mathrm{e}^{-\frac{\gamma}{2}t} \qquad (t_1 < t < t_2) \,,$$

where $K_{\delta\alpha}^{(1)}$, the collisional kernel due to the first collision, is given by

$$K_{\delta\alpha}^{(1)} = \mathrm{e}^{-2\pi \mathrm{i}\,(\alpha - \delta)\,\nu_{\mathrm{L}} t_1} \left[\sum_{i=1}^{3} D_{\delta i}^{(1)} \, \mathrm{e}^{\mathrm{i}\phi_i^{(1)}} \, D_{\alpha i}^{(1)\,*} \right] , \tag{5.183}$$

with the direction cosines $D_{\delta i}^{(1)}$ defined as in Eq. (5.178). Similarly, for the time interval (t_n, t_{n+1}) one has

$$x_\alpha(t) = \sum_{\delta\epsilon\varphi\ldots\rho} A_\delta \, K_{\delta\epsilon}^{(1)} \, K_{\epsilon\varphi}^{(2)} \ldots K_{\rho\alpha}^{(n)} \, \mathrm{e}^{-2\pi \mathrm{i}\,(\nu_0 - \alpha\nu_{\mathrm{L}})\,t} \; \mathrm{e}^{-\frac{\gamma}{2}t} \qquad (t_n < t < t_{n+1}) \,.$$

To shorten notations we define the cumulative collisional kernel due to the first n collisions as

$$\mathcal{K}_{\delta\alpha}^{(n)} = \sum_{\epsilon\varphi\ldots\rho} K_{\delta\epsilon}^{(0)} \, K_{\epsilon\varphi}^{(1)} \ldots K_{\rho\alpha}^{(n)} \tag{5.184}$$

with

$$\mathcal{K}_{\alpha\beta}^{(0)} = K_{\alpha\beta}^{(0)} = \delta_{\alpha\beta} \,, \tag{5.185}$$

and we can write

$$x_\alpha(t) = \sum_\delta A_\delta \, \mathcal{K}_{\delta\alpha}^{(n)} \, \mathrm{e}^{-2\pi \mathrm{i}\,(\nu_0 - \alpha\nu_{\mathrm{L}})\,t} \; \mathrm{e}^{-\frac{\gamma}{2}t} \qquad (t_n < t < t_{n+1}) \,,$$

a general formula which includes Eq. (5.182).

The function $x_\alpha(t)$ can be expanded in Fourier series,

$$x_\alpha(t) = \int_{-\infty}^{\infty} \mathcal{F}_\alpha(\nu)\ \mathrm{e}^{-2\pi \mathrm{i}\nu t}\ \mathrm{d}\nu\ ,$$

where[1]

$$\mathcal{F}_\alpha(\nu) = \int_0^\infty x_\alpha(t)\ \mathrm{e}^{2\pi\mathrm{i}\nu t}\ \mathrm{d}t = \sum_{n=0}^{\infty} \sum_\delta A_\delta\, \mathcal{K}_{\delta\alpha}^{(n)} \int_{t_n}^{t_{n+1}} \mathrm{e}^{-\left[2\pi\mathrm{i}\,(\nu_0 - \alpha\nu_\mathrm{L} - \nu) + \frac{\gamma}{2}\right]t}\ \mathrm{d}t$$

$$= \sum_{n=0}^{\infty} \sum_\delta A_\delta\, \mathcal{K}_{\delta\alpha}^{(n)}\ \frac{\mathrm{e}^{-N_\alpha t_n} - \mathrm{e}^{-N_\alpha t_{n+1}}}{N_\alpha}\ , \tag{5.186}$$

with

$$N_\alpha = 2\pi\mathrm{i}\,(\nu_0 - \alpha\nu_\mathrm{L} - \nu) + \frac{\gamma}{2} = 2\pi\mathrm{i}\left[(\nu_0 - \alpha\nu_\mathrm{L} - \nu) - \mathrm{i}\Gamma\right]\ . \tag{5.187}$$

To investigate how the Zeeman effect and resonance polarization are affected by perturbing collisions we must start from Eqs. (3.34) and (5.75), respectively. Owing to the different definition of the Fourier transforms $\mathcal{F}_\alpha(\nu)$ and $F_\alpha(\nu)$, these two equations must be rewritten in the form

$$J_{ij}(r) = \frac{16\pi^4 e_0^2}{r^2 c^4} \sum_{\alpha\beta} C_{\alpha i}^*\, C_{\beta j}\, \frac{1}{\tau} \int_{-\infty}^{\infty} \nu^4\, \mathcal{F}_\alpha(\nu)^*\, \mathcal{F}_\beta(\nu)\ \mathrm{d}\nu \tag{5.188}$$

and

$$\mathrm{d}\tilde{I}_{ij}(\vec{\Omega}) = \frac{2\pi^3 e_0^2}{c^3}\ \mathrm{d}\Omega \sum_{\alpha\beta} C_{\alpha i}^*\, C_{\beta j}\, \frac{1}{\tau} \int_{-\infty}^{\infty} \nu^4\, \mathcal{F}_\alpha(\nu)^*\, \mathcal{F}_\beta(\nu)\ \mathrm{d}\nu\ , \tag{5.189}$$

respectively.

From Eq. (5.186) we have

$$\mathcal{F}_\alpha(\nu)^*\, \mathcal{F}_\beta(\nu) =$$

$$= \sum_{n=0}^{\infty} \sum_{n'=0}^{\infty} \sum_{\delta\epsilon} A_\delta^* A_\epsilon\, \mathcal{K}_{\delta\alpha}^{(n)\,*}\, \mathcal{K}_{\epsilon\beta}^{(n')}$$

$$\times\ \frac{\left[\mathrm{e}^{-N_\alpha^* t_n} - \mathrm{e}^{-N_\alpha^* t_{n+1}}\right]\left[\mathrm{e}^{-N_\beta t_{n'}} - \mathrm{e}^{-N_\beta t_{n'+1}}\right]}{N_\alpha^*\, N_\beta}\ . \tag{5.190}$$

[1] The Fourier transform $\mathcal{F}_\alpha(\nu)$ differs from $F_\alpha(\nu)$ defined in Eq. (3.32) for the presence of the amplitudes A_δ. In the special case of no collisions ($\phi_i^{(n)} = 0$, $\mathcal{K}_{\alpha\beta}^{(n)} = \delta_{\alpha\beta}$) we have

$$\mathcal{F}_\alpha(\nu) = A_\alpha\, F_\alpha(\nu)\ .$$

This expression refers to a particular sequence of collisional events. Now we must average over all the possible collision directions and over all the possible collision times $t_1, t_2, \ldots\ t_n, \ldots$

First of all, we observe that the phase shifts $\phi_i^{(n)}$ relative to the n-th collision are totally uncorrelated with the phase shifts $\phi_j^{(n')}$ relative to the n'-th collision. This reduces the double sum in Eq. (5.190) to a single sum ($n' = n$). Then we consider the average of the collisional kernels over an isotropic velocity distribution of perturbing particles. These statistical averages are performed in some detail in the following section. Borrowing from there Eq. (5.200), we have

$$\begin{aligned}
&\mathcal{F}_\alpha(\nu)^*\,\mathcal{F}_\beta(\nu) = \\
&= \sum_{n=0}^{\infty}\sum_{\delta\epsilon} A_\delta^* A_\epsilon\,(-1)^{\delta-\alpha}\sum_{KQ} r_K^n\,(2K+1)\begin{pmatrix}1 & 1 & K\\ \epsilon & -\delta & Q\end{pmatrix}\begin{pmatrix}1 & 1 & K\\ \beta & -\alpha & Q\end{pmatrix} \\
&\qquad\times\frac{\left[\mathrm{e}^{-N_\alpha^* t_n}-\mathrm{e}^{-N_\alpha^* t_{n+1}}\right]\left[\mathrm{e}^{-N_\beta t_n}-\mathrm{e}^{-N_\beta t_{n+1}}\right]}{N_\alpha^* N_\beta}\,,
\end{aligned}$$

where the symbol r_K is defined in Eq. (5.199).

Finally, we average over all the possible collision times. To this aim we must evaluate the multiple integral (see footnote 1 on p. 223)

$$\int_0^\infty f\,\mathrm{d}t_1\int_{t_1}^\infty f\,\mathrm{d}t_2\cdots\int_{t_n}^\infty f\,\mathrm{d}t_{n+1}\ \mathrm{e}^{-f t_{n+1}}\ \mathcal{F}_\alpha(\nu)^*\,\mathcal{F}_\beta(\nu)\,,$$

where f is the frequency of perturbing collisions. The evaluation of the integral is elementary and leads to

$$\begin{aligned}
&\mathcal{F}_\alpha(\nu)^*\,\mathcal{F}_\beta(\nu) = \\
&= \sum_{n=0}^{\infty}\sum_{\delta\epsilon} A_\delta^* A_\epsilon\,(-1)^{\delta-\alpha}\sum_{KQ} r_K^n\,(2K+1)\begin{pmatrix}1 & 1 & K\\ \epsilon & -\delta & Q\end{pmatrix}\begin{pmatrix}1 & 1 & K\\ \beta & -\alpha & Q\end{pmatrix} \\
&\qquad\times\frac{f^n\,(N_\alpha^*+N_\beta+2f)}{(N_\alpha^*+N_\beta+f)^{n+1}\,(N_\alpha^*+f)\,(N_\beta+f)}\,.
\end{aligned}$$

Performing the sum over n, and using the expressions of N_α^* and N_β given in Eq. (5.187), one finally obtains

$$\begin{aligned}
&\mathcal{F}_\alpha(\nu)^*\,\mathcal{F}_\beta(\nu) = \\
&= \frac{1}{4\pi^2}\sum_{\delta\epsilon} A_\delta^* A_\epsilon\,(-1)^{\delta-\alpha}\,\frac{\frac{\Gamma'}{\Gamma}+\mathrm{i}\,(\alpha-\beta)H}{\left[(\nu_0-\alpha\nu_{\mathrm{L}}-\nu)+\mathrm{i}\Gamma'\right]\left[(\nu_0-\beta\nu_{\mathrm{L}}-\nu)-\mathrm{i}\Gamma'\right]} \\
&\qquad\times\sum_{KQ}(2K+1)\begin{pmatrix}1 & 1 & K\\ \epsilon & -\delta & Q\end{pmatrix}\begin{pmatrix}1 & 1 & K\\ \beta & -\alpha & Q\end{pmatrix} \\
&\qquad\qquad\times\left[\frac{\Gamma+\Gamma_{\mathrm{c}}\,(1-r_K)}{\Gamma}+\mathrm{i}\,(\alpha-\beta)H\right]^{-1}\,,
\end{aligned}\tag{5.191}$$

where the various damping coefficients are given by

$$\Gamma = \frac{\gamma}{4\pi}\,, \qquad \Gamma_{\rm c} = \frac{f}{4\pi}\,, \qquad \Gamma' = \Gamma + 2\Gamma_{\rm c}\,, \qquad H = \frac{2\pi\nu_{\rm L}}{\gamma} = \frac{e_0 B}{2mc\gamma}\,.$$

As far as the Zeeman effect is concerned, if we restrict attention – as in Sect. 3.2 – to the case of natural excitation, we must replace $A^*_\delta A_\epsilon$ by $\overline{|A|^2}\,\delta_{\delta\epsilon}$ in Eq. (5.191). Using Eq. (2.26a) we can write

$$\delta_{\delta\epsilon}\,(-1)^{\delta-\alpha} = 3\begin{pmatrix}1 & 1 & 0\\ \epsilon & -\delta & 0\end{pmatrix}\begin{pmatrix}1 & 1 & 0\\ \alpha & -\alpha & 0\end{pmatrix}\,.$$

Application of the orthogonality relation (2.23a) shows that the only non-zero contribution originates from the $K = 0$ term. Thus we obtain, with the help of Eqs. (2.26a) and (5.199)

$$\mathcal{F}_\alpha(\nu)^*\,\mathcal{F}_\beta(\nu) = \delta_{\alpha\beta}\,\frac{1}{4\pi^2}\,\overline{|A|^2}\,\frac{\Gamma'}{\Gamma}\,\frac{1}{(\nu_0 - \alpha\nu_{\rm L} - \nu)^2 + \Gamma'^2}\,. \tag{5.192}$$

Since Eq. (3.35) – which relates the amplitude $\overline{|A|^2}$ to the average energy $\bar{E}$ contained in each oscillator – is still valid, from Eqs. (3.36), (5.188), and (5.192) we obtain for the emission coefficient in tensorial form the expression (3.37) with Γ replaced by Γ'. In other words, the effect of perturbing collisions on the Zeeman effect is nothing but a broadening of the profile. This is consistent with what we found for the radiative transfer of polarized radiation.

As far as resonance polarization and the Hanle effect are concerned, the situation is very different. Since the Fourier transform $\mathcal{F}_\alpha(\nu)$ is substantially non-zero only for $\nu \approx \nu_0$, we can extract the factor ν^4 from the integral over frequency in Eq. (5.189). Using the residue theorem, we then obtain from Eq. (5.191)

$$\begin{aligned}\int_{-\infty}^{\infty} \mathcal{F}_\alpha(\nu)^*\,\mathcal{F}_\beta(\nu)\,{\rm d}\nu &= \\ = \frac{1}{4\pi\Gamma}\sum_{\delta\epsilon} A^*_\delta A_\epsilon\,(-1)^{\delta-\alpha}\sum_{KQ}(2K+1)\begin{pmatrix}1 & 1 & K\\ \epsilon & -\delta & Q\end{pmatrix}\begin{pmatrix}1 & 1 & K\\ \beta & -\alpha & Q\end{pmatrix}& \\ \times\left[\frac{\Gamma + \Gamma_{\rm c}\,(1-r_K)}{\Gamma} + {\rm i}\,(\alpha-\beta)H\right]^{-1}&\end{aligned}$$

(which is consistent, under the limit $f \to 0$, with Eq. (5.83)). Repeating the same arguments leading to Eq. (5.87), one finds that this equation must be replaced by the following

$$\begin{aligned}T_{ij,kl}(\vec{\Omega},\vec{\Omega}';\vec{B},f) = \frac{3}{2}\sum_{\alpha\beta\delta\epsilon}(-1)^{\delta-\alpha}\,C^*_{\alpha i}\,C_{\beta j}\,C'_{\delta k}\,C'^*_{\epsilon l}& \\ \times\sum_{KQ}(2K+1)\begin{pmatrix}1 & 1 & K\\ \epsilon & -\delta & Q\end{pmatrix}\begin{pmatrix}1 & 1 & K\\ \beta & -\alpha & Q\end{pmatrix}& \\ \times\left[\frac{\Gamma + \Gamma_{\rm c}\,(1-r_K)}{\Gamma} + {\rm i}\,(\alpha-\beta)H\right]^{-1}\,,&\end{aligned}$$

which is the general expression for the scattering phase matrix of the polarization tensor in the presence of perturbing collisions. It can be easily seen that properties (5.88) and (5.89) are still satisfied.

The scattering phase matrix for the Stokes parameters in the presence of collisions is given by the analogue of Eq. (5.92), namely

$$R_{ij}(\vec{\Omega},\vec{\Omega}';\vec{B},f) = \frac{1}{2}\sum_{klmn}(\sigma_i)_{lk}\,(\sigma_j)_{mn}\,T_{kl,mn}(\vec{\Omega},\vec{\Omega}';\vec{B},f)\;.$$

Again, properties (5.93) and (5.94) still hold.

The effect of perturbing collisions can be better understood if irreducible tensors are introduced (see Sect. 5.10). Repeating the same arguments leading to Eq. (5.121) one finds that this equation must be replaced by

$$\begin{aligned} T_{\mu\nu,\rho\sigma}(\vec{\Omega},\vec{\Omega}';\vec{B},f) = \frac{3}{2}\sum_{qq'pp'}(-1)^{p-q}\,\mathcal{E}_{qq'}(\mu,\nu,\vec{\Omega})\,\mathcal{E}_{p'p}(\sigma,\rho,\vec{\Omega}') \\ \times\sum_{KQ}(2K+1)\begin{pmatrix}1 & 1 & K\\ p' & -p & Q\end{pmatrix}\begin{pmatrix}1 & 1 & K\\ q' & -q & Q\end{pmatrix} \\ \times\left[\frac{\Gamma+\Gamma_{\rm c}\,(1-r_K)}{\Gamma}+\mathrm{i}\,(q-q')H\right]^{-1}. \end{aligned}$$

Using then Eqs. (5.125) and (2.23a) one obtains

$$\begin{aligned} &T_{\mu\nu,\rho\sigma}(\vec{\Omega},\vec{\Omega}';\vec{B},f) = \\ &= \frac{1}{2}\sum_{KQ}(-1)^Q\,\mathcal{E}^K_Q(\mu,\nu,\vec{\Omega})\,\mathcal{E}^K_{-Q}(\sigma,\rho,\vec{\Omega}')\left[\frac{\Gamma+\Gamma_{\rm c}\,(1-r_K)}{\Gamma}+\mathrm{i}\,QH\right]^{-1}, \end{aligned}$$

which is the same as Eq. (5.127) with the only substitution

$$\left[1+\mathrm{i}\,QH\right]^{-1}\rightarrow\left[\frac{\Gamma+\Gamma_{\rm c}\,(1-r_K)}{\Gamma}+\mathrm{i}\,QH\right]^{-1}.$$

Similarly, one finds that Eq. (5.133), which gives the scattering phase matrix for the Stokes parameters, must be replaced by

$$R_{ij}(\vec{\Omega},\vec{\Omega}';\vec{B},f) = \sum_{KQ}(-1)^Q\,\mathcal{T}^K_Q(i,\vec{\Omega})\,\mathcal{T}^K_{-Q}(j,\vec{\Omega}')\,\left[\frac{\Gamma+\Gamma_{\rm c}\,(1-r_K)}{\Gamma}+\mathrm{i}\,QH\right]^{-1}.$$

These expressions show the substantial difference between magnetic field and collisions as depolarizing agents in resonance scattering. Collisions affect *all* the K-pole components (except that with $K=0$, as it will be seen shortly), while the magnetic field does not affect the $Q=0$ components. It has been mentioned in

Sect. 5.13 – and will be shown in detail in Chap. 10 – that this feature is related to the fact that the magnetic field can alter the coherences but not the populations of the atomic levels, whereas collisions can alter both. In terms of classical dipoles this means that collisions affect both phase correlations and amplitude differences between oscillations, while the magnetic field affects only the former.

To discuss the results just obtained, we can write the depolarization factor in the form

$$\left[\frac{\Gamma + \Gamma_{\rm c}\,(1 - r_K)}{\Gamma} + {\rm i}\,QH\right]^{-1} = \frac{1}{1 + \delta_K + {\rm i}\,QH} = \frac{1}{1 + \delta_K}\,\frac{1}{1 + {\rm i}\,QH'_K}\ , \quad (5.193)$$

where

$$\delta_K = \frac{\Gamma_{\rm c}}{\Gamma}\,(1 - r_K) = \frac{f}{\gamma}\,(1 - r_K)$$

$$H'_K = \frac{H}{1 + \delta_K} = \frac{2\pi\nu_{\rm L}}{\gamma + f\,(1 - r_K)}\ . \quad (5.194)$$

This expression shows that the effect of collisions is twofold. First, each K-pole contribution to the scattering phase matrix is reduced by the factor $(1 + \delta_K)$, where δ_K is a parameter proportional to the frequency of perturbing collisions or, in other words, to the density of perturbers. It will be shown in the next section that the values of δ_K depend on the specific assumptions which are made about the phase shifts induced by perturbing collisions. The model considered here leads to the values (see Eq. (5.199) of next section)

$$\delta_0 = 0\ , \qquad \delta_1 = \frac{f}{\gamma}\ , \qquad \delta_2 = \frac{3}{5}\,\frac{f}{\gamma}\ .$$

Thus

$$\frac{\delta_1}{\delta_2} = \frac{5}{3}\ , \quad (5.195)$$

a result deduced through a quantum-mechanical calculation by Omont (1965) for the case of Van der Waals, dipole-dipole interactions.

Moreover, perturbing collisions reduce the efficiency of the magnetic field in depolarizing (or in polarizing) the scattered radiation, the reduction being larger for $K = 1$ than for $K = 2$.

As a specific example, let us consider the scattering geometry illustrated in Fig. 5.10. In the absence of collisions the multipole components of the scattering phase matrix are given by Eqs. (5.139). In the presence of collisions, one finds that the matrix $\boldsymbol{R}^{(1)}$ must be divided by the factor $(1 + \delta_1)$, and the quantity C_1 appearing in its expression must be replaced by

$$C'_1 = \cos\alpha'_1\,\cos\bigl(\alpha'_1 + \chi' - \chi\bigr)\ ,$$

with α'_1 defined by

$$\tan\alpha'_1 = H'_1\ .$$

Similarly, the matrix $\boldsymbol{R}^{(2)}$ must be divided by the factor $(1+\delta_2)$, and the quantities C_1, S_1, C_2, S_2 must be replaced by

$$C_1'' = \cos\alpha_1''\,\cos\bigl(\alpha_1'' + \chi' - \chi\bigr) \qquad S_1'' = \cos\alpha_1''\,\sin\bigl(\alpha_1'' + \chi' - \chi\bigr)$$
$$C_2'' = \cos\alpha_2''\,\cos\bigl(\alpha_2'' + 2(\chi' - \chi)\bigr) \qquad S_2'' = \cos\alpha_2''\,\sin\bigl(\alpha_2'' + 2(\chi' - \chi)\bigr)\ ,$$

with

$$\tan\alpha_1'' = H_2'\ , \qquad \tan\alpha_2'' = 2H_2'\ .$$

Finally, we want to recall that the theory presented in this section is based on rather restrictive assumptions, and that it could in principle be generalized by considering the effects of weak collisions, the existence of correlations between different phase shifts, and so on.

5.15. Some Properties of the Collisional Kernels

We evaluate in this section – under the assumption of an isotropic velocity distribution of colliding particles – the average over all collision directions of the quantity

$$\mathcal{K}_{\delta\alpha}^{(n)\,*}\,\mathcal{K}_{\epsilon\beta}^{(n)}\ ,$$

where the kernels are defined in Eq. (5.184).

Starting from the kernel relative to the first collision, we have from Eqs. (5.185) and (5.183)

$$\mathcal{K}_{\delta\alpha}^{(1)\,*}\,\mathcal{K}_{\epsilon\beta}^{(1)} = K_{\delta\alpha}^{(1)\,*}\,K_{\epsilon\beta}^{(1)}$$
$$= \mathrm{e}^{2\pi\mathrm{i}\,(\alpha-\delta-\beta+\epsilon)\,\nu_{\mathrm{L}}t_1}\left[\sum_{i=1}^{3} D_{\delta i}^{(1)\,*}\,\mathrm{e}^{-\mathrm{i}\phi_i^{(1)}}\,D_{\alpha i}^{(1)}\right]\left[\sum_{j=1}^{3} D_{\epsilon j}^{(1)}\,\mathrm{e}^{\mathrm{i}\phi_j^{(1)}}\,D_{\beta j}^{(1)\,*}\right]. \qquad (5.196)$$

According to our hypotheses on perturbing collisions, the phase shifts relative to the i-direction are totally uncorrelated with those relative to the j-direction. Thus the double sum reduces to a single sum of the form

$$S = \sum_{i=1}^{3} D_{\epsilon i}\,D_{\delta i}^{*}\,D_{\alpha i}\,D_{\beta i}^{*}\ ,$$

where

$$D_{\alpha i} = \vec{u}_\alpha\cdot\vec{t}_i^{\,*} = \vec{u}_\alpha\cdot\vec{t}_i\ .$$

Since we must average over all the possible orientations of the unit vectors $\vec{t}_i$, and since, on the other hand, these three unit vectors are equivalent, we have

$$\bigl\langle S\bigr\rangle = 3\,\bigl\langle D_{\epsilon i}\,D_{\delta i}^{*}\,D_{\alpha i}\,D_{\beta i}^{*}\bigr\rangle\ , \qquad (5.197)$$

where $i = 1$, or 2, or 3.

The average is easily evaluated using spherical tensors. In the reference system of the magnetic field $(\vec{u}_r, \vec{u}_s, \vec{u}_0)$ we have, with the help of Eqs. (5.111), (5.112), and (5.120)

$$D_{\epsilon i} = \sum_q (u_\epsilon)_q \, (t_i)^*_q = \sum_q \delta_{\epsilon q} \, (t_i)^*_q = (t_i)^*_\epsilon \, .$$

From Eq. (5.116), identifying the unit vectors $\vec{t}_1$, $\vec{t}_2$, $\vec{t}_3$ with $\vec{a}$, $\vec{b}$, $\vec{c}$, respectively, we have

$$(t_\alpha)_q = \mathcal{D}^1_{\alpha q}(R) \, ,$$

where R is the rotation bringing $(\vec{t}_1, \vec{t}_2, \vec{t}_3)$ into $(\vec{u}_r, \vec{u}_s, \vec{u}_0)$. Since in Eq. (5.197) the index i can be chosen arbitrarily, taking $i = 3$ one has

$$\begin{aligned} \langle S \rangle &= 3 \left\langle D_{\epsilon 3} \, D^*_{\delta 3} \, D_{\alpha 3} \, D^*_{\beta 3} \right\rangle = 3 \left\langle (t_0)^*_\epsilon \, (t_0)_\delta \, (t_0)^*_\alpha \, (t_0)_\beta \right\rangle \\ &= 3 \left\langle \mathcal{D}^1_{0\epsilon}(R)^* \, \mathcal{D}^1_{0\delta}(R) \, \mathcal{D}^1_{0\alpha}(R)^* \, \mathcal{D}^1_{0\beta}(R) \right\rangle \, . \end{aligned}$$

To evaluate this expression we use twice Eq. (2.77) and then Eq. (2.73) and the Weyl theorem (2.76) to get

$$\langle S \rangle = (-1)^{\delta - \alpha} \sum_{KQ} r_K \, (2K+1) \begin{pmatrix} 1 & 1 & K \\ \epsilon & -\delta & Q \end{pmatrix} \begin{pmatrix} 1 & 1 & K \\ \beta & -\alpha & Q \end{pmatrix} \, , \tag{5.198}$$

where

$$r_K = 3 \begin{pmatrix} 1 & 1 & K \\ 0 & 0 & 0 \end{pmatrix}^2 = \begin{cases} 1 & \text{for } K = 0 \\ 0 & \text{for } K = 1 \\ 2/5 & \text{for } K = 2 \, . \end{cases} \tag{5.199}$$

Substitution into Eq. (5.196) gives

$$\left\langle \mathcal{K}^{(1)\,*}_{\delta\alpha} \, \mathcal{K}^{(1)}_{\epsilon\beta} \right\rangle = (-1)^{\delta - \alpha} \sum_{KQ} r_K \, (2K+1) \begin{pmatrix} 1 & 1 & K \\ \epsilon & -\delta & Q \end{pmatrix} \begin{pmatrix} 1 & 1 & K \\ \beta & -\alpha & Q \end{pmatrix} \, .$$

The collisional kernels of higher degree can be evaluated by a recursive procedure. Assuming the complete independence of successive collisions one obtains

$$\begin{aligned} &\left\langle \mathcal{K}^{(n)\,*}_{\delta\alpha} \, \mathcal{K}^{(n)}_{\epsilon\beta} \right\rangle = \\ &= (-1)^{\delta - \alpha} \sum_{KQ} r^n_K \, (2K+1) \begin{pmatrix} 1 & 1 & K \\ \epsilon & -\delta & Q \end{pmatrix} \begin{pmatrix} 1 & 1 & K \\ \beta & -\alpha & Q \end{pmatrix} \, , \end{aligned} \tag{5.200}$$

which – recalling the orthogonality relations (2.23b) – is valid also for $n = 0$.

It should be remarked that the expression for r_K given in Eq. (5.199) is strictly related to the assumptions on the phase shifts ϕ_i that we have made at the beginning of Sect. 5.14. The motion of the atomic oscillator has been expanded into three oscillations along a triplet of *real*, *orthogonal* unit vectors $\vec{t}_i$, and the phase shifts ϕ_i

induced by a perturbing collision have been assumed to refer to such oscillations. If we choose a different triplet of unit vectors, and retain the assumption of the complete independence of the phase shifts along each of them, the final results will generally be different. This is no wonder, as the choice of a specific triplet of unit vectors is equivalent to a definite physical assumption on the effects of perturbing collisions.

For example, let us choose the triplet of unit vectors

$$\begin{aligned} \vec{t}_{-1} &= \frac{1}{\sqrt{2}} \left(\vec{t}_1 + \mathrm{i}\, \vec{t}_2 \right) \\ \vec{t}_0 &= \vec{t}_3 \\ \vec{t}_{+1} &= \frac{1}{\sqrt{2}} \left(-\vec{t}_1 + \mathrm{i}\, \vec{t}_2 \right) , \end{aligned} \tag{5.201}$$

with $(\vec{t}_1, \vec{t}_2, \vec{t}_3)$ the usual triplet of real, orthogonal unit vectors. One finds the same results as before, except that Eq. (5.197) must be replaced by the following

$$\left\langle S \right\rangle = \sum_{\mu} \left\langle D_{\epsilon\mu}\, D^*_{\delta\mu}\, D_{\alpha\mu}\, D^*_{\beta\mu} \right\rangle$$

(obviously the three unit vectors of Eq. (5.201) cannot be considered equivalent). In terms of rotation matrices we have

$$\left\langle S \right\rangle = \sum_{\mu} \left\langle \mathcal{D}^1_{\mu\epsilon}(R)^*\, \mathcal{D}^1_{\mu\delta}(R)\, \mathcal{D}^1_{\mu\alpha}(R)^*\, \mathcal{D}^1_{\mu\beta}(R) \right\rangle ,$$

and we obtain the same equation as Eq. (5.198) with

$$r_K = \frac{1}{2K+1} = \begin{cases} 1 & \text{for } K = 0 \\ 1/3 & \text{for } K = 1 \\ 1/5 & \text{for } K = 2\,. \end{cases}$$

Thus Eq. (5.195) becomes

$$\frac{\delta_1}{\delta_2} = \frac{5}{6} ,$$

which is just half the value obtained from the previous model.

5.16. Classification of the Physical Regimes

We have seen in this chapter how it is possible to describe in classical terms some of the different phenomena which are able to induce polarization in spectral lines or to affect its characteristics. In particular, we have seen that polarization can be originated either by the presence of a magnetic field – which induces a frequency splitting between the different classical dipoles – or by the presence of an intrinsic

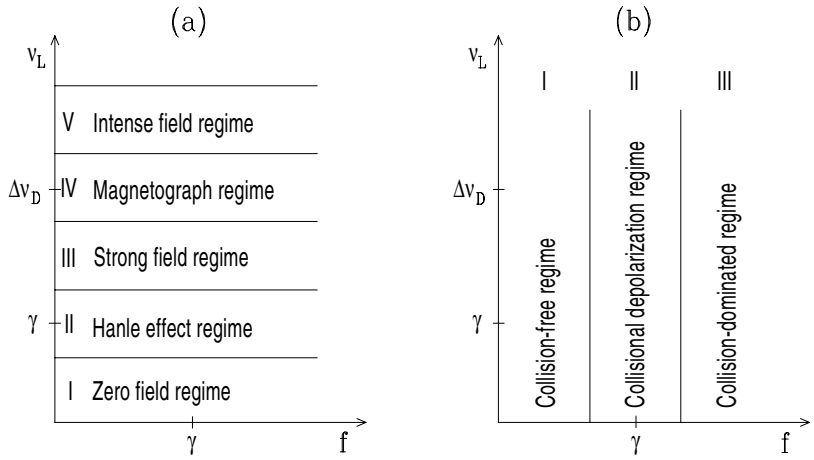

Fig.5.18. A classification scheme for polarization phenomena in spectral lines (the meaning of the symbols is explained in the text).

anisotropy in the radiation field which is illuminating the atom. The anisotropy of the radiation field, that is in general related both to its angular distribution and to its polarization state, can induce amplitude differences between the oscillations of the dipoles and well-defined phase correlations (or coherences) between such oscillations. We have also seen that a magnetic field has the further effect of reducing such phase correlations, and that collisions with an isotropic distribution of perturbers produce a relaxation of the amplitude differences and of the phase correlations.

All these phenomena, that will in general act simultaneously in a magnetized plasma, can be characterized by four different parameters all having the dimensions of frequency. These parameters are the following:
a) $\nu_{\rm L}$, the Larmor frequency, proportional to the magnetic field magnitude, which is defined in Eq. (3.10);
b) $\Delta\nu_{\rm D}$, the Doppler width, which depends on the temperature of the plasma (and on its microturbulent velocity), defined in Eqs. (5.43) and (5.48);
c) γ, the oscillator damping constant, which has its quantum analogue in the Einstein A coefficient for spontaneous emission from the upper level;
d) f, the frequency of depolarizing collisions, which is proportional to the number density of perturbers.

According to the relative values of these four parameters we have different physical regimes that can be suitably classified in a two-dimensional diagram (Landi Degl'Innocenti, 1983). Such diagram, shown in Fig. 5.18, bears a magnetic field indicator (the Larmor frequency) on the vertical axis and a density indicator (the frequency of collisions) on the horizontal axis.

In drawing the diagram we have assumed $\Delta\nu_{\rm D} \gg \gamma$. In terms of the thermal velocity $w_{\rm T}$ we have indeed

$$\frac{\Delta\nu_{\rm D}}{\gamma} = \frac{w_{\rm T}}{\lambda\gamma} \,,$$

where λ is the line wavelength. Substituting typical values relative to a spectral line of optical wavelength formed in a stellar atmosphere ($w_{\rm T} = 2$ km s^{-1}, $\lambda = 5000$ Å, $\gamma = 10^7$ s^{-1}) we get

$$\frac{\Delta\nu_{\rm D}}{\gamma} = 4.0 \times 10^2 \ .$$

The various physical regimes are sketched in Fig. 5.18; each of them can be assigned a specific denomination.[1] As far as the magnetic field is concerned, we have the following five regimes:

Ia) *Zero field regime* ($\nu_{\rm L} \ll \gamma$): the magnetic field is so weak as to induce a negligible Zeeman splitting and a negligible relaxation effect on phase correlations. In this regime the magnetic field can just be ignored.

IIa) *Hanle effect regime* ($\gamma \approx 2\pi\nu_{\rm L} \ll \Delta\nu_{\rm D}$): the magnetic field is strong enough to reduce the phase correlations between different oscillators. By contrast, the Zeeman splitting is still very small and can be neglected.

IIIa) *Strong field regime* ($\gamma \ll \nu_{\rm L} < \Delta\nu_{\rm D}$): the relaxation of coherences is now complete, so that the different oscillators can be treated as independent. The Zeeman splitting is a small fraction of $\Delta\nu_{\rm D}$ and is able to produce an observable (although weak) polarization signal.

IVa) *Magnetograph* (or *intermediate*) *regime* ($\gamma \ll \nu_{\rm L} \approx \Delta\nu_{\rm D}$): the Zeeman splitting is comparable with the Doppler width, which results in a strong polarization signal; the different Zeeman components are, however, still unresolved. The observations performed by solar or stellar magnetographs usually fall in this regime.

Va) *Intense field regime* ($\nu_{\rm L} > \Delta\nu_{\rm D}$): the Zeeman splitting is now so large that the different components are well-separated in the spectrum.

To sum up, we have that the Zeeman splitting can be neglected in regimes Ia and IIa, while in regimes IIIa, IVa, and Va coherences are completely relaxed and can be ignored. As far as the amplitude differences between oscillators are concerned, the magnetic field has no effect on them.

Turning now to the influence of collisions, we have three different regimes:

Ib) *Collision-free regime* ($f \ll \gamma$): depolarizing collisions have a negligible influence on atomic polarization and can be disregarded.

IIb) *Collisional depolarization regime* ($f \approx \gamma$): depolarizing collisions are important in reducing atomic polarization (both coherences and amplitude differences between oscillators) but not so strong as to produce a complete relaxation. In this regime a detailed knowledge of the depolarizing rates is essential for a correct description of the physical situation.

IIIb) *Collision-dominated regime* ($f \gg \gamma$): the effect of depolarizing collisions is so strong that atomic polarization is totally destroyed. In this regime there are no coherences between different dipoles and the oscillation amplitudes are equal; in other words, the classical dipoles are thermalized.

[1] The denominations used here are slightly different from those in Landi Degl'Innocenti (1983).

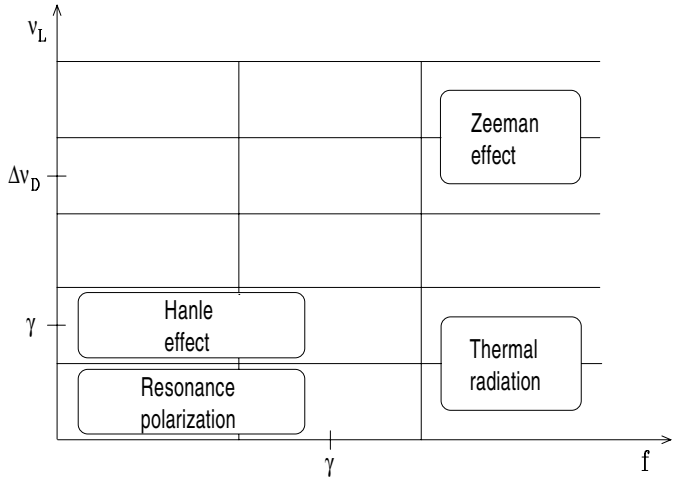

Fig.5.19. The (ν_L - f) diagram is divided into fifteen different regions resulting from the intersection of the physical regimes sketched in Fig.5.18.

By combining the five magnetic regimes and the three collisional regimes, one finds out that there are 15 characteristic regimes for polarization in spectral lines,[1] each occupying a well-defined region in the (ν_L - f) diagram. Figure 5.19 points out the regions of the diagram where conventional laboratory experiments are usually performed.

It is important to remark that the classical description given above can be transposed into quantum-mechanical terms. As outlined at the end of Sect. 5.13, the phase correlations between different dipoles have their quantum analogue in the off-diagonal density-matrix elements, while the oscillation amplitudes of the single dipoles have their analogue in the diagonal matrix elements. Finally, the oscillator damping constant γ has its quantum equivalent in the Einstein A coefficient for spontaneous emission.

[1] Indeed, regime (Ia-IIIb) is equivalent to (IIa-IIIb).

This page intentionally left blank

CHAPTER 6

INTERACTION OF MATERIAL SYSTEMS WITH POLARIZED RADIATION (THE QUANTUM APPROACH)

We derive in this chapter the basic equations describing the interaction of a material system with a polarized radiation field. These equations consist essentially of two distinct sets, one for the material system (*statistical equilibrium equations*) and the other for the radiation field (*radiative transfer equations*). But the two sets are coupled, as the properties of the material system turn out to be affected by the radiation field, and vice versa. From this point of view, the theory presented in the following can be regarded as the basis for a generalized theory of Non Local Thermodynamic Equilibrium which takes the polarization characteristics of the material system and of radiation into account.

The two sets of equations are deduced by strictly similar procedures, which start from the very principles of Quantum Mechanics and are based on the use of the density operator. The radiation field is described with the formalism of (non-relativistic) second quantization, while the material system is characterized by its own Hamiltonian which does not need to be specified in detail. The interaction is also treated under the non-relativistic approximation, and explicit formulae for electric-dipole and magnetic-dipole transitions are derived.

The formalism used in this chapter is rather complicated, but the preceding outlines of density operator and second quantization theories (Chaps. 3 and 4, respectively) should enable the reader to follow all the developments. We also tried to point out, whenever possible, the physical meaning of the various equations and the analogies with the classical treatment presented in Chap. 5.

The results that will be obtained in this chapter suffer from some basic limitations that arise both from the formalism itself and from the different approximations introduced in the derivation. Indeed, such results cannot be applied when coherences between non-degenerate levels are present, unless the spectrum of the radiation incident on the material system is flat across a range wider than the frequency separation of those levels. Similarly, if coherences between degenerate levels are present, the results provide an exact description of scattering phenomena only if the spectrum of the incident radiation is flat across a frequency range wider than the inverse lifetime of the levels.

These limitations are analogous – in the polarized case – to those contained in the 'complete frequency redistribution' approach of the standard non-LTE theory (see e.g. Mihalas, 1978). They are ultimately related to the fact that two consecutive interactions of the material system with the radiation field are considered as independent: this means, for instance, that when an emission event takes place, no memory is kept of the frequency of the photon that induced the previous absorption event.

Notwithstanding its basic limitations, the theory has a wide range of physical and astrophysical applications because, in many cases, the spectrum of the incident radiation is in fact flat across the relevant frequency range. Usually coherences are important as long as the separation between energy levels is less than about $10^8\,\mathrm{s}^{-1}$ (a typical value of the spontaneous de-excitation Einstein coefficient), and such frequency interval – which corresponds to 1 mÅ in the visible – is much smaller than the typical Doppler widths of spectral lines.

However, there are some phenomena that cannot be fully described by the formalism presented in this chapter, like the quantum-interference polarization observed in the CaII H and K lines at the solar limb (Stenflo, 1980). In that case, coherences between energy levels separated by a very large interval (about 50 Å) are found to play a major role, and the incident radiation field is definitely not flat across such interval. In these cases a more general formalism, able to encompass *frequency redistribution effects*, is required. Although some results have indeed been obtained on this subject (Stenflo, 1994; Bommier, 1997a,b; Landi Degl'Innocenti et al., 1997), the underlying theory is still in a preliminary phase and remains outside the scope of this book.

This chapter is based on previous works by the authors and collaborators (Landi Degl'Innocenti and Landi Degl'Innocenti, 1972, 1975; Landi Degl'Innocenti et al., 1976; Landi Degl'Innocenti, 1983). The same method has been reconsidered and illustrated in some detail by Cannon (1985), Trujillo Bueno (1990), and Stenflo (1994).

6.1. Equations of Motion

According to the principles of Quantum Mechanics (see e.g. Messiah, 1961) the state of a physical system at time t is described by a vector in the Hilbert space, $|\,\psi(t)\rangle$, which satisfies the normalization condition

$$\langle\psi(t)\,|\,\psi(t)\rangle = 1\ .$$

The time evolution of the system is governed by the well-known Schrödinger equation

$$\mathrm{i}\,\frac{h}{2\pi}\,\frac{\mathrm{d}}{\mathrm{d}t}\,|\,\psi(t)\rangle = H\,|\,\psi(t)\rangle\ ,$$

where i is the imaginary unit, h is the Planck constant, and H is the Hamiltonian operator that we suppose here independent of time.

On the other hand, any observable of the system is described by a linear, Hermitian operator acting on the same Hilbert space. The expectation value of the observable (i.e. the average value of the measurement of the observable ideally performed on an infinite number of 'copies' of the same physical system) is given by

$$O(t) = \langle\psi(t)\,|\,\hat{O}\,|\,\psi(t)\rangle\ ,$$

where $\hat{O}$ is the quantum operator corresponding to the observable O.

However, there are many physical situations where the state of the system cannot be described by a pure state $|\,\psi(t)\rangle$ (nor by a superposition of pure states), but a detailed quantum-statistical description is necessary. This can be achieved in a very natural way using the concept of density (or statistical) operator (see Sect. 3.6). We recall that the expectation value of the observable O is related to the density operator ρ by the expression (see Eq. (3.86))

$$O(t) = \mathrm{Tr}\left\{\hat{O}\rho\right\} . \tag{6.1}$$

The time evolution of $O(t)$ can be easily obtained from Eq. (6.1). We have

$$\frac{\mathrm{d}}{\mathrm{d}t}\,O(t) = \mathrm{Tr}\left\{\frac{\mathrm{d}\hat{O}}{\mathrm{d}t}\,\rho\right\} + \mathrm{Tr}\left\{\hat{O}\,\frac{\mathrm{d}\rho}{\mathrm{d}t}\right\} , \tag{6.2}$$

where the first term is non-zero only when the operator $\hat{O}$ depends explicitly on time. This equation can be rewritten, with the help of Eq. (3.88), in the form

$$\frac{\mathrm{d}}{\mathrm{d}t}\,O(t) = \mathrm{Tr}\left\{\frac{\mathrm{d}\hat{O}}{\mathrm{d}t}\,\rho\right\} - \frac{2\pi\mathrm{i}}{h}\,\mathrm{Tr}\left\{\hat{O}\left[H,\rho\right]\right\} ,$$

or, using the cyclic property of the trace, in the more convenient form

$$\frac{\mathrm{d}}{\mathrm{d}t}\,O(t) = \mathrm{Tr}\left\{\frac{\mathrm{d}\hat{O}}{\mathrm{d}t}\,\rho\right\} - \frac{2\pi\mathrm{i}}{h}\,\mathrm{Tr}\left\{\left[\hat{O},H\right]\rho\right\} . \tag{6.3}$$

In many cases the total Hamiltonian H of the system can be expressed as the sum of two terms,

$$H = H_0 + V , \tag{6.4}$$

where H_0 is the so-called *unperturbed* Hamiltonian and V is the *interaction* Hamiltonian. In such cases it is in many respects useful to introduce a different representation for the quantum phenomena, called the *interaction picture*. This is obtained from the usual *Schrödinger picture* – which has been employed so far – by the following unitary transformation

a) for the state vectors:

$$|\,\psi(t)\rangle_{\mathrm{I}} = \mathrm{e}^{\,\mathrm{i}\frac{2\pi}{h}H_0 t}\,|\,\psi(t)\rangle$$

b) for the operators:

$$\hat{O}_{\mathrm{I}}(t) = \mathrm{e}^{\,\mathrm{i}\frac{2\pi}{h}H_0 t}\;\hat{O}\;\mathrm{e}^{\,-\mathrm{i}\frac{2\pi}{h}H_0 t} , \tag{6.5}$$

where the index I means that the corresponding symbol (operator, or state vector) is defined in the interaction picture.

The equation of motion for the density operator expressed in the interaction picture can be easily obtained from Eq. (6.5). Using Eqs. (3.88) and (6.4) we get

$$\frac{\mathrm{d}}{\mathrm{d}t}\,\rho_{\mathrm{I}}(t) = -\frac{2\pi\mathrm{i}}{h}\,\left[V_{\mathrm{I}}(t),\rho_{\mathrm{I}}(t)\right] , \tag{6.6}$$

where

$$V_{\rm I}(t) = {\rm e}^{{\rm i}\frac{2\pi}{h}H_0 t}\, V\, {\rm e}^{-{\rm i}\frac{2\pi}{h}H_0 t} \tag{6.7}$$

is the interaction Hamiltonian expressed in the interaction picture.

Substitution of Eq. (6.6) into Eq. (6.2) leads to

$$\frac{\rm d}{{\rm d}t}\,O(t) = {\rm Tr}\left\{\left(\frac{\rm d}{{\rm d}t}\hat{O}_{\rm I}(t)\right)\rho_{\rm I}(t)\right\} - \frac{2\pi{\rm i}}{h}\,{\rm Tr}\left\{\left[\hat{O}_{\rm I}(t), V_{\rm I}(t)\right]\rho_{\rm I}(t)\right\}. \tag{6.8}$$

Comparison of Eqs. (6.8) and (6.3) shows that when the interaction picture is used, the time evolution of the expectation value $O(t)$ is determined by the interaction Hamiltonian only (rather than the total Hamiltonian, as in the Schrödinger picture). When the interaction Hamiltonian is small in comparison with the unperturbed Hamiltonian,[1] Eq. (6.8) can be usefully expanded as follows. Integration of Eq. (6.6) between 0 and t gives

$$\rho_{\rm I}(t) = \rho_{\rm I}(0) - \frac{2\pi{\rm i}}{h}\int_0^t \left[V_{\rm I}(t'), \rho_{\rm I}(t')\right]{\rm d}t'\,,$$

which can be substituted into Eq. (6.8) to obtain, using the cyclic property of the trace

$$\begin{aligned}\frac{\rm d}{{\rm d}t}\,O(t) = {}& {\rm Tr}\left\{\left(\frac{\rm d}{{\rm d}t}\hat{O}_{\rm I}(t)\right)\rho_{\rm I}(t)\right\} - \frac{2\pi{\rm i}}{h}\,{\rm Tr}\left\{\left[\hat{O}_{\rm I}(t), V_{\rm I}(t)\right]\rho_{\rm I}(0)\right\} \\ & - \frac{4\pi^2}{h^2}\,{\rm Tr}\left\{\int_0^t \left[\left[\hat{O}_{\rm I}(t), V_{\rm I}(t)\right], V_{\rm I}(t')\right]\rho_{\rm I}(t')\,{\rm d}t'\right\}. \end{aligned} \tag{6.9}$$

This is an exact equation describing the time evolution of the observable $O(t)$ produced by the interaction Hamiltonian. In the following sections it will be applied to describe the interaction between a material system and the radiation field.

6.2. The Interaction Hamiltonian

We consider the interaction between an arbitrary material system and the radiation field. The material system is here schematized as the collection of N independent subsystems (that will be called 'atoms') occupying a definite volume $\mathcal{V}$ in the ordinary three-dimensional space. The total Hamiltonian of the coupled system composed of one atom and the radiation field can be written, in the Schrödinger picture, in the form

$$H = H_0 + V\,,$$

[1] 'Small' means here that the typical matrix elements of V are much smaller than the matrix elements of H_0.

where H_0 – the unperturbed Hamiltonian – is the sum of the Hamiltonians of the free radiation field and of the atom,

$$H_0 = H_{\rm R} + H_{\rm A} \ . \tag{6.10}$$

The expression for $H_{\rm R}$ has already been deduced in Chap. 4, where the formalism of second quantization has been introduced. From Eq. (4.34) we have

$$H_{\rm R} = \sum_{\nu\vec{\Omega}\lambda} h\nu \ a^\dagger(\nu,\vec{\Omega},\lambda)\, a(\nu,\vec{\Omega},\lambda) \ , \tag{6.11}$$

where $a(\nu,\vec{\Omega},\lambda)$ and $a^\dagger(\nu,\vec{\Omega},\lambda)$ are, respectively, the destruction and creation operators associated with the mode of frequency ν, direction $\vec{\Omega}$, and polarization state characterized by the unit vector $\vec{e}_\lambda$ ($\lambda = 1, 2$), and where the sum runs over all the possible modes of the radiation field.

The expression of the atomic Hamiltonian $H_{\rm A}$ depends on the particular atomic system and on the possible presence of external agents (like, for instance, a static, electric or magnetic field). For the time being we make no specific assumption on $H_{\rm A}$. However, we suppose to know its normalized eigenstates $|\, n\rangle$ and energy eigenvalues E_n, solution of the stationary Schrödinger equation

$$H_{\rm A}\,|\, n\rangle = E_n |\, n\rangle \ , \tag{6.12}$$

with

$$\langle n \,|\, m\rangle = \delta_{nm} \tag{6.13}$$

and

$$\sum_n \ |\, n\rangle\langle n \,| = 1 \ . \tag{6.14}$$

The interaction Hamiltonian V can be deduced using the standard methods of Quantum Electrodynamics. According to Cohen-Tannoudji et al. (1977, 1987) the expression for V is given, in the non-relativistic approximation, by the expression

$$V = \frac{e_0}{mc} \sum_i \vec{p}_i \cdot \vec{A}(\vec{r}_i) + \frac{e_0}{mc} \sum_i \vec{s}_i \cdot \vec{B}(\vec{r}_i) + \frac{e_0^2}{2mc^2} \sum_i \Big(\vec{A}(\vec{r}_i)\Big)^2 \ , \tag{6.15}$$

where $\vec{r}_i$, $\vec{p}_i$, and $\vec{s}_i$ are the position, momentum, and spin operators of the i-th optical electron of the atom, and where $\vec{A}(\vec{r})$ and $\vec{B}(\vec{r})$ are the operators corresponding to the vector potential and to the magnetic field vector of the radiation field, respectively.

Writing the different contributions to V in the form

$$V = V_1 + V_2 + V_3 \ ,$$

we can easily find the order of magnitude of the various terms. We have just to recall that, as an order of magnitude

$$p \approx \frac{h}{2\pi a_0} \ , \qquad A \approx \frac{c}{2\pi\nu}\, E \ , \qquad s \approx \frac{h}{2\pi} \ , \qquad B \approx E \ ,$$

where E and ν are the electric field and the frequency of the radiation field, respectively, and where a_0 is the Bohr radius. Moreover, for the atomic Hamiltonian $H_{\rm A}$ we have

$$\left\langle H_{\rm A} \right\rangle \approx \frac{p^2}{m} \approx \frac{e_0^2}{a_0} \, ,$$

so that we obtain

$$\frac{\left\langle V_1 \right\rangle}{\left\langle H_{\rm A} \right\rangle} \approx \frac{\left\langle V_3 \right\rangle}{\left\langle V_1 \right\rangle} \approx \frac{e_0 E a_0}{h\nu} \, , \qquad \frac{\left\langle V_2 \right\rangle}{\left\langle V_1 \right\rangle} \approx \frac{2\pi a_0}{\lambda} \, . \tag{6.16}$$

At optical wavelengths the quantity $h\nu$ is comparable with the atomic energy, so that we can also write

$$\frac{\left\langle V_1 \right\rangle}{\left\langle H_{\rm A} \right\rangle} \approx \frac{\left\langle V_3 \right\rangle}{\left\langle V_1 \right\rangle} \approx \frac{e_0 E a_0}{e_0 E_{\rm at} a_0} = \frac{E}{E_{\rm at}} \, ,$$

where $E_{\rm at}$ is a typical interatomic electric field. Thus when the ratio between the radiation electric field and the typical interatomic electric fields is small, V_1 can be considered a perturbation in comparison with $H_{\rm A}$, and V_3 a perturbation (of the same order) in comparison with V_1. On the other hand, Eq. (6.16) shows that V_2, at optical wavelengths, is also much smaller (by about four orders of magnitude) than V_1. It follows that if we restrict attention to typical astrophysical or laboratory plasmas, where the inequality $E/E_{\rm at} \ll 1$ is always well-satisfied,[1] and to wavelengths λ such that $\lambda \gg a_0$, we can simply write the interaction Hamiltonian in the form

$$V = \frac{e_0}{mc} \sum_i \vec{p}_i \cdot \vec{A}(\vec{r}_i) \, . \tag{6.17}$$

This is the form that will be actually used in the following to describe the interaction between the atomic system and the radiation field.

Substituting the expression of the operator $\vec{A}(\vec{r})$ in terms of destruction and creation operators (Eq. (4.30)) into Eq. (6.17), we obtain

$$V = \sum_{\nu \vec{\Omega} \lambda} \left\{ Q(\nu, \vec{\Omega}, \lambda) \, a(\nu, \vec{\Omega}, \lambda) + Q^\dagger(\nu, \vec{\Omega}, \lambda) \, a^\dagger(\nu, \vec{\Omega}, \lambda) \right\} , \tag{6.18}$$

where the operator $Q(\nu, \vec{\Omega}, \lambda)$ and its adjoint $Q^\dagger(\nu, \vec{\Omega}, \lambda)$ are given by[2]

$$Q(\nu, \vec{\Omega}, \lambda) = d_\nu \sum_i \vec{p}_i \cdot \vec{e}_\lambda(\vec{\Omega}) \; {\rm e}^{\,{\rm i}\vec{k}\cdot\vec{r}_i}$$

$$Q^\dagger(\nu, \vec{\Omega}, \lambda) = d_\nu \sum_i \vec{p}_i \cdot \vec{e}_\lambda(\vec{\Omega})^* \; {\rm e}^{\,-{\rm i}\vec{k}\cdot\vec{r}_i} \, ,$$

---

[1] This inequality is not satisfied in optical experiments performed with high-power lasers, giving rise to non-linear optics phenomena.

[2] To prove that the operator multiplying $a^\dagger(\nu, \vec{\Omega}, \lambda)$ in Eq. (6.18) is just the adjoint of $Q(\nu, \vec{\Omega}, \lambda)$ one needs the commutation rule

$$[\, \vec{p} \cdot \vec{e}_\lambda(\vec{\Omega}) \, , \, {\rm e}^{{\rm i}\vec{k}\cdot\vec{r}} \,] = 0 \, ,$$

which follows from the commutation rule $[r_j, p_k] = {\rm i}\hbar \, \delta_{jk}$ and from Eq. (4.31).

with

$$d_\nu = \frac{e_0}{m}\sqrt{\frac{h}{2\pi\nu\mathcal{V}}}\,. \tag{6.19}$$

The interaction Hamiltonian given in Eq. (6.18) is expressed in the Schrödinger picture. To derive its expression in the interaction picture, it should be noticed that the operators $Q(\nu,\vec{\Omega},\lambda)$ and $Q^\dagger(\nu,\vec{\Omega},\lambda)$ act only on the atomic system, while the operators $a(\nu,\vec{\Omega},\lambda)$ and $a^\dagger(\nu,\vec{\Omega},\lambda)$ act only on the radiation field, which implies

$$\big[H_{\rm R}, Q(\nu,\vec{\Omega},\lambda)\big] = \big[H_{\rm A}, a(\nu,\vec{\Omega},\lambda)\big] = \big[H_{\rm R}, H_{\rm A}\big] = 0.$$

We thus obtain from Eq. (6.7)

$$V_{\rm I}(t) = \mathrm{e}^{\mathrm{i}\frac{2\pi}{h}H_0 t}\; V\; \mathrm{e}^{-\mathrm{i}\frac{2\pi}{h}H_0 t} = B(t) + B^\dagger(t)\,, \tag{6.20}$$

where

$$B(t) = \sum_{\nu\vec{\Omega}\lambda}\left\{\mathrm{e}^{\mathrm{i}\frac{2\pi}{h}H_{\rm A}t}\; Q(\nu,\vec{\Omega},\lambda)\; \mathrm{e}^{-\mathrm{i}\frac{2\pi}{h}H_{\rm A}t}\right\}\left\{\mathrm{e}^{\mathrm{i}\frac{2\pi}{h}H_{\rm R}t}\; a(\nu,\vec{\Omega},\lambda)\; \mathrm{e}^{-\mathrm{i}\frac{2\pi}{h}H_{\rm R}t}\right\}. \tag{6.21}$$

Denoting by $P(t)$ the operator resulting from the second curly bracket, we can easily prove that

$$P(t) = \mathrm{e}^{-2\pi\mathrm{i}\nu t}\; a(\nu,\vec{\Omega},\lambda)\,. \tag{6.22}$$

The formal proof is as follows. For $t = 0$ we have

$$P(0) = a(\nu,\vec{\Omega},\lambda)\,, \tag{6.23}$$

and the time derivative of $P(t)$ is

$$\frac{\mathrm{d}}{\mathrm{d}t}P(t) = \frac{2\pi\mathrm{i}}{h}\; \mathrm{e}^{\mathrm{i}\frac{2\pi}{h}H_{\rm R}t}\; \big[H_{\rm R}, a(\nu,\vec{\Omega},\lambda)\big]\; \mathrm{e}^{-\mathrm{i}\frac{2\pi}{h}H_{\rm R}t}\,.$$

On the other hand, taking into account the expression for $H_{\rm R}$ (Eq. (6.11)) and the commutation properties of the operators a and $a^\dagger$ (Eqs. (4.32)), one gets

$$\big[H_{\rm R}, a(\nu,\vec{\Omega},\lambda)\big] = -h\nu\; a(\nu,\vec{\Omega},\lambda)\,,$$

so that

$$\frac{\mathrm{d}}{\mathrm{d}t}\,P(t) = -2\pi\mathrm{i}\,\nu\,P(t)\,.$$

Integration of this differential equation with the initial condition (6.23) leads to expression (6.22).

As far as the first curly bracket is concerned, we can express it in a more convenient form by introducing the complete set of eigenvectors $\{|\, n\rangle\}$ of the atomic Hamiltonian defined in Eqs. (6.12)-(6.14). We have

$$\begin{aligned} & \mathrm{e}^{\mathrm{i}\frac{2\pi}{h}H_{\mathrm{A}}t}\ Q(\nu,\vec{\Omega},\lambda)\ \mathrm{e}^{-\mathrm{i}\frac{2\pi}{h}H_{\mathrm{A}}t} = \\ & = \sum_{nm}\ \mathrm{e}^{\mathrm{i}\frac{2\pi}{h}H_{\mathrm{A}}t}\,|\, n\rangle\langle n\,|\, Q(\nu,\vec{\Omega},\lambda)\,|\, m\rangle\langle m\,|\,\mathrm{e}^{-\mathrm{i}\frac{2\pi}{h}H_{\mathrm{A}}t} \\ & = \sum_{nm}\ d_\nu\big[q(\nu,\vec{\Omega},\lambda)\big]_{nm}\ \mathrm{e}^{2\pi\mathrm{i}\,\nu_{nm}t}\ \,|\, n\rangle\langle m\,|\,, \end{aligned} \tag{6.24}$$

where ν_{nm} are the Bohr frequencies

$$\nu_{nm} = \frac{E_n - E_m}{h}\ , \tag{6.25}$$

and where the matrix elements $[q(\nu,\vec{\Omega},\lambda)]_{nm}$ are given by

$$\big[q(\nu,\vec{\Omega},\lambda)\big]_{nm} = \langle n\,|\sum_i\ \vec{p}_i\cdot\vec{e}_\lambda(\vec{\Omega})\ \mathrm{e}^{\mathrm{i}\,\vec{k}\cdot\vec{r}_i}\,|\, m\rangle\ . \tag{6.26}$$

Substituting Eqs. (6.24) and (6.22) into Eq. (6.21) we get

$$B(t) = \sum_{\nu\vec{\Omega}\lambda}\sum_{nm} d_\nu\,\big[q(\nu,\vec{\Omega},\lambda)\big]_{nm}\,|\, n\rangle\langle m\,|\, a(\nu,\vec{\Omega},\lambda)\ \mathrm{e}^{2\pi\mathrm{i}\,(\nu_{nm}-\nu)\,t} \tag{6.27}$$

and, similarly

$$B^\dagger(t) = \sum_{\nu\vec{\Omega}\lambda}\sum_{nm} d_\nu\,\big[q^\dagger(\nu,\vec{\Omega},\lambda)\big]_{nm}\,|\, n\rangle\langle m\,|\, a^\dagger(\nu,\vec{\Omega},\lambda)\ \mathrm{e}^{2\pi\mathrm{i}\,(\nu_{nm}+\nu)\,t}\ , \tag{6.28}$$

where

$$\big[q^\dagger(\nu,\vec{\Omega},\lambda)\big]_{nm} = \langle n\,|\sum_i\ \vec{p}_i\cdot\vec{e}_\lambda(\vec{\Omega})^*\ \mathrm{e}^{-\mathrm{i}\,\vec{k}\cdot\vec{r}_i}\,|\, m\rangle = \big[q(\nu,\vec{\Omega},\lambda)\big]^*_{mn}\ .$$

6.3. The Dipole Approximation

The matrix element $[q(\nu,\vec{\Omega},\lambda)]_{nm}$ defined in Eq. (6.26) can be somewhat simplified by a series of transformations that are discussed here in some detail.

First we observe that the coordinate $\vec{r}_i$ of the i-th electron is measured from an arbitrary origin. Introducing the relative coordinate $\vec{x}_i$, measured from the center of mass of the atomic system, we have

$$\vec{r}_i = \vec{X} + \vec{x}_i\ ,$$

where $\vec{X}$ is the coordinate of the center of mass. With this position, the exponential appearing in the definition of $[q(\nu,\vec{\Omega},\lambda)]_{nm}$ can be written as

$$\mathrm{e}^{\mathrm{i}\vec{k}\cdot\vec{r}_i} = \mathrm{e}^{\mathrm{i}\vec{k}\cdot\vec{X}}\,\mathrm{e}^{\mathrm{i}\vec{k}\cdot\vec{x}_i}\,,$$

and expanding the last exponential in power series

$$\mathrm{e}^{\mathrm{i}\vec{k}\cdot\vec{r}_i} = \mathrm{e}^{\mathrm{i}\vec{k}\cdot\vec{X}}\left[1+\mathrm{i}\,\vec{k}\cdot\vec{x}_i-\frac{1}{2}\left(\vec{k}\cdot\vec{x}_i\right)^2+\cdots\right]. \tag{6.29}$$

Since at optical wavelengths

$$\vec{k}\cdot\vec{x}_i \approx \frac{2\pi a_0}{\lambda} \ll 1\,,$$

we can simply write (*long-wavelength approximation*)

$$\mathrm{e}^{\mathrm{i}\vec{k}\cdot\vec{r}_i} = \mathrm{e}^{\mathrm{i}\vec{k}\cdot\vec{X}}\,, \tag{6.30}$$

which is consistent with our previous approximation of neglecting V_2 in the general expression for the interaction Hamiltonian (see Eq. (6.16)).

To avoid the introduction of a heavier formalism, we suppose the center of mass of the atomic system to be at rest, so that, taking $\vec{X}=0$, we get

$$\left[q(\nu,\vec{\Omega},\lambda)\right]_{nm} = \left\langle n\,\middle|\,\sum_i \vec{p}_i\cdot\vec{e}_\lambda(\vec{\Omega})\,\middle|\,m\right\rangle. \tag{6.31}$$

It should be remarked, however, that the theory presented in the following cannot give – because of the assumption $\vec{X}=$ const. – a consistent description of the phenomena associated with the motion of the atomic system (Doppler effect). We observe that if the coordinate $\vec{X}$ is considered as an ordinary variable describing the physical state of the atomic system (like the relative coordinates $\vec{x}_i$ of the optical electrons) the formalism of Quantum Electrodynamics is able to provide an elegant derivation of the fundamental formulae of the Doppler effect – which basically result from the laws of conservation of momentum and energy. The reader is referred to Louisell (1973) for an example of such derivation; the original idea of deducing the Doppler effect from the momentum-energy conservation is due to Fermi (1932).

Equation (6.31) can be further simplified by considering the expression of the atomic Hamiltonian H_{A}. Neglecting relativistic corrections, we have

$$H_{\mathrm{A}} = \sum_i \frac{p_i^2}{2m} + V_{\mathrm{Coul}}\,,$$

where V_{Coul} represents the electrostatic energy of the electrons which depends on the coordinates $\vec{x}_i$. Using the commutation rule of the operators $\vec{p}_i$ and $\vec{x}_i$, and defining

$$\vec{x} = \sum_i \vec{x}_i\,,$$

we have

$$\left[H_{\rm A}, \vec{x}\right] = -{\rm i}\,\frac{h}{2\pi m}\sum_i \vec{p}_i\,,$$

thus Eq. (6.31) can be written in the form

$$\left[q(\nu,\vec{\Omega},\lambda)\right]_{nm} = 2\pi m\,{\rm i}\,\nu_{nm}\,\langle n\,|\,\vec{x}\cdot\vec{e}_\lambda(\vec{\Omega})|\,m\rangle\,, \tag{6.32}$$

where ν_{nm} is the Bohr frequency defined in Eq. (6.25). This new expression involves the matrix elements of the operator $\vec{x}$, which coincides, apart from the factor -e_0, with the dipole operator

$$\vec{d} = -e_0\,\vec{x}\,.$$

This justifies the alternative name of (*electric*) *dipole approximation* that is given to the long-wavelength approximation (Eq. (6.30)).

An important point concerning the dipole approximation should be explicitly stressed. Substitution of Eq. (6.32) into Eq. (6.27) gives

$$\left[B(t)\right]_{\rm e.d.} = \sum_{\nu\vec{\Omega}\lambda}\sum_{nm}\ {\rm i}\,e_0\nu_{nm}\sqrt{\frac{2\pi h}{\nu\mathcal{V}}}\ \langle n\,|\,\vec{x}\cdot\vec{e}_\lambda(\vec{\Omega})|\,m\rangle \times |\,n\rangle\langle m\,|\,a(\nu,\vec{\Omega},\lambda)\ {\rm e}^{2\pi{\rm i}\,(\nu_{nm}-\nu)\,t}\,, \tag{6.33}$$

where Eq. (6.19) has been used. This expression can be compared with a similar expression that is obtained by assuming a priori that the interaction Hamiltonian has the form

$$V' = \sum_i e_0\,\vec{x}_i\cdot\vec{E}(\vec{r}_i)$$

instead of the form (6.17). Substituting Eq. (4.33) for $\vec{E}(\vec{r}_i)$, passing to the interaction picture, and adopting again the long-wavelength approximation, we get

$$V'_{\rm I}(t) = {\rm e}^{{\rm i}\frac{2\pi}{h}H_0 t}\ V'\ {\rm e}^{-{\rm i}\frac{2\pi}{h}H_0 t} = B'(t) + B'^{\dagger}(t)\,,$$

where

$$B'(t) = \sum_{\nu\vec{\Omega}\lambda}\sum_{nm}\ {\rm i}\,e_0\sqrt{\frac{2\pi\nu h}{\mathcal{V}}}\ \langle n\,|\,\vec{x}\cdot\vec{e}_\lambda(\vec{\Omega})|\,m\rangle \times |\,n\rangle\langle m\,|\,a(\nu,\vec{\Omega},\lambda)\ {\rm e}^{2\pi{\rm i}\,(\nu_{nm}-\nu)\,t}\,. \tag{6.34}$$

Comparison of Eqs. (6.33) and (6.34) shows that $B'(t)$ can be obtained from $[B(t)]_{\rm e.d.}$ by replacing the factor ν_{nm} with ν. In most physical applications the distinction between these two forms of the interaction Hamiltonian is insignificant. Roughly speaking, this is due to the presence of the rapidly oscillating factor $\exp\left[2\pi{\rm i}\,(\nu_{nm}-\nu)\,t\right]$ which, for large values of t, is zero unless $\nu_{nm} = \nu$. A full

discussion on this subject, together with a formal proof on how the two different Hamiltonians can be connected by a similarity transformation (the so-called *Göppert-Mayer transformation*) can be found in Cohen-Tannoudji et al. (1987). In this book we will take for $B(t)$ the more compact expression of Eq. (6.34). The final form of the interaction Hamiltonian is therefore

$$V_{\mathrm{I}}(t) = \big[B(t)\big]_{\mathrm{e.d.}} + \big[B^{\dagger}(t)\big]_{\mathrm{e.d.}} ,$$

where

$$\begin{aligned}
\big[B(t)\big]_{\mathrm{e.d.}} &= -\mathrm{i}\sum_{\nu\vec{\Omega}\lambda}\sum_{nm} c_{\nu}\,\big[\vec{d}\cdot\vec{e}_{\lambda}(\vec{\Omega})\big]_{nm}\,|\,n\rangle\langle m\,|\,a(\nu,\vec{\Omega},\lambda)\;\mathrm{e}^{2\pi\mathrm{i}\,(\nu_{nm}-\nu)\,t} \\
\big[B^{\dagger}(t)\big]_{\mathrm{e.d.}} &= \mathrm{i}\sum_{\nu\vec{\Omega}\lambda}\sum_{nm} c_{\nu}\,\big[\vec{d}\cdot\vec{e}_{\lambda}(\vec{\Omega})^{*}\big]_{nm}\,|\,n\rangle\langle m\,|\,a^{\dagger}(\nu,\vec{\Omega},\lambda)\;\mathrm{e}^{2\pi\mathrm{i}\,(\nu_{nm}+\nu)\,t}
\end{aligned} \tag{6.35}$$

with

$$\begin{aligned}
c_{\nu} &= \sqrt{\frac{2\pi\nu h}{\mathcal{V}}} \\
\vec{d} &= -e_0\sum_{j}\vec{x}_j = -e_0\,\vec{x} \\
\big[\vec{d}\cdot\vec{e}_{\lambda}(\vec{\Omega})\big]_{nm} &= \langle n\,|\,\vec{d}\cdot\vec{e}_{\lambda}(\vec{\Omega})|\,m\rangle = \langle n\,|\,\vec{d}\,|\,m\rangle\cdot\vec{e}_{\lambda}(\vec{\Omega}) \\
&= (\vec{d}\,)_{nm}\cdot\vec{e}_{\lambda}(\vec{\Omega}) \\
\big[\vec{d}\cdot\vec{e}_{\lambda}(\vec{\Omega})^{*}\big]_{nm} &= \langle n\,|\,\vec{d}\cdot\vec{e}_{\lambda}(\vec{\Omega})^{*}|\,m\rangle = \langle n\,|\,\vec{d}\,|\,m\rangle\cdot\vec{e}_{\lambda}(\vec{\Omega})^{*} \\
&= (\vec{d}\,)_{nm}\cdot\vec{e}_{\lambda}(\vec{\Omega})^{*}
\end{aligned} \tag{6.36}$$

and with

$$\big[\vec{d}\cdot\vec{e}_{\lambda}(\vec{\Omega})^{*}\big]_{nm} = \big[\vec{d}\cdot\vec{e}_{\lambda}(\vec{\Omega})\big]^{*}_{mn} . \tag{6.37}$$

In some cases, the dipole matrix elements between two particular levels $|\,n\rangle$ and $|\,m\rangle$ may well be zero. This means that the electric dipole approximation gives no contribution to the transition between such levels, and one must go back to those parts of the interaction Hamiltonian that have been neglected so far. The various terms neglected in the Taylor expansion (6.29) give rise to the *electric quadrupole*, *electric octupole*, etc., Hamiltonians and to those parts of the magnetic-multipole Hamiltonian related to the orbital angular momentum of the electrons, while the second term in the right-hand side of Eq. (6.15) gives rise to those parts of the magnetic-multipole Hamiltonian related to the electron spin.

In particular, let us consider the so-called *magnetic-dipole* transitions. Setting again $\vec{X} = 0$, the contribution of the second term of the expansion (6.29) to the interaction Hamiltonian can still be written in the form of Eq. (6.18) with the

substitutions[1]

$$Q(\nu,\vec{\Omega},\lambda) \to Q_1(\nu,\vec{\Omega},\lambda) = \\ = \frac{\mathrm{i}}{2}\, d_\nu \sum_i \left[\vec{p}_i\cdot\vec{e}_\lambda(\vec{\Omega})\ \vec{k}\cdot\vec{x}_i \ +\ \vec{k}\cdot\vec{x}_i\ \vec{p}_i\cdot\vec{e}_\lambda(\vec{\Omega})\right]$$

$$Q^\dagger(\nu,\vec{\Omega},\lambda) \to Q_1^\dagger(\nu,\vec{\Omega},\lambda) = \\ = -\frac{\mathrm{i}}{2}\, d_\nu \sum_i \left[\vec{p}_i\cdot\vec{e}_\lambda(\vec{\Omega})^*\ \vec{k}\cdot\vec{x}_i \ +\ \vec{k}\cdot\vec{x}_i\ \vec{p}_i\cdot\vec{e}_\lambda(\vec{\Omega})^*\right]. \qquad (6.38)$$

Introducing the orbital angular momentum of the i-th electron,

$$\vec{l}_i = \vec{x}_i \times \vec{p}_i\ ,$$

it can be easily shown that

$$\vec{p}_i\cdot\vec{e}_\lambda(\vec{\Omega})\ \vec{k}\cdot\vec{x}_i \ +\ \vec{k}\cdot\vec{x}_i\ \vec{p}_i\cdot\vec{e}_\lambda(\vec{\Omega}) = \vec{l}_i\cdot\vec{k}\times\vec{e}_\lambda(\vec{\Omega}) \\ + \left[\vec{k}\cdot\vec{x}_i\ \vec{p}_i\cdot\vec{e}_\lambda(\vec{\Omega}) \ +\ \vec{k}\cdot\vec{p}_i\ \vec{x}_i\cdot\vec{e}_\lambda(\vec{\Omega})\right].$$

Recalling that $\vec{k} = 2\pi\nu\,\vec{\Omega}/c$, we obtain

$$Q_1(\nu,\vec{\Omega},\lambda) = \mathrm{i}\, c_\nu \frac{e_0}{2mc}\left\{\sum_i\ \vec{l}_i\cdot\vec{\Omega}\times\vec{e}_\lambda(\vec{\Omega}) \right. \\ \left. + \sum_i\left[\vec{\Omega}\cdot\vec{x}_i\ \vec{p}_i\cdot\vec{e}_\lambda(\vec{\Omega}) + \vec{\Omega}\cdot\vec{p}_i\ \vec{x}_i\cdot\vec{e}_\lambda(\vec{\Omega})\right]\right\}$$

$$Q_1^\dagger(\nu,\vec{\Omega},\lambda) = -\mathrm{i}\, c_\nu \frac{e_0}{2mc}\left\{\sum_i\ \vec{l}_i\cdot\vec{\Omega}\times\vec{e}_\lambda(\vec{\Omega})^* \right. \\ \left. + \sum_i\left[\vec{\Omega}\cdot\vec{x}_i\ \vec{p}_i\cdot\vec{e}_\lambda(\vec{\Omega})^* + \vec{\Omega}\cdot\vec{p}_i\ \vec{x}_i\cdot\vec{e}_\lambda(\vec{\Omega})^*\right]\right\}, \qquad (6.39)$$

where the definitions of d_ν and c_ν (Eqs. (6.19), (6.36)) have been used.

Consider now the second term of the interaction Hamiltonian in Eq. (6.15). Using expression (4.33) for $\vec{B}(\vec{r}\,)$, and adopting the long-wavelength approximation (6.30) with $\vec{X} = 0$, we see that this term can also be written in the form of Eq. (6.18) with the substitutions

$$Q(\nu,\vec{\Omega},\lambda) \to Q_2(\nu,\vec{\Omega},\lambda) = \mathrm{i}\, c_\nu \frac{e_0}{mc}\sum_i\ \vec{s}_i\cdot\vec{\Omega}\times\vec{e}_\lambda(\vec{\Omega})$$

$$Q^\dagger(\nu,\vec{\Omega},\lambda) \to Q_2^\dagger(\nu,\vec{\Omega},\lambda) = -\mathrm{i}\, c_\nu \frac{e_0}{mc}\sum_i\ \vec{s}_i\cdot\vec{\Omega}\times\vec{e}_\lambda(\vec{\Omega})^*\ . \qquad (6.40)$$

[1] It can be easily shown that the operators $\vec{p}_i\cdot\vec{e}_\lambda(\vec{\Omega})$ and $\vec{k}\cdot\vec{x}_i$ commute (cf. footnote 2 on p.242). However, the symmetrized forms in Eqs. (6.38) lead in the most straightforward way to the correct decomposition of the interaction Hamiltonian into the electric-quadrupole and magnetic-dipole terms (see e.g. Shu, 1991).

The terms in square brackets of Eqs. (6.39) are responsible for electric-quadrupole transitions, while the first terms, combined with those in Eqs. (6.40), are responsible for magnetic-dipole transitions. Passing to the interaction picture, the magnetic-dipole Hamiltonian can thus be written in the form

$$\left[V_{\mathrm{I}}(t)\right]_{\mathrm{m.d.}} = \left[B(t)\right]_{\mathrm{m.d.}} + \left[B^{\dagger}(t)\right]_{\mathrm{m.d.}} ,$$

where

$$\left[B(t)\right]_{\mathrm{m.d.}} = -\mathrm{i} \sum_{\nu \vec{\Omega} \lambda} \sum_{nm} c_{\nu} \left[\vec{\mu} \cdot \vec{\Omega} \times \vec{e}_{\lambda}(\vec{\Omega})\right]_{nm} \times |\, n \rangle \langle m \,|\, a(\nu, \vec{\Omega}, \lambda)\, \mathrm{e}^{2\pi \mathrm{i}\,(\nu_{nm} - \nu)\, t}$$

$$\left[B^{\dagger}(t)\right]_{\mathrm{m.d.}} = \mathrm{i} \sum_{\nu \vec{\Omega} \lambda} \sum_{nm} c_{\nu} \left[\vec{\mu} \cdot \vec{\Omega} \times \vec{e}_{\lambda}(\vec{\Omega})^{*}\right]_{nm} \times |\, n \rangle \langle m \,|\, a^{\dagger}(\nu, \vec{\Omega}, \lambda)\, \mathrm{e}^{2\pi \mathrm{i}\,(\nu_{nm} + \nu)\, t} . \tag{6.41}$$

In these expressions the quantity

$$\vec{\mu} = -\frac{e_0}{2mc} \sum_i \left(\vec{l}_i + 2\vec{s}_i\right)$$

is the magnetic moment associated with the electrons, and the matrix elements are defined in strict analogy with Eqs. (6.36).

Comparison of Eqs. (6.41) and (6.35) shows that the magnetic-dipole Hamiltonian can be simply obtained from the electric-dipole Hamiltonian by the formal substitutions

$$\vec{d} \to \vec{\mu} , \qquad \vec{e}_{\lambda}(\vec{\Omega}) \to \vec{\Omega} \times \vec{e}_{\lambda}(\vec{\Omega}) . \tag{6.42}$$

6.4. Approximate Equations of Motion

Substituting Eq. (6.20) into Eq. (6.9), the time variation of any physical observable can be written as

$$\begin{aligned} \frac{\mathrm{d}}{\mathrm{d}t} O(t) = {} & \mathrm{Tr} \left\{ \left(\frac{\mathrm{d}}{\mathrm{d}t} \hat{O}_{\mathrm{I}}(t) \right) \rho_{\mathrm{I}}(t) \right\} - \frac{2\pi \mathrm{i}}{h} \mathrm{Tr} \left\{ \left[\hat{O}_{\mathrm{I}}(t), B(t)\right] \rho_{\mathrm{I}}(0) \right\} \\ & - \frac{2\pi \mathrm{i}}{h} \mathrm{Tr} \left\{ \left[\hat{O}_{\mathrm{I}}(t), B^{\dagger}(t)\right] \rho_{\mathrm{I}}(0) \right\} \\ & - \frac{4\pi^2}{h^2} \mathrm{Tr} \left\{ \int_0^t \left[\left[\hat{O}_{\mathrm{I}}(t), B(t)\right], B(t') \right] \rho_{\mathrm{I}}(t')\, \mathrm{d}t' \right\} + \end{aligned}$$

$$
\begin{aligned}
&- \frac{4\pi^2}{h^2}\,\mathrm{Tr}\left\{ \int_0^t \left[\left[\hat{O}_{\mathrm{I}}(t), B(t) \right], B^{\dagger}(t') \right] \rho_{\mathrm{I}}(t')\,\mathrm{d}t' \right\} \\
&- \frac{4\pi^2}{h^2}\,\mathrm{Tr}\left\{ \int_0^t \left[\left[\hat{O}_{\mathrm{I}}(t), B^{\dagger}(t) \right], B(t') \right] \rho_{\mathrm{I}}(t')\,\mathrm{d}t' \right\} \\
&- \frac{4\pi^2}{h^2}\,\mathrm{Tr}\left\{ \int_0^t \left[\left[\hat{O}_{\mathrm{I}}(t), B^{\dagger}(t) \right], B^{\dagger}(t') \right] \rho_{\mathrm{I}}(t')\,\mathrm{d}t' \right\} . \qquad (6.43)
\end{aligned}
$$

It should be emphasized that this is a very general, exact equation that follows directly from the principles of Quantum Mechanics. Now we are going to introduce a number of assumptions which will enable us to derive a self-contained set of evolution equations for the physical quantities characterizing the interaction of an atomic system with the radiation field.

First of all we suppose that the density operator of the full system is the direct product of the density operators of the individual systems,

$$
\rho_{\mathrm{I}}(t) = \rho_{\mathrm{I}}^{(\mathrm{R})}(t) \otimes \rho_{\mathrm{I}}^{(\mathrm{A})}(t) \qquad \text{for} \quad t \geq 0 \, . \qquad (6.44)
$$

In other words, if $\hat{O}^{(\mathrm{R})}$ is an operator acting only on the radiation field, and $\hat{O}^{(\mathrm{A})}$ is an operator acting only on the atomic system, we assume that the expectation value of their product is equal to the product of their expectation values,

$$
\mathrm{Tr}\left\{ \hat{O}_{\mathrm{I}}^{(\mathrm{R})}\, \hat{O}_{\mathrm{I}}^{(\mathrm{A})}\, \rho_{\mathrm{I}} \right\} = \mathrm{Tr}^{(\mathrm{R})}\left\{ \hat{O}_{\mathrm{I}}^{(\mathrm{R})} \rho_{\mathrm{I}}^{(\mathrm{R})} \right\} \mathrm{Tr}^{(\mathrm{A})}\left\{ \hat{O}_{\mathrm{I}}^{(\mathrm{A})} \rho_{\mathrm{I}}^{(\mathrm{A})} \right\} ,
$$

where $\mathrm{Tr}^{(\mathrm{R})}$ and $\mathrm{Tr}^{(\mathrm{A})}$ denote tracing over the states of the radiation field and of the atomic system, respectively.

The physical meaning of this approximation is that the radiation field and the atomic system are supposed to be uncorrelated. At time $t = 0$ (when the interaction starts) this is indeed a reasonable approximation to describe the interaction between light and matter in an environment like a stellar atmosphere. In such an environment an atom interacts with radiation quanta that have been emitted at typical distances of the order of many kilometers, so that atom-radiation correlations can be safely neglected. The above approximation is also valid in laboratory experiments, provided the light source is physically separated from the cell (or analogous device) containing the atoms. By contrast, the approximation breaks down in other physical conditions (like for instance in lasers, where atom-radiation correlations play a major role).

Equation (6.44) postulates, however, that the uncorrelation between the radiation field and the atomic system persists for $t > 0$. When Eq. (6.44) is substituted into Eq. (6.43), we obtain an equation which can be considered as the lowest-order approximation to the exact equation of motion. This approximation is justified when the relaxation time of the density operator, t_{r}, is much longer than the typical temporal factors which appear in Eq. (6.43) when the explicit expressions of

$B(t)$ and $B^\dagger(t)$ are used (Eqs. (6.27)-(6.28), or (6.35)-(6.36) in the dipole approximation).

Our second assumption concerns the properties of the radiation field, and can be expressed by the set of conditions

$$\mathrm{Tr}^{(\mathrm{R})}\left\{a(\nu,\vec{\Omega},\lambda)\;\rho_{\mathrm{I}}^{(\mathrm{R})}(t)\right\} = \mathrm{Tr}^{(\mathrm{R})}\left\{a^\dagger(\nu,\vec{\Omega},\lambda)\;\rho_{\mathrm{I}}^{(\mathrm{R})}(t)\right\} = 0 \tag{6.45}$$

$$\mathrm{Tr}^{(\mathrm{R})}\left\{a(\nu,\vec{\Omega},\lambda)\,a(\nu',\vec{\Omega}',\lambda')\;\rho_{\mathrm{I}}^{(\mathrm{R})}(t)\right\} = 0 \tag{6.46a}$$

$$\mathrm{Tr}^{(\mathrm{R})}\left\{a^\dagger(\nu,\vec{\Omega},\lambda)\,a^\dagger(\nu',\vec{\Omega}',\lambda')\;\rho_{\mathrm{I}}^{(\mathrm{R})}(t)\right\} = 0 \tag{6.46b}$$

$$\mathrm{Tr}^{(\mathrm{R})}\left\{a^\dagger(\nu,\vec{\Omega},\lambda)\,a(\nu',\vec{\Omega}',\lambda')\;\rho_{\mathrm{I}}^{(\mathrm{R})}(t)\right\} = 0 \quad \text{unless} \quad \nu=\nu',\,\vec{\Omega}=\vec{\Omega}'\,. \tag{6.47}$$

Equation (6.45) means that the expectation value of any observable which is linear either in the destruction or the creation operator of the radiation field is zero. If we consider, for instance, the expectation value of the electric or magnetic field (whose associated operators are given, in the Schrödinger picture, by Eqs. (4.33)) we have

$$\left\langle\vec{E}(\vec{r},t)\right\rangle = \mathrm{Tr}^{(\mathrm{R})}\left\{\mathrm{e}^{\mathrm{i}\frac{2\pi}{h}H_0 t}\;\vec{E}(\vec{r})\;\mathrm{e}^{-\mathrm{i}\frac{2\pi}{h}H_0 t}\;\rho_{\mathrm{I}}^{(\mathrm{R})}(t)\right\} = 0$$

and, similarly

$$\left\langle\vec{B}(\vec{r},t)\right\rangle = 0\,.$$

We thus obtain the analogue of the classical result that the statistical average of such quantities is zero as long as the electromagnetic field can be regarded as the incoherent superposition of different wavetrains with random phases.

Equation (6.45) is, however, somewhat restrictive in that it prevents the consideration of processes involving coherent states of the radiation field (see e.g. Glauber, 1964, for an introduction to these concepts). Nevertheless, this approximation is quite reliable to describe the radiation field typical of a stellar atmosphere, where optical-coherent phenomena are believed to play a totally insignificant role. The same is true for a quite large variety of laboratory experiments.

The meaning of Eqs. (6.46) is similar; indeed, the left-hand side of Eq. (6.46a) represents, up to a factor, the statistical average of the quantity $c_{\vec{k}\lambda}(t)\,c_{\vec{k}'\lambda'}(t)$, where $c_{\vec{k}\lambda}(t)$ is the amplitude of the Fourier component of the electric field vector associated with a particular mode (see Eq. (4.20)). Similarly, the left-hand side of Eq. (6.46b) represents the statistical average of the quantity $c_{\vec{k}\lambda}(t)^* c_{\vec{k}'\lambda'}(t)^*$. Again, the approximation of Eqs. (6.46) is fully justified for electromagnetic fields that can be described as the incoherent superposition of different wavetrains with random phases.

Finally, assumption (6.47) means that no correlations exist between different modes of the radiation field, except for correlations between polarization states within each mode.

Using approximations (6.44)-(6.46) we can considerably simplify Eq. (6.43) for two important classes of operators $\hat{O}_{\mathrm{I}}(t)$, namely the operators acting only on the

atomic system and the operators acting only on the radiation field and having the form $a^\dagger(\nu, \vec{\Omega}, \lambda)\, a(\nu', \vec{\Omega}', \lambda')$. It can be easily shown that for such operators, owing to the form of $B(t)$ and $B^\dagger(t)$ (Eqs. (6.27)-(6.28)), Eq. (6.43) reduces to

$$\begin{aligned}\frac{\mathrm{d}}{\mathrm{d}t} O(t) = \mathrm{Tr}\left\{\left(\frac{\mathrm{d}}{\mathrm{d}t}\hat{O}_\mathrm{I}(t)\right)\rho_\mathrm{I}(t)\right\} \\ - \frac{4\pi^2}{h^2}\,\mathrm{Tr}\left\{\int_0^t \left[\left[\hat{O}_\mathrm{I}(t), B(t)\right], B^\dagger(t')\right]\rho_\mathrm{I}(t')\,\mathrm{d}t'\right\} \\ - \frac{4\pi^2}{h^2}\,\mathrm{Tr}\left\{\int_0^t \left[\left[\hat{O}_\mathrm{I}(t), B^\dagger(t)\right], B(t')\right]\rho_\mathrm{I}(t')\,\mathrm{d}t'\right\}.\end{aligned}$$

Because of the Hermitian character of the density operator and of the cyclic property of the trace, this equation can be rewritten as

$$\begin{aligned}\frac{\mathrm{d}}{\mathrm{d}t} O(t) = \mathrm{Tr}\left\{\left(\frac{\mathrm{d}}{\mathrm{d}t}\hat{O}_\mathrm{I}(t)\right)\rho_\mathrm{I}(t)\right\} \\ - \frac{4\pi^2}{h^2}\,\mathrm{Tr}\left\{\int_0^t \left[\left[\hat{O}_\mathrm{I}(t), B(t)\right], B^\dagger(t')\right]\rho_\mathrm{I}(t')\,\mathrm{d}t'\right\} \\ + \text{c.c.}\left\{\hat{O}_\mathrm{I}(t) \to \hat{O}_\mathrm{I}^\dagger(t)\right\},\end{aligned} \tag{6.48}$$

where the last symbol denotes the quantity that is obtained by taking the complex conjugate of the previous term and by replacing the operator $\hat{O}_\mathrm{I}(t)$ with its adjoint $\hat{O}_\mathrm{I}^\dagger(t)$.

This is the basic equation that will be used in the following to derive the time evolution of the radiation field and of the material system resulting from their mutual interaction.

6.5. Evolution Equations for the Atomic System

A complete description of the atomic system can be obtained through the knowledge of the instantaneous value of the matrix elements of the density operator $\rho^{(\mathrm{A})}(t)$,

$$\rho_{mm'}(t) \equiv \langle m \,|\, \rho^{(\mathrm{A})}(t) \,|\, m' \rangle = \mathrm{Tr}^{(\mathrm{A})}\left\{|\, m' \rangle\langle m \,|\, \rho^{(\mathrm{A})}(t)\right\}, \tag{6.49}$$

where $|\, m \rangle$ and $|\, m' \rangle$ are two arbitrary eigenvectors of the atomic Hamiltonian, and $\rho^{(\mathrm{A})}(t)$ is the time-dependent density operator of the atomic system expressed in the Schrödinger picture.

From Eq. (3.87) we have

$$\rho^{(\mathrm{A})}(t) = \mathrm{Tr}^{(\mathrm{R})}\left\{\rho(t)\right\},$$

where $\rho(t)$ is the density operator of the whole system, so that we can also write

$$\rho_{mm'}(t) = \mathrm{Tr}\left\{ |\, m' \rangle \langle m \,|\, \rho(t) \right\} .$$

If we now pass to the interaction picture, we get

$$\rho_{mm'}(t) = \mathrm{Tr}\left\{ \hat{O}_{\mathrm{I}}(t)\, \rho_{\mathrm{I}}(t) \right\} , \tag{6.50}$$

where $\hat{O}_{\mathrm{I}}(t)$ is given by (see Eqs. (6.5) and (6.10))

$$\hat{O}_{\mathrm{I}}(t) = \mathrm{e}^{\mathrm{i}\frac{2\pi}{h} H_{\mathrm{A}} t}\ |\, m' \rangle \langle m \,|\ \mathrm{e}^{-\mathrm{i}\frac{2\pi}{h} H_{\mathrm{A}} t} = |\, m' \rangle \langle m \,|\ \mathrm{e}^{2\pi \mathrm{i}\, \nu_{m'm} t} . \tag{6.51}$$

Thus the density-matrix element $\rho_{mm'}(t)$ represents the expectation value of an operator given by $\hat{O} = |\, m' \rangle \langle m \,|$ in the Schrödinger picture, and by Eq. (6.51) in the interaction picture.

To derive the time evolution of $\rho_{mm'}(t)$ we will now apply Eq. (6.48), taking for $B(t)$ and $B^{\dagger}(t)$ their expressions in the electric-dipole approximation (Eqs. (6.35)). The first term is easily evaluated; from Eqs. (6.51) and (6.50) we get

$$\begin{aligned} \mathrm{Tr}\left\{ \left(\frac{\mathrm{d}}{\mathrm{d}t} \hat{O}_{\mathrm{I}}(t) \right) \rho_{\mathrm{I}}(t) \right\} &= 2\pi\, \mathrm{i}\, \nu_{m'm}\ \mathrm{Tr}\left\{ |\, m' \rangle \langle m \,|\ \mathrm{e}^{2\pi \mathrm{i}\, \nu_{m'm} t}\ \rho_{\mathrm{I}}(t) \right\} \\ &= 2\pi\, \mathrm{i}\, \nu_{m'm}\ \ \rho_{mm'}(t) . \end{aligned} \tag{6.52}$$

For the second term we have, on the contrary, a rather involved expression

$$\begin{aligned} &\left[\left[\hat{O}_{\mathrm{I}}(t), B(t) \right], B^{\dagger}(t') \right] = \\ &= \sum_{\nu \vec{\Omega} \lambda} \sum_{\nu' \vec{\Omega}' \lambda'} c_{\nu} c_{\nu'} \sum_{nn'} \sum_{rr'} \left[\vec{d} \cdot \vec{e}_{\lambda}(\vec{\Omega}) \right]_{nn'} \left[\vec{d} \cdot \vec{e}_{\lambda'}(\vec{\Omega}')^{*} \right]_{rr'} \\ &\qquad \times\ \mathrm{e}^{2\pi \mathrm{i}\, (\nu_{m'm} + \nu_{nn'} - \nu)\, t + 2\pi \mathrm{i}\, (\nu_{rr'} + \nu')\, t'}\ \ \mathcal{C} , \end{aligned} \tag{6.53}$$

where $\mathcal{C}$ is the double commutator

$$\mathcal{C} = \left[\left[|\, m' \rangle \langle m \,|\, , |\, n \rangle \langle n' \,|\, a(\nu, \vec{\Omega}, \lambda) \right] , |\, r \rangle \langle r' \,|\, a^{\dagger}(\nu', \vec{\Omega}', \lambda') \right] .$$

$\mathcal{C}$ can be easily evaluated using the commutation rule of the creation and destruction operators (Eq. (4.32)), and the commutation rule of the projection operators

$$\left[|\, a \rangle \langle b \,|\, , |\, c \rangle \langle d \,| \right] = \delta_{bc}\, |\, a \rangle \langle d \,| - \delta_{ad}\, |\, c \rangle \langle b \,| .$$

After some algebra, rearranging the final result in such a way that $a^\dagger$-operators precede a-operators, we get

$$\begin{aligned}\mathcal{C} = \; & \delta_{mn}\,\delta_{n'r}\,|\,m'\rangle\langle r'\,|\,\Big(a^\dagger(\nu',\vec{\Omega}',\lambda')\,a(\nu,\vec{\Omega},\lambda) \;+\; \delta_{\nu\nu'}\,\delta_{\vec{\Omega}\vec{\Omega}'}\,\delta_{\lambda\lambda'}\Big) \\ & - \delta_{mn}\,\delta_{m'r'}\,|\,r\rangle\langle n'\,|\,a^\dagger(\nu',\vec{\Omega}',\lambda')\,a(\nu,\vec{\Omega},\lambda) \\ & - \delta_{m'n'}\,\delta_{mr}\,|\,n\rangle\langle r'\,|\,\Big(a^\dagger(\nu',\vec{\Omega}',\lambda')\,a(\nu,\vec{\Omega},\lambda) \;+\; \delta_{\nu\nu'}\,\delta_{\vec{\Omega}\vec{\Omega}'}\,\delta_{\lambda\lambda'}\Big) \\ & + \delta_{m'n'}\,\delta_{nr'}\,|\,r\rangle\langle m\,|\,a^\dagger(\nu',\vec{\Omega}',\lambda')\,a(\nu,\vec{\Omega},\lambda)\;. \end{aligned} \tag{6.54}$$

Substituting this expression into Eq. (6.53) and renaming the summation indices in the first line of Eq. (6.54) according to

$$n' = r \to n\,, \qquad r' \to m''\,,$$

we obtain

$$\begin{aligned}&\Big[\big[\hat{O}_{\rm I}(t),B(t)\big],B^\dagger(t')\Big] = \\ &= \sum_{\nu\vec{\Omega}\lambda}\sum_{\nu'\vec{\Omega}'\lambda'} c_\nu c_{\nu'} \sum_{nm''} \big[\vec{d}\cdot\vec{e}_\lambda(\vec{\Omega})\big]_{mn}\big[\vec{d}\cdot\vec{e}_{\lambda'}(\vec{\Omega}')^*\big]_{nm''} \\ &\qquad\qquad \times\; {\rm e}^{2\pi{\rm i}\,(\nu_{m'n}-\nu)\,t\,+\,2\pi{\rm i}\,(\nu_{nm''}+\nu')\,t'}\;\;|\,m'\rangle\langle m''\,| \\ &\qquad\qquad \times\Big(a^\dagger(\nu'\vec{\Omega}'\lambda')\,a(\nu,\vec{\Omega},\lambda) + \delta_{\nu\nu'}\,\delta_{\vec{\Omega}\vec{\Omega}'}\,\delta_{\lambda\lambda'}\Big) \\ &\quad + (\text{other terms})\;, \end{aligned} \tag{6.55}$$

where '(other terms)' denotes the contribution arising from the other lines of Eq. (6.54).

Now we multiply Eq. (6.55) by $\rho_{\rm I}(t')$ and evaluate the trace. Using the approximations of Eqs. (6.44) and (6.47), and observing that

$$\nu_{nm''} = \nu_{m'm''} - \nu_{m'n}\;,$$

we get

$$\begin{aligned}&{\rm Tr}\,\Big\{\Big[\big[\hat{O}_{\rm I}(t),B(t)\big],B^\dagger(t')\Big]\,\rho_{\rm I}(t')\Big\} = \\ &= \sum_{\nu\vec{\Omega}\lambda\lambda'} c_\nu^2 \sum_{nm''} \big[\vec{d}\cdot\vec{e}_\lambda(\vec{\Omega})\big]_{mn}\big[\vec{d}\cdot\vec{e}_{\lambda'}(\vec{\Omega})^*\big]_{nm''}\;{\rm e}^{2\pi{\rm i}\,(\nu_{m'n}-\nu)(t-t')} \\ &\qquad\qquad \times {\rm Tr}^{(\rm A)}\Big\{|\,m'\rangle\langle m''\,|\;{\rm e}^{2\pi{\rm i}\,\nu_{m'm''}t'}\;\rho_{\rm I}^{(\rm A)}(t')\Big\} \\ &\qquad\qquad \times {\rm Tr}^{(\rm R)}\Big\{\big(a^\dagger(\nu,\vec{\Omega},\lambda')\,a(\nu,\vec{\Omega},\lambda) \;+\; \delta_{\lambda\lambda'}\big)\;\rho_{\rm I}^{(\rm R)}(t')\Big\} \\ &\quad + (\text{other terms})\;. \end{aligned} \tag{6.56}$$

The two separate traces appearing in this equation can be easily identified in terms of physical observables. The trace over (A) is nothing but the density-matrix element $\rho_{m''m'}(t')$ (see Eqs. (6.49), (6.50) and (6.51)), while from Eq. (4.37) we have[1]

$$\mathrm{Tr}^{(\mathrm{R})}\left\{\left(a^{\dagger}(\nu,\vec{\Omega},\lambda')\,a(\nu,\vec{\Omega},\lambda)\,+\,\delta_{\lambda\lambda'}\right)\rho_{\mathrm{I}}^{(\mathrm{R})}(t')\right\}=\frac{c^2}{h\nu^3}\,\left[I_{\lambda'\lambda}(\nu,\vec{\Omega})\right]_{t'}+\delta_{\lambda\lambda'}\,,$$

where $[I_{\lambda'\lambda}(\nu,\vec{\Omega})]_{t'}$ is the polarization tensor of the radiation of frequency ν propagating in the direction $\vec{\Omega}$ at time t'.

Now we have to perform the integral in $\mathrm{d}t'$, between 0 and t, of Eq. (6.56). A possible way to evaluate the integral is to assume that the relaxation time t_{r} characterizing the evolution of the physical quantities of the coupled system is much longer than the typical time-scale over which the oscillating factor

$$\mathrm{e}^{2\pi\mathrm{i}\,(\nu_{m'n}-\nu)(t-t')}$$

varies. Under this assumption we can extract the quantities $\rho_{m''m'}$ and $I_{\lambda'\lambda}$ from the integral (and drop their explicit time dependence) to get

$$\begin{aligned}
&-\frac{4\pi^2}{h^2}\,\mathrm{Tr}\left\{\int_0^t\left[\left[\hat{O}_{\mathrm{I}}(t),B(t)\right],B^{\dagger}(t')\right]\rho_{\mathrm{I}}(t')\,\mathrm{d}t'\right\}=\\
&=-\sum_{\nu\vec{\Omega}\lambda\lambda'}\frac{8\pi^3c^2}{h^2\nu^2\mathcal{V}}\sum_{nm''}\left[\vec{d}\cdot\vec{e}_{\lambda}(\vec{\Omega})\right]_{mn}\left[\vec{d}\cdot\vec{e}_{\lambda'}(\vec{\Omega})^{*}\right]_{nm''}\;\rho_{m''m'}\\
&\qquad\qquad\times\left[I_{\lambda'\lambda}(\nu,\vec{\Omega})\,+\,\frac{h\nu^3}{c^2}\,\delta_{\lambda\lambda'}\right]\int_0^t\mathrm{e}^{2\pi\mathrm{i}\,(\nu_{m'n}-\nu)(t-t')}\,\mathrm{d}t'\\
&\quad+(\text{other terms})\,,
\end{aligned}$$

where the expression of c_ν^2 has been used (see Eqs. (6.36)).

The last integral can be evaluated by standard methods; moreover, because of the above assumption, it is natural to take its asymptotic value for $t\to\infty$. We have

$$\lim_{t\to\infty}\int_0^t\mathrm{e}^{2\pi\mathrm{i}\,(\nu_{ab}-\nu)(t-t')}\,\mathrm{d}t'=\frac{1}{2}\;\delta(\nu_{ab}-\nu)\,+\,\frac{\mathrm{i}}{2\pi}\;\mathrm{P}\frac{1}{\nu_{ab}-\nu}\,,$$

where $\delta(x)$ is the Dirac delta-function and $\mathrm{P}(x)$ means the principal part in the sense of distribution theory.

If we define the complex profile $\Phi(\nu_0-\nu)$ to be

$$\Phi(\nu_0-\nu)=\,\phi(\nu_0-\nu)\,+\,\mathrm{i}\,\psi(\nu_0-\nu)=\,\delta(\nu_0-\nu)\,+\,\frac{\mathrm{i}}{\pi}\;\mathrm{P}\frac{1}{\nu_0-\nu}\,,\qquad(6.57)$$

[1] It follows from Eq. (6.22) that the operator $a^{\dagger}(\nu,\vec{\Omega},\lambda')\,a(\nu,\vec{\Omega},\lambda)$ has the same form in the Schrödinger picture and in the interaction picture.

and transform the summation over the various modes of the radiation field into a double integral via Eq. (4.35), we obtain

$$
\begin{aligned}
&-\frac{4\pi^2}{h^2}\,\mathrm{Tr}\left\{\int_0^t \left[\left[\hat{O}_{\mathrm{I}}(t), B(t)\right], B^{\dagger}(t')\right] \rho_{\mathrm{I}}(t')\,\mathrm{d}t'\right\} = \\
&= -\frac{16\,\pi^4}{h^2 c}\sum_{\lambda\lambda'}\sum_{nm''}\rho_{m''m'}\oint\frac{\mathrm{d}\Omega}{4\pi}\int_0^{\infty}\mathrm{d}\nu\;\left[\vec{d}\cdot\vec{e}_{\lambda}(\vec{\Omega})\right]_{mn}\left[\vec{d}\cdot\vec{e}_{\lambda'}(\vec{\Omega})^*\right]_{nm''} \\
&\qquad\qquad \times\left[I_{\lambda'\lambda}(\nu,\vec{\Omega})+\frac{h\nu^3}{c^2}\,\delta_{\lambda\lambda'}\right]\Phi(\nu_{m'n}-\nu) \\
&\quad + (\text{other terms})\,. \qquad (6.58)
\end{aligned}
$$

This procedure can however be criticized from several points of view. First of all, by assuming $\rho_{m''m'}(t')$ to be independent of t', we give up the possibility of describing those aspects of the phenomena which depend on the 'history' of the density-matrix elements. This is the so-called *secular approximation* (cf. Cohen-Tannoudji et al., 1988), a special case of the *Markov approximation*, which makes impossible the treatment of correlation effects in successive interactions, e.g., frequency redistribution effects in the absorption and re-emission process.

Furthermore, we should realize that the exact time evolution of the density-matrix element $\rho_{mm'}$ is affected by several complicated phenomena that cannot be accounted for by our approach, which is based on a lowest-order expansion in the framework of Quantum Electrodynamics: the finite width of energy levels, their energy shift due to interactions with real and virtual photons, and – when the levels m and m' are non-degenerate – the so-called quantum beats. The last phenomenon consists in oscillations of $\rho_{mm'}$ whose frequencies depend on the spectral characteristics of the incident radiation.

The first two phenomena (finite width and shift of the energy levels) can be taken into account, in a phenomenological way, by replacing the complex profile of Eq. (6.57) with the following

$$
\begin{aligned}
\Phi(\nu_{ab}-\nu) &= \phi(\nu_{ab}-\nu) + \mathrm{i}\,\psi(\nu_{ab}-\nu) \\
&= \frac{1}{\pi}\,\frac{\Gamma_{ab}}{\Gamma_{ab}^2+(\nu_{ab}+\Delta_{ab}-\nu)^2} + \frac{\mathrm{i}}{\pi}\,\frac{\nu_{ab}+\Delta_{ab}-\nu}{\Gamma_{ab}^2+(\nu_{ab}+\Delta_{ab}-\nu)^2}\,, \qquad (6.59a)
\end{aligned}
$$

where

$$
\Gamma_{ab} = \frac{\gamma_{ab}}{4\pi} = \frac{\gamma_a+\gamma_b}{4\pi}\,, \qquad \Delta_{ab} = \Delta_a - \Delta_b\,, \qquad (6.59b)
$$

with γ_a, γ_b the probabilities per unit time that the atom leaves level $|\,a\rangle$ or $|\,b\rangle$, respectively, via spontaneous or stimulated transitions, and Δ_a, Δ_b the frequency shifts of the two levels. Note that the real part of the profile satisfies the normalization

$$
\int_{-\infty}^{\infty}\phi(\nu_{ab}-\nu)\,\mathrm{d}\nu = 1\,. \qquad (6.59c)
$$

The existence of quantum beats affects Eq. (6.58) in such a way that, when off-diagonal density-matrix elements connecting non-degenerate levels are present, the central frequency $\nu_{m'n}$ of the Φ profile is in fact an oscillating quantity. Therefore, the equations obtained from our simple treatment remain valid when the precise frequency position of the Φ profile is not crucial. This requires that the incident radiation field should be flat, i.e. independent of frequency, across a spectral interval $\Delta\nu$ larger than the Bohr frequencies connecting the different m levels and, moreover, larger than the inverse lifetime of each m level. Under this assumption (*flat-spectrum approximation*), the integral over frequency of the first term in the square bracket of Eq. (6.58) is seen to be proportional to

$$I_{\lambda'\lambda}(\nu_{m^*n}, \vec{\Omega}) \ ,$$

where m^* stands equivalently for m, m', or m'' since $I_{\lambda'\lambda}(\nu_{mn}, \vec{\Omega}) = I_{\lambda'\lambda}(\nu_{m'n}, \vec{\Omega}) = I_{\lambda'\lambda}(\nu_{m''n}, \vec{\Omega})$.

Two special cases are worth to be treated separately because, in principle, they do not require the introduction of the flat-spectrum approximation. These are the cases where:

i) all the m levels involved are degenerate;

ii) all the off-diagonal density-matrix elements are zero.

In both cases quantum beats are ineffective, and the first term in the square bracket of Eq. (6.58) leads to an integral of the form

$$\int_0^\infty I_{\lambda'\lambda}(\nu, \vec{\Omega}) \ \Phi(\nu_{m'n} - \nu) \, \mathrm{d}\nu \ .$$

In order to describe both the general case and these two special cases by a unique equation, we write the result of the integration over frequency in the form

$$I_{\lambda'\lambda}(\nu_{\overline{m}n}, \vec{\Omega}) \ ,$$

where the 'mean' Bohr frequency $\nu_{\overline{m}n}$ is given by

$$\nu_{\overline{m}n} = \frac{1}{3} \left(\nu_{mn} + \nu_{m'n} + \nu_{m''n} \right) \ . \tag{6.60}$$

Obviously, the introduction of the 'mean' Bohr frequency is just a formal artifice. In the general case (non-zero density-matrix elements connecting non-degenerate levels), $\nu_{\overline{m}n}$ is a 'label' which reminds that the radiation field at *any* of the Bohr frequencies ν_{mn}, $\nu_{m'n}$, $\nu_{m''n}$ should be considered; in the special cases i) and ii), $\nu_{\overline{m}n}$ reduces to the true Bohr frequency ν_{mn}.

Let's now consider the second term in the square bracket of Eq. (6.58). This term leads to an integral over frequency whose real part is easily evaluated. Taking

into account that the real part of the Φ profile is practically a Dirac delta-function centered at the frequency $\nu_{\overline{m}n}$, we obtain

$$\begin{cases} \frac{h}{c^2}\,\nu_{\overline{m}n}^3 & \text{if} \quad \nu_{\overline{m}n} > 0 \\ 0 & \text{if} \quad \nu_{\overline{m}n} < 0\,. \end{cases}$$

The imaginary part of the Φ profile leads, on the contrary, to a diverging integral. Integrals of such kind are commonly encountered in Quantum Electrodynamics, and describe the finite widths and the shifts of the energy levels due to the interaction of the atom with virtual photons. The actual calculation of the shift of a given level (Lamb shift) involves the removal of the divergence of the integral by standard procedures based on the concept of *mass renormalization*. An example of such calculation for the simple case of the hydrogen atom can be found in Bethe and Salpeter (1957). In the following, these terms related to the Lamb shift will be simply neglected in our equations. Obviously, they can be reintroduced a posteriori in the theory by supposing that the eigenvalues E_n of the atomic Hamiltonian represent the exact energies (including the Lamb shift) of the atomic levels.

The above reasoning allows Eq. (6.58) to be rewritten in the form

$$\begin{aligned} &-\frac{4\pi^2}{h^2}\,\mathrm{Tr}\left\{\int_0^t \Big[\big[\hat{O}_{\mathrm{I}}(t), B(t)\big], B^\dagger(t')\Big]\,\rho_{\mathrm{I}}(t')\,\mathrm{d}t'\right\} = \\ &= -\frac{16\,\pi^4}{h^2 c}\sum_{\lambda\lambda'}\sum_{nm''}\rho_{m''m'}\oint\frac{\mathrm{d}\Omega}{4\pi}\,\big[\vec{d}\cdot\vec{e}_\lambda(\vec{\Omega})\big]_{mn}\big[\vec{d}\cdot\vec{e}_{\lambda'}(\vec{\Omega})^*\big]_{nm''} \\ &\qquad\qquad \times\; I_{\lambda'\lambda}(\nu_{\overline{m}n}, \vec{\Omega}) \\ &\quad -\frac{16\,\pi^4}{hc^3}\sum_{\lambda}\sum_{m''}\rho_{m''m'}\sum_{n}\nu_{\overline{m}n}^3\,\Theta(\nu_{\overline{m}n}) \\ &\qquad\qquad \times\oint\frac{\mathrm{d}\Omega}{4\pi}\,\big[\vec{d}\cdot\vec{e}_\lambda(\vec{\Omega})\big]_{mn}\big[\vec{d}\cdot\vec{e}_\lambda(\vec{\Omega})^*\big]_{nm''} \\ &\quad +\,(\text{other terms})\,, \end{aligned} \tag{6.61}$$

where $\Theta(x)$ is the step-function, which is equal to 1 for positive values of the argument and to 0 otherwise.

The '(other terms)' appearing in this equation are those arising from the second, third, and fourth line of Eq. (6.54). The evaluation of these terms requires calculations quite similar to those developed above. Once these terms have been evaluated (by introducing the relevant 'mean' Bohr frequencies as in Eq. (6.60)), we substitute Eqs. (6.61) and (6.52) into Eq. (6.48) and we add the term resulting from the complex conjugate of Eq. (6.61) with the interchange $m \rightleftarrows m'$ (this interchange transforms the operator $\hat{O}_{\mathrm{I}}(t)$ defined in Eq. (6.51) into $\hat{O}_{\mathrm{I}}^\dagger(t)$).

After some algebra, which involves several operations of index renaming, we obtain the evolution equations for the density-matrix elements $\rho_{mm'}$ (usually called

the *statistical equilibrium equations*) in the form[1]

$$\begin{aligned}\frac{\mathrm{d}}{\mathrm{d}t}\,\rho_{mm'} &= -2\pi\,\mathrm{i}\,\nu_{mm'}\,\rho_{mm'}\\ &\quad+\sum_{nn'}\,\rho_{nn'}\,T_{\mathrm{A}}(m,m',n,n')\\ &\quad+\sum_{pp'}\,\rho_{pp'}\,T_{\mathrm{E}}(m,m',p,p')\\ &\quad+\sum_{pp'}\,\rho_{pp'}\,T_{\mathrm{S}}(m,m',p,p')\\ &\quad-\sum_{m''}\Big[\rho_{mm''}\,R_{\mathrm{A}}(m,m',m'')\,+\,\rho_{m''m'}\,R_{\mathrm{A}}(m',m'',m)\Big]\\ &\quad-\sum_{m''}\Big[\rho_{mm''}\,R_{\mathrm{E}}(m'',m,m')+\,\rho_{m''m'}\,R_{\mathrm{E}}(m,m',m'')\Big]\\ &\quad-\sum_{m''}\Big[\rho_{mm''}\,R_{\mathrm{S}}(m'',m,m')\,+\,\rho_{m''m'}\,R_{\mathrm{S}}(m,m',m'')\Big]\,,\end{aligned}\tag{6.62}$$

where

$$T_{\mathrm{A}}(m,m',n,n')=\frac{32\pi^4}{h^2c}\sum_{\lambda\lambda'}\oint\frac{\mathrm{d}\Omega}{4\pi}\,\big[\vec{d}\cdot\vec{e}_\lambda(\vec{\Omega})\big]_{mn}\big[\vec{d}\cdot\vec{e}_{\lambda'}(\vec{\Omega})^*\big]_{n'm'}\times I_{\lambda'\lambda}(\nu_{\overline{mn}},\vec{\Omega})$$

$$T_{\mathrm{E}}(m,m',p,p')=\frac{32\pi^4}{hc^3}\sum_{\lambda}\oint\frac{\mathrm{d}\Omega}{4\pi}\,\big[\vec{d}\cdot\vec{e}_\lambda(\vec{\Omega})\big]_{p'm'}\big[\vec{d}\cdot\vec{e}_{\lambda}(\vec{\Omega})^*\big]_{mp}\times \nu^3_{\overline{pm}}\,\Theta(\nu_{\overline{pm}})$$

$$T_{\mathrm{S}}(m,m',p,p')=\frac{32\pi^4}{h^2c}\sum_{\lambda\lambda'}\oint\frac{\mathrm{d}\Omega}{4\pi}\,\big[\vec{d}\cdot\vec{e}_\lambda(\vec{\Omega})\big]_{p'm'}\big[\vec{d}\cdot\vec{e}_{\lambda'}(\vec{\Omega})^*\big]_{mp}\times I_{\lambda'\lambda}(\nu_{\overline{pm}},\vec{\Omega})$$

$$R_{\mathrm{A}}(m,m',m'')=\sum_{p}\frac{16\pi^4}{h^2c}\sum_{\lambda\lambda'}\oint\frac{\mathrm{d}\Omega}{4\pi}\,\big[\vec{d}\cdot\vec{e}_\lambda(\vec{\Omega})\big]_{pm'}\big[\vec{d}\cdot\vec{e}_{\lambda'}(\vec{\Omega})^*\big]_{m''p}\times I_{\lambda'\lambda}(\nu_{\overline{pm}},\vec{\Omega})$$

[1] It should be recalled that from Eqs. (1.37), (3.80), and (6.37) one has the relations

$$I_{\lambda\lambda'}(\nu,\vec{\Omega})^*=I_{\lambda'\lambda}(\nu,\vec{\Omega})\,,\qquad \rho^*_{ab}=\rho_{ba}\,,\qquad [\,\vec{d}\cdot\vec{e}_\lambda(\vec{\Omega})]^*_{ab}=[\,\vec{d}\cdot\vec{e}_\lambda(\vec{\Omega})^*]_{ba}\,.$$

$$R_{\rm E}(m,m',m'') = \sum_n \frac{16\pi^4}{hc^3} \sum_\lambda \oint \frac{{\rm d}\Omega}{4\pi} \left[\vec{d}\cdot\vec{e}_\lambda(\vec{\Omega})\right]_{mn} \left[\vec{d}\cdot\vec{e}_\lambda(\vec{\Omega})^*\right]_{nm''} \times \nu_{\overline{mn}}^3 \, \Theta(\nu_{\overline{mn}})$$

$$R_{\rm S}(m,m',m'') = \sum_n \frac{16\pi^4}{h^2c} \sum_{\lambda\lambda'} \oint \frac{{\rm d}\Omega}{4\pi} \left[\vec{d}\cdot\vec{e}_\lambda(\vec{\Omega})\right]_{mn} \left[\vec{d}\cdot\vec{e}_{\lambda'}(\vec{\Omega})^*\right]_{nm''} \times I_{\lambda'\lambda}(\nu_{\overline{mn}},\vec{\Omega}) \,, \tag{6.63}$$

with

$$\nu_{\overline{rs}} = \frac{1}{4}\left(\nu_{rs} + \nu_{rs'} + \nu_{r's} + \nu_{r's'}\right)$$

$$\nu_{r\overline{s}} = \frac{1}{3}\left(\nu_{rs} + \nu_{rs'} + \nu_{rs''}\right)$$

$$\nu_{\overline{r}s} = \frac{1}{3}\left(\nu_{rs} + \nu_{r's} + \nu_{r''s}\right) . \tag{6.64}$$

The physical meaning of the various terms in Eq. (6.62) can be easily understood. The first term in the right-hand side describes a relaxation of the coherence $\rho_{mm'}$ due to the energy difference between levels $|\, m\rangle$ and $|\, m'\rangle$. This term,which is obviously zero for the coherences between degenerate levels (and in particular for the diagonal elements ρ_{mm} representing the populations), produces in general a relaxation of the coherence $\rho_{mm'}$ which is the stronger, the larger the energy separation between the corresponding levels. Roughly speaking, the coherence between levels $|\, m\rangle$ and $|\, m'\rangle$ turns out to be practically zero when the corresponding Bohr frequency $2\pi\,\nu_{mm'}$ is much larger than the typical rates T and R appearing in the right-hand side of Eq. (6.62). As these rates are usually of order $10^9\,{\rm s}^{-1}$ or smaller, we obtain the following criterion for the disappearance of coherences between levels $|\, m\rangle$ and $|\, m'\rangle$

$$|\,\nu_{mm'}| \gg 1.6\times 10^8 \text{ Hz}$$

or, in other words

$$|\,E_m - E_{m'}| \gg 7\times 10^{-7} \text{ eV} \,. \tag{6.65}$$

The other terms in the right-hand side of Eq. (6.62) represent the rates at which the coherence $\rho_{mm'}$ either increases as a result of *coherence-transfer* from different levels or decreases as a result of *coherence-relaxation* to different levels. Coherence-transfer rates are denoted by the symbol T and all bear a positive sign. These terms are due to absorption from lower levels ($T_{\rm A}$), to spontaneous emission from upper levels ($T_{\rm E}$), and to stimulated emission from upper levels ($T_{\rm S}$). Similarly, coherence-relaxation rates – denoted by the symbol R – are due to absorption towards upper levels ($R_{\rm A}$), to spontaneous emission towards lower levels ($R_{\rm E}$), and to stimulated emission towards lower levels ($R_{\rm S}$). All these rates bear a negative sign. The rates $R_{\rm S}$ and $R_{\rm E}$ originate from the first line of Eq. (6.54); the rate $T_{\rm A}$ from the second,

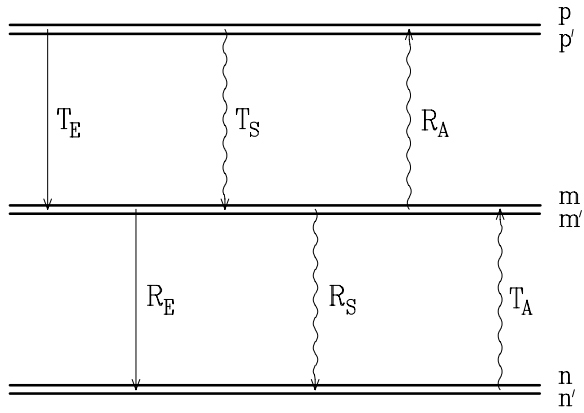

Fig.6.1. The radiative processes contributing to the time evolution of the coherence $\rho_{mm'}$ are schematized in this simplified Grotrian diagram. Straight lines refer to spontaneous emission while wavy lines refer to absorption (arrows pointing upward) or stimulated emission (arrows pointing downward). Coherence-transfer rates are represented by transitions ending in the couple of levels (m, m') while coherence-relaxation rates are represented by transitions originating from these levels. Each process is labelled with the symbol of the corresponding rate.

the rates $T_{\rm S}$ and $T_{\rm E}$ from the third, and the rate $R_{\rm A}$ from the fourth line. The processes described by the different rates are schematically shown in Fig. 6.1.

From the explicit expressions of the various rates (Eqs. (6.63)) it is possible to prove some important properties. With easy transformations, one obtains the conjugation relations

$$
\begin{aligned}
T_{\rm A}(m,m',n,n')^* &= T_{\rm A}(m',m,n',n) \\
T_{\rm E}(m,m',p,p')^* &= T_{\rm E}(m',m,p',p) \\
T_{\rm S}(m,m',p,p')^* &= T_{\rm S}(m',m,p',p) \\
R_{\rm A}(m,m',m'')^* &= R_{\rm A}(m,m'',m') \\
R_{\rm E}(m,m',m'')^* &= R_{\rm E}(m'',m',m) \\
R_{\rm S}(m,m',m'')^* &= R_{\rm S}(m'',m',m)\ .
\end{aligned}
$$

Another property concerns the time evolution of the trace of the density operator. Setting $m' = m$ in Eq. (6.62) and summing over m one finds, after some algebra which involves several operations of index renaming, that the term arising from $T_{\rm A}$ exactly cancels out with the terms arising from $R_{\rm A}$, and, similarly, $T_{\rm E}$ cancels out with $R_{\rm E}$, and $T_{\rm S}$ cancels out with $R_{\rm S}$, so that

$$
\frac{\mathrm{d}}{\mathrm{d}t}\left(\sum_m \rho_{mm}\right) = 0\ .
$$

This property – which should be expected on the basis of Eq. (3.83) – implies that the trace of the density operator of the atomic system can be fixed once and for

all. In many cases the density operator is normalized through the equation

$$\sum_m \rho_{mm} = 1 \,,$$

but different normalizations can be safely employed. Equation (6.62), being linear in the density-matrix elements, is independent of the particular normalization condition employed.

The expressions for the various rates given in Eqs. (6.63) contain matrix elements of the form $[\vec{d}\cdot\vec{e}_\lambda(\vec{\Omega})]_{mn}$. The evaluation of these matrix elements is generally easier using the spherical components of the dipole operator (rather than its Cartesian components).[1] From Eq. (2.83) we have

$$\vec{d}\cdot\vec{e}_\lambda(\vec{\Omega}) = \sum_q (-1)^q \, d_{-q} \left(e_\lambda(\vec{\Omega})\right)_q \,,$$

whence

$$\left[\vec{d}\cdot\vec{e}_\lambda(\vec{\Omega})\right]_{mn} = \sum_q (-1)^q \, (d_{-q})_{mn} \left(e_\lambda(\vec{\Omega})\right)_q \tag{6.66}$$

and, similarly

$$\left[\vec{d}\cdot\vec{e}_{\lambda'}(\vec{\Omega})^*\right]_{mn} = \left[\vec{d}\cdot\vec{e}_{\lambda'}(\vec{\Omega})\right]^*_{nm} = \left[\sum_q (-1)^q \, (d_{-q})_{nm} \left(e_{\lambda'}(\vec{\Omega})\right)_q\right]^* .$$

To shorten notations we introduce the symbols

$$(d_{-q})^*_{nm} \equiv \left[(d_{-q})_{nm}\right]^* , \qquad \left(e_{\lambda'}(\vec{\Omega})\right)^*_q \equiv \left[\left(e_{\lambda'}(\vec{\Omega})\right)_q\right]^* ,$$

so that

$$\left[\vec{d}\cdot\vec{e}_{\lambda'}(\vec{\Omega})^*\right]_{mn} = \sum_q (-1)^q \, (d_{-q})^*_{nm} \left(e_{\lambda'}(\vec{\Omega})\right)^*_q . \tag{6.67}$$

At this point we choose a specific form for the unit vectors $\vec{e}_\lambda(\vec{\Omega})$, which up to now were just the unit vectors – satisfying the relations (4.31) – used to expand the vector potential. From now on we require that these vectors have the form of Eq. (5.141). This choice provides the simplest expression for their spherical components and, moreover, it allows us to use the spherical tensors already introduced in Sect. 5.11.

As a first consequence, we can easily evaluate the angular integrals appearing in the expressions for the rates $T_{\rm E}$ and $R_{\rm E}$ related to spontaneous emission (see Eqs. (6.63)). From Eqs. (6.66), (6.67), (5.140) and (5.143) we have

[1] This is basically related to the Wigner-Eckart theorem, see Sect. 2.8.

$$\sum_{\lambda} \oint \frac{\mathrm{d}\Omega}{4\pi} \left[\vec{d}\cdot\vec{e}_{\lambda}(\vec{\Omega})\right]_{ab} \left[\vec{d}\cdot\vec{e}_{\lambda}(\vec{\Omega})^{*}\right]_{cd} =$$

$$= \sum_{\alpha=\pm 1} \oint \frac{\mathrm{d}\Omega}{4\pi} \sum_{qq'} (-1)^{q+q'} (d_{-q})_{ab} \, (d_{-q'})^{*}_{dc} \left(e_{\alpha}(\vec{\Omega})\right)_{q} \left(e_{\alpha}(\vec{\Omega})\right)^{*}_{q'}$$

$$= \sum_{qq'} (-1)^{q+q'} (d_{-q})_{ab} \, (d_{-q'})^{*}_{dc} \sum_{\alpha=\pm 1} \oint \frac{\mathrm{d}\Omega}{4\pi} \; \mathcal{E}_{qq'}(\alpha,\alpha,\vec{\Omega})$$

$$= \frac{2}{3} \sum_{q} (d_{-q})_{ab} \, (d_{-q})^{*}_{dc} \, . \tag{6.68}$$

Next, recalling the definition of the radiation field tensor $J_{qq'}(\nu)$ (see Eqs. (5.150) and (5.153)), we can rewrite the rates appearing in the statistical equilibrium equations in the more compact form

$$T_{\mathrm{A}}(m,m',n,n') = \frac{32\pi^4}{h^2 c} \sum_{qq'} (-1)^{q+q'} \, (d_{-q})_{mn} \, (d_{-q'})^{*}_{m'n'} \; J_{qq'}(\nu_{\overline{mn}})$$

$$T_{\mathrm{E}}(m,m',p,p') = \frac{64\pi^4}{3hc^3} \sum_{q} \; (d_{-q})_{p'm'} \, (d_{-q})^{*}_{pm} \; \nu^{3}_{\overline{pm}} \, \Theta(\nu_{\overline{pm}})$$

$$T_{\mathrm{S}}(m,m',p,p') = \frac{32\pi^4}{h^2 c} \sum_{qq'} (-1)^{q+q'} \, (d_{-q})_{p'm'} \, (d_{-q'})^{*}_{pm} \; J_{qq'}(\nu_{\overline{pm}})$$

$$R_{\mathrm{A}}(m,m',m'') = \sum_{p} \frac{16\pi^4}{h^2 c} \sum_{qq'} (-1)^{q+q'} \, (d_{-q})_{pm'} \, (d_{-q'})^{*}_{pm''} \; J_{qq'}(\nu_{p\overline{m}})$$

$$R_{\mathrm{E}}(m,m',m'') = \sum_{n} \frac{32\pi^4}{3hc^3} \sum_{q} \; (d_{-q})_{mn} \, (d_{-q})^{*}_{m''n} \; \nu^{3}_{\overline{mn}} \, \Theta(\nu_{\overline{mn}})$$

$$R_{\mathrm{S}}(m,m',m'') = \sum_{n} \frac{16\pi^4}{h^2 c} \sum_{qq'} (-1)^{q+q'} \, (d_{-q})_{mn} \, (d_{-q'})^{*}_{m''n} \; J_{qq'}(\nu_{\overline{mn}}) \, , \tag{6.69}$$

where the various 'mean' Bohr frequencies are defined in Eqs. (6.64).

An important remark should be made about the limit of the statistical equilibrium equations under the hypothesis of neglecting polarization phenomena in the atomic system and of neglecting polarization and anisotropy effects in the radiation field. Let us assume that

$$\rho_{ab} = \rho_a \, \delta_{ab} \, , \qquad I_{\lambda'\lambda}(\nu,\vec{\Omega}) = \frac{1}{2} \, I(\nu) \; \delta_{\lambda'\lambda} \, ,$$

where ρ_a is the population of level $|\, a\rangle$ and $I(\nu)$ is the radiation field intensity. From Eq. (6.62) we have

$$\frac{\mathrm{d}}{\mathrm{d}t} \, \rho_m = \sum_{n} \rho_n \, T_{\mathrm{A}}(m,m,n,n) + \sum_{p} \rho_p \left[T_{\mathrm{E}}(m,m,p,p) + T_{\mathrm{S}}(m,m,p,p)\right]$$

$$- 2 \, \rho_m \left[R_{\mathrm{A}}(m,m,m) + R_{\mathrm{E}}(m,m,m) + R_{\mathrm{S}}(m,m,m)\right] \, .$$

From Eqs. (5.150), (5.153) and (5.143) the radiation field tensor is found to be

$$J_{qq'}(\nu) = \frac{1}{3}\, I(\nu)\ \delta_{qq'}\ .$$

According to Eqs. (6.69) the coherence-transfer rate $T_{\rm A}$ becomes

$$T_{\rm A}(m,m,n,n) = \frac{32\pi^4}{3h^2c}\ |\vec{d}_{mn}|^2\ I(\nu_{mn})\ ,$$

where (see Eq. (2.82))

$$|\vec{d}_{mn}|^2 = |\vec{d}_{nm}|^2 = \vec{d}_{mn}\cdot\vec{d}_{nm} = \sum_q\ |(d_q)_{mn}|^2\ . \tag{6.70}$$

Introducing the Einstein B_{nm} coefficient for the transition from the initial state $|\,n\rangle$ to the final state $|\,m\rangle$ by the standard definition

$$B_{nm} = \frac{32}{3}\frac{\pi^4}{h^2c}\ |\vec{d}_{nm}|^2\ , \tag{6.71}$$

one obtains

$$T_{\rm A}(m,m,n,n) = B_{nm}\, I(\nu_{mn})\ .$$

Performing the same kind of calculations on the other rates one finally gets

$$\begin{aligned}\frac{\rm d}{{\rm d}t}\,\rho_m\ =& \sum_n\ \rho_n\ B_{nm}\, I(\nu_{mn})\\ &+\sum_p\ \rho_p\left[A_{pm} + B_{pm}\, I(\nu_{pm})\right]\\ &-\sum_p\ \rho_m\ B_{mp}\, I(\nu_{pm})\\ &-\sum_n\ \rho_m\left[A_{mn} + B_{mn}\, I(\nu_{mn})\right]\ ,\end{aligned} \tag{6.72}$$

where

$$A_{mn} = \frac{64\pi^4}{3hc^3}\ \nu_{mn}^3\ |\vec{d}_{mn}|^2 = \frac{2h\nu_{mn}^3}{c^2}\ B_{mn} \tag{6.73}$$

is the Einstein coefficient for spontaneous emission from the upper level $|\,m\rangle$ to the lower level $|\,n\rangle$.

Equations (6.72) are the standard statistical equilibrium equations whose derivation, based on heuristic arguments, can be found in various textbooks (see e.g. Mihalas, 1978). They are just a special case of a more general set of equations (Eqs. (6.62)) which have been derived here directly from the principles of Quantum Electrodynamics. Equations (6.62) reduce to Eqs. (6.72) when polarization and anisotropy phenomena are neglected.

6.6. Evolution Equations for the Radiation Field

We derive here the evolution equations for the radiation field by essentially the same method just employed for the atomic system. In particular, we are interested in the time evolution of the polarization tensor $I_{\alpha\beta}(\nu,\vec{\Omega})$ related to a given frequency ν and a given direction $\vec{\Omega}$, whose associated quantum operator is given by Eq. (4.37). As this operator remains unchanged in the interaction picture (see footnote on p. 255), we have just to apply Eq. (6.48) with the operator $\hat{O}_{\rm I}(t)$ given by

$$\hat{O}_{\rm I}(t) = \frac{h\nu^3}{c^2}\, a^\dagger(\nu,\vec{\Omega},\alpha)\, a(\nu,\vec{\Omega},\beta)\ .$$

Since $\mathrm{d}\hat{O}_{\rm I}(t)/\mathrm{d}t = 0$, and since the adjoint operator $\hat{O}_{\rm I}^\dagger(t)$ is obtained from $\hat{O}_{\rm I}(t)$ by exchange of the indices α and β, we get

$$\begin{aligned}
&\frac{\mathrm{d}}{\mathrm{d}t}\, I_{\alpha\beta}(\nu,\vec{\Omega}) = \\
&= -\frac{4\pi^2\nu^3}{hc^2}\ \mathrm{Tr}\left\{ \int_0^t \Big[\big[a^\dagger(\nu,\vec{\Omega},\alpha)\, a(\nu,\vec{\Omega},\beta)\,, B(t)\big], B^\dagger(t')\Big]\, \rho_{\rm I}(t')\,\mathrm{d}t' \right\} \\
&\qquad + \text{c.c.}\ \big\{\alpha \rightleftarrows \beta\big\}\ . \qquad (6.74)
\end{aligned}$$

We start by evaluating the inner commutator, with $B(t)$ given by Eq. (6.35). We have

$$\begin{aligned}
&\big[a^\dagger(\nu,\vec{\Omega},\alpha)\, a(\nu,\vec{\Omega},\beta)\,, B(t)\big] = \\
&= -\mathrm{i} \sum_{\nu'\vec{\Omega}'\lambda'} \sum_{mn} c_{\nu'} \big[\vec{d}\cdot\vec{e}_{\lambda'}(\vec{\Omega}')\big]_{mn} \\
&\qquad\qquad \times |\, m\rangle\langle n\,| \big[a^\dagger(\nu,\vec{\Omega},\alpha)\, a(\nu,\vec{\Omega},\beta)\,, a(\nu',\vec{\Omega}',\lambda')\big]\ \mathrm{e}^{2\pi\mathrm{i}\,(\nu_{mn}-\nu')\,t}\ ,
\end{aligned}$$

and using the commutation properties of the operators a and $a^\dagger$ (Eq. (4.32)) we get

$$\begin{aligned}
\big[a^\dagger(\nu,\vec{\Omega},\alpha)\, a(\nu,\vec{\Omega},\beta)\,, B(t)\big] &= \mathrm{i}\, c_\nu \sum_{mn} \big[\vec{d}\cdot\vec{e}_\alpha(\vec{\Omega})\big]_{mn} \\
&\qquad \times |\, m\rangle\langle n\,|\, a(\nu,\vec{\Omega},\beta)\ \mathrm{e}^{2\pi\mathrm{i}\,(\nu_{mn}-\nu)\,t}\ .
\end{aligned}$$

Thus the double commutator can be written as

$$\begin{aligned}
&\Big[\big[a^\dagger(\nu,\vec{\Omega},\alpha)\, a(\nu,\vec{\Omega},\beta)\,, B(t)\big], B^\dagger(t')\Big] = \\
&= -\sum_{\nu'\vec{\Omega}'\lambda'} \sum_{mn}\sum_{rs} c_\nu c_{\nu'} \big[\vec{d}\cdot\vec{e}_\alpha(\vec{\Omega})\big]_{mn} \big[\vec{d}\cdot\vec{e}_{\lambda'}(\vec{\Omega}')^*\big]_{rs} \\
&\qquad\qquad \times \mathrm{e}^{2\pi\mathrm{i}\,(\nu_{mn}-\nu)\,t + 2\pi\mathrm{i}\,(\nu_{rs}+\nu')\,t'}\ \mathcal{C}\ , \qquad (6.75)
\end{aligned}$$

where $\mathcal{C}$ is the commutator

$$\mathcal{C} = \left[\, |\, m\rangle\langle n\,|\, a(\nu,\vec{\Omega},\beta)\;,\; |\, r\rangle\langle s\,|\, a^\dagger(\nu',\vec{\Omega}',\lambda')\,\right]\;.$$

With some easy algebra, and rearranging the final result in such a way that $a^\dagger$-operators precede a-operators, we obtain

$$\begin{aligned}\mathcal{C} = {} & \delta_{nr}\;|\, m\rangle\langle s\,|\,\Big(a^\dagger(\nu',\vec{\Omega}',\lambda')\,a(\nu,\vec{\Omega},\beta)\;+\;\delta_{\nu\nu'}\,\delta_{\vec{\Omega}\vec{\Omega}'}\,\delta_{\lambda'\beta}\Big)\\ & -\,\delta_{sm}\;|\, r\rangle\langle n\,|\; a^\dagger(\nu',\vec{\Omega}',\lambda')\,a(\nu,\vec{\Omega},\beta)\;. \end{aligned}\tag{6.76}$$

Now we substitute Eq. (6.76) into Eq. (6.75), multiply by $\rho_{\mathrm{I}}(t')$ and take the trace of the resulting operator. With the help of Eqs. (6.44) and (6.47) we obtain

$$\begin{aligned}&\mathrm{Tr}\left\{\Big[\big[a^\dagger(\nu,\vec{\Omega},\alpha)\,a(\nu,\vec{\Omega},\beta)\,,B(t)\big],B^\dagger(t')\Big]\;\rho_{\mathrm{I}}(t')\right\} =\\ &= -\sum_\lambda\sum_{mns} c_\nu^2\;\big[\vec{d}\cdot\vec{e}_\alpha(\vec{\Omega})\big]_{mn}\big[\vec{d}\cdot\vec{e}_\lambda(\vec{\Omega})^*\big]_{ns}\;\mathrm{e}^{\,2\pi\mathrm{i}\,(\nu_{mn}-\nu)(t-t')}\\ &\qquad\times\mathrm{Tr}^{(\mathrm{A})}\Big\{|\, m\rangle\langle s\,|\;\mathrm{e}^{\,2\pi\mathrm{i}\,\nu_{ms}t'}\;\rho_{\mathrm{I}}^{(\mathrm{A})}(t')\Big\}\\ &\qquad\times\mathrm{Tr}^{(\mathrm{R})}\Big\{\big(a^\dagger(\nu,\vec{\Omega},\lambda)\,a(\nu,\vec{\Omega},\beta)\;+\;\delta_{\lambda\beta}\big)\;\rho_{\mathrm{I}}^{(\mathrm{R})}(t')\Big\}\\ &\quad+\sum_\lambda\sum_{mnr} c_\nu^2\;\big[\vec{d}\cdot\vec{e}_\alpha(\vec{\Omega})\big]_{mn}\big[\vec{d}\cdot\vec{e}_\lambda(\vec{\Omega})^*\big]_{rm}\;\mathrm{e}^{\,2\pi\mathrm{i}\,(\nu_{mn}-\nu)(t-t')}\\ &\qquad\times\mathrm{Tr}^{(\mathrm{A})}\Big\{|\, r\rangle\langle n\,|\;\mathrm{e}^{\,2\pi\mathrm{i}\,\nu_{rn}t'}\;\rho_{\mathrm{I}}^{(\mathrm{A})}(t')\Big\}\\ &\qquad\times\mathrm{Tr}^{(\mathrm{R})}\Big\{a^\dagger(\nu,\vec{\Omega},\lambda)\,a(\nu,\vec{\Omega},\beta)\;\rho_{\mathrm{I}}^{(\mathrm{R})}(t')\Big\}\;. \end{aligned}$$

Similarly to the previous section, we identify the various traces in this equation with the corresponding physical observables. Next we perform the integral in $\mathrm{d}t'$ between 0 and t (for $t\to\infty$) and we substitute into Eq. (6.74) to obtain, after some index renaming

$$\begin{aligned}&\frac{\mathrm{d}}{\mathrm{d}t}\,I_{\alpha\beta}(\nu,\vec{\Omega}) =\\ &= \left\{\frac{4\pi^3\nu}{h\mathcal{V}}\sum_\gamma\sum_{mm'n}\;\big[\vec{d}\cdot\vec{e}_\alpha(\vec{\Omega})\big]_{mn}\big[\vec{d}\cdot\vec{e}_\gamma(\vec{\Omega})^*\big]_{nm'}\;\rho_{m'm}\right.\\ &\qquad\left.\times\,\Phi(\nu_{mn}-\nu)\;I_{\gamma\beta}(\nu,\vec{\Omega})\right.\\ &\quad+\frac{4\pi^3\nu^4}{c^2\mathcal{V}}\sum_{mm'n}\;\big[\vec{d}\cdot\vec{e}_\alpha(\vec{\Omega})\big]_{mn}\big[\vec{d}\cdot\vec{e}_\beta(\vec{\Omega})^*\big]_{nm'}\;\rho_{m'm}\,\Phi(\nu_{mn}-\nu)\;+ \end{aligned}$$

$$- \frac{4\pi^3\nu}{h\mathcal{V}} \sum_{\gamma} \sum_{mnn'} \left[\vec{d}\cdot\vec{e}_{\alpha}(\vec{\Omega})\right]_{mn} \left[\vec{d}\cdot\vec{e}_{\gamma}(\vec{\Omega})^*\right]_{n'm} \rho_{nn'} \times \Phi(\nu_{mn}-\nu)\, I_{\gamma\beta}(\nu,\vec{\Omega}) \Bigg\}$$

$$+ \text{c.c.} \left\{\alpha \rightleftarrows \beta\right\} , \tag{6.77}$$

where the complex profile Φ is given by Eq. (6.57).

However, the above derivation is not fully justified, because it neglects the finite widths and the shifts of the atomic energy levels due to interactions with real and virtual photons, and quantum beats (see the analogous discussion following Eq. (6.58)). The first two phenomena can be taken into account, in a phenomenological way, by assuming the Φ profile in Eq. (6.77) to have the form of Eq. (6.59a) rather than Eq. (6.57). Even with this substitution, the validity of Eq. (6.77) is subjected to a basic restriction related to the existence of quantum beats: in order that our formalism can be consistent, the density-matrix elements appearing in the equation must be deduced from the statistical equilibrium equations under the secular approximation, which implies the flat-spectrum approximation illustrated in the preceding section. Obviously, the formalism presented here cannot describe frequency-redistribution phenomena.

Equation (6.77) must be interpreted as an evolution equation for the polarization tensor in the phase space of the photon occupation numbers. To express it as an evolution equation in the ordinary three-dimensional space, we attach an explicit time and space dependence to the polarization tensor. In other words, we replace $I_{\alpha\beta}(\nu,\vec{\Omega})$ by $I_{\alpha\beta}(\nu,\vec{\Omega}\,;t,\vec{x}\,)$ and we regard it as the polarization tensor that is propagating at time t through the point P of coordinate $\vec{x}$ in the direction $\vec{\Omega}$, at frequency ν. The time derivative calculated in Eq. (6.77) is nothing but

$$\lim_{\Delta t\to 0} \frac{I_{\alpha\beta}(\nu,\vec{\Omega}\,;t+\Delta t,\vec{x}+\vec{\Omega}\,c\,\Delta t) - I_{\alpha\beta}(\nu,\vec{\Omega}\,;t,\vec{x}\,)}{\Delta t} = \\ = \frac{\partial}{\partial t} I_{\alpha\beta}(\nu,\vec{\Omega}\,;t,\vec{x}\,) + c\,\vec{\Omega}\cdot\operatorname{grad} I_{\alpha\beta}(\nu,\vec{\Omega}\,;t,\vec{x}\,) .$$

Denoting by s the spatial coordinate along the direction $\vec{\Omega}$, we can thus replace the time derivative in Eq. (6.77) with

$$\frac{\mathrm{d}}{\mathrm{d}t} \to \frac{\partial}{\partial t} + c\,\frac{\mathrm{d}}{\mathrm{d}s} .$$

Next we observe that Eq. (6.77) has been obtained under the assumption that the radiation field, defined in the normalization box of volume $\mathcal{V}$, interacts with a single atomic system. For an ensemble of uncorrelated atomic systems we have just to multiply the right-hand side by the number of such systems, with the result that the factor $1/\mathcal{V}$ is replaced by the number density $\mathcal{N}$. Equation (6.77) can then be

cast into the form of a radiative transfer equation

$$\left(\frac{1}{c}\,\frac{\partial}{\partial t} + \frac{\mathrm{d}}{\mathrm{d}s}\right) I_{\alpha\beta}(\nu,\vec{\Omega}) = -\sum_{\gamma}\left[g_{\alpha\gamma}\, I_{\gamma\beta}(\nu,\vec{\Omega}) \;+\; g^{*}_{\beta\gamma}\, I_{\alpha\gamma}(\nu,\vec{\Omega})\right] + \sum_{\gamma}\left[h_{\alpha\gamma}\, I_{\gamma\beta}(\nu,\vec{\Omega}) \;+\; h^{*}_{\beta\gamma}\, I_{\alpha\gamma}(\nu,\vec{\Omega})\right] + \frac{1}{2}\left[f_{\alpha\beta} + f^{*}_{\beta\alpha}\right], \tag{6.78}$$

where

$$\begin{aligned} g_{\alpha\beta} &= \frac{4\pi^3\nu}{ch}\,\mathcal{N}\sum_{mnn'}\left[\vec{d}\cdot\vec{e}_{\alpha}(\vec{\Omega})\right]_{mn}\left[\vec{d}\cdot\vec{e}_{\beta}(\vec{\Omega})^{*}\right]_{n'm}\;\rho_{nn'}\,\Phi(\nu_{mn}-\nu) \\ h_{\alpha\beta} &= \frac{4\pi^3\nu}{ch}\,\mathcal{N}\sum_{mm'n}\left[\vec{d}\cdot\vec{e}_{\alpha}(\vec{\Omega})\right]_{mn}\left[\vec{d}\cdot\vec{e}_{\beta}(\vec{\Omega})^{*}\right]_{nm'}\;\rho_{m'm}\,\Phi(\nu_{mn}-\nu) \\ f_{\alpha\beta} &= \frac{2h\nu^3}{c^2}\;h_{\alpha\beta}\;. \end{aligned} \tag{6.79}$$

The physical interpretation of the terms in the right-hand side of Eq. (6.78) is straightforward. The first term, which bears a negative sign and which results from the third line in Eq. (6.77), describes the transfer effects produced by the absorption of radiation. It is proportional to the coherence $\rho_{nn'}$ between two levels $|\,n\rangle$ and $|\,n'\rangle$ which are connected to the upper level $|\,m\rangle$ by dipole transitions. The imaginary part of the complex Φ profile describes the associated anomalous dispersion effects.

In Chap. 5 we already found – using the formalism of classical electrodynamics – a transfer equation for the polarization tensor (cf. Eq. (5.24)).[1] Comparison with Eq. (6.78) shows that the tensor $\boldsymbol{g}$ is just the quantum analogue of the propagation tensor $\boldsymbol{G}$ defined in Eq. (5.22) (with $\boldsymbol{G} \rightarrow \boldsymbol{g}^{*}$). This analogy provides an interesting relation between the refractive index and the matrix elements of the dipole operator between eigenstates of the atomic system.

The second term in Eq. (6.78), which bears a positive sign and which results from the first line in Eq. (6.77), describes the transfer effects produced by stimulated emission of radiation. This term is proportional to the coherence $\rho_{m'm}$ between two levels $|\,m'\rangle$ and $|\,m\rangle$ which are connected to the lower level $|\,n\rangle$ by dipole transitions. We see the appearance, via the imaginary part of the complex Φ profile, of anomalous dispersion effects associated with stimulated emission of radiation. This term has no analogue in the classical equation, an obvious consequence of the quantum nature of stimulated emission.

Finally, the third term in Eq. (6.78), which again bears a positive sign and which results from the second line in Eq. (6.77), describes the transfer effects produced

[1] Equation (5.24) involves the tensor $\boldsymbol{J}$, while Eq. (6.78) involves the tensor $\boldsymbol{I}$. We recall that $\boldsymbol{I}$ and $\boldsymbol{J}$ are proportional (see Eq. (1.36)).

by spontaneous emission of radiation. The classical analogue of this term has been deduced for the special case of an atom in the presence of a magnetic field (see Eq. (3.37)).

As in the preceding section, it is convenient to express the dipole matrix elements appearing in Eqs. (6.79) in terms of spherical tensors, assuming at the same time that the polarization unit vectors have the form of Eq. (5.141). Using Eqs. (6.66), (6.67), and (5.140) we can easily rewrite the tensors $\boldsymbol{g}$, $\boldsymbol{h}$, $\boldsymbol{f}$ in the form

$$g_{\alpha\beta} = \frac{4\pi^3\nu}{ch}\mathcal{N}\sum_{mnn'}\sum_{qq'}(-1)^{q+q'}\,(d_{-q})_{mn}\,(d_{-q'})^*_{mn'} \times \mathcal{E}_{qq'}(\alpha,\beta,\vec{\Omega})\;\rho_{nn'}\,\Phi(\nu_{mn}-\nu)$$

$$h_{\alpha\beta} = \frac{4\pi^3\nu}{ch}\mathcal{N}\sum_{mm'n}\sum_{qq'}(-1)^{q+q'}\,(d_{-q})_{mn}\,(d_{-q'})^*_{m'n} \times \mathcal{E}_{qq'}(\alpha,\beta,\vec{\Omega})\;\rho_{m'm}\,\Phi(\nu_{mn}-\nu)$$

$$f_{\alpha\beta} = \frac{2h\nu^3}{c^2}\,h_{\alpha\beta}\,. \tag{6.80}$$

An important remark on the radiative transfer equations concerns the special case where polarization is neglected both in the radiation field and in the atomic system. If we suppose that

$$I_{\alpha\beta}(\nu,\vec{\Omega}) = \frac{1}{2}\,I(\nu,\vec{\Omega})\,\delta_{\alpha\beta}\,, \qquad \rho_{nn'} = \rho_n\,\delta_{nn'}\,,$$

we get

$$\begin{aligned}\left(\frac{1}{c}\frac{\partial}{\partial t}+\frac{\mathrm{d}}{\mathrm{d}s}\right)I(\nu,\vec{\Omega}) &= \left(\frac{1}{c}\frac{\partial}{\partial t}+\frac{\mathrm{d}}{\mathrm{d}s}\right)\sum_\alpha I_{\alpha\alpha}(\nu,\vec{\Omega})\\ &= -\sum_\alpha\frac{1}{2}\left(g_{\alpha\alpha}+g^*_{\alpha\alpha}\right)I(\nu,\vec{\Omega})\\ &\quad+\sum_\alpha\frac{1}{2}\left(h_{\alpha\alpha}+h^*_{\alpha\alpha}\right)I(\nu,\vec{\Omega})\\ &\quad+\sum_\alpha\frac{1}{2}\left(f_{\alpha\alpha}+f^*_{\alpha\alpha}\right),\end{aligned} \tag{6.81}$$

where

$$\sum_\alpha g_{\alpha\alpha} = \frac{4\pi^3\nu}{ch}\mathcal{N}\sum_{mn}\sum_\alpha\sum_{qq'}(-1)^{q+q'}\,(d_{-q})_{mn}\,(d_{-q'})^*_{mn} \times \mathcal{E}_{qq'}(\alpha,\alpha,\vec{\Omega})\;\rho_n\,\Phi(\nu_{mn}-\nu)\,,$$

etc. Now we 'average over all the possible orientations of the atom', which is equivalent to keeping the atom fixed and averaging over all the $\vec{\Omega}$ directions entering the tensor $\mathcal{E}_{qq'}$. Using Eq. (6.68) we obtain[1]

$$\sum_{\alpha} g_{\alpha\alpha} = \frac{8\pi^3\nu}{3ch}\mathcal{N}\sum_{mn}|\vec{d}_{mn}|^2\,\rho_n\,\Phi(\nu_{mn}-\nu)\;, \tag{6.82}$$

where $|\vec{d}_{mn}|^2$ is defined in Eq. (6.70). Performing similar calculations for the other terms of Eq. (6.81) and bearing in mind the definition of the Einstein coefficients (Eqs. (6.71) and (6.73)) we easily obtain

$$\left(\frac{1}{c}\frac{\partial}{\partial t}+\frac{\mathrm{d}}{\mathrm{d}s}\right)I(\nu,\vec{\Omega}) = -k_\nu\,I(\nu,\vec{\Omega})\,+\,\varepsilon_\nu\;,$$

where[2]

$$k_\nu = \frac{h\nu}{4\pi}\sum_{nm}B_{nm}\left(\rho_n-\rho_m\right)\,\phi(\nu_{mn}-\nu)\,\mathcal{N}$$
$$\varepsilon_\nu = \frac{h\nu}{4\pi}\sum_{nm}A_{mn}\,\rho_m\,\phi(\nu_{mn}-\nu)\,\mathcal{N}\;.$$

This is the usual radiative transfer equation whose derivation, generally based on heuristic arguments, can be found in several textbooks (see for instance Mihalas, 1978). The quantities k_ν and ε_ν are the line absorption coefficient (corrected for stimulated emission) and the emission coefficient, respectively. The special case now considered shows that the tensors $\boldsymbol{g}$, $\boldsymbol{h}$, and $\boldsymbol{f}$ defined in Eqs. (6.79) are just the generalization of the absorption coefficient, the negative absorption coefficient due to stimulated emission, and the emission coefficient, respectively. These quantities, and the structure itself of the transfer equations, have been derived in this section directly from the principles of Quantum Electrodynamics.

6.7. Evolution Equations for the Stokes Parameters

Equations (6.78) describe the radiative transfer of polarized radiation in terms of the polarization tensor $I_{\alpha\beta}(\nu,\vec{\Omega})$. To turn them into transfer equations for the

[1] Equation (6.82) is correct only when the atomic system is evenly populated in *all the degenerate sublevels* of a given energy level. Even in that case, it does not hold in the presence of any kind of anisotropy (e.g., in the presence of a magnetic field).

[2] The above expression for ε_ν is obtained by noticing that, because of the presence of the profile $\phi(\nu_{mn}-\nu)$, the Einstein coefficient A_{mn} can also be written as

$$A_{mn} = \frac{2h\nu^3}{c^2}\,B_{mn}\;.$$

Stokes parameters $S_i(\nu,\vec{\Omega})$ we have just to fix the form of the polarization unit vectors. If we choose the unit vectors of Eqs. (5.141) – so that expressions (6.80) can be used for the tensors $\boldsymbol{f}$, $\boldsymbol{g}$, $\boldsymbol{h}$ – the polarization tensor is connected with the Stokes parameters by the transformation (5.129).[1] Thus we can write

$$\left(\frac{1}{c}\frac{\partial}{\partial t}+\frac{\mathrm{d}}{\mathrm{d}s}\right)S_i(\nu,\vec{\Omega})=\sum_{\alpha\beta}(\hat{\sigma}_i)_{\alpha\beta}\left(\frac{1}{c}\frac{\partial}{\partial t}+\frac{\mathrm{d}}{\mathrm{d}s}\right)I_{\beta\alpha}(\nu,\vec{\Omega}) \qquad \begin{matrix}(\alpha,\beta=\pm 1)\\ (i=0,1,2,3)\,,\end{matrix}$$

where $\hat{\boldsymbol{\sigma}}_i$ are the Pauli spin matrices of Eqs. (5.128). Substituting Eqs. (6.78), and using the conjugation relation (5.147) and the cyclic property of the trace, one obtains after some algebra

$$\left(\frac{1}{c}\frac{\partial}{\partial t}+\frac{\mathrm{d}}{\mathrm{d}s}\right)S_i(\nu,\vec{\Omega})=-\sum_{j=0}^{3}K_{ij}^{\mathrm{A}}\,S_j(\nu,\vec{\Omega})+\sum_{j=0}^{3}K_{ij}^{\mathrm{S}}\,S_j(\nu,\vec{\Omega})+\varepsilon_i\,, \tag{6.83}$$

where[2]

$$\begin{aligned}K_{ij}^{\mathrm{A}}&=\mathrm{Re}\big[\,\mathrm{Tr}\,(\hat{\boldsymbol{\sigma}}_j\,\hat{\boldsymbol{\sigma}}_i\,\boldsymbol{g})\big]\\ K_{ij}^{\mathrm{S}}&=\mathrm{Re}\big[\,\mathrm{Tr}\,(\hat{\boldsymbol{\sigma}}_j\,\hat{\boldsymbol{\sigma}}_i\,\boldsymbol{h})\big]\\ \varepsilon_i\ &=\mathrm{Re}\big[\,\mathrm{Tr}\,(\hat{\boldsymbol{\sigma}}_i\,\boldsymbol{f})\big]\,.\end{aligned} \tag{6.84}$$

This equation can be rewritten in the explicit matrix form

$$\begin{aligned}\left(c\frac{\partial}{\partial t}+\frac{\mathrm{d}}{\mathrm{d}s}\right)\begin{pmatrix}I\\Q\\U\\V\end{pmatrix}=&-\begin{pmatrix}\eta_I^{\mathrm{A}}&\eta_Q^{\mathrm{A}}&\eta_U^{\mathrm{A}}&\eta_V^{\mathrm{A}}\\ \eta_Q^{\mathrm{A}}&\eta_I^{\mathrm{A}}&\rho_V^{\mathrm{A}}&-\rho_U^{\mathrm{A}}\\ \eta_U^{\mathrm{A}}&-\rho_V^{\mathrm{A}}&\eta_I^{\mathrm{A}}&\rho_Q^{\mathrm{A}}\\ \eta_V^{\mathrm{A}}&\rho_U^{\mathrm{A}}&-\rho_Q^{\mathrm{A}}&\eta_I^{\mathrm{A}}\end{pmatrix}\begin{pmatrix}I\\Q\\U\\V\end{pmatrix}\\ &+\begin{pmatrix}\eta_I^{\mathrm{S}}&\eta_Q^{\mathrm{S}}&\eta_U^{\mathrm{S}}&\eta_V^{\mathrm{S}}\\ \eta_Q^{\mathrm{S}}&\eta_I^{\mathrm{S}}&\rho_V^{\mathrm{S}}&-\rho_U^{\mathrm{S}}\\ \eta_U^{\mathrm{S}}&-\rho_V^{\mathrm{S}}&\eta_I^{\mathrm{S}}&\rho_Q^{\mathrm{S}}\\ \eta_V^{\mathrm{S}}&\rho_U^{\mathrm{S}}&-\rho_Q^{\mathrm{S}}&\eta_I^{\mathrm{S}}\end{pmatrix}\begin{pmatrix}I\\Q\\U\\V\end{pmatrix}+\begin{pmatrix}\varepsilon_I\\ \varepsilon_Q\\ \varepsilon_U\\ \varepsilon_V\end{pmatrix}\,,\end{aligned} \tag{6.85}$$

where

$$\begin{aligned}\eta_I^{\mathrm{A}}&=K_{00}^{\mathrm{A}}=K_{11}^{\mathrm{A}}=K_{22}^{\mathrm{A}}=K_{33}^{\mathrm{A}}=\mathrm{Re}\big[\,\mathrm{Tr}\,(\boldsymbol{g})\big]=\mathrm{Re}\,\big(g_{++}+g_{--}\big)\\ \eta_Q^{\mathrm{A}}&=K_{01}^{\mathrm{A}}=K_{10}^{\mathrm{A}}=\mathrm{Re}\big[\,\mathrm{Tr}\,(\hat{\boldsymbol{\sigma}}_1\,\boldsymbol{g})\big]=-\mathrm{Re}\,\big(g_{+-}+g_{-+}\big)\end{aligned}$$

[1] Note that a similar transformation on the transfer equations has been performed in Sect. 5.2, although using a different basis of polarization unit vectors.

[2] It is understood that the components of the tensors $\boldsymbol{f}$, $\boldsymbol{g}$, $\boldsymbol{h}$ are labelled in the same way as the spin matrices $\hat{\boldsymbol{\sigma}}_i$ (see the remark following Eq. (5.128)).

$$
\begin{aligned}
\eta_U^{\mathrm{A}} &= K_{02}^{\mathrm{A}} = K_{20}^{\mathrm{A}} = \mathrm{Re}\big[\,\mathrm{Tr}\,(\hat{\boldsymbol{\sigma}}_2\,\boldsymbol{g})\big] = \mathrm{Im}\,\big(g_{+-} - g_{-+}\big) \\
\eta_V^{\mathrm{A}} &= K_{03}^{\mathrm{A}} = K_{30}^{\mathrm{A}} = \mathrm{Re}\big[\,\mathrm{Tr}\,(\hat{\boldsymbol{\sigma}}_3\,\boldsymbol{g})\big] = \mathrm{Re}\,\big(g_{++} - g_{--}\big) \\
\rho_Q^{\mathrm{A}} &= K_{23}^{\mathrm{A}} = -K_{32}^{\mathrm{A}} = \mathrm{Im}\big[\,\mathrm{Tr}\,(\hat{\boldsymbol{\sigma}}_1\,\boldsymbol{g})\big] = -\mathrm{Im}\,\big(g_{+-} + g_{-+}\big) \\
\rho_U^{\mathrm{A}} &= K_{31}^{\mathrm{A}} = -K_{13}^{\mathrm{A}} = \mathrm{Im}\big[\,\mathrm{Tr}\,(\hat{\boldsymbol{\sigma}}_2\,\boldsymbol{g})\big] = -\mathrm{Re}\,\big(g_{+-} - g_{-+}\big) \\
\rho_V^{\mathrm{A}} &= K_{12}^{\mathrm{A}} = -K_{21}^{\mathrm{A}} = \mathrm{Im}\big[\,\mathrm{Tr}\,(\hat{\boldsymbol{\sigma}}_3\,\boldsymbol{g})\big] = \mathrm{Im}\,\big(g_{++} - g_{--}\big) \\
\varepsilon_I &= \varepsilon_0 = \mathrm{Re}\big[\,\mathrm{Tr}\,(\boldsymbol{f})\big] = \mathrm{Re}\,\big(f_{++} + f_{--}\big) \\
\varepsilon_Q &= \varepsilon_1 = \mathrm{Re}\big[\,\mathrm{Tr}\,(\hat{\boldsymbol{\sigma}}_1\,\boldsymbol{f})\big] = -\mathrm{Re}\,\big(f_{+-} + f_{-+}\big) \\
\varepsilon_U &= \varepsilon_2 = \mathrm{Re}\big[\,\mathrm{Tr}\,(\hat{\boldsymbol{\sigma}}_2\,\boldsymbol{f})\big] = \mathrm{Im}\,\big(f_{+-} - f_{-+}\big) \\
\varepsilon_V &= \varepsilon_3 = \mathrm{Re}\big[\,\mathrm{Tr}\,(\hat{\boldsymbol{\sigma}}_3\,\boldsymbol{f})\big] = \mathrm{Re}\,\big(f_{++} - f_{--}\big)\,, \qquad (6.86)
\end{aligned}
$$

and where $\eta_I^{\mathrm{S}}, \ldots, \rho_V^{\mathrm{S}}$ have the same expressions as $\eta_I^{\mathrm{A}}, \ldots, \rho_V^{\mathrm{A}}$ with $h_{\alpha\beta}$ substituted for $g_{\alpha\beta}$. All these quantities can be easily written in terms of the reducible spherical tensor $\mathcal{T}_{qq'}(i,\vec{\Omega})$ introduced in Chap. 5 (Eq. (5.146)). Defining the formal vectors

$$
\begin{aligned}
\eta_i^{\mathrm{A}} &= (\eta_I^{\mathrm{A}}, \eta_Q^{\mathrm{A}}, \eta_U^{\mathrm{A}}, \eta_V^{\mathrm{A}}) \qquad (i = 0,1,2,3) \\
\eta_i^{\mathrm{S}} &= (\eta_I^{\mathrm{S}}, \eta_Q^{\mathrm{S}}, \eta_U^{\mathrm{S}}, \eta_V^{\mathrm{S}}) \qquad (i = 0,1,2,3) \\
\rho_i^{\mathrm{A}} &= (\rho_Q^{\mathrm{A}}, \rho_U^{\mathrm{A}}, \rho_V^{\mathrm{A}}) \qquad (i = 1,2,3) \\
\rho_i^{\mathrm{S}} &= (\rho_Q^{\mathrm{S}}, \rho_U^{\mathrm{S}}, \rho_V^{\mathrm{S}}) \qquad (i = 1,2,3)\,, \qquad (6.87)
\end{aligned}
$$

we have from Eqs. (6.80)

$$
\begin{aligned}
\eta_i^{\mathrm{A}}(\nu,\vec{\Omega}) = {} & \frac{8\pi^3\nu}{ch}\,\mathcal{N} \sum_{mnn'} \sum_{qq'} (-1)^{q+q'} \\
& \times \mathrm{Re}\left[(d_{-q})_{mn}\,(d_{-q'})^*_{mn'}\;\mathcal{T}_{qq'}(i,\vec{\Omega})\;\rho_{nn'}\;\Phi(\nu_{mn}-\nu)\right] \\
\eta_i^{\mathrm{S}}(\nu,\vec{\Omega}) = {} & \frac{8\pi^3\nu}{ch}\,\mathcal{N} \sum_{mm'n} \sum_{qq'} (-1)^{q+q'} \\
& \times \mathrm{Re}\left[(d_{-q})_{mn}\,(d_{-q'})^*_{m'n}\;\mathcal{T}_{qq'}(i,\vec{\Omega})\;\rho_{m'm}\;\Phi(\nu_{mn}-\nu)\right] \\
\rho_i^{\mathrm{A}}(\nu,\vec{\Omega}) = {} & \eta_i^{\mathrm{A}}(\nu,\vec{\Omega})\;\big\{\mathrm{Re}\to\mathrm{Im}\big\} \\
\rho_i^{\mathrm{S}}(\nu,\vec{\Omega}) = {} & \eta_i^{\mathrm{S}}(\nu,\vec{\Omega})\;\big\{\mathrm{Re}\to\mathrm{Im}\big\} \\
\varepsilon_i(\nu,\vec{\Omega}) = {} & \frac{2h\nu^3}{c^2}\;\eta_i^{\mathrm{S}}(\nu,\vec{\Omega})\,, \qquad (6.88)
\end{aligned}
$$

where the symbol $\{\mathrm{Re}\to\mathrm{Im}\}$ means that ρ_i is obtained from the corresponding η_i by substitution of the imaginary part for the real part.

The radiative transfer equations become much simpler in the special case of Local Thermodynamic Equilibrium, since the density-matrix elements of the atomic system reduce to the expression (Boltzmann law)

$$\rho_{nn'} = \delta_{nn'} \frac{\mathrm{e}^{-\frac{E_n}{k_\mathrm{B}T}}}{Z(T)} ,$$

where k_B is the Boltzmann constant, T the absolute temperature of the medium, and $Z(T)$ the partition function. With the use of the conjugation relation (5.148), we have from Eqs. (6.88)

$$\eta_i^\mathrm{A}(\nu,\vec{\Omega}) = \frac{8\pi^3\nu}{ch}\mathcal{N}\sum_{mn}\sum_{qq'}(-1)^{q+q'} \times (d_{-q})_{mn}\,(d_{-q'})^*_{mn}\,\mathcal{T}_{qq'}(i,\vec{\Omega})\,\frac{\mathrm{e}^{-\frac{E_n}{k_\mathrm{B}T}}}{Z(T)}\,\phi(\nu_{mn}-\nu)$$

$$\eta_i^\mathrm{S}(\nu,\vec{\Omega}) = \frac{8\pi^3\nu}{ch}\mathcal{N}\sum_{mn}\sum_{qq'}(-1)^{q+q'} \times (d_{-q})_{mn}\,(d_{-q'})^*_{mn}\,\mathcal{T}_{qq'}(i,\vec{\Omega})\,\frac{\mathrm{e}^{-\frac{E_m}{k_\mathrm{B}T}}}{Z(T)}\,\phi(\nu_{mn}-\nu) ,$$

and since the profiles $\phi(\nu_{mn}-\nu)$ are practically Dirac delta-functions

$$\eta_i^\mathrm{S}(\nu,\vec{\Omega}) = \mathrm{e}^{-\frac{h\nu}{k_\mathrm{B}T}}\,\eta_i^\mathrm{A}(\nu,\vec{\Omega})$$

$$\varepsilon_i(\nu,\vec{\Omega}) = \frac{2h\nu^3}{c^2}\,\mathrm{e}^{-\frac{h\nu}{k_\mathrm{B}T}}\,\eta_i^\mathrm{A}(\nu,\vec{\Omega}) = \left(\eta_i^\mathrm{A}(\nu,\vec{\Omega}) - \eta_i^\mathrm{S}(\nu,\vec{\Omega})\right) B_\mathrm{P} , \tag{6.89}$$

where

$$B_\mathrm{P} = \frac{2h\nu^3}{c^2}\,\frac{1}{\mathrm{e}^{\frac{h\nu}{k_\mathrm{B}T}}-1}$$

is the Planck function. Thus the radiative transfer equations can be written in the compact form

$$\left(\frac{1}{c}\,\frac{\partial}{\partial t} + \frac{\mathrm{d}}{\mathrm{d}s}\right) S_i = -\sum_{j=0}^{3} K_{ij}\left(S_j - B_\mathrm{P}\,U_j\right) ,$$

where[1]

$$K_{ij} = K_{ij}^\mathrm{A} - K_{ij}^\mathrm{S}$$

[1] Note that the relation between the quantities ρ_i^A and ρ_i^S analogous to the first of Eqs. (6.89),

$$\rho_i^\mathrm{S}(\nu,\vec{\Omega}) = \mathrm{e}^{-\frac{h\nu}{k_\mathrm{B}T}}\,\rho_i^\mathrm{A}(\nu,\vec{\Omega}) ,$$

is only approximately satisfied. Under such approximation we can write

$$K_{ij} = K_{ij}^\mathrm{A}\left(1 - \mathrm{e}^{-\frac{h\nu}{k_\mathrm{B}T}}\right) .$$

is the propagation matrix corrected for stimulated emission, and

$$U_j = \delta_{j0}$$

is the unity vector $\boldsymbol{U} = (1,0,0,0)^\dagger$. In matrix form the equation reads

$$\left(\frac{1}{c}\frac{\partial}{\partial t} + \frac{\mathrm{d}}{\mathrm{d}s}\right)\begin{pmatrix} I \\ Q \\ U \\ V \end{pmatrix} = -\begin{pmatrix} \eta_I & \eta_Q & \eta_U & \eta_V \\ \eta_Q & \eta_I & \rho_V & -\rho_U \\ \eta_U & -\rho_V & \eta_I & \rho_Q \\ \eta_V & \rho_U & -\rho_Q & \eta_I \end{pmatrix}\begin{pmatrix} I - B_\mathrm{P} \\ Q \\ U \\ V \end{pmatrix},$$

with $\eta_I = \eta_I^\mathrm{A} - \eta_I^\mathrm{S}$, $\eta_Q = \eta_Q^\mathrm{A} - \eta_Q^\mathrm{S}$, etc.

6.8. Magnetic Dipole Transitions

The statistical equilibrium equations and the radiative transfer equations have been derived in the preceding sections under the assumption of electric-dipole transitions, but they can be easily rewritten for magnetic-dipole transitions. As shown at the end of Sect. 6.3, we have just to change the interaction Hamiltonian according to Eqs. (6.42).

It immediately follows that the basic equations (6.62) and (6.78) remain unchanged, while the matrix elements in the expressions of the radiative rates (Eqs. (6.63)) and in the expressions of the tensors $\boldsymbol{f}$, $\boldsymbol{g}$, $\boldsymbol{h}$ (Eqs. (6.79)) must be replaced according to

$$\left[\vec{d}\cdot\vec{e}_\lambda(\vec{\Omega})\right]_{nm} \rightarrow \left[\vec{\mu}\cdot\vec{\Omega}\times\vec{e}_\lambda(\vec{\Omega})\right]_{nm}.$$

When spherical tensors are introduced, it can be easily seen that the matrix elements of the form $(d_q)_{nm}$ must be replaced by $(\mu_q)_{nm}$, and the tensor $\mathcal{E}_{qq'}(\alpha,\beta,\vec{\Omega})$ by

$$\left[\mathcal{E}_{qq'}(\alpha,\beta,\vec{\Omega})\right]_{\mathrm{m.d.}} = \left(\vec{\Omega}\times\vec{e}_\alpha(\vec{\Omega})\right)_q \left(\vec{\Omega}\times\vec{e}_\beta(\vec{\Omega})\right)^*_{q'} \qquad (\alpha,\beta = \pm 1),$$

which can also be written in the form

$$\left[\mathcal{E}_{qq'}(\alpha,\beta,\vec{\Omega})\right]_{\mathrm{m.d.}} = \alpha\,\beta\;\mathcal{E}_{qq'}(\alpha,\beta,\vec{\Omega})$$

since the unit vectors $\vec{e}_\alpha$ satisfy the relation

$$\vec{\Omega}\times\vec{e}_\alpha(\vec{\Omega}) = \mathrm{i}\,\alpha\;\vec{e}_\alpha(\vec{\Omega}).$$

It follows that the tensor $\mathcal{T}_{qq'}(i,\vec{\Omega})$ defined in Eq. (5.146) must be replaced by

$$\begin{aligned}
\left[\mathcal{T}_{qq'}(0,\vec{\Omega})\right]_{\mathrm{m.d.}} &= \mathcal{T}_{qq'}(0,\vec{\Omega}) \\
\left[\mathcal{T}_{qq'}(1,\vec{\Omega})\right]_{\mathrm{m.d.}} &= -\mathcal{T}_{qq'}(1,\vec{\Omega}) \\
\left[\mathcal{T}_{qq'}(2,\vec{\Omega})\right]_{\mathrm{m.d.}} &= -\mathcal{T}_{qq'}(2,\vec{\Omega}) \\
\left[\mathcal{T}_{qq'}(3,\vec{\Omega})\right]_{\mathrm{m.d.}} &= \mathcal{T}_{qq'}(3,\vec{\Omega}).
\end{aligned}$$

As far as the statistical equilibrium equations are concerned, we have therefore that the radiation field tensor $J_{qq'}(\nu)$ (defined in Eq. (5.153)) to be used in Eqs. (6.69) for magnetic-dipole transitions is obtained from the corresponding tensor for electric-dipole transitions by changing the sign of the linear polarization Stokes parameters Q and U.

As to the radiative transfer equations, it appears from Eqs. (6.80) that the quantities $g_{\alpha\beta}$, $h_{\alpha\beta}$, $f_{\alpha\beta}$ must be replaced by

$$
\begin{aligned}
[\, g_{\alpha\beta}\,]_{\mathrm{m.d.}} &= \alpha\,\beta\ g_{\alpha\beta}\ \{\vec{d} \to \vec{\mu}\} \\
[\, h_{\alpha\beta}\,]_{\mathrm{m.d.}} &= \alpha\,\beta\ h_{\alpha\beta}\ \{\vec{d} \to \vec{\mu}\} \\
[\, f_{\alpha\beta}\,]_{\mathrm{m.d.}} &= \alpha\,\beta\ f_{\alpha\beta}\ \{\vec{d} \to \vec{\mu}\} \qquad\qquad (\alpha, \beta = \pm 1)\ ,
\end{aligned}
$$

where the symbol in curly bracket means the substitution of the matrix elements $(\mu_q)_{nm}$ for $(d_q)_{nm}$. If we consider the matrix form (6.85) of the transfer equations, we have therefore – besides the just mentioned substitution – a sign change of the quantities η_Q^{A}, η_U^{A}, ρ_Q^{A}, ρ_U^{A}, η_Q^{S}, η_U^{S}, ρ_Q^{S}, ρ_U^{S}, ε_Q, ε_U.

This page intentionally left blank

CHAPTER 7

STATISTICAL EQUILIBRIUM EQUATIONS AND RADIATIVE TRANSFER COEFFICIENTS FOR ATOMIC SYSTEMS

In this chapter we will apply the basic equations derived in Chap. 6 (statistical equilibrium and radiative transfer equations) to the special case where the material system interacting with the radiation field is an atom – or, more properly, an ensemble of uncorrelated identical atoms. We will also assume the atoms to be embedded in an external, static magnetic field, on account of the great importance of this topic in astrophysical plasmas. Obviously, the results that will be derived in this chapter are subjected to the limitations outlined in the introduction to Chap. 6.

The two sets of equations depend on the atomic system through the quantities:
i) $\rho_{nm} = \langle n \,|\, \rho \,|\, m \rangle$, the matrix elements of the atomic density operator between energy eigenstates, describing populations ($n = m$) and coherences ($n \neq m$);
ii) $\nu_{nm} = (E_n - E_m)/h$, the corresponding Bohr frequencies;
iii) $\langle n \,|\, \vec{d} \,|\, m \rangle$ (or $\langle n \,|\, \vec{\mu} \,|\, m \rangle$), the matrix elements of the electric (or magnetic) dipole operator between energy eigenstates. In these expressions $|\, n \rangle$ and E_n are the eigenvectors and eigenvalues of the Hamiltonian of the unperturbed atom, plus the Hamiltonian describing the interaction with the external magnetic field.

The quantities $|\, n \rangle$ and E_n depend on the spectral properties of the atom and on the intensity of the magnetic field (L-S or different coupling schemes, possible presence of hyperfine structure, Zeeman or Paschen-Back effect regime, etc.). Moreover, one should in principle consider the coherences between *any* couple of levels $|\, n \rangle$, $|\, m \rangle$, which would make the problem extremely involved. However, depending on the specific atomic structure and magnetic field value, certain coherences can be disregarded. This is related to a general property of the statistical equilibrium equations, according to which the coherence ρ_{nm} is the smaller, the larger the energy difference between levels $|\, n \rangle$ and $|\, m \rangle$.

We consider in the following three schematic situations, which cover most cases of interest for practical applications:
i) atom with no hyperfine structure, Zeeman effect regime, coherences between magnetic sublevels (M, M') of each (αJ)-level (neglecting those between different levels): Sects. 7.1-7.4;
ii) atom with no hyperfine structure, L-S coupling scheme, incomplete Paschen-Back effect regime, coherences between magnetic sublevels (M, M') of each (βLSJ) level *and* between magnetic sublevels of different levels (βLSJ), $(\beta LSJ')$ belonging to the same term (neglecting coherences between different terms): Sects. 7.5-7.8;
iii) atom with hyperfine structure, incomplete Paschen-Back effect regime (of hyperfine structure), coherences between magnetic sublevels (f, f') of each hyperfine level (αJIF) *and* between magnetic sublevels of different hyperfine levels (αJIF),

$(\alpha JIF')$ belonging to the same level (neglecting coherences between different levels): Sect. 7.9.

The statistical equilibrium and the radiative transfer equations will be written both in the standard representation of the atomic density operator (which is easier to work with, starting from the formalism of Chap. 6) and in the spherical statistical tensor representation, which leads to more compact and physically significant expressions.

At the end of the chapter we will also study the effect of collisions on the statistical equilibrium equations, under the assumption of an isotropic distribution of colliding particles.

7.1. The Multi-Level Atom in the Standard Representation

We consider an atomic system devoid of hyperfine structure, whose energy levels are characterized by the quantum numbers α and J, where J is the total angular momentum and α is a set of quantum numbers related to different physical properties of the energy level (in particular, for an atom described in the Russel-Saunders coupling scheme, α could represent the set of quantum numbers (β, L, S) which describe the electronic configuration, the total orbital angular momentum, and the total electronic spin, respectively).

Assuming that the magnetic field is sufficiently weak for the Zeeman effect regime to hold (see the discussion in Sects. 3.1 and 3.4), and aligning the z-direction of the reference system along the magnetic field, we have for the eigenvectors and eigenvalues of the atomic Hamiltonian

$$H_{\mathrm{A}} \, |\alpha JM\rangle = \left(E_{\alpha J} + \mu_0 \, g_{\alpha J} B \, M\right) |\alpha JM\rangle \; ,$$

where all the symbols have the same meaning as in Sect. 3.1.

The formalism presented in Chap. 6 can now be applied to this particular system. To begin with the simplest case, we will neglect here all coherences between magnetic sublevels that do not belong to the same (αJ)-level. In other words, we suppose that all the atomic density-matrix elements of the form[1] $\langle \alpha JM| \, \rho \, |\alpha' J' M'\rangle$ are zero except for $(\alpha J) = (\alpha' J')$,

$$\langle \alpha JM| \, \rho \, |\alpha' J' M'\rangle = \; \delta_{\alpha\alpha'} \, \delta_{JJ'} \, \langle \alpha JM| \, \rho \, |\alpha JM'\rangle \; . \tag{7.1}$$

This approximation is usually justified when the energy separation between two different levels – say (αJ) and $(\alpha' J')$ – is sufficiently large that the corresponding Bohr frequency

$$\nu_{\alpha J, \, \alpha' J'} = \frac{E_{\alpha J} - E_{\alpha' J'}}{h} \tag{7.2}$$

[1] In this chapter we denote by ρ the atomic density operator $\rho^{(\mathrm{A})}$.

is much larger (in absolute value) than the Einstein A coefficient for spontaneous emission.[1] Under such approximation all the different atomic levels are decoupled and the atomic system is referred to as a *multi-level atom*. For this system, the flat-spectrum approximation discussed in Sect. 6.5 requires that the radiation field incident on the atom should be constant across frequency intervals wider than the Zeeman separations and than the inverse lifetimes of the relevant magnetic sublevels. Therefore, it is sufficient to specify the incident radiation field at the Bohr frequencies (7.2) relating different levels.

We can apply the formalism of Chap. 6 to the multi-level atom in the presence of a magnetic field by performing the following substitutions

i) for the energy eigenvectors:

$$|\, n\rangle \rightarrow |\alpha J M\rangle \; ;$$

ii) for the corresponding energy eigenvalues:

$$E_n \rightarrow E_{\alpha J} + \mu_0 \, g_{\alpha J} B \, M \; ,$$

whence

iii) for the Bohr frequencies:

$$\nu_{nm} = \frac{E_n - E_m}{h} \rightarrow \nu_{\alpha J M, \, \alpha' J' M'} = \nu_{\alpha J, \, \alpha' J'} + \nu_{\mathrm{L}} \, (g_{\alpha J} \, M - g_{\alpha' J'} \, M') \; , \qquad (7.3)$$

where $\nu_{\alpha J, \alpha' J'}$ is defined in Eq. (7.2) and ν_{L} is the Larmor frequency (cf. Eq. (3.10));

iv) for the matrix elements of the spherical components of the dipole operator:

$$\begin{aligned} (d_q)_{nm} = \langle n \,|\, d_q \,|\, m \rangle \rightarrow (d_q)_{\alpha J M, \, \alpha' J' M'} = \langle \alpha J M |\, d_q \,| \alpha' J' M' \rangle = \\ = (-1)^{J' + M + 1} \sqrt{2J+1} \begin{pmatrix} J & J' & 1 \\ -M & M' & q \end{pmatrix} \langle \alpha J \| \vec{d} \, \| \alpha' J' \rangle \; , \qquad (7.4) \end{aligned}$$

where we have applied the Wigner-Eckart theorem (Eq. (2.96));

v) finally, for the atomic density-matrix elements:

$$\begin{aligned} \rho_{nm} = \langle n \,|\, \rho \,|\, m \rangle \rightarrow \langle \alpha J M |\, \rho \,| \alpha' J' M' \rangle = \\ = \; \delta_{\alpha \alpha'} \, \delta_{J J'} \, \langle \alpha J M |\, \rho \,| \alpha J M' \rangle = \; \delta_{\alpha \alpha'} \, \delta_{J J'} \, \rho_{\alpha J}(M, M') \; , \end{aligned}$$

where we have used the assumption (7.1) and we have introduced the notation of Eq. (3.91a).

[1] We will see however in the following (see Sect. 10.17) that the coherences between different J-levels are fundamental to explain certain polarization phenomena in multiplets even when $\nu_{\alpha J, \, \alpha' J'} \gg A$.

By means of substitutions i) to v) the statistical equilibrium equations and the radiative transfer equations for the multi-level atom can be directly deduced from the corresponding equations of Chap. 6.

7.1.a Statistical Equilibrium Equations

In Eqs. (6.62) and (6.69) we substitute (see also Fig. 6.1)

$$\begin{array}{lll} m \to \alpha J M & & \\ m' \to \alpha J M' & n \to \alpha_\ell J_\ell M_\ell & p \to \alpha_u J_u M_u \\ m'' \to \alpha J M'' & n' \to \alpha_\ell J_\ell M'_\ell & p' \to \alpha_u J_u M'_u \,, \end{array}$$

where the indices ℓ (for 'lower') and u (for 'upper') denote any level of energy lower (or higher, respectively) than $E_{\alpha J}$. We obtain

$$\begin{aligned} \frac{\mathrm{d}}{\mathrm{d}t}\,\rho_{\alpha J}(M,M') &= -2\pi \mathrm{i}\,\nu_\mathrm{L}\; g_{\alpha J}\;(M-M')\;\rho_{\alpha J}(M,M') \\ &+ \sum_{\alpha_\ell J_\ell} \sum_{M_\ell M'_\ell} \rho_{\alpha_\ell J_\ell}(M_\ell, M'_\ell)\; T_\mathrm{A}(\alpha J M M', \alpha_\ell J_\ell M_\ell M'_\ell) \\ &+ \sum_{\alpha_u J_u} \sum_{M_u M'_u} \rho_{\alpha_u J_u}(M_u, M'_u) \Big[T_\mathrm{E}(\alpha J M M', \alpha_u J_u M_u M'_u) \\ &\qquad + T_\mathrm{S}(\alpha J M M', \alpha_u J_u M_u M'_u) \Big] \\ &- \sum_{M''} \Big\{ \rho_{\alpha J}(M,M'') \Big[R_\mathrm{A}(\alpha J M' M'') + R_\mathrm{E}(\alpha J M'' M') \\ &\qquad + R_\mathrm{S}(\alpha J M'' M') \Big] \\ &\quad + \rho_{\alpha J}(M'',M') \Big[R_\mathrm{A}(\alpha J M'' M) + R_\mathrm{E}(\alpha J M M'') \\ &\qquad + R_\mathrm{S}(\alpha J M M'') \Big] \Big\} \,, \end{aligned} \tag{7.5}$$

where the various rates (for which we have introduced shorthand notations) are given by

$$\begin{aligned} &T_\mathrm{A}(\alpha J M M', \alpha_\ell J_\ell M_\ell M'_\ell) = \\ &= \frac{32\pi^4}{h^2 c} \sum_{qq'} (-1)^{q+q'}\, (d_{-q})_{\alpha J M,\, \alpha_\ell J_\ell M_\ell}\; (d_{-q'})^*_{\alpha J M',\, \alpha_\ell J_\ell M'_\ell}\;\; J_{qq'}(\nu_{\alpha J,\, \alpha_\ell J_\ell}) \end{aligned}$$

$$\begin{aligned} &T_\mathrm{E}(\alpha J M M', \alpha_u J_u M_u M'_u) = \\ &= \frac{64\pi^4}{3hc^3} \sum_{q} (d_{-q})_{\alpha_u J_u M'_u,\, \alpha J M'}\; (d_{-q})^*_{\alpha_u J_u M_u,\, \alpha J M}\;\; \nu^3_{\alpha_u J_u,\, \alpha J} \end{aligned}$$

$$T_{\rm S}(\alpha JMM', \alpha_u J_u M_u M'_u) =$$
$$= \frac{32\pi^4}{h^2 c} \sum_{qq'} (-1)^{q+q'} \, (d_{-q})_{\alpha_u J_u M'_u, \, \alpha JM'} \, (d_{-q'})^*_{\alpha_u J_u M_u, \, \alpha JM} \;\; J_{qq'}(\nu_{\alpha_u J_u, \, \alpha J})$$

$$R_{\rm A}(\alpha JMM') =$$
$$= \sum_{\alpha_u J_u M_u} \frac{16\pi^4}{h^2 c} \sum_{qq'} (-1)^{q+q'} \, (d_{-q})_{\alpha_u J_u M_u, \, \alpha JM} \, (d_{-q'})^*_{\alpha_u J_u M_u, \, \alpha JM'} \;\; J_{qq'}(\nu_{\alpha_u J_u, \, \alpha J})$$

$$R_{\rm E}(\alpha JMM') =$$
$$= \sum_{\alpha_\ell J_\ell M_\ell} \frac{32\pi^4}{3hc^3} \sum_{q} (d_{-q})_{\alpha JM, \, \alpha_\ell J_\ell M_\ell} \, (d_{-q})^*_{\alpha JM', \, \alpha_\ell J_\ell M_\ell} \;\; \nu^3_{\alpha J, \, \alpha_\ell J_\ell}$$

$$R_{\rm S}(\alpha JMM') =$$
$$= \sum_{\alpha_\ell J_\ell M_\ell} \frac{16\pi^4}{h^2 c} \sum_{qq'} (-1)^{q+q'} \, (d_{-q})_{\alpha JM, \, \alpha_\ell J_\ell M_\ell} \, (d_{-q'})^*_{\alpha JM', \, \alpha_\ell J_\ell M_\ell} \;\; J_{qq'}(\nu_{\alpha J, \, \alpha_\ell J_\ell}) \, .$$

Because of Eq. (7.4), the expressions for the rates contain the square modulus of the reduced matrix element of the dipole operator between the (αJ)-level and one of the lower or upper levels,

$$|\langle \alpha J \| \vec{d} \, \| \alpha_\ell J_\ell \rangle|^2 \quad \text{or} \quad |\langle \alpha_u J_u \| \vec{d} \, \| \alpha J \rangle|^2 \, .$$

These quantities can be easily expressed in terms of the Einstein coefficients for transitions between different levels. Given two levels $(\alpha_\ell J_\ell)$ and $(\alpha_u J_u)$, with $E_{\alpha_u J_u} > E_{\alpha_\ell J_\ell}$, the *line strength* of the transition is defined by the symmetrical expression

$$\begin{aligned} \mathcal{S}(\alpha_\ell J_\ell, \alpha_u J_u) = \mathcal{S}(\alpha_u J_u, \alpha_\ell J_\ell) &= (2J_\ell + 1) \, |\langle \alpha_\ell J_\ell \| \vec{d} \, \| \alpha_u J_u \rangle|^2 \\ &= (2J_u + 1) \, |\langle \alpha_u J_u \| \vec{d} \, \| \alpha_\ell J_\ell \rangle|^2 \, , \end{aligned} \tag{7.6}$$

where the last equality follows from Eq. (2.101). The Einstein coefficients for spontaneous and stimulated emission and for absorption are connected with the line strength by the relations[1]

$$\begin{aligned} (2J_u + 1) \, A(\alpha_u J_u \to \alpha_\ell J_\ell) &= \frac{64\pi^4}{3hc^3} \;\; \nu^3_{\alpha_u J_u, \, \alpha_\ell J_\ell} \; \mathcal{S}(\alpha_u J_u, \alpha_\ell J_\ell) \\ (2J_u + 1) \, B(\alpha_u J_u \to \alpha_\ell J_\ell) &= \frac{32\pi^4}{3h^2 c} \; \mathcal{S}(\alpha_u J_u, \alpha_\ell J_\ell) \\ (2J_\ell + 1) \, B(\alpha_\ell J_\ell \to \alpha_u J_u) &= \frac{32\pi^4}{3h^2 c} \; \mathcal{S}(\alpha_\ell J_\ell, \alpha_u J_u) \, , \end{aligned} \tag{7.7}$$

[1] Note that from Eqs. (6.71) and (6.73) the Einstein coefficients for the transition between

with

$$A(\alpha_u J_u \to \alpha_\ell J_\ell) = \frac{2h}{c^2}\,\nu^3_{\alpha_u J_u,\,\alpha_\ell J_\ell}\,B(\alpha_u J_u \to \alpha_\ell J_\ell)$$
$$(2J_\ell+1)\,B(\alpha_\ell J_\ell \to \alpha_u J_u) = (2J_u+1)\,B(\alpha_u J_u \to \alpha_\ell J_\ell)\,. \tag{7.8}$$

Using these relations, we can rewrite the expressions of the rates in the form

$$T_{\rm A}(\alpha J M M', \alpha_\ell J_\ell M_\ell M'_\ell) = (2J_\ell+1)\,B(\alpha_\ell J_\ell \to \alpha J)$$
$$\times \sum_{qq'} 3\,(-1)^{M_\ell - M'_\ell} \begin{pmatrix} J & J_\ell & 1 \\ -M & M_\ell & -q \end{pmatrix} \begin{pmatrix} J & J_\ell & 1 \\ -M' & M'_\ell & -q' \end{pmatrix}$$
$$\times\ J_{qq'}(\nu_{\alpha J,\,\alpha_\ell J_\ell}) \tag{7.9a}$$

$$T_{\rm E}(\alpha J M M', \alpha_u J_u M_u M'_u) = (2J_u+1)\,A(\alpha_u J_u \to \alpha J)$$
$$\times \sum_{q} (-1)^{M_u - M'_u} \begin{pmatrix} J_u & J & 1 \\ -M'_u & M' & -q \end{pmatrix} \begin{pmatrix} J_u & J & 1 \\ -M_u & M & -q \end{pmatrix} \tag{7.9b}$$

$$T_{\rm S}(\alpha J M M', \alpha_u J_u M_u M'_u) = (2J_u+1)\,B(\alpha_u J_u \to \alpha J)$$
$$\times \sum_{qq'} 3\,(-1)^{M' - M} \begin{pmatrix} J_u & J & 1 \\ -M'_u & M' & -q \end{pmatrix} \begin{pmatrix} J_u & J & 1 \\ -M_u & M & -q' \end{pmatrix}$$
$$\times\ J_{qq'}(\nu_{\alpha_u J_u,\,\alpha J}) \tag{7.9c}$$

---

the individual magnetic sublevels $(\alpha_\ell J_\ell M_\ell)$ and $(\alpha_u J_u M_u)$ are given by

$$A_{\alpha_u J_u M_u,\,\alpha_\ell J_\ell M_\ell} = \frac{64\pi^4}{3hc^3}\,\nu^3_{\alpha_u J_u M_u,\,\alpha_\ell J_\ell M_\ell}\,|\langle\!\langle \alpha_u J_u M_u|\,\vec{d}\,|\alpha_\ell J_\ell M_\ell \rangle\!\rangle|^2$$
$$B_{\alpha_u J_u M_u,\,\alpha_\ell J_\ell M_\ell} = \frac{32\pi^4}{3h^2c}\,|\langle\!\langle \alpha_u J_u M_u|\,\vec{d}\,|\alpha_\ell J_\ell M_\ell \rangle\!\rangle|^2$$
$$B_{\alpha_\ell J_\ell M_\ell,\,\alpha_u J_u M_u} = \frac{32\pi^4}{3h^2c}\,|\langle\!\langle \alpha_\ell J_\ell M_\ell|\,\vec{d}\,|\alpha_u J_u M_u \rangle\!\rangle|^2\,.$$

Using Eqs. (6.70), (7.4), (2.23a) and (7.6) we get

$$\textstyle\sum_{M_\ell} A_{\alpha_u J_u M_u,\,\alpha_\ell J_\ell M_\ell} = A(\alpha_u J_u \to \alpha_\ell J_\ell)$$
$$\textstyle\sum_{M_\ell} B_{\alpha_u J_u M_u,\,\alpha_\ell J_\ell M_\ell} = B(\alpha_u J_u \to \alpha_\ell J_\ell)\,, \qquad \sum_{M_u} B_{\alpha_\ell J_\ell M_\ell,\,\alpha_u J_u M_u} = B(\alpha_\ell J_\ell \to \alpha_u J_u)$$

(the first relation implies indeed the approximation

$$\nu^3_{\alpha_u J_u M_u,\,\alpha_\ell J_\ell M_\ell} = \nu^3_{\alpha_u J_u,\,\alpha_\ell J_\ell}\,)\,.$$

$$R_{\rm A}(\alpha JMM') = \frac{1}{2}\sum_{\alpha_u J_u}(2J+1)\,B(\alpha J\to\alpha_u J_u) \times\sum_{qq'M_u} 3\,(-1)^{M-M'}\begin{pmatrix} J_u & J & 1\\ -M_u & M & -q\end{pmatrix}\begin{pmatrix} J_u & J & 1\\ -M_u & M' & -q'\end{pmatrix} \times J_{qq'}(\nu_{\alpha_u J_u,\,\alpha J}) \tag{7.9d}$$

$$R_{\rm E}(\alpha JMM') = \frac{1}{2}\sum_{\alpha_\ell J_\ell}(2J+1)\,A(\alpha J\to\alpha_\ell J_\ell) \times\sum_{qM_\ell}(-1)^{M-M'}\begin{pmatrix} J & J_\ell & 1\\ -M & M_\ell & -q\end{pmatrix}\begin{pmatrix} J & J_\ell & 1\\ -M' & M_\ell & -q\end{pmatrix} = \frac{1}{2}\,\delta_{MM'}\sum_{\alpha_\ell J_\ell} A(\alpha J\to\alpha_\ell J_\ell) \tag{7.9e}$$

$$R_{\rm S}(\alpha JMM') = \frac{1}{2}\sum_{\alpha_\ell J_\ell}(2J+1)\,B(\alpha J\to\alpha_\ell J_\ell) \times\sum_{qq'M_\ell} 3\begin{pmatrix} J & J_\ell & 1\\ -M & M_\ell & -q\end{pmatrix}\begin{pmatrix} J & J_\ell & 1\\ -M' & M_\ell & -q'\end{pmatrix} \times J_{qq'}(\nu_{\alpha J,\,\alpha_\ell J_\ell})\,. \tag{7.9f}$$

7.1.b Radiative Transfer Coefficients

Quite similar transformations can be applied to the different quantities entering the radiative transfer equations – which will be simply referred to as the *radiative transfer coefficients*. Substituting in Eqs. (6.88)

$$\begin{array}{ll} m\to\alpha_u J_u M_u & n\to\alpha_\ell J_\ell M_\ell\\ m'\to\alpha_u J_u M'_u & n'\to\alpha_\ell J_\ell M'_\ell\,,\end{array}$$

we obtain[1]

$$\eta_i^{\rm A}(\nu,\vec{\Omega}) = \frac{h\nu}{4\pi}\mathcal{N}\sum_{\alpha_\ell J_\ell}\sum_{\alpha_u J_u}(2J_\ell+1)\,B(\alpha_\ell J_\ell\to\alpha_u J_u) \times\sum_{M_\ell M'_\ell M_u qq'}(-1)^{M_\ell-M'_\ell}\;3\begin{pmatrix} J_u & J_\ell & 1\\ -M_u & M_\ell & -q\end{pmatrix}\begin{pmatrix} J_u & J_\ell & 1\\ -M_u & M'_\ell & -q'\end{pmatrix} \times\;{\rm Re}\Big[\,\mathcal{T}_{qq'}(i,\vec{\Omega})\;\rho_{\alpha_\ell J_\ell}(M_\ell,M'_\ell)\;\Phi(\nu_{\alpha_u J_u M_u,\,\alpha_\ell J_\ell M_\ell}-\nu)\Big] \tag{7.10a}$$

[1] The second expression for $\varepsilon_i(\nu,\vec{\Omega})$ should be multiplied by the factor $\nu^3/\nu^3_{\alpha_u J_u,\,\alpha_\ell J_\ell}$, which is however very close to unity because of the presence of the Φ profile.

$$\eta_i^{\rm S}(\nu,\vec{\Omega}) = \frac{h\nu}{4\pi}\mathcal{N}\sum_{\alpha_\ell J_\ell}\sum_{\alpha_u J_u}(2J_u+1)\,B(\alpha_u J_u\rightarrow\alpha_\ell J_\ell)$$
$$\times\sum_{M_u M_u' M_\ell q q'} 3\begin{pmatrix} J_u & J_\ell & 1\\ -M_u & M_\ell & -q\end{pmatrix}\begin{pmatrix} J_u & J_\ell & 1\\ -M_u' & M_\ell & -q'\end{pmatrix}$$
$$\times\ {\rm Re}\Big[\,\mathcal{T}_{qq'}(i,\vec{\Omega})\ \rho_{\alpha_u J_u}(M_u',M_u)\ \Phi(\nu_{\alpha_u J_u M_u,\,\alpha_\ell J_\ell M_\ell}-\nu)\Big] \tag{7.10b}$$

$$\rho_i^{\rm A}(\nu,\vec{\Omega}) = \eta_i^{\rm A}(\nu,\vec{\Omega})\Big\{{\rm Re}\rightarrow{\rm Im}\Big\} \tag{7.10c}$$

$$\rho_i^{\rm S}(\nu,\vec{\Omega}) = \eta_i^{\rm S}(\nu,\vec{\Omega})\Big\{{\rm Re}\rightarrow{\rm Im}\Big\} \tag{7.10d}$$

$$\varepsilon_i(\nu,\vec{\Omega}) = \frac{2h\nu^3}{c^2}\ \eta_i^{\rm S}(\nu,\vec{\Omega})$$
$$= \frac{h\nu}{4\pi}\mathcal{N}\sum_{\alpha_\ell J_\ell}\sum_{\alpha_u J_u}(2J_u+1)\,A(\alpha_u J_u\rightarrow\alpha_\ell J_\ell)$$
$$\times\sum_{M_u M_u' M_\ell q q'} 3\begin{pmatrix} J_u & J_\ell & 1\\ -M_u & M_\ell & -q\end{pmatrix}\begin{pmatrix} J_u & J_\ell & 1\\ -M_u' & M_\ell & -q'\end{pmatrix}$$
$$\times\ {\rm Re}\Big[\,\mathcal{T}_{qq'}(i,\vec{\Omega})\ \rho_{\alpha_u J_u}(M_u',M_u)\ \Phi(\nu_{\alpha_u J_u M_u,\,\alpha_\ell J_\ell M_\ell}-\nu)\Big]\,. \tag{7.10e}$$

7.2. The Multi-Level Atom in the Spherical Statistical Tensor Representation

We will now convert the equations of the previous section into the spherical statistical tensor representation.

7.2.a Statistical Equilibrium Equations

Multiplying both sides of Eq. (7.5) by

$$(-1)^{J-M}\sqrt{2K+1}\begin{pmatrix} J & J & K\\ M & -M' & -Q\end{pmatrix}$$

and carrying out the summation over M and M' we obtain, with the use of Eqs. (3.97) and (3.99)

$$\frac{\rm d}{{\rm d}t}\,\rho_Q^K(\alpha J) = -2\pi{\rm i}\,\nu_{\rm L}\ g_{\alpha J}\ Q\ \rho_Q^K(\alpha J)$$
$$+\sum_{\alpha_\ell J_\ell}\sum_{K_\ell Q_\ell}\rho_{Q_\ell}^{K_\ell}(\alpha_\ell J_\ell)\ \mathbb{T}_{\rm A}(\alpha J K Q,\alpha_\ell J_\ell K_\ell Q_\ell)+$$

$$+\sum_{\alpha_u J_u}\sum_{K_u Q_u}\rho^{K_u}_{Q_u}(\alpha_u J_u)\Big[\mathbb{T}_{\mathrm{E}}(\alpha JKQ,\alpha_u J_u K_u Q_u) + \mathbb{T}_{\mathrm{S}}(\alpha JKQ,\alpha_u J_u K_u Q_u)\Big]$$

$$-\sum_{K'Q'}\rho^{K'}_{Q'}(\alpha J)\Big[\mathbb{R}_{\mathrm{A}}(\alpha JKQK'Q') + \mathbb{R}_{\mathrm{E}}(\alpha JKQK'Q') + \mathbb{R}_{\mathrm{S}}(\alpha JKQK'Q')\Big], \tag{7.11}$$

where

$$\mathbb{T}_{\mathrm{A}}(\alpha JKQ,\alpha_\ell J_\ell K_\ell Q_\ell) = \sqrt{(2K+1)(2K_\ell+1)} \times \sum_{MM'}\sum_{M_\ell M'_\ell}(-1)^{J-M+J_\ell-M_\ell}\begin{pmatrix} J & J & K\\ M & -M' & -Q\end{pmatrix}\begin{pmatrix} J_\ell & J_\ell & K_\ell\\ M_\ell & -M'_\ell & -Q_\ell\end{pmatrix} \times T_{\mathrm{A}}(\alpha JMM',\alpha_\ell J_\ell M_\ell M'_\ell)$$

$$\mathbb{T}_{\mathrm{E}}(\alpha JKQ,\alpha_u J_u K_u Q_u) = \sqrt{(2K+1)(2K_u+1)} \times \sum_{MM'}\sum_{M_u M'_u}(-1)^{J-M+J_u-M_u}\begin{pmatrix} J & J & K\\ M & -M' & -Q\end{pmatrix}\begin{pmatrix} J_u & J_u & K_u\\ M_u & -M'_u & -Q_u\end{pmatrix} \times T_{\mathrm{E}}(\alpha JMM',\alpha_u J_u M_u M'_u)$$

$$\mathbb{T}_{\mathrm{S}}(\alpha JKQ,\alpha_u J_u K_u Q_u) = \sqrt{(2K+1)(2K_u+1)} \times \sum_{MM'}\sum_{M_u M'_u}(-1)^{J-M+J_u-M_u}\begin{pmatrix} J & J & K\\ M & -M' & -Q\end{pmatrix}\begin{pmatrix} J_u & J_u & K_u\\ M_u & -M'_u & -Q_u\end{pmatrix} \times T_{\mathrm{S}}(\alpha JMM',\alpha_u J_u M_u M'_u)$$

$$\mathbb{R}_{\mathrm{A}}(\alpha JKQK'Q') = \sqrt{(2K+1)(2K'+1)} \times \sum_{MM'M''}\begin{pmatrix} J & J & K\\ M & -M' & -Q\end{pmatrix} \times\left\{\begin{pmatrix} J & J & K'\\ M & -M'' & -Q'\end{pmatrix} R_{\mathrm{A}}(\alpha JM'M'') + (-1)^{Q'-Q}\begin{pmatrix} J & J & K'\\ M'' & -M' & -Q'\end{pmatrix} R_{\mathrm{A}}(\alpha JM''M)\right\}$$

$$\mathbb{R}_{\mathrm{E}}(\alpha JKQK'Q') = \sqrt{(2K+1)(2K'+1)}$$
$$\times \sum_{MM'M''} \begin{pmatrix} J & J & K \\ M & -M' & -Q \end{pmatrix}$$
$$\times \left\{ \begin{pmatrix} J & J & K' \\ M & -M'' & -Q' \end{pmatrix} R_{\mathrm{E}}(\alpha JM''M') \right.$$
$$\left. + (-1)^{Q'-Q} \begin{pmatrix} J & J & K' \\ M'' & -M' & -Q' \end{pmatrix} R_{\mathrm{E}}(\alpha JMM'') \right\}$$

$$\mathbb{R}_{\mathrm{S}}(\alpha JKQK'Q') = \sqrt{(2K+1)(2K'+1)}$$
$$\times \sum_{MM'M''} \begin{pmatrix} J & J & K \\ M & -M' & -Q \end{pmatrix}$$
$$\times \left\{ \begin{pmatrix} J & J & K' \\ M & -M'' & -Q' \end{pmatrix} R_{\mathrm{S}}(\alpha JM''M') \right.$$
$$\left. + (-1)^{Q'-Q} \begin{pmatrix} J & J & K' \\ M'' & -M' & -Q' \end{pmatrix} R_{\mathrm{S}}(\alpha JMM'') \right\} .$$

These expressions can be further developed by substitution of Eqs. (7.9). For the rate $\mathbb{T}_{\mathrm{A}}$ we have

$$\mathbb{T}_{\mathrm{A}}(\alpha JKQ, \alpha_\ell J_\ell K_\ell Q_\ell) = 3\,(2J_\ell+1)\,B(\alpha_\ell J_\ell \rightarrow \alpha J)\,\sqrt{(2K+1)(2K_\ell+1)}$$
$$\times \sum_{MM'M_\ell M'_\ell qq'} (-1)^{J-M+J_\ell-M'_\ell} \begin{pmatrix} J & J & K \\ M & -M' & -Q \end{pmatrix} \begin{pmatrix} J_\ell & J_\ell & K_\ell \\ M_\ell & -M'_\ell & -Q_\ell \end{pmatrix}$$
$$\times \begin{pmatrix} J & J_\ell & 1 \\ -M & M_\ell & -q \end{pmatrix} \begin{pmatrix} J & J_\ell & 1 \\ -M' & M'_\ell & -q' \end{pmatrix}$$
$$\times J_{qq'}(\nu_{\alpha J,\, \alpha_\ell J_\ell}) \,. \tag{7.12}$$

We can now introduce the irreducible radiation field tensor $J^K_Q(\nu)$ using Eq. (5.156), which gives

$$J_{qq'}(\nu) = \sum_{K_{\mathrm{r}} Q_{\mathrm{r}}} (-1)^{1+q} \sqrt{\frac{2K_{\mathrm{r}}+1}{3}} \begin{pmatrix} 1 & 1 & K_{\mathrm{r}} \\ q & -q' & -Q_{\mathrm{r}} \end{pmatrix} J^{K_{\mathrm{r}}}_{Q_{\mathrm{r}}}(\nu) \,. \tag{7.13}$$

Substitution into Eq. (7.12) yields[1]

[1] To arrange the sign factor in this expression it should be kept in mind that – as apparent from the various 3-j symbols – the indices K, Q, K_ℓ, Q_ℓ, K_{r}, Q_{r} are integers.

$$\mathbb{T}_{\rm A}(\alpha JKQ,\alpha_\ell J_\ell K_\ell Q_\ell) = (2J_\ell+1)\,B(\alpha_\ell J_\ell\to\alpha J)$$
$$\times\sum_{K_{\rm r}Q_{\rm r}}\sqrt{3(2K+1)(2K_\ell+1)(2K_{\rm r}+1)}$$
$$\times\sum_{MM'M_\ell M'_\ell qq'}(-1)^{1+J-J_\ell+Q_\ell}\begin{pmatrix}J&J&K\\M&-M'&-Q\end{pmatrix}\begin{pmatrix}J_\ell&J_\ell&K_\ell\\M_\ell&-M'_\ell&-Q_\ell\end{pmatrix}$$
$$\times\begin{pmatrix}J&J_\ell&1\\-M&M_\ell&-q\end{pmatrix}\begin{pmatrix}J&J_\ell&1\\-M'&M'_\ell&-q'\end{pmatrix}\begin{pmatrix}1&1&K_{\rm r}\\q&-q'&-Q_{\rm r}\end{pmatrix}$$
$$\times J^{K_{\rm r}}_{Q_{\rm r}}(\nu_{\alpha J,\,\alpha_\ell J_\ell})\,.$$

The sum of the product of the five 3-j symbols can be evaluated via Eq. (2.52). After some manipulations similar to those of App. 2 we obtain[1]

$$\mathbb{T}_{\rm A}(\alpha JKQ,\alpha_\ell J_\ell K_\ell Q_\ell) = (2J_\ell+1)\,B(\alpha_\ell J_\ell\to\alpha J)$$
$$\times\sum_{K_{\rm r}Q_{\rm r}}\sqrt{3(2K+1)(2K_\ell+1)(2K_{\rm r}+1)}$$
$$\times(-1)^{K_\ell+Q_\ell}\begin{Bmatrix}J&J_\ell&1\\J&J_\ell&1\\K&K_\ell&K_{\rm r}\end{Bmatrix}\begin{pmatrix}K&K_\ell&K_{\rm r}\\-Q&Q_\ell&-Q_{\rm r}\end{pmatrix}J^{K_{\rm r}}_{Q_{\rm r}}(\nu_{\alpha J,\,\alpha_\ell J_\ell})\,. \tag{7.14a}$$

With analogous procedures involving the use of Eq. (2.34) for $\mathbb{T}_{\rm E}$, Eq. (2.52) for $\mathbb{T}_{\rm S}$, Eq. (2.23a) for $\mathbb{R}_{\rm E}$, and Eq. (2.42) – applied twice – for $\mathbb{R}_{\rm A}$ and $\mathbb{R}_{\rm S}$, we get

$$\mathbb{T}_{\rm E}(\alpha JKQ,\alpha_u J_u K_u Q_u) = \delta_{KK_u}\,\delta_{QQ_u}\,(2J_u+1)\,A(\alpha_u J_u\to\alpha J)$$
$$\times(-1)^{1+J+J_u+K}\begin{Bmatrix}J_u&J_u&K\\J&J&1\end{Bmatrix} \tag{7.14b}$$

$$\mathbb{T}_{\rm S}(\alpha JKQ,\alpha_u J_u K_u Q_u) = (2J_u+1)\,B(\alpha_u J_u\to\alpha J)$$
$$\times\sum_{K_{\rm r}Q_{\rm r}}\sqrt{3(2K+1)(2K_u+1)(2K_{\rm r}+1)}$$
$$\times(-1)^{K_{\rm r}+K_u+Q_u}\begin{Bmatrix}J&J_u&1\\J&J_u&1\\K&K_u&K_{\rm r}\end{Bmatrix}\begin{pmatrix}K&K_u&K_{\rm r}\\-Q&Q_u&-Q_{\rm r}\end{pmatrix}J^{K_{\rm r}}_{Q_{\rm r}}(\nu_{\alpha_u J_u,\,\alpha J}) \tag{7.14c}$$

[1] Note that the sign factor appearing in this formula, $(-1)^{K_\ell+Q_\ell}$, can be written in various different ways. As Q_ℓ is an integer, we can also write $(-1)^{K_\ell-Q_\ell}$. As the 9-j symbol is zero unless $(K+K_\ell+K_{\rm r})$ is an even integer (because of the symmetry properties following Eq. (2.48)), the sign factor can also be written $(-1)^{K+K_{\rm r}+Q_\ell}$; etc.

$$\mathbb{R}_{\rm A}(\alpha JKQK'Q') = (2J+1)\sum_{\alpha_u J_u} B(\alpha J \rightarrow \alpha_u J_u)$$
$$\times \sum_{K_{\rm r}Q_{\rm r}} \sqrt{3(2K+1)(2K'+1)(2K_{\rm r}+1)}$$
$$\times (-1)^{1+J_u-J+K_{\rm r}+Q'} \begin{Bmatrix} K & K' & K_{\rm r} \\ J & J & J \end{Bmatrix} \begin{Bmatrix} 1 & 1 & K_{\rm r} \\ J & J & J_u \end{Bmatrix} \begin{pmatrix} K & K' & K_{\rm r} \\ Q & -Q' & Q_{\rm r} \end{pmatrix}$$
$$\times \ \zeta_+ \ J^{K_{\rm r}}_{Q_{\rm r}}(\nu_{\alpha_u J_u, \alpha J}) \tag{7.14d}$$

$$\mathbb{R}_{\rm E}(\alpha JKQK'Q') = \ \delta_{KK'}\,\delta_{QQ'} \sum_{\alpha_\ell J_\ell} A(\alpha J \rightarrow \alpha_\ell J_\ell) \tag{7.14e}$$

$$\mathbb{R}_{\rm S}(\alpha JKQK'Q') = (2J+1)\sum_{\alpha_\ell J_\ell} B(\alpha J \rightarrow \alpha_\ell J_\ell)$$
$$\times \sum_{K_{\rm r}Q_{\rm r}} \sqrt{3(2K+1)(2K'+1)(2K_{\rm r}+1)}$$
$$\times (-1)^{1+J_\ell-J+Q'} \begin{Bmatrix} K & K' & K_{\rm r} \\ J & J & J \end{Bmatrix} \begin{Bmatrix} 1 & 1 & K_{\rm r} \\ J & J & J_\ell \end{Bmatrix} \begin{pmatrix} K & K' & K_{\rm r} \\ Q & -Q' & Q_{\rm r} \end{pmatrix}$$
$$\times \ \zeta_+ \ J^{K_{\rm r}}_{Q_{\rm r}}(\nu_{\alpha J, \alpha_\ell J_\ell}) \ , \tag{7.14f}$$

where[1]

$$\zeta_+ = \frac{1}{2}\left[1 + \ (-1)^{K+K'+K_{\rm r}}\right] .$$

The equations above were first deduced by Bommier and Sahal-Bréchot (1978). Bommier (1977) had formerly derived the corresponding equations in the standard representation.

7.2.b Radiative Transfer Coefficients

The radiative transfer coefficients can be easily expressed in the spherical statistical tensor representation. Using again Eq. (3.99) and writing $\mathcal{T}_{qq'}(i,\vec{\Omega})$ in terms of the irreducible spherical tensor $\mathcal{T}^K_Q(i,\vec{\Omega})$ via Eq. (5.156), we obtain from Eqs. (7.10)

$$\eta^{\rm A}_i(\nu,\vec{\Omega}) = \frac{h\nu}{4\pi}\mathcal{N} \sum_{\alpha_\ell J_\ell} \sum_{\alpha_u J_u} (2J_\ell+1)\, B(\alpha_\ell J_\ell \rightarrow \alpha_u J_u)$$
$$\times \sum_{KQK_\ell Q_\ell} \sqrt{3(2K+1)(2K_\ell+1)} \ \times$$

[1] Note that the quantity ζ_+ is 1 or 0 according as the integer $(K+K'+K_{\rm r})$ is even or odd, respectively.

$$\times \sum_{M_\ell M'_\ell M_u q q'} (-1)^{1+J_\ell-M_\ell+q'} \begin{pmatrix} J_u & J_\ell & 1 \\ -M_u & M_\ell & -q \end{pmatrix} \begin{pmatrix} J_u & J_\ell & 1 \\ -M_u & M'_\ell & -q' \end{pmatrix}$$
$$\times \begin{pmatrix} 1 & 1 & K \\ q & -q' & -Q \end{pmatrix} \begin{pmatrix} J_\ell & J_\ell & K_\ell \\ M_\ell & -M'_\ell & -Q_\ell \end{pmatrix}$$
$$\times \mathrm{Re}\Big[\mathcal{T}^K_Q(i,\vec{\Omega})\ \rho^{K_\ell}_{Q_\ell}(\alpha_\ell J_\ell)\ \Phi(\nu_{\alpha_u J_u M_u,\, \alpha_\ell J_\ell M_\ell} - \nu) \Big] \quad (7.15a)$$

$$\eta^{\mathrm{S}}_i(\nu,\vec{\Omega}) = \frac{h\nu}{4\pi} \mathcal{N} \sum_{\alpha_\ell J_\ell} \sum_{\alpha_u J_u} (2J_u+1)\, B(\alpha_u J_u \to \alpha_\ell J_\ell)$$
$$\times \sum_{K Q K_u Q_u} \sqrt{3(2K+1)(2K_u+1)}$$
$$\times \sum_{M_u M'_u M_\ell q q'} (-1)^{1+J_u-M_u+q'} \begin{pmatrix} J_u & J_\ell & 1 \\ -M_u & M_\ell & -q \end{pmatrix} \begin{pmatrix} J_u & J_\ell & 1 \\ -M'_u & M_\ell & -q' \end{pmatrix}$$
$$\times \begin{pmatrix} 1 & 1 & K \\ q & -q' & -Q \end{pmatrix} \begin{pmatrix} J_u & J_u & K_u \\ M'_u & -M_u & -Q_u \end{pmatrix}$$
$$\times \mathrm{Re}\Big[\mathcal{T}^K_Q(i,\vec{\Omega})\ \rho^{K_u}_{Q_u}(\alpha_u J_u)\ \Phi(\nu_{\alpha_u J_u M_u,\, \alpha_\ell J_\ell M_\ell} - \nu) \Big] \quad (7.15b)$$

$$\rho^{\mathrm{A}}_i(\nu,\vec{\Omega}) = \eta^{\mathrm{A}}_i(\nu,\vec{\Omega}) \Big\{ \mathrm{Re} \to \mathrm{Im} \Big\} \quad (7.15c)$$

$$\rho^{\mathrm{S}}_i(\nu,\vec{\Omega}) = \eta^{\mathrm{S}}_i(\nu,\vec{\Omega}) \Big\{ \mathrm{Re} \to \mathrm{Im} \Big\} \quad (7.15d)$$

$$\varepsilon_i(\nu,\vec{\Omega}) = \frac{2h\nu^3}{c^2}\ \eta^{\mathrm{S}}_i(\nu,\vec{\Omega})\ . \quad (7.15e)$$

These expressions simplify considerably when the dependence of the Φ profiles on the magnetic quantum numbers can be neglected. This occurs, for instance, when the line width is much larger than the Zeeman splitting (the physical regimes Ia and IIa of the classification scheme presented in Sect. 5.16), or when low-resolution observations of the radiation emitted by a thin plasma are to be interpreted. Substituting in Eqs. (7.15)

$$\Phi(\nu_{\alpha_u J_u M_u,\, \alpha_\ell J_\ell M_\ell} - \nu) \to \Phi(\nu_{\alpha_u J_u,\, \alpha_\ell J_\ell} - \nu)\ ,$$

the summations over the magnetic quantum numbers can be carried out using Eq. (2.34). Taking also into account that the quantity $\sum_Q \mathcal{T}^K_Q(i,\vec{\Omega})\ \rho^K_Q(\alpha J)$ is real – as apparent from the conjugation properties (3.102) and (5.158) – one gets

$$\eta^{\mathrm{A}}_i(\nu,\vec{\Omega}) = \frac{h\nu}{4\pi} \mathcal{N} \sum_{\alpha_\ell J_\ell} \sum_{\alpha_u J_u} (2J_\ell+1)\, B(\alpha_\ell J_\ell \to \alpha_u J_u) \times$$

$$\times \sum_{KQ} \sqrt{3}\ (-1)^{1+J_\ell+J_u+K} \begin{Bmatrix} 1 & 1 & K \\ J_\ell & J_\ell & J_u \end{Bmatrix} \mathcal{T}^K_Q(i,\vec{\Omega})\ \rho^K_Q(\alpha_\ell J_\ell)$$
$$\times\ \phi(\nu_{\alpha_u J_u,\,\alpha_\ell J_\ell} - \nu) \tag{7.16a}$$

$$\eta^{\mathrm{S}}_i(\nu,\vec{\Omega}) = \frac{h\nu}{4\pi}\mathcal{N} \sum_{\alpha_\ell J_\ell} \sum_{\alpha_u J_u} (2J_u+1)\, B(\alpha_u J_u \to \alpha_\ell J_\ell)$$
$$\times \sum_{KQ} \sqrt{3}\ (-1)^{1+J_\ell+J_u} \begin{Bmatrix} 1 & 1 & K \\ J_u & J_u & J_\ell \end{Bmatrix} \mathcal{T}^K_Q(i,\vec{\Omega})\ \rho^K_Q(\alpha_u J_u)$$
$$\times\ \phi(\nu_{\alpha_u J_u,\,\alpha_\ell J_\ell} - \nu) \tag{7.16b}$$

$$\rho^{\mathrm{A}}_i(\nu,\vec{\Omega}) = \eta^{\mathrm{A}}_i(\nu,\vec{\Omega}) \left\{ \phi(\nu_{\alpha_u J_u,\,\alpha_\ell J_\ell} - \nu) \to \psi(\nu_{\alpha_u J_u,\,\alpha_\ell J_\ell} - \nu) \right\} \tag{7.16c}$$

$$\rho^{\mathrm{S}}_i(\nu,\vec{\Omega}) = \eta^{\mathrm{S}}_i(\nu,\vec{\Omega}) \left\{ \phi(\nu_{\alpha_u J_u,\,\alpha_\ell J_\ell} - \nu) \to \psi(\nu_{\alpha_u J_u,\,\alpha_\ell J_\ell} - \nu) \right\} \tag{7.16d}$$

$$\varepsilon_i(\nu,\vec{\Omega}) = \frac{2h\nu^3}{c^2}\ \eta^{\mathrm{S}}_i(\nu,\vec{\Omega})\ , \tag{7.16e}$$

where the profiles ϕ and ψ are defined in Eq. (6.59a).

7.3. Conjugation Properties of the Rates

The physical meaning of the various rates defined in Sect. 7.1.a is strictly analogous to that of the more general rates introduced in Chap. 6 (see the discussion following Eq. (6.65)). For instance, the quantity $T_{\mathrm{A}}(\alpha JMM', \alpha_\ell J_\ell M_\ell M'_\ell)$ represents the transfer rate, due to absorption, from the 'lower-level coherence' $\rho_{\alpha_\ell J_\ell}(M_\ell, M'_\ell)$ to the coherence $\rho_{\alpha J}(M, M')$. Similarly, the quantity $R_{\mathrm{A}}(\alpha JM'M'')$ represents the relaxation rate, due to absorption to upper levels, connecting the coherence $\rho_{\alpha J}(M, M')$ with the coherence $\rho_{\alpha J}(M, M'')$. The rates introduced in Sect. 7.2.a have a similar physical interpretation. The quantity $\mathbb{T}_{\mathrm{A}}(\alpha JKQ, \alpha_\ell J_\ell K_\ell Q_\ell)$, for instance, represents the transfer rate, due to absorption, from the spherical statistical tensor of the lower level $\rho^{K_\ell}_{Q_\ell}(\alpha_\ell J_\ell)$ to the spherical statistical tensor $\rho^K_Q(\alpha J)$.

We can easily find the conjugation properties of the different rates. Bearing in mind Eq. (5.154), we have from Eqs. (7.9)

$$T_{\mathrm{A}}(\alpha JMM', \alpha_\ell J_\ell M_\ell M'_\ell)^* = T_{\mathrm{A}}(\alpha JM'M, \alpha_\ell J_\ell M'_\ell M_\ell)$$
$$T_{\mathrm{E}}(\alpha JMM', \alpha_u J_u M_u M'_u)^* = T_{\mathrm{E}}(\alpha JM'M, \alpha_u J_u M'_u M_u)$$
$$= T_{\mathrm{E}}(\alpha JMM', \alpha_u J_u M_u M'_u)$$
$$T_{\mathrm{S}}(\alpha JMM', \alpha_u J_u M_u M'_u)^* = T_{\mathrm{S}}(\alpha JM'M, \alpha_u J_u M'_u M_u)$$

$$R_{\mathrm{A}}(\alpha JMM')^* = R_{\mathrm{A}}(\alpha JM'M)$$

$$R_{\mathrm{E}}(\alpha JMM')^* = R_{\mathrm{E}}(\alpha JM'M) = R_{\mathrm{E}}(\alpha JMM')$$

$$R_{\mathrm{S}}(\alpha JMM')^* = R_{\mathrm{S}}(\alpha JM'M)\ .$$

As to the rates in the spherical statistical tensor representation, we obtain from Eqs. (7.14), with the help of Eqs. (5.158)

$$\mathbb{T}_{\mathrm{A}}(\alpha JKQ, \alpha_\ell J_\ell K_\ell Q_\ell)^* = (-1)^{Q+Q_\ell}\ \mathbb{T}_{\mathrm{A}}(\alpha JK\ -Q, \alpha_\ell J_\ell K_\ell\ -Q_\ell)$$

$$\mathbb{T}_{\mathrm{E}}(\alpha JKQ, \alpha_u J_u K_u Q_u)^* = (-1)^{Q+Q_u}\ \mathbb{T}_{\mathrm{E}}(\alpha JK\ -Q, \alpha_u J_u K_u\ -Q_u)$$

$$= \mathbb{T}_{\mathrm{E}}(\alpha JKQ, \alpha_u J_u K_u Q_u)$$

$$\mathbb{T}_{\mathrm{S}}(\alpha JKQ, \alpha_u J_u K_u Q_u)^* = (-1)^{Q+Q_u}\ \mathbb{T}_{\mathrm{S}}(\alpha JK\ -Q, \alpha_u J_u K_u\ -Q_u)$$

$$\mathbb{R}_{\mathrm{A}}(\alpha JKQK'Q')^* = (-1)^{Q+Q'}\ \mathbb{R}_{\mathrm{A}}(\alpha JK\ -QK'\ -Q')$$

$$\mathbb{R}_{\mathrm{E}}(\alpha JKQK'Q')^* = (-1)^{Q+Q'}\ \mathbb{R}_{\mathrm{E}}(\alpha JK\ -QK'\ -Q') = \mathbb{R}_{\mathrm{E}}(\alpha JKQK'Q')$$

$$\mathbb{R}_{\mathrm{S}}(\alpha JKQK'Q')^* = (-1)^{Q+Q'}\ \mathbb{R}_{\mathrm{S}}(\alpha JK\ -QK'\ -Q')\ .$$

7.4. The No-Coherence Case

The equations derived in Sects. 7.1 and 7.2 are rather involved, which is quite natural as they describe a complex physical situation. It is interesting to consider in detail the special case where atomic polarization can be disregarded; obviously, the equations become considerably simpler in this case.

Let us assume that coherences between Zeeman sublevels can be neglected or, in other words, that the atomic density matrix is diagonal. This case – which will be referred to as *no-coherence case* – covers the union (in the sense of the mathematical set theory) of the physical regimes IIIa, IVa, Va, IIIb outlined in Sect. 5.16. The statistical equilibrium equations in the standard representation might be deduced directly from Eq. (7.5). However, the resulting equations would be of limited use because of the severe assumption on the spectrum of the incident radiation. Since no coherences between magnetic sublevels are present, we can now make – still consistently with the flat-spectrum approximation – the less restrictive assumption that the incident radiation field is flat across frequency intervals wider than the inverse lifetimes of the magnetic sublevels, allowing for its dependence on the individual Bohr frequencies $\nu_{\alpha JM,\,\alpha' J' M'}$. Performing in Eqs. (6.62), (6.69) the same substitutions as in Sect. 7.1.a and introducing shorthand notations for the

rates, we have[1]

$$\frac{\mathrm{d}}{\mathrm{d}t}\,\rho_{\alpha J}(M) = \sum_{\alpha_\ell J_\ell M_\ell} \rho_{\alpha_\ell J_\ell}(M_\ell)\; t_{\mathrm{A}}(\alpha JM, \alpha_\ell J_\ell M_\ell) + \sum_{\alpha_u J_u M_u} \rho_{\alpha_u J_u}(M_u) \Big[t_{\mathrm{E}}(\alpha JM, \alpha_u J_u M_u) + t_{\mathrm{S}}(\alpha JM, \alpha_u J_u M_u) \Big] - \rho_{\alpha J}(M) \Big[r_{\mathrm{A}}(\alpha JM) + r_{\mathrm{E}}(\alpha JM) + r_{\mathrm{S}}(\alpha JM) \Big] , \tag{7.17}$$

where

$$t_{\mathrm{A}}(\alpha JM, \alpha_\ell J_\ell M_\ell) = (2J_\ell + 1)\, B(\alpha_\ell J_\ell \to \alpha J) \times \sum_q 3 \begin{pmatrix} J & J_\ell & 1 \\ -M & M_\ell & -q \end{pmatrix}^2 J_{qq}(\nu_{\alpha JM,\, \alpha_\ell J_\ell M_\ell}) \tag{7.18a}$$

$$t_{\mathrm{E}}(\alpha JM, \alpha_u J_u M_u) = (2J_u + 1)\, A(\alpha_u J_u \to \alpha J) \sum_q \begin{pmatrix} J_u & J & 1 \\ -M_u & M & -q \end{pmatrix}^2 \tag{7.18b}$$

$$t_{\mathrm{S}}(\alpha JM, \alpha_u J_u M_u) = (2J_u + 1)\, B(\alpha_u J_u \to \alpha J) \times \sum_q 3 \begin{pmatrix} J_u & J & 1 \\ -M_u & M & -q \end{pmatrix}^2 J_{qq}(\nu_{\alpha_u J_u M_u,\, \alpha JM}) \tag{7.18c}$$

$$r_{\mathrm{A}}(\alpha JM) = \sum_{\alpha_u J_u} (2J + 1)\, B(\alpha J \to \alpha_u J_u) \times \sum_{qM_u} 3 \begin{pmatrix} J_u & J & 1 \\ -M_u & M & -q \end{pmatrix}^2 J_{qq}(\nu_{\alpha_u J_u M_u,\, \alpha JM}) \tag{7.18d}$$

$$r_{\mathrm{E}}(\alpha JM) = \sum_{\alpha_\ell J_\ell} A(\alpha J \to \alpha_\ell J_\ell) \tag{7.18e}$$

$$r_{\mathrm{S}}(\alpha JM) = \sum_{\alpha_\ell J_\ell} (2J + 1)\, B(\alpha J \to \alpha_\ell J_\ell) \times \sum_{qM_\ell} 3 \begin{pmatrix} J & J_\ell & 1 \\ -M & M_\ell & -q \end{pmatrix}^2 J_{qq}(\nu_{\alpha JM,\, \alpha_\ell J_\ell M_\ell}) , \tag{7.18f}$$

where Eq. (3.91b) has been used.

[1] The expressions for $t_{\mathrm{E}}(\alpha JM, \alpha_u J_u M_u)$ and $r_{\mathrm{E}}(\alpha JM)$ imply, respectively, the approximations

$$\nu^3_{\alpha_u J_u M_u,\, \alpha JM} = \nu^3_{\alpha_u J_u,\, \alpha J} , \qquad \nu^3_{\alpha JM,\, \alpha_\ell J_\ell M_\ell} = \nu^3_{\alpha J,\, \alpha_\ell J_\ell} .$$

For the radiative transfer coefficients we obtain from Eqs. (7.10), with the help of Eq. (5.148)

$$\eta_i^{\mathrm{A}}(\nu,\vec{\Omega}) = \frac{h\nu}{4\pi}\mathcal{N}\sum_{\alpha_\ell J_\ell}\sum_{\alpha_u J_u}(2J_\ell+1)\,B(\alpha_\ell J_\ell\rightarrow\alpha_u J_u)$$
$$\times\sum_{M_\ell M_u q} 3\begin{pmatrix} J_u & J_\ell & 1\\ -M_u & M_\ell & -q\end{pmatrix}^2 \mathcal{T}_{qq}(i,\vec{\Omega})\;\rho_{\alpha_\ell J_\ell}(M_\ell)$$
$$\times\;\phi(\nu_{\alpha_u J_u M_u,\alpha_\ell J_\ell M_\ell}-\nu) \tag{7.19a}$$

$$\eta_i^{\mathrm{S}}(\nu,\vec{\Omega}) = \frac{h\nu}{4\pi}\mathcal{N}\sum_{\alpha_\ell J_\ell}\sum_{\alpha_u J_u}(2J_u+1)\,B(\alpha_u J_u\rightarrow\alpha_\ell J_\ell)$$
$$\times\sum_{M_\ell M_u q} 3\begin{pmatrix} J_u & J_\ell & 1\\ -M_u & M_\ell & -q\end{pmatrix}^2 \mathcal{T}_{qq}(i,\vec{\Omega})\;\rho_{\alpha_u J_u}(M_u)$$
$$\times\;\phi(\nu_{\alpha_u J_u M_u,\alpha_\ell J_\ell M_\ell}-\nu) \tag{7.19b}$$

$$\rho_i^{\mathrm{A}}(\nu,\vec{\Omega}) = \eta_i^{\mathrm{A}}(\nu,\vec{\Omega})\left\{\phi(\nu_{\alpha_u J_u M_u,\alpha_\ell J_\ell M_\ell}-\nu)\rightarrow\psi(\nu_{\alpha_u J_u M_u,\alpha_\ell J_\ell M_\ell}-\nu)\right\} \tag{7.19c}$$

$$\rho_i^{\mathrm{S}}(\nu,\vec{\Omega}) = \eta_i^{\mathrm{S}}(\nu,\vec{\Omega})\left\{\phi(\nu_{\alpha_u J_u M_u,\alpha_\ell J_\ell M_\ell}-\nu)\rightarrow\psi(\nu_{\alpha_u J_u M_u,\alpha_\ell J_\ell M_\ell}-\nu)\right\} \tag{7.19d}$$

$$\varepsilon_i(\nu,\vec{\Omega}) = \frac{2h\nu^3}{c^2}\;\eta_i^{\mathrm{S}}(\nu,\vec{\Omega})\;. \tag{7.19e}$$

Similar simplifications occur in the equations written in the spherical statistical tensor representation. The no-coherence hypothesis results here in the fact that all the components of the multipole moments ρ^K_Q vanish except those having $Q=0$, as apparent from the definition (3.101). Multiplying both sides of Eq. (7.17) by

$$(-1)^{J-M}\sqrt{2K+1}\begin{pmatrix} J & J & K\\ M & -M & 0\end{pmatrix},$$

carrying out the summation over M, and using Eqs. (3.99), (3.101) and (7.13), we obtain the following simplified statistical equilibrium equations[1]

$$\frac{\mathrm{d}}{\mathrm{d}t}\,\rho_0^K(\alpha J) = \sum_{\alpha_\ell J_\ell K_\ell}\rho_0^{K_\ell}(\alpha_\ell J_\ell)\;t_{\mathrm{A}}(\alpha JK,\alpha_\ell J_\ell K_\ell)$$
$$+\sum_{\alpha_u J_u K_u}\rho_0^{K_u}(\alpha_u J_u)\left[t_{\mathrm{E}}(\alpha JK,\alpha_u J_u K_u)+\,t_{\mathrm{S}}(\alpha JK,\alpha_u J_u K_u)\right]$$
$$-\sum_{K'}\rho_0^{K'}(\alpha J)\left[r_{\mathrm{A}}(\alpha JKK')+\,r_{\mathrm{E}}(\alpha JKK')+\,r_{\mathrm{S}}(\alpha JKK')\right],$$

[1] The expressions for the rates $t_{\mathrm{E}}(\alpha JK,\alpha_u J_u K_u)$ and $r_{\mathrm{E}}(\alpha JKK')$ are derived with the help of Eqs. (2.34) and (2.23a), respectively.

where

$$t_{\rm A}(\alpha JK,\alpha_\ell J_\ell K_\ell) = (2J_\ell+1)\,B(\alpha_\ell J_\ell\to\alpha J)\sum_{K_{\rm r}}\sqrt{3(2K+1)(2K_\ell+1)(2K_{\rm r}+1)}$$
$$\times\sum_{MM_\ell q}(-1)^{1+J-J_\ell}\begin{pmatrix}J & J & K\\ M & -M & 0\end{pmatrix}\begin{pmatrix}J_\ell & J_\ell & K_\ell\\ M_\ell & -M_\ell & 0\end{pmatrix}$$
$$\times\begin{pmatrix}J & J_\ell & 1\\ -M & M_\ell & -q\end{pmatrix}^2\begin{pmatrix}1 & 1 & K_{\rm r}\\ q & -q & 0\end{pmatrix}J_0^{K_{\rm r}}(\nu_{\alpha JM,\,\alpha_\ell J_\ell M_\ell}) \tag{7.20a}$$

$$t_{\rm E}(\alpha JK,\alpha_u J_u K_u) = \delta_{KK_u}\,(2J_u+1)\,A(\alpha_u J_u\to\alpha J)$$
$$\times(-1)^{1+J+J_u+K}\begin{Bmatrix}J_u & J_u & K\\ J & J & 1\end{Bmatrix} \tag{7.20b}$$

$$t_{\rm S}(\alpha JK,\alpha_u J_u K_u) = (2J_u+1)\,B(\alpha_u J_u\to\alpha J)\sum_{K_{\rm r}}\sqrt{3(2K+1)(2K_u+1)(2K_{\rm r}+1)}$$
$$\times\sum_{MM_u q}(-1)^{1+J-J_u}\begin{pmatrix}J & J & K\\ M & -M & 0\end{pmatrix}\begin{pmatrix}J_u & J_u & K_u\\ M_u & -M_u & 0\end{pmatrix}$$
$$\times\begin{pmatrix}J_u & J & 1\\ -M_u & M & -q\end{pmatrix}^2\begin{pmatrix}1 & 1 & K_{\rm r}\\ q & -q & 0\end{pmatrix}J_0^{K_{\rm r}}(\nu_{\alpha_u J_u M_u,\,\alpha JM}) \tag{7.20c}$$

$$r_{\rm A}(\alpha JKK') = (2J+1)\sum_{\alpha_u J_u}B(\alpha J\to\alpha_u J_u)\sum_{K_{\rm r}}\sqrt{3(2K+1)(2K'+1)(2K_{\rm r}+1)}$$
$$\times\sum_{MM_u q}(-1)^{1+q}\begin{pmatrix}J & J & K\\ M & -M & 0\end{pmatrix}\begin{pmatrix}J & J & K'\\ M & -M & 0\end{pmatrix}$$
$$\times\begin{pmatrix}J_u & J & 1\\ -M_u & M & -q\end{pmatrix}^2\begin{pmatrix}1 & 1 & K_{\rm r}\\ q & -q & 0\end{pmatrix}J_0^{K_{\rm r}}(\nu_{\alpha_u J_u M_u,\,\alpha JM}) \tag{7.20d}$$

$$r_{\rm E}(\alpha JKK') = \delta_{KK'}\sum_{\alpha_\ell J_\ell}A(\alpha J\to\alpha_\ell J_\ell) \tag{7.20e}$$

$$r_{\rm S}(\alpha JKK') = (2J+1)\sum_{\alpha_\ell J_\ell}B(\alpha J\to\alpha_\ell J_\ell)\sum_{K_{\rm r}}\sqrt{3(2K+1)(2K'+1)(2K_{\rm r}+1)}$$
$$\times\sum_{MM_\ell q}(-1)^{1+q}\begin{pmatrix}J & J & K\\ M & -M & 0\end{pmatrix}\begin{pmatrix}J & J & K'\\ M & -M & 0\end{pmatrix}$$
$$\times\begin{pmatrix}J & J_\ell & 1\\ -M & M_\ell & -q\end{pmatrix}^2\begin{pmatrix}1 & 1 & K_{\rm r}\\ q & -q & 0\end{pmatrix}J_0^{K_{\rm r}}(\nu_{\alpha JM,\,\alpha_\ell J_\ell M_\ell})\,. \tag{7.20f}$$

For the radiative transfer coefficients we have from Eqs. (7.15), with the use of the conjugation relations (3.102) and (5.158)

$$\eta_i^{\mathrm{A}}(\nu,\vec{\Omega}) = \frac{h\nu}{4\pi}\mathcal{N}\sum_{\alpha_\ell J_\ell}\sum_{\alpha_u J_u}(2J_\ell+1)\,B(\alpha_\ell J_\ell\to\alpha_u J_u)\sum_{KK_\ell}\sqrt{3(2K+1)(2K_\ell+1)}$$
$$\times\sum_{M_\ell M_u q}(-1)^{1+J_\ell-M_\ell+q}\begin{pmatrix}J_u & J_\ell & 1\\ -M_u & M_\ell & -q\end{pmatrix}^2\begin{pmatrix}1 & 1 & K\\ q & -q & 0\end{pmatrix}\begin{pmatrix}J_\ell & J_\ell & K_\ell\\ M_\ell & -M_\ell & 0\end{pmatrix}$$
$$\times\,\mathcal{T}_0^K(i,\vec{\Omega})\;\rho_0^{K_\ell}(\alpha_\ell J_\ell)\;\phi(\nu_{\alpha_u J_u M_u,\,\alpha_\ell J_\ell M_\ell}-\nu) \tag{7.21a}$$

$$\eta_i^{\mathrm{S}}(\nu,\vec{\Omega}) = \frac{h\nu}{4\pi}\mathcal{N}\sum_{\alpha_\ell J_\ell}\sum_{\alpha_u J_u}(2J_u+1)\,B(\alpha_u J_u\to\alpha_\ell J_\ell)\sum_{KK_u}\sqrt{3(2K+1)(2K_u+1)}$$
$$\times\sum_{M_\ell M_u q}(-1)^{1+J_u-M_u+q}\begin{pmatrix}J_u & J_\ell & 1\\ -M_u & M_\ell & -q\end{pmatrix}^2\begin{pmatrix}1 & 1 & K\\ q & -q & 0\end{pmatrix}\begin{pmatrix}J_u & J_u & K_u\\ M_u & -M_u & 0\end{pmatrix}$$
$$\times\,\mathcal{T}_0^K(i,\vec{\Omega})\;\rho_0^{K_u}(\alpha_u J_u)\;\phi(\nu_{\alpha_u J_u M_u,\,\alpha_\ell J_\ell M_\ell}-\nu) \tag{7.21b}$$

$$\rho_i^{\mathrm{A}}(\nu,\vec{\Omega}) = \eta_i^{\mathrm{A}}(\nu,\vec{\Omega})\left\{\phi(\nu_{\alpha_u J_u M_u,\,\alpha_\ell J_\ell M_\ell}-\nu)\to\psi(\nu_{\alpha_u J_u M_u,\,\alpha_\ell J_\ell M_\ell}-\nu)\right\} \tag{7.21c}$$

$$\rho_i^{\mathrm{S}}(\nu,\vec{\Omega}) = \eta_i^{\mathrm{S}}(\nu,\vec{\Omega})\left\{\phi(\nu_{\alpha_u J_u M_u,\,\alpha_\ell J_\ell M_\ell}-\nu)\to\psi(\nu_{\alpha_u J_u M_u,\,\alpha_\ell J_\ell M_\ell}-\nu)\right\} \tag{7.21d}$$

$$\varepsilon_i(\nu,\vec{\Omega}) = \frac{2h\nu^3}{c^2}\;\eta_i^{\mathrm{S}}(\nu,\vec{\Omega})\;. \tag{7.21e}$$

7.5. The Multi-Term Atom in the Energy-Eigenvector Representation

We will now consider the interaction of an atomic system with a polarized radiation field in more general terms, dropping some of the basic restrictions adopted so far. First, we will allow for coherences between *different* J-levels, besides those between magnetic sublevels of any individual J-level. Second, we will drop the limitation on the magnetic field intensity,[1] so that the validity of the new equations is not restricted to the Zeeman effect regime. The only restrictions that will be retained are the following:

a) the atom is devoid of hyperfine structure;

b) the atom is described by the L-S coupling scheme (cf. Sect. 3.1), so that the different J-levels are grouped in *terms*, each term being characterized by the quantum numbers β, L, and S;

c) coherences between J-levels pertaining to different terms are negligible.

[1] The magnetic field must be however sufficiently weak for the diamagnetic term in the atomic Hamiltonian to be negligible. This implies $B \ll 10^{10}$G (see the discussion in Sect. 3.1).

The model atom described by these approximations will be named in the following the *multi-term atom*. For such system, the flat-spectrum approximation discussed in Sect. 6.5 requires that the radiation field incident on the atom should be constant across frequency intervals larger than the frequency separation between different levels belonging to the same term. The radiation field can thus be characterized by specifying its value at the Bohr frequencies

$$\nu_{\beta LS,\,\beta' L' S'} = \frac{E(\beta LS) - E(\beta' L' S')}{h} \,, \tag{7.22}$$

where $E(\beta LS)$, $E(\beta' L' S')$ are the energies of the relevant terms (which disregard both the spin-orbit and the magnetic Hamiltonian). This approximation is indeed rather restrictive, but it can only be released within the framework of more general theories able to encompass frequency redistribution effects (see the introductory discussion to Chap. 6).

We now apply the equations derived in Chap. 6 to the multi-term atom embedded in an arbitrary magnetic field. To this aim we must go back to the results obtained in Sect. 3.4 for the Paschen-Back effect regime – which obviously describe, as a particular case, also the Zeeman effect regime. Using the notations of Sect. 3.4 (which implies that the z-axis of the reference system is in the magnetic field direction) we have for the eigenvectors and eigenvalues of the atomic Hamiltonian

$$H_{\rm A}\,|\beta LSjM\rangle = \left[E(\beta LS) + \lambda_j(\beta LS, M)\right] |\beta LSjM\rangle \,,$$

where the eigenvectors are given by (see Eq. (3.58))

$$|\beta LSjM\rangle = \sum_J C_J^j(\beta LS, M)\,|\beta LSJM\rangle \,. \tag{7.23}$$

Therefore, we have to modify the formalism of Chap. 6 according to the following substitutions

i) for the energy eigenvectors:

$$|\,n\rangle \rightarrow |\beta LSjM\rangle \,; \tag{7.24}$$

ii) for the corresponding energy eigenvalues:

$$E_n \rightarrow E(\beta LS) + \lambda_j(\beta LS, M) \,, \tag{7.25}$$

whence

iii) for the Bohr frequencies:

$$\begin{aligned} \nu_{nm} = \frac{E_n - E_m}{h} \rightarrow \;& \nu_{\beta LSjM,\,\beta' L' S' j' M'} = \\ &= \nu_{\beta LS,\,\beta' L' S'} + \frac{\lambda_j(\beta LS, M) - \lambda_{j'}(\beta' L' S', M')}{h} \,; \end{aligned} \tag{7.26}$$

iv) for the matrix elements of the spherical components of the dipole operator:

$$
\begin{aligned}
(d_q)_{nm} = \langle n \,|\, d_q \,|\, m \rangle \rightarrow (d_q)_{\beta LSjM,\,\beta' L'S'j'M'} &= \langle \beta LSjM |\, d_q \,| \beta' L'S'j'M' \rangle = \\
&= \sum_{JJ'} C_J^j(\beta LS, M)\, C_{J'}^{j'}(\beta' L'S', M')\, \langle \beta LSJM |\, d_q \,| \beta' L'S'J'M' \rangle \\
&= \sum_{JJ'} C_J^j(\beta LS, M)\, C_{J'}^{j'}(\beta' L'S', M') \\
&\qquad \times (-1)^{J'+M+1} \sqrt{2J+1} \begin{pmatrix} J & J' & 1 \\ -M & M' & q \end{pmatrix} \langle \beta LSJ \| \vec{d} \,\| \beta' L'S'J' \rangle \\
&= \sum_{JJ'} C_J^j(\beta LS, M)\, C_{J'}^{j'}(\beta' L'S', M') \\
&\qquad \times (-1)^{L+S-M} \sqrt{(2L+1)(2J+1)(2J'+1)} \\
&\qquad \times \begin{pmatrix} J & J' & 1 \\ -M & M' & q \end{pmatrix} \begin{Bmatrix} L & L' & 1 \\ J' & J & S \end{Bmatrix} \langle \beta L \| \vec{d} \,\| \beta' L' \rangle\, \delta_{SS'} \,, \qquad (7.27)
\end{aligned}
$$

where we have used the reality of the C_J^j coefficients (cf. Sect. 3.4), the Wigner-Eckart theorem (Eq. (2.96)), and Eq. (2.108);

v) finally, for the atomic density-matrix elements:

$$
\begin{aligned}
\rho_{nm} = \langle n \,|\, \rho \,|\, m \rangle \rightarrow \langle \beta LSjM |\, \rho \,| \beta' L'S'j'M' \rangle &= \\
&= \delta_{\beta\beta'}\, \delta_{LL'}\, \delta_{SS'}\, \langle \beta LSjM |\, \rho \,| \beta LSj'M' \rangle \\
&= \delta_{\beta\beta'}\, \delta_{LL'}\, \delta_{SS'}\, \rho_{\beta LS}(jM, j'M') \,, \qquad (7.28)
\end{aligned}
$$

where we have used assumption c).

By means of substitutions i) to v) the statistical equilibrium equations and the radiative transfer equations for the multi-term atom in an arbitrary magnetic field can be directly deduced from the corresponding equations of Chap. 6.

7.5.a Statistical Equilibrium Equations

Observing that dipole transitions are only allowed between terms having the same S-value (as apparent from the factor $\delta_{SS'}$ in Eq. (7.27)), we replace in Eqs. (6.62) and (6.69) (see also Fig. 6.1)

$$
\begin{aligned}
&m \rightarrow \beta LSjM \\
&m' \rightarrow \beta LSj'M' \\
&m'' \rightarrow \beta LSj''M''
\end{aligned}
\qquad
\begin{aligned}
&n \rightarrow \beta_\ell L_\ell S j_\ell M_\ell \\
&n' \rightarrow \beta_\ell L_\ell S j'_\ell M'_\ell
\end{aligned}
\qquad
\begin{aligned}
&p \rightarrow \beta_u L_u S j_u M_u \\
&p' \rightarrow \beta_u L_u S j'_u M'_u \,,
\end{aligned}
$$

where the quantum numbers $(\beta_\ell L_\ell S)$ and $(\beta_u L_u S)$ refer to any term of energy lower or higher, respectively, than $E(\beta LS)$. We obtain

$$\frac{\mathrm{d}}{\mathrm{d}t}\,\rho_{\beta LS}(jM,j'M') = -2\pi\mathrm{i}\,\nu_{\beta LS}(jM,j'M')\;\rho_{\beta LS}(jM,j'M')$$
$$+\sum_{\beta_\ell L_\ell j_\ell M_\ell j'_\ell M'_\ell}\rho_{\beta_\ell L_\ell S}(j_\ell M_\ell,j'_\ell M'_\ell)\;T_{\mathrm{A}}(\beta LSjMj'M',\beta_\ell L_\ell S j_\ell M_\ell j'_\ell M'_\ell)$$
$$+\sum_{\beta_u L_u j_u M_u j'_u M'_u}\rho_{\beta_u L_u S}(j_u M_u,j'_u M'_u)\Big[T_{\mathrm{E}}(\beta LSjMj'M',\beta_u L_u S j_u M_u j'_u M'_u)$$
$$+T_{\mathrm{S}}(\beta LSjMj'M',\beta_u L_u S j_u M_u j'_u M'_u)\Big]$$
$$-\sum_{j''M''}\Big\{\rho_{\beta LS}(jM,j''M'')\Big[R_{\mathrm{A}}(\beta LSj'M'j''M'')$$
$$+R_{\mathrm{E}}(\beta LSj''M''j'M')+R_{\mathrm{S}}(\beta LSj''M''j'M')\Big]$$
$$+\rho_{\beta LS}(j''M'',j'M')\Big[R_{\mathrm{A}}(\beta LSj''M''jM)$$
$$+R_{\mathrm{E}}(\beta LSjMj''M'')+R_{\mathrm{S}}(\beta LSjMj''M'')\Big]\Big\}\,, \qquad (7.29)$$

where

$$\nu_{\beta LS}(jM,j'M') = \frac{\lambda_j(\beta LS,M)-\lambda_{j'}(\beta LS,M')}{h}\,. \qquad (7.30)$$

Similarly to Sect. 7.1.a, we now define the line strength of the (electric-dipole) transition between two terms $(\beta_\ell L_\ell S)$ and $(\beta_u L_u S)$ – with $E(\beta_u L_u S) > E(\beta_\ell L_\ell S)$ – by the symmetrical expression

$$\mathcal{S}(\beta_\ell L_\ell S,\beta_u L_u S) = \mathcal{S}(\beta_u L_u S,\beta_\ell L_\ell S) = (2L_\ell+1)\,|\langle\beta_\ell L_\ell\|\vec{d}\,\|\beta_u L_u\rangle|^2$$
$$= (2L_u+1)\,|\langle\beta_u L_u\|\vec{d}\,\|\beta_\ell L_\ell\rangle|^2\,. \qquad (7.31)$$

The Einstein coefficients for spontaneous and stimulated emission and for absorption are connected with the line strength by the relations[1]

[1] Starting from Eqs. (6.71) and (6.73), it can be proved that the Einstein coefficients for the transition between the individual levels $(\beta_\ell L_\ell S j_\ell M_\ell)$ and $(\beta_u L_u S j_u M_u)$ are connected with the Einstein coefficients defined here by the relations

$$\textstyle\sum_{j_\ell M_\ell} A_{\beta_u L_u S j_u M_u,\,\beta_\ell L_\ell S j_\ell M_\ell} = A(\beta_u L_u S\to\beta_\ell L_\ell S)$$
$$\textstyle\sum_{j_\ell M_\ell} B_{\beta_u L_u S j_u M_u,\,\beta_\ell L_\ell S j_\ell M_\ell} = B(\beta_u L_u S\to\beta_\ell L_\ell S)$$
$$\textstyle\sum_{j_u M_u} B_{\beta_\ell L_\ell S j_\ell M_\ell,\,\beta_u L_u S j_u M_u} = B(\beta_\ell L_\ell S\to\beta_u L_u S)$$

(the first relation holds only under the limit

$$\nu^3_{\beta_u L_u S j_u M_u,\,\beta_\ell L_\ell S j_\ell M_\ell} = \nu^3_{\beta_u L_u S,\,\beta_\ell L_\ell S}\,)\,.$$

The proof can be carried out with the help of Eqs. (7.27), (3.62), (2.23a) and (2.39).

$$(2L_u+1)\,A(\beta_u L_u S \to \beta_\ell L_\ell S) = \frac{64\pi^4}{3hc^3}\,\nu^3_{\beta_u L_u S,\,\beta_\ell L_\ell S}\;\mathcal{S}(\beta_u L_u S, \beta_\ell L_\ell S)$$

$$(2L_u+1)\,B(\beta_u L_u S \to \beta_\ell L_\ell S) = \frac{32\pi^4}{3h^2c}\;\mathcal{S}(\beta_u L_u S, \beta_\ell L_\ell S)$$

$$(2L_\ell+1)\,B(\beta_\ell L_\ell S \to \beta_u L_u S) = \frac{32\pi^4}{3h^2c}\;\mathcal{S}(\beta_\ell L_\ell S, \beta_u L_u S)\;, \tag{7.32}$$

with

$$A(\beta_u L_u S \to \beta_\ell L_\ell S) = \frac{2h}{c^2}\,\nu^3_{\beta_u L_u S,\,\beta_\ell L_\ell S}\;B(\beta_u L_u S \to \beta_\ell L_\ell S)$$

$$(2L_\ell+1)\,B(\beta_\ell L_\ell S \to \beta_u L_u S) = (2L_u+1)\,B(\beta_u L_u S \to \beta_\ell L_\ell S)\;. \tag{7.33}$$

Performing the substitutions outlined above, we obtain after some algebra

$$T_{\rm A}(\beta LSjMj'M', \beta_\ell L_\ell S j_\ell M_\ell j'_\ell M'_\ell) = (2L_\ell+1)\,B(\beta_\ell L_\ell S \to \beta LS)$$

$$\times \sum_{JJ'J_\ell J'_\ell} \sum_{qq'} 3\,(-1)^{M_\ell - M'_\ell}\; C^j_J(\beta LS, M)\, C^{j'}_{J'}(\beta LS, M')$$

$$\times C^{j_\ell}_{J_\ell}(\beta_\ell L_\ell S, M_\ell)\, C^{j'_\ell}_{J'_\ell}(\beta_\ell L_\ell S, M'_\ell)\,\sqrt{(2J+1)(2J'+1)(2J_\ell+1)(2J'_\ell+1)}$$

$$\times \begin{pmatrix} J & J_\ell & 1 \\ -M & M_\ell & -q \end{pmatrix} \begin{pmatrix} J' & J'_\ell & 1 \\ -M' & M'_\ell & -q' \end{pmatrix} \begin{Bmatrix} L & L_\ell & 1 \\ J_\ell & J & S \end{Bmatrix} \begin{Bmatrix} L & L_\ell & 1 \\ J'_\ell & J' & S \end{Bmatrix}$$

$$\times\; J_{qq'}(\nu_{\beta LS,\,\beta_\ell L_\ell S}) \tag{7.34a}$$

$$T_{\rm E}(\beta LSjMj'M', \beta_u L_u S j_u M_u j'_u M'_u) = (2L_u+1)\,A(\beta_u L_u S \to \beta LS)$$

$$\times \sum_{JJ'J_u J'_u} \sum_{q} (-1)^{M_u - M'_u}\; C^j_J(\beta LS, M)\, C^{j'}_{J'}(\beta LS, M')$$

$$\times C^{j_u}_{J_u}(\beta_u L_u S, M_u)\, C^{j'_u}_{J'_u}(\beta_u L_u S, M'_u)\,\sqrt{(2J+1)(2J'+1)(2J_u+1)(2J'_u+1)}$$

$$\times \begin{pmatrix} J_u & J & 1 \\ -M_u & M & -q \end{pmatrix} \begin{pmatrix} J'_u & J' & 1 \\ -M'_u & M' & -q \end{pmatrix} \begin{Bmatrix} L_u & L & 1 \\ J & J_u & S \end{Bmatrix} \begin{Bmatrix} L_u & L & 1 \\ J' & J'_u & S \end{Bmatrix} \tag{7.34b}$$

$$T_{\rm S}(\beta LSjMj'M', \beta_u L_u S j_u M_u j'_u M'_u) = (2L_u+1)\,B(\beta_u L_u S \to \beta LS)$$

$$\times \sum_{JJ'J_u J'_u} \sum_{qq'} 3\,(-1)^{M - M'}\; C^j_J(\beta LS, M)\, C^{j'}_{J'}(\beta LS, M')\;\times$$

$$\times\, C^{j_u}_{J_u}(\beta_u L_u S, M_u)\, C^{j'_u}_{J'_u}(\beta_u L_u S, M'_u)\, \sqrt{(2J+1)(2J'+1)(2J_u+1)(2J'_u+1)}$$
$$\times \begin{pmatrix} J_u & J & 1 \\ -M_u & M & -q' \end{pmatrix} \begin{pmatrix} J'_u & J' & 1 \\ -M'_u & M' & -q \end{pmatrix} \begin{Bmatrix} L_u & L & 1 \\ J & J_u & S \end{Bmatrix} \begin{Bmatrix} L_u & L & 1 \\ J' & J'_u & S \end{Bmatrix}$$
$$\times\, J_{qq'}(\nu_{\beta_u L_u S,\, \beta LS}) \tag{7.34c}$$

$$R_{\mathrm{A}}(\beta LSjMj'M') = \frac{1}{2} \sum_{\beta_u L_u} (2L+1)\, B(\beta LS \rightarrow \beta_u L_u S)$$
$$\times \sum_{JJ'J_u} \sum_{qq'M_u} 3\,(-1)^{q+q'}\, C^{j}_{J}(\beta LS, M)\, C^{j'}_{J'}(\beta LS, M')$$
$$\times \sqrt{(2J+1)(2J'+1)}\ (2J_u+1) \begin{pmatrix} J_u & J & 1 \\ -M_u & M & -q \end{pmatrix} \begin{pmatrix} J_u & J' & 1 \\ -M_u & M' & -q' \end{pmatrix}$$
$$\times \begin{Bmatrix} L_u & L & 1 \\ J & J_u & S \end{Bmatrix} \begin{Bmatrix} L_u & L & 1 \\ J' & J_u & S \end{Bmatrix} J_{qq'}(\nu_{\beta_u L_u S,\, \beta LS}) \tag{7.34d}$$

$$R_{\mathrm{E}}(\beta LSjMj'M') = \frac{1}{2}\, \delta_{jj'}\, \delta_{MM'} \sum_{\beta_\ell L_\ell} A(\beta LS \rightarrow \beta_\ell L_\ell S) \tag{7.34e}$$

$$R_{\mathrm{S}}(\beta LSjMj'M') = \frac{1}{2} \sum_{\beta_\ell L_\ell} (2L+1)\, B(\beta LS \rightarrow \beta_\ell L_\ell S)$$
$$\times \sum_{JJ'J_\ell} \sum_{qq'M_\ell} 3\, C^{j}_{J}(\beta LS, M)\, C^{j'}_{J'}(\beta LS, M')$$
$$\times \sqrt{(2J+1)(2J'+1)}\ (2J_\ell+1) \begin{pmatrix} J & J_\ell & 1 \\ -M & M_\ell & -q \end{pmatrix} \begin{pmatrix} J' & J_\ell & 1 \\ -M' & M_\ell & -q' \end{pmatrix}$$
$$\times \begin{Bmatrix} L & L_\ell & 1 \\ J_\ell & J & S \end{Bmatrix} \begin{Bmatrix} L & L_\ell & 1 \\ J_\ell & J' & S \end{Bmatrix} J_{qq'}(\nu_{\beta LS,\, \beta_\ell L_\ell S})\,. \tag{7.34f}$$

The expressions for R_{A} and R_{S} have been derived using Eq. (3.62b); the expression for R_{E} using Eqs. (3.62b), (2.23a), (2.39), and (3.62a).

7.5.b Radiative Transfer Coefficients

Substituting in Eqs. (6.88)

$$\begin{aligned} m &\rightarrow \beta_u L_u S j_u M_u \qquad & n &\rightarrow \beta_\ell L_\ell S j_\ell M_\ell \\ m' &\rightarrow \beta_u L_u S j'_u M'_u \qquad & n' &\rightarrow \beta_\ell L_\ell S j'_\ell M'_\ell\,, \end{aligned}$$

we obtain by similar transformations

$$\eta_i^{\mathrm{A}}(\nu,\vec{\Omega}) = \frac{h\nu}{4\pi}\mathcal{N} \sum_{\beta_\ell L_\ell S \beta_u L_u} (2L_\ell+1)\, B(\beta_\ell L_\ell S \to \beta_u L_u S)$$
$$\times \sum_{j_\ell j'_\ell J_\ell J'_\ell j_u J_u J'_u} \sum_{M_\ell M'_\ell M_u q q'} 3\,(-1)^{q+q'}\, C^{j_\ell}_{J_\ell}(\beta_\ell L_\ell S, M_\ell)\, C^{j'_\ell}_{J'_\ell}(\beta_\ell L_\ell S, M'_\ell)$$
$$\times C^{j_u}_{J_u}(\beta_u L_u S, M_u)\, C^{j_u}_{J'_u}(\beta_u L_u S, M_u) \sqrt{(2J_\ell+1)(2J'_\ell+1)(2J_u+1)(2J'_u+1)}$$
$$\times \begin{pmatrix} J_u & J_\ell & 1 \\ -M_u & M_\ell & -q \end{pmatrix} \begin{pmatrix} J'_u & J'_\ell & 1 \\ -M_u & M'_\ell & -q' \end{pmatrix} \begin{Bmatrix} L_u & L_\ell & 1 \\ J_\ell & J_u & S \end{Bmatrix} \begin{Bmatrix} L_u & L_\ell & 1 \\ J'_\ell & J'_u & S \end{Bmatrix}$$
$$\times \mathrm{Re}\Big[\, \mathcal{T}_{qq'}(i,\vec{\Omega})\ \rho_{\beta_\ell L_\ell S}(j_\ell M_\ell, j'_\ell M'_\ell)\ \Phi(\nu_{\beta_u L_u S j_u M_u,\, \beta_\ell L_\ell S j_\ell M_\ell} - \nu)\Big] \tag{7.35a}$$

$$\eta_i^{\mathrm{S}}(\nu,\vec{\Omega}) = \frac{h\nu}{4\pi}\mathcal{N} \sum_{\beta_u L_u S \beta_\ell L_\ell} (2L_u+1)\, B(\beta_u L_u S \to \beta_\ell L_\ell S)$$
$$\times \sum_{j_u j'_u J_u J'_u j_\ell J_\ell J'_\ell} \sum_{M_u M'_u M_\ell q q'} 3\, C^{j_\ell}_{J_\ell}(\beta_\ell L_\ell S, M_\ell)\, C^{j_\ell}_{J'_\ell}(\beta_\ell L_\ell S, M_\ell)$$
$$\times C^{j_u}_{J_u}(\beta_u L_u S, M_u)\, C^{j'_u}_{J'_u}(\beta_u L_u S, M'_u) \sqrt{(2J_\ell+1)(2J'_\ell+1)(2J_u+1)(2J'_u+1)}$$
$$\times \begin{pmatrix} J_u & J_\ell & 1 \\ -M_u & M_\ell & -q \end{pmatrix} \begin{pmatrix} J'_u & J'_\ell & 1 \\ -M'_u & M_\ell & -q' \end{pmatrix} \begin{Bmatrix} L_u & L_\ell & 1 \\ J_\ell & J_u & S \end{Bmatrix} \begin{Bmatrix} L_u & L_\ell & 1 \\ J'_\ell & J'_u & S \end{Bmatrix}$$
$$\times \mathrm{Re}\Big[\, \mathcal{T}_{qq'}(i,\vec{\Omega})\ \rho_{\beta_u L_u S}(j'_u M'_u, j_u M_u)\ \Phi(\nu_{\beta_u L_u S j_u M_u,\, \beta_\ell L_\ell S j_\ell M_\ell} - \nu)\Big] \tag{7.35b}$$

$$\rho_i^{\mathrm{A}}(\nu,\vec{\Omega}) = \eta_i^{\mathrm{A}}(\nu,\vec{\Omega}) \Big\{ \mathrm{Re} \to \mathrm{Im} \Big\} \tag{7.35c}$$

$$\rho_i^{\mathrm{S}}(\nu,\vec{\Omega}) = \eta_i^{\mathrm{S}}(\nu,\vec{\Omega}) \Big\{ \mathrm{Re} \to \mathrm{Im} \Big\} \tag{7.35d}$$

$$\varepsilon_i(\nu,\vec{\Omega}) = \frac{2h\nu^3}{c^2}\ \eta_i^{\mathrm{S}}(\nu,\vec{\Omega})\ . \tag{7.35e}$$

7.6. The Multi-Term Atom in the Spherical Statistical Tensor Representation

It is worth pointing out an important difference between the case of the multi-level atom considered in Sect. 7.1 and the case of the multi-term atom of Sect. 7.5. In the former case, because of the Zeeman effect regime assumption, the energy eigenvectors coincide with the eigenvectors of angular momentum, so that there is no

difference between energy-eigenvector representation and standard representation of the atomic density operator. In the latter case, on the contrary – where the limitation on the magnetic field intensity is dropped (Paschen-Back effect regime) – the two representations are distinct, which leads to the appearance of the C^j_J coefficients of Eq. (7.23) in the expressions of the rates (Eqs. (7.34)) and of the radiative transfer coefficients (Eqs. (7.35)). This fact, together with the consideration of coherences between different J-levels, is responsible for the much greater complexity of the equations of Sect. 7.5 compared with those of Sect. 7.1.

It is a simple task to rewrite the equations for the multi-term atom either in the standard representation or in the spherical statistical tensor representation. We recall that the various representations are connected by the linear relations (see Eqs. (7.23) and (3.99))

$$\rho_{\beta LS}(jM,j'M') = \sum_{JJ'} C^j_J(\beta LS,M)\, C^{j'}_{J'}(\beta LS,M')\ \rho_{\beta LS}(JM,J'M')$$

$$\begin{aligned}\rho_{\beta LS}(jM,j'M') &= \sum_{JJ'} C^j_J(\beta LS,M)\, C^{j'}_{J'}(\beta LS,M') \\ &\times \sum_{KQ} (-1)^{J-M}\sqrt{2K+1}\begin{pmatrix} J & J' & K \\ M & -M' & -Q\end{pmatrix} {}^{\beta LS}\rho^K_Q(J,J')\end{aligned} \tag{7.36}$$

with the inverse formulae, that can be deduced using Eqs. (3.62b) and (3.97)

$$\rho_{\beta LS}(JM,J'M') = \sum_{jj'} C^j_J(\beta LS,M)\, C^{j'}_{J'}(\beta LS,M')\ \rho_{\beta LS}(jM,j'M')$$

$$\begin{aligned}{}^{\beta LS}\rho^K_Q(J,J') &= \sum_{jMj'M'} C^j_J(\beta LS,M)\, C^{j'}_{J'}(\beta LS,M') \\ &\times (-1)^{J-M}\sqrt{2K+1}\begin{pmatrix} J & J' & K \\ M & -M' & -Q\end{pmatrix} \rho_{\beta LS}(jM,j'M')\ .\end{aligned} \tag{7.37}$$

In the following we derive the statistical equilibrium equations and the radiative transfer coefficients directly in the spherical statistical tensor representation.

7.6.a Statistical Equilibrium Equations

Multiplication of both sides of Eq. (7.29) by

$$C^j_J(\beta LS,M)\, C^{j'}_{J'}(\beta LS,M')\ (-1)^{J-M}\sqrt{2K+1}\begin{pmatrix} J & J' & K \\ M & -M' & -Q\end{pmatrix}$$

followed by summation over j, M, j', M' yields, with the use of Eqs. (7.36)-(7.37)

$$\frac{\mathrm{d}}{\mathrm{d}t}\,{}^{\beta LS}\rho^{K}_{Q}(J,J') = -2\pi\mathrm{i}\sum_{K'Q'}\sum_{J''J'''} N_{\beta LS}(KQJJ',K'Q'J''J''')\;{}^{\beta LS}\rho^{K'}_{Q'}(J'',J''')$$
$$+\sum_{\beta_\ell L_\ell K_\ell Q_\ell J_\ell J'_\ell}{}^{\beta_\ell L_\ell S}\rho^{K_\ell}_{Q_\ell}(J_\ell,J'_\ell)\;\mathbb{T}_{\mathrm{A}}(\beta LSKQJJ',\beta_\ell L_\ell SK_\ell Q_\ell J_\ell J'_\ell)$$
$$+\sum_{\beta_u L_u K_u Q_u J_u J'_u}{}^{\beta_u L_u S}\rho^{K_u}_{Q_u}(J_u,J'_u)\Big[\mathbb{T}_{\mathrm{E}}(\beta LSKQJJ',\beta_u L_u SK_u Q_u J_u J'_u)$$
$$+\mathbb{T}_{\mathrm{S}}(\beta LSKQJJ',\beta_u L_u SK_u Q_u J_u J'_u)\Big]$$
$$-\sum_{K'Q'J''J'''}{}^{\beta LS}\rho^{K'}_{Q'}(J'',J''')\Big[\mathbb{R}_{\mathrm{A}}(\beta LSKQJJ'K'Q'J''J''')$$
$$+\mathbb{R}_{\mathrm{E}}(\beta LSKQJJ'K'Q'J''J''')+\mathbb{R}_{\mathrm{S}}(\beta LSKQJJ'K'Q'J''J''')\Big]\,, \quad (7.38)$$

where

$$N_{\beta LS}(KQJJ',K'Q'J''J''') =$$
$$=\sum_{jMj'M'} C^{j}_{J}(\beta LS,M)\,C^{j'}_{J'}(\beta LS,M')\,C^{j}_{J''}(\beta LS,M)\,C^{j'}_{J'''}(\beta LS,M')$$
$$\times(-1)^{J-J''}\sqrt{(2K+1)(2K'+1)}$$
$$\times\begin{pmatrix} J & J' & K\\ M & -M' & -Q\end{pmatrix}\begin{pmatrix} J'' & J''' & K'\\ M & -M' & -Q'\end{pmatrix}\nu_{\beta LS}(jM,j'M') \quad (7.39)$$

$$\mathbb{T}_{\mathrm{A}}(\beta LSKQJJ',\beta_\ell L_\ell SK_\ell Q_\ell J_\ell J'_\ell) =$$
$$=\sum_{jMj'M'j_\ell M_\ell j'_\ell M'_\ell} C^{j}_{J}(\beta LS,M)\,C^{j'}_{J'}(\beta LS,M')\,C^{j_\ell}_{J_\ell}(\beta_\ell L_\ell S,M_\ell)\,C^{j'_\ell}_{J'_\ell}(\beta_\ell L_\ell S,M'_\ell)$$
$$\times(-1)^{J-M+J_\ell-M_\ell}\sqrt{(2K+1)(2K_\ell+1)}\begin{pmatrix} J & J' & K\\ M & -M' & -Q\end{pmatrix}$$
$$\times\begin{pmatrix} J_\ell & J'_\ell & K_\ell\\ M_\ell & -M'_\ell & -Q_\ell\end{pmatrix}T_{\mathrm{A}}(\beta LSjMj'M',\beta_\ell L_\ell Sj_\ell M_\ell j'_\ell M'_\ell) \quad (7.40a)$$

$$\mathbb{T}_{\mathrm{E}}(\beta LSKQJJ',\beta_u L_u SK_u Q_u J_u J'_u) =$$
$$=\sum_{jMj'M'j_u M_u j'_u M'_u} C^{j}_{J}(\beta LS,M)\,C^{j'}_{J'}(\beta LS,M')\,C^{j_u}_{J_u}(\beta_u L_u S,M_u)\,C^{j'_u}_{J'_u}(\beta_u L_u S,M'_u)$$
$$\times(-1)^{J-M+J_u-M_u}\sqrt{(2K+1)(2K_u+1)}\begin{pmatrix} J & J' & K\\ M & -M' & -Q\end{pmatrix}$$
$$\times\begin{pmatrix} J_u & J'_u & K_u\\ M_u & -M'_u & -Q_u\end{pmatrix}T_{\mathrm{E}}(\beta LSjMj'M',\beta_u L_u Sj_u M_u j'_u M'_u) \quad (7.40b)$$

$$\mathbb{R}_{\rm A}(\beta LSKQJJ'K'Q'J''J''') =$$
$$= \sum_{jMj'M'j''M''} C^{j}_{J}(\beta LS,M)\, C^{j'}_{J'}(\beta LS,M')$$
$$\times (-1)^{J-J''}\sqrt{(2K+1)(2K'+1)}\begin{pmatrix} J & J' & K \\ M & -M' & -Q\end{pmatrix}$$
$$\times \Bigg[C^{j}_{J''}(\beta LS,M)\, C^{j''}_{J'''}(\beta LS,M'')$$
$$\times \begin{pmatrix} J'' & J''' & K' \\ M & -M'' & -Q'\end{pmatrix} R_{\rm A}(\beta LSj'M'j''M'')$$
$$+ (-1)^{M''-M}\, C^{j''}_{J''}(\beta LS,M'')\, C^{j'}_{J'''}(\beta LS,M')$$
$$\times \begin{pmatrix} J'' & J''' & K' \\ M'' & -M' & -Q'\end{pmatrix} R_{\rm A}(\beta LSj''M''jM)\Bigg] \qquad (7.40c)$$

$$\mathbb{R}_{\rm E}(\beta LSKQJJ'K'Q'J''J''') =$$
$$= \sum_{jMj'M'j''M''} C^{j}_{J}(\beta LS,M)\, C^{j'}_{J'}(\beta LS,M')$$
$$\times (-1)^{J-J''}\sqrt{(2K+1)(2K'+1)}\begin{pmatrix} J & J' & K \\ M & -M' & -Q\end{pmatrix}$$
$$\times \Bigg[C^{j}_{J''}(\beta LS,M)\, C^{j''}_{J'''}(\beta LS,M'')$$
$$\times \begin{pmatrix} J'' & J''' & K' \\ M & -M'' & -Q'\end{pmatrix} R_{\rm E}(\beta LSj''M''j'M')$$
$$+ (-1)^{M''-M}\, C^{j''}_{J''}(\beta LS,M'')\, C^{j'}_{J'''}(\beta LS,M')$$
$$\times \begin{pmatrix} J'' & J''' & K' \\ M'' & -M' & -Q'\end{pmatrix} R_{\rm E}(\beta LSjMj''M'')\Bigg] \qquad (7.40d)$$

(the relation between $\mathbb{T}_{\rm S}$ and $T_{\rm S}$ is identical to the relation between $\mathbb{T}_{\rm E}$ and $T_{\rm E}$, as obvious from the structure of Eq. (7.29); the same holds for the relation between $\mathbb{R}_{\rm S}$ and $R_{\rm S}$, which is identical to the relation between $\mathbb{R}_{\rm E}$ and $R_{\rm E}$).

The term N defined in Eq. (7.39) can be evaluated in greater detail. Using Eqs. (7.30) and (3.62b,c) we have

$$N_{\beta LS}(KQJJ',K'Q'J''J''') = \delta_{QQ'}\,(-1)^{J-J''}\sqrt{(2K+1)(2K'+1)}$$
$$\times \frac{1}{h}\Bigg[\delta_{J'J'''}\sum_{MM'}\begin{pmatrix} J & J' & K \\ M & -M' & -Q\end{pmatrix}\begin{pmatrix} J'' & J' & K' \\ M & -M' & -Q\end{pmatrix}$$
$$\times \langle \beta LSJM|H_{\rm so}+H_B|\beta LSJ''M\rangle \;+$$

$$- \delta_{JJ''} \sum_{MM'} \begin{pmatrix} J & J' & K \\ M & -M' & -Q \end{pmatrix} \begin{pmatrix} J & J''' & K' \\ M & -M' & -Q \end{pmatrix} \times \left\langle \beta LSJ'M' | H_{\rm so} + H_B | \beta LSJ'''M' \right\rangle \Bigg] ,$$

where $H_{\rm so}$ is the spin-orbit Hamiltonian and H_B the magnetic Hamiltonian. The matrix elements in the right-hand side can be easily evaluated. Taking into account that $H_{\rm so}$ is diagonal with respect to J, expressing the matrix elements of H_B via Eq. (3.57), and performing the summation over M and M' by means of Eqs. (2.23a), (3.42) and (2.42), we obtain after some algebra

$$\begin{aligned} N_{\beta LS}(KQJJ', K'Q'J''J''') = {} & \delta_{KK'} \, \delta_{QQ'} \, \delta_{JJ''} \, \delta_{J'J'''} \, \nu_{\beta LSJ,\, \beta LSJ'} \\ & + \delta_{QQ'} \, \nu_{\rm L} \, (-1)^{J+J'-Q} \sqrt{(2K+1)(2K'+1)} \begin{pmatrix} K & K' & 1 \\ -Q & Q & 0 \end{pmatrix} \\ & \times \Bigg[\delta_{J'J'''} \, \Gamma_{LS}(J, J'') \begin{Bmatrix} K & K' & 1 \\ J'' & J & J' \end{Bmatrix} \\ & \quad + \delta_{JJ''} \, (-1)^{K-K'} \, \Gamma_{LS}(J''', J') \begin{Bmatrix} K & K' & 1 \\ J''' & J' & J \end{Bmatrix} \Bigg] , \end{aligned} \tag{7.41}$$

where

$$\begin{aligned} \Gamma_{LS}(J, J') &= (-1)^{J-J'} \, \Gamma_{LS}(J', J) \\ &= \delta_{JJ'} \sqrt{J(J+1)(2J+1)} \\ &\quad + (-1)^{1+L+S+J} \sqrt{(2J+1)(2J'+1)S(S+1)(2S+1)} \begin{Bmatrix} J & J' & 1 \\ S & S & L \end{Bmatrix} \end{aligned} \tag{7.42}$$

and where

$$\nu_{\beta LSJ,\, \beta LSJ'} = \frac{E_{\beta LS}(J) - E_{\beta LS}(J')}{h} , \tag{7.43}$$

with $E_{\beta LS}(J)$ defined in Eq. (3.60). The quantity $\Gamma_{LS}(J, J')$ is a sort of generalized Landé factor. Use of Eq. (2.36d) shows that

$$\Gamma_{LS}(J, J) = \sqrt{J(J+1)(2J+1)} \; g_{LS}(J) , \tag{7.44}$$

where $g_{LS}(J)$ is the usual Landé factor introduced in Eq. (3.8).

The expressions for the different rates can be further developed by substituting Eqs. (7.34) into Eqs. (7.40). Performing the summations over the indices j, j', j_ℓ, j'_ℓ etc. with the use of Eqs. (3.62b), and substituting Eq. (7.13), the calculations reduce to evaluating the sums over angular momentum components of products of several 3-j symbols. This can be done using Eq. (2.52) for the rates $\mathbb{T}_{\rm A}$ and $\mathbb{T}_{\rm S}$,

Eq. (2.34) for $\mathbb{T}_{\rm E}$, Eq. (2.42) applied twice for $\mathbb{R}_{\rm A}$ and $\mathbb{R}_{\rm S}$, and Eq. (2.23a), also applied twice, for $\mathbb{R}_{\rm E}$. The final results are the following

$$\mathbb{T}_{\rm A}(\beta LSKQJJ',\beta_\ell L_\ell S K_\ell Q_\ell J_\ell J'_\ell) = (2L_\ell+1)\,B(\beta_\ell L_\ell S\to\beta LS)$$
$$\times\sum_{K_{\rm r}Q_{\rm r}}\sqrt{3(2J+1)(2J'+1)(2J_\ell+1)(2J'_\ell+1)(2K+1)(2K_\ell+1)(2K_{\rm r}+1)}$$
$$\times(-1)^{K_\ell+Q_\ell+J'_\ell-J_\ell}\begin{Bmatrix} J & J_\ell & 1\\ J' & J'_\ell & 1\\ K & K_\ell & K_{\rm r}\end{Bmatrix}\begin{Bmatrix} L & L_\ell & 1\\ J_\ell & J & S\end{Bmatrix}$$
$$\times\begin{Bmatrix} L & L_\ell & 1\\ J'_\ell & J' & S\end{Bmatrix}\begin{pmatrix} K & K_\ell & K_{\rm r}\\ -Q & Q_\ell & -Q_{\rm r}\end{pmatrix} J^{K_{\rm r}}_{Q_{\rm r}}(\nu_{\beta LS,\,\beta_\ell L_\ell S}) \tag{7.45a}$$

$$\mathbb{T}_{\rm E}(\beta LSKQJJ',\beta_u L_u S K_u Q_u J_u J'_u) = \delta_{KK_u}\,\delta_{QQ_u}\,(2L_u+1)\,A(\beta_u L_u S\to\beta LS)$$
$$\times\sqrt{(2J+1)(2J'+1)(2J_u+1)(2J'_u+1)}$$
$$\times(-1)^{1+K+J'+J'_u}\begin{Bmatrix} J & J' & K\\ J'_u & J_u & 1\end{Bmatrix}\begin{Bmatrix} L_u & L & 1\\ J & J_u & S\end{Bmatrix}\begin{Bmatrix} L_u & L & 1\\ J' & J'_u & S\end{Bmatrix} \tag{7.45b}$$

$$\mathbb{T}_{\rm S}(\beta LSKQJJ',\beta_u L_u S K_u Q_u J_u J'_u) = (2L_u+1)\,B(\beta_u L_u S\to\beta LS)$$
$$\times\sum_{K_{\rm r}Q_{\rm r}}\sqrt{3(2J+1)(2J'+1)(2J_u+1)(2J'_u+1)(2K+1)(2K_u+1)(2K_{\rm r}+1)}$$
$$\times(-1)^{K_{\rm r}+K_u+Q_u+J'_u-J_u}\begin{Bmatrix} J & J_u & 1\\ J' & J'_u & 1\\ K & K_u & K_{\rm r}\end{Bmatrix}\begin{Bmatrix} L_u & L & 1\\ J & J_u & S\end{Bmatrix}$$
$$\times\begin{Bmatrix} L_u & L & 1\\ J' & J'_u & S\end{Bmatrix}\begin{pmatrix} K & K_u & K_{\rm r}\\ -Q & Q_u & -Q_{\rm r}\end{pmatrix} J^{K_{\rm r}}_{Q_{\rm r}}(\nu_{\beta_u L_u S,\,\beta LS}) \tag{7.45c}$$

$$\mathbb{R}_{\rm A}(\beta LSKQJJ'K'Q'J''J''') = (2L+1)\sum_{\beta_u L_u J_u}(2J_u+1)\,B(\beta LS\to\beta_u L_u S)$$
$$\times\sum_{K_{\rm r}Q_{\rm r}}\sqrt{3(2K+1)(2K'+1)(2K_{\rm r}+1)}\;(-1)^{1+J_u-J'+K_{\rm r}+Q'}\begin{pmatrix} K & K' & K_{\rm r}\\ Q & -Q' & Q_{\rm r}\end{pmatrix}$$
$$\times\frac{1}{2}\Bigg[\delta_{JJ''}\,\sqrt{(2J'+1)(2J'''+1)}$$
$$\times(-1)^{J-J'''}\begin{Bmatrix} L_u & L & 1\\ J' & J_u & S\end{Bmatrix}\begin{Bmatrix} L_u & L & 1\\ J''' & J_u & S\end{Bmatrix}$$
$$\times\begin{Bmatrix} K & K' & K_{\rm r}\\ J''' & J' & J\end{Bmatrix}\begin{Bmatrix} 1 & 1 & K_{\rm r}\\ J''' & J' & J_u\end{Bmatrix}\;+$$

$$
\begin{aligned}
&+ \delta_{J'J'''}\,\sqrt{(2J+1)(2J''+1)} \\
&\quad\times (-1)^{K+K'+K_{\rm r}} \left\{ \begin{array}{ccc} L_u & L & 1 \\ J & J_u & S \end{array} \right\} \left\{ \begin{array}{ccc} L_u & L & 1 \\ J'' & J_u & S \end{array} \right\} \\
&\quad\times \left\{ \begin{array}{ccc} K & K' & K_{\rm r} \\ J'' & J & J' \end{array} \right\} \left\{ \begin{array}{ccc} 1 & 1 & K_{\rm r} \\ J'' & J & J_u \end{array} \right\} \Bigg]\, J^{K_{\rm r}}_{Q_{\rm r}}(\nu_{\beta_u L_u S,\,\beta LS})
\end{aligned}
\tag{7.45d}
$$

$$
\begin{aligned}
\mathbb{R}_{\rm E}(\beta LSKQJJ'K'Q'J''J''') &= \delta_{KK'}\,\delta_{QQ'}\,\delta_{JJ''}\,\delta_{J'J'''} \\
&\times (2L+1) \sum_{\beta_\ell L_\ell J_\ell} A(\beta LS \to \beta_\ell L_\ell S)\,(2J_\ell+1) \\
&\qquad\times \frac{1}{2}\Bigg[\left\{ \begin{array}{ccc} L & L_\ell & 1 \\ J_\ell & J & S \end{array} \right\}^2 + \left\{ \begin{array}{ccc} L & L_\ell & 1 \\ J_\ell & J' & S \end{array} \right\}^2 \Bigg]
\end{aligned}
\tag{7.45e}
$$

$$
\begin{aligned}
\mathbb{R}_{\rm S}(\beta LSKQJJ'K'Q'J''J''') &= (2L+1) \sum_{\beta_\ell L_\ell J_\ell} (2J_\ell+1)\, B(\beta LS \to \beta_\ell L_\ell S) \\
&\times \sum_{K_{\rm r}Q_{\rm r}} \sqrt{3(2K+1)(2K'+1)(2K_{\rm r}+1)}\; (-1)^{1+J_\ell-J'+Q'} \begin{pmatrix} K & K' & K_{\rm r} \\ Q & -Q' & Q_{\rm r} \end{pmatrix} \\
&\times \frac{1}{2}\Bigg[\delta_{JJ''}\,\sqrt{(2J'+1)(2J'''+1)} \\
&\qquad\times (-1)^{J-J'''} \left\{ \begin{array}{ccc} L & L_\ell & 1 \\ J_\ell & J' & S \end{array} \right\} \left\{ \begin{array}{ccc} L & L_\ell & 1 \\ J_\ell & J''' & S \end{array} \right\} \\
&\qquad\times \left\{ \begin{array}{ccc} K & K' & K_{\rm r} \\ J''' & J' & J \end{array} \right\} \left\{ \begin{array}{ccc} 1 & 1 & K_{\rm r} \\ J''' & J' & J_\ell \end{array} \right\} \\
&\quad + \delta_{J'J'''}\,\sqrt{(2J+1)(2J''+1)} \\
&\qquad\times (-1)^{K+K'+K_{\rm r}} \left\{ \begin{array}{ccc} L & L_\ell & 1 \\ J_\ell & J & S \end{array} \right\} \left\{ \begin{array}{ccc} L & L_\ell & 1 \\ J_\ell & J'' & S \end{array} \right\} \\
&\qquad\times \left\{ \begin{array}{ccc} K & K' & K_{\rm r} \\ J'' & J & J' \end{array} \right\} \left\{ \begin{array}{ccc} 1 & 1 & K_{\rm r} \\ J'' & J & J_\ell \end{array} \right\} \Bigg]\, J^{K_{\rm r}}_{Q_{\rm r}}(\nu_{\beta LS,\,\beta_\ell L_\ell S})\,.
\end{aligned}
\tag{7.45f}
$$

The above expressions for the relaxation rates can be further simplified by carrying out the summations on the J quantum numbers. Using Eq. (2.41) for $\mathbb{R}_{\rm A}$ and $\mathbb{R}_{\rm S}$, and Eq. (2.39) for $\mathbb{R}_{\rm E}$ we obtain

$$
\begin{aligned}
\mathbb{R}_{\rm A}(\beta LSKQJJ'K'Q'J''J''') &= (2L+1) \sum_{\beta_u L_u} B(\beta LS \to \beta_u L_u S) \\
&\times \sum_{K_{\rm r}Q_{\rm r}} \sqrt{3(2K+1)(2K'+1)(2K_{\rm r}+1)} \\
&\times (-1)^{1+L_u-S+J+Q'} \left\{ \begin{array}{ccc} L & L & K_{\rm r} \\ 1 & 1 & L_u \end{array} \right\} \begin{pmatrix} K & K' & K_{\rm r} \\ Q & -Q' & Q_{\rm r} \end{pmatrix} \times
\end{aligned}
$$

$$\times \frac{1}{2}\Bigg[\delta_{JJ''} \sqrt{(2J'+1)(2J'''+1)} \times \begin{Bmatrix} L & L & K_{\rm r} \\ J''' & J' & S \end{Bmatrix} \begin{Bmatrix} K & K' & K_{\rm r} \\ J''' & J' & J \end{Bmatrix} + \delta_{J'J'''} \sqrt{(2J+1)(2J''+1)}\ (-1)^{J''-J'+K+K'+K_{\rm r}} \times \begin{Bmatrix} L & L & K_{\rm r} \\ J'' & J & S \end{Bmatrix} \begin{Bmatrix} K & K' & K_{\rm r} \\ J'' & J & J' \end{Bmatrix} \Bigg] J^{K_{\rm r}}_{Q_{\rm r}}(\nu_{\beta_u L_u S,\, \beta L S}) \tag{7.46a}$$

$$\mathbb{R}_{\rm E}(\beta L S K Q J J' K' Q' J'' J''') = \delta_{KK'}\, \delta_{QQ'}\, \delta_{JJ''}\, \delta_{J'J'''} \times \sum_{\beta_\ell L_\ell} A(\beta L S \rightarrow \beta_\ell L_\ell S) \tag{7.46b}$$

$$\mathbb{R}_{\rm S}(\beta L S K Q J J' K' Q' J'' J''') = (2L+1) \sum_{\beta_\ell L_\ell} B(\beta L S \rightarrow \beta_\ell L_\ell S) \times \sum_{K_{\rm r} Q_{\rm r}} \sqrt{3(2K+1)(2K'+1)(2K_{\rm r}+1)} \times (-1)^{1+L_\ell - S + J + K_{\rm r} + Q'} \begin{Bmatrix} L & L & K_{\rm r} \\ 1 & 1 & L_\ell \end{Bmatrix} \begin{pmatrix} K & K' & K_{\rm r} \\ Q & -Q' & Q_{\rm r} \end{pmatrix} \times \frac{1}{2}\Bigg[\delta_{JJ''} \sqrt{(2J'+1)(2J'''+1)} \times \begin{Bmatrix} L & L & K_{\rm r} \\ J''' & J' & S \end{Bmatrix} \begin{Bmatrix} K & K' & K_{\rm r} \\ J''' & J' & J \end{Bmatrix} + \delta_{J'J'''} \sqrt{(2J+1)(2J''+1)}\ (-1)^{J''-J'+K+K'+K_{\rm r}} \times \begin{Bmatrix} L & L & K_{\rm r} \\ J'' & J & S \end{Bmatrix} \begin{Bmatrix} K & K' & K_{\rm r} \\ J'' & J & J' \end{Bmatrix} \Bigg] J^{K_{\rm r}}_{Q_{\rm r}}(\nu_{\beta L S,\, \beta_\ell L_\ell S})\ . \tag{7.46c}$$

Expressions (7.45a-c) and (7.46a-c) have been given by Landi Degl'Innocenti (1982b).[1] The statistical equilibrium equations for the multi-term atom in the standard representation of the atomic density operator have been derived by Bommier (1980).

7.6.b Radiative Transfer Coefficients

Substitution of Eqs. (7.36) and (5.156) – applied to the tensor $\mathcal{T}_{qq'}(i,\vec{\Omega})$ – into Eqs. (7.35) leads, with the help of Eq. (3.62b), to the following expressions

[1] The expressions appearing in that paper contain indeed some additional terms, due to the tensor $F^{K_{\rm r}}_{Q_{\rm r}}$, in the rates $\mathbb{R}_{\rm A}$ and $\mathbb{R}_{\rm S}$. These terms are of very limited importance and their presence is not justified in the flat-spectrum approximation.

$$\eta_i^{\mathrm{A}}(\nu,\vec{\Omega}) = \frac{h\nu}{4\pi}\mathcal{N}\sum_{\beta_\ell L_\ell S\beta_u L_u}(2L_\ell+1)\,B(\beta_\ell L_\ell S\to\beta_u L_u S)$$
$$\times\sum_{KQK_\ell Q_\ell}\sqrt{3(2K+1)(2K_\ell+1)}$$
$$\times\sum_{j_\ell J_\ell J'_\ell J''_\ell j_u J_u J'_u}\ \sum_{M_\ell M'_\ell M_u qq'}(-1)^{1+J''_\ell-M_\ell+q'}\ C^{j_\ell}_{J_\ell}(\beta_\ell L_\ell S,M_\ell)\,C^{j_\ell}_{J''_\ell}(\beta_\ell L_\ell S,M_\ell)$$
$$\times C^{j_u}_{J_u}(\beta_u L_u S,M_u)\,C^{j_u}_{J''_u}(\beta_u L_u S,M_u)\sqrt{(2J_\ell+1)(2J'_\ell+1)(2J_u+1)(2J'_u+1)}$$
$$\times\begin{pmatrix}J_u & J_\ell & 1\\ -M_u & M_\ell & -q\end{pmatrix}\begin{pmatrix}J'_u & J'_\ell & 1\\ -M_u & M'_\ell & -q'\end{pmatrix}\begin{pmatrix}1 & 1 & K\\ q & -q' & -Q\end{pmatrix}$$
$$\times\begin{pmatrix}J''_\ell & J'_\ell & K_\ell\\ M_\ell & -M'_\ell & -Q_\ell\end{pmatrix}\begin{Bmatrix}L_u & L_\ell & 1\\ J_\ell & J_u & S\end{Bmatrix}\begin{Bmatrix}L_u & L_\ell & 1\\ J'_\ell & J'_u & S\end{Bmatrix}$$
$$\times\mathrm{Re}\Big[\,\mathcal{T}^K_Q(i,\vec{\Omega})\ {}^{\beta_\ell L_\ell S}\rho^{K_\ell}_{Q_\ell}(J''_\ell,J'_\ell)\ \Phi(\nu_{\beta_u L_u S j_u M_u,\beta_\ell L_\ell S j_\ell M_\ell}-\nu)\Big] \tag{7.47a}$$

$$\eta_i^{\mathrm{S}}(\nu,\vec{\Omega}) = \frac{h\nu}{4\pi}\mathcal{N}\sum_{\beta_u L_u S\beta_\ell L_\ell}(2L_u+1)\,B(\beta_u L_u S\to\beta_\ell L_\ell S)$$
$$\times\sum_{KQK_u Q_u}\sqrt{3(2K+1)(2K_u+1)}$$
$$\times\sum_{j_u J_u J'_u J''_u j_\ell J_\ell J'_\ell}\ \sum_{M_u M'_u M_\ell qq'}(-1)^{1+J'_u-M_u+q'}\ C^{j_\ell}_{J_\ell}(\beta_\ell L_\ell S,M_\ell)\,C^{j_\ell}_{J'_\ell}(\beta_\ell L_\ell S,M_\ell)$$
$$\times C^{j_u}_{J_u}(\beta_u L_u S,M_u)\,C^{j_u}_{J''_u}(\beta_u L_u S,M_u)\sqrt{(2J_\ell+1)(2J'_\ell+1)(2J_u+1)(2J'_u+1)}$$
$$\times\begin{pmatrix}J_u & J_\ell & 1\\ -M_u & M_\ell & -q\end{pmatrix}\begin{pmatrix}J'_u & J'_\ell & 1\\ -M'_u & M_\ell & -q'\end{pmatrix}\begin{pmatrix}1 & 1 & K\\ q & -q' & -Q\end{pmatrix}$$
$$\times\begin{pmatrix}J'_u & J''_u & K_u\\ M'_u & -M_u & -Q_u\end{pmatrix}\begin{Bmatrix}L_u & L_\ell & 1\\ J_\ell & J_u & S\end{Bmatrix}\begin{Bmatrix}L_u & L_\ell & 1\\ J'_\ell & J'_u & S\end{Bmatrix}$$
$$\times\mathrm{Re}\Big[\,\mathcal{T}^K_Q(i,\vec{\Omega})\ {}^{\beta_u L_u S}\rho^{K_u}_{Q_u}(J'_u,J''_u)\ \Phi(\nu_{\beta_u L_u S j_u M_u,\beta_\ell L_\ell S j_\ell M_\ell}-\nu)\Big] \tag{7.47b}$$

$$\rho_i^{\mathrm{A}}(\nu,\vec{\Omega}) = \eta_i^{\mathrm{A}}(\nu,\vec{\Omega})\Big\{\mathrm{Re}\to\mathrm{Im}\Big\} \tag{7.47c}$$

$$\rho_i^{\mathrm{S}}(\nu,\vec{\Omega}) = \eta_i^{\mathrm{S}}(\nu,\vec{\Omega})\Big\{\mathrm{Re}\to\mathrm{Im}\Big\} \tag{7.47d}$$

$$\varepsilon_i(\nu,\vec{\Omega}) = \frac{2h\nu^3}{c^2}\ \eta_i^{\mathrm{S}}(\nu,\vec{\Omega})\,. \tag{7.47e}$$

These expressions become much simpler when the frequency splittings – due to fine structure and to the magnetic field – of the lines of each multiplet can be neglected (see the analogous case discussed at the end of Sect. 7.2.b). Replacing the profiles

$$\Phi(\nu_{\beta_u L_u S j_u M_u,\, \beta_\ell L_\ell S j_\ell M_\ell} - \nu)$$

in Eqs. (7.47) by a single profile

$$\Phi(\nu_{\beta_u L_u S,\, \beta_\ell L_\ell S} - \nu)\ ,$$

and using Eqs. (3.62b), (2.34), (3.100) and (5.158), one obtains

$$\begin{aligned}\eta_i^{\rm A}(\nu,\vec{\Omega}) = \frac{h\nu}{4\pi}\mathcal{N} \sum_{\beta_\ell L_\ell S \beta_u L_u} (2L_\ell+1)\, B(\beta_\ell L_\ell S \rightarrow \beta_u L_u S) \\ \times \sum_{KQ} \sum_{J_\ell J'_\ell J_u} (-1)^{1+J_u+J_\ell+K}\, (2J_u+1)\, \sqrt{3(2J_\ell+1)(2J'_\ell+1)} \\ \times \left\{ \begin{array}{ccc} L_u & L_\ell & 1 \\ J_\ell & J_u & S \end{array} \right\} \left\{ \begin{array}{ccc} L_u & L_\ell & 1 \\ J'_\ell & J_u & S \end{array} \right\} \left\{ \begin{array}{ccc} 1 & 1 & K \\ J_\ell & J'_\ell & J_u \end{array} \right\} \\ \times \mathcal{T}^K_Q(i,\vec{\Omega})\ {}^{\beta_\ell L_\ell S}\rho^K_Q(J_\ell, J'_\ell)\ \phi(\nu_{\beta_u L_u S,\, \beta_\ell L_\ell S} - \nu) \end{aligned} \tag{7.48a}$$

or, performing the summation over J_u via Eq. (2.41)

$$\begin{aligned}\eta_i^{\rm A}(\nu,\vec{\Omega}) = \frac{h\nu}{4\pi}\mathcal{N} \sum_{\beta_\ell L_\ell S \beta_u L_u} (2L_\ell+1)\, B(\beta_\ell L_\ell S \rightarrow \beta_u L_u S) \\ \times \sum_{KQ} \sum_{J_\ell J'_\ell} (-1)^{1-L_u+S+J'_\ell}\, \sqrt{3(2J_\ell+1)(2J'_\ell+1)} \\ \times \left\{ \begin{array}{ccc} L_\ell & L_\ell & K \\ J_\ell & J'_\ell & S \end{array} \right\} \left\{ \begin{array}{ccc} 1 & 1 & K \\ L_\ell & L_\ell & L_u \end{array} \right\} \\ \times \mathcal{T}^K_Q(i,\vec{\Omega})\ {}^{\beta_\ell L_\ell S}\rho^K_Q(J_\ell, J'_\ell)\ \phi(\nu_{\beta_u L_u S,\, \beta_\ell L_\ell S} - \nu)\ . \end{aligned} \tag{7.48b}$$

Similarly

$$\begin{aligned}\eta_i^{\rm S}(\nu,\vec{\Omega}) = \frac{h\nu}{4\pi}\mathcal{N} \sum_{\beta_u L_u S \beta_\ell L_\ell} (2L_u+1)\, B(\beta_u L_u S \rightarrow \beta_\ell L_\ell S) \\ \times \sum_{KQ} \sum_{J_u J'_u J_\ell} (-1)^{1+J_\ell+J'_u}\, (2J_\ell+1)\, \sqrt{3(2J_u+1)(2J'_u+1)} \\ \times \left\{ \begin{array}{ccc} L_u & L_\ell & 1 \\ J_\ell & J_u & S \end{array} \right\} \left\{ \begin{array}{ccc} L_u & L_\ell & 1 \\ J_\ell & J'_u & S \end{array} \right\} \left\{ \begin{array}{ccc} 1 & 1 & K \\ J_u & J'_u & J_\ell \end{array} \right\} \\ \times \mathcal{T}^K_Q(i,\vec{\Omega})\ {}^{\beta_u L_u S}\rho^K_Q(J'_u, J_u)\ \phi(\nu_{\beta_u L_u S,\, \beta_\ell L_\ell S} - \nu) \end{aligned} \tag{7.48c}$$

or, performing the summation over J_ℓ via Eq. (2.41)

$$\eta_i^{\mathrm{S}}(\nu,\vec{\Omega}) = \frac{h\nu}{4\pi}\mathcal{N}\sum_{\beta_u L_u S \beta_\ell L_\ell}(2L_u+1)\,B(\beta_u L_u S \to \beta_\ell L_\ell S)$$
$$\times \sum_{KQ}\sum_{J_u J_u'}(-1)^{1-L_\ell+S+J_u+K}\sqrt{3(2J_u+1)(2J_u'+1)}$$
$$\times \begin{Bmatrix} L_u & L_u & K \\ J_u & J_u' & S \end{Bmatrix}\begin{Bmatrix} 1 & 1 & K \\ L_u & L_u & L_\ell \end{Bmatrix}$$
$$\times \mathcal{T}_Q^K(i,\vec{\Omega})\ {}^{\beta_u L_u S}\rho_Q^K(J_u',J_u)\ \phi(\nu_{\beta_u L_u S,\,\beta_\ell L_\ell S}-\nu)\,. \qquad (7.48\mathrm{d})$$

The same calculations show that

$$\rho_i^{\mathrm{A}}(\nu,\vec{\Omega}) = \eta_i^{\mathrm{A}}(\nu,\vec{\Omega})\left\{\phi(\nu_{\beta_u L_u S,\,\beta_\ell L_\ell S}-\nu) \to \psi(\nu_{\beta_u L_u S,\,\beta_\ell L_\ell S}-\nu)\right\} \qquad (7.48\mathrm{e})$$

$$\rho_i^{\mathrm{S}}(\nu,\vec{\Omega}) = \eta_i^{\mathrm{S}}(\nu,\vec{\Omega})\left\{\phi(\nu_{\beta_u L_u S,\,\beta_\ell L_\ell S}-\nu) \to \psi(\nu_{\beta_u L_u S,\,\beta_\ell L_\ell S}-\nu)\right\} \qquad (7.48\mathrm{f})$$

$$\varepsilon_i(\nu,\vec{\Omega}) = \frac{2h\nu^3}{c^2}\ \eta_i^{\mathrm{S}}(\nu,\vec{\Omega})\,. \qquad (7.48\mathrm{g})$$

7.7. Conjugation Properties of the Rates

The radiative rates appearing in the statistical equilibrium equations for the multiterm atom have simple conjugation properties. In the energy-eigenvector representation, we have from Eqs. (7.34), using Eq. (5.154) and the reality of the C_J^j coefficients (see Sect. 3.4)

$$T_{\mathrm{A}}(\beta LSjMj'M',\beta_\ell L_\ell S j_\ell M_\ell j_\ell' M_\ell')^* = T_{\mathrm{A}}(\beta LSj'M'jM,\beta_\ell L_\ell S j_\ell' M_\ell' j_\ell M_\ell)$$
$$T_{\mathrm{E}}(\beta LSjMj'M',\beta_u L_u S j_u M_u j_u' M_u')^* = T_{\mathrm{E}}(\beta LSj'M'jM,\beta_u L_u S j_u' M_u' j_u M_u)\,,$$

with an analogous relation for T_{S};

$$R_{\mathrm{A}}(\beta LSjMj'M')^* = R_{\mathrm{A}}(\beta LSj'M'jM)\,,$$

with analogous relations for R_{E} and R_{S}; moreover, the rates T_{E} and R_{E} are real. In the spherical statistical tensor representation, we have from Eqs. (7.45a-c) and (7.46a-c), with the help of Eqs. (5.158)[1]

$$\mathbb{T}_{\mathrm{A}}(\beta LSKQJJ',\beta_\ell L_\ell S K_\ell Q_\ell J_\ell J_\ell')^* =$$
$$= (-1)^{J-J'+Q+J_\ell-J_\ell'+Q_\ell}\ \mathbb{T}_{\mathrm{A}}(\beta LSK\ -QJ'J,\beta_\ell L_\ell S K_\ell\ -Q_\ell J_\ell' J_\ell)$$

[1] To arrange the sign factors in these equations, one should bear in mind that the quantum numbers J, J', J'', J''' are all integers or all half-integers, and that the indices K, Q, K', Q' K_ℓ, Q_ℓ, K_u, Q_u are integers (see footnote on p.123).

$$\mathbb{T}_{\rm E}(\beta LSKQJJ', \beta_u L_u S K_u Q_u J_u J'_u)^* =$$
$$= (-1)^{J-J'+Q+J_u-J'_u+Q_u}\ \mathbb{T}_{\rm E}(\beta LSK\ -QJ'J, \beta_u L_u S K_u\ -Q_u J'_u J_u)\ ,$$

with an analogous relation for $\mathbb{T}_{\rm S}$;

$$\mathbb{R}_{\rm A}(\beta LSKQJJ'K'Q'J''J''')^* =$$
$$= (-1)^{J-J'+Q+J''-J'''+Q'}\ \mathbb{R}_{\rm A}(\beta LSK\ -QJ'JK'\ -Q'J'''J'')\ ,$$

with analogous relations for $\mathbb{R}_{\rm E}$ and $\mathbb{R}_{\rm S}$; moreover, the rates $\mathbb{T}_{\rm E}$ and $\mathbb{R}_{\rm E}$ are real.

7.8. The Multi-Level Atom as a Special Case of the Multi-Term Atom

As apparent from Sects. 7.5 and 7.6, the description of the multi-term atom requires much more complicated equations than the multi-level atom treated previously: this is basically related to the fact that *two* types of coherences (between different J-levels and between magnetic sublevels of each J-level) are considered in this model. It can be easily realized that if we neglect coherences between J-levels, retaining only those between magnetic sublevels of individual J-levels, the case of the multi-term atom becomes very similar to the case of the multi-level atom. In fact, after the formal identifications

$$\alpha \equiv (\beta LS)\ , \qquad \alpha_\ell \equiv (\beta_\ell L_\ell S)\ , \qquad \alpha_u \equiv (\beta_u L_u S)\ , \tag{7.49}$$

the statistical equilibrium equations for the two cases must indeed coincide provided the incident radiation field is such that

$$J^K_Q(\nu_{\alpha_u J_u, \alpha_\ell J_\ell}) \equiv J^K_Q(\nu_{\beta_u L_u S J_u, \beta_\ell L_\ell S J_\ell}) = J^K_Q(\nu_{\beta_u L_u S, \beta_\ell L_\ell S}) \tag{7.50}$$

for each multiplet. The radiative transfer coefficients for the two cases must also coincide provided the frequency splittings of the Φ profiles due to fine structure are neglected,

$$\Phi(\nu_{\alpha_u J_u, \alpha_\ell J_\ell} - \nu) \equiv \Phi(\nu_{\beta_u L_u S J_u, \beta_\ell L_\ell S J_\ell} - \nu) = \Phi(\nu_{\beta_u L_u S, \beta_\ell L_\ell S} - \nu)\ . \tag{7.51}$$

To check this property – which is a proof of consistency of the formalism – we substitute into Eq. (7.38)

$${}^{\beta LS}\rho^K_Q(J, J') = \delta_{JJ'}\ {}^{\beta LS}\rho^K_Q(J, J) = \delta_{JJ'}\ {}^{\beta LS}\rho^K_Q(J)\ , \tag{7.52}$$

and we get

$$\frac{\mathrm{d}}{\mathrm{d}t}\,{}^{\beta LS}\rho^{K}_{Q}(J) = -2\pi\mathrm{i}\sum_{K'Q'}\sum_{J'} N_{\beta LS}(KQJJ,K'Q'J'J')\;{}^{\beta LS}\rho^{K'}_{Q'}(J')$$
$$+\sum_{\beta_\ell L_\ell K_\ell Q_\ell J_\ell}{}^{\beta_\ell L_\ell S}\rho^{K_\ell}_{Q_\ell}(J_\ell)\;\mathbb{T}_{\mathrm{A}}(\beta LSKQJJ,\beta_\ell L_\ell S K_\ell Q_\ell J_\ell J_\ell)$$
$$+\sum_{\beta_u L_u K_u Q_u J_u}{}^{\beta_u L_u S}\rho^{K_u}_{Q_u}(J_u)\Big[\mathbb{T}_{\mathrm{E}}(\beta LSKQJJ,\beta_u L_u S K_u Q_u J_u J_u) + \mathbb{T}_{\mathrm{S}}(\beta LSKQJJ,\beta_u L_u S K_u Q_u J_u J_u)\Big]$$
$$-\sum_{K'Q'J'}{}^{\beta LS}\rho^{K'}_{Q'}(J')\Big[\mathbb{R}_{\mathrm{A}}(\beta LSKQJJK'Q'J'J') + \mathbb{R}_{\mathrm{E}}(\beta LSKQJJK'Q'J'J') + \mathbb{R}_{\mathrm{S}}(\beta LSKQJJK'Q'J'J')\Big]\,. \tag{7.53}$$

From Eqs. (7.41) and (7.44) we have

$$N_{\beta LS}(KQJJ,K'Q'J'J') = \\ = \delta_{QQ'}\,\nu_{\mathrm{L}}\,(-1)^{2J-Q}\sqrt{(2K+1)(2K'+1)}\begin{pmatrix} K & K' & 1\\ -Q & Q & 0\end{pmatrix} \\ \times\,\delta_{JJ'}\sqrt{J(J+1)(2J+1)}\left[1+(-1)^{K-K'}\right]\begin{Bmatrix} K & K' & 1\\ J & J & J\end{Bmatrix} g_{LS}(J)\,,$$

which can be transformed using some Racah algebra. Because of the triangular condition $(K,K',1)$ we can write

$$\left[1+(-1)^{K-K'}\right] = 2\,\delta_{KK'}\,,$$

and using Eqs. (2.26d) and (2.36d) we obtain

$$N_{\beta LS}(KQJJ,K'Q'J'J') = \delta_{KK'}\,\delta_{QQ'}\,\delta_{JJ'}\,\nu_{\mathrm{L}}\,Q\,g_{LS}(J)\,, \tag{7.54}$$

which makes the first term in the right-hand side of Eq. (7.53) equal to the corresponding term in Eq. (7.11).[1]

As far as the other terms are concerned, it is readily seen that Eq. (7.53) – with the identifications (7.49) – has the same form as Eq. (7.11), thus we have just to compare the expressions for the rates. From Eq. (7.45a) we have

$$\mathbb{T}_{\mathrm{A}}(\beta LSKQJJ,\beta_\ell L_\ell S K_\ell Q_\ell J_\ell J_\ell) = (2L_\ell+1)\,B(\beta_\ell L_\ell S\to\beta LS) \\ \times\sum_{K_{\mathrm{r}}Q_{\mathrm{r}}}(2J+1)\,(2J_\ell+1)\sqrt{3(2K+1)(2K_\ell+1)(2K_{\mathrm{r}}+1)} \\ \times(-1)^{K_\ell+Q_\ell}\begin{Bmatrix} J & J_\ell & 1\\ J & J_\ell & 1\\ K & K_\ell & K_{\mathrm{r}}\end{Bmatrix}\begin{Bmatrix} L & L_\ell & 1\\ J_\ell & J & S\end{Bmatrix}^2\begin{pmatrix} K & K_\ell & K_{\mathrm{r}}\\ -Q & Q_\ell & -Q_{\mathrm{r}}\end{pmatrix} \\ \times J^{K_{\mathrm{r}}}_{Q_{\mathrm{r}}}(\nu_{\beta LS,\,\beta_\ell L_\ell S})\,, \tag{7.55}$$

[1] Of course, Eq. (7.54) contains the Landé factor evaluated in the L-S coupling scheme, while Eq. (7.11) contains the more general Landé factor defined in Eq. (3.7).

which should be compared with Eq. (7.14a). To this end we need the relation between the Einstein coefficient for the transition between two terms and the Einstein coefficients for the transition between two individual J-levels.

Equation (7.6) with substitutions (7.49) gives

$$\mathcal{S}(\beta_\ell L_\ell S J_\ell, \beta_u L_u S J_u) = (2J_\ell + 1)\, |\langle \beta_\ell L_\ell S J_\ell \| \vec{d} \, \| \beta_u L_u S J_u \rangle|^2 \,,$$

and using Eqs. (2.108) and (7.31) we obtain the relation connecting the strengths[1]

$$\begin{aligned} \mathcal{S}(\beta_\ell L_\ell S J_\ell, \beta_u L_u S J_u) = (2J_\ell + 1)\,(2J_u + 1) \begin{Bmatrix} L_u & L_\ell & 1 \\ J_\ell & J_u & S \end{Bmatrix}^2 \\ \times\, \mathcal{S}(\beta_\ell L_\ell S, \beta_u L_u S) \,. \end{aligned} \tag{7.56}$$

Finally, from Eqs. (7.7) and (7.32) we get

$$\begin{aligned} B(\beta_\ell L_\ell S J_\ell \to \beta_u L_u S J_u) = (2L_\ell + 1)\,(2J_u + 1) \begin{Bmatrix} L_u & L_\ell & 1 \\ J_\ell & J_u & S \end{Bmatrix}^2 \\ \times\, B(\beta_\ell L_\ell S \to \beta_u L_u S) \,. \end{aligned} \tag{7.57a}$$

Substitution into Eq. (7.55) shows that the expressions in the right-hand side of Eqs. (7.55) and (7.14a) are identical when approximation (7.50) is satisfied.

Quite similar calculations can be performed for the other rates. Using the further relations between Einstein coefficients[2]

$$\begin{aligned} B(\beta_u L_u S J_u \to \beta_\ell L_\ell S J_\ell) = (2L_u + 1)\,(2J_\ell + 1) \begin{Bmatrix} L_u & L_\ell & 1 \\ J_\ell & J_u & S \end{Bmatrix}^2 \\ \times\, B(\beta_u L_u S \to \beta_\ell L_\ell S) \end{aligned} \tag{7.57b}$$

---

[1] From Eq. (7.56) we have, with the help of Eq. (2.39)

$$\textstyle\sum_{J_\ell J_u} \mathcal{S}(\beta_\ell L_\ell S J_\ell, \beta_u L_u S J_u) = (2S+1)\;\mathcal{S}(\beta_\ell L_\ell S, \beta_u L_u S) \,,$$

therefore the relative strengths of the multiplet, normalized to unity, are given by

$$S^{J_\ell, J_u} = \frac{(2J_\ell + 1)(2J_u + 1)}{2S + 1} \begin{Bmatrix} L_u & L_\ell & 1 \\ J_\ell & J_u & S \end{Bmatrix}^2 \,,$$

which is just Eq. (3.65).

[2] Note that Eq. (7.57c) implies the approximation

$$\nu^3_{\beta_u L_u S J_u,\, \beta_\ell L_\ell S J_\ell} \,/\, \nu^3_{\beta_u L_u S,\, \beta_\ell L_\ell S} = 1 \,.$$

Note also that the Einstein coefficients in Eqs. (7.57) are related by the equations

$$\begin{aligned} \textstyle\sum_{J_\ell} A(\beta_u L_u S J_u \to \beta_\ell L_\ell S J_\ell) &= A(\beta_u L_u S \to \beta_\ell L_\ell S) \\ \textstyle\sum_{J_\ell} B(\beta_u L_u S J_u \to \beta_\ell L_\ell S J_\ell) &= B(\beta_u L_u S \to \beta_\ell L_\ell S) \\ \textstyle\sum_{J_u} B(\beta_\ell L_\ell S J_\ell \to \beta_u L_u S J_u) &= B(\beta_\ell L_\ell S \to \beta_u L_u S) \,, \end{aligned}$$

which are easily derived with the use of Eq. (2.39).

$$A(\beta_u L_u S J_u \to \beta_\ell L_\ell S J_\ell) = (2L_u+1)(2J_\ell+1) \begin{Bmatrix} L_u & L_\ell & 1 \\ J_\ell & J_u & S \end{Bmatrix}^2 \times A(\beta_u L_u S \to \beta_\ell L_\ell S) \,, \tag{7.57c}$$

one finds that all the rates in Eq. (7.53) coincide with the corresponding rates of Eqs. (7.14), which proves that the statistical equilibrium equations for the multi-term atom reduce to the equations for the multi-level atom under the assumptions mentioned above.

The same check can be repeated for the radiative transfer coefficients. Substitution of Eq. (7.52) into Eqs. (7.48) and use of approximation (7.51) yields exactly the same expressions derived for the multi-level atom (Eqs. (7.16)).

7.9. The Multi-Level Atom with Hyperfine Structure

In the preceding sections of this chapter we have developed the basic equations for a standard atom devoid of hyperfine structure. Now we are going to generalize the description of the atomic system by including this further degree of freedom.

If I is the nuclear spin of a given atomic species, the energy eigenvectors – in the absence of magnetic fields – have the form $|\alpha JIFf\rangle$ (cf. Sect. 3.5 for the meaning of symbols). In principle, one could develop the statistical equilibrium equations and the radiative transfer equations for the general case implying coherences of the form

$$\langle \alpha JIFf | \, \rho \, | \alpha J' I F' f' \rangle \,.$$

However, with the exception of the hydrogen atom (which presents, moreover, an additional degeneracy of the eigenvalues with respect to the azimuthal quantum number l, and therefore requires a more involved formalism), it is in most cases sufficient to restrict the description of the atom with hyperfine structure to the J-diagonal density-matrix elements

$$\langle \alpha JIFf | \, \rho \, | \alpha JIF' f' \rangle = \rho_{\alpha JI}(Ff, F'f') \,.$$

The model atom described by this approximation will be called in the following the *multi-level atom with hyperfine structure*. For such system, the flat-spectrum approximation (cf. Sect. 6.5) implies that the radiation field incident on the atom should be constant across a frequency interval wider than the frequency shifts and inverse lifetimes of the hyperfine-structure sublevels involved. This means that the radiation field can be characterized by specifying its value at the Bohr frequencies

$$\nu_{\alpha J,\, \alpha' J'} = \frac{E_{\alpha J} - E_{\alpha' J'}}{h} \,,$$

where $E_{\alpha J}$, $E_{\alpha' J'}$ are the energies of the relevant levels (which disregard both the hyperfine-structure and the magnetic Hamiltonian). This approximation is usually well-satisfied in astrophysical plasmas.

We now apply the equations derived in Chap. 6 to such an atom embedded in a magnetic field. If we choose a reference system with the z-axis pointing in the magnetic field direction, we have for the eigenvectors and eigenvalues of the atomic Hamiltonian

$$H_{\rm A}\,|\alpha JIif\rangle = \left[E_{\alpha J} + \lambda_i(\alpha JI, f)\right]|\alpha JIif\rangle\ ,$$

where (see Eq. (3.74))

$$|\alpha JIif\rangle = \sum_F C_F^i(\alpha JI, f)\,|\alpha JIFf\rangle\ . \tag{7.58}$$

Thus we modify the formalism of Chap. 6 according to the following substitutions

i) for the energy eigenvectors:

$$|\,n\rangle \to |\alpha JIif\rangle\ ; \tag{7.59}$$

ii) for the corresponding energy eigenvalues:

$$E_n \to E_{\alpha J} + \lambda_i(\alpha JI, f)\ , \tag{7.60}$$

whence

iii) for the Bohr frequencies:

$$\begin{aligned}\nu_{nm} = \frac{E_n - E_m}{h} \to\ & \nu_{\alpha JIif,\,\alpha' J' Ii' f'} = \\ & = \nu_{\alpha J,\,\alpha' J'} + \frac{\lambda_i(\alpha JI, f) - \lambda_{i'}(\alpha' J' I, f')}{h}\ ;\end{aligned} \tag{7.61}$$

iv) for the matrix elements of the spherical components of the dipole operator (see the analogous derivation of Eq. (7.27)):

$$\begin{aligned}(d_q)_{nm} = \langle n\,|\,d_q\,|\,m\rangle \to (d_q)_{\alpha JIif,\,\alpha' J' Ii' f'} = \langle \alpha JIif|\,d_q\,|\alpha' J' Ii' f'\rangle = \\ = \sum_{FF'} C_F^i(\alpha JI, f)\,C_{F'}^{i'}(\alpha' J' I, f') \\ \times (-1)^{J+I-f}\sqrt{(2J+1)(2F+1)(2F'+1)} \\ \times \begin{pmatrix} F & F' & 1 \\ -f & f' & q \end{pmatrix} \begin{Bmatrix} J & J' & 1 \\ F' & F & I \end{Bmatrix} \langle \alpha J\|\vec{d}\,\|\alpha' J'\rangle\ ;\end{aligned} \tag{7.62}$$

v) finally, for the atomic density-matrix elements:

$$\begin{aligned}\rho_{nm} = \langle n\,|\,\rho\,|\,m\rangle \to \langle \alpha JIif|\,\rho\,|\alpha' J' Ii' f'\rangle = \\ = \delta_{\alpha\alpha'}\,\delta_{JJ'}\langle \alpha JIif|\,\rho\,|\alpha JIi' f'\rangle = \delta_{\alpha\alpha'}\,\delta_{JJ'}\,\rho_{\alpha JI}(if, i' f')\ .\end{aligned} \tag{7.63}$$

If we now compare Eqs. (7.59)-(7.63) with Eqs. (7.24)-(7.28), we see that the equations for the multi-level atom with hyperfine structure can be deduced from the corresponding equations of the multi-term atom by means of the formal substitutions

$$\begin{array}{lll} \beta \to \alpha & S \to I & j \to i \\ L \to J & J \to F & M \to f\ . \end{array} \tag{7.64}$$

Thus the statistical equilibrium equations and the radiative transfer coefficients for the multi-level atom with hyperfine structure, expressed in the energy-eigenvector representation, are simply given by Eqs. (7.29),[1] (7.34) and (7.35) with the formal substitutions (7.64).

The conversion to the spherical statistical tensor representation is also straightforward. Using Eqs. (7.58) and (3.103) we obtain the relation

$$\begin{aligned} \rho_{\alpha JI}(if, i'f') &= \sum_{FF'} C_F^i(\alpha JI, f)\, C_{F'}^{i'}(\alpha JI, f')\, \rho_{\alpha JI}(Ff, F'f') \\ &= \sum_{FF'} C_F^i(\alpha JI, f)\, C_{F'}^{i'}(\alpha JI, f') \\ &\quad \times \sum_{KQ} (-1)^{F-f} \sqrt{2K+1} \begin{pmatrix} F & F' & K \\ f & -f' & -Q \end{pmatrix} {}^{\alpha JI}\rho_Q^K(F, F')\ , \end{aligned}$$

which is just the same as Eq. (7.36) with substitutions (7.64). It follows that the equations for the multi-level atom with hyperfine structure, expressed in the spherical statistical tensor representation, can be easily deduced from the corresponding equations for the multi-term atom by performing the same substitutions.

For the statistical equilibrium equations we have (cf. Eq. (7.38))

$$\begin{aligned} \frac{\mathrm{d}}{\mathrm{d}t}\, {}^{\alpha JI}\rho_Q^K(F, F') &= -2\pi \mathrm{i} \sum_{K'Q'} \sum_{F''F'''} \tilde{N}_{\alpha JI}(KQFF', K'Q'F''F''')\, {}^{\alpha JI}\rho_{Q'}^{K'}(F'', F''') \\ &+ \sum_{\alpha_\ell J_\ell K_\ell Q_\ell F_\ell F'_\ell} {}^{\alpha_\ell J_\ell I}\rho_{Q_\ell}^{K_\ell}(F_\ell, F'_\ell)\, \mathbb{T}_{\mathrm{A}}(\alpha JIKQFF', \alpha_\ell J_\ell I K_\ell Q_\ell F_\ell F'_\ell) \\ &+ \sum_{\alpha_u J_u K_u Q_u F_u F'_u} {}^{\alpha_u J_u I}\rho_{Q_u}^{K_u}(F_u, F'_u) \Big[\mathbb{T}_{\mathrm{E}}(\alpha JIKQFF', \alpha_u J_u I K_u Q_u F_u F'_u) \\ &\qquad + \mathbb{T}_{\mathrm{S}}(\alpha JIKQFF', \alpha_u J_u I K_u Q_u F_u F'_u) \Big] \\ &- \sum_{K'Q'F''F'''} {}^{\alpha JI}\rho_{Q'}^{K'}(F'', F''') \Big[\mathbb{R}_{\mathrm{A}}(\alpha JIKQFF'K'Q'F''F''') \\ &\qquad + \mathbb{R}_{\mathrm{E}}(\alpha JIKQFF'K'Q'F''F''') + \mathbb{R}_{\mathrm{S}}(\alpha JIKQFF'K'Q'F''F''') \Big]. \end{aligned} \tag{7.65}$$

[1] The term in Eq. (7.30) is discussed later in greater detail.

The only term which cannot be deduced by direct substitution of Eqs. (7.64) is the first term in the right-hand side, as expected because of the intrinsic difference between the fine-structure and the hyperfine-structure Hamiltonians. To evaluate this term we must go back to Eqs. (7.39) and (7.30). Applying substitutions (7.64) and using Eqs. (3.76b,c) we get

$$\begin{aligned}\tilde{N}_{\alpha JI}(KQFF', K'Q'F''F''') = \delta_{QQ'}\,(-1)^{F-F''}\sqrt{(2K+1)(2K'+1)}\\ \times\frac{1}{h}\Bigg[\delta_{F'F'''}\sum_{ff'}\begin{pmatrix} F & F' & K\\ f & -f' & -Q\end{pmatrix}\begin{pmatrix} F'' & F' & K'\\ f & -f' & -Q\end{pmatrix}\\ \times\langle\alpha JIFf|H^{(1)}_{\rm hfs}+H^{(2)}_{\rm hfs}+H_B|\alpha JIF''f\rangle\\ -\delta_{FF''}\sum_{ff'}\begin{pmatrix} F & F' & K\\ f & -f' & -Q\end{pmatrix}\begin{pmatrix} F & F''' & K'\\ f & -f' & -Q\end{pmatrix}\\ \times\langle\alpha JIF'f'|H^{(1)}_{\rm hfs}+H^{(2)}_{\rm hfs}+H_B|\alpha JIF'''f'\rangle\Bigg],\end{aligned}$$

with the Hamiltonians $H^{(1)}_{\rm hfs}$ and $H^{(2)}_{\rm hfs}$ given by Eqs. (3.70) and (3.71). The matrix elements in the right-hand side can be evaluated using Eqs. (3.70) and (3.72). Carrying out the summations over f and f' via Eqs. (2.23a) and (2.42) one obtains

$$\begin{aligned}\tilde{N}_{\alpha JI}(KQFF', K'Q'F''F''') = \delta_{KK'}\,\delta_{QQ'}\,\delta_{FF''}\,\delta_{F'F'''}\,\nu_{\alpha JIF,\,\alpha JIF'}\\ +\delta_{QQ'}\,\nu_{\rm L}\,g_{\alpha J}\,(-1)^{F'+F''+Q}\sqrt{(2K+1)(2K'+1)}\begin{pmatrix} K & K' & 1\\ -Q & Q & 0\end{pmatrix}\\ \times\Bigg[\delta_{F'F'''}\,\Gamma_{JI}(F,F'')\begin{Bmatrix} K & K' & 1\\ F'' & F & F'\end{Bmatrix}\\ +\delta_{FF''}\,(-1)^{K-K'}\,\Gamma_{JI}(F',F''')\begin{Bmatrix} K & K' & 1\\ F''' & F' & F\end{Bmatrix}\Bigg],\end{aligned}\tag{7.66}$$

where

$$\begin{aligned}\nu_{\alpha JIF,\,\alpha JIF'} &= \frac{E_{\alpha JI}(F)-E_{\alpha JI}(F')}{h}\\ &= \frac{1}{h}\Big[\langle\alpha JIFf|H^{(1)}_{\rm hfs}+H^{(2)}_{\rm hfs}|\alpha JIFf\rangle-\langle\alpha JIF'f|H^{(1)}_{\rm hfs}+H^{(2)}_{\rm hfs}|\alpha JIF'f\rangle\Big]\end{aligned}\tag{7.67}$$

and where we have introduced a generalized Landé factor for hyperfine structure through the position[1]

[1] A slightly different generalized Landé factor has been introduced by Landolfi and Landi Degl'Innocenti (1985). Note the similarity of Eq. (7.68) with Eq. (7.42). Note also that

$$\Gamma_{JI}(F,F) = \sqrt{F(F+1)(2F+1)}\;\; g_{\rm hfs}(F)\,,$$

where $g_{\rm hfs}(F)$ is given in Eq. (3.73).

$$\Gamma_{JI}(F,F') = (-1)^{F-F'}\,\Gamma_{JI}(F',F)$$
$$= (-1)^{1+J+I+F}\sqrt{J(J+1)(2J+1)(2F+1)(2F'+1)}\begin{Bmatrix} F & F' & 1 \\ J & J & I \end{Bmatrix}. \qquad (7.68)$$

All the other terms in Eq. (7.65) can be derived by carrying out the substitutions (7.64). We write down here, for future reference, the expressions for the radiative rates (cf. Eqs. (7.45a-c) and (7.46a-c))

$$\mathbb{T}_{\rm A}(\alpha JIKQFF', \alpha_\ell J_\ell I K_\ell Q_\ell F_\ell F'_\ell) = (2J_\ell+1)\,B(\alpha_\ell J_\ell \to \alpha J)$$
$$\times \sum_{K_{\rm r}Q_{\rm r}} \sqrt{3(2F+1)(2F'+1)(2F_\ell+1)(2F'_\ell+1)(2K+1)(2K_\ell+1)(2K_{\rm r}+1)}$$
$$\times (-1)^{K_\ell+Q_\ell+F'_\ell-F_\ell}\begin{Bmatrix} F & F_\ell & 1 \\ F' & F'_\ell & 1 \\ K & K_\ell & K_{\rm r} \end{Bmatrix}\begin{Bmatrix} J & J_\ell & 1 \\ F_\ell & F & I \end{Bmatrix}$$
$$\times \begin{Bmatrix} J & J_\ell & 1 \\ F'_\ell & F' & I \end{Bmatrix}\begin{pmatrix} K & K_\ell & K_{\rm r} \\ -Q & Q_\ell & -Q_{\rm r} \end{pmatrix} J^{K_{\rm r}}_{Q_{\rm r}}(\nu_{\alpha J,\,\alpha_\ell J_\ell}) \qquad (7.69a)$$

$$\mathbb{T}_{\rm E}(\alpha JIKQFF', \alpha_u J_u I K_u Q_u F_u F'_u) = \delta_{KK_u}\,\delta_{QQ_u}\,(2J_u+1)\,A(\alpha_u J_u \to \alpha J)$$
$$\times \sqrt{(2F+1)(2F'+1)(2F_u+1)(2F'_u+1)}$$
$$\times (-1)^{1+K+F'+F'_u}\begin{Bmatrix} F & F' & K \\ F'_u & F_u & 1 \end{Bmatrix}\begin{Bmatrix} J_u & J & 1 \\ F & F_u & I \end{Bmatrix}\begin{Bmatrix} J_u & J & 1 \\ F' & F'_u & I \end{Bmatrix} \qquad (7.69b)$$

$$\mathbb{T}_{\rm S}(\alpha JIKQFF', \alpha_u J_u I K_u Q_u F_u F'_u) = (2J_u+1)\,B(\alpha_u J_u \to \alpha J)$$
$$\times \sum_{K_{\rm r}Q_{\rm r}} \sqrt{3(2F+1)(2F'+1)(2F_u+1)(2F'_u+1)(2K+1)(2K_u+1)(2K_{\rm r}+1)}$$
$$\times (-1)^{K_{\rm r}+K_u+Q_u+F'_u-F_u}\begin{Bmatrix} F & F_u & 1 \\ F' & F'_u & 1 \\ K & K_u & K_{\rm r} \end{Bmatrix}\begin{Bmatrix} J_u & J & 1 \\ F & F_u & I \end{Bmatrix}$$
$$\times \begin{Bmatrix} J_u & J & 1 \\ F' & F'_u & I \end{Bmatrix}\begin{pmatrix} K & K_u & K_{\rm r} \\ -Q & Q_u & -Q_{\rm r} \end{pmatrix} J^{K_{\rm r}}_{Q_{\rm r}}(\nu_{\alpha_u J_u,\,\alpha J}) \qquad (7.69c)$$

$$\mathbb{R}_{\rm A}(\alpha JIKQFF'K'Q'F''F''') = (2J+1)\sum_{\alpha_u J_u} B(\alpha J \to \alpha_u J_u)$$
$$\times \sum_{K_{\rm r}Q_{\rm r}} \sqrt{3(2K+1)(2K'+1)(2K_{\rm r}+1)}$$
$$\times (-1)^{1+J_u-I+F+Q'}\begin{Bmatrix} J & J & K_{\rm r} \\ 1 & 1 & J_u \end{Bmatrix}\begin{pmatrix} K & K' & K_{\rm r} \\ Q & -Q' & Q_{\rm r} \end{pmatrix} \times$$

$$\times \frac{1}{2}\Bigg[\delta_{FF''} \sqrt{(2F'+1)(2F'''+1)} \times \begin{Bmatrix} J & J & K_{\rm r} \\ F''' & F' & I \end{Bmatrix} \begin{Bmatrix} K & K' & K_{\rm r} \\ F''' & F' & F \end{Bmatrix} + \delta_{F'F'''} \sqrt{(2F+1)(2F''+1)}\ (-1)^{F''-F'+K+K'+K_{\rm r}} \times \begin{Bmatrix} J & J & K_{\rm r} \\ F'' & F & I \end{Bmatrix} \begin{Bmatrix} K & K' & K_{\rm r} \\ F'' & F & F' \end{Bmatrix} \Bigg] J^{K_{\rm r}}_{Q_{\rm r}}(\nu_{\alpha_u J_u, \alpha J}) \tag{7.69d}$$

$$\mathbb{R}_{\rm E}(\alpha J I K Q F F' K' Q' F'' F''') = \delta_{KK'}\, \delta_{QQ'}\, \delta_{FF''}\, \delta_{F'F'''} \times \sum_{\alpha_\ell J_\ell} A(\alpha J \rightarrow \alpha_\ell J_\ell) \tag{7.69e}$$

$$\mathbb{R}_{\rm S}(\alpha J I K Q F F' K' Q' F'' F''') = (2J+1) \sum_{\alpha_\ell J_\ell} B(\alpha J \rightarrow \alpha_\ell J_\ell) \times \sum_{K_{\rm r} Q_{\rm r}} \sqrt{3(2K+1)(2K'+1)(2K_{\rm r}+1)} \times (-1)^{1+J_\ell-I+F+K_{\rm r}+Q'} \begin{Bmatrix} J & J & K_{\rm r} \\ 1 & 1 & J_\ell \end{Bmatrix} \begin{pmatrix} K & K' & K_{\rm r} \\ Q & -Q' & Q_{\rm r} \end{pmatrix} \times \frac{1}{2}\Bigg[\delta_{FF''} \sqrt{(2F'+1)(2F'''+1)} \times \begin{Bmatrix} J & J & K_{\rm r} \\ F''' & F' & I \end{Bmatrix} \begin{Bmatrix} K & K' & K_{\rm r} \\ F''' & F' & F \end{Bmatrix} + \delta_{F'F'''} \sqrt{(2F+1)(2F''+1)}\ (-1)^{F''-F'+K+K'+K_{\rm r}} \times \begin{Bmatrix} J & J & K_{\rm r} \\ F'' & F & I \end{Bmatrix} \begin{Bmatrix} K & K' & K_{\rm r} \\ F'' & F & F' \end{Bmatrix} \Bigg] J^{K_{\rm r}}_{Q_{\rm r}}(\nu_{\alpha J, \alpha_\ell J_\ell})\,. \tag{7.69f}$$

Finally, the radiative transfer coefficients can be obtained by applying the same substitutions to Eqs. (7.47). In the special case where all the profiles of the various hyperfine components can be considered coincident, we have from Eqs. (7.48)

$$\eta^{\rm A}_i(\nu, \vec{\Omega}) = \frac{h\nu}{4\pi} \mathcal{N} \sum_{\alpha_\ell J_\ell \alpha_u J_u} (2J_\ell+1)\, B(\alpha_\ell J_\ell \rightarrow \alpha_u J_u) \times \sum_{KQ} \sum_{F_\ell F'_\ell} (-1)^{1-J_u+I+F'_\ell} \sqrt{3(2F_\ell+1)(2F'_\ell+1)}\ \times$$

$$\times \left\{ \begin{array}{ccc} J_\ell & J_\ell & K \\ F_\ell & F'_\ell & I \end{array} \right\} \left\{ \begin{array}{ccc} 1 & 1 & K \\ J_\ell & J_\ell & J_u \end{array} \right\}$$

$$\times \mathcal{T}^K_Q(i,\vec{\Omega})\ {}^{\alpha_\ell J_\ell I}\rho^K_Q(F_\ell, F'_\ell)\ \phi(\nu_{\alpha_u J_u,\, \alpha_\ell J_\ell} - \nu) \tag{7.70a}$$

$$\eta^{\mathrm{S}}_i(\nu,\vec{\Omega}) = \frac{h\nu}{4\pi}\mathcal{N} \sum_{\alpha_u J_u \alpha_\ell J_\ell} (2J_u+1)\, B(\alpha_u J_u \to \alpha_\ell J_\ell)$$

$$\times \sum_{KQ} \sum_{F_u F'_u} (-1)^{1-J_\ell+I+F_u+K} \sqrt{3(2F_u+1)(2F'_u+1)}$$

$$\times \left\{ \begin{array}{ccc} J_u & J_u & K \\ F_u & F'_u & I \end{array} \right\} \left\{ \begin{array}{ccc} 1 & 1 & K \\ J_u & J_u & J_\ell \end{array} \right\}$$

$$\times \mathcal{T}^K_Q(i,\vec{\Omega})\ {}^{\alpha_u J_u I}\rho^K_Q(F'_u, F_u)\ \phi(\nu_{\alpha_u J_u,\, \alpha_\ell J_\ell} - \nu) \tag{7.70b}$$

$$\rho^{\mathrm{A}}_i(\nu,\vec{\Omega}) = \eta^{\mathrm{A}}_i(\nu,\vec{\Omega}) \left\{ \phi(\nu_{\alpha_u J_u,\, \alpha_\ell J_\ell} - \nu) \to \psi(\nu_{\alpha_u J_u,\, \alpha_\ell J_\ell} - \nu) \right\} \tag{7.70c}$$

$$\rho^{\mathrm{S}}_i(\nu,\vec{\Omega}) = \eta^{\mathrm{S}}_i(\nu,\vec{\Omega}) \left\{ \phi(\nu_{\alpha_u J_u,\, \alpha_\ell J_\ell} - \nu) \to \psi(\nu_{\alpha_u J_u,\, \alpha_\ell J_\ell} - \nu) \right\} \tag{7.70d}$$

$$\varepsilon_i(\nu,\vec{\Omega}) = \frac{2h\nu^3}{c^2}\ \eta^{\mathrm{S}}_i(\nu,\vec{\Omega})\ . \tag{7.70e}$$

7.10. The Principle of Spectroscopic Stability

The equations obtained in the previous section for the multi-level atom with hyperfine structure must be compatible with the corresponding equations derived in Sect. 7.2 for the multi-level atom without hyperfine structure. By this we mean that when hyperfine structure has a negligible effect (strictly speaking, when the two constants $\mathcal{A}$ and $\mathcal{B}$ in Eqs. (3.70) are zero), it should be possible to get back the equations of Sect. 7.2 from those of Sect. 7.9. This is what we are going to prove here, thus obtaining – in a particular case – a confirmation of the *principle of spectroscopic stability*. Among the several possible formulations of this principle, the most satisfactory is the following: 'If two different descriptions are used to characterize a quantum system – a detailed description which takes an inner quantum number into account and a simplified description which disregards it – the predicted results must be the same in all physical experiments where the structure described by the inner quantum number is unimportant'. In the particular case that we are considering here, the inner quantum numbers are the nuclear spin quantum numbers (I, M_I).

We will now derive from Eq. (7.65) the corresponding equation for the multipole moments $\rho^K_Q(\alpha J)$ describing the atom irrespective of its hyperfine structure.

Equation (3.104) shows that the time evolution of $\rho^K_Q(\alpha J)$ can be obtained by

multiplication of Eq. (7.65) by the factor

$$(-1)^{J+I+F'+K}\sqrt{(2F+1)(2F'+1)}\begin{Bmatrix} F & F' & K \\ J & J & I \end{Bmatrix}$$

followed by summation over F and F'. We thus obtain

$$\frac{\mathrm{d}}{\mathrm{d}t}\rho_Q^K(\alpha J) = \sum_{FF'}(-1)^{J+I+F'+K}\sqrt{(2F+1)(2F'+1)}\begin{Bmatrix} F & F' & K \\ J & J & I \end{Bmatrix} \times \Big[\text{Right-Hand Side of Eq. (7.65)}\Big] . \tag{7.71}$$

Now we perform the summation over F and F' for the various terms in the right-hand side of Eq. (7.65). For the term containing $\mathbb{T}_{\mathrm{A}}$ we obtain from Eq. (7.69a) the following expression

$$\begin{aligned}
&\sum_{FF'}(-1)^{J+I+F'+K}\sqrt{(2F+1)(2F'+1)}\begin{Bmatrix} F & F' & K \\ J & J & I \end{Bmatrix} \\
&\quad\times \sum_{\alpha_\ell J_\ell K_\ell Q_\ell F_\ell F'_\ell} {}^{\alpha_\ell J_\ell I}\rho_{Q_\ell}^{K_\ell}(F_\ell, F'_\ell)\ (2J_\ell+1)\, B(\alpha_\ell J_\ell \to \alpha J) \\
&\quad\times \sum_{K_{\mathrm{r}}Q_{\mathrm{r}}} \sqrt{3(2F+1)(2F'+1)(2F_\ell+1)(2F'_\ell+1)(2K+1)(2K_\ell+1)(2K_{\mathrm{r}}+1)} \\
&\qquad\times (-1)^{K_\ell+Q_\ell+F'_\ell-F_\ell}\begin{Bmatrix} F & F_\ell & 1 \\ F' & F'_\ell & 1 \\ K & K_\ell & K_{\mathrm{r}} \end{Bmatrix}\begin{Bmatrix} J & J_\ell & 1 \\ F_\ell & F & I \end{Bmatrix}\begin{Bmatrix} J & J_\ell & 1 \\ F'_\ell & F' & I \end{Bmatrix} \\
&\qquad\times \begin{pmatrix} K & K_\ell & K_{\mathrm{r}} \\ -Q & Q_\ell & -Q_{\mathrm{r}} \end{pmatrix} J_{Q_{\mathrm{r}}}^{K_{\mathrm{r}}}(\nu_{\alpha J,\,\alpha_\ell J_\ell}) .
\end{aligned}$$

The summation over F and F' can be performed with the help of Eq. (2.56), and the expression above reduces to

$$\begin{aligned}
&\sum_{\alpha_\ell J_\ell K_\ell Q_\ell F_\ell F'_\ell}(-1)^{J_\ell+I+F'_\ell+K_\ell}\sqrt{(2F_\ell+1)(2F'_\ell+1)}\begin{Bmatrix} F_\ell & F'_\ell & K_\ell \\ J_\ell & J_\ell & I \end{Bmatrix} \\
&\qquad\times\ {}^{\alpha_\ell J_\ell I}\rho_{Q_\ell}^{K_\ell}(F_\ell, F'_\ell)\ (2J_\ell+1)\, B(\alpha_\ell J_\ell \to \alpha J) \\
&\qquad\times \sum_{K_{\mathrm{r}}Q_{\mathrm{r}}}\sqrt{3(2K+1)(2K_\ell+1)(2K_{\mathrm{r}}+1)}\ (-1)^{K_\ell+Q_\ell}\begin{Bmatrix} J & J_\ell & 1 \\ J & J_\ell & 1 \\ K & K_\ell & K_{\mathrm{r}} \end{Bmatrix} \\
&\qquad\qquad\times \begin{pmatrix} K & K_\ell & K_{\mathrm{r}} \\ -Q & Q_\ell & -Q_{\mathrm{r}} \end{pmatrix} J_{Q_{\mathrm{r}}}^{K_{\mathrm{r}}}(\nu_{\alpha J,\,\alpha_\ell J_\ell})
\end{aligned}$$

which, using again Eq. (3.104), can be cast into the form

$$\sum_{\alpha_\ell J_\ell K_\ell Q_\ell}\rho_{Q_\ell}^{K_\ell}(\alpha_\ell J_\ell)\ \mathbb{T}_{\mathrm{A}}(\alpha J K Q, \alpha_\ell J_\ell K_\ell Q_\ell) ,$$

where $\mathbb{T}_{\rm A}(\alpha JKQ, \alpha_\ell J_\ell K_\ell Q_\ell)$ is the rate defined in Eq. (7.14a).

By similar calculations – which involve the use of Eqs. (2.48), (2.55), (2.56) and (2.41) – we obtain from Eq. (7.71)

$$\begin{aligned}
\frac{\mathrm{d}}{\mathrm{d}t}\,\rho^K_Q(\alpha J) = {} & \sum_{FF'} (-1)^{J+I+F'+K} \sqrt{(2F+1)(2F'+1)} \begin{Bmatrix} F & F' & K \\ J & J & I \end{Bmatrix} \\
& \times (-2\pi\mathrm{i}) \sum_{K'Q'} \sum_{F''F'''} \tilde{N}_{\alpha JI}(KQFF', K'Q'F''F''')\ {}^{\alpha JI}\rho^{K'}_{Q'}(F'', F''') \\
& + \sum_{\alpha_\ell J_\ell} \sum_{K_\ell Q_\ell} \rho^{K_\ell}_{Q_\ell}(\alpha_\ell J_\ell)\ \mathbb{T}_{\rm A}(\alpha JKQ, \alpha_\ell J_\ell K_\ell Q_\ell) \\
& + \sum_{\alpha_u J_u} \sum_{K_u Q_u} \rho^{K_u}_{Q_u}(\alpha_u J_u) \left[\mathbb{T}_{\rm E}(\alpha JKQ, \alpha_u J_u K_u Q_u) + \mathbb{T}_{\rm S}(\alpha JKQ, \alpha_u J_u K_u Q_u) \right] \\
& - \sum_{K'Q'} \rho^{K'}_{Q'}(\alpha J) \left[\mathbb{R}_{\rm A}(\alpha JKQK'Q') + \mathbb{R}_{\rm E}(\alpha JKQK'Q') + \mathbb{R}_{\rm S}(\alpha JKQK'Q') \right],
\end{aligned}$$

where all the rates are exactly the same as those of Eqs. (7.14).

Finally, we evaluate the first term in the right-hand side using the expression for $\tilde{N}$ given in Eq. (7.66). With the help of Eqs. (2.41), (2.26d) and (2.36d) we get

$$\begin{aligned}
\frac{\mathrm{d}}{\mathrm{d}t}\,\rho^K_Q(\alpha J) = {} & -2\pi\mathrm{i} \sum_{FF'} (-1)^{J+I+F'+K} \sqrt{(2F+1)(2F'+1)} \begin{Bmatrix} F & F' & K \\ J & J & I \end{Bmatrix} \\
& \times\ \nu_{\alpha JIF,\,\alpha JIF'}\ {}^{\alpha JI}\rho^K_Q(F, F') \\
& - 2\pi\mathrm{i}\,\nu_{\rm L}\, g_{\alpha J}\, Q\, \rho^K_Q(\alpha J) \\
& + \sum_{\alpha_\ell J_\ell} \sum_{K_\ell Q_\ell} \rho^{K_\ell}_{Q_\ell}(\alpha_\ell J_\ell)\ \mathbb{T}_{\rm A}(\alpha JKQ, \alpha_\ell J_\ell K_\ell Q_\ell) \\
& + \sum_{\alpha_u J_u} \sum_{K_u Q_u} \rho^{K_u}_{Q_u}(\alpha_u J_u) \left[\mathbb{T}_{\rm E}(\alpha JKQ, \alpha_u J_u K_u Q_u) + \mathbb{T}_{\rm S}(\alpha JKQ, \alpha_u J_u K_u Q_u) \right] \\
& - \sum_{K'Q'} \rho^{K'}_{Q'}(\alpha J) \left[\mathbb{R}_{\rm A}(\alpha JKQK'Q') + \mathbb{R}_{\rm E}(\alpha JKQK'Q') \right. \\
& \qquad \left. + \mathbb{R}_{\rm S}(\alpha JKQK'Q') \right].
\end{aligned} \tag{7.72}$$

When hyperfine structure is negligible, the Bohr frequencies $\nu_{\alpha JIF,\,\alpha JIF'}$ are zero (cf. Eq. (7.67)), and Eqs. (7.72) reduce to the statistical equilibrium equations for the multi-level atom without hyperfine structure (Eq. (7.11)) – which confirms the principle of spectroscopic stability. Equation (7.72) also shows that the 'inner' description of the atomic system involving hyperfine structure can be avoided whenever the frequency shifts among the F-sublevels of each (αJ)-level are negligible in comparison with the relaxation rates of the same level (roughly speaking,

when they are much smaller than the inverse lifetime of the level). This provides a quantitative criterion to ascertain whether hyperfine structure can be neglected in a real physical problem.

As far as the radiative transfer coefficients are concerned, a direct application of Eq. (3.104) shows that Eqs. (7.70), which have just been obtained by neglecting the frequency shifts between hyperfine components, are nothing but Eqs. (7.16) written in a different form. Referring for instance to the expression for $\eta_i^{\rm A}(\nu,\vec{\Omega})$ in Eq. (7.70a), and recalling that, according to Eq. (3.104)

$$\rho^K_Q(\alpha_\ell J_\ell) =$$

$$= \sum_{F_\ell F'_\ell} (-1)^{J_\ell+I+F'_\ell+K} \sqrt{(2F_\ell+1)(2F'_\ell+1)} \left\{ \begin{array}{ccc} F_\ell & F'_\ell & K \\ J_\ell & J_\ell & I \end{array} \right\} {}^{\alpha_\ell J_\ell I}\rho^K_Q(F_\ell, F'_\ell) \,,$$

we obtain

$$\begin{aligned} \eta_i^{\rm A}(\nu,\vec{\Omega}) = & \frac{h\nu}{4\pi} \mathcal{N} \sum_{\alpha_\ell J_\ell} \sum_{\alpha_u J_u} (2J_\ell+1)\, B(\alpha_\ell J_\ell \rightarrow \alpha_u J_u) \\ & \times \sum_{KQ} \sqrt{3}\ (-1)^{1-J_\ell-J_u-K} \left\{ \begin{array}{ccc} 1 & 1 & K \\ J_\ell & J_\ell & J_u \end{array} \right\} \mathcal{T}^K_Q(i,\vec{\Omega})\ \rho^K_Q(\alpha_\ell J_\ell) \\ & \times\ \phi(\nu_{\alpha_u J_u,\, \alpha_\ell J_\ell} - \nu) \,, \end{aligned}$$

which coincides with the corresponding expression in Eq. (7.16a). This is a further aspect of the principle of spectroscopic stability.

The same reasoning followed about hyperfine structure can be repeated for fine structure, which is – in terms of the principle of spectroscopic stability – the 'inner' structure of the atom due to the electronic spin. According to this principle, the equations describing the multi-term atom should exactly reduce to the equations for the 'spinless atom' when the effects due to the presence of spin are negligible.

To check this property we start from Eq. (7.38), with N given by Eqs. (7.41)-(7.43) and the rates by Eqs. (7.45a-c) and (7.46a-c), and – bearing in mind Eq. (3.105) – we multiply both sides by the factor

$$(-1)^{L+S+J'+K} \sqrt{(2J+1)(2J'+1)} \left\{ \begin{array}{ccc} J & J' & K \\ L & L & S \end{array} \right\}$$

and sum over J and J'. Neglecting the fine-structure shifts $\nu_{\beta LSJ,\, \beta LSJ'}$ in the final result, we obtain the equation[1]

[1] The first term in the right-hand side can be deduced using the Racah-algebra relation

$$\sqrt{c\,(c+1)(2c+1)} \left\{ \begin{array}{ccc} a & b & 1 \\ c & c & d \end{array} \right\} + (-1)^{a-b} \sqrt{d\,(d+1)(2d+1)} \left\{ \begin{array}{ccc} a & b & 1 \\ d & d & c \end{array} \right\} =$$

$$= \delta_{ab}\ (-1)^{a+c+d+1} \sqrt{a\,(a+1)} \,\Big/ \sqrt{2a+1} \,,$$

which follows from Eqs. (2.36d) and (2.36f).

$$\frac{\mathrm{d}}{\mathrm{d}t}\,\rho^K_Q(\beta L) = -2\pi\mathrm{i}\,\nu_\mathrm{L}\,Q\,\rho^K_Q(\beta L)$$
$$+\sum_{\beta_\ell L_\ell}\sum_{K_\ell Q_\ell}\rho^{K_\ell}_{Q_\ell}(\beta_\ell L_\ell)\;\mathbb{T}_\mathrm{A}(\beta LKQ,\beta_\ell L_\ell K_\ell Q_\ell)$$
$$+\sum_{\beta_u L_u}\sum_{K_u Q_u}\rho^{K_u}_{Q_u}(\beta_u L_u)\left[\mathbb{T}_\mathrm{E}(\beta LKQ,\beta_u L_u K_u Q_u)+\mathbb{T}_\mathrm{S}(\beta LKQ,\beta_u L_u K_u Q_u)\right]$$
$$-\sum_{K'Q'}\rho^{K'}_{Q'}(\beta L)\left[\mathbb{R}_\mathrm{A}(\beta LKQK'Q')+\mathbb{R}_\mathrm{E}(\beta LKQK'Q')\right.$$
$$\left.+\,\mathbb{R}_\mathrm{S}(\beta LKQK'Q')\right], \tag{7.73}$$

where all the rates are the same as those in Eqs. (7.14) with the formal substitutions

$$\begin{array}{lll}\alpha\to\beta & \alpha_\ell\to\beta_\ell & \alpha_u\to\beta_u\\ J\to L & J_\ell\to L_\ell & J_u\to L_u\,.\end{array} \tag{7.74}$$

It is easily seen that, performing these substitutions, Eq. (7.73) is identical to Eq. (7.11) except for the presence, in the latter equation, of the Landé factor $g_{\alpha J}$, which is however equal to unity when spin is neglected.

Similarly, it can be seen using Eq. (3.105) that the expressions (7.48) for the radiative transfer coefficients (which have been obtained by neglecting the frequency shifts due to fine structure) are identical to Eqs. (7.16) with substitutions (7.74).

7.11. Selection Rules

All the expressions derived in the preceding sections for the radiative rates and for the radiative transfer coefficients involve some 3-j, or 6-j, or 9-j symbols which are responsible for the appearance of several selection rules. These rules originate from the electric-dipole approximation and can be considered as an obvious generalization of the selection rules that are usually met in conventional spectroscopy.

In the following we list the selection rules for the radiative rates written in the spherical statistical tensor representation. The list is divided into three parts, which refer to the different atomic models considered previously. We recall that – as apparent from Eqs. (5.153) and (5.155) – the only non-zero components of the radiation field tensor $J^{K_\mathrm{r}}_{Q_\mathrm{r}}$ are those with $K_\mathrm{r} = 0,\,1,\,2$.

1) Multi-Level Atom (Eqs. (7.14))[1]

a) Transfer rate due to absorption from lower levels, $\mathbb{T}_{\mathrm{A}}(\alpha JKQ, \alpha_\ell J_\ell K_\ell Q_\ell)$:

$$\Delta J = J - J_\ell = 0, \pm 1;\ 0 \nrightarrow 0$$

$$\Delta K = K - K_\ell = \begin{cases} 0 & \text{for } K_{\mathrm{r}} = 0 \\ 0, \pm 1;\ 0 \nrightarrow 0 & \text{for } K_{\mathrm{r}} = 1 \\ 0, \pm 2;\ 0 \nrightarrow 0 & \text{for } K_{\mathrm{r}} = 2 \end{cases}$$

b) Transfer rate due to spontaneous emission from upper levels, $\mathbb{T}_{\mathrm{E}}(\alpha JKQ, \alpha_u J_u K_u Q_u)$:

$$\Delta J = J_u - J = 0, \pm 1;\ 0 \nrightarrow 0$$

$$\Delta K = K_u - K = 0$$

c) Transfer rate due to stimulated emission from upper levels, $\mathbb{T}_{\mathrm{S}}(\alpha JKQ, \alpha_u J_u K_u Q_u)$:

$$\Delta J = J_u - J = 0, \pm 1;\ 0 \nrightarrow 0$$

$$\Delta K = K_u - K = \begin{cases} 0 & \text{for } K_{\mathrm{r}} = 0 \\ 0, \pm 1;\ 0 \nrightarrow 0 & \text{for } K_{\mathrm{r}} = 1 \\ 0, \pm 2;\ 0 \nrightarrow 0 & \text{for } K_{\mathrm{r}} = 2 \end{cases}$$

d) Relaxation rate due to absorption towards upper levels, $\mathbb{R}_{\mathrm{A}}(\alpha JKQK'Q')$:

$$\Delta K = K' - K = \begin{cases} 0 & \text{for } K_{\mathrm{r}} = 0 \\ 0, \pm 1;\ 0 \nrightarrow 0 & \text{for } K_{\mathrm{r}} = 1 \\ 0, \pm 2;\ 0 \nrightarrow 0 & \text{for } K_{\mathrm{r}} = 2 \end{cases}$$

e) Relaxation rate due to spontaneous emission towards lower levels, $\mathbb{R}_{\mathrm{E}}(\alpha JKQK'Q')$:

$$\Delta K = K' - K = 0$$

f) Relaxation rate due to stimulated emission towards lower levels, $\mathbb{R}_{\mathrm{S}}(\alpha JKQK'Q')$:

$$\Delta K = K' - K = \begin{cases} 0 & \text{for } K_{\mathrm{r}} = 0 \\ 0, \pm 1;\ 0 \nrightarrow 0 & \text{for } K_{\mathrm{r}} = 1 \\ 0, \pm 2;\ 0 \nrightarrow 0 & \text{for } K_{\mathrm{r}} = 2 \end{cases}$$

[1] Note that, for $K_{\mathrm{r}} = 2$, the values $\Delta K = \pm 1$ are forbidden. For $\mathbb{T}_{\mathrm{A}}$ and $\mathbb{T}_{\mathrm{S}}$, this property follows from the presence of the 9-j symbol (cf. footnote on p.287); for $\mathbb{R}_{\mathrm{A}}$ and $\mathbb{R}_{\mathrm{S}}$, it follows from the presence of the factor ζ_+.

2) Multi-Term Atom (Eqs. (7.45a-c) and (7.46a-c))

a) Transfer rate due to absorption from lower terms, $\mathbb{T}_{\mathrm{A}}(\beta LSKQJJ', \beta_\ell L_\ell S K_\ell Q_\ell J_\ell J'_\ell)$:

$$\Delta L = L - L_\ell = 0, \pm 1;\ 0 \nrightarrow 0$$
$$\Delta J = J - J_\ell = 0, \pm 1;\ 0 \nrightarrow 0$$
$$\Delta J' = J' - J'_\ell = 0, \pm 1;\ 0 \nrightarrow 0$$
$$\Delta K = K - K_\ell = \begin{cases} 0 & \text{for } K_{\mathrm{r}} = 0 \\ 0, \pm 1;\ 0 \nrightarrow 0 & \text{for } K_{\mathrm{r}} = 1 \\ 0, \pm 1, \pm 2;\ 0 \nrightarrow 0, 0 \nrightarrow 1, 1 \nrightarrow 0 & \text{for } K_{\mathrm{r}} = 2 \end{cases}$$

b) Transfer rate due to spontaneous emission from upper terms, $\mathbb{T}_{\mathrm{E}}(\beta LSKQJJ', \beta_u L_u S K_u Q_u J_u J'_u)$:

$$\Delta L = L_u - L = 0, \pm 1;\ 0 \nrightarrow 0$$
$$\Delta J = J_u - J = 0, \pm 1;\ 0 \nrightarrow 0$$
$$\Delta J' = J'_u - J' = 0, \pm 1;\ 0 \nrightarrow 0$$
$$\Delta K = K_u - K = 0$$

c) Transfer rate due to stimulated emission from upper terms, $\mathbb{T}_{\mathrm{S}}(\beta LSKQJJ', \beta_u L_u S K_u Q_u J_u J'_u)$:

$$\Delta L = L_u - L = 0, \pm 1;\ 0 \nrightarrow 0$$
$$\Delta J = J_u - J = 0, \pm 1;\ 0 \nrightarrow 0$$
$$\Delta J' = J'_u - J' = 0, \pm 1;\ 0 \nrightarrow 0$$
$$\Delta K = K_u - K = \begin{cases} 0 & \text{for } K_{\mathrm{r}} = 0 \\ 0, \pm 1;\ 0 \nrightarrow 0 & \text{for } K_{\mathrm{r}} = 1 \\ 0, \pm 1, \pm 2;\ 0 \nrightarrow 0, 0 \nrightarrow 1, 1 \nrightarrow 0 & \text{for } K_{\mathrm{r}} = 2 \end{cases}$$

d) Relaxation rate due to absorption towards upper terms, $\mathbb{R}_{\mathrm{A}}(\beta LSKQJJ'K'Q'J''J''')$:

$$\Delta J = J'' - J = 0 \ \text{ and } \ \Delta J' = J''' - J' = \begin{cases} 0 & \text{for } K_{\mathrm{r}} = 0 \\ 0, \pm 1;\ 0 \nrightarrow 0 & \text{for } K_{\mathrm{r}} = 1 \\ 0, \pm 1, \pm 2;\ 0 \nrightarrow 0, 0 \nrightarrow 1, 1 \nrightarrow 0 & \text{for } K_{\mathrm{r}} = 2 \end{cases}$$

or

$$\Delta J' = J''' - J' = 0 \ \text{ and } \ \Delta J = J'' - J = \begin{cases} 0 & \text{for } K_{\mathrm{r}} = 0 \\ 0, \pm 1;\ 0 \nrightarrow 0 & \text{for } K_{\mathrm{r}} = 1 \\ 0, \pm 1, \pm 2;\ 0 \nrightarrow 0, 0 \nrightarrow 1, 1 \nrightarrow 0 & \text{for } K_{\mathrm{r}} = 2; \end{cases}$$

$$\Delta K = K' - K = \begin{cases} 0 & \text{for } K_{\mathrm{r}} = 0 \\ 0, \pm 1;\ 0 \nrightarrow 0 & \text{for } K_{\mathrm{r}} = 1 \\ 0, \pm 1, \pm 2;\ 0 \nrightarrow 0, 0 \nrightarrow 1, 1 \nrightarrow 0 & \text{for } K_{\mathrm{r}} = 2 \end{cases}$$

e) Relaxation rate due to spontaneous emission towards lower terms, $\mathbb{R}_{\mathrm{E}}(\beta LSKQJJ'K'Q'J''J''')$:

$$\Delta J = J'' - J = 0$$

$$\Delta J' = J''' - J' = 0$$

$$\Delta K = K' - K = 0$$

f) Relaxation rate due to stimulated emission towards lower terms, $\mathbb{R}_{\mathrm{S}}(\beta LSKQJJ'K'Q'J''J''')$:

$$\Delta J = J'' - J = 0 \text{ and } \Delta J' = J''' - J' = \begin{cases} 0 & \text{for } K_{\mathrm{r}} = 0 \\ 0, \pm 1;\ 0 \nrightarrow 0 & \text{for } K_{\mathrm{r}} = 1 \\ 0, \pm 1, \pm 2;\ 0 \nrightarrow 0, 0 \nrightarrow 1, 1 \nrightarrow 0 & \text{for } K_{\mathrm{r}} = 2 \end{cases}$$

or

$$\Delta J' = J''' - J' = 0 \text{ and } \Delta J = J'' - J = \begin{cases} 0 & \text{for } K_{\mathrm{r}} = 0 \\ 0, \pm 1;\ 0 \nrightarrow 0 & \text{for } K_{\mathrm{r}} = 1 \\ 0, \pm 1, \pm 2;\ 0 \nrightarrow 0, 0 \nrightarrow 1, 1 \nrightarrow 0 & \text{for } K_{\mathrm{r}} = 2; \end{cases}$$

$$\Delta K = K' - K = \begin{cases} 0 & \text{for } K_{\mathrm{r}} = 0 \\ 0, \pm 1;\ 0 \nrightarrow 0 & \text{for } K_{\mathrm{r}} = 1 \\ 0, \pm 1, \pm 2;\ 0 \nrightarrow 0, 0 \nrightarrow 1, 1 \nrightarrow 0 & \text{for } K_{\mathrm{r}} = 2 \end{cases}$$

3) Multi-Level Atom with Hyperfine Structure (Eqs. (7.69))

The selection rules are here strictly analogous to those for the multi-term atom; they can be simply derived by substituting $L \to J$, $J \to F$.

7.12. Changing the Reference System

All the equations of the former sections have been derived in a reference system having its z-axis (i.e. the quantization axis for angular momentum) in the magnetic field direction – obviously, the z-axis direction is arbitrary for zero magnetic field. It is now important to discuss how these equations are modified when a different reference system is chosen.

Consider first the statistical equilibrium equations. The procedure to obtain these equations in a reference system other than the 'magnetic' reference system (the one with the z-axis parallel to the magnetic field) is straightforward. One has just to consider the equations written in the 'old' system and to express the density-matrix elements as functions of the density-matrix elements in the 'new' system.

This procedure can be formalized as follows: we introduce a formal vector $\boldsymbol{\rho}$, having dimension N, whose N components are the density-matrix elements of the model atom considered, and we observe that the statistical equilibrium equations can be written in the condensed form

$$\frac{\mathrm{d}}{\mathrm{d}t}\,\boldsymbol{\rho} = \boldsymbol{A}\,\boldsymbol{\rho}\ ,$$

where $\boldsymbol{A}$ is an $N \times N$ matrix that will be called in the following the *rate matrix*. Since the density-matrix elements change under rotation according to linear relations (see e.g. Eqs. (3.95) or (3.98)), we can write

$$\boldsymbol{\rho}^{(\mathrm{new})} = \boldsymbol{S}\,\boldsymbol{\rho}^{(\mathrm{old})} \tag{7.75}$$

with the inverse formula

$$\boldsymbol{\rho}^{(\mathrm{old})} = \boldsymbol{S}^{-1}\,\boldsymbol{\rho}^{(\mathrm{new})}\ ,$$

where $\boldsymbol{S}$ is the $N \times N$ transformation matrix that depends on the rotation. It follows that

$$\frac{\mathrm{d}}{\mathrm{d}t}\,\boldsymbol{\rho}^{(\mathrm{new})} = \boldsymbol{A}^{(\mathrm{new})}\,\boldsymbol{\rho}^{(\mathrm{new})}\ ,$$

where

$$\boldsymbol{A}^{(\mathrm{new})} = \boldsymbol{S}\,\boldsymbol{A}^{(\mathrm{old})}\ \boldsymbol{S}^{-1}\ .$$

This is the transformation law for the rate matrix under rotation of the reference system.

To give an example, let us consider the statistical equilibrium equations for the multi-level atom in the spherical statistical tensor representation (Eq. (7.11)). If R is the rotation which carries the old reference system into the new one, we have from Eq. (3.98)

$$\left[\rho^K_Q(\alpha J)\right]_{\mathrm{new}} = \sum_{Q'} \left[\rho^K_{Q'}(\alpha J)\right]_{\mathrm{old}} \mathcal{D}^K_{Q'Q}(R)^*\ , \tag{7.76}$$

with the inverse transformation (that can be easily deduced using Eqs. (2.72))

$$\left[\rho^K_Q(\alpha J)\right]_{\mathrm{old}} = \sum_{Q'} \left[\rho^K_{Q'}(\alpha J)\right]_{\mathrm{new}} \mathcal{D}^K_{QQ'}(R)\ . \tag{7.77}$$

Note that these transformations imply that the $\boldsymbol{S}$ matrix defined above is block-diagonal, with its non-zero elements connecting only statistical tensors of the same level and of the same rank.

With the help of some algebra it is easily shown that the statistical equilibrium equations in the new reference system are the following

$$\begin{aligned}
\frac{\mathrm{d}}{\mathrm{d}t}\Big[\rho_Q^K(\alpha J)\Big]_{\mathrm{new}} &= -2\pi\mathrm{i}\,\nu_{\mathrm{L}}\; g_{\alpha J} \sum_{Q'} \mathcal{K}^K_{QQ'}\,\Big[\rho^K_{Q'}(\alpha J)\Big]_{\mathrm{new}} \\
&+ \sum_{\alpha_\ell J_\ell} \sum_{K_\ell Q_\ell} \Big[\rho^{K_\ell}_{Q_\ell}(\alpha_\ell J_\ell)\Big]_{\mathrm{new}} \Big[\mathbb{T}_{\mathrm{A}}(\alpha JKQ, \alpha_\ell J_\ell K_\ell Q_\ell)\Big]_{\mathrm{new}} \\
&+ \sum_{\alpha_u J_u} \sum_{K_u Q_u} \Big[\rho^{K_u}_{Q_u}(\alpha_u J_u)\Big]_{\mathrm{new}} \Big\{ \Big[\mathbb{T}_{\mathrm{E}}(\alpha JKQ, \alpha_u J_u K_u Q_u)\Big]_{\mathrm{new}} \\
&\qquad + \Big[\mathbb{T}_{\mathrm{S}}(\alpha JKQ, \alpha_u J_u K_u Q_u)\Big]_{\mathrm{new}}\Big\} \\
&- \sum_{K'Q'} \Big[\rho^{K'}_{Q'}(\alpha J)\Big]_{\mathrm{new}} \Big\{ \Big[\mathbb{R}_{\mathrm{A}}(\alpha JKQK'Q')\Big]_{\mathrm{new}} + \Big[\mathbb{R}_{\mathrm{E}}(\alpha JKQK'Q')\Big]_{\mathrm{new}} \\
&\qquad + \Big[\mathbb{R}_{\mathrm{S}}(\alpha JKQK'Q')\Big]_{\mathrm{new}}\Big\}\,, \qquad (7.78)
\end{aligned}$$

where the kernel $\mathcal{K}^K_{QQ'}$ is given by

$$\mathcal{K}^K_{QQ'} = \sum_{Q''} \mathcal{D}^K_{Q''Q}(R)^*\; Q''\; \mathcal{D}^K_{Q''Q'}(R) \qquad (7.79)$$

and where

$$\begin{aligned}
&\Big[\mathbb{T}_{\mathrm{A}}(\alpha JKQ, \alpha_\ell J_\ell K_\ell Q_\ell)\Big]_{\mathrm{new}} = \\
&\qquad = \sum_{Q'Q'_\ell} \mathcal{D}^K_{Q'Q}(R)^* \Big[\mathbb{T}_{\mathrm{A}}(\alpha JKQ', \alpha_\ell J_\ell K_\ell Q'_\ell)\Big]_{\mathrm{old}} \mathcal{D}^{K_\ell}_{Q'_\ell Q_\ell}(R) \\
&\Big[\mathbb{T}_{\mathrm{E,S}}(\alpha JKQ, \alpha_u J_u K_u Q_u)\Big]_{\mathrm{new}} = \\
&\qquad = \sum_{Q'Q'_u} \mathcal{D}^K_{Q'Q}(R)^* \Big[\mathbb{T}_{\mathrm{E,S}}(\alpha JKQ', \alpha_u J_u K_u Q'_u)\Big]_{\mathrm{old}} \mathcal{D}^{K_u}_{Q'_u Q_u}(R) \\
&\Big[\mathbb{R}_{\mathrm{A,E,S}}(\alpha JKQK'Q')\Big]_{\mathrm{new}} = \\
&\qquad = \sum_{Q''Q'''} \mathcal{D}^K_{Q''Q}(R)^* \Big[\mathbb{R}_{\mathrm{A,E,S}}(\alpha JKQ''K'Q''')\Big]_{\mathrm{old}} \mathcal{D}^{K'}_{Q'''Q'}(R)\,. \qquad (7.80)
\end{aligned}$$

It can be proved that the expressions for the radiative rates are formally invariant. Consider for instance Eq. (7.14a); from Eqs. (7.80) we have

$$\Big[\mathbb{T}_{\rm A}(\alpha JKQ,\alpha_\ell J_\ell K_\ell Q_\ell)\Big]_{\rm new} =$$

$$= \sum_{Q'Q'_\ell} \mathcal{D}^{K}_{Q'Q}(R)^*\, \mathcal{D}^{K_\ell}_{Q'_\ell Q_\ell}(R)\ (2J_\ell+1)\, B(\alpha_\ell J_\ell \rightarrow \alpha J)$$

$$\times \sum_{K_{\rm r}Q_{\rm r}} \sqrt{3(2K+1)(2K_\ell+1)(2K_{\rm r}+1)}$$

$$\times (-1)^{K_\ell+Q'_\ell} \begin{Bmatrix} J & J_\ell & 1 \\ J & J_\ell & 1 \\ K & K_\ell & K_{\rm r} \end{Bmatrix} \begin{pmatrix} K & K_\ell & K_{\rm r} \\ -Q' & Q'_\ell & -Q_{\rm r} \end{pmatrix} \Big[J^{K_{\rm r}}_{Q_{\rm r}}(\nu_{\alpha J,\,\alpha_\ell J_\ell})\Big]_{\rm old} ,$$

where $\big[J^{K_{\rm r}}_{Q_{\rm r}}(\nu_{\alpha J,\,\alpha_\ell J_\ell})\big]_{\rm old}$ is the radiation field tensor evaluated in the old reference system. After some algebra, which involves the use of Eqs. (2.77), (2.23a) and (2.73), one obtains the expression

$$\Big[\mathbb{T}_{\rm A}(\alpha JKQ,\alpha_\ell J_\ell K_\ell Q_\ell)\Big]_{\rm new} = (2J_\ell+1)\, B(\alpha_\ell J_\ell \rightarrow \alpha J)$$

$$\times \sum_{K_{\rm r}Q_{\rm r}} \sqrt{3(2K+1)(2K_\ell+1)(2K_{\rm r}+1)}$$

$$\times (-1)^{K_\ell+Q_\ell} \begin{Bmatrix} J & J_\ell & 1 \\ J & J_\ell & 1 \\ K & K_\ell & K_{\rm r} \end{Bmatrix} \begin{pmatrix} K & K_\ell & K_{\rm r} \\ -Q & Q_\ell & -Q'_{\rm r} \end{pmatrix} \mathcal{D}^{K_{\rm r}}_{Q_{\rm r}Q'_{\rm r}}(R) \Big[J^{K_{\rm r}}_{Q_{\rm r}}(\nu_{\alpha J,\,\alpha_\ell J_\ell})\Big]_{\rm old} ,$$

and since from Eq. (2.78)

$$\sum_{Q_{\rm r}} \mathcal{D}^{K_{\rm r}}_{Q_{\rm r}Q'_{\rm r}}(R) \Big[J^{K_{\rm r}}_{Q_{\rm r}}(\nu_{\alpha J,\,\alpha_\ell J_\ell})\Big]_{\rm old} = \Big[J^{K_{\rm r}}_{Q'_{\rm r}}(\nu_{\alpha J,\,\alpha_\ell J_\ell})\Big]_{\rm new} , \tag{7.81}$$

we see that the rate $\mathbb{T}_{\rm A}$ has the same expression in the old and new reference systems.

It can be easily proved that this property holds for the other rates as well. Thus we can state that *all the radiative rates entering the statistical equilibrium equations are invariant under rotation of the reference system.*[1]

This result – which has been deduced here for the multi-level atom – is also valid for the other model atoms considered in this chapter, namely the multi-term and the multi-level atom with hyperfine structure. This means that the radiative rates of Eqs. (7.45a-c), (7.46a-c) and (7.69) are formally invariant under rotation of the reference system.

[1] This is of course a *formal* invariance. The actual value of the rates $\mathbb{T}_{\rm A}$, $\mathbb{T}_{\rm S}$, $\mathbb{R}_{\rm A}$, $\mathbb{R}_{\rm S}$ for an assigned incident radiation field does depend on the reference system because the radiation field tensor J^K_Q changes according to Eq. (7.81).

Moreover, this result is valid irrespective of the representation used for the density operator. We have proved it here for the equations written in the spherical statistical tensor representation, but it is also valid in the standard representation. The proof is of course more involved, since the transformation law of the density-matrix elements under rotation of the reference system is more complicated than the transformation law of multipole moments (cf. Eqs. (3.96) and (3.98)).[1]

It should be remarked that, in spite of the formal invariance of the radiative rates, the statistical equilibrium equations in a reference system other than the 'magnetic' system are in general more involved because of the presence of the magnetic term (Eq. (7.79)).[2] This term has its simplest expression in the reference system having the z-axis in the magnetic field direction.

The radiative transfer coefficients, like the radiative rates, have always been expressed in the 'magnetic' reference system in the former sections; thus we are again faced with the problem of finding their expressions in a different system.

Referring, for instance, to the emission coefficient $\varepsilon_i(\nu, \vec{\Omega})$, its expression in the 'magnetic' reference system can be formally written as the scalar product

$$\varepsilon_i(\nu, \vec{\Omega}) = \boldsymbol{C}_i^{\dagger} \cdot \boldsymbol{\rho} \,,$$

where $\boldsymbol{C}_i$ is a vector having dimension N. In the new reference system, one has from Eq. (7.75)

$$\varepsilon_i(\nu, \vec{\Omega}) = \boldsymbol{C}_i^{\dagger\,(\mathrm{new})} \cdot \boldsymbol{\rho}^{(\mathrm{new})} \,,$$

where

$$\boldsymbol{C}_i^{\dagger\,(\mathrm{new})} = \boldsymbol{C}_i^{\dagger\,(\mathrm{old})}\, \boldsymbol{S}^{-1} \,.$$

This is the general transformation law for the vector $\boldsymbol{C}_i^{\dagger}$.

To give an example, let us consider the expression of $\varepsilon_i(\nu, \vec{\Omega})$ for the multi-level atom in the approximation of neglecting the dependence of the Φ profiles on the magnetic quantum numbers (Eq. (7.16e)). Recalling Eqs. (7.8) and (7.77) we can write

$$\begin{aligned}
\varepsilon_i(\nu, \vec{\Omega}) = \frac{h\nu}{4\pi} \mathcal{N} & \sum_{\alpha_\ell J_\ell} \sum_{\alpha_u J_u} (2J_u + 1)\, A(\alpha_u J_u \rightarrow \alpha_\ell J_\ell) \\
& \times \sum_{KQ} \sqrt{3}\ (-1)^{1+J_\ell+J_u} \left\{ \begin{array}{ccc} 1 & 1 & K \\ J_u & J_u & J_\ell \end{array} \right\} \left[\mathcal{T}_Q^K(i, \vec{\Omega}) \right]_{\mathrm{old}} \\
& \times \sum_{Q'} \left[\rho_{Q'}^K(\alpha_u J_u) \right]_{\mathrm{new}} \mathcal{D}_{QQ'}^K(R)\ \phi(\nu_{\alpha_u J_u, \alpha_\ell J_\ell} - \nu) \,,
\end{aligned}$$

[1] The proof is however straightforward. Considering for instance the multi-level atom, one should start from Eq. (7.5), multiply both sides by the factor $\mathcal{D}_{MN}^J(R)^*\, \mathcal{D}_{M'N'}^J(R)$ and sum over M and M' to get, using Eq. (3.96) and its inverse, the statistical equilibrium equations in the new reference system. The expressions for the rates in the old system are given by Eqs. (7.9). The corresponding expressions in the new system can then be derived via several Racah-algebra calculations.

[2] An exception occurs when the radiation field is cylindrically symmetrical about an axis. In that case it may be simpler to write the statistical equilibrium equations in a reference system having the z-axis directed along this symmetry axis (see e.g. Sect. 10.8).

where R is the rotation which carries the 'magnetic' reference system into the new one. Since from Eq. (2.78)

$$\sum_Q \left[\mathcal{T}^K_Q(i,\vec{\Omega})\right]_{\rm old} \mathcal{D}^K_{QQ'}(R) = \left[\mathcal{T}^K_{Q'}(i,\vec{\Omega})\right]_{\rm new} ,$$

we see that $\varepsilon_i(\nu,\vec{\Omega})$ has the same expression in the old and new reference systems. As this property holds for the other radiative transfer coefficients too, we conclude that *when the dependence of the Φ profiles on the magnetic quantum numbers can be neglected, all the radiative transfer coefficients are invariant under rotation of the reference system.*[1]

Similar invariance properties can be proved for the multi-term atom and for the multi-level atom with hyperfine structure (Eqs. (7.48) and (7.70)).

7.13. Collisional Rates

In the previous sections we have derived the statistical equilibrium equations for the atomic density-matrix elements by considering only the interaction of the atomic system with the radiation field. In real plasmas atoms are also subjected, in general, to a wide variety of collisions both with particles of several species (like electrons, ions, and different atoms) and – in the case of laboratory experiments – with the walls of the cell containing the plasma.

A detailed theory of collisions is beyond the aim of this book. Here we want just to deduce some general results about the effect of collisions on the physical state of the atomic system under the assumption of an isotropic distribution of colliding particles.

In Chap. 5 (see Sects. 5.14 and 5.15) we presented a thorough discussion, based on classical physics, of the role of collisions in polarization phenomena. The distinction there introduced between 'exciting' and 'perturbing' collisions can be transferred to the quantum description of collisional interactions.

Let us consider a multi-level atom with energy eigenvectors of the form $|\alpha JM\rangle$, and let us suppose, for the time being, that no magnetic field (nor any other anisotropic agent) is present in the physical environment. The energy eigenvectors will then be degenerate with respect to the magnetic quantum number M. We can divide collisions into *inelastic* and *elastic*. Inelastic collisions induce transitions between the level $|\alpha JM\rangle$ and an upper level $|\alpha_u J_u M_u\rangle$ with a corresponding energy loss of the colliding particle. Such collisions, which are the quantum analogue

[1] Contrary to the radiative rates, this is a *real* – not just a formal – invariance. It is clear that once the multipole moments in an assigned reference system are given, the radiative transfer coefficients are univocally determined. If the reference system is rotated, both the multipole moments and the components of the tensor $\mathcal{T}^K_Q(i,\vec{\Omega})$ are changed, but the quantity

$$\textstyle\sum_Q \mathcal{T}^K_Q(i,\vec{\Omega})\ \rho^K_Q(\alpha J)$$

is invariant.

of the (classical) 'exciting' collisions, have their inverse process in the so-called *superelastic* collisions, which induce transitions between the level $|\alpha JM\rangle$ and a lower level $|\alpha_\ell J_\ell M_\ell\rangle$ with a corresponding energy increase of the colliding particle. Elastic collisions induce transitions between the level $|\alpha JM\rangle$ and levels of the form $|\alpha JM'\rangle$ or, in other words, between magnetic sublevels belonging to the same (αJ)-level. In these collisions, which are the quantum analogue of the (classical) 'perturbing' collisions, the energy of the colliding particle does not change during the interaction.

The effect of all these collisions on the physical state of the atomic system can be described by suitable rates (which will be divided into *transfer* and *relaxation* collisional rates, with the same meaning as the radiative rates) appearing in the statistical equilibrium equations for the density-matrix elements of the atomic system. We will now derive some properties of these rates which follow from general physical principles under the hypothesis of an isotropic distribution of colliding particles.

7.13.a Collisional Rates due to Inelastic and Superelastic Collisions

Consider first the transfer rate due to inelastic collisions which contribute to the time evolution of a particular density-matrix element. In an assigned – although arbitrary – reference system we can write, with self-evident notations

$$\frac{\mathrm{d}}{\mathrm{d}t}\,\rho_{\alpha J}(M,M') = \sum_{\alpha_\ell J_\ell M_\ell M'_\ell} C_{\mathrm{I}}(\alpha JMM', \alpha_\ell J_\ell M_\ell M'_\ell)\ \rho_{\alpha_\ell J_\ell}(M_\ell, M'_\ell)\ , \qquad (7.82)$$

where the quantum numbers $(\alpha_\ell J_\ell)$ denote any atomic level having energy lower than the level (αJ).

We now consider a new reference system obtained from the old one by the rotation R. Using Eq. (3.96) and its inverse, we have

$$\begin{aligned}
&\frac{\mathrm{d}}{\mathrm{d}t}\left[\rho_{\alpha J}(M,M')\right]_{\mathrm{new}} = \\
&= \sum_{\alpha_\ell J_\ell M_\ell M'_\ell} \left\{ \sum_{NN'N_\ell N'_\ell} \mathcal{D}^J_{NM}(R)^*\ \mathcal{D}^J_{N'M'}(R)\ \mathcal{D}^{J_\ell}_{N_\ell M_\ell}(R)\ \mathcal{D}^{J_\ell}_{N'_\ell M'_\ell}(R)^* \right. \\
&\qquad \left. \times\, C_{\mathrm{I}}(\alpha JNN', \alpha_\ell J_\ell N_\ell N'_\ell) \right\} \left[\rho_{\alpha_\ell J_\ell}(M_\ell, M'_\ell)\right]_{\mathrm{new}} . \qquad (7.83)
\end{aligned}$$

On the other hand, the assumption of isotropic collisions implies that all quantization directions are equivalent, therefore Eqs. (7.82) and (7.83) have to be identical. It follows that the collisional rates must satisfy the relation

$$\begin{aligned}
C_{\mathrm{I}}(\alpha JMM', \alpha_\ell J_\ell M_\ell M'_\ell) = &\sum_{NN'N_\ell N'_\ell} \mathcal{D}^J_{NM}(R)^*\ \mathcal{D}^J_{N'M'}(R)\ \mathcal{D}^{J_\ell}_{N_\ell M_\ell}(R)\ \mathcal{D}^{J_\ell}_{N'_\ell M'_\ell}(R)^* \\
&\times C_{\mathrm{I}}(\alpha JNN', \alpha_\ell J_\ell N_\ell N'_\ell) \qquad (7.84)
\end{aligned}$$

whatever the rotation R.

The right-hand side of this equation can be transformed using Eq. (2.77) and the complex conjugate of Eq. (2.75). Writing

$$\mathcal{D}^{J}_{N'M'}(R)\,\mathcal{D}^{J}_{NM}(R)^* = $$
$$= (-1)^{N-M}\sum_K (2K+1)\begin{pmatrix} J & J & K \\ N' & -N & P\end{pmatrix}\begin{pmatrix} J & J & K \\ M' & -M & Q\end{pmatrix}\mathcal{D}^{K}_{PQ}(R)^*\,,$$

$$\mathcal{D}^{J_\ell}_{N_\ell M_\ell}(R)\,\mathcal{D}^{J_\ell}_{N'_\ell M'_\ell}(R)^* = $$
$$= (-1)^{N'_\ell - M'_\ell}\sum_{K'} (2K'+1)\begin{pmatrix} J_\ell & J_\ell & K' \\ N_\ell & -N'_\ell & P'\end{pmatrix}\begin{pmatrix} J_\ell & J_\ell & K' \\ M_\ell & -M'_\ell & Q'\end{pmatrix}\mathcal{D}^{K'}_{P'Q'}(R)^*\,,$$

$$\mathcal{D}^{K}_{PQ}(R)^*\,\mathcal{D}^{K'}_{P'Q'}(R)^* = $$
$$= \sum_{K''} (2K''+1)\begin{pmatrix} K & K' & K'' \\ P & P' & P''\end{pmatrix}\begin{pmatrix} K & K' & K'' \\ Q & Q' & Q''\end{pmatrix}\mathcal{D}^{K''}_{P''Q''}(R)\,, \tag{7.85}$$

one gets

$$C_{\mathrm{I}}(\alpha JMM', \alpha_\ell J_\ell M_\ell M'_\ell) = \sum_{NN'N_\ell N'_\ell} C_{\mathrm{I}}(\alpha JNN', \alpha_\ell J_\ell N_\ell N'_\ell)$$
$$\times \sum_{KK'K''} (2K+1)(2K'+1)(2K''+1)\ (-1)^{N-M+N'_\ell - M'_\ell}$$
$$\times \begin{pmatrix} J & J & K \\ N' & -N & P\end{pmatrix}\begin{pmatrix} J & J & K \\ M' & -M & Q\end{pmatrix}\begin{pmatrix} J_\ell & J_\ell & K' \\ N_\ell & -N'_\ell & P'\end{pmatrix}$$
$$\times \begin{pmatrix} J_\ell & J_\ell & K' \\ M_\ell & -M'_\ell & Q'\end{pmatrix}\begin{pmatrix} K & K' & K'' \\ P & P' & P''\end{pmatrix}\begin{pmatrix} K & K' & K'' \\ Q & Q' & Q''\end{pmatrix}\mathcal{D}^{K''}_{P''Q''}(R)\,.$$

As the right-hand side must be independent of the rotation R, the index K'' can only take the value $K''=0$. This implies $K=K'$, $P=-P'$, $Q=-Q'$. We thus obtain, with the help of Eq. (2.26a)[1]

$$C_{\mathrm{I}}(\alpha JMM', \alpha_\ell J_\ell M_\ell M'_\ell) = (-1)^{J-M'+J_\ell - M'_\ell}\sqrt{\frac{2J_\ell+1}{2J+1}}$$
$$\times \sum_K (2K+1)\begin{pmatrix} J & J & K \\ M' & -M & Q\end{pmatrix}\begin{pmatrix} J_\ell & J_\ell & K \\ M'_\ell & -M_\ell & Q\end{pmatrix} C^{(K)}_{\mathrm{I}}(\alpha J, \alpha_\ell J_\ell)\,, \tag{7.86}$$

[1] The factor

$$\sqrt{2J_\ell+1}\ \Big/\ \sqrt{2J+1}$$

is introduced in Eq. (7.86) to get simpler relations between these rates and the usual collisional rates connecting atomic populations (see below).

where we have defined the *multipole components of the inelastic collisional rates* by the equation

$$C_{\rm I}^{(K)}(\alpha J,\alpha_\ell J_\ell)=\sqrt{\frac{2J+1}{2J_\ell+1}}$$
$$\times\sum_{NN'N_\ell N'_\ell P}(-1)^{J-N'+J_\ell-N'_\ell}\begin{pmatrix}J&J&K\\N'&-N&P\end{pmatrix}\begin{pmatrix}J_\ell&J_\ell&K\\N'_\ell&-N_\ell&P\end{pmatrix}$$
$$\times C_{\rm I}(\alpha JNN',\alpha_\ell J_\ell N_\ell N'_\ell)\ . \tag{7.87}$$

Equation (7.86) shows that the transfer collisional rates due to inelastic collisions take a quite simple form as a result of the isotropy of the colliding particles.

Some properties of the multipole components $C_{\rm I}^{(K)}(\alpha J,\alpha_\ell J_\ell)$ follow directly from Eq. (7.87). Taking the complex conjugate of Eq. (7.82) we have, with the use of Eq. (3.80)

$$C_{\rm I}(\alpha JMM',\alpha_\ell J_\ell M_\ell M'_\ell)^*=C_{\rm I}(\alpha JM'M,\alpha_\ell J_\ell M'_\ell M_\ell)\ ,$$

so that, recalling the symmetry properties of the 3-j symbols

$$C_{\rm I}^{(K)}(\alpha J,\alpha_\ell J_\ell)^*=C_{\rm I}^{(K)}(\alpha J,\alpha_\ell J_\ell)\ ,$$

which shows the reality of the multipole components. Moreover, setting $K=0$ in Eq. (7.87) we obtain via Eq. (2.26a)

$$C_{\rm I}^{(0)}(\alpha J,\alpha_\ell J_\ell)=\frac{1}{2J_\ell+1}\sum_{NN_\ell}C_{\rm I}(\alpha JNN,\alpha_\ell J_\ell N_\ell N_\ell)\ .$$

The rate $C_{\rm I}(\alpha JNN,\alpha_\ell J_\ell N_\ell N_\ell)$ represents, by definition of transfer rate, the probability that a collisional transition occurs from the level $|\alpha_\ell J_\ell N_\ell\rangle$ to the level $|\alpha JN\rangle$, therefore it is non-negative. It follows that the zero-rank multipole component is also non-negative,

$$C_{\rm I}^{(0)}(\alpha J,\alpha_\ell J_\ell)\geq 0\ .$$

A strictly similar line of reasoning can be followed for the transfer rates due to superelastic collisions. These rates contribute to the time evolution of a particular density-matrix element via the equation (cf. Eq. (7.82))

$$\frac{\rm d}{{\rm d}t}\,\rho_{\alpha J}(M,M')=\sum_{\alpha_u J_u M_u M'_u}C_{\rm S}(\alpha JMM',\alpha_u J_u M_u M'_u)\ \rho_{\alpha_u J_u}(M_u,M'_u)\ , \tag{7.88}$$

and can be written, under the assumption of isotropic collisions, in the form

$$C_{\rm S}(\alpha JMM',\alpha_u J_u M_u M'_u)=(-1)^{J-M'+J_u-M'_u}\sqrt{\frac{2J_u+1}{2J+1}}$$
$$\times\sum_K(2K+1)\begin{pmatrix}J&J&K\\M'&-M&Q\end{pmatrix}\begin{pmatrix}J_u&J_u&K\\M'_u&-M_u&Q\end{pmatrix}C_{\rm S}^{(K)}(\alpha J,\alpha_u J_u)\ ,$$

where

$$C_{\rm S}^{(K)}(\alpha J,\alpha_u J_u)=\sqrt{\frac{2J+1}{2J_u+1}}$$
$$\times\sum_{NN'N_uN_u'P}(-1)^{J-N'+J_u-N_u'}\begin{pmatrix}J & J & K\\ N' & -N & P\end{pmatrix}\begin{pmatrix}J_u & J_u & K\\ N_u' & -N_u & P\end{pmatrix}$$
$$\times C_{\rm S}(\alpha JNN',\alpha_u J_u N_u N_u') \tag{7.89}$$

are the *multipole components of the superelastic collisional rates*. These quantities are real and $C_{\rm S}^{(0)}(\alpha J,\alpha_u J_u)$ is non-negative.

Let's now discuss the relaxation rates due to inelastic and superelastic collisions. In a given reference system, these rates contribute to the time evolution of a particular density-matrix element via an equation of the form

$$\frac{\rm d}{{\rm d}t}\,\rho_{\alpha J}(M,M')=-\sum_{M''}\Big[\,f(\alpha JMM'M'')\;\rho_{\alpha J}(M,M'')$$
$$+\,g(\alpha JMM'M'')\;\rho_{\alpha J}(M'',M')\Big]\,.$$

The conjugation properties of the density-matrix elements (Eq. (3.80)) require that

$$g(\alpha JMM'M'')=f(\alpha JM'MM'')^*\;,$$

thus we can write

$$\frac{\rm d}{{\rm d}t}\,\rho_{\alpha J}(M,M')=-\sum_{M''}\left[\,\frac{1}{2}\,S(\alpha JMM'M'')\;\rho_{\alpha J}(M,M'')\right.$$
$$\left.+\,\frac{1}{2}\,S(\alpha JM'MM'')^*\;\rho_{\alpha J}(M'',M')\right]\,. \tag{7.90}$$

As above, we consider a new reference system obtained from the former by an arbitrary rotation R. In the new system Eq. (7.90) becomes

$$\frac{\rm d}{{\rm d}t}\left[\rho_{\alpha J}(M,M')\right]_{\rm new}=$$
$$=-\sum_{M''M'''}\left\{\frac{1}{2}\sum_{NN'N''}\mathcal{D}^J_{NM}(R)^*\,\mathcal{D}^J_{N'M'}(R)\;S(\alpha JNN'N'')\right.$$
$$\times\,\mathcal{D}^J_{NM'''}(R)\,\mathcal{D}^J_{N''M''}(R)^*\left[\rho_{\alpha J}(M''',M'')\right]_{\rm new}$$
$$+\,\frac{1}{2}\sum_{NN'N''}\mathcal{D}^J_{NM}(R)^*\,\mathcal{D}^J_{N'M'}(R)\;S(\alpha JN'NN'')^*$$
$$\left.\times\,\mathcal{D}^J_{N''M''}(R)\,\mathcal{D}^J_{N'M'''}(R)^*\left[\rho_{\alpha J}(M'',M''')\right]_{\rm new}\right\}. \tag{7.91}$$

Owing to the isotropy of collisions, Eqs. (7.90) and (7.91) must be identical, therefore

$$S(\alpha JMM'M'')\,\delta_{MM'''} =$$
$$= \sum_{NN'N''} \mathcal{D}^J_{NM}(R)^*\,\mathcal{D}^J_{N'M'}(R)\;S(\alpha JNN'N'')\;\mathcal{D}^J_{NM'''}(R)\,\mathcal{D}^J_{N''M''}(R)^* \qquad (7.92)$$

whatever the rotation R. This requires the rate $S(\alpha JNN'N'')$ to be independent of the quantum number N. As a consequence, we can carry out the summation over N via Eqs. (2.72) to get

$$S(\alpha JM'M'') = \sum_{N'N''} S(\alpha JN'N'')\;\mathcal{D}^J_{N'M'}(R)\,\mathcal{D}^J_{N''M''}(R)^*$$

or, using Eq. (2.77)

$$S(\alpha JM'M'') = \sum_{N'N''} S(\alpha JN'N'')\;(-1)^{N''-M''}$$
$$\times \sum_K (2K+1) \begin{pmatrix} J & J & K \\ N' & -N'' & Q \end{pmatrix} \begin{pmatrix} J & J & K \\ M' & -M'' & Q' \end{pmatrix} \mathcal{D}^K_{QQ'}(R)^* \,.$$

Since the right-hand side must be independent of the rotation R, the index K can only take the value $K = 0$. This implies $M' = M''$, $N' = N''$, and using Eq. (2.26a) one gets

$$S(\alpha JM'M'') = \delta_{M'M''}\;\frac{1}{2J+1}\sum_{N'} S(\alpha JN'N') \,.$$

Substitution into Eq. (7.90) gives

$$\frac{\mathrm{d}}{\mathrm{d}t}\,\rho_{\alpha J}(M,M') = -\,S_0(\alpha J)\;\rho_{\alpha J}(M,M') \,,$$

where the relaxation collisional rate

$$S_0(\alpha J) = \frac{1}{2J+1}\,\mathrm{Re}\Big[\sum_M S(\alpha JMM)\Big]$$

is real and independent of the magnetic quantum numbers.

Collecting together transfer and relaxation rates, the statistical equilibrium equations for the density-matrix elements turn out to be

$$\frac{\mathrm{d}}{\mathrm{d}t}\,\rho_{\alpha J}(M,M') = \sum_{\alpha_\ell J_\ell M_\ell M'_\ell} \sum_K (-1)^{J-M'+J_\ell-M'_\ell} \sqrt{\frac{2J_\ell+1}{2J+1}}$$
$$\times (2K+1) \begin{pmatrix} J & J & K \\ M' & -M & Q \end{pmatrix} \begin{pmatrix} J_\ell & J_\ell & K \\ M'_\ell & -M_\ell & Q \end{pmatrix}$$
$$\times C^{(K)}_{\mathrm{I}}(\alpha J, \alpha_\ell J_\ell)\;\rho_{\alpha_\ell J_\ell}(M_\ell, M'_\ell) \;+$$

$$+ \sum_{\alpha_u J_u M_u M'_u} \sum_K (-1)^{J-M'+J_u-M'_u} \sqrt{\frac{2J_u+1}{2J+1}} \times (2K+1) \begin{pmatrix} J & J & K \\ M' & -M & Q \end{pmatrix} \begin{pmatrix} J_u & J_u & K \\ M'_u & -M_u & Q \end{pmatrix} \times C_{\mathrm{S}}^{(K)}(\alpha J, \alpha_u J_u)\ \rho_{\alpha_u J_u}(M_u, M'_u)$$

$$- S_0(\alpha J)\ \rho_{\alpha J}(M, M') \,. \tag{7.93}$$

The conservation of the total number of atoms implies that the quantities $C_{\mathrm{I}}^{(K)}$, $C_{\mathrm{S}}^{(K)}$ and S_0 are not independent. Denoting by $n_{\alpha J}$ the population of the level (αJ), we require that (cf. Eq. (3.89))

$$\frac{\mathrm{d}}{\mathrm{d}t} \sum_{\alpha J}\ n_{\alpha J} = \sum_{\alpha J} \frac{\mathrm{d}}{\mathrm{d}t} \Big[\sum_M\ \rho_{\alpha J}(M, M) \Big] = 0 \,. \tag{7.94}$$

Using Eq. (7.93) and the relation (see Eqs. (2.23a) and (2.26a))

$$\sum_M (-1)^{J-M} \begin{pmatrix} J & J & K \\ M & -M & Q \end{pmatrix} =$$

$$= \sqrt{2J+1}\ \sum_M \begin{pmatrix} J & J & K \\ M & -M & Q \end{pmatrix} \begin{pmatrix} J & J & 0 \\ M & -M & 0 \end{pmatrix} = \sqrt{2J+1}\ \ \delta_{K0}\, \delta_{Q0} \,, \tag{7.95}$$

we obtain

$$\frac{\mathrm{d}}{\mathrm{d}t}\, n_{\alpha J} = \sum_{\alpha_\ell J_\ell} C_{\mathrm{I}}^{(0)}(\alpha J, \alpha_\ell J_\ell)\ n_{\alpha_\ell J_\ell} + \sum_{\alpha_u J_u} C_{\mathrm{S}}^{(0)}(\alpha J, \alpha_u J_u)\ n_{\alpha_u J_u} - S_0(\alpha J)\ n_{\alpha J} \,, \tag{7.96}$$

thus the condition (7.94) becomes

$$\sum_{\alpha J} \sum_{\alpha_\ell J_\ell < \alpha J} C_{\mathrm{I}}^{(0)}(\alpha J, \alpha_\ell J_\ell)\ n_{\alpha_\ell J_\ell} + \sum_{\alpha J} \sum_{\alpha_u J_u > \alpha J} C_{\mathrm{S}}^{(0)}(\alpha J, \alpha_u J_u)\ n_{\alpha_u J_u} =$$

$$= \sum_{\alpha J} S_0(\alpha J)\ n_{\alpha J} \,.$$

In the first term we replace (αJ) by $(\alpha_u J_u)$ and $(\alpha_\ell J_\ell)$ by (αJ), and in the second term we replace (αJ) by $(\alpha_\ell J_\ell)$ and $(\alpha_u J_u)$ by (αJ). This yields

$$S_0(\alpha J) = \sum_{\alpha_u J_u} C_{\mathrm{I}}^{(0)}(\alpha_u J_u, \alpha J) + \sum_{\alpha_\ell J_\ell} C_{\mathrm{S}}^{(0)}(\alpha_\ell J_\ell, \alpha J) \,, \tag{7.97}$$

which is the above mentioned relation between $C_{\rm I}^{(0)}$, $C_{\rm S}^{(0)}$ and S_0.

Substitution of Eq. (7.97) into Eq. (7.96) gives

$$\frac{\mathrm{d}}{\mathrm{d}t}\, n_{\alpha J} = \sum_{\alpha_\ell J_\ell} C_{\rm I}^{(0)}(\alpha J, \alpha_\ell J_\ell)\; n_{\alpha_\ell J_\ell} + \sum_{\alpha_u J_u} C_{\rm S}^{(0)}(\alpha J, \alpha_u J_u)\; n_{\alpha_u J_u} - \left[\sum_{\alpha_u J_u} C_{\rm I}^{(0)}(\alpha_u J_u, \alpha J) + \sum_{\alpha_\ell J_\ell} C_{\rm S}^{(0)}(\alpha_\ell J_\ell, \alpha J) \right] n_{\alpha J} \; .$$

This equation can be compared with the standard statistical equilibrium equation that is found in many classical textbooks, like for instance in Mihalas (1978). One finds an exact correspondence between the two formulations, which allows a direct comparison of the different rates. In the notation used by Mihalas, $\mathcal{C}_{\ell u}$ denotes the inelastic collisional rate for the transition from the lower level ℓ to the upper level u, while $\mathcal{C}_{u\ell}$ denotes the superelastic collisional rate for the transition from the level u to the level ℓ. The relation with our quantities is the following

$$\mathcal{C}_{\ell u} = C_{\rm I}^{(0)}(\alpha_u J_u, \alpha_\ell J_\ell) \; , \qquad \mathcal{C}_{u\ell} = C_{\rm S}^{(0)}(\alpha_\ell J_\ell, \alpha_u J_u) \; .$$

Because of this simple relation, we can directly apply the results derived in Mihalas (1978) to the zero-rank multipole components of the collisional rates. In particular, if the colliders are electrons with a velocity distribution $f(v)$, such that

$$\int_0^\infty f(v)\; \mathrm{d}v = 1 \; ,$$

we have

$$C_{\rm I}^{(0)}(\alpha_u J_u, \alpha_\ell J_\ell) = N_{\rm e} \int_{v_0}^\infty \sigma_{\alpha_\ell J_\ell,\, \alpha_u J_u}(v)\; f(v)\; v\, \mathrm{d}v \; ,$$

where $N_{\rm e}$ is the electron density, $\sigma_{\alpha_\ell J_\ell,\, \alpha_u J_u}(v)$ is the cross-section for electron excitation from the level $(\alpha_\ell J_\ell)$ to the level $(\alpha_u J_u)$, and v_0 is the threshold velocity defined, for non-relativistic electrons, by the equation

$$\frac{1}{2}\, m\, v_0^2 = E_{\alpha_u J_u} - E_{\alpha_\ell J_\ell} \; ,$$

with m the electron mass and $E_{\alpha_\ell J_\ell}$, $E_{\alpha_u J_u}$ the energies of the two levels.

If the colliding particles have a Maxwellian distribution of velocities, a simple relation can be established between the zero-rank multipole components $C_{\rm I}^{(0)}$ and $C_{\rm S}^{(0)}$. From detailed-balance arguments one gets the following *Einstein-Milne relation*

$$C_{\rm S}^{(0)}(\alpha_\ell J_\ell, \alpha_u J_u) = \frac{2J_\ell + 1}{2J_u + 1}\; \mathrm{e}^{\frac{E_{\alpha_u J_u} - E_{\alpha_\ell J_\ell}}{k_{\rm B}\, T_{\rm c}}}\; C_{\rm I}^{(0)}(\alpha_u J_u, \alpha_\ell J_\ell) \; , \tag{7.98}$$

where k_B is the Boltzmann constant and T_c is the absolute temperature characterizing the Maxwellian distribution of the colliders.

Collisional rates for atom-electron interactions have been (and still are) widely investigated both from the theoretical and from the experimental point of view, and an extended collection of results is now available. These results can be directly applied to the study of polarization phenomena but, in general, they provide only the $K = 0$ multipole component of the collisional rates. To find the other components one must go back to a detailed study of the atom-collider interaction. In App. 4 we show how it is possible to relate, in some particular cases, the components $C_I^{(K)}$ and $C_S^{(K)}$ with the corresponding components $C_I^{(0)}$ and $C_S^{(0)}$.

7.13.b Collisional Rates due to Elastic Collisions

Elastic collisions induce transitions between degenerate energy sublevels of the form $|\alpha JM\rangle$, $|\alpha JM'\rangle$. The contribution of these collisions to the time evolution of the density-matrix element $\rho_{\alpha J}(M, M')$ can be written, by analogy with Eqs. (7.82), (7.88) and (7.90), as

$$\frac{\mathrm{d}}{\mathrm{d}t}\,\rho_{\alpha J}(M,M') = \sum_{M''M'''} C_E(\alpha JMM', \alpha JM''M''')\;\rho_{\alpha J}(M'',M''') - \sum_{M''}\left[\frac{1}{2}\,\mathcal{S}(\alpha JMM'M'')\;\rho_{\alpha J}(M,M'') + \frac{1}{2}\,\mathcal{S}(\alpha JM'MM'')^*\;\rho_{\alpha J}(M'',M')\right].$$

If collisions are isotropic one finds, similarly to the preceding subsection, that this equation can be cast into the form

$$\frac{\mathrm{d}}{\mathrm{d}t}\,\rho_{\alpha J}(M,M') = \sum_{M''M'''}\sum_{K}(-1)^{M'''-M'}\,(2K+1)\begin{pmatrix} J & J & K \\ M' & -M & Q\end{pmatrix} \times \begin{pmatrix} J & J & K \\ M''' & -M'' & Q\end{pmatrix} C_E^{(K)}(\alpha J)\;\rho_{\alpha J}(M'',M''') - C_E^{(0)}(\alpha J)\;\rho_{\alpha J}(M,M')\,, \tag{7.99}$$

where

$$C_E^{(K)}(\alpha J) = \sum_{NN'N''N'''P}(-1)^{N'''-N'}\begin{pmatrix} J & J & K \\ N' & -N & P\end{pmatrix}\begin{pmatrix} J & J & K \\ N''' & -N'' & P\end{pmatrix} \times C_E(\alpha JNN', \alpha JN''N''') \tag{7.100}$$

are the *multipole components of the elastic collisional rates*, which satisfy the properties

$$C_E^{(K)}(\alpha J)^* = C_E^{(K)}(\alpha J)\,, \qquad C_E^{(0)}(\alpha J) \geq 0\,.$$

From Eq. (7.99) one can prove, using Eq. (7.95), that

$$\frac{\mathrm{d}}{\mathrm{d}t}\, n_{\alpha J} \,=\, \frac{\mathrm{d}}{\mathrm{d}t}\left[\sum_{M} \rho_{\alpha J}(M,M)\right] = 0\ ,$$

as expected because the overall population of the (αJ)-level is not affected by elastic collisions.

The collisional rates due to elastic collisions are discussed in greater detail in the following subsection.

7.13.c Collisional Rates in the Spherical Statistical Tensor Representation

Adding together the contributions of inelastic, superelastic, and elastic collisions, we can write the statistical equilibrium equations in the form (see Eqs. (7.93), (7.97), and (7.99))

$$\begin{aligned}
\frac{\mathrm{d}}{\mathrm{d}t}\,\rho_{\alpha J}(M,M') = {} & \sum_{\alpha_\ell J_\ell M_\ell M'_\ell} \sum_{K} (-1)^{J-M'+J_\ell-M'_\ell} \sqrt{\frac{2J_\ell+1}{2J+1}} \\
& \times (2K+1) \begin{pmatrix} J & J & K \\ M' & -M & Q \end{pmatrix} \begin{pmatrix} J_\ell & J_\ell & K \\ M'_\ell & -M_\ell & Q \end{pmatrix} \\
& \times C_{\mathrm{I}}^{(K)}(\alpha J, \alpha_\ell J_\ell)\ \rho_{\alpha_\ell J_\ell}(M_\ell, M'_\ell) \\
& + \sum_{\alpha_u J_u M_u M'_u} \sum_{K} (-1)^{J-M'+J_u-M'_u} \sqrt{\frac{2J_u+1}{2J+1}} \\
& \times (2K+1) \begin{pmatrix} J & J & K \\ M' & -M & Q \end{pmatrix} \begin{pmatrix} J_u & J_u & K \\ M'_u & -M_u & Q \end{pmatrix} \\
& \times C_{\mathrm{S}}^{(K)}(\alpha J, \alpha_u J_u)\ \rho_{\alpha_u J_u}(M_u, M'_u) \\
& + \sum_{M'' M'''} \sum_{K} (-1)^{M'''-M'} \\
& \times (2K+1) \begin{pmatrix} J & J & K \\ M' & -M & Q \end{pmatrix} \begin{pmatrix} J & J & K \\ M''' & -M'' & Q \end{pmatrix} \\
& \times C_{\mathrm{E}}^{(K)}(\alpha J)\ \rho_{\alpha J}(M'', M''') \\
& - \left[\sum_{\alpha_u J_u} C_{\mathrm{I}}^{(0)}(\alpha_u J_u, \alpha J) + \sum_{\alpha_\ell J_\ell} C_{\mathrm{S}}^{(0)}(\alpha_\ell J_\ell, \alpha J) \,+\, C_{\mathrm{E}}^{(0)}(\alpha J)\right] \\
& \times\ \rho_{\alpha J}(M, M')\ .
\end{aligned}$$

The conversion to the spherical statistical tensor representation is easily performed. Use of Eqs. (3.101) and (2.23a) gives

$$\frac{\mathrm{d}}{\mathrm{d}t}\,\rho^K_Q(\alpha J) = \sum_{\alpha_\ell J_\ell} \sqrt{\frac{2J_\ell+1}{2J+1}}\, C^{(K)}_{\mathrm{I}}(\alpha J, \alpha_\ell J_\ell)\ \rho^K_Q(\alpha_\ell J_\ell) + \sum_{\alpha_u J_u} \sqrt{\frac{2J_u+1}{2J+1}}\, C^{(K)}_{\mathrm{S}}(\alpha J, \alpha_u J_u)\ \rho^K_Q(\alpha_u J_u) - \Bigg[\sum_{\alpha_u J_u} C^{(0)}_{\mathrm{I}}(\alpha_u J_u, \alpha J) + \sum_{\alpha_\ell J_\ell} C^{(0)}_{\mathrm{S}}(\alpha_\ell J_\ell, \alpha J) + D^{(K)}(\alpha J)\Bigg]\, \rho^K_Q(\alpha J)\ , \tag{7.101}$$

where we have introduced the *depolarizing rates* due to elastic collisions defined by[1]

$$D^{(K)}(\alpha J) = C^{(0)}_{\mathrm{E}}(\alpha J) - C^{(K)}_{\mathrm{E}}(\alpha J)\ . \tag{7.102}$$

Equation (7.101) shows that, under the assumption of isotropic collisions, only spherical statistical tensors with the same K and Q value are coupled by collisional transitions.

Depolarizing rates have received little attention both from the experimental and from the theoretical point of view.[2] This is obviously due to the fact that the actual values of depolarizing rates are needed only for the interpretation of polarization phenomena. A detailed discussion of depolarizing rates can be found in Lamb and ter Haar (1971). According to these authors, the main contribution to depolarizing rates in astrophysical plasmas arises from long-range collisions with neutral perturbers (generally hydrogen atoms). In such collisions, the interaction between atom and perturber is described by a Van der Waals potential, which depends on the atom-perturber distance R as

$$V_{\mathrm{VdW}} = h\, C_6(\alpha J)\ R^{-6}\ ,$$

where h is the Planck constant and $C_6(\alpha J)$ is the Van der Waals constant for the level in question.

Let us consider a particular collision having impact parameter b. If $\bar{v}_{\mathrm{r}}$ is the average relative velocity between atom and collider, the interaction energy varies with time according to

$$V_{\mathrm{VdW}}(t) = h\, C_6(\alpha J)\ \frac{1}{(b^2 + \bar{v}_{\mathrm{r}}^2\ t^2\ )^3}\ ,$$

[1] It follows that $D^{(0)}(\alpha J) = 0$, which shows at once that the population of the (αJ)-level is unaffected by elastic collisions (see Eq. (3.107)).

[2] Some theoretical results on depolarizing rates by isotropic collisions with hydrogen atoms have recently appeared in the literature. Applications to NaI and other atoms of the same isoelectronic sequence can be found in Kerkeni (2002) and Kerkeni et al. (2003). Applications to p states of neutral atoms have been presented by Derouich et al. (2003).

where $t = 0$ is the time of closest approach.

The typical collision time t_c is of order $b/\bar{v}_r$, and for astrophysical plasmas it is much shorter than the other typical times characterizing the evolution of the atomic system. This means that the collisional interaction produces a phase shift ϕ in the eigenfunction of the atomic system whose order of magnitude is given by

$$\phi = \frac{2\pi}{h} \int_{-\infty}^{\infty} V_{\mathrm{VdW}}(t)\, \mathrm{d}t = \frac{3\pi^2}{4}\, \frac{C_6(\alpha J)}{b^5\, \bar{v}_r} \,. \tag{7.103}$$

The cumulative effect of these phase shifts is responsible for the depolarizing rates via a mechanism similar to that illustrated in Sect. 5.14 for classical oscillators.

We can give a rough estimate of the depolarizing rate by writing $D^{(K)}$ in the form

$$D^{(K)} \approx f = \sigma\, \bar{v}_r\, n_H \,,$$

where f is the collision frequency, n_H the number density of hydrogen atoms, and σ – the *depolarizing cross-section* – is given by

$$\sigma = \pi\, b_c^2 \,,$$

b_c being the critical impact parameter which produces a phase shift equal to some large value $\phi_0 \simeq 1$. This approximation is equivalent to assuming that all collisions having $b < b_c$ are totally effective in depolarizing the atom, while the others can be neglected. Taking for ϕ_0 the value 0.61,[1] one gets from Eq. (7.103)

$$b_c = 1.65 \left[\frac{C_6(\alpha J)}{\bar{v}_r}\right]^{0.2} \,, \tag{7.104}$$

whence

$$f = 8.5 \left[C_6(\alpha J)\right]^{0.4}\, \bar{v}_r^{\,0.6}\, n_H \,. \tag{7.105}$$

To get a rough estimate of $C_6(\alpha J)$ we can use the expression given by Aller (1963)

$$C_6(\alpha J) = \frac{e_0^2}{h}\, p\, \left\langle r^2(\alpha J)\right\rangle \,,$$

where e_0 is the electron charge, h the Planck constant, p the polarizability of the hydrogen atom, and $\left\langle r^2(\alpha J)\right\rangle$ the mean square radius of the electronic cloud in the level (αJ). Since $p \simeq 6.7 \times 10^{-25}$ cm^3 (Allen, 1973), one gets, expressing $\left\langle r^2(\alpha J)\right\rangle$ in atomic units

$$C_6(\alpha J) \simeq 6.5 \times 10^{-34} \left\langle r^2(\alpha J)\right\rangle \ \mathrm{cm^6\, s^{-1}} \,. \tag{7.106}$$

[1] This value is discussed in some detail by Aller (1963) in connection with the frequency of collisions responsible for the broadening of spectral lines.

Values for $\langle r^2(\alpha J)\rangle$ can be deduced by means of scaled Fermi-Thomas potentials (see e.g. Warner, 1969); otherwise one can refer to an approximate expression which, for neutral atoms, reduces to (Unsöld, 1955)

$$\langle r^2(\alpha J)\rangle = \frac{5}{2}\left(\frac{13.6}{I - E_{\alpha J}}\right)^2 ,$$

where I is the ionization potential of the atom and $E_{\alpha J}$ is the excitation energy of the (αJ)-level, both expressed in eV.

On the other hand, assuming a Maxwellian distribution of velocities at temperature T, the average relative velocity is

$$\bar{v}_{\rm r} = \sqrt{\frac{8k_{\rm B}T}{\pi\, m_{\rm H}}\left(1 + \frac{1}{\mu}\right)} , \tag{7.107}$$

where $k_{\rm B}$ is the Boltzmann constant, $m_{\rm H}$ is the mass of the hydrogen atom, and μ is the atomic weight of the atom.[1] Substitution of Eqs. (7.106) and (7.107) into Eq. (7.105) gives

$$f \simeq 1.4 \times 10^{-10}\left[\langle r^2(\alpha J)\rangle\right]^{0.4}\left[T\left(1 + \frac{1}{\mu}\right)\right]^{0.3} n_{\rm H} \quad {\rm s}^{-1} , \tag{7.108}$$

where T is in K and $n_{\rm H}$ in cm^{-3}.

Particularly interesting is the ratio $D^{(1)}(\alpha J)/D^{(2)}(\alpha J)$, that is the ratio of depolarizing rates for orientation and alignment (see Sect. 3.7), because it is strongly dependent on the type of interaction between atom and collider. We have shown in App. 4 that – for isotropic collisions – the interaction can be expanded into a series of tensor operators of different rank. Equations (7.102), (A4.3) and (2.36a) give

$$D^{(K)}(\alpha J) = \\ = (2J+1)\sum_{K'=1}^{2J}(-1)^{2J+K'}\left[\begin{Bmatrix} J & J & 0 \\ J & J & K' \end{Bmatrix} - (-1)^K \begin{Bmatrix} J & J & K \\ J & J & K' \end{Bmatrix}\right] I_{\rm E}^{(K')}(\alpha J) ,$$

which shows that depolarizing rates are unaffected by a zero-rank tensor operator. If the interaction is described by a single tensor operator of rank 1 (or by a tensor operator of rank 1 plus a tensor operator of rank 0) we have, using Eq. (2.36d)

$$\frac{D^{(1)}(\alpha J)}{D^{(2)}(\alpha J)} = \frac{1}{3} \qquad \left(J \neq 0,\, \frac{1}{2}\right) ,$$

[1] It is worth noticing that Eqs. (7.104), (7.106) and (7.107) give for the collision time

$$t_{\rm c} = b_{\rm c}\,/\,\bar{v}_{\rm r} \simeq 3.8 \times 10^{-12}\left[\langle r^2(\alpha J)\rangle\right]^{0.2}\left[T\left(1 + \frac{1}{\mu}\right)\right]^{-0.6} \quad {\rm s} ,$$

thus $t_{\rm c} \simeq 10^{-13}$ - 10^{-14} s for a typical stellar atmosphere.

whereas for a single tensor operator of rank 2 (or a tensor operator of rank 2 plus a tensor operator of rank 0) we have, using Eq. (2.36h)

$$\frac{D^{(1)}(\alpha J)}{D^{(2)}(\alpha J)} = \frac{1}{3}\,\frac{4J^2+4J-3}{4J^2+4J-7} \qquad \left(J \neq 0,\, \frac{1}{2}\right) . \tag{7.109}$$

In particular, the Van der Waals interaction depends on the atomic variables through the quadrupolar momentum of the atomic cloud, which is a symmetric Cartesian tensor that can be decomposed into the sum of a spherical tensor of rank 0 plus a spherical tensor of rank 2, so that the ratio $D^{(1)}(\alpha J)/D^{(2)}(\alpha J)$ is given by Eq. (7.109). We can compare this expression with the results obtained in Sect. 5.14, where the atom was schematized as a collection of classical oscillators. The corresponding ratio (δ_1/δ_2) was found to be (see Eq. (5.195))

$$\frac{\delta_1}{\delta_2} = \frac{5}{3} ,$$

which is just the value given by Eq. (7.109) for $J = 1$ (the only quantum-mechanical atomic level for which the classical analogy works).

7.13.d Collisional Rates in the Presence of a Magnetic Field

Collisional rates have been discussed in this section under the assumption that colliders have an isotropic velocity distribution, and that no physical agent able to break the spherical symmetry of the problem is present (otherwise Eqs. (7.84) and (7.92) could not be deduced). In the presence of a magnetic field the latter requirement is not satisfied, and we can wonder whether the previous results are still valid or not.

In typical astrophysical plasmas the inelastic and superelastic collisional rates are due to thermal electrons. Therefore they depend only on the velocity distribution of electrons and on the eigenfunctions of the atomic levels involved in the (collisional) transition. If we restrict attention to the Zeeman effect regime, the eigenfunctions are not altered by the presence of a magnetic field, and the collisional rates remain the same as in the zero-field case provided

$$h\,\nu_{\rm L} \ll k_{\rm B}\,T$$

(with $\nu_{\rm L}$ the Larmor frequency and $k_{\rm B}$ the Boltzmann constant), or, numerically

$$B \ll 1.5 \times 10^4\ T\ , \tag{7.110}$$

where B is in G and T in K. This inequality is well-satisfied both for the sun and for magnetic stars.

As far as depolarizing rates are concerned, the situation is more involved. Besides the condition of Eq. (7.110) (which still must be satisfied), there is the further constraint that the typical collision time $t_{\rm c}$ should be much smaller than the Larmor time $(2\pi\nu_{\rm L})^{-1}$. Thus

$$B \ll 1.1 \times 10^{-7}\ t_{\rm c}^{-1}\ ,$$

where B is in G and t_c in s. This condition is also well-satisfied both for the sun and for magnetic stars (see footnote on p. 345).

7.13.e Concluding Remarks

The treatment of collisional rates presented in this section has been restricted to the multi-level atom, but it could be generalized to the multi-term atom. Considering for instance the inelastic collisional transitions between two terms $(\beta_\ell L_\ell S_\ell)$ and (βLS), one could write an equation of the form

$$\frac{\mathrm{d}}{\mathrm{d}t}\ {}^{\beta LS}\rho(JM, J'M') = \sum_{\beta_\ell L_\ell S_\ell} \sum_{J_\ell M_\ell J'_\ell M'_\ell} C_{\mathrm{I}}(\beta LSJMJ'M', \beta_\ell L_\ell S_\ell J_\ell M_\ell J'_\ell M'_\ell) \times {}^{\beta_\ell L_\ell S_\ell}\rho(J_\ell M_\ell, J'_\ell M'_\ell) \ .$$

Assuming that collisions are isotropic and that no magnetic field is present (or that the magnetic field is sufficiently weak to satisfy the constraints discussed in Sect. 7.13.d), one could derive, along the same lines of the former subsections, the general properties of the rates $C_{\mathrm{I}}(\beta LSJMJ'M', \beta_\ell L_\ell S_\ell J_\ell M_\ell J'_\ell M'_\ell)$. However, this more complicated type of collisional rates will not be studied in this book.

A major point concerning collisional rates is that, under a wide variety of astrophysical and laboratory conditions, they *can be simply added* to the corresponding radiative rates in the statistical equilibrium equations; symbolically

$$\frac{\mathrm{d}}{\mathrm{d}t}\Big[\text{Density-Matrix Element}\Big] = \\ = \sum \Big[\text{Radiative Rates} + \text{Collisional Rates}\Big] \times \Big[\text{Density-Matrix Element}\Big] \ .$$

Although this equation may seem physically evident, it is indeed correct only when the so-called impact approximation is valid (see Lamb and ter Haar, 1971, for a thorough discussion of this subject). The impact approximation – that we have already encountered in Sect. 5.14, see Eq. (5.176) – requires that the collision time is much smaller than the relaxation time due to radiative rates, a condition that is generally well-satisfied both in laboratory plasmas and in stellar atmospheres.

This page intentionally left blank

CHAPTER 8

RADIATIVE TRANSFER FOR POLARIZED RADIATION

In previous sections of this book we have derived the radiative transfer equations for polarized radiation from general principles. In Sect. 5.2 the derivation was based on a classical approach involving the familiar concept of index of refraction, while in Sect. 6.7 it was based on a more powerful quantum-electrodynamical approach. As already remarked, the structure of the resulting equations is obviously the same. In Sect. 5.5 we have indeed outlined how this structure is intimately connected with very general physical principles.

This chapter is devoted to the solution of the radiative transfer equations for polarized radiation in their most general formulation. We will also consider some particular cases where the solution can be expressed in purely analytical form.

Most practical applications of radiative transfer for polarized radiation concern the problem of line formation in a magnetic field, and the consequent analysis of polarimetric observations of solar active regions or of magnetic stars. These special aspects of the general problem of radiative transfer for polarized radiation will be discussed in the following chapters.

8.1. Generalities

The radiative transfer equations for polarized radiation have been derived from the principles of Quantum Electrodynamics in Chap. 6. For a stationary medium (i.e. a medium whose properties do not vary over time) we have from Eq. (6.83)

$$\frac{\mathrm{d}}{\mathrm{d}s}\, S_i(\nu,\vec{\Omega}) = -\sum_{j=0}^{3} K^{\mathrm{A}}_{ij}\, S_j(\nu,\vec{\Omega}) + \sum_{j=0}^{3} K^{\mathrm{S}}_{ij}\, S_j(\nu,\vec{\Omega}) + \varepsilon_i \quad (i=0,1,2,3)\,, \quad (8.1)$$

where s is the coordinate measured along the ray path, $S_i(\nu,\vec{\Omega})$ is the Stokes vector of the radiation of frequency ν propagating along the direction $\vec{\Omega}$, K^{A}_{ij} and K^{S}_{ij} are the propagation matrices due to absorption and stimulated emission, respectively, and ε_i is the emission vector.

For our present purposes it is convenient to cast Eq. (8.1) into matrix form. Introducing the propagation matrix tout court

$$K_{ij} = K^{\mathrm{A}}_{ij} - K^{\mathrm{S}}_{ij}\,,$$

and stressing the explicit dependence of the various quantities on the coordinate s, we have

$$\frac{\mathrm{d}}{\mathrm{d}s}\, \boldsymbol{I}(s) = -\boldsymbol{K}(s)\, \boldsymbol{I}(s) + \boldsymbol{\varepsilon}(s)\,, \quad (8.2)$$

where[1]

$$\boldsymbol{I}(s) = \begin{pmatrix} S_0(s) \\ S_1(s) \\ S_2(s) \\ S_3(s) \end{pmatrix} = \begin{pmatrix} I(s) \\ Q(s) \\ U(s) \\ V(s) \end{pmatrix} .$$

The matrix $\boldsymbol{K}$, as deduced both from classical and from quantum physics, has the form (see Eqs. (5.25) and (6.85))

$$\boldsymbol{K} = \begin{pmatrix} \eta_I & \eta_Q & \eta_U & \eta_V \\ \eta_Q & \eta_I & \rho_V & -\rho_U \\ \eta_U & -\rho_V & \eta_I & \rho_Q \\ \eta_V & \rho_U & -\rho_Q & \eta_I \end{pmatrix} , \tag{8.3}$$

where the seven independent quantities $\eta_I, \eta_Q, \ldots, \rho_V$ are related to the (direction-dependent) properties of the medium by Eqs. (5.26) (for the classical case) or Eqs. (6.86) (for the quantum-mechanical case). The general expression for the emission vector $\boldsymbol{\varepsilon}$, derived from Quantum Mechanics, is given in Eqs. (6.86). Another expression, obtained from classical physics for the special case of an atomic vapor embedded in a magnetic field, is given in Eqs. (5.38).

It is quite interesting to compare Eq. (8.2) with the usual transfer equation for 'unpolarized' radiation (see for instance Mihalas, 1978)

$$\frac{\mathrm{d}}{\mathrm{d}s} I(s) = -k(s)\, I(s) \, + \, \varepsilon(s) \, , \tag{8.4}$$

where I is the intensity of the beam and where k and ε are the absorption and emission coefficients, respectively. It is seen that the two equations have a similar structure, with the obvious difference that the scalar quantities I and ε of Eq. (8.4) are replaced, in the 'polarized' case, by the four-component vectors $\boldsymbol{I}$ and $\boldsymbol{\varepsilon}$, while the scalar absorption coefficient k is replaced by the 4×4 propagation matrix $\boldsymbol{K}$. The peculiarity of the transfer of polarized radiation originates just from the matrix character of Eq. (8.2), which produces a typical effect of *ordering* that will be explained in the following section.

8.2. Formal Solution of the Radiative Transfer Equations: the Evolution Operator

To find a formal solution to Eq. (8.2), we start by considering the homogeneous equation

$$\frac{\mathrm{d}}{\mathrm{d}s} \boldsymbol{I}(s) = -\boldsymbol{K}(s)\, \boldsymbol{I}(s) \, , \tag{8.5}$$

[1] In this chapter we denote the Stokes vector by the symbol $\boldsymbol{I}$ (instead of $\boldsymbol{S}$) to avoid confusion with the source-function vector that will be introduced later.

which describes the transfer of radiation through a purely absorbing medium.

We define the *evolution operator*[1] $\boldsymbol{O}(s, s')$ as the 4×4 real matrix which, when applied to the Stokes vector at point s', yields the Stokes vector at point s (with $s \geq s'$)

$$\boldsymbol{I}(s) = \boldsymbol{O}(s, s')\, \boldsymbol{I}(s') \,. \tag{8.6}$$

Obviously, the evolution operator obeys the condition

$$\boldsymbol{O}(s, s) = \boldsymbol{1} \,, \tag{8.7}$$

$\boldsymbol{1}$ being the 4×4 identity matrix, and the composition law

$$\boldsymbol{O}(s, s'') = \boldsymbol{O}(s, s')\, \boldsymbol{O}(s', s'') \qquad (s \geq s' \geq s'') \,. \tag{8.8}$$

Derivation of Eq. (8.6) with respect to s and use of Eq. (8.5) show that the evolution operator satisfies the differential equation

$$\frac{\mathrm{d}}{\mathrm{d}s}\, \boldsymbol{O}(s, s') = -\boldsymbol{K}(s)\, \boldsymbol{O}(s, s') \,. \tag{8.9}$$

In a similar way we get

$$\frac{\mathrm{d}}{\mathrm{d}s'}\, \boldsymbol{O}(s, s') = \boldsymbol{O}(s, s')\, \boldsymbol{K}(s') \,. \tag{8.10}$$

Equation (8.9) can be formally integrated to give

$$\boldsymbol{O}(s, s') = \boldsymbol{1} - \int_{s'}^{s} \boldsymbol{K}(s_1)\, \boldsymbol{O}(s_1, s')\, \mathrm{d}s_1 \,. \tag{8.11}$$

The operator $\boldsymbol{O}(s_1, s')$ in the right-hand side can in turn be expressed via Eq. (8.11), and iterating the procedure we obtain

$$\boldsymbol{O}(s, s') = \boldsymbol{1} + \sum_{n=1}^{\infty} (-1)^n \int_{s'}^{s} \mathrm{d}s_1 \int_{s'}^{s_1} \mathrm{d}s_2 \cdots \int_{s'}^{s_{n-1}} \mathrm{d}s_n \;\; \boldsymbol{K}(s_1)\, \boldsymbol{K}(s_2) \cdots \boldsymbol{K}(s_n) \,.$$

This equation can be rewritten in the form

$$\boldsymbol{O}(s, s') = \\ = \boldsymbol{1} + \sum_{n=1}^{\infty} \frac{(-1)^n}{n!} \int_{s'}^{s} \mathrm{d}s_1 \int_{s'}^{s} \mathrm{d}s_2 \cdots \int_{s'}^{s} \mathrm{d}s_n \;\; \mathbb{P}\Big\{ \boldsymbol{K}(s_1)\, \boldsymbol{K}(s_2) \cdots \boldsymbol{K}(s_n) \Big\} \,, \tag{8.12}$$

[1] The concept of evolution operator expressed as a 4×4 real matrix was introduced by Landi Degl'Innocenti and Landi Degl'Innocenti (1985). A similar concept in terms of 2×2 complex matrices is due to Van Ballegooijen (1985, 1987) and is developed in Sects. 8.8 and 8.9. The presentation given here follows rather closely the derivation by Landi Degl'Innocenti (1987). It appears that the general concept of evolution operator has been known for a long time in matrix theory (see e.g. Gantmacher, 1966, where it is referred to as *matricant*).

where we have introduced the *Dyson chronological product* of the n matrices $\boldsymbol{K}(s_1)$, $\boldsymbol{K}(s_2)$, ... , $\boldsymbol{K}(s_n)$, defined by

$$\mathbb{P}\Big\{\boldsymbol{K}(s_1)\,\boldsymbol{K}(s_2)\,\cdots\,\boldsymbol{K}(s_n)\Big\} = \boldsymbol{K}(s_i)\,\boldsymbol{K}(s_j)\,\cdots\,\boldsymbol{K}(s_k)\;, \tag{8.13}$$

where $(i, j, \ldots, k)$ is a permutation of the integers $(1, 2, \ldots, n)$ such that

$$s_i \geq s_j \geq \ldots \geq s_k\;.$$

In other words, the chronological product orders the matrices in the bracket in such a way that larger values of the argument s stand to the left of smaller values.

The formal solution of the non-homogeneous transfer equation (Eq. (8.2)) can be easily expressed in terms of the evolution operator $\boldsymbol{O}(s, s')$. Bearing in mind Eqs. (8.7) and (8.9), it is seen that the expression

$$\boldsymbol{I}(s) = \int_{s'}^{s} \boldsymbol{O}(s, s'')\,\boldsymbol{\varepsilon}(s'')\,\mathrm{d}s'' \,+\, \boldsymbol{O}(s, s')\,\boldsymbol{I}(s') \tag{8.14}$$

satisfies Eq. (8.2). The physical interpretation of this equation is straightforward. Let us consider a slab extending between points s' and s along the ray path. The Stokes vector at the exit of the slab, $\boldsymbol{I}(s)$, results from the addition of two terms. The latter is just the Stokes vector entering the slab, $\boldsymbol{I}(s')$, transformed by the evolution operator associated with the whole slab, $\boldsymbol{O}(s, s')$. The former results from the contribution of the emission in each infinitesimal interval of the slab, $\boldsymbol{\varepsilon}(s'')\,\mathrm{d}s''$, transformed by the evolution operator associated with the fraction of the slab crossed by the radiation, $\boldsymbol{O}(s, s'')$.

Equation (8.14) can be directly applied to the case of a slab extending to infinity in one direction (semi-infinite atmosphere). Provided the emission vector does not grow above reasonable limits when $s' \to -\infty$, or, more properly, provided

$$\lim_{s' \to -\infty} \boldsymbol{O}(s, s')\,\boldsymbol{\varepsilon}(s') = 0\;,$$

the formal solution of Eq. (8.2) is simply given by

$$\boldsymbol{I}(s) = \int_{-\infty}^{s} \boldsymbol{O}(s, s')\,\boldsymbol{\varepsilon}(s')\,\mathrm{d}s'\;. \tag{8.15}$$

The operator $\boldsymbol{O}(s, s')$ introduced in this section is nothing but the generalization to the radiative transfer problem for polarized radiation of the usual attenuation operator

$$o(s, s') = \mathrm{e}^{-\int_{s'}^{s} k(s'')\,\mathrm{d}s''} \tag{8.16}$$

that solves the transfer equation for 'unpolarized' radiation (Eq. (8.4)). It can be easily proved that the homogeneous equation

$$\frac{\mathrm{d}}{\mathrm{d}s}\, I(s) = -k(s)\, I(s)$$

has the solution

$$I(s) = o(s, s')\, I(s')\ , \tag{8.17}$$

and that the non-homogeneous equation has the solution

$$I(s) = \int_{s'}^{s} o(s, s'')\, \varepsilon(s'')\, \mathrm{d}s'' + o(s, s')\, I(s')\ . \tag{8.18}$$

Comparison of Eqs. (8.17)-(8.18) with Eqs. (8.6)-(8.14) shows the strict correspondence between the operators $\boldsymbol{O}(s, s')$ and $o(s, s')$. However, Eq. (8.12) – contrary to Eq. (8.16) – contains a chronological product. This peculiarity is intimately connected with the physical fact that two slabs, A and B, acting differently on the polarization properties of a radiation beam, do not 'commute': in other words, the emerging polarization is in general different if slab A is located in front of slab B or vice versa. On the contrary, the ordering of a train of absorbing slabs does not matter for 'unpolarized' radiation.

8.3. Analytical Expressions for the Evolution Operator

Owing to the presence of a chronological product in Eq. (8.12), the expression for the evolution operator $\boldsymbol{O}(s, s')$ cannot be reduced, in general, to simpler forms. An important exception occurs when the propagation matrix $\boldsymbol{K}(s)$ at a particular point s_1 commutes with the same matrix at any other point s_2,

$$\big[\boldsymbol{K}(s_1), \boldsymbol{K}(s_2)\big] = \boldsymbol{K}(s_1)\, \boldsymbol{K}(s_2) - \boldsymbol{K}(s_2)\, \boldsymbol{K}(s_1) = 0. \tag{8.19}$$

In such case the chronological product reduces to an ordinary product, so that Eq. (8.12) becomes

$$\boldsymbol{O}(s, s') = \boldsymbol{1} + \sum_{n=1}^{\infty} \frac{(-1)^n}{n!} \left[\int_{s'}^{s} \boldsymbol{K}(s'')\, \mathrm{d}s'' \right]^n . \tag{8.20}$$

Let's now recall the definition of function of a matrix. If $\boldsymbol{A}$ is a square matrix, and $f(z)$ an arbitrary function of the variable z with Taylor expansion

$$f(z) = \sum_{n=0}^{\infty} \frac{1}{n!} \left(\frac{\mathrm{d}^n f}{\mathrm{d}z^n} \right)_{z=0} z^n \ = \sum_{n=0}^{\infty} f_n\, z^n\ ,$$

the matrix $\boldsymbol{F} = f(\boldsymbol{A})$ is defined to be

$$\boldsymbol{F} = f(\boldsymbol{A}) = \sum_{n=0}^{\infty} f_n \, \boldsymbol{A}^n \ ,$$

with $\boldsymbol{A}^0 \equiv \boldsymbol{1}$. In particular

$$\mathrm{e}^{-\boldsymbol{A}} = \sum_{n=0}^{\infty} \frac{(-1)^n}{n!} \, \boldsymbol{A}^n \ , \tag{8.21}$$

so that Eq. (8.20) can be rewritten in the form

$$\boldsymbol{O}(s, s') = \mathrm{e}^{-\int_{s'}^{s} \boldsymbol{K}(s'') \, \mathrm{d}s''} \ . \tag{8.22}$$

There are three remarkable cases where Eq. (8.19) holds and, therefore, Eq. (8.22) can be applied. These are the following:
a) the matrix $\boldsymbol{K}$ is independent of s;
b) the matrix $\boldsymbol{K}$ can be written in the form

$$\boldsymbol{K}(s) = c_1(s) \, \boldsymbol{1} + c_2(s) \, \boldsymbol{H}$$

with $\boldsymbol{H}$ independent of s;[1]
c) the matrix $\boldsymbol{K}$ has an arbitrary dependence on s but it has a particular structure, with several elements identically zero.

8.3.a Propagation matrix independent of s

The integral appearing in Eq. (8.22) can be immediately performed to give

$$\boldsymbol{O}(s, s') = \mathrm{e}^{-(s-s') \, \boldsymbol{K}} \ .$$

This expression can be transformed, with some algebra, in the linear combination of four matrices, each multiplied by a suitable exponential factor. The relevant calculations are carried out in App. 5 and allow the evolution operator to be written in the form

$$\begin{aligned}
\boldsymbol{O}(s, s') = {} & \mathrm{e}^{-(s-s') \, \eta_I} \\
& \times \left\{ \frac{1}{2} \Big[\cosh\big[(s-s') \, \Lambda_+(\vec{\eta}, \vec{\rho})\big] + \cos\big[(s-s') \, \Lambda_-(\vec{\eta}, \vec{\rho})\big] \Big] \boldsymbol{M}_1(\vec{\eta}, \vec{\rho}) \right. \\
& \quad - \sin\big[(s-s') \, \Lambda_-(\vec{\eta}, \vec{\rho})\big] \, \boldsymbol{M}_2(\vec{\eta}, \vec{\rho}) \\
& \quad - \sinh\big[(s-s') \, \Lambda_+(\vec{\eta}, \vec{\rho})\big] \, \boldsymbol{M}_3(\vec{\eta}, \vec{\rho}) \\
& \quad \left. + \frac{1}{2} \Big[\cosh\big[(s-s') \, \Lambda_+(\vec{\eta}, \vec{\rho})\big] - \cos\big[(s-s') \, \Lambda_-(\vec{\eta}, \vec{\rho})\big] \Big] \boldsymbol{M}_4(\vec{\eta}, \vec{\rho}) \right\}
\end{aligned} \tag{8.23}$$

[1] Obviously a) is a special case of b). The two cases will be however treated separately, as both of them have important applications.

or, alternatively

$$\boldsymbol{O}(s,s') = \mathrm{e}^{-(s-s')\,[\,\eta_I + \Lambda_+(\vec{\eta},\vec{\rho})\,]}\,\boldsymbol{N}_1(\vec{\eta},\vec{\rho}) + \mathrm{e}^{-(s-s')\,[\,\eta_I - \Lambda_+(\vec{\eta},\vec{\rho})\,]}\,\boldsymbol{N}_2(\vec{\eta},\vec{\rho}) + \mathrm{e}^{-(s-s')\,[\,\eta_I + \mathrm{i}\,\Lambda_-(\vec{\eta},\vec{\rho})\,]}\,\boldsymbol{N}_3(\vec{\eta},\vec{\rho}) + \mathrm{e}^{-(s-s')\,[\,\eta_I - \mathrm{i}\,\Lambda_-(\vec{\eta},\vec{\rho})\,]}\,\boldsymbol{N}_4(\vec{\eta},\vec{\rho})\,,$$

where the quantities $\Lambda_\pm(\vec{\eta},\vec{\rho})$ and the matrices $\boldsymbol{M}_i(\vec{\eta},\vec{\rho})$ and $\boldsymbol{N}_i(\vec{\eta},\vec{\rho})$ are given in App. 5. In the special case

$$\Lambda_+(\vec{\eta},\vec{\rho}) = \Lambda_-(\vec{\eta},\vec{\rho}) = 0$$

the expressions above should be replaced by the following

$$\boldsymbol{O}(s,s') = \mathrm{e}^{-(s-s')\,\eta_I}\left[\,\boldsymbol{1} - (s-s')\,\boldsymbol{G}(\vec{\eta},\vec{\rho}) + \frac{1}{2}\,(s-s')^2\,\boldsymbol{G}(\vec{\eta},\vec{\rho})^2\right],$$

with $\boldsymbol{G}$ given by Eq. (A5.25).

8.3.b Propagation matrix of the form $[\,c_1(s)\,\boldsymbol{1} + c_2(s)\,\boldsymbol{H}\,]$*, with* $\boldsymbol{H}$ *independent of* s

Equation (8.22) gives, with the help of Eq. (A5.6)

$$\boldsymbol{O}(s,s') = \mathrm{e}^{-C_1(s,s')\;\boldsymbol{1}}\;\mathrm{e}^{-C_2(s,s')\,\boldsymbol{H}} = \mathrm{e}^{-C_1(s,s')}\;\mathrm{e}^{-C_2(s,s')\,\boldsymbol{H}}\,,$$

where

$$C_1(s,s') = \int_{s'}^{s} c_1(s'')\,\mathrm{d}s''\,, \qquad C_2(s,s') = \int_{s'}^{s} c_2(s'')\,\mathrm{d}s''\,.$$

Obviously the matrix $\boldsymbol{H}$ has the same structure as the matrix $\boldsymbol{K}$. Writing

$$\boldsymbol{H} = \begin{pmatrix} h_I & h_Q & h_U & h_V \\ h_Q & h_I & r_V & -r_U \\ h_U & -r_V & h_I & r_Q \\ h_V & r_U & -r_Q & h_I \end{pmatrix},$$

we obtain from Eq. (A5.20)

$$\begin{aligned}\boldsymbol{O}(s,s') = {} & \mathrm{e}^{-[C_1(s,s') + C_2(s,s')\,h_I]} \\ & \times \left\{ \frac{1}{2}\Big[\cosh\big[C_2(s,s')\;\Lambda_+(\vec{h},\vec{r})\big] + \cos\big[C_2(s,s')\;\Lambda_-(\vec{h},\vec{r})\big]\Big]\boldsymbol{M}_1(\vec{h},\vec{r}) \right. \\ & \quad - \sin\big[C_2(s,s')\;\Lambda_-(\vec{h},\vec{r})\big]\,\boldsymbol{M}_2(\vec{h},\vec{r}) \\ & \quad - \sinh\big[C_2(s,s')\;\Lambda_+(\vec{h},\vec{r})\big]\,\boldsymbol{M}_3(\vec{h},\vec{r}) \\ & \quad \left. + \frac{1}{2}\Big[\cosh\big[C_2(s,s')\;\Lambda_+(\vec{h},\vec{r})\big] - \cos\big[C_2(s,s')\;\Lambda_-(\vec{h},\vec{r})\big]\Big]\boldsymbol{M}_4(\vec{h},\vec{r}) \right\}\end{aligned}$$

or, from Eq. (A5.23)

$$\begin{aligned}\boldsymbol{O}(s,s') = \mathrm{e}^{-C_1(s,s')}\Big\{&\mathrm{e}^{-C_2(s,s')\,[\,h_I+\Lambda_+(\vec{h},\vec{r})\,]}\,\boldsymbol{N}_1(\vec{h},\vec{r})\\ &+\mathrm{e}^{-C_2(s,s')\,[\,h_I-\Lambda_+(\vec{h},\vec{r})\,]}\,\boldsymbol{N}_2(\vec{h},\vec{r})\\ &+\mathrm{e}^{-C_2(s,s')\,[\,h_I+\mathrm{i}\,\Lambda_-(\vec{h},\vec{r})\,]}\,\boldsymbol{N}_3(\vec{h},\vec{r})\\ &+\mathrm{e}^{-C_2(s,s')\,[\,h_I-\mathrm{i}\,\Lambda_-(\vec{h},\vec{r})\,]}\,\boldsymbol{N}_4(\vec{h},\vec{r})\Big\}\,.\end{aligned}$$

If $\Lambda_+(\vec{h},\vec{r}) = \Lambda_-(\vec{h},\vec{r}) = 0$, these expressions must be replaced by

$$\boldsymbol{O}(s,s') = \mathrm{e}^{-[C_1(s,s')+C_2(s,s')\,h_I]}\,\Big[\boldsymbol{1} - C_2(s,s')\,\boldsymbol{G}(\vec{h},\vec{r}) + \frac{1}{2}\,C_2(s,s')^2\,\boldsymbol{G}(\vec{h},\vec{r})^2\Big]\,,$$

with $\boldsymbol{G}$ given by Eq. (A5.25).

8.3.c Propagation matrix with peculiar form

There are some particular cases where the matrix $\boldsymbol{K}(s)$ has only few non-zero elements, so that, even if these elements are arbitrary functions of s, Eq. (8.19) is satisfied. As an example, let us consider the following particular case

$$\boldsymbol{K}(s) = \begin{pmatrix}\eta_I(s) & 0 & 0 & \eta_V(s)\\ 0 & \eta_I(s) & \rho_V(s) & 0\\ 0 & -\rho_V(s) & \eta_I(s) & 0\\ \eta_V(s) & 0 & 0 & \eta_I(s)\end{pmatrix}\,. \tag{8.24}$$

Using the matrices $\boldsymbol{A}_3$ and $\boldsymbol{B}_3$ defined in App. 5 (Eq. (A5.1c)) we can write

$$\boldsymbol{K}(s) = \eta_I(s)\,\boldsymbol{1} + a_3(s)\,\boldsymbol{A}_3 + b_3(s)\,\boldsymbol{B}_3\,, \tag{8.25}$$

where

$$a_3(s) = \frac{1}{2}\Big[\eta_V(s) + \mathrm{i}\,\rho_V(s)\Big]\,, \qquad b_3(s) = a_3(s)^* = \frac{1}{2}\Big[\eta_V(s) - \mathrm{i}\,\rho_V(s)\Big]\,.$$

As the three matrices in the right-hand side of Eq. (8.25) are commuting matrices (see Eq. (A5.3)), the matrix $\boldsymbol{K}(s)$ satisfies Eq. (8.19), thus the evolution operator is given by Eq. (8.22). Using Eq. (A5.6) we get

$$\boldsymbol{O}(s,s') = \mathrm{e}^{-H_I\,\boldsymbol{1}}\;\;\mathrm{e}^{-\frac{1}{2}\,(H_V+\mathrm{i}\,R_V)\,\boldsymbol{A}_3}\;\;\mathrm{e}^{-\frac{1}{2}\,(H_V-\mathrm{i}\,R_V)\,\boldsymbol{B}_3}\,,$$

where

$$H_I = \int_{s'}^{s}\eta_I(s'')\,\mathrm{d}s''\,, \qquad H_V = \int_{s'}^{s}\eta_V(s'')\,\mathrm{d}s''\,, \qquad R_V = \int_{s'}^{s}\rho_V(s'')\,\mathrm{d}s''\,. \tag{8.26}$$

Expanding the exponentials as in App. 5, we obtain after some algebra

$$\boldsymbol{O}(s,s') = \mathrm{e}^{-H_I} \begin{pmatrix} \cosh H_V & 0 & 0 & -\sinh H_V \\ 0 & \cos R_V & -\sin R_V & 0 \\ 0 & \sin R_V & \cos R_V & 0 \\ -\sinh H_V & 0 & 0 & \cosh H_V \end{pmatrix} . \tag{8.27}$$

In a similar way it can be shown that a propagation matrix of the form

$$\boldsymbol{K}(s) = \begin{pmatrix} \eta_I(s) & \eta_Q(s) & 0 & 0 \\ \eta_Q(s) & \eta_I(s) & 0 & 0 \\ 0 & 0 & \eta_I(s) & \rho_Q(s) \\ 0 & 0 & -\rho_Q(s) & \eta_I(s) \end{pmatrix} \tag{8.28}$$

leads to the evolution operator

$$\boldsymbol{O}(s,s') = \mathrm{e}^{-H_I} \begin{pmatrix} \cosh H_Q & -\sinh H_Q & 0 & 0 \\ -\sinh H_Q & \cosh H_Q & 0 & 0 \\ 0 & 0 & \cos R_Q & -\sin R_Q \\ 0 & 0 & \sin R_Q & \cos R_Q \end{pmatrix} ,$$

with H_I given by Eq. (8.26) and

$$H_Q = \int_{s'}^{s} \eta_Q(s'')\, \mathrm{d}s'' , \qquad R_Q = \int_{s'}^{s} \rho_Q(s'')\, \mathrm{d}s'' .$$

Finally, if

$$\boldsymbol{K}(s) = \begin{pmatrix} \eta_I(s) & 0 & \eta_U(s) & 0 \\ 0 & \eta_I(s) & 0 & -\rho_U(s) \\ \eta_U(s) & 0 & \eta_I(s) & 0 \\ 0 & \rho_U(s) & 0 & \eta_I(s) \end{pmatrix} \tag{8.29}$$

one gets

$$\boldsymbol{O}(s,s') = \mathrm{e}^{-H_I} \begin{pmatrix} \cosh H_U & 0 & -\sinh H_U & 0 \\ 0 & \cos R_U & 0 & \sin R_U \\ -\sinh H_U & 0 & \cosh H_U & 0 \\ 0 & -\sin R_U & 0 & \cos R_U \end{pmatrix} ,$$

where

$$H_U = \int_{s'}^{s} \eta_U(s'')\, \mathrm{d}s'' , \qquad R_U = \int_{s'}^{s} \rho_U(s'')\, \mathrm{d}s'' .$$

8.4. Solution of the Radiative Transfer Equations by Diagonalization

A different way to find a formal solution to the radiative transfer equations is provided by the diagonalization method. This method was first introduced by Kjeldseth-Moe (1968) for the case of a simplified propagation matrix ($\rho_Q = \rho_U = \rho_V = 0$) and was later generalized by Katz (1971) and Šidlichovsky (1976).

Let us consider the eigenvalue equation for the propagation matrix $\boldsymbol{K}$ at point s,

$$\boldsymbol{K}\,\boldsymbol{u}^{(i)} = \lambda_i\,\boldsymbol{u}^{(i)} \qquad (i = 1, 2, 3, 4)\,.$$

The eigenvalues λ_i are obtained by solution of the equation

$$\det\,(\boldsymbol{K} - \lambda\,\boldsymbol{1}) = 0. \tag{8.30}$$

Introducing the formal vectors

$$\vec{\eta} = (\eta_Q, \eta_U, \eta_V)\,, \qquad \vec{\rho} = (\rho_Q, \rho_U, \rho_V)\,, \tag{8.31}$$

Eq. (8.30) leads to the fourth-degree algebraic equation in λ

$$(\eta_I - \lambda)^4 - (\eta^2 - \rho^2)\,(\eta_I - \lambda)^2 - (\vec{\eta}\cdot\vec{\rho})^2 = 0\,, \tag{8.32}$$

whose solution is

$$\begin{aligned}
\lambda_1 &= \eta_I + \Lambda_+(\vec{\eta},\vec{\rho}) \\
\lambda_2 &= \eta_I - \Lambda_+(\vec{\eta},\vec{\rho}) \\
\lambda_3 &= \eta_I + \mathrm{i}\,\Lambda_-(\vec{\eta},\vec{\rho}) \\
\lambda_4 &= \eta_I - \mathrm{i}\,\Lambda_-(\vec{\eta},\vec{\rho})\,,
\end{aligned} \tag{8.33}$$

where $\Lambda_+(\vec{\eta},\vec{\rho})$ and $\Lambda_-(\vec{\eta},\vec{\rho})$ are the quantities – which now acquire a more precise significance – defined in Eqs. (A5.18).

If both $\Lambda_+(\vec{\eta},\vec{\rho})$ and $\Lambda_-(\vec{\eta},\vec{\rho})$ are non-zero (so that the four eigenvalues λ_i are distinct), we can consider the matrix $\boldsymbol{X}$ such that

$$\boldsymbol{X}^{-1}\,\boldsymbol{K}\,\boldsymbol{X} = \boldsymbol{K}'\,, \tag{8.34}$$

where $\boldsymbol{K}'$ is the diagonal matrix[1]

$$K'_{ij} = \lambda_i\,\delta_{ij}\,.$$

[1] If $\Lambda_+(\vec{\eta},\vec{\rho}) = 0$ and/or $\Lambda_-(\vec{\eta},\vec{\rho}) = 0$, the matrix $\boldsymbol{K}$ cannot be reduced, in general, to diagonal form. In such cases the method described in this section cannot be applied. A similar method, based on a different reduction for $\boldsymbol{K}$, could indeed be employed (see e.g. Heading, 1958, p.63), but it will not be considered here. Note that the case $\rho_Q = \rho_U = \rho_V = 0$, which implies $\Lambda_-(\vec{\eta},\vec{\rho}) = 0$, is a special one: $\boldsymbol{K}$ becomes a symmetric matrix and can be diagonalized.

Multiplying Eq. (8.2) by $\boldsymbol{X}^{-1}$ from the left, and introducing the identity $\boldsymbol{X}\boldsymbol{X}^{-1} = \boldsymbol{1}$ between $\boldsymbol{K}(s)$ and $\boldsymbol{I}(s)$, we get

$$\boldsymbol{X}^{-1} \frac{\mathrm{d}}{\mathrm{d}s} \boldsymbol{I}(s) = -\boldsymbol{K}'(s)\, \boldsymbol{X}^{-1}\, \boldsymbol{I}(s) + \boldsymbol{X}^{-1}\, \boldsymbol{\varepsilon}(s) \,. \tag{8.35}$$

Since $\boldsymbol{K}$ depends in general on s, the matrix $\boldsymbol{X}$ depends also on s, thus it does not commute with the operator $\mathrm{d}/\mathrm{d}s$. In the special case where $\boldsymbol{X}$ is independent of s, Eq. (8.35) becomes

$$\frac{\mathrm{d}}{\mathrm{d}s} \boldsymbol{I}'(s) = -\boldsymbol{K}'(s)\, \boldsymbol{I}'(s) + \boldsymbol{\varepsilon}'(s) \,, \tag{8.36}$$

where

$$\boldsymbol{I}'(s) = \boldsymbol{X}^{-1}\, \boldsymbol{I}(s) \tag{8.37a}$$

$$\boldsymbol{\varepsilon}'(s) = \boldsymbol{X}^{-1}\, \boldsymbol{\varepsilon}(s) \,. \tag{8.37b}$$

As the matrix $\boldsymbol{K}'(s)$ is diagonal, Eq. (8.36) represents a set of four *decoupled* differential equations (in other words, the linear combinations of Stokes parameters given in Eq. (8.37a) are the *eigenvectors of the radiative transfer equations*). Thus they have the solution (cf. Eqs. (8.4), (8.18) and (8.16))

$$\boldsymbol{I}'(s) = \int_{s'}^{s} \boldsymbol{O}'(s, s'')\, \boldsymbol{\varepsilon}'(s'')\, \mathrm{d}s'' + \boldsymbol{O}'(s, s')\, \boldsymbol{I}'(s') \,,$$

where $\boldsymbol{O}'(s, s')$ is the diagonal matrix

$$\boldsymbol{O}'(s, s') = \begin{pmatrix} e_1(s, s') & 0 & 0 & 0 \\ 0 & e_2(s, s') & 0 & 0 \\ 0 & 0 & e_3(s, s') & 0 \\ 0 & 0 & 0 & e_4(s, s') \end{pmatrix} \tag{8.38}$$

with

$$e_i(s, s') = \mathrm{e}^{-\int_{s'}^{s} \lambda_i(s'')\, \mathrm{d}s''} \qquad (i = 1, 2, 3, 4) \,.$$

Inversion of Eq. (8.37a) yields the solution of the radiative transfer equations in the form

$$\boldsymbol{I}(s) = \boldsymbol{X}\, \boldsymbol{I}'(s) = \int_{s'}^{s} \boldsymbol{X}\, \boldsymbol{O}'(s, s'')\, \boldsymbol{\varepsilon}'(s'')\, \mathrm{d}s'' + \boldsymbol{X}\, \boldsymbol{O}'(s, s')\, \boldsymbol{I}'(s') \,. \tag{8.39}$$

It is easily seen that this expression, although different from the solution based on the evolution operator (Eq. (8.14)), is however strictly connected with it. Comparison of Eqs. (8.39) and (8.14) shows, with the help of Eqs. (8.37), that the evolution

operator $\boldsymbol{O}(s,s')$ and the matrix $\boldsymbol{O}'(s,s')$ defined in Eq. (8.38) are connected by the relation

$$\boldsymbol{O}(s,s') = \boldsymbol{X}\,\boldsymbol{O}'(s,s')\,\boldsymbol{X}^{-1}\,. \tag{8.40}$$

It should be emphasized that the assumption $\boldsymbol{X}$ independent of s, which is at the basis of the diagonalization method, implies that condition (8.19) is satisfied. This is easily seen by inversion of Eq. (8.34), which gives

$$\begin{aligned}\big[\boldsymbol{K}(s_1),\boldsymbol{K}(s_2)\big] &= \boldsymbol{X}\,\boldsymbol{K}'(s_1)\,\boldsymbol{X}^{-1}\,\boldsymbol{X}\,\boldsymbol{K}'(s_2)\,\boldsymbol{X}^{-1} - \boldsymbol{X}\,\boldsymbol{K}'(s_2)\,\boldsymbol{X}^{-1}\,\boldsymbol{X}\,\boldsymbol{K}'(s_1)\,\boldsymbol{X}^{-1}\\ &= \boldsymbol{X}\,\big[\boldsymbol{K}'(s_1),\boldsymbol{K}'(s_2)\big]\,\boldsymbol{X}^{-1} = 0\,,\end{aligned}$$

because the matrix $\boldsymbol{K}'$ is diagonal. It follows that the solution of the radiative transfer equations based on the diagonalization of the propagation matrix is equivalent to the solution based on the evolution operator *with the evolution operator given by Eq. (8.22).*

The actual calculation of the matrices $\boldsymbol{X}$ and $\boldsymbol{X}^{-1}$ can be performed by a standard method that is presented in App. 6. We give here the final results.

Defining the formal vectors

$$\vec{\zeta} = \vec{\eta}\times\vec{\rho} \equiv (\eta_U\rho_V - \eta_V\rho_U\,,\eta_V\rho_Q - \eta_Q\rho_V\,,\eta_Q\rho_U - \eta_U\rho_Q) \tag{8.41}$$

$$\begin{aligned}\vec{f}^{\,(1)} &= \Lambda_+^2\,\vec{\eta} - \Lambda_+\,\vec{\zeta} + (\vec{\eta}\cdot\vec{\rho})\,\vec{\rho}\\ \vec{f}^{\,(2)} &= \Lambda_+^2\,\vec{\eta} + \Lambda_+\,\vec{\zeta} + (\vec{\eta}\cdot\vec{\rho})\,\vec{\rho}\\ \vec{f}^{\,(3)} &= -\Lambda_-^2\,\vec{\eta} - \mathrm{i}\,\Lambda_-\,\vec{\zeta} + (\vec{\eta}\cdot\vec{\rho})\,\vec{\rho}\\ \vec{f}^{\,(4)} &= -\Lambda_-^2\,\vec{\eta} + \mathrm{i}\,\Lambda_-\,\vec{\zeta} + (\vec{\eta}\cdot\vec{\rho})\,\vec{\rho}\end{aligned}$$

and the scalar quantities

$$\begin{aligned}g_+ &= \frac{1}{2}\,\frac{1}{\Lambda_+^4\,\eta^2 + 2\,\Lambda_+^2\,(\vec{\eta}\cdot\vec{\rho})^2 + \rho^2\,(\vec{\eta}\cdot\vec{\rho})^2}\\ g_- &= \frac{1}{2}\,\frac{1}{\Lambda_-^4\,\eta^2 - 2\,\Lambda_-^2\,(\vec{\eta}\cdot\vec{\rho})^2 + \rho^2\,(\vec{\eta}\cdot\vec{\rho})^2}\\ l_+ &= \Lambda_+\big(\rho^2 + \Lambda_+^2\big)\\ l_- &= \Lambda_-\big(\rho^2 - \Lambda_-^2\big)\,,\end{aligned}$$

one has (under the restrictions specified at the end of App. 6)

$$\boldsymbol{X}^{-1} = \begin{pmatrix} l_+ & f_1^{(1)} & f_2^{(1)} & f_3^{(1)}\\ -l_+ & f_1^{(2)} & f_2^{(2)} & f_3^{(2)}\\ \mathrm{i}\,l_- & f_1^{(3)} & f_2^{(3)} & f_3^{(3)}\\ -\mathrm{i}\,l_- & f_1^{(4)} & f_2^{(4)} & f_3^{(4)}\end{pmatrix} \tag{8.42a}$$

$$\boldsymbol{X} = \begin{pmatrix} g_+ l_+ & -g_+ l_+ & \mathrm{i}\, g_- l_- & -\mathrm{i}\, g_- l_- \\ g_+ f_1^{(2)} & g_+ f_1^{(1)} & g_- f_1^{(4)} & g_- f_1^{(3)} \\ g_+ f_2^{(2)} & g_+ f_2^{(1)} & g_- f_2^{(4)} & g_- f_2^{(3)} \\ g_+ f_3^{(2)} & g_+ f_3^{(1)} & g_- f_3^{(4)} & g_- f_3^{(3)} \end{pmatrix} . \tag{8.42b}$$

Substitution of Eqs. (8.42) into Eq. (8.37a) yields explicit expressions for the eigenvectors of the radiative transfer equations. These are the linear combinations (two real and two complex)

$$\begin{aligned} I'_1 &= l_+ I + f_1^{(1)} Q + f_2^{(1)} U + f_3^{(1)} V \qquad \text{with eigenvalue} \quad \left(\eta_I + \Lambda_+\right) \\ I'_2 &= -l_+ I + f_1^{(2)} Q + f_2^{(2)} U + f_3^{(2)} V \qquad \text{with eigenvalue} \quad \left(\eta_I - \Lambda_+\right) \\ I'_3 &= \mathrm{i}\, l_- I + f_1^{(3)} Q + f_2^{(3)} U + f_3^{(3)} V \qquad \text{with eigenvalue} \quad \left(\eta_I + \mathrm{i}\,\Lambda_-\right) \\ I'_4 &= -\mathrm{i}\, l_- I + f_1^{(4)} Q + f_2^{(4)} U + f_3^{(4)} V \qquad \text{with eigenvalue} \quad \left(\eta_I - \mathrm{i}\,\Lambda_-\right) . \end{aligned}$$

If the propagation matrix is constant, so that the elements of the matrix $\boldsymbol{O'}(s, s')$ defined in Eq. (8.38) reduce to

$$e_i(s, s') = \mathrm{e}^{-(s-s')\,\lambda_i}$$

(with λ_i independent of s), the expression for the evolution operator obtained by substitution of Eqs. (8.42) into Eq. (8.40) must coincide with Eq. (8.23). The formal proof is however rather involved; moreover, it should be kept in mind that Eqs. (8.42) are ill-defined in several particular cases (see App. 6).

Finally, we want to remark that the diagonalization method is particularly suitable to solve the radiative transfer equations in the special cases that have been collected in Sect. 8.3.c. Let us suppose, for instance, that the propagation matrix has the form of Eq. (8.24). It is easily shown that the radiative transfer equations for the linear combinations of Stokes parameters

$$\begin{aligned} I'_1 &= \frac{1}{2}\left(I + V\right) \qquad & I'_3 &= \frac{1}{2}\left(Q + \mathrm{i}\, U\right) \\ I'_2 &= \frac{1}{2}\left(I - V\right) \qquad & I'_4 &= \frac{1}{2}\left(Q - \mathrm{i}\, U\right) \end{aligned} \tag{8.43}$$

are

$$\begin{aligned} \frac{\mathrm{d}}{\mathrm{d}s} I'_1 &= -\left(\eta_I + \eta_V\right) I'_1 + \frac{1}{2}\left(\varepsilon_I + \varepsilon_V\right) \\ \frac{\mathrm{d}}{\mathrm{d}s} I'_2 &= -\left(\eta_I - \eta_V\right) I'_2 + \frac{1}{2}\left(\varepsilon_I - \varepsilon_V\right) \\ \frac{\mathrm{d}}{\mathrm{d}s} I'_3 &= -\left(\eta_I - \mathrm{i}\,\rho_V\right) I'_3 + \frac{1}{2}\left(\varepsilon_Q + \mathrm{i}\,\varepsilon_U\right) \\ \frac{\mathrm{d}}{\mathrm{d}s} I'_4 &= -\left(\eta_I + \mathrm{i}\,\rho_V\right) I'_4 + \frac{1}{2}\left(\varepsilon_Q - \mathrm{i}\,\varepsilon_U\right) , \end{aligned} \tag{8.44}$$

which is a set of four decoupled equations. The solution to these equations is trivial (cf. Eqs. (8.4), (8.18) and (8.16)), and the solution for the Stokes parameters is readily obtained by inversion of Eqs. (8.43).[1] This is of course the same solution that is obtained from Eq. (8.14) with the evolution operator of Eq. (8.27). It is important to stress that the eigenvectors of the radiative transfer equations have in this case a simple physical meaning: the combinations I'_1 and I'_2 in Eq. (8.43) are just the amount of right and left circular polarization contained in the radiation beam.

Analogous considerations can be repeated for the propagation matrices described by Eqs. (8.28) and (8.29). In these cases the eigenvectors of the transfer equations represent the amount of linear polarization along different directions.

8.5. Evolution Operator for Purely Dichroic or Purely Dispersive Media

The analytical expression for the evolution operator derived in Sect. 8.3.a takes a simpler form when the medium where the radiation is propagated is either purely dichroic ($\rho_Q = \rho_U = \rho_V = 0$) or purely dispersive ($\eta_I = \eta_Q = \eta_U = \eta_V = 0$).

The purely dichroic case is seldom encountered in practice. Its analysis is however important because, in some cases, it can be useful to tackle a transfer problem neglecting – as a first-order approximation – the influence of anomalous dispersion (this leads in general to considerable simplifications). The opposite case of a purely dispersive medium is met in some astrophysical applications (the propagation of radio waves in a magnetized plasma is a typical example). Further examples of purely dichroic or purely dispersive media can be found in laboratory optics: an ideal (dichroic) polarizer is composed of a purely dichroic medium, while an ideal retarder is composed of a purely dispersive medium.

a) *purely dichroic media*

From Eqs. (A5.18) one has

$$\Lambda_+(\vec{\eta}, 0) = \sqrt{\eta^2} = \sqrt{\eta_Q^2 + \eta_U^2 + \eta_V^2} = \eta$$

$$\Lambda_-(\vec{\eta}, 0) = 0 \,,$$

and the evolution operator can be written, using Eqs. (8.23) and (A5.21), in the form

[1] Note that in this case, being

$$\eta^2 \rho^2 = \eta_V^2 \rho_V^2 = (\vec{\eta} \cdot \vec{\rho})^2 \,,$$

the condition of Eq. (A6.14) is not satisfied, thus the matrices $\boldsymbol{X}$, $\boldsymbol{X}^{-1}$ in Eqs. (8.42) are ill-defined (actually the denominator of the quantity g_- vanishes).

$$\boldsymbol{O}(s,s') = \mathrm{e}^{-x\,\eta_I}\left\{\frac{1}{\eta^2}\begin{pmatrix} 0 & 0 & 0 & 0 \\ 0 & \eta_U^2+\eta_V^2 & -\eta_Q\eta_U & -\eta_V\eta_Q \\ 0 & -\eta_Q\eta_U & \eta_V^2+\eta_Q^2 & -\eta_U\eta_V \\ 0 & -\eta_V\eta_Q & -\eta_U\eta_V & \eta_Q^2+\eta_U^2 \end{pmatrix}\right.$$

$$+\cosh(x\eta)\,\frac{1}{\eta^2}\begin{pmatrix} \eta^2 & 0 & 0 & 0 \\ 0 & \eta_Q^2 & \eta_Q\eta_U & \eta_V\eta_Q \\ 0 & \eta_Q\eta_U & \eta_U^2 & \eta_U\eta_V \\ 0 & \eta_V\eta_Q & \eta_U\eta_V & \eta_V^2 \end{pmatrix}$$

$$\left.-\sinh(x\eta)\,\frac{1}{\eta}\begin{pmatrix} 0 & \eta_Q & \eta_U & \eta_V \\ \eta_Q & 0 & 0 & 0 \\ \eta_U & 0 & 0 & 0 \\ \eta_V & 0 & 0 & 0 \end{pmatrix}\right\}, \tag{8.45}$$

where $x = (s - s')$.

b) *purely dispersive media*

In this case one has

$$\Lambda_+(0,\vec{\rho}) = 0$$

$$\Lambda_-(0,\vec{\rho}) = \sqrt{\rho^2} = \sqrt{\rho_Q^2+\rho_U^2+\rho_V^2} = \rho\,,$$

and the evolution operator is

$$\boldsymbol{O}(s,s') = \frac{1}{\rho^2}\begin{pmatrix} \rho^2 & 0 & 0 & 0 \\ 0 & \rho_Q^2 & \rho_Q\rho_U & \rho_V\rho_Q \\ 0 & \rho_Q\rho_U & \rho_U^2 & \rho_U\rho_V \\ 0 & \rho_V\rho_Q & \rho_U\rho_V & \rho_V^2 \end{pmatrix}$$

$$+\cos(x\rho)\,\frac{1}{\rho^2}\begin{pmatrix} 0 & 0 & 0 & 0 \\ 0 & \rho_U^2+\rho_V^2 & -\rho_Q\rho_U & -\rho_V\rho_Q \\ 0 & -\rho_Q\rho_U & \rho_V^2+\rho_Q^2 & -\rho_U\rho_V \\ 0 & -\rho_V\rho_Q & -\rho_U\rho_V & \rho_Q^2+\rho_U^2 \end{pmatrix}$$

$$-\sin(x\rho)\,\frac{1}{\rho}\begin{pmatrix} 0 & 0 & 0 & 0 \\ 0 & 0 & \rho_V & -\rho_U \\ 0 & -\rho_V & 0 & \rho_Q \\ 0 & \rho_U & -\rho_Q & 0 \end{pmatrix}, \tag{8.46}$$

where $x = (s - s')$.

8.6. Evolution Operator and Mueller Matrices

The concept of Mueller matrix is a very useful tool that is often used to characterize, from a mathematical point of view, the properties of an optical device with respect to the polarization of the light that is crossing the device itself. If $\boldsymbol{I}'$ is the Stokes vector of the light beam that is entering the device, and $\boldsymbol{I}$ the Stokes vector at the exit of the device, the *Mueller matrix* is defined by

$$\boldsymbol{I} = \boldsymbol{M}\, \boldsymbol{I}' \,. \tag{8.47}$$

This concept, introduced by Mueller (1948), provides a matrix-algebraic method – the so-called *Mueller calculus* – for computing the effect of a train of several devices on a light beam. If $\boldsymbol{M}_{\mathrm{A}}$, $\boldsymbol{M}_{\mathrm{B}}$, ..., $\boldsymbol{M}_{\mathrm{N}}$ are the Mueller matrices of the single optical devices, and if the light beam crosses the train in the order A, B, ..., N, we have, with evident notations

$$\boldsymbol{I} = \boldsymbol{M}_{\mathrm{N}} \cdots \boldsymbol{M}_{\mathrm{B}}\, \boldsymbol{M}_{\mathrm{A}}\, \boldsymbol{I}' \,. \tag{8.48}$$

Comparison of Eq. (8.47) or (8.48) with Eq. (8.6) shows that the Mueller matrix of an optical device is nothing but the evolution operator describing the propagation of radiation inside the material medium of which the device is composed.[1] Therefore, the expression of the Mueller matrix can be deduced once the geometrical and optical properties of the medium are specified.

As an example, let us consider the case of a dichroic linear polarizer of geometrical thickness l. The medium composing the polarizer can be characterized by a triplet of real, orthogonal unit vectors $(\vec{u}_{\mathrm{t}}, \vec{u}_{\mathrm{a}}, \vec{u}_{\mathrm{p}})$ – parallel to the transmission axis, the 'absorption' axis and the propagation direction, respectively – such that the corresponding indices of refraction are

$$n_{\mathrm{t}} = 1 + \mathrm{i}\, k_{\mathrm{t}} \,, \qquad n_{\mathrm{a}} = 1 + \mathrm{i}\, k_{\mathrm{a}}$$

(the index n_{p} is unimportant). Using the notations of Sect. 5.1, the unit vectors $\vec{u}'_\alpha$ are given by[2]

$$\vec{u}'_\alpha = \vec{u}_\alpha \qquad (\alpha = \mathrm{t}, \mathrm{a}, \mathrm{p}) \,.$$

Aligning the reference direction with the unit vector $\vec{u}_{\mathrm{t}}$, we obtain for the propagation tensor (see Eq. (5.22))

$$G_{11} = -2\pi\, \mathrm{i}\, \frac{\nu}{c}\, n_{\mathrm{t}} \,, \qquad G_{22} = -2\pi\, \mathrm{i}\, \frac{\nu}{c}\, n_{\mathrm{a}} \,, \qquad G_{12} = G_{21} = 0 \,,$$

[1] Actually, the concept of Mueller matrix is broader, because it can also be used to characterize optical devices where light is partially reflected or deviated laterally. Of course the identification of Mueller matrix and evolution operator does not hold in these cases.

[2] Note that the medium composing a dichroic polarizer is a very special case of an absorbing anisotropic medium.

so that Eqs. (5.26) give

$$\eta_I = 2\pi\,\frac{\nu}{c}\,\left(k_{\rm t} + k_{\rm a}\right), \qquad \eta_Q = 2\pi\,\frac{\nu}{c}\,\left(k_{\rm t} - k_{\rm a}\right)$$
$$\eta_U = \eta_V = \rho_Q = \rho_U = \rho_V = 0\,.$$

The Mueller matrix of the polarizer, $\boldsymbol{M}_{\rm P}$, can be deduced directly from Eq. (8.45) by substituting l for x. We obtain

$$\boldsymbol{M}_{\rm P} = {\rm e}^{-l\,\eta_I}\left\{\begin{pmatrix}0&0&0&0\\0&0&0&0\\0&0&1&0\\0&0&0&1\end{pmatrix} + \cosh(l\,\eta_Q)\begin{pmatrix}1&0&0&0\\0&1&0&0\\0&0&0&0\\0&0&0&0\end{pmatrix} - \sinh(l\,\eta_Q)\begin{pmatrix}0&1&0&0\\1&0&0&0\\0&0&0&0\\0&0&0&0\end{pmatrix}\right\}$$

$$= \frac{1}{2}\begin{pmatrix}K_{\rm t}+K_{\rm a} & K_{\rm t}-K_{\rm a} & 0 & 0\\ K_{\rm t}-K_{\rm a} & K_{\rm t}+K_{\rm a} & 0 & 0\\ 0 & 0 & 2\sqrt{K_{\rm t}K_{\rm a}} & 0\\ 0 & 0 & 0 & 2\sqrt{K_{\rm t}K_{\rm a}}\end{pmatrix},$$

where

$$K_{\rm t} = {\rm e}^{-4\pi\,\frac{\nu}{c}\,k_{\rm t}\,l}\,, \qquad K_{\rm a} = {\rm e}^{-4\pi\,\frac{\nu}{c}\,k_{\rm a}\,l}\,.$$

For an *ideal* polarizer, one has $K_{\rm t} = 1$ (no absorption along the transmission axis) and $K_{\rm a} = 0$ (complete absorption along the orthogonal axis), thus

$$\boldsymbol{M}_{\rm P} = \frac{1}{2}\begin{pmatrix}1&1&0&0\\1&1&0&0\\0&0&0&0\\0&0&0&0\end{pmatrix},$$

which is the correct Mueller matrix for an ideal polarizer with its transmission axis parallel to the reference direction (see e.g. Clarke and Grainger, 1971).

As a further example, let us consider the Mueller matrix of a retarder. In this case the medium is characterized by a triplet of real, orthogonal unit vectors $(\vec{u}_{\rm f}\,,\vec{u}_{\rm s}\,,\vec{u}_{\rm p})$ – parallel to the fast axis, the slow axis and the propagation direction – such that the corresponding indices of refraction are given by

$$n_{\rm f} = 1 + \delta_{\rm f}\,, \qquad n_{\rm s} = 1 + \delta_{\rm s}$$

with $\delta_{\rm s} > \delta_{\rm f}$ (again the index $n_{\rm p}$ is unimportant). Aligning the reference direction with the unit vector $\vec{u}_{\rm f}$, we have from Eq. (5.22)

$$G_{11} = -2\pi\,{\rm i}\,\frac{\nu}{c}\,n_{\rm f}\,, \qquad G_{22} = -2\pi\,{\rm i}\,\frac{\nu}{c}\,n_{\rm s}\,, \qquad G_{12} = G_{21} = 0\,,$$

and from Eqs. (5.26)

$$\rho_Q = -\,2\pi\,\frac{\nu}{c}\,\left(\delta_{\rm s} - \delta_{\rm f}\right)$$
$$\eta_I = \eta_Q = \eta_U = \eta_V = \rho_U = \rho_V = 0\;.$$

The Mueller matrix of the retarder, $\boldsymbol{M}_{\rm R}$, is derived from Eq. (8.46). After some easy algebra we get

$$\boldsymbol{M}_{\rm R} = \begin{pmatrix} 1 & 0 & 0 & 0 \\ 0 & 1 & 0 & 0 \\ 0 & 0 & \cos\delta & \sin\delta \\ 0 & 0 & -\sin\delta & \cos\delta \end{pmatrix}\;,$$

where δ is the retardance defined in Eq. (1.28)

$$\delta = -\rho_Q\, l \,=\, 2\pi\,\frac{\nu}{c}\,\left(\delta_{\rm s} - \delta_{\rm f}\right) l \,=\, 2\pi\left(n_{\rm s} - n_{\rm f}\right)\frac{l}{\lambda}$$

(l is the thickness of the retarder).

Using the method outlined above, it is possible to obtain the Mueller matrix of any optical device once the geometrical and optical properties of its constituents are known.

8.7. Perturbative Solution of the Radiative Transfer Equations

In many practical applications, it is convenient to express the propagation matrix $\boldsymbol{K}$ and the emission vector $\boldsymbol{\varepsilon}$ as the sum of a leading (or zero-order) term plus a perturbation,

$$\boldsymbol{K}(s) = \boldsymbol{K}_0(s) + \delta\boldsymbol{K}(s)$$
$$\boldsymbol{\varepsilon}(s) = \boldsymbol{\varepsilon}_0(s) + \delta\boldsymbol{\varepsilon}(s)\;.$$

Equation (8.2) takes then the form

$$\frac{\mathrm{d}}{\mathrm{d}s}\,\boldsymbol{I}(s) = -\left[\boldsymbol{K}_0(s) + \delta\boldsymbol{K}(s)\right]\boldsymbol{I}(s) + \left[\boldsymbol{\varepsilon}_0(s) + \delta\boldsymbol{\varepsilon}(s)\right]\;. \tag{8.49}$$

We look for a solution to this equation of the form

$$\boldsymbol{I}(s) = \boldsymbol{I}_0(s) + \delta\boldsymbol{I}(s)\;,$$

where $\boldsymbol{I}_0(s)$ is the solution of the 'zero-order' equation

$$\frac{\mathrm{d}}{\mathrm{d}s}\,\boldsymbol{I}_0(s) = -\boldsymbol{K}_0(s)\,\boldsymbol{I}_0(s) + \boldsymbol{\varepsilon}_0(s) \tag{8.50}$$

and where $\delta \boldsymbol{I}(s)$ satisfies the equation (resulting from Eqs. (8.49) and (8.50))

$$\frac{\mathrm{d}}{\mathrm{d}s}\,\delta \boldsymbol{I}(s) = -\,\boldsymbol{K}_0(s)\,\delta \boldsymbol{I}(s) \;-\; \delta \boldsymbol{K}(s)\,\boldsymbol{I}_0(s) \;-\; \delta \boldsymbol{K}(s)\,\delta \boldsymbol{I}(s) \;+\; \delta \boldsymbol{\varepsilon}(s)\;. \tag{8.51}$$

If the perturbation is 'everywhere small', or, in other words, if

$$\delta \boldsymbol{K}(s) \ll \boldsymbol{K}_0(s) \quad \text{and} \quad \delta \boldsymbol{\varepsilon}(s) \ll \boldsymbol{\varepsilon}_0(s)$$

for any s, we should expect that

$$\delta \boldsymbol{I}(s) \ll \boldsymbol{I}_0(s)\;,$$

so that the third term in the right-hand side of Eq. (8.51), being a 'second-order' term, can be neglected. We have therefore

$$\frac{\mathrm{d}}{\mathrm{d}s}\,\delta \boldsymbol{I}(s) = -\,\boldsymbol{K}_0(s)\,\delta \boldsymbol{I}(s) \;+\; \left[\,\delta \boldsymbol{\varepsilon}(s) \;-\; \delta \boldsymbol{K}(s)\,\boldsymbol{I}_0(s)\right]\;. \tag{8.52}$$

Equations (8.50) and (8.52) can be solved using the evolution operator $\boldsymbol{O}_0(s, s')$ associated with the unperturbed propagation matrix $\boldsymbol{K}_0(s)$. For a medium extending in s' from $-\infty$ to s, one gets from Eq. (8.15)

$$\boldsymbol{I}_0(s) = \int_{-\infty}^{s} \boldsymbol{O}_0(s, s')\,\boldsymbol{\varepsilon}_0(s')\;\mathrm{d}s' \tag{8.53}$$

$$\begin{aligned}
\delta \boldsymbol{I}(s) &= \int_{-\infty}^{s} \boldsymbol{O}_0(s, s')\left[\delta \boldsymbol{\varepsilon}(s') \;-\; \delta \boldsymbol{K}(s')\,\boldsymbol{I}_0(s')\right]\mathrm{d}s' \\
&= \int_{-\infty}^{s} \boldsymbol{O}_0(s, s')\,\delta \boldsymbol{\varepsilon}(s')\;\mathrm{d}s' \\
&\quad - \int_{-\infty}^{s} \mathrm{d}s'\;\boldsymbol{O}_0(s, s')\,\delta \boldsymbol{K}(s') \int_{-\infty}^{s'} \mathrm{d}s''\;\boldsymbol{O}_0(s', s'')\,\boldsymbol{\varepsilon}_0(s'')\;.
\end{aligned} \tag{8.54}$$

Equations (8.53) and (8.54) solve, in a perturbative way, the transfer problem. This method of solution is especially useful when the operator $\boldsymbol{O}_0$ can be written in analytical form. Moreover, through an adaptation of this same method, it is possible to introduce the concept of *response function*, which will be done in the following chapter (see Sect. 9.16) in connection with the problem of line formation in a magnetic field.

8.8. An Alternative Form of the Radiative Transfer Equations

The transfer equation (8.2) can be cast into a different form by introducing, in the place of the Stokes vector $\boldsymbol{I}$, a 2×2 matrix which is strictly related to the polarization tensor. Indeed, both the classical derivation of Sect. 5.2 and the quantum-mechanical derivation of Sect. 6.6 lead quite naturally to a transfer equation for the polarization tensor (cf. Eqs. (5.24) and (6.78)). These equations were later converted into a transfer equation for the Stokes vector, which in both cases resulted in being of the form of Eq. (8.2).

In this section we will proceed in the opposite direction, showing in full generality how it is possible to transform Eq. (8.2) into a transfer equation having the form of Eq. (5.24) or (6.78).

From the Stokes vector $\boldsymbol{I}$ we define the tensor $\tilde{\boldsymbol{I}}$ via the equation (cf. Eqs. (1.40) and (5.129))

$$\tilde{I}_{\alpha\beta} = \frac{1}{2} \sum_{i=0}^{3} (\tau_i)_{\alpha\beta} \, I_i \qquad (\alpha, \beta = 1, 2) \, , \tag{8.55}$$

where the matrices $\boldsymbol{\tau}_i$ are *any* representation of the Pauli spin matrices. In particular, we can take $\boldsymbol{\tau}_i = \boldsymbol{\sigma}_i$ or $\boldsymbol{\tau}_i = \hat{\boldsymbol{\sigma}}_i$ (where $\boldsymbol{\sigma}_i$ and $\hat{\boldsymbol{\sigma}}_i$ are given by Eqs. (1.17) and (5.128), respectively) or, more generally, $\boldsymbol{\tau}_i = \boldsymbol{x} \, \boldsymbol{\sigma}_i \, \boldsymbol{x}^{-1}$, where $\boldsymbol{x}$ is any unitary 2×2 matrix ($\boldsymbol{x}^{-1} = \boldsymbol{x}^{\dagger}$).[1]

Whatever representation is chosen, the matrices $\boldsymbol{\tau}_i$ are Hermitian,

$$\boldsymbol{\tau}_i{}^{\dagger} = \left(\boldsymbol{x} \, \boldsymbol{\sigma}_i \, \boldsymbol{x}^{-1} \right)^{\dagger} = \left(\boldsymbol{x}^{-1} \right)^{\dagger} \boldsymbol{\sigma}_i^{\dagger} \, \boldsymbol{x}^{\dagger} = \boldsymbol{x} \, \boldsymbol{\sigma}_i \, \boldsymbol{x}^{-1} = \boldsymbol{\tau}_i \, ,$$

thus the tensor $\tilde{\boldsymbol{I}}$ is also Hermitian

$$\tilde{I}^{*}_{\alpha\beta} = \frac{1}{2} \sum_{i=0}^{3} (\tau_i)^{*}_{\alpha\beta} \, I_i \, = \, \frac{1}{2} \sum_{i=0}^{3} (\tau_i)_{\beta\alpha} \, I_i \, = \tilde{I}_{\beta\alpha} \, .$$

Moreover, from Eq. (1.18) we have

$$\begin{aligned} \boldsymbol{\tau}_j \, \boldsymbol{\tau}_k &= \boldsymbol{x} \, \boldsymbol{\sigma}_j \, \boldsymbol{x}^{-1} \, \boldsymbol{x} \, \boldsymbol{\sigma}_k \, \boldsymbol{x}^{-1} = \boldsymbol{x} \left[\delta_{jk} \, \boldsymbol{\sigma}_0 + \mathrm{i} \sum_l \epsilon_{jkl} \, \boldsymbol{\sigma}_l \right] \boldsymbol{x}^{-1} \\ &= \delta_{jk} \, \boldsymbol{\tau}_0 + \mathrm{i} \sum_l \epsilon_{jkl} \, \boldsymbol{\tau}_l \qquad\qquad (j, k, l = 1, 2, 3) \, , \end{aligned} \tag{8.56}$$

where $\boldsymbol{\tau}_0$ is the 2×2 identity matrix, and from Eq. (1.19)

$$\begin{aligned} \mathrm{Tr} \left(\boldsymbol{\tau}_j \, \boldsymbol{\tau}_k \right) &= \mathrm{Tr} \left(\boldsymbol{x} \, \boldsymbol{\sigma}_j \, \boldsymbol{x}^{-1} \, \boldsymbol{x} \, \boldsymbol{\sigma}_k \, \boldsymbol{x}^{-1} \right) = \mathrm{Tr} \left(\boldsymbol{x}^{-1} \boldsymbol{x} \, \boldsymbol{\sigma}_j \, \boldsymbol{\sigma}_k \right) \\ &= 2 \, \delta_{jk} \qquad\qquad (j, k = 0, 1, 2, 3) \, , \end{aligned} \tag{8.57}$$

[1] The arbitrariness of the matrices $\boldsymbol{\tau}_i$ is strictly connected with the arbitrariness of the choice of the unit vectors defining the polarization tensor (cf. Sect. 1.8).

which allows to find the inverse relation of Eq. (8.55)

$$I_i = \sum_{\alpha\beta} (\tau_i)_{\alpha\beta}\, \tilde{I}_{\beta\alpha} \ . \tag{8.58}$$

Deriving Eq. (8.55) with respect to s , and using Eqs. (8.2) and (8.58), one obtains the transfer equation for $\tilde{I}_{\alpha\beta}$

$$\frac{\mathrm{d}}{\mathrm{d}s}\, \tilde{I}_{\alpha\beta}(s) = -\frac{1}{2} \sum_{\gamma\delta} \left[\sum_{i=0}^{3} \sum_{j=0}^{3} (\tau_i)_{\alpha\beta}\, (\tau_j)_{\gamma\delta}\, K_{ij}(s) \right] \tilde{I}_{\delta\gamma}(s) \ + \ e_{\alpha\beta}(s) \ , \tag{8.59}$$

where

$$e_{\alpha\beta}(s) = \frac{1}{2} \sum_{i=0}^{3} (\tau_i)_{\alpha\beta}\ \varepsilon_i(s) \ .$$

We now observe that, because of its symmetry (and reality) properties, the matrix $\boldsymbol{K}$ can be written in the following form, suggested by Eq. (6.84)

$$K_{ij} = \mathrm{Re}\left[\mathrm{Tr}\,(\boldsymbol{\tau}_j\, \boldsymbol{\tau}_i\, \boldsymbol{q}) \right] \ , \tag{8.60}$$

where $\boldsymbol{q}$ is a 2×2 matrix implicitly defined by this equation. The expression of $\boldsymbol{q}$ can be obtained by inversion of Eq. (8.60). This can be done in the easiest way by noticing that any representation of the Pauli spin matrices forms a complete basis for the 2×2 matrices. Writing then

$$\boldsymbol{q} = \sum_{k=0}^{3} a_k\, \boldsymbol{\tau}_k \tag{8.61}$$

one gets

$$K_{ij} = \sum_{k=0}^{3} \mathrm{Re}\left[a_k\, \mathrm{Tr}\,(\boldsymbol{\tau}_j\, \boldsymbol{\tau}_i\, \boldsymbol{\tau}_k) \right] \ .$$

The trace is easily evaluated from Eqs. (8.56) and (8.57), which give

$$\mathrm{Tr}\,(\boldsymbol{\tau}_m\, \boldsymbol{\tau}_n\, \boldsymbol{\tau}_p) = \ 2\ \mathrm{i}\ \epsilon_{mnp} \qquad (m, n, p = 1, 2, 3) \tag{8.62}$$

(if one of the indices is zero, the trace is given directly from Eq. (8.57)). We obtain

$$\begin{aligned}
\eta_I &= K_{00} = K_{11} = K_{22} = K_{33} = 2\ \mathrm{Re}\,(a_0) \\
\eta_Q &= K_{01} = K_{10} = 2\ \mathrm{Re}\,(a_1) \\
\eta_U &= K_{02} = K_{20} = 2\ \mathrm{Re}\,(a_2) \\
\eta_V &= K_{03} = K_{30} = 2\ \mathrm{Re}\,(a_3) \\
\rho_Q &= K_{23} = -K_{32} = 2\ \mathrm{Im}\,(a_1) \\
\rho_U &= K_{31} = -K_{13} = 2\ \mathrm{Im}\,(a_2) \\
\rho_V &= K_{12} = -K_{21} = 2\ \mathrm{Im}\,(a_3) \ ,
\end{aligned}$$

or[1]

$$a_0 = \frac{1}{2}\,\eta_I \qquad a_2 = \frac{1}{2}\,(\eta_U + \mathrm{i}\,\rho_U)$$
$$a_1 = \frac{1}{2}\,(\eta_Q + \mathrm{i}\,\rho_Q) \qquad a_3 = \frac{1}{2}\,(\eta_V + \mathrm{i}\,\rho_V)\ . \tag{8.63}$$

Substituting Eq. (8.60) into Eq. (8.59), and using the remarkable property of the Pauli spin matrices

$$\sum_{i=0}^{3} (\tau_i)_{\alpha\beta}\,(\tau_i)_{\mu\nu} = 2\,\delta_{\alpha\nu}\,\delta_{\beta\mu}\ , \tag{8.64}$$

one finds after some algebra

$$\frac{\mathrm{d}}{\mathrm{d}s}\,\tilde{I}_{\alpha\beta}(s) = -\sum_{\gamma}\left[\,q_{\alpha\gamma}(s)\,\tilde{I}_{\gamma\beta}(s) + q_{\beta\gamma}(s)^*\,\tilde{I}_{\alpha\gamma}(s)\,\right] + e_{\alpha\beta}(s)\ ,$$

or, in matrix form

$$\frac{\mathrm{d}}{\mathrm{d}s}\,\tilde{\boldsymbol{I}}(s) = -\,\boldsymbol{q}(s)\,\tilde{\boldsymbol{I}}(s) - \tilde{\boldsymbol{I}}(s)\,\boldsymbol{q}^{\dagger}(s) + \boldsymbol{e}(s)\ , \tag{8.65}$$

where $\boldsymbol{q}^{\dagger}$, the transpose conjugate of $\boldsymbol{q}$ ($q^{\dagger}_{\alpha\beta} = q^*_{\beta\alpha}$), is

$$\boldsymbol{q}^{\dagger} = \sum_{k=0}^{3} a_k^*\,\boldsymbol{\tau}_k\ .$$

The above derivation shows that the radiative transfer equation (8.65) is fully equivalent to Eq. (8.2).

8.9. Solution of the Alternative Form of the Radiative Transfer Equations

Equation (8.65) can be formally solved by the introduction of an evolution operator, similarly to what done in Sect. 8.2 for the solution of Eq. (8.2). This operator – which will be referred to in the following as *reduced evolution operator* – has been introduced by Van Ballegooijen (1985, 1987) for a particular representation of the Pauli spin matrices.

[1] The inversion of Eq. (8.60) leaves unspecified the imaginary part of a_0. From the mathematical point of view this indetermination is not surprising, because the complex 2×2 matrix $\boldsymbol{q}$ is defined by eight real numbers, while the matrix $\boldsymbol{K}$ contains just seven independent (real) quantities. From the physical point of view, the indetermination is related to the fact that the transfer equations do not depend on the absolute phases of the components of the electric field. In Eqs. (8.63) we have set $\mathrm{Im}\,(a_0) = 0$, but the following results are unaffected by the value of $\mathrm{Im}\,(a_0)$.

Considering first the homogeneous equation

$$\frac{\mathrm{d}}{\mathrm{d}s}\,\tilde{\boldsymbol{I}}(s) = -\,\boldsymbol{q}(s)\,\tilde{\boldsymbol{I}}(s) \;-\; \tilde{\boldsymbol{I}}(s)\,\boldsymbol{q}^{\dagger}(s)\;, \tag{8.66}$$

we define the reduced evolution operator $\boldsymbol{E}(s,s')$ as the 2×2 complex matrix which, acting on $\tilde{\boldsymbol{I}}(s')$, gives $\tilde{\boldsymbol{I}}(s)$ (with $s \geq s'$) through the expression

$$\tilde{\boldsymbol{I}}(s) = \boldsymbol{E}(s,s')\,\tilde{\boldsymbol{I}}(s')\,\boldsymbol{E}^{\dagger}(s,s')\;, \tag{8.67}$$

with

$$\boldsymbol{E}(s,s) = \boldsymbol{1} \tag{8.68}$$

($\boldsymbol{1}$ being the 2×2 identity matrix) and

$$\boldsymbol{E}(s,s'') = \boldsymbol{E}(s,s')\,\boldsymbol{E}(s',s'') \qquad (s \geq s' \geq s'')\;.$$

Derivation of Eq. (8.67) with respect to s gives

$$\frac{\mathrm{d}}{\mathrm{d}s}\,\tilde{\boldsymbol{I}}(s) = \left[\frac{\mathrm{d}}{\mathrm{d}s}\,\boldsymbol{E}(s,s')\right]\tilde{\boldsymbol{I}}(s')\,\boldsymbol{E}^{\dagger}(s,s') \;+\; \boldsymbol{E}(s,s')\,\tilde{\boldsymbol{I}}(s')\left[\frac{\mathrm{d}}{\mathrm{d}s}\,\boldsymbol{E}^{\dagger}(s,s')\right]\;,$$

while substitution of Eq. (8.67) into the right-hand side of Eq. (8.66) gives

$$\frac{\mathrm{d}}{\mathrm{d}s}\,\tilde{\boldsymbol{I}}(s) = -\,\boldsymbol{q}(s)\,\boldsymbol{E}(s,s')\,\tilde{\boldsymbol{I}}(s')\,\boldsymbol{E}^{\dagger}(s,s') \;-\; \boldsymbol{E}(s,s')\,\tilde{\boldsymbol{I}}(s')\,\boldsymbol{E}^{\dagger}(s,s')\,\boldsymbol{q}^{\dagger}(s)\;.$$

Comparison of these two equations yields

$$\frac{\mathrm{d}}{\mathrm{d}s}\,\boldsymbol{E}(s,s') = -\,\boldsymbol{q}(s)\,\boldsymbol{E}(s,s')\;. \tag{8.69}$$

In a similar way one finds

$$\frac{\mathrm{d}}{\mathrm{d}s'}\,\boldsymbol{E}(s,s') = \boldsymbol{E}(s,s')\,\boldsymbol{q}(s')\;. \tag{8.70}$$

Because of the strict analogy between Eqs. (8.69)-(8.70) and Eqs. (8.9)-(8.10), we can expand the operator $\boldsymbol{E}(s,s')$ in the form (cf. Eq. (8.12))

$$\boldsymbol{E}(s,s') = \boldsymbol{1} + \sum_{n=1}^{\infty}\frac{(-1)^n}{n!}\int_{s'}^{s}\mathrm{d}s_1\int_{s'}^{s}\mathrm{d}s_2\cdots\int_{s'}^{s}\mathrm{d}s_n\;\mathbb{P}\Big\{\boldsymbol{q}(s_1)\,\boldsymbol{q}(s_2)\cdots\boldsymbol{q}(s_n)\Big\}\;,$$

where $\mathbb{P}$ is the Dyson chronological product defined in Eq. (8.13). Moreover, it can be easily proved, with the help of Eqs. (8.68) and (8.69), that the formal solution of the non-homogeneous equation (Eq. (8.65)) is

$$\tilde{\boldsymbol{I}}(s) = \int_{s'}^{s}\boldsymbol{E}(s,s'')\,\boldsymbol{e}(s'')\,\boldsymbol{E}^{\dagger}(s,s'')\,\mathrm{d}s'' + \boldsymbol{E}(s,s')\,\tilde{\boldsymbol{I}}(s')\,\boldsymbol{E}^{\dagger}(s,s')\;.$$

Analytical forms of the reduced evolution operator $\boldsymbol{E}(s,s')$ can be found whenever

$$\big[\,\boldsymbol{q}(s_1),\boldsymbol{q}(s_2)\,\big]=0 \tag{8.71}$$

for any couple of points $s_1\,,\ s_2$ in the interval (s',s). In this case one gets (cf. Eq. (8.22))

$$\boldsymbol{E}(s,s')=\mathrm{e}^{-\int_{s'}^{s}\boldsymbol{q}(s'')\,\mathrm{d}s''}\ . \tag{8.72}$$

Similarly to Sect. 8.3, one can distinguish three different cases where Eq. (8.71) is satisfied. As an example, let us consider the case $\boldsymbol{q}=$ const., where Eq. (8.72) reduces to

$$\boldsymbol{E}(s,s')=\mathrm{e}^{-(s-s')\,\boldsymbol{q}}\ .$$

Use of Eqs. (8.61) and (A5.6) gives

$$\boldsymbol{E}(s,s')=\mathrm{e}^{-(s-s')\,a_0}\ \mathrm{e}^{-(s-s')\,\vec{a}\cdot\vec{\boldsymbol{\tau}}}\ , \tag{8.73}$$

where

$$\vec{a}\,=(a_1\,,a_2\,,a_3)\,,\qquad \vec{\boldsymbol{\tau}}=(\boldsymbol{\tau}_1\,,\boldsymbol{\tau}_2\,,\boldsymbol{\tau}_3)\,,$$

with a_i given by Eqs. (8.63). The exponential in the right-hand side of Eq. (8.73) can be expanded by a method similar to that of App. 5. The result is[1]

$$\boldsymbol{E}(s,s')=\mathrm{e}^{-\frac{1}{2}\,x\,\eta_I}\left[\cosh(xa)\,\boldsymbol{1}-\frac{\sinh(xa)}{a}\ \vec{a}\cdot\vec{\boldsymbol{\tau}}\ \right]\,, \tag{8.74}$$

where

$$\begin{aligned}x&=(s-s')\\ a&=\sqrt{a^2}\,=\,\frac{1}{2}\left[\Lambda_+(\vec{\eta},\vec{\rho})+\,\mathrm{i}\,\sigma\,\Lambda_-(\vec{\eta},\vec{\rho})\right]\end{aligned}$$

with $\Lambda_\pm(\vec{\eta},\vec{\rho})$ and σ defined in Eqs. (A5.18) and (A5.19), respectively.

The reduced evolution operator $\boldsymbol{E}(s,s')$ is of course related to the evolution operator $\boldsymbol{O}(s,s')$ defined in Sect. 8.2. To find this relation we start from Eq. (8.58), written at point s, and substitute for $\tilde{\boldsymbol{I}}(s)$ its expression in terms of the reduced evolution operator (Eq. (8.67)). Next we use Eq. (8.55), written at point s', and compare with the definition (8.6) to obtain

$$O_{ij}(s,s')=\frac{1}{2}\ \mathrm{Tr}\left[\,\boldsymbol{\tau}_i\ \boldsymbol{E}(s,s')\,\boldsymbol{\tau}_j\ \boldsymbol{E}^{\dagger}(s,s')\,\right]\qquad(i,j=0,1,2,3)\,. \tag{8.75}$$

This formula shows that the 16 real elements O_{ij} are bilinear combinations of the 4 complex elements $E_{\alpha\beta}$. The explicit expressions are rather cumbersome and depend on the representation used for the matrices $\boldsymbol{\tau}_i$.

---

[1] If $(\eta^2-\rho^2)=\vec{\eta}\cdot\vec{\rho}=0$ (so that $\Lambda_+(\vec{\eta},\vec{\rho})=\Lambda_-(\vec{\eta},\vec{\rho})=0$), Eq. (8.74) should be replaced by

$$\boldsymbol{E}(s,s')=\mathrm{e}^{-\frac{1}{2}\,x\,\eta_I}\left[\,\boldsymbol{1}-x\,\vec{a}\cdot\vec{\boldsymbol{\tau}}\,\right]\,.$$

On the other hand, $\boldsymbol{E}(s,s')$ depends also on the representation because of its dependence on the matrix $\boldsymbol{q}$ (see Eqs. (8.69) and (8.61)). It is however possible to obtain an 'intrinsic' relation (i.e. a relation independent of the representation) between the operators $\boldsymbol{O}(s,s')$ and $\boldsymbol{E}(s,s')$ by expanding the latter on the basis $\{\boldsymbol{\tau}_i\}$,[1]

$$\boldsymbol{E}(s,s') = \sum_{k=0}^{3} E^{(k)}(s,s')\,\boldsymbol{\tau}_k\ . \tag{8.76}$$

Substitution into Eq. (8.75) gives

$$O_{ij}(s,s') = \frac{1}{2}\sum_{k=0}^{3}\sum_{l=0}^{3} E^{(k)}(s,s')\,E^{(l)}(s,s')^*\ \mathrm{Tr}\left(\boldsymbol{\tau}_i\,\boldsymbol{\tau}_k\,\boldsymbol{\tau}_j\,\boldsymbol{\tau}_l\right)\ , \tag{8.77}$$

which clearly does not depend on the representation.

Equation (8.76) suggests a further important remark. Using Eq. (8.57), the coefficients $E^{(k)}(s,s')$ can be written in the form

$$E^{(k)}(s,s') = \frac{1}{2}\ \mathrm{Tr}\left[\,\boldsymbol{\tau}_k\ \boldsymbol{E}(s,s')\,\right]\ .$$

Derivation with respect to s leads, with the help of Eqs. (8.69), (8.61) and (8.76), to the set of differential equations (independent of the representation)

$$\frac{\mathrm{d}}{\mathrm{d}s}\,E^{(k)}(s,s') = -\frac{1}{2}\sum_{i=0}^{3}\sum_{j=0}^{3} a_i\,E^{(j)}(s,s')\ \mathrm{Tr}\left(\boldsymbol{\tau}_i\,\boldsymbol{\tau}_j\,\boldsymbol{\tau}_k\right)\ . \tag{8.78}$$

It follows that the general problem of finding the evolution operator is equivalent to solving a system of 8 linear, homogeneous, real differential equations in the 8 unknowns

$$\mathrm{Re}\left[\,E^{(k)}(s,s')\,\right]\,,\qquad \mathrm{Im}\left[\,E^{(k)}(s,s')\,\right]\qquad (k=0,1,2,3)\ ,$$

subjected to the boundary condition (see Eqs. (8.68) and (8.76))

$$\mathrm{Re}\left[\,E^{(k)}(s',s')\,\right] = \delta_{k0}\ ,\qquad \mathrm{Im}\left[\,E^{(k)}(s',s')\,\right] = 0\ .$$

Once the system is solved, the reduced evolution operator $\boldsymbol{E}(s,s')$ can be computed from Eq. (8.76), and the evolution operator $\boldsymbol{O}(s,s')$ from Eq. (8.77).

Equations (8.78) and (8.77) are developed in detail in App. 7. Similar equations have been obtained, with a different formalism, by Sánchez Almeida (1992).

---

[1] In the case $\boldsymbol{q}$ = const. considered above, $\boldsymbol{E}(s,s')$ is already expressed in this form (see Eq. (8.74)).

This page intentionally left blank

CHAPTER 9

LINE FORMATION IN A MAGNETIC FIELD

The problem of line formation in a magnetic field is a classical one in the theory of stellar atmospheres.[1] In its most general formulation it consists in the following. Consider a wavelength interval of the electromagnetic spectrum where one or several spectral lines are present. The radiation contained in the interval flows through a stellar atmosphere permeated by a magnetic field and interacts with the atoms (responsible for those spectral lines) via the usual processes of absorption, emission (spontaneous and stimulated) and scattering. The result is, quite generally, the formation of absorption (or emission) lines with typical polarization features. The problem is to relate the polarization features of the emerging radiation, described by its Stokes parameters, to the physical properties of the atmosphere and to the magnetic field vector.

The overall problem is extremely complicated and ultimately requires a full non-equilibrium (or non-LTE) approach, whose basic physics will be outlined in Chap. 14. However, in most astrophysical applications only the deepest layers of stellar atmospheres are involved. In that case, depolarizing collisions can be assumed to be sufficiently strong to destroy any atomic polarization that might be induced by the (anisotropic and polarized) radiation field. As we will see in the following, this assumption greatly simplifies the general problem and, in particular, allows the emission term in the radiative transfer equation to be described by a scalar source function (which reduces to the Planck function in LTE). The present chapter is devoted to the subject of line formation in a magnetic field under the assumption of complete atomic depolarization.

9.1. Transfer Equation for Polarized Radiation in a Magnetized Stellar Atmosphere

Consider a radiation beam of frequency ν that is flowing in a stellar atmosphere along the direction $\vec{\Omega}$. If the frequency ν is close to the frequency ν_0 of a spectral line (produced by an atomic species present in the atmosphere), the radiation beam undergoes two different kinds of interactions with the ambient medium: absorption and emission processes due to the continuum, and the corresponding processes due to the spectral line.

[1] In this chapter we use the term 'stellar atmosphere' in a rather broad sense. Many of the results that will be derived in the following sections can as well be applied to laboratory or astrophysical plasmas of arbitrary geometrical shape, like slabs, cylinders, etc. In many cases, these can indeed be regarded as 'pieces' of a stellar atmosphere.

The theory of the continuum absorption coefficient in stellar atmospheres is described in detail in several books and will not be repeated here (see e.g. Mihalas, 1978). Although such theory has been developed for non-magnetic atmospheres, it can be shown that the presence of a magnetic field does not alter the frequency dependence of the continuum absorption coefficient and does not introduce dichroism or anomalous dispersion effects.[1] Since this is also true for the emission coefficient, the contribution of continuum processes to the radiative transfer equation for polarized radiation is of the form

$$\frac{\mathrm{d}}{\mathrm{d}s}\begin{pmatrix} I \\ Q \\ U \\ V \end{pmatrix} = -\begin{pmatrix} k_{\mathrm{c}} & 0 & 0 & 0 \\ 0 & k_{\mathrm{c}} & 0 & 0 \\ 0 & 0 & k_{\mathrm{c}} & 0 \\ 0 & 0 & 0 & k_{\mathrm{c}} \end{pmatrix}\begin{pmatrix} I - S_{\mathrm{c}} \\ Q \\ U \\ V \end{pmatrix}, \tag{9.1}$$

where I, Q, U, and V are the Stokes parameters of the radiation of frequency ν flowing along the direction $\vec{\Omega}$, s is the coordinate measured along the ray path, k_{c} is the local continuum absorption coefficient (corrected for stimulated emission) at frequency ν and, finally, S_{c} is the continuum source function that, in most cases, can be equated to the local Planck function B_{P}.

We must now add to the transfer equation the contribution of the absorption and emission processes in the spectral line. For electric-dipole transitions, this contribution is given by Eq. (6.85), with the substitution

$$\left(c\frac{\partial}{\partial t} + \frac{\mathrm{d}}{\mathrm{d}s}\right) \rightarrow \frac{\mathrm{d}}{\mathrm{d}s}$$

which applies to a stationary radiation field. The coefficients of this equation depend – as illustrated in Chap. 7 – both on the physical characteristics of the line and on the value of the magnetic field. The line can be 'unstructured' or formed by the superposition of several fine-structure (or hyperfine-structure) components. On the other hand, the splitting of the atomic levels will be described by the Zeeman or Paschen-Back effect regime, depending on the magnetic field value (see Chap. 3).

Throughout this chapter – except Sect. 9.23, dealing with 'structured' lines – we shall be concerned with the simplest situation, where absorption and emission at frequency ν involve an *isolated* spectral line originating in the transition between two levels $(\alpha_\ell J_\ell)$ and $(\alpha_u J_u)$ of an atom devoid of hyperfine structure. We will further assume that the magnetic field is weak enough for the Zeeman effect regime to hold, and that no atomic polarization is present in the two levels. The latter assumption means that the atomic density matrix in the subspace of the magnetic quantum numbers is diagonal and proportional to the unit matrix.

This is a special case of the model that has been denoted in Chap. 7 as 'multilevel atom'. The radiative transfer coefficients in the standard representation are

[1] This is indeed valid for the magnetic fields that are typically found in the solar atmosphere or in magnetic, non-degenerate stars. The case of magnetic white dwarfs (where $B \geq 10^7$ G) is quite different (cf. Kemp, 1970; Lamb and Sutherland, 1974).

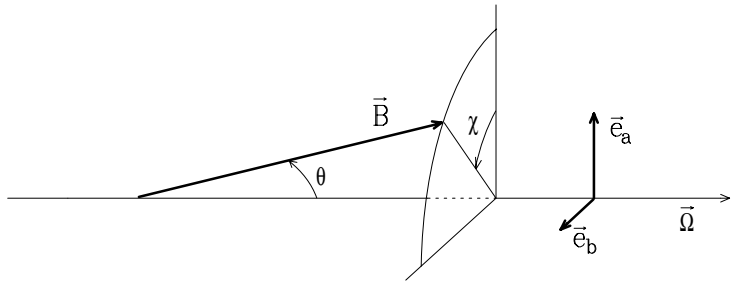

Fig.9.1. The magnetic field direction is specified by the angles θ and χ. $\vec{\Omega}$ is the propagation direction of the radiation while $\vec{e}_a$ is the reference unit vector.

given by Eqs. (7.19), where (because of the isolated spectral line assumption) the summations over the atomic levels are limited to one lower level $(\alpha_\ell J_\ell)$ and one upper level $(\alpha_u J_u)$, and where (because of the no-atomic-polarization assumption) we have to substitute

$$\mathcal{N}\,(2J_\ell+1)\;\rho_{\alpha_\ell J_\ell}(M_\ell) \to \mathcal{N}_\ell$$
$$\mathcal{N}\,(2J_u+1)\;\rho_{\alpha_u J_u}(M_u) \to \mathcal{N}_u\ ,$$

$\mathcal{N}_\ell$ and $\mathcal{N}_u$ being the number of atoms per unit volume in the lower and upper level, respectively. Equation (7.19a) reduces to

$$\eta_i^{\mathrm{A}}(\nu,\vec{\Omega}) = \frac{h\nu}{4\pi}\,\mathcal{N}_\ell\;B(\alpha_\ell J_\ell \to \alpha_u J_u)$$
$$\times \sum_{M_\ell M_u\, q} 3 \begin{pmatrix} J_u & J_\ell & 1 \\ -M_u & M_\ell & -q \end{pmatrix}^2 \mathcal{T}_{qq}(i,\vec{\Omega})\;\phi(\nu_{\alpha_u J_u M_u,\,\alpha_\ell J_\ell M_\ell} - \nu)\ , \quad (9.2)$$

where, according to Eq. (7.3)

$$\nu_{\alpha_u J_u M_u,\alpha_\ell J_\ell M_\ell} = \nu_0 + \nu_{\mathrm{L}}\,(g_u M_u - g_\ell M_\ell)\ , \quad (9.3)$$

with ν_0 the unperturbed frequency of the transition, ν_{L} the Larmor frequency, g_u and g_ℓ the Landé factors of the upper and lower level, respectively.

The quantities $\mathcal{T}_{qq}(i,\vec{\Omega})$ depend on the geometrical relations between the (local) magnetic field vector, the propagation direction $\vec{\Omega}$, and the reference direction chosen to define the Stokes parameters. Let us denote by θ and χ the inclination and azimuth angles of the magnetic field (see Fig. 9.1). Recalling the definitions in Sect. 5.11, we have to find the Euler angles of the rotation that brings the triplet of unit vectors $(\vec{e}_a, \vec{e}_b, \vec{\Omega})$ into a right-handed coordinate system (xyz) having the z-axis along the magnetic field direction (our quantization axis). From Fig. 9.1 we get

$$R \equiv (\chi, \theta, \gamma)\ ,$$

where γ is an arbitrary angle (specifying the orientation of the x and y axes) which does not enter the expressions of $\mathcal{T}_{qq}(i,\vec{\Omega})$. These expressions can be deduced from Table 5.3 which, however, refers to the rotation $R \equiv (-\gamma, -\theta, -\chi)$. Performing the substitutions ($\gamma \rightarrow -\chi$, $\theta \rightarrow -\theta$, $\chi \rightarrow -\gamma$), we obtain

$$\begin{aligned}
&\mathcal{T}_{-1-1}(0,\vec{\Omega}) = \mathcal{T}_{11}(0,\vec{\Omega}) = \frac{1}{4}\left(1+\cos^2\theta\right)\\
&\mathcal{T}_{-1-1}(1,\vec{\Omega}) = \mathcal{T}_{11}(1,\vec{\Omega}) = -\frac{1}{4}\,\sin^2\theta\,\cos 2\chi\\
&\mathcal{T}_{-1-1}(2,\vec{\Omega}) = \mathcal{T}_{11}(2,\vec{\Omega}) = -\frac{1}{4}\,\sin^2\theta\,\sin 2\chi\\
&\mathcal{T}_{-1-1}(3,\vec{\Omega}) = -\mathcal{T}_{11}(3,\vec{\Omega}) = -\frac{1}{2}\,\cos\theta\\
&\mathcal{T}_{00}(0,\vec{\Omega}) = \frac{1}{2}\,\sin^2\theta\\
&\mathcal{T}_{00}(1,\vec{\Omega}) = \frac{1}{2}\,\sin^2\theta\,\cos 2\chi\\
&\mathcal{T}_{00}(2,\vec{\Omega}) = \frac{1}{2}\,\sin^2\theta\,\sin 2\chi\\
&\mathcal{T}_{00}(3,\vec{\Omega}) = 0\ .
\end{aligned}$$

Equation (9.2) can then be cast into the form (see also Eqs. (6.87))

$$\begin{aligned}
\eta_0^{\rm A}(\nu,\vec{\Omega}) =&\ \eta_I^{\rm A}(\nu,\vec{\Omega}) = k_{\rm L}^{\rm A}\,\frac{1}{2}\left[\phi_0\sin^2\theta + \frac{\phi_{-1}+\phi_1}{2}\,(1+\cos^2\theta)\right]\\
\eta_1^{\rm A}(\nu,\vec{\Omega}) =&\ \eta_Q^{\rm A}(\nu,\vec{\Omega}) = k_{\rm L}^{\rm A}\,\frac{1}{2}\left[\phi_0 - \frac{\phi_{-1}+\phi_1}{2}\right]\sin^2\theta\,\cos 2\chi\\
\eta_2^{\rm A}(\nu,\vec{\Omega}) =&\ \eta_U^{\rm A}(\nu,\vec{\Omega}) = k_{\rm L}^{\rm A}\,\frac{1}{2}\left[\phi_0 - \frac{\phi_{-1}+\phi_1}{2}\right]\sin^2\theta\,\sin 2\chi\\
\eta_3^{\rm A}(\nu,\vec{\Omega}) =&\ \eta_V^{\rm A}(\nu,\vec{\Omega}) = k_{\rm L}^{\rm A}\,\frac{1}{2}\left[\phi_1 - \phi_{-1}\right]\cos\theta\ ,
\end{aligned} \tag{9.4}$$

where

$$k_{\rm L}^{\rm A} \;=\; \frac{h\nu}{4\pi}\,\mathcal{N}_\ell\ B(\alpha_\ell J_\ell \rightarrow \alpha_u J_u) \tag{9.5}$$

is the frequency-integrated absorption coefficient in the line[1] and where

$$\phi_q = \sum_{M_\ell M_u} 3\begin{pmatrix} J_u & J_\ell & 1\\ -M_u & M_\ell & -q\end{pmatrix}^2 \phi(\nu_{\alpha_u J_u M_u,\,\alpha_\ell J_\ell M_\ell} - \nu) \qquad (q=-1,0,+1)\,. \tag{9.6}$$

[1] Since the ϕ_q profiles are normalized to unity in frequency (cf. Eqs. (6.59c) and (2.23a)), we have

$$\int_{\rm line} \eta_I^{\rm A}(\nu,\vec{\Omega})\,{\rm d}\nu \;=\; k_{\rm L}^{\rm A}\ .$$

With strictly analogous substitutions one finds from Eq. (7.19c)

$$\begin{aligned}
\rho_1^{\mathrm{A}}(\nu,\vec{\Omega}) &= \rho_Q^{\mathrm{A}}(\nu,\vec{\Omega}) = k_{\mathrm{L}}^{\mathrm{A}}\,\frac{1}{2}\left[\psi_0 - \frac{\psi_{-1}+\psi_1}{2}\right]\sin^2\theta\,\cos 2\chi \\
\rho_2^{\mathrm{A}}(\nu,\vec{\Omega}) &= \rho_U^{\mathrm{A}}(\nu,\vec{\Omega}) = k_{\mathrm{L}}^{\mathrm{A}}\,\frac{1}{2}\left[\psi_0 - \frac{\psi_{-1}+\psi_1}{2}\right]\sin^2\theta\,\sin 2\chi \\
\rho_3^{\mathrm{A}}(\nu,\vec{\Omega}) &= \rho_V^{\mathrm{A}}(\nu,\vec{\Omega}) = k_{\mathrm{L}}^{\mathrm{A}}\,\frac{1}{2}\left[\psi_1 - \psi_{-1}\right]\cos\theta\,,
\end{aligned} \tag{9.7}$$

where

$$\psi_q = \sum_{M_\ell M_u} 3\begin{pmatrix} J_u & J_\ell & 1 \\ -M_u & M_\ell & -q \end{pmatrix}^2 \psi(\nu_{\alpha_u J_u M_u,\,\alpha_\ell J_\ell M_\ell} - \nu) \qquad (q=-1,0,+1). \tag{9.8}$$

Equations (9.4) and (9.7) can be conveniently rewritten in the form

$$\begin{aligned}
\eta_I^{\mathrm{A}}(\nu,\vec{\Omega}) &= k_{\mathrm{L}}^{\mathrm{A}}\,\phi_I(\nu,\vec{\Omega}) \\
\eta_Q^{\mathrm{A}}(\nu,\vec{\Omega}) &= k_{\mathrm{L}}^{\mathrm{A}}\,\phi_Q(\nu,\vec{\Omega}) & \rho_Q^{\mathrm{A}}(\nu,\vec{\Omega}) &= k_{\mathrm{L}}^{\mathrm{A}}\,\psi_Q(\nu,\vec{\Omega}) \\
\eta_U^{\mathrm{A}}(\nu,\vec{\Omega}) &= k_{\mathrm{L}}^{\mathrm{A}}\,\phi_U(\nu,\vec{\Omega}) & \rho_U^{\mathrm{A}}(\nu,\vec{\Omega}) &= k_{\mathrm{L}}^{\mathrm{A}}\,\psi_U(\nu,\vec{\Omega}) \\
\eta_V^{\mathrm{A}}(\nu,\vec{\Omega}) &= k_{\mathrm{L}}^{\mathrm{A}}\,\phi_V(\nu,\vec{\Omega}) & \rho_V^{\mathrm{A}}(\nu,\vec{\Omega}) &= k_{\mathrm{L}}^{\mathrm{A}}\,\psi_V(\nu,\vec{\Omega})\,,
\end{aligned}$$

with

$$\begin{aligned}
\phi_I(\nu,\vec{\Omega}) &= \frac{1}{2}\left[\phi_0\sin^2\theta + \frac{\phi_{-1}+\phi_1}{2}\,(1+\cos^2\theta)\right] \\
\phi_Q(\nu,\vec{\Omega}) &= \frac{1}{2}\left[\phi_0 - \frac{\phi_{-1}+\phi_1}{2}\right]\sin^2\theta\,\cos 2\chi \\
\phi_U(\nu,\vec{\Omega}) &= \frac{1}{2}\left[\phi_0 - \frac{\phi_{-1}+\phi_1}{2}\right]\sin^2\theta\,\sin 2\chi \\
\phi_V(\nu,\vec{\Omega}) &= \frac{1}{2}\left[\phi_1 - \phi_{-1}\right]\cos\theta \\
\psi_Q(\nu,\vec{\Omega}) &= \frac{1}{2}\left[\psi_0 - \frac{\psi_{-1}+\psi_1}{2}\right]\sin^2\theta\,\cos 2\chi \\
\psi_U(\nu,\vec{\Omega}) &= \frac{1}{2}\left[\psi_0 - \frac{\psi_{-1}+\psi_1}{2}\right]\sin^2\theta\,\sin 2\chi \\
\psi_V(\nu,\vec{\Omega}) &= \frac{1}{2}\left[\psi_1 - \psi_{-1}\right]\cos\theta\,.
\end{aligned} \tag{9.9}$$

Using these notations, one gets for the stimulated emission coefficients (Eqs. (7.19b) and (7.19d))

$$
\begin{aligned}
\eta_0^{\rm S}(\nu,\vec{\Omega}) = \eta_I^{\rm S}(\nu,\vec{\Omega}) &= k_{\rm L}^{\rm S}\,\phi_I(\nu,\vec{\Omega}) \\
\eta_1^{\rm S}(\nu,\vec{\Omega}) = \eta_Q^{\rm S}(\nu,\vec{\Omega}) &= k_{\rm L}^{\rm S}\,\phi_Q(\nu,\vec{\Omega}) \\
\eta_2^{\rm S}(\nu,\vec{\Omega}) = \eta_U^{\rm S}(\nu,\vec{\Omega}) &= k_{\rm L}^{\rm S}\,\phi_U(\nu,\vec{\Omega}) \\
\eta_3^{\rm S}(\nu,\vec{\Omega}) = \eta_V^{\rm S}(\nu,\vec{\Omega}) &= k_{\rm L}^{\rm S}\,\phi_V(\nu,\vec{\Omega}) \\
\rho_1^{\rm S}(\nu,\vec{\Omega}) = \rho_Q^{\rm S}(\nu,\vec{\Omega}) &= k_{\rm L}^{\rm S}\,\psi_Q(\nu,\vec{\Omega}) \\
\rho_2^{\rm S}(\nu,\vec{\Omega}) = \rho_U^{\rm S}(\nu,\vec{\Omega}) &= k_{\rm L}^{\rm S}\,\psi_U(\nu,\vec{\Omega}) \\
\rho_3^{\rm S}(\nu,\vec{\Omega}) = \rho_V^{\rm S}(\nu,\vec{\Omega}) &= k_{\rm L}^{\rm S}\,\psi_V(\nu,\vec{\Omega})\,,
\end{aligned}
$$

where

$$
k_{\rm L}^{\rm S} = \frac{h\nu}{4\pi}\,\mathcal{N}_u\;B(\alpha_u J_u \rightarrow \alpha_\ell J_\ell)\,,
$$

and for the spontaneous emission coefficients (Eq. (7.19e); see also Eqs. (7.8))

$$
\begin{aligned}
\varepsilon_0(\nu,\vec{\Omega}) = \varepsilon_I(\nu,\vec{\Omega}) &= \varepsilon_{\rm L}\,\phi_I(\nu,\vec{\Omega}) \\
\varepsilon_1(\nu,\vec{\Omega}) = \varepsilon_Q(\nu,\vec{\Omega}) &= \varepsilon_{\rm L}\,\phi_Q(\nu,\vec{\Omega}) \\
\varepsilon_2(\nu,\vec{\Omega}) = \varepsilon_U(\nu,\vec{\Omega}) &= \varepsilon_{\rm L}\,\phi_U(\nu,\vec{\Omega}) \\
\varepsilon_3(\nu,\vec{\Omega}) = \varepsilon_V(\nu,\vec{\Omega}) &= \varepsilon_{\rm L}\,\phi_V(\nu,\vec{\Omega})\,,
\end{aligned}
\tag{9.10}
$$

where

$$
\varepsilon_{\rm L} = \frac{h\nu}{4\pi}\,\mathcal{N}_u\;A(\alpha_u J_u \rightarrow \alpha_\ell J_\ell)\,. \tag{9.11}
$$

Collecting all the various terms, the contribution of the line to the radiative transfer equation for polarized radiation takes the form

$$
\frac{\rm d}{{\rm d}s}\begin{pmatrix} I \\ Q \\ U \\ V \end{pmatrix} = -\,k_{\rm L}\begin{pmatrix} \phi_I & \phi_Q & \phi_U & \phi_V \\ \phi_Q & \phi_I & \psi_V & -\psi_U \\ \phi_U & -\psi_V & \phi_I & \psi_Q \\ \phi_V & \psi_U & -\psi_Q & \phi_I \end{pmatrix}\begin{pmatrix} I - S_{\rm L} \\ Q \\ U \\ V \end{pmatrix}, \tag{9.12}
$$

where

$$
k_{\rm L} = k_{\rm L}^{\rm A} - k_{\rm L}^{\rm S}
$$

is the (frequency-integrated) line absorption coefficient corrected for stimulated emission, and where

$$
S_{\rm L} = \frac{\varepsilon_{\rm L}}{k_{\rm L}^{\rm A} - k_{\rm L}^{\rm S}} \tag{9.13}
$$

is the line source function. Using the well-known relations among the Einstein coefficients (see Eqs. (7.8)), these two quantities can be rewritten as

$$
k_{\rm L} = k_{\rm L}^{\rm A}\left(1 - \frac{\mathcal{N}_u}{\mathcal{N}_\ell}\,\frac{\tilde{g}_\ell}{\tilde{g}_u}\right), \qquad S_{\rm L} = \frac{2h\nu_0^3}{c^2}\left(\frac{\mathcal{N}_\ell}{\mathcal{N}_u}\,\frac{\tilde{g}_u}{\tilde{g}_\ell} - 1\right)^{-1}, \tag{9.14}
$$

where $\tilde{g}_\ell = (2J_\ell + 1)$ and $\tilde{g}_u = (2J_u + 1)$ are the degeneracies of the lower and upper level, respectively. In the particular case of LTE, one simply gets

$$k_{\rm L} = k_{\rm L}^{\rm A}\left(1 - {\rm e}^{-\frac{h\nu_0}{k_{\rm B}T}}\right), \qquad S_{\rm L} = \frac{2h\nu_0^3}{c^2}\left({\rm e}^{\frac{h\nu_0}{k_{\rm B}T}} - 1\right)^{-1} = B_{\rm P}(\nu_0)\,.$$

Adding the contributions of continuum processes and line processes, one obtains from Eqs. (9.1) and (9.12)

$$\frac{\rm d}{{\rm d}s}\begin{pmatrix} I \\ Q \\ U \\ V \end{pmatrix} = -\,k_{\rm c}\begin{pmatrix} 1 & 0 & 0 & 0 \\ 0 & 1 & 0 & 0 \\ 0 & 0 & 1 & 0 \\ 0 & 0 & 0 & 1 \end{pmatrix}\begin{pmatrix} I - S_{\rm c} \\ Q \\ U \\ V \end{pmatrix}$$
$$-\,k_{\rm L}\begin{pmatrix} \phi_I & \phi_Q & \phi_U & \phi_V \\ \phi_Q & \phi_I & \psi_V & -\psi_U \\ \phi_U & -\psi_V & \phi_I & \psi_Q \\ \phi_V & \psi_U & -\psi_Q & \phi_I \end{pmatrix}\begin{pmatrix} I - S_{\rm L} \\ Q \\ U \\ V \end{pmatrix}. \qquad (9.15)$$

It should be noticed that the equations derived in this section prove some properties of the Zeeman patterns that were anticipated in Sect. 3.1. First of all, the ϕ_q and ψ_q profiles in Eqs. (9.6) and (9.8) can be written in the form

$$\phi_q = \sum_{M_\ell M_u} S_q^{J_\ell J_u}(M_\ell, M_u)\ \phi(\nu_{\alpha_u J_u M_u, \alpha_\ell J_\ell M_\ell} - \nu)$$
$$\psi_q = \sum_{M_\ell M_u} S_q^{J_\ell J_u}(M_\ell, M_u)\ \psi(\nu_{\alpha_u J_u M_u, \alpha_\ell J_\ell M_\ell} - \nu)\,, \qquad (9.16)$$

where Eq. (3.16) has been used. Thus the quantity $S_q^{J_\ell J_u}(M_\ell, M_u)$ is indeed the relative strength of the Zeeman component ($\sigma_{\rm b}$, π or $\sigma_{\rm r}$ according as $q = -1$, 0, $+1$, respectively) connecting the sublevels $(J_\ell M_\ell)$ and $(J_u M_u)$. The strengths are normalized as in Eq. (3.17) and satisfy the relations (3.18)-(3.19). Furthermore, the polarization features of the radiation emitted by each type of component can be deduced from Eq. (9.10), and it is easily seen that they are just as illustrated in Sect. 3.1 (cf. Figs. 9.1 and 3.1).

9.2. Comparison with the Classical Theory

We are now in a position to compare the line transfer equation derived from Quantum Mechanics with the corresponding equation derived from classical physics in Chap. 5. Direct comparison of Eqs. (9.12) and (5.39) shows that the structure of the two equations is exactly the same and allows us to relate the line source

function $S_{\rm L}$, as given by Eq. (9.14), with the 'classical' source function defined in Eq. (5.40). Equating the two expressions (and neglecting in $S_{\rm L}$ the contribution due to stimulated emission, a phenomenon that has no classical analogue) one finds a relationship between the average energy per degree of freedom of the classical oscillator, $\bar{E}$, and the number density of atoms in the lower and upper level

$$\bar{E} = h\nu_0 \, \frac{\mathcal{N}_u / \tilde{g}_u}{\mathcal{N}_\ell / \tilde{g}_\ell} \, .$$

This is just the expression that is obtained for a two-level atom having a probability $\mathcal{N}_u/\tilde{g}_u$ of being found in the upper level (of energy $h\nu_0$) and a much larger probability $\mathcal{N}_\ell/\tilde{g}_\ell$ of being found in the lower level (of zero energy).

Comparison of Eqs. (9.12) and (5.39) also shows that the elements of the propagation matrix coincide provided the following transformations are performed (see Eqs. (9.9) and (5.36), and Figs. 9.1 and 5.1)

$$\frac{\pi e_0^2}{mc} \, N \to k_{\rm L} \tag{9.17}$$

and

$$\begin{aligned} \phi_{\rm b} &\to \phi_{-1} \qquad & \psi_{\rm b} &\to \psi_{-1} \\ \phi_{\rm p} &\to \phi_0 \qquad & \psi_{\rm p} &\to \psi_0 \\ \phi_{\rm r} &\to \phi_1 \qquad & \psi_{\rm r} &\to \psi_1 \, . \end{aligned} \tag{9.18}$$

Transformation (9.17) can be easily interpreted if we neglect again stimulated emission and write the frequency-integrated line absorption coefficient in the form

$$k_{\rm L} \to k_{\rm L}^{\rm A} = \frac{\pi e_0^2}{mc} \, \mathcal{N}_\ell \; f(\alpha_\ell J_\ell \to \alpha_u J_u) \, , \tag{9.19}$$

where $f(\alpha_\ell J_\ell \to \alpha_u J_u)$ is the *oscillator strength* of the transition. The dimensionless parameter f can be regarded as an efficiency parameter for the transition: multiplication of the number of atoms in the lower level by f yields the equivalent number of classical oscillators. Comparison of Eqs. (9.19) and (9.5) shows that the oscillator strength is given by

$$f(\alpha_\ell J_\ell \to \alpha_u J_u) = \frac{h\nu \, mc}{4\pi^2 \, e_0^2} \; B(\alpha_\ell J_\ell \to \alpha_u J_u) \, ,$$

or, using Eqs. (7.6) and (7.7)

$$\begin{aligned} f(\alpha_\ell J_\ell \to \alpha_u J_u) &= \frac{8\pi^2}{3} \, \frac{m\,\nu}{h\, e_0^2} \; |\langle \alpha_\ell J_\ell \| \vec{d} \, \| \alpha_u J_u \rangle|^2 \\ &= \frac{1}{8\pi^2} \, \frac{mc^3}{e_0^2 \, \nu^2} \, \frac{2J_u + 1}{2J_\ell + 1} \, A(\alpha_u J_u \to \alpha_\ell J_\ell) \, . \end{aligned} \tag{9.20}$$

The oscillator strength is generally a quite small number which can attain a value of order unity only for the strongest spectral lines.

The correspondence between classical oscillators and atomic transitions also appears from transformation (9.18). Some qualitative aspects of this correspondence have been anticipated in Sect. 3.2. More quantitatively, recalling Eqs. (9.3) and (6.59a), and neglecting the frequency shifts, we have from Eqs. (9.16)

$$\phi_q = \sum_{M_\ell M_u} S_q^{J_\ell J_u}(M_\ell, M_u)\ \frac{1}{\pi}\ \frac{\Gamma}{\Gamma^2 + [\,\nu_0 + \nu_{\rm L}\,(g_u M_u - g_\ell M_\ell) - \nu\,]^2}$$

$$\psi_q = \sum_{M_\ell M_u} S_q^{J_\ell J_u}(M_\ell, M_u)\ \frac{1}{\pi}\ \frac{\nu_0 + \nu_{\rm L}\,(g_u M_u - g_\ell M_\ell) - \nu}{\Gamma^2 + [\,\nu_0 + \nu_{\rm L}\,(g_u M_u - g_\ell M_\ell) - \nu\,]^2}\ , \qquad (9.21)$$

where Γ, defined in Eq. (6.59b), is the natural width of the line

$$\Gamma = \frac{\gamma_\ell + \gamma_u}{4\pi}\ ,$$

with γ_ℓ and γ_u the inverse lifetimes of the lower and upper level, respectively. In particular, for a normal Zeeman triplet having unit Landé factor ($g_\ell = 1$ if $J_u = 0$, or $g_u = 1$ if $J_\ell = 0$), we simply have

$$\nu_0 + \nu_{\rm L}\,(g_u M_u - g_\ell M_\ell) - \nu \;=\; \nu_0 + \nu_{\rm L}\,(M_u - M_\ell) - \nu \;=\; \nu_0 - \nu_{\rm L}\,q - \nu\ ,$$

and performing the sum over M_ℓ and M_u via Eq. (3.17)

$$\phi_q = \frac{1}{\pi}\ \frac{\Gamma}{\Gamma^2 + (\nu_0 - \nu_{\rm L}\,q - \nu)^2}$$

$$\psi_q = \frac{1}{\pi}\ \frac{\nu_0 - \nu_{\rm L}\,q - \nu}{\Gamma^2 + (\nu_0 - \nu_{\rm L}\,q - \nu)^2}\ .$$

Since the components $\sigma_{\rm b}$, π, $\sigma_{\rm r}$ correspond to $q = -1,\ 0,\ +1$ respectively, these profiles are just the same as the 'classical' profiles given by Eqs. (5.37).

Therefore, as far as the absorption and anomalous dispersion profiles are concerned, the theory developed from the principles of Quantum Electrodynamics leads, for the case of a normal Zeeman triplet with unit Landé factor, to the same results as the classical theory. The latter is however unable to describe the more general case of anomalous Zeeman patterns. This can only be done by considering the strengths and splittings of the different components, as derived from the quantum-mechanical theory.

9.3. Collisional and Doppler Broadening

The absorption and anomalous dispersion profiles given by Eqs. (9.21) are still inadequate to describe the physical situation of a stellar atmosphere. This is because the quantum theory presented in Chap. 6 is based on the assumption that

the material system (the atom in this case) interacting with the radiation field is isolated and at rest. The obvious consequence is that the absorption and anomalous dispersion profiles are broadened by a single mechanism, namely *natural* (or *radiation*) *damping*.

Collisional broadening can be carried into our formalism in a rather straightforward way. The effect of collisions is simply described by replacing Γ, the natural line width appearing in Eqs. (9.21), with the sum Γ' of the natural and collisional width, defined by

$$\Gamma' = \Gamma + 2\Gamma_{\rm c} \, . \tag{9.22}$$

This result has been proved in Sect. 5.14 within the framework of the classical theory (see Eq. (5.180)). It still holds, however, when more refined, quantum-mechanical models of the atom-radiation interaction are considered (see for instance Loudon, 1983).

To get an estimate of the collisional width, we recall that $\Gamma_{\rm c}$ is proportional to the frequency f of perturbing collisions ($\Gamma_{\rm c} = f/4\pi$, see Sect. 5.14), and that f has already been estimated in Sect. 7.13.c in connection with our discussion of depolarizing rates.[1] If we assume that perturbing collisions are mainly due to long-range interactions with neutral perturbers (hydrogen atoms),[2] we get from Eqs. (5.181) and (7.105)[3]

$$\Gamma_{\rm c} = 0.68 \left[C_6(\alpha_u J_u)\right]^{0.4} \, \bar{v}_{\rm r}^{0.6} \, n_{\rm H} \, ,$$

where $C_6(\alpha_u J_u)$ is the Van der Waals constant for the upper level involved in the transition, $\bar{v}_{\rm r}$ the average relative velocity atom-perturber, and $n_{\rm H}$ the number density of hydrogen atoms. Using Eq. (7.108) we can also write

$$\Gamma_{\rm c} \simeq 1.1 \times 10^{-11} \left[\left\langle r^2(\alpha_u J_u)\right\rangle\right]^{0.4} \left[T\left(1+\frac{1}{\mu}\right)\right]^{0.3} n_{\rm H} \quad {\rm s}^{-1} \, ,$$

where $\left\langle r^2(\alpha_u J_u)\right\rangle$ is the mean square radius of the electronic cloud in the level $(\alpha_u J_u)$ expressed in atomic units, T is the temperature in K, μ is the atomic weight of the atom, and $n_{\rm H}$ is expressed in cm^{-3}.

When collisions are taken into account, the profiles ϕ_q and ψ_q in Eqs. (9.21) become

---

1 It should be remarked that both the phenomena of collisional broadening and atomic-level depolarization are basically due to the same physical mechanism, as shown in Sect. 5.14.

2 By so doing, we neglect collisions with electrons and ions. In typical stellar atmospheres, their contribution to collisional line broadening is quite modest (with the exception of hydrogen and helium lines). An excellent discussion of collisional broadening due to charged particles can be found in Mihalas (1978) or in Griem (1974).

3 This result agrees with the often quoted expression of Unsöld (1955)

$$\Gamma_{\rm U} \simeq 17 \; C_6^{2/5} \, \bar{v}_{\rm r}^{3/5} \, n_{\rm H} \, .$$

The definition of $\Gamma_{\rm U}$ is such that $\Gamma_{\rm U} = 8\pi\,\Gamma_{\rm c}$.

$$\phi_q = \sum_{M_\ell M_u} S_q^{J_\ell J_u}(M_\ell, M_u)\ \frac{1}{\pi}\ \frac{\Gamma'}{\Gamma'^2 + [\,\nu_0 + \nu_{\rm L}\,(g_u M_u - g_\ell M_\ell) - \nu\,]^2}$$

$$\psi_q = \sum_{M_\ell M_u} S_q^{J_\ell J_u}(M_\ell, M_u)\ \frac{1}{\pi}\ \frac{\nu_0 + \nu_{\rm L}\,(g_u M_u - g_\ell M_\ell) - \nu}{\Gamma'^2 + [\,\nu_0 + \nu_{\rm L}\,(g_u M_u - g_\ell M_\ell) - \nu\,]^2}\ ,$$

where

$$\Gamma' = \Gamma + 2\Gamma_{\rm c}\ .$$

As far as the motion of the atomic system is concerned, we already noticed (see the discussion following Eq. (6.31)) that the quantum theory presented in Chap. 6 cannot account for the Doppler effect. However, this effect can be reintroduced in our formalism by the same arguments outlined in Sect. 5.4. By so doing we obtain

$$\phi_q = \sum_{M_\ell M_u} S_q^{J_\ell J_u}(M_\ell, M_u)\ \frac{1}{\sqrt{\pi}}\ \frac{1}{\Delta\nu_{\rm D}}\ H\big(v - v_{\rm A} + v_B\,(g_u M_u - g_\ell M_\ell),\, a\big)$$

$$\psi_q = \sum_{M_\ell M_u} S_q^{J_\ell J_u}(M_\ell, M_u)\ \frac{1}{\sqrt{\pi}}\ \frac{1}{\Delta\nu_{\rm D}}\ L\big(v - v_{\rm A} + v_B\,(g_u M_u - g_\ell M_\ell),\, a\big)\ , \qquad (9.23)$$

where the functions $H(v,a)$ and $L(v,a)$ are defined in Eqs. (5.45), and where

$$\Delta\nu_{\rm D} = \nu_0\,\frac{w_{\rm T}}{c}\ , \qquad a = \frac{\Gamma'}{\Delta\nu_{\rm D}}$$

$$v_B = \frac{\nu_{\rm L}}{\Delta\nu_{\rm D}}\ , \qquad v_{\rm A} = \frac{w_{\rm A}}{w_{\rm T}} = \frac{\nu_0\,w_{\rm A}}{c\,\Delta\nu_{\rm D}}\ , \qquad v = \frac{\nu_0 - \nu}{\Delta\nu_{\rm D}}\ . \qquad (9.24)$$

Note that these equations are the same as Eqs. (5.43) except for the definition of the damping constant a, where Γ' is substituted for Γ in order to allow for collisional broadening. We recall that $w_{\rm A}$ and $w_{\rm T}$ represent the line-of-sight component of the bulk velocity of the ambient medium and the thermal velocity, respectively.

As mentioned in Sect. 5.4, the various quantities entering the definitions of the dimensionless parameters v, $v_{\rm A}$, v_B, a can be expressed in wavelength units rather than in frequency units. Introducing the Doppler width in wavelength units

$$\Delta\lambda_{\rm D} = \frac{\lambda_0^2}{c}\,\Delta\nu_{\rm D} = \lambda_0\,\frac{w_{\rm T}}{c}\ , \qquad (9.25)$$

we can write (cf. Eqs. (5.47))

$$v = \frac{\lambda - \lambda_0}{\Delta\lambda_{\rm D}}\ , \qquad a = \frac{\lambda_0^2\,\Gamma'}{c\,\Delta\lambda_{\rm D}}\ , \qquad v_{\rm A} = \frac{\lambda_0\,w_{\rm A}}{c\,\Delta\lambda_{\rm D}}$$

$$v_B = \frac{\lambda_0^2\,\nu_{\rm L}}{c\,\Delta\lambda_{\rm D}} = \frac{\lambda_0^2\,e_0\,B}{4\pi mc^2\,\Delta\lambda_{\rm D}} = \frac{\Delta\lambda_B}{\Delta\lambda_{\rm D}}\ . \qquad (9.26)$$

A numerical expression for v_B is given in Eq. (5.49).

9.4. Different Forms of the Transfer Equation

For practical applications, and especially for those concerning the diagnostics of magnetic fields in the solar and stellar atmospheres, it may be convenient to write the transfer equation (9.15) in other forms, using different definitions for the absorption and anomalous dispersion profiles and/or substituting optical depth for geometrical depth.

Consider first the propagation matrix multiplying $k_{\rm L}$ in the right-hand side of Eq. (9.15). This matrix contains the seven independent quantities ϕ_I, ϕ_Q, ϕ_U, ϕ_V, ψ_Q, ψ_U, ψ_V defined in Eqs. (9.9), which are linear combinations of the profiles ϕ_q or ψ_q defined in Eqs. (9.23). It can be easily shown via Eqs. (3.17) and (5.60) that the profiles ϕ_q are normalized to unity in frequency,

$$\int_{-\infty}^{\infty} \phi_q \, {\rm d}\nu = 1 \ .$$

It is customary to introduce different profiles, η_q, normalized to unity in v, the reduced frequency (or wavelength) defined in Eqs. (9.24)-(9.26). Setting

$$\begin{aligned} \eta_q &= \Delta\nu_{\rm D} \, \phi_q \\ &= \sum_{M_\ell M_u} S_q^{J_\ell J_u}(M_\ell, M_u) \ \frac{1}{\sqrt{\pi}} \, H\big(v - v_{\rm A} + v_B \, (g_u M_u - g_\ell M_\ell), \, a\big) \end{aligned} \tag{9.27a}$$

and, by analogy

$$\begin{aligned} \rho_q &= \Delta\nu_{\rm D} \, \psi_q \\ &= \sum_{M_\ell M_u} S_q^{J_\ell J_u}(M_\ell, M_u) \ \frac{1}{\sqrt{\pi}} \, L\big(v - v_{\rm A} + v_B \, (g_u M_u - g_\ell M_\ell), \, a\big) \ , \end{aligned} \tag{9.27b}$$

we obviously have

$$\int_{-\infty}^{\infty} \eta_q \, {\rm d}v = 1 \ , \tag{9.28}$$

and introducing the notation

$$\begin{aligned} \eta_{\rm b} &= \eta_{-1} \qquad & \rho_{\rm b} &= \rho_{-1} \\ \eta_{\rm p} &= \eta_0 \qquad & \rho_{\rm p} &= \rho_0 \\ \eta_{\rm r} &= \eta_1 \qquad & \rho_{\rm r} &= \rho_1 \ , \end{aligned} \tag{9.29}$$

the transfer equation for polarized radiation can be written in the form

$$\frac{\mathrm{d}}{\mathrm{d}s}\begin{pmatrix} I \\ Q \\ U \\ V \end{pmatrix} = -k_{\mathrm{c}}\left\{\begin{pmatrix} 1 & 0 & 0 & 0 \\ 0 & 1 & 0 & 0 \\ 0 & 0 & 1 & 0 \\ 0 & 0 & 0 & 1 \end{pmatrix}\begin{pmatrix} I - S_{\mathrm{c}} \\ Q \\ U \\ V \end{pmatrix}\right.$$
$$\left. + \kappa_{\mathrm{L}}\begin{pmatrix} h_I & h_Q & h_U & h_V \\ h_Q & h_I & r_V & -r_U \\ h_U & -r_V & h_I & r_Q \\ h_V & r_U & -r_Q & h_I \end{pmatrix}\begin{pmatrix} I - S_{\mathrm{L}} \\ Q \\ U \\ V \end{pmatrix}\right\}, \qquad (9.30)$$

where κ_{L}, the ratio between the frequency-integrated line absorption coefficient (corrected for stimulated emission and expressed in Doppler width units) and the continuum absorption coefficient at the line wavelength, is given by (see Eqs. (9.14) and (9.19))

$$\kappa_{\mathrm{L}} = \frac{k_{\mathrm{L}}}{k_{\mathrm{c}}\,\Delta\nu_{\mathrm{D}}} = \frac{\pi e_0^2}{mc}\,\frac{\mathcal{N}_\ell\; f(\alpha_\ell J_\ell \rightarrow \alpha_u J_u)}{k_{\mathrm{c}}\,\Delta\nu_{\mathrm{D}}}\left(1 - \frac{\mathcal{N}_u}{\mathcal{N}_\ell}\,\frac{\tilde{g}_\ell}{\tilde{g}_u}\right), \qquad (9.31)$$

and where

$$\begin{aligned} h_I &= \frac{1}{2}\left[\eta_{\mathrm{p}}\sin^2\theta + \frac{\eta_{\mathrm{b}} + \eta_{\mathrm{r}}}{2}\left(1 + \cos^2\theta\right)\right] \\ h_Q &= \frac{1}{2}\left[\eta_{\mathrm{p}} - \frac{\eta_{\mathrm{b}} + \eta_{\mathrm{r}}}{2}\right]\sin^2\theta\,\cos 2\chi \\ h_U &= \frac{1}{2}\left[\eta_{\mathrm{p}} - \frac{\eta_{\mathrm{b}} + \eta_{\mathrm{r}}}{2}\right]\sin^2\theta\,\sin 2\chi \\ h_V &= \frac{1}{2}\left[\eta_{\mathrm{r}} - \eta_{\mathrm{b}}\right]\cos\theta \\ r_Q &= \frac{1}{2}\left[\rho_{\mathrm{p}} - \frac{\rho_{\mathrm{b}} + \rho_{\mathrm{r}}}{2}\right]\sin^2\theta\,\cos 2\chi \\ r_U &= \frac{1}{2}\left[\rho_{\mathrm{p}} - \frac{\rho_{\mathrm{b}} + \rho_{\mathrm{r}}}{2}\right]\sin^2\theta\,\sin 2\chi \\ r_V &= \frac{1}{2}\left[\rho_{\mathrm{r}} - \rho_{\mathrm{b}}\right]\cos\theta\,. \end{aligned} \qquad (9.32)$$

With the present definitions,[1] the ratio between the line absorption coefficient at line center and the continuum absorption coefficient is given, for zero magnetic field

[1] Note that κ_{L}, as well as h_I, h_Q, h_U, h_V, r_Q, r_U, r_V, are dimensionless quantities. For the sake of brevity, the parameter κ_{L} will be sometimes referred to in the following as the 'ratio between line and continuum absorption coefficients'.

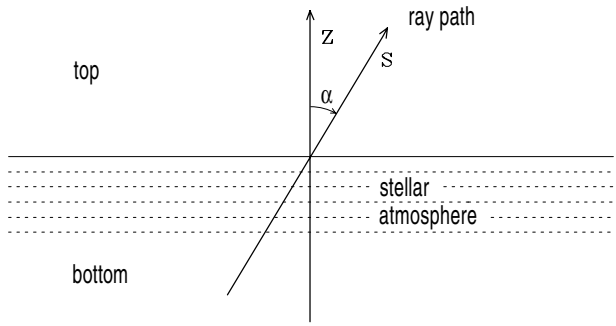

Fig.9.2. The coordinates s and z generally used for radiative transfer in stellar atmospheres.

and no damping, by $\kappa_{\rm L}\,/\sqrt{\pi}$ (see Eqs. (5.55), (9.27), (3.17) and (9.32)). Different definitions can be found in the literature, where the symbol η_0 is often used to represent the ratio $k_{\rm L}\,/(k_{\rm c}\,\Delta\nu_{\rm D}\,\sqrt{\pi}\,)$ (thus resulting a factor $\sqrt{\pi}$ smaller than $\kappa_{\rm L}$), and where the profiles $\eta_{\rm b}\,,\ \eta_{\rm p}\,,\ \eta_{\rm r}\,,\ \rho_{\rm b}\,,\ \rho_{\rm p}\,,\ \rho_{\rm r}$ are defined as in Eqs. (9.29) and (9.27) *without* the factor $1\,/\sqrt{\pi}$ (thus resulting a factor $\sqrt{\pi}$ larger than ours).

When dealing with radiative transfer in astrophysical plasmas, it is generally convenient to refer to the familiar concept of optical depth. The coordinate s measured along the ray path can be replaced by the optical depth $\tau_{\rm c}$ in the continuum adjacent to the line, or by the optical depth $\tau_{\rm r}$ in the continuum at a given reference frequency $\nu_{\rm r}$, or by the optical depth $\tau_{\rm L}$ in the line. These quantities are defined by

$$\mathrm{d}\tau_{\rm c} = -k_{\rm c}(\nu_0)\,\mathrm{d}s\ , \qquad \mathrm{d}\tau_{\rm r} = -k_{\rm c}(\nu_{\rm r})\,\mathrm{d}s\ , \qquad \mathrm{d}\tau_{\rm L} = -\frac{k_{\rm L}}{\Delta\nu_{\rm D}}\,\mathrm{d}s\ , \tag{9.33}$$

where the minus sign means that the increasing direction for optical depth is opposite to the propagation direction. For plane-parallel atmospheres, optical depths can be referred to the coordinate z measured outward along the vertical to the atmosphere. If we denote by t such optical depths and if α is the angle defined in Fig. 9.2, we obviously have

$$\begin{aligned} \mathrm{d}t_{\rm c} &= -k_{\rm c}(\nu_0)\,\mathrm{d}z = \mu\,\mathrm{d}\tau_{\rm c} \\ \mathrm{d}t_{\rm r} &= -k_{\rm c}(\nu_{\rm r})\,\mathrm{d}z = \mu\,\mathrm{d}\tau_{\rm r} \\ \mathrm{d}t_{\rm L} &= -\frac{k_{\rm L}}{\Delta\nu_{\rm D}}\,\mathrm{d}z = \mu\,\mathrm{d}\tau_{\rm L}\ , \end{aligned} \tag{9.34}$$

where $\mu = \cos\alpha$.

Introducing, for instance, the optical depth $\tau_{\rm c}$, Eq. (9.30) becomes

$$\frac{\mathrm{d}}{\mathrm{d}\tau_{\rm c}} \begin{pmatrix} I \\ Q \\ U \\ V \end{pmatrix} = \begin{pmatrix} 1 & 0 & 0 & 0 \\ 0 & 1 & 0 & 0 \\ 0 & 0 & 1 & 0 \\ 0 & 0 & 0 & 1 \end{pmatrix} \begin{pmatrix} I - S_{\rm c} \\ Q \\ U \\ V \end{pmatrix} +$$

$$+\ \kappa_{\rm L}\begin{pmatrix} h_I & h_Q & h_U & h_V \\ h_Q & h_I & r_V & -r_U \\ h_U & -r_V & h_I & r_Q \\ h_V & r_U & -r_Q & h_I \end{pmatrix}\begin{pmatrix} I-S_{\rm L} \\ Q \\ U \\ V \end{pmatrix}\ , \tag{9.35}$$

while introducing the optical depth $\tau_{\rm L}$ we have

$$\frac{\rm d}{{\rm d}\tau_{\rm L}}\begin{pmatrix} I \\ Q \\ U \\ V \end{pmatrix} = \kappa_{\rm c}\begin{pmatrix} 1 & 0 & 0 & 0 \\ 0 & 1 & 0 & 0 \\ 0 & 0 & 1 & 0 \\ 0 & 0 & 0 & 1 \end{pmatrix}\begin{pmatrix} I-S_{\rm c} \\ Q \\ U \\ V \end{pmatrix}$$
$$+\begin{pmatrix} h_I & h_Q & h_U & h_V \\ h_Q & h_I & r_V & -r_U \\ h_U & -r_V & h_I & r_Q \\ h_V & r_U & -r_Q & h_I \end{pmatrix}\begin{pmatrix} I-S_{\rm L} \\ Q \\ U \\ V \end{pmatrix}\ , \tag{9.36}$$

where

$$\kappa_{\rm c} = \frac{1}{\kappa_{\rm L}} = \frac{k_{\rm c}(\nu_0)\ \Delta\nu_{\rm D}}{k_{\rm L}}\ . \tag{9.37}$$

Particularly important is the case of LTE, where both the source functions $S_{\rm c}$ and $S_{\rm L}$ reduce to the Planck function $B_{\rm P}$; in this case Eq. (9.35) can be written in the form

$$\frac{\rm d}{{\rm d}\tau_{\rm c}}\begin{pmatrix} I \\ Q \\ U \\ V \end{pmatrix} = \begin{pmatrix} 1+k_I & k_Q & k_U & k_V \\ k_Q & 1+k_I & f_V & -f_U \\ k_U & -f_V & 1+k_I & f_Q \\ k_V & f_U & -f_Q & 1+k_I \end{pmatrix}\begin{pmatrix} I-B_{\rm P} \\ Q \\ U \\ V \end{pmatrix}\ , \tag{9.38}$$

where

$$\begin{aligned} k_I &= \kappa_{\rm L}\, h_I \\ k_Q &= \kappa_{\rm L}\, h_Q \qquad & f_Q &= \kappa_{\rm L}\, r_Q \\ k_U &= \kappa_{\rm L}\, h_U \qquad & f_U &= \kappa_{\rm L}\, r_U \\ k_V &= \kappa_{\rm L}\, h_V \qquad & f_V &= \kappa_{\rm L}\, r_V\ , \end{aligned} \tag{9.39}$$

with h_I, h_Q, h_U, h_V, r_Q, r_U, r_V given by Eqs. (9.32).

9.5. Generalities and Symmetry Properties of the Transfer Equation

Let us consider the transfer equation in the form (9.35). For any wavelength λ, Eq. (9.35) is a system of four linear, first-order, ordinary differential equations in

the Stokes parameters $I(\tau_c)$, $Q(\tau_c)$, $U(\tau_c)$, $V(\tau_c)$ characterizing a radiation beam flowing along a given direction $\vec{\Omega}$. The solution to the system requires a set of boundary conditions, which depend of course on the specific physical situation. Here we restrict attention to the case of a semi-infinite stellar atmosphere.

If the atmosphere is not illuminated from outside (obviously this is not the case for a star in a binary system), the boundary conditions at the outermost layer are simply

$$I(\tau_c = 0) = Q(\tau_c = 0) = U(\tau_c = 0) = V(\tau_c = 0) = 0 \tag{9.40}$$

for any λ and any inward propagation direction ($\vec{\Omega} \cdot \vec{k} < 0$, with $\vec{k}$ the outward-directed unit vector perpendicular to the stellar surface). The boundary conditions in the deep layers are more delicate and require a previous discussion of the source functions S_c and S_L. It is reasonable to assume that the atmospheric plasma at large optical depths is in thermodynamic equilibrium, so that

$$\lim_{\tau_c \to \infty} S_c(\tau_c) = \lim_{\tau_c \to \infty} S_L(\tau_c) = B_P\big(T(\tau_c)\big) \ . \tag{9.41}$$

The boundary conditions for the Stokes parameters are then

$$\begin{aligned} &\lim_{\tau_c \to \infty} I(\tau_c) = B_P\big(T(\tau_c)\big) \\ &\lim_{\tau_c \to \infty} Q(\tau_c) = \lim_{\tau_c \to \infty} U(\tau_c) = \lim_{\tau_c \to \infty} V(\tau_c) = 0 \end{aligned} \tag{9.42}$$

for any λ and any $\vec{\Omega}$. Equations (9.40)-(9.42) still hold if the optical depth τ_c is replaced by any of the optical depths considered in Sect. 9.4.

Once the propagation direction and the boundary conditions are specified, the Stokes parameters at any assigned optical depth depend on the coefficients of Eq. (9.35), which, in general, are themselves functions of optical depth. Inspection of Eqs. (9.35), (9.32), (9.29), (9.27) and (9.26) shows that the value of the Stokes parameters for a specific spectral line at a given distance $(\lambda - \lambda_0)$ from line center is determined by the following parameters:
– the continuum source function S_c , which is generally well-approximated by the local Planck function B_P ;
– the line source function S_L , which reduces to the Planck function only when the LTE approximation is valid;
– the ratio κ_L between line and continuum absorption coefficient;
– the magnetic field intensity B, entering the definition of v_B ;
– the inclination angle θ of the magnetic field vector defined in Fig. 9.1;
– the azimuth angle χ of the magnetic field vector, also defined in Fig. 9.1;
– the Doppler width of the line $\Delta\lambda_D$, entering the definitions of the reduced wavelength v, the damping constant a, and the quantities v_A and v_B ;
– the natural plus collisional width Γ', defined in Eq. (9.22), entering the damping constant a ;
– the line-of-sight component of the macroscopic velocity of the ambient medium w_A , entering the definition of v_A .

In addition, the Stokes parameters depend on the Zeeman pattern of the line and on the wavelength λ_0 which affects the parameters v_B , $v_{\rm A}$ and a.

In the special case where the parameter $w_{\rm A}$ is independent of optical depth, its effect on the Stokes parameters profiles is just a global wavelength shift of the spectrum. It may then be convenient to neglect the term $v_{\rm A}$ in Eqs. (9.27) and use a different definition for the reduced wavelength,

$$v' \equiv v - v_{\rm A} = \frac{\lambda - \lambda'_0}{\Delta\lambda_{\rm D}} , \tag{9.43}$$

where

$$\lambda'_0 = \lambda_0 \left(1 + \frac{w_{\rm A}}{c}\right) . \tag{9.44}$$

This case will be referred to in the following as the *constant velocity case*.[1] The opposite case, where $w_{\rm A}$ is variable with optical depth, will be referred to as the *velocity gradient case*, although, more properly, one should speak of 'the case where the line-of-sight component of the bulk velocity of the ambient medium is variable with optical depth'.

The wavelength dependence of the Stokes parameters emerging from a stellar atmosphere reflects, broadly speaking, the wavelength dependence of the quantities h_I , h_Q , h_U , h_V , r_Q , r_U , r_V defined in Eqs. (9.32). As an illustrative example, Fig. 9.3 shows this dependence for different Zeeman patterns and for assigned values of the relevant parameters. The quantities h_U and r_U , not shown in the figure, vanish identically since the azimuth angle χ has been set to zero.

The existence of wavelength symmetries about line center appears clearly from Fig. 9.3, and a general proof of this fact can be easily obtained. From Eqs. (9.27) we get, with the help of Eqs. (3.18), (5.59), and (9.26)

$$\eta_q(-\Delta\lambda) = \eta_{-q}(\Delta\lambda) , \qquad \rho_q(-\Delta\lambda) = -\rho_{-q}(\Delta\lambda) ,$$

where

$$\Delta\lambda = \lambda - \lambda_0\Big(1 + \frac{w_{\rm A}}{c}\Big) \tag{9.45}$$

is the wavelength distance from (local) line center. Thus from Eqs. (9.29)

$$\begin{aligned} &\eta_{\rm b}(-\Delta\lambda) = \eta_{\rm r}(\Delta\lambda) && \eta_{\rm p}(-\Delta\lambda) = \eta_{\rm p}(\Delta\lambda) \\ &\rho_{\rm b}(-\Delta\lambda) = -\rho_{\rm r}(\Delta\lambda) && \rho_{\rm p}(-\Delta\lambda) = -\rho_{\rm p}(\Delta\lambda) , \end{aligned} \tag{9.46}$$

and substituting into Eqs. (9.32) we obtain

$$\begin{aligned} &h_I(-\Delta\lambda) = h_I(\Delta\lambda) && \\ &h_Q(-\Delta\lambda) = h_Q(\Delta\lambda) && r_Q(-\Delta\lambda) = -r_Q(\Delta\lambda) \\ &h_U(-\Delta\lambda) = h_U(\Delta\lambda) && r_U(-\Delta\lambda) = -r_U(\Delta\lambda) \\ &h_V(-\Delta\lambda) = -h_V(\Delta\lambda) && r_V(-\Delta\lambda) = r_V(\Delta\lambda) , \end{aligned} \tag{9.47}$$

[1] Obviously, it includes the more restrictive case of a static atmosphere ($w_{\rm A} = 0$).

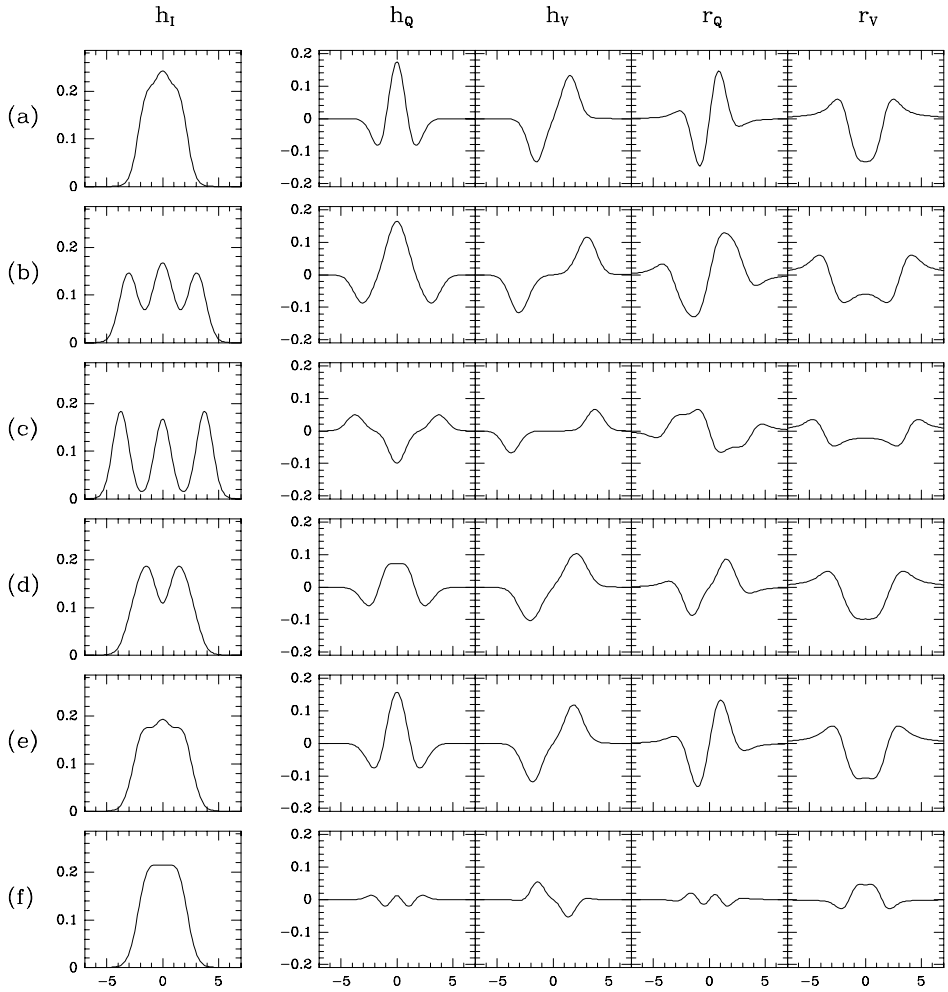

Fig.9.3. The elements of the propagation matrix are plotted as functions of the reduced wavelength for the following transitions (cf. Fig.3.2 on p. 83): (a) ${}^1\mathrm{S}_0 - {}^1\mathrm{P}_1$ (normal Zeeman triplet); (b) ${}^5\mathrm{D}_2 - {}^7\mathrm{D}_3$; (c) ${}^5\mathrm{P}_1 - {}^5\mathrm{F}_1$; (d) ${}^5\mathrm{D}_3 - {}^5\mathrm{F}_3$; (e) ${}^5\mathrm{P}_3 - {}^5\mathrm{D}_4$; (f) ${}^5\mathrm{D}_1 - {}^5\mathrm{G}_2$. The relevant parameters are: $v_\mathrm{A} = 0$, $v_B = 1.5$, $\theta = 60°$, $\chi = 0°$, $a = 0.05$. Note that cases (c) and (f) show characteristic reversals in h_Q , h_V , r_Q , r_V relative to the other cases. Transition (c) corresponds to $\bar{g} > 0$ and $\bar{G} < 0$ (see Sect. 9.6), while transition (f) corresponds to $\bar{g} < 0$ and $\bar{G} < 0$.

which are just the symmetry properties shown by Fig. 9.3.

These properties are very important because they entail – under certain assumptions – definite symmetry characteristics of the solutions to the transfer equation.[1]

[1] A different proof of the properties expressed by Eqs. (9.54) and (9.56), based on the analogy between the transfer equation and the motion of the representative point in the Poincaré sphere, has been presented by Landi Degl'Innocenti and Landi Degl'Innocenti (1981).

Consider again Eq. (9.35), which we rewrite in the compact matrix form

$$\frac{\mathrm{d}\boldsymbol{I}}{\mathrm{d}\tau_{\mathrm{c}}} = \boldsymbol{I} - S_{\mathrm{c}}\,\boldsymbol{U} + \kappa_{\mathrm{L}}\,\boldsymbol{H}\left[\,\boldsymbol{I} - S_{\mathrm{L}}\boldsymbol{U}\,\right], \tag{9.48}$$

where

$$\begin{aligned}\boldsymbol{I} &= (I,\,Q,\,U,\,V)^{\dagger}\\ \boldsymbol{U} &= (1,\,0,\,0,\,0)^{\dagger}\end{aligned} \tag{9.49}$$

and

$$\boldsymbol{H} = \begin{pmatrix} h_I & h_Q & h_U & h_V \\ h_Q & h_I & r_V & -r_U \\ h_U & -r_V & h_I & r_Q \\ h_V & r_U & -r_Q & h_I \end{pmatrix}. \tag{9.50}$$

Equations (9.47) show that wavelength inversion about (local) line center corresponds to a unitary similarity transformation of the matrix $\boldsymbol{H}$

$$\boldsymbol{H}(-\Delta\lambda) = \boldsymbol{X}^{-1}\,\boldsymbol{H}(\Delta\lambda)\,\boldsymbol{X}\,, \tag{9.51}$$

where $\boldsymbol{X}$ is the diagonal matrix

$$\boldsymbol{X} = \boldsymbol{X}^{-1} = \begin{pmatrix} 1 & 0 & 0 & 0 \\ 0 & 1 & 0 & 0 \\ 0 & 0 & 1 & 0 \\ 0 & 0 & 0 & -1 \end{pmatrix}. \tag{9.52}$$

Let us now consider the constant velocity case. The quantity $\Delta\lambda$ defined in Eq. (9.45) is now independent of optical depth, thus it can be used in the place of λ to describe the wavelength dependence of the Stokes profiles. The transfer equations for $\boldsymbol{I}(\Delta\lambda)$ and $\boldsymbol{I}(-\Delta\lambda)$ are, from Eq. (9.48)

$$\frac{\mathrm{d}}{\mathrm{d}\tau_{\mathrm{c}}}\,\boldsymbol{I}(\Delta\lambda) = \boldsymbol{I}(\Delta\lambda) - S_{\mathrm{c}}\,\boldsymbol{U} + \kappa_{\mathrm{L}}\,\boldsymbol{H}(\Delta\lambda)\left[\,\boldsymbol{I}(\Delta\lambda) - S_{\mathrm{L}}\boldsymbol{U}\,\right] \tag{9.53a}$$

$$\frac{\mathrm{d}}{\mathrm{d}\tau_{\mathrm{c}}}\,\boldsymbol{I}(-\Delta\lambda) = \boldsymbol{I}(-\Delta\lambda) - S_{\mathrm{c}}\,\boldsymbol{U} + \kappa_{\mathrm{L}}\,\boldsymbol{H}(-\Delta\lambda)\left[\,\boldsymbol{I}(-\Delta\lambda) - S_{\mathrm{L}}\boldsymbol{U}\,\right]. \tag{9.53b}$$

In the latter equation we substitute Eq. (9.51) and multiply both sides by $\boldsymbol{X}$ from the left. Since $\boldsymbol{X}\boldsymbol{U} = \boldsymbol{U}$, we get

$$\frac{\mathrm{d}}{\mathrm{d}\tau_{\mathrm{c}}}\left[\boldsymbol{X}\,\boldsymbol{I}(-\Delta\lambda)\right] = \boldsymbol{X}\,\boldsymbol{I}(-\Delta\lambda) - S_{\mathrm{c}}\,\boldsymbol{U} + \kappa_{\mathrm{L}}\,\boldsymbol{H}(\Delta\lambda)\left[\,\boldsymbol{X}\,\boldsymbol{I}(-\Delta\lambda) - S_{\mathrm{L}}\boldsymbol{U}\,\right].$$

Comparison with Eq. (9.53a) shows that the two vectors $\boldsymbol{X}\,\boldsymbol{I}(-\Delta\lambda)$ and $\boldsymbol{I}(\Delta\lambda)$ obey the same differential equation. If the boundary values $\boldsymbol{I}^{(\mathrm{b})}$ are such that[1]

[1] This is always the case for the radiation emerging from a semi-infinite stellar atmosphere (see Eqs. (9.42)).

$\boldsymbol{X}\,\boldsymbol{I}^{(\mathrm{b})}(-\Delta\lambda) = \boldsymbol{I}^{(\mathrm{b})}(\Delta\lambda)$, we can conclude that the two vectors coincide, or, in other words

$$\begin{aligned} I(-\Delta\lambda) &= I(\Delta\lambda) \\ Q(-\Delta\lambda) &= Q(\Delta\lambda) \\ U(-\Delta\lambda) &= U(\Delta\lambda) \\ V(-\Delta\lambda) &= -V(\Delta\lambda) \end{aligned} \tag{9.54}$$

at any optical depth.

Another general property of the solutions to the transfer equation can be proved under certain assumptions. It concerns the local inversion of the magnetic field direction at each point along the ray path,

$$\vec{B}(\tau_{\mathrm{c}}) \rightarrow \vec{B}'(\tau_{\mathrm{c}}) = -\vec{B}(\tau_{\mathrm{c}})\ .$$

This transformation implies, at any optical depth (cf. Fig. 9.1)

$$\theta' = \pi - \theta\ , \qquad \chi' = \pi + \chi\ ,$$

hence from Eqs. (9.32)

$$\begin{aligned} h'_I &= h_I & & \\ h'_Q &= h_Q & r'_Q &= r_Q \\ h'_U &= h_U & r'_U &= r_U \\ h'_V &= -h_V & r'_V &= -r_V\ . \end{aligned}$$

The relation between the propagation matrices $\boldsymbol{H}$ and $\boldsymbol{H}'$ can be expressed in terms of a unitary similarity transformation

$$\boldsymbol{H}' = \boldsymbol{Y}^{-1}\,\boldsymbol{H}\,\boldsymbol{Y}\ . \tag{9.55}$$

It can be shown with some matrix algebra that the most general matrix satisfying Eq. (9.55) has the form

$$\boldsymbol{Y} = \boldsymbol{Y}^{-1} = \begin{pmatrix} 1 & 0 & 0 & 0 \\ 0 & \cos 4\chi & \sin 4\chi & 0 \\ 0 & \sin 4\chi & -\cos 4\chi & 0 \\ 0 & 0 & 0 & -1 \end{pmatrix}\ .$$

If we now assume this matrix (that is, the χ angle) to be independent of optical depth, we can follow the same line of reasoning which leads from Eqs. (9.53) to Eqs. (9.54). We deduce that inversion of the magnetic field direction changes the Stokes parameters into $\boldsymbol{I}' = \boldsymbol{Y}\,\boldsymbol{I}$, or, explicitly

$$\begin{aligned} I' &= I \\ Q' &= \cos 4\chi\, Q + \sin 4\chi\, U \\ U' &= \sin 4\chi\, Q - \cos 4\chi\, U \\ V' &= -V\ , \end{aligned} \tag{9.56}$$

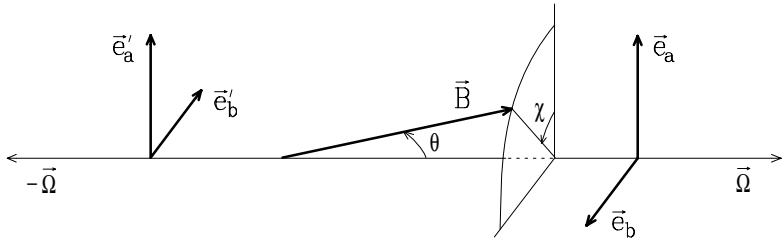

Fig.9.4. The angles θ and χ specifying the magnetic field direction are referred to the right-handed orthogonal system $(\vec{e}_a, \vec{e}_b, \vec{\Omega})$. The unit vector $\vec{e}'_a$ is parallel to $\vec{e}_a$.

provided the boundary values $\boldsymbol{I}^{(\mathrm{b})}$, $\boldsymbol{I}'^{(\mathrm{b})}$ are themselves connected by these relations. In the preferred reference frame (Sect. 5.5) we simply have a sign switch of the Stokes parameters U and V. It should be remarked that, while the magnetic field strength and inclination (as well as the other parameters affecting the transfer equation) are allowed to vary with optical depth, the azimuth angle must be constant in order for Eqs. (9.56) to hold.

A further symmetry property of the solutions to the transfer equation concerns the 180° rotation of the magnetic field vector about the propagation direction, at each point along the ray path. This transformation, corresponding to

$$\chi(\tau_{\mathrm{c}}) \rightarrow \pi + \chi(\tau_{\mathrm{c}}) \,, \tag{9.57}$$

leaves the propagation matrix unchanged, so that the Stokes parameters are also unchanged. This is an obvious consequence of the invariance of the Stokes parameters under a 180° rotation of the reference frame about the propagation direction.

Finally, we point out a symmetry property relating the transfer equations of two radiation beams flowing in opposite directions. Let $(\vec{e}_a, \vec{e}_b)$ and $(\vec{e}'_a, \vec{e}'_b)$ denote the unit vectors defining the Stokes parameters for the directions $\vec{\Omega}$ and $-\vec{\Omega}$, respectively. We choose the reference directions $\vec{e}_a$ and $\vec{e}'_a$ to be the same. If the magnetic field vector at a given point is specified in the reference system $(\vec{e}_a, \vec{e}_b, \vec{\Omega})$ by the angles θ and χ (see Fig. 9.4), the corresponding angles in the system $(\vec{e}'_a, \vec{e}'_b, -\vec{\Omega})$ are given by

$$\theta' = \pi - \theta \,, \qquad \chi' = -\chi \,. \tag{9.58}$$

If, in addition, a macroscopic velocity field is present, having a component w_{A} along the direction $\vec{\Omega}$, its component along the opposite direction is $w'_{\mathrm{A}} = -w_{\mathrm{A}}$. The relation between the propagation matrices $\boldsymbol{H}'$ and $\boldsymbol{H}$ (referring to $-\vec{\Omega}$ and $\vec{\Omega}$, respectively) can be easily deduced. From Eqs. (9.27) we obtain, with the help of Eqs. (5.59) and (3.18)

$$\eta'_q(\Delta\lambda) = \eta_{-q}(-\Delta\lambda) \,, \qquad \rho'_q(\Delta\lambda) = -\rho_{-q}(-\Delta\lambda) \,,$$

where

$$\Delta\lambda = \lambda - \lambda_0 \tag{9.59}$$

is the wavelength distance from the rest line center. Bearing in mind Eqs. (9.29) and (9.58), we have from Eqs. (9.32)

$$\begin{aligned} h'_I(\Delta\lambda) &= h_I(-\Delta\lambda) & & \\ h'_Q(\Delta\lambda) &= h_Q(-\Delta\lambda) & r'_Q(\Delta\lambda) &= -r_Q(-\Delta\lambda) \\ h'_U(\Delta\lambda) &= -h_U(-\Delta\lambda) & r'_U(\Delta\lambda) &= r_U(-\Delta\lambda) \\ h'_V(\Delta\lambda) &= h_V(-\Delta\lambda) & r'_V(\Delta\lambda) &= -r_V(-\Delta\lambda)\ . \end{aligned}$$

It can be shown with some matrix algebra that this transformation can be written as a unitary similarity transformation

$$\boldsymbol{H}'(\Delta\lambda) = \boldsymbol{Z}^{-1}\,\boldsymbol{H}(-\Delta\lambda)\,\boldsymbol{Z}\ , \tag{9.60}$$

where

$$\boldsymbol{Z} = \boldsymbol{Z}^{-1} = \begin{pmatrix} 1 & 0 & 0 & 0 \\ 0 & 1 & 0 & 0 \\ 0 & 0 & -1 & 0 \\ 0 & 0 & 0 & 1 \end{pmatrix}\ .$$

Denoting by $\boldsymbol{I}'$ and $\boldsymbol{I}$ the Stokes vectors of the radiation beams flowing in the directions $-\vec{\Omega}$ and $\vec{\Omega}$ respectively, we have from Eq. (9.48)

$$\frac{\mathrm{d}}{\mathrm{d}\tau'_\mathrm{c}}\,\boldsymbol{I}'(\Delta\lambda) = \boldsymbol{I}'(\Delta\lambda) - S_\mathrm{c}\,\boldsymbol{U} + \kappa_\mathrm{L}\,\boldsymbol{H}'(\Delta\lambda)\left[\,\boldsymbol{I}'(\Delta\lambda) - S_\mathrm{L}\boldsymbol{U}\,\right]\ ,$$

where τ'_c is the continuum optical depth measured along $-\vec{\Omega}$. Left-multiplication by $\boldsymbol{Z}$ gives, with the use of Eq. (9.60)

$$\frac{\mathrm{d}}{\mathrm{d}\tau'_\mathrm{c}}\left[\boldsymbol{Z}\,\boldsymbol{I}'(\Delta\lambda)\right] = \boldsymbol{Z}\,\boldsymbol{I}'(\Delta\lambda) - S_\mathrm{c}\,\boldsymbol{U} + \kappa_\mathrm{L}\,\boldsymbol{H}(-\Delta\lambda)\left[\boldsymbol{Z}\,\boldsymbol{I}'(\Delta\lambda) - S_\mathrm{L}\boldsymbol{U}\right]\ ,$$

since $\boldsymbol{Z}\boldsymbol{U} = \boldsymbol{U}$. Defining now the formal vector

$$\tilde{\boldsymbol{I}}' = \boldsymbol{Z}\,\boldsymbol{I}' = (I',\, Q',\, -U',\, V')^\dagger\ ,$$

and noting that $\mathrm{d}\tau'_\mathrm{c} = -\,\mathrm{d}\tau_\mathrm{c}$, we have

$$\frac{\mathrm{d}}{\mathrm{d}\tau_\mathrm{c}}\,\tilde{\boldsymbol{I}}'(\Delta\lambda) = -\left\{\tilde{\boldsymbol{I}}'(\Delta\lambda) - S_\mathrm{c}\,\boldsymbol{U} + \kappa_\mathrm{L}\,\boldsymbol{H}(-\Delta\lambda)\left[\,\tilde{\boldsymbol{I}}'(\Delta\lambda) - S_\mathrm{L}\boldsymbol{U}\,\right]\right\}\ . \tag{9.61}$$

It follows that the transfer equations for $\tilde{\boldsymbol{I}}'(\Delta\lambda)$ and $\boldsymbol{I}(-\Delta\lambda)$ are the same except for a sign switch.

9.6. The Weak Field Approximation

When the magnetic field is weak or, more precisely, when the Zeeman splitting is much smaller than the typical width of the profiles η_q and ρ_q defined in Eqs. (9.27), it is possible to deduce some properties of the solutions to the transfer equation without actually solving it. The above condition means

$$\bar{g}\, v_B = \bar{g}\, \frac{\Delta\lambda_B}{\Delta\lambda_{\rm D}} \ll 1 \,,$$

where $\bar{g}$ is the effective Landé factor. This sets an upper bound to the magnetic field strength, which depends (see Eq. (5.49)) both on the spectral line (through its wavelength and the atomic weight of the element) and on the ambient medium (through its kinetic temperature and microturbulent velocity). For instance, for an iron line of optical wavelength formed in the solar atmosphere, we have from Eq. (5.49)

$$\bar{g}\, B \ll 2500 \text{ G} \,.$$

The following derivation is based on an original, perturbative scheme presented by Landi Degl'Innocenti and Landi Degl'Innocenti (1973) and later extended by Jefferies et al. (1989).

Let us consider a radiation beam flowing along a given direction in a stellar atmosphere, and let us denote by $\vec{B}(\tau_{\rm c})$ the magnetic field vector at optical depth $\tau_{\rm c}$ along the ray path. The transfer equation is given by Eq. (9.35). Now suppose this reference (or 'true') atmosphere is replaced by a 'fictitious' atmosphere identical to the former except for the substitution

$$\vec{B}(\tau_{\rm c}) \to \alpha\, \vec{B}(\tau_{\rm c}) \,, \tag{9.62}$$

which entails

$$v_B(\tau_{\rm c}) \to \alpha\, v_B(\tau_{\rm c}) \,,$$

where α is a dimensionless, real parameter which at the end of the calculation will be set to 1. All the quantities in Eq. (9.35) – except the source functions and the ratio $\kappa_{\rm L}$ between line and continuum absorption coefficient – become functions of α, hence they can be expanded in power series of α. For the Stokes parameters we can write[1]

$$\begin{aligned} I &= I_0 + I_1\,\alpha + I_2\,\alpha^2 + I_3\,\alpha^3 + \cdots \\ Q &= Q_0 + Q_1\,\alpha + Q_2\,\alpha^2 + Q_3\,\alpha^3 + \cdots \end{aligned} \tag{9.63}$$

with similar equations for U and V. To obtain the series expansions of the elements of the propagation matrix, we write the η_q and ρ_q profiles in the form

$$\eta_q = \sum_{n=0}^{\infty} \left[\frac{\partial^n \eta_q}{\partial \alpha^n}\right]_{\alpha=0} \frac{\alpha^n}{n!} \,, \qquad \rho_q = \sum_{n=0}^{\infty} \left[\frac{\partial^n \rho_q}{\partial \alpha^n}\right]_{\alpha=0} \frac{\alpha^n}{n!} \,. \tag{9.64}$$

[1] In this section we denote by $I_0\,, I_1\,, I_2\,\ldots$ the coefficients of the power series expansion of the intensity I (first Stokes parameter). These should not be confused with the symbols $(I_0\,, I_1\,, I_2\,, I_3)$ used in other sections to denote the full Stokes vector (I, Q, U, V).

The zero-order coefficients are given by (see Eqs. (9.27) and (3.17))

$$\begin{aligned}\left[\eta_q\right]_{\alpha=0} &= \frac{1}{\sqrt{\pi}}\; H(v-v_{\rm A}\,,a) \;\equiv\; \eta \\ \left[\rho_q\right]_{\alpha=0} &= \frac{1}{\sqrt{\pi}}\; L(v-v_{\rm A}\,,a) \;\equiv\; \rho\,, \end{aligned} \tag{9.65}$$

thus they are simply the absorption profile and the associated dispersion profile for zero magnetic field. The higher-order coefficients can be expressed in terms of derivatives of η and ρ with respect to wavelength. From Eqs. (9.27) and (9.26) we have

$$\begin{aligned}\left[\frac{\partial^n \eta_q}{\partial \alpha^n}\right]_{\alpha=0} &= \sum_{M_\ell M_u} S_q^{J_\ell J_u}(M_\ell\,,M_u)\;(g_u M_u - g_\ell M_\ell)^n\;\Delta\lambda_B^n\;\frac{\partial^n \eta}{\partial \lambda^n} \\ \left[\frac{\partial^n \rho_q}{\partial \alpha^n}\right]_{\alpha=0} &= \sum_{M_\ell M_u} S_q^{J_\ell J_u}(M_\ell\,,M_u)\;(g_u M_u - g_\ell M_\ell)^n\;\Delta\lambda_B^n\;\frac{\partial^n \rho}{\partial \lambda^n}\,, \end{aligned} \tag{9.66}$$

where

$$\begin{aligned}\frac{\partial^n \eta}{\partial \lambda^n} &= \frac{1}{\Delta\lambda_{\rm D}^n\;\sqrt{\pi}}\;\frac{\partial^n}{\partial v^n}\,H(v-v_{\rm A}\,,a) \\ \frac{\partial^n \rho}{\partial \lambda^n} &= \frac{1}{\Delta\lambda_{\rm D}^n\;\sqrt{\pi}}\;\frac{\partial^n}{\partial v^n}\,L(v-v_{\rm A}\,,a)\,. \end{aligned} \tag{9.67}$$

The sum over M_ℓ and M_u appearing in Eqs. (9.66) has already been calculated in Sect. 3.3. Using Eqs. (3.53), (3.20) and (3.54) we get

$$\begin{aligned}\left[\frac{\partial^n \eta_q}{\partial \alpha^n}\right]_{\alpha=0} &= (-1)^n\;G_q^{(n)}(J_\ell\,,J_u)\;\;\Delta\lambda_B^n\;\frac{\partial^n \eta}{\partial \lambda^n} \\ \left[\frac{\partial^n \rho_q}{\partial \alpha^n}\right]_{\alpha=0} &= (-1)^n\;G_q^{(n)}(J_\ell\,,J_u)\;\;\Delta\lambda_B^n\;\frac{\partial^n \rho}{\partial \lambda^n}\,, \end{aligned} \tag{9.68}$$

where the symbols $G_q^{(n)}$, defined in Eq. (3.55), are expressed analytically (up to $n=4$) in Table 3.4. Substituting into Eqs. (9.64) and bearing in mind Eqs. (9.29), we obtain from Eqs. (9.32) the following expansions up to third-order terms in α

$$\begin{aligned} h_I &= \eta + \frac{1}{4}\,\alpha^2\,\Delta\lambda_B^2\;\eta''\left[G_0^{(2)}\sin^2\theta + G_1^{(2)}\,(1+\cos^2\theta)\right] + \cdots \\ h_Q &= \frac{1}{4}\,\alpha^2\,\Delta\lambda_B^2\;\eta''\left[G_0^{(2)} - G_1^{(2)}\right]\sin^2\theta\cos 2\chi + \cdots \\ h_U &= \frac{1}{4}\,\alpha^2\,\Delta\lambda_B^2\;\eta''\left[G_0^{(2)} - G_1^{(2)}\right]\sin^2\theta\sin 2\chi + \cdots \\ h_V &= -\,\alpha\;\Delta\lambda_B\;\eta'\;G_1^{(1)}\cos\theta - \frac{1}{6}\,\alpha^3\,\Delta\lambda_B^3\;\eta'''\;G_1^{(3)}\cos\theta + \cdots \end{aligned}$$

$$
\begin{aligned}
r_Q &= \frac{1}{4}\,\alpha^2\,\Delta\lambda_B^2\;\rho''\left[G_0^{(2)} - G_1^{(2)}\right]\sin^2\theta\cos 2\chi + \cdots \\
r_U &= \frac{1}{4}\,\alpha^2\,\Delta\lambda_B^2\;\rho''\left[G_0^{(2)} - G_1^{(2)}\right]\sin^2\theta\sin 2\chi + \cdots \\
r_V &= -\,\alpha\,\Delta\lambda_B\;\rho'\,G_1^{(1)}\cos\theta - \frac{1}{6}\,\alpha^3\,\Delta\lambda_B^3\;\rho'''\,G_1^{(3)}\cos\theta + \cdots\,,
\end{aligned}
\tag{9.69}
$$

where

$$
\eta' = \frac{\partial\eta}{\partial\lambda}\,, \qquad \rho' = \frac{\partial\rho}{\partial\lambda}\,, \qquad \eta'' = \frac{\partial^2\eta}{\partial\lambda^2}\,, \qquad \text{etc.} \tag{9.70}
$$

Substitution of the series expansions (9.69) and (9.63) into the transfer equation (9.35) leads to four equations each representing an equality between two power series in α. Since α is arbitrary, the coefficients of each power must separately be equal. To the lowest perturbative order we have

$$
\begin{aligned}
&\frac{\mathrm{d}I_0}{\mathrm{d}\tau_{\mathrm{c}}} = I_0 - S_{\mathrm{c}} + \kappa_{\mathrm{L}}\,\eta\,(I_0 - S_{\mathrm{L}}) && \frac{\mathrm{d}U_0}{\mathrm{d}\tau_{\mathrm{c}}} = (1+\kappa_{\mathrm{L}}\,\eta)\,U_0 \\
&\frac{\mathrm{d}Q_0}{\mathrm{d}\tau_{\mathrm{c}}} = (1+\kappa_{\mathrm{L}}\,\eta)\,Q_0 && \frac{\mathrm{d}V_0}{\mathrm{d}\tau_{\mathrm{c}}} = (1+\kappa_{\mathrm{L}}\,\eta)\,V_0\,.
\end{aligned}
\tag{9.71}
$$

Boundary conditions should now be considered. For a semi-infinite atmosphere – the case to which we restrict attention from now on – the equations resulting from the substitution of Eqs. (9.63) into Eqs. (9.42) must hold for any value of α. Therefore, the boundary conditions at the bottom of the atmosphere are[1]

$$
\begin{aligned}
&\lim_{\tau_{\mathrm{c}}\to\infty} I_0(\tau_{\mathrm{c}}) = B_{\mathrm{P}}\big(T(\tau_{\mathrm{c}})\big) \\
&\lim_{\tau_{\mathrm{c}}\to\infty} I_1(\tau_{\mathrm{c}}) = \lim_{\tau_{\mathrm{c}}\to\infty} I_2(\tau_{\mathrm{c}}) = \ldots = \lim_{\tau_{\mathrm{c}}\to\infty} Q_0(\tau_{\mathrm{c}}) = \lim_{\tau_{\mathrm{c}}\to\infty} Q_1(\tau_{\mathrm{c}}) = \ldots \\
&= \lim_{\tau_{\mathrm{c}}\to\infty} U_0(\tau_{\mathrm{c}}) = \lim_{\tau_{\mathrm{c}}\to\infty} U_1(\tau_{\mathrm{c}}) = \ldots = \lim_{\tau_{\mathrm{c}}\to\infty} V_0(\tau_{\mathrm{c}}) = \lim_{\tau_{\mathrm{c}}\to\infty} V_1(\tau_{\mathrm{c}}) = \\
&\ldots = 0\,.
\end{aligned}
\tag{9.72}
$$

It follows from Eqs. (9.71)-(9.72) that the zero-order Stokes parameters Q_0, U_0, and V_0, obeying a linear homogeneous differential equation (without source terms) and being identically zero at the boundary of the atmosphere, are identically zero everywhere. As far as I_0 is concerned, we observe that it obeys the same differential equation as the intensity $\bar{I}$ of a radiation beam travelling through the same atmosphere with no magnetic field.[2] We conclude that, to the lowest perturbative order, the polarization is zero and the intensity equals, at any optical depth and for

[1] For the radiation flowing inward, one has to consider the boundary conditions at the top of the atmosphere. For an isolated star, all terms in Eqs. (9.63) are identically zero at $\tau_{\mathrm{c}} = 0$.

[2] By 'same atmosphere' we mean that the line source function S_{L} is also the same. This remark is not trivial for non-LTE lines, since the presence of a magnetic field may alter the line source function.

any direction, the intensity that would be present in the same atmosphere without magnetic field. This was to be expected since, according to Eqs. (9.63) and (9.62), the zero-order terms correspond to a non-magnetic atmosphere.

Proceeding along the same lines, we obtain a system of differential equations for each perturbative order. The results up to the third order are the following:

– *Zero order*

$$I_0 = \bar{I}$$
$$Q_0 = U_0 = V_0 = 0 \, .$$

– *First order*

$$\frac{\mathrm{d}V_1}{\mathrm{d}\tau_\mathrm{c}} = (1 + \kappa_\mathrm{L}\,\eta)\,V_1 - \Delta\lambda_B\; G_1^{(1)} \cos\theta\;\; \kappa_\mathrm{L}\;\eta'\;(I_0 - \; S_\mathrm{L})$$
$$I_1 = Q_1 = U_1 = 0 \, .$$

– *Second order*

$$\frac{\mathrm{d}I_2}{\mathrm{d}\tau_\mathrm{c}} = (1 + \kappa_\mathrm{L}\,\eta)\,I_2 + \frac{1}{4}\;\Delta\lambda_B^2 \left[G_0^{(2)} \sin^2\theta + \; G_1^{(2)}\,(1 + \cos^2\theta)\right] \kappa_\mathrm{L}\;\eta''\;(I_0 - \; S_\mathrm{L})$$
$$- \Delta\lambda_B\; G_1^{(1)} \cos\theta\;\; \kappa_\mathrm{L}\;\eta'\;V_1$$

$$\frac{\mathrm{d}Q_2}{\mathrm{d}\tau_\mathrm{c}} = (1 + \kappa_\mathrm{L}\,\eta)\,Q_2 + \frac{1}{4}\;\Delta\lambda_B^2 \left[G_0^{(2)} - \; G_1^{(2)}\right] \sin^2\theta \cos 2\chi\;\; \kappa_\mathrm{L}\;\eta''\;(I_0 - \; S_\mathrm{L})$$

$$\frac{\mathrm{d}U_2}{\mathrm{d}\tau_\mathrm{c}} = (1 + \kappa_\mathrm{L}\,\eta)\,U_2 + \frac{1}{4}\;\Delta\lambda_B^2 \left[G_0^{(2)} - \; G_1^{(2)}\right] \sin^2\theta \sin 2\chi\;\; \kappa_\mathrm{L}\;\eta''\;(I_0 - \; S_\mathrm{L})$$

$$V_2 = 0 \, .$$

– *Third order*

$$I_3 = 0$$

$$\frac{\mathrm{d}Q_3}{\mathrm{d}\tau_\mathrm{c}} = (1 + \kappa_\mathrm{L}\,\eta)\,Q_3 - \Delta\lambda_B\; G_1^{(1)} \cos\theta\;\; \kappa_\mathrm{L}\;\rho'\;U_2$$
$$- \frac{1}{4}\;\Delta\lambda_B^2 \left[G_0^{(2)} - \; G_1^{(2)}\right] \sin^2\theta \sin 2\chi\;\; \kappa_\mathrm{L}\;\rho''\;V_1$$

$$\frac{\mathrm{d}U_3}{\mathrm{d}\tau_\mathrm{c}} = (1 + \kappa_\mathrm{L}\,\eta)\,U_3 + \Delta\lambda_B\; G_1^{(1)} \cos\theta\;\; \kappa_\mathrm{L}\;\rho'\;Q_2$$
$$+ \frac{1}{4}\;\Delta\lambda_B^2 \left[G_0^{(2)} - \; G_1^{(2)}\right] \sin^2\theta \cos 2\chi\;\; \kappa_\mathrm{L}\;\rho''\;V_1$$

$$\frac{\mathrm{d}V_3}{\mathrm{d}\tau_\mathrm{c}} = (1 + \kappa_\mathrm{L}\,\eta)\,V_3 - \frac{1}{6}\;\Delta\lambda_B^3\; G_1^{(3)} \cos\theta\;\; \kappa_\mathrm{L}\;\eta'''\;(I_0 - \; S_\mathrm{L})$$
$$- \Delta\lambda_B\; G_1^{(1)} \cos\theta\;\; \kappa_\mathrm{L}\;\eta'\;I_2$$
$$+ \frac{1}{4}\;\Delta\lambda_B^2 \left[G_0^{(2)} \sin^2\theta + \; G_1^{(2)}\,(1 + \cos^2\theta)\right] \kappa_\mathrm{L}\;\eta''\;V_1 \, .$$

These equations suggest two general remarks:
a) Each of the coefficients of the power series expansions (9.63), if non-zero, obeys a differential equation of the form

$$\frac{\mathrm{d}C_n}{\mathrm{d}\tau_\mathrm{c}} = (1+\kappa_\mathrm{L}\,\eta)\,C_n \;+\; (\text{source term})\;,$$

where the source term is proportional (see Eqs. (9.67)) to $v_B^n = (\Delta\lambda_B/\Delta\lambda_\mathrm{D})^n$. Thus, I_0 is of order 0 in v_B ; V_1 is proportional to v_B ; I_2 , Q_2 and U_2 are proportional to v_B^2 , and so on.
b) Anomalous dispersion effects enter the perturbative equations only from the third order on. This means that for weak magnetic field they are negligible.

The perturbative expansion considered in this section is obviously meaningful only in the limiting case of weak magnetic field ($v_B \to 0$). If, for each Stokes parameter, we retain only the lowest-order non-zero term in Eqs. (9.63), we have, setting $\alpha = 1$

$$I = I_0\;, \qquad Q = Q_2\;, \qquad U = U_2\;, \qquad V = V_1\;. \tag{9.73}$$

Thus the transfer equation for the Stokes parameters reduces, under the limit of weak magnetic field, to the following system

$$\frac{\mathrm{d}I}{\mathrm{d}\tau_\mathrm{c}} = (1+\kappa_\mathrm{L}\,\eta)\,I - (S_\mathrm{c} + \kappa_\mathrm{L}\,\eta\,S_\mathrm{L}) \tag{9.74a}$$

$$\frac{\mathrm{d}V}{\mathrm{d}\tau_\mathrm{c}} = (1+\kappa_\mathrm{L}\,\eta)\,V - \Delta\lambda_B\;\bar{g}\,\cos\theta\,\kappa_\mathrm{L}\,\eta'\,(I - S_\mathrm{L}) \tag{9.74b}$$

$$\frac{\mathrm{d}Q}{\mathrm{d}\tau_\mathrm{c}} = (1+\kappa_\mathrm{L}\,\eta)\,Q - \frac{1}{4}\,\Delta\lambda_B^2\,\bar{G}\,\sin^2\theta\cos 2\chi\;\kappa_\mathrm{L}\,\eta''\,(I - S_\mathrm{L}) \tag{9.74c}$$

$$\frac{\mathrm{d}U}{\mathrm{d}\tau_\mathrm{c}} = (1+\kappa_\mathrm{L}\,\eta)\,U - \frac{1}{4}\,\Delta\lambda_B^2\,\bar{G}\,\sin^2\theta\sin 2\chi\;\kappa_\mathrm{L}\,\eta''\,(I - S_\mathrm{L})\;, \tag{9.74d}$$

where we have taken into account (see Table 3.4) that

$$G_1^{(1)} = \bar{g}\;, \tag{9.75}$$

with $\bar{g}$ the effective Landé factor of the line defined in Eq. (3.44), and where

$$\bar{G} = G_1^{(2)} - G_0^{(2)}\;. \tag{9.76}$$

Note that the quantity $\bar{G}$ can be written in the form

$$\bar{G} = \bar{g}^2 - \delta\;, \tag{9.77}$$

where, using the notations of Table 3.4

$$\delta = \frac{1}{80}\,g_d^2\;(16s - 7d^2 - 4)\;. \tag{9.78}$$

A number of interesting results can be derived from Eqs. (9.74):

i) Since $S_{\rm c}$, $S_{\rm L}$ and $\kappa_{\rm L}$ are practically wavelength-independent, derivation of Eq. (9.74a) with respect to wavelength yields

$$\frac{\mathrm{d}}{\mathrm{d}\tau_{\rm c}}\left(\frac{\partial I}{\partial\lambda}\right) = (1+\kappa_{\rm L}\,\eta)\,\frac{\partial I}{\partial\lambda} \;+\; \kappa_{\rm L}\,\eta'\,(I-\;S_{\rm L})\;, \tag{9.79}$$

where the notation of Eq. (9.70) has been used. Multiplying both sides by the factor $-\Delta\lambda_B\;\bar{g}\,\cos\theta$, and assuming this factor (i.e. the line-of-sight component of the magnetic field) to be independent of optical depth, we see that the resulting equation is formally identical to Eq. (9.74b), which means that the functions

$$V \qquad \text{and} \qquad -\,\Delta\lambda_B\;\bar{g}\,\cos\theta\;\frac{\partial I}{\partial\lambda}$$

obey the same differential equation. On the other hand, since from Eqs. (9.73) and (9.72)

$$\lim_{\tau_{\rm c}\to\infty} V(\tau_{\rm c}) = 0\;, \qquad \lim_{\tau_{\rm c}\to\infty}\;\frac{\partial I}{\partial\lambda} = \frac{\partial}{\partial\lambda}\,B_{\rm P}\big(T(\tau_{\rm c})\big) = 0\;,$$

they also satisfy the same boundary conditions. We conclude that, at any optical depth

$$V(\lambda) = -\,\Delta\lambda_B\;\bar{g}\,\cos\theta\;\frac{\partial I}{\partial\lambda}\;. \tag{9.80}$$

ii) Next consider Eqs. (9.74c) and (9.74d). Multiplying the former by $\sin 2\chi$, the latter by $\cos 2\chi$, subtracting the resulting equations and assuming χ to be independent of optical depth, we get

$$\frac{\mathrm{d}}{\mathrm{d}\tau_{\rm c}}\left(\sin 2\chi\;\,Q-\cos 2\chi\;\,U\right) = \;(1+\kappa_{\rm L}\,\eta)\left(\sin 2\chi\;\,Q-\cos 2\chi\;\,U\right)\;,$$

and since from Eqs. (9.73) and (9.72)

$$\lim_{\tau_{\rm c}\to\infty} Q(\tau_{\rm c}) = \lim_{\tau_{\rm c}\to\infty} U(\tau_{\rm c}) = 0\;,$$

we deduce that, at any optical depth

$$\sin 2\chi\;\,Q-\cos 2\chi\;\,U = 0\;,$$

or, for $Q\neq 0$

$$\frac{U(\lambda)}{Q(\lambda)} = \;\tan 2\chi\;. \tag{9.81}$$

iii) If we retain the assumption $\chi = \text{const.}$, we can choose to measure the Stokes parameters in the preferred frame (so that $\chi = 0$; see Sect. 5.5). Denoting by $\tilde{Q}$ and $\tilde{U}$ the Stokes parameters in this frame, we have from Eqs. (9.74c) and (9.81)

$$\frac{\mathrm{d}\tilde{Q}}{\mathrm{d}\tau_\mathrm{c}} = (1 + \kappa_\mathrm{L}\,\eta)\,\tilde{Q} - \frac{1}{4}\,\Delta\lambda_B^2\,\bar{G}\,\sin^2\theta\;\kappa_\mathrm{L}\,\eta''\,(I - S_\mathrm{L})$$

$$\tilde{U} = 0\,. \tag{9.82}$$

On the other hand, derivation of Eq. (9.79) with respect to wavelength yields

$$\frac{\mathrm{d}}{\mathrm{d}\tau_\mathrm{c}}\left(\frac{\partial^2 I}{\partial\lambda^2}\right) = \left(1 + \kappa_\mathrm{L}\,\eta\right)\frac{\partial^2 I}{\partial\lambda^2} + \kappa_\mathrm{L}\,\eta''\,(I - S_\mathrm{L}) + 2\,\kappa_\mathrm{L}\,\eta'\,\frac{\partial I}{\partial\lambda}\,.$$

In the constant velocity case, the last term vanishes at the wavelength λ_0' corresponding to line center (see Eqs. (9.44) and (9.67)). Multiplying the resulting equation by the factor $-\Delta\lambda_B^2\,\bar{G}\,\sin^2\theta/4$ and assuming this factor (hence the transverse component of the magnetic field) to be independent of optical depth, we obtain by comparison with the first of Eqs. (9.82) that the two functions

$$\tilde{Q}(\lambda_0') \qquad \text{and} \qquad -\frac{1}{4}\,\Delta\lambda_B^2\,\bar{G}\,\sin^2\theta\left[\frac{\partial^2 I}{\partial\lambda^2}\right]_{\lambda=\lambda_0'}$$

satisfy the same differential equation. As the boundary conditions are also the same, we deduce that, at any optical depth

$$\tilde{Q}(\lambda_0') = -\frac{1}{4}\,\Delta\lambda_B^2\,\bar{G}\,\sin^2\theta\left[\frac{\partial^2 I}{\partial\lambda^2}\right]_{\lambda=\lambda_0'}\,. \tag{9.83}$$

iv) Another expression for $\tilde{Q}$, valid for any λ, can be obtained under a set of more restrictive assumptions. Consider Eq. (9.79) and multiply both sides by the factor

$$-\frac{1}{4}\,\Delta\lambda_B^2\,\bar{G}\,\sin^2\theta\;\frac{\eta''}{\eta'}\,.$$

If this factor is independent of optical depth, which requires the τ_c-independence of:
a) the transverse component of the magnetic field;
b) the line-of-sight velocity w_A;
c) the parameters $\Delta\lambda_\mathrm{D}$ and Γ' controlling the shape of the η profile,
then we see by comparison with the first of Eqs. (9.82) that, at any optical depth[1]

$$\tilde{Q}(\lambda) = -\frac{1}{4}\,\Delta\lambda_B^2\,\bar{G}\,\sin^2\theta\;\frac{\eta''}{\eta'}\,\frac{\partial I}{\partial\lambda}\,. \tag{9.84}$$

[1] Note that Eq. (9.84) is meaningless at line center, since Eqs. (9.67) and (9.54) yield

$$\left[\frac{\partial\eta}{\partial\lambda}\right]_{\lambda=\lambda_0'} = \left[\frac{\partial I}{\partial\lambda}\right]_{\lambda=\lambda_0'} = 0.$$

The value of $\tilde{Q}(\lambda_0')$ is however given by the (more general) equation (9.83).

TABLE 9.1

Expressions for the Stokes parameters in the weak field limit. The expressions are valid provided the physical parameters marked by a star are independent of optical depth. $B_\parallel$ and $B_\perp$ stand for $B\cos\theta$ and $B\sin\theta$, respectively.

Expression	Eq.	$B_\parallel$	$B_\perp$	χ	$w_{\rm A}$	$\Delta\lambda_{\rm D}$	Γ'	Domain
$V(\lambda) = -\Delta\lambda_B\, \bar{g}\, \cos\theta \left(\frac{\partial I}{\partial \lambda}\right)$	(9.80)	$\star$						any λ
$\frac{U(\lambda)}{Q(\lambda)} = \tan 2\chi$	(9.81)			$\star$				any λ
$\tilde{Q}(\lambda_0') = -\frac{1}{4}\, \Delta\lambda_B^2\, \bar{G}\, \sin^2\theta \left(\frac{\partial^2 I}{\partial \lambda^2}\right)_{\lambda_0'}$	(9.83)		$\star$	$\star$	$\star$			line center
$\tilde{Q}(\lambda) = -\frac{1}{4}\, \Delta\lambda_B^2\, \bar{G}\, \sin^2\theta\, \frac{\eta''}{\eta'} \left(\frac{\partial I}{\partial \lambda}\right)$	(9.84)		$\star$	$\star$	$\star$	$\star$	$\star$	any λ
$\tilde{Q}(\lambda_{\rm w}) = \frac{3}{4}\, \Delta\lambda_B^2\, \bar{G}\, \sin^2\theta\, \frac{1}{\lambda_{\rm w} - \lambda_0'} \left(\frac{\partial I}{\partial \lambda}\right)_{\lambda_{\rm w}}$	(9.85)		$\star$	$\star$	$\star$			line wings

v) If we restrict ourselves to the line wings, assumption c) above is unnecessary in order for Eq. (9.84) to hold. In fact, denoting by $\lambda_{\rm w}$ a particular wavelength far away in the wing, or, more precisely, such that

$$\left|\lambda_{\rm w} - \lambda_0'\right| \gg \Delta\lambda_{\rm D} \qquad \text{and} \qquad \left|\lambda_{\rm w} - \lambda_0'\right| \gg a\, \Delta\lambda_{\rm D}\ ,$$

the profile η can be written in the form (see Eqs. (9.65), (9.43), and (5.57))

$$\eta = \frac{1}{\pi}\, \frac{a\, \Delta\lambda_{\rm D}^2}{(\lambda_{\rm w} - \lambda_0')^2}\ ,$$

so that

$$\frac{\eta''}{\eta'} = -\, \frac{3}{\lambda_{\rm w} - \lambda_0'}\ .$$

This ratio is independent of $\Delta\lambda_{\rm D}$ and Γ', therefore assumption c) can be dropped and Eq. (9.84) becomes

$$\tilde{Q}(\lambda_{\rm w}) = \frac{3}{4}\, \Delta\lambda_B^2\, \bar{G}\, \sin^2\theta\, \frac{1}{\lambda_{\rm w} - \lambda_0'} \left[\frac{\partial I}{\partial \lambda}\right]_{\lambda = \lambda_{\rm w}}\ . \tag{9.85}$$

The results just derived are summarized in Table 9.1, together with the assumptions required – in addition to the weak field hypothesis – for the various expressions to hold. In particular, it should be emphasized that Eq. (9.80) is rather general and that it can also be applied in the 'velocity gradient case' (see Sect. 9.5).

Some general features of the Stokes parameters profiles arise from the analytical expressions in Table 9.1. First we consider Eq. (9.80), and we refer to a typical stellar atmosphere where both line and continuum source functions are monotonically increasing functions of optical depth. Such atmosphere produces absorption

lines and, for any line, the quantity $\partial I/\partial\lambda$ is negative in the blue wing and positive in the red wing. For any propagation direction making an angle $\theta < \pi/2$ with the magnetic field direction, it follows that the V Stokes parameter is positive in the blue wing and negative in the red wing, while the opposite holds for $\theta > \pi/2$.[1] It also follows that there is a particular wavelength (more precisely, an odd number of wavelengths) where the V profile vanishes.

Another consequence of Eq. (9.80) concerns the dependence of circular polarization on the characteristics of spectral lines. Let us suppose that the intensity profile emerging from a static stellar atmosphere can be written in the form[2]

$$I(\lambda) = I_{\rm c}\left[1 - d_{\rm c}\ \frac{\eta(\lambda)}{\eta(\lambda_0)}\right], \tag{9.86}$$

where $I_{\rm c}$ is the intensity of the continuum adjacent to the line and where

$$d_{\rm c} = \frac{I_{\rm c} - I(\lambda_0)}{I_{\rm c}}$$

is the line central depression in units of $I_{\rm c}$. Assuming a depth-independent Doppler width, from Eqs. (9.86), (9.67) and (9.80) we have, as an order of magnitude

$$\frac{V}{I_{\rm c}} \approx \frac{\Delta\lambda_B}{\Delta\lambda_{\rm D}}\ \cos\theta\ \bar{g}\ d_{\rm c}\ . \tag{9.87}$$

This formula shows that $V/I_{\rm c}$ is inversely proportional to $\Delta\lambda_{\rm D}$, which means that circular polarization in narrow lines is larger than in broad lines. Furthermore, it is larger in lines of heavy elements compared with light elements, because $\Delta\lambda_{\rm D}$ decreases with increasing atomic weight (see Eqs. (9.25) and (5.48)). For a given element, the largest circular polarization is produced by lines having the largest effective Landé factor $\bar{g}$, the largest central depression $d_{\rm c}$, and the largest wavelength λ_0. This last effect stems from the fact that $\Delta\lambda_B$ scales as λ_0^2 (Eqs. (9.26)) while $\Delta\lambda_{\rm D}$ scales as λ_0 (Eq. (9.25)).

The above properties suggest the introduction of a dimensionless parameter, the *circular polarization sensitivity index* of a spectral line, having the form

$$s_V = \left(\frac{\lambda_0}{\lambda_{\rm ref}}\right)\ \bar{g}\ d_{\rm c}\ , \tag{9.88}$$

where $\lambda_{\rm ref}$ is a reference wavelength, like for instance 5000 Å. A search for the most sensitive lines in the FeI solar spectrum (restricted to the list of about 400

[1] We consider here the most frequent case of $\bar{g} > 0$. For the very few lines having $\bar{g} < 0$ the situation is reversed.

[2] This is generally an acceptable approximation for unsaturated absorption lines. The following remarks also apply, as a rule, to the more general case where $\eta(\lambda)$ in Eq. (9.86) is replaced by a bell-shaped profile having a typical width $\Delta\lambda_{\rm p}$. For saturated lines one usually has $\Delta\lambda_{\rm p} > \Delta\lambda_{\rm D}$.

TABLE 9.2

The lines of the FeI solar spectrum are listed in order of decreasing circular polarization sensitivity index (computed from Eq.(9.88) with $\lambda_{\rm ref} = 5000$ Å). The value of $\bar{g}$ is calculated according to L-S coupling. Zeeman triplets are identified by a star in the last column.

λ_0(Å)	Multiplet	Transition	$\bar{g}$	s_V	
5250.21	1	$^5\mathrm{D}_0 - {}^7\mathrm{D}_1$	3.000	2.249	⋆
6302.50	816	$^5\mathrm{P}_1 - {}^5\mathrm{D}_0$	2.500	2.058	⋆
6173.34	62	$^5\mathrm{P}_1 - {}^5\mathrm{D}_0$	2.500	1.923	⋆
5506.78	15	$^5\mathrm{F}_2 - {}^5\mathrm{D}_3$	2.000	1.808	
6336.83	816	$^5\mathrm{P}_1 - {}^5\mathrm{D}_1$	2.000	1.769	
5225.53	1	$^5\mathrm{D}_1 - {}^7\mathrm{D}_1$	2.250	1.764	
4690.14	820	$^5\mathrm{P}_1 - {}^7\mathrm{D}_1$	2.750	1.708	
5501.47	15	$^5\mathrm{F}_3 - {}^5\mathrm{D}_4$	1.875	1.669	
6213.43	62	$^5\mathrm{P}_1 - {}^5\mathrm{D}_1$	2.000	1.665	
4938.82	318	$^7\mathrm{F}_2 - {}^7\mathrm{D}_3$	2.000	1.661	

unblended lines in the interval 4365-6859 Å given by Stenflo and Lindegren, 1977) yields the list in Table 9.2.

Let us now turn to the discussion of linear polarization, described by Eqs. (9.83), (9.84), and (9.85). For an absorption line the quantity $[\partial^2 I/\partial\lambda^2]_{\lambda=\lambda'_0}$ is positive, so that, according to Eq. (9.83), $\tilde{Q}(\lambda'_0)$ is negative when $\bar{G}$ is positive and vice versa. Equation (9.85) shows that the sign of $\tilde{Q}$ in the wings is opposite to the sign at line center. It follows that the $\tilde{Q}$ profile vanishes at two particular wavelengths (more precisely, at an even number of wavelengths). These wavelengths can be easily found only when Eq. (9.84) holds (which implies however more restrictive assumptions – see Table 9.1). In that case they are the solutions to the equation $\eta'' = 0$, which, using Eqs. (9.65) and (5.58), can be written in the form[1]

$$\frac{2a}{\sqrt{\pi}} - (1 + 2a^2 - 2v^2)\, H(v,a) - 4av\, L(v,a) = 0\,.$$

For zero damping ($a = 0$) this equation has the two solutions $v_0 = \pm 1/\sqrt{2}$. For $a \neq 0$ one can find an analytical, approximate solution if $a \ll 1$. The calculation, that is left as an exercise to the reader, leads to the following result

$$v_0 = \pm \left(\frac{1}{\sqrt{2}} + \alpha\, a \right)\,,$$

where, denoting by $D(x)$ the Dawson function defined in Eq. (5.56),

$$\alpha = \sqrt{\frac{\mathrm{e}}{2\pi}} \left[2\sqrt{2}\; D\!\left(\frac{1}{\sqrt{2}}\right) - 1 \right] \simeq 0.2957\,.$$

[1] We assume here, to avoid formal complications, that the ambient medium velocity $w_{\rm A}$ is zero. In any case, $w_{\rm A}$ must be constant for Eq. (9.84) to hold.

Another consequence of Eq. (9.84) concerns the special case where the intensity profile $I(\lambda)$ has the form of Eq. (9.86). Since in that case

$$\frac{\eta''}{\eta'} = \frac{\partial^2 I}{\partial \lambda^2} \Big/ \frac{\partial I}{\partial \lambda} ,$$

Eq. (9.84) becomes

$$\tilde{Q}(\lambda) = -\frac{1}{4}\, \Delta\lambda_B^2\, \bar{G}\, \sin^2\theta\, \frac{\partial^2 I}{\partial \lambda^2} ,$$

which 'extends' the validity of expression (9.83) to all wavelengths (of course this holds only for weak, unsaturated lines). Use of Eq. (9.67) yields, as an order of magnitude (cf. Eq. (9.87))

$$\frac{\tilde{Q}}{I_{\rm c}} \approx \frac{\Delta\lambda_B^2}{\Delta\lambda_{\rm D}^2}\, \sin^2\theta\, \bar{G}\, d_{\rm c} ,$$

which suggests the introduction of the (dimensionless) *linear polarization sensitivity index* of a spectral line

$$s_Q = \left(\frac{\lambda_0}{\lambda_{\rm ref}}\right)^2 \bar{G}\, d_{\rm c} . \tag{9.89}$$

The parameter $\bar{G}$ clearly plays for linear polarization the same role as the effective Landé factor $\bar{g}$ does for circular polarization. As $\bar{G}$ is connected with the second-order moments of Zeeman components, it can quite naturally be called the *second order effective Landé factor*. Its main properties can be deduced from Eqs. (9.77) and (9.78). Since for electric-dipole transitions the quantity δ defined in Eq. (9.78) is non-negative for any Zeeman pattern and zero for triplets (normal or anomalous), one can draw the conclusion that $\bar{G} = \bar{g}^2$ for triplets, while $\bar{G} < \bar{g}^2$ for any other Zeeman pattern.

Although most lines have $\bar{G} > 0$, there are several with $\bar{G} < 0$. Analysis of the list of FeI lines quoted above shows[1] that about 8% have $\bar{G} \leq 0$, and that the average value is $\langle \bar{G} \rangle = 1.60$. A search in the same list for which lines produce the largest linear polarization yields the results shown in Table 9.3. Note that the first three spectral lines in Tables 9.3 and 9.2 are the same.

For certain applications, it may be useful to know which transitions produce – because of their intrinsic structure – small polarization, or no polarization at all. Table 9.4 shows a list of transitions with $\bar{g} = 0$ or $\bar{G} = 0$ (the former are the same as in Table 3.2). The list collects all the transitions between L-S levels having $S \leq 7/2$ and $L \leq 5$, and satisfying the conditions

$$\Delta J = 0, \pm 1 , \qquad \Delta S = 0, \pm 1 , \qquad \Delta L = 0, \pm 1, \pm 2 .$$

It appears from Table 9.4 that both $\bar{g}$ and $\bar{G}$ are zero in some cases. It can be easily shown that this property, combined with the selection rule $\Delta J = 0, \pm 1$, implies

[1] The analysis has been performed using L-S Landé factors; the average $\langle \bar{G} \rangle$ was obtained by weighting the $\bar{G}$ factors of individual lines by their central depression.

TABLE 9.3

The lines of the FeI solar spectrum are listed in order of decreasing linear polarization sensitivity index (computed from Eq.(9.89) with $\lambda_{\rm ref} = 5000$ Å; upper panel). The lower panel lists the most sensitive lines with $\bar{G} < 0$. $\bar{G}$ is calculated in L-S coupling. A star in the last column identifies Zeeman triplets.

λ_0(Å)	Multiplet	Transition	$\bar{G}$	s_Q	
5250.21	1	$^5\mathrm{D}_0 - {}^7\mathrm{D}_1$	9.000	7.085	⋆
6302.50	816	$^5\mathrm{P}_1 - {}^5\mathrm{D}_0$	6.250	6.485	⋆
6173.34	62	$^5\mathrm{P}_1 - {}^5\mathrm{D}_0$	6.250	5.936	⋆
4690.14	820	$^5\mathrm{P}_1 - {}^7\mathrm{D}_1$	7.375	4.296	
6232.64	816	$^5\mathrm{P}_2 - {}^5\mathrm{D}_1$	3.983	3.974	
6842.69	1197	$^5\mathrm{P}_1 - {}^5\mathrm{P}_1$	6.250	3.921	⋆
4704.95	821	$^5\mathrm{P}_1 - {}^5\mathrm{D}_0$	6.250	3.885	⋆
5506.78	15	$^5\mathrm{F}_2 - {}^5\mathrm{D}_3$	3.900	3.884	
6136.99	62	$^5\mathrm{P}_2 - {}^5\mathrm{D}_1$	3.983	3.673	
6336.83	816	$^5\mathrm{P}_1 - {}^5\mathrm{D}_1$	3.250	3.644	
5197.93	1091	$^5\mathrm{F}_1 - {}^5\mathrm{P}_1$	−3.125	−1.351	
4598.12	554	$^5\mathrm{D}_1 - {}^5\mathrm{F}_1$	−1.125	−0.740	
5705.46	1087	$^5\mathrm{F}_1 - {}^5\mathrm{D}_1$	−1.125	−0.583	
5432.95	1143	$^5\mathrm{G}_2 - {}^5\mathrm{F}_2$	−0.600	−0.453	
5916.25	170	$^3\mathrm{H}_4 - {}^3\mathrm{F}_4$	−0.559	−0.422	

TABLE 9.4

A star identifies the transitions having $\bar{g} = 0$ or $\bar{G} = 0$. The Landé factors are calculated in L-S coupling. The list includes all the transitions obeying the constraints specified in the text.

Transition	$\bar{g}=0$	$\bar{G}=0$	Transition	$\bar{g}=0$	$\bar{G}=0$	Transition	$\bar{g}=0$	$\bar{G}=0$
$^2\mathrm{S}_{\frac{1}{2}} - {}^4\mathrm{D}_{\frac{1}{2}}$		⋆	$^5\mathrm{D}_2 - {}^3\mathrm{G}_3$	⋆		$^7\mathrm{F}_2 - {}^7\mathrm{H}_3$	⋆	
$^2\mathrm{P}_{\frac{1}{2}} - {}^4\mathrm{D}_{\frac{1}{2}}$		⋆	$^6\mathrm{D}_{\frac{1}{2}} - {}^6\mathrm{G}_{\frac{3}{2}}$		⋆	$^7\mathrm{F}_3 - {}^5\mathrm{H}_4$	⋆	
$^3\mathrm{P}_0 - {}^5\mathrm{F}_1$	⋆	⋆	$^7\mathrm{D}_1 - {}^5\mathrm{F}_2$	⋆		$^8\mathrm{F}_{\frac{1}{2}} - {}^6\mathrm{G}_{\frac{3}{2}}$		⋆
$^4\mathrm{P}_{\frac{1}{2}} - {}^4\mathrm{D}_{\frac{1}{2}}$		⋆	$^8\mathrm{D}_{\frac{5}{2}} - {}^6\mathrm{G}_{\frac{7}{2}}$	⋆		$^8\mathrm{F}_{\frac{3}{2}} - {}^6\mathrm{G}_{\frac{5}{2}}$	⋆	
$^6\mathrm{P}_{\frac{3}{2}} - {}^4\mathrm{F}_{\frac{5}{2}}$	⋆		$^4\mathrm{F}_{\frac{7}{2}} - {}^6\mathrm{H}_{\frac{7}{2}}$		⋆	$^8\mathrm{F}_{\frac{5}{2}} - {}^6\mathrm{G}_{\frac{7}{2}}$		⋆
$^4\mathrm{D}_{\frac{1}{2}} - {}^4\mathrm{D}_{\frac{1}{2}}$	⋆	⋆	$^5\mathrm{F}_1 - {}^5\mathrm{F}_1$	⋆	⋆	$^6\mathrm{G}_{\frac{3}{2}} - {}^6\mathrm{G}_{\frac{3}{2}}$	⋆	⋆
$^4\mathrm{D}_{\frac{1}{2}} - {}^6\mathrm{D}_{\frac{1}{2}}$		⋆	$^5\mathrm{F}_1 - {}^7\mathrm{F}_0$	⋆	⋆	$^6\mathrm{G}_{\frac{3}{2}} - {}^8\mathrm{G}_{\frac{1}{2}}$		⋆
$^4\mathrm{D}_{\frac{1}{2}} - {}^6\mathrm{F}_{\frac{1}{2}}$		⋆	$^5\mathrm{F}_1 - {}^7\mathrm{H}_2$	⋆	⋆	$^7\mathrm{H}_2 - {}^7\mathrm{H}_2$	⋆	⋆
$^4\mathrm{D}_{\frac{1}{2}} - {}^6\mathrm{G}_{\frac{3}{2}}$	⋆	⋆	$^5\mathrm{F}_2 - {}^5\mathrm{H}_3$	⋆				
$^5\mathrm{D}_0 - {}^5\mathrm{F}_1$	⋆	⋆	$^6\mathrm{F}_{\frac{1}{2}} - {}^6\mathrm{G}_{\frac{3}{2}}$		⋆			

that the Landé factors of both the upper and lower level are zero. Therefore, these transitions produce no polarization *whatever* the magnetic field strength.

As for the transitions with $\bar{g} = 0$ and $\bar{G} \neq 0$, it can be proved that the Landé factors of both levels are non-zero. According to Eq. (9.80), such transitions produce no circular polarization under the weak field limit. They can produce circular polarization if the magnetic field is not weak.

According to Eq. (9.84), the transitions with $\bar{G} = 0$ and $\bar{g} \neq 0$ produce no linear polarization in the weak field limit. They can in principle give rise to linear polarization when the magnetic field is strong. However, as shown by Sánchez Almeida and Vela Villahoz (1993), all the transitions in Table 9.4 involving the terms ${}^4\mathrm{D}_{1/2}$ or ${}^6\mathrm{G}_{3/2}$ are characterized by peculiar Zeeman patterns where a compensation occurs between σ and π components, which eventually causes the elements h_Q , h_U , r_Q , r_U of the propagation matrix to be identically zero. It follows (cf. Eq. (9.35)) that the transfer equations for the Stokes parameters Q and U are decoupled from those for I and V; if the boundary values for Q and U are also zero (Eqs. (9.42)), the linear polarization for such transitions is zero *whatever* the magnetic field strength.

As a concluding remark, we emphasize that most of the results contained in this section, and especially those related to the shape of the Stokes profiles and to the dependence of polarization on the characteristics of spectral lines, remain qualitatively valid even when the weak field assumption is dropped, that is when $\Delta\lambda_B \approx \Delta\lambda_\mathrm{D}$.

9.7. Formal Solution through the Evolution Operator

Consider again the transfer equation in the form (9.35). A formal solution to this equation is easily obtained by adjusting the formalism of the evolution operator developed in Sect. 8.2. For this purpose it is convenient to cast Eq. (9.35) in the matrix form[1]

$$\frac{\mathrm{d}}{\mathrm{d}\tau_\mathrm{c}} \boldsymbol{I}(\tau_\mathrm{c}) = \boldsymbol{C}(\tau_\mathrm{c})\, \boldsymbol{I}(\tau_\mathrm{c}) - \boldsymbol{j}(\tau_\mathrm{c}) \,, \tag{9.90}$$

where

$$\boldsymbol{I} = \begin{pmatrix} I \\ Q \\ U \\ V \end{pmatrix}$$

$$\boldsymbol{C} = \boldsymbol{1} + \kappa_\mathrm{L}\, \boldsymbol{H} = \begin{pmatrix} 1+k_I & k_Q & k_U & k_V \\ k_Q & 1+k_I & f_V & -f_U \\ k_U & -f_V & 1+k_I & f_Q \\ k_V & f_U & -f_Q & 1+k_I \end{pmatrix} \tag{9.91}$$

[1] The notation used here is rather uncommon: the matrix $\boldsymbol{C}$ appearing in this equation is often denoted in the literature with the symbol $\boldsymbol{K}$. We use this notation to avoid confusion with the matrix $\boldsymbol{K}$ introduced in Chap. 8 (see Eq. (8.2)).

$$\boldsymbol{j} = \left(S_{\rm c}\,\boldsymbol{1} + \kappa_{\rm L}\,S_{\rm L}\,\boldsymbol{H}\right)\boldsymbol{U} = \begin{pmatrix} S_{\rm c} + k_I\,S_{\rm L} \\ k_Q\,S_{\rm L} \\ k_U\,S_{\rm L} \\ k_V\,S_{\rm L} \end{pmatrix} , \tag{9.92}$$

with $\boldsymbol{U}$ and $\boldsymbol{H}$ given by Eqs. (9.49) and (9.50), and the coefficients k_I , k_Q , k_U , k_V , f_Q , f_U , f_V by Eqs. (9.39).

Equation (9.90) is formally identical to Eq. (8.2), except for a sign switch due to the use of the optical depth (which increases in the direction opposite to propagation) as independent variable. Thus we can define an evolution operator $\boldsymbol{O}(\tau_{\rm c}\,,\tau_{\rm c}')$ via the equation (cf. Eq. (8.6))

$$\boldsymbol{I}(\tau_{\rm c}) = \boldsymbol{O}(\tau_{\rm c}\,,\tau_{\rm c}')\;\boldsymbol{I}(\tau_{\rm c}') \qquad (\tau_{\rm c} \le \tau_{\rm c}') \,, \tag{9.93}$$

which has the properties (cf. Eqs. (8.7)-(8.10))

$$\boldsymbol{O}(\tau_{\rm c}\,,\tau_{\rm c}) = \boldsymbol{1} \tag{9.94}$$

$$\boldsymbol{O}(\tau_{\rm c}\,,\tau_{\rm c}'') = \boldsymbol{O}(\tau_{\rm c}\,,\tau_{\rm c}')\,\boldsymbol{O}(\tau_{\rm c}'\,,\tau_{\rm c}'') \qquad (\tau_{\rm c} \le \tau_{\rm c}' \le \tau_{\rm c}'') \tag{9.95}$$

$$\frac{\rm d}{{\rm d}\tau_{\rm c}}\,\boldsymbol{O}(\tau_{\rm c}\,,\tau_{\rm c}') = \boldsymbol{C}(\tau_{\rm c})\,\boldsymbol{O}(\tau_{\rm c}\,,\tau_{\rm c}') \tag{9.96}$$

$$\frac{\rm d}{{\rm d}\tau_{\rm c}'}\,\boldsymbol{O}(\tau_{\rm c}\,,\tau_{\rm c}') = -\,\boldsymbol{O}(\tau_{\rm c}\,,\tau_{\rm c}')\,\boldsymbol{C}(\tau_{\rm c}') \,, \tag{9.97}$$

and which can be written in the form (cf. Eq. (8.12))

$$\boldsymbol{O}(\tau_{\rm c}\,,\tau_{\rm c}') = \boldsymbol{1} + \sum_{n=1}^{\infty}\,\frac{(-1)^n}{n!}\int_{\tau_{\rm c}}^{\tau_{\rm c}'}\!{\rm d}\tau_1\int_{\tau_{\rm c}}^{\tau_{\rm c}'}\!{\rm d}\tau_2\,\cdots\int_{\tau_{\rm c}}^{\tau_{\rm c}'}\!{\rm d}\tau_n\;\mathbb{P}\Big\{\boldsymbol{C}(\tau_1)\,\boldsymbol{C}(\tau_2)\,\cdots\,\boldsymbol{C}(\tau_n)\Big\} \,,$$

where $\mathbb{P}$ is the Dyson chronological product

$$\mathbb{P}\Big\{\boldsymbol{C}(\tau_1)\,\boldsymbol{C}(\tau_2)\,\cdots\,\boldsymbol{C}(\tau_n)\Big\} = \boldsymbol{C}(\tau_i)\,\boldsymbol{C}(\tau_j)\,\cdots\,\boldsymbol{C}(\tau_k) \,, \tag{9.98}$$

$(i,j,\ldots,k)$ being a permutation of the integers $(1,2,\ldots,n)$ such that

$$\tau_i \le \tau_j \le\,\cdots\,\le \tau_k \,. \tag{9.99}$$

The formal solution to Eq. (9.90) is given by (cf. Eq. (8.14))

$$\boldsymbol{I}(\tau_{\rm c}) = \int_{\tau_{\rm c}}^{\tau_{\rm c}'}\!\boldsymbol{O}(\tau_{\rm c}\,,\tau_{\rm c}'')\;\boldsymbol{j}(\tau_{\rm c}'')\;{\rm d}\tau_{\rm c}'' \;+\; \boldsymbol{O}(\tau_{\rm c}\,,\tau_{\rm c}')\;\boldsymbol{I}(\tau_{\rm c}') \,, \tag{9.100}$$

which for a semi-infinite atmosphere reduces to

$$\boldsymbol{I}(\tau_{\rm c}) = \int_{\tau_{\rm c}}^{\infty} \boldsymbol{O}(\tau_{\rm c}\,,\tau_{\rm c}')\ \boldsymbol{j}(\tau_{\rm c}')\,{\rm d}\tau_{\rm c}' \tag{9.101}$$

provided

$$\lim_{\tau_{\rm c}'\to\infty} \boldsymbol{O}(\tau_{\rm c}\,,\tau_{\rm c}')\ \boldsymbol{j}(\tau_{\rm c}') = 0\ . \tag{9.102}$$

It can be easily proved, by the same arguments used in Sect. 8.3, that the evolution operator corresponding to a $\boldsymbol{C}$ matrix independent of optical depth is

$$\boldsymbol{O}(\tau_{\rm c}\,,\tau_{\rm c}') = {\rm e}^{-(\tau_{\rm c}'-\tau_{\rm c})\,\boldsymbol{C}}\ , \tag{9.103}$$

while for a matrix of the form $\boldsymbol{C} = c_1(\tau_{\rm c})\,\boldsymbol{1} + c_2(\tau_{\rm c})\,\boldsymbol{H}$, with $\boldsymbol{H}$ independent of optical depth, one has

$$\boldsymbol{O}(\tau_{\rm c}\,,\tau_{\rm c}') = {\rm e}^{-\int_{\tau_{\rm c}}^{\tau_{\rm c}'} c_1(\tau_{\rm c}'')\,{\rm d}\tau_{\rm c}''}\ \ {\rm e}^{-\int_{\tau_{\rm c}}^{\tau_{\rm c}'} c_2(\tau_{\rm c}'')\,{\rm d}\tau_{\rm c}''\ \boldsymbol{H}}\ . \tag{9.104}$$

9.8. The Unno-Rachkovsky Solution

The formal solution derived in the previous section allows us to express the Stokes parameters of the radiation propagating along any direction at any specified point of a magnetized stellar atmosphere in terms of the physical characteristics of the atmosphere itself. To specify such characteristics means to give a *model* of the atmosphere or, in other words, a set of mathematical functions which fix, at any point in the atmosphere, the value of all the physical quantities affecting the propagation matrix and the emission vector.

Probably the simplest atmospheric model[1] is the so-called *Milne-Eddington model* which results from the following set of assumptions:
a) the atmosphere is plane-parallel, semi-infinite, and in LTE ($S_{\rm c} = S_{\rm L} = B_{\rm P}$);
b) all the quantities affecting the propagation matrix $\boldsymbol{C}$, namely $\kappa_{\rm L}$, B, θ, χ, $\Delta\lambda_{\rm D}$, Γ', $w_{\rm A}$ are depth-independent, so that, for any propagation direction, $\boldsymbol{C}$ is constant;
c) the Planck function is linear in $t_{\rm c}$, the continuum optical depth measured along the vertical

$$B_{\rm P} = B_0 + B_1\,t_{\rm c} = B_0\,(1+\beta\,t_{\rm c})\ . \tag{9.105}$$

Under these assumptions we can easily find, using the formulae of the previous section, an analytical solution to the transfer equation.

[1] The even simpler reversing-layer model that leads to the Seares formulae (see Sect. 9.13) should be considered, more properly, a slab model.

Owing to assumptions a) and c), Eq. (9.92) reduces to (see also Eq. (9.91))

$$\boldsymbol{j}(t_{\rm c}) = B_0\,(1+\beta\,t_{\rm c})\,\boldsymbol{C}\,\boldsymbol{U}\ ,$$

and using assumption b) we obtain from Eqs. (9.103), (9.101) and (9.100)[1]

$$\boldsymbol{I}(t_{\rm c}\,,\mu) = B_0 \int\limits_{t_{\rm c}}^{\infty} {\rm e}^{-\frac{t'_{\rm c}-t_{\rm c}}{\mu}\,\boldsymbol{C}}\ (1+\beta\,t'_{\rm c})\,\boldsymbol{C}\,\boldsymbol{U}\ \frac{{\rm d}t'_{\rm c}}{\mu} \qquad (\mu>0)$$

$$\boldsymbol{I}(t_{\rm c}\,,\mu) = B_0 \int\limits_{0}^{t_{\rm c}} {\rm e}^{-\frac{t_{\rm c}-t'_{\rm c}}{|\mu|}\,\boldsymbol{C}}\ (1+\beta\,t'_{\rm c})\,\boldsymbol{C}\,\boldsymbol{U}\ \frac{{\rm d}t'_{\rm c}}{|\mu|} \qquad (\mu<0)\ ,$$

with $\mu = \cos\alpha$ and α defined in Fig. 9.2. Both integrals can be performed by means of the substitution $(t'_{\rm c}-t_{\rm c})/\mu = x$. Bearing in mind the definition of the exponential of a matrix (Eq. (8.21)), it can be easily proved that

$$\int\limits_a^b {\rm e}^{-x\,\boldsymbol{C}}\ {\rm d}x = \Big[\,{\rm e}^{-a\,\boldsymbol{C}}\ -\ {\rm e}^{-b\,\boldsymbol{C}}\,\Big]\,\boldsymbol{C}^{-1} \tag{9.106}$$

$$\int\limits_a^b {\rm e}^{-x\,\boldsymbol{C}}\ x\ {\rm d}x = \Big[\,\big(a\,\boldsymbol{1}+\boldsymbol{C}^{-1}\big)\,{\rm e}^{-a\,\boldsymbol{C}}\ -\ \big(b\,\boldsymbol{1}+\boldsymbol{C}^{-1}\big)\,{\rm e}^{-b\,\boldsymbol{C}}\,\Big]\,\boldsymbol{C}^{-1}\ , \tag{9.107}$$

where $\boldsymbol{C}^{-1}$ is the inverse of the matrix $\boldsymbol{C}$,

$$\boldsymbol{C}\,\boldsymbol{C}^{-1} = \boldsymbol{C}^{-1}\,\boldsymbol{C} = \boldsymbol{1}\ .$$

Use of Eqs. (9.106) and (9.107) leads to the expressions

$$\boldsymbol{I}(t_{\rm c}\,,\mu) = B_0\Big[\,(1+\beta\,t_{\rm c})\,\boldsymbol{1}\ +\ \beta\mu\,\boldsymbol{C}^{-1}\,\Big]\,\boldsymbol{U} \qquad (\mu>0)$$

$$\begin{aligned}\boldsymbol{I}(t_{\rm c}\,,\mu) = B_0\Big[\,&(1+\beta\,t_{\rm c})\,\boldsymbol{1}\ -\ \beta\,|\mu|\,\boldsymbol{C}^{-1}\\ &-\big(\boldsymbol{1}-\beta\,|\mu|\,\boldsymbol{C}^{-1}\big)\,{\rm e}^{-\frac{t_{\rm c}}{|\mu|}\,\boldsymbol{C}}\,\Big]\,\boldsymbol{U} \qquad (\mu<0)\ .\end{aligned} \tag{9.108}$$

In particular, the radiation emerging from the atmosphere ($t_{\rm c}=0\,,\ \mu>0$) is given by

$$\boldsymbol{I}(0,\mu) = B_0\,\big[\,\boldsymbol{1}\ +\ \beta\mu\,\boldsymbol{C}^{-1}\,\big]\,\boldsymbol{U}\ . \tag{9.109}$$

[1] It is understood that the boundary condition at $t_{\rm c}=0$ is $\boldsymbol{I}\,(\mu<0)=0$; using Eqs. (A5.23) and (9.111) it can be shown that condition (9.102) is also satisfied.

TABLE 9.5

Analytical expressions for the elements of the matrix $\boldsymbol{C}^{-1}$

$$
\begin{aligned}
(C^{-1})_{00} &= \Delta^{-1}(1+k_I)\left[(1+k_I)^2+f_Q^2+f_U^2+f_V^2\right]\\
(C^{-1})_{01} &= -\Delta^{-1}\left[(1+k_I)^2k_Q+(1+k_I)(k_Uf_V-k_Vf_U)+f_Q(k_Qf_Q+k_Uf_U+k_Vf_V)\right]\\
(C^{-1})_{02} &= -\Delta^{-1}\left[(1+k_I)^2k_U+(1+k_I)(k_Vf_Q-k_Qf_V)+f_U(k_Qf_Q+k_Uf_U+k_Vf_V)\right]\\
(C^{-1})_{03} &= -\Delta^{-1}\left[(1+k_I)^2k_V+(1+k_I)(k_Qf_U-k_Uf_Q)+f_V(k_Qf_Q+k_Uf_U+k_Vf_V)\right]\\
(C^{-1})_{10} &= -\Delta^{-1}\left[(1+k_I)^2k_Q-(1+k_I)(k_Uf_V-k_Vf_U)+f_Q(k_Qf_Q+k_Uf_U+k_Vf_V)\right]\\
(C^{-1})_{11} &= \Delta^{-1}(1+k_I)\left[(1+k_I)^2+f_Q^2-k_U^2-k_V^2\right]\\
(C^{-1})_{12} &= -\Delta^{-1}\left[(1+k_I)^2f_V-(1+k_I)(k_Qk_U+f_Qf_U)-k_V(k_Qf_Q+k_Uf_U+k_Vf_V)\right]\\
(C^{-1})_{13} &= \Delta^{-1}\left[(1+k_I)^2f_U+(1+k_I)(k_Vk_Q+f_Vf_Q)-k_U(k_Qf_Q+k_Uf_U+k_Vf_V)\right]\\
(C^{-1})_{20} &= -\Delta^{-1}\left[(1+k_I)^2k_U-(1+k_I)(k_Vf_Q-k_Qf_V)+f_U(k_Qf_Q+k_Uf_U+k_Vf_V)\right]\\
(C^{-1})_{21} &= \Delta^{-1}\left[(1+k_I)^2f_V+(1+k_I)(k_Qk_U+f_Qf_U)-k_V(k_Qf_Q+k_Uf_U+k_Vf_V)\right]\\
(C^{-1})_{22} &= \Delta^{-1}(1+k_I)\left[(1+k_I)^2+f_U^2-k_V^2-k_Q^2\right]\\
(C^{-1})_{23} &= -\Delta^{-1}\left[(1+k_I)^2f_Q-(1+k_I)(k_Uk_V+f_Uf_V)-k_Q(k_Qf_Q+k_Uf_U+k_Vf_V)\right]\\
(C^{-1})_{30} &= -\Delta^{-1}\left[(1+k_I)^2k_V-(1+k_I)(k_Qf_U-k_Uf_Q)+f_V(k_Qf_Q+k_Uf_U+k_Vf_V)\right]\\
(C^{-1})_{31} &= -\Delta^{-1}\left[(1+k_I)^2f_U-(1+k_I)(k_Vk_Q+f_Vf_Q)-k_U(k_Qf_Q+k_Uf_U+k_Vf_V)\right]\\
(C^{-1})_{32} &= \Delta^{-1}\left[(1+k_I)^2f_Q+(1+k_I)(k_Uk_V+f_Uf_V)-k_Q(k_Qf_Q+k_Uf_U+k_Vf_V)\right]\\
(C^{-1})_{33} &= \Delta^{-1}(1+k_I)\left[(1+k_I)^2+f_V^2-k_Q^2-k_U^2\right]
\end{aligned}
$$

where

$$\Delta = (1+k_I)^4+(1+k_I)^2\left(f_Q^2+f_U^2+f_V^2-k_Q^2-k_U^2-k_V^2\right)-(k_Qf_Q+k_Uf_U+k_Vf_V)^2$$

The matrix $\boldsymbol{C}^{-1}$ can be calculated analytically from the expression of the matrix $\boldsymbol{C}$ given in Eq. (9.91). A straightforward calculation yields the expressions contained in Table 9.5, whence one gets the so-called *Unno-Rachkovsky solutions*[1]

$$I(0,\mu) = B_0\left\{1+\beta\mu\,\Delta^{-1}(1+k_I)\left[(1+k_I)^2+f_Q^2+f_U^2+f_V^2\right]\right\}$$

$$\begin{aligned}Q(0,\mu) = -B_0\,\beta\mu\,\Delta^{-1}\Big\{&(1+k_I)^2\,k_Q-(1+k_I)\,(k_Uf_V-k_Vf_U)\\&+f_Q\,(k_Qf_Q+k_Uf_U+k_Vf_V)\Big\}\end{aligned}$$

[1] Note that the quantity $(k_Qf_U-k_Uf_Q)$ appearing in the expression of $V(0,\mu)$ – and of the matrix elements $(C^{-1})_{03}$ and $(C^{-1})_{30}$ – has been written down just to point out the 'cyclic' character of the formulae for Q, U, V; however, as obvious from Eqs. (9.39) and (9.32), it is identically zero.

$$U(0,\mu) = -B_0\,\beta\mu\,\Delta^{-1}\Big\{(1+k_I)^2\,k_U - (1+k_I)\,(k_V f_Q - k_Q f_V) + f_U\,(k_Q f_Q + k_U f_U + k_V f_V)\Big\}$$

$$V(0,\mu) = -B_0\,\beta\mu\,\Delta^{-1}\Big\{(1+k_I)^2\,k_V - (1+k_I)\,(k_Q f_U - k_U f_Q) + f_V\,(k_Q f_Q + k_U f_U + k_V f_V)\Big\}\,. \qquad (9.110)$$

As far as the quantity Δ (which is the determinant of the matrix $\boldsymbol{C}$) is concerned, it is worth noticing that the inequality

$$(k_Q f_Q + k_U f_U + k_V f_V)^2 \le (k_Q^2 + k_U^2 + k_V^2)\,(f_Q^2 + f_U^2 + f_V^2) \qquad (9.111)$$

implies

$$\Delta \ge \left[\,(1+k_I)^2 + (f_Q^2 + f_U^2 + f_V^2)\,\right]\left[\,(1+k_I)^2 - (k_Q^2 + k_U^2 + k_V^2)\,\right]\,.$$

On the other hand, it can be shown via Eqs. (9.39) and (9.32) that the term in the second bracket is positive. It follows that, whatever the values of the various parameters, one always has $\Delta > 0$.

Equations (9.110) are particularly important because they provide simple analytical expressions for the Stokes parameters profiles of the line radiation emerging from a magnetized stellar atmosphere. Although the Milne-Eddington model (summarized by approximations a), b) and c) at the beginning of this section) is indeed the simplest schematization of a real stellar atmosphere, the Unno-Rachkovsky formulae contain the basic physics of radiative transfer for polarized radiation and have been widely used in astrophysical applications. They were first derived by Unno (1956) who neglected, however, magneto-optical effects. By setting $f_Q = f_U = f_V = 0$ in Eqs. (9.110), one obtains the simplified *Unno solutions*

$$\begin{aligned} I(0,\mu) &= B_0\left[\,1 + \beta\mu\,\Delta_0^{-1}\,(1+k_I)\,\right] \\ Q(0,\mu) &= -B_0\,\beta\mu\,\Delta_0^{-1}\;k_Q \\ U(0,\mu) &= -B_0\,\beta\mu\,\Delta_0^{-1}\;k_U \\ V(0,\mu) &= -B_0\,\beta\mu\,\Delta_0^{-1}\;k_V\,, \end{aligned}$$

where

$$\Delta_0 = (1+k_I)^2 - k_Q^2 - k_U^2 - k_V^2\,.$$

The equations acquired their standard form with the introduction of magneto-optical effects by Rachkovsky (1962b).

The Stokes parameters profiles given by the Unno-Rachkovsky solutions depend on 9 different parameters: the seven quoted under point b) above plus the coefficients B_0 and β representing the surface value and the slope of the Planck function. Obviously there is a further dependence on the Zeeman pattern and on the rest

wavelength of the spectral line. The dependence on the parameter B_0 can be dropped by normalizing the profiles to the intensity $I_c(0,\mu)$ of the nearby continuum. Since in the continuum all the coefficients k and f vanish, we have from Eqs. (9.110)

$$I_c(0,\mu) = B_0\,(1+\beta\mu)\ .$$

A frequently used normalization is the following

$$\begin{aligned}
\mathcal{R}_I(0,\mu) &= \frac{I_c(0,\mu) - I(0,\mu)}{I_c(0,\mu)} \\
&= \frac{\beta\mu}{1+\beta\mu}\Big\{1 - \Delta^{-1}\,(1+k_I)\left[(1+k_I)^2 + f_Q^2 + f_U^2 + f_V^2\right]\Big\} \\
\mathcal{R}_Q(0,\mu) &= \frac{Q(0,\mu)}{I_c(0,\mu)} = -\,\frac{\beta\mu}{1+\beta\mu}\,\Delta^{-1} \\
&\times\Big\{(1+k_I)^2\,k_Q - (1+k_I)(k_U f_V - k_V f_U) + f_Q\,(k_Q f_Q + k_U f_U + k_V f_V)\Big\} \\
\mathcal{R}_U(0,\mu) &= \frac{U(0,\mu)}{I_c(0,\mu)} = -\,\frac{\beta\mu}{1+\beta\mu}\,\Delta^{-1} \\
&\times\Big\{(1+k_I)^2\,k_U - (1+k_I)(k_V f_Q - k_Q f_V) + f_U\,(k_Q f_Q + k_U f_U + k_V f_V)\Big\} \\
\mathcal{R}_V(0,\mu) &= \frac{V(0,\mu)}{I_c(0,\mu)} \\
&= -\,\frac{\beta\mu}{1+\beta\mu}\,\Delta^{-1}\Big\{(1+k_I)^2\,k_V + f_V\,(k_Q f_Q + k_U f_U + k_V f_V)\Big\}\,. \qquad (9.112)
\end{aligned}$$

Because of the large number of parameters on which the Unno-Rachkovsky solutions depend, we show in Figs. 9.5 and 9.6 just a few illustrative examples.[1] Figure 9.5 shows the Stokes profiles for six different Zeeman patterns (the same as in Figs. 3.2 and 9.3) and for a fixed set of parameters' values (which will be referred to as 'standard case'). Figure 9.6 refers to a normal Zeeman triplet (panel (a) in Fig. 9.5) and shows how the Stokes profiles change when the different parameters are varied one at a time.

As apparent from panel (d) of Fig. 9.6, the I and V profiles are unaffected by a variation of the azimuth angle χ, while Q and U tend to change into each other. Since χ is independent of optical depth, such behavior is implied by the definition itself of the Stokes parameters: a variation $\Delta\chi$ is equivalent to a rotation of the reference direction through an angle $\alpha = -\Delta\chi$. This property is in fact contained in Eqs. (9.110): bearing in mind Eqs. (9.39) and (9.32), it can be easily seen that I and V are independent of χ, while Q and U change according to the law (cf.

[1] An atlas of Stokes profiles, based on the Unno-Rachkovsky formulae, has been presented by Arena and Landi Degl'Innocenti (1982).

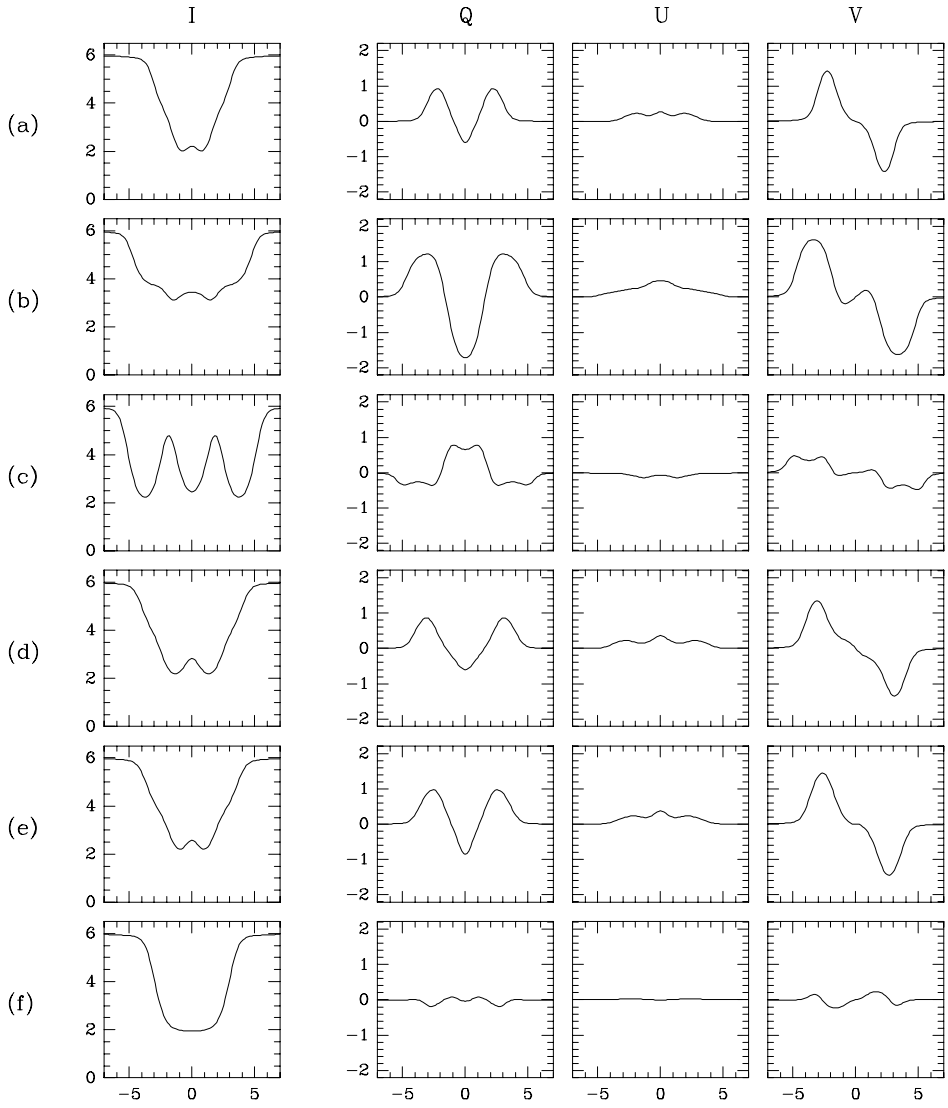

Fig.9.5. The Stokes parameters profiles, as given by the Unno-Rachkovsky formulae (9.110), are plotted as functions of the reduced wavelength for the same transitions considered in Fig.9.3. The profiles are normalized to B_0, and the values of the relevant parameters are the following ('standard case'): $\beta\mu = 5$, $\kappa_{\rm L} = 20$, $v_{\rm A} = 0$, $v_B = 1.5$, $\theta = 60^\circ$, $\chi = 0^\circ$, $a = 0.05$ (the last 5 values are the same as in Fig.9.3).

Eqs. (1.45))

$$Q(\chi + \Delta\chi) = \cos(2\,\Delta\chi)\; Q(\chi) \;-\; \sin(2\,\Delta\chi)\; U(\chi)$$
$$U(\chi + \Delta\chi) = \sin(2\,\Delta\chi)\; Q(\chi) \;+\; \cos(2\,\Delta\chi)\; U(\chi)\;.$$

It should be remarked that Eqs. (9.110) provide analytical expressions for the

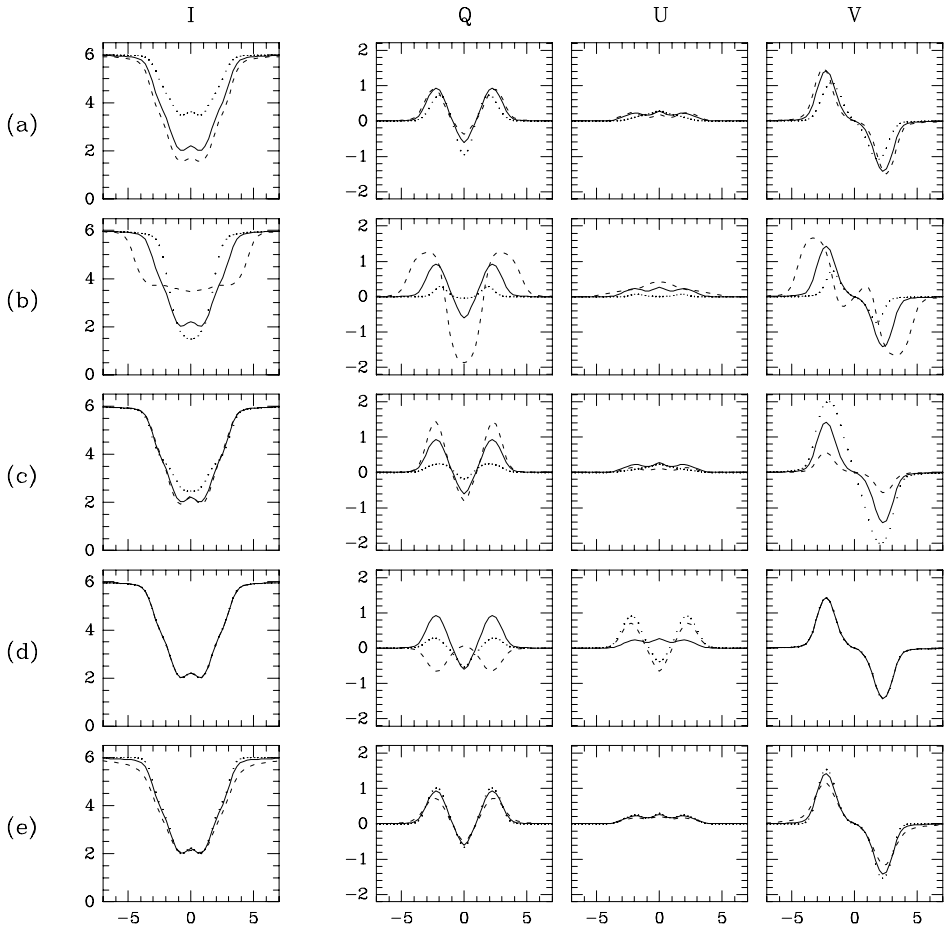

Fig.9.6. Influence of the different parameters, varied one at a time, on the Stokes profiles. The profiles refer to a Zeeman triplet and are calculated as in Fig.9.5; the full line corresponds to the 'standard case'. (a) $\kappa_{\rm L} = 5$ (dotted), $\kappa_{\rm L} = 40$ (dashed); (b) $v_B = 0.5$ (dotted), $v_B = 3$ (dashed); (c) $\theta = 30^\circ$ (dotted), $\theta = 80^\circ$ (dashed); (d) $\chi = 30^\circ$ (dotted), $\chi = 60^\circ$ (dashed); (e) $a = 0.0$ (dotted), $a = 0.2$ (dashed).

emerging Stokes parameters profiles ($t_{\rm c} = 0$, $\mu > 0$). To obtain analytical expressions valid for any optical depth and direction we must resort to Eqs. (9.108). The result for $\mu > 0$ is trivial

$$
\begin{aligned}
I(t_{\rm c}\,,\mu) &= I(0,\mu) + B_0\,\beta\,t_{\rm c} \\
Q(t_{\rm c}\,,\mu) &= Q(0,\mu) \\
U(t_{\rm c}\,,\mu) &= U(0,\mu) \\
V(t_{\rm c}\,,\mu) &= V(0,\mu)\ ,
\end{aligned}
$$

while for $\mu < 0$ one needs the expressions for the matrix elements of $\boldsymbol{C}^{-1}$ contained

in Table 9.5 and those for the exponential of a matrix deduced in App. 5. The resulting formulae are rather involved and will not be given here.

9.9. More General Analytical Solutions

The Milne-Eddington atmosphere, which is at the basis of the Unno-Rachkovsky solution to the radiative transfer equation, is in many cases a too rough approximation for a real stellar atmosphere. The main limitations of the model are the LTE assumption, the linearity of the Planck function with optical depth, and the assumption of a depth-independent $\kappa_{\rm L}$ (the ratio between line and continuum opacity).

If we drop these approximations, but retain all the other assumptions of the Milne-Eddington model, it is still possible to obtain a fully analytical solution to the transfer equation. To be definite, let us make the following (somewhat more realistic) assumptions:

a′) the atmosphere where the line is formed is plane-parallel and semi-infinite;

b′) the quantities B, θ, χ, $\Delta\lambda_{\rm D}$, Γ', $w_{\rm A}$ are depth-independent throughout the whole atmosphere.

Assumption b′) means that the magnetic field vector and the absorption and anomalous dispersion profiles are independent of optical depth. It follows that the propagation matrix $\boldsymbol{C}$ defined in Eq. (9.91) has the form

$$\boldsymbol{C}(t_{\rm c}) = \boldsymbol{1} + \kappa_{\rm L}(t_{\rm c})\, \boldsymbol{H} \ ,$$

with $\boldsymbol{H} = \text{const}$. According to Eqs. (9.104), (9.101), (9.102) and (9.92), the emerging Stokes parameters are given by

$$\boldsymbol{I}(0,\mu) = \int_0^\infty \mathrm{e}^{-\frac{t_{\rm c}}{\mu}}\ \mathrm{e}^{-\frac{K_{\rm L}(t_{\rm c})}{\mu}\boldsymbol{H}}\ \left[\, S_{\rm c}(t_{\rm c})\, \boldsymbol{1} + \kappa_{\rm L}(t_{\rm c})\, S_{\rm L}(t_{\rm c})\ \boldsymbol{H}\,\right] \boldsymbol{U}\ \frac{\mathrm{d}t_{\rm c}}{\mu}\ , \qquad (9.113)$$

where

$$K_{\rm L}(t_{\rm c}) = \int_0^{t_{\rm c}} \kappa_{\rm L}(t'_{\rm c})\ \mathrm{d}t'_{\rm c}\ ,$$

provided

$$\lim_{t_{\rm c}\to\infty}\ \mathrm{e}^{-\frac{t_{\rm c}}{\mu}}\ \mathrm{e}^{-\frac{K_{\rm L}(t_{\rm c})}{\mu}\boldsymbol{H}}\ \left[\, S_{\rm c}(t_{\rm c})\, \boldsymbol{1} + \kappa_{\rm L}(t_{\rm c})\, S_{\rm L}(t_{\rm c})\ \boldsymbol{H}\,\right] \boldsymbol{U} = 0\ . \qquad (9.114)$$

Using Eq. (9.113), explicit expressions for $\boldsymbol{I}(0,\mu)$ can be obtained once the functions $S_{\rm c}(t_{\rm c})$, $S_{\rm L}(t_{\rm c})$, and $\kappa_{\rm L}(t_{\rm c})$ are specified.

For example, let us consider a simple generalization of the Milne-Eddington model which is suitable to describe a chromospheric temperature rise at low optical depths. Assuming

$$\begin{aligned} &\kappa_{\rm L} = \text{const.} \\ &S_{\rm c}(t_{\rm c}) = B_0\,(1+\beta\,t_{\rm c}) \,+\, A_1\,{\rm e}^{-\alpha_1\,t_{\rm c}} \\ &S_{\rm L}(t_{\rm c}) = B_0\,(1+\beta\,t_{\rm c}) \,+\, A_1\,{\rm e}^{-\alpha_1\,t_{\rm c}} \,-\, A_2\,{\rm e}^{-\alpha_2\,t_{\rm c}} \end{aligned} \tag{9.115}$$

with α_1 and α_2 positive, so that Eq. (9.114) is satisfied, one has the possibility of adjusting the various parameters so as to simulate a variety of different behaviors for the continuum and line source functions. In particular, the last term in $S_{\rm L}(t_{\rm c})$ allows for a drop of the line source function below the continuum source function at optical depths $t_{\rm c} \le 1/\alpha_2$.

The integral resulting from the substitution of Eqs. (9.115) into Eq. (9.113) can be carried out with the help of Eqs. (9.106) and (9.107). After some algebra we obtain

$$\begin{aligned} \boldsymbol{I}(0,\mu) = \Big\{ & B_0\,\big[\,\boldsymbol{1} + \beta\mu\,\boldsymbol{C}^{-1}\,\big] + A_1\,\big[\,\boldsymbol{1} - \alpha_1\mu\,(\alpha_1\mu\,\boldsymbol{1}+\boldsymbol{C})^{-1}\,\big] \\ & - A_2\,\big[\,\boldsymbol{1} - (1+\alpha_2\mu)\,(\alpha_2\mu\,\boldsymbol{1}+\boldsymbol{C})^{-1}\,\big]\Big\}\,\boldsymbol{U}\;, \end{aligned} \tag{9.116}$$

which of course reduces to the Unno-Rachkovsky solution (9.109) for $A_1 = A_2 = 0$. Figure 9.7 shows the Stokes parameters profiles deduced from Eq. (9.116) in some particular cases. The profiles are normalized to the intensity of the nearby continuum, which is given by

$$I_{\rm c}(0,\mu) = B_0\,(1+\beta\mu) \,+\, \frac{A_1}{1+\alpha_1\mu}\;.$$

A remarkable expression for the emerging Stokes parameters can be obtained if, in addition to assumptions a′) and b′) specified above, we adopt the LTE hypothesis. To derive this expression we use the line optical depth $t_{\rm L}$ (instead of $t_{\rm c}$) as independent variable.

Using Eqs. (9.36) and (9.34), we can write the transfer equation in the form

$$\mu\,\frac{{\rm d}\boldsymbol{I}}{{\rm d}t_{\rm L}} = (\kappa_{\rm c}\,\boldsymbol{1} \,+\, \boldsymbol{H})\,\boldsymbol{I} - (\kappa_{\rm c}\,S_{\rm c}\,\boldsymbol{1} \,+\, S_{\rm L}\,\boldsymbol{H})\,\boldsymbol{U}\;,$$

where $\kappa_{\rm c}$ is given by Eq. (9.37) and $\boldsymbol{H}$ by Eq. (9.50). According to Eqs. (9.104), (9.101) and (9.102), the emerging Stokes parameters are given by

$$\boldsymbol{I}(0,\mu) = \int_0^\infty {\rm e}^{-\frac{K_{\rm c}(t_{\rm L})}{\mu}}\;\; {\rm e}^{-\frac{t_{\rm L}}{\mu}\,\boldsymbol{H}}\;\big[\,\kappa_{\rm c}(t_{\rm L})\,S_{\rm c}(t_{\rm L})\,\boldsymbol{1} \,+\, S_{\rm L}(t_{\rm L})\,\boldsymbol{H}\,\big]\,\boldsymbol{U}\;\frac{{\rm d}t_{\rm L}}{\mu}\;, \tag{9.117}$$

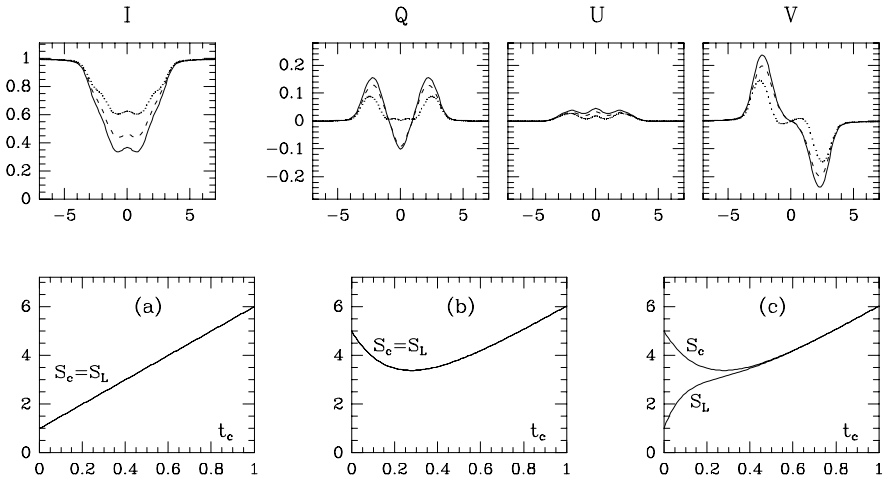

Fig.9.7. Stokes parameters profiles as functions of reduced wavelength, computed from Eq.(9.116) for a normal Zeeman triplet and the source functions $S_{\rm c}$ and $S_{\rm L}$ plotted in the lower part of the figure. The profiles are normalized to the continuum intensity, the source functions to B_0. Full line: $A_1 = A_2 = 0$ (model (a), i.e. a Milne-Eddington atmosphere); dotted line: $A_1/B_0 = 4$, $\alpha_1 = 5$, $A_2 = 0$ (model (b)); dashed line: $A_1/B_0 = A_2/B_0 = 4$, $\alpha_1 = 5$, $\alpha_2 = 10$ (model (c)). The parameters β and μ are set to 5 and 1 respectively. The remaining parameters have the same values as in Fig.9.5.

with

$$K_{\rm c}(t_{\rm L}) = \int_0^{t_{\rm L}} \kappa_{\rm c}(t'_{\rm L})\ {\rm d}t'_{\rm L}\ ,$$

provided

$$\lim_{t_{\rm L}\to\infty}\ {\rm e}^{-\frac{K_{\rm c}(t_{\rm L})}{\mu}}\ \ {\rm e}^{-\frac{t_{\rm L}}{\mu}\boldsymbol{H}}\ \left[\,\kappa_{\rm c}(t_{\rm L})\,S_{\rm c}(t_{\rm L})\,\boldsymbol{1}\ +\ S_{\rm L}(t_{\rm L})\,\boldsymbol{H}\,\right]\boldsymbol{U} = 0\ .$$

Equation (9.117), which is basically equivalent to Eq. (9.113), can be further developed in the LTE case, where

$$S_{\rm c}(t_{\rm L}) = S_{\rm L}(t_{\rm L}) = B_{\rm P}(t_{\rm L})\ .$$

Since

$${\rm e}^{-\frac{K_{\rm c}(t_{\rm L})}{\mu}}\ \ {\rm e}^{-\frac{t_{\rm L}}{\mu}\boldsymbol{H}}\ \left[\kappa_{\rm c}(t_{\rm L})\,\boldsymbol{1}\ +\ \boldsymbol{H}\,\right] = -\,\mu\,\frac{\rm d}{{\rm d}t_{\rm L}}\left\{{\rm e}^{-\frac{K_{\rm c}(t_{\rm L})}{\mu}}\ \ {\rm e}^{-\frac{t_{\rm L}}{\mu}\boldsymbol{H}}\right\}\ ,$$

integration by parts of Eq. (9.117) yields

$$\boldsymbol{I}(0,\mu) = \left\{B_{\rm P}(0)\,\boldsymbol{1} + \int_0^{\infty} {\rm e}^{-\frac{K_{\rm c}(t_{\rm L})}{\mu}}\ \ {\rm e}^{-\frac{t_{\rm L}}{\mu}\boldsymbol{H}}\ \ \frac{{\rm d}B_{\rm P}}{{\rm d}t_{\rm L}}\ {\rm d}t_{\rm L}\right\}\boldsymbol{U}\ , \qquad (9.118)$$

where $B_{\rm P}(0) = B_{\rm P}(t_{\rm L} = 0)$. Using Eq. (A5.23), the matrix $\exp(-t_{\rm L}\,\boldsymbol{H}/\mu)$ can be written in the form

$$\mathrm{e}^{-\frac{t_{\rm L}}{\mu}\,\boldsymbol{H}} \;=\; \sum_{i=1}^{4}\; \mathrm{e}^{-\frac{t_{\rm L}}{\mu}\,\lambda_i(\,\vec{h},\vec{r}\,)}\;\; \boldsymbol{N}_i(\,\vec{h},\vec{r}\,)\;, \tag{9.119}$$

where the matrices $\boldsymbol{N}_i$ are given by Eqs. (A5.24) and λ_i are the eigenvalues of the matrix $\boldsymbol{H}$ (cf. Sect. 8.4)

$$\begin{aligned} \lambda_1(\,\vec{h},\vec{r}\,) &= h_I + \Lambda_+(\,\vec{h},\vec{r}\,) \qquad & \lambda_3(\,\vec{h},\vec{r}\,) &= h_I + \mathrm{i}\,\Lambda_-(\,\vec{h},\vec{r}\,) \\ \lambda_2(\,\vec{h},\vec{r}\,) &= h_I - \Lambda_+(\,\vec{h},\vec{r}\,) \qquad & \lambda_4(\,\vec{h},\vec{r}\,) &= h_I - \mathrm{i}\,\Lambda_-(\,\vec{h},\vec{r}\,)\;, \end{aligned}$$

with $\Lambda_\pm(\,\vec{h},\vec{r}\,)$ given by Eqs. (A5.18). Equation (9.119) enables the emerging Stokes parameters to be expressed in terms of Laplace transforms. We recall that the Laplace transform of the function $f(x\,;\mu)$ is defined, in the half plane $\mathrm{Re}\,p > 0$, by

$$\mathrm{L}(p\,;\mu) = \int_0^\infty \mathrm{e}^{-px}\; f(x\,;\mu)\;\mathrm{d}x\;.$$

Substitution of Eq. (9.119) into Eq. (9.118) yields[1]

$$\boldsymbol{I}(0,\mu) = \left\{ B_{\rm P}(0)\,\boldsymbol{1} + \sum_{i=1}^{4}\; \mathrm{L}\!\left(\frac{\lambda_i(\,\vec{h},\vec{r}\,)}{\mu}\,;\,\mu\right) \boldsymbol{N}_i(\,\vec{h},\vec{r}\,) \right\} \boldsymbol{U}\;, \tag{9.120}$$

where L is the Laplace transform of the function

$$f(x\,;\mu) = \;\mathrm{e}^{-\frac{K_{\rm c}(x)}{\mu}}\;\; \frac{\mathrm{d}B_{\rm P}}{\mathrm{d}x}\;.$$

Equation (9.120) is rather general and provides analytical expressions for the emerging Stokes parameters for a wide variety of model atmospheres. As observed in App. 5, the matrices $\boldsymbol{N}_i$ are ill-defined when $\Lambda_+ = \Lambda_- = 0$. In that case Eq. (9.120) should be replaced by the following

$$\boldsymbol{I}(0,\mu) = \left\{ \left[B_{\rm P}(0) + \mathrm{L}\!\left(\frac{h_I}{\mu}\,;\mu\right)\right]\boldsymbol{1} - \mathrm{L}_1\!\left(\frac{h_I}{\mu}\,;\mu\right)\boldsymbol{G}(\,\vec{h},\vec{r}\,) + \frac{1}{2}\,\mathrm{L}_2\!\left(\frac{h_I}{\mu}\,;\mu\right)\boldsymbol{G}(\,\vec{h},\vec{r}\,)^2 \right\}\boldsymbol{U},$$

where the matrix $\boldsymbol{G}$ is given by Eq. (A5.25), and where $\mathrm{L}_1(p\,;\mu)$ and $\mathrm{L}_2(p\,;\mu)$ are the Laplace transforms of the functions

$$f_1(x\,;\mu) = \;\frac{x}{\mu}\;\mathrm{e}^{-\frac{K_{\rm c}(x)}{\mu}}\;\; \frac{\mathrm{d}B_{\rm P}}{\mathrm{d}x}\;, \qquad f_2(x\,;\mu) = \;\left(\frac{x}{\mu}\right)^2\;\mathrm{e}^{-\frac{K_{\rm c}(x)}{\mu}}\;\; \frac{\mathrm{d}B_{\rm P}}{\mathrm{d}x}\;,$$

respectively.

---

[1] The condition $\mathrm{Re}\;p > 0$ is clearly satisfied for the eigenvalues λ_1, λ_3 and λ_4. Using the inequality

$$(\,\vec{h}\cdot\vec{r}\,)^2 \le h^2 r^2\;,$$

it can be easily proved via Eqs. (A5.18) and (9.32) that it is also satisfied for λ_2.

9.10. Solutions for Special Magnetic Field Orientations

As outlined in Sect. 8.3.c, there are some special cases where, because certain elements of the propagation matrix are zero, the transfer equation can be solved in closed form without any additional assumption. Two such cases occur when, at each point along the ray path, the magnetic field vector is parallel or perpendicular to the propagation direction.

Let us consider the former case ($\theta = 0°$ or $180°$ in Fig. 9.1). From Eqs. (9.32) we have

$$\begin{aligned} h_I &= \frac{1}{2}\left(\eta_\mathrm{b} + \eta_\mathrm{r}\right) \\ h_Q &= h_U = 0 & r_Q &= r_U = 0 \\ h_V &= \pm\frac{1}{2}\left(\eta_\mathrm{r} - \eta_\mathrm{b}\right) & r_V &= \pm\frac{1}{2}\left(\rho_\mathrm{r} - \rho_\mathrm{b}\right), \end{aligned} \tag{9.121}$$

where the plus sign in the expressions of h_V and r_V refers to $\theta = 0°$ and the minus sign to $\theta = 180°$. Substitution into the transfer equation (9.35) yields

$$\begin{aligned} \frac{\mathrm{d}I}{\mathrm{d}\tau_\mathrm{c}} &= \left(1 + \kappa_\mathrm{L}\, h_I\right) I + \kappa_\mathrm{L}\, h_V\, V - \left(S_\mathrm{c} + \kappa_\mathrm{L}\, h_I\, S_\mathrm{L}\right) \\ \frac{\mathrm{d}Q}{\mathrm{d}\tau_\mathrm{c}} &= \left(1 + \kappa_\mathrm{L}\, h_I\right) Q + \kappa_\mathrm{L}\, r_V\, U \\ \frac{\mathrm{d}U}{\mathrm{d}\tau_\mathrm{c}} &= \left(1 + \kappa_\mathrm{L}\, h_I\right) U - \kappa_\mathrm{L}\, r_V\, Q \\ \frac{\mathrm{d}V}{\mathrm{d}\tau_\mathrm{c}} &= \left(1 + \kappa_\mathrm{L}\, h_I\right) V + \kappa_\mathrm{L}\, h_V\, I - \kappa_\mathrm{L}\, h_V\, S_\mathrm{L}\,. \end{aligned} \tag{9.122}$$

These equations can be solved either by the evolution operator technique (cf. Eq. (8.27) which refers to a similar case) or by diagonalization. We apply here the second method, which is very simple in this case (cf. Eqs. (8.43) and (8.44)).

As apparent from Eqs. (9.122), the Stokes parameters Q and U are only coupled with each other: since the equations for Q and U do not contain source terms, we have, at any optical depth[1]

$$Q = U = 0$$

provided the boundary values of Q and U are also zero. As far as I and V are concerned, summation and subtraction of the first and fourth of Eqs. (9.122) gives,

[1] Note that Eqs. (8.44) do not imply the solution $Q = U = 0$, although the propagation matrix has the same form. This is because all atomic coherences are neglected in the present chapter, so that the condition $h_Q = h_U = 0$ implies that the Q and U components of the emission vector are zero (see Eq. (9.92)).

in the $\theta = 0^\circ$ case[1]

$$\frac{\mathrm{d}}{\mathrm{d}\tau_\mathrm{c}}\,(I+V) = (1+\kappa_\mathrm{L}\,\eta_\mathrm{r})\,(I+V) - (S_\mathrm{c} + \kappa_\mathrm{L}\,\eta_\mathrm{r}\,S_\mathrm{L})$$
$$\frac{\mathrm{d}}{\mathrm{d}\tau_\mathrm{c}}\,(I-V) = (1+\kappa_\mathrm{L}\,\eta_\mathrm{b})\,(I-V) - (S_\mathrm{c} + \kappa_\mathrm{L}\,\eta_\mathrm{b}\,S_\mathrm{L})\;, \qquad (9.123)$$

where Eqs. (9.121) have been used. These equations are uncoupled and have the formal solutions (cf. Eqs. (8.4) and (8.18))

$$(I+V)_{\tau_\mathrm{c}=0} = \int_0^\infty \mathrm{e}^{-\int_0^{\tau_\mathrm{c}} \left[1+\kappa_\mathrm{L}(\tau_\mathrm{c}')\,\eta_\mathrm{r}(\tau_\mathrm{c}')\right]\mathrm{d}\tau_\mathrm{c}'} \times \left[S_\mathrm{c}(\tau_\mathrm{c}) + \kappa_\mathrm{L}(\tau_\mathrm{c})\,\eta_\mathrm{r}(\tau_\mathrm{c})\,S_\mathrm{L}(\tau_\mathrm{c})\right]\mathrm{d}\tau_\mathrm{c}$$

$$(I-V)_{\tau_\mathrm{c}=0} = \int_0^\infty \mathrm{e}^{-\int_0^{\tau_\mathrm{c}} \left[1+\kappa_\mathrm{L}(\tau_\mathrm{c}')\,\eta_\mathrm{b}(\tau_\mathrm{c}')\right]\mathrm{d}\tau_\mathrm{c}'} \times \left[S_\mathrm{c}(\tau_\mathrm{c}) + \kappa_\mathrm{L}(\tau_\mathrm{c})\,\eta_\mathrm{b}(\tau_\mathrm{c})\,S_\mathrm{L}(\tau_\mathrm{c})\right]\mathrm{d}\tau_\mathrm{c}\;, \qquad (9.124)$$

which allow the emerging I and V Stokes parameters to be written in the form

$$I(0) = \frac{1}{2}\left[(I+V)_{\tau_\mathrm{c}=0} + (I-V)_{\tau_\mathrm{c}=0}\right]$$
$$V(0) = \frac{1}{2}\left[(I+V)_{\tau_\mathrm{c}=0} - (I-V)_{\tau_\mathrm{c}=0}\right]\;. \qquad (9.125)$$

Equations (9.123) show that magneto-optical effects do not influence the transfer of radiation: this is indeed one of the few cases where these effects can a priori be neglected (cf. Sect. 9.22). It also appears that the quantity $(I+V)$ – which represents twice the amount of right circular polarization contained in the radiation beam, see Sect. 1.6) – obeys the same transfer equation as the intensity of an (unpolarized) beam propagating through a non-magnetic atmosphere, with the only difference that the profile η_r would be replaced, in the latter case, be the profile η defined in Eq. (9.65). The same holds for $(I-V)$, with η_b playing the role of η_r. If we restrict attention to a Zeeman *triplet* (normal or anomalous), the η_r and η_b profiles are nothing but the η profile shifted in wavelength by the amount $g\,\Delta\lambda_B$ to the red or to the blue, respectively[2] (see Eqs. (9.26), (9.27) and (9.29)). Therefore, if the *amplitude* (besides the direction) of the magnetic field is constant along the ray path, and if suitable boundary conditions (like those in Eqs. (9.42))

[1] The case $\theta = 180^\circ$ leads to the same equations with the interchange of η_r and η_b.

[2] Obviously, the opposite shifts occur if the Landé factor is negative.

hold, we have, at any optical depth[1]

$$I(\lambda) = \frac{1}{2}\left[\,\bar{I}(\lambda - g\,\Delta\lambda_B) \,+\, \bar{I}(\lambda + g\,\Delta\lambda_B)\right]$$
$$V(\lambda) = \frac{1}{2}\left[\,\bar{I}(\lambda - g\,\Delta\lambda_B) \,-\, \bar{I}(\lambda + g\,\Delta\lambda_B)\right], \tag{9.126}$$

where $\bar{I}(\lambda)$ is the intensity that would be observed if the magnetic field were switched off leaving unchanged all the other physical parameters (including the source functions).

Let's now turn to the case where the magnetic field vector is perpendicular to the propagation direction. For $\theta = 90°$, Eqs. (9.32) reduce to

$$h_I = \frac{1}{2}\left[\eta_\mathrm{p} + \frac{\eta_\mathrm{b} + \eta_\mathrm{r}}{2}\right]$$
$$h_Q = \frac{1}{2}\left[\eta_\mathrm{p} - \frac{\eta_\mathrm{b} + \eta_\mathrm{r}}{2}\right]\cos 2\chi \qquad r_Q = \frac{1}{2}\left[\rho_\mathrm{p} - \frac{\rho_\mathrm{b} + \rho_\mathrm{r}}{2}\right]\cos 2\chi$$
$$h_U = \frac{1}{2}\left[\eta_\mathrm{p} - \frac{\eta_\mathrm{b} + \eta_\mathrm{r}}{2}\right]\sin 2\chi \qquad r_U = \frac{1}{2}\left[\rho_\mathrm{p} - \frac{\rho_\mathrm{b} + \rho_\mathrm{r}}{2}\right]\sin 2\chi$$
$$h_V = 0 \qquad r_V = 0\,,$$

and Eqs. (9.35) now read

$$\frac{\mathrm{d}I}{\mathrm{d}\tau_\mathrm{c}} = (1 + \kappa_\mathrm{L}\,h_I)\,I + \kappa_\mathrm{L}\,h_Q\,Q + \kappa_\mathrm{L}\,h_U\,U - (S_\mathrm{c} + \kappa_\mathrm{L}\,h_I\,S_\mathrm{L})$$
$$\frac{\mathrm{d}Q}{\mathrm{d}\tau_\mathrm{c}} = (1 + \kappa_\mathrm{L}\,h_I)\,Q + \kappa_\mathrm{L}\,h_Q\,I - \kappa_\mathrm{L}\,r_U\,V - \kappa_\mathrm{L}\,h_Q\,S_\mathrm{L}$$
$$\frac{\mathrm{d}U}{\mathrm{d}\tau_\mathrm{c}} = (1 + \kappa_\mathrm{L}\,h_I)\,U + \kappa_\mathrm{L}\,h_U\,I + \kappa_\mathrm{L}\,r_Q\,V - \kappa_\mathrm{L}\,h_U\,S_\mathrm{L}$$
$$\frac{\mathrm{d}V}{\mathrm{d}\tau_\mathrm{c}} = (1 + \kappa_\mathrm{L}\,h_I)\,V + \kappa_\mathrm{L}\,r_U\,Q - \kappa_\mathrm{L}\,r_Q\,U\,.$$

These equations can be solved by diagonalization provided the azimuth angle χ is constant along the ray path. Introducing the linear combinations[2]

$$\tilde{Q} = Q\,\cos 2\chi \,+\, U\,\sin 2\chi$$
$$\tilde{U} = U\,\cos 2\chi \,-\, Q\,\sin 2\chi\,, \tag{9.127}$$

[1] The case $\theta = 180°$ yields a sign switch in the expression of $V(\lambda)$.

[2] These combinations are nothing but the Stokes parameters defined in the preferred frame (see Sect. 5.5).

and setting

$$h_W = h_Q(\theta = 90^\circ, \chi = 0^\circ) = \frac{1}{2}\left[\eta_\mathrm{p} - \frac{\eta_\mathrm{b} + \eta_\mathrm{r}}{2}\right]$$
$$r_W = r_Q(\theta = 90^\circ, \chi = 0^\circ) = \frac{1}{2}\left[\rho_\mathrm{p} - \frac{\rho_\mathrm{b} + \rho_\mathrm{r}}{2}\right],$$

one gets

$$\frac{\mathrm{d}I}{\mathrm{d}\tau_\mathrm{c}} = (1 + \kappa_\mathrm{L}\, h_I)\, I + \kappa_\mathrm{L}\, h_W\, \tilde{Q} - (S_\mathrm{c} + \kappa_\mathrm{L}\, h_I\, S_\mathrm{L})$$
$$\frac{\mathrm{d}\tilde{Q}}{\mathrm{d}\tau_\mathrm{c}} = (1 + \kappa_\mathrm{L}\, h_I)\, \tilde{Q} + \kappa_\mathrm{L}\, h_W\, I - \kappa_\mathrm{L}\, h_W\, S_\mathrm{L}$$
$$\frac{\mathrm{d}\tilde{U}}{\mathrm{d}\tau_\mathrm{c}} = (1 + \kappa_\mathrm{L}\, h_I)\, \tilde{U} + \kappa_\mathrm{L}\, r_W\, V$$
$$\frac{\mathrm{d}V}{\mathrm{d}\tau_\mathrm{c}} = (1 + \kappa_\mathrm{L}\, h_I)\, V - \kappa_\mathrm{L}\, r_W\, \tilde{U}\,.$$

These are strictly similar to Eqs. (9.122) and can be solved by the same method. Since $\tilde{U}$ and V are only coupled with each other and no source term is present in their equations, one has

$$\tilde{U} = V = 0\,.$$

On the other hand, summation and subtraction of the first two equations yields the decoupled equations

$$\frac{\mathrm{d}}{\mathrm{d}\tau_\mathrm{c}}(I + \tilde{Q}) = \left(1 + \kappa_\mathrm{L}\, \eta_\mathrm{p}\right)(I + \tilde{Q}) - \left(S_\mathrm{c} + \kappa_\mathrm{L}\, \eta_\mathrm{p}\, S_\mathrm{L}\right)$$
$$\frac{\mathrm{d}}{\mathrm{d}\tau_\mathrm{c}}(I - \tilde{Q}) = \left(1 + \kappa_\mathrm{L}\, \frac{\eta_\mathrm{b} + \eta_\mathrm{r}}{2}\right)(I - \tilde{Q}) - \left(S_\mathrm{c} + \kappa_\mathrm{L}\, \frac{\eta_\mathrm{b} + \eta_\mathrm{r}}{2}\, S_\mathrm{L}\right),$$

whose solutions are

$$(I + \tilde{Q})_{\tau_\mathrm{c}=0} = \int_0^\infty \mathrm{e}^{-\int_0^{\tau_\mathrm{c}} \left[1 + \kappa_\mathrm{L}(\tau_\mathrm{c}')\, \eta_\mathrm{p}(\tau_\mathrm{c}')\right] \mathrm{d}\tau_\mathrm{c}'} \times \left[S_\mathrm{c}(\tau_\mathrm{c}) + \kappa_\mathrm{L}(\tau_\mathrm{c})\, \eta_\mathrm{p}(\tau_\mathrm{c})\, S_\mathrm{L}(\tau_\mathrm{c})\right] \mathrm{d}\tau_\mathrm{c}$$

$$(I - \tilde{Q})_{\tau_\mathrm{c}=0} = \int_0^\infty \mathrm{e}^{-\int_0^{\tau_\mathrm{c}} \left[1 + \kappa_\mathrm{L}(\tau_\mathrm{c}')\, \frac{\eta_\mathrm{b}(\tau_\mathrm{c}') + \eta_\mathrm{r}(\tau_\mathrm{c}')}{2}\right] \mathrm{d}\tau_\mathrm{c}'} \times \left[S_\mathrm{c}(\tau_\mathrm{c}) + \kappa_\mathrm{L}(\tau_\mathrm{c})\, \frac{\eta_\mathrm{b}(\tau_\mathrm{c}) + \eta_\mathrm{r}(\tau_\mathrm{c})}{2}\, S_\mathrm{L}(\tau_\mathrm{c})\right] \mathrm{d}\tau_\mathrm{c}\,. \qquad (9.128)$$

Finally, inversion of Eqs. (9.127) leads to the following expressions for the emerging Stokes parameters

$$
\begin{aligned}
I(0) &= \frac{1}{2}\left[(I+\tilde{Q})_{\tau_{\rm c}=0} + (I-\tilde{Q})_{\tau_{\rm c}=0} \right] \\
Q(0) &= \frac{1}{2}\left[(I+\tilde{Q})_{\tau_{\rm c}=0} - (I-\tilde{Q})_{\tau_{\rm c}=0} \right] \cos 2\chi \\
U(0) &= \frac{1}{2}\left[(I+\tilde{Q})_{\tau_{\rm c}=0} - (I-\tilde{Q})_{\tau_{\rm c}=0} \right] \sin 2\chi \\
V(0) &= 0 \; .
\end{aligned}
$$

The above equations show that magneto-optical effects do not affect the Stokes parameters in this case either.

9.11. The Stepanov Solution

In the early days of polarized radiative transfer, the importance of magneto-optical effects was not completely realized, and the transfer equations were often considered in the simplified form resulting from the drastic approximation $r_Q = r_U = r_V = 0$. Under this approximation, Eqs. (9.35) reduce to

$$
\begin{aligned}
\frac{{\rm d}I}{{\rm d}\tau_{\rm c}} &= I - S_{\rm c} + \kappa_{\rm L}\left[h_I\,(I-S_{\rm L}) + h_Q Q + h_U U + h_V V \right] \\
\frac{{\rm d}Q}{{\rm d}\tau_{\rm c}} &= Q + \kappa_{\rm L}\left[h_Q\,(I-S_{\rm L}) + h_I Q \right] \\
\frac{{\rm d}U}{{\rm d}\tau_{\rm c}} &= U + \kappa_{\rm L}\left[h_U\,(I-S_{\rm L}) + h_I U \right] \\
\frac{{\rm d}V}{{\rm d}\tau_{\rm c}} &= V + \kappa_{\rm L}\left[h_V\,(I-S_{\rm L}) + h_I V \right] \; .
\end{aligned}
\tag{9.129}
$$

Bearing in mind Eqs. (9.32), we can write

$$
h_Q = a\,\cos 2\chi \; , \qquad h_U = a\,\sin 2\chi \; , \qquad h_V = b \; ,
$$

with

$$
a = \frac{1}{2}\left[\eta_{\rm p} - \frac{\eta_{\rm b}+\eta_{\rm r}}{2} \right] \sin^2\theta \; , \qquad b = \frac{1}{2}\left[\eta_{\rm r} - \eta_{\rm b} \right] \cos\theta \; .
\tag{9.130}
$$

Setting

$$
\frac{a}{\sqrt{a^2+b^2}} = \cos\delta \; , \qquad \frac{b}{\sqrt{a^2+b^2}} = \sin\delta \; ,
\tag{9.131}
$$

we have

$$h_Q = \cos\delta\, \cos 2\chi \sqrt{h_Q^2 + h_U^2 + h_V^2}$$

$$h_U = \cos\delta\, \sin 2\chi \sqrt{h_Q^2 + h_U^2 + h_V^2}$$

$$h_V = \sin\delta \sqrt{h_Q^2 + h_U^2 + h_V^2} \ . \tag{9.132}$$

The Stepanov solution derives from the assumption that both χ and δ are independent of $\tau_{\rm c}$: this assumption enables Eqs. (9.129) to be cast into diagonal form.

Contrary to the angle χ (the azimuth of the magnetic field vector defined in Fig. 9.1), the angle δ, which depends on wavelength, has no precise physical meaning. However, as apparent from Eqs. (9.130) and (9.131), the assumption $\delta = \text{const.}$ implies that the parameters B, θ, $\Delta\lambda_{\rm D}$, Γ', $w_{\rm A}$ should be independent of optical depth. Thus the approximations underlying the Stepanov solution are equivalent to approximation b') considered in Sect. 9.9 plus the additional approximation of neglecting magneto-optical effects.

Let us substitute Eqs. (9.132) into Eqs. (9.129), and let us replace the last three equations by the linear combinations obtained by summation of the second, third, and fourth equation multiplied, respectively, by the factors $\cos\delta\cos 2\chi$, $\cos\delta\sin 2\chi$, $\sin\delta$; then by the factors $\sin\delta\cos 2\chi$, $\sin\delta\sin 2\chi$, $-\cos\delta$; and finally by the factors $\sin 2\chi$, $-\cos 2\chi$, 0. The following set of equations is obtained

$$\frac{\mathrm{d}}{\mathrm{d}\tau_{\rm c}} I = I - S_{\rm c} + \kappa_{\rm L} \left[h_I \,(I - S_{\rm L}) \ + \ \sqrt{h_Q^2 + h_U^2 + h_V^2} \ P_A \right]$$

$$\frac{\mathrm{d}}{\mathrm{d}\tau_{\rm c}} P_A = P_A + \kappa_{\rm L} \left[\sqrt{h_Q^2 + h_U^2 + h_V^2} \ (I - S_{\rm L}) \ + \ h_I P_A \right]$$

$$\frac{\mathrm{d}}{\mathrm{d}\tau_{\rm c}} P_B = (1 + \kappa_{\rm L}\, h_I)\, P_B$$

$$\frac{\mathrm{d}}{\mathrm{d}\tau_{\rm c}} P_C = (1 + \kappa_{\rm L}\, h_I)\, P_C \ , \tag{9.133}$$

where

$$P_A = \cos\delta\, \cos 2\chi \ Q \ + \ \cos\delta\, \sin 2\chi \ U \ + \ \sin\delta \ V$$

$$P_B = \sin\delta\, \cos 2\chi \ Q \ + \ \sin\delta\, \sin 2\chi \ U \ - \ \cos\delta \ V$$

$$P_C = \sin 2\chi \ Q \ - \ \cos 2\chi \ U \ . \tag{9.134}$$

The last two equations in the set (9.133) show that, provided Q , U, and V are zero at the boundary,

$$P_B = P_C = 0 \ . \tag{9.135}$$

The solution to the algebraic system (9.134) with the condition (9.135) is

$$Q = \cos\delta\, \cos 2\chi \ P_A \ , \qquad U = \cos\delta\, \sin 2\chi \ P_A \ , \qquad V = \sin\delta \ P_A \ .$$

Finally, by summing and subtracting the first two equations in the set (9.133) one gets the decoupled equations

$$\frac{\mathrm{d}I^{(+)}}{\mathrm{d}\tau_{\mathrm{c}}} = \left(1 + \kappa_{\mathrm{L}}\, h^{(+)}\right) I^{(+)} - \left(S_{\mathrm{c}} + \kappa_{\mathrm{L}}\, h^{(+)}\, S_{\mathrm{L}}\right)$$
$$\frac{\mathrm{d}I^{(-)}}{\mathrm{d}\tau_{\mathrm{c}}} = \left(1 + \kappa_{\mathrm{L}}\, h^{(-)}\right) I^{(-)} - \left(S_{\mathrm{c}} + \kappa_{\mathrm{L}}\, h^{(-)}\, S_{\mathrm{L}}\right) , \tag{9.136}$$

where

$$I^{(+)} = I + P_A \qquad h^{(+)} = h_I + \sqrt{h_Q^2 + h_U^2 + h_V^2}$$
$$I^{(-)} = I - P_A \qquad h^{(-)} = h_I - \sqrt{h_Q^2 + h_U^2 + h_V^2} \ .$$

Equations (9.136) are the so-called *Stepanov equations* (Stepanov, 1958), and can be easily integrated (cf. the analogous solutions (9.124) or (9.128)). The Stepanov equations are seldom used in modern research. They have been illustrated mainly because of their historical importance in the problem of line formation in a magnetic field.

9.12. The Intense Field Solution

In the limiting case of very strong magnetic field, the various Zeeman components spread out considerably in wavelength and the spectral line consists of a number of independent components, each associated with the corresponding Zeeman component.[1]

This physical situation, which will be referred to as 'intense field' and which is characterized by the inequality (see Eqs. (9.26))

$$v_B = \frac{\Delta\lambda_B}{\Delta\lambda_{\mathrm{D}}} \gg 1 \ ,$$

is easily achieved in laboratory plasmas where it is currently used to illustrate the Zeeman effect and to measure Landé factors. In astrophysical plasmas, on the contrary, the Doppler broadening is generally quite large, so that really strong fields are needed for the above inequality to hold. According to the discussion at the beginning of Sect. 9.6, the magnetic field strength should be of order 10^4-10^5 G for optical lines; in the far infrared, however, considerably weaker fields are sufficient, because v_B is proportional to the line wavelength (see Eqs. (9.25) and (9.26)).

The problem of line formation in an intense magnetic field can be dealt with by introducing a drastic approximation. This consists in the assumption that, for

[1] According to the basic hypotheses of this chapter (Sect. 9.1), the magnetic splitting – although large – is assumed to follow the Zeeman effect regime, and the spectral line is assumed to be 'unstructured'.

any assigned wavelength, only one Zeeman component contributes to the elements of the propagation matrix. In other words, we assume that the expressions of the profiles η_q and ρ_q in a wavelength interval about the Zeeman component connecting two specific sublevels $(J_\ell M_\ell)$ and $(J_u M_u)$ are (cf. Eqs. (9.27))

$$\begin{aligned}
\eta_q &= S_q^{J_\ell J_u}(M_\ell, M_u)\ \frac{1}{\sqrt{\pi}}\ H\big(v - v_{\rm A} + v_B\,(g_u M_u - g_\ell M_\ell),\, a\big) \\
\rho_q &= S_q^{J_\ell J_u}(M_\ell, M_u)\ \frac{1}{\sqrt{\pi}}\ L\big(v - v_{\rm A} + v_B\,(g_u M_u - g_\ell M_\ell),\, a\big)\ ,
\end{aligned} \tag{9.137}$$

with $q = (M_\ell - M_u) = -1,\ 0,\ +1$ for $\sigma_{\rm b}$, π, and $\sigma_{\rm r}$ components respectively.

This approximation requires some comments. First of all, there are Zeeman patterns where two or more components overlap irrespective of the magnetic field strength. An example is given by the transition ${}^5{\rm P}_1 - {}^5{\rm F}_1$ (panel (c) in Fig. 3.2), where overlappings of σ and π components and of two σ components occur. These special cases would deserve a separate discussion but, being rather uncommon, they will not be considered in the following. Second, it should be kept in mind that the dispersion profiles have very broad wings, as apparent from Eqs. (5.57) (see also Fig. 5.3). Since the distance between Zeeman components is roughly $\Delta\lambda_B$, our present approximation introduces in ρ_q an error of order $\Delta\lambda_{\rm D}/\Delta\lambda_B$ (the corresponding error in η_q is much smaller being of order $a\,\Delta\lambda_{\rm D}^2/\Delta\lambda_B^2$). Finally, the approximation can hold at any optical depth only if there are no 'contaminations' between different Zeeman components: these could be caused either by a magnetic field gradient or by a line-of-sight velocity gradient. If $\delta(\Delta\lambda_B)$ represents the variation of $\Delta\lambda_B$ between – say – the atmospheric layers $\tau_{\rm c} = 0$ and $\tau_{\rm c} = 1$, and if $\delta(w_{\rm A})$ has the same meaning for $w_{\rm A}$, we should thus require

$$\delta(\Delta\lambda_B) \ll \Delta\lambda_B\ , \qquad \frac{\lambda_0}{c}\ \delta(w_{\rm A}) \ll \Delta\lambda_B\ . \tag{9.138}$$

Let us consider the transfer equation in the form of Eq. (9.35), and let us restrict attention to a wavelength interval about the Zeeman component connecting two particular sublevels $(J_\ell M_\ell)$ and $(J_u M_u)$. This component – $\sigma_{\rm b}$, π or $\sigma_{\rm r}$ according to the value of $(M_\ell - M_u)$ – will be referred to as the *i-component*. Using assumption (9.137), the elements of the propagation matrix can be written in the form (see Eqs. (9.29) and (9.32))

$$\begin{aligned}
h_I &= \alpha_I^{(i)}\ s_i\ \eta^{(i)} \\
h_Q &= \alpha_Q^{(i)}\ s_i\ \eta^{(i)} \qquad & r_Q &= \alpha_Q^{(i)}\ s_i\ \rho^{(i)} \\
h_U &= \alpha_U^{(i)}\ s_i\ \eta^{(i)} \qquad & r_U &= \alpha_U^{(i)}\ s_i\ \rho^{(i)} \\
h_V &= \alpha_V^{(i)}\ s_i\ \eta^{(i)} \qquad & r_V &= \alpha_V^{(i)}\ s_i\ \rho^{(i)}\ ,
\end{aligned} \tag{9.139}$$

TABLE 9.6

Expressions of the angular factors for different types of Zeeman components

	$\alpha_I^{(i)}$	$\alpha_Q^{(i)}$	$\alpha_U^{(i)}$	$\alpha_V^{(i)}$
$\sigma_{\rm b}$	$\frac{1}{4}\,(1+\cos^2\theta)$	$-\frac{1}{4}\,\sin^2\theta\,\cos 2\chi$	$-\frac{1}{4}\,\sin^2\theta\,\sin 2\chi$	$-\frac{1}{2}\,\cos\theta$
π	$\frac{1}{2}\,\sin^2\theta$	$\frac{1}{2}\,\sin^2\theta\,\cos 2\chi$	$\frac{1}{2}\,\sin^2\theta\,\sin 2\chi$	0
$\sigma_{\rm r}$	$\frac{1}{4}\,(1+\cos^2\theta)$	$-\frac{1}{4}\,\sin^2\theta\,\cos 2\chi$	$-\frac{1}{4}\,\sin^2\theta\,\sin 2\chi$	$\frac{1}{2}\,\cos\theta$

where

$$
\begin{aligned}
s_i &= S_q^{J_\ell J_u}(M_\ell, M_u) \\
\eta^{(i)} &= \frac{1}{\sqrt{\pi}}\, H\big(v - v_{\rm A} + v_B\,(g_u M_u - g_\ell M_\ell),\, a\big) \\
\rho^{(i)} &= \frac{1}{\sqrt{\pi}}\, L\big(v - v_{\rm A} + v_B\,(g_u M_u - g_\ell M_\ell),\, a\big)\,, \qquad (9.140)
\end{aligned}
$$

and where the angular factors $\alpha_I^{(i)}$, $\alpha_Q^{(i)}$, $\alpha_U^{(i)}$, $\alpha_V^{(i)}$ are defined in Table 9.6. We will now show that the transfer equation can be cast into diagonal form if the ratios

$$
\frac{\alpha_Q^{(i)}}{\alpha_I^{(i)}}\,, \qquad \frac{\alpha_U^{(i)}}{\alpha_I^{(i)}}\,, \qquad \frac{\alpha_V^{(i)}}{\alpha_I^{(i)}}
$$

are assumed to be independent of optical depth. As apparent from Table 9.6, this means that the direction of the magnetic field vector is assumed to be constant along the ray path.

Setting

$$
Q = \frac{\alpha_Q^{(i)}}{\alpha_I^{(i)}}\, P\,, \qquad U = \frac{\alpha_U^{(i)}}{\alpha_I^{(i)}}\, P\,, \qquad V = \frac{\alpha_V^{(i)}}{\alpha_I^{(i)}}\, P\,, \qquad (9.141)
$$

and noticing that, both for σ and π components

$$
\big[\,\alpha_Q^{(i)}\,\big]^2 + \big[\,\alpha_U^{(i)}\,\big]^2 + \big[\,\alpha_V^{(i)}\,\big]^2 = \big[\,\alpha_I^{(i)}\,\big]^2\,,
$$

we obtain from Eqs. (9.35)

$$
\begin{aligned}
\frac{{\rm d}I}{{\rm d}\tau_{\rm c}} &= I - S_{\rm c} + \kappa_{\rm L}\,\alpha_I^{(i)}\, s_i\, \eta^{(i)}\, (I + P - S_{\rm L}) \\
\frac{{\rm d}P}{{\rm d}\tau_{\rm c}} &= P + \kappa_{\rm L}\,\alpha_I^{(i)}\, s_i\, \eta^{(i)}\, (I + P - S_{\rm L})\,.
\end{aligned}
$$

Summation and subtraction of these two equations yields the decoupled equations

$$
\begin{aligned}
\frac{\rm d}{{\rm d}\tau_{\rm c}}\,(I+P) &= \big(1 + 2\kappa_{\rm L}\,\alpha_I^{(i)}\, s_i\, \eta^{(i)}\big)\,(I+P) - \big(S_{\rm c} + 2\,\kappa_{\rm L}\,\alpha_I^{(i)}\, s_i\, \eta^{(i)}\, S_{\rm L}\big) \\
\frac{\rm d}{{\rm d}\tau_{\rm c}}\,(I-P) &= (I-P) - S_{\rm c}\,. \qquad (9.142)
\end{aligned}
$$

It is interesting to note that the latter of Eqs. (9.142) has the same form as the transfer equation for the continuum intensity $I_{\rm c}$, while the former is just the transfer equation for the intensity $I_{\rm f}^{(i)}$ of a fictitious, non-magnetic line having a ratio $\kappa_{\rm f}^{(i)}$ between line and continuum absorption coefficient given by

$$\kappa_{\rm f}^{(i)} = 2\,\kappa_{\rm L}\,\alpha_I^{(i)}\,s_i \tag{9.143}$$

and line source function $S_{\rm L}$. Setting

$$I - P = I_{\rm c}\ , \qquad (I + P) = I_{\rm f}^{(i)}\ ,$$

and using Eqs. (9.141), we can write for the Stokes parameters in a wavelength interval about the i-component

$$\begin{aligned}
I^{(i)}(\tau_{\rm c}) &= \frac{1}{2}\left[\,I_{\rm c}(\tau_{\rm c}) + I_{\rm f}^{(i)}(\tau_{\rm c})\,\right] \\
Q^{(i)}(\tau_{\rm c}) &= -\frac{1}{2}\,\frac{\alpha_Q^{(i)}}{\alpha_I^{(i)}}\left[\,I_{\rm c}(\tau_{\rm c}) - I_{\rm f}^{(i)}(\tau_{\rm c})\,\right] \\
U^{(i)}(\tau_{\rm c}) &= -\frac{1}{2}\,\frac{\alpha_U^{(i)}}{\alpha_I^{(i)}}\left[\,I_{\rm c}(\tau_{\rm c}) - I_{\rm f}^{(i)}(\tau_{\rm c})\,\right] \\
V^{(i)}(\tau_{\rm c}) &= -\frac{1}{2}\,\frac{\alpha_V^{(i)}}{\alpha_I^{(i)}}\left[\,I_{\rm c}(\tau_{\rm c}) - I_{\rm f}^{(i)}(\tau_{\rm c})\,\right]\ ,
\end{aligned} \tag{9.144}$$

where

$$\begin{aligned}
I_{\rm c}(\tau_{\rm c}) &= \int_{\tau_{\rm c}}^{\infty} S_{\rm c}(\tau_{\rm c}')\ \ {\rm e}^{-(\tau_{\rm c}' - \tau_{\rm c})}\ \ {\rm d}\tau_{\rm c}' \\
I_{\rm f}^{(i)}(\tau_{\rm c}) &= \int_{\tau_{\rm c}}^{\infty} \left(S_{\rm c} + \kappa_{\rm f}^{(i)}\,\eta^{(i)}\,S_{\rm L}\right)_{\tau_{\rm c}'}\ \ {\rm e}^{-\int_{\tau_{\rm c}}^{\tau_{\rm c}'}\left[\,1\,+\,\kappa_{\rm f}^{(i)}\,\eta^{(i)}\,\right]_{\tau_{\rm c}''}\ {\rm d}\tau_{\rm c}''}\ \ {\rm d}\tau_{\rm c}'\ .
\end{aligned} \tag{9.145}$$

The equations above show that magneto-optical effects do not affect the Stokes parameters. This is a direct consequence of the two basic assumptions of this section, namely that the magnetic field is very strong and has a fixed direction. Bearing in mind the geometrical interpretation of the transfer equation presented in Sect. 5.6, we see from Eqs. (9.139) that the formal vectors $\vec{\eta}$ and $\vec{\rho}$ point in the same (or the opposite) direction in the Poincaré space (Q/I, U/I, V/I); furthermore, since the angles θ and χ are assumed to be constant, this direction is fixed. It follows that the formal vector $\vec{p}$ is also parallel to the same direction, so that the term $\vec{\rho} \times \vec{p}$ in Eq. (5.74b) – the only term due to magneto-optical effects – is zero.

In the special case of the Milne-Eddington model atmosphere, the expressions for the emerging Stokes parameters in a wavelength interval about the i-component become very simple. We write them down because they will be needed in subsequent applications (see Sects. 9.19, 9.20 and 9.21). According to assumptions a), b) and c) of Sect. 9.8, we have

$$S_{\rm c} = S_{\rm L} = B_0\,(1+\beta\,t_{\rm c})\;, \qquad \kappa_{\rm f}^{(i)} = \text{const.}\;, \qquad \eta^{(i)} = \text{const.}\;,$$

and Eqs. (9.145) reduce to

$$\begin{aligned} I_{\rm c}(0,\mu) &= B_0\,(1+\beta\mu) \\ I_{\rm f}^{(i)}(0,\mu) &= B_0\left[1+\beta\mu\,\frac{1}{1+\kappa_{\rm f}^{(i)}\,\eta^{(i)}}\right]. \end{aligned}$$

Substituting into Eqs. (9.144) and adopting the normalization of Eqs. (9.112), we obtain

$$\begin{aligned} \mathcal{R}_I^{(i)}(0,\mu) &= \frac{I_{\rm c}(0,\mu)-I(0,\mu)}{I_{\rm c}(0,\mu)} = \frac{1}{2}\,\frac{\beta\mu}{1+\beta\mu}\,\frac{\kappa_{\rm f}^{(i)}\,\eta^{(i)}}{1+\kappa_{\rm f}^{(i)}\,\eta^{(i)}} \\ \mathcal{R}_Q^{(i)}(0,\mu) &= \frac{Q(0,\mu)}{I_{\rm c}(0,\mu)} = -\frac{1}{2}\,\frac{\beta\mu}{1+\beta\mu}\,\frac{\alpha_Q^{(i)}}{\alpha_I^{(i)}}\,\frac{\kappa_{\rm f}^{(i)}\,\eta^{(i)}}{1+\kappa_{\rm f}^{(i)}\,\eta^{(i)}} \\ \mathcal{R}_U^{(i)}(0,\mu) &= \frac{U(0,\mu)}{I_{\rm c}(0,\mu)} = -\frac{1}{2}\,\frac{\beta\mu}{1+\beta\mu}\,\frac{\alpha_U^{(i)}}{\alpha_I^{(i)}}\,\frac{\kappa_{\rm f}^{(i)}\,\eta^{(i)}}{1+\kappa_{\rm f}^{(i)}\,\eta^{(i)}} \\ \mathcal{R}_V^{(i)}(0,\mu) &= \frac{V(0,\mu)}{I_{\rm c}(0,\mu)} = -\frac{1}{2}\,\frac{\beta\mu}{1+\beta\mu}\,\frac{\alpha_V^{(i)}}{\alpha_I^{(i)}}\,\frac{\kappa_{\rm f}^{(i)}\,\eta^{(i)}}{1+\kappa_{\rm f}^{(i)}\,\eta^{(i)}}\;. \end{aligned} \tag{9.146}$$

These formulae can also be obtained by direct substitution into Eqs. (9.112) of the following expressions (resulting from Eqs. (9.39), (9.139) and (9.143)) for the elements of the propagation matrix

$$\begin{aligned} k_I &= \frac{1}{2}\,\kappa_{\rm f}^{(i)}\,\eta^{(i)} \\ k_Q &= \frac{1}{2}\,\frac{\alpha_Q^{(i)}}{\alpha_I^{(i)}}\,\kappa_{\rm f}^{(i)}\,\eta^{(i)} & f_Q &= \frac{1}{2}\,\frac{\alpha_Q^{(i)}}{\alpha_I^{(i)}}\,\kappa_{\rm f}^{(i)}\,\rho^{(i)} \\ k_U &= \frac{1}{2}\,\frac{\alpha_U^{(i)}}{\alpha_I^{(i)}}\,\kappa_{\rm f}^{(i)}\,\eta^{(i)} & f_U &= \frac{1}{2}\,\frac{\alpha_U^{(i)}}{\alpha_I^{(i)}}\,\kappa_{\rm f}^{(i)}\,\rho^{(i)} \\ k_V &= \frac{1}{2}\,\frac{\alpha_V^{(i)}}{\alpha_I^{(i)}}\,\kappa_{\rm f}^{(i)}\,\eta^{(i)} & f_V &= \frac{1}{2}\,\frac{\alpha_V^{(i)}}{\alpha_I^{(i)}}\,\kappa_{\rm f}^{(i)}\,\rho^{(i)}\;. \end{aligned} \tag{9.147}$$

9.13. The Seares Formulae

The solution to the radiative transfer equation is particularly simple when dealing with optically thin, homogeneous slabs rather than semi-infinite atmospheres. To be definite, let us consider a cold, absorbing slab superposed on a deeper layer which emits continuum, unpolarized radiation. The slab is assumed to absorb only in the line (not in the continuum), and to have zero emission and small optical thickness. This schematic situation (the *reversing layer model*) was used in the early decades of this century to represent a stellar atmosphere. Nowadays, it should be regarded as a slab model rather than a real model atmosphere.

In the reversing layer – that we assume magnetized – the transfer of radiation can be described using Eq. (9.36) with $\kappa_c = 0$ (no continuum absorption) and $S_L = 0$ (no emission). Let $\Delta\tau_L$ and $I_c^{(b)}$ denote, respectively, the optical thickness of the slab and the intensity of the continuum radiation (at the line wavelength) entering the slab from the lower boundary. Since $\Delta\tau_L \ll 1$, we can replace the Stokes vector in the right-hand side of Eq. (9.36) by the Stokes vector at the boundary $(I_c^{(b)}, 0, 0, 0)^\dagger$. Hence we obtain

$$\frac{\Delta I}{\Delta\tau_L} \equiv \frac{I_c^{(b)} - I}{\Delta\tau_L} = h_I\, I_c^{(b)} \qquad \frac{\Delta U}{\Delta\tau_L} \equiv -\frac{U}{\Delta\tau_L} = h_U\, I_c^{(b)}$$

$$\frac{\Delta Q}{\Delta\tau_L} \equiv -\frac{Q}{\Delta\tau_L} = h_Q\, I_c^{(b)} \qquad \frac{\Delta V}{\Delta\tau_L} \equiv -\frac{V}{\Delta\tau_L} = h_V\, I_c^{(b)} \ ,$$

where I, Q, U, V are the emerging Stokes parameters. Use of Eqs. (9.32) yields

$$I = I_c^{(b)} \left\{ 1 - \Delta\tau_L\, \frac{1}{2} \left[\eta_p \sin^2\theta + \frac{\eta_b + \eta_r}{2} \left(1 + \cos^2\theta\right) \right] \right\}$$

$$Q = -I_c^{(b)}\, \Delta\tau_L\, \frac{1}{2} \left[\eta_p - \frac{\eta_b + \eta_r}{2} \right] \sin^2\theta\, \cos 2\chi$$

$$U = -I_c^{(b)}\, \Delta\tau_L\, \frac{1}{2} \left[\eta_p - \frac{\eta_b + \eta_r}{2} \right] \sin^2\theta\, \sin 2\chi$$

$$V = -I_c^{(b)}\, \Delta\tau_L\, \frac{1}{2} \left[\eta_r - \eta_b \right] \cos\theta \ . \tag{9.148}$$

These are the so-called *Seares formulae* (Seares, 1913). They give Stokes parameters profiles which match exactly the corresponding dichroic profiles.

It should be remarked that the same result is predicted by the Unno-Rachkovsky solutions under the limit of weak spectral lines ($\kappa_L \ll 1$). Recalling Eqs. (9.39), we obtain by series expansion of Eqs. (9.110) up to first order in κ_L

$$I(0,\mu) = B_0 \left[(1 + \beta\mu) - \beta\mu\, \kappa_L\, h_I \right]$$

$$Q(0,\mu) = -B_0\, \beta\mu\, \kappa_L\, h_Q$$

$$U(0,\mu) = -B_0\, \beta\mu\, \kappa_L\, h_U$$

$$V(0,\mu) = -B_0\, \beta\mu\, \kappa_L\, h_V \ , \tag{9.149}$$

which coincide with Eqs. (9.148) after the formal substitutions

$$B_0\,(1+\beta\mu) \to I_{\rm c}^{\rm (b)}\ , \qquad\qquad \frac{\beta\mu}{1+\beta\mu}\,\kappa_{\rm L} \to \Delta\tau_{\rm L}\ .$$

The Seares formulae have a very restricted domain of applicability. They are mainly important from a historical point of view, being at the basis of the first methods used for the diagnostics of magnetic fields in the solar atmosphere.

For weak spectral lines, we can find an approximate solution to the radiative transfer equation which is valid for a semi-infinite atmosphere instead of a slab. This solution can be regarded as a generalization of the Seares formulae.

Let us consider the transfer equation in the form (9.38).[1] Using Eqs. (9.39) we can write

$$\frac{{\rm d}\boldsymbol{I}}{{\rm d}\tau_{\rm c}} = \left(\boldsymbol{1}+\kappa_{\rm L}\,\boldsymbol{H}\right)\boldsymbol{I}\,-\,B_{\rm P}\left(\boldsymbol{1}+\kappa_{\rm L}\,\boldsymbol{H}\right)\boldsymbol{U}\ , \tag{9.150}$$

with $\boldsymbol{H}$ and $\boldsymbol{U}$ given by Eqs. (9.50) and (9.49), respectively. Since $\kappa_{\rm L} \ll 1$, we can apply a perturbative technique (cf. Sect. 8.7) and look for a solution to this equation of the form

$$\boldsymbol{I}(\tau_{\rm c}) = \boldsymbol{I}_0(\tau_{\rm c})\,+\,\delta\boldsymbol{I}(\tau_{\rm c})\ ,$$

where $\boldsymbol{I}_0$ corresponds to $\kappa_{\rm L}=0$ (no spectral line) and $\delta\boldsymbol{I}$ is a first-order correction. We thus replace Eq. (9.150) by the zero-order and first-order equations

$$\frac{\rm d}{{\rm d}\tau_{\rm c}}\,\boldsymbol{I}_0 = \boldsymbol{I}_0\,-\,B_{\rm P}\,\boldsymbol{U}$$

$$\frac{\rm d}{{\rm d}\tau_{\rm c}}\,\delta\boldsymbol{I} = \delta\boldsymbol{I}\,-\,\kappa_{\rm L}\,\boldsymbol{H}\,\left(B_{\rm P}\boldsymbol{U}\,-\,\boldsymbol{I}_0\right)\ .$$

The evolution operator corresponding to these equations is (cf. Eqs. (9.90) and (9.103))

$$\boldsymbol{O}(\tau_{\rm c}\,,\tau_{\rm c}') = {\rm e}^{\,-(\tau_{\rm c}'-\,\tau_{\rm c})}\ \boldsymbol{1}\ ,$$

so that according to Eq. (9.101) we obtain the solutions

$$\boldsymbol{I}_0(\tau_{\rm c}) = \int_{\tau_{\rm c}}^{\infty} {\rm e}^{\,-(\tau_{\rm c}'-\,\tau_{\rm c})}\ B_{\rm P}(\tau_{\rm c}')\,\boldsymbol{U}\ {\rm d}\tau_{\rm c}' = I_{\rm c}(\tau_{\rm c})\,\boldsymbol{U}$$

$$\delta\boldsymbol{I}(\tau_{\rm c}) = \int_{\tau_{\rm c}}^{\infty} {\rm e}^{\,-(\tau_{\rm c}'-\,\tau_{\rm c})}\ \kappa_{\rm L}(\tau_{\rm c}')\,\boldsymbol{H}(\tau_{\rm c}')\left[\,B_{\rm P}(\tau_{\rm c}')-I_{\rm c}(\tau_{\rm c}')\,\right]\boldsymbol{U}\ {\rm d}\tau_{\rm c}'\ ,$$

where $I_{\rm c}$ is the continuum intensity at the line wavelength. The emerging Stokes parameters are therefore given by

$$\boldsymbol{I}(0) = \boldsymbol{I}_0(0)\,+\,\delta\boldsymbol{I}(0)$$

[1] We restrict attention to the LTE transfer equation rather than the more general equation (9.35). This is justified by the fact that LTE is generally a very good approximation for weak lines.

with

$$\boldsymbol{I}_0(0) = \int_0^\infty \mathrm{e}^{-\tau_\mathrm{c}}\ B_\mathrm{P}(\tau_\mathrm{c})\,\boldsymbol{U}\,\mathrm{d}\tau_\mathrm{c} \;=\; I_\mathrm{c}(0)\,\boldsymbol{U}$$

$$\delta\boldsymbol{I}(0) = \int_0^\infty \mathrm{e}^{-\tau_\mathrm{c}}\ \kappa_\mathrm{L}(\tau_\mathrm{c})\,\boldsymbol{H}(\tau_\mathrm{c}) \times \left[B_\mathrm{P}(\tau_\mathrm{c}) - \int_{\tau_\mathrm{c}}^\infty \mathrm{e}^{-(\tau_\mathrm{c}'-\,\tau_\mathrm{c})}\ B_\mathrm{P}(\tau_\mathrm{c}')\,\mathrm{d}\tau_\mathrm{c}'\right]\boldsymbol{U}\,\mathrm{d}\tau_\mathrm{c}\ . \tag{9.151}$$

These expressions will be referred to as the *generalized Seares formulae*. They reduce to Eqs. (9.149) for the Milne-Eddington model atmosphere, where $\kappa_\mathrm{L} = \text{const.}$, $\boldsymbol{H} = \text{const.}$, $B_\mathrm{P}(\tau_\mathrm{c}) = B_0\,(1 + \beta\mu\,\tau_\mathrm{c})$. It should be noticed that magneto-optical effects are unimportant when the spectral line is weak.

9.14. The Magnetic Field with Variable Azimuth

The problem of line formation in a magnetic field whose azimuth is variable with optical depth can be reduced to the corresponding problem in a magnetic field with constant azimuth via a simple transformation on the propagation matrix.

To illustrate this statement, we consider a radiation beam flowing in a stellar atmosphere along the direction $\vec{\Omega}$, and take the transfer equation in the form (9.35). We denote by $\boldsymbol{I}$ the Stokes vector in a fixed reference system – say, the system $(\vec{e}_a\,, \vec{e}_b\,, \vec{\Omega})$ of Fig. 9.1 – and by $\boldsymbol{I}'$ the Stokes vector in the depth-dependent system whose reference unit vector $\vec{e}_a'$ points in the direction of the transverse component of the local magnetic field vector. It follows that the azimuth angle of the magnetic field is $\chi(\tau_\mathrm{c})$ in the fixed system and $\chi = 0^\circ$ in the depth-dependent system.

The Stokes vectors $\boldsymbol{I}$ and $\boldsymbol{I}'$ are related by the transformation (see Eqs. (1.45))

$$\boldsymbol{I}' = \boldsymbol{R}\,\boldsymbol{I}\ , \tag{9.152}$$

where

$$\boldsymbol{R} = \begin{pmatrix} 1 & 0 & 0 & 0 \\ 0 & \cos\big[2\chi(\tau_\mathrm{c})\big] & \sin\big[2\chi(\tau_\mathrm{c})\big] & 0 \\ 0 & -\sin\big[2\chi(\tau_\mathrm{c})\big] & \cos\big[2\chi(\tau_\mathrm{c})\big] & 0 \\ 0 & 0 & 0 & 1 \end{pmatrix}\ .$$

Writing Eq. (9.35) in the matrix form

$$\frac{\mathrm{d}\boldsymbol{I}}{\mathrm{d}\tau_\mathrm{c}} = \big(\boldsymbol{1} + \kappa_\mathrm{L}\,\boldsymbol{H}\big)\,\boldsymbol{I} \;-\; \big(S_\mathrm{c}\,\boldsymbol{1} + \kappa_\mathrm{L} S_\mathrm{L}\,\boldsymbol{H}\big)\,\boldsymbol{U} \tag{9.153}$$

(with $\boldsymbol{H}$ and $\boldsymbol{U}$ given by Eqs. (9.50) and (9.49)), and deriving Eq. (9.152) with respect to $\tau_{\rm c}$, we obtain

$$\frac{{\rm d}\boldsymbol{I}'}{{\rm d}\tau_{\rm c}} = \frac{{\rm d}\boldsymbol{R}}{{\rm d}\tau_{\rm c}}\,\boldsymbol{I} + \boldsymbol{R}\,\frac{{\rm d}\boldsymbol{I}}{{\rm d}\tau_{\rm c}} = \frac{{\rm d}\boldsymbol{R}}{{\rm d}\tau_{\rm c}}\,\boldsymbol{I} + \boldsymbol{R}\left(\boldsymbol{1} + \kappa_{\rm L}\,\boldsymbol{H}\right)\boldsymbol{I} - \boldsymbol{R}\left(S_{\rm c}\,\boldsymbol{1} + \kappa_{\rm L}\,S_{\rm L}\,\boldsymbol{H}\right)\boldsymbol{U}\ .$$

The Stokes vector $\boldsymbol{I}$ in the right-hand side can be expressed in terms of $\boldsymbol{I}'$ via the inverse transformation of Eq. (9.152)

$$\boldsymbol{I} = \boldsymbol{R}^{-1}\,\boldsymbol{I}'\ , \tag{9.154}$$

which leads to

$$\frac{{\rm d}\boldsymbol{I}'}{{\rm d}\tau_{\rm c}} = \left[\,\frac{{\rm d}\boldsymbol{R}}{{\rm d}\tau_{\rm c}}\,\boldsymbol{R}^{-1} + \boldsymbol{1} + \kappa_{\rm L}\,\boldsymbol{R}\,\boldsymbol{H}\,\boldsymbol{R}^{-1}\right]\boldsymbol{I}' - \left[S_{\rm c}\,\boldsymbol{1} + \kappa_{\rm L}S_{\rm L}\,\boldsymbol{R}\,\boldsymbol{H}\,\boldsymbol{R}^{-1}\right]\boldsymbol{R}\,\boldsymbol{U}\ . \tag{9.155}$$

A direct calculation shows that

$$\boldsymbol{R}^{-1} = \begin{pmatrix} 1 & 0 & 0 & 0 \\ 0 & \cos\big[2\chi(\tau_{\rm c})\big] & -\sin\big[2\chi(\tau_{\rm c})\big] & 0 \\ 0 & \sin\big[2\chi(\tau_{\rm c})\big] & \cos\big[2\chi(\tau_{\rm c})\big] & 0 \\ 0 & 0 & 0 & 1 \end{pmatrix}\ ,$$

whence we easily obtain

$$\frac{{\rm d}\boldsymbol{R}}{{\rm d}\tau_{\rm c}}\,\boldsymbol{R}^{-1} = 2\,\frac{{\rm d}\chi}{{\rm d}\tau_{\rm c}}\,\boldsymbol{Z}\ ,$$

with

$$\boldsymbol{Z} = \begin{pmatrix} 0 & 0 & 0 & 0 \\ 0 & 0 & 1 & 0 \\ 0 & -1 & 0 & 0 \\ 0 & 0 & 0 & 0 \end{pmatrix}\ ,$$

and, using Eqs. (9.32)

$$\boldsymbol{R}\,\boldsymbol{H}\,\boldsymbol{R}^{-1} = \begin{pmatrix} h_I & h_{\tilde{Q}} & 0 & h_V \\ h_{\tilde{Q}} & h_I & r_V & 0 \\ 0 & -r_V & h_I & r_{\tilde{Q}} \\ h_V & 0 & -r_{\tilde{Q}} & h_I \end{pmatrix}\ , \tag{9.156}$$

where[1]

$$\begin{aligned} h_{\tilde{Q}} = h_Q(\chi = 0^\circ) &= \frac{1}{2}\left[\,\eta_{\rm p} - \frac{\eta_{\rm b} + \eta_{\rm r}}{2}\right]\sin^2\theta \\ r_{\tilde{Q}} = r_Q(\chi = 0^\circ) &= \frac{1}{2}\left[\,\rho_{\rm p} - \frac{\rho_{\rm b} + \rho_{\rm r}}{2}\right]\sin^2\theta\ . \end{aligned} \tag{9.157}$$

[1] Note that the matrix in Eq. (9.156) is nothing but the propagation matrix for a magnetic field having $\chi = 0^\circ$.

Since, moreover

$$\boldsymbol{R}\,\boldsymbol{U} = \boldsymbol{U}\ , \qquad \boldsymbol{Z}\,\boldsymbol{U} = 0\ ,$$

Eq. (9.155) can be rewritten in the form

$$\frac{\mathrm{d}\boldsymbol{I}'}{\mathrm{d}\tau_{\mathrm{c}}} = \left(\boldsymbol{1} + \kappa_{\mathrm{L}}\,\boldsymbol{H}'\right)\boldsymbol{I}' - \left(S_{\mathrm{c}}\,\boldsymbol{1} + \kappa_{\mathrm{L}}\,S_{\mathrm{L}}\,\boldsymbol{H}'\right)\boldsymbol{U}\ , \tag{9.158}$$

where

$$\boldsymbol{H}' = \boldsymbol{R}\,\boldsymbol{H}\,\boldsymbol{R}^{-1} + \frac{2}{\kappa_{\mathrm{L}}}\,\frac{\mathrm{d}\chi}{\mathrm{d}\tau_{\mathrm{c}}}\,\boldsymbol{Z} = \begin{pmatrix} h_I & h_{\tilde{Q}} & 0 & h_V \\ h_{\tilde{Q}} & h_I & r'_V & 0 \\ 0 & -r'_V & h_I & r_{\tilde{Q}} \\ h_V & 0 & -r_{\tilde{Q}} & h_I \end{pmatrix}\ , \tag{9.159}$$

with

$$r'_V = r_V + \frac{2}{\kappa_{\mathrm{L}}}\,\frac{\mathrm{d}\chi}{\mathrm{d}\tau_{\mathrm{c}}} = r_V + 2\,\frac{\mathrm{d}\chi}{\mathrm{d}\tau_{\mathrm{L}}} \tag{9.160}$$

(Eqs. (9.31) and (9.33) have been used to derive the last expression).

Comparison of Eqs. (9.158) and (9.153) shows that the transfer equation for $\boldsymbol{I}'$ is obtained from the transfer equation for $\boldsymbol{I}$ by substituting the matrix $\boldsymbol{H}'$ for the matrix $\boldsymbol{H}$. As apparent from Eqs. (9.159) and (9.160), this means that the depth dependence of the azimuth of the magnetic field can be taken into account by setting $\chi = 0°$ at any optical depth and by adding the (wavelength-independent) term $2\,(\mathrm{d}\chi/\mathrm{d}\tau_{\mathrm{L}})$ to the Faraday rotation coefficient r_V. This result was first derived by Staude (1969). Obviously, once Eq. (9.158) is solved, the Stokes vector $\boldsymbol{I}$ is obtained by applying the transformation (9.154).

The influence of the depth dependence of the azimuth angle on the Stokes parameters profiles is illustrated in Fig. 9.8, in the form of Unno-Rachkovsky solution to the radiative transfer equation. Of course, such solution can only be used under the assumption that $(\mathrm{d}\chi/\mathrm{d}\tau_{\mathrm{L}})$ is independent of optical depth (in addition to the assumptions listed at the beginning of Sect. 9.8). As expected, the main effect of azimuth variability is a decrease of linear polarization.

9.15. Numerical Solutions

In the preceding sections of this chapter we have considered several cases where the transfer equation can be solved in closed form thanks to certain assumptions about the structure of the medium where propagation occurs. In a real stellar atmosphere, or in detailed model atmospheres (like for instance the solar models given by Gingerich et al., 1971, or Vernazza et al., 1981), these assumptions are generally not satisfied, so that the approximate solutions presented so far cannot be used reliably. This does not mean, however, that such solutions are pointless, since it should be borne in mind that the sophisticated models which are nowadays available are themselves based on specific assumptions about the physics and

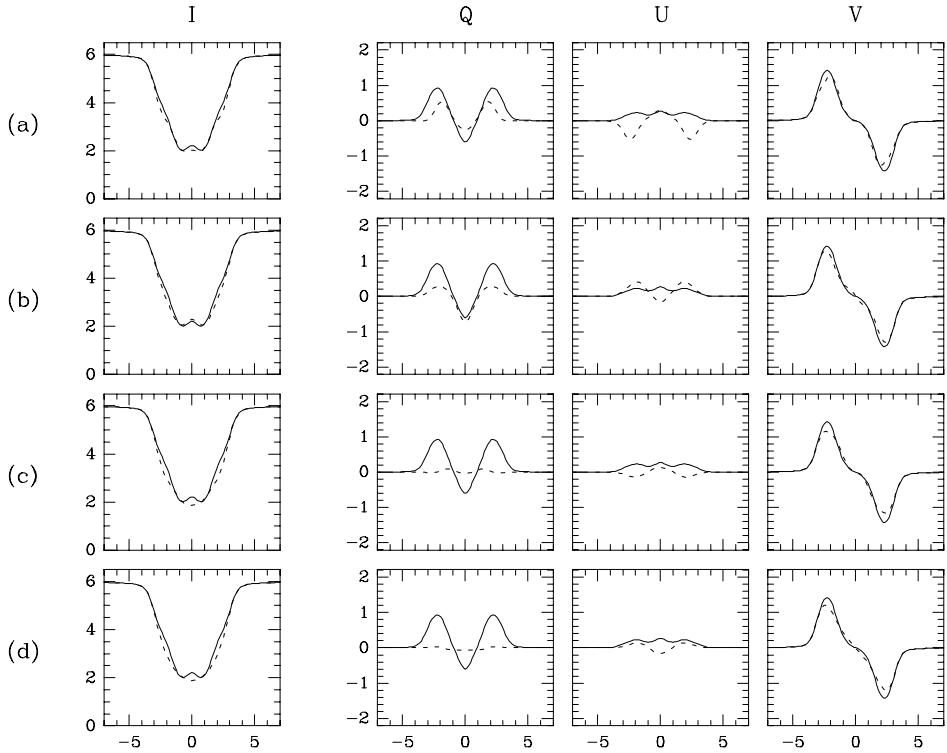

Fig.9.8. Stokes parameters profiles for the normal Zeeman triplet ${}^1S_0 - {}^1P_1$ emerging from an atmosphere with depth-dependent magnetic field's azimuth. The profiles are computed using Eqs.(9.110) with $f_V = \kappa_L\, r'_V$ and r'_V given by Eq.(9.160). They are normalized to B_0 and plotted against the reduced wavelength. The reference direction is parallel to the transverse component of the magnetic field at $\tau_c = 0$. The values of the relevant parameters are those of the 'standard case' (see Fig.9.5). The full line, drawn for reference, corresponds to $d\chi/d\tau_L = 0$. The dotted line corresponds to the following values of $d\chi/d\tau_L$: -0.1 (a); $+0.1$ (b); -0.5 (c); $+0.5$ (d).

geometry of real atmospheres. The interpretation of an observed phenomenon may result clearer, and in some cases even more precise, if a rough model like the Milne-Eddington is used instead of a detailed model. This is particularly true for magnetic stellar atmospheres because the theoretical construction of fully consistent magneto-hydrodynamic models is still in a preliminary phase and, on the other hand, the deduction of empirical models is hampered by the inadequate knowledge of the magnetic structure.

Detailed models for plane-parallel atmospheres generally consist of a table of numbers giving the run of several physical quantities (such as temperature, partial pressures, microturbulent velocity, magnetic field vector, etc.) with depth. Models can also be constructed for more complicated (non plane-parallel) atmospheres. One could consider for instance a composite atmosphere formed by magnetic structures (like sunspots or flux-tubes) embedded in a plane-parallel atmosphere. This would be a three-dimensional model and the actual run of the physical quantities

with depth would depend on the individual ray path.

Different depth indicators are used in different models, the most common being the geometrical depth, the column mass, and the continuum optical depth at a reference frequency $\nu_{\rm r}$ (typically the frequency corresponding to 5000 Å). Standard calculations enable the conversion between different indicators. Such calculations involve the equation of state of the atmospheric plasma and require the knowledge of its chemical composition and of the processes which contribute to the continuum opacity (see e.g. Unsöld, 1955; Aller, 1963; Mihalas, 1978).

Let us consider the radiative transfer problem in the case where the properties of the medium are specified through a numerical model atmosphere. Without loosing in generality, we assume that the model is given in terms of $\tau_{\rm r}$, the continuum optical depth at the reference frequency $\nu_{\rm r}$ measured along the ray path (see Eqs. (9.33)). The transfer equation (9.30) reads

$$\frac{\mathrm{d}}{\mathrm{d}\tau_{\rm r}} \begin{pmatrix} I \\ Q \\ U \\ V \end{pmatrix} = \kappa_{\rm r} \begin{pmatrix} 1 & 0 & 0 & 0 \\ 0 & 1 & 0 & 0 \\ 0 & 0 & 1 & 0 \\ 0 & 0 & 0 & 1 \end{pmatrix} \begin{pmatrix} I - S_{\rm c} \\ Q \\ U \\ V \end{pmatrix} + \kappa_{\rm R} \begin{pmatrix} h_I & h_Q & h_U & h_V \\ h_Q & h_I & r_V & -r_U \\ h_U & -r_V & h_I & r_Q \\ h_V & r_U & -r_Q & h_I \end{pmatrix} \begin{pmatrix} I - S_{\rm L} \\ Q \\ U \\ V \end{pmatrix} , \tag{9.161}$$

$\kappa_{\rm r}$ and $\kappa_{\rm R}$ being the dimensionless quantities (see Eq. (9.31))

$$\kappa_{\rm r} = \frac{k_{\rm c}(\nu_0)}{k_{\rm c}(\nu_{\rm r})} , \qquad \kappa_{\rm R} = \frac{k_{\rm L}}{k_{\rm c}(\nu_{\rm r})\, \Delta\nu_{\rm D}} , \tag{9.162}$$

or, in matrix form[1]

$$\frac{\mathrm{d}}{\mathrm{d}\tau_{\rm r}} \boldsymbol{I}(\tau_{\rm r}) = \boldsymbol{A}(\tau_{\rm r})\, \boldsymbol{I}(\tau_{\rm r}) - \boldsymbol{b}(\tau_{\rm r}) , \tag{9.163}$$

where

$$\begin{aligned} \boldsymbol{A} &= \kappa_{\rm r}\, \boldsymbol{1} + \kappa_{\rm R}\, \boldsymbol{H} \\ \boldsymbol{b} &= \left[\kappa_{\rm r}\, S_{\rm c}\, \boldsymbol{1} + \kappa_{\rm R}\, S_{\rm L}\, \boldsymbol{H} \right] \boldsymbol{U} , \end{aligned} \tag{9.164}$$

with $\boldsymbol{H}$ and $\boldsymbol{U}$ given by Eqs. (9.50) and (9.49), respectively.

The quantity $\kappa_{\rm r}$ and the elements of the matrix $\boldsymbol{H}$ can be evaluated numerically, at each optical depth and for any wavelength, via the standard computations

[1] Obviously, Eq. (9.163) is identical, from the mathematical point of view, to Eq. (9.90). The difference between the matrices $\boldsymbol{A}$ and $\boldsymbol{C}$ and the vectors $\boldsymbol{b}$ and $\boldsymbol{j}$ is only due to the use of different depth indicators.

mentioned above. In the case of LTE, this is also true for the source functions ($S_{\rm c} = S_{\rm L} = B_{\rm P}$) and for the quantity $\kappa_{\rm R}$. For non-LTE situations, we assume here that $S_{\rm c}$, $S_{\rm L}$ and $\kappa_{\rm R}$ (or the ratio $\mathcal{N}_u/\mathcal{N}_\ell$, see Eqs. (9.14)) are known, i.e. given together with the model. (The problem of non-LTE will be considered in more generality in Chap. 14).

Equation (9.163) can be formally solved by the evolution operator method. Similarly to Eq. (9.100), we have

$$\boldsymbol{I}(\tau_{\rm r}) = \int_{\tau_{\rm r}}^{\tau_{\rm r}'} \boldsymbol{O}(\tau_{\rm r}\,,\tau_{\rm r}'')\,\boldsymbol{b}(\tau_{\rm r}'')\,{\rm d}\tau_{\rm r}'' \;+\; \boldsymbol{O}(\tau_{\rm r}\,,\tau_{\rm r}')\,\boldsymbol{I}(\tau_{\rm r}')\;, \tag{9.165}$$

and, for the Stokes parameters emerging from a semi-infinite atmosphere

$$\boldsymbol{I}(0) = \int_0^\infty \boldsymbol{O}(0,\tau_{\rm r})\,\boldsymbol{b}(\tau_{\rm r})\,{\rm d}\tau_{\rm r}\;, \tag{9.166}$$

provided

$$\lim_{\tau_{\rm r}\to\infty} \boldsymbol{O}(0,\tau_{\rm r})\,\boldsymbol{b}(\tau_{\rm r}) = 0\;.$$

The evolution operator $\boldsymbol{O}(\tau_{\rm r}\,,\tau_{\rm r}')$ satisfies the analogues of Eqs. (9.94)-(9.97) and can be written in the form

$$\begin{aligned}&\boldsymbol{O}(\tau_{\rm r}\,,\tau_{\rm r}') = \\ &= \boldsymbol{1} + \sum_{n=1}^{\infty} \frac{(-1)^n}{n!} \int_{\tau_{\rm r}}^{\tau_{\rm r}'} {\rm d}\tau_1 \int_{\tau_{\rm r}}^{\tau_{\rm r}'} {\rm d}\tau_2 \cdots \int_{\tau_{\rm r}}^{\tau_{\rm r}'} {\rm d}\tau_n\; \mathbb{P}\Big\{\boldsymbol{A}(\tau_1)\,\boldsymbol{A}(\tau_2)\cdots\boldsymbol{A}(\tau_n)\Big\}\;,\end{aligned} \tag{9.167}$$

$\mathbb{P}$ being the chronological ordering operator defined in Eqs. (9.98)-(9.99).

Unfortunately, Eq. (9.167) is too involved from the mathematical point of view to provide a convenient method for the numerical computation of the evolution operator. Alternative algorithms have been proposed for the solution of the transfer equation (9.163). In this section we give a brief account of these methods and of their main advantages and disadvantages. We point out, however, that an exhaustive discussion of the numerical accuracy and computing time typical of each method is beyond the aim of this book.

A numerical technique that has been widely used for the solution of Eq. (9.163) is the so-called *4-th order Runge-Kutta method* (Beckers, 1969a; Wittmann, 1974; Landi Degl'Innocenti, 1976). This method, whose mathematical description can be found in Collatz (1966), requires – for each wavelength at which the equation is to be solved – the division of the integration domain into a number N of intervals, not necessarily equal, from $\tau_{\rm r} = \tau_{\rm min}$ (the smallest $\tau_{\rm r}$-value where the model is specified or suitably extrapolated) to $\tau_{\rm r} = \tau_{\rm b}$ (an appropriate boundary value): this defines a grid of points $\tau_0 = \tau_{\rm min}\,, \tau_1\,, \tau_2\,, \ldots, \tau_N = \tau_{\rm b}$. Boundary values for

the Stokes parameters at the optical depth $\tau_{\rm b}$ are then chosen.[1] The integration starts at $\tau_{\rm b}$ and proceeds outwards, step by step, the Stokes parameters at the k-th grid-point being related to those at the $(k+1)$-th point by the equations

$$\boldsymbol{I}(\tau_k) = \boldsymbol{I}(\tau_{k+1}) - \frac{1}{6}\left[\Delta\boldsymbol{I}^{(1)} + 2\,\Delta\boldsymbol{I}^{(2)} + 2\,\Delta\boldsymbol{I}^{(3)} + \Delta\boldsymbol{I}^{(4)}\right], \tag{9.168}$$

where

$$\begin{aligned}
\Delta\boldsymbol{I}^{(1)} &= (\tau_{k+1} - \tau_k)\left\{\boldsymbol{A}(\tau_{k+1})\,\boldsymbol{I}(\tau_{k+1}) - \boldsymbol{b}(\tau_{k+1})\right\} \\
\Delta\boldsymbol{I}^{(2)} &= (\tau_{k+1} - \tau_k)\left\{\boldsymbol{A}(\tilde{\tau}_k)\left[\boldsymbol{I}(\tau_{k+1}) - \frac{1}{2}\Delta\boldsymbol{I}^{(1)}\right] - \boldsymbol{b}(\tilde{\tau}_k)\right\} \\
\Delta\boldsymbol{I}^{(3)} &= (\tau_{k+1} - \tau_k)\left\{\boldsymbol{A}(\tilde{\tau}_k)\left[\boldsymbol{I}(\tau_{k+1}) - \frac{1}{2}\Delta\boldsymbol{I}^{(2)}\right] - \boldsymbol{b}(\tilde{\tau}_k)\right\} \\
\Delta\boldsymbol{I}^{(4)} &= (\tau_{k+1} - \tau_k)\left\{\boldsymbol{A}(\tau_k)\left[\boldsymbol{I}(\tau_{k+1}) - \Delta\boldsymbol{I}^{(3)}\right] - \boldsymbol{b}(\tau_k)\right\},
\end{aligned} \tag{9.169}$$

with $\tilde{\tau}_k$ the midpoint of the $(k+1)$-th interval

$$\tilde{\tau}_k = \frac{\tau_k + \tau_{k+1}}{2} \ .$$

The accuracy of the Runge-Kutta integration is strictly related to the length of the intervals. There are two distinct reasons why the intervals should be kept small. The first is that the variation of $\boldsymbol{A}$ and $\boldsymbol{b}$ in a 'large' interval could be too large: in other words, the three-point sampling of $\boldsymbol{A}$ and $\boldsymbol{b}$ performed in Eqs. (9.169) – at the ends and midpoint of the interval – might be insufficient. This is usually a minor drawback, because the grid of a well-constructed numerical model is in general sufficiently close for the physical quantities to show very smooth point-to-point variations. In such cases an integration grid everywhere equal to (or finer than) the model grid may be adequate.[2]

The second reason for keeping the integration intervals small becomes evident by fully expanding Eq. (9.168) and by writing it in the form

$$\boldsymbol{I}_k = \boldsymbol{p}_k + \boldsymbol{\Pi}_k\,\boldsymbol{I}_{k+1} \ , \tag{9.170}$$

where

$$\boldsymbol{I}_k = \boldsymbol{I}(\tau_k) \ , \qquad \boldsymbol{I}_{k+1} = \boldsymbol{I}(\tau_{k+1}) \ .$$

[1] One generally takes the Unno-Rachkovsky solutions resulting from the assumption that, for $\tau_{\rm r} > \tau_{\rm b}$, the propagation matrix is constant and the source functions (coincident with the Planck function at large optical depth) are linear in $\tau_{\rm r}$.

[2] Note that this is a very qualitative statement. To the authors' knowledge, a systematic analysis of the influence of the $\tau_{\rm r}$-variation of $\boldsymbol{A}$ and $\boldsymbol{b}$ on the numerical accuracy of the Runge-Kutta integration has never been carried out.

We obtain

$$\begin{aligned}
\boldsymbol{p}_k &= \frac{1}{6}\,\delta_k \Big[\, \boldsymbol{b}(\tau_{k+1}) \,+\, 4\,\boldsymbol{b}(\tilde{\tau}_k) \,+\, \boldsymbol{b}(\tau_k) \Big] \\
&\quad - \frac{1}{6}\,\delta_k^2 \Big[\, \boldsymbol{A}(\tilde{\tau}_k)\,\boldsymbol{b}(\tau_{k+1}) \,+\, \boldsymbol{A}(\tilde{\tau}_k)\,\boldsymbol{b}(\tilde{\tau}_k) \,+\, \boldsymbol{A}(\tau_k)\,\boldsymbol{b}(\tilde{\tau}_k) \Big] \\
&\quad + \frac{1}{12}\,\delta_k^3 \Big[\, \boldsymbol{A}^2(\tilde{\tau}_k)\,\boldsymbol{b}(\tau_{k+1}) \,+\, \boldsymbol{A}(\tau_k)\,\boldsymbol{A}(\tilde{\tau}_k)\,\boldsymbol{b}(\tilde{\tau}_k) \Big] \\
&\quad - \frac{1}{24}\,\delta_k^4 \;\boldsymbol{A}(\tau_k)\,\boldsymbol{A}^2(\tilde{\tau}_k)\,\boldsymbol{b}(\tau_{k+1}) \;, \\
\boldsymbol{\Pi}_k &= \boldsymbol{1} - \frac{1}{6}\,\delta_k \Big[\, \boldsymbol{A}(\tau_{k+1}) \,+\, 4\,\boldsymbol{A}(\tilde{\tau}_k) \,+\, \boldsymbol{A}(\tau_k) \Big] \\
&\quad + \frac{1}{6}\,\delta_k^2 \Big[\, \boldsymbol{A}(\tilde{\tau}_k)\,\boldsymbol{A}(\tau_{k+1}) \,+\, \boldsymbol{A}^2(\tilde{\tau}_k) \,+\, \boldsymbol{A}(\tau_k)\,\boldsymbol{A}(\tilde{\tau}_k) \Big] \\
&\quad - \frac{1}{12}\,\delta_k^3 \Big[\, \boldsymbol{A}^2(\tilde{\tau}_k)\,\boldsymbol{A}(\tau_{k+1}) \,+\, \boldsymbol{A}(\tau_k)\,\boldsymbol{A}^2(\tilde{\tau}_k) \Big] \\
&\quad + \frac{1}{24}\,\delta_k^4 \;\boldsymbol{A}(\tau_k)\,\boldsymbol{A}^2(\tilde{\tau}_k)\,\boldsymbol{A}(\tau_{k+1}) \;,
\end{aligned} \tag{9.171}$$

where δ_k is the length of the $(k+1)$-th interval

$$\delta_k = \tau_{k+1} - \tau_k \;.$$

Comparison of Eqs. (9.170) and (9.165) shows that the matrix $\boldsymbol{\Pi}_k$ provides a numerical representation of the evolution operator associated with the interval $(\tau_k\,,\tau_{k+1})$,

$$\boldsymbol{\Pi}_k \approx \boldsymbol{O}(\tau_k\,,\tau_{k+1}) \;.$$

To test the accuracy of the Runge-Kutta integration against the step length, we can thus adopt the following criterion: assume the propagation matrix $\boldsymbol{A}$ to be constant in the interval $(\tau_k\,,\tau_{k+1})$ and compare the exact analytical expression of the evolution operator with its numerical representation $\boldsymbol{\Pi}_k$. Equations (9.103) and (9.171) yield

$$\boldsymbol{O}(\tau_k\,,\tau_{k+1}) = \mathrm{e}^{\,-\delta_k\,\boldsymbol{A}} \tag{9.172}$$

$$\boldsymbol{\Pi}_k = \boldsymbol{1} - \delta_k\,\boldsymbol{A} + \frac{1}{2!}\,\delta_k^2\,\boldsymbol{A}^2 - \frac{1}{3!}\,\delta_k^3\,\boldsymbol{A}^3 + \frac{1}{4!}\,\delta_k^4\,\boldsymbol{A}^4 \;. \tag{9.173}$$

It follows that the 4-th order Runge-Kutta method gives a Taylor expansion of the analytical result which is correct up to fourth-order terms in the quantity $\delta_k\,\boldsymbol{A}$.

Consider now the eigenvalues of the matrix $\boldsymbol{A}$. From Eqs. (8.33) and (9.164) we have

$$\begin{aligned}
\lambda_1 &= \kappa_{\mathrm{r}} + \kappa_{\mathrm{R}} \big[\, h_I \,+\, \Lambda_+(\vec{h},\vec{r}\,) \big] \\
\lambda_2 &= \kappa_{\mathrm{r}} + \kappa_{\mathrm{R}} \big[\, h_I \,-\, \Lambda_+(\vec{h},\vec{r}\,) \big] \\
\lambda_3 &= \kappa_{\mathrm{r}} + \kappa_{\mathrm{R}} \big[\, h_I \,+\, \mathrm{i}\,\Lambda_-(\vec{h},\vec{r}\,) \big] \\
\lambda_4 &= \kappa_{\mathrm{r}} + \kappa_{\mathrm{R}} \big[\, h_I \,-\, \mathrm{i}\,\Lambda_-(\vec{h},\vec{r}\,) \big] \;,
\end{aligned} \tag{9.174}$$

where $\Lambda_+(\vec{h},\vec{r})$ and $\Lambda_-(\vec{h},\vec{r})$ are given by Eqs. (A5.18). Since each of the quantities $\kappa_{\rm r}$, $\kappa_{\rm R}$, h_I, Λ_+ and Λ_- is non-negative, the modulus of the eigenvalue having the largest modulus (that will be simply referred to as maximum eigenvalue) is

$$\lambda_{\max} = \max\left(\lambda_1, |\lambda_3|\right) = \max\left(\lambda_1, |\lambda_4|\right)$$

$$= \max\left\{\kappa_{\rm r} + \kappa_{\rm R}\left[h_I + \Lambda_+(\vec{h},\vec{r})\right], \sqrt{\left[\kappa_{\rm r} + \kappa_{\rm R}\, h_I\right]^2 + \left[\kappa_{\rm R}\,\Lambda_-(\vec{h},\vec{r})\right]^2}\right\}. \quad (9.175)$$

Similarly, the minimum eigenvalue is

$$\lambda_{\min} = \lambda_2 = \kappa_{\rm r} + \kappa_{\rm R}\left[h_I - \Lambda_+(\vec{h},\vec{r})\right]. \quad (9.176)$$

Comparison of Eqs. (9.172) and (9.173) suggests the following criterion to choose the length of the integration step. The error made in substituting the series expansion (9.173) for the exact expression (9.172) is of order $(\delta_k\,\lambda_{\max})^5 / 120$. If we want to keep this error less than an assigned small number ϵ, we must require

$$\delta_k \le \frac{(120\,\epsilon)^{1/5}}{\lambda_{\max}}, \quad (9.177)$$

which shows how the step length should be controlled by the local value of the maximum eigenvalue.

As far as the choice of $\tau_{\rm b}$ is concerned, we must make sure that the solution does not 'feel' possible inexactitudes in the boundary condition. Bearing in mind Eq. (9.165), this leads to a constraint on the evolution operator $\boldsymbol{O}(\tau_{\min}, \tau_{\rm b})$. This constraint can be expressed in the form[1]

$$\mathrm{e}^{-\int_{\tau_{\min}}^{\tau_{\rm b}} \lambda_{\min}(\tau_{\rm r})\,\mathrm{d}\tau_{\rm r}} \le \epsilon'$$

or

$$\int_{\tau_{\min}}^{\tau_{\rm b}} \lambda_{\min}(\tau_{\rm r})\,\mathrm{d}\tau_{\rm r} \ge -\ln\epsilon', \quad (9.178)$$

where ϵ' is a given small number.

It follows from Eqs. (9.177) and (9.178) that the total number of steps, N, is determined essentially by the ratio

$$\ell = \frac{\lambda_{\max}}{\lambda_{\min}}.$$

Using the Cauchy mean-value theorem we have in fact

$$N \approx \int_{\tau_{\min}}^{\tau_{\rm b}} \frac{1}{\delta_k}\,\mathrm{d}\tau_{\rm r} \ge \int_{\tau_{\min}}^{\tau_{\rm b}} \frac{\lambda_{\max}(\tau_{\rm r})}{(120\,\epsilon)^{1/5}}\,\mathrm{d}\tau_{\rm r} \approx \frac{\langle\,\ell\,\rangle}{(120\,\epsilon)^{1/5}} \int_{\tau_{\min}}^{\tau_{\rm b}} \lambda_{\min}(\tau_{\rm r})\,\mathrm{d}\tau_{\rm r}$$

$$\ge -\frac{\ln\epsilon'}{(120\,\epsilon)^{1/5}}\,\langle\,\ell\,\rangle. \quad (9.179)$$

[1] The quantity $\lambda_{\min}$ is always positive (see footnote on p.421).

Setting for instance $\epsilon = \epsilon' = 10^{-3}$, we have

$$N \geq 10.6 \left\langle \ell \right\rangle ,$$

and it is easily seen that this number may be very large at certain wavelengths, especially for strong lines ($\kappa_{\rm R} \gg \kappa_{\rm r}$). This is the main disadvantage of the Runge-Kutta method.

Beside being used to solve the radiative transfer equation, this method can also be used to compute numerically the evolution operator. In particular, Grossmann-Doerth et al. (1988a) and Sánchez Almeida (1992) have applied the 4-th order Runge-Kutta technique to evaluate the reduced evolution operator (see Sect. 8.9 and App. 7).

Another numerical technique that has been used to solve Eq. (9.163) is the so-called *Feautrier method*. This is the direct generalization to the polarized case of the method proposed by Feautrier (1964) to solve the 'scalar' transfer equation for the intensity. It has been developed by Auer et al. (1977a) in the simplified case where magneto-optical effects are neglected and later generalized by Rees and Murphy (1987) to include these effects. The approach consists in writing the transfer equation as a second-order differential equation with boundary conditions at both ends of the integration interval.

Let us suppose the model atmosphere is given, and let us recall the property of the radiative transfer equation considered at the end of Sect. 9.5 and summarized by Eq. (9.61). Denoting by $\vec{\Omega}$ an arbitrary *outward* direction, and by $-\vec{\Omega}$ the opposite (*inward*) direction, we have from Eq. (9.163)

$$\begin{aligned} &\frac{\mathrm{d}}{\mathrm{d}\tau_{\rm r}} \boldsymbol{I}(\tau_{\rm r}\,, \Delta\lambda) = \boldsymbol{A}(\tau_{\rm r}\,, \Delta\lambda)\; \boldsymbol{I}(\tau_{\rm r}\,, \Delta\lambda) \;-\; \boldsymbol{b}(\tau_{\rm r}\,, \Delta\lambda) \\ &-\frac{\mathrm{d}}{\mathrm{d}\tau_{\rm r}} \tilde{\boldsymbol{I}}'(\tau_{\rm r}\,, -\Delta\lambda) = \boldsymbol{A}(\tau_{\rm r}\,, \Delta\lambda)\; \tilde{\boldsymbol{I}}'(\tau_{\rm r}\,, -\Delta\lambda) \;-\; \boldsymbol{b}(\tau_{\rm r}\,, \Delta\lambda)\;, \end{aligned} \tag{9.180}$$

where the vectors $\boldsymbol{I} = (I,\, Q,\, U,\, V)^{\dagger}$ and $\tilde{\boldsymbol{I}}' = (I',\, Q',\, -U',\, V')^{\dagger}$ refer to the radiation travelling in the directions $\vec{\Omega}$ and $-\vec{\Omega}$ respectively, $\Delta\lambda$ is given by Eq. (9.59), and the reference direction unit vectors are as in Fig. 9.4. Introducing the formal vectors

$$\begin{aligned} \boldsymbol{F}(\tau_{\rm r}\,, \Delta\lambda) &= \frac{1}{2}\Big[\, \boldsymbol{I}(\tau_{\rm r}\,, \Delta\lambda) \;-\; \tilde{\boldsymbol{I}}'(\tau_{\rm r}\,, -\Delta\lambda)\,\Big] \\ \boldsymbol{G}(\tau_{\rm r}\,, \Delta\lambda) &= \frac{1}{2}\Big[\, \boldsymbol{I}(\tau_{\rm r}\,, \Delta\lambda) \;+\; \tilde{\boldsymbol{I}}'(\tau_{\rm r}\,, -\Delta\lambda)\,\Big]\;, \end{aligned} \tag{9.181}$$

and omitting the arguments of the various functions for conciseness, we have using Eqs. (9.180)

$$\frac{\mathrm{d}\boldsymbol{F}}{\mathrm{d}\tau_{\rm r}} = \boldsymbol{A}\,\boldsymbol{G} \;-\; \boldsymbol{b}\;, \qquad\qquad \frac{\mathrm{d}\boldsymbol{G}}{\mathrm{d}\tau_{\rm r}} = \boldsymbol{A}\,\boldsymbol{F}\;, \tag{9.182}$$

whence the following second-order differential equation for $\boldsymbol{G}$ is obtained

$$\frac{\mathrm{d}}{\mathrm{d}\tau_{\mathrm{r}}}\left[\boldsymbol{A}^{-1}\,\frac{\mathrm{d}\boldsymbol{G}}{\mathrm{d}\tau_{\mathrm{r}}}\right] = \boldsymbol{A}\,\boldsymbol{G} - \boldsymbol{b}\,. \tag{9.183}$$

We must now specify the boundary conditions at $\tau_{\mathrm{r}} = 0$ and $\tau_{\mathrm{r}} = \tau_{\mathrm{b}}$. At $\tau_{\mathrm{r}} = 0$, for an atmosphere not illuminated from above (the case to which we restrict attention), we have

$$I' = Q' = U' = V' = 0\,, \tag{9.184}$$

so that Eqs. (9.181) yield $\boldsymbol{F} = \boldsymbol{G}$. Using the second of Eqs. (9.182) we get

$$\boldsymbol{A}^{-1}\,\frac{\mathrm{d}\boldsymbol{G}}{\mathrm{d}\tau_{\mathrm{r}}} = \boldsymbol{G} \qquad\qquad (\tau_{\mathrm{r}} = 0)\,. \tag{9.185}$$

At $\tau_{\mathrm{r}} = \tau_{\mathrm{b}}$ we take $\boldsymbol{I} = \boldsymbol{I}^{(\mathrm{b})}$, where $\boldsymbol{I}^{(\mathrm{b})}$ is for instance the Unno-Rachkovsky solution obtained as specified in footnote 1 on p. 441. Use of Eqs. (9.182) and (9.181) yields

$$\boldsymbol{A}^{-1}\,\frac{\mathrm{d}\boldsymbol{G}}{\mathrm{d}\tau_{\mathrm{r}}} = -\,\boldsymbol{G} + \boldsymbol{I}^{(\mathrm{b})} \qquad\qquad (\tau_{\mathrm{r}} = \tau_{\mathrm{b}})\,. \tag{9.186}$$

The numerical solution of Eq. (9.183), subjected to the boundary conditions (9.185) and (9.186), can be carried out by standard methods of numerical analysis which imply the solution of a tridiagonal system of linear equations. The mathematical details are developed in App. 8 for the case – considered by Auer et al., 1977a, and Rees and Murphy, 1987 – where derivatives are replaced by difference formulae having second-order accuracy. The results of App. 8 show that the Feautrier solution (obtained with such difference formulae) is equivalent, from the point of view of numerical accuracy, to a second-order Runge-Kutta. This obviously implies that the length of the integration step should be controlled by the local value of the 'maximum eigenvalue'.

The same arguments developed for the Runge-Kutta solution show that Eqs. (9.177) and (9.179) must be replaced by

$$\delta_k \le \frac{(6\,\epsilon)^{1/3}}{\lambda_{\max}}\,, \qquad\qquad N \ge -\,\frac{\ln\epsilon'}{(6\,\epsilon)^{1/3}}\,\langle\,\ell\,\rangle\,,$$

respectively. Note that for $\epsilon = \epsilon' = 10^{-3}$ the latter gives $N \ge 38.0\,\langle\,\ell\,\rangle$, or a number of steps almost 4 times larger than in the 4-th order Runge-Kutta solution. Difference formulae having higher-order accuracy can in principle be used within the Feautrier method. References for the solution of the 'scalar' transfer equation are given by Mihalas (1978, p.155).

Another method that has been proposed for the numerical solution of Eq. (9.163) is the so-called *diagonal element lambda-operator* (or *DELO*) *method* (Rees and Murphy, 1987; Rees et al., 1989). The transfer equation is reformulated by taking

advantage of the fact that the four diagonal elements of the propagation matrix $\boldsymbol{A}$ are equal. This enables Eq. (9.163) to be cast into the form

$$\frac{\mathrm{d}}{\mathrm{d}\tau_\mathrm{r}}\,\boldsymbol{I}(\tau_\mathrm{r}) = a_I(\tau_\mathrm{r})\left\{\left[\,\boldsymbol{1} + \boldsymbol{A}'(\tau_\mathrm{r})\,\right]\boldsymbol{I}(\tau_\mathrm{r}) - \boldsymbol{b}'(\tau_\mathrm{r})\right\}, \tag{9.187}$$

where

$$\begin{aligned} a_I &= \kappa_\mathrm{r} + \kappa_\mathrm{R}\, h_I \\ \boldsymbol{A}'(\tau_\mathrm{r}) &= \frac{\boldsymbol{A}(\tau_\mathrm{r})}{a_I(\tau_\mathrm{r})} - \boldsymbol{1} = \frac{\kappa_\mathrm{R}\,[\,\boldsymbol{H} - h_I\,\boldsymbol{1}\,]}{\kappa_\mathrm{r} + \kappa_\mathrm{R}\, h_I} \\ \boldsymbol{b}'(\tau_\mathrm{r}) &= \frac{\boldsymbol{b}(\tau_\mathrm{r})}{a_I(\tau_\mathrm{r})} = \frac{[\,\kappa_\mathrm{r}\, S_\mathrm{c}\,\boldsymbol{1} + \kappa_\mathrm{R}\, S_\mathrm{L}\,\boldsymbol{H}\,]\,\boldsymbol{U}}{\kappa_\mathrm{r} + \kappa_\mathrm{R}\, h_I}\ . \end{aligned} \tag{9.188}$$

Equation (9.187) can be rewritten in the form

$$\frac{\mathrm{d}}{\mathrm{d}\tau_\mathrm{r}}\,\boldsymbol{I}(\tau_\mathrm{r}) = a_I(\tau_\mathrm{r})\left[\,\boldsymbol{I}(\tau_\mathrm{r}) - \boldsymbol{s}(\tau_\mathrm{r})\,\right], \tag{9.189}$$

where

$$\boldsymbol{s}(\tau_\mathrm{r}) = \boldsymbol{b}'(\tau_\mathrm{r}) - \boldsymbol{A}'(\tau_\mathrm{r})\,\boldsymbol{I}(\tau_\mathrm{r}) \tag{9.190}$$

is a 'modified source vector' which is a function of the Stokes vector itself.

The formal solution to Eq. (9.189)

$$\boldsymbol{I}(\tau_\mathrm{r}) = \int_{\tau_\mathrm{r}}^{\infty} \mathrm{e}^{-\int_{\tau_\mathrm{r}}^{\tau'_\mathrm{r}} a_I(\tau''_\mathrm{r})\,\mathrm{d}\tau''_\mathrm{r}}\; a_I(\tau'_\mathrm{r})\,\boldsymbol{s}(\tau'_\mathrm{r})\,\mathrm{d}\tau'_\mathrm{r} \tag{9.191}$$

is an integral Volterra equation for $\boldsymbol{I}(\tau_\mathrm{r})$. It can be solved via an iterative procedure, called *lambda-iteration*,[1] as done by Staude (1969). The numerical method proposed by Rees and Murphy (1987), whose details are developed in App. 9, has the advantage of avoiding the slow convergence of the lambda-iteration.

The results contained in App. 9 show that the integration grid must be locally controlled also for the DELO method. The criterion to choose the step length

[1] The concepts of lambda-operator and lambda-iteration are basic tools of the theory of (scalar) radiative transfer (see e.g. Mihalas, 1978). Recalling Eq. (9.190), Eq. (9.191) can be written in the form

$$\boldsymbol{I}(\tau_\mathrm{r}) = \boldsymbol{\Lambda}(\,\boldsymbol{I}\,;\tau_\mathrm{r}) + \boldsymbol{\Lambda}'(\boldsymbol{b}\,;\tau_\mathrm{r})\,,$$

where $\boldsymbol{\Lambda}$ and $\boldsymbol{\Lambda}'$ are integral operators acting, respectively, on the vectors $\boldsymbol{I}$ (unknown) and $\boldsymbol{b}$ (known). The usual lambda-iteration consists in starting with the zero-order solution $\boldsymbol{I}^{(0)}(\tau_\mathrm{r}) = 0$ and evaluating repeatedly the left-hand side of the equation by substituting in the right-hand side the value $\boldsymbol{I}^{(k)}(\tau_\mathrm{r})$ obtained in the previous iteration. The procedure is stopped when convergence is reached. Lambda-iterations generally converge very slowly.

is suggested by Eq. (A9.9). The eigenvalues of the matrix $(\boldsymbol{A} - a_I\,\boldsymbol{1})$ are (cf. Eqs. (9.164), (9.188) and (8.33))

$$\lambda'_1 = \kappa_{\rm R}\,\Lambda_+(\vec{h},\vec{r}) \qquad \lambda'_3 = \mathrm{i}\,\kappa_{\rm R}\,\Lambda_-(\vec{h},\vec{r})$$
$$\lambda'_2 = -\kappa_{\rm R}\,\Lambda_+(\vec{h},\vec{r}) \qquad \lambda'_4 = -\mathrm{i}\,\kappa_{\rm R}\,\Lambda_-(\vec{h},\vec{r})\ .$$

Defining

$$\lambda'_{\max} = \max\left[\,\kappa_{\rm R}\,\Lambda_+(\vec{h},\vec{r})\ ,\ \kappa_{\rm R}\,\Lambda_-(\vec{h},\vec{r})\,\right]\ , \tag{9.192}$$

the error introduced at each step by the DELO integration is of order

$$\frac{\delta_k^3}{12}\left(\lambda'_{\max}\right)^3\left(1+\frac{a_I}{\lambda'_{\max}}\right)^2\ .$$

If we want to keep this error less than ϵ, we must require

$$\delta_k \ \le\ \frac{(12\,\epsilon)^{1/3}}{\lambda'_{\max}\left(1+\dfrac{a_I}{\lambda'_{\max}}\right)^{2/3}}\ . \tag{9.193}$$

The number of steps necessary for the integration is therefore (cf. the derivation of Eq. (9.179))

$$N\ \ge\ -\frac{\ln\epsilon'}{(12\,\epsilon)^{1/3}}\left\langle\,\ell'\,\right\rangle\ ,$$

where

$$\ell'\ =\ \frac{\lambda'_{\max}}{\lambda_{\min}}\left(1+\frac{a_I}{\lambda'_{\max}}\right)^{2/3}\ ,$$

with $\lambda_{\min}$ given by Eq. (9.176).

The performance of the DELO method against the Runge-Kutta method can be examined by comparing the corresponding step lengths. Taking for instance $\epsilon = 10^{-3}$, we have from Eqs. (9.177) and (9.193)

$$\frac{(\delta_k)_{\rm R.K.}}{(\delta_k)_{\rm DELO}}\ \approx\ 2.9\ \frac{\left(\lambda'_{\max}\right)^{1/3}\left(a_I+\lambda'_{\max}\right)^{2/3}}{\lambda_{\max}}\ ,$$

with $\lambda_{\max}$ given by Eq. (9.175). If the propagation matrix $\boldsymbol{A}$ is 'almost diagonal', we have from Eqs. (9.174), (9.188) and (9.192)

$$\lambda'_{\max}\ \ll\ a_I\ , \qquad\qquad \lambda_{\max}\ \approx\ a_I\ ,$$

thus the DELO method is more efficient. When $\lambda'_{\max}$ and a_I are comparable (which is often the case in most practical applications), it is difficult to establish which method is more efficient.

The last integration method that we discuss here is based on the direct application of the concept of evolution operator. The method, already presented in a slightly different form in Landi Degl'Innocenti (1987), will be referred to as the *piecemeal evolution operator* (or *PEO*) *method*. It consists in the following.

We introduce a grid of N points $(\tau_1\,,\tau_2\,,\ldots,\tau_N)$ not necessarily evenly spaced. In each interval we assume that the matrix $\boldsymbol{H}$ is constant and equal to the average of the values at the end points of the interval,

$$\overline{\boldsymbol{H}}_k = \frac{1}{2}\left[\,\boldsymbol{H}(\tau_k) \,+\, \boldsymbol{H}(\tau_{k+1})\right]. \tag{9.194}$$

According to Eqs. (9.164) and (9.104), the evolution operator associated with the interval $(\tau_k\,,\tau_{k+1})$ is

$$\boldsymbol{O}(\tau_k\,,\tau_{k+1}) \equiv \boldsymbol{O}_k = \mathrm{e}^{-K_\mathrm{r}(\tau_k\,,\tau_{k+1})}\;\mathrm{e}^{-K_\mathrm{R}(\tau_k\,,\tau_{k+1})\,\overline{\boldsymbol{H}}_k} \qquad (k=1,2,\ldots,N-1)\,,$$

where

$$K_\mathrm{r}(\tau,\tau') = \int_\tau^{\tau'} \kappa_\mathrm{r}(\tau_\mathrm{r})\,\mathrm{d}\tau_\mathrm{r}\,, \qquad K_\mathrm{R}(\tau,\tau') = \int_\tau^{\tau'} \kappa_\mathrm{R}(\tau_\mathrm{r})\,\mathrm{d}\tau_\mathrm{r}\,, \tag{9.195}$$

and where the exponential of the matrix can be conveniently expressed via Eqs. (A5.20) or (A5.23).

Iterative application of Eq. (9.165) enables the emerging Stokes vector to be written in the form

$$\boldsymbol{I}(\tau_1) = \boldsymbol{W}_1 + \boldsymbol{O}_1\big(\boldsymbol{W}_2 + \boldsymbol{O}_2\big(\boldsymbol{W}_3 + \boldsymbol{O}_3\big(\ldots\;\big(\boldsymbol{W}_{N-1} \,+\, \boldsymbol{O}_{N-1}\,\boldsymbol{W}_N\big)\;\ldots\big)\big)\big)$$

or

$$\boldsymbol{I}(\tau_1) = \boldsymbol{W}_1 \,+\, \sum_{k=2}^{N} \boldsymbol{O}_1\,\boldsymbol{O}_2\,\cdots\,\boldsymbol{O}_{k-1}\,\boldsymbol{W}_k\,,$$

where, using Eqs. (9.164)

$$\begin{aligned}
\boldsymbol{W}_k &= \int_{\tau_k}^{\tau_{k+1}} \boldsymbol{O}(\tau_k\,,\tau_\mathrm{r})\,\boldsymbol{b}(\tau_\mathrm{r})\,\mathrm{d}\tau_\mathrm{r} \\
&= \int_{\tau_k}^{\tau_{k+1}} \mathrm{e}^{-K_\mathrm{r}(\tau_k\,,\tau_\mathrm{r})}\;\mathrm{e}^{-K_\mathrm{R}(\tau_k\,,\tau_\mathrm{r})\,\overline{\boldsymbol{H}}_k} \\
&\qquad \times \left[\,\kappa_\mathrm{r}(\tau_\mathrm{r})\,S_\mathrm{c}(\tau_\mathrm{r})\,\boldsymbol{1} \,+\, \kappa_\mathrm{R}(\tau_\mathrm{r})\,S_\mathrm{L}(\tau_\mathrm{r})\,\overline{\boldsymbol{H}}_k\,\right]\boldsymbol{U}\,\mathrm{d}\tau_\mathrm{r}
\end{aligned} \tag{9.196}$$

for $k = 1,\,2,\,\ldots,N-1$, and

$$\boldsymbol{W}_N \,=\, \boldsymbol{I}(\tau_N) \,=\, \boldsymbol{I}^{(\mathrm{b})}\,,$$

with $\boldsymbol{I}^{(\mathrm{b})}$ the boundary Stokes vector (see footnote 1 on p. 441).

The run with τ_{r} of the quantities κ_{r}, κ_{R}, S_{c} and S_{L} is deduced from the atmospheric model at the grid points where the model is specified. Values in intermediate points can be computed by usual interpolation methods. The integrals in Eqs. (9.195) and (9.196) can then be evaluated by standard numerical techniques.

Obviously, for a hypothetic atmosphere where the matrix $\boldsymbol{H}$ is constant, the PEO method provides the *exact* solution to the transfer equation irrespective of the number and length of the integration steps. It is also obvious that the criterion used to evaluate the accuracy of the preceding methods (comparison between the numerical and analytical expressions of the evolution operator) is meaningless for the PEO method. What is important for this method is not the local value of the maximum eigenvalue, but the rate of variation of the matrix $\boldsymbol{H}$ with optical depth. For instance, if $\boldsymbol{H}$ has a smooth variation in a certain interval, a relatively large integration step can be chosen even if the maximum eigenvalue of $\boldsymbol{H}$ is 'large'.

It should be pointed out that the accuracy of the PEO method can be improved through an algorithm based on the concept of perturbative solution introduced in Sect. 8.7. The solution previously obtained – with the matrix $\boldsymbol{H}$ assumed constant in each interval – can be considered as the 'zero-order solution'. The 'perturbation' consists in assuming the matrix $\boldsymbol{H}$ linear in τ_{r} in the interval $(\tau_k\,,\tau_{k+1})$,

$$\delta\boldsymbol{H}(\tau_{\mathrm{r}}) = \boldsymbol{H}(\tau_{\mathrm{r}}) - \overline{\boldsymbol{H}}_k = \left[\boldsymbol{H}(\tau_{k+1}) - \boldsymbol{H}(\tau_k)\right] \frac{2\tau_{\mathrm{r}} - \tau_{k+1} - \tau_k}{2\,(\tau_{k+1} - \tau_k)} \qquad (\tau_k \le \tau_{\mathrm{r}} \le \tau_{k+1})\,,$$

where Eq. (9.194) has been used. Calculations similar to those in Sect. 8.7 show that the correction to the zero-order solution can be written in the form

$$\delta\boldsymbol{I}(\tau_1) = \int_{\tau_1}^{\infty} \boldsymbol{O}_0(\tau_1\,,\tau_{\mathrm{r}})\;\kappa_{\mathrm{R}}(\tau_{\mathrm{r}})\;\delta\boldsymbol{H}(\tau_{\mathrm{r}})\;\left[\,S_{\mathrm{L}}(\tau_{\mathrm{r}})\,\boldsymbol{U} \;-\; \boldsymbol{I}_0(\tau_{\mathrm{r}})\,\right]\,\mathrm{d}\tau_{\mathrm{r}}\;,$$

where $\boldsymbol{O}_0$ and $\boldsymbol{I}_0$ are the evolution operator and the solution to the zero-order equation, respectively. The integral in the right-hand side is rather involved, but it can be easily performed under suitable assumptions. Since $\delta\boldsymbol{I}(\tau_1)$ is in general a small correction to $\boldsymbol{I}_0(\tau_1)$, even a crude approximation is justified. An adequate approximation is to consider the 'effective source vector' $[S_{\mathrm{L}}(\tau_{\mathrm{r}})\boldsymbol{U} - \boldsymbol{I}_0(\tau_{\mathrm{r}})]$ as a linear function of τ_{r} in each interval $(\tau_k\,,\tau_{k+1})$. This allows the integral to be evaluated by standard numerical techniques.

It should be mentioned that a numerical method quite similar to the PEO method has been presented by Van Ballegooijen (1987) to solve the transfer equation in the form of Eq. (8.65).

9.16. Response Functions

The concept of response function is particularly important in the problem of line formation in a magnetic field since it clarifies the role played by the different phys-

ical parameters in determining the characteristics of the Stokes parameters profiles emerging from a magnetized stellar atmosphere. The concept was introduced by Beckers and Milkey (1975) – see also Mein, 1971 – for non-magnetic lines, and was later generalized to magnetic lines by Landi Degl'Innocenti and Landi Degl'Innocenti (1977). Although response functions may in principle be defined also for non-LTE lines, the following discussion will be restricted to the simpler case of LTE.

Let us consider the transfer equation in the form (9.161) or (9.163). Because of the LTE assumption, the emission vector defined in Eqs. (9.164) reduces to

$$\boldsymbol{b}(\tau_{\rm r}) = \boldsymbol{A}(\tau_{\rm r})\, B_{\rm P}(\tau_{\rm r})\, \boldsymbol{U} \ ,$$

with $B_{\rm P}(\tau_{\rm r})$ the Planck function, and the transfer equation becomes

$$\frac{\mathrm{d}}{\mathrm{d}\tau_{\rm r}}\, \boldsymbol{I}(\tau_{\rm r}) \ = \ \boldsymbol{A}(\tau_{\rm r}) \left[\, \boldsymbol{I}(\tau_{\rm r}) - B_{\rm P}(\tau_{\rm r})\, \boldsymbol{U} \, \right] \ , \tag{9.197}$$

where $\boldsymbol{A}(\tau_{\rm r})$ is given by Eqs. (9.164). For a semi-infinite atmosphere, the formal solution to this equation is (cf. Eq. (9.165))

$$\boldsymbol{I}(\tau_{\rm r}) = \int_{\tau_{\rm r}}^{\infty} \boldsymbol{O}(\tau_{\rm r}\,, \tau_{\rm r}')\, \boldsymbol{A}(\tau_{\rm r}')\, B_{\rm P}(\tau_{\rm r}')\, \boldsymbol{U}\ \mathrm{d}\tau_{\rm r}' \ , \tag{9.198}$$

with the evolution operator $\boldsymbol{O}(\tau_{\rm r}\,, \tau_{\rm r}')$ given by Eq. (9.167).

We now observe that the quantities $\boldsymbol{A}(\tau_{\rm r})$ and $B_{\rm P}(\tau_{\rm r})$ depend on the local[1] value of a set of physical parameters $\{\zeta_i\}$, where $i = 1, 2, \ldots, p$. These parameters might in principle be divided in two groups, the independent and the dependent parameters. If the chemical composition of the atmosphere is fixed, the independent parameters are only the temperature, the gas pressure, the magnetic field vector and the line-of-sight component of the velocity field, the last resulting both from the microturbulent velocity and from the bulk velocity of the ambient medium. Otherwise, the element abundances play also the role of independent parameters. The dependent parameters are quantities (like the Doppler width, the damping constant, the continuum and line absorption coefficients) which depend on the parameters of the first group. In other words, they can be evaluated (by a simple formula or a series of calculations) once the independent parameters are known. In the following we just assume that the set $\{\zeta_i\}$ contains a number p of physical parameters that are *independent of each other*. A set composed of the magnetic field intensity and the Doppler width is a particular example of a set with $p = 2$.

Given a stellar atmosphere where the p physical parameters ζ_i vary with optical depth, we consider a 'perturbed' atmosphere characterized by the parameters

$$\zeta_i'(\tau_{\rm r}) = \zeta_i(\tau_{\rm r}) \ + \ \delta\zeta_i(\tau_{\rm r}) \qquad (i = 1, 2, \ldots, p) \ .$$

[1] In the non-LTE case, the source functions $S_{\rm c}(\tau_{\rm r})$ and $S_{\rm L}(\tau_{\rm r})$ have a non-local dependence on the physical parameters. This makes difficult the generalization of the concept of response function to that case.

If the 'increments' $\delta\zeta_i(\tau_{\rm r})$ are small, we can express the propagation matrix and the Planck function by a first-order expansion

$$\boldsymbol{A}'(\tau_{\rm r}) = \boldsymbol{A}(\tau_{\rm r}) + \delta\boldsymbol{A}(\tau_{\rm r}) = \boldsymbol{A}(\tau_{\rm r}) + \sum_{i=1}^{p} \left(\frac{\partial \boldsymbol{A}}{\partial \zeta_i}\right)_{\tau_{\rm r}} \delta\zeta_i(\tau_{\rm r})$$

$$B'_{\rm P}(\tau_{\rm r}) = B_{\rm P}(\tau_{\rm r}) + \delta B_{\rm P}(\tau_{\rm r}) = B_{\rm P}(\tau_{\rm r}) + \sum_{i=1}^{p} \left(\frac{\partial B_{\rm P}}{\partial \zeta_i}\right)_{\tau_{\rm r}} \delta\zeta_i(\tau_{\rm r}) \,. \qquad (9.199)$$

Some remarks are necessary here. A variation of the physical parameters entails, in general, a variation of the continuum absorption coefficient. Therefore, the optical-depth scales in the unperturbed and perturbed atmosphere are different. In the following, the optical-depth scale of the unperturbed atmosphere will always be used. This implies that the partial derivatives in Eqs. (9.199) should be performed by keeping constant the value of the absorption coefficient $k_{\rm c}(\nu_{\rm r})$ which enters the definitions of $\kappa_{\rm r}$ and $\kappa_{\rm R}$ (see Eqs. (9.162)). The second remark concerns the expression of $\delta B_{\rm P}$ in Eqs. (9.199). Since $B_{\rm P}$ depends only on temperature, $\delta B_{\rm P}$ is identically zero if the temperature is not contained in the set $\{\zeta_i\}$.

Substituting Eqs. (9.199) into Eq. (9.197), writing the Stokes parameters for the perturbed atmosphere in the form

$$\boldsymbol{I}'(\tau_{\rm r}) = \boldsymbol{I}(\tau_{\rm r}) + \delta\boldsymbol{I}(\tau_{\rm r}) \,, \qquad (9.200)$$

and considering only the first-order terms in the resulting equation, we get for $\delta\boldsymbol{I}$ the transfer equation

$$\frac{\mathrm{d}}{\mathrm{d}\tau_{\rm r}} \delta\boldsymbol{I}(\tau_{\rm r}) = \boldsymbol{A}(\tau_{\rm r})\, \delta\boldsymbol{I}(\tau_{\rm r}) - \left\{ \boldsymbol{A}(\tau_{\rm r}) \sum_{i=1}^{p} \left(\frac{\partial B_{\rm P}}{\partial \zeta_i}\right)_{\tau_{\rm r}} \delta\zeta_i(\tau_{\rm r})\, \boldsymbol{U} - \sum_{i=1}^{p} \left(\frac{\partial \boldsymbol{A}}{\partial \zeta_i}\right)_{\tau_{\rm r}} \delta\zeta_i(\tau_{\rm r}) \left[\, \boldsymbol{I}(\tau_{\rm r}) - B_{\rm P}(\tau_{\rm r})\, \boldsymbol{U} \,\right] \right\} .$$

The correction to the Stokes parameters emerging from the perturbed atmosphere can thus be written in the form

$$\delta\boldsymbol{I}(0) = \sum_{i=1}^{p} \int_0^{\infty} \boldsymbol{O}(0,\tau_{\rm r}) \left\{ \boldsymbol{A}(\tau_{\rm r}) \left(\frac{\partial B_{\rm P}}{\partial \zeta_i}\right)_{\tau_{\rm r}} \boldsymbol{U} - \left(\frac{\partial \boldsymbol{A}}{\partial \zeta_i}\right)_{\tau_{\rm r}} \left[\, \boldsymbol{I}(\tau_{\rm r}) - B_{\rm P}(\tau_{\rm r})\, \boldsymbol{U} \,\right] \right\} \delta\zeta_i(\tau_{\rm r})\, \mathrm{d}\tau_{\rm r} \,, \qquad (9.201)$$

where $\boldsymbol{I}(\tau_{\rm r})$ is given by Eq. (9.198).

The concept of response function is suggested quite naturally by Eq. (9.201): the response function for the physical parameter ζ_i, $\boldsymbol{R}_{\rm F}(\zeta_i\,;\tau_{\rm r})$, is defined to be the i-th term in the integrand of Eq. (9.201),

$$\boldsymbol{R}_{\rm F}(\zeta_i\,;\,\tau_{\rm r}) = \boldsymbol{O}(0,\tau_{\rm r}) \left\{ \boldsymbol{A}(\tau_{\rm r}) \left(\frac{\partial B_{\rm P}}{\partial \zeta_i}\right)_{\tau_{\rm r}} \boldsymbol{U} - \left(\frac{\partial \boldsymbol{A}}{\partial \zeta_i}\right)_{\tau_{\rm r}} \left[\, \boldsymbol{I}(\tau_{\rm r}) - B_{\rm P}(\tau_{\rm r})\, \boldsymbol{U} \,\right] \right\} . \qquad (9.202)$$

Obviously, it depends on wavelength and on the model atmosphere. Using this definition, Eq. (9.201) reads

$$\delta \boldsymbol{I}(0) = \sum_{i=1}^{p} \int_0^\infty \boldsymbol{R}_{\rm F}(\zeta_i\,;\,\tau_{\rm r})\;\delta\zeta_i(\tau_{\rm r})\;{\rm d}\tau_{\rm r}\;. \tag{9.203}$$

The physical meaning of response functions follows directly from Eq. (9.203). If $\Delta\tau_{\rm r}$ is a small optical-depth interval centered at $\tau_{\rm r}$, and $\delta\zeta_i$ is a small variation of the physical parameter ζ_i in that interval, one gets

$$\boldsymbol{R}_{\rm F}(\zeta_i\,;\,\tau_{\rm r}) = \frac{\delta \boldsymbol{I}(0)}{\delta\zeta_i\;\Delta\tau_{\rm r}}\;,$$

which shows that response functions can be regarded as a sort of partial derivatives of the emerging Stokes parameters with respect to the physical parameters (Ruiz Cobo and del Toro Iniesta, 1994). Equation (9.203) also gives an 'operational definition' of response functions: in principle, they could be measured by changing the value of a physical parameter in a small region of a stellar atmosphere and by observing the corresponding variation of the emerging Stokes parameters. Although this is obviously a *Gedankenexperiment*, it shows that response functions are correctly defined from the physical point of view.

Response functions satisfy the important integral property

$$\int_0^\infty \boldsymbol{R}_{\rm F}(\zeta_i\,;\,\tau_{\rm r})\;{\rm d}\tau_{\rm r} \;=\; \frac{\partial \boldsymbol{I}(0)}{\partial\zeta_i}\;,$$

which follows directly from Eq. (9.203) by considering an increment $\delta\zeta_i$ independent of optical depth.

Equation (9.202) shows that response functions can be expressed in analytical form whenever the same property holds for the evolution operator. As an example we can consider the case of the Milne-Eddington atmosphere that has been developed in Sect. 9.8.

First of all, it is convenient to rewrite Eq. (9.202) in terms of the optical depth $\tau_{\rm c}$ rather than $\tau_{\rm r}$, so that the expressions derived in Sect. 9.8 can be applied. Starting at Eq. (9.203) we obtain, with the help of Eqs. (9.33), (9.162), (9.164) and (9.31)[1]

$$\boldsymbol{R}_{\rm F}(\zeta_i\,;\,\tau_{\rm c}) = \boldsymbol{O}(0,\tau_{\rm c})\left\{\boldsymbol{C}(\tau_{\rm c})\left(\frac{\partial B_{\rm P}}{\partial\zeta_i}\right)_{\tau_{\rm c}}\boldsymbol{U} \;-\; \left(\frac{\partial \boldsymbol{C}}{\partial\zeta_i}\right)_{\tau_{\rm c}}\left[\,\boldsymbol{I}(\tau_{\rm c}) - B_{\rm P}(\tau_{\rm c})\,\boldsymbol{U}\,\right]\right\},$$

where $\boldsymbol{C}(\tau_{\rm c})$ is defined in Eq. (9.91). In the Milne-Eddington atmosphere $\boldsymbol{C}$ is constant, the evolution operator is given by Eqs. (9.103), $B_{\rm P}$ by Eq. (9.105) and

[1] Use of $\tau_{\rm c}$ instead of $\tau_{\rm r}$ as independent variable makes more complicated the formal treatment of response functions for physical variables affecting the continuum absorption coefficient, since in that case the ratio $\kappa_{\rm r}$ defined in Eqs. (9.162) is unity by definition. This is the reason why our general discussion of response functions is based on $\tau_{\rm r}$.

$\boldsymbol{I}(t_{\rm c}\,,\mu)$, the Stokes parameters of the radiation flowing along the μ-direction at optical depth $t_{\rm c} = \mu\,\tau_{\rm c}$, by Eqs. (9.108). The response function for any physical parameter ζ_i except temperature[1] is therefore

$$\boldsymbol{R}_{\rm F}(\zeta_i\,;\,t_{\rm c}\,,\mu) = -B_0\,\beta\mu\;\mathrm{e}^{-\frac{t_{\rm c}}{\mu}\boldsymbol{C}}\;\frac{\partial \boldsymbol{C}}{\partial \zeta_i}\;\boldsymbol{C}^{-1}\,\boldsymbol{U}\;,$$

and the correction to the emerging Stokes parameters due to the 'perturbations' $\delta\zeta_i(t_{\rm c})$ is

$$\delta\boldsymbol{I}(0,\mu) = \sum_{i=1}^{p}\;\int_0^{\infty}\boldsymbol{R}_{\rm F}(\zeta_i\,;\,t_{\rm c}\,,\mu)\;\delta\zeta_i(t_{\rm c})\;\frac{\mathrm{d}t_{\rm c}}{\mu}\;.$$

Explicit expressions for $\delta\boldsymbol{I}(0,\mu)$ can be derived for different forms of the functions $\delta\zeta_i(t_{\rm c})$. Assuming, for instance, a linear behavior of the perturbation (Landolfi, 1987)

$$\delta\zeta_i(t_{\rm c}) = a_i + b_i\,t_{\rm c}\;,$$

we obtain with the help of Eqs. (9.106) and (9.107)

$$\delta\boldsymbol{I}(0,\mu) = -B_0\,\beta\mu\sum_{i=1}^{p}\left[a_i\,\boldsymbol{C}^{-1}\,\frac{\partial\boldsymbol{C}}{\partial\zeta_i}\,\boldsymbol{C}^{-1} + \mu\,b_i\left(\boldsymbol{C}^{-1}\right)^2\,\frac{\partial\boldsymbol{C}}{\partial\zeta_i}\,\boldsymbol{C}^{-1}\right]\boldsymbol{U}\;,$$

or, observing that

$$\frac{\partial\,\boldsymbol{C}^{-1}}{\partial\zeta_i} = -\,\boldsymbol{C}^{-1}\,\frac{\partial\boldsymbol{C}}{\partial\zeta_i}\,\boldsymbol{C}^{-1}\;, \tag{9.204}$$

$$\delta\boldsymbol{I}(0,\mu) = B_0\,\beta\mu\sum_{i=1}^{p}\left(a_i\,\boldsymbol{1} + \mu\,b_i\,\boldsymbol{C}^{-1}\right)\frac{\partial\,\boldsymbol{C}^{-1}}{\partial\zeta_i}\,\boldsymbol{U}\;. \tag{9.205}$$

Bearing in mind the expression of the 'unperturbed' emerging Stokes parameters (Eqs. (9.108)), we can also write

$$\delta\boldsymbol{I}(0,\mu) = \sum_{i=1}^{p}\left(a_i\,\boldsymbol{1} + \mu\,b_i\,\boldsymbol{C}^{-1}\right)\frac{\partial}{\partial\zeta_i}\,\boldsymbol{I}(0,\mu)\;.$$

Similarly, assuming an exponential behavior

$$\delta\zeta_i(t_{\rm c}) = A_i\;\mathrm{e}^{-\alpha_i\,t_{\rm c}}\;,$$

we get

$$\delta\boldsymbol{I}(0,\mu) = -B_0\,\beta\mu\sum_{i=1}^{p}A_i\left(\boldsymbol{C} + \mu\,\alpha_i\,\boldsymbol{1}\right)^{-1}\,\frac{\partial\boldsymbol{C}}{\partial\zeta_i}\,\boldsymbol{C}^{-1}\,\boldsymbol{U}\;,$$

[1] In a Milne-Eddington atmosphere the partial derivative $\partial B_{\rm P}\,/\,\partial T$ is meaningless because of the parameterization adopted for $B_{\rm P}$.

or, in a different form

$$\delta \boldsymbol{I}(0,\mu) = B_0\,\beta\mu \sum_{i=1}^{p} A_i \left[\boldsymbol{1} - \mu\,\alpha_i \left(\boldsymbol{C} + \mu\,\alpha_i\,\boldsymbol{1} \right)^{-1} \right] \frac{\partial\,\boldsymbol{C}^{-1}}{\partial \zeta_i}\,\boldsymbol{U}$$

$$= \sum_{i=1}^{p} A_i \left[\boldsymbol{1} - \mu\,\alpha_i \left(\boldsymbol{C} + \mu\,\alpha_i\,\boldsymbol{1} \right)^{-1} \right] \frac{\partial}{\partial \zeta_i}\,\boldsymbol{I}(0,\mu)\ .$$

If the unperturbed atmosphere is static – or, more generally, in the 'constant velocity case' defined in Sect. 9.5 – the response functions for a given physical parameter evaluated at two wavelengths symmetrical about line center are related by interesting symmetry properties, which follow directly from Eqs. (9.202). Defining $\Delta\lambda$ as in Eq. (9.45), the propagation matrix $\boldsymbol{A}$ and the Stokes vector $\boldsymbol{I}$ satisfy, at any optical depth, the relations (cf. Eqs. (9.51) and (9.54))

$$\boldsymbol{A}(\tau_{\rm r}\,;\,-\Delta\lambda) \;=\; \boldsymbol{X}\;\boldsymbol{A}(\tau_{\rm r}\,;\,\Delta\lambda)\;\boldsymbol{X}^{-1}$$

$$\boldsymbol{I}(\tau_{\rm r}\,;\,-\Delta\lambda) \;=\; \boldsymbol{X}\;\boldsymbol{I}(\tau_{\rm r}\,;\,\Delta\lambda)\ , \tag{9.206}$$

where the matrix $\boldsymbol{X}$ is defined in Eq. (9.52). On the other hand, the series expansion of the evolution operator given in Eq. (9.167) shows that

$$\boldsymbol{O}(0,\tau_{\rm r}\,;\,-\Delta\lambda) \;=\; \boldsymbol{X}\;\boldsymbol{O}(0,\tau_{\rm r}\,;\,\Delta\lambda)\;\boldsymbol{X}^{-1}\ . \tag{9.207}$$

The relation between the matrices $(\partial\boldsymbol{A}\,/\,\partial\zeta_i)_{\tau_{\rm r}}$ evaluated at $\Delta\lambda$ and $-\Delta\lambda$ depends on the physical parameter ζ_i. It is necessary to divide the physical parameters in two groups, (a) and (b). Group (a) includes temperature, pressure, magnetic field (B, θ, χ), Doppler width and damping constant: in other words, all the parameters except the line-of-sight component $w_{\rm A}$ of the bulk velocity. Group (b) contains $w_{\rm A}$ alone. It can be proved from the explicit expression of $\boldsymbol{A}$ (see Eqs. (9.164), (9.162), (9.50), (9.32), (9.27), (9.29) and (9.26)) that

$$\left[\frac{\partial}{\partial\zeta_{\rm a}}\,\boldsymbol{A}(-\Delta\lambda)\right]_{\tau_{\rm r}} \;=\; \boldsymbol{X}\;\left[\frac{\partial}{\partial\zeta_{\rm a}}\,\boldsymbol{A}(\Delta\lambda)\right]_{\tau_{\rm r}}\boldsymbol{X}^{-1}$$

$$\left[\frac{\partial}{\partial\zeta_{\rm b}}\,\boldsymbol{A}(-\Delta\lambda)\right]_{\tau_{\rm r}} = -\,\boldsymbol{X}\;\left[\frac{\partial}{\partial\zeta_{\rm b}}\,\boldsymbol{A}(\Delta\lambda)\right]_{\tau_{\rm r}}\boldsymbol{X}^{-1}\ , \tag{9.208}$$

where $\zeta_{\rm a}$ is any physical parameter of group (a), and $\zeta_{\rm b} = w_{\rm A}$. Using Eqs. (9.206)-(9.208), and observing that

$$\left(\frac{\partial B_{\rm P}}{\partial\zeta_{\rm b}}\right)_{\tau_{\rm r}} \;=\; 0\ , \qquad\qquad \boldsymbol{X}^{-1}\,\boldsymbol{U} \;=\; \boldsymbol{U}\ ,$$

one easily obtains from Eq. (9.202)

$$\boldsymbol{R}_{\rm F}(\zeta_{\rm a}\,;\,\tau_{\rm r}\,,\,-\Delta\lambda) \;=\; \boldsymbol{X}\;\boldsymbol{R}_{\rm F}(\zeta_{\rm a}\,;\,\tau_{\rm r}\,,\,\Delta\lambda)$$

$$\boldsymbol{R}_{\rm F}(\zeta_{\rm b}\,;\,\tau_{\rm r}\,,\,-\Delta\lambda) \;=\; -\,\boldsymbol{X}\;\boldsymbol{R}_{\rm F}(\zeta_{\rm b}\,;\,\tau_{\rm r}\,,\,\Delta\lambda)\ . \tag{9.209}$$

According to Eq. (9.203), the corrections $\delta\boldsymbol{I}(0,\Delta\lambda)$ and $\delta\boldsymbol{I}(0,-\Delta\lambda)$ satisfy symmetry relations of the same form as Eqs. (9.209). It follows that only a variation of the physical parameter $w_{\rm A}$ with optical depth can alter the symmetry characteristics of the Stokes parameters expressed by Eqs. (9.54).[1] The (first-order) corrections produced by such variation have the opposite symmetry of the corresponding Stokes parameters,

$$\begin{aligned}
\delta I(0,-\Delta\lambda) &= -\,\delta I(0,\Delta\lambda)\\
\delta Q(0,-\Delta\lambda) &= -\,\delta Q(0,\Delta\lambda)\\
\delta U(0,-\Delta\lambda) &= -\,\delta U(0,\Delta\lambda)\\
\delta V(0,-\Delta\lambda) &= \delta V(0,\Delta\lambda)\ .
\end{aligned}$$

Finally, we want to remark that the concept of response function can be easily generalized to any observable quantity obtained by a mathematical transformation on the emerging Stokes parameters $\boldsymbol{I}(0,\lambda)$. As an example, let us consider the *line-integrated Stokes parameters* defined by[2]

$$\boldsymbol{\mathcal{I}} = (\mathcal{I},\,\mathcal{Q}\,,\mathcal{U},\,\mathcal{V})^{\dagger} = \int_{\rm line} \left[\,\boldsymbol{I}(0,\lambda) \,-\, I_{\rm c}(0)\,\boldsymbol{U}\,\right] {\rm d}\lambda\,, \tag{9.210}$$

where $I_{\rm c}(0)$ is the emerging intensity in the continuum adjacent to the line ($I_{\rm c}(0)\,\boldsymbol{U} = \boldsymbol{I}(0,\lambda_{\rm c})$, with $\lambda_{\rm c}$ a wavelength sufficiently far in the line wing), and the integral is over the line profile. Following our perturbative scheme, we have from Eq. (9.203)

$$\delta\boldsymbol{\mathcal{I}} = \int_{\rm line} \left\{ \sum_{i=1}^{p} \int_0^{\infty} \left[\,\boldsymbol{R}_{\rm F}(\zeta_i\,;\,\tau_{\rm r}\,,\lambda) \,-\, \boldsymbol{R}_{\rm F}(\zeta_i\,;\,\tau_{\rm r}\,,\lambda_{\rm c})\,\right] \delta\zeta_i(\tau_{\rm r})\ {\rm d}\tau_{\rm r} \right\} {\rm d}\lambda\,.$$

Inverting the order of the integrals, this equation can be cast into the form

$$\delta\boldsymbol{\mathcal{I}} = \sum_{i=1}^{p} \int_0^{\infty} \boldsymbol{\mathcal{R}}_{\rm F}(\zeta_i\,;\,\tau_{\rm r})\ \delta\zeta_i(\tau_{\rm r})\ {\rm d}\tau_{\rm r}\ \ ,$$

where the *line-integrated response function* is defined by

$$\boldsymbol{\mathcal{R}}_{\rm F}(\zeta_i\,;\,\tau_{\rm r}) = \int_{\rm line} \left[\,\boldsymbol{R}_{\rm F}(\zeta_i\,;\,\tau_{\rm r}\,,\lambda) \,-\, \boldsymbol{R}_{\rm F}(\zeta_i\,;\,\tau_{\rm r}\,,\lambda_{\rm c})\,\right] {\rm d}\lambda\,.$$

Further examples of 'generalized' response functions can be found in Landi Degl'Innocenti and Landolfi (1983), Grossmann-Doerth et al. (1988a), Ruiz Cobo and

[1] These characteristics can also be altered by fine or hyperfine structure effects (see Sect. 9.23), or by atomic polarization effects (see Sect. 10.5).

[2] Note that $\mathcal{I}$ is proportional to the line equivalent width W. In fact $\mathcal{I} = -I_{\rm c}(0)\ W$.

del Toro Iniesta (1994). In this last paper the concept is precisely stated from the mathematical point of view.

9.17. Contribution Functions

Contribution functions are a rather controversial subject in the theory of radiative transfer, both in the 'classical' formulation that neglects polarization phenomena and, even more, in the case of polarized radiation. The underlying idea is to find an expression, defined in terms of opacities and source functions, whose dependence on optical depth should represent the contribution of the different atmospheric layers to the emerging intensity, or to the line depression, or to some other observable spectral feature.

Although this idea seems rather simple and intuitive, difficulties usually arise when trying to express it into a quantitative form. This is demonstrated by the large number of papers dealing with the subject and by the even larger number of contribution functions proposed in the literature (see e.g. Caccin et al., 1977; Magain, 1986; Achmad et al., 1991, and references therein). Moreover, most of the work has been devoted to contribution functions for the scalar case (no magnetic field), where physical intuition can be more helpful in checking the soundness of the definitions: contribution functions for polarized radiation are usually obtained by direct generalization of the corresponding scalar expressions. Without entering into the details of the controversy, we limit ourselves to give a few examples of contribution functions for the Stokes parameters.

Equation (9.166), rewritten in the form

$$\boldsymbol{I}(0) = \int_0^\infty \boldsymbol{C}_{\rm F}(\tau_{\rm r})\, {\rm d}\tau_{\rm r} \;, \tag{9.211}$$

provides the possibility of defining a contribution function for the Stokes parameters in the form (Van Ballegooijen, 1985)

$$\boldsymbol{C}_{\rm F}(\tau_{\rm r}) = \boldsymbol{O}(0,\tau_{\rm r}) \left[\kappa_{\rm r}\, S_{\rm c}\, \boldsymbol{1} \,+\, \kappa_{\rm R}\, S_{\rm L}\, \boldsymbol{H} \right] \boldsymbol{U} \;.$$

This contribution function has a very intuitive physical meaning, but has the drawback of mixing the contributions of the continuum and of the spectral line. To overcome this difficulty one can define the contribution function for the *line depression* $[I_{\rm c}(0)\,\boldsymbol{U} - \boldsymbol{I}(0)]$, or the contribution function for the *normalized line depression*[1] defined by

$$\boldsymbol{D}(0) = \frac{I_{\rm c}(0)\,\boldsymbol{U} \,-\, \boldsymbol{I}(0)}{I_{\rm c}(0)} = \boldsymbol{U} \,-\, \frac{\boldsymbol{I}(0)}{I_{\rm c}(0)} \;. \tag{9.212}$$

[1] The term 'line depression' is applied here to the four Stokes parameters, although, more properly, it should only be applied to the intensity.

Let us consider the second possibility. According to Magain (1986), a correct definition of the contribution function requires the following procedure: one should write a transfer equation for the quantity $\boldsymbol{D}(\tau_{\rm r})$, find a formal solution to the equation, and identify the integrand with the contribution function itself. From Eq. (9.163) and from the transfer equation for the continuum intensity

$$\frac{{\rm d}I_{\rm c}}{{\rm d}\tau_{\rm r}} = \kappa_{\rm r} \left(I_{\rm c} - S_{\rm c} \right) \tag{9.213}$$

one obtains, with the use of Eqs. (9.164), the transfer equation

$$\frac{{\rm d}\boldsymbol{D}}{{\rm d}\tau_{\rm r}} = \left(\kappa_{\rm r} \frac{S_{\rm c}}{I_{\rm c}} \, \boldsymbol{1} + \kappa_{\rm R} \boldsymbol{H} \right) \boldsymbol{D} - \kappa_{\rm R} \left(1 - \frac{S_{\rm L}}{I_{\rm c}} \right) \boldsymbol{H} \boldsymbol{U} \, .$$

This is formally similar to any of the transfer equations considered previously, with the only difference that, in the present case, the propagation matrix and the emission vector depend also on the local value of the continuum intensity. Defining

$$\boldsymbol{A}_{\rm D} = \kappa_{\rm r} \frac{S_{\rm c}}{I_{\rm c}} \, \boldsymbol{1} + \kappa_{\rm R} \boldsymbol{H} = \boldsymbol{A} - \kappa_{\rm r} \left(1 - \frac{S_{\rm c}}{I_{\rm c}} \right) \boldsymbol{1} \, ,$$

with $\boldsymbol{A}$ given by Eqs. (9.164), the value of $\boldsymbol{A}_{\rm D}$ at any optical depth can be evaluated using the solution to Eq. (9.213). We can then calculate the evolution operator $\boldsymbol{O}_{\rm D}$ corresponding to the propagation matrix $\boldsymbol{A}_{\rm D}$, and finally write

$$\boldsymbol{D}(0) = \int_0^\infty \boldsymbol{\mathcal{C}}_{\rm F}(\tau_{\rm r}) \, {\rm d}\tau_{\rm r} \, , \tag{9.214}$$

where $\boldsymbol{\mathcal{C}}_{\rm F}(\tau_{\rm r})$, the *contribution function to the normalized line depression*, is defined by (Grossmann-Doerth et al., 1988a; Rees et al., 1989)

$$\boldsymbol{\mathcal{C}}_{\rm F}(\tau_{\rm r}) = \boldsymbol{O}_{\rm D}(0, \tau_{\rm r}) \, \kappa_{\rm R} \left(1 - \frac{S_{\rm L}}{I_{\rm c}} \right) \boldsymbol{H} \boldsymbol{U} \, .$$

The main drawback of contribution functions is indeed implicit in their definition. As apparent from Eqs. (9.211) or (9.214), these functions are invariant under a kind of 'gauge transformation' of the form

$$\boldsymbol{\mathcal{C}}_{\rm F}(\tau_{\rm r}) \rightarrow \boldsymbol{\mathcal{C}}_{\rm F}(\tau_{\rm r}) + \boldsymbol{g}(\tau_{\rm r}) \, ,$$

where $\boldsymbol{g}(\tau_{\rm r})$ is an arbitrary function such that

$$\int_0^\infty \boldsymbol{g}(\tau_{\rm r}) \, {\rm d}\tau_{\rm r} = 0 \, .$$

The choice of the gauge is more or less arbitrary, although in some cases it can be suggested by physical considerations. We believe that no real progress can be achieved in this subject until a clear, operational definition of contribution function is given.

A possible way out could be to replace the concept of contribution function by an appropriate response function, like the response function to the logarithm of the line oscillator strength, defined by (see Eq. (9.203))[1]

$$\delta \boldsymbol{I}(0) = \int_0^\infty \boldsymbol{R}_{\rm F}(\,\ln f\,;\,\tau_{\rm r})\;\delta \ln f(\tau_{\rm r})\,{\rm d}\tau_{\rm r}\;.$$

According to Eq. (9.212), the correction to the normalized line depression produced by the 'perturbation' $\delta \ln f(\tau_{\rm r})$ is given by

$$\delta {\rm D}(0) = -\,\frac{\delta \boldsymbol{I}(0)}{I_{\rm c}(0)}\;,$$

because the continuum intensity is unaffected by a variation of the line opacity. If we introduce a (generalized) response function $\boldsymbol{\mathcal{R}}_{\rm F}(\,\ln f\,;\,\tau_{\rm r})$ such that

$$\delta \boldsymbol{D}(0) = \int_0^\infty \boldsymbol{\mathcal{R}}_{\rm F}(\,\ln f\,;\,\tau_{\rm r})\;\delta \ln f(\tau_{\rm r})\,{\rm d}\tau_{\rm r}\;,$$

we have from the above equations

$$\boldsymbol{\mathcal{R}}_{\rm F}(\,\ln f\,;\,\tau_{\rm r}) = -\,\frac{\boldsymbol{R}_{\rm F}(\,\ln f\,;\,\tau_{\rm r})}{I_{\rm c}(0)}\;. \tag{9.215}$$

Since

$$\left(\frac{\partial B_{\rm P}}{\partial(\ln f)}\right)_{\tau_{\rm r}} = 0$$

and, using Eqs. (9.164), (9.162) and (9.19)

$$\left(\frac{\partial \boldsymbol{A}}{\partial(\ln f)}\right)_{\tau_{\rm r}} = \kappa_{\rm R}(\tau_{\rm r})\;\boldsymbol{H}(\tau_{\rm r})\;,$$

we obtain from Eqs. (9.202) and (9.215) the remarkable expression

$$\boldsymbol{\mathcal{R}}_{\rm F}(\,\ln f\,;\,\tau_{\rm r}) \;=\; \frac{1}{I_{\rm c}(0)}\left\{\kappa_{\rm R}(\tau_{\rm r})\,\boldsymbol{O}(0,\tau_{\rm r})\,\boldsymbol{H}(\tau_{\rm r})\left[\,\boldsymbol{I}(\tau_{\rm r}) \;-\; B_{\rm P}(\tau_{\rm r})\,\boldsymbol{U}\,\right]\right\}.$$

[1] We restrict ourselves to the LTE case since our definition of response function does not apply to non-LTE lines – see the discussion in the previous section.

Finally, it should be noticed that all the contribution functions defined in this section, as well as the response functions defined in the former section, are referred to the optical-depth scale $\tau_{\rm r}$. When a different depth indicator x is used, the new contribution function is obtained through the obvious transformation

$$\boldsymbol{C}_{\rm F}(x) = \boldsymbol{C}_{\rm F}(\tau_{\rm r}) \, \frac{{\rm d}\tau_{\rm r}}{{\rm d}x} \, ,$$

with a similar relation for $\boldsymbol{R}_{\rm F}(x)$. Assuming for instance $x = {\rm Log}\, \tau_{\rm r}$, one has

$$\boldsymbol{C}_{\rm F}(x) = \ln(10) \; \tau_{\rm r} \, \boldsymbol{C}_{\rm F}(\tau_{\rm r}) \, .$$

The scale ${\rm Log}\, \tau_{\rm r}$ is generally convenient for plotting contribution and response functions against optical depth.

9.18. Blends

Blends are a common feature of stellar spectra. They simply result from the fact that, in a given section of the spectrum, two or more lines, generally belonging to different elements, may overlap to give rise to a complicated spectral feature. The most common case is the presence of a weak line in the blue or in the red wing of a stronger line.

When the individual lines are *independent*, which means that they belong either to different elements or to different multiplets of the same element, their cumulative effect can be simply described by adding in the transfer equation the contributions of each line. When the blending lines are the fine-structure or hyperfine-structure components of a single 'parent' line, the situation is more complex and requires a different approach (see Sect. 9.23).

For an ensemble of N independent lines, each characterized by its own $\kappa_{\rm L}^{(i)}$ (the ratio between line and continuum absorption coefficient defined in Eq. (9.31)) and $S_{\rm L}^{(i)}$ (the line source function defined in Eq. (9.14)), Eq. (9.35) generalizes into the following

$$\frac{\rm d}{{\rm d}\tau_{\rm c}} \begin{pmatrix} I \\ Q \\ U \\ V \end{pmatrix} = \begin{pmatrix} 1 & 0 & 0 & 0 \\ 0 & 1 & 0 & 0 \\ 0 & 0 & 1 & 0 \\ 0 & 0 & 0 & 1 \end{pmatrix} \begin{pmatrix} I - S_{\rm c} \\ Q \\ U \\ V \end{pmatrix} + \sum_{i=1}^{N} \kappa_{\rm L}^{(i)} \begin{pmatrix} h_I^{(i)} & h_Q^{(i)} & h_U^{(i)} & h_V^{(i)} \\ h_Q^{(i)} & h_I^{(i)} & r_V^{(i)} & -r_U^{(i)} \\ h_U^{(i)} & -r_V^{(i)} & h_I^{(i)} & r_Q^{(i)} \\ h_V^{(i)} & r_U^{(i)} & -r_Q^{(i)} & h_I^{(i)} \end{pmatrix} \begin{pmatrix} I - S_{\rm L}^{(i)} \\ Q \\ U \\ V \end{pmatrix} , \qquad (9.216)$$

or, in matrix form

$$\frac{\mathrm{d}\boldsymbol{I}}{\mathrm{d}\tau_{\mathrm{c}}} = \left[\boldsymbol{1} + \sum_{i=1}^{N} \kappa_{\mathrm{L}}^{(i)}\, \boldsymbol{H}^{(i)} \right] \boldsymbol{I} - \left[S_{\mathrm{c}}\, \boldsymbol{1} + \sum_{i=1}^{N} \kappa_{\mathrm{L}}^{(i)}\, S_{\mathrm{L}}^{(i)}\, \boldsymbol{H}^{(i)} \right] \boldsymbol{U} \,, \qquad (9.217)$$

where the elements $h_I^{(i)}$, $h_Q^{(i)}$, $h_U^{(i)}$, $h_V^{(i)}$, $r_Q^{(i)}$, $r_U^{(i)}$, $r_V^{(i)}$ of the matrix $\boldsymbol{H}^{(i)}$ are defined as in Eqs. (9.32). Obviously each line has its own central wavelength, Zeeman pattern, Doppler width and damping constant.

Many of the results derived in this chapter for single spectral lines can be easily generalized to blends. In particular, the Stokes parameters emerging from a Milne-Eddington atmosphere are still given by Eq. (9.109), with the matrix $\boldsymbol{C}$ given by

$$\boldsymbol{C} = \boldsymbol{1} + \sum_{i=1}^{N} \kappa_{\mathrm{L}}^{(i)}\, \boldsymbol{H}^{(i)} \,.$$

Figure 9.9 shows the emerging Stokes parameters, calculated according to Eq. (9.109), for a blend of two lines. The line on the left is the normal Zeeman triplet of Fig. 9.5 (a), the other one is weaker but has a larger sensitivity to the magnetic field (normal triplet with $g = 2$). Panels (a) to (d) are obtained by reducing the wavelength separation of the lines. The Stokes parameters are normalized to B_0 and are plotted against the reduced wavelength $v = (\lambda - \bar{\lambda}_0) / \Delta\lambda_{\mathrm{D}}$, where $\bar{\lambda}_0 = (\lambda_0^{(1)} + \lambda_0^{(2)}) / 2$ and $\Delta\lambda_{\mathrm{D}}$ is the (common) Doppler width of the two lines. The figure shows quite clearly that blends break the symmetry characteristics of Stokes profiles about line center. The 'distortion' is particularly evident in the Q profile, panels (a) and (b).

In the quite common case of a weak line lying on the wing of a stronger line, the emerging Stokes parameters can be obtained by a perturbative solution of the transfer equation (9.217). If the index 1 refers to the stronger line and the index 2 to the weaker, one can first solve the equation

$$\frac{\mathrm{d}\boldsymbol{I}_0}{\mathrm{d}\tau_{\mathrm{c}}} = \left[\boldsymbol{1} + \kappa_{\mathrm{L}}^{(1)}\, \boldsymbol{H}^{(1)} \right] \boldsymbol{I}_0 - \left[S_{\mathrm{c}}\, \boldsymbol{1} + \kappa_{\mathrm{L}}^{(1)}\, S_{\mathrm{L}}^{(1)}\, \boldsymbol{H}^{(1)} \right] \boldsymbol{U}$$

to obtain the 'zero-order' Stokes vector $\boldsymbol{I}_0(\tau_{\mathrm{c}})$. The correction $\delta\boldsymbol{I}$ is then found by solving the approximate equation

$$\frac{\mathrm{d}}{\mathrm{d}\tau_{\mathrm{c}}}\, \delta\boldsymbol{I} = \left[\boldsymbol{1} + \kappa_{\mathrm{L}}^{(1)}\, \boldsymbol{H}^{(1)} \right] \delta\boldsymbol{I} - \kappa_{\mathrm{L}}^{(2)}\, \boldsymbol{H}^{(2)} \left[S_{\mathrm{L}}^{(2)}\, \boldsymbol{U} - \boldsymbol{I}_0 \right] .$$

Obviously, such perturbative solution is justified only if $\kappa_{\mathrm{L}}^{(2)}\, H_{ij}^{(2)} \ll \kappa_{\mathrm{L}}^{(1)}\, H_{ij}^{(1)}$.

9.19. The Magnetic Intensification Mechanism

Let us consider a spectral line formed in the radiation flowing along a particular direction in a given stellar atmosphere. If no magnetic field is present in the

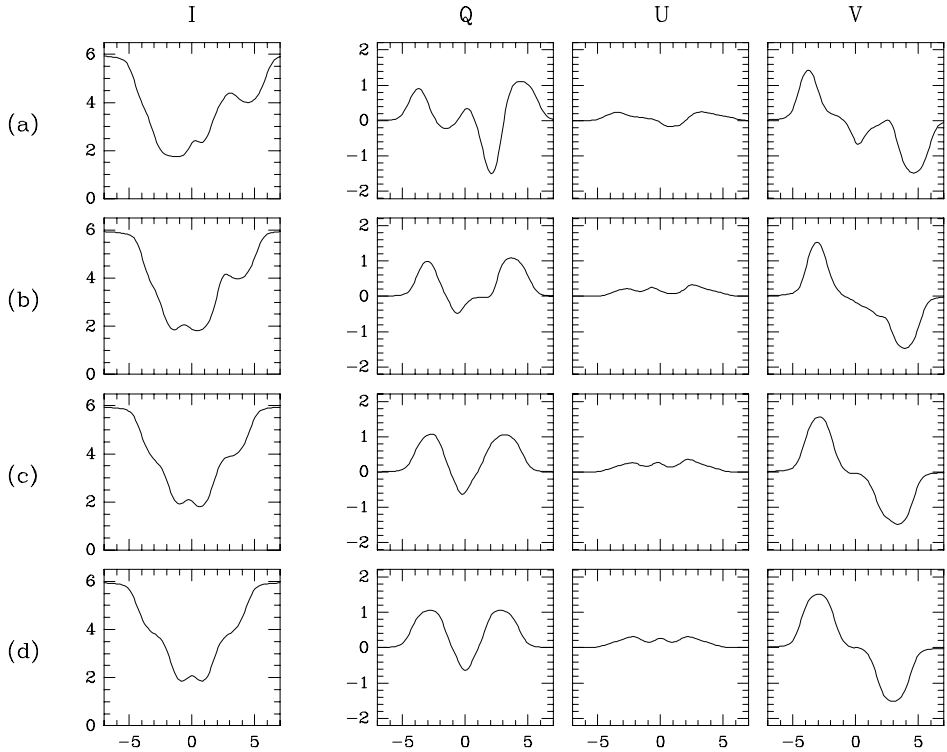

Fig.9.9. Stokes parameters profiles for a blend of two lines, computed for a Milne-Eddington atmosphere. The profiles are normalized to B_0 and are plotted against the reduced wavelength defined in the text. The lines have different strength ($\kappa_{\rm L}^{(1)} = 20$, $\kappa_{\rm L}^{(2)} = 10$) and magnetic sensitivity (normal Zeeman triplets with $g^{(1)} = 1$, $g^{(2)} = 2$). The values of the remaining parameters are those of the 'standard case' (see Fig.9.5). The four panels correspond to different wavelength separation of the lines, parameterized through $\Delta v = (\lambda_0^{(2)} - \lambda_0^{(1)})/\Delta\lambda_{\rm D}$ with $\Delta\lambda_{\rm D}$ the (common) Doppler width. Panel (a) $\Delta v = 3$; (b) $\Delta v = 1.5$; (c) $\Delta v = 0.5$; (d) $\Delta v = 0$.

atmosphere, the line will be characterized by a zero-field equivalent width W_0 defined by

$$W_0 = \frac{1}{I_{\rm c}(0)} \int_{\rm line} \left[I_{\rm c}(0) - \bar{I}(0) \right] {\rm d}\lambda \,, \tag{9.218}$$

where $I_{\rm c}(0)$ is the emerging intensity in the nearby continuum and $\bar{I}(0)$ is the zero-field, wavelength-dependent emerging intensity.

In a sort of *Gedankenexperiment*, let us now suppose a constant magnetic field is switched on throughout the whole atmosphere, all the other physical parameters remaining unchanged. The new atmosphere will be characterized by the same continuum intensity[1] but a different line intensity, and this will result in a different

[1] See footnote on p.376.

equivalent width for the line considered. Defining the new equivalent width as

$$W = \frac{1}{I_{\rm c}(0)} \int\limits_{\rm line} \left[I_{\rm c}(0) - I(0) \right] {\rm d}\lambda \, , \tag{9.219}$$

where $I(0)$ is the intensity emerging from the magnetic atmosphere, the influence of the magnetic field on the equivalent width can be characterized by the dimensionless parameter

$$\mathcal{M} = \frac{W}{W_0} \, , \tag{9.220}$$

that we will call the *magnetic intensification parameter*. In most stellar atmospheres and for most spectral lines, this parameter is larger than 1: in other words, the equivalent width in a magnetic atmosphere is usually larger than the equivalent width in the corresponding (in the sense specified above) non-magnetic atmosphere.

This fact has a very simple physical explanation, which can be understood with the help of the classical theory of the equivalent width developed, for instance, in Aller (1963) or in Mihalas (1978). Consider a line in the flat part of the curve of growth, where saturation phenomena are important. In the presence of a magnetic field the line splits into its Zeeman components and, as soon as the Zeeman splitting becomes of the order of the Doppler width ($\Delta\lambda_B \approx \Delta\lambda_{\rm D}$), it broadens – thus increasing its equivalent width – and desaturates. This desaturation process increases with increasing magnetic field strength and reaches its maximum when all the Zeeman components are well-separated ($\Delta\lambda_B \gg \Delta\lambda_{\rm D}$). In this process the line intensifies, which justifies the name of *magnetic intensification* given to this physical mechanism.

Ten Bruggencate and von Klüber (1939) were the first to suggest that such mechanism may be effective in sunspots. Further contributions to this subject were given by Babcock (1949) and Boyarchuk et al. (1961).

Even in the simple case of an atmosphere with constant magnetic field, the magnetic intensification parameter defined in Eq. (9.220) depends on many quantities. Besides the magnetic field intensity and direction, it depends on the spectral line (the structure of the Zeeman pattern being of crucial importance), on the full set of physical quantities specifying the properties of the atmosphere, and on the direction of the emerging radiation.

We can obtain an approximate expression for $\mathcal{M}$ by assuming the atmosphere to be described by the Milne-Eddington model. Although this may seem a very rough approximation, it should be remarked that the equivalent width of a spectral line has a rather weak dependence on the detailed structure of the atmosphere, and this holds especially for the magnetic intensification parameter which is the ratio of two equivalent widths. Recalling Eqs. (9.218)-(9.220) and Eq. (9.112), we obtain

$$\mathcal{M} = \frac{\displaystyle\int_{-\infty}^{\infty} \left\{ 1 - \Delta^{-1} \, (1+k_I) \left[\, (1+k_I)^2 + f_Q^2 + f_U^2 + f_V^2 \, \right] \right\} {\rm d}\lambda}{\displaystyle\int_{-\infty}^{\infty} \left\{ 1 - \, (1+\kappa_{\rm L} \, \eta)^{-1} \right\} {\rm d}\lambda} \, , \tag{9.221}$$

where Δ is defined in Table 9.5, η is the normalized absorption profile for zero magnetic field

$$\eta = \frac{1}{\sqrt{\pi}} H\left(\frac{\lambda - \lambda_0}{\Delta\lambda_{\rm D}}, a\right),$$

and the remaining quantities are given by Eqs. (9.31) and (9.39).

Despite the substantial simplification introduced by the Milne-Eddington model, $\mathcal{M}$ still remains a complicated function of the Zeeman pattern and of the four parameters[1] v_B, θ, $\kappa_{\rm L}$, a. Only a few properties of $\mathcal{M}$ can be deduced analytically from Eq. (9.221). These are the following:

a) Under the limit of weak, unsaturated lines, the magnetic intensification parameter is equal to 1,

$$\lim_{\kappa_{\rm L}\to 0} \mathcal{M} = \frac{\kappa_{\rm L}\int_{-\infty}^{\infty} h_I \, {\rm d}\lambda}{\kappa_{\rm L}\int_{-\infty}^{\infty} \eta \, {\rm d}\lambda} = 1 .$$

In other words, the line-broadening mechanism due to the magnetic field is ineffective in this particular case. The proof is easily obtained by series expansion of the integrands in Eq. (9.221) and use of the normalization (9.28).

b) Under the limit of weak magnetic field ($\Delta\lambda_B \ll \Delta\lambda_{\rm D}$), the numerator of Eq. (9.221) can be expanded in power series of $\Delta\lambda_B$ with the help of Eqs. (9.69). After some algebra we obtain, up to second-order terms

$$\mathcal{M} = 1 + v_B^2 \, \frac{\frac{1}{4}\left[G_0^{(2)}\sin^2\theta + G_1^{(2)}(1+\cos^2\theta)\right]\mathcal{I}_2(\kappa_{\rm L}, a) - \left[G_1^{(1)}\right]^2 \cos^2\theta \; \mathcal{I}_3(\kappa_{\rm L}, a)}{\mathcal{I}_1(\kappa_{\rm L}, a)} ,$$

where the integrals $\mathcal{I}_1$, $\mathcal{I}_2$, $\mathcal{I}_3$ are given by

$$\mathcal{I}_1(\kappa_{\rm L}, a) = \int_{-\infty}^{\infty} \frac{\kappa_{\rm L}\,\eta}{1+\kappa_{\rm L}\,\eta} \, {\rm d}v$$

$$\mathcal{I}_2(\kappa_{\rm L}, a) = \int_{-\infty}^{\infty} \frac{\kappa_{\rm L}\,\ddot{\eta}}{(1+\kappa_{\rm L}\,\eta)^2} \, {\rm d}v$$

$$\mathcal{I}_3(\kappa_{\rm L}, a) = \int_{-\infty}^{\infty} \frac{\kappa_{\rm L}^2\,\dot{\eta}^2}{(1+\kappa_{\rm L}\,\eta)^3} \, {\rm d}v , \qquad (9.222)$$

with v the reduced wavelength defined in Eqs. (9.26) and

[1] The dependence on χ, the azimuth angle of the magnetic field vector, disappears for obvious symmetry reasons.

$$\dot{\eta} \,=\, \frac{\partial \eta}{\partial v} \,=\, \Delta\lambda_{\rm D}\, \frac{\partial \eta}{\partial \lambda}\,, \qquad\qquad \ddot{\eta} \,=\, \frac{\partial^2 \eta}{\partial v^2} \,=\, \Delta\lambda_{\rm D}^2\, \frac{\partial^2 \eta}{\partial \lambda^2}\,. \tag{9.223}$$

Integration by parts of $\mathcal{I}_2(\kappa_{\rm L}\,,a)$ shows that

$$\mathcal{I}_2(\kappa_{\rm L}\,,a) \,=\, 2\,\mathcal{I}_3(\kappa_{\rm L}\,,a)\,, \tag{9.224}$$

hence

$$\mathcal{M} \,=\, 1 + \,v_B^2\;\Gamma(\theta)\;\frac{\mathcal{I}_3(\kappa_{\rm L}\,,a)}{\mathcal{I}_1(\kappa_{\rm L}\,,a)}\;, \tag{9.225}$$

where

$$\Gamma(\theta) \,=\, \frac{1}{2}\left[\,G_0^{(2)}\sin^2\!\theta \,+\, G_1^{(2)}\,(1+\cos^2\!\theta)\right] - \left[G_1^{(1)}\right]^2\cos^2\!\theta\,.$$

The function $\Gamma(\theta)$ can be transformed by substituting the expressions for the quantities $G_q^{(n)}$ contained in Table 3.4. With some easy algebra one gets

$$\Gamma(\theta) \,=\, \frac{1}{2}\,\left(\,\bar{g}^2 \,+\, \delta\,\right)\sin^2\!\theta \,+\, \delta'\,, \tag{9.226}$$

where $\bar{g}$ is the effective Landé factor defined in Eq. (3.44), δ is defined in Eq. (9.78) and δ' is given by

$$\delta' \,=\, \frac{1}{80}\;g_d^2\;\left(8s \,-\, d^2 \,-\, 12\right). \tag{9.227}$$

For electric-dipole transitions, the quantity δ' is – like δ, see Sect. 9.6 – a non-negative quantity that vanishes only for Zeeman triplets (and for transitions $J = 1/2 \rightarrow J' = 1/2$).

Since both integrals $\mathcal{I}_1$ and $\mathcal{I}_3$ are positive, substitution of Eq. (9.226) into Eq. (9.225) shows that the following conclusions can be drawn about the magnetic intensification parameter in the weak field limit: i) it increases quadratically with the magnetic field strength; ii) it increases linearly with $\sin^2\!\theta$, reaching its maximum value for transverse fields ($\theta = 90°$); iii) in a longitudinal field ($\theta = 0°$ or $180°$), it is always equal to 1 for Zeeman triplets and for transitions $J = 1/2 \rightarrow J' = 1/2$;[1] iv) its dependence on $\kappa_{\rm L}$ and a is neither affected by the magnetic field nor by the Zeeman pattern of the spectral line, and is fully described by the function $\mathcal{I}_3\,/\,\mathcal{I}_1$. The functions $\mathcal{I}_1$, $\mathcal{I}_3$ and the ratio $\mathcal{I}_3\,/\,\mathcal{I}_1$ are plotted in Fig. 9.10. Note that $\mathcal{I}_1$ is proportional to the equivalent width of a non-magnetic line expressed in the Milne-Eddington approximation. From Eqs. (9.218), (9.112) and (9.222) we have in fact

$$W_0(\mu) = \Delta\lambda_{\rm D}\;\frac{\beta\mu}{1+\beta\mu}\;\mathcal{I}_1(\kappa_{\rm L}\,,a)\,. \tag{9.228}$$

[1] This property holds even if the magnetic field is not weak, as it can be easily realized from the discussion presented in Sect. 9.10 (cf. Eqs. (9.126)).

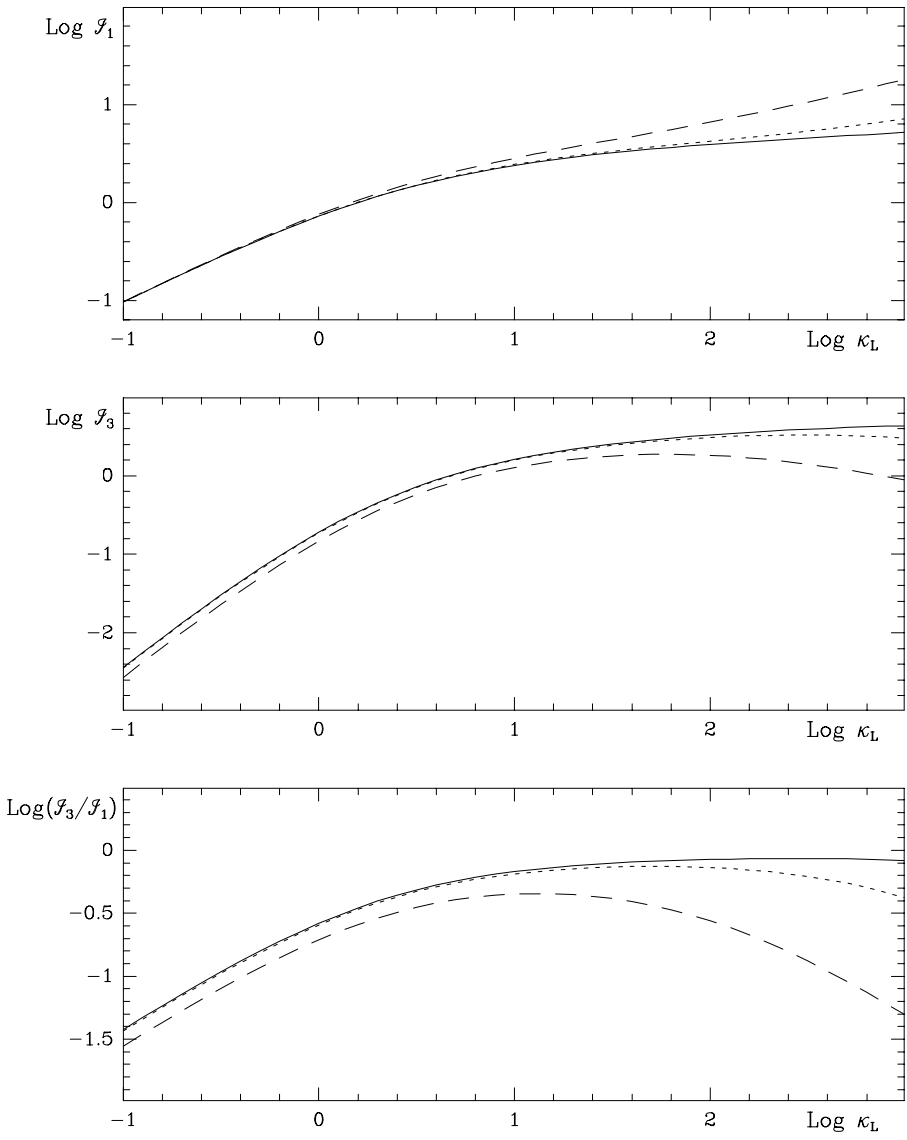

Fig.9.10. The functions $\mathcal{I}_1(\kappa_L\,, a)$ and $\mathcal{I}_3(\kappa_L\,, a)$ are plotted against κ_L on a Log-Log scale, for different values of the damping constant: $a = 10^{-3}$ (full line), $a = 10^{-2}$ (short dash), $a = 10^{-1}$ (long dash). Note that $\mathcal{I}_1(\kappa_L\,, a)$ represents the standard curve of growth for non-magnetic lines. According to Eq.(9.225), the ratio $\mathcal{I}_3\,/\,\mathcal{I}_1$ describes the dependence on κ_L and a of the magnetic intensification parameter $\mathcal{M}$.

c) Under the limit of very large magnetic field ($\Delta\lambda_B \gg \Delta\lambda_D$), when the profiles of the different Zeeman components are completely separated and do not overlap, each component can be treated independently. Its contribution is easily obtained with the help of the results derived in Sect. 9.12. Equations (9.220), (9.219), (9.228)

and (9.146) yield, for the Milne-Eddington atmosphere

$$\mathcal{M} = \frac{1}{W_0(\mu)} \sum_{i=1}^{N} \int_{\text{line}} \mathcal{R}_I^{(i)}(0,\mu)\, \mathrm{d}\lambda = \frac{1}{2\,\mathcal{I}_1(\kappa_\mathrm{L}\,, a)} \sum_{i=1}^{N} \int_{-\infty}^{\infty} \frac{\kappa_\mathrm{f}^{(i)}\, \eta^{(i)}}{1+\kappa_\mathrm{f}^{(i)}\, \eta^{(i)}}\ \mathrm{d}v\ ,$$

where $\kappa_\mathrm{f}^{(i)}$ is given by Eq. (9.143), $\eta^{(i)}$ by Eqs. (9.140), and N is the total number of Zeeman components. Recalling the definition of $\mathcal{I}_1$ (Eqs. (9.222)) and dividing the Zeeman components into π and σ, we obtain, with the use of the expressions in Table 9.6

$$\mathcal{M} = \frac{1}{2}\ \frac{\displaystyle\sum_{i=1}^{N_\pi} \mathcal{I}_1\Big(\kappa_\mathrm{L}\, s_i\, \sin^2\theta, a\Big) + \sum_{i=1}^{N_\sigma} \mathcal{I}_1\Big(\kappa_\mathrm{L}\, s_i\, \frac{1+\cos^2\theta}{2}\,, a\Big)}{\mathcal{I}_1(\kappa_\mathrm{L}\,, a)}\ , \qquad (9.229)$$

where s_i is the strength of the i-component defined in Eqs. (9.140) and the two summations refer to π and σ components, respectively ($N_\pi + N_\sigma = N$). It follows from Eq. (9.229) that, when κ_L is increased, the magnetic intensification parameter tends to a maximum asymptotic value given by[1] (Babcock, 1949)

$$\mathcal{M} = \frac{N_\pi\ +\ N_\sigma}{2}\ =\ \frac{N}{2}\ ,$$

which clearly shows the importance of the Zeeman pattern in determining the value of the magnetic intensification parameter.

All the properties discussed above are confirmed by detailed numerical calculations. Sample results are shown in Fig. 9.11.

9.20. Net Linear Polarization in Spectral Lines: the Differential Saturation Mechanism

Saturation effects in magnetic spectral lines not only increase their equivalent width (as shown in the former section) but also produce a net amount of linear polarization in the line.

It is easily seen that weak, unsaturated magnetic lines cannot produce net linear polarization. According to the generalized Seares formulae (9.151), which are valid for weak lines in an arbitrary atmosphere, the emerging Q Stokes parameter is given by

$$Q(0) = \int_0^\infty \mathrm{e}^{-\tau_\mathrm{c}}\ \kappa_\mathrm{L}(\tau_\mathrm{c})\, h_Q(\tau_\mathrm{c}) \left[B_\mathrm{P}(\tau_\mathrm{c}) - \int_{\tau_\mathrm{c}}^\infty \mathrm{e}^{-(\tau_\mathrm{c}'-\tau_\mathrm{c})}\ B_\mathrm{P}(\tau_\mathrm{c}')\, \mathrm{d}\tau_\mathrm{c}' \right] \mathrm{d}\tau_\mathrm{c}\ ,$$

[1] If θ is close to 0° or 180°, the 'fictitious opacity' in the π components ($\kappa_\mathrm{L}\, s_i\, \sin^2\theta$) is small. For such inclination angles the asymptotic value for $\mathcal{M}$ is $N_\sigma\,/\,2$ instead of $N\,/\,2$. This shows again that $\mathcal{M} = 1$ for Zeeman triplets when the magnetic field is parallel or antiparallel to the propagation direction (the magnetic intensification mechanism is ineffective).

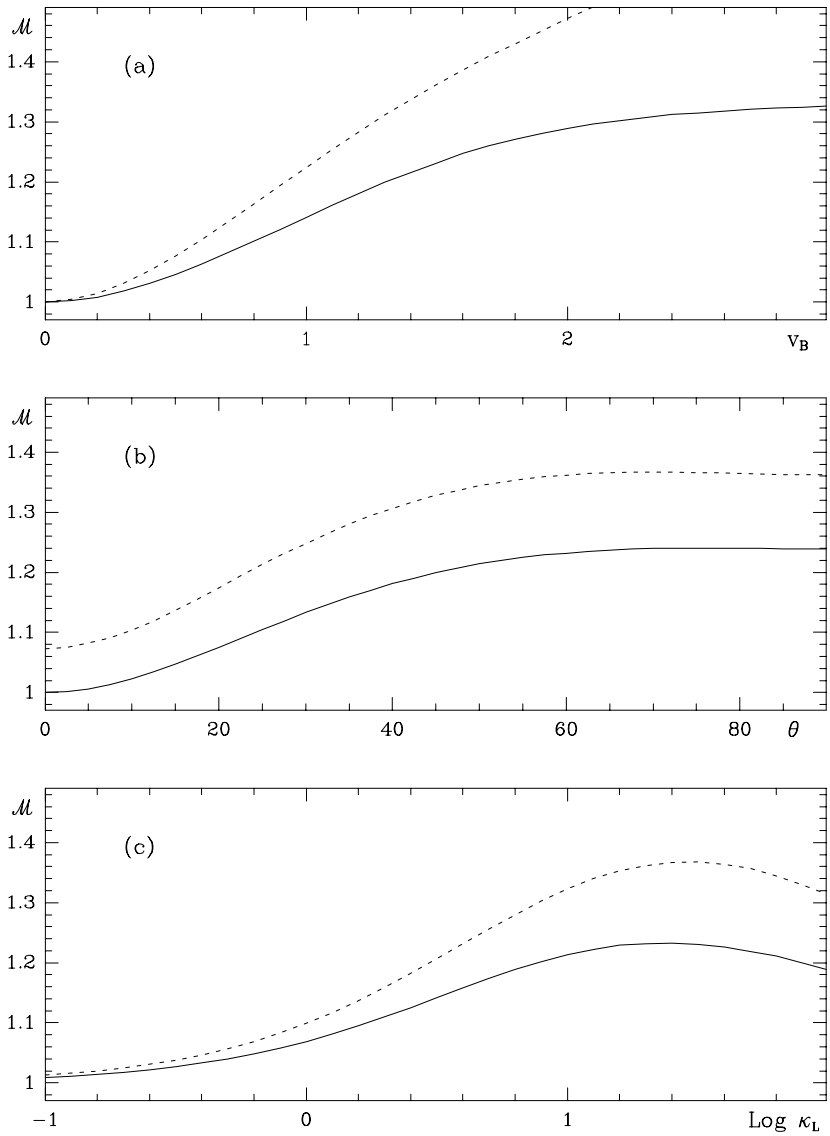

Fig.9.11. Numerical results for the magnetic intensification parameter $\mathcal{M}$ computed according to Eq.(9.221). The solid line refers to a normal Zeeman triplet ($^1S_0 - {}^1P_1$), while the dashed line refers to a more complicated Zeeman pattern ($^5P_3 - {}^5D_4$, see Fig.3.2). Panel (a): $\mathcal{M}$ versus v_B for $\theta = 60°$, $\kappa_L = 20$, $a = 0.05$. Panel (b): $\mathcal{M}$ versus θ for $v_B = 1.5$, $\kappa_L = 20$, $a = 0.05$. Panel (c): $\mathcal{M}$ versus $\mathrm{Log}\,\kappa_L$ for $v_B = 1.5$, $\theta = 60°$, $a = 0.05$.

with a similar expression for $U(0)$. Since from Eqs. (9.32), (9.29) and (9.28)

$$\int_{\text{line}} h_Q \, \mathrm{d}\lambda = \int_{\text{line}} h_U \, \mathrm{d}\lambda = 0 \,,$$

the line-integrated Stokes parameters $\mathcal{Q}$ and $\mathcal{U}$ defined in Eq. (9.210)

$$\mathcal{Q} = \int_{\text{line}} Q(0,\lambda)\,\mathrm{d}\lambda\,, \qquad\qquad \mathcal{U} = \int_{\text{line}} U(0,\lambda)\,\mathrm{d}\lambda$$

are both zero.

This property breaks down when saturation effects are important. In that case, the contributions of π and σ components (which affect linear polarization in opposite ways) no longer compensate each other, because saturation effects are in general different for either type. It follows that $\mathcal{Q} \neq 0$ and $\mathcal{U} \neq 0$. This is the so-called mechanism of *differential saturation* (of π and σ components). Being due to saturation effects, it is strictly related to the magnetic intensification mechanism studied in the previous section. In the first papers dealing with net linear polarization in magnetic lines (Leroy, 1962; Calamai et al., 1975) the term 'magnetic intensification' was indeed used to denote both mechanisms.

In order to describe the net amount of linear polarization in a spectral line, it is convenient to introduce dimensionless quantities by normalizing $\mathcal{Q}$ and $\mathcal{U}$ to the net amount of continuum radiation subtracted by the line. Thus we introduce the *net linear polarization parameters*

$$\mathfrak{q} = -\frac{\mathcal{Q}}{\mathcal{I}} = \frac{\mathcal{Q}}{I_{\mathrm{c}}(0)\,W}\,, \qquad\qquad \mathfrak{u} = -\frac{\mathcal{U}}{\mathcal{I}} = \frac{\mathcal{U}}{I_{\mathrm{c}}(0)\,W}\,, \tag{9.230}$$

where $\mathcal{I}$ is defined in Eq. (9.210) and W is the equivalent width given by Eq. (9.219).

As in the case of the magnetic intensification parameter $\mathcal{M}$, a good approximation for $\mathfrak{q}$ and $\mathfrak{u}$ is obtained by assuming the Milne-Eddington model atmosphere. It is also convenient to express the net linear polarization parameters in the preferred reference frame (see Sect. 5.5). Setting

$$\tilde{\mathfrak{q}} = \mathfrak{q}\,(\chi = 0^\circ)\,, \qquad\qquad \tilde{\mathfrak{u}} = \mathfrak{u}\,(\chi = 0^\circ)\,,$$

we have from Eqs. (9.230), (9.219) and (9.112)

$$\tilde{\mathfrak{q}} = -\frac{\displaystyle\int_{-\infty}^{\infty} \Delta^{-1}\left[\,(1+k_I)^2\,k_{\tilde{Q}} \;+\; f_{\tilde{Q}}\,(k_{\tilde{Q}} f_{\tilde{Q}} + k_V f_V)\,\right]\mathrm{d}\lambda}{\displaystyle\int_{-\infty}^{\infty} \left\{1 - \Delta^{-1}\,(1+k_I)\left[(1+k_I)^2 + f_{\tilde{Q}}^2 + f_V^2\,\right]\right\}\mathrm{d}\lambda}$$

$$\tilde{\mathfrak{u}} = \frac{\displaystyle\int_{-\infty}^{\infty} \Delta^{-1}\,(1+k_I)\,(k_V f_{\tilde{Q}} - k_{\tilde{Q}} f_V)\,\mathrm{d}\lambda}{\displaystyle\int_{-\infty}^{\infty} \left\{1 - \Delta^{-1}\,(1+k_I)\left[(1+k_I)^2 + f_{\tilde{Q}}^2 + f_V^2\,\right]\right\}\mathrm{d}\lambda}\,, \tag{9.231}$$

where

$$\Delta = (1+k_I)^4 + (1+k_I)^2\,(f_{\tilde{Q}}^2 + f_V^2 - k_{\tilde{Q}}^2 - k_V^2) - (k_{\tilde{Q}} f_{\tilde{Q}} + k_V f_V)^2$$

and (see Eqs. (9.39) and (9.157))

$$k_{\tilde{Q}} = \kappa_{\rm L}\, h_{\tilde{Q}} \,, \qquad\qquad f_{\tilde{Q}} = \kappa_{\rm L}\, r_{\tilde{Q}} \,. \tag{9.232}$$

The quantities Π and Φ, implicitly defined by

$$\tilde{\mathfrak{q}} = \Pi \cos 2\Phi \,, \qquad\qquad \tilde{\mathfrak{u}} = \Pi \sin 2\Phi$$

with Φ ranging from 0 to π, are sometimes used in the place of $\tilde{\mathfrak{q}}$ and $\tilde{\mathfrak{u}}$. Inversion of these relations gives (cf. Eqs. (1.8))

$$\Pi = \sqrt{\tilde{\mathfrak{q}}^2 + \tilde{\mathfrak{u}}^2}$$

and, for $\tilde{\mathfrak{q}} \neq 0$

$$\Phi = \frac{1}{2} \arctan\left(\frac{\tilde{\mathfrak{u}}}{\tilde{\mathfrak{q}}}\right) + \Phi_0$$

with

$$\Phi_0 = \begin{cases} 0 & \text{if } \tilde{\mathfrak{q}} > 0 \text{ and } \tilde{\mathfrak{u}} \geq 0 \\ \pi & \text{if } \tilde{\mathfrak{q}} > 0 \text{ and } \tilde{\mathfrak{u}} < 0 \\ \pi/2 & \text{if } \tilde{\mathfrak{q}} < 0 \,, \end{cases}$$

while for $\tilde{\mathfrak{q}} = 0$

$$\Phi = \begin{cases} \frac{1}{4}\pi & \text{if } \tilde{\mathfrak{u}} > 0 \\ \frac{3}{4}\pi & \text{if } \tilde{\mathfrak{u}} < 0 \,. \end{cases}$$

The relation between the net linear polarization parameters expressed in an arbitrary frame (rather than the preferred frame) and the set (Π, Φ) is easily obtained from the transformation law of the Stokes parameters under rotation of the reference direction. Equations (1.45) yield

$$\mathfrak{q} = \Pi \cos 2(\Phi + \chi) \,, \qquad\qquad \mathfrak{u} = \Pi \sin 2(\Phi + \chi) \,.$$

The physical meaning of Π and Φ is obvious: Π is the net linear polarization degree, Φ is the angle between the direction of maximum net linear polarization and the transverse component of the magnetic field.

The net linear polarization parameters $\tilde{\mathfrak{q}}$ and $\tilde{\mathfrak{u}}$ (or the quantities Π and Φ) depend on the four parameters v_B, θ, $\kappa_{\rm L}$, a and on the structure of the Zeeman pattern. Because of the involved form of Eqs. (9.231), only a few analytical results can be obtained. These are the following:

a) Symmetry properties: if we consider the transformation $\theta \to \pi - \theta$, we have from Eqs. (9.32)

$$\begin{aligned} &\tilde{\mathfrak{q}}\,(\pi - \theta) = \tilde{\mathfrak{q}}\,(\theta) \qquad &&\Pi(\pi - \theta) = \Pi(\theta) \\ &\tilde{\mathfrak{u}}\,(\pi - \theta) = -\,\tilde{\mathfrak{u}}\,(\theta) \qquad &&\Phi(\pi - \theta) = \pi - \Phi(\theta) \,. \end{aligned}$$

b) Under the limit of weak, unsaturated lines ($\kappa_{\rm L} \ll 1$), expansion of Eqs. (9.231) into power series of $\kappa_{\rm L}$ yields, with the help of Eqs. (9.32), (9.29) and (9.28)

$$\tilde{\mathfrak{q}} = 2\,\kappa_{\rm L} \int_{-\infty}^{\infty} h_{\bar{Q}}\, h_I \, {\rm d}v \;, \qquad \tilde{\mathfrak{u}} = \kappa_{\rm L} \int_{-\infty}^{\infty} \left(h_V \, r_{\bar{Q}} \, - \, h_{\bar{Q}} \, r_V \right) {\rm d}v \;,$$

where v is the reduced wavelength defined in Eqs. (9.26). These equations show that $\mathit{\Pi}$ grows linearly with $\kappa_{\rm L}$ and that $\mathit{\Phi}$ attains a finite value for $\kappa_{\rm L} \rightarrow 0$.

c) Under the limit of weak magnetic field ($\mathit{\Delta}\lambda_B \ll \mathit{\Delta}\lambda_{\rm D}$) we can expand the integrands in Eqs. (9.231) by using Eqs. (9.69). To the lowest order in v_B we obtain, with the help of Eqs. (9.76), (9.224) and Table 3.4

$$\tilde{\mathfrak{q}} = \frac{1}{2}\, v_B^2 \;\; \bar{G}\, \sin^2\theta \;\; \frac{\mathcal{I}_3(\kappa_{\rm L}\,,a)}{\mathcal{I}_1(\kappa_{\rm L}\,,a)}$$

$$\tilde{\mathfrak{u}} = \frac{1}{4}\, v_B^3 \;\; \bar{g}\,\bar{G}\, \sin^2\theta\, \cos\theta \;\; \frac{\mathcal{I}_4(\kappa_{\rm L}\,,a)}{\mathcal{I}_1(\kappa_{\rm L}\,,a)} \;, \qquad (9.233)$$

where $\mathcal{I}_1$ and $\mathcal{I}_3$ are defined in Eqs. (9.222) and where

$$\mathcal{I}_4(\kappa_{\rm L}\,,a) = \int_{-\infty}^{\infty} \frac{\kappa_{\rm L}^2 \; (\dot{\eta}\,\ddot{\rho} \, - \, \ddot{\eta}\,\dot{\rho})}{(1+\kappa_{\rm L}\,\eta)^3} \;\; {\rm d}v \;,$$

with $\dot{\eta}$, $\ddot{\eta}$ given by Eqs. (9.223) and, similarly

$$\dot{\rho} \, = \frac{\partial \rho}{\partial v} = \mathit{\Delta}\lambda_{\rm D} \, \frac{\partial \rho}{\partial \lambda} \;, \qquad \ddot{\rho} \, = \frac{\partial^2 \rho}{\partial v^2} = \mathit{\Delta}\lambda_{\rm D}^2 \;\; \frac{\partial^2 \rho}{\partial \lambda^2} \;.$$

Equations (9.233) show that, for weak fields, the net linear polarization grows quadratically with the magnetic field strength and linearly with $\sin^2\theta$. The direction of maximum polarization is determined by the sign of $\tilde{\mathfrak{q}}$, hence (since both $\mathcal{I}_1$ and $\mathcal{I}_3$ are positive) by the sign of $\bar{G}$. Most spectral lines have $\bar{G} > 0$, which implies that the net linear polarization is parallel to the transverse component of the magnetic field. The opposite holds for the lines with $\bar{G} < 0$ (net linear polarization perpendicular to the transverse component of the magnetic field). Comparison of the expression for $\tilde{\mathfrak{q}}$ given by Eqs. (9.233) with Eqs. (9.83) and (9.85) shows that the sign of $\tilde{\mathfrak{q}}$ is the same as the sign of the $\tilde{Q}$ profile in the wings and is opposite to the sign of $\tilde{Q}$ in the line core. This means that, for weak fields, σ components are always less saturated than π components.

d) Under the limit of very large magnetic field ($\mathit{\Delta}\lambda_B \gg \mathit{\Delta}\lambda_{\rm D}$), we can use the results developed in Sect. 9.12. The following expressions are obtained (see Eq. (9.229)

for a similar derivation)

$$\tilde{\mathfrak{q}} = \frac{\dfrac{\sin^2\theta}{1+\cos^2\theta}\displaystyle\sum_{i=1}^{N_\sigma}\mathcal{I}_1\Big(\kappa_{\rm L}\,s_i\,\frac{1+\cos^2\theta}{2}\,,\,a\Big) - \sum_{i=1}^{N_\pi}\mathcal{I}_1\Big(\kappa_{\rm L}\,s_i\,\sin^2\theta,\,a\Big)}{\displaystyle\sum_{i=1}^{N_\sigma}\mathcal{I}_1\Big(\kappa_{\rm L}\,s_i\,\frac{1+\cos^2\theta}{2}\,,\,a\Big) + \sum_{i=1}^{N_\pi}\mathcal{I}_1\Big(\kappa_{\rm L}\,s_i\,\sin^2\theta,\,a\Big)}$$

$$\tilde{\mathfrak{u}} = 0\ ,$$

where N_σ and N_π are the total number of σ and π components, respectively. It follows that, for saturated lines lying on the flat part of the curve of growth (and excluding θ values close to 0° or 180°), $\tilde{\mathfrak{q}}$ is roughly given by the expression

$$\tilde{\mathfrak{q}} = \frac{\sin^2\theta}{1+\cos^2\theta}\,\frac{N_\sigma}{N} - \frac{N_\pi}{N}\ , \tag{9.234}$$

with $N = N_\pi + N_\sigma$. Therefore, $\tilde{\mathfrak{q}}$ is negative for small values of $\sin^2\theta$ (net linear polarization perpendicular to the transverse component of the magnetic field, π components more saturated than σ components), while it is positive for large values of $\sin^2\theta$ (polarization parallel to the transverse component of the magnetic field, π components less saturated than σ components). Obviously, there are two values of θ such that the net linear polarization is zero,

$$\theta_{\rm z} = \arccos\sqrt{\frac{N_\sigma - N_\pi}{N}} \qquad \text{and} \qquad \theta'_{\rm z} = 180^\circ - \theta_{\rm z}\ .$$

Note that in the most common case where $N_\sigma = 2\,N_\pi$,[1]

$$\theta_{\rm z} = \arccos\sqrt{\frac{1}{3}} = \theta_{\rm V}\ ,$$

where $\theta_{\rm V}$ is the Van Vleck angle defined in Eqs. (5.100)-(5.101). Equation (9.234) also shows that for $\theta = 90^\circ$ (transverse field), $\tilde{\mathfrak{q}}$ reaches its maximum value

$$\tilde{\mathfrak{q}}_{\rm max} = \frac{N_\sigma - N_\pi}{N}\ ,$$

or, for most Zeeman patterns

$$\tilde{\mathfrak{q}}_{\rm max} = \frac{1}{3}\ .$$

[1] For electric-dipole transitions, the relation $N_\sigma = 2N_\pi$ is always valid except when the lower and upper level have the same half-integral J quantum number. In that case $N_\pi = 2J+1$ and $N_\sigma = 4J$, hence

$$\theta_{\rm z} = \arccos\sqrt{\frac{2J-1}{6J+1}}\ .$$

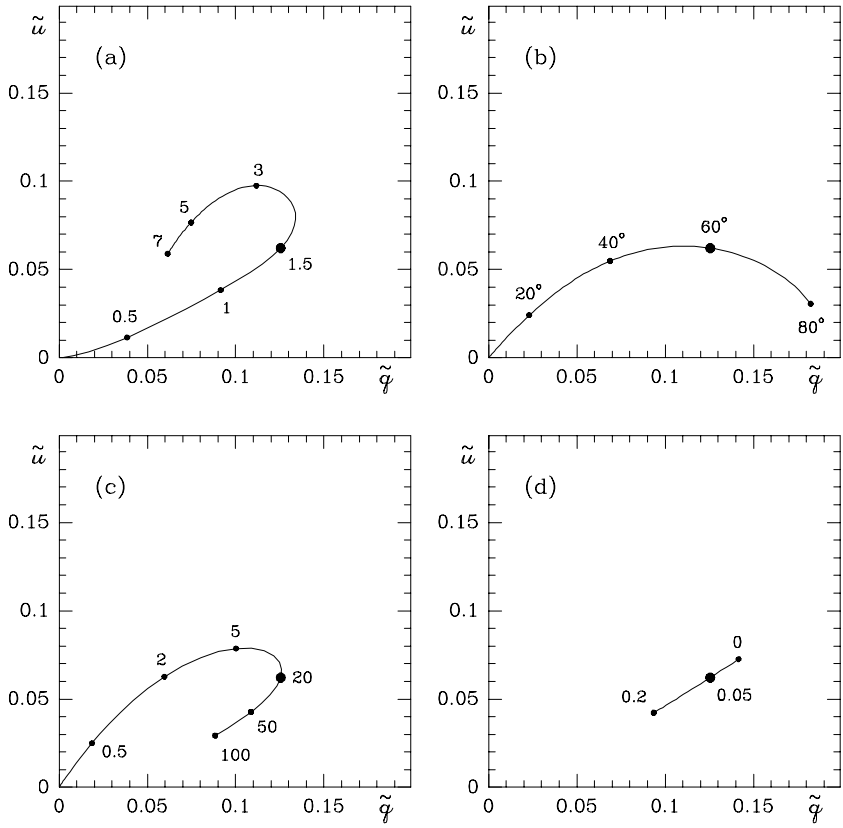

Fig.9.12. Numerical results for the differential saturation mechanism. The net linear polarization parameters $\tilde{\mathfrak{q}}$ and $\tilde{\mathfrak{u}}$ are calculated from Eqs.(9.231) for the normal Zeeman triplet ${}^1S_0 - {}^1P_1$. The big dot corresponds to the 'standard case' values $v_B = 1.5$, $\theta = 60°$, $\kappa_L = 20$, $a = 0.05$. The four curves are obtained by varying one parameter at a time, namely: v_B (a); θ (b); κ_L (c); a (d). Values of the varying parameter are marked by small dots.

The analytical results presented above are only valid within a limited region of the hyperspace of the four parameters v_B, θ, κ_L, a. In general, the calculation of the net linear polarization requires (under the Milne-Eddington assumptions) a numerical evaluation of the integrals in Eqs. (9.231). Sample results are shown in Fig. 9.12. It is seen that, except in the limiting cases of very weak and very strong magnetic field, the parameter $\tilde{\mathfrak{u}}$ makes an important contribution to the net linear polarization. Since this parameter vanishes when magneto-optical effects are neglected (see Eqs. (9.231)), it follows that these effects play a major role in the mechanism of differential saturation. Numerical results on the net linear polarization have been presented by Calamai et al. (1975), Landi Degl'Innocenti and Calamai (1982), Calamai and Landi Degl'Innocenti (1983), and Bagnulo (1993). In these works the line strength is parameterized through the quantity η_0 which is connected with κ_L by the relation $\eta_0 = \kappa_L / \sqrt{\pi}$ (see the remarks following Eqs. (9.32)).

Finally, it should be pointed out that differential saturation of π and σ compo-

nents is the only mechanism that can introduce net linear polarization in spectral lines when atomic polarization effects are neglected. We will see in the following (Sect. 10.5) that if the alignment components of the atomic density matrix are non-zero, there is an extra-contribution to net linear polarization. The definition of alignment and its physical meaning are discussed in Sect. 3.7.

9.21. Net Circular Polarization in Spectral Lines

In the two previous sections we have seen that saturation effects in magnetic lines produce an increase of equivalent width and the appearance of net linear polarization. For circular polarization the situation is quite different, because saturation effects are *necessary but not sufficient* for the appearance of a net contribution from a given spectral line.

The proof of this statement is straightforward. For the first part (saturation effects are necessary) it is enough to consider the generalized Seares formulae (Eqs. (9.151)) that we rewrite here for the emerging V Stokes parameter

$$V(0) = \int_0^\infty \mathrm{e}^{-\tau_\mathrm{c}}\ \kappa_\mathrm{L}(\tau_\mathrm{c})\, h_V(\tau_\mathrm{c}) \left[B_\mathrm{P}(\tau_\mathrm{c}) - \int_{\tau_\mathrm{c}}^\infty \mathrm{e}^{-(\tau_\mathrm{c}'-\tau_\mathrm{c})}\ B_\mathrm{P}(\tau_\mathrm{c}')\, \mathrm{d}\tau_\mathrm{c}' \right] \mathrm{d}\tau_\mathrm{c}\ .$$

Since from Eqs. (9.32), (9.29) and (9.28)

$$\int_\mathrm{line} h_V\ \mathrm{d}\lambda\ = 0\ ,$$

the line-integrated V Stokes parameter in a weak (unsaturated) line is zero,

$$\mathcal{V} = \int_\mathrm{line} V(0,\lambda)\ \mathrm{d}\lambda\ = 0\ .$$

The second part of the statement (saturation effects are not sufficient) is directly proved by the wavelength symmetry properties of the Stokes parameters outlined in Sect. 9.5 and summarized in Eqs. (9.54): for a static (or constant-velocity) atmosphere we find again $\mathcal{V} = 0$.

These arguments suggest that, in order to obtain net circular polarization in magnetic spectral lines, it is necessary to have saturation effects combined with a velocity gradient.

Similarly to Eqs. (9.230), we define the (dimensionless) *net circular polarization parameter* to be

$$\mathfrak{v} = -\frac{\mathcal{V}}{\mathcal{I}} = \frac{\mathcal{V}}{I_\mathrm{c}(0)\, W}\ , \tag{9.235}$$

with $\mathcal{I}$ and W given by Eqs. (9.210) and (9.219) respectively, and $I_\mathrm{c}(0)$ the emerging continuum intensity. This parameter has a very complicated dependence on

the physical quantities specifying the stellar atmosphere (including the velocity gradient) and on the Zeeman pattern of the line. This makes extremely difficult to derive its general properties except in some special cases based on drastic approximations. Obviously, it is impossible to use the Milne-Eddington solution to the transfer equation (as done in the former section for the net linear polarization) because the Milne-Eddington model atmosphere is static.

In the following we consider three special cases where analytical expressions for the parameter $\mathfrak{v}$ can be derived:
i) a zero-order Milne-Eddington atmosphere is 'perturbed' by a (small) velocity gradient;
ii) an arbitrary atmosphere with vertical magnetic field presents a velocity gradient associated with a gradient of the magnetic field intensity;
iii) the atmosphere is composed of two superposed Milne-Eddington atmospheres with a discontinuity of all the physical parameters (including velocity) at the transition layer.

In case i) the velocity gradient is small and continuous and it is not associated with other gradients. In case ii) the velocity gradient is continuous and not necessarily small, and it is associated with a gradient of the magnetic field intensity. Finally, in case iii) the velocity gradient is discontinuous (being mathematically described by a Dirac delta-function) and it is associated with discontinuous gradients of the other physical quantities.

Before we analyze these special cases, some general remarks about the line-of-sight velocity gradient are necessary. Given a *stationary* stellar atmosphere where a macroscopic velocity field $\vec{w}_{\rm A}$ is present, we introduce the terms[1]

$$\begin{aligned} &\textit{expanding atmosphere} \qquad \text{if} \quad \operatorname{div} \vec{w}_{\rm A} > 0 \\ &\textit{compressing atmosphere} \quad \text{if} \quad \operatorname{div} \vec{w}_{\rm A} < 0 \,. \end{aligned}$$

The reason for these terms is the following. Denoting by ρ the mass density of the medium, its total (Eulerian) time derivative is given by

$$\frac{\mathrm{d}\rho}{\mathrm{d}t} = \vec{w}_{\rm A} \cdot \operatorname{grad} \rho \,,$$

since the atmosphere is stationary ($\partial\rho/\partial t = 0$). Combining this relation with the mass conservation equation

$$\operatorname{div} (\rho \, \vec{w}_{\rm A}) = \vec{w}_{\rm A} \cdot \operatorname{grad} \rho \, + \, \rho \operatorname{div} \vec{w}_{\rm A} = 0 \,,$$

we get

$$\frac{\mathrm{d}\rho}{\mathrm{d}t} = - \, \rho \operatorname{div} \vec{w}_{\rm A} \,,$$

[1] For simplicity, we assume that $\operatorname{div} \vec{w}_{\rm A}$ has the same sign throughout the whole atmosphere. Note that a similar terminology was first introduced by Skumanich and Lites (1987).

so that $\mathrm{d}\rho/\mathrm{d}t$ is negative for an 'expanding' atmosphere and positive for a 'compressing' atmosphere. It follows that each plasma element goes across regions of *decreasing* density in the former case and of *increasing* density in the latter.

In the particular case of a plane-parallel atmosphere with a vertical (upward or downward) velocity field, all the physical quantities, including $\vec{w}_{\rm A}$, depend only on the geometrical depth z defined in Fig. 9.2. For a radiation beam travelling along the direction $\vec{\Omega}$, the line-of-sight component of the velocity $\vec{w}_{\rm A}$ – which we keep on denoting by $w_{\rm A}$ – is, according to the sign astrophysical convention (see Sect. 5.4)

$$w_{\rm A} = -\,\vec{\Omega}\cdot\vec{w}_{\rm A}\ .$$

If s is the coordinate measured along the ray path and $\mu = \cos\alpha$, with α defined in Fig. 9.2, we get from the two equations above

$$\frac{\mathrm{d}w_{\rm A}}{\mathrm{d}s} = -\,\vec{\Omega}\cdot\frac{\mathrm{d}\vec{w}_{\rm A}}{\mathrm{d}s} = -\,\mu\ \vec{\Omega}\cdot\frac{\partial\vec{w}_{\rm A}}{\partial z} = -\,\mu^2\ \mathrm{div}\ \vec{w}_{\rm A}\ .$$

In terms of the optical depths $\tau_{\rm c}$ or $t_{\rm c}$ defined in Eqs. (9.33) and (9.34) we have

$$\frac{\mathrm{d}w_{\rm A}}{\mathrm{d}\tau_{\rm c}} = \frac{\mu^2}{k_{\rm c}}\ \mathrm{div}\ \vec{w}_{\rm A}\ , \qquad\qquad \frac{\mathrm{d}w_{\rm A}}{\mathrm{d}t_{\rm c}} = \frac{\mu}{k_{\rm c}}\ \mathrm{div}\ \vec{w}_{\rm A}\ .$$

Therefore, under the conditions specified above (plane-parallel atmosphere, vertical velocity field, astrophysical convention for $w_{\rm A}$), equivalent definitions of 'expanding' atmosphere are provided by the inequalities

$$\frac{\mathrm{d}w_{\rm A}}{\mathrm{d}\tau_{\rm c}} > 0$$

or

$$\frac{\mathrm{d}w_{\rm A}}{\mathrm{d}t_{\rm c}} > 0 \quad \text{for radiation travelling } \textit{outward}.$$

It should be remarked that the distinction between 'expanding' and 'compressing' atmosphere only involves the sign of the velocity gradient, not the sign of the velocity itself. In fact, as recalled at the beginning of this section, the addition of a constant velocity field simply produces an overall wavelength shift of the Stokes profiles and has no effect on the net circular polarization parameter $\mathfrak{v}$.

Let's now turn to the analysis of the three schematic models listed above.[1]

Case i) We consider a Milne-Eddington atmosphere, characterized by the constant propagation matrix $\boldsymbol{C}$ defined in Eq. (9.91). The atmosphere is perturbed by a vertical velocity field which varies linearly with optical depth. For a radiation beam flowing along an assigned μ-direction, we describe the line-of-sight velocity by the equation

$$w_{\rm A}(t_{\rm c}) = w_{\rm A}^{(0)} + w_{\rm A}^{(1)}\ t_{\rm c}\ ,$$

[1] A similar analysis has been presented in Landolfi and Landi Degl'Innocenti (1996).

where t_c is the optical depth measured along the vertical (Eqs. (9.34)).

We now make the further assumption that the perturbation is everywhere small, that is (cf. Eqs. (9.26))

$$v_A(t_c) = \frac{w_A(t_c)}{c}\,\frac{\lambda_0}{\Delta\lambda_D} \ll 1$$

or

$$w_A^{(0)}\ ,\ w_A^{(1)} \ll w_T\ , \tag{9.236}$$

where w_T is the thermal velocity defined in Eqs. (5.42) and (5.46). This assumption enables the first-order correction to the emerging V Stokes parameter to be evaluated using the appropriate response function. Similarly to Eq. (9.200), we can write

$$V'(0,\mu) = V(0,\mu) + \delta V(0,\mu)\ , \tag{9.237}$$

where the zero-order term $V(0,\mu)$, corresponding to the static atmosphere, makes no contribution to the net circular polarization parameter, which thus reduces to (see Eqs. (9.235) and (9.210))

$$\mathfrak{v} = \frac{1}{I_c(0)\,W}\int_{-\infty}^{\infty}\delta V(0,\mu)\,\mathrm{d}\lambda\ . \tag{9.238}$$

On the other hand, Eqs. (9.39), (9.32), (9.29), (9.27) and (9.26) show that

$$\frac{\partial\,\boldsymbol{C}^{-1}}{\partial w_A} = \frac{\lambda_0}{c\,\Delta\lambda_D}\,\frac{\partial\,\boldsymbol{C}^{-1}}{\partial v_A} = -\frac{\lambda_0}{c\,\Delta\lambda_D}\,\frac{\partial\,\boldsymbol{C}^{-1}}{\partial v} = -\frac{\lambda_0}{c}\,\frac{\partial\,\boldsymbol{C}^{-1}}{\partial\lambda}\ ,$$

thus we can apply Eq. (9.205) to obtain

$$\delta V(0,\mu) = -B_0\,\beta\mu\,\frac{\lambda_0}{c} \times\left[w_A^{(0)}\,\frac{\partial}{\partial\lambda}\big(C^{-1}\big)_{30} + \mu\,w_A^{(1)}\sum_{i=0}^{3}\big(C^{-1}\big)_{3i}\,\frac{\partial}{\partial\lambda}\big(C^{-1}\big)_{i0}\right]. \tag{9.239}$$

Since from Table 9.5

$$\lim_{\lambda\to\pm\infty}\big(C^{-1}\big)_{ij} = 0 \qquad \text{for} \qquad i\neq j\ ,$$

we have[1]

$$\int_{-\infty}^{\infty}\frac{\partial}{\partial\lambda}\big(C^{-1}\big)_{30}\,\mathrm{d}\lambda = 0\ . \tag{9.240}$$

[1] Equation (9.240) shows that the term $w_A^{(0)}$ does not affect the net circular polarization. The condition $w_A^{(0)} \ll w_T$ in Eq. (9.236) is necessary only if we want to regard $V(0,\mu)$ in Eq. (9.237) as the solution corresponding to the static atmosphere. However, $V(0,\mu)$ could as well be regarded as the solution corresponding to a constant-velocity atmosphere with line-of-sight velocity $w_A^{(0)}$, which again proves that the condition $w_A^{(0)} \ll w_T$ is indeed unnecessary for the following results (in particular Eq. (9.241)) to hold.

Integrating by parts the last term in Eq. (9.239) we have

$$\int_{-\infty}^{\infty} \sum_{i=0}^{3} \left(C^{-1}\right)_{3i} \frac{\partial}{\partial\lambda}\left(C^{-1}\right)_{i0} \,\mathrm{d}\lambda = -\int_{-\infty}^{\infty} \sum_{i=0}^{3} \left[\frac{\partial}{\partial\lambda}\left(C^{-1}\right)_{3i}\right]\left(C^{-1}\right)_{i0} \,\mathrm{d}\lambda\,,$$

whence

$$\int_{-\infty}^{\infty} \sum_{i=0}^{3} \left(C^{-1}\right)_{3i} \frac{\partial}{\partial\lambda}\left(C^{-1}\right)_{i0} \,\mathrm{d}\lambda = -\frac{1}{2}\int_{-\infty}^{\infty} \left[\frac{\partial \boldsymbol{C}^{-1}}{\partial\lambda}\,,\, \boldsymbol{C}^{-1}\right]_{30} \mathrm{d}\lambda\,,$$

where the integrand in the right-hand side is the element $(3,0)$ of the commutator of the two matrices. The denominator of Eq. (9.238) is easily evaluated using Eqs. (9.219) and (9.109). To the lowest order we obtain

$$I_{\mathrm{c}}(0)\, W = B_0\, \beta\mu \int_{-\infty}^{\infty} \left[1 - \left(C^{-1}\right)_{00}\right] \mathrm{d}\lambda\,.$$

Substitution of the above equations into Eq. (9.238) yields

$$\mathfrak{v} = \frac{1}{2}\,\mu\,\frac{\lambda_0}{c}\; w_{\mathrm{A}}^{(1)}\; \frac{\displaystyle\int_{-\infty}^{\infty} \left[\frac{\partial \boldsymbol{C}^{-1}}{\partial\lambda}\,,\, \boldsymbol{C}^{-1}\right]_{30} \mathrm{d}\lambda}{\displaystyle\int_{-\infty}^{\infty} \left[1 - \left(C^{-1}\right)_{00}\right] \mathrm{d}\lambda}\;. \tag{9.241}$$

The analytical calculation can be further developed by substituting the expressions for the elements of the matrix $\boldsymbol{C}^{-1}$ given in Table 9.5. If the calculation is performed in the preferred frame (the Stokes parameter V is independent of the choice of the reference direction), the following expression is obtained

$$\mathfrak{v} = \mu\,\frac{w_{\mathrm{A}}^{(1)}}{c}\,\frac{\lambda_0}{\Delta\lambda_{\mathrm{D}}}\; \frac{\displaystyle\int_{-\infty}^{\infty} \Delta^{-2}\,\mathcal{A}\;\mathrm{d}v}{\displaystyle\int_{-\infty}^{\infty} \left\{1 - \Delta^{-1}\,(1+k_I)\left[\,(1+k_I)^2 + f_{\tilde{Q}}^2 + f_V^2\,\right]\right\} \mathrm{d}v}\;, \tag{9.242}$$

where $\Delta\lambda_{\mathrm{D}}$ is the Doppler width, v the reduced wavelength defined in Eqs. (9.26), and

$$\begin{aligned}
\mathcal{A} = {} & \Big\{(1+k_I)^3\,(k_{\tilde{Q}}k_V + f_{\tilde{Q}}f_V) \\
& + (1+k_I)\left[-k_{\tilde{Q}}k_V\left(f_{\tilde{Q}}^2 - f_V^2\right) + f_{\tilde{Q}}f_V\left(k_{\tilde{Q}}^2 - k_V^2\right)\right]\Big\}\frac{\partial k_{\tilde{Q}}}{\partial v} \\
& - (1+k_I)^3\left(k_{\tilde{Q}}^2 + f_{\tilde{Q}}^2\right)\frac{\partial k_V}{\partial v} \\
& + \Big\{(1+k_I)^3\,(k_V f_{\tilde{Q}} - k_{\tilde{Q}}f_V) \\
& \quad + (1+k_I)\left[\,k_{\tilde{Q}}f_V\left(k_V^2 + f_{\tilde{Q}}^2\right) + k_V f_{\tilde{Q}}\left(k_{\tilde{Q}}^2 + f_V^2\right)\right]\Big\}\frac{\partial f_{\tilde{Q}}}{\partial v} \\
& - (1+k_I)\,(k_{\tilde{Q}}f_{\tilde{Q}} + k_V f_V)\left(k_{\tilde{Q}}^2 + f_{\tilde{Q}}^2\right)\frac{\partial f_V}{\partial v}\;;
\end{aligned} \tag{9.243}$$

the quantities $k_{\tilde{Q}}$ and $f_{\tilde{Q}}$ are given by (cf. Eqs. (9.232))

$$k_{\tilde{Q}} = k_Q(\chi = 0^\circ) = \kappa_{\rm L}\, h_{\tilde{Q}} \,, \qquad\qquad f_{\tilde{Q}} = f_Q(\chi = 0^\circ) = \kappa_{\rm L}\, r_{\tilde{Q}} \,.$$

Equations (9.242)-(9.243) show that the net circular polarization parameter depends on the four quantities v_B, θ, $\kappa_{\rm L}$, a and on the structure of the Zeeman pattern. Moreover, it is proportional to the line-of-sight velocity gradient $\mu\, w_{\rm A}^{(1)}$, so that its sign changes if the velocity gradient is inverted ($w_{\rm A}^{(1)} \rightarrow - \, w_{\rm A}^{(1)}$). Because of the involved structure of the expression, only a few results can be derived analytically. These are the following:

a) It is easily seen, with the help of Eqs. (9.32), that $\mathfrak{v} = 0$ for $\theta = 0^\circ$ and $\theta = 180^\circ$, and that

$$\mathfrak{v}\,(180^\circ - \theta) = - \, \mathfrak{v}\,(\theta) \,,$$

which implies in particular $\mathfrak{v}\,(\theta = 90^\circ) = 0$. In other words, under the assumption of weak velocity gradient considered here, the net circular polarization vanishes for longitudinal and transverse magnetic fields.

b) Under the limit of weak magnetic field ($\Delta\lambda_B \ll \Delta\lambda_{\rm D}$), the expansions in Eqs. (9.69) can be used. Recalling Eqs. (9.75) and (9.76) one obtains, to the lowest order in v_B

$$\mathfrak{v} \, = - \, \frac{1}{16} \, \mu \, \frac{w_{\rm A}^{(1)}}{c} \, \frac{\lambda_0}{\Delta\lambda_{\rm D}} \; \bar{g}\, \bar{G}^2 \;\; v_B^5 \;\; \sin^4\!\theta \cos\theta \;\; \frac{\mathcal{I}_5(\kappa_{\rm L}\,, a)}{\mathcal{I}_1(\kappa_{\rm L}\,, a)} \;\; , \tag{9.244}$$

where $\mathcal{I}_1(\kappa_{\rm L}\,, a)$ is defined in Eqs. (9.222) and

$$\mathcal{I}_5(\kappa_{\rm L}\,, a) = \int\limits_{-\infty}^{\infty} \frac{\kappa_{\rm L}^5 \left[\, (\ddot{\eta}\, \dot{\eta} \, + \ddot{\rho}\, \dot{\rho}) \, \dddot{\eta} \; - \; (\ddot{\eta}^{\,2} + \ddot{\rho}^{\,2}) \, \ddot{\eta} \; + \; (\dot{\eta}\, \ddot{\rho} - \ddot{\eta}\, \dot{\rho}) \, \dddot{\rho} \, \right]}{(1 + \kappa_{\rm L}\, \eta)^5} \;\; {\rm d}v \;\, ,$$

with η and ρ given by Eqs. (9.65) and with the dots denoting derivatives with respect to the reduced wavelength (cf. Eqs. (9.223)).

A numerical analysis of the integral $\mathcal{I}_5$ shows that, excluding weak lines ($\kappa_{\rm L}$ less than about 1.5), it is a positive quantity. This implies that the net circular polarization parameter has the same sign as the red wing of the V Stokes profile[1] for 'expanding' atmospheres ($w_{\rm A}^{(1)} > 0$), while it has the sign of the blue wing for 'compressing' atmospheres ($w_{\rm A}^{(1)} < 0$). It must be pointed out that magneto-optical terms play a crucial role in determining the value of $\mathfrak{v}$: neglect of these terms results in a sign switch of the integral $\mathcal{I}_5$ for practically all values of the parameters $\kappa_{\rm L}$ and a.

Another important consequence of Eq. (9.244) is the explicit dependence of $\mathfrak{v}$ on the inclination angle θ. The net circular polarization is maximum for

$$\theta_1 = \, \arccos\left(\frac{1}{\sqrt{5}}\right) \simeq \, 63^\circ.4 \,, \qquad\qquad \theta_2 = 180^\circ - \, \theta_1 \simeq \, 116^\circ.6 \;\, .$$

[1] According to Eq. (9.80), the sign of the red wing of the V profile is the sign of the quantity $(-\, \bar{g} \, \cos\theta)$.

Finally, the proportionality to the factor $\bar{g}\,\bar{G}^2$ shows that, for electric-dipole transitions of assigned effective Landé factor, the net circular polarization is maximum for Zeeman triplets (see Sect. 9.6).

c) Under the limit of very large magnetic field ($\Delta\lambda_B \gg \Delta\lambda_{\rm D}$), direct substitution of Eqs. (9.147) into Eq. (9.242) shows that $\mathfrak{v} = 0$.[1]

When the magnetic field is neither weak nor strong, one must resort to a numerical evaluation of Eq. (9.242). Some results are shown in Fig. 9.13 for the quantity $\mathfrak{v}/\mathfrak{v}_0$, where $\mathfrak{v}_0 = \mu\, w_{\rm A}^{(1)}\, \lambda_0 /(c\, \Delta\lambda_{\rm D})$ is the perturbative parameter ($\mathfrak{v}_0 \ll 1$ for Eq. (9.242) to hold).

Case ii) Given an arbitrary stellar atmosphere, let us consider the radiation flowing along a given outward direction, and let us suppose that the magnetic field vector at each point along the ray path is parallel to the propagation direction ($\theta = 0°$) or antiparallel ($\theta = 180°$). The results obtained in Sect. 9.10 and summarized by Eqs. (9.124) and (9.125) allow the net circular polarization parameter to be written in the form (see Eqs. (9.235), (9.210) and (9.219))

$$\mathfrak{v} \,=\, \sigma\, \frac{W_{\rm b} - W_{\rm r}}{W_{\rm b} + W_{\rm r}} \;, \tag{9.245}$$

where $W_{\rm b}$ and $W_{\rm r}$ are the equivalent widths of two 'fictitious' lines formed in the same atmosphere, and having the same $\kappa_{\rm L}$ as the real line, and absorption profiles $\eta_{\rm b}$ and $\eta_{\rm r}$, respectively; σ is a sign factor given by

$$\sigma = \begin{cases} +1 & \text{for } \theta = 0° \\ -1 & \text{for } \theta = 180° \;. \end{cases} \tag{9.246}$$

To analyze the behavior of the net circular polarization parameter, we consider the simplest case of a Zeeman triplet. In this case the expressions for $\eta_{\rm b}$ and $\eta_{\rm r}$ are particularly simple. From Eqs. (9.29) and (9.27) we have

$$\eta_{\rm b} = \frac{1}{\sqrt{\pi}}\; H(v - v_{\rm A} + g\, v_B\,, a)$$

$$\eta_{\rm r} = \frac{1}{\sqrt{\pi}}\; H(v - v_{\rm A} - g\, v_B\,, a)\;,$$

which show that $\eta_{\rm b}$ and $\eta_{\rm r}$ are identical profiles centered, respectively, at the wavelengths $\lambda_{\rm b}$ and $\lambda_{\rm r}$ given by (see Eqs. (9.26))

$$\lambda_{\rm b} \,=\, \lambda_0 \,+\, \Delta\lambda_{\rm A} \,-\, g\, \Delta\lambda_B$$

$$\lambda_{\rm r} \,=\, \lambda_0 \,+\, \Delta\lambda_{\rm A} \,+\, g\, \Delta\lambda_B \;,$$

[1] Note that the two conditions in Eqs. (9.138) are satisfied since, by assumption, the magnetic field is constant and large and the velocity gradient is small.

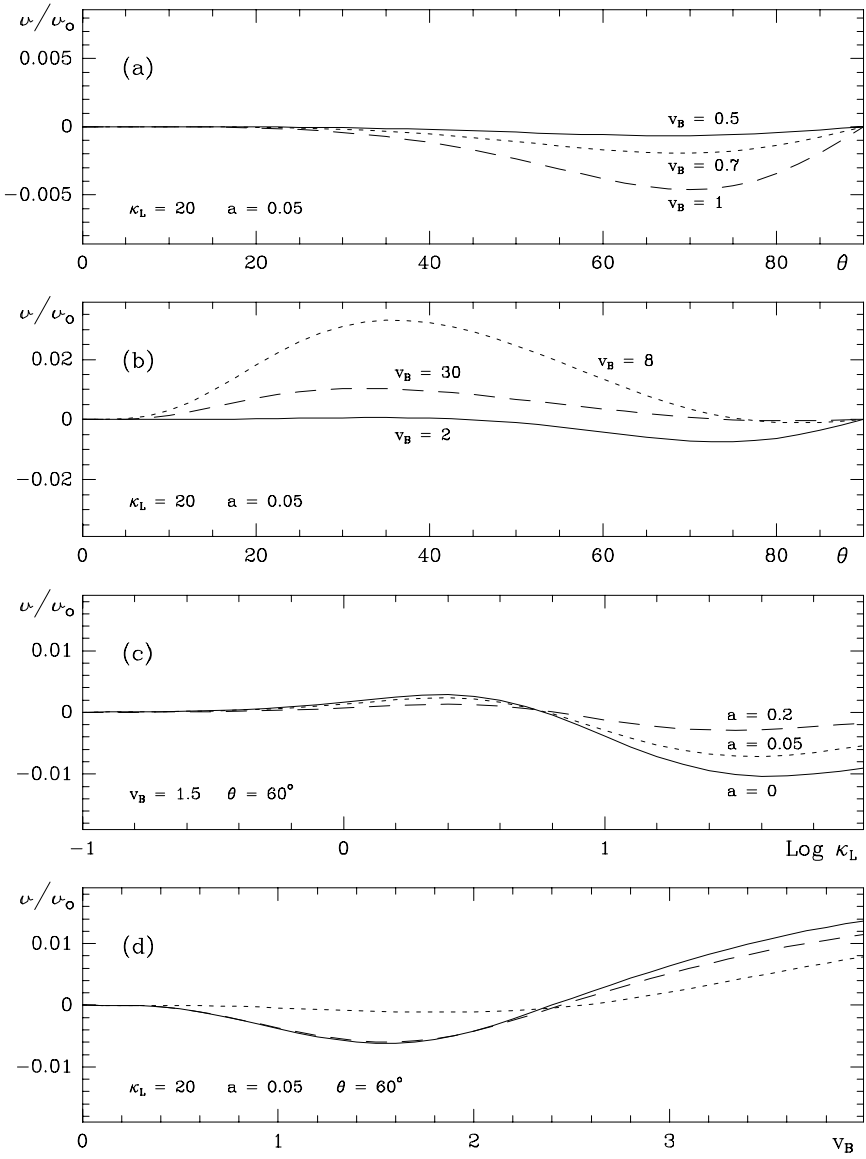

Fig.9.13. The net circular polarization computed from Eq.(9.242) is plotted versus different parameters. Panels (a), (b) and (c) refer to the normal Zeeman triplet ${}^1S_0 - {}^1P_1$. Panel (d) refers to three different transitions having $\bar{g} = 1$: ${}^1S_0 - {}^1P_1$ ($\bar{G} = 1$, full line), ${}^3P_1 - {}^3D_1$ ($\bar{G} = 0.250$, short dash), ${}^3D_2 - {}^3F_3$ ($\bar{G} = 0.997$, long dash).

where $\Delta\lambda_A = \lambda_0 \, w_A / c$.

Let us now suppose that both the magnetic field intensity and the line-of-sight component of the macroscopic velocity of the medium vary with optical depth. It follows that the wavelengths λ_b and λ_r are themselves functions of optical depth,

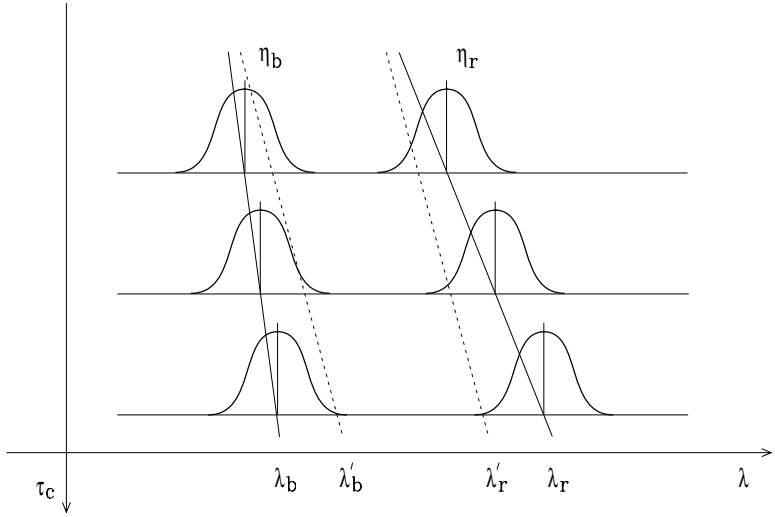

Fig.9.14. The combined effect of a velocity gradient and a magnetic field gradient on the absorption profiles η_b and η_r. For an 'expanding' atmosphere ($\Delta\lambda_A^{(1)} > 0$), at each τ_c the profiles would be centered at the wavelengths λ_b' and λ_r' (dashed lines) if the magnetic field were constant. If, on the contrary, the intensity of the magnetic field increases with τ_c ($\Delta\lambda_B^{(1)} > 0$), the profiles are centered at the wavelengths λ_b and λ_r (solid lines). The η_r profiles at different τ_c are less overlapped than the η_b profiles, thus $W_r > W_b$.

and this affects the equivalent widths of the two 'fictitious' lines. The effect will in general be different for W_b and W_r, which eventually results in a net amount of circular polarization.

General properties of $\mathfrak{v}$ cannot be established without a knowledge of the dependence of $\Delta\lambda_A$ and $\Delta\lambda_B$ on optical depth. Here we restrict attention to the simplest case of linear variations[1]

$$\begin{aligned} \Delta\lambda_A(\tau_c) &= \Delta\lambda_A^{(0)} + \Delta\lambda_A^{(1)}\ \tau_c \\ \Delta\lambda_B(\tau_c) &= \Delta\lambda_B^{(0)} + \Delta\lambda_B^{(1)}\ \tau_c\ , \end{aligned} \tag{9.247}$$

whence

$$\begin{aligned} \lambda_b &= \lambda_b^{(0)} + \left(\Delta\lambda_A^{(1)} - g\,\Delta\lambda_B^{(1)}\right)\tau_c \\ \lambda_r &= \lambda_r^{(0)} + \left(\Delta\lambda_A^{(1)} + g\,\Delta\lambda_B^{(1)}\right)\tau_c\ , \end{aligned} \tag{9.248}$$

where $\lambda_b^{(0)}$ and $\lambda_r^{(0)}$ are the values of λ_b and λ_r at $\tau_c = 0$.

If the atmosphere is 'standard' (i.e. if temperature is a monotonic increasing function of optical depth, so that absorption lines are formed), the equivalent width should be expected to be larger, the larger is the wavelength shift of the absorption profile between two assigned optical depths, because saturation effects are reduced (see Fig. 9.14). It follows that

[1] Note that $\Delta\lambda_B$ is, by definition, a positive quantity. If $\Delta\lambda_B^{(1)}$ is negative, Eqs. (9.247) lead to negative values of $\Delta\lambda_B$ for large τ_c. Obviously, we assume that these atmospheric layers do not contribute to the emerging radiation.

$$\begin{cases} W_{\rm r} > W_{\rm b} & \text{if} \quad |\,\Delta\lambda_{\rm A}^{(1)} + g\,\Delta\lambda_B^{(1)}\,| > |\,\Delta\lambda_{\rm A}^{(1)} - g\,\Delta\lambda_B^{(1)}\,| \\ W_{\rm r} = W_{\rm b} & \text{if} \quad |\,\Delta\lambda_{\rm A}^{(1)} + g\,\Delta\lambda_B^{(1)}\,| = |\,\Delta\lambda_{\rm A}^{(1)} - g\,\Delta\lambda_B^{(1)}\,| \\ W_{\rm r} < W_{\rm b} & \text{if} \quad |\,\Delta\lambda_{\rm A}^{(1)} + g\,\Delta\lambda_B^{(1)}\,| < |\,\Delta\lambda_{\rm A}^{(1)} - g\,\Delta\lambda_B^{(1)}\,| \,. \end{cases} \tag{9.249}$$

These relations show that: (a) $W_{\rm r} = W_{\rm b}$ if either $\Delta\lambda_{\rm A}^{(1)} = 0$ (no velocity gradient) or $\Delta\lambda_B^{(1)} = 0$ (no magnetic field gradient); (b) $W_{\rm r} > W_{\rm b}$ if $\Delta\lambda_{\rm A}^{(1)}$ and $g\,\Delta\lambda_B^{(1)}$ have the same sign; (c) $W_{\rm r} < W_{\rm b}$ if $\Delta\lambda_{\rm A}^{(1)}$ and $g\,\Delta\lambda_B^{(1)}$ have opposite signs. Equations (9.249) can be rewritten in the form[1]

$$\text{sign}\left(W_{\rm r} - W_{\rm b}\right) = \text{sign}\left[\, g\,\Delta\lambda_{\rm A}^{(1)}\,\Delta\lambda_B^{(1)}\,\right],$$

or, in terms of $\mathfrak{v}$

$$\text{sign}\,(\mathfrak{v}\,) = \text{sign}\left[-\sigma\, g\,\Delta\lambda_{\rm A}^{(1)}\,\Delta\lambda_B^{(1)}\,\right], \tag{9.250}$$

with σ defined in Eq. (9.246).

A quantitative confirmation of this result can be obtained by introducing further approximations. Following Sánchez Almeida et al. (1989), we assume both the velocity gradient and the magnetic field gradient to be small ($\Delta\lambda_{\rm A}^{(1)}$ and $\Delta\lambda_B^{(1)}$ much smaller than the Doppler width $\Delta\lambda_{\rm D}$), so that the transfer equation can be solved by a perturbative expansion. By further assuming a Milne-Eddington model atmosphere, one obtains a closed expression for the equivalent width. These calculations are carried out in App. 10 and show that, up to the second order, the equivalent widths $W_{\rm r}$ and $W_{\rm b}$ can be written in the form (see Eqs. (A10.8), (9.248) and (A10.7))

$$W_{\rm r,b} = \Delta\lambda_{\rm D}\,\frac{\beta}{1+\beta}\left[\mathcal{I}_1(\kappa_{\rm L}\,,a) + \left(\frac{\Delta\lambda_{\rm A}^{(1)} \pm g\,\Delta\lambda_B^{(1)}}{\Delta\lambda_{\rm D}}\right)^2 \mathcal{I}_6(\kappa_{\rm L}\,,a)\right],$$

where the plus and minus signs refer to the red and blue component respectively, $\mathcal{I}_1(\kappa_{\rm L}\,,a)$ is given by Eqs. (9.222) and $\mathcal{I}_6(\kappa_{\rm L}\,,a)$ by Eq. (A10.9). Substitution into Eq. (9.245) yields, to the lowest order

$$\mathfrak{v} = -\,2\,\sigma\, g\;\frac{\Delta\lambda_{\rm A}^{(1)}\,\Delta\lambda_B^{(1)}}{\Delta\lambda_{\rm D}^2}\;\frac{\mathcal{I}_6(\kappa_{\rm L}\,,a)}{\mathcal{I}_1(\kappa_{\rm L}\,,a)}\;,$$

which confirms Eq. (9.250) since both $\mathcal{I}_1(\kappa_{\rm L}\,,a)$ and $\mathcal{I}_6(\kappa_{\rm L}\,,a)$ are positive. Note that this expression is valid irrespective of the magnetic field strength: only the gradients ($\Delta\lambda_{\rm A}^{(1)}$ and $\Delta\lambda_B^{(1)}$) are required to be small. A similar expression has been given by Pavlov and Shibanov (1978).

Case iii) Let us consider the following discontinuous model atmosphere. A thin slab with a vertical velocity field is superposed on an arbitrary, static atmosphere;

[1] A similar expression has been derived by Solanki and Pahlke (1988).

both the slab and the underlying atmosphere are magnetized, the magnetic field vectors being in general different.[1] We restrict attention to the radiation travelling in the vertical, outward direction, and denote by $t_{\rm s}$ the continuum optical thickness of the slab ($t_{\rm s} \ll 1$), by $w_{\rm A}^{(\rm s)}$ the line-of-sight component of the velocity field (defined, as usual, according to the astrophysical convention), and by $\vec{B}_{\rm s} \equiv (B_{\rm s}\,, \theta_{\rm s}\,, \chi_{\rm s})$ and $\vec{B} \equiv (B, \theta, \chi)$, respectively, the magnetic field vectors in the slab and in the underlying atmosphere.

The transfer of radiation across the slab is described by Eq. (9.90), where the propagation matrix $\boldsymbol{C}^{(\rm s)}$ and the emission vector $\boldsymbol{j}^{(\rm s)}$ can be considered constant because $t_{\rm s} \ll 1$. The emerging Stokes parameters can be easily calculated by integration of Eq. (9.90)

$$\boldsymbol{I}(0) = \left[\, \boldsymbol{1} \,-\, t_{\rm s}\, \boldsymbol{C}^{(\rm s)} \,\right] \boldsymbol{I}^{(\rm b)} \,+\, t_{\rm s}\, \boldsymbol{j}^{(\rm s)}\,, \tag{9.251}$$

where $\boldsymbol{I}^{(\rm b)}$ is the boundary Stokes vector resulting from the lower atmosphere.

As far as the V Stokes parameter is concerned, the first and third term in Eq. (9.251) give rise to antisymmetrical profiles that make no contribution to the line-integrated circular polarization, which reduces to

$$\mathcal{V} = -\, t_{\rm s} \int_{-\infty}^{\infty} \sum_{i=0}^{3} C_{3i}^{(\rm s)}\; I_i^{(\rm b)}\; {\rm d}\lambda\,.$$

To the lowest order in $t_{\rm s}$, the net circular polarization parameter is therefore (see Eqs. (9.235), (9.219), (9.91) and (9.39))

$$\mathfrak{v} \,=\, -\, t_{\rm s}\; \kappa_{\rm L}^{(\rm s)}\; \frac{\displaystyle\int_{-\infty}^{\infty} \left[h_V^{(\rm s)}\, I^{(\rm b)} \,+\, r_U^{(\rm s)}\, Q^{(\rm b)} \,-\, r_Q^{(\rm s)}\, U^{(\rm b)} \,+\, h_I^{(\rm s)}\, V^{(\rm b)} \right] {\rm d}\lambda}{\displaystyle\int_{-\infty}^{\infty} \left[I_{\rm c}^{(\rm b)} - I^{(\rm b)} \right] {\rm d}\lambda}\;, \tag{9.252}$$

where $I_{\rm c}^{(\rm b)}$ is the continuum intensity emerging from the underlying atmosphere. Note that the Stokes profiles $I^{(\rm b)}$, $Q^{(\rm b)}$, $U^{(\rm b)}$, $V^{(\rm b)}$ are centered at the rest wavelength λ_0, while the profiles $h_V^{(\rm s)}$, $r_U^{(\rm s)}$, $r_Q^{(\rm s)}$, $h_I^{(\rm s)}$ are centered at the wavelength

$$\lambda_0 \,+\, \Delta\lambda_{\rm A}^{(\rm s)} \,=\, \lambda_0 \left(1 + \frac{w_{\rm A}^{(\rm s)}}{c} \right).$$

The symmetry properties (9.47) and (9.54) show that $\mathfrak{v}$ is zero both when $\Delta\lambda_{\rm A}^{(\rm s)}$ is zero and when it is so large that the profiles $I^{(\rm b)}, \ldots, V^{(\rm b)}$ and $h_V^{(\rm s)}, \ldots, h_I^{(\rm s)}$ do

[1] This model was proposed by Illing et al. (1975) to explain the broad-band circular polarization observed in sunspots, and it is often referred to as the *Illing* (or *Illing, Landman and Mickey*) *model*. Some quantitative estimates of the net circular polarization produced by the model have been given by Auer and Heasley (1978).

not overlap. It is therefore to be expected that the maximum value of $\mathfrak{v}$ is attained when $\Delta\lambda_{\rm A}^{(\rm s)}$ and the widths of the profiles are comparable.

The integrand in the numerator of Eq. (9.252) is rather involved and it is practically impossible to obtain any quantitative conclusion about $\mathfrak{v}$ without introducing further approximations. Even if the Unno-Rachkovsky solution is used to express the boundary Stokes vector, the integrand remains too involved. Therefore, we make the drastic approximation that the boundary Stokes profiles are described by the Seares formulae (we recall that the Unno-Rachkovsky formulae reduce to the Seares formulae for weak spectral lines, cf. Sect. 9.13). Substituting Eqs. (9.149) – with $\mu = 1$ – into Eq. (9.252), we obtain

$$\mathfrak{v} \,=\, \frac{t_{\rm s}\,\kappa_{\rm L}^{(\rm s)}}{\Delta\lambda_{\rm D}} \int\limits_{-\infty}^{\infty} \Big[h_V^{(\rm s)}\, h_I \,+\, r_U^{(\rm s)}\, h_Q \,-\, r_Q^{(\rm s)}\, h_U \,+\, h_I^{(\rm s)}\, h_V \Big]\, {\rm d}\lambda$$

where the quantities $h_I\,,\ \ldots,\ h_V$ and the Doppler width $\Delta\lambda_{\rm D}$ refer to the lower atmosphere. Use of Eqs. (9.32) yields, with evident notations

$$\begin{aligned}
\mathfrak{v} \,=\, & \frac{1}{4}\,\frac{t_{\rm s}\,\kappa_{\rm L}^{(\rm s)}}{\Delta\lambda_{\rm D}} \\
\times \Bigg\{ & \frac{1}{2}\Big[\cos\theta_{\rm s}\,(1+\cos^2\theta) + \cos\theta\,(1+\cos^2\theta_{\rm s})\Big] \int\limits_{-\infty}^{\infty} \Big[\eta_{\rm r}^{(\rm s)}\eta_{\rm r} - \eta_{\rm b}^{(\rm s)}\eta_{\rm b}\Big]{\rm d}\lambda \\
& + \cos\theta_{\rm s}\sin^2\theta \int\limits_{-\infty}^{\infty} \Big[\eta_{\rm r}^{(\rm s)} - \eta_{\rm b}^{(\rm s)}\Big]\eta_{\rm p}\,{\rm d}\lambda \,+\, \cos\theta\sin^2\theta_{\rm s} \int\limits_{-\infty}^{\infty} \eta_{\rm p}^{(\rm s)}\Big[\eta_{\rm r} - \eta_{\rm b}\Big]{\rm d}\lambda \\
& + \frac{1}{2}\Big[\cos\theta_{\rm s}\,(1+\cos^2\theta) - \cos\theta\,(1+\cos^2\theta_{\rm s})\Big] \int\limits_{-\infty}^{\infty} \Big[\eta_{\rm r}^{(\rm s)}\eta_{\rm b} - \eta_{\rm b}^{(\rm s)}\eta_{\rm r}\Big]{\rm d}\lambda \\
& - \sin^2\theta_{\rm s}\sin^2\theta\sin 2(\chi-\chi_{\rm s}) \int\limits_{-\infty}^{\infty} \left[\rho_{\rm p}^{(\rm s)} - \frac{\rho_{\rm b}^{(\rm s)} + \rho_{\rm r}^{(\rm s)}}{2}\right]\left[\eta_{\rm p} - \frac{\eta_{\rm b}+\eta_{\rm r}}{2}\right]{\rm d}\lambda \Bigg\}. \qquad (9.253)
\end{aligned}$$

Two general properties of $\mathfrak{v}$ follow from this expression. The first is that magneto-optical effects are important only if the azimuth angles of the magnetic field in the slab and in the underlying atmosphere are different. The second, which can be easily deduced with the help of Eqs. (9.46), is that $\mathfrak{v}$ is zero if the magnetic field gradient is zero ($\vec{B}_{\rm s} = \vec{B}$), even in the presence of a velocity gradient ($w_{\rm A}^{(\rm s)} \neq 0$). This could seem inconsistent with the results of Case i) considered above, but is really quite logical because saturation effects are neglected in the present model: the slab is by assumption optically thin and the Seares formulae describe a weak, unsaturated spectral line.

In the following we analyze separately the effects of the velocity gradient combined with a discontinuity at the boundary layer of: (a) the modulus of the

magnetic field (*ΔB-effect*); (b) the inclination angle (*Δθ-effect*); (c) the azimuth angle (*Δχ-effect*).

In case (a), being $\theta_{\rm s} = \theta$ and $\chi_{\rm s} = \chi$, only the first two lines of Eq. (9.253) are non-zero. Thus we obtain

$$\mathfrak{v} = \frac{1}{4}\,\frac{t_{\rm s}\,\kappa_{\rm L}^{(\rm s)}}{\Delta\lambda_{\rm D}}\,\cos\theta\,\left\{(1+\cos^2\theta)\int_{-\infty}^{\infty}\left[\eta_{\rm r}^{(\rm s)}\eta_{\rm r} - \eta_{\rm b}^{(\rm s)}\eta_{\rm b}\right]{\rm d}\lambda\right.$$
$$\left. + \sin^2\theta\int_{-\infty}^{\infty}\left[\eta_{\rm r}^{(\rm s)}\eta_{\rm p} + \eta_{\rm p}^{(\rm s)}\eta_{\rm r} - \eta_{\rm b}^{(\rm s)}\eta_{\rm p} - \eta_{\rm p}^{(\rm s)}\eta_{\rm b}\right]{\rm d}\lambda\right\}. \quad (9.254)$$

For simplicity, we restrict attention to Zeeman triplets and we assume that the Doppler width and the damping constant in the slab and in the lower atmosphere are the same. The integrals in Eq. (9.254) can be performed analytically via Eqs. (5.64). Using Eqs. (9.29) and (9.27), and denoting by $\Delta\lambda_B^{(\rm s)}$ and $\Delta\lambda_B$ the Zeeman splittings in the slab and in the atmosphere, respectively, we get

$$\mathfrak{v} = \frac{1}{4\sqrt{2\pi}}\,t_{\rm s}\,\kappa_{\rm L}^{(\rm s)}\,\cos\theta$$
$$\times\left\{(1+\cos^2\theta)\left[H(\hat{v}_{\rm rr}\,,\hat{a}) - H(\hat{v}_{\rm bb}\,,\hat{a})\right]\right.$$
$$\left. + \sin^2\theta\left[H(\hat{v}_{\rm rp}\,,\hat{a}) + H(\hat{v}_{\rm pr}\,,\hat{a}) - H(\hat{v}_{\rm bp}\,,\hat{a}) - H(\hat{v}_{\rm pb}\,,\hat{a})\right]\right\}, \quad (9.255)$$

where (some additional symbols are defined for future reference)

$$\hat{v}_{\rm rr} = \frac{1}{\sqrt{2}\,\Delta\lambda_{\rm D}}\left[\Delta\lambda_{\rm A}^{(\rm s)} + g\,\left(\Delta\lambda_B^{(\rm s)} - \Delta\lambda_B\right)\right]$$
$$\hat{v}_{\rm bb} = \frac{1}{\sqrt{2}\,\Delta\lambda_{\rm D}}\left[\Delta\lambda_{\rm A}^{(\rm s)} - g\,\left(\Delta\lambda_B^{(\rm s)} - \Delta\lambda_B\right)\right]$$
$$\hat{v}_{\rm rp} = \frac{1}{\sqrt{2}\,\Delta\lambda_{\rm D}}\left[\Delta\lambda_{\rm A}^{(\rm s)} + g\,\Delta\lambda_B^{(\rm s)}\right]$$
$$\hat{v}_{\rm bp} = \frac{1}{\sqrt{2}\,\Delta\lambda_{\rm D}}\left[\Delta\lambda_{\rm A}^{(\rm s)} - g\,\Delta\lambda_B^{(\rm s)}\right]$$
$$\hat{v}_{\rm pr} = \frac{1}{\sqrt{2}\,\Delta\lambda_{\rm D}}\left[\Delta\lambda_{\rm A}^{(\rm s)} - g\,\Delta\lambda_B\right]$$
$$\hat{v}_{\rm pb} = \frac{1}{\sqrt{2}\,\Delta\lambda_{\rm D}}\left[\Delta\lambda_{\rm A}^{(\rm s)} + g\,\Delta\lambda_B\right]$$
$$\hat{v}_{\rm rb} = \frac{1}{\sqrt{2}\,\Delta\lambda_{\rm D}}\left[\Delta\lambda_{\rm A}^{(\rm s)} + g\,\left(\Delta\lambda_B^{(\rm s)} + \Delta\lambda_B\right)\right]$$

$$\hat{v}_{\rm br} = \frac{1}{\sqrt{2}\,\Delta\lambda_{\rm D}}\left[\Delta\lambda_{\rm A}^{(\rm s)} - g\left(\Delta\lambda_B^{(\rm s)} + \Delta\lambda_B\right)\right]$$

$$\hat{v}_{\rm pp} = \frac{1}{\sqrt{2}\,\Delta\lambda_{\rm D}}\;\Delta\lambda_{\rm A}^{(\rm s)}$$

$$\hat{a} \,=\, \sqrt{2}\;a\;.$$

If we separate the contributions of the first and second line of Eq. (9.255) by writing

$$\mathfrak{v} \,=\, (1+\cos^2\theta)\;\mathfrak{v}^{(1)} \,+\, \sin^2\theta\;\;\mathfrak{v}^{(2)}\;, \tag{9.256}$$

the sign of $\mathfrak{v}^{(1)}$ can be easily deduced. Since $H(v,a)$ is a monotonically decreasing function of $|v|$, we have

$$\mathrm{sign}\left(\mathfrak{v}^{(1)}\right) = \mathrm{sign}\left[\cos\theta\; g\;\Delta\lambda_{\rm A}^{(\rm s)}\;\left(\Delta\lambda_B - \Delta\lambda_B^{(\rm s)}\right)\right], \tag{9.257}$$

which agrees with the result obtained previously for continuous gradients and vertical magnetic field (cf. Eq. (9.250)).[1] For slightly inclined magnetic field ($\sin^2\theta \ll 1$), Eq. (9.257) gives the sign of the net circular polarization. By contrast, no general rule can be established for the sign of $\mathfrak{v}^{(2)}$. When either $\Delta\lambda_B^{(\rm s)} = 0$ (non-magnetic slab superposed on a magnetic atmosphere) or $\Delta\lambda_B = 0$ (magnetic slab superposed on a non-magnetic atmosphere), it can be easily shown that $\mathfrak{v}^{(2)} = \mathfrak{v}^{(1)}$. However, there are cases where the signs of $\mathfrak{v}^{(2)}$ and $\mathfrak{v}^{(1)}$ are opposite.

Let us now consider the $\Delta\theta$-effect. Being now $B_{\rm s} = B$ and $\chi_{\rm s} = \chi$, only the second and third line of Eq. (9.253) are non-zero. Under the same assumptions as before (Zeeman triplet, same Doppler width and damping constant in the slab and in the atmosphere), one obtains

$$\begin{aligned}\mathfrak{v} \,=\, & \frac{1}{4\sqrt{2\pi}}\;\;t_{\rm s}\;\kappa_{\rm L}^{(\rm s)} \\ & \times\left\{\left[\cos\theta_{\rm s}\sin^2\theta - \cos\theta\sin^2\theta_{\rm s}\,\right]\left[\,H(\hat{v}_{\rm rp}\,,\hat{a}) - H(\hat{v}_{\rm bp}\,,\hat{a})\,\right]\right. \\ & \left. \quad + \frac{1}{2}\left[\,\cos\theta_{\rm s}\,(1+\cos^2\theta) - \cos\theta\,(1+\cos^2\theta_{\rm s})\,\right]\left[\,H(\hat{v}_{\rm rb}\,,\hat{a}) - H(\hat{v}_{\rm br}\,,\hat{a})\,\right]\right\}.\end{aligned}$$

It can be easily shown that both the factors containing $\theta_{\rm s}$ and θ are positive when $\theta > \theta_{\rm s}$ and negative when $\theta < \theta_{\rm s}$, and that both the factors containing the Voigt functions are positive when $g\;\Delta\lambda_{\rm A}^{(\rm s)} < 0$ and negative when $g\;\Delta\lambda_{\rm A}^{(\rm s)} > 0$. Therefore, we have the sign rule

$$\mathrm{sign}\,(\mathfrak{v}\,) = \mathrm{sign}\left[-\,g\;\Delta\lambda_{\rm A}^{(\rm s)}\;\left(\theta - \theta_{\rm s}\right)\right]. \tag{9.258}$$

[1] Note that positive values of $\Delta\lambda_B^{(1)}$ and $\Delta\lambda_{\rm A}^{(1)}$ in Eq. (9.250) are equivalent to $\Delta\lambda_B > \Delta\lambda_B^{(\rm s)}$ and $\Delta\lambda_{\rm A}^{(\rm s)} < 0$ in Eq. (9.257).

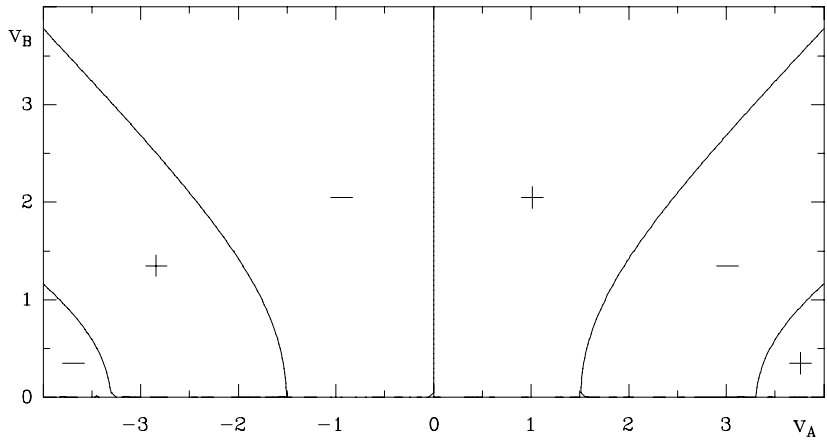

Fig.9.15. Contour plot of the function in square brackets of Eq.(9.259) in the plane $(v_{\rm A}\,, v_B) = (\Delta\lambda_{\rm A}^{\rm (s)}/\Delta\lambda_{\rm D}\,, \Delta\lambda_B/\Delta\lambda_{\rm D})$. The plus and minus signs denote the regions where the function is positive or negative. The value of the damping constant is $a = 0$ (the contour plot depends very slightly on a).

It is interesting to compare this relation with Eq. (9.257). It appears that a magnetic field of constant orientation whose modulus increases with optical depth, and a magnetic field of constant modulus whose longitudinal component increases (in absolute value) with optical depth, produce the same effect on the net circular polarization parameter. This result has been deduced by Solanki and Montavon (1993) with numerical computations. Sánchez Almeida and Lites (1992), who proposed for the θ-gradient effect the name *$\Delta\theta$-mechanism*, pointed out that it is more effective than the ΔB-effect when the magnetic field is highly inclined, while the opposite holds when the field is slightly inclined.

Finally, we consider the $\Delta\chi$-effect.[1] In this case, being $B_{\rm s} = B$ and $\theta_{\rm s} = \theta$, only the fourth line of Eq. (9.253) is non-zero. Under the same assumptions as before, and using Eqs. (5.64) to evaluate the convolutions of Voigt functions and dispersion profiles, we obtain the expression

$$\mathfrak{v} = \frac{1}{4\sqrt{2\pi}}\; t_{\rm s}\,\kappa_{\rm L}^{\rm (s)}\;\sin^4\theta\,\sin 2(\chi-\chi_{\rm s})$$

$$\times\left[\frac{3}{2}\,L(\hat{v}_{\rm pp}\,,\hat{a}) - L(\hat{v}_{\rm rp}\,,\hat{a}) - L(\hat{v}_{\rm bp}\,,\hat{a}) + \frac{1}{4}\,L(\hat{v}_{\rm rb}\,,\hat{a}) + \frac{1}{4}\,L(\hat{v}_{\rm br}\,,\hat{a})\right]. \quad (9.259)$$

It is important to remark that the presence of the factor $\sin^4\theta$ in this equation makes the $\Delta\chi$-effect particularly sensitive to transverse magnetic fields.

A numerical analysis of the term in square brackets of Eq. (9.259) is presented in Fig. 9.15, which shows that no simple rule can be established for the sign of this

[1] The possibility that this mechanism might be effective in sunspots was first suggested by Makita (1986).

term. However, if we exclude values of $|\Delta\lambda_{\rm A}^{(\rm s)}|$ larger than approximately 1.5 $\Delta\lambda_{\rm D}$, we get the rule

$$\text{sign}\,(\mathfrak{v}\,) = \text{sign}\left[\,\Delta\lambda_{\rm A}^{(\rm s)}\,\left(\chi - \chi_{\rm s}\right)\,\right]. \qquad (9.260)$$

Contrary to Eqs. (9.257) and (9.258), the sign rule (9.260) is independent of the Landé factor. This property enables in principle the $\Delta\chi$-effect to be disentangled from the two previous effects by using a couple of spectral lines having a positive and a negative Landé factor respectively. According to Eq. (9.260), the sign of $\mathfrak{v}$ depends on the sign of the velocity gradient and on the twisting direction of the magnetic field. Thus we have the following rule for the $\Delta\chi$-effect: an expanding atmosphere ($\Delta\lambda_{\rm A}^{(\rm s)} < 0$) and a magnetic field winding as the thread of a right-handed screw ($\chi < \chi_{\rm s}$) give rise to positive net circular polarization.

The results presented in this section show that the phenomenon of net circular polarization in spectral lines is extremely complex. Furthermore, it should be stressed that the net circular polarization discussed above is due to velocity and/or magnetic field gradients only, while blends and atomic orientation have not been considered.

Blends between independent lines, or between different components of a multiplet, can indeed produce net circular polarization (cf. Figs. 9.9 and 9.18). Further remarks on this topic are presented in App. 11. The effect of atomic orientation will be discussed in Sect. 10.5. We just point out that atomic orientation can be set up both in isolated atomic levels (through a mechanism which involves the simultaneous presence of magnetic fields and velocity gradients; see Landi Degl'Innocenti, 1985b) and in fine-structured or hyperfine-structured atomic levels (through a mechanism of 'alignment-to-orientation conversion' due to anisotropic illumination; see Sect. 10.20). Net circular polarization in spectral lines can also be produced by velocity-magnetic field correlations in stochastic media. This phenomenon will be discussed in Sect. 9.24.

9.22. The Importance of Magneto-Optical Effects

In the early days of polarized radiative transfer, the importance of magneto-optical effects was basically underestimated and, in many applications, these effects were simply neglected. Now we know that they are a fundamental ingredient of polarized radiative transfer, and we have seen that they arise quite naturally both in the classical derivation (Sects. 5.1-5.2) and in the quantum derivation (Sects. 6.6-6.7) of the transfer equation.

However, since this equation considerably simplifies when magneto-optical effects are ignored, it is important to point out those physical situations where such approximation is justified. These are the following:

a) *Weak field limit* ($\Delta\lambda_B \ll \Delta\lambda_{\rm D}$).
Extension of the perturbative scheme described in Sect. 9.6 up to the fifth order

shows that magneto-optical effects yield, in general, corrections of order

$$\left(\frac{\Delta\lambda_B}{\Delta\lambda_\mathrm{D}}\right)^5, \qquad \left(\frac{\Delta\lambda_B}{\Delta\lambda_\mathrm{D}}\right)^4, \qquad \left(\frac{\Delta\lambda_B}{\Delta\lambda_\mathrm{D}}\right)$$

on the Stokes parameters I, V, and Q-U, respectively.

b) *Intense field limit ($\Delta\lambda_B \gg \Delta\lambda_\mathrm{D}$).*
In Sect. 9.12 it has been shown that under this limit, and under the supplementary condition of a magnetic field having the same direction at any optical depth ($\theta =$ const., $\chi =$ const.), magneto-optical effects can be neglected.

c) *Longitudinal field ($\theta = 0^\circ$ or 180°) or transverse field ($\theta = 90^\circ$).*
In these special cases magneto-optical effects do not influence the Stokes parameters, as shown in Sect. 9.10. When $\theta = 90^\circ$, however, the supplementary condition of constant azimuth ($\chi =$ const.) is also necessary.

Except for the particular cases listed above, magneto-optical effects must be taken into account and give rise to characteristic signatures in the Stokes parameters profiles. A comparison between typical profiles emerging from a Milne-Eddington atmosphere, computed with and without magneto-optical effects, is shown in Fig. 9.16. From the figure, and from similar results obtained for different values of the relevant parameters, the following qualitative conclusions can be drawn:
i) As pointed out by Wittmann (1971), magneto-optical effects can introduce a reversal in the V profile around line center (*magneto-optical undulation*). This feature is rather sensitive to the intensity and inclination of the magnetic field, and also to the structure of the Zeeman pattern: in the case of triplets, it appears only for $g\,\Delta\lambda_B$ of the order or larger than $2\,\Delta\lambda_\mathrm{D}$ and for rather inclined fields (approximately $40^\circ \leq \theta \leq 140^\circ$ – see e.g. panel (b) of Fig. 9.5).
ii) The Stokes parameters which are relatively more affected by magneto-optical effects are the linear polarization parameters Q and U. This point is better illustrated by considering (under the assumption that the azimuth of the magnetic field is constant with optical depth) $\tilde{Q}$ and $\tilde{U}$, the Stokes parameters defined in the 'preferred frame'. The profile $\tilde{U}$ vanishes at all wavelengths if magneto-optical effects are neglected (because the transfer equation for $\tilde{U}$ is decoupled from the others, see Eq. (9.35)). As a rule, the sign of $\tilde{U}$ is the same at all wavelengths and depends on the magnetic field polarity, being positive for $0^\circ \leq \theta \leq 90^\circ$ and negative for $90^\circ \leq \theta \leq 180^\circ$.[1] Magneto-optical effects also change the shape of $\tilde{Q}$ by reducing, in general, the amplitude of its central depression and by moving the lateral lobes closer to line center.

The influence of magneto-optical effects on the linear polarization profiles can also be illustrated by diagrams like the one shown in Fig. 9.17. Proceeding from the line center to the line wing, the representative point draws in the Q-U plane a curve that is typical of magneto-optical effects. If these were neglected, the curve would

[1] Exceptions to this simple rule can be found, especially for 'exotic' Zeeman patterns. In some cases $\tilde{U}$ can even change sign across the line profile.

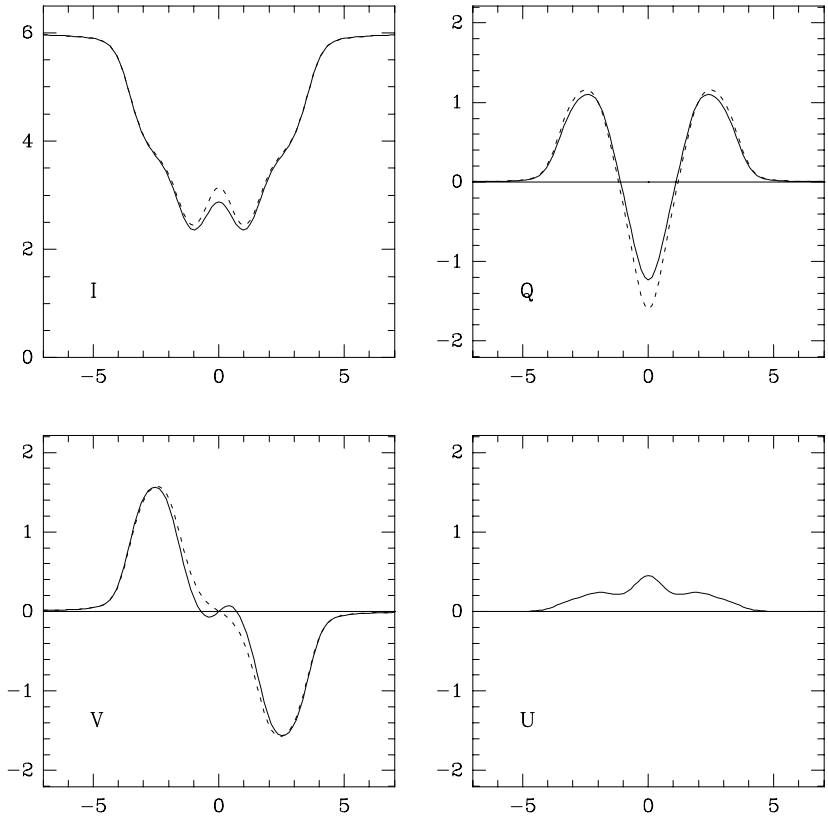

Fig.9.16. The Stokes parameters profiles, as given by the Unno-Rachkovsky solutions (9.110), are plotted against reduced wavelength for the normal Zeeman triplet ${}^1\mathrm{S}_0 - {}^1\mathrm{P}_1$. The profiles are normalized to B_0 and the relevant parameters have the same values as in the 'standard case' (see Fig.9.5) except for $v_B = 2$. Full line: with magneto-optical effects; dashed line: without magneto-optical effects (U is identically zero).

reduce – for $\chi = \text{const.}$ – to a straight line through the origin, partially covered twice, having angular coefficient $\tan 2\chi$. These diagrams, introduced by Kawakami (1983), clearly show that the importance of magneto-optical effects decreases in the wings.

iii) Finally, magneto-optical effects have also a (small) influence on the intensity profile. By scrambling the polarization among Q, U, and V, they reduce the importance of saturation, which eventually leads to a deeper profile and to a slight increase of the equivalent width.

The influence of magneto-optical effects is even more pronounced on the net (line-integrated) polarization. As evident from our thorough discussion in Sect. 9.20, net linear polarization is dramatically affected by magneto-optical effects. Referring for instance to Fig. 9.12, all the representative points would lie on the $\tilde{\mathfrak{q}}$-axis if magneto-optical effects were neglected. Similar conclusions can be drawn for the net circular polarization. In the absence of magneto-optical effects, the net circular

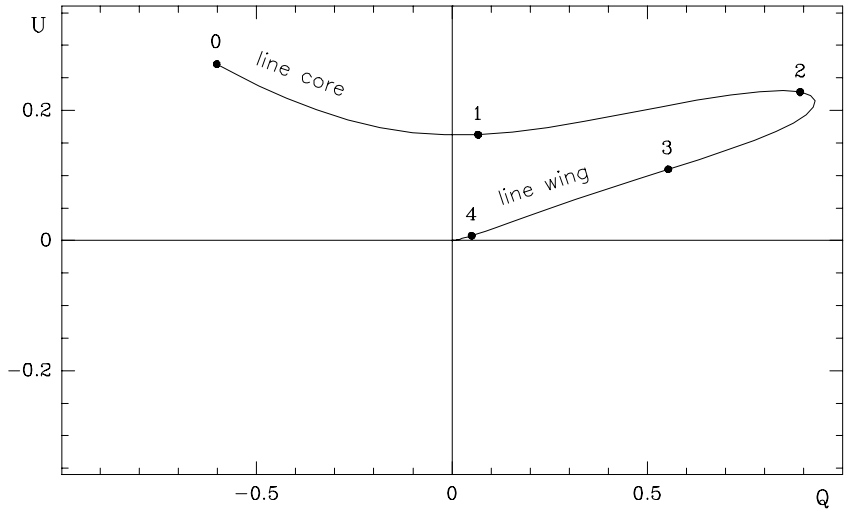

Fig.9.17. Polarization diagram ($U(\lambda)$ vs. $Q(\lambda)$) for the normal Zeeman triplet ${}^1\mathrm{S}_0 - {}^1\mathrm{P}_1$. The Stokes parameters are computed from the Unno-Rachkovsky solutions (9.110) with the 'standard' values of the relevant parameters (see Fig.9.5). The dots indicate distance from line center in Doppler width units.

polarization obtained for small velocity gradient and weak magnetic field would have the opposite sign (see the comments following Eq. (9.244)), and the $\Delta\chi$-effect discussed at the end of Sect. 9.21 would simply disappear.

9.23. Transfer Equation for Fine-Structured and Hyperfine-Structured Lines

The transfer equation that we have considered throughout this chapter refers to an isolated spectral line originating in the transition between two atomic levels whose magnetic splitting is described by the Zeeman effect regime. For a line multiplet composed of different fine-structure or hyperfine-structure components, the equation must be modified. The modifications do not concern, of course, the form of the transfer equation – which is still given by Eq. (6.85) – but only its coefficients: in other words, we have to find the new expressions for the elements of the propagation matrix and of the emission vector.

Let us consider the multi-term model atom discussed in Sect. 7.5 embedded in an arbitrary magnetic field. The radiative transfer coefficients, expressed in the energy-eigenvector representation of the atomic density operator, are given by Eqs. (7.35). Similarly to Sect. 9.1, we assume that only two atomic terms contribute to absorption and emission at frequency ν (the analogue of the isolated spectral line hypothesis), and that no atomic polarization is present in either term. The former assumption implies that the summation over the terms in Eqs. (7.35) is limited to one lower term ($\beta_\ell L_\ell S$) and one upper term ($\beta_u L_u S$); the latter implies

the substitutions

$$\mathcal{N}\,(2L_\ell+1)\;\rho_{\beta_\ell L_\ell S}(j_\ell M_\ell, j'_\ell M'_\ell) \rightarrow \frac{\mathbb{N}_\ell}{2S+1}\;\delta_{j_\ell j'_\ell}\;\delta_{M_\ell M'_\ell}$$

$$\mathcal{N}\,(2L_u+1)\;\rho_{\beta_u L_u S}(j_u M_u, j'_u M'_u) \rightarrow \frac{\mathbb{N}_u}{2S+1}\;\delta_{j_u j'_u}\;\delta_{M_u M'_u}\;,$$

where $\mathbb{N}_\ell$ and $\mathbb{N}_u$ are the overall number of atoms per unit volume in the lower and upper term, respectively.

Using these assumptions, and recalling Eq. (5.148), Eq. (7.35a) reduces to the following

$$\begin{aligned}
\eta_i^{\mathrm{A}}(\nu,\vec{\Omega}) = {} & \frac{h\nu}{4\pi}\;\frac{\mathbb{N}_\ell}{2S+1}\;B(\beta_\ell L_\ell S \rightarrow \beta_u L_u S) \\
& \times \sum_{j_\ell J_\ell J'_\ell\, j_u J_u J'_u} \sum_{M_\ell M_u\, q} 3\, C^{j_\ell}_{J_\ell}(\beta_\ell L_\ell S, M_\ell)\, C^{j_\ell}_{J'_\ell}(\beta_\ell L_\ell S, M_\ell) \\
& \times C^{j_u}_{J_u}(\beta_u L_u S, M_u)\, C^{j_u}_{J'_u}(\beta_u L_u S, M_u) \sqrt{(2J_\ell+1)(2J'_\ell+1)(2J_u+1)(2J'_u+1)} \\
& \times \begin{pmatrix} J_u & J_\ell & 1 \\ -M_u & M_\ell & -q \end{pmatrix} \begin{pmatrix} J'_u & J'_\ell & 1 \\ -M_u & M_\ell & -q \end{pmatrix} \begin{Bmatrix} L_u & L_\ell & 1 \\ J_\ell & J_u & S \end{Bmatrix} \begin{Bmatrix} L_u & L_\ell & 1 \\ J'_\ell & J'_u & S \end{Bmatrix} \\
& \times\; \mathcal{T}_{qq}(i,\vec{\Omega})\;\phi(\nu_{\beta_u L_u S j_u M_u, \beta_\ell L_\ell S j_\ell M_\ell} - \nu)\;,
\end{aligned}$$

which can be cast into a simpler form by introducing the normalized strengths of the multiplet components defined in Eq. (3.64). Taking into account the symmetry properties of the 3-j and 6-j coefficients, we have

$$\begin{aligned}
\eta_i^{\mathrm{A}}(\nu,\vec{\Omega}) = {} & \frac{h\nu}{4\pi}\,\mathbb{N}_\ell\;B(\beta_\ell L_\ell S \rightarrow \beta_u L_u S) \\
& \times \sum_{j_\ell j_u} \sum_{M_\ell M_u\, q} S_q^{j_\ell M_\ell, j_u M_u}\;\mathcal{T}_{qq}(i,\vec{\Omega})\;\phi(\nu_{\beta_u L_u S j_u M_u, \beta_\ell L_\ell S j_\ell M_\ell} - \nu)\;.
\end{aligned}$$

Comparison with Eq. (9.2) – see also Eq. (3.16) – shows a remarkable similarity. Since the same similarities are also found for the other radiative transfer coefficients, we conclude that the transfer equation for polarized radiation in a fine-structure multiplet can be obtained from the corresponding equation for an isolated spectral line by performing the following formal substitutions

i) for the absorption coefficient:

k_{L}, the frequency-integrated line absorption coefficient defined in Eqs. (9.14) and (9.5), must be replaced by k_{M}, the frequency-integrated multiplet absorption coefficient defined by

$$\begin{aligned}
k_{\mathrm{M}} = {} & k_{\mathrm{M}}^{\mathrm{A}} - k_{\mathrm{M}}^{\mathrm{S}} = \frac{h\nu}{4\pi}\,\mathbb{N}_\ell\;B(\beta_\ell L_\ell S \rightarrow \beta_u L_u S) - \frac{h\nu}{4\pi}\,\mathbb{N}_u\;B(\beta_u L_u S \rightarrow \beta_\ell L_\ell S) \\
= {} & \frac{h\nu}{4\pi}\,\mathbb{N}_\ell\;B(\beta_\ell L_\ell S \rightarrow \beta_u L_u S)\left(1 - \frac{\mathbb{N}_u}{\mathbb{N}_\ell}\,\frac{\tilde{\omega}_\ell}{\tilde{\omega}_u}\right),
\end{aligned}$$

where $\tilde{\omega}_\ell = (2L_\ell + 1)(2S + 1)$ is the degeneracy of the lower term and $\tilde{\omega}_u = (2L_u + 1)(2S + 1)$ the degeneracy of the upper term.

ii) for the source function:
$S_{\rm L}$, the line source function defined in Eqs. (9.14), must be replaced by $S_{\rm M}$, the multiplet source function defined by

$$S_{\rm M} = \frac{2h\nu_0^3}{c^2} \left(\frac{\mathbb{N}_\ell}{\mathbb{N}_u} \frac{\tilde{\omega}_u}{\tilde{\omega}_\ell} - 1 \right)^{-1} ,$$

where $\nu_0 = \nu_{\beta_u L_u S, \beta_\ell L_\ell S}$ is the 'central frequency' of the multiplet defined in Eq. (7.22).

iii) for the strengths of the components:
$S_q^{J_\ell J_u}(M_\ell, M_u)$, the normalized strength of the Zeeman component connecting the lower level $|\alpha_\ell J_\ell M_\ell\rangle$ with the upper level $|\alpha_u J_u M_u\rangle$, must be replaced by $S_q^{j_\ell M_\ell, j_u M_u}$, the normalized strength of the multiplet component connecting the lower level $|\beta_\ell L_\ell S j_\ell M_\ell\rangle$ with the upper level $|\beta_u L_u S j_u M_u\rangle$. This strength is given by Eq. (3.64) and its explicit calculation requires the numerical diagonalization of the spin-orbit plus magnetic Hamiltonians, as explained in Sect. 3.4.

iv) for the splitting of the components:
the splitting $\nu_{\rm L}(g_u M_u - g_\ell M_\ell)$, associated with the transition $|\alpha_\ell J_\ell M_\ell\rangle \rightarrow |\alpha_u J_u M_u\rangle$, must be replaced by the splitting $(\nu_{\beta_u L_u S j_u M_u, \beta_\ell L_\ell S j_\ell M_\ell} - \nu_0)$ associated with the transition $|\beta_\ell L_\ell S j_\ell M_\ell\rangle \rightarrow |\beta_u L_u S j_u M_u\rangle$. This quantity is defined in Eq. (3.68) (see also Eq. (7.26)); its value is also deduced by diagonalization of the above Hamiltonians.

Once these substitutions are carried out, any fine-structure multiplet can be treated as a usual Zeeman multiplet, with the only difference that the structure of the 'equivalent Zeeman pattern' is generally more complicated.

Hyperfine-structure multiplets can be handled in a strictly similar way. As noticed in Sects. 3.5 and 7.9, there is indeed a very strict analogy – both physical and formal – between fine-structure and hyperfine-structure multiplets. If we refer to an atom having nuclear spin I and consider the transition between the lower level $(\alpha_\ell J_\ell)$ and the upper level $(\alpha_u J_u)$, the assumption of complete depolarization of both levels implies

$$\mathcal{N}\,(2J_\ell + 1)\ \rho_{\alpha_\ell J_\ell I}(i_\ell f_\ell, i'_\ell f'_\ell) \rightarrow \frac{\mathcal{N}_\ell}{2I+1}\ \delta_{i_\ell i'_\ell}\ \delta_{f_\ell f'_\ell}$$

$$\mathcal{N}\,(2J_u + 1)\ \rho_{\alpha_u J_u I}(i_u f_u, i'_u f'_u) \rightarrow \frac{\mathcal{N}_u}{2I+1}\ \delta_{i_u i'_u}\ \delta_{f_u f'_u} , \qquad (9.261)$$

where $\mathcal{N}_\ell$ and $\mathcal{N}_u$ are the overall number densities of atoms in the lower and upper level, respectively, and where the density-matrix elements are defined in Eq. (7.63). Using Eqs. (9.261), one easily finds that the transfer equation for polarized radiation in a hyperfine-structure multiplet can be obtained from the corresponding

equation for a non-structured spectral line by simple substitution of the appropriate 'equivalent Zeeman pattern'. The normalized strengths and the splittings of the hyperfine components are given by Eqs. (3.75) and (3.78), respectively.

Most of the results obtained in this chapter can be applied both to fine-structure and to hyperfine-structure multiplets. The most important difference is that the 'equivalent Zeeman pattern' of a multiplet does not show the characteristic symmetry properties of usual Zeeman patterns expressed by Eqs. (3.18) and (3.21). This means that *even in the constant velocity case, the symmetry properties (9.54) of the Stokes parameters are no longer valid for multiplets*, which eventually leads to the appearance of net circular polarization, as noticed at the end of Sect. 9.21.

A remarkable property of the 'equivalent Zeeman patterns', concerning the frequency shifts of the $\sigma_{\rm r}$, $\sigma_{\rm b}$, and π components, has been proved in Chap. 3. It is expressed by Eq. (3.66) for fine-structure multiplets, and by Eq. (3.77) for hyperfine-structure multiplets. An important consequence of this property can be derived via a perturbative expansion similar to that of Sect. 9.6. Let us consider a spectral line resulting from a multiplet whose components, in the absence of magnetic field, have wavelength separations much smaller than the Doppler width $\Delta\lambda_{\rm D}$. This means, for fine-structure multiplets

$$\zeta \ll \frac{hc}{\lambda_0^2}\ \Delta\lambda_{\rm D}\ , \tag{9.262}$$

and for hyperfine-structure multiplets

$$\mathcal{A} \ll \frac{hc}{\lambda_0^2}\ \Delta\lambda_{\rm D}\ , \qquad \mathcal{B} \ll \frac{hc}{\lambda_0^2}\ \Delta\lambda_{\rm D}\ , \tag{9.263}$$

where λ_0 is the central wavelength of the multiplet and where ζ and $\mathcal{A}$, $\mathcal{B}$ are defined in Eqs. (3.59) and (3.70), respectively. In the presence of a weak magnetic field ($\Delta\lambda_B \ll \Delta\lambda_{\rm D}$) one obtains, using the above-mentioned property, a relation between the Stokes parameters V and I of the form of Eq. (9.80), namely

$$V = -\,\Delta\lambda_B\ \cos\theta\ \frac{\partial I}{\partial\lambda}$$

for fine-structure multiplets, and

$$V = -\,\Delta\lambda_B\ \bar{g}\ \cos\theta\ \frac{\partial I}{\partial\lambda}\ ,$$

with $\bar{g}$ defined in Eq. (3.44), for hyperfine-structure multiplets. It follows that when inequality (9.262) or (9.263) is satisfied, the presence of fine or hyperfine structure does not change – relative to the case where the 'inner structure' is neglected – the relation existing between V and I in the weak field regime.[1]

[1] Note that this result is non-trivial and is not a direct consequence of the principle of spectroscopic stability. For this principle to be applicable, one should also assume $\zeta \ll hc\ \Delta\lambda_B/\lambda_0^2$ for fine-structure multiplets and $\mathcal{A}, \mathcal{B} \ll hc\ \Delta\lambda_B/\lambda_0^2$ for hyperfine-structure multiplets. Were these last inequalities satisfied, Eqs. (9.83), (9.84) and (9.85) would also be valid (with $\bar{G} = 1$ for fine-structure multiplets).

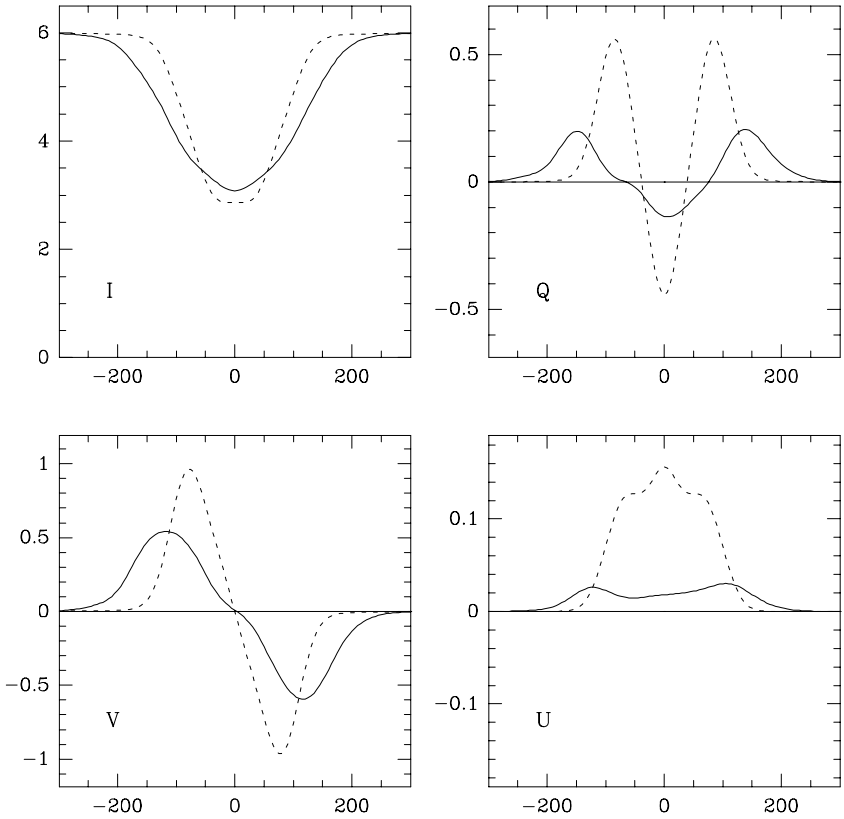

Fig.9.18. The Stokes parameters profiles of the line $\lambda\,5420.362$ of MnI are plotted against wavelength distance from line center in mÅ (solid line). They are computed according to Eqs.(9.110) and are normalized to B_0. The relevant parameters are the following: $\Delta\lambda_{\rm D} = 40$ mÅ, $B = 3000$ G (whence $v_B = 1.029$), $\theta = 60°$, $\chi = 0°$, $\kappa_{\rm L} = 7$, $a = 0.05$, $\beta\mu = 5$. The 'equivalent Zeeman pattern' is computed using the values of the hyperfine-structure constants given by Brix and Kopfermann (1952). The dashed line refers to the Stokes parameters profiles computed neglecting hyperfine structure.

Figure 9.18 shows the Stokes parameters profiles, as deduced from the Unno-Rachkovsky solution, for a typical hyperfine-structure multiplet. Note the characteristic broadening of the profiles and the 'asymmetries' introduced by hyperfine structure.

9.24. Line Formation in Stochastic Media

In this chapter we have treated several aspects of the problem of line formation in a magnetic field. In all cases, it was understood that the physical parameters affecting the transfer of radiation through the ambient medium were deterministic: in other words, they were assumed to take well-defined values in any volume element

of the medium. Here we assume, on the contrary, that the medium is stochastic. By this we mean that the physical parameters are random variables having, locally, a certain probability distribution (with possible correlations between different parameters) and, non-locally, a typical autocorrelation length.

The idea of a non-deterministic ambient medium is indeed realistic. For instance, the analysis of spectral lines in stellar atmospheres has shown for a long time the existence of turbulent velocity fields: this suggests quite naturally that the magnetic field (and other physical variables) may also be present in a turbulent form. Furthermore, one can easily imagine the existence of correlation effects in this turbulent medium. As an example, one might consider the possibility that the magnetic field is larger-than-average when the turbulent velocity is directed outward and smaller-than-average when it is directed inward (or vice versa).

Writing the transfer equation in its general form (9.163)

$$\frac{\mathrm{d}\boldsymbol{I}}{\mathrm{d}\tau_{\mathrm{r}}} \;=\; \boldsymbol{A}(\tau_{\mathrm{r}})\,\boldsymbol{I} \;-\; \boldsymbol{b}(\tau_{\mathrm{r}})\;, \tag{9.264}$$

one is faced with the problem of solving a linear stochastic equation, that is a linear equation with random coefficients.[1] The general problem is extremely complex; however, it is possible to obtain a quite simple analytical solution under a set of restrictive assumptions. Following Auvergne et al. (1973), who solved the simpler problem of the transfer of unpolarized radiation in a turbulent velocity field, we make the following hypotheses:

a) We assume the line is formed in LTE, with a Planck function linear in τ_{r}. This allows us to write the emission coefficient $\boldsymbol{b}(\tau_{\mathrm{r}})$, defined in Eqs. (9.164), in the form[2]

$$\boldsymbol{b}(\tau_{\mathrm{r}}) = B_{\mathrm{P}}(\tau_{\mathrm{r}})\,\boldsymbol{A}(\tau_{\mathrm{r}})\,\boldsymbol{U} = B_0\,(1+\beta'\tau_{\mathrm{r}})\,\boldsymbol{A}(\tau_{\mathrm{r}})\,\boldsymbol{U}\;. \tag{9.265}$$

b) We assume the physical parameters $\{\zeta_i\}$ (with $i = 1, \ldots, p$), on which the propagation matrix $\boldsymbol{A}(\tau_{\mathrm{r}})$ depends – see the discussion at the beginning of Sect. 9.16 – to have a stochastic distribution described by the function $f(\zeta_1, \zeta_2\,, \ldots, \zeta_p)$. The probability $\mathrm{d}P$ of finding the first parameter in the interval $(\zeta_1, \zeta_1 + \mathrm{d}\zeta_1)$, the second in the interval $(\zeta_2\,, \zeta_2 + \mathrm{d}\zeta_2)$, etc., is given by

$$\mathrm{d}P = f(\zeta_1, \zeta_2\,, \ldots, \zeta_p)\;\mathrm{d}\zeta_1\;\mathrm{d}\zeta_2\;\cdots\;\mathrm{d}\zeta_p\;\;, \tag{9.266}$$

with

$$\int \mathrm{d}\zeta_1 \int \mathrm{d}\zeta_2\;\cdots \int \mathrm{d}\zeta_p\;\; f(\zeta_1, \zeta_2\,, \ldots, \zeta_p) \;=\; 1\;.$$

---

[1] The optical depth τ_{r} in Eq. (9.264) should be considered a deterministic variable. For a stochastic medium where the continuum absorption coefficient at the reference frequency, $k_{\mathrm{c}}(\nu_{\mathrm{r}})$, is also a stochastic variable, the definition of τ_{r} given in Eqs. (9.33) must be replaced by $\mathrm{d}\tau_{\mathrm{r}} = -\langle k_{\mathrm{c}}(\nu_{\mathrm{r}})\rangle\,\mathrm{d}s$, where the meaning of the symbol $\langle\cdots\rangle$ is explained below (see Eq. (9.271)).

[2] The slope of the Planck function is here denoted by β' to distinguish it from the quantity β defined in Eq. (9.105). For a plane-parallel atmosphere with a constant ratio of the absorption coefficients $k_{\mathrm{c}}(\nu_{\mathrm{r}})$ and $k_{\mathrm{c}}(\nu_0)$, the two quantities are related by the simple equation $\beta' = \beta\mu\;k_{\mathrm{c}}(\nu_0)\,/\,k_{\mathrm{c}}(\nu_{\mathrm{r}})$.

c) We assume that each given ray path crosses a sequence of independent 'eddies'. The n-th eddy covers the optical depth interval ($\tau_{\rm r} = \tau_{n-1}$, $\tau_{\rm r} = \tau_n$), with $\tau_0 = 0$. In each interval the physical parameters are constant and their values are drawn at random from the probability distribution $f(\zeta_1, \zeta_2, \ldots, \zeta_p)$. Accordingly, the propagation matrix in the n-th interval is constant and will be denoted by $\boldsymbol{A}_n$. Obviously there is no correlation between the matrix $\boldsymbol{A}_i$ in the i-th interval and the matrix $\boldsymbol{A}_j$ in the j-th interval.
d) We finally assume the 'jumping points' τ_1 , τ_2 , ..., τ_n , ... to be distributed according to a Poisson law characterized by the frequency $1/\tau_{\rm e}$ or, in other words, by the mean length of the eddies $\tau_{\rm e}$. The probability $\mathrm{d}Q$ that the first jumping point is found in the interval $(\tau_1 , \tau_1 + \mathrm{d}\tau_1)$, the second in the interval $(\tau_2 , \tau_2 + \mathrm{d}\tau_2)$, etc., is given by

$$\mathrm{d}Q = \mathrm{e}^{-\frac{\tau_1 - \tau_0}{\tau_{\rm e}}} \; \mathrm{e}^{-\frac{\tau_2 - \tau_1}{\tau_{\rm e}}} \; \cdots \; \mathrm{e}^{-\frac{\tau_n - \tau_{n-1}}{\tau_{\rm e}}} \; \cdots \; \frac{\mathrm{d}\tau_1}{\tau_{\rm e}} \, \frac{\mathrm{d}\tau_2}{\tau_{\rm e}} \cdots \frac{\mathrm{d}\tau_n}{\tau_{\rm e}} \cdots , \qquad (9.267)$$

with

$$\int \mathrm{d}Q = \int_{\tau_0}^{\infty} \frac{\mathrm{d}\tau_1}{\tau_{\rm e}} \int_{\tau_1}^{\infty} \frac{\mathrm{d}\tau_2}{\tau_{\rm e}} \cdots \int_{\tau_{n-1}}^{\infty} \frac{\mathrm{d}\tau_n}{\tau_{\rm e}} \cdots \mathrm{e}^{-\frac{\tau_1 - \tau_0}{\tau_{\rm e}}} \; \mathrm{e}^{-\frac{\tau_2 - \tau_1}{\tau_{\rm e}}} \; \cdots \; \mathrm{e}^{-\frac{\tau_n - \tau_{n-1}}{\tau_{\rm e}}} \; \cdots = 1 \, .$$

Hypotheses b), c), and d) characterize what is often referred to as a Poisson-step or Kubo-Anderson process (see Brissaud and Frisch, 1971).

The transfer equation can be easily solved with the help of the assumptions above (see Landi Degl'Innocenti, 1994). Let us first go back to Eq. (9.166), which in LTE reduces to (see Eqs. (9.164))

$$\boldsymbol{I}(0) = \int_0^{\infty} \boldsymbol{O}(0, \tau_{\rm r}) \, \boldsymbol{A}(\tau_{\rm r}) \, B_{\rm P}(\tau_{\rm r}) \, \boldsymbol{U} \, \mathrm{d}\tau_{\rm r} \, . \qquad (9.268)$$

Using the analogues of Eqs. (9.97)-(9.94) for the evolution operator $\boldsymbol{O}(\tau_{\rm r} , \tau'_{\rm r})$ and integrating by parts, we get

$$\boldsymbol{I}(0) = B_{\rm P}(0) \left[\boldsymbol{1} + \int_0^{\infty} \boldsymbol{O}(0, \tau_{\rm r}) \, \frac{\mathrm{d}B_{\rm P}(\tau_{\rm r})}{\mathrm{d}\tau_{\rm r}} \, \mathrm{d}\tau_{\rm r} \right] \boldsymbol{U} \, ,$$

and for a linear Planck function (assumption (a))

$$\boldsymbol{I}(0) = B_0 \left[\boldsymbol{1} + \beta' \int_0^{\infty} \boldsymbol{O}(0, \tau_{\rm r}) \, \mathrm{d}\tau_{\rm r} \right] \boldsymbol{U} \, . \qquad (9.269)$$

Consider now a particular realization of the jumping points $(\tau_1, \tau_2, \ldots, \tau_n, \ldots)$ and of the propagation matrices in the various intervals $(\boldsymbol{A}_1, \boldsymbol{A}_2, \ldots, \boldsymbol{A}_n, \ldots)$. Using the analogues of Eqs. (9.95) and (9.103), we have

$$\int_0^\infty \boldsymbol{O}(0,\tau_{\rm r})\,{\rm d}\tau_{\rm r} = \sum_{n=1}^{\infty} \int_{\tau_{n-1}}^{\tau_n} \boldsymbol{O}(0,\tau_{\rm r})\,{\rm d}\tau_{\rm r}$$

$$= \sum_{n=1}^{\infty} {\rm e}^{-(\tau_1-\tau_0)\,\boldsymbol{A}_1}\ {\rm e}^{-(\tau_2-\tau_1)\,\boldsymbol{A}_2}\ \cdots\ {\rm e}^{-(\tau_{n-1}-\tau_{n-2})\,\boldsymbol{A}_{n-1}} \int_{\tau_{n-1}}^{\tau_n} {\rm e}^{-(\tau_{\rm r}-\tau_{n-1})\,\boldsymbol{A}_n}\,{\rm d}\tau_{\rm r}\ .$$

The integral in the right-hand side can be evaluated via Eq. (9.106). Substitution into Eq. (9.269) yields

$$\boldsymbol{I}(0) = B_0 \Bigg\{ \boldsymbol{1} + \beta' \sum_{n=1}^{\infty} {\rm e}^{-(\tau_1-\tau_0)\,\boldsymbol{A}_1}\ {\rm e}^{-(\tau_2-\tau_1)\,\boldsymbol{A}_2}\ \cdots\ {\rm e}^{-(\tau_{n-1}-\tau_{n-2})\,\boldsymbol{A}_{n-1}} \times \Big[\boldsymbol{1} - {\rm e}^{-(\tau_n-\tau_{n-1})\,\boldsymbol{A}_n}\Big]\boldsymbol{A}_n^{-1} \Bigg\} \boldsymbol{U}\ . \tag{9.270}$$

We now multiply both sides by the probability ${\rm d}Q$ defined in Eq. (9.267) and integrate over all possible realizations of the jumping points. Using again Eq. (9.106), we obtain

$$\int \boldsymbol{I}(0)\,{\rm d}Q = B_0 \Bigg\{ \boldsymbol{1} + \beta' \sum_{n=1}^{\infty} (\boldsymbol{1}+\tau_{\rm e}\,\boldsymbol{A}_1)^{-1}\,(\boldsymbol{1}+\tau_{\rm e}\,\boldsymbol{A}_2)^{-1}\,\cdots\,(\boldsymbol{1}+\tau_{\rm e}\,\boldsymbol{A}_{n-1})^{-1} \times \Big[\boldsymbol{1} - (\boldsymbol{1}+\tau_{\rm e}\,\boldsymbol{A}_n)^{-1}\Big]\boldsymbol{A}_n^{-1} \Bigg\} \boldsymbol{U}\ .$$

Finally, we average over the distribution of the physical parameters $\{\zeta_i\}$. Let us denote by $\langle\, g\,\rangle$ the mean value of any given function $g(\zeta_1, \zeta_2, \ldots, \zeta_p)$ over the distribution function $f(\zeta_1, \zeta_2, \ldots, \zeta_p)$ defined in Eq. (9.266),

$$\langle\, g\,\rangle = \int {\rm d}\zeta_1 \int {\rm d}\zeta_2 \cdots \int {\rm d}\zeta_p\ \ g(\zeta_1, \zeta_2, \ldots, \zeta_p)\ f(\zeta_1, \zeta_2, \ldots, \zeta_p)\ . \tag{9.271}$$

Since by assumption c) the values of the physical parameters in different eddies are uncorrelated, we obtain for the statistical average of the emerging Stokes parameters[1]

$$\big[\,\boldsymbol{I}(0)\,\big]_{\rm av} = B_0 \Bigg\{ \boldsymbol{1} + \beta' \Bigg[\sum_{n=1}^{\infty} \big\langle\, (\boldsymbol{1}+\tau_{\rm e}\,\boldsymbol{A})^{-1}\,\big\rangle^{n-1} \Bigg] \times \Big[\big\langle \boldsymbol{A}^{-1} \big\rangle - \big\langle\, (\boldsymbol{1}+\tau_{\rm e}\,\boldsymbol{A})^{-1}\ \boldsymbol{A}^{-1}\,\big\rangle \Big] \Bigg\} \boldsymbol{U}\ . \tag{9.272}$$

[1] Note that the term corresponding to $n = 1$ in the sum over n is the identity matrix $\boldsymbol{1}$.

This expression can be further developed as follows. Given an arbitrary matrix $\boldsymbol{B}$, expansion of $(\boldsymbol{1} - \boldsymbol{B})^{-1}$ into power series of $\boldsymbol{B}$ and use of the relation

$$(\boldsymbol{1} - \boldsymbol{B})^{-1} \, (\boldsymbol{1} - \boldsymbol{B}) = \boldsymbol{1}$$

yields

$$(\boldsymbol{1} - \boldsymbol{B})^{-1} \, = \sum_{k=0}^{\infty} \, \boldsymbol{B}^k \, .$$

Hence the sum over n in Eq. (9.272) can be written in the form

$$\sum_{n=1}^{\infty} \left\langle \, (\boldsymbol{1} + \tau_{\mathrm{e}} \, \boldsymbol{A})^{-1} \, \right\rangle^{n-1} \, = \left[\, \boldsymbol{1} - \left\langle \, (\boldsymbol{1} + \tau_{\mathrm{e}} \, \boldsymbol{A})^{-1} \, \right\rangle \right]^{-1}$$

$$= \left\langle \, \boldsymbol{1} - \, (\boldsymbol{1} + \tau_{\mathrm{e}} \, \boldsymbol{A})^{-1} \, \right\rangle^{-1} \, = \, \frac{1}{\tau_{\mathrm{e}}} \left\langle \, \boldsymbol{A} \, (\boldsymbol{1} + \tau_{\mathrm{e}} \, \boldsymbol{A})^{-1} \, \right\rangle^{-1} \, . \tag{9.273}$$

On the other hand, we have

$$\left\langle \boldsymbol{A}^{-1} \right\rangle - \left\langle \, (\boldsymbol{1} + \tau_{\mathrm{e}} \, \boldsymbol{A})^{-1} \, \boldsymbol{A}^{-1} \, \right\rangle = \left\langle \boldsymbol{A}^{-1} \, - \, \boldsymbol{A}^{-1} \, (\boldsymbol{1} + \tau_{\mathrm{e}} \, \boldsymbol{A})^{-1} \, \right\rangle$$

$$= \left\langle \boldsymbol{A}^{-1} \left[\, \boldsymbol{1} - \, (\boldsymbol{1} + \tau_{\mathrm{e}} \, \boldsymbol{A})^{-1} \, \right] \right\rangle = \, \tau_{\mathrm{e}} \left\langle \, (\boldsymbol{1} + \tau_{\mathrm{e}} \, \boldsymbol{A})^{-1} \, \right\rangle .$$

Substitution of these relations into Eq. (9.272) leads to the expression

$$\left[\, \boldsymbol{I}(0) \, \right]_{\mathrm{av}} \, = B_0 \left[\, \boldsymbol{1} \, + \, \beta' \left\langle \boldsymbol{A} \, (\boldsymbol{1} + \tau_{\mathrm{e}} \, \boldsymbol{A})^{-1} \, \right\rangle^{-1} \, \left\langle \, (\boldsymbol{1} + \tau_{\mathrm{e}} \, \boldsymbol{A})^{-1} \, \right\rangle \right] \boldsymbol{U} \, . \tag{9.274}$$

This formula contains, as particular cases, some interesting limits:

i) If the physical parameters are deterministic, the symbols $\langle \cdots \rangle$ can be removed and one obtains

$$\left[\, \boldsymbol{I}(0) \, \right]_{\mathrm{av}} \, = B_0 \left[\, \boldsymbol{1} \, + \, \beta' \, \boldsymbol{A}^{-1} \right] \boldsymbol{U} \, , \tag{9.275}$$

which is nothing but the Unno-Rachkovsky solution.[1]

ii) Microturbulent limit: under the limit $\tau_{\mathrm{e}} \to 0$ (microscopic eddies) one gets

$$\left[\, \boldsymbol{I}(0) \, \right]_{\mathrm{av}} \, = B_0 \left[\, \boldsymbol{1} \, + \, \beta' \left\langle \, \boldsymbol{A} \, \right\rangle^{-1} \right] \boldsymbol{U} \, , \tag{9.276}$$

or, in other words, the Unno-Rachkovsky solution of the deterministic case with the matrix $\boldsymbol{A}$ replaced by $\langle \boldsymbol{A} \rangle$.

iii) Macroturbulent limit: under the limit $\tau_{\mathrm{e}} \to \infty$ (very large eddies) one obtains

$$\left[\, \boldsymbol{I}(0) \, \right]_{\mathrm{av}} \, = B_0 \left[\, \boldsymbol{1} \, + \, \beta' \left\langle \boldsymbol{A}^{-1} \right\rangle \right] \boldsymbol{U} \, , \tag{9.277}$$

[1] The connection with the Unno-Rachkovsky solution will be discussed more precisely in the following.

which is again the Unno-Rachkovsky solution with the matrix $\boldsymbol{A}^{-1}$ replaced by $\langle \boldsymbol{A}^{-1} \rangle$.

iv) Finally, for non-magnetic media the matrix $\boldsymbol{A}$ is proportional to the unit matrix,

$$\boldsymbol{A} = (\kappa_{\rm r} + \kappa_{\rm R}\, \eta)\, \boldsymbol{1} = \kappa\, \boldsymbol{1}\,, \tag{9.278}$$

with η defined in Eqs. (9.65). The intensity (the other Stokes parameters are obviously zero) is given by

$$\big[\, I(0) \,\big]_{\rm av} = B_0 \left[1 + \beta' \left\langle \frac{1}{1+\tau_{\rm e}\,\kappa} \right\rangle \Big/ \left\langle \frac{\kappa}{1+\tau_{\rm e}\,\kappa} \right\rangle \right], \tag{9.279}$$

a formula derived by Auvergne et al. (1973) for the case of turbulent velocity fields.

For a plane-parallel atmosphere, we can rewrite Eq. (9.274) in a form more similar to the Unno-Rachkovsky solution (9.109) by identifying the reference frequency $\nu_{\rm r}$ with the line frequency ν_0. Let us denote by $t_{\rm e}$ the mean length of the eddies measured along the vertical to the atmosphere. Bearing in mind footnote 2 on p. 496, the emerging Stokes profiles for a radiation beam travelling in the μ-direction are given by

$$\big[\, \boldsymbol{I}(0) \,\big]_{\rm av} = B_0 \left[\boldsymbol{1} + \beta\mu \left\langle \boldsymbol{C} \left(\boldsymbol{1} + \frac{t_{\rm e}}{\mu}\, \boldsymbol{C} \right)^{-1} \right\rangle^{-1} \left\langle \left(\boldsymbol{1} + \frac{t_{\rm e}}{\mu}\, \boldsymbol{C} \right)^{-1} \right\rangle \right] \boldsymbol{U}, \tag{9.280}$$

where β and $\boldsymbol{C}$ are defined in Eqs. (9.105) and (9.91), respectively.[1]

Figures 9.19 and 9.20 show some numerical results for the case where all the physical parameters are deterministic except for the magnetic field intensity and the line-of-sight component of the velocity field, which are characterized by a bimodal distribution of the form (Martin, 1971)

$$f(v_B\,, v_A) = \frac{{\rm e}^{-\alpha}}{2\pi \sqrt{1-\rho^2}\;\; \Delta v_B\, \Delta v_{\rm A}}\;, \tag{9.281}$$

where

$$\alpha = \frac{1}{1-\rho^2} \left\{ \frac{1}{2} \left[\frac{v_B - v_B^{(0)}}{\Delta v_B} \right]^2 + \frac{1}{2} \left[\frac{v_{\rm A} - v_{\rm A}^{(0)}}{\Delta v_{\rm A}} \right]^2 - \rho\, \frac{\big(v_B - v_B^{(0)}\big)\big(v_{\rm A} - v_{\rm A}^{(0)}\big)}{\Delta v_B\, \Delta v_{\rm A}} \right\}.$$

In these equations, v_B and $v_{\rm A}$ are defined by Eqs. (9.26), the Doppler width $\Delta\lambda_{\rm D}$ being due to the thermal velocity only. The quantity ρ is the *correlation parameter*

[1] Note, however, that stochastic variations of the continuum absorption coefficient cannot be considered if the matrix $\boldsymbol{C}$ has the form of Eq. (9.91). Such variations can be allowed for if $\boldsymbol{C}$ in Eq. (9.280) is defined to be

$$\boldsymbol{C} = \frac{k_{\rm c}(\nu_0)}{\langle\, k_{\rm c}(\nu_0)\,\rangle} \left[\boldsymbol{1} + \kappa_{\rm L}\, \boldsymbol{H} \right].$$

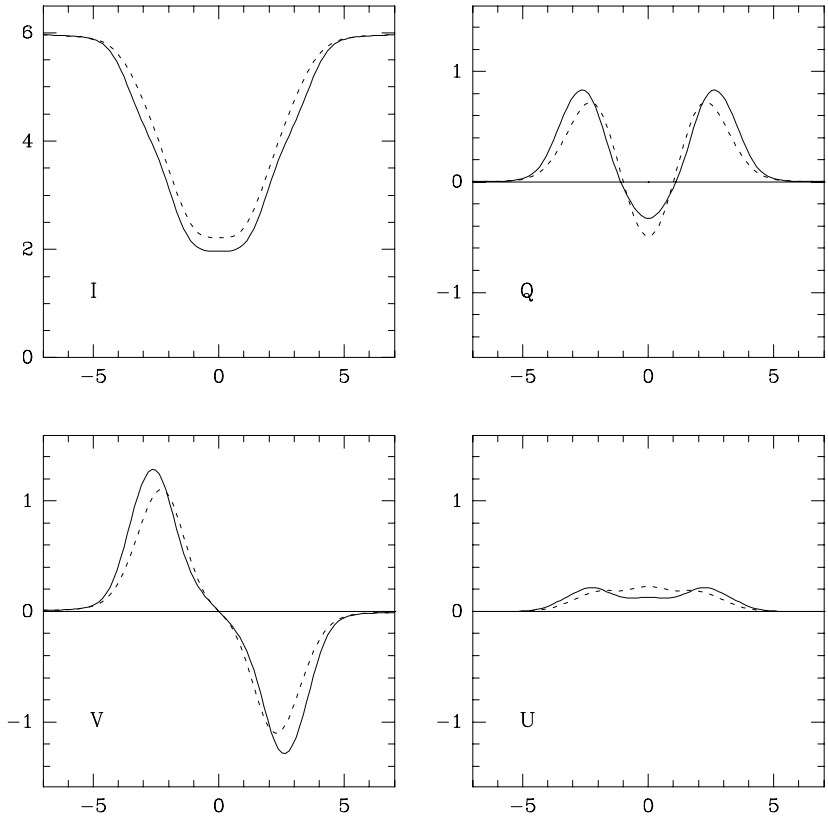

Fig.9.19. Stokes parameters profiles computed from Eq.(9.280) for the Zeeman triplet ${}^1\mathrm{S}_0 - {}^1\mathrm{P}_1$ and the bimodal distribution (9.281). The profiles are normalized to B_0. The values of the parameters specifying the distribution are: $\rho = 0$, $v_B^{(0)} = 1.5$, $\Delta v_B = 0.5$, $v_\mathrm{A}^{(0)} = 0$, $\Delta v_\mathrm{A} = 0.5$. The values of the remaining parameters are: $\kappa_\mathrm{L} = 20$, $\theta = 60°$, $\chi = 0°$, $a = 0.05$, $\beta\mu = 5$. Full line: microturbulent limit ($t_\mathrm{e} = 0$); dashed line: macroturbulent limit ($t_\mathrm{e} = 1000$).

($-1 < \rho < 1$). When $\rho = 0$ the distribution function reduces to the product of two Gaussian distributions, one for v_B (centered at $v_B^{(0)}$ and having standard deviation Δv_B) and the other for v_A (centered at $v_\mathrm{A}^{(0)}$ and having standard deviation Δv_A). By simple algebra it can be proved that the distribution (9.281) is normalized to unity,

$$\int_{-\infty}^{\infty} \mathrm{d}v_B \int_{-\infty}^{\infty} \mathrm{d}v_\mathrm{A} \quad f(v_B\,, v_\mathrm{A}) = 1\,.$$

Both figures refer to the normal Zeeman triplet ${}^1\mathrm{S}_0 - {}^1\mathrm{P}_1$. Figure 9.19 gives the emerging Stokes profiles computed for $\rho = 0$ (absence of correlations). Comparison with panel (a) of Fig. 9.5 clearly shows the broadening of the profiles introduced by the Gaussian distributions of magnetic field intensity and of turbulent velocity. The remarkable effects of correlations are shown in Fig. 9.20, computed for $\rho = 0.7$. Correlations between magnetic field intensity and line-of-sight velocity are able to

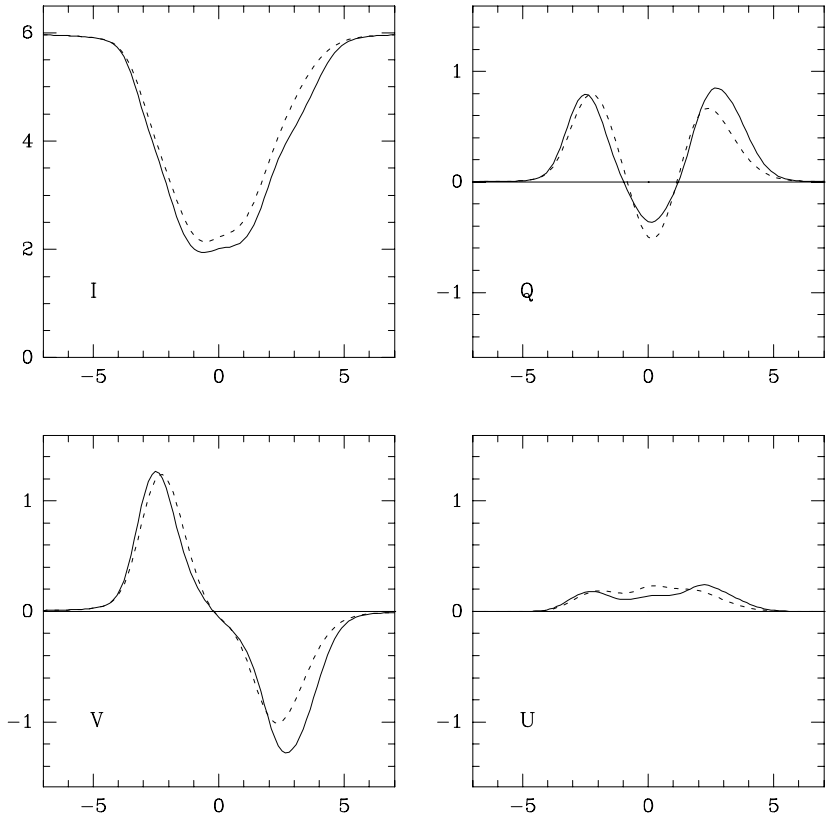

Fig.9.20. Same as Fig.9.19 with $\rho = 0.7$.

produce asymmetric profiles and a definite amount of net circular polarization (except in the macroturbulent limit $t_{\rm e} \to \infty$).

According to Eq. (9.265), the Planck function – hence the temperature of the medium – has been assumed to be a deterministic variable: therefore, correlations involving temperature (like temperature-velocity or temperature-magnetic field) cannot be treated via Eqs. (9.274) or (9.280). A simple generalization of these equations, which allows for such correlations, can be obtained by writing the Planck function in the form

$$B_{\rm P}(\tau_{\rm r}) = B_0 \, (1 + \beta' \tau_{\rm r}) \, + \, \Delta B_{\rm P} \ , \tag{9.282}$$

where $\Delta B_{\rm P}$ satisfies assumptions b), c) and d) above – in other words, is itself a Kubo-Anderson process.

Let us denote by $(\Delta B_1 \, , \Delta B_2 \, , \ldots , \Delta B_n \, , \ldots)$ a particular realization of $\Delta B_{\rm P}$ in the intervals $(\tau_0 \, , \tau_1)$, $(\tau_1 \, , \tau_2)$, $\ldots$, $(\tau_{n-1} \, , \tau_n)$, $\ldots$. Following the same line of reasoning, it is easily seen that the additional term $\Delta B_{\rm P}$ in Eq. (9.282) makes an

additional contribution to Eq. (9.268) of the form

$$\boldsymbol{I}_{\mathrm{a.c.}}(0) = \sum_{n=1}^{\infty} \int_{\tau_{n-1}}^{\tau_n} \boldsymbol{O}(0,\tau_{\mathrm{r}})\, \boldsymbol{A}(\tau_{\mathrm{r}})\, \Delta B_n\, \boldsymbol{U}\ \mathrm{d}\tau_{\mathrm{r}}\ .$$

Using Eqs. (9.97), (9.95) and (9.103) we obtain

$$\boldsymbol{I}_{\mathrm{a.c.}}(0) = \sum_{n=1}^{\infty}\ \Delta B_n\ \mathrm{e}^{-(\tau_1-\tau_0)\,\boldsymbol{A}_1}\ \mathrm{e}^{-(\tau_2-\tau_1)\,\boldsymbol{A}_2}\ \cdots\ \mathrm{e}^{-(\tau_{n-1}-\tau_{n-2})\,\boldsymbol{A}_{n-1}}$$
$$\times \left[\boldsymbol{1}\ -\ \mathrm{e}^{-(\tau_n-\tau_{n-1})\,\boldsymbol{A}_n}\right] \boldsymbol{U}\ ,$$

which is the additional contribution to Eq. (9.270). Integration over the Poisson distribution of the jumping points and over the distribution of the physical parameters yields

$$\left[\boldsymbol{I}_{\mathrm{a.c.}}(0)\right]_{\mathrm{av}} = \sum_{n=1}^{\infty} \Big[\left\langle \Delta B \right\rangle \left\langle\, (\boldsymbol{1}+\tau_{\mathrm{e}}\,\boldsymbol{A})^{-1}\,\right\rangle^{n-1}$$
$$- \left\langle\, (\boldsymbol{1}+\tau_{\mathrm{e}}\,\boldsymbol{A})^{-1}\,\right\rangle^{n-1} \left\langle \Delta B\ (\boldsymbol{1}+\tau_{\mathrm{e}}\,\boldsymbol{A})^{-1}\,\right\rangle \Big]\, \boldsymbol{U}\ .$$

Since

$$\left\langle \Delta B \right\rangle \boldsymbol{1}\ -\ \left\langle \Delta B\ (\boldsymbol{1}+\tau_{\mathrm{e}}\,\boldsymbol{A})^{-1}\,\right\rangle\ =\ \tau_{\mathrm{e}}\left\langle \Delta B\ \ \boldsymbol{A}\,(\boldsymbol{1}+\tau_{\mathrm{e}}\,\boldsymbol{A})^{-1}\,\right\rangle,$$

we finally obtain, with the help of Eq. (9.273)

$$\left[\boldsymbol{I}_{\mathrm{a.c.}}(0)\right]_{\mathrm{av}} = \left\langle \boldsymbol{A}\,(\boldsymbol{1}+\tau_{\mathrm{e}}\,\boldsymbol{A})^{-1}\,\right\rangle^{-1}\ \left\langle \Delta B\ \ \boldsymbol{A}\,(\boldsymbol{1}+\tau_{\mathrm{e}}\,\boldsymbol{A})^{-1}\,\right\rangle \boldsymbol{U}\ . \tag{9.283}$$

This formula contains the following special cases (cf. Eqs. (9.275)-(9.279)):

i) Deterministic limit

$$\left[\boldsymbol{I}_{\mathrm{a.c.}}(0)\right]_{\mathrm{av}}\ =\ \Delta B\ \ \boldsymbol{U}\ .$$

ii) Microturbulent limit

$$\lim_{\tau_{\mathrm{e}}\to 0} \left[\boldsymbol{I}_{\mathrm{a.c.}}(0)\right]_{\mathrm{av}}\ = \left\langle\, \boldsymbol{A}\,\right\rangle^{-1}\ \left\langle \Delta B\ \boldsymbol{A}\right\rangle \boldsymbol{U}\ .$$

iii) Macroturbulent limit

$$\lim_{\tau_{\mathrm{e}}\to\infty} \left[\boldsymbol{I}_{\mathrm{a.c.}}(0)\right]_{\mathrm{av}}\ = \left\langle \Delta B \right\rangle \boldsymbol{U}\ .$$

iv) Scalar case

$$\left[\boldsymbol{I}_{\mathrm{a.c.}}(0) \right]_{\mathrm{av}} = \left[\left\langle \frac{\Delta B \ \kappa}{1 + \tau_{\mathrm{e}} \ \kappa} \right\rangle \Big/ \left\langle \frac{\kappa}{1 + \tau_{\mathrm{e}} \ \kappa} \right\rangle \right] \boldsymbol{U} \ ,$$

where κ is defined in Eq. (9.278).

Adding Eqs. (9.274) and (9.283) we obtain the expression

$$\left[\boldsymbol{I}(0) \right]_{\mathrm{av}} = \Big[B_0 \ \boldsymbol{1} \ + \ \left\langle \boldsymbol{A} \ (\boldsymbol{1} + \tau_{\mathrm{e}} \ \boldsymbol{A})^{-1} \right\rangle^{-1} \times \left\langle \ (B_0 \ \beta' \ \boldsymbol{1} \ + \ \Delta B \ \boldsymbol{A}) \ (\boldsymbol{1} + \tau_{\mathrm{e}} \ \boldsymbol{A})^{-1} \right\rangle \Big] \boldsymbol{U} \ , \qquad (9.284)$$

which generalizes Eq. (9.274) by allowing for the stochastic behavior of the Planck function.[1]

The procedure followed in this section to find an analytical solution to the transfer equation (9.264) for a Kubo-Anderson process can also be applied to solve the homogeneous transfer equation

$$\frac{\mathrm{d}\boldsymbol{I}}{\mathrm{d}\tau_{\mathrm{r}}} = \boldsymbol{A}(\tau_{\mathrm{r}}) \ \boldsymbol{I} \ . \qquad (9.285)$$

The calculations are developed in App. 12 and lead to a closed analytical form for the stochastic average of the evolution operator.

It should be mentioned that the problem of line formation in a stochastic magnetic field has been tackled, with a completely different approach, by Faulstich (1980). This approach is a generalization of the method developed by Gail et al. (1980) for the non-polarized case and is based on the assumption that the intensity of the magnetic field is constant while its direction changes along the ray path according to a Markov process. The stochastic average of the emerging Stokes parameters is found by solving a Fokker-Planck equation for the probability $P(x, \vec{\Omega}, \boldsymbol{I})$ of finding, at point x along the ray path, the magnetic field in the solid angle $\mathrm{d}\Omega$ about the direction $\vec{\Omega}$ and the Stokes parameters in the interval $(\boldsymbol{I}, \boldsymbol{I} + \mathrm{d}\boldsymbol{I})$.

9.25. Isotropic, Microturbulent Magnetic Field

In the former section and in App. 12 we have found that, under the microturbulent limit, radiative transfer for polarized radiation can be simply described by replacing the propagation matrix $\boldsymbol{A}$ with its stochastic average $\langle \boldsymbol{A} \rangle$ (see Eqs. (9.276) and (A12.8)). This result is valid well beyond the set of assumptions outlined in the

[1] Note that a stochastic behavior of the Planck function implies a stochastic behavior of the temperature, which obviously affects the propagation matrix $\boldsymbol{A}$. In other words, the symbols $\langle \cdots \rangle$ in Eq. (9.284) mean an average over a distribution function $f(\zeta_1, \zeta_2, \ldots, \zeta_p)$ which includes temperature among its arguments.

former section. In fact, it holds whenever the correlation lengths of the stochastic physical parameters are much smaller than the typical scales of the radiative transfer problem (determined by the eigenvalues of the propagation matrix), irrespective of the type of process – Kubo-Anderson, Markov, etc. – characterizing the stochastic behavior (see e.g. Stenflo, 1971).

Here we want to consider the effect of a microturbulent, isotropic magnetic field on the propagation matrix, under the assumption that the field modulus B, characterized by a normalized distribution $f(B)$, is the only stochastic variable (except for microturbulent velocity, assumed uncorrelated with it).[1]

Since the continuum and line absorption coefficients are not affected by the magnetic field, the average propagation matrix reduces to (see Eqs. (9.164))

$$\langle \boldsymbol{A} \rangle = \kappa_{\mathrm{r}} \boldsymbol{1} + \kappa_{\mathrm{R}} \langle \boldsymbol{H} \rangle \, .$$

On the other hand, the off-diagonal elements of the matrix $\langle \boldsymbol{H} \rangle$ vanish because of the isotropy of the magnetic field.[2] From Eqs. (9.50) and (9.32), being

$$\langle \cos\theta \rangle = \langle \sin^2\theta \cos 2\chi \rangle = \langle \sin^2\theta \sin 2\chi \rangle = 0$$

and

$$\langle \sin^2\theta \rangle = \frac{2}{3} \, , \qquad \langle \cos^2\theta \rangle = \frac{1}{3} \, ,$$

we get

$$\langle \boldsymbol{H} \rangle = \langle \, h_I \, \rangle \boldsymbol{1} = \frac{1}{3} \left[\langle \, \eta_{\mathrm{b}} \, \rangle + \langle \, \eta_{\mathrm{p}} \, \rangle + \langle \, \eta_{\mathrm{r}} \, \rangle \right] \boldsymbol{1} \, , \tag{9.286}$$

where

$$\langle \, \eta_{\mathrm{b,p,r}} \, \rangle = \int_0^\infty \eta_{\mathrm{b,p,r}}(B) \, f(B) \, \mathrm{d}B \, . \tag{9.287}$$

If we now take for $f(B)$ a Gaussian distribution characterized by the r.m.s. value B_{t} (the 'turbulent' field),

$$f(B) = \sqrt{\frac{2}{\pi}} \, \frac{B^2}{B_{\mathrm{t}}^3} \, \mathrm{e}^{-\frac{1}{2}\left[\frac{B}{B_{\mathrm{t}}}\right]^2} \, , \tag{9.288}$$

we can easily find an analytical expression for the matrix $\langle \boldsymbol{H} \rangle$.

Let us first assume the turbulent field is weak, that is (cf. Eqs. (9.26))

$$\Delta\lambda_B^{(\mathrm{t})} \equiv \frac{\lambda_0^2 \, e_0 \, B_{\mathrm{t}}}{4\pi \, mc^2} \ll \Delta\lambda_{\mathrm{D}} \, , \tag{9.289}$$

[1] More complicated magnetic field distributions have been considered by Dolginov and Pavlov (1972).

[2] It follows that the radiation emerging from a semi-infinite atmosphere where a microturbulent, isotropic magnetic field is present, is unpolarized.

with $\Delta\lambda_{\rm D}$ the Doppler width. From Eqs. (9.64) and (9.68) we have, up to second-order terms in $\Delta\lambda_B$

$$\eta_q = G_q^{(0)}\,\eta - G_q^{(1)}\,\Delta\lambda_B\,\eta' + \frac{1}{2}\,G_q^{(2)}\,\Delta\lambda_B^2\,\eta'' \qquad (q=-1,0,+1)\,, \tag{9.290}$$

where η is defined in Eqs. (9.65), η' and η'' in Eqs. (9.70), and

$$\Delta\lambda_B = \frac{\lambda_0^2\,e_0\,B}{4\pi\,mc^2} \ll \Delta\lambda_{\rm D}\ .$$

Recalling Eqs. (9.29), and using Eqs. (9.290) and (9.288), the integrals in Eq. (9.287) can be performed. Substituting the expressions for $G_q^{(n)}$ given in Table 3.4 we finally obtain

$$\langle\, h_I \,\rangle = \eta + \bar{G}_{\rm t}\left[\,\Delta\lambda_B^{(\rm t)}\,\right]^2\eta''\,, \tag{9.291}$$

where $\bar{G}_{\rm t}$, the *second-order effective Landé factor for turbulent fields*, is given by

$$\bar{G}_{\rm t} = \frac{1}{2}\,G_0^{(2)} + G_1^{(2)} = \bar{g}^2 + \delta''\,,$$

with[1]

$$\delta'' = \frac{1}{16}\,g_d^2\,(4s - d^2 - 4)\,.$$

It can be easily shown that δ'' is a non-negative quantity that vanishes only for Zeeman triplets (normal or anomalous). Consequently, $\bar{G}_{\rm t}$ is also a non-negative quantity.

Equation (9.291) can be cast into a more significant form. Let us define a 'total Doppler width' $\Delta\lambda_{\rm T}$ as

$$\Delta\lambda_{\rm T} = \sqrt{\Delta\lambda_{\rm D}^2 + 4\,\bar{G}_{\rm t}\left[\,\Delta\lambda_B^{(\rm t)}\,\right]^2}\ ,$$

where $\Delta\lambda_B^{(\rm t)}$ satisfies the condition (9.289). Using the relation

$$\frac{\partial^2 H(v,a)}{\partial v^2} = -\,2\left[H(v,a) + v\,\frac{\partial H(v,a)}{\partial v} + a\,\frac{\partial H(v,a)}{\partial a}\right],$$

which follows directly from Eqs. (5.58), it can be easily proved that, up to second-order terms in $\Delta\lambda_B^{(\rm t)}$, we can write

$$\langle\, h_I \,\rangle = \frac{\Delta\lambda_{\rm D}}{\Delta\lambda_{\rm T}}\ \frac{1}{\sqrt{\pi}}\ H\!\left(\frac{\lambda-\lambda_0'}{\Delta\lambda_{\rm T}}\,,\ \frac{a\,\Delta\lambda_{\rm D}}{\Delta\lambda_{\rm T}}\right)\,,$$

[1] Note that $\delta'' = (\delta + 3\,\delta')\,/\,2$, where δ and δ' are defined in Eqs. (9.78) and (9.227), respectively.

where λ_0' is defined in Eq. (9.44). We conclude that a weak, turbulent magnetic field described by the distribution (9.288) produces a broadening of the absorption profile which is the same as the broadening produced by a velocity field of amplitude

$$w_{\rm eq} = \sqrt{\bar{G}_{\rm t}}\ \ \frac{\lambda_0\, e_0\, B_{\rm t}}{2\pi\, mc}\ ,$$

or, numerically

$$w_{\rm eq} = 1.4 \times 10^{-3}\ \sqrt{\bar{G}_{\rm t}}\ \left(\frac{\lambda_0}{5000}\right) B_{\rm t}\ ,$$

where λ_0 is expressed in Å, $B_{\rm t}$ in G, and $w_{\rm eq}$ in km s^{-1}.

For arbitrary values of $B_{\rm t}$, when inequality (9.289) is no longer satisfied, it is still possible to find an analytical expression for $\langle\, h_I \,\rangle$. Let us consider the case of a Zeeman triplet. Bearing in mind Eqs. (9.29), (9.27a) and (9.26), we have from Eqs. (9.286)-(9.288)

$$\begin{aligned}\langle\, h_I \,\rangle = {} & \frac{1}{3\,\sqrt{\pi}}\ H\!\left(\frac{\lambda-\lambda_0'}{\Delta\lambda_{\rm D}}\,,\, a\right) \\ & + \frac{\sqrt{2}}{3\pi}\ \int_0^\infty \left[H\!\left(\frac{\lambda-\lambda_0'+g\,\Delta\lambda_B}{\Delta\lambda_{\rm D}}\,,\, a\right) + H\!\left(\frac{\lambda-\lambda_0'-g\,\Delta\lambda_B}{\Delta\lambda_{\rm D}}\,,\, a\right)\right] \\ & \qquad \times \left[\frac{\Delta\lambda_B}{\Delta\lambda_B^{(\rm t)}}\right]^2\ {\rm e}^{-\frac{1}{2}\left[\Delta\lambda_B\,/\,\Delta\lambda_B^{(\rm t)}\right]^2}\ \ \frac{{\rm d}\,(\Delta\lambda_B)}{\Delta\lambda_B^{(\rm t)}}\ . \end{aligned} \tag{9.292}$$

Since the integrand is an even function of $\Delta\lambda_B$, the integral can be evaluated by extending it from $-\infty$ to $+\infty$ and dividing by 2. Then we make use of the relation

$$\left[\frac{y}{y_0}\right]^2\ {\rm e}^{-\frac{1}{2}\left[\frac{y}{y_0}\right]^2}\ = H\!\left(\frac{y}{\sqrt{2}\,y_0}\,,\,0\right)\ +\ y_0^2\ \lim_{x\to 0}\left[\frac{\partial^2}{\partial x^2}\ H\!\left(\frac{y-x}{\sqrt{2}\,y_0}\,,\,0\right)\right],$$

which can be proved with the help of Eqs. (5.55). The evaluation of the integral in Eq. (9.292) is thus reduced to the evaluation of convolutions of Voigt functions with different widths, which can be easily done – using the symmetry property (5.59) – via Eqs. (5.65). The final result is

$$\begin{aligned}\langle\, h_I \,\rangle = {} & \frac{1}{3\,\sqrt{\pi}}\ H\!\left(\frac{\lambda-\lambda_0'}{\Delta\lambda_{\rm D}}\,,\, a\right) + \frac{2}{3\,\sqrt{\pi}}\ \frac{\Delta\lambda_{\rm D}}{\Delta\lambda_{\rm T}'}\ H\!\left(\frac{\lambda-\lambda_0'}{\Delta\lambda_{\rm T}'}\,,\,\frac{a\,\Delta\lambda_{\rm D}}{\Delta\lambda_{\rm T}'}\right) \\ & + \frac{2}{3\,\sqrt{\pi}}\ \frac{\Delta\lambda_{\rm D}}{\Delta\lambda_{\rm T}'}\ g^2\left[\,\Delta\lambda_B^{(\rm t)}\,\right]^2\ \frac{\partial^2}{\partial\lambda^2}\ H\!\left(\frac{\lambda-\lambda_0'}{\Delta\lambda_{\rm T}'}\,,\,\frac{a\,\Delta\lambda_{\rm D}}{\Delta\lambda_{\rm T}'}\right), \end{aligned}$$

where

$$\Delta\lambda_{\rm T}' = \sqrt{\Delta\lambda_{\rm D}^2\ +\ 2\,g^2\left[\,\Delta\lambda_B^{(\rm t)}\,\right]^2}\ .$$

This formula could be generalized to more complicated Zeeman patterns, but we will not develop the relevant calculations.

This page intentionally left blank

CHAPTER 10

NON-EQUILIBRIUM ATOMIC PHYSICS

Let us consider a typical astrophysical plasma (like, for instance, a stellar atmosphere) and let us focus our attention on a particular atom belonging to a given volume element of the plasma. The atom experiences a continuous series of interactions with the photons propagating inside the plasma, with the surrounding particles and, if the plasma is magnetized, with the magnetic field. Except for a few very special cases, the atom will be in a typical non-equilibrium situation: the distribution of level populations will differ from the Saha-Boltzmann distribution, and each individual level will have a definite amount of atomic polarization. The aim of this chapter is to describe the main aspects of these non-equilibrium phenomena, by showing how the most important atomic properties – like the emissivity and the absorptivity – depend in a critical way on the physical characteristics of the environment.

Once such physical characteristics are specified, the state of the atom is obtained by solving the statistical equilibrium equations. In stationary situations, these equations form a system of linear, algebraic equations whose unknowns are the atomic density-matrix elements (or those linear combinations of density-matrix elements representing the multipole moments or spherical statistical tensors). The number of equations (and of unknowns) depends on the model atom considered, the coefficients depend both on the model atom and on the physical environment (characteristics of the incident radiation field, presence or absence of a magnetic field and/or of collisions). In practice, one is faced with very complicated equations even for relatively simple model atoms and physical situations. Therefore, although the calculation of the atomic state under given physical conditions is in principle a trivial task (it just requires the solution of a system of linear, algebraic equations), it is in fact extremely difficult to understand the role played by the different factors in determining such state.

In the general case, there is no way out of this situation: once the model atom and the physical environment are given, the statistical equilibrium equations have to be solved numerically. This is however of little help to understand the physics of the different phenomena. Therefore, rather than illustrating a variety of sample cases obtained by numerical solutions to the equations, we consider in this chapter a number of simplified physical situations, by introducing certain approximations which, in many cases, lead to analytical expressions for the atomic density-matrix elements.

The basic approximation used throughout this chapter is to consider model atoms having just *two* energy states, an upper and a lower state, between which transitions take place. All the three model atoms described in Chap. 7 (multi-level, multi-term, and multi-level with hyperfine structure) will be studied, but they will

be 'restricted' to two-level or two-term model atoms. The only exceptions are Sects. 10.10, 10.11, and 10.12, where three-level model atoms are considered in order to point out some peculiar phenomena.

The second, frequently used approximation is to neglect the atomic polarization of the lower level (or term). In general, this is a reasonable assumption provided depolarizing collisions are present and the radiation field is sufficiently weak (see Sect. 10.7). Accordingly, stimulation effects are systematically neglected whenever this approximation is made.

Two further assumptions introduced in some sections concern the radiation field. Instead of an arbitrary field, we sometimes consider either an unpolarized field having cylindrical symmetry about a given direction, or a weakly anisotropic field. Both cases lead to major simplifications in the statistical equilibrium equations; on the other hand, such radiation fields are rather common both in laboratory and astrophysical situations.

As far as collisions (either inelastic/superelastic or depolarizing) and the magnetic field are concerned, we will treat a number of different situations, in order to illustrate their specific effects on the atomic density matrix. However, collisions will only be considered when dealing with the multi-level atom, because the theory of collisions presented in Chap. 7 was not explicitly developed for the multi-term model atom.

In order to make the study of individual sections easier, the various assumptions are briefly recalled by subheadings or 'keywords' at the beginning of each section.

Whenever analytical expressions for the atomic density matrix are worked out, they can be substituted into the expressions of the radiative transfer coefficients. This yields explicit formulae relating, for instance, the atomic emissivity in the four Stokes parameters to the radiation field impinging on the atom and to the other physical properties of the environment (collisions, magnetic field). In several cases such relations turn out to be linear, in the sense that the emission coefficient in the i-th Stokes parameter for the direction $\vec{\Omega}$ is linearly related to the j-th Stokes parameter of the radiation impinging on the atom from the direction $\vec{\Omega}'$. This provides the possibility of defining suitable redistribution matrices for scattering processes. Such procedure was first introduced by Landi Degl'Innocenti (1984).

The validity of the results derived in this chapter is obviously subjected to the limitation outlined in the introduction to Chap. 6 and thoroughly discussed in Sect. 6.5. This limitation concerns the spectral characteristics of the radiation field that is illuminating the atom, which must satisfy the so-called flat-spectrum approximation.

10.1. The Two-Level Atom: Generalities

We consider a simple atomic model consisting of two levels: a lower and an upper level characterized by the quantum numbers[1] (α_ℓ, J_ℓ) and (α_u, J_u), respectively.

[1] The spectroscopic notation is the same as that used throughout the whole book. J is the

The atom is interacting with an anisotropic, polarized radiation field characterized, for any given direction $\vec{\Omega}$ and any frequency ν, by the Stokes vector $I_i(\nu,\vec{\Omega})$.[1] It is also interacting with a collection of perturbers (or colliders) whose velocity distribution is assumed to be isotropic and Maxwellian, and which produce elastic, inelastic, and superelastic collisions (see Sect. 7.13). A magnetic field is present, with associated Larmor frequency $\nu_{\rm L}$ (see Eq. (3.10)) and direction $\vec{\Omega}_B$. We adopt the flat-spectrum approximation by assuming that the radiation field has no spectral structure across a frequency interval $\Delta\nu$ centered at the frequency ν_0 (corresponding to the energy separation between the two levels) and larger both than $\nu_{\rm L}$ and than the width (in frequency units) of the levels.

We fix a reference system having the z-axis in the magnetic field direction, and we describe the atom by the multipole moments of the density matrix. Collecting the results on the radiative and collisional rates derived in Chap. 7 (see Eqs. (7.11) and (7.101), and the discussion in Sects. 7.13d and 7.13e), one gets for the time evolution of the multipole moments of the upper level

$$\begin{aligned}\frac{\mathrm{d}}{\mathrm{d}t}\,\rho^K_Q(\alpha_u J_u) &= -2\pi\mathrm{i}\,\nu_{\rm L}\,g_{\alpha_u J_u}\,Q\,\rho^K_Q(\alpha_u J_u)\\ &+\sum_{K'Q'}\mathbb{T}_{\rm A}(\alpha_u J_u KQ,\alpha_\ell J_\ell K'Q')\,\rho^{K'}_{Q'}(\alpha_\ell J_\ell)\\ &-\sum_{K'Q'}\Big[\mathbb{R}_{\rm E}(\alpha_u J_u KQK'Q')+\mathbb{R}_{\rm S}(\alpha_u J_u KQK'Q')\Big]\,\rho^{K'}_{Q'}(\alpha_u J_u)\\ &+\sqrt{\frac{2J_\ell+1}{2J_u+1}}\;C^{(K)}_{\rm I}(\alpha_u J_u,\alpha_\ell J_\ell)\,\rho^K_Q(\alpha_\ell J_\ell)\\ &-\Big[C^{(0)}_{\rm S}(\alpha_\ell J_\ell,\alpha_u J_u)\,+\,D^{(K)}(\alpha_u J_u)\Big]\,\rho^K_Q(\alpha_u J_u)\;, \end{aligned}\tag{10.1}$$

and for the lower level

$$\begin{aligned}\frac{\mathrm{d}}{\mathrm{d}t}\,\rho^K_Q(\alpha_\ell J_\ell) &= -2\pi\mathrm{i}\,\nu_{\rm L}\,g_{\alpha_\ell J_\ell}\,Q\,\rho^K_Q(\alpha_\ell J_\ell)\\ &+\sum_{K'Q'}\Big[\mathbb{T}_{\rm E}(\alpha_\ell J_\ell KQ,\alpha_u J_u K'Q')+\mathbb{T}_{\rm S}(\alpha_\ell J_\ell KQ,\alpha_u J_u K'Q')\Big]\,\rho^{K'}_{Q'}(\alpha_u J_u)\\ &-\sum_{K'Q'}\mathbb{R}_{\rm A}(\alpha_\ell J_\ell KQK'Q')\,\rho^{K'}_{Q'}(\alpha_\ell J_\ell)\\ &+\sqrt{\frac{2J_u+1}{2J_\ell+1}}\;C^{(K)}_{\rm S}(\alpha_\ell J_\ell,\alpha_u J_u)\,\rho^K_Q(\alpha_u J_u)\\ &-\Big[C^{(0)}_{\rm I}(\alpha_u J_u,\alpha_\ell J_\ell)\,+\,D^{(K)}(\alpha_\ell J_\ell)\Big]\,\rho^K_Q(\alpha_\ell J_\ell)\;. \end{aligned}\tag{10.2}$$

total (orbital + spin) angular momentum quantum number of the electronic cloud, while α is a collection of inner quantum numbers (see Sect. 3.1).

[1] Throughout this chapter the Stokes vector will be denoted by the symbol I_i (with $i=0,1,2,3$) rather than S_i used in preceding chapters.

All the rates appearing in these equations have been introduced and discussed in Chap. 7 (see Sect. 7.2 for the radiative rates and Sect. 7.13 for the collisional rates). Here we just recall that $\mathbb{T}_{\rm A}$, $\mathbb{T}_{\rm E}$, and $\mathbb{T}_{\rm S}$ are the radiative transfer rates due to absorption, spontaneous emission and stimulated emission, respectively, while $\mathbb{R}_{\rm A}$, $\mathbb{R}_{\rm E}$, and $\mathbb{R}_{\rm S}$ are the corresponding relaxation rates. $C_{\rm I}$ and $C_{\rm S}$ are the rates due to inelastic and superelastic collisions, respectively. Finally, D are the relaxation rates due to depolarizing elastic collisions.

Equations (10.1) and (10.2) form a system of linear, homogeneous, differential equations in the unknowns $\rho^K_Q(\alpha_\ell J_\ell)$ and $\rho^K_Q(\alpha_u J_u)$. In stationary situations, the left-hand sides of both equations are zero and the system reduces to a set of linear, homogeneous, algebraic equations. The number of equations (and of unknowns) is given by

$$N_{\rm eq} = (2J_\ell + 1)^2 + (2J_u + 1)^2 \; . \tag{10.3}$$

On the other hand, the determinant of the system is zero,[1] so that the multipole moments can be determined up to a multiplicative factor. This factor can be found by considering the trace equation, which for the two-level atom reads (see Eqs. (3.84) and (3.108))

$$\sqrt{2J_\ell + 1}\;\; \rho^0_0(\alpha_\ell J_\ell) \; + \sqrt{2J_u + 1}\;\; \rho^0_0(\alpha_u J_u) = 1 \; , \tag{10.4}$$

or, introducing the number density of atoms $\mathcal{N}$

$$\mathcal{N}_\ell + \mathcal{N}_u = \mathcal{N} \; , \tag{10.5}$$

where

$$\mathcal{N}_\ell = \mathcal{N}\sqrt{2J_\ell + 1}\;\; \rho^0_0(\alpha_\ell J_\ell) \; , \qquad \mathcal{N}_u = \mathcal{N}\sqrt{2J_u + 1}\;\; \rho^0_0(\alpha_u J_u) \; . \tag{10.6}$$

Once the statistical equilibrium equations are solved, the radiative transfer coefficients can be found from Eqs. (7.15).

In general, it is impossible to obtain a closed analytical expression for the solution to Eqs. (10.1)-(10.2). An important exception is provided by the case where the lower level is unpolarized (or naturally populated) so that its multipole moments are given by

$$\rho^K_Q(\alpha_\ell J_\ell) = \; \delta_{K0}\; \delta_{Q0}\;\; \rho^0_0(\alpha_\ell J_\ell) \; . \tag{10.7}$$

This relation is approximately satisfied when the lower-level radiative rates are much smaller than the lower-level collisional rates, which is often true in the presence of a very weak (or 'diluted') radiation field (see the discussion in Sect. 10.7). Obviously, Eq. (10.7) is identically satisfied in the special case where the lower level

[1] It can easily be shown, with the help of Eqs. (7.14), (2.36a) and (2.49), that the equations for the time derivatives of

$$\sqrt{2J_u + 1}\;\; \rho^0_0(\alpha_u J_u) \qquad \text{and} \qquad -\sqrt{2J_\ell + 1}\;\; \rho^0_0(\alpha_\ell J_\ell)$$

are identical.

has $J_\ell = 0$, since in that case $\rho^0_0(\alpha_\ell J_\ell)$ is the only non-zero multipole moment (cf. Eq. (3.101)).

Consider the statistical equilibrium equations for the upper level (Eq. (10.1)) under the assumption that Eq. (10.7) – the *unpolarized lower level* hypothesis – is valid. In stationary situations, and neglecting the rate for stimulated emission, we immediately get an analytical expression for $\rho^K_Q(\alpha_u J_u)$. Bearing in mind the expression for $\mathbb{R}_{\rm E}$ (Eq. (7.14e)) we obtain

$$\rho^K_Q(\alpha_u J_u) = \frac{\mathbb{T}_{\rm A}(\alpha_u J_u K Q, \alpha_\ell J_\ell\, 0\, 0) + \sqrt{\frac{2J_\ell+1}{2J_u+1}}\; C^{(0)}_{\rm I}(\alpha_u J_u, \alpha_\ell J_\ell)\; \delta_{K0}\; \delta_{Q0}}{2\pi {\rm i}\, \nu_{\rm L}\; g_{\alpha_u J_u}\, Q + A(\alpha_u J_u \rightarrow \alpha_\ell J_\ell) + C^{(0)}_{\rm S}(\alpha_\ell J_\ell, \alpha_u J_u) + D^{(K)}(\alpha_u J_u)}$$

$$\times\; \rho^0_0(\alpha_\ell J_\ell)\;, \tag{10.8}$$

where, from Eq. (7.14a) and using Eqs. (2.26a) and (2.49)

$$\mathbb{T}_{\rm A}(\alpha_u J_u K Q, \alpha_\ell J_\ell\, 0\, 0) = \sqrt{3(2J_\ell+1)}\; B(\alpha_\ell J_\ell \rightarrow \alpha_u J_u)$$

$$\times\; (-1)^{1+J_\ell+J_u+Q} \left\{ \begin{array}{ccc} 1 & 1 & K \\ J_u & J_u & J_\ell \end{array} \right\} J^K_{-Q}(\nu_0)\;. \tag{10.9}$$

In the following we will apply Eq. (10.8) to different physical regimes, characterized by the relative order of magnitude of the different parameters.

10.2. The Two-Level Atom: Resonance Polarization

(*unpolarized lower level - no magnetic field - no collisions*)

The ideal case of resonance polarization is obtained by neglecting in Eq. (10.8) both the effect of the magnetic field and the effect of collisions. Setting in Eq. (10.8)

$$\nu_{\rm L} = C^{(0)}_{\rm I}(\alpha_u J_u, \alpha_\ell J_\ell) = C^{(0)}_{\rm S}(\alpha_\ell J_\ell, \alpha_u J_u) = D^{(K)}(\alpha_u J_u) = 0\;,$$

and substituting Eq. (10.9), we have[1]

$$\rho^K_Q(\alpha_u J_u) = \sqrt{3(2J_\ell+1)}\; \frac{B(\alpha_\ell J_\ell \rightarrow \alpha_u J_u)}{A(\alpha_u J_u \rightarrow \alpha_\ell J_\ell)}$$

$$\times\; (-1)^{1+J_\ell+J_u+Q} \left\{ \begin{array}{ccc} 1 & 1 & K \\ J_u & J_u & J_\ell \end{array} \right\} J^K_{-Q}(\nu_0)\; \rho^0_0(\alpha_\ell J_\ell)\;. \tag{10.10}$$

It is convenient to introduce the symbol $w^{(K)}_{J_u J_\ell}$ defined by[2]

$$w^{(K)}_{J_u J_\ell} = (-1)^{1+J_\ell+J_u} \sqrt{3(2J_u+1)} \left\{ \begin{array}{ccc} 1 & 1 & K \\ J_u & J_u & J_\ell \end{array} \right\}\;, \tag{10.11}$$

[1] Note that Eq. (10.10) is valid in an arbitrary reference system, since the magnetic field is zero.

[2] The symbol was first introduced by Landi Degl'Innocenti (1984).

or, equivalently (see Eq. (2.36a))

$$w^{(K)}_{J_u J_\ell} = \frac{\left\{ \begin{array}{ccc} 1 & 1 & K \\ J_u & J_u & J_\ell \end{array} \right\}}{\left\{ \begin{array}{ccc} 1 & 1 & 0 \\ J_u & J_u & J_\ell \end{array} \right\}} \, . \tag{10.12}$$

With this new symbol, Eq. (10.10) takes the more compact form

$$\rho^K_Q(\alpha_u J_u) = \sqrt{\frac{2J_\ell + 1}{2J_u + 1}} \; \frac{B(\alpha_\ell J_\ell \to \alpha_u J_u)}{A(\alpha_u J_u \to \alpha_\ell J_\ell)} \; w^{(K)}_{J_u J_\ell} \; (-1)^Q \, J^K_{-Q}(\nu_0) \; \rho^0_0(\alpha_\ell J_\ell) \, . \tag{10.13}$$

This expression shows that the upper-level multipole moment $\rho^K_Q(\alpha_u J_u)$ is proportional to the corresponding multipole component of the radiation field tensor.[1] As the latter has a limited number of components ($K \leq 2$, see Eq. (5.155)), it follows that only the multipole moments $\rho^K_Q(\alpha_u J_u)$ with $K \leq 2$ can be excited by the radiation field.

Equation (10.13) also points out the meaning of the symbol $w^{(K)}_{J_u J_\ell}$. It is a sort of 'efficiency factor' characterizing the transfer of the K-th order multipole from the radiation field to the atomic density matrix in the absorption process from the lower level $(\alpha_\ell J_\ell)$ to the upper level $(\alpha_u J_u)$. The symbol $w^{(K)}_{J_u J_\ell}$ is defined for any dipole transition ($J_u - J_\ell = 0, \pm 1 \, ; \, 0 \nrightarrow 0$) with K ranging from 0 to 2. For $K = 0$ one obviously has, from Eq. (10.12)

$$w^{(0)}_{J_u J_\ell} = 1 \, . \tag{10.14}$$

Numerical values of $w^{(K)}_{J_u J_\ell}$ for $K = 1$ and $K = 2$ are given in Table 10.1, together with the values of other symbols that will be introduced later on.

Using the expression of the upper-level statistical tensors given in Eq. (10.13), the emission coefficient can be easily deduced. Since by assumption the magnetic field is zero, the emission coefficient is given by Eq. (7.16e), which can be rewritten in the form[2]

$$\begin{aligned} \varepsilon_i(\nu, \vec{\Omega}) = \frac{h\nu}{4\pi} \mathcal{N} \sqrt{2J_u + 1} \; A(\alpha_u J_u \to \alpha_\ell J_\ell) \\ \times \sum_{KQ} \; w^{(K)}_{J_u J_\ell} \; \mathcal{T}^K_Q(i, \vec{\Omega}) \; \rho^K_Q(\alpha_u J_u) \; \phi(\nu_0 - \nu) \, , \end{aligned} \tag{10.15}$$

---

[1] The sign difference in the subscript Q and the factor $(-1)^Q$ arise from the fact that J^K_Q is a true irreducible tensor (which, under rotation of the reference system, changes according to Eq. (2.78)), while ρ^K_Q is not (it changes according to Eq. (3.98)). The conjugate $(\rho^K_Q)^*$ – and not ρ^K_Q itself – is an irreducible tensor. The conjugation property (3.102) explains the above differences.

[2] The right-hand side should indeed be multiplied by the factor ν^3/ν_0^3 (cf. footnote on p.283).

TABLE 10.1

Values of the quantities $w^{(K)}_{J_u J_\ell}$, $W_K(J_\ell, J_u)$, $(p_Q)_{\max}$, $|p_V|_{\max}$ for different transitions

J_ℓ	J_u	$w^{(1)}_{J_u J_\ell}$	$W_1(J_\ell, J_u)$	$w^{(2)}_{J_u J_\ell}$	$W_2(J_\ell, J_u)$	$\left(p_Q\right)_{\max}$	$\left\|p_V\right\|_{\max}$
0	1	−1.	1.	1.	1.	1.	1.
1/2	1/2	−0.816	0.667	0.	0.	0.	1.
1/2	3/2	−0.913	0.833	0.707	0.5	0.429	1.
1	0	0.	0.	0.	0.	0.	0.
1	1	−0.5	0.25	−0.5	0.25	0.2	0.333
1	2	−0.866	0.75	0.592	0.35	0.288	0.957
3/2	1/2	0.408	0.167	0.	0.	0.	0.25
3/2	3/2	−0.365	0.133	−0.566	0.32	0.261	0.172
3/2	5/2	−0.837	0.7	0.529	0.28	0.226	0.921
2	1	0.5	0.25	0.1	0.01	0.008	0.373
2	2	−0.289	0.083	−0.592	0.35	0.288	0.106
2	3	−0.816	0.667	0.490	0.24	0.191	0.893
5/2	3/2	0.548	0.3	0.141	0.02	0.015	0.446
5/2	5/2	−0.239	0.057	−0.605	0.366	0.302	0.072
5/2	7/2	−0.802	0.643	0.463	0.214	0.170	0.871
3	2	0.577	0.333	0.169	0.029	0.022	0.493
3	3	−0.204	0.042	−0.612	0.375	0.310	0.053
3	4	−0.791	0.625	0.443	0.196	0.155	0.854
7/2	5/2	0.598	0.357	0.189	0.036	0.027	0.526
7/2	7/2	−0.178	0.032	−0.617	0.381	0.316	0.04
7/2	9/2	−0.782	0.611	0.428	0.183	0.144	0.840
4	3	0.612	0.375	0.204	0.042	0.032	0.551
4	4	−0.158	0.025	−0.620	0.385	0.320	0.031
4	5	−0.775	0.6	0.416	0.173	0.136	0.828
9/2	7/2	0.624	0.389	0.216	0.047	0.035	0.570
9/2	9/2	−0.142	0.020	−0.623	0.388	0.322	0.025
9/2	11/2	−0.769	0.591	0.407	0.165	0.129	0.819
5	4	0.632	0.4	0.226	0.051	0.039	0.585
5	5	−0.129	0.017	−0.624	0.39	0.324	0.021
5	6	−0.764	0.583	0.399	0.159	0.124	0.811
11/2	9/2	0.640	0.409	0.234	0.055	0.041	0.597
11/2	11/2	−0.118	0.014	−0.626	0.392	0.326	0.018
11/2	13/2	−0.760	0.577	0.392	0.154	0.12	0.804
6	5	0.645	0.417	0.240	0.058	0.044	0.607
6	6	−0.109	0.012	−0.627	0.393	0.327	0.015
6	7	−0.756	0.571	0.387	0.149	0.116	0.798

TABLE 10.1

(continued)

J_ℓ	J_u	$w^{(1)}_{J_u J_\ell}$	$W_1(J_\ell, J_u)$	$w^{(2)}_{J_u J_\ell}$	$W_2(J_\ell, J_u)$	$\left(p_Q\right)_{\max}$	$\left\|p_V\right\|_{\max}$
13/2	11/2	0.650	0.423	0.246	0.060	0.046	0.616
13/2	13/2	−0.101	0.010	−0.628	0.394	0.328	0.013
13/2	15/2	−0.753	0.567	0.382	0.146	0.113	0.792
7	6	0.655	0.429	0.251	0.063	0.048	0.623
7	7	−0.094	0.009	−0.628	0.395	0.328	0.011
7	8	−0.75	0.562	0.377	0.142	0.111	0.788
15/2	13/2	0.658	0.433	0.255	0.065	0.050	0.630
15/2	15/2	−0.089	0.008	−0.629	0.395	0.329	0.010
8	7	0.661	0.437	0.259	0.067	0.051	0.635
8	8	−0.083	0.007	−0.629	0.396	0.329	0.009

where Eqs. (10.11) and (7.8) have been used. We recall that $\mathcal{N}$ is the number density of atoms, and that the tensor $\mathcal{T}^K_Q(i,\vec{\Omega})$ is defined in Eq. (5.159) – see Table 5.6 for the explicit expressions of its components. Substitution of Eq. (10.13) into Eq. (10.15) leads, with the help of Eqs. (10.6), to the expression

$$\varepsilon_i(\nu,\vec{\Omega}) = \frac{h\nu}{4\pi}\mathcal{N}_\ell\, B(\alpha_\ell J_\ell \rightarrow \alpha_u J_u)\ \phi(\nu_0-\nu) \times \sum_{KQ} W_K(J_\ell, J_u)\ (-1)^Q\ \mathcal{T}^K_Q(i,\vec{\Omega})\ J^K_{-Q}(\nu_0)\ , \tag{10.16}$$

where the new symbol $W_K(J_\ell, J_u)$ is defined to be (see Eq. (2.36a))

$$W_K(J_\ell, J_u) = \left(w^{(K)}_{J_u J_\ell}\right)^2 = 3(2J_u+1)\begin{Bmatrix} 1 & 1 & K \\ J_u & J_u & J_\ell \end{Bmatrix}^2 = \frac{\begin{Bmatrix} 1 & 1 & K \\ J_u & J_u & J_\ell \end{Bmatrix}^2}{\begin{Bmatrix} 1 & 1 & 0 \\ J_u & J_u & J_\ell \end{Bmatrix}^2}\ . \tag{10.17}$$

Numerical values of $W_K(J_\ell, J_u)$ for $K=1$ and $K=2$ are given in Table 10.1. For $K=0$, we simply have

$$W_0(J_\ell, J_u) = 1\ . \tag{10.18}$$

Equation (10.16) gives, for the two-level atom under the approximations considered in this section, the Stokes parameters of the radiation emitted in a scattering process as a function of the incident radiation field. A still more significant expression can be obtained by writing the radiation field tensor in terms of the Stokes parameters of the incoming radiation. Bearing in mind the definition of $k^{\rm A}_{\rm L}$, the

frequency-integrated line absorption coefficient defined in Eq. (9.5), we obtain via Eqs. (5.157)

$$\varepsilon_i(\nu,\vec{\Omega}) = k_{\rm L}^{\rm A}\,\phi(\nu_0-\nu)\oint\frac{{\rm d}\Omega'}{4\pi}\sum_{j=0}^{3}P_{ij}(\vec{\Omega},\vec{\Omega}')\,I_j(\nu_0,\vec{\Omega}')\;, \tag{10.19}$$

where $P_{ij}(\vec{\Omega},\vec{\Omega}')$, the (quantum-mechanical) scattering phase matrix, is given by

$$P_{ij}(\vec{\Omega},\vec{\Omega}') = \sum_{KQ} W_K(J_\ell,J_u)\;(-1)^Q\;\mathcal{T}^K_Q(i,\vec{\Omega})\;\mathcal{T}^K_{-Q}(j,\vec{\Omega}')\;. \tag{10.20}$$

This result, first derived by Hamilton (1947) – see also Chandrasekhar (1950)[1] – generalizes to Quantum Mechanics the expression for the scattering phase matrix $R_{ij}(\vec{\Omega},\vec{\Omega}')$ that we have obtained by a 'classical' derivation (see Sects. 5.7 and 5.10). The relation between $P_{ij}(\vec{\Omega},\vec{\Omega}')$ and $R_{ij}(\vec{\Omega},\vec{\Omega}')$ can easily be established. From Eqs. (5.137)-(5.138) we have

$$\begin{aligned} R_{ij}(\vec{\Omega},\vec{\Omega}') \equiv R_{ij}(\vec{\Omega},\vec{\Omega}';0) &= \sum_K R^{(K)}_{ij}(\vec{\Omega},\vec{\Omega}';0) \\ &= \sum_K\Big[\sum_Q(-1)^Q\;\mathcal{T}^K_Q(i,\vec{\Omega})\;\mathcal{T}^K_{-Q}(j,\vec{\Omega}')\Big]\;, \end{aligned} \tag{10.21}$$

hence

$$P_{ij}(\vec{\Omega},\vec{\Omega}') = \sum_K W_K(J_\ell,J_u)\;R^{(K)}_{ij}(\vec{\Omega},\vec{\Omega}';0)\;. \tag{10.22}$$

In other words, the quantum-mechanical scattering phase matrix is obtained by summation of the multipole components of the classical matrix multiplied by the corresponding W_K factors. It is interesting to note that for the transition $(J_\ell=0,J_u=1)$ all the W_K are unity, and that such a property is valid *only* for this transition (see Table 10.1). We thus find a further confirmation of the fact that $(J_\ell=0,J_u=1)$ is the only transition properly described by the classical theory.

Various properties of the matrix $R_{ij}(\vec{\Omega},\vec{\Omega}')$ have been proved in Chap. 5. These properties can be easily extended to the matrix $P_{ij}(\vec{\Omega},\vec{\Omega}')$. First of all, $P_{ij}(\vec{\Omega},\vec{\Omega}')$ is real: this is obvious from Eq. (10.19) – where all the other quantities are real – but can directly be checked from the definition in Eq. (10.20) with the help of Eqs. (5.158). From Eq. (10.20) it follows also that $P_{ij}(\vec{\Omega},\vec{\Omega}')$ satisfies the Helmoltz principle of reciprocity for a scattering process,

$$P_{ij}(\vec{\Omega},\vec{\Omega}') = P_{ji}(\vec{\Omega}',\vec{\Omega})\;,$$

[1] Chandrasekhar introduces the symbols E_1, E_2, and E_3 instead of W_1 and W_2. The relationship is the following

$$E_1 = W_2\;,\quad E_2 = 1-W_2\;,\quad E_3 = W_1\;.$$

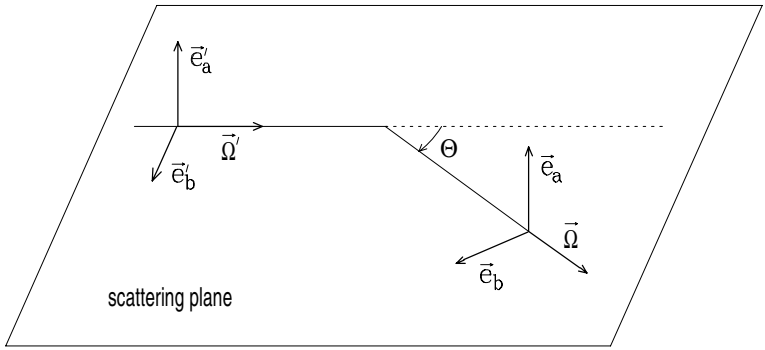

Fig.10.1. Geometry of a scattering process. The unit vectors $\vec{e}'_a$ and $\vec{e}_a$, which define the positive Q direction for the incident and the scattered beam, respectively, are perpendicular to the scattering plane $(\vec{\Omega}', \vec{\Omega})$.

which generalizes Eq. (5.95). Finally, from Eq. (10.22), using the second expression in Eq. (5.138) – with $H = 0$ – and Eq. (2.74), we obtain

$$P_{ij}(\vec{\Omega}, \vec{\Omega}') = \sum_{KPP'} W_K(J_\ell, J_u)\ t^K_P(i)\ t^K_{P'}(j)^*\ \mathcal{D}^K_{PP'}(R)\ , \tag{10.23}$$

where the symbol t^K_P is defined in Eq. (5.160) and R is the rotation carrying the reference frame $(\vec{e}_a(\vec{\Omega}), \vec{e}_b(\vec{\Omega}), \vec{\Omega})$ into the frame $(\vec{e}'_a(\vec{\Omega}'), \vec{e}'_b(\vec{\Omega}'), \vec{\Omega}')$. Equation (10.23) is the quantum-mechanical generalization of Eq. (5.168).

The physical meaning of the symbol $W_K(J_\ell, J_u)$ can be better illustrated by considering the polarization of the emitted radiation in a scattering process. Let us consider the scattering geometry of Fig. 10.1. The phase matrix can be obtained from Eqs. (10.22) and (5.139) by setting in the latter[1] $\mu = \mu' = 0$, $C_1 = \cos\Theta$, $S_1 = -\sin\Theta$, $C_2 = \cos 2\Theta$, $S_2 = -\sin 2\Theta$. One gets, with the use of Eq. (10.18)

$$\boldsymbol{P}(\vec{\Omega}, \vec{\Omega}') =$$

$$= \begin{pmatrix} 1 - \frac{1}{4}W_2\,(1 - 3\cos^2\Theta) & \frac{3}{4}W_2\ \sin^2\Theta & 0 & 0 \\ \frac{3}{4}W_2\ \sin^2\Theta & \frac{3}{4}W_2\,(1 + \cos^2\Theta) & 0 & 0 \\ 0 & 0 & \frac{3}{2}W_2\ \cos\Theta & 0 \\ 0 & 0 & 0 & \frac{3}{2}W_1\cos\Theta \end{pmatrix}. \tag{10.24}$$

For an unpolarized incident beam, the scattered radiation is found to be linearly polarized with fractional polarization given by

$$p_Q \equiv \frac{\varepsilon_Q(\nu, \vec{\Omega})}{\varepsilon_I(\nu, \vec{\Omega})} = \frac{P_{10}(\vec{\Omega}, \vec{\Omega}')}{P_{00}(\vec{\Omega}, \vec{\Omega}')} = \frac{3\,W_2\ \sin^2\Theta}{4 - W_2 + 3\,W_2\cos^2\Theta}$$

$$p_U \equiv \frac{\varepsilon_U(\nu, \vec{\Omega})}{\varepsilon_I(\nu, \vec{\Omega})} = \frac{P_{20}(\vec{\Omega}, \vec{\Omega}')}{P_{00}(\vec{\Omega}, \vec{\Omega}')} = 0\ . \tag{10.25}$$

[1] We recall that Eqs. (5.139) refer to the geometry of Fig. 5.10. The geometry of Fig. 10.1 is recovered by setting $\theta = \theta' = 90°$, $\chi - \chi' = \Theta$. The corresponding values of μ, μ', C_1, S_1, C_2, S_2 are then obtained from Eqs. (5.84), (5.98) and (5.97).

TABLE 10.2

Analytical expressions of the quantities $W_K(J_\ell, J_u)$, $(p_Q)_{\max}$, $|p_V|_{\max}$

	$W_1(J_\ell, J_u)$	$W_2(J_\ell, J_u)$	$\big(p_Q\big)_{\max}$	$\big\lvert p_V\big\rvert_{\max}$
$J_u = J_\ell + 1$	$\frac{J_\ell + 2}{2\,(J_\ell + 1)}$	$\frac{(2J_\ell + 5)(J_\ell + 2)}{10\,(J_\ell + 1)(2J_\ell + 1)}$	$\frac{(2J_\ell + 5)(J_\ell + 2)}{26J_\ell^2 + 37J_\ell + 10}$	$\frac{5\,(J_\ell + 2)(2J_\ell + 1)}{14J_\ell^2 + 23J_\ell + 10}$
$J_u = J_\ell$	$\frac{1}{2\,J_\ell(J_\ell + 1)}$	$\frac{(2J_\ell - 1)(2J_\ell + 3)}{10\,J_\ell(J_\ell + 1)}$	$\frac{(2J_\ell - 1)(2J_\ell + 3)}{12J_\ell^2 + 12J_\ell + 1}$	$\frac{5}{8J_\ell^2 + 8J_\ell - 1}$
$J_u = J_\ell - 1$	$\frac{J_\ell - 1}{2\,J_\ell}$	$\frac{(2J_\ell - 3)(J_\ell - 1)}{10\,J_\ell(2J_\ell + 1)}$	$\frac{(J_\ell - 1)(2J_\ell - 3)}{26J_\ell^2 + 15J_\ell - 1}$	$\frac{5\,(J_\ell - 1)(2J_\ell + 1)}{14J_\ell^2 + 5J_\ell + 1}$

Since W_2 values range from 0 to 1, p_Q is always positive, which means that the polarization is perpendicular to the scattering plane. Its maximum value is found for $\Theta = 90°$ and is given by

$$\big(p_Q\big)_{\max} = \frac{3\,W_2}{4 - W_2}\,. \tag{10.26}$$

This is an increasing function of W_2. The factor W_2 can thus be regarded as an efficiency factor for the generation of linear polarization from unpolarized radiation in scattering processes.

The parameter W_1, on the contrary, is only related to circular polarization. In the geometry of Fig. 10.1, assuming that the incident radiation is totally circularly polarized (say positively), the fractional circular polarization of the scattered radiation is given by

$$p_V \equiv \frac{\varepsilon_V(\nu, \vec{\Omega})}{\varepsilon_I(\nu, \vec{\Omega})} = \frac{P_{33}(\vec{\Omega}, \vec{\Omega}')}{P_{00}(\vec{\Omega}, \vec{\Omega}')} = \frac{6\,W_1 \cos\Theta}{4 - W_2 + 3\,W_2\,\cos^2\Theta}\,.$$

Since W_1 is non-negative, the handedness of the scattered circular polarization is the same as that of the incident radiation for $\Theta < 90°$, the opposite for $\Theta > 90°$ (p_V vanishes for $\Theta = 90°$). The maximum absolute value of p_V is found for $\Theta = 0°$ (forward scattering) and for $\Theta = 180°$ (backward scattering), and is given by

$$\big\lvert p_V\big\rvert_{\max} = \frac{3\,W_1}{2 + W_2}\,.$$

This formula shows that W_1 can be considered as an efficiency factor for the generation of circular (from circular) polarization in scattering processes.

Numerical values of $(p_Q)_{\max}$ and $|p_V|_{\max}$ for different transitions are given in Table 10.1. It is important to notice that W_2 – hence $(p_Q)_{\max}$ – vanishes for any transition having $J_u = 0$ or $J_u = 1/2$. On the contrary, W_1 – hence $|p_V|_{\max}$ – vanishes only for the transition $(J_\ell = 1, J_u = 0)$.

Table 10.2 gives the analytical expressions of W_1, W_2, $(p_Q)_{\max}$ and $|p_V|_{\max}$ for dipole transitions. Such expressions can be obtained from Eq. (10.17) with the help of Eqs. (2.36d) and (2.36h).

10.3. The Two-Level Atom: the Hanle Effect

(*unpolarized lower level - no collisions*)

The basic characteristics of the Hanle effect are obtained from Eq. (10.8) by retaining the 'magnetic' term (first term in the denominator, which was set to zero in the preceding section).[1] In order to further simplify our treatment, we still neglect – as in the preceding section – the effects of collisions (this matter is deferred until Sect. 10.6). Using Eqs. (10.9) and (10.11), we can rewrite Eq. (10.8) in the form

$$\rho^K_Q(\alpha_u J_u) = \sqrt{\frac{2J_\ell+1}{2J_u+1}}\ \frac{B(\alpha_\ell J_\ell \to \alpha_u J_u)}{A(\alpha_u J_u \to \alpha_\ell J_\ell) + 2\pi \mathrm{i}\,\nu_\mathrm{L}\, g_{\alpha_u J_u} Q} \times\ w^{(K)}_{J_u J_\ell}\ (-1)^Q\, J^K_{-Q}(\nu_0)\ \rho^0_0(\alpha_\ell J_\ell)\ . \tag{10.27}$$

We recall that the statistical tensors are defined in a reference system having the z-axis in the magnetic field direction. Comparison with the corresponding expression obtained for the non-magnetic regime (Eq. (10.13)) shows that the effect of the magnetic field is to *reduce and dephase*, via the imaginary term in the denominator, *all the multipole moments with* $Q \neq 0$. The efficiency of this relaxation process is controlled by the dimensionless parameter H_u defined by

$$H_u = \frac{2\pi\nu_\mathrm{L}\, g_{\alpha_u J_u}}{A(\alpha_u J_u \to \alpha_\ell J_\ell)}\ . \tag{10.28}$$

This parameter is the quantum-mechanical analogue of the parameter H introduced in the classical derivation of the Hanle effect (see Eq. (5.84)).[2] Numerically, one has (cf. Eq. (5.85))

$$H_u = \frac{0.879\, g_{\alpha_u J_u} B}{A(\alpha_u J_u \to \alpha_\ell J_\ell)}\ , \tag{10.29}$$

where B is in G and $A(\alpha_u J_u \to \alpha_\ell J_\ell)$ in $10^7\,\mathrm{s}^{-1}$.

Using H_u, Eq. (10.27) can be expressed in the form

$$\rho^K_Q(\alpha_u J_u) = \frac{1}{1+\mathrm{i}\,Q H_u}\left[\rho^K_Q(\alpha_u J_u)\right]_{B=0}\ , \tag{10.30}$$

where $[\rho^K_Q(\alpha_u J_u)]_{B=0}$ are the multipole moments for the non-magnetic case (in the presence of the same radiation field and defined in the same reference system). Equation (10.30) summarizes the 'essence' of the Hanle effect. It shows that coherences with $Q = 0$ (those connected with the populations of the Zeeman sublevels, see Eq. (3.101)) are unaffected by the magnetic field, while those with

[1] Note that we are still using the unpolarized lower level assumption and we are neglecting, accordingly, stimulated emission effects.

[2] The classical damping constant γ, defined in Eq. (5.28), has its obvious quantum-mechanical counterpart in the Einstein coefficient A.

$Q \neq 0$ are reduced, with respect to the non-magnetic case, by a factor $\sqrt{1+Q^2H_u^2}$. The magnetic field has the additional effect of introducing a phase factor, given by $\arctan(QH_u)$, in the latter. Such conclusions were anticipated in Sect. 5.13 where an intuitive description of the Hanle effect, based on classical physics, was presented.

The radiation emitted by the atom along a given direction is obtained by substitution of Eq. (10.27) into Eq. (7.15e) – adapted to the case of our two-level atom. The resulting expression is quite involved, and will be studied in detail in the next section. Here we disregard the spectral details of the emitted radiation, and we restrict attention to the frequency-integrated emission coefficient, defined by

$$\tilde{\varepsilon}_i(\vec{\Omega}) = \int_{\Delta\nu} \varepsilon_i(\nu, \vec{\Omega})\, \mathrm{d}\nu \,,$$

where the interval $\Delta\nu$ is sufficiently broad to fully cover all the Zeeman components of the line. Taking into account that all the profiles $\Phi(\nu_{\alpha_u J_u M_u,\, \alpha_\ell J_\ell M_\ell} - \nu)$ are normalized to unity in frequency (see Eqs. (6.59a-c)), we obtain, along the same lines leading from Eq. (7.15e) to Eq. (7.16e)

$$\begin{aligned}\tilde{\varepsilon}_i(\vec{\Omega}) = {} & \frac{h^2\nu^4}{2\pi c^2}\, \mathcal{N}\, (2J_u+1)\, B(\alpha_u J_u \rightarrow \alpha_\ell J_\ell) \\ & \times \sum_{KQ} \sqrt{3}\ (-1)^{1+J_\ell+J_u} \left\{ \begin{array}{ccc} 1 & 1 & K \\ J_u & J_u & J_\ell \end{array} \right\} \mathcal{T}^K_Q(i, \vec{\Omega})\, \rho^K_Q(\alpha_u J_u) \,,\end{aligned}$$

or, with the use of Eqs. (7.8) and (10.11)

$$\tilde{\varepsilon}_i(\vec{\Omega}) = \frac{h\nu}{4\pi}\, \mathcal{N}\sqrt{2J_u+1}\ A(\alpha_u J_u \rightarrow \alpha_\ell J_\ell) \sum_{KQ} w^{(K)}_{J_u J_\ell}\, \mathcal{T}^K_Q(i, \vec{\Omega})\, \rho^K_Q(\alpha_u J_u) \,. \quad (10.31)$$

Substitution of Eq. (10.27) into Eq. (10.31) yields, with the help of Eqs. (5.157), (9.5), (10.6), (10.17) and (10.28)

$$\tilde{\varepsilon}_i(\vec{\Omega}) = k^{\mathrm{A}}_{\mathrm{L}} \oint \frac{\mathrm{d}\Omega'}{4\pi} \sum_{j=0}^{3} P_{ij}(\vec{\Omega}, \vec{\Omega}'; \vec{B})\, I_j(\nu_0, \vec{\Omega}') \,, \quad (10.32)$$

where $P_{ij}(\vec{\Omega}, \vec{\Omega}'; \vec{B})$, the quantum-mechanical scattering phase matrix in the presence of a magnetic field, is given by[1]

$$P_{ij}(\vec{\Omega}, \vec{\Omega}'; \vec{B}) = \sum_{KQ} W_K(J_\ell, J_u)\ (-1)^Q\, \mathcal{T}^K_Q(i, \vec{\Omega})\, \mathcal{T}^K_{-Q}(j, \vec{\Omega}')\, \frac{1}{1 + \mathrm{i}\, QH_u} \,. \quad (10.33)$$

[1] The expression in Eq. (10.33) was first derived by Landi Degl'Innocenti (1985c).

This expression generalizes to Quantum Mechanics the result that we have derived in Chap. 5 from the classical theory of the electron (Eq. (5.133)). The difference from the classical result is twofold: the factor W_K comes into play, and the classical parameter H is replaced by H_u (note that both W_K and H_u depend on the atomic transition). As expected, the quantum-mechanical and the classical phase matrix coincide for the transition ($J_\ell = 0, J_u = 1$) with $g_{\alpha_u J_u} = 1$ (normal Zeeman triplet), provided the classical damping constant γ is identified with the Einstein coefficient $A(\alpha_u J_u \rightarrow \alpha_\ell J_\ell)$ – we recall that $W_K(0,1) = 1$ for $K = 0, 1, 2$ (see Table 10.1). In general, the quantum-mechanical scattering matrix is formally related to the multipole components of the classical matrix by the expression

$$P_{ij}(\vec{\Omega}, \vec{\Omega}'; \vec{B}) = \sum_K W_K(J_\ell, J_u)\; R_{ij}^{(K)}(\vec{\Omega}, \vec{\Omega}'; \vec{B}) \;, \tag{10.34}$$

where $R_{ij}^{(K)}(\vec{\Omega}, \vec{\Omega}'; \vec{B})$ is defined as in Eq. (5.138) with H replaced by H_u.

Several properties proved in Chap. 5 for the classical scattering phase matrix are valid for the quantum-mechanical matrix as well. It can easily be shown that $P_{ij}(\vec{\Omega}, \vec{\Omega}'; \vec{B})$ is real and satisfies the relation[1]

$$P_{ij}(\vec{\Omega}, \vec{\Omega}'; -\vec{B}) = P_{ji}(\vec{\Omega}', \vec{\Omega}; \vec{B}) \;, \tag{10.35}$$

analogous to Eq. (5.94). It can also be shown, using Eq. (10.34), that the value of the Van Vleck angle (Eq. (5.100)) is independent of the atomic transition – except of course for $J_u = 0$ or $J_u = 1/2$ since in those cases the linear polarization of the scattered radiation is zero. This property is basically due to the fact that the values of W_2 are limited between 0 and 1. The other properties proved in Sect. 5.12 for the classical matrix are easily extended to the quantum-mechanical matrix. In particular, we can consider the average of the scattering matrix over an isotropic distribution of magnetic fields, defined by

$$\left\langle P_{ij}(\vec{\Omega}, \vec{\Omega}'; \vec{B}) \right\rangle = \frac{1}{4\pi} \int_0^{2\pi} \mathrm{d}\chi_B \int_0^{\pi} \sin\theta_B \; P_{ij}(\vec{\Omega}, \vec{\Omega}'; \vec{B}) \; \mathrm{d}\theta_B \;,$$

where θ_B and χ_B are the polar and azimuth angle, respectively, of the magnetic field vector in a given reference frame (see Fig. 5.9). Along the same lines of Sect. 5.12 we obtain

$$\left\langle P_{ij}(\vec{\Omega}, \vec{\Omega}'; \vec{B}) \right\rangle = \sum_K W_K(J_\ell, J_u)\; \mu_K \, R_{ij}^{(K)}(\vec{\Omega}, \vec{\Omega}'; 0) \;, \tag{10.36}$$

where the multipole components $R_{ij}^{(K)}(\vec{\Omega}, \vec{\Omega}'; 0)$ are defined in Eq. (10.21) and the quantities μ_K are given by Eq. (5.172) with the substitution $H \rightarrow H_u$. Equation (10.36) is the quantum analogue of Eq. (5.174); as expected, the two expressions

[1] Equation (10.35) can be proved with the help of Eqs. (5.137), (5.138), (5.165) and (5.169).

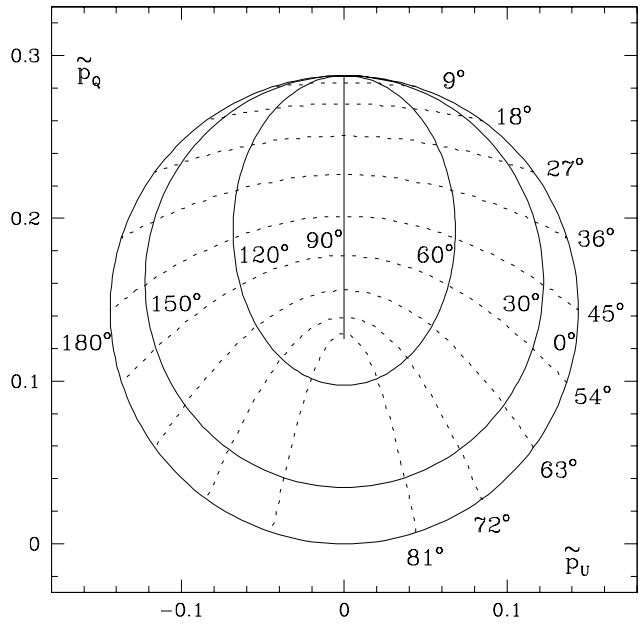

Fig.10.2. Polarization (or Hanle) diagram for the transition ($J_\ell = 1$, $J_u = 2$), relative to the scattering process illustrated in Fig.5.11. Full lines correspond to $\beta = \text{const.}$, dashed lines to constant magnetic field strength, parameterized through the angle α_2 (see Eqs.(10.28) and (10.38)). Note the scale difference from the classical Hanle diagram of Fig.5.12.

coincide for the transition ($J_\ell = 0, J_u = 1$) with $g_{\alpha_u J_u} = 1$ (see Table 10.1 and footnote 2 on p. 520).

In order to illustrate the Hanle effect in a specific case, let us consider the scattering geometry of Fig. 5.11. The polarization of the scattered radiation is given by Eq. (10.32) with the phase matrix of Eq. (10.34). The multipole components $R_{ij}^{(K)}(\vec{\Omega}, \vec{\Omega}'; \vec{B})$ are given by Eqs. (5.139).[1] The resulting fractional (frequency-integrated) linear polarization is found to be

$$\tilde{p}_Q \equiv \frac{\tilde{\varepsilon}_Q(\vec{\Omega})}{\tilde{\varepsilon}_I(\vec{\Omega})} = \frac{3\,W_2\left[\sin^2\beta + (1+\cos^2\beta)\cos^2\alpha_2\right]}{8 + W_2\,(1 - 3\cos^2\beta - 3\sin^2\beta\cos^2\alpha_2)}$$

$$\tilde{p}_U \equiv \frac{\tilde{\varepsilon}_U(\vec{\Omega})}{\tilde{\varepsilon}_I(\vec{\Omega})} = \frac{6\,W_2\,\cos\beta\,\sin\alpha_2\cos\alpha_2}{8 + W_2\,(1 - 3\cos^2\beta - 3\sin^2\beta\cos^2\alpha_2)}\,, \qquad (10.37)$$

where

$$\tan\alpha_2 = 2H_u\,. \qquad (10.38)$$

Figure 10.2 shows the polarization diagram predicted by Eqs. (10.37) for the transition ($J_\ell = 1, J_u = 2$), which has a W_2 value of 0.35 (see Table 10.1). Note that

[1] Note that the scattering geometry of Fig. 5.11 is a special case of the geometry of Fig. 5.10 (which is implied by Eqs. (5.139)) corresponding to $\mu = \cos\beta$, $\mu' = 0$, $\chi - \chi' = 90°$. The values of μ, μ', C_1, S_1, C_2, S_2 are given by Eqs. (5.97) and (5.98) – in the latter, H is replaced by H_u.

the diagram is quite similar to the classical Hanle diagram shown in Fig. 5.12 (cf. Eqs. (5.102)), apart from a scale factor due to the smaller polarizing efficiency of the transition (the maximum fractional polarization, corresponding to zero magnetic field, is $21/73 \simeq 0.288$ – see Table 10.2 – instead of 1). The shape of the Hanle diagrams can be appropriately characterized by the relative height, r, of the 'center' of the diagram (defined as the point corresponding to $\alpha_2 = 90°$, $\beta = 90°$). The parameter r is just the ratio of the scattered polarization for infinitely large magnetic field to the polarization for zero field, in the 90° scattering of an unpolarized beam with the magnetic field perpendicular to the scattering plane,

$$r = \frac{\tilde{p}_Q(\alpha_2 = 90°, \beta = 90°)}{\tilde{p}_Q(\alpha_2 = 0°)} \ .$$

From Eqs. (10.37) we have

$$r = \frac{4 - W_2}{8 + W_2} \ ,$$

thus r varies from 1/3 for $W_2 = 1$ to 1/2 for $W_2 \to 0$ (minimum polarizing efficiency). For the transition $(J_\ell = 1, J_u = 2)$ we get $r \simeq 0.437$.

10.4. The Two-Level Atom: Spectral Details of the Hanle Effect

(*unpolarized lower level - no collisions*)

In this section we analyze in some detail the frequency dependence of the emitted radiation in the Hanle effect. It is important to recall that the results presented in the following are valid under the flat-spectrum approximation for the incident radiation field. As in the preceding section, we assume that the lower level is unpolarized and we neglect collisions.

The emission coefficient in the four Stokes parameters, as a function of frequency, is obtained by substitution of Eq. (10.27) into Eq. (7.15e). Before performing the substitution, it is convenient to rewrite the latter in the form

$$\varepsilon_i(\nu, \vec{\Omega}) = \frac{h\nu}{4\pi} \mathcal{N} \sqrt{2J_u + 1} \ A(\alpha_u J_u \to \alpha_\ell J_\ell) \times \sum_{KK'Q} \mathcal{T}_Q^{K'}(i, \vec{\Omega}) \ \rho_Q^K(\alpha_u J_u) \ \Phi_Q^{KK'}(J_\ell, J_u; \nu) \ , \qquad (10.39)$$

where the *generalized profile* $\Phi_Q^{KK'}(J_\ell, J_u; \nu)$ is given by[1]

[1] The symbol was introduced by Landi Degl'Innocenti et al. (1991).

$$\Phi_Q^{KK'}(J_\ell, J_u; \nu) = \sqrt{3(2J_u+1)(2K+1)(2K'+1)}$$
$$\times \sum_{M_u M'_u M_\ell q q'} (-1)^{1+J_u-M_u+q'} \begin{pmatrix} J_u & J_\ell & 1 \\ -M_u & M_\ell & -q \end{pmatrix} \begin{pmatrix} J_u & J_\ell & 1 \\ -M'_u & M_\ell & -q' \end{pmatrix}$$
$$\times \begin{pmatrix} J_u & J_u & K \\ M'_u & -M_u & -Q \end{pmatrix} \begin{pmatrix} 1 & 1 & K' \\ q & -q' & -Q \end{pmatrix}$$
$$\times \frac{1}{2}\left[\Phi(\nu_{\alpha_u J_u M_u, \alpha_\ell J_\ell M_\ell} - \nu) + \Phi(\nu_{\alpha_u J_u M'_u, \alpha_\ell J_\ell M_\ell} - \nu)^*\right] . \quad (10.40)$$

Equation (10.39) shows that the generalized profile is a frequency-dependent coupling coefficient connecting the (K, Q) multipole moment of the atomic density matrix with the (K', Q) multipole component of the emitted radiation. Its main properties, including the proof of Eq. (10.39), are given in App. 13.

Substitution of Eq. (10.27) into Eq. (10.39) yields, with the help of Eqs. (5.157), (9.5), (10.6) and (10.28)

$$\varepsilon_i(\nu, \vec{\Omega}) = k_{\rm L}^{\rm A} \sum_{KK'Q} \Phi_Q^{KK'}(J_\ell, J_u; \nu)$$
$$\times \oint \frac{{\rm d}\Omega'}{4\pi} \sum_{j=0}^{3} w_{J_u J_\ell}^{(K)} (-1)^Q \mathcal{T}_Q^{K'}(i, \vec{\Omega}) \mathcal{T}_{-Q}^{K}(j, \vec{\Omega}') \frac{1}{1 + {\rm i}\, Q H_u} I_j(\nu_0, \vec{\Omega}') . \quad (10.41)$$

Obviously, Eq. (10.41) reduces to Eq. (10.32) after integration over frequency (see Eqs. (A13.3) and (10.17)).

A remarkable result can be deduced from Eq. (10.41): provided the width of the lower level is much smaller than the width of the upper level (which requires a sufficiently weak incident radiation field), *the Hanle effect vanishes in the far wings of the line*. In other words, resonance scattering in the line wings is unaffected by the presence of the magnetic field.

To prove this property, we go back to Eq. (6.59a). Neglecting frequency shifts, we can write

$$\Phi(\nu_{\alpha_u J_u M_u, \alpha_\ell J_\ell M_\ell} - \nu) = \frac{1}{\pi} \frac{1}{\Gamma - {\rm i}\,(\nu_{\alpha_u J_u M_u, \alpha_\ell J_\ell M_\ell} - \nu)} ,$$

where (see Eq. (7.3))

$$\nu_{\alpha_u J_u M_u, \alpha_\ell J_\ell M_\ell} = \nu_0 + \nu_{\rm L} (g_{\alpha_u J_u} M_u - g_{\alpha_\ell J_\ell} M_\ell) .$$

It follows that

$$\frac{1}{2}\left[\Phi(\nu_{\alpha_u J_u M_u, \alpha_\ell J_\ell M_\ell} - \nu) + \Phi(\nu_{\alpha_u J_u M'_u, \alpha_\ell J_\ell M_\ell} - \nu)^*\right] =$$
$$= \frac{1}{2\pi} \frac{2\Gamma + {\rm i}\,\nu_{\rm L}\, g_{\alpha_u J_u} (M'_u - M_u)}{\left[\Gamma - {\rm i}\,(\nu_{\alpha_u J_u M_u, \alpha_\ell J_\ell M_\ell} - \nu)\right]\left[\Gamma + {\rm i}\,(\nu_{\alpha_u J_u M'_u, \alpha_\ell J_\ell M_\ell} - \nu)\right]} . \quad (10.42)$$

In the far wings ($|\nu_0-\nu| \gg \Gamma$ and $|\nu_0-\nu| \gg \nu_{\rm L}$) we obtain

$$\frac{1}{2}\left[\Phi(\nu_{\alpha_u J_u M_u,\,\alpha_\ell J_\ell M_\ell}-\nu)+\Phi(\nu_{\alpha_u J_u M'_u,\,\alpha_\ell J_\ell M_\ell}-\nu)^*\right] \approx$$

$$\approx \left[1+\mathrm{i}\,\frac{\nu_{\rm L}\, g_{\alpha_u J_u}}{2\Gamma}\,(M'_u-M_u)\right]\frac{1}{\pi}\,\frac{\Gamma}{\Gamma^2+(\nu_0-\nu)^2}\ .$$

Substitution into Eq. (10.40) yields, owing to the presence of the third 3-j symbol

$$\begin{aligned}\Phi_Q^{KK'}(J_\ell,J_u;\nu) \approx{}& \left[1+\mathrm{i}\,Q\,\frac{\nu_{\rm L}\, g_{\alpha_u J_u}}{2\Gamma}\right]\frac{1}{\pi}\frac{\Gamma}{\Gamma^2+(\nu_0-\nu)^2}\\ &\times\sqrt{3(2J_u+1)(2K+1)(2K'+1)}\\ &\times\sum_{M_u M'_u M_\ell q q'}(-1)^{1+J_u-M_u+q'}\begin{pmatrix}J_u & J_\ell & 1\\ -M_u & M_\ell & -q\end{pmatrix}\begin{pmatrix}J_u & J_\ell & 1\\ -M'_u & M_\ell & -q'\end{pmatrix}\\ &\times\begin{pmatrix}J_u & J_u & K\\ M'_u & -M_u & -Q\end{pmatrix}\begin{pmatrix}1 & 1 & K'\\ q & -q' & -Q\end{pmatrix}\ .\end{aligned}$$

The summation can easily be evaluated (see the derivation of Eq. (A13.3)). If the width of the lower level is negligible compared to the width of the upper level, we have from Eqs. (6.59b) – see footnote 2 on p. 520

$$\Gamma=\frac{A(\alpha_u J_u\to\alpha_\ell J_\ell)}{4\pi}\ , \tag{10.43}$$

and recalling Eq. (10.28) we finally obtain

$$\Phi_Q^{KK'}(J_\ell,J_u;\nu)\approx\ \delta_{KK'}\ w^{(K)}_{J_u J_\ell}\,(1+\mathrm{i}\,Q H_u)\ \phi(\nu_0-\nu)\ .$$

Substitution into Eq. (10.41) shows that the dependence on the magnetic field disappears – in fact, Eq. (10.41) reduces to Eq. (10.19). This proves that the Hanle effect vanishes in the line wings.

To get a deeper insight into Eq. (10.41), let us consider a specific scattering process. We refer again to the geometry of Fig. 5.11, and we set $\beta = 0°$ (the magnetic field points in the direction of the outgoing radiation) and denote by I' and $\Delta\Omega'$, respectively, the intensity and the (infinitesimal) angular spread of the incoming, unpolarized beam. The tensors $\mathcal{T}^K_Q$ can be evaluated from Table 5.6.[1] For the sake of simplicity we consider the transition ($J_\ell = 0, J_u = 1$) with $g_{\alpha_u J_u} = 1$.

[1] A possible choice for the angles appearing in Table 5.6 is: $\theta = 0°$, χ, $\gamma = 90°$ for the emitted radiation; $\theta' = 90°$, $\chi' = \chi$ for the incident radiation. An equivalent choice – cf. footnote on p.523 – is: $\theta = 0°$, χ, $\gamma = 0°$; $\theta' = 90°$, $\chi' = \chi - 90°$.

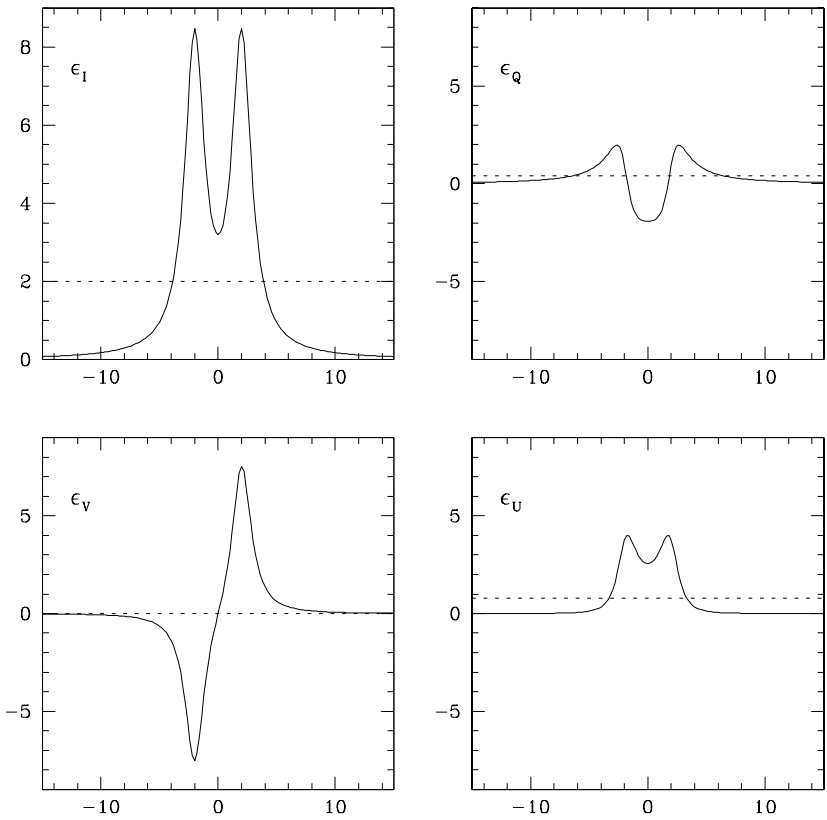

Fig.10.3. The emission coefficients of Eqs.(10.44), normalized to $(3/8)\, k_{\rm L}^{\rm A} \Delta\Omega'\, I'$, are plotted in units of $10^8\,{\rm s}^{-1}$ against the 'reduced' frequency $(\nu_0 - \nu)/\Gamma$. The relevant parameters are: $A(\alpha_u J_u \to \alpha_\ell J_\ell) = 5 \times 10^7\,{\rm s}^{-1}$, $H_u = 1$ (hence $\Gamma = 3.98 \times 10^6\,{\rm s}^{-1}$, $B = 5.69\,{\rm G}$). The dashed lines represent the values obtained from frequency-integrated observations. Note that the full frequency range corresponds to 1 mÅ for a line at 5000 Å.

After some algebra we obtain, with the help of Eqs. (A13.11) and Table 10.1

$$
\begin{aligned}
\varepsilon_0(\nu, \vec{\Omega}) &= \frac{3}{8}\, k_{\rm L}^{\rm A}\, \Delta\Omega'\, I' \left[\phi_{-1} + \phi_1 \right] \\
\varepsilon_1(\nu, \vec{\Omega}) &= \frac{3}{8}\, k_{\rm L}^{\rm A}\, \Delta\Omega'\, I' \left[\frac{1}{1+4H_u^2} \left(\phi_{-1} + \phi_1 \right) - \frac{2H_u}{1+4H_u^2} \left(\psi_{-1} - \psi_1 \right) \right] \\
\varepsilon_2(\nu, \vec{\Omega}) &= \frac{3}{8}\, k_{\rm L}^{\rm A}\, \Delta\Omega'\, I' \left[\frac{2H_u}{1+4H_u^2} \left(\phi_{-1} + \phi_1 \right) + \frac{1}{1+4H_u^2} \left(\psi_{-1} - \psi_1 \right) \right] \\
\varepsilon_3(\nu, \vec{\Omega}) &= -\frac{3}{8}\, k_{\rm L}^{\rm A}\, \Delta\Omega'\, I' \left[\phi_{-1} - \phi_1 \right] ,
\end{aligned}
\tag{10.44}
$$

where the profiles ϕ_{-1}, ϕ_1, ψ_{-1}, ψ_1 are defined in Eqs. (A13.10).

The emission coefficients in the four Stokes parameters predicted by Eqs. (10.44) are shown in Fig. 10.3. One can note the presence of circular polarization – due

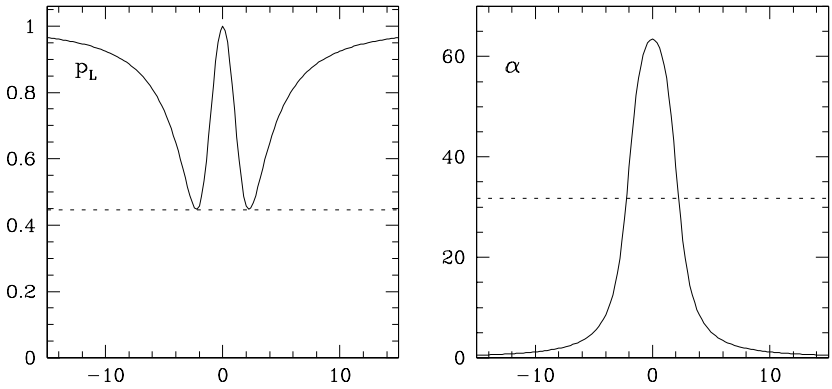

Fig.10.4. The linear polarization degree $p_{\rm L}$ and the rotation angle α (in degrees) corresponding to the emission coefficients of Fig.10.3. The dashed lines have the same meaning as in Fig.10.3.

to the Zeeman effect – and the complex shape of the linear polarization profiles. From Eqs. (10.44) it can easily be shown that the scattered radiation is totally polarized at every single frequency. Some features of the linear polarization are better appreciated in Fig. 10.4, where the polarization degree $p_{\rm L}$ and the rotation angle α, given by

$$p_{\rm L} = \frac{\sqrt{\varepsilon_1^2 + \varepsilon_2^2}}{\varepsilon_0} \,, \qquad \alpha = \frac{1}{2} \arctan\Big(\frac{\varepsilon_2}{\varepsilon_1}\Big) + \alpha_0$$

(with α_0 defined as in Eqs. (1.8b,c)) are plotted against frequency. At line center the polarization degree is unity while the direction of maximum polarization is rotated through a large angle ($\simeq 63^\circ$) from the zero-field direction. In the far wings, $p_{\rm L}$ tends again to unity while α tends to zero, according to the property proved earlier that the Hanle effect vanishes. In fact, the asymptotic values of the fractional emission coefficients derived from Eqs. (10.44) for $|\nu_0 - \nu| \to \infty$ are

$$p_Q = 1 \,, \qquad p_U = p_V = 0 \,.$$

10.5. The Two-Level Atom: Resonance Polarization for Strong Magnetic Fields

(*unpolarized lower level - no collisions*)

In this section we consider the interaction of a two-level atom with the radiation field in the presence of a strong magnetic field, in order to illustrate an important, general concept: atomic polarization can be produced not only by the anisotropy and/or polarization of the incident radiation, but also by the spectral structure of the radiation itself. For the sake of simplicity we assume (as in the former sections) the lower level to be unpolarized and we neglect collisions.

In the strong field regime, the Zeeman splitting is much larger than the natural line width. This implies $H_u \gg 1$ (see Eq. (10.28)) so that, according to Eq. (10.30), the upper-level statistical tensors with $Q \neq 0$ can be neglected.[1] In other words, all coherences are zero and atomic polarization can only involve differences between the populations of Zeeman sublevels (cf. Eq. (3.101)). Under this approximation Eq. (10.27) reduces to

$$\rho^K_Q(\alpha_u J_u) = \delta_{Q0} \sqrt{\frac{2J_\ell + 1}{2J_u + 1}} \frac{B(\alpha_\ell J_\ell \to \alpha_u J_u)}{A(\alpha_u J_u \to \alpha_\ell J_\ell)} \; w^{(K)}_{J_u J_\ell} \; J^K_0(\nu_0) \; \rho^0_0(\alpha_\ell J_\ell) \; .$$

Substitution into Eq. (10.39) gives the corresponding expression for the emission coefficient. Using Eqs. (5.157), (9.5) and (10.6) we obtain

$$\varepsilon_i(\nu, \vec{\Omega}) = k^{\rm A}_{\rm L} \sum_{KK'} \Phi^{KK'}_0(J_\ell, J_u; \nu) \times \oint \frac{{\rm d}\Omega'}{4\pi} \sum_{j=0}^{3} w^{(K)}_{J_u J_\ell} \; \mathcal{T}^{K'}_0(i, \vec{\Omega}) \; \mathcal{T}^K_0(j, \vec{\Omega}') \; I_j(\nu_0, \vec{\Omega}') \; ,$$

which is a special case of Eq. (10.41).

The above derivation assumes the incident radiation field to be flat across the *whole* line width, i.e., across a frequency interval $\Delta\nu$ larger than the overall Zeeman splitting of the line. Since in the strong-field regime coherences between Zeeman sublevels are negligible, we can investigate, still within the flat-spectrum approximation, the more general case where the incident radiation is different in different Zeeman components, yet being practically constant (over frequency intervals of the order of the natural line width) across each component. Such case has been analyzed in Sect. 7.4.

To handle this physical situation, it is convenient to use the standard (rather than the statistical tensor) representation of the density matrix. In this representation the atom is described by the diagonal density-matrix elements $\rho_{\alpha J}(M)$ giving the population of the magnetic sublevel M of level (αJ) – cf. Eq. (3.91b).

The relevant statistical equilibrium equations are given by Eq. (7.17). We write such equations for the upper level of a two-level atom neglecting stimulated emission. Taking into account the expressions for the rates $t_{\rm A}$ and $r_{\rm E}$ (Eqs. (7.18a,e)) we obtain, in stationary situations

$$\rho_{\alpha_u J_u}(M_u) = \frac{(2J_\ell + 1) \, B(\alpha_\ell J_\ell \to \alpha_u J_u)}{A(\alpha_u J_u \to \alpha_\ell J_\ell)} \sum_{M_\ell \, q} 3 \begin{pmatrix} J_u & J_\ell & 1 \\ -M_u & M_\ell & -q \end{pmatrix}^2 \times J_{qq}(\nu_{\alpha_u J_u M_u, \alpha_\ell J_\ell M_\ell}) \; \rho_{\alpha_\ell J_\ell}(M_\ell) \; . \tag{10.45}$$

[1] Obviously, this statement holds only in a reference system having the z-axis along the magnetic field direction. It should be remarked that neglecting the statistical tensors with $Q \neq 0$ is, in any case, an approximation which makes impossible to account for certain phenomena typical of line wings (like the disappearance of the Hanle effect described in the previous section).

Introducing the number density of atoms $\mathcal{N}$, the assumption of unpolarized lower level gives (see Eqs. (3.84), (3.89) and (10.5))

$$\rho_{\alpha_\ell J_\ell}(M_\ell) = \frac{\mathcal{N}_\ell}{\mathcal{N}} \frac{1}{2J_\ell + 1} .$$

Substitution into Eq. (10.45) yields, with the use of Eqs. (7.8) and (5.153)

$$\rho_{\alpha_u J_u}(M_u) = \frac{2J_u + 1}{2J_\ell + 1} \frac{\mathcal{N}_\ell}{\mathcal{N}} \frac{c^2}{2h\nu_0^3} \sum_{M_\ell\, q} 3 \begin{pmatrix} J_u & J_\ell & 1 \\ -M_u & M_\ell & -q \end{pmatrix}^2$$

$$\times \oint \frac{\mathrm{d}\Omega'}{4\pi} \sum_{j=0}^{3} \mathcal{T}_{qq}(j, \vec{\Omega}')\, I_j(\nu_{\alpha_u J_u M_u, \alpha_\ell J_\ell M_\ell}, \vec{\Omega}') . \qquad (10.46)$$

This expression gives the populations of the Zeeman sublevels of the upper level as determined by a radiation field which can be anisotropic, polarized, and frequency-dependent (within the limitations specified above). Its implications are best illustrated by comparison with the extreme case where the radiation field is isotropic, unpolarized, and flat across the whole frequency interval spanned by the spectral line,

$$I_j(\nu_{\alpha_u J_u M_u, \alpha_\ell J_\ell M_\ell}, \vec{\Omega}') = \delta_{j0}\, J ,$$

where J is the field intensity. In such case the integral over the solid angle can be evaluated with the help of Eqs. (5.146), (5.128) and (5.143),

$$\oint \frac{\mathrm{d}\Omega'}{4\pi} \mathcal{T}_{qq}(0, \vec{\Omega}') = \frac{1}{3} ,$$

and the summation over M_ℓ and q can be performed via Eq. (2.23a). The result is

$$\rho_{\alpha_u J_u}(M_u) = \frac{\mathcal{N}_\ell}{\mathcal{N}} \frac{1}{2J_\ell + 1} \frac{c^2}{2h\nu_0^3} J ,$$

which shows that all the Zeeman sublevels of the upper level are evenly populated (unpolarized upper level).

If *any* of the above conditions is not met, a certain amount of atomic polarization (population unbalances) will form in the upper level, because of a mechanism of *selective pumping* of the different Zeeman sublevels. There may exist selective pumping due to anisotropy (and/or polarization) of the incident radiation, or selective pumping due to spectral structure of the incident radiation, or both. Obviously, the second mechanism is effective only when the Zeeman sublevels are split because of the presence of a magnetic field. In the preceding sections of this chapter only the first mechanism has been considered.[1]

[1] It should be remarked that the strong-field regime analyzed in this section is one of the few cases where a frequency-structured radiation field can be treated *within the flat-spectrum approximation* (such possibility is related to the fact that the atomic density matrix is diagonal). If the Zeeman separation is comparable with the natural line width and the radiation field is significantly structured across that width, the theory developed in this book cannot be applied (see Sect. 6.5).

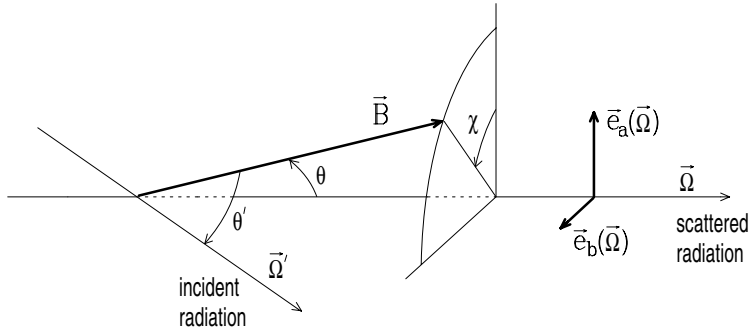

Fig.10.5. An unpolarized radiation beam, having direction $\vec{\Omega}'$, is scattered into the direction $\vec{\Omega}$. The direction of the magnetic field $\vec{B}$ is specified by the angles θ and χ in the reference frame $(\vec{e}_a(\vec{\Omega}), \vec{e}_b(\vec{\Omega}), \vec{\Omega})$. The angle between $\vec{\Omega}'$ and $\vec{B}$ is θ'.

Let us apply Eq. (10.46) to a specific case. A two-level atom with $J_\ell = 0$, $J_u = 1$, and $g_{\alpha_u J_u} = 1$ is illuminated by an unpolarized radiation beam having intensity $I'(\nu)$, angular spread $\Delta\Omega'$, and making an angle θ' with the direction of the magnetic field (see Fig. 10.5). Equations (10.46) yield, with the help of Eq. (2.26a) and Table 5.3

$$\begin{aligned} \rho_{\mp 1} \equiv \rho_{\alpha_u J_u}(\mp 1) &= \frac{3}{4}\frac{\mathcal{N}_\ell}{\mathcal{N}}\frac{c^2}{2h\nu_0^3}\frac{\Delta\Omega'}{4\pi}\left(1+\cos^2\theta'\right) I'(\nu_0 \mp \nu_{\rm L}) \\ \rho_0 \equiv \rho_{\alpha_u J_u}(0) &= \frac{3}{4}\frac{\mathcal{N}_\ell}{\mathcal{N}}\frac{c^2}{2h\nu_0^3}\frac{\Delta\Omega'}{4\pi}\, 2\sin^2\theta'\, I'(\nu_0)\,. \end{aligned} \tag{10.47}$$

These formulae show that by suitably choosing the angle θ' and the spectrum of the incident radiation, the three Zeeman sublevels *can be arbitrarily populated*. Note, however, that if the spectrum of the incident radiation is symmetrical about line center – in particular, if it is flat across the whole spectral line – the populations of the sublevels $M_u = 1$ and $M_u = -1$ are the same (the atom is 'aligned' but not 'oriented', see Sect. 3.7 and Table 3.6): atomic orientation can arise only if $I'(\nu_0 - \nu_{\rm L})$ and $I'(\nu_0 + \nu_{\rm L})$ are different.

Next we evaluate the radiation scattered by the atom in the direction $\vec{\Omega}$ (see Fig. 10.5). The emission coefficient can be obtained from Eq. (7.19e), with the tensors $\mathcal{T}_{qq}(i, \vec{\Omega})$ given by Table 5.3 (with $\theta \to \theta$, $\gamma \to 180° - \chi$). Using Eqs. (7.8), (3.107) and (10.6), and the shorthand notations for $\rho_{\alpha_u J_u}(M_u)$ of Eqs. (10.47), we obtain

$$\begin{aligned} \varepsilon_0(\nu, \vec{\Omega}) &= \varepsilon_{\rm L}\,\frac{3}{\rho_{-1}+\rho_0+\rho_1}\,\frac{1}{2}\left[\rho_0\phi_0\,\sin^2\theta + \frac{\rho_1\phi_{-1}+\rho_{-1}\phi_1}{2}\left(1+\cos^2\theta\right)\right] \\ \varepsilon_1(\nu, \vec{\Omega}) &= \varepsilon_{\rm L}\,\frac{3}{\rho_{-1}+\rho_0+\rho_1}\,\frac{1}{2}\left[\rho_0\phi_0 - \frac{\rho_1\phi_{-1}+\rho_{-1}\phi_1}{2}\right]\sin^2\theta\cos 2\chi \\ \varepsilon_2(\nu, \vec{\Omega}) &= \varepsilon_{\rm L}\,\frac{3}{\rho_{-1}+\rho_0+\rho_1}\,\frac{1}{2}\left[\rho_0\phi_0 - \frac{\rho_1\phi_{-1}+\rho_{-1}\phi_1}{2}\right]\sin^2\theta\sin 2\chi \end{aligned}$$

$$\varepsilon_3(\nu,\vec{\Omega}) = \varepsilon_{\rm L}\,\frac{3}{\rho_{-1}+\rho_0+\rho_1}\,\frac{1}{2}\Big[\rho_{-1}\phi_1-\rho_1\phi_{-1}\Big]\cos\theta\,, \tag{10.48}$$

where $\varepsilon_{\rm L}$ is defined in Eq. (9.11) and the profiles ϕ_{-1}, ϕ_0, ϕ_1 in Eq. (A13.10).

If the atom is unpolarized ($\rho_{-1}=\rho_0=\rho_1$), Eqs. (10.48) reduce to Eqs. (9.10) written for the transition ($J_\ell=0, J_u=1$). In such case two remarkable spectral properties hold: a) the frequency profile of ε_0, ε_1, ε_2 is symmetrical about line center, the frequency profile of ε_3 is antisymmetrical; b) the integral over frequency of ε_1, ε_2 and ε_3 is zero. As obvious from Eqs. (10.48), none of these properties is any longer valid if atomic polarization is present. In particular, the symmetry characteristics of the profiles about line center are broken if the atom is oriented ($\rho_{-1}\neq\rho_1$). The frequency-integrated linear polarization turns out to be proportional to the amount of atomic alignment, the frequency-integrated circular polarization to the amount of atomic orientation (cf. Table 3.6).

It should be remarked that the formal invariance of Eqs. (10.48) under the transformation $\chi\rightarrow\pi+\chi$ (rotation through 180° of the magnetic field vector about the direction of the scattered radiation) does *not* mean that the scattered radiation is unaffected by such transformation – this is only true when the atom is unpolarized. In general, the populations ρ_{-1}, ρ_0, ρ_1 depend on the angle θ' (see Eqs. (10.47)) which is not invariant for $\chi\rightarrow\pi+\chi$.

10.6. The Two-Level Atom: the Role of Collisions

(*unpolarized lower level*)

Resonance polarization and the Hanle effect are deeply modified by the presence of collisions. In this section we illustrate their effects for the two-level atom, under the restrictive assumption that the lower level is unpolarized. Thus we refer again to Eq. (10.8), and we recall that the collisional rates for inelastic and superelastic collisions are connected by the Einstein-Milne relation (Eq. (7.98))

$$C_{\rm I}^{(0)}(\alpha_u J_u,\alpha_\ell J_\ell) = \frac{2J_u+1}{2J_\ell+1}\;\;{\rm e}^{-\frac{h\nu_0}{k_{\rm B}T_{\rm c}}}\;\;C_{\rm S}^{(0)}(\alpha_\ell J_\ell,\alpha_u J_u)\,, \tag{10.49}$$

since by assumption the colliding particles are characterized by a Maxwellian distribution of velocities with temperature $T_{\rm c}$.

Substitution of Eq. (10.9) into Eq. (10.8) and use of Eqs. (7.8), (10.11) and (10.28) yields

$$\rho_Q^K(\alpha_u J_u) = \sqrt{\frac{2J_\ell+1}{2J_u+1}}\,\frac{B(\alpha_\ell J_\ell\rightarrow\alpha_u J_u)}{A(\alpha_u J_u\rightarrow\alpha_\ell J_\ell)} \times\frac{\epsilon\,B_{\rm P}(T_{\rm c})\,\delta_{K0}\,\delta_{Q0}\,+\,w^{(K)}_{J_uJ_\ell}\,(-1)^Q\,J^K_{-Q}(\nu_0)}{1+{\rm i}\,Q H_u+\epsilon+\delta_u^{(K)}}\,\rho_0^0(\alpha_\ell J_\ell)\,, \tag{10.50}$$

where

$$\epsilon = \frac{C_{\rm S}^{(0)}(\alpha_\ell J_\ell, \alpha_u J_u)}{A(\alpha_u J_u \to \alpha_\ell J_\ell)} \,, \qquad \delta_u^{(K)} = \frac{D^{(K)}(\alpha_u J_u)}{A(\alpha_u J_u \to \alpha_\ell J_\ell)} \,, \tag{10.51}$$

and where

$$B_{\rm P}(T_{\rm c}) = \frac{2h\nu_0^3}{c^2} \; {\rm e}^{-\frac{h\nu_0}{k_{\rm B} T_{\rm c}}}$$

is the Planck function (in the Wien limit, where stimulated emission is neglected) at the temperature $T_{\rm c}$.

The physical meaning of the quantities introduced in Eqs. (10.51) is quite obvious. ϵ represents the ratio of collisional to radiative de-excitation rates of the upper level, whereas $\delta_u^{(K)}$ – with $\delta_u^{(0)} = 0$, see Eq. (7.102) – represents the effective number of depolarizing collisions (for the statistical tensors of rank K) taking place during the lifetime of the excited level. It is worth noticing that, under the limit $\delta_u^{(K)} \to \infty$, Eq. (10.50) predicts that all the $\rho^K_Q(\alpha_u J_u)$ with $K \neq 0$ vanish. The only non-zero statistical tensor is $\rho^0_0(\alpha_u J_u)$, and Eq. (10.50) can be cast into the form

$$\sqrt{\frac{2J_u+1}{2J_\ell+1}} \; \frac{A(\alpha_u J_u \to \alpha_\ell J_\ell)}{B(\alpha_\ell J_\ell \to \alpha_u J_u)} \; \frac{\rho^0_0(\alpha_u J_u)}{\rho^0_0(\alpha_\ell J_\ell)} = \frac{\epsilon}{1+\epsilon} \, B_{\rm P}(T_{\rm c}) + \frac{1}{1+\epsilon} \, J^0_0(\nu_0) \,. \tag{10.52}$$

This relation is easily recognized as the usual statistical equilibrium equation of the 'scalar' (unpolarized) case, once the left-hand side is interpreted as the line source function (see Eqs. (9.5), (9.11), (9.13) and (10.6)).[1]

To obtain the radiation emitted by the atom along a given direction $\vec{\Omega}$, we have to substitute Eq. (10.50) into Eq. (10.39) or, if one is only interested in the frequency-integrated radiation, into Eq. (10.31). Let us consider the latter case first. Use of Eqs. (9.5), (10.6), (10.17), (5.157) and Table 5.6 yields

$$\begin{aligned} \tilde{\varepsilon}_i(\vec{\Omega}) = \; & k_{\rm L}^{\rm A} \left[\frac{\epsilon}{1+\epsilon} \, B_{\rm P}(T_{\rm c}) \, \delta_{i0} \right. \\ & \left. + \oint \frac{{\rm d}\Omega'}{4\pi} \sum_{j=0}^{3} P_{ij}(\vec{\Omega}, \vec{\Omega}'; \vec{B}, \epsilon, \delta_u^{(K)}) \; I_j(\nu_0, \vec{\Omega}') \right] , \end{aligned} \tag{10.53}$$

where the generalized scattering phase matrix (i.e. the phase matrix in the presence of a magnetic field *and* collisions) is given by

$$\begin{aligned} P_{ij}(\vec{\Omega}, \vec{\Omega}'; \vec{B}, \epsilon, \delta_u^{(K)}) = & \sum_{KQ} W_K(J_\ell, J_u) \; (-1)^Q \, \mathcal{T}^K_Q(i, \vec{\Omega}) \, \mathcal{T}^K_{-Q}(j, \vec{\Omega}') \\ & \times \frac{1}{1 + {\rm i}\, Q H_u + \epsilon + \delta_u^{(K)}} \,. \end{aligned} \tag{10.54}$$

[1] The right-hand side is often written in the slightly different form

$$\epsilon' \, B_{\rm P}(T_{\rm c}) + (1-\epsilon') \, J^0_0(\nu_0) \,,$$

where $\epsilon' = \epsilon \,/(1+\epsilon)$.

Equations (10.53) and (10.54) show the double role played by collisions in resonance scattering. On the one hand, inelastic (and superelastic) collisions introduce an additional term in the emission coefficient. This term affects only intensity, not polarization, and is proportional to $\epsilon/(1+\epsilon)$ or, in other words, to the branching ratio

$$\frac{C_{\rm S}^{(0)}(\alpha_\ell J_\ell, \alpha_u J_u)}{A(\alpha_u J_u \rightarrow \alpha_\ell J_\ell) + C_{\rm S}^{(0)}(\alpha_\ell J_\ell, \alpha_u J_u)} ,$$

which represents the collisional de-excitation probability divided by the total de-excitation probability of the upper level. The unpolarized character of the emitted radiation is a consequence of the fact that we have assumed an isotropic distribution of colliders, which prevents the possibility of describing impact polarization.

On the other hand, collisional rates affect the scattering phase matrix via the factor

$$\frac{1}{1 + {\rm i}\, Q H_u + \epsilon + \delta_u^{(K)}} , \tag{10.55}$$

which involves both inelastic and elastic collisions. This factor describes the so-called *quenching* of resonance polarization (see Mitchell and Zemanski, 1934). Its effects are easily understood by rewriting Eq. (10.55) in the form (cf. Eqs. (5.193), (5.194) for a similar 'classical' expression)

$$\frac{1}{1 + {\rm i}\, Q H_u + \epsilon + \delta_u^{(K)}} = \frac{1}{1 + \epsilon + \delta_u^{(K)}} \, \frac{1}{1 + {\rm i}\, Q H'_u(K)} , \tag{10.56}$$

where, using Eqs. (10.28) and (10.51)

$$H'_u(K) = \frac{H_u}{1 + \epsilon + \delta_u^{(K)}} = \frac{2\pi\nu_{\rm L}\, g_{\alpha_u J_u}}{A(\alpha_u J_u \rightarrow \alpha_\ell J_\ell) + C_{\rm S}^{(0)}(\alpha_\ell J_\ell, \alpha_u J_u) + D^{(K)}(\alpha_u J_u)} .$$

Equations (10.54) and (10.56) show that the generalized phase matrix can be formally deduced from the Hanle phase matrix (Eq. (10.33)) by the substitutions

$$W_K(J_\ell, J_u) \rightarrow \frac{W_K(J_\ell, J_u)}{1 + \epsilon + \delta_u^{(K)}} , \qquad H_u \rightarrow H'_u(K) .$$

Thus the quenching of resonance polarization consists both in a net reduction of the scattered polarization and in a reduction of the efficiency of the magnetic field as depolarizing agent in the Hanle effect.

If the dependence of the scattered radiation on frequency is considered, a further effect of collisions comes into play, i.e., the broadening of the individual profiles $\Phi(\nu_{\alpha_u J_u M_u, \alpha_\ell J_\ell M_\ell} - \nu)$. Neglecting frequency shifts, these profiles are given by

$$\Phi(\nu_{\alpha_u J_u M_u, \alpha_\ell J_\ell M_\ell} - \nu) = \frac{1}{\pi} \frac{\Gamma'}{\Gamma'^2 + (\nu_{\alpha_u J_u M_u, \alpha_\ell J_\ell M_\ell} - \nu)^2} + \frac{\rm i}{\pi} \frac{\nu_{\alpha_u J_u M_u, \alpha_\ell J_\ell M_\ell} - \nu}{\Gamma'^2 + (\nu_{\alpha_u J_u M_u, \alpha_\ell J_\ell M_\ell} - \nu)^2} ,$$

where (see Eqs. (6.59b) and (5.180))

$$\Gamma' = \Gamma + 2\Gamma_{\rm c} = \frac{\gamma_u + \gamma_\ell}{4\pi} + \frac{f}{2\pi} \ ,$$

γ_u and γ_ℓ being the inverse lifetimes of the upper and lower level, respectively, and f the frequency of elastic collisions. For the two-level atom, neglecting the width of the lower level, we have

$$\Gamma' = \frac{A(\alpha_u J_u \rightarrow \alpha_\ell J_\ell) + C_{\rm S}^{(0)}(\alpha_\ell J_\ell, \alpha_u J_u)}{4\pi} + \frac{f}{2\pi} \ .$$

The form of the profiles $\Phi(\nu_{\alpha_u J_u M_u, \alpha_\ell J_\ell M_\ell} - \nu)$ is the same as in the collisionless regime except for the replacement $\Gamma \rightarrow \Gamma'$. Thus, in the presence of collisions, we can still define the generalized profiles as in Eq. (10.40), and the expression of the emission coefficient is formally identical with Eq. (10.39). Substitution of Eq. (10.50) into Eq. (10.39) leads, using again Eqs. (9.5), (10.6) and (5.157), to the following expression

$$\begin{aligned}\varepsilon_i(\nu, \vec{\Omega}) = \ k_{\rm L}^{\rm A} \Bigg[& \frac{\epsilon}{1+\epsilon} B_{\rm P}(T_{\rm c}) \sum_K \Phi_0^{0K}(J_\ell, J_u; \nu) \, \mathcal{T}_0^K(i, \vec{\Omega}) \\ & + \sum_{KK'Q} \Phi_Q^{KK'}(J_\ell, J_u; \nu) \oint \frac{{\rm d}\Omega'}{4\pi} \sum_{j=0}^{3} w_{J_u J_\ell}^{(K)} \ (-1)^Q \, \mathcal{T}_Q^{K'}(i, \vec{\Omega}) \, \mathcal{T}_{-Q}^K(j, \vec{\Omega}') \\ & \times \frac{1}{1 + {\rm i}\, Q H_u + \epsilon + \delta_u^{(K)}} \, I_j(\nu_0, \vec{\Omega}') \Bigg] \ . \end{aligned} \tag{10.57}$$

The broadening of the profiles due to collisions has important consequences and, in particular, it breaks down a property proved in Sect. 10.4 for the collisionless regime: while in the latter resonance scattering in the far wings of a spectral line is unaffected by the magnetic field, this is no longer true in the presence of collisions.

For $\epsilon \rightarrow \infty$ only the first term of Eq. (10.57) is non-zero. It can easily be shown that under this limit Eq. (10.57) reduces to Eqs. (9.10) written for LTE.

10.7. The Two-Level Atom: the Role of Lower-Level Polarization

(*cylindrical symmetry - no magnetic field - no stimulated emission - no inelastic collisions*)

Up to now we have systematically ignored the possibility that some atomic polarization may form in the lower level of a two-level atom under the action of the incident radiation field: all the results derived in Sects. 10.2 to 10.6 are based on the unpolarized lower level approximation. Here we release this approximation, in order to illustrate how the former results are modified when lower-level atomic polarization is allowed for.

As already mentioned in Sect. 10.1, the statistical equilibrium equations become remarkably more complicated as soon as lower-level polarization is taken into account, and closed analytical solutions to these equations can hardly be found even for the simplest cases. If we want to get such solutions (at least for a few sample cases), so as to be able to understand in detail the role of lower-level polarization, we are therefore forced to introduce some other approximation.

An interesting possibility is offered by the so-called weak anisotropy approximation: this will be discussed in Sects. 10.13 and 10.14. However, as obvious from the denomination, such approximation is not applicable when the incoming radiation field is markedly anisotropic – in particular, when it is just a beam. In the present section we adopt an assumption on the incident radiation field which in a sense is complementary to the weak anisotropy approximation: we assume the radiation to be *unpolarized and cylindrically symmetrical about a fixed direction*. For the sake of simplicity, we also adopt the following additional assumptions: absence of inelastic and superelastic collisions (whereas depolarizing collisions are taken into account); absence of the magnetic field (this will be considered in the next section); absence of stimulated emission (which will be considered in Sect. 10.9).

The simplification introduced by the above assumptions (in particular, those concerning the incoming radiation and the magnetic field) can easily be understood. If the symmetry axis of the radiation field is taken as the z-axis of our reference system, and if the radiation is frequency-independent across the line width (flat-spectrum approximation), two single quantities are sufficient to fully specify the incoming radiation, i.e., the multipole components $J^0_0(\nu_0)$ and $J^2_0(\nu_0)$ – see Eqs. (5.164). This implies that, in stationary situations, the only non-zero statistical tensors are those with K even and $Q = 0$.

This property can be proved directly from the statistical equilibrium equations (10.1) and (10.2) by keeping in mind the expressions of the radiative rates given in Eqs. (7.14).[1] Since the multipole components $J^{K_\mathrm{r}}_{Q_\mathrm{r}}(\nu_0)$ with $Q_\mathrm{r} \neq 0$ are zero, all the radiative rates in Eqs. (10.1) and (10.2) are zero unless $Q = Q'$: this is due to the presence of a 3-j symbol of the form

$$\begin{pmatrix} K & K' & K_\mathrm{r} \\ Q & -Q' & Q_\mathrm{r} \end{pmatrix} \tag{10.58}$$

in the expressions of the rates $\mathbb{T}_\mathrm{A}$ and $\mathbb{R}_\mathrm{A}$ – on the other hand, the rates $\mathbb{T}_\mathrm{E}$ and $\mathbb{R}_\mathrm{E}$ are proportional to the Kronecker symbol $\delta_{QQ'}$. Thus the overall set of equations is decoupled into separate subsets characterized by a fixed Q value. As the trace equation (10.4) – the only non-homogeneous equation – involves only statistical tensors with $Q = 0$, all the other ones are identically zero. Note, incidentally, that this means that all coherences between magnetic sublevels are zero (see Eq. (3.101)): under the assumptions adopted in this section, atomic polarization can only consist in population differences of the magnetic sublevels. On the other side, since the

[1] As obvious from the following argument, the property is valid even if inelastic and superelastic collisions and/or stimulated emission are taken into account. It also holds for the multi-level (not just the two-level) model atom.

multipole components $J^{K_\mathrm{r}}_{Q_\mathrm{r}}(\nu_0)$ with $K_\mathrm{r} = 1$ are zero, all the radiative rates vanish unless $(K - K') = 0$ or $(K - K') = \pm 2$: as far as $\mathbb{T}_\mathrm{A}$ and $\mathbb{R}_\mathrm{A}$ are concerned, this is again due to the 3-j symbol in Eq. (10.58) which, for $Q = Q' = Q_\mathrm{r} = 0$, is zero unless $(K + K' + K_\mathrm{r})$ is even (see Eq. (2.25)); as for $\mathbb{T}_\mathrm{E}$ and $\mathbb{R}_\mathrm{E}$, both are proportional to the Kronecker symbol $\delta_{KK'}$. It follows that the remaining set of equations (involving the statistical tensors with $Q = 0$) is in turn decoupled into two separate subsets relating statistical tensors of even and odd rank, respectively. As the latter do not appear in the trace equation, the corresponding subset is identically solved by the null solution.

Because of the above property, the number of equations to be solved is largely reduced. It can be shown that such number is

$$N_\mathrm{eq} = \begin{cases} J_\ell + J_u + 2 & \text{for } J_\ell, J_u \text{ integers} \\ J_\ell + J_u + 1 & \text{for } J_\ell, J_u \text{ half-integers}\,, \end{cases} \tag{10.59}$$

to be compared with Eq. (10.3).

Let us rewrite Eqs. (10.1) and (10.2) for the physical situation considered in this section. Using Eqs. (7.14b) and (7.14e) we get

$$\begin{aligned} \frac{\mathrm{d}}{\mathrm{d}t}\,\rho^K_0(\alpha_u J_u) = &-\Big[A(\alpha_u J_u \to \alpha_\ell J_\ell) + D^{(K)}(\alpha_u J_u)\Big]\,\rho^K_0(\alpha_u J_u) \\ &+ \sum_{K' \text{ even}} \mathbb{T}_\mathrm{A}(\alpha_u J_u K\,0, \alpha_\ell J_\ell K'\,0)\;\rho^{K'}_0(\alpha_\ell J_\ell) \end{aligned}$$

$$\begin{aligned} \frac{\mathrm{d}}{\mathrm{d}t}\,\rho^K_0(\alpha_\ell J_\ell) = &\,(2J_u + 1)\,A(\alpha_u J_u \to \alpha_\ell J_\ell)\,(-1)^{1+J_\ell+J_u} \begin{Bmatrix} J_u & J_u & K \\ J_\ell & J_\ell & 1 \end{Bmatrix} \rho^K_0(\alpha_u J_u) \\ &- \sum_{K' \text{ even}} \Big[\mathbb{R}_\mathrm{A}(\alpha_\ell J_\ell K\,0\,K'\,0) + \delta_{KK'}\,D^{(K)}(\alpha_\ell J_\ell)\Big]\,\rho^{K'}_0(\alpha_\ell J_\ell)\,, \end{aligned} \tag{10.60}$$

where K is even. The rates $\mathbb{T}_\mathrm{A}$ and $\mathbb{R}_\mathrm{A}$, given by Eqs. (7.14a) and (7.14d) respectively, reduce, with the help of Eqs. (2.26a), (2.36a) and (2.49), to the following

$$\begin{aligned} \mathbb{T}_\mathrm{A}(\alpha_u J_u K\,0, \alpha_\ell J_\ell K'\,0) = &\,(2J_\ell + 1)\,B(\alpha_\ell J_\ell \to \alpha_u J_u) \\ &\times \Bigg[\delta_{KK'}\,(-1)^{1+J_\ell+J_u} \begin{Bmatrix} J_u & J_u & K \\ J_\ell & J_\ell & 1 \end{Bmatrix} J^0_0(\nu_0) \\ &+ \sqrt{15(2K+1)(2K'+1)} \begin{Bmatrix} J_u & J_\ell & 1 \\ J_u & J_\ell & 1 \\ K & K' & 2 \end{Bmatrix} \begin{pmatrix} K & K' & 2 \\ 0 & 0 & 0 \end{pmatrix} J^2_0(\nu_0) \Bigg] \end{aligned}$$

$$\mathbb{R}_{\rm A}(\alpha_\ell J_\ell K\,0\,K'\,0) = (2J_\ell+1)\,B(\alpha_\ell J_\ell \to \alpha_u J_u)$$
$$\times \left[\delta_{KK'}\,\frac{1}{2J_\ell+1}\,J_0^0(\nu_0) + (-1)^{1-J_\ell+J_u}\,\sqrt{15(2K+1)(2K'+1)} \right.$$
$$\left. \times \begin{Bmatrix} K & K' & 2 \\ J_\ell & J_\ell & J_\ell \end{Bmatrix} \begin{Bmatrix} 1 & 1 & 2 \\ J_\ell & J_\ell & J_u \end{Bmatrix} \begin{pmatrix} K & K' & 2 \\ 0 & 0 & 0 \end{pmatrix} J_0^2(\nu_0) \right]. \quad (10.61)$$

In view of practical applications, it is convenient to cast Eqs. (10.60) in dimensionless form, by dividing both sides by the Einstein coefficient $A(\alpha_u J_u \to \alpha_\ell J_\ell)$ and by introducing the parameters

$$\frac{(2J_\ell+1)\,B(\alpha_\ell J_\ell \to \alpha_u J_u)}{(2J_u+1)\,A(\alpha_u J_u \to \alpha_\ell J_\ell)}\,J_0^0(\nu_0) = \frac{c^2}{2h\nu_0^3}\,J_0^0(\nu_0) = \bar{n}$$
$$\frac{J_0^2(\nu_0)}{J_0^0(\nu_0)} = \frac{w}{\sqrt{2}}$$
$$\frac{D^{(K)}(\alpha_u J_u)}{A(\alpha_u J_u \to \alpha_\ell J_\ell)} = \delta_u^{(K)}$$
$$\frac{D^{(K)}(\alpha_\ell J_\ell)}{B(\alpha_\ell J_\ell \to \alpha_u J_u)\,J_0^0(\nu_0)} = \delta_\ell^{(K)} \quad (10.62)$$

(Eqs. (7.8) have been used in the first relation). Their meaning is the following. The parameter $\bar{n}$ represents the solid-angle average of the number of photons per mode at frequency ν_0 (see Eqs. (4.36), (5.157) and Table 5.7); in the present case it is much less than unity, since we have assumed stimulated emission to be negligible. The parameter w, satisfying the condition $-1/2 \le w \le 1$ under the conditions considered in this section, is the so-called *anisotropy factor*. Its value is unity for a unidirectional (unpolarized) radiation beam, and zero for an isotropic (unpolarized) radiation field – see Eqs. (5.164). Finally, $\delta_u^{(K)}$, already introduced in Eqs. (10.51), represents the effective number of depolarizing collisions (for the statistical tensors of rank K) taking place during the lifetime of the upper level, while $\delta_\ell^{(K)}$ is the corresponding quantity for the lower level. Note that, by combining the first and the last of Eqs. (10.62), we can write

$$\delta_\ell^{(K)} = \frac{2J_\ell+1}{2J_u+1}\,\frac{D^{(K)}(\alpha_\ell J_\ell)}{\bar{n}\,A(\alpha_u J_u \to \alpha_\ell J_\ell)}\,; \quad (10.63)$$

since $D^{(K)}(\alpha_\ell J_\ell)$ and $D^{(K)}(\alpha_u J_u)$ are of the same order of magnitude and $\bar{n} \ll 1$, it follows that

$$\delta_\ell^{(K)} \gg \delta_u^{(K)}\,.$$

In the following we apply Eqs. (10.60) to a few simple cases. We begin with the transition ($J_\ell = 1, J_u = 0$) which is the simplest transition where lower-level polarization plays a role. After some calculations, involving the numerical evaluation of

several 3-j, 6-j, and 9-j symbols, one gets the following independent equations[1]

$$\frac{1}{A(\alpha_u J_u \to \alpha_\ell J_\ell)} \frac{\mathrm{d}}{\mathrm{d}t} \rho_0^0(\alpha_u J_u) = -\rho_0^0(\alpha_u J_u) + \frac{1}{\sqrt{3}} \bar{n} \rho_0^0(\alpha_\ell J_\ell) + \frac{1}{\sqrt{6}} \bar{n} w \rho_0^2(\alpha_\ell J_\ell)$$
$$\frac{1}{A(\alpha_u J_u \to \alpha_\ell J_\ell)} \frac{\mathrm{d}}{\mathrm{d}t} \rho_0^2(\alpha_\ell J_\ell) = -\frac{1}{3} \bar{n} \left[1 - \frac{1}{2} w + \delta_\ell^{(2)}\right] \rho_0^2(\alpha_\ell J_\ell) - \frac{1}{3\sqrt{2}} \bar{n} w \rho_0^0(\alpha_\ell J_\ell) ,$$

where the parameters defined in Eqs. (10.62) have been introduced. In stationary situations, the solution can be written in the form[2]

$$\sigma_0^2(\alpha_\ell J_\ell) \equiv \frac{\rho_0^2(\alpha_\ell J_\ell)}{\rho_0^0(\alpha_\ell J_\ell)} = -\sqrt{2} \frac{w}{2 - w + 2\,\delta_\ell^{(2)}}$$
$$\frac{\rho_0^0(\alpha_u J_u)}{\rho_0^0(\alpha_\ell J_\ell)} = \frac{1}{\sqrt{3}} \bar{n} \left[1 - \frac{w^2}{2 - w + 2\,\delta_\ell^{(2)}}\right] . \tag{10.64}$$

These expressions exhibit several interesting aspects. First of all, atomic polarization, as well as the ratio of the upper to the lower level population, depend in a non-linear way on the anisotropy factor w: this is generally the case when lower-level polarization is allowed for.

Secondly, atomic polarization is zero if $w = 0$, which is quite obvious because in that case the physical environment is completely isotropic (we recall that in our treatment collisions are isotropic by assumption). Apart from this special case, atomic polarization tends to zero for $\delta_\ell^{(2)} \to \infty$: in general, the approximation of the unpolarized lower level is strictly justified only under such limit. On the other hand, according to Eq. (10.63), $\delta_\ell^{(2)}$ is inversely proportional to $\bar{n}$, or to the intensity of the radiation field. Thus we can also say that lower-level atomic polarization increases as the intensity of the radiation field is increased. This is easily understood if we consider that the radiative rates (which are responsible for atomic polarization) are proportional to the intensity of the radiation field, while the collisional rates are independent of it (they only depend on the density of the colliders).

Another peculiar aspect of Eqs. (10.64) is that for $w = 1$ and $\delta_\ell^{(2)} = 0$ (unidirectional, unpolarized radiation beam and no collisions) we have

$$\sigma_0^2(\alpha_\ell J_\ell) = -\sqrt{2} , \qquad \rho_0^0(\alpha_u J_u) = 0 . \tag{10.65}$$

The second result means that the upper level is completely depopulated (the atom is perfectly transparent to the incident radiation), which looks rather surprising

[1] We recall that the equations for the time derivatives of $\rho_0^0(\alpha_\ell J_\ell)$ and $\rho_0^0(\alpha_u J_u)$ are not independent: see footnote on p.512.

[2] The symbol $\sigma_Q^K(\alpha J) = \rho_Q^K(\alpha J)/\rho_0^0(\alpha J)$, sometimes referred to as *reduced statistical tensor*, will be often used in the following.

at first sight. However, one should bear in mind that a unidirectional, unpolarized radiation beam induces only transitions with $\Delta M = \pm 1$.[1] The Zeeman sublevels $M_\ell = \pm 1$ of the lower level are therefore depopulated by the incident radiation, while the sublevel $M_\ell = 0$ is not. On the other hand, the upper level $(J_u = 0, M_u = 0)$ de-excites with the same probability to each of the three sublevels of the lower level. The result of this cycle is that all the atoms are eventually pumped into the sublevel $M_\ell = 0$ of the lower level, which explains both the factor $-\sqrt{2}$ for the relative amount of alignment (cf. Table 3.6) and the total absence of population in the upper level.

Finally, Eqs. (10.64) show that depolarizing collisions affect the ratio of the upper level to the lower level population, which may look surprising because such collisions are elastic (see Sect. 7.13). The reason for this is that depolarizing collisions tend to mix up the populations of the Zeeman sublevels of each (αJ)-level, thus affecting (indirectly) the absorption and emission of radiation. Such effect is clearly illustrated by the example just considered of a unidirectional, unpolarized incident beam: in stationary situations and under the limit $\delta_\ell^{(2)} = 0$, all the atoms are in the sublevel $M_\ell = 0$ of the lower level whence absorption can no longer take place, so that the upper level is completely depopulated (Eqs. (10.65)). But if depolarizing collisions are present, some of the atoms are forced to move from the $M_\ell = 0$ to the $M_\ell = \pm 1$ sublevels whence absorption is possible, which eventually leads to a non-null value for the population of the upper level.

The transition $(J_\ell = 1, J_u = 0)$, though interesting under several aspects, is not so illuminating under the point of view of resonance polarization: since $J_u = 0$, the emitted radiation is unpolarized irrespective of the presence of lower-level atomic polarization. The latter can only affect the *absorption* properties of the atom, an argument that we are not going to pursue here but that might be easily handled by substituting the expressions of the statistical tensors of the lower level into Eqs. (7.15a,c) applied to the two-level atom.

We now analyze the simplest transition where atomic polarization can be present both in the lower and the upper level, namely the transition $(J_\ell = 1, J_u = 1)$. Application of Eqs. (10.60) to this case yields the following set of independent equations

$$\frac{1}{A(\alpha_u J_u \to \alpha_\ell J_\ell)} \frac{\mathrm{d}}{\mathrm{d}t} \rho_0^0(\alpha_u J_u) = -\rho_0^0(\alpha_u J_u) + \bar{n}\, \rho_0^0(\alpha_\ell J_\ell) - \frac{1}{2\sqrt{2}}\, \bar{n} w\, \rho_0^2(\alpha_\ell J_\ell)$$

$$\frac{1}{A(\alpha_u J_u \to \alpha_\ell J_\ell)} \frac{\mathrm{d}}{\mathrm{d}t} \rho_0^2(\alpha_u J_u) = -\left[1 + \delta_u^{(2)}\right] \rho_0^2(\alpha_u J_u) - \frac{1}{2\sqrt{2}}\, \bar{n} w\, \rho_0^0(\alpha_\ell J_\ell) - \frac{1}{2}\, \bar{n} \left[1 + w\right] \rho_0^2(\alpha_\ell J_\ell)$$

[1] This fact can be easily verified by considering the statistical equilibrium equations in the standard representation and the corresponding expressions of the radiative rates (Eqs. (7.5) and (7.9), respectively). It is sufficient to recall that for a unidirectional, unpolarized radiation beam the only non-zero components of the (reducible) radiation field tensor are $J_{11}(\nu_0)$ and $J_{-1-1}(\nu_0)$ – cf. Eqs. (5.153) and Table 5.4.

$$\frac{1}{A(\alpha_u J_u \rightarrow \alpha_\ell J_\ell)} \frac{\mathrm{d}}{\mathrm{d}t} \rho^2_0(\alpha_\ell J_\ell) = -\frac{1}{2} \rho^2_0(\alpha_u J_u) + \frac{1}{2\sqrt{2}} \bar{n} w \, \rho^0_0(\alpha_\ell J_\ell) - \bar{n} \left[1 + \frac{1}{4} w + \delta^{(2)}_\ell\right] \rho^2_0(\alpha_\ell J_\ell) \, ,$$

where the notations of Eqs. (10.62) have been used. In stationary situations, the solution can be written in the form

$$\sigma^2_0(\alpha_u J_u) = -\sqrt{2}\, w \, \frac{6 + 3w + 4\,\delta^{(2)}_\ell}{4\left[(1+\delta^{(2)}_u)(4 + w + 4\,\delta^{(2)}_\ell) - (1+w)\right] - w^2(3 + 2\,\delta^{(2)}_u)}$$

$$\sigma^2_0(\alpha_\ell J_\ell) = \sqrt{2}\, w \, \frac{3 + 2\,\delta^{(2)}_u}{2\left[(1+\delta^{(2)}_u)(4 + w + 4\,\delta^{(2)}_\ell) - (1+w)\right]}$$

$$\frac{\rho^0_0(\alpha_u J_u)}{\rho^0_0(\alpha_\ell J_\ell)} = \bar{n} \, \frac{4\left[(1+\delta^{(2)}_u)(4 + w + 4\,\delta^{(2)}_\ell) - (1+w)\right] - w^2(3 + 2\,\delta^{(2)}_u)}{4\left[(1+\delta^{(2)}_u)(4 + w + 4\,\delta^{(2)}_\ell) - (1+w)\right]} \, . \qquad (10.66)$$

These expressions are rather involved and clearly show the intricate dependence of atomic polarization on the different parameters. However, it is easily seen that the basic characteristics found for the transition ($J_\ell = 1, J_u = 0$) are confirmed: atomic polarization (of both the upper and the lower level) depends non-linearly on the anisotropy factor w, and vanishes for $w = 0$; the ratio of the upper to the lower level population also depends non-linearly on w, and is affected by the presence of depolarizing collisions.

Consider now the limit $\delta^{(2)}_\ell \rightarrow \infty$. Equations (10.66) reduce to

$$\sigma^2_0(\alpha_u J_u) = -\frac{\sqrt{2}}{4} \frac{w}{1 + \delta^{(2)}_u} \, , \qquad \sigma^2_0(\alpha_\ell J_\ell) = 0 \, , \qquad \frac{\rho^0_0(\alpha_u J_u)}{\rho^0_0(\alpha_\ell J_\ell)} = \bar{n} \, . \qquad (10.67)$$

These can be compared with the corresponding expressions derived in Sect. 10.6 for the two-level atom under the unpolarized lower level approximation. Setting $\epsilon = H_u = 0$ (the conditions considered in the present section) into Eq. (10.50) we obtain, for an arbitrary transition (J_ℓ, J_u)

$$\left[\sigma^2_0(\alpha_u J_u)\right]_{\text{u.l.l.}} = \frac{w^{(2)}_{J_u J_\ell}}{\sqrt{2}\,\left(1 + \delta^{(2)}_u\right)} \, w \, , \qquad \left[\frac{\rho^0_0(\alpha_u J_u)}{\rho^0_0(\alpha_\ell J_\ell)}\right]_{\text{u.l.l.}} = \sqrt{\frac{2J_u + 1}{2J_\ell + 1}} \, \bar{n} \, , \quad (10.68)$$

where 'u.l.l.' stands for 'unpolarized lower level', and where we have used the notations of Eqs. (10.62). For the transition ($J_\ell = 1, J_u = 1$), Eqs. (10.68) give the same results as Eqs. (10.67) – see Table 10.1. Once again we see that the unpolarized lower level approximation is correct under the limit $\delta^{(K)}_\ell \rightarrow \infty$ – a statement which, on the other hand, is suggested by the structure itself of the statistical equilibrium equations. It is important to remark that the condition $\delta^{(K)}_\ell \gg 1$ occurs not only when $D^{(K)} \gg A(\alpha_u J_u \rightarrow \alpha_\ell J_\ell)$ – in which case $\delta^{(K)}_u \gg 1$, so that the polarization of the upper level tends to zero as well – but also when $\bar{n} \ll 1$ (see Eq. (10.63)). Therefore *the unpolarized lower level approximation is especially*

appropriate in the presence of depolarizing collisions and a radiation field of low intensity. It should also be noticed that, according to Eqs. (10.68), the atomic polarization of the upper level depends linearly on w, contrary to Eqs. (10.66).

Finally, it is instructive to consider the special case $\delta_\ell^{(2)} = \delta_u^{(2)} = 0$, $w = 1$ (absence of depolarizing collisions, atom illuminated by a unidirectional, unpolarized beam). Equations (10.66) yield

$$\sigma_0^2(\alpha_u J_u) = -\sqrt{2}\,, \qquad \sigma_0^2(\alpha_\ell J_\ell) = \frac{1}{\sqrt{2}}\,, \qquad \frac{\rho_0^0(\alpha_u J_u)}{\rho_0^0(\alpha_\ell J_\ell)} = \frac{3}{4}\,\bar{n}\,.$$

According to Table 3.6, this means that the Zeeman sublevels of the upper level with $M_u = \pm 1$, and the Zeeman sublevel of the lower level with $M_\ell = 0$ are completely depopulated. The populations of the remaining sublevels, normalized to unity, are

$$\rho_{\alpha_u J_u}(0) = \frac{3\,\bar{n}}{4 + 3\,\bar{n}}\,, \qquad \rho_{\alpha_\ell J_\ell}(\pm 1) = \frac{2}{4 + 3\,\bar{n}}\,.$$

The analytical results obtained for the two simple cases ($J_\ell = 1, J_u = 0$) and ($J_\ell = 1, J_u = 1$) might in principle be extended to transitions involving larger J values. However, the algebraic system to be solved becomes of course more and more complicated; at the same time, the dependence of atomic polarization on the various parameters becomes so intricate that no real insight into the physics of the scattering process can be gained. In order to give an idea of the atomic polarization arising in different transitions, we collect in Table 10.3 the values of the reduced statistical tensors

$$\sigma_0^K(\alpha_u J_u) = \frac{\rho_0^K(\alpha_u J_u)}{\rho_0^0(\alpha_u J_u)}\,, \qquad \sigma_0^K(\alpha_\ell J_\ell) = \frac{\rho_0^K(\alpha_\ell J_\ell)}{\rho_0^0(\alpha_\ell J_\ell)}$$

obtained by a numerical code for the collisionless, maximum anisotropy regime ($\delta_\ell^{(K)} = \delta_u^{(K)} = 0$, $w = 1$, corresponding to the irradiation of the atom by a unidirectional, unpolarized beam). For comparison, we also report the value of

$$\left[\sigma_0^2(\alpha_u J_u)\right]_{\text{u.l.l.}} = \frac{w^{(2)}_{J_u J_\ell}}{\sqrt{2}}$$

obtained for the same physical conditions plus the assumption of the unpolarized lower level (cf. Eqs. (10.68)). The last two columns of Table 10.3 show, respectively, the fractional linear polarization p_Q expected in a 90° scattering process, and the same quantity evaluated under the additional assumption of the unpolarized lower level, $[p_Q]_{\text{u.l.l.}}$. The expression of the former can be deduced from Eq. (10.15). Defining the positive Q direction as the perpendicular to the scattering plane, we obtain, with the help of Table 5.6 (with $\theta = 90°$, $\gamma = 90°$) and Eq. (10.14)

$$p_Q = \frac{\varepsilon_Q(90°)}{\varepsilon_I(90°)} = \frac{3\,w^{(2)}_{J_u J_\ell}\,\sigma_0^2(\alpha_u J_u)}{2\sqrt{2} - w^{(2)}_{J_u J_\ell}\,\sigma_0^2(\alpha_u J_u)}\,. \tag{10.69}$$

TABLE 10.3

Atomic polarization for different transitions in the collisionless, maximum anisotropy regime. The letters u and ℓ denote the upper and lower level, respectively. The last two columns give the fractional linear polarization in a 90° scattering. The label u.l.l. means 'unpolarized lower level'.

J_ℓ	J_u	$\sigma_0^2(u)$ $\sigma_0^2(\ell)$	$\sigma_0^4(u)$ $\sigma_0^4(\ell)$	$\sigma_0^6(u)$ $\sigma_0^6(\ell)$	$\sigma_0^8(u)$ $\sigma_0^8(\ell)$	$\sigma_0^{10}(u)$ $\sigma_0^{10}(\ell)$	$[\sigma_0^2(u)]_{\text{u.l.l.}}$	p_Q	$[p_Q]_{\text{u.l.l.}}$
0	1	0.707 –	–	–	–	–	0.707	1.	1.
1/2	1/2	– –	–	–	–	–	–	0.	0.
1/2	3/2	0.5 –	–	–	–	–	0.5	0.429	0.429
1	0	– −1.414	–	–	–	–	–	0.	0.
1	1	−1.414 0.707	–	–	–	–	−0.354	1.	0.2
1	2	0.622 0.321	0.214 –	–	–	–	0.418	0.448	0.288
3/2	1/2	– −0.5	–	–	–	–	–	0.	0.
3/2	3/2	−0.526 0.308	–	–	–	–	−0.4	0.353	0.261
3/2	5/2	0.764 0.5	0.265 –	–	–	–	0.374	0.5	0.226
2	1	−0.202 −0.489	– 0.146	–	–	–	0.071	−0.021	0.008
2	2	−0.460 0.272	−0.247 0.146	–	–	–	−0.418	0.319	0.288
2	3	0.903 0.659	0.354 0.137	0.089 –	–	–	0.346	0.556	0.191
5/2	3/2	−0.357 −0.541	– 0.141	–	–	–	0.1	−0.053	0.015
5/2	5/2	−0.408 0.244	−0.109 0.065	–	–	–	−0.428	0.287	0.302
5/2	7/2	1.035 0.809	0.458 0.242	0.132 –	–	–	0.327	0.611	0.170

TABLE 10.3

(continued)

J_ℓ	J_u	$\sigma_0^2(u)$ $\sigma_0^2(\ell)$	$\sigma_0^4(u)$ $\sigma_0^4(\ell)$	$\sigma_0^6(u)$ $\sigma_0^6(\ell)$	$\sigma_0^8(u)$ $\sigma_0^8(\ell)$	$\sigma_0^{10}(u)$ $\sigma_0^{10}(\ell)$	$[\sigma_0^2(u)]_{\text{u.l.l.}}$	p_Q	$[p_Q]_{\text{u.l.l.}}$
3	2	−0.452 −0.590	0.054 0.164	– −0.027	– –	– –	0.120	−0.079	0.022
3	3	−0.388 0.233	−0.092 0.055	−0.047 0.028	– –	– –	−0.433	0.275	0.310
3	4	1.156 0.948	0.569 0.352	0.186 0.060	0.037 –	– –	0.313	0.664	0.155
7/2	5/2	−0.522 −0.632	0.100 0.196	– −0.036	– –	– –	0.134	−0.101	0.027
7/2	7/2	−0.376 0.226	−0.080 0.048	−0.021 0.013	– –	– –	−0.436	0.268	0.316
7/2	9/2	1.266 1.077	0.683 0.466	0.248 0.114	0.062 –	– –	0.303	0.711	0.144
4	3	−0.579 −0.670	0.143 0.230	−0.013 −0.047	– 0.005	– –	0.144	−0.120	0.032
4	4	−0.369 0.222	−0.075 0.045	−0.018 0.011	−0.009 0.005	– –	−0.439	0.264	0.320
4	5	1.363 1.195	0.797 0.584	0.318 0.175	0.091 0.025	0.015 –	0.294	0.753	0.136
9/2	7/2	−0.628 −0.704	0.183 0.263	−0.026 −0.061	– 0.009	– –	0.153	−0.137	0.035
9/2	9/2	−0.364 0.219	−0.071 0.043	−0.015 0.009	−0.004 0.002	– –	−0.440	0.261	0.322
9/2	11/2	1.449 1.300	0.908 0.701	0.392 0.242	0.125 0.051	0.027 –	0.288	0.790	0.129
5	4	−0.669 −0.733	0.222 0.296	−0.040 −0.076	0.003 0.012	– −0.001	0.160	−0.152	0.039
5	5	−0.360 0.217	−0.069 0.042	−0.014 0.008	−0.003 0.002	−0.002 0.001	−0.442	0.259	0.324
11/2	9/2	−0.704 −0.759	0.259 0.327	−0.056 −0.093	0.006 0.017	– −0.002	0.165	−0.165	0.041
11/2	11/2	−0.358 0.216	−0.068 0.041	−0.013 0.008	−0.003 0.002	−0.001 0.000	−0.442	0.258	0.326

In the special case of unpolarized lower level, this expression reduces to

$$\left[p_Q\right]_{\text{u.l.l.}} = \frac{3\,W_2(J_\ell, J_u)}{4 - W_2(J_\ell, J_u)}\,, \tag{10.70}$$

where Eqs. (10.68) and (10.17) have been used. Note that expression (10.70) has already been derived in Sect. 10.2 (Eq. (10.26)).

It is interesting to observe that, with some exceptions, the linear polarization of the scattered radiation is larger (in absolute value) when the atomic polarization of the lower level is taken into account. The exceptions are provided by transitions having $\Delta J = J_u - J_\ell = 0$ (and $J_\ell > 2$), for which the difference between the last two columns of Table 10.3 is, however, rather small. It is also interesting to notice that for transitions with $\Delta J = -1$ the polarization of the scattered radiation is negative (polarization direction parallel to the scattering plane) when the atomic polarization of the lower level is taken into account.

The results in Table 10.3 can also be used to reconstruct the relative populations of the Zeeman sublevels via Eq. (3.99). Referring for instance to the transition $(J_\ell = 1, J_u = 2)$, one can easily find that the relative populations are $9/22$ $(M_\ell = \pm 1)$ and $4/22$ $(M_\ell = 0)$ for the lower level, and $9/25$ $(M_u = \pm 2)$, $2/25$ $(M_u = \pm 1)$, $3/25$ $(M_u = 0)$ for the upper level.[1]

10.8. The Two-Level Atom: the Hanle Effect with Lower-Level Polarization

(*cylindrical symmetry - no stimulated emission - no inelastic collisions*)

The results of the previous section can be generalized by allowing for the presence of a magnetic field: this leads to an investigation of the Hanle effect in more general terms than in Sect. 10.3, since lower-level atomic polarization is now taken into account. In order to simplify the problem, we adopt exactly the same assumptions as in the preceding section (except of course for the presence of the magnetic field): we neglect stimulated emission as well as inelastic and superelastic collisions, and we assume the incoming radiation to be unpolarized and cylindrically symmetrical about a given direction. The flat-spectrum approximation requires now the radiation to be unstructured across a frequency interval centered at the transition frequency ν_0 and larger than the Zeeman splitting of the line.

Since there are two preferred directions (the magnetic field vector and the symmetry axis of the radiation field), it is convenient to write the statistical equilibrium equations in a reference system whose z-axis is parallel to one of them. Either choice has its own advantages and disadvantages. In the frame with the z-axis

[1] In terms of rational numbers, one has

$$\sigma^2_0(\alpha_\ell J_\ell) = \frac{5\sqrt{2}}{22}\,, \qquad \sigma^2_0(\alpha_u J_u) = \frac{13\sqrt{70}}{175}\,, \qquad \sigma^4_0(\alpha_u J_u) = \frac{2\sqrt{14}}{35}\,.$$

along the magnetic field direction, one can apply directly Eq. (7.11). The magnetic contribution to the equations is very simple (being diagonal), but the expressions of the transfer and relaxation rates are rather complicated because the radiation field has no special symmetry characteristics about the magnetic field's direction. In the frame with the z-axis parallel to the symmetry axis of the radiation field, the expressions of the rates are much simpler (because the radiation field tensor has only two non-zero components, $J^0_0(\nu_0)$ and $J^2_0(\nu_0)$), whereas the magnetic term involves a kernel connecting different statistical tensors (see Eqs. (7.78) and (7.79)).

In the following we choose the latter reference frame. It can easily be proved that, in stationary situations, the only non-null statistical tensors are those with K even (see Sect. 10.7). Owing to the presence of the magnetic kernel, which mixes up statistical tensors of the same rank but with different Q values, the statistical tensors with $Q \neq 0$ are in general non-zero. Therefore, contrary to the previous section, atomic polarization involves *both* population unbalances *and* coherences between Zeeman sublevels. The number of equations (and of unknowns) is now given by (cf. Eq. (10.59))

$$N_{\rm eq} = \begin{cases} (J_\ell+1)(2J_\ell+1) + (J_u+1)(2J_u+1) & \text{for } J_\ell, J_u \text{ integers} \\ J_\ell(2J_\ell+1) + J_u(2J_u+1) & \text{for } J_\ell, J_u \text{ half-integers}\,. \end{cases} \tag{10.71}$$

The statistical equilibrium equations for the two-level atom, under the physical conditions specified above, can be obtained from Eq. (7.78) by adding the contribution of depolarizing collisions (Eq. (7.101)). Bearing in mind the formal invariance of the radiative rates proved in Sect. 7.12 – which implies that such rates are still given by Eqs. (7.14) – we get, with the help of Eqs. (2.26a), (2.36a) and (2.49)[1]

$$\begin{aligned} \frac{\mathrm{d}}{\mathrm{d}t}\,\rho^K_Q(\alpha_u J_u) = &-2\pi\mathrm{i}\,\nu_{\rm L}\; g_{\alpha_u J_u} \sum_{Q'} \; \mathcal{K}^K_{QQ'} \;\; \rho^K_{Q'}(\alpha_u J_u) \\ &- \Big[A(\alpha_u J_u \rightarrow \alpha_\ell J_\ell) + D^{(K)}(\alpha_u J_u)\Big]\; \rho^K_Q(\alpha_u J_u) \\ &+ \sum_{K' \text{ even}} \mathbb{T}_{\rm A}(\alpha_u J_u K Q, \alpha_\ell J_\ell K' Q) \;\; \rho^{K'}_Q(\alpha_\ell J_\ell) \end{aligned}$$

$$\begin{aligned} \frac{\mathrm{d}}{\mathrm{d}t}\,\rho^K_Q(\alpha_\ell J_\ell) = &-2\pi\mathrm{i}\,\nu_{\rm L}\; g_{\alpha_\ell J_\ell} \sum_{Q'} \; \mathcal{K}^K_{QQ'} \;\; \rho^K_{Q'}(\alpha_\ell J_\ell) \\ &+ (2J_u+1)\, A(\alpha_u J_u \rightarrow \alpha_\ell J_\ell) \;\; (-1)^{1+J_\ell+J_u} \left\{ \begin{array}{ccc} J_u & J_u & K \\ J_\ell & J_\ell & 1 \end{array} \right\} \rho^K_Q(\alpha_u J_u) \\ &- \sum_{K' \text{ even}} \Big[\mathbb{R}_{\rm A}(\alpha_\ell J_\ell K Q K' Q) + \delta_{KK'}\, D^{(K)}(\alpha_\ell J_\ell)\Big]\; \rho^{K'}_Q(\alpha_\ell J_\ell)\,, \end{aligned} \tag{10.72}$$

where K is even, and where

[1] The rates $D^{(K)}(\alpha J)$ are obviously invariant, because of the isotropic distribution of the colliding particles. Such invariance can be formally proved with the help of Eqs. (2.72).

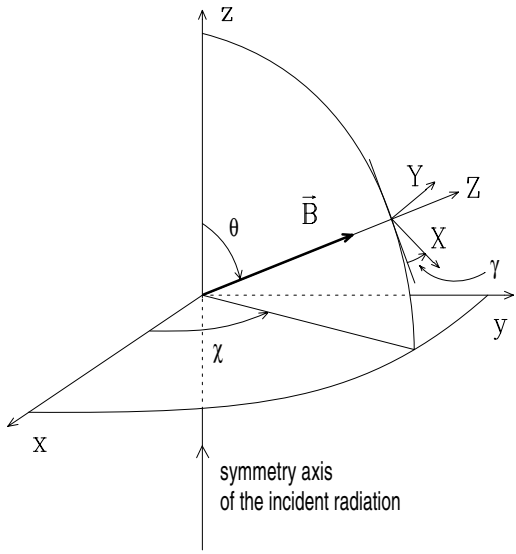

Fig.10.6. The rotation R appearing in Eqs.(10.73) and (10.74) carries the reference system (XYZ) into (xyz).

$$\mathbb{T}_{\rm A}(\alpha_u J_u K Q, \alpha_\ell J_\ell K' Q) = (2J_\ell + 1)\, B(\alpha_\ell J_\ell \to \alpha_u J_u)$$
$$\times \left[\delta_{KK'}\, (-1)^{1+J_\ell+J_u} \begin{Bmatrix} J_u & J_u & K \\ J_\ell & J_\ell & 1 \end{Bmatrix} J_0^0(\nu_0) \right.$$
$$\left. + (-1)^Q \sqrt{15(2K+1)(2K'+1)} \begin{Bmatrix} J_u & J_\ell & 1 \\ J_u & J_\ell & 1 \\ K & K' & 2 \end{Bmatrix} \begin{pmatrix} K & K' & 2 \\ -Q & Q & 0 \end{pmatrix} J_0^2(\nu_0) \right]$$

$$\mathbb{R}_{\rm A}(\alpha_\ell J_\ell K Q K' Q) = (2J_\ell + 1)\, B(\alpha_\ell J_\ell \to \alpha_u J_u)$$
$$\times \left[\delta_{KK'}\, \frac{1}{2J_\ell + 1}\, J_0^0(\nu_0) \,+\, (-1)^{1-J_\ell+J_u+Q} \sqrt{15(2K+1)(2K'+1)} \right.$$
$$\left. \times \begin{Bmatrix} K & K' & 2 \\ J_\ell & J_\ell & J_\ell \end{Bmatrix} \begin{Bmatrix} 1 & 1 & 2 \\ J_\ell & J_\ell & J_u \end{Bmatrix} \begin{pmatrix} K & K' & 2 \\ Q & -Q & 0 \end{pmatrix} J_0^2(\nu_0) \right],$$

and

$$\mathcal{K}^K_{QQ'} = \sum_{Q''} \mathcal{D}^K_{Q''Q}(R)^*\, Q''\, \mathcal{D}^K_{Q''Q'}(R)\,, \tag{10.73}$$

R being the rotation which carries the reference system with the z-axis directed along the magnetic field into the reference system with the z-axis directed along the symmetry axis of the radiation field.

The expression of the kernel $\mathcal{K}^K_{QQ'}$ can be somewhat simplified. Referring to Fig. 10.6, the rotation R is given, in terms of Euler angles, by

$$R \equiv (-\gamma, -\theta, -\chi) \; .$$

Expression (10.73) is independent of the angle γ, as obvious from Eq. (2.68). The summation over Q'' can be performed by expressing Q'' via Eq. (2.26d),

$$Q'' = \sqrt{K(K+1)(2K+1)} \; (-1)^{K-Q''} \begin{pmatrix} K & K & 1 \\ Q'' & -Q'' & 0 \end{pmatrix} \; ,$$

and the product of two rotation matrices via Eq. (2.77). With the help of Eqs. (2.23a) and (2.73) we obtain the simpler expression

$$\mathcal{K}^K_{QQ'} = \sqrt{K(K+1)(2K+1)} \; (-1)^{K-Q'} \begin{pmatrix} K & K & 1 \\ Q & -Q' & q \end{pmatrix} \mathcal{D}^1_{0q}(R) \; . \qquad (10.74)$$

Even for the simplest transitions, Eqs. (10.72) are so involved that it isn't worth trying to solve them (in stationary situations) analytically: for instance, according to Eq. (10.71), the transition $(J_\ell = 1, J_u = 1)$ is described by a system of 12 equations in 12 unknowns. It is therefore necessary to resort to a numerical solution.

Once the solution is found, the radiation emitted in a given direction can be evaluated via Eq. (10.39), or via Eq. (10.31) if only the frequency-integrated radiation is required. To give an example, we refer to the geometry of Fig. 10.6 and we evaluate the frequency-integrated fractional polarization of the radiation emitted in the x-direction (i.e., at 90° from the symmetry axis of the incoming radiation), taking the y-axis as the positive Q direction. Using the expressions of $\mathcal{T}^K_Q(i, \vec{\Omega})$ in Table 5.6 (with $\theta = 90°$, $\chi = 0°$, $\gamma = 90°$) we obtain from Eq. (10.31), with the help of Eqs. (3.102) and (10.14)

$$\tilde{p}_Q = \frac{\tilde{\varepsilon}_Q}{\tilde{\varepsilon}_I} = \frac{w^{(2)}_{J_u J_\ell} \left[\, 3\,\sigma^2_0 + \sqrt{6}\,\mathrm{Re}(\sigma^2_2) \, \right]}{2\sqrt{2} - w^{(2)}_{J_u J_\ell} \left[\, \sigma^2_0 - \sqrt{6}\,\mathrm{Re}(\sigma^2_2) \, \right]}$$

$$\tilde{p}_U = \frac{\tilde{\varepsilon}_U}{\tilde{\varepsilon}_I} = -\frac{2\sqrt{6}\;\; w^{(2)}_{J_u J_\ell}\;\; \mathrm{Im}(\sigma^2_1)}{2\sqrt{2} - w^{(2)}_{J_u J_\ell} \left[\, \sigma^2_0 - \sqrt{6}\,\mathrm{Re}(\sigma^2_2) \, \right]} \; , \qquad (10.75)$$

where σ^K_Q are the reduced statistical tensors of the upper level.

Figures 10.7 and 10.8 show the Hanle diagrams for the transitions $(J_\ell = 1, J_u = 1)$ and $(J_\ell = 1, J_u = 2)$, respectively.[1] They are obtained from Eqs. (10.75), with the values of the statistical tensors derived by solving numerically Eqs. (10.72) – written for stationary situations – together with the trace equation (10.4), under the following conditions: the magnetic field vector lies in the x-y plane ($\theta = 90°$ in Fig. 10.6); the incoming radiation is a unidirectional, unpolarized beam travelling in the z-direction; its intensity is very weak; depolarizing collisions are negligible.

[1] Hanle diagrams for other transitions have been presented by Landolfi and Landi Degl'Innocenti (1986).

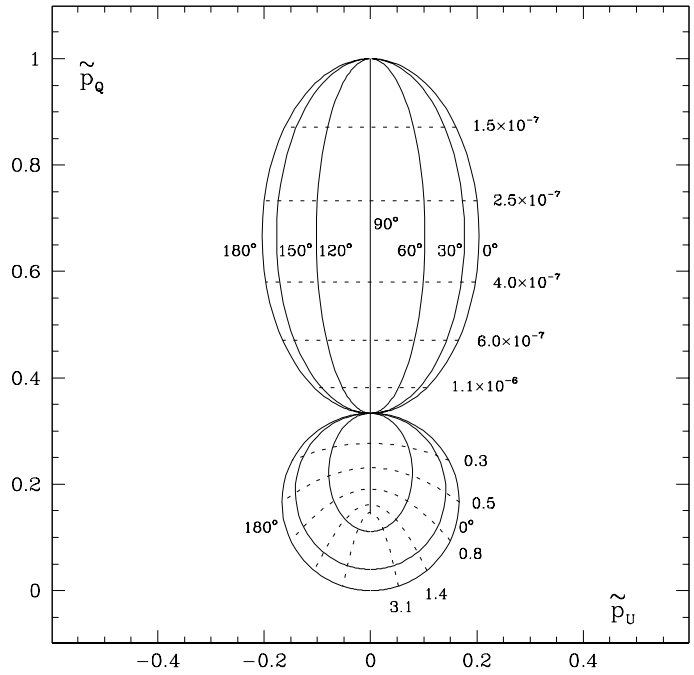

Fig.10.7. Polarization diagram for the transition ($J_\ell = 1, J_u = 1$) corresponding to the geometry of Fig.10.6 with $\theta = 90°$. The scattering direction is the x-axis. Lower-level atomic polarization is taken into account. The relevant parameters are: $w = 1$, $\bar{n} = 10^{-6}$, $\delta_u^{(K)} = \delta_\ell^{(K)} = 0$ (see Eqs.(10.62)). Full lines correspond to $\chi = \text{const.}$, dashed lines to constant magnetic field strength ($H_u = \text{const.}$, see Eq.(10.28); the Landé factors of the upper and lower level are assumed to be the same).

In terms of the parameters defined in Eqs. (10.62) the last three conditions read: $w = 1$, $\bar{n} \ll 1$, $\delta_u^{(K)} = \delta_\ell^{(K)} = 0$.

If the diagrams in Fig. 10.7 or 10.8 are compared with a 'usual' Hanle diagram (see e.g. Fig. 10.2), an obvious difference comes out: the latter consists of a unique 'lobe', while the former are split into two distinct lobes. Such lobes correspond to the relaxation of the lower-level coherences (*lower-level Hanle effect*) and of the upper-level coherences ('usual' Hanle effect), respectively. The order of magnitude of the magnetic field strength in either lobe is different, because – as suggested by Eqs. (10.72) – the typical field which depolarizes the lower level is such that

$$2\pi\nu_{\rm L}\, g_{\alpha_\ell J_\ell} \approx B(\alpha_\ell J_\ell \to \alpha_u J_u)\, J_0^0(\nu_0)\ ,$$

whereas the typical field which depolarizes the upper level is such that

$$2\pi\nu_{\rm L}\, g_{\alpha_u J_u} \approx A(\alpha_u J_u \to \alpha_\ell J_\ell)\ .$$

Since from Eqs. (10.62)

$$\frac{B(\alpha_\ell J_\ell \to \alpha_u J_u)\, J_0^0(\nu_0)}{A(\alpha_u J_u \to \alpha_\ell J_\ell)} = \frac{2J_u + 1}{2J_\ell + 1}\ \bar{n}\ ,$$

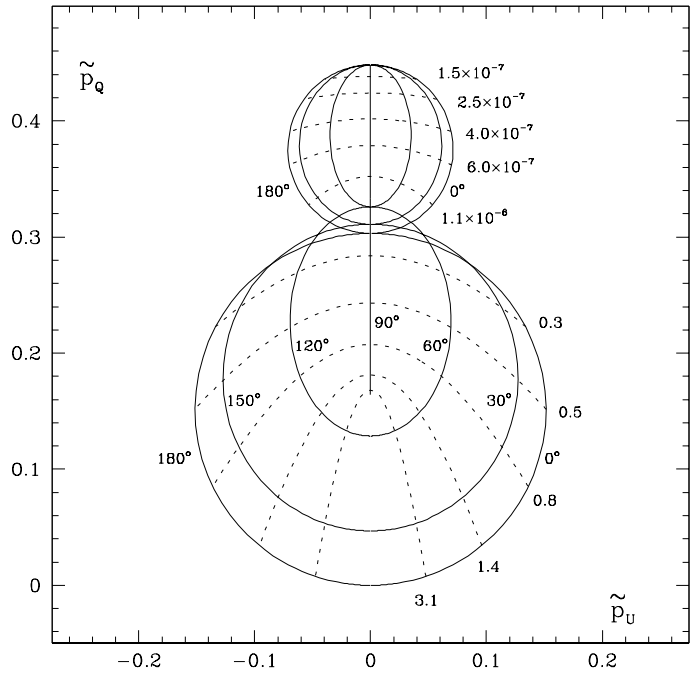

Fig.10.8. Same as Fig.10.7 for the transition ($J_\ell = 1, J_u = 2$).

it follows that the former is approximately $\bar{n}$ times smaller than the latter. The lower-level and the 'usual' Hanle effect are clearly separated in Figs. 10.7 and 10.8 because the incident radiation is extremely diluted ($\bar{n} = 10^{-6}$). The shape of the diagrams will however remain the same provided $\bar{n} \ll 1$. For $\bar{n} \simeq 1$ the two regimes tend to overlap; but a correct treatment of this case requires that the stimulated emission rates be included in the statistical equilibrium equations (see the next section).

Let us compare the diagrams in Figs. 10.8 and 10.2 more closely. They refer to the same transition and the same geometrical and physical conditions: the only difference is the atomic polarization of the lower level, which is allowed for in Fig. 10.8 and neglected in Fig. 10.2 (unpolarized lower level approximation). For zero magnetic field, the value of $\tilde{p}_Q$ in Fig. 10.8 is larger than the value in Fig. 10.2 (approximately 0.45 and 0.29, respectively: see Table 10.3), consistently with the results presented at the end of Sect. 10.7. The value of $\tilde{p}_Q$ corresponding to the relaxation of the lower-level coherences (the 'transition region' between the two lobes of Fig. 10.8) depends on the value of the angle χ, ranging approximately from 0.30 for $\chi = 0°$ or 180° to 0.33 for $\chi = 90°$. In any case, this value is larger than $\tilde{p}_Q \simeq 0.29$ of Fig. 10.2, where lower-level atomic polarization is neglected a priori. The same characteristic appears from Fig. 10.7, where the value of $\tilde{p}_Q$ corresponding to the transition between the two lobes (independent of χ in this case) is about 0.33, to be compared with $\tilde{p}_Q = 0.2$ given in Table 10.3 for the transition ($J_\ell = 1, J_u = 1$) under the unpolarized lower level approximation. These examples

show that *atomic polarization of the lower level is reduced, but not completely removed, by the magnetic field*. The complete cancellation of lower-level polarization can only occur in the presence of depolarizing collisions.

10.9. The Two-Level Atom: the Role of Stimulated Emission

(*cylindrical symmetry - no inelastic collisions*)

In this section we further enlarge the treatment of resonance polarization in a two-level atom by taking stimulated emission (besides lower-level atomic polarization) into account. Apart from this generalization, the physical conditions under which the phenomenon is studied are the same as in the two previous sections: the incoming radiation is assumed to be unpolarized and cylindrically symmetrical about a fixed direction, and to satisfy the flat-spectrum approximation; inelastic and superelastic collisions are neglected. As far as the magnetic field is concerned, we will consider separately the (simpler) non-magnetic and the magnetic case.[1]

We begin with the non-magnetic case, and we choose a reference system with the z-axis parallel to the symmetry axis of the radiation field. As shown in Sect. 10.7, the only non-zero components of the radiation field tensor are $J^0_0(\nu_0)$ and $J^2_0(\nu_0)$, and the only non-zero statistical tensors are those with K even and $Q = 0$. The statistical equilibrium equations (identical with Eqs. (10.60) except for the presence of the stimulated emission rates) are easily deduced from Eqs. (10.1) and (10.2)

$$\begin{aligned}
\frac{\mathrm{d}}{\mathrm{d}t}\,\rho^K_0(\alpha_u J_u) &= -\Big[A(\alpha_u J_u \to \alpha_\ell J_\ell) + D^{(K)}(\alpha_u J_u)\Big]\ \rho^K_0(\alpha_u J_u) \\
&\quad + \sum_{K' \text{ even}} \mathbb{T}_{\mathrm{A}}(\alpha_u J_u K\, 0, \alpha_\ell J_\ell K' 0)\ \rho^{K'}_0(\alpha_\ell J_\ell) \\
&\quad - \sum_{K' \text{ even}} \mathbb{R}_{\mathrm{S}}(\alpha_u J_u K\, 0\, K' 0)\ \rho^{K'}_0(\alpha_u J_u) \\
\frac{\mathrm{d}}{\mathrm{d}t}\,\rho^K_0(\alpha_\ell J_\ell) &= (2J_u+1)\, A(\alpha_u J_u \to \alpha_\ell J_\ell)\ (-1)^{1+J_\ell+J_u} \begin{Bmatrix} J_u & J_u & K \\ J_\ell & J_\ell & 1 \end{Bmatrix} \rho^K_0(\alpha_u J_u) \\
&\quad - \sum_{K' \text{ even}} \Big[\mathbb{R}_{\mathrm{A}}(\alpha_\ell J_\ell K\, 0\, K' 0) + \delta_{KK'}\, D^{(K)}(\alpha_\ell J_\ell)\Big]\ \rho^{K'}_0(\alpha_\ell J_\ell) \\
&\quad + \sum_{K' \text{ even}} \mathbb{T}_{\mathrm{S}}(\alpha_\ell J_\ell K\, 0, \alpha_u J_u K' 0)\ \rho^{K'}_0(\alpha_u J_u)\,, \qquad (10.76)
\end{aligned}$$

where K is even and the rates $\mathbb{T}_{\mathrm{A}}$ and $\mathbb{R}_{\mathrm{A}}$ are given by Eqs. (10.61), while the rates $\mathbb{T}_{\mathrm{S}}$ and $\mathbb{R}_{\mathrm{S}}$ can be obtained from Eqs. (7.14c,f) with the help of Eqs. (2.26a), (2.36a) and (2.49)

[1] The precise meaning of the flat-spectrum approximation is different in the two cases: see Sects. 10.7 and 10.8.

$$\mathbb{T}_{\rm S}(\alpha_\ell J_\ell K\,0, \alpha_u J_u K'\,0) = (2J_u+1)\,B(\alpha_u J_u \rightarrow \alpha_\ell J_\ell)$$
$$\times \left[\delta_{KK'}\,(-1)^{1+J_\ell+J_u} \begin{Bmatrix} J_\ell & J_\ell & K \\ J_u & J_u & 1 \end{Bmatrix} J_0^0(\nu_0) \right.$$
$$\left. + \sqrt{15(2K+1)(2K'+1)} \begin{Bmatrix} J_\ell & J_u & 1 \\ J_\ell & J_u & 1 \\ K & K' & 2 \end{Bmatrix} \begin{pmatrix} K & K' & 2 \\ 0 & 0 & 0 \end{pmatrix} J_0^2(\nu_0) \right]$$

$$\mathbb{R}_{\rm S}(\alpha_u J_u K\,0\,K'\,0) = (2J_u+1)\,B(\alpha_u J_u \rightarrow \alpha_\ell J_\ell)$$
$$\times \left[\delta_{KK'}\,\frac{1}{2J_u+1}\,J_0^0(\nu_0) + (-1)^{1+J_\ell-J_u}\sqrt{15(2K+1)(2K'+1)} \right.$$
$$\left. \times \begin{Bmatrix} K & K' & 2 \\ J_u & J_u & J_u \end{Bmatrix} \begin{Bmatrix} 1 & 1 & 2 \\ J_u & J_u & J_\ell \end{Bmatrix} \begin{pmatrix} K & K' & 2 \\ 0 & 0 & 0 \end{pmatrix} J_0^2(\nu_0) \right].$$

In order to illustrate the effects of stimulated emission, we apply Eqs. (10.76) to a few sample transitions, beginning with the simple case ($J_\ell = 0, J_u = 1$). The obvious advantage of this transition is that lower-level atomic polarization is zero by definition.[1] It should be emphasized that, in general, *lower-level polarization should not be neglected when stimulated emission starts becoming important*. This is because the radiative lifetime of the lower level becomes comparable with that of the upper level and, even invoking depolarizing collisions, it is impossible to find a physical regime where the upper level is polarized while the lower level is unpolarized. For the transition ($J_\ell = 0, J_u = 1$) we obtain from the first of Eqs. (10.76), recalling Eqs. (7.8)

$$\frac{1}{A(\alpha_u J_u \rightarrow \alpha_\ell J_\ell)}\,\frac{\mathrm{d}}{\mathrm{d}t}\,\rho_0^0(\alpha_u J_u) = -\left[1+\bar{n}\right]\rho_0^0(\alpha_u J_u) + \sqrt{3}\,\bar{n}\;\rho_0^0(\alpha_\ell J_\ell)$$
$$-\frac{1}{\sqrt{2}}\,\bar{n}w\;\rho_0^2(\alpha_u J_u)$$

$$\frac{1}{A(\alpha_u J_u \rightarrow \alpha_\ell J_\ell)}\,\frac{\mathrm{d}}{\mathrm{d}t}\,\rho_0^2(\alpha_u J_u) = -\left[1+\bar{n}-\frac{1}{2}\,\bar{n}w+\delta_u^{(2)}\right]\rho_0^2(\alpha_u J_u)$$
$$-\frac{1}{\sqrt{2}}\,\bar{n}w\;\rho_0^0(\alpha_u J_u) + \sqrt{\frac{3}{2}}\;\bar{n}w\;\rho_0^0(\alpha_\ell J_\ell)\,,$$

[1] The same simplification occurs for the transitions ($J_\ell = 1/2, J_u = 1/2$) and ($J_\ell = 1/2, J_u = 3/2$), where lower-level polarization is zero in the presence of an unpolarized, cylindrically symmetrical radiation field. In fact, the only statistical tensors that can be defined for $J = 1/2$ are ρ_0^0 and ρ_Q^1, and the latter are zero because K is odd.

where the notations of Eqs. (10.62) have been used. In stationary situations, the solution can be written in the form

$$\sigma_0^2(\alpha_u J_u) = \frac{1}{\sqrt{2}}\ \frac{w}{1+\bar{n}\left[1-\frac{1}{2}\,w-\frac{1}{2}\,w^2\right]+\delta_u^{(2)}}$$

$$\frac{\rho_0^0(\alpha_u J_u)}{\rho_0^0(\alpha_\ell J_\ell)} = \sqrt{3}\ \bar{n}\ \frac{1+\bar{n}\left[1-\frac{1}{2}\,w-\frac{1}{2}\,w^2\right]+\delta_u^{(2)}}{\left[1+\bar{n}\right]\left[1+\bar{n}-\frac{1}{2}\,\bar{n}w+\delta_u^{(2)}\right]-\frac{1}{2}\,\bar{n}^2w^2}\ . \tag{10.77}$$

Obviously, we get back previous results if we neglect stimulated emission: for $\bar{n} \ll 1$ we have

$$\sigma_0^2(\alpha_u J_u) = \frac{1}{\sqrt{2}}\ \frac{w}{1+\ \delta_u^{(2)}}\ , \qquad \frac{\rho_0^0(\alpha_u J_u)}{\rho_0^0(\alpha_\ell J_\ell)} = \sqrt{3}\ \bar{n}\ ,$$

which are the same expressions obtained from Eqs. (10.50) under the physical conditions considered here ($\epsilon = 0$, $H_u = 0$, $J_Q^K = 0$ except for J_0^0 and J_0^2).

In general, the first of Eqs. (10.77) shows that stimulated emission reduces the atomic polarization of the upper level, except in the special case $w = 1$ (unidirectional, unpolarized beam) where it has no effect. The second equation yields the classical value $\sqrt{3}\,\bar{n}\,/(1+\bar{n})$ either for an isotropic, unpolarized radiation field ($w = 0$), or under the limit of extremely strong collisional rates ($\delta_u^{(2)} \to \infty$). In general, it shows that – even for the simple transition ($J_\ell = 0, J_u = 1$) and for a quantity that may be expected to be rather insensitive to anisotropy phenomena (the ratio of the upper to the lower level population) – the interplay of the anisotropy itself, the intensity of the radiation field and depolarizing collisions is very complicated and can produce large differences from the case where polarization phenomena are neglected.

Next we consider the simplest transition where lower-level atomic polarization plays a role, i.e., ($J_\ell = 1, J_u = 0$). From Eqs. (10.76) we obtain, using again Eqs. (7.8) and (10.62)

$$\frac{1}{A(\alpha_u J_u \to \alpha_\ell J_\ell)}\ \frac{\mathrm{d}}{\mathrm{d}t}\,\rho_0^0(\alpha_u J_u) = -\left[1+\bar{n}\right]\rho_0^0(\alpha_u J_u) + \frac{1}{\sqrt{3}}\ \bar{n}\ \rho_0^0(\alpha_\ell J_\ell) + \frac{1}{\sqrt{6}}\ \bar{n}w\ \rho_0^2(\alpha_\ell J_\ell)$$

$$\frac{1}{A(\alpha_u J_u \to \alpha_\ell J_\ell)}\ \frac{\mathrm{d}}{\mathrm{d}t}\,\rho_0^2(\alpha_\ell J_\ell) = -\frac{1}{3}\ \bar{n}\Big[1-\frac{1}{2}\,w+\delta_\ell^{(2)}\Big]\rho_0^2(\alpha_\ell J_\ell) - \frac{1}{3\sqrt{2}}\ \bar{n}w\ \rho_0^0(\alpha_\ell J_\ell) + \frac{1}{\sqrt{6}}\ \bar{n}w\ \rho_0^0(\alpha_u J_u)\ .$$

In stationary situations, the solution can be written in the form

$$\sigma_0^2(\alpha_\ell J_\ell) = -\sqrt{2}\ \frac{w}{2-w+2\,\delta_\ell^{(2)}+\bar{n}\left[2-w-w^2+2\,\delta_\ell^{(2)}\right]}$$

$$\frac{\rho_0^0(\alpha_u J_u)}{\rho_0^0(\alpha_\ell J_\ell)} = \frac{1}{\sqrt{3}}\ \bar{n}\ \frac{2-w-w^2+2\,\delta_\ell^{(2)}}{2-w+2\,\delta_\ell^{(2)}+\bar{n}\left[2-w-w^2+2\,\delta_\ell^{(2)}\right]}\ . \tag{10.78}$$

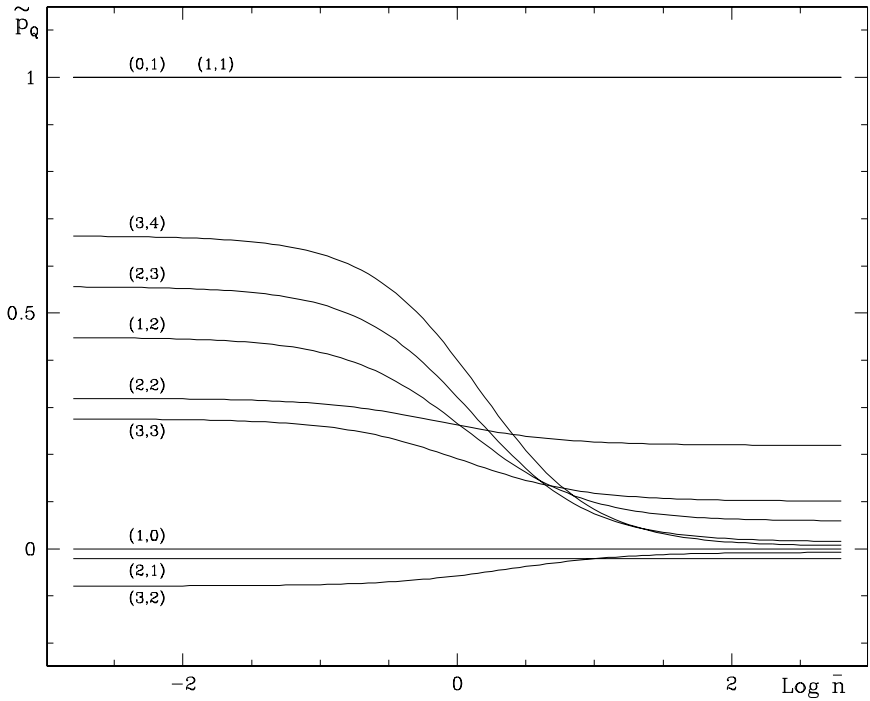

Fig.10.9. Fractional polarization of the radiation scattered at 90° from the incident (unpolarized) beam as a function of the beam intensity, for different atomic transitions (J_ℓ, J_u) involving integral J values.

Comparison with Eqs. (10.64) shows that stimulated emission reduces the polarization of the lower level (except in the extreme case $w = 1$ *and* $\delta_\ell^{(2)} = 0$). The ratio of the upper to the lower level population depends again in a complicated way on the different parameters (anisotropy factor, intensity, depolarizing collisions). Only for an isotropic, unpolarized radiation field ($w = 0$), or for strong collisional rates ($\delta_\ell^{(2)} \to \infty$), the second of Eqs. (10.78) yields the classical value $(1/\sqrt{3})\,\bar{n}\,/(1+\bar{n})$.

For more complicated transitions, the influence of stimulation effects on atomic polarization can be evaluated numerically, by solving Eqs. (10.76) – in stationary situations – together with the trace equation (10.4). Rather than atomic polarization itself, it is probably more instructive to examine the polarization of the radiation scattered by the atom in a given direction. If we refer for instance to the geometry of Fig. 10.6 (with $\vec{B} = 0$) and consider the frequency-integrated fractional polarization scattered in the x-direction (i.e., at 90° from the symmetry axis of the incident radiation), taking the y-axis as reference direction for Q, we have from Eqs. (10.75)

$$\tilde{p}_Q = \frac{3\, w^{(2)}_{J_u J_\ell}\, \sigma_0^2(\alpha_u J_u)}{2\sqrt{2} - w^{(2)}_{J_u J_\ell}\, \sigma_0^2(\alpha_u J_u)}\,, \qquad \tilde{p}_U = 0\,.$$

Figures 10.9 and 10.10 show the results of such calculations for several atomic

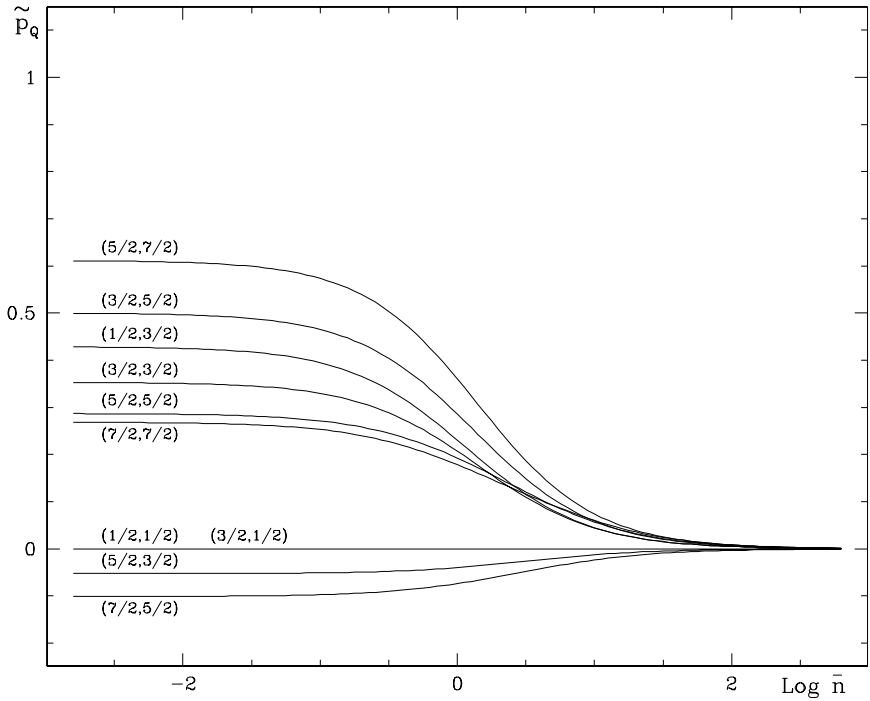

Fig.10.10. Same as Fig.10.9 for transitions involving half-integral J values.

transitions. Both figures refer to the collisionless, maximum anisotropy regime ($\delta_u^{(K)} = \delta_\ell^{(K)} = 0$, $w = 1$: see Eqs. (10.62)). Except for a few special cases, the polarization of the scattered radiation *decreases* (in absolute value) *with increasing* $\bar{n}$. However, an outstanding difference comes out between transitions involving integral and half-integral J values: for $\bar{n} \to \infty$ the polarization tends to a non-zero value (dependent on the individual transition) in the former case, while it tends to zero for all transitions in the latter.

The decrease of atomic polarization due to stimulated emission is not surprising. Atomic polarization is due to the fact that, in an anisotropic environment, the transitions between certain magnetic sublevels of the upper and lower level (characterized by their own quantum numbers M_u, M_ℓ) are more efficient than the others in absorbing radiation, which results in a population unbalance. When stimulated emission is important, however, just the *same* transitions are more efficient in *emitting* radiation, and the population unbalance is thus reduced.

Let's now examine how the above results are modified by the presence of a magnetic field. To obtain the statistical equilibrium equations in a reference system with the z-axis parallel to the symmetry axis of the incoming radiation, we have just to add in the right-hand sides of Eqs. (10.72) the contributions of stimulated emission, i.e., the term (see Eq. (10.1))

$$- \sum_{K' \text{ even}} \mathbb{R}_S(\alpha_u J_u K Q K' Q)\, \rho^{K'}_Q(\alpha_u J_u)$$

in the first equation, and the term (see Eq. (10.2))

$$+ \sum_{K' \text{ even}} \mathbb{T}_{\rm S}(\alpha_\ell J_\ell K Q, \alpha_u J_u K' Q)\, \rho^{K'}_{Q}(\alpha_u J_u)$$

in the second. The expressions of the rates $\mathbb{T}_{\rm S}$ and $\mathbb{R}_{\rm S}$ can be derived from Eqs. (7.14c,f) with the help of Eqs. (2.26a), (2.36a) and (2.49), bearing in mind that the index K is an even integer and that the only non-zero components of the radiation field tensor are $J^0_0(\nu_0)$ and $J^2_0(\nu_0)$

$$\mathbb{R}_{\rm S}(\alpha_u J_u K Q K' Q) = (2J_u+1)\, B(\alpha_u J_u \rightarrow \alpha_\ell J_\ell)$$
$$\times \left[\delta_{KK'}\, \frac{1}{2J_u+1}\, J^0_0(\nu_0) + (-1)^{1+J_\ell-J_u+Q} \sqrt{15(2K+1)(2K'+1)} \right.$$
$$\left. \times \begin{Bmatrix} K & K' & 2 \\ J_u & J_u & J_u \end{Bmatrix} \begin{Bmatrix} 1 & 1 & 2 \\ J_u & J_u & J_\ell \end{Bmatrix} \begin{pmatrix} K & K' & 2 \\ Q & -Q & 0 \end{pmatrix} J^2_0(\nu_0) \right]$$

$$\mathbb{T}_{\rm S}(\alpha_\ell J_\ell K Q, \alpha_u J_u K' Q) = (2J_u+1)\, B(\alpha_u J_u \rightarrow \alpha_\ell J_\ell)$$
$$\times \left[\delta_{KK'}\, (-1)^{1+J_\ell+J_u} \begin{Bmatrix} J_\ell & J_\ell & K \\ J_u & J_u & 1 \end{Bmatrix} J^0_0(\nu_0) \right.$$
$$\left. + (-1)^Q \sqrt{15(2K+1)(2K'+1)} \begin{Bmatrix} J_\ell & J_u & 1 \\ J_\ell & J_u & 1 \\ K & K' & 2 \end{Bmatrix} \begin{pmatrix} K & K' & 2 \\ -Q & Q & 0 \end{pmatrix} J^2_0(\nu_0) \right].$$

In stationary situations, the statistical equilibrium equations can be solved numerically for any given transition (J_ℓ, J_u), and the polarization of the scattered radiation can then be evaluated. As an example, we present in Fig. 10.11 the results of such calculations for the transition $(J_\ell = 1, J_u = 2)$. The scattering geometry is the same as in Figs. 10.7-10.8, and the polarization of the scattered radiation has been computed from Eqs. (10.75). The figure is directly comparable with Fig. 10.8 (collisionless, maximum anisotropy regime; same Landé factors for the upper and lower level), with the only difference that the intensity of the incident (unpolarized) beam is now 'large' ($\bar{n} = 0.5$), so that stimulation effects are important. One can notice the overall reduction of the polarization (consistent with the results of Fig. 10.9) and the disappearance of the double-lobe shape of the diagram. The lower-level Hanle effect mixes with the 'usual' Hanle effect because the lifetimes of the upper and lower level are now of the same order of magnitude.

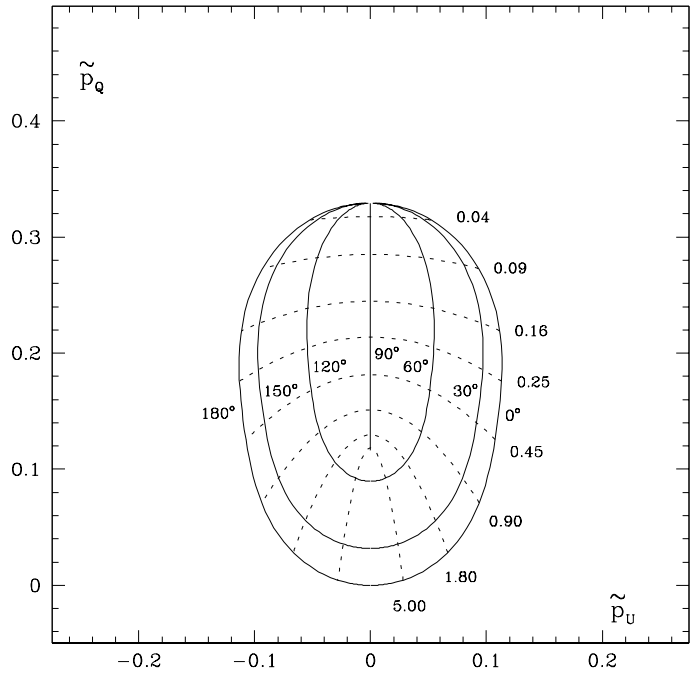

Fig.10.11. Same as Fig.10.8 for $\bar{n} = 0.5$ (intense irradiation of the model atom).

10.10. Three-Level Atoms: the Stepwise Excitation

For model atoms composed of more than two levels, the statistical equilibrium equations become more and more involved and depend on a growing number of physical parameters. However, according to the specific model atom and to the characteristics of the incoming radiation, it is sometimes possible to simplify considerably the problem. One of such cases, which can even be treated analytically, is illustrated in this section.

Consider the three-level model atom of Fig. 10.12, where, by assumption, transitions between levels a,b and between levels b,c are allowed, while the transition between levels a,c is forbidden. We assume the incident radiation field at each of the Bohr frequencies $\nu_{\rm ba}$, $\nu_{\rm cb}$ to be very diluted,

$$\bar{n}_{\rm ba} \ll 1 \,, \qquad \bar{n}_{\rm cb} \ll 1 \,, \tag{10.79}$$

where $\bar{n}_{\rm ba}$, $\bar{n}_{\rm cb}$ are the average numbers of photons per mode at frequencies $\nu_{\rm ba}$, $\nu_{\rm cb}$ respectively. This situation is often referred to as *stepwise excitation*. For simplicity, we assume that there is no magnetic field and we neglect inelastic and superelastic collisions, while we retain depolarizing collisions.

An order-of-magnitude estimate shows that the statistical tensors of levels a, b, c are of order

$$1 \,, \qquad \bar{n}_{\rm ba} \,, \qquad \bar{n}_{\rm ba}\, \bar{n}_{\rm cb} \,,$$

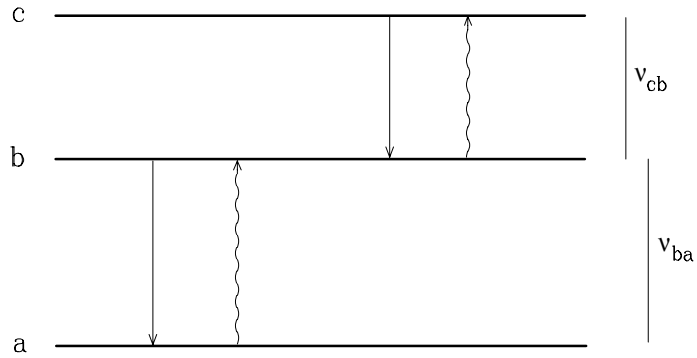

Fig.10.12. Three-level model atom for stepwise excitation.

respectively. Let us consider the statistical equilibrium equation for the statistical tensors of the intermediate level (level b). From Eqs. (7.11) and (7.101) we have, using shorthand notations

$$\frac{\mathrm{d}}{\mathrm{d}t}\,\rho_{\mathrm{b}} = \mathbb{T}_{\mathrm{A}}\,\rho_{\mathrm{a}} + \left(\mathbb{T}_{\mathrm{E}} + \mathbb{T}_{\mathrm{S}}\right)\rho_{\mathrm{c}} - \left(\mathbb{R}_{\mathrm{A}} + \mathbb{R}_{\mathrm{E}} + \mathbb{R}_{\mathrm{S}}\right)\rho_{\mathrm{b}} - D\,\rho_{\mathrm{b}}\;. \tag{10.80}$$

The order of magnitude of the different terms is the following (see Eqs. (7.14) and (10.62))

$$\begin{aligned}
&\mathbb{T}_{\mathrm{A}}\,\rho_{\mathrm{a}} \approx A_{\mathrm{ba}}\,\bar{n}_{\mathrm{ba}} && \mathbb{R}_{\mathrm{A}}\,\rho_{\mathrm{b}} \approx A_{\mathrm{cb}}\,\bar{n}_{\mathrm{ba}}\,\bar{n}_{\mathrm{cb}} \\
&\mathbb{T}_{\mathrm{E}}\,\rho_{\mathrm{c}} \approx A_{\mathrm{cb}}\,\bar{n}_{\mathrm{ba}}\,\bar{n}_{\mathrm{cb}} && \mathbb{R}_{\mathrm{E}}\,\rho_{\mathrm{b}} \approx A_{\mathrm{ba}}\,\bar{n}_{\mathrm{ba}} \\
&\mathbb{T}_{\mathrm{S}}\,\rho_{\mathrm{c}} \approx A_{\mathrm{cb}}\,\bar{n}_{\mathrm{ba}}\,\bar{n}^2_{\mathrm{cb}} && \mathbb{R}_{\mathrm{S}}\,\rho_{\mathrm{b}} \approx A_{\mathrm{ba}}\,\bar{n}^2_{\mathrm{ba}} \qquad D\,\rho_{\mathrm{b}} \approx D\,\bar{n}_{\mathrm{ba}}\;,
\end{aligned} \tag{10.81}$$

where A_{ba} and A_{cb} are the Einstein coefficients for spontaneous emission of the transitions (a,b) and (b,c), respectively. Equations (10.80)-(10.81) show that, to first order in the number of photons per mode, only the rates $\mathbb{T}_{\mathrm{A}}$, $\mathbb{R}_{\mathrm{E}}$ and D make a contribution to the time derivative of ρ_{b}: it follows that level b is only coupled with the lower level a.[1] The same reasoning shows that stimulated emission can be disregarded in both transitions (a,b) and (b,c). The three-level model atom considered can therefore be regarded as the combination of two 'superposed' two-level atoms. In stationary situations, the statistical tensors $\rho^K_Q(\mathrm{b})$ are obtained as the solution to the statistical equilibrium equations for the two-level atom (a,b). The statistical tensors $\rho^K_Q(\mathrm{c})$ are then obtained as the solution to the statistical equilibrium equations for the two-level atom (b,c), with $\rho^K_Q(\mathrm{b})$ known from the previous solution.

As an illustration, we consider a three-level model atom with $J_{\mathrm{a}} = 0$, $J_{\mathrm{b}} = 1$, $J_{\mathrm{c}} = 2$. We assume for simplicity that the incoming radiation (frequency-independent around the Bohr frequencies ν_{ba} and ν_{cb}) is unpolarized and cylindrically

[1] This approximation implies indeed the further condition $A_{\mathrm{cb}}\,\bar{n}_{\mathrm{cb}} \ll A_{\mathrm{ba}}$, which follows from Eq. (10.79) provided the order of magnitude of the two Einstein coefficients is the same.

symmetrical about a fixed direction: this implies, as shown in Sect. 10.7, that only the statistical tensors with K even and $Q = 0$ are non-zero. Following Eqs. (10.62), we introduce the anisotropy factors in the two lines

$$\frac{w_{\rm ba}}{\sqrt{2}} = \frac{J_0^2(\nu_{\rm ba})}{J_0^0(\nu_{\rm ba})} \,, \qquad \frac{w_{\rm cb}}{\sqrt{2}} = \frac{J_0^2(\nu_{\rm cb})}{J_0^0(\nu_{\rm cb})} \,.$$

In stationary situations, the statistical tensors of level b – considered as the upper level of the two-level atom (a, b) – are obtained from Eqs. (10.68)

$$\frac{\rho_0^2(\alpha_{\rm b} J_{\rm b})}{\rho_0^0(\alpha_{\rm b} J_{\rm b})} = \frac{w_{\rm ba}}{\sqrt{2}\,\big(1 + \delta_{\rm b}^{(2)}\big)} \,, \qquad \frac{\rho_0^0(\alpha_{\rm b} J_{\rm b})}{\rho_0^0(\alpha_{\rm a} J_{\rm a})} = \sqrt{3}\ \bar{n}_{\rm ba} \,, \tag{10.82}$$

where we have used the value $w_{10}^{(2)} = 1$ given by Table 10.1 and where, according to Eqs. (10.62)

$$\delta_{\rm b}^{(2)} = \frac{D^{(2)}(\alpha_{\rm b} J_{\rm b})}{A_{\rm ba}} \,.$$

The statistical equilibrium equations for level c – considered as the upper level of the two-level atom (b, c) – are given by the first of Eqs. (10.60). Using Eqs. (10.61) and (10.62) we obtain, after some algebra

$$\begin{aligned}
\frac{1}{A_{\rm cb}}\,\frac{\mathrm{d}}{\mathrm{d}t}\,\rho_0^0(\alpha_{\rm c} J_{\rm c}) &= -\,\rho_0^0(\alpha_{\rm c} J_{\rm c}) + \sqrt{\frac{5}{3}}\,\bar{n}_{\rm cb}\,\rho_0^0(\alpha_{\rm b} J_{\rm b}) + \frac{1}{2\sqrt{30}}\,\bar{n}_{\rm cb} w_{\rm cb}\,\rho_0^2(\alpha_{\rm b} J_{\rm b}) \\
\frac{1}{A_{\rm cb}}\,\frac{\mathrm{d}}{\mathrm{d}t}\,\rho_0^2(\alpha_{\rm c} J_{\rm c}) &= -\,\Big[1 + \delta_{\rm c}^{(2)}\Big]\,\rho_0^2(\alpha_{\rm c} J_{\rm c}) + \frac{1}{2}\sqrt{\frac{7}{6}}\,\bar{n}_{\rm cb} w_{\rm cb}\,\rho_0^0(\alpha_{\rm b} J_{\rm b}) \\
&\qquad + \frac{1}{2}\sqrt{\frac{7}{3}}\,\bar{n}_{\rm cb}\,\Big[1 + \frac{1}{7}\,w_{\rm cb}\Big]\,\rho_0^2(\alpha_{\rm b} J_{\rm b}) \\
\frac{1}{A_{\rm cb}}\,\frac{\mathrm{d}}{\mathrm{d}t}\,\rho_0^4(\alpha_{\rm c} J_{\rm c}) &= -\,\Big[1 + \delta_{\rm c}^{(4)}\Big]\,\rho_0^4(\alpha_{\rm c} J_{\rm c}) + 3\sqrt{\frac{3}{35}}\,\bar{n}_{\rm cb} w_{\rm cb}\,\rho_0^2(\alpha_{\rm b} J_{\rm b}) \,,
\end{aligned}$$

where

$$\delta_{\rm c}^{(K)} = \frac{D^{(K)}(\alpha_{\rm c} J_{\rm c})}{A_{\rm cb}} \,.$$

In stationary situations, eliminating $\rho_0^0(\alpha_{\rm b} J_{\rm b})$ and $\rho_0^2(\alpha_{\rm b} J_{\rm b})$ via Eqs. (10.82), one finally gets

$$\begin{aligned}
\sigma_0^2(\alpha_{\rm c} J_{\rm c}) &= \frac{1}{2}\sqrt{\frac{7}{10}}\ \frac{w_{\rm cb}\big[1 + \delta_{\rm b}^{(2)}\big] + w_{\rm ba}\big[1 + \frac{1}{7}\,w_{\rm cb}\big]}{1 + \delta_{\rm b}^{(2)} + \frac{1}{20}\,w_{\rm cb}\,w_{\rm ba}}\ \frac{1}{1 + \delta_{\rm c}^{(2)}} \\
\sigma_0^4(\alpha_{\rm c} J_{\rm c}) &= \frac{9}{5\sqrt{14}}\ \frac{w_{\rm cb}\,w_{\rm ba}}{1 + \delta_{\rm b}^{(2)} + \frac{1}{20}\,w_{\rm cb}\,w_{\rm ba}}\ \frac{1}{1 + \delta_{\rm c}^{(4)}} \\
\frac{\rho_0^0(\alpha_{\rm c} J_{\rm c})}{\rho_0^0(\alpha_{\rm a} J_{\rm a})} &= \sqrt{5}\ \bar{n}_{\rm cb}\,\bar{n}_{\rm ba}\Big[1 + \frac{1}{20}\,\frac{w_{\rm cb}\,w_{\rm ba}}{1 + \delta_{\rm b}^{(2)}}\Big] \,.
\end{aligned} \tag{10.83}$$

These expressions show that the amount of atomic polarization of level c depends on the anisotropy factors in both transitions and on the depolarizing rates of levels b and c, while it is independent of the intensity of the radiation field in either transition (this is due to the basic characteristics of stepwise excitation $\bar{n}_{\rm ba}$, $\bar{n}_{\rm cb} \ll 1$, $A_{\rm cb}\,\bar{n}_{\rm cb} \ll A_{\rm ba}$). Note that $\sigma^2_0(\alpha_{\rm c} J_{\rm c})$ – contrary to $\sigma^4_0(\alpha_{\rm c} J_{\rm c})$ – is non-zero even if the radiation field at the frequency $\nu_{\rm cb}$ of the upper transition is isotropic ($w_{\rm cb} = 0$).

In the extreme case of maximum anisotropy ($w_{\rm ba} = w_{\rm cb} = 1$) and no depolarizing collisions ($\delta^{(2)}_{\rm b} = \delta^{(2)}_{\rm c} = \delta^{(4)}_{\rm c} = 0$), Eqs. (10.83) give

$$\sigma^2_0(\alpha_{\rm c} J_{\rm c}) = \frac{5}{7}\sqrt{\frac{10}{7}}\,, \qquad \sigma^4_0(\alpha_{\rm c} J_{\rm c}) = \frac{6}{7}\sqrt{\frac{2}{7}}\,. \tag{10.84}$$

The populations of the Zeeman sublevels of level c can be found by substituting Eqs. (10.84) into Eq. (3.99). The relative populations turn out to be 3/7 ($M_{\rm c} = \pm 2$), 1/7 ($M_{\rm c} = 0$), and 0 ($M_{\rm c} = \pm 1$). This result is easily understood if we recall that for $w = 1$ only transitions with $\Delta M = \pm 1$ can be excited by the incident radiation (cf. footnote on p. 540). Since $w_{\rm ba} = 1$, in level b only the sublevels $M_{\rm b} = \pm 1$ are populated;[1] and since $w_{\rm cb} = 1$, in level c only the sublevels $M_{\rm c} = 0, \pm 2$ are populated. The relative populations are determined by the strength of the Zeeman transitions. As the transition from the (lower) sublevel $M_{\rm b} = 1$ to the (upper) sublevel $M_{\rm c} = 2$ is six times stronger than the transition from $M_{\rm b} = 1$ to $M_{\rm c} = 0$ (see Eq. (3.16)), the above result is straightforward.

The fractional polarization of the radiation emitted in the upper transition at 90° from the symmetry axis of the radiation field is obtained by substituting the value of $\sigma^2_0(\alpha_{\rm c} J_{\rm c})$ into Eq. (10.69). In particular, for the maximum anisotropy, collisionless case we get, with the help of Eqs. (10.84) and Table 10.1

$$p_Q \simeq 0.652\,.$$

This figure can be compared with the value 0.448, corresponding to the two-level atom ($J_\ell = 1, J_u = 2$), and with the value 0.288 corresponding to the same model atom with unpolarized lower level (see Table 10.3). The basic result of stepwise excitation for the three-level atom considered is to increase the polarization of the radiation scattered in the upper transition.

10.11. Three-Level Atoms: the Raman Effect

Another special case of three-level model atom leading to simple and interesting results is illustrated in Fig. 10.13. There are two 'lower' levels, a and b, but absorption processes can only take place between one of them (say, level a) and the upper level c. Level c can then decay to both levels a and b, giving rise to resonance

[1] This is consistent with the value $\sigma^2_0(\alpha_{\rm b} J_{\rm b}) = 1/\sqrt{2}$ deduced from Eqs. (10.82) for $w_{\rm ba} = 1$ and $\delta^{(2)}_{\rm b} = 0$. According to Table 3.6, such value means that the sublevel $M_{\rm b} = 0$ is depopulated.

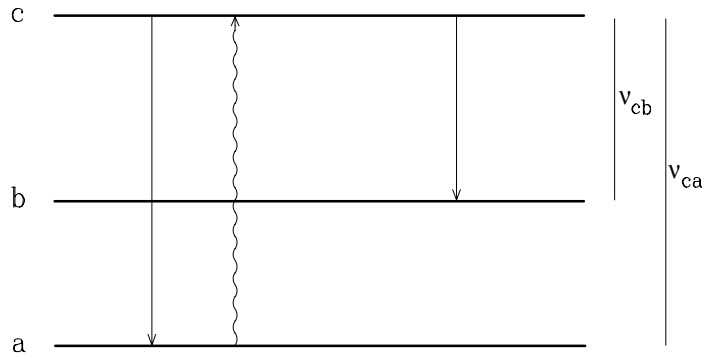

Fig.10.13. Three-level model atom for Raman scattering.

scattering radiation and to Raman scattering radiation, respectively. In practice, the atom is pumped at frequency $\nu_{\rm ca}$ and two lines are scattered, at frequencies $\nu_{\rm ca}$ and $\nu_{\rm cb}$ respectively. The Raman line (at frequency $\nu_{\rm cb}$) is called a *Stokes line* if $\nu_{\rm cb} < \nu_{\rm ca}$ or an *anti-Stokes line* if $\nu_{\rm cb} > \nu_{\rm ca}$.

It should be remarked that this phenomenon can be easily produced in the laboratory by selecting the spectral range of the pumping radiation. In astrophysical plasmas, the situation where level c is pumped by the radiation field in both lines at the same time is much more common.

The model atom of Fig. 10.13 can be handled at different levels of sophistication. Here we wish to deduce the main properties of Raman scattering under the simplest physical conditions. Thus we make the following assumptions: there is no magnetic field; the incoming radiation (frequency-independent about $\nu_{\rm ca}$) is sufficiently diluted to induce negligible stimulation effects; level a is unpolarized; the collisional rates in the statistical equilibrium equations for the upper level c can be neglected. Under these assumptions, we have from Eq. (7.11)

$$\frac{\mathrm{d}}{\mathrm{d}t}\,\rho^K_Q(\alpha_{\rm c}J_{\rm c}) = \mathbb{T}_{\rm A}(\alpha_{\rm c}J_{\rm c}KQ, \alpha_{\rm a}J_{\rm a}\,0\,0)\;\rho^0_0(\alpha_{\rm a}J_{\rm a}) - \sum_{K'Q'} \mathbb{R}_{\rm E}(\alpha_{\rm c}J_{\rm c}KQK'Q')\;\rho^{K'}_{Q'}(\alpha_{\rm c}J_{\rm c})\;.$$

In stationary situations we obtain, with the use of Eqs. (7.14e), (10.9) and (10.11)[1]

$$\rho^K_Q(\alpha_{\rm c}J_{\rm c}) = \sqrt{\frac{2J_{\rm a}+1}{2J_{\rm c}+1}}\;\frac{B(\alpha_{\rm a}J_{\rm a}\rightarrow\alpha_{\rm c}J_{\rm c})}{A(\alpha_{\rm c}J_{\rm c}\rightarrow\alpha_{\rm a}J_{\rm a})+A(\alpha_{\rm c}J_{\rm c}\rightarrow\alpha_{\rm b}J_{\rm b})}\;w^{(K)}_{J_{\rm c}J_{\rm a}} \times (-1)^Q\;J^K_{-Q}(\nu_{\rm ca})\;\rho^0_0(\alpha_{\rm a}J_{\rm a})\;. \qquad (10.85)$$

[1] Obviously, the schematic model of Fig. 10.13 is not self-consistent: in stationary situations, all the atoms would be in level b. Here it is understood that level b is coupled (for instance collisionally) to level a.

The emission coefficient in the Raman line is given by Eq. (10.15), which now reads

$$\varepsilon_i(\nu,\vec{\Omega}) = \frac{h\nu}{4\pi}\mathcal{N}\,\sqrt{2J_\mathrm{c}+1}\;A(\alpha_\mathrm{c}J_\mathrm{c}\rightarrow\alpha_\mathrm{b}J_\mathrm{b}) \\ \times\sum_{KQ} w^{(K)}_{J_\mathrm{c}J_\mathrm{b}}\;\mathcal{T}^K_Q(i,\vec{\Omega})\;\rho^K_Q(\alpha_\mathrm{c}J_\mathrm{c})\;\phi(\nu_\mathrm{cb}-\nu)\;. \tag{10.86}$$

Substitution of Eq. (10.85) into Eq. (10.86) yields, with the help of Eq. (10.6)

$$\varepsilon_i(\nu,\vec{\Omega}) = \frac{h\nu}{4\pi}\mathcal{N}_\mathrm{a}\;B(\alpha_\mathrm{a}J_\mathrm{a}\rightarrow\alpha_\mathrm{c}J_\mathrm{c})\;b_\mathrm{r}\;\phi(\nu_\mathrm{cb}-\nu) \\ \times\sum_{KQ} W_K(J_\mathrm{a},J_\mathrm{c},J_\mathrm{b})\;(-1)^Q\;\mathcal{T}^K_Q(i,\vec{\Omega})\;J^K_{-Q}(\nu_\mathrm{ca})\;, \tag{10.87}$$

where $\mathcal{N}_\mathrm{a}$ is the overall population of level a, b_r is the branching ratio

$$b_\mathrm{r} = \frac{A(\alpha_\mathrm{c}J_\mathrm{c}\rightarrow\alpha_\mathrm{b}J_\mathrm{b})}{A(\alpha_\mathrm{c}J_\mathrm{c}\rightarrow\alpha_\mathrm{a}J_\mathrm{a})+A(\alpha_\mathrm{c}J_\mathrm{c}\rightarrow\alpha_\mathrm{b}J_\mathrm{b})}\;,$$

and the new symbol $W_K(J_\ell,J_u,J'_\ell)$ is defined by (see Eq. (10.11))[1]

$$W_K(J_\ell,J_u,J'_\ell) = w^{(K)}_{J_uJ_\ell}\;w^{(K)}_{J_uJ'_\ell} \\ = (-1)^{J_\ell-J'_\ell}\;3(2J_u+1)\begin{Bmatrix}1 & 1 & K\\ J_u & J_u & J_\ell\end{Bmatrix}\begin{Bmatrix}1 & 1 & K\\ J_u & J_u & J'_\ell\end{Bmatrix}. \tag{10.88}$$

Comparison of Eqs. (10.87) and (10.16) shows that, apart from the obvious presence of the branching ratio and the frequency change of the emitted radiation, Raman scattering is described by an expression strictly similar to that for resonance scattering. The only difference is that the symbol $W_K(J_\ell,J_u)$ of resonance scattering is replaced by the symbol $W_K(J_\ell,J_u,J'_\ell)$. This difference is non-trivial because for certain combinations of the three J quantum numbers, $W_2(J_\ell,J_u,J'_\ell)$ turns out to be negative. In such cases, the direction of Raman scattering polarization produced by unpolarized incident radiation is parallel to the scattering plane (although the lower level a is by assumption unpolarized).[2]

Numerical values of the symbol $W_K(J_\ell,J_u,J'_\ell)$ can be obtained from Eq. (10.88) and Table 10.1. It is worth noticing that $w^{(2)}_{J_uJ_\ell}$ is negative for $J_\ell=J_u$ (except the special case $J_\ell=J_u=1/2$ for which $w^{(2)}_{J_uJ_\ell}=0$) and positive for $J_\ell\neq J_u$: therefore $W_2(J_\ell,J_u,J'_\ell)$ is negative when $J_\ell\neq J'_\ell$ and either $J_u=J_\ell$ or $J_u=J'_\ell$. From Eqs. (10.14) and (10.17) it follows that

$$W_0(J_\ell,J_u,J'_\ell)=1\;,\qquad W_K(J_\ell,J_u,J_\ell)=W_K(J_\ell,J_u)\;.$$

[1] The symbol $W_K(J_\ell,J_u,J'_\ell)$ was first introduced by Landi Degl'Innocenti (1984).

[2] We recall that resonance scattering polarization, for unpolarized lower level and unpolarized incident radiation, is always perpendicular to the scattering plane (see Sect 10.2).

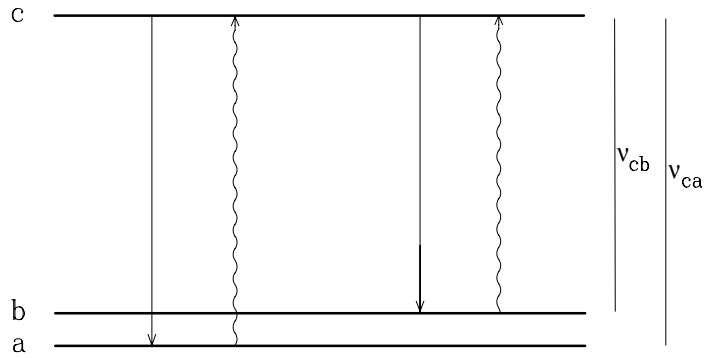

Fig.10.14. Three-level model atom leading to population inversion.

10.12. Three-Level Atoms: an Example Leading to Population Inversion

A particularly interesting three-level model atom is illustrated in Fig. 10.14. There are two lower levels (a and b), both connected to the upper level c by radiative transitions at the frequencies $\nu_{\rm ca}$ and $\nu_{\rm cb}$, respectively. The Einstein coefficient for the transition between a and b is assumed to be very small, so that such transition can be disregarded in the statistical equilibrium equations for levels a and b.

We study this model atom under the following set of assumptions: no magnetic field; no inelastic and superelastic collisions; the radiation field is frequency-independent about $\nu_{\rm ca}$ and $\nu_{\rm cb}$, although its intensity at the two frequencies may be different; it is unpolarized and cylindrically symmetrical about a fixed direction, although the amount of anisotropy at either frequency may be different; finally, it is sufficiently diluted to produce negligible stimulation effects. We recall from Sect. 10.7 that under such conditions, if we choose a reference system with the z-axis parallel to the symmetry axis of the radiation field, the only non-zero components of the radiation field tensor are J^0_0 and J^2_0, and that in stationary situations the only non-zero statistical tensors are those with K even and $Q = 0$.

The statistical equilibrium equations are easily deduced from Eqs. (7.11) and (7.101). With the help of Eqs. (7.14b,e) we obtain

$$\begin{aligned}\frac{\mathrm{d}}{\mathrm{d}t}\,\rho^K_0(\alpha_{\rm c}J_{\rm c}) = &-\Big[A(\alpha_{\rm c}J_{\rm c}\to\alpha_{\rm a}J_{\rm a})+A(\alpha_{\rm c}J_{\rm c}\to\alpha_{\rm b}J_{\rm b})+D^{(K)}(\alpha_{\rm c}J_{\rm c})\Big]\,\rho^K_0(\alpha_{\rm c}J_{\rm c})\\ &+\sum_{K'\,\text{even}}\mathbb{T}_{\rm A}(\alpha_{\rm c}J_{\rm c}K\,0,\alpha_{\rm a}J_{\rm a}K'\,0)\;\rho^{K'}_0(\alpha_{\rm a}J_{\rm a})\\ &+\sum_{K'\,\text{even}}\mathbb{T}_{\rm A}(\alpha_{\rm c}J_{\rm c}K\,0,\alpha_{\rm b}J_{\rm b}K'\,0)\;\rho^{K'}_0(\alpha_{\rm b}J_{\rm b})\end{aligned}$$

$$\begin{aligned}\frac{\mathrm{d}}{\mathrm{d}t}\,\rho^K_0(\alpha_{\rm a}J_{\rm a}) = &\,(-1)^{1+J_{\rm a}+J_{\rm c}}\,(2J_{\rm c}+1)\,A(\alpha_{\rm c}J_{\rm c}\to\alpha_{\rm a}J_{\rm a})\begin{Bmatrix}J_{\rm c}&J_{\rm c}&K\\J_{\rm a}&J_{\rm a}&1\end{Bmatrix}\rho^K_0(\alpha_{\rm c}J_{\rm c})\\ &-\sum_{K'\,\text{even}}\Big[\mathbb{R}_{\rm A}(\alpha_{\rm a}J_{\rm a}K\,0\,K'\,0)+\delta_{KK'}\,D^{(K)}(\alpha_{\rm a}J_{\rm a})\Big]\,\rho^{K'}_0(\alpha_{\rm a}J_{\rm a})\;,\end{aligned}$$

where K is even and where the rates $\mathbb{T}_{\rm A}$ and $\mathbb{R}_{\rm A}$ are given by Eqs. (10.61); the equation for $\mathrm{d}\rho_0^K(\alpha_{\rm b}J_{\rm b})/\mathrm{d}t$ is the same as that for $\mathrm{d}\rho_0^K(\alpha_{\rm a}J_{\rm a})/\mathrm{d}t$ with the substitutions $\alpha_{\rm a}\to\alpha_{\rm b}$, $J_{\rm a}\to J_{\rm b}$.

We wish to illustrate the typical results arising from the solution of the statistical equilibrium equations on a particularly simple example. Assuming $J_{\rm a}=1/2$, $J_{\rm b}=3/2$, $J_{\rm c}=1/2$, the atom is described by the four statistical tensors $\rho_0^0(J_{\rm a})$, $\rho_0^0(J_{\rm b})$, $\rho_0^2(J_{\rm b})$, $\rho_0^0(J_{\rm c})$. After some algebra we obtain the following equations

$$\frac{1}{A(\alpha_{\rm c}J_{\rm c}\to\alpha_{\rm a}J_{\rm a})}\,\frac{\mathrm{d}}{\mathrm{d}t}\,\rho_0^0(\alpha_{\rm a}J_{\rm a})=\rho_0^0(\alpha_{\rm c}J_{\rm c})-\bar{n}_{\rm ca}\,\rho_0^0(\alpha_{\rm a}J_{\rm a})$$

$$\frac{1}{A(\alpha_{\rm c}J_{\rm c}\to\alpha_{\rm b}J_{\rm b})}\,\frac{\mathrm{d}}{\mathrm{d}t}\,\rho_0^0(\alpha_{\rm b}J_{\rm b})=\frac{1}{\sqrt{2}}\,\rho_0^0(\alpha_{\rm c}J_{\rm c})-\frac{1}{2}\,\bar{n}_{\rm cb}\,\rho_0^0(\alpha_{\rm b}J_{\rm b})$$
$$-\frac{1}{4}\,\bar{n}_{\rm cb}w_{\rm cb}\,\rho_0^2(\alpha_{\rm b}J_{\rm b})$$

$$\frac{1}{A(\alpha_{\rm c}J_{\rm c}\to\alpha_{\rm b}J_{\rm b})}\,\frac{\mathrm{d}}{\mathrm{d}t}\,\rho_0^2(\alpha_{\rm b}J_{\rm b})=-\frac{1}{4}\,\bar{n}_{\rm cb}w_{\rm cb}\,\rho_0^0(\alpha_{\rm b}J_{\rm b})-\frac{1}{2}\,\bar{n}_{\rm cb}\left[1+\delta_{\rm b}^{(2)}\right]\rho_0^2(\alpha_{\rm b}J_{\rm b})\,,$$

where, according to Eqs. (10.62) and (10.63), we have introduced the anisotropy factor

$$\frac{w_{\rm cb}}{\sqrt{2}}=\frac{J_0^2(\nu_{\rm cb})}{J_0^0(\nu_{\rm cb})}\,,$$

the average numbers of photons per mode (much less than unity by assumption)

$$\bar{n}_{\rm ca}=\frac{B(\alpha_{\rm a}J_{\rm a}\to\alpha_{\rm c}J_{\rm c})}{A(\alpha_{\rm c}J_{\rm c}\to\alpha_{\rm a}J_{\rm a})}\,J_0^0(\nu_{\rm ca})\,,\qquad \bar{n}_{\rm cb}=2\,\frac{B(\alpha_{\rm b}J_{\rm b}\to\alpha_{\rm c}J_{\rm c})}{A(\alpha_{\rm c}J_{\rm c}\to\alpha_{\rm b}J_{\rm b})}\,J_0^0(\nu_{\rm cb})\,,$$

and the quantity

$$\delta_{\rm b}^{(2)}=2\,\frac{D^{(2)}(\alpha_{\rm b}J_{\rm b})}{\bar{n}_{\rm cb}\,A(\alpha_{\rm c}J_{\rm c}\to\alpha_{\rm b}J_{\rm b})}\,.$$

In stationary situations, the solution to these equations can be written in the form

$$\frac{\rho_0^0(\alpha_{\rm b}J_{\rm b})}{\rho_0^0(\alpha_{\rm a}J_{\rm a})}=\frac{4\sqrt{2}\,\left(1+\delta_{\rm b}^{(2)}\right)}{4\left(1+\delta_{\rm b}^{(2)}\right)-w_{\rm cb}^2}\,\frac{\bar{n}_{\rm ca}}{\bar{n}_{\rm cb}} \tag{10.89a}$$

$$\sigma_0^2(\alpha_{\rm b}J_{\rm b})=-\frac{w_{\rm cb}}{2\left(1+\delta_{\rm b}^{(2)}\right)} \tag{10.89b}$$

$$\frac{\rho_0^0(\alpha_{\rm c}J_{\rm c})}{\rho_0^0(\alpha_{\rm a}J_{\rm a})}=\bar{n}_{\rm ca}\,. \tag{10.89c}$$

These expressions are very interesting since they predict that, depending on the physical situation, different 'kinds' of population inversion between the lower levels a and b may occur.

From Eqs. (10.89a) and (3.108), the ratio of the overall populations of levels a and b is given by

$$\frac{n_{\alpha_{\rm b}J_{\rm b}}}{n_{\alpha_{\rm a}J_{\rm a}}}=\frac{8\left(1+\delta_{\rm b}^{(2)}\right)}{4\left(1+\delta_{\rm b}^{(2)}\right)-w_{\rm cb}^2}\,\frac{\bar{n}_{\rm ca}}{\bar{n}_{\rm cb}}\,. \tag{10.90}$$

If the incident radiation is isotropic ($w_{\rm cb} = 0$), the populations of the two levels are proportional to the corresponding statistical weights when $\bar{n}_{\rm ca} = \bar{n}_{\rm cb}$,

$$\frac{n_{\alpha_{\rm b} J_{\rm b}}}{n_{\alpha_{\rm a} J_{\rm a}}} = 2 \; ;$$

for $\bar{n}_{\rm ca} > \bar{n}_{\rm cb}$ there is an overall population inversion.

However, in astrophysical situations $\bar{n}_{\rm ca}$ is usually smaller than $\bar{n}_{\rm cb}$. Consider for instance the case where the atom is irradiated, within a solid angle Ω, by a black-body radiation at temperature T. In that case we have

$$\bar{n}_{\rm ca} = \frac{\Omega}{4\pi} \; {\rm e}^{-\frac{h\nu_{\rm ca}}{k_{\rm B} T}} \; , \qquad \bar{n}_{\rm cb} = \frac{\Omega}{4\pi} \; {\rm e}^{-\frac{h\nu_{\rm cb}}{k_{\rm B} T}} \; ,$$

where the Wien limit has been taken consistently with the assumption of neglecting stimulated emission in the radiative rates. Thus

$$\frac{\bar{n}_{\rm ca}}{\bar{n}_{\rm cb}} = {\rm e}^{-\frac{h\nu_{\rm ba}}{k_{\rm B} T}} \; ,$$

or

$$\frac{\bar{n}_{\rm ca}}{\bar{n}_{\rm cb}} \approx 1 - \frac{h\nu_{\rm ba}}{k_{\rm B} T}$$

when the energy difference between levels a and b is very small.

On the other hand, Eq. (10.90) shows that, in the presence of anisotropic incident radiation ($w_{\rm cb} > 0$), population inversion between levels a and b can take place even if $\bar{n}_{\rm ca} < \bar{n}_{\rm cb}$. This occurs when

$$w_{\rm cb} > 2 \sqrt{\left(1 + \delta_{\rm b}^{(2)}\right) \left(1 - \frac{\bar{n}_{\rm ca}}{\bar{n}_{\rm cb}}\right)} \; .$$

In a low-density medium where depolarizing collisions are negligible, this condition becomes

$$w_{\rm cb} > 2 \sqrt{\frac{h\nu_{\rm ba}}{k_{\rm B} T}} \; , \tag{10.91}$$

which shows that a weak anisotropy of the incident radiation can easily induce population inversion of levels a and b, provided the two levels are sufficiently close in energy.

It is interesting to consider the relative populations of the Zeeman sublevels of levels a and b for given values of $w_{\rm cb}$, $\delta_{\rm b}^{(2)}$ and $\bar{n}_{\rm ca}/\bar{n}_{\rm cb}$. From Eqs. (3.99) and (10.89a,b) we obtain

$$\begin{aligned}
\frac{\rho(\alpha_{\rm b} J_{\rm b}, M_{\rm b} = \pm 1/2)}{\rho(\alpha_{\rm a} J_{\rm a}, M_{\rm a} = \pm 1/2)} &= \left[1 + \frac{w_{\rm cb}}{2\left(1 + \delta_{\rm b}^{(2)}\right)}\right] \frac{4\left(1 + \delta_{\rm b}^{(2)}\right)}{4\left(1 + \delta_{\rm b}^{(2)}\right) - w_{\rm cb}^2} \; \frac{\bar{n}_{\rm ca}}{\bar{n}_{\rm cb}} \\
\frac{\rho(\alpha_{\rm b} J_{\rm b}, M_{\rm b} = \pm 3/2)}{\rho(\alpha_{\rm a} J_{\rm a}, M_{\rm a} = \pm 1/2)} &= \left[1 - \frac{w_{\rm cb}}{2\left(1 + \delta_{\rm b}^{(2)}\right)}\right] \frac{4\left(1 + \delta_{\rm b}^{(2)}\right)}{4\left(1 + \delta_{\rm b}^{(2)}\right) - w_{\rm cb}^2} \; \frac{\bar{n}_{\rm ca}}{\bar{n}_{\rm cb}} \; .
\end{aligned} \tag{10.92}$$

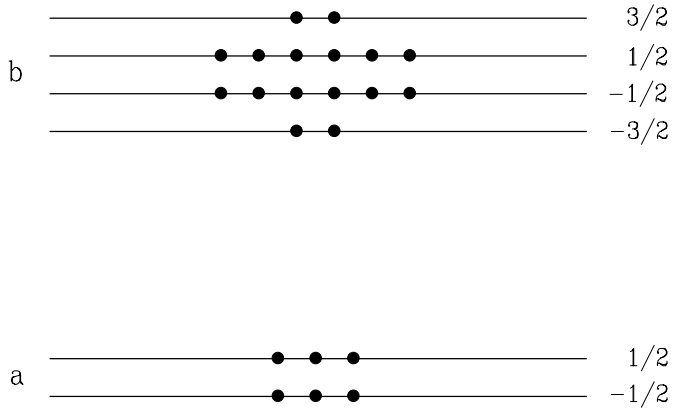

Fig.10.15. The Zeeman sublevels (artificially split) corresponding to levels a and b of the model atom of Fig.10.14, for $J_{\rm a} = 1/2$, $J_{\rm b} = 3/2$, $J_{\rm c} = 1/2$. Under the conditions specified in the text, their populations are proportional to the number of dots drawn on each of them.

In the extreme case $w_{\rm cb} = 1,\ \delta_{\rm b}^{(2)} = 0,\ \bar{n}_{\rm ca} = \bar{n}_{\rm cb}$ we have

$$\frac{\rho(\alpha_{\rm a} J_{\rm a}, M_{\rm a} = \pm 1/2)}{3} = \frac{\rho(\alpha_{\rm b} J_{\rm b}, M_{\rm b} = \pm 1/2)}{6} = \frac{\rho(\alpha_{\rm b} J_{\rm b}, M_{\rm b} = \pm 3/2)}{2} \ .$$

A pictorial representation of this situation is given in Fig. 10.15, which clearly shows that, in this case, it is more appropriate to speak about *selective* population inversion rather than population inversion tout court. In fact, the sublevels $M_{\rm b} = \pm 1/2$ of level b are overpopulated compared to those of the lower level a, while the sublevels $M_{\rm b} = \pm 3/2$ are not.

In the case illustrated in Fig. 10.15, selective population inversion occurs together with an overall population inversion of levels a and b ($n_{\alpha_{\rm b} J_{\rm b}} / n_{\alpha_{\rm a} J_{\rm a}} = 8/3 > 2$). However, under suitable physical conditions, it is possible to have selective population inversion without overall population inversion. According to Eqs. (10.92) and (10.90), this occurs when

$$\sqrt{\left(\frac{\bar{n}_{\rm ca}}{\bar{n}_{\rm cb}}\right)^2 + 4\left(1 + \delta_{\rm b}^{(2)}\right)\left(1 - \frac{\bar{n}_{\rm ca}}{\bar{n}_{\rm cb}}\right)} - \frac{\bar{n}_{\rm ca}}{\bar{n}_{\rm cb}} < w_{\rm cb} < 2\sqrt{\left(1 + \delta_{\rm b}^{(2)}\right)\left(1 - \frac{\bar{n}_{\rm ca}}{\bar{n}_{\rm cb}}\right)} \ ,$$

which for low-density media ($\delta_{\rm b}^{(2)} = 0$) reduces to (cf. Eq. (10.91))

$$2\,\frac{h\nu_{\rm ba}}{k_{\rm B} T} < w_{\rm cb} < 2\sqrt{\frac{h\nu_{\rm ba}}{k_{\rm B} T}} \ .$$

The presence of selective population inversion may have important consequences on the polarization of the radiation, which can be amplified through maser action in the transition between levels a and b.

The mechanism for selective population inversion described in this section is very robust. Inspection of Eqs. (10.89a,b) shows that, if depolarizing collisions

are negligible, the results are independent of the values of the Einstein coefficients of the transitions connecting the lower levels a,b with the upper level c. Under the same condition, the results are not affected by the radiation intensity at the individual frequencies $\nu_{\rm ca}$ and $\nu_{\rm cb}$, they only depend on their ratio. It follows that, provided this ratio is not too far from unity, selective population inversion can take place irrespective of the distance between the atom and the radiating source.

It should be remarked that selective population inversion (without overall population inversion) can easily arise also in the 'inverted' three-level model atom having $J_{\rm a} = 3/2$, $J_{\rm b} = 1/2$, $J_{\rm c} = 1/2$. In the case of maximum anisotropy, neglecting depolarizing collisions and assuming $\bar{n}_{\rm ca}/\bar{n}_{\rm cb} = 1$, one obtains the same result as in Fig. 10.15 except for the exchanged energy position of the two levels. The sublevels $M = \pm 1/2$ of the (upper) level $J = 1/2$ show population inversion with respect to the levels $M = \pm 3/2$ of the (lower) level $J = 3/2$.

10.13. The Weak Anisotropy Approximation

In some environments of astrophysical interest, like for instance in stellar atmospheres, the anisotropy of the radiation field interacting with the atomic systems is rather weak. This means that the 'off-diagonal' components of the radiation field tensor are much smaller (in absolute value) than the mean intensity $J^0_0(\nu)$. In formulae, defining

$$s^K_Q(\nu) = \frac{J^K_Q(\nu)}{J^0_0(\nu)} \,, \tag{10.93}$$

we have

$$\left| s^K_Q(\nu) \right| \ll 1 \qquad (K = 1, 2) \tag{10.94}$$

at all frequencies of interest.

In this situation it is possible to simplify considerably the statistical equilibrium equations (written in the spherical statistical tensor representation) via a perturbative expansion. This can formally be obtained by multiplying the components $J^1_Q(\nu)$ and $J^2_Q(\nu)$ by the real parameter λ (which at the end of the calculations will be set to 1) and by expanding the statistical tensors as a function of λ. Referring for instance to the equations for the multi-level atom written in the 'magnetic' frame (Eq. (7.11) supplemented in the right-hand side with the collisional rates of Eq. (7.101)), we set

$$\rho^K_Q(\alpha J) = \sum_{n=0}^{\infty} \left[\rho^K_Q(\alpha J)\right]^{(n)} \lambda^n \,, \tag{10.95}$$

where $[\rho^K_Q(\alpha J)]^{(n)}$ is the n-th order contribution to the statistical tensor $\rho^K_Q(\alpha J)$. Substitution of Eq. (10.95) into the statistical equilibrium equations leads to an equality between two power series in λ. Since λ is arbitrary, the coefficients of each power must separately be equal.

To the lowest order, the radiative rates $\mathbb{T}_{\rm A}$, $\mathbb{T}_{\rm S}$, $\mathbb{R}_{\rm A}$, $\mathbb{R}_{\rm S}$ (the only rates connecting statistical tensors with different K, Q values) contain only the J^0_0 component of

the radiation field tensor. Bearing in mind their expressions (Eqs. (7.14)), it is easily seen that the statistical equilibrium equations split into separate systems of equations, each one involving statistical tensors with the same value for K and Q. Since the trace equation involves only populations (proportional to ρ^0_0), in stationary situations all the statistical tensors with $K \neq 0$ are zero. For $K = 0$ we obtain, with the use of Eqs. (7.14), (2.26a), (2.36a) and (2.49)

$$\begin{aligned}
\frac{\mathrm{d}}{\mathrm{d}t}\sqrt{2J+1}\left[\rho^0_0(\alpha J)\right]^{(0)} &= \sum_{\alpha_\ell J_\ell} B(\alpha_\ell J_\ell \rightarrow \alpha J)\, J^0_0(\nu_{\alpha J,\,\alpha_\ell J_\ell})\,\sqrt{2J_\ell+1}\,\left[\rho^0_0(\alpha_\ell J_\ell)\right]^{(0)} \\
&+ \sum_{\alpha_u J_u}\Big[A(\alpha_u J_u \rightarrow \alpha J) + B(\alpha_u J_u \rightarrow \alpha J)\, J^0_0(\nu_{\alpha_u J_u,\,\alpha J})\Big]\sqrt{2J_u+1}\,\left[\rho^0_0(\alpha_u J_u)\right]^{(0)} \\
&- \Big[\sum_{\alpha_u J_u} B(\alpha J \rightarrow \alpha_u J_u)\, J^0_0(\nu_{\alpha_u J_u,\,\alpha J}) + \sum_{\alpha_\ell J_\ell} A(\alpha J \rightarrow \alpha_\ell J_\ell) \\
&\qquad + \sum_{\alpha_\ell J_\ell} B(\alpha J \rightarrow \alpha_\ell J_\ell)\, J^0_0(\nu_{\alpha J,\,\alpha_\ell J_\ell})\Big]\sqrt{2J+1}\,\left[\rho^0_0(\alpha J)\right]^{(0)} \\
&+ \sum_{\alpha_\ell J_\ell} C^{(0)}_{\mathrm{I}}(\alpha J, \alpha_\ell J_\ell)\,\sqrt{2J_\ell+1}\,\left[\rho^0_0(\alpha_\ell J_\ell)\right]^{(0)} \\
&+ \sum_{\alpha_u J_u} C^{(0)}_{\mathrm{S}}(\alpha J, \alpha_u J_u)\,\sqrt{2J_u+1}\,\left[\rho^0_0(\alpha_u J_u)\right]^{(0)} \\
&- \Big[\sum_{\alpha_u J_u} C^{(0)}_{\mathrm{I}}(\alpha_u J_u, \alpha J) + \sum_{\alpha_\ell J_\ell} C^{(0)}_{\mathrm{S}}(\alpha_\ell J_\ell, \alpha J)\Big]\sqrt{2J+1}\,\left[\rho^0_0(\alpha J)\right]^{(0)}\,, \qquad (10.96)
\end{aligned}$$

and the trace equation reads (see Eqs. (3.84) and (3.108))

$$\sum_{\alpha J}\left[n_{\alpha J}\right]^{(0)} = \sum_{\alpha J}\sqrt{2J+1}\,\left[\rho^0_0(\alpha J)\right]^{(0)} = 1\,.$$

Thus the zero-order equations coincide with the usual statistical equilibrium equations for the level populations of the scalar (unpolarized) case – see e.g. Mihalas, 1978).

Passing to the first order, it is convenient to consider separately the equations for $\mathrm{d}\left[\rho^0_0(\alpha J)\right]^{(1)}/\mathrm{d}t$ and for $\mathrm{d}\left[\rho^K_Q(\alpha J)\right]^{(1)}/\mathrm{d}t$ with $K \neq 0$. The former turn out to be formally identical to Eqs. (10.96), but the trace equation is now

$$\sum_{\alpha J}\sqrt{2J+1}\,\left[\rho^0_0(\alpha J)\right]^{(1)} = 0\,.$$

This means that, in stationary situations, the first-order correction to $\rho^0_0(\alpha J)$ is identically zero. For $K \neq 0$ we obtain, using again Eqs. (7.14), (2.26a), (2.36a) and (2.49)

$$
\begin{aligned}
\frac{\mathrm{d}}{\mathrm{d}t}\left[\rho_Q^K(\alpha J)\right]^{(1)} &= -2\pi\mathrm{i}\,\nu_{\mathrm{L}}\,g_{\alpha J}\,Q\left[\rho_Q^K(\alpha J)\right]^{(1)} \\
&+ \sum_{\alpha_\ell J_\ell}\sqrt{\frac{2J_\ell+1}{2J+1}}\,B(\alpha_\ell J_\ell\to\alpha J)\Big\{\,y_{JJ_\ell}^{(K)}\,J_0^0(\nu_{\alpha J,\,\alpha_\ell J_\ell})\left[\rho_Q^K(\alpha_\ell J_\ell)\right]^{(1)} \\
&\qquad\qquad + w_{JJ_\ell}^{(K)}\,(-1)^Q\,J_{-Q}^K(\nu_{\alpha J,\,\alpha_\ell J_\ell})\left[\rho_0^0(\alpha_\ell J_\ell)\right]^{(0)}\Big\} \\
&+ \sum_{\alpha_u J_u}\sqrt{\frac{2J_u+1}{2J+1}}\,A(\alpha_u J_u\to\alpha J)\,y_{J_uJ}^{(K)}\left[\rho_Q^K(\alpha_u J_u)\right]^{(1)} \\
&+ \sum_{\alpha_u J_u}\sqrt{\frac{2J_u+1}{2J+1}}\,B(\alpha_u J_u\to\alpha J)\Big\{\,y_{JJ_u}^{(K)}\,J_0^0(\nu_{\alpha_u J_u,\,\alpha J})\left[\rho_Q^K(\alpha_u J_u)\right]^{(1)} \\
&\qquad\qquad + w_{JJ_u}^{(K)}\,(-1)^{K+Q}\,J_{-Q}^K(\nu_{\alpha_u J_u,\,\alpha J})\left[\rho_0^0(\alpha_u J_u)\right]^{(0)}\Big\} \\
&- \sum_{\alpha_u J_u} B(\alpha J\to\alpha_u J_u)\Big\{J_0^0(\nu_{\alpha_u J_u,\,\alpha J})\left[\rho_Q^K(\alpha J)\right]^{(1)} \\
&\qquad\qquad + w_{JJ_u}^{(K)}\,(-1)^{K+Q}\,J_{-Q}^K(\nu_{\alpha_u J_u,\,\alpha J})\left[\rho_0^0(\alpha J)\right]^{(0)}\Big\} \\
&- \sum_{\alpha_\ell J_\ell} A(\alpha J\to\alpha_\ell J_\ell)\left[\rho_Q^K(\alpha J)\right]^{(1)} \\
&- \sum_{\alpha_\ell J_\ell} B(\alpha J\to\alpha_\ell J_\ell)\Big\{J_0^0(\nu_{\alpha J,\,\alpha_\ell J_\ell})\left[\rho_Q^K(\alpha J)\right]^{(1)} \\
&\qquad\qquad + w_{JJ_\ell}^{(K)}\,(-1)^Q\,J_{-Q}^K(\nu_{\alpha J,\,\alpha_\ell J_\ell})\left[\rho_0^0(\alpha J)\right]^{(0)}\Big\} \\
&+ \sum_{\alpha_\ell J_\ell}\sqrt{\frac{2J_\ell+1}{2J+1}}\;C_{\mathrm{I}}^{(K)}(\alpha J,\alpha_\ell J_\ell)\left[\rho_Q^K(\alpha_\ell J_\ell)\right]^{(1)} \\
&+ \sum_{\alpha_u J_u}\sqrt{\frac{2J_u+1}{2J+1}}\;C_{\mathrm{S}}^{(K)}(\alpha J,\alpha_u J_u)\left[\rho_Q^K(\alpha_u J_u)\right]^{(1)} \\
&- \Big\{\sum_{\alpha_u J_u} C_{\mathrm{I}}^{(0)}(\alpha_u J_u,\alpha J)+\sum_{\alpha_\ell J_\ell} C_{\mathrm{S}}^{(0)}(\alpha_\ell J_\ell,\alpha J)+D^{(K)}(\alpha J)\Big\}\left[\rho_Q^K(\alpha J)\right]^{(1)}. \qquad (10.97)
\end{aligned}
$$

In this equation, the symbol $w_{JJ'}^{(K)}$ is defined as in Eq. (10.11),

$$
w_{JJ'}^{(K)} = (-1)^{1+J+J'}\sqrt{3(2J+1)}\begin{Bmatrix} 1 & 1 & K \\ J & J & J' \end{Bmatrix}, \qquad (10.98)
$$

while the symbol $y_{JJ'}^{(K)}$, invariant under interchange of J and J', is defined by

$$
y_{JJ'}^{(K)} = y_{J'J}^{(K)} = (-1)^{1+J+J'+K}\sqrt{(2J+1)(2J'+1)}\begin{Bmatrix} J' & J' & K \\ J & J & 1 \end{Bmatrix}, \qquad (10.99)
$$

or, using Eq. (2.36a)

$$y_{JJ'}^{(K)} = (-1)^K \frac{\begin{Bmatrix} J' & J' & K \\ J & J & 1 \end{Bmatrix}}{\begin{Bmatrix} J' & J' & 0 \\ J & J & 1 \end{Bmatrix}} ,$$

which shows that $y_{JJ'}^{(0)} = 1$.

Equation (10.97) has a very peculiar structure. In compact notation it can be written in the form

$$\frac{\mathrm{d}}{\mathrm{d}t} \left[\rho_Q^K(\alpha_i J_i)\right]^{(1)} = \sum_j a_{ij} \left[\rho_Q^K(\alpha_j J_j)\right]^{(1)} + \sum_j b_{ij} \left[\rho_0^0(\alpha_j J_j)\right]^{(0)} \qquad (K \neq 0) , \tag{10.100}$$

where the indices i and j run over all the atomic levels (excluding, obviously, those for which the multipole moment ρ_Q^K is undefined). The coefficients a_{ij} contain the contributions of the magnetic field, of collisions, and of the radiative rates: the last one, however, is restricted to terms involving the only component J_0^0 of the radiation field tensor (evaluated at the Bohr frequency connecting levels i and j). The coefficients b_{ij} contain only contributions of the radiative rates (absorption and stimulated emission) restricted to terms involving the components J_{-Q}^K of the radiation field tensor with $K \neq 0$.

The structure of Eq. (10.100) immediately suggests the method to solve (in stationary situations, and up to the first order) the statistical equilibrium equations under the weak anisotropy approximation. First, the values of $[\rho_0^0(\alpha_j J_j)]^{(0)}$ are obtained by solving Eq. (10.96) – the statistical equilibrium equations for the level populations. These values are then substituted into the right-hand side of Eq. (10.100) which reduces to an algebraic, inhomogeneous system in the unknowns $[\rho_Q^K(\alpha_i J_i)]^{(1)}$ with $K \neq 0$. The substantial simplification introduced by the weak anisotropy approximation is that this system is formed by a set of *uncoupled* subsystems, each characterized by its own K, Q values.

As apparent from the structure of Eq. (10.100), the solutions $[\rho_Q^K(\alpha_i J_i)]^{(1)}$ will be linear combinations of the multipole components J_{-Q}^K (evaluated at the different Bohr frequencies of the model atom considered) with the *same* K, Q values. An obvious consequence of this fact is that *in the weak anisotropy approximation only statistical tensors with* $K \leq 2$ *can be non-zero* (to first order).

10.14. The Two-Level Atom in the Weak Anisotropy Approximation

In this section we go back to the two-level model atom, already analyzed from several points of view, and we solve the statistical equilibrium equations under the assumption of weak anisotropy of the radiation field. Following the method outlined

in the former section, we will first determine (from the zero-order equations) the statistical tensors ρ^0_0, then (from the first-order equations) the statistical tensors ρ^K_Q with $K \neq 0$, both for the upper and the lower level.

From Eqs. (10.96) we obtain, in stationary situations

$$\frac{\rho^0_0(\alpha_u J_u)}{\rho^0_0(\alpha_\ell J_\ell)} = \sqrt{\frac{2J_\ell+1}{2J_u+1}} \times \frac{B(\alpha_\ell J_\ell \to \alpha_u J_u)\, J^0_0(\nu_0) + C^{(0)}_{\rm I}(\alpha_u J_u, \alpha_\ell J_\ell)}{A(\alpha_u J_u \to \alpha_\ell J_\ell) + B(\alpha_u J_u \to \alpha_\ell J_\ell)\, J^0_0(\nu_0) + C^{(0)}_{\rm S}(\alpha_\ell J_\ell, \alpha_u J_u)} ,$$

where ν_0 is the transition frequency and where, for conciseness, the index $^{(0)}$ of the statistical tensors has been omitted. This expression can be simplified by dividing numerator and denominator by the Einstein coefficient $A(\alpha_u J_u \to \alpha_\ell J_\ell)$. Using Eqs. (7.8) and the Einstein-Milne relation between inelastic and superelastic collisional rates (Eq. (7.98), valid for a Maxwellian distribution of velocities), we get

$$\frac{\rho^0_0(\alpha_u J_u)}{\rho^0_0(\alpha_\ell J_\ell)} = \sqrt{\frac{2J_u+1}{2J_\ell+1}}\ \frac{\bar{n} + \epsilon\, b(T_{\rm c})}{1+\bar{n}+\epsilon} , \qquad (10.101)$$

where the dimensionless parameters $\bar{n}$ and ϵ are given by Eqs. (10.62) and (10.51), respectively, and where $b(T_{\rm c})$ is the Boltzmann factor

$$b(T_{\rm c}) = {\rm e}^{-\frac{h\nu_0}{k_{\rm B} T_{\rm c}}} ,$$

with $T_{\rm c}$ the temperature characterizing the distribution of the colliding particles.

Next we write down Eq. (10.97) for the upper and lower atomic level, and we make use of Eq. (10.101). This leads, in stationary situations, to an algebraic system of two equations in the unknowns $[\rho^K_Q(\alpha_u J_u)]^{(1)}$ and $[\rho^K_Q(\alpha_\ell J_\ell)]^{(1)}$. Omitting the index $^{(1)}$ and introducing the reduced statistical tensors $\sigma^K_Q = \rho^K_Q/\rho^0_0$, the solution can be written in the compact form[1]

$$\sigma^K_Q(\alpha_u J_u) = \frac{\bar{n}\left[1+\epsilon-\epsilon\, b(T_{\rm c})\right]}{\bar{n}+\epsilon\, b(T_{\rm c})}\ \frac{1}{\Delta}\left\{ w^{(K)}_{J_u J_\ell}\left[\bar{n}\left(1+\delta^{(K)}_\ell + {\rm i}\, H_\ell\, Q\right) + \epsilon\, b(T_{\rm c})\right] - (-1)^K\, w^{(K)}_{J_\ell J_u}\ \bar{n}\left[\, y^{(K)}_{J_u J_\ell} + \epsilon^{(K)}_\ell\,\right]\right\} (-1)^Q\, s^K_{-Q}(\nu_0)$$

$$\sigma^K_Q(\alpha_\ell J_\ell) = \frac{\bar{n}\left[1+\epsilon-\epsilon\, b(T_{\rm c})\right]}{1+\bar{n}+\epsilon}\ \frac{1}{\Delta}\left\{ w^{(K)}_{J_u J_\ell}\left[\, y^{(K)}_{J_u J_\ell}\left(1+\bar{n}\right) + \epsilon^{(K)}_u\,\right] - (-1)^K\, w^{(K)}_{J_\ell J_u}\left[1+\bar{n}+\epsilon+\delta^{(K)}_u + {\rm i}\, H_u\, Q\right]\right\} (-1)^Q\, s^K_{-Q}(\nu_0) , \qquad (10.102)$$

[1] We recall that $y^{(K)}_{J_u J_\ell} = y^{(K)}_{J_\ell J_u}$ (see Eq. (10.99)).

where $K = 1, 2$ and

$$\Delta = \Big[1 + \bar{n} + \epsilon + \delta_u^{(K)} + \mathrm{i}\, H_u\, Q\Big] \Big[\, \bar{n}\, \big(1 + \delta_\ell^{(K)} + \mathrm{i}\, H_\ell\, Q\big) + \epsilon\, b(T_\mathrm{c})\Big] - \bar{n}\, \Big[\, y^{(K)}_{J_u J_\ell}\, \big(1 + \bar{n}\big) + \epsilon_u^{(K)}\, \Big] \Big[\, y^{(K)}_{J_u J_\ell} + \epsilon_\ell^{(K)}\, \Big]\ .$$

In these expressions, all the symbols denote dimensionless quantities: $s^K_Q(\nu_0)$ is defined in Eq. (10.93); $w^{(K)}_{JJ'}$ and $y^{(K)}_{JJ'}$ in Eqs. (10.98) and (10.99), respectively; H_u, $\delta_u^{(K)}$ and $\delta_\ell^{(K)}$ in Eqs. (10.28), (10.51) and (10.63), respectively. The remaining symbols are defined as follows

$$\epsilon_u^{(K)} = \frac{C_\mathrm{S}^{(K)}(\alpha_\ell J_\ell, \alpha_u J_u)}{A(\alpha_u J_u \to \alpha_\ell J_\ell)}$$

$$\epsilon_\ell^{(K)} = \frac{C_\mathrm{I}^{(K)}(\alpha_u J_u, \alpha_\ell J_\ell)}{B(\alpha_\ell J_\ell \to \alpha_u J_u)\ J_0^0(\nu_0)} = \frac{2J_\ell + 1}{2J_u + 1}\ \frac{C_\mathrm{I}^{(K)}(\alpha_u J_u, \alpha_\ell J_\ell)}{\bar{n}\ A(\alpha_u J_u \to \alpha_\ell J_\ell)}$$

$$H_\ell = \frac{2\pi\nu_\mathrm{L}\ g_{\alpha_\ell J_\ell}}{B(\alpha_\ell J_\ell \to \alpha_u J_u)\ J_0^0(\nu_0)} = \frac{2J_\ell + 1}{2J_u + 1}\ \frac{2\pi\nu_\mathrm{L}\ g_{\alpha_\ell J_\ell}}{\bar{n}\ A(\alpha_u J_u \to \alpha_\ell J_\ell)}\ . \qquad (10.103)$$

The physical meaning of these new quantities is immediate. $\epsilon_u^{(K)}$ represents the number of superelastic collisions (for the statistical tensors of rank K) taking place during the lifetime of the upper level and, similarly, $\epsilon_\ell^{(K)}$ the number of inelastic collisions (for the statistical tensors of rank K) taking place during the lifetime of the lower level; H_ℓ (the analogue of H_u) quantifies the efficiency of the relaxation process of the lower level due to the magnetic field. Note that the quantities $\epsilon_u^{(K)}$ and $\epsilon_\ell^{(K)}$ are related to ϵ by the expressions (see Eq. (10.49))

$$\epsilon_u^{(K)} = \frac{C_\mathrm{S}^{(K)}(\alpha_\ell J_\ell, \alpha_u J_u)}{C_\mathrm{S}^{(0)}(\alpha_\ell J_\ell, \alpha_u J_u)}\ \epsilon\ , \qquad \epsilon_\ell^{(K)} = \frac{C_\mathrm{I}^{(K)}(\alpha_u J_u, \alpha_\ell J_\ell)}{C_\mathrm{I}^{(0)}(\alpha_u J_u, \alpha_\ell J_\ell)}\ \frac{b(T_\mathrm{c})}{\bar{n}}\ \epsilon\ .$$

In the following we study in detail the solutions (10.101) and (10.102), considering separately the effects of depolarizing collisions, of the magnetic field and of stimulated emission, and pointing out the analogies (and differences) with previous results concerning the two-level model atom.

10.14.a No magnetic field - no collisions - no stimulated emission

This is the simplest case that can be considered. Setting ϵ, $\epsilon_u^{(K)}$, $\epsilon_\ell^{(K)}$, $\delta_u^{(K)}$, $\delta_\ell^{(K)}$, H_u and H_ℓ to zero, and assuming $\bar{n} \ll 1$, Eq. (10.101) reduces to

$$\frac{\rho^0_0(\alpha_u J_u)}{\rho^0_0(\alpha_\ell J_\ell)} = \sqrt{\frac{2J_u + 1}{2J_\ell + 1}}\ \bar{n}\ , \qquad (10.104)$$

and Eqs. (10.102) yield the remarkably symmetrical expressions

$$\sigma^K_Q(\alpha_u J_u) = x^{(K)}_{J_u J_\ell}\ \ (-1)^Q\, s^K_{-Q}(\nu_0)$$

$$\sigma^K_Q(\alpha_\ell J_\ell) = (-1)^{1+K}\ x^{(K)}_{J_\ell J_u}\ \ (-1)^Q\, s^K_{-Q}(\nu_0)\ , \qquad (10.105)$$

where the new symbol $x^{(K)}_{JJ'}$ is given by[1]

$$x^{(K)}_{JJ'} = \frac{w^{(K)}_{JJ'} - (-1)^K\, w^{(K)}_{J'J}\; y^{(K)}_{JJ'}}{1 - \left[\, y^{(K)}_{JJ'} \,\right]^2} = (-1)^{1+J+J'} \sqrt{3(2J+1)}$$

$$\times \frac{\left\{ \begin{array}{ccc} 1 & 1 & K \\ J & J & J' \end{array} \right\} + (-1)^{J+J'} (2J'+1) \left\{ \begin{array}{ccc} 1 & 1 & K \\ J' & J' & J \end{array} \right\} \left\{ \begin{array}{ccc} J & J & K \\ J' & J' & 1 \end{array} \right\}}{1 - (2J+1)(2J'+1) \left\{ \begin{array}{ccc} J & J & K \\ J' & J' & 1 \end{array} \right\}^2} . \quad (10.106)$$

Using Eqs. (10.104), (10.62) and (10.93), the first of Eqs. (10.105) can be rewritten in the form

$$\rho^K_Q(\alpha_u J_u) = \sqrt{\frac{2J_\ell + 1}{2J_u + 1}}\; \frac{B(\alpha_\ell J_\ell \rightarrow \alpha_u J_u)}{A(\alpha_u J_u \rightarrow \alpha_\ell J_\ell)}\; x^{(K)}_{J_u J_\ell}\; (-1)^Q\, J^K_{-Q}(\nu_0)\; \rho^0_0(\alpha_\ell J_\ell) \, .$$

This is identical with Eq. (10.13) except for the presence of the quantity $x^{(K)}_{J_u J_\ell}$ in the place of $w^{(K)}_{J_u J_\ell}$. It follows that for the two-level atom under the weak anisotropy approximation, resonance scattering is still described by Eq. (10.19), where the scattering phase matrix is now given by

$$P_{ij}(\vec{\Omega}, \vec{\Omega}') = \sum_{KQ} X_K(J_\ell, J_u)\; (-1)^Q\, \mathcal{T}^K_Q(i, \vec{\Omega})\, \mathcal{T}^K_{-Q}(j, \vec{\Omega}') \, , \quad (10.107)$$

with

$$X_K(J, J') = w^{(K)}_{J'J}\; x^{(K)}_{J'J} = 3(2J'+1)$$

$$\times \frac{\left\{ \begin{array}{ccc} 1 & 1 & K \\ J' & J' & J \end{array} \right\}^2 + (-1)^{J+J'} (2J+1) \left\{ \begin{array}{ccc} 1 & 1 & K \\ J' & J' & J \end{array} \right\} \left\{ \begin{array}{ccc} 1 & 1 & K \\ J & J & J' \end{array} \right\} \left\{ \begin{array}{ccc} J & J & K \\ J' & J' & 1 \end{array} \right\}}{1 - (2J+1)(2J'+1) \left\{ \begin{array}{ccc} J & J & K \\ J' & J' & 1 \end{array} \right\}^2}$$

for $K = 1, 2$, and

$$X_0(J, J') \equiv 1 \, . \quad (10.108)$$

Obviously, it should be kept in mind that the incident radiation field in the right-hand side of Eq. (10.19) has now to satisfy the weak anisotropy approximation described by Eq. (10.94). For instance, we cannot use Eq. (10.19) with the phase matrix of Eq. (10.107) to describe the scattering of a radiation *beam*, because the weak anisotropy approximation does not hold in that case.

[1] Note that for $K = 0$ the symbol is indeterminate (being of the form 0/0). This is not surprising, since Eqs. (10.105) are a special case of Eqs. (10.102), which hold for $K = 1, 2$. Equations (10.105) are correct also for $K = 0$ if we set by definition $x^{(0)}_{J_u J_\ell} = 1$ in the former and $x^{(0)}_{J_\ell J_u} = -1$ in the latter.

Numerical values of the symbols $y^{(K)}_{J'J}$, $x^{(K)}_{J'J}$ and $X_K(J,J')$ are given, for different transitions, in Table 10.4. Table 10.5 collects the analytical expressions of $X_1(J,J')$ and $X_2(J,J')$ obtained via Eqs. (2.36d) and (2.36h). Note that, contrary to the symbols W_1 and W_2, which satisfy the inequality $0 \leq W_K \leq 1$, the symbols X_1 and X_2 can be negative as well as larger than unity. In particular, X_2 is negative for all transitions having $J_u = J_\ell - 1$ (except $(J_\ell = 1, J_u = 0)$ and $(J_\ell = 3/2, J_u = 1/2)$ for which X_2 is zero). As illustrated at the end of Sect. 10.7, this is due to the presence of lower-level atomic polarization.

10.14.b No magnetic field - no inelastic collisions - no stimulated emission

Consider now the effect of depolarizing collisions. Neglecting inelastic and superelastic collisions ($\epsilon = \epsilon^{(K)}_u = \epsilon^{(K)}_\ell = 0$), the magnetic field ($H_u = H_\ell = 0$) and stimulated emission ($\bar{n} \ll 1$), Eq. (10.101) reduces again to Eq. (10.104), while Eqs. (10.102) take the form

$$\sigma^K_Q(\alpha_u J_u) = \frac{w^{(K)}_{J_u J_\ell}\left(1+\delta^{(K)}_\ell\right) - (-1)^K\, w^{(K)}_{J_\ell J_u}\; y^{(K)}_{J_u J_\ell}}{\left(1+\delta^{(K)}_u\right)\left(1+\delta^{(K)}_\ell\right) - \left[\, y^{(K)}_{J_u J_\ell}\,\right]^2}\; (-1)^Q\, s^K_{-Q}(\nu_0)$$

$$\sigma^K_Q(\alpha_\ell J_\ell) = (-1)^{1+K} \times \frac{w^{(K)}_{J_\ell J_u}\left(1+\delta^{(K)}_u\right) - (-1)^K\, w^{(K)}_{J_u J_\ell}\; y^{(K)}_{J_\ell J_u}}{\left(1+\delta^{(K)}_u\right)\left(1+\delta^{(K)}_\ell\right) - \left[\, y^{(K)}_{J_\ell J_u}\,\right]^2}\; (-1)^Q\, s^K_{-Q}(\nu_0)\,. \qquad (10.109)$$

Substitution of Eqs. (10.104), (10.62) and (10.93) into the first of Eqs. (10.109) yields, for $K \neq 0$

$$\rho^K_Q(\alpha_u J_u) = \sqrt{\frac{2J_\ell+1}{2J_u+1}}\; \frac{B(\alpha_\ell J_\ell \to \alpha_u J_u)}{A(\alpha_u J_u \to \alpha_\ell J_\ell)} \times \frac{w^{(K)}_{J_u J_\ell}\left(1+\delta^{(K)}_\ell\right) - (-1)^K\, w^{(K)}_{J_\ell J_u}\; y^{(K)}_{J_u J_\ell}}{\left(1+\delta^{(K)}_u\right)\left(1+\delta^{(K)}_\ell\right) - \left[\, y^{(K)}_{J_u J_\ell}\,\right]^2}\; (-1)^Q\, J^K_{-Q}(\nu_0)\; \rho^0_0(\alpha_\ell J_\ell)\,.$$

Comparison with Eq. (10.13) shows that resonance scattering is still described by Eq. (10.19), with a phase matrix given by

$$P_{ij}(\vec{\Omega},\vec{\Omega}') = \sum_{KQ} \left[X_K(J_\ell,J_u)\right]_{\rm d.c.}\, (-1)^Q\, \mathcal{T}^K_Q(i,\vec{\Omega})\, \mathcal{T}^K_{-Q}(j,\vec{\Omega}')\,,$$

where the new symbol (the symbol $X_K(J_\ell,J_u)$ 'modified by depolarizing collisions') is defined to be

$$\left[X_K(J_\ell,J_u)\right]_{\rm d.c.} = \frac{\left[\, w^{(K)}_{J_u J_\ell}\,\right]^2\left(1+\delta^{(K)}_\ell\right) - (-1)^K\, w^{(K)}_{J_u J_\ell}\; w^{(K)}_{J_\ell J_u}\; y^{(K)}_{J_u J_\ell}}{\left(1+\delta^{(K)}_u\right)\left(1+\delta^{(K)}_\ell\right) - \left[\, y^{(K)}_{J_u J_\ell}\,\right]^2} \qquad (K=1,2)$$

$$\left[X_0(J_\ell,J_u)\right]_{\rm d.c.} \equiv 1\,. \qquad (10.110)$$

TABLE 10.4

Values of the quantities $y^{(K)}_{J'J}$, $x^{(K)}_{J'J}$, $X_K(J,J')$ for different transitions

J	J'	$y^{(1)}_{J'J}$	$x^{(1)}_{J'J}$	$X_1(J,J')$	$y^{(2)}_{J'J}$	$x^{(2)}_{J'J}$	$X_2(J,J')$
0	1	0.	−1.	1.	0.	1.	1.
1/2	1/2	−0.333	−0.612	0.5	0.	0.	0.
1/2	3/2	0.745	−1.369	1.25	0.	0.707	0.5
1	0	0.	0.	0.	0.	0.	0.
1	1	0.5	−1.	0.5	−0.5	−1.	0.5
1	2	0.866	−1.732	1.5	0.592	0.819	0.485
3/2	1/2	0.745	−0.612	−0.25	0.	0.	0.
3/2	3/2	0.733	−1.369	0.5	0.2	−0.471	0.267
3/2	5/2	0.917	−2.092	1.75	0.748	0.962	0.509
2	1	0.866	−1.	−0.5	0.592	−0.385	−0.038
2	2	0.833	−1.732	0.5	0.5	−0.394	0.233
2	3	0.943	−2.449	2.	0.828	1.113	0.545
5/2	3/2	0.917	−1.369	−0.75	0.748	−0.579	−0.082
5/2	5/2	0.886	−2.092	0.5	0.657	−0.365	0.221
5/2	7/2	0.958	−2.806	2.25	0.875	1.268	0.587
3	2	0.943	−1.732	−1.	0.828	−0.753	−0.127
3	3	0.917	−2.449	0.5	0.75	−0.350	0.214
3	4	0.968	−3.162	2.5	0.905	1.424	0.631
7/2	5/2	0.958	−2.092	−1.25	0.875	−0.920	−0.174
7/2	7/2	0.937	−2.806	0.5	0.810	−0.341	0.211
7/2	9/2	0.975	−3.518	2.75	0.925	1.581	0.677
4	3	0.968	−2.449	−1.5	0.905	−1.084	−0.221
4	4	0.95	−3.162	0.5	0.85	−0.335	0.208
4	5	0.980	−3.873	3.	0.939	1.738	0.724
9/2	7/2	0.975	−2.806	−1.75	0.925	−1.246	−0.269
9/2	9/2	0.960	−3.518	0.5	0.879	−0.331	0.206
9/2	11/2	0.983	−4.228	3.25	0.950	1.896	0.771
5	4	0.980	−3.162	−2.	0.939	−1.407	−0.318
5	5	0.967	−3.873	0.5	0.9	−0.329	0.205
5	6	0.986	−4.583	3.5	0.958	2.054	0.819
11/2	9/2	0.983	−3.518	−2.25	0.950	−1.568	−0.366
11/2	11/2	0.972	−4.228	0.5	0.916	−0.327	0.204
11/2	13/2	0.988	−4.937	3.75	0.964	2.212	0.867
6	5	0.986	−3.873	−2.5	0.958	−1.727	−0.415
6	6	0.976	−4.583	0.5	0.929	−0.325	0.204
6	7	0.990	−5.292	4.	0.969	2.370	0.916

TABLE 10.4

(continued)

J	J'	$y^{(1)}_{J'J}$	$x^{(1)}_{J'J}$	$X_1(J,J')$	$y^{(2)}_{J'J}$	$x^{(2)}_{J'J}$	$X_2(J,J')$
13/2	11/2	0.988	−4.228	−2.75	0.964	−1.887	−0.464
13/2	13/2	0.979	−4.937	0.5	0.938	−0.324	0.203
13/2	15/2	0.991	−5.646	4.25	0.973	2.528	0.965
7	6	0.990	−4.583	−3.	0.969	−2.046	−0.513
7	7	0.982	−5.292	0.5	0.946	−0.323	0.203
7	8	0.992	−6.	4.5	0.976	2.686	1.014
15/2	13/2	0.991	−4.937	−3.25	0.973	−2.205	−0.562
15/2	15/2	0.984	−5.646	0.5	0.953	−0.322	0.202
8	7	0.992	−5.292	−3.5	0.976	−2.364	−0.611
8	8	0.986	−6.	0.5	0.958	−0.321	0.202

TABLE 10.5

Analytical expressions of the quantities $X_K(J,J')$

	$X_1(J,J')$	$X_2(J,J')$
$J'=J+1$	$\frac{J+2}{2}$	$\frac{(J+2)(2J+1)(2J+5)}{10\,(4J^2+8J+1)}$
$J'=J$	$\frac{1}{2}$	$\frac{(2J-1)(2J+3)}{10\,(2J^2+2J-3)}$
$J'=J-1$	$-\frac{J-1}{2}$	$-\frac{(J-1)(2J+1)(2J-3)}{10\,(4J^2-3)}$

This symbol satisfies the obvious relations (cf. Eqs. (10.106), (10.108), (10.17), (10.54))

$$\lim_{\substack{\delta_\ell^{(K)}\to 0\\ \delta_u^{(K)}\to 0}} \left[X_K(J_\ell,J_u)\right]_{\text{d.c.}} = X_K(J_\ell,J_u)$$

$$\lim_{\substack{\delta_\ell^{(K)}\to \infty\\ \delta_u^{(K)}\to 0}} \left[X_K(J_\ell,J_u)\right]_{\text{d.c.}} = W_K(J_\ell,J_u)$$

$$\lim_{\delta_\ell^{(K)}\to \infty} \left[X_K(J_\ell,J_u)\right]_{\text{d.c.}} = \frac{W_K(J_\ell,J_u)}{1+\delta_u^{(K)}}\ .$$

It is worth noticing that analytical results similar to those of Eqs. (10.104) and (10.109) have already been obtained, for specific transitions, in Sect. 10.7. Consider for instance Eqs. (10.64) or Eqs. (10.66), which refer to the transitions $(J_\ell=1, J_u=0)$ and $(J_\ell=1, J_u=1)$, respectively. They give the atomic polarization of a two-level atom under the same physical conditions considered here (no

inelastic and superelastic collisions, no magnetic field, no stimulated emission) except for the incident radiation field: in Sect. 10.7 the only non-zero components of the radiation field tensor are J^0_0 and $J^2_0 = J^0_0\, w/\sqrt{2}$, whereas in the present section any component of the radiation field tensor can be non-zero but it must satisfy the weak anisotropy approximation $|J^K_Q| \ll J^0_0$. It is obvious that Eqs. (10.64) and (10.66) should give the same results as Eqs. (10.104) and (10.109) for $w \ll 1$.[1] As an example, consider the first of Eqs. (10.66). To first order in w, it reduces to

$$\sigma^2_0(\alpha_u J_u) = -\frac{w}{\sqrt{2}}\, \frac{3 + 2\,\delta^{(2)}_\ell}{4\big(1+\delta^{(2)}_u\big)\big(1+\delta^{(2)}_\ell\big) - 1}\,,$$

which is consistent with the first of Eqs. (10.109) since (see Eq. (10.93) and Tables 10.1, 10.4) $s^2_0 = w/\sqrt{2}\,,\ w^{(2)}_{11} = y^{(2)}_{11} = -1/2\,.$

10.14.c No inelastic collisions - no stimulated emission

Consider now the effect of the magnetic field. Neglecting inelastic and superelastic collisions and stimulation effects ($\epsilon = \epsilon^{(K)}_u = \epsilon^{(K)}_\ell = 0\,;\ \bar{n} \ll 1$), Eq. (10.101) reduces to Eq. (10.104) while Eqs. (10.102) become

$$\sigma^K_Q(\alpha_u J_u) = \frac{w^{(K)}_{J_u J_\ell}\big(1+\delta^{(K)}_\ell + \mathrm{i}\,H_\ell\,Q\big) - (-1)^K\, w^{(K)}_{J_\ell J_u}\, y^{(K)}_{J_u J_\ell}}{\big(1+\delta^{(K)}_u + \mathrm{i}\,H_u\,Q\big)\big(1+\delta^{(K)}_\ell + \mathrm{i}\,H_\ell\,Q\big) - \big[\,y^{(K)}_{J_u J_\ell}\,\big]^2}\ (-1)^Q\, s^K_{-Q}(\nu_0)$$

$$\sigma^K_Q(\alpha_\ell J_\ell) = (-1)^{1+K} \times \frac{w^{(K)}_{J_\ell J_u}\big(1+\delta^{(K)}_u + \mathrm{i}\,H_u\,Q\big) - (-1)^K\, w^{(K)}_{J_u J_\ell}\, y^{(K)}_{J_\ell J_u}}{\big(1+\delta^{(K)}_u + \mathrm{i}\,H_u\,Q\big)\big(1+\delta^{(K)}_\ell + \mathrm{i}\,H_\ell\,Q\big) - \big[\,y^{(K)}_{J_\ell J_u}\,\big]^2}\ (-1)^Q\, s^K_{-Q}(\nu_0)\,. \quad (10.111)$$

Using Eqs. (10.104), (10.62) and (10.93), the first of Eqs. (10.111) can be rewritten in the form

$$\rho^K_Q(\alpha_u J_u) = \sqrt{\frac{2J_\ell+1}{2J_u+1}}\, \frac{B(\alpha_\ell J_\ell \to \alpha_u J_u)}{A(\alpha_u J_u \to \alpha_\ell J_\ell)} \times \frac{w^{(K)}_{J_u J_\ell}\big(1+\delta^{(K)}_\ell + \mathrm{i}\,H_\ell\,Q\big) - (-1)^K\, w^{(K)}_{J_\ell J_u}\, y^{(K)}_{J_u J_\ell}}{\big(1+\delta^{(K)}_u + \mathrm{i}\,H_u\,Q\big)\big(1+\delta^{(K)}_\ell + \mathrm{i}\,H_\ell\,Q\big) - \big[\,y^{(K)}_{J_u J_\ell}\,\big]^2}\ (-1)^Q\, J^K_{-Q}(\nu_0)\ \rho^0_0(\alpha_\ell J_\ell)\,.$$

Comparison with Eq. (10.27) shows that the frequency-integrated radiation emitted in a scattering process is still given by Eq. (10.32), where the phase matrix is now

$$P_{ij}(\vec{\Omega}, \vec{\Omega}'; \vec{B}\,) = \sum_{KQ} \big[X_{KQ}(J_\ell, J_u; B)\big]_{\mathrm{d.c.}}\ (-1)^Q\, \mathcal{T}^K_Q(i, \vec{\Omega})\, \mathcal{T}^K_{-Q}(j, \vec{\Omega}')\,, \quad (10.112)$$

[1] The comparison must of course be restricted to statistical tensors of the form ρ^0_0 or ρ^2_0. We recall that, when the radiation field is characterized by the only components J^0_0 and J^2_0 and the magnetic field is zero, the only non-null statistical tensors are those with K even and $Q = 0$; by contrast, under the weak anisotropy approximation, the only non-null statistical tensors are those with $K \leq 2$ and any Q.

with the symbol $[X_{KQ}(J_\ell, J_u; B)]_{\rm d.c.}$ – which, contrary to the symbols $X_K(J_\ell, J_u)$ and $[X_K(J_\ell, J_u)]_{\rm d.c.}$, depends also on the quantum number Q – defined by

$$\big[X_{KQ}(J_\ell, J_u; B)\big]_{\rm d.c.} =$$

$$= \frac{\big[\, w^{(K)}_{J_u J_\ell}\,\big]^2 \big(1 + \delta^{(K)}_\ell + {\rm i}\, H_\ell\, Q\big) - (-1)^K\, w^{(K)}_{J_u J_\ell}\;\, w^{(K)}_{J_\ell J_u}\;\, y^{(K)}_{J_u J_\ell}}{\big(1 + \delta^{(K)}_u + {\rm i}\, H_u\, Q\big)\big(1 + \delta^{(K)}_\ell + {\rm i}\, H_\ell\, Q\big) - \big[\, y^{(K)}_{J_u J_\ell}\,\big]^2} \qquad (K = 1, 2)$$

$$\big[X_{00}(J_\ell, J_u; B)\big]_{\rm d.c.} \equiv 1\ . \tag{10.113}$$

As an application of Eq. (10.112), we can evaluate the average of the scattering phase matrix over an isotropic distribution of magnetic fields. Along the lines of Sect. 5.12 we obtain (cf. Eq. (10.36))

$$\langle P_{ij}(\vec\Omega, \vec\Omega'; \vec B\,)\rangle = \sum_K\, M_K(B)\; R^{(K)}_{ij}(\vec\Omega, \vec\Omega'; 0)\ ,$$

where the matrix $R^{(K)}_{ij}(\vec\Omega, \vec\Omega'; 0)$ is defined in Eq. (10.21) and the quantity $M_K(B)$ – the quantum analogue of the factor μ_K defined in Eq. (5.172) – is the average of $[X_{KQ}(J_\ell, J_u; B)]_{\rm d.c.}$ over all possible values of Q

$$M_K(B) = \frac{1}{2K+1}\ \sum_Q\, \big[X_{KQ}(J_\ell, J_u; B)\big]_{\rm d.c.}\ .$$

Let us rewrite the first of Eqs. (10.113) in the form

$$\big[X_{KQ}(J_\ell, J_u; B)\big]_{\rm d.c.} = \frac{a + {\rm i}\, b\, Q}{c + {\rm i}\, d\, Q + e\, Q^2}\ ,$$

where[1]

$$\begin{aligned}
a &= \big[\, w^{(K)}_{J_u J_\ell}\,\big]^2 \big(1 + \delta^{(K)}_\ell\big) - (-1)^K\, w^{(K)}_{J_u J_\ell}\;\, w^{(K)}_{J_\ell J_u}\;\, y^{(K)}_{J_u J_\ell} \\
b &= \big[\, w^{(K)}_{J_u J_\ell}\,\big]^2\, H_\ell \\
c &= \big(1 + \delta^{(K)}_u\big)\big(1 + \delta^{(K)}_\ell\big) - \big[\, y^{(K)}_{J_u J_\ell}\,\big]^2 \\
d &= \big(1 + \delta^{(K)}_u\big)\, H_\ell + \big(1 + \delta^{(K)}_\ell\big)\, H_u \\
e &= -H_\ell\, H_u\ .
\end{aligned}$$

After some algebra we obtain

$$\begin{aligned}
M_0(B) &= 1 \\
M_1(B) &= \frac{1}{3}\left[\frac{a}{c} + 2\,\frac{a(c+e) + bd}{(c+e)^2 + d^2}\right] \\
M_2(B) &= \frac{1}{5}\left[\frac{a}{c} + 2\,\frac{a(c+e) + bd}{(c+e)^2 + d^2} + 2\,\frac{a(c+4e) + 4bd}{(c+4e)^2 + 4d^2}\right]\ .
\end{aligned} \tag{10.114}$$

[1] Note that the quantities a, b, c, d depend on K.

We can consider some interesting limits of these expressions. For the transition ($J_\ell = 0, J_u = 1$), neglecting depolarizing collisions, Eqs. (10.114) give the 'classical' result of Eqs. (5.173) with H_u in the place of H (see Eqs. (10.103) and Tables 10.1 and 10.4). For zero magnetic field, Eqs. (10.114) obviously reduce to Eqs. (10.110),

$$\lim_{B\to 0} M_K(B) = \left[X_K(J_\ell, J_u)\right]_{\text{d.c.}} .$$

For $H_\ell \to \infty$ (complete relaxation of lower-level coherences) we obtain, with the use of Eq. (10.17)

$$\lim_{H_\ell\to\infty} M_1(B) = \frac{1}{3}\left\{ \left[X_1(J_\ell, J_u)\right]_{\text{d.c.}} + 2\,\frac{W_1(J_\ell, J_u)\,\left(1+\delta_u^{(1)}\right)}{\left(1+\delta_u^{(1)}\right)^2 + H_u^2} \right\}$$

$$\lim_{H_\ell\to\infty} M_2(B) = \frac{1}{5}\left\{ \left[X_2(J_\ell, J_u)\right]_{\text{d.c.}} + 2\,\frac{W_2(J_\ell, J_u)\,\left(1+\delta_u^{(2)}\right)}{\left(1+\delta_u^{(2)}\right)^2 + H_u^2} + 2\,\frac{W_2(J_\ell, J_u)\,\left(1+\delta_u^{(2)}\right)}{\left(1+\delta_u^{(2)}\right)^2 + 4H_u^2} \right\} .$$

For $H_u \to \infty$ (complete relaxation of both upper and lower level coherences), we have[1]

$$\lim_{H_u\to\infty} M_1(B) = \frac{1}{3}\left[X_1(J_\ell, J_u)\right]_{\text{d.c.}} , \qquad \lim_{H_u\to\infty} M_2(B) = \frac{1}{5}\left[X_2(J_\ell, J_u)\right]_{\text{d.c.}} .$$

10.14.d No inelastic collisions

Finally, we examine how atomic polarization is affected by stimulated emission. Neglecting inelastic and superelastic collisions ($\epsilon = \epsilon_u^{(K)} = \epsilon_\ell^{(K)} = 0$), Eq. (10.101) reads

$$\frac{\rho_0^0(\alpha_u J_u)}{\rho_0^0(\alpha_\ell J_\ell)} = \sqrt{\frac{2J_u+1}{2J_\ell+1}}\;\frac{\bar{n}}{1+\bar{n}} ,$$

and Eqs. (10.102) can be written in the form

$$\sigma_Q^K(\alpha_u J_u) = \frac{w^{(K)}_{J_u J_\ell}\left(1+\delta_\ell^{(K)} + \mathrm{i}\,H_\ell\,Q\right) - (-1)^K\, w^{(K)}_{J_\ell J_u}\, y^{(K)}_{J_u J_\ell}}{\left(1+\delta_u'^{(K)} + \mathrm{i}\,H_u'\,Q\right)\left(1+\delta_\ell^{(K)} + \mathrm{i}\,H_\ell\,Q\right) - \left[\,y^{(K)}_{J_u J_\ell}\,\right]^2}\;\frac{(-1)^Q\, s^K_{-Q}(\nu_0)}{1+\bar{n}}$$

$$\sigma_Q^K(\alpha_\ell J_\ell) = (-1)^{1+K} \times \frac{w^{(K)}_{J_\ell J_u}\left(1+\delta_u'^{(K)} + \mathrm{i}\,H_u'\,Q\right) - (-1)^K\, w^{(K)}_{J_u J_\ell}\, y^{(K)}_{J_\ell J_u}}{\left(1+\delta_u'^{(K)} + \mathrm{i}\,H_u'\,Q\right)\left(1+\delta_\ell^{(K)} + \mathrm{i}\,H_\ell\,Q\right) - \left[\,y^{(K)}_{J_\ell J_u}\,\right]^2}\;\frac{(-1)^Q\, s^K_{-Q}(\nu_0)}{1+\bar{n}} ,$$

[1] We recall that Eq. (10.112) is valid for $\bar{n} \ll 1$, which implies $H_\ell \gg H_u$.

where

$$\delta_u'^{(K)} = \frac{\delta_u^{(K)}}{1+\bar{n}} \,, \qquad H_u' = \frac{H_u}{1+\bar{n}} \,.$$

Comparison with Eqs. (10.111) shows that the effect of stimulated emission is twofold. On the one hand, the efficiency of collisions and of the magnetic field in depolarizing the upper level is reduced:[1] this is a consequence of the fact that the lifetime of the upper level is now shorter. On the other hand, atomic polarization is globally decreased by a factor $(1+\bar{n})$. This is consistent with the results derived in Sect. 10.9.

10.15. The Two-Term Atom: Generalities

In the previous sections of this chapter we have studied the interaction of an atomic system with the radiation field by referring to the simplest model atom, that we denoted as multi-level. In that model the atomic energy states are 'uncorrelated' J-levels, and atomic transitions take place between two such levels. Now we extend this study to the so-called multi-term atom considered in Sects. 7.5-7.7, which describes the atomic structure by taking into account (under the assumption of L-S coupling) the spin-orbit interaction. In this model, transitions involve an upper and a lower *term*, i.e., two 'groups' of J-levels, each characterized by the same values of the quantum numbers L and S. Transitions are now associated with a *set* of spectral lines (the components of the multiplet) rather than with a single line. Atomic polarization involves coherences *both* between magnetic sublevels of each J-level *and* between magnetic sublevels of the different J-levels of each term. Coherences of the latter kind (which do not exist, by definition, in the multi-level atom) are responsible for several remarkable phenomena, both in the presence and in the absence of a magnetic field.

The following treatment of the multi-term atom is strictly analogous to our previous treatment of the multi-level atom. In particular, we restrict attention to a simplified atomic model composed of just *two* terms. However, two important points should be emphasized. The first one concerns collisions, which – contrary to the previous case – will not be considered. This is because the theory of collisions developed in Chap. 7 is only valid for the multi-level atom. Extension of such theory to the multi-term atom is rather complicated and is outside the aims of this book. The second point concerns the flat-spectrum approximation. We still assume that the radiation impinging on the atomic system satisfies such approximation – this is indeed required by the general equations (statistical equilibrium and radiative transfer) established in Chap. 6: from this point of view, there is no difference from the multi-level case. However, the range over which the radiation field must be frequency-independent is much larger in the present case: neglecting the magnetic field, it basically coincides with the entire frequency range spanned by

[1] A similar effect is also present in the lower level, since the quantities $\delta_\ell^{(K)}$ and H_ℓ are inversely proportional to $\bar{n}$ (cf. Eqs. (10.63) and (10.103)).

the multiplet, to be compared with the (natural plus collisional) frequency width of a single line in the multi-level case. For instance, the relevant wavelength range for the CaII doublet is about 100 Å (see Sect. 10.17). These two points (exclusion of collisions and flat-spectrum approximation) obviously set severe constraints to the applicability of the following results to real cases.

As in the multi-level case, we will often introduce certain approximations (concerning either the atomic system or the radiation field) in order to simplify the equations and to obtain analytical expressions for the atomic polarization and for the radiation emitted in scattering processes. These approximations are briefly recalled by subheadings at the beginning of each section.

Let us consider a two-term model atom, and let us denote by $(\beta_\ell L_\ell S)$ and $(\beta_u L_u S)$ the quantum numbers characterizing the lower and upper term, respectively (both in L-S coupling).[1] The atom is interacting with an anisotropic, polarized radiation field specified by the Stokes vector $I_i(\nu, \vec{\Omega})$. A magnetic field is present, with associated Larmor frequency $\nu_{\rm L}$ (see Eq. (3.10)) and direction $\vec{\Omega}_B$. The flat-spectrum approximation requires that the radiation field is frequency-independent across an interval $\Delta\nu$ centered at $\nu_{\beta_u L_u S, \beta_\ell L_\ell S}$ (the Bohr frequency corresponding to the transition between the two terms, see Eq. (7.22)) and encompassing the Bohr frequencies of all the transitions between the different magnetic sublevels originating, in the Paschen-Back effect regime, from the two terms.[2] We fix a reference system with the z-axis along the magnetic field direction, and we describe the atom through the multipole moments of the density matrix. From Eq. (7.38) we get, for the upper term

$$\begin{aligned}
\frac{\mathrm{d}}{\mathrm{d}t}\,{}^{\beta_u L_u S}\rho^K_Q(J_u, J'_u) &= -2\pi\mathrm{i} \sum_{K'Q'J''_uJ'''_u} N_{\beta_u L_u S}(KQJ_uJ'_u, K'Q'J''_uJ'''_u)\,{}^{\beta_u L_u S}\rho^{K'}_{Q'}(J''_u, J'''_u) \\
&+ \sum_{K'Q'J_\ell J'_\ell} \mathbb{T}_{\rm A}(\beta_u L_u SKQJ_uJ'_u, \beta_\ell L_\ell SK'Q'J_\ell J'_\ell)\,{}^{\beta_\ell L_\ell S}\rho^{K'}_{Q'}(J_\ell, J'_\ell) \\
&- \sum_{K'Q'J''_uJ'''_u} \Big[\mathbb{R}_{\rm E}(\beta_u L_u SKQJ_uJ'_uK'Q'J''_uJ'''_u) \\
&\qquad + \mathbb{R}_{\rm S}(\beta_u L_u SKQJ_uJ'_uK'Q'J''_uJ'''_u) \Big]\,{}^{\beta_u L_u S}\rho^{K'}_{Q'}(J''_u, J'''_u)\,, \qquad (10.115)
\end{aligned}$$

and for the lower term

$$\begin{aligned}
\frac{\mathrm{d}}{\mathrm{d}t}\,{}^{\beta_\ell L_\ell S}\rho^K_Q(J_\ell, J'_\ell) &= -2\pi\mathrm{i} \sum_{K'Q'J''_\ell J'''_\ell} N_{\beta_\ell L_\ell S}(KQJ_\ell J'_\ell, K'Q'J''_\ell J'''_\ell)\,{}^{\beta_\ell L_\ell S}\rho^{K'}_{Q'}(J''_\ell, J'''_\ell) \\
&+ \sum_{K'Q'J_uJ'_u} \Big[\mathbb{T}_{\rm E}(\beta_\ell L_\ell SKQJ_\ell J'_\ell, \beta_u L_u SK'Q'J_uJ'_u) +
\end{aligned}$$

[1] The spectroscopic notation is the same as that employed in the whole book: L is the orbital angular momentum quantum number of the electronic cloud and S is the spin, while β describes the electronic configuration. The spin of the lower and upper term is the same, so that a dipole transition is allowed between them.

[2] Such frequencies, denoted by $\nu_{\beta_u L_u S j_u M_u, \beta_\ell L_\ell S j_\ell M_\ell}$, are defined in Eq. (7.26).

$$+ \mathbb{T}_{\rm S}(\beta_\ell L_\ell SKQJ_\ell J'_\ell, \beta_u L_u SK'Q'J_u J'_u)\Big]\ {}^{\beta_u L_u S}\rho^{K'}_{Q'}(J_u, J'_u)$$

$$- \sum_{K'Q'J''_\ell J'''_\ell} \mathbb{R}_{\rm A}(\beta_\ell L_\ell SKQJ_\ell J'_\ell K'Q'J''_\ell J'''_\ell)\ {}^{\beta_\ell L_\ell S}\rho^{K'}_{Q'}(J''_\ell, J'''_\ell)\ . \qquad (10.116)$$

The expressions of the rates are given in Sect. 7.6. We remind the reader that $\mathbb{T}_{\rm A}$, $\mathbb{T}_{\rm E}$, and $\mathbb{T}_{\rm S}$ are the radiative transfer rates due to absorption, spontaneous emission and stimulated emission, respectively, while $\mathbb{R}_{\rm A}$, $\mathbb{R}_{\rm E}$, and $\mathbb{R}_{\rm S}$ are the corresponding relaxation rates. N is the kernel containing the contributions of fine structure and of the magnetic field.

Equations (10.115) and (10.116) form a system of linear, differential equations in the unknowns ${}^{\beta_\ell L_\ell S}\rho^K_Q(J_\ell, J'_\ell)$ and ${}^{\beta_u L_u S}\rho^K_Q(J_u, J'_u)$. In stationary situations the left-hand sides are zero, and the equations reduce to an algebraic, linear, homogeneous system. The number of equations (and of unknowns) is given by

$$N_{\rm eq} = (2S+1)^2\ \left[(2L_\ell+1)^2 + (2L_u+1)^2\right]\ , \qquad (10.117)$$

and the determinant of the system is zero.[1] The normalization condition is provided by the trace equation, which reads (see Eqs. (3.84), (3.101), (3.108))

$$\sum_{J_\ell} \sqrt{2J_\ell+1}\ {}^{\beta_\ell L_\ell S}\rho^0_0(J_\ell, J_\ell) + \sum_{J_u} \sqrt{2J_u+1}\ {}^{\beta_u L_u S}\rho^0_0(J_u, J_u) = 1\ , \qquad (10.118)$$

or, introducing the number density of atoms $\mathcal{N}$,

$$\mathbb{N}_\ell + \mathbb{N}_u = \mathcal{N}\ ,$$

with

$$\mathbb{N}_\ell = \mathcal{N} \sum_{J_\ell} \sqrt{2J_\ell+1}\ {}^{\beta_\ell L_\ell S}\rho^0_0(J_\ell, J_\ell)$$

$$\mathbb{N}_u = \mathcal{N} \sum_{J_u} \sqrt{2J_u+1}\ {}^{\beta_u L_u S}\rho^0_0(J_u, J_u)\ . \qquad (10.119)$$

Once the statistical equilibrium equations are solved, the radiative transfer coefficients can be found from Eqs. (7.47).

As obvious from Eq. (10.117), the system contains a large number of equations even for the simplest transitions. Analytical solutions are therefore impracticable unless some approximation is introduced. One of the most natural and fruitful

[1] Using the expressions of the rates and of the kernel N, it can be shown directly that the equations for the time derivatives of the linear combinations

$$\textstyle\sum_{J_\ell} \sqrt{2J_\ell+1}\ {}^{\beta_\ell L_\ell S}\rho^0_0(J_\ell, J_\ell) \qquad \text{and} \qquad \sum_{J_u} \sqrt{2J_u+1}\ {}^{\beta_u L_u S}\rho^0_0(J_u, J_u)$$

(the populations of the lower and upper term) are identical, except for the opposite sign.

approximations, that will often be used in the following sections, is to neglect the atomic polarization of the lower term. Although collisions are not included in Eqs. (10.115)-(10.116), it is reasonable to believe, by analogy with the two-level case (cf. Sect. 10.7), that such *unpolarized lower term approximation* is roughly satisfied in the presence of depolarizing collisions and a weak radiation field (which also implies that stimulation effects should be neglected).

Let us examine how the statistical equilibrium equations are modified by this approximation. The condition that all the sublevels of the lower term are evenly populated and that no coherence is present between them can be written in the form

$$\rho_{\beta_\ell L_\ell S}(j_\ell M_\ell, j'_\ell M'_\ell) = \delta_{j_\ell j'_\ell}\, \delta_{M_\ell M'_\ell}\; C\;, \tag{10.120}$$

where $\rho_{\beta_\ell L_\ell S}(j_\ell M_\ell, j'_\ell M'_\ell)$ is the density-matrix element in the energy-eigenvector representation (see Sect. 7.5) and C is a constant (independent of j_ℓ and M_ℓ). The statistical tensors of the lower term can be easily deduced by substituting Eq. (10.120) into Eq. (7.37) and by using Eqs. (3.62b), (2.26a) and (2.23a). One gets

$${}^{\beta_\ell L_\ell S}\rho^K_Q(J_\ell, J'_\ell) = \delta_{K0}\, \delta_{Q0}\, \delta_{J_\ell J'_\ell}\, \sqrt{2J_\ell + 1}\;\; C\;. \tag{10.121}$$

The constant C is proportional to the overall population of the lower term. Substitution of Eq. (10.121) into the first of Eqs. (10.119) yields

$$C = \frac{1}{(2S+1)(2L_\ell+1)}\;\frac{\mathbb{N}_\ell}{\mathcal{N}}\;. \tag{10.122}$$

The equations for the statistical tensors of the upper term can now be derived from Eq. (10.115) by neglecting the relaxation rate due to stimulated emission and by making use of Eqs. (10.121) and (10.122). Recalling Eq. (7.46b) we obtain, in stationary situations

$$\begin{aligned} &A(\beta_u L_u S \to \beta_\ell L_\ell S)\; {}^{\beta_u L_u S}\rho^K_Q(J_u, J'_u) + \\ &\quad + 2\pi \mathrm{i} \sum_{K' Q' J''_u J'''_u} N_{\beta_u L_u S}(KQJ_uJ'_u, K'Q'J''_uJ'''_u)\; {}^{\beta_u L_u S}\rho^{K'}_{Q'}(J''_u, J'''_u) = \\ &\quad = \sum_{J_\ell} T_{\mathrm{A}}(\beta_u L_u S K Q J_u J'_u, \beta_\ell L_\ell S\, 0\, 0 J_\ell J_\ell)\;\frac{\sqrt{2J_\ell+1}}{(2S+1)(2L_\ell+1)}\;\frac{\mathbb{N}_\ell}{\mathcal{N}}\;, \end{aligned} \tag{10.123}$$

where the kernel N is given by Eq. (7.41) and the transfer rate T_{A} by Eq. (7.45a). Taking into account Eqs. (2.26a) and (2.49), the latter can be rewritten in the form

$$\begin{aligned} &T_{\mathrm{A}}(\beta_u L_u S K Q J_u J'_u, \beta_\ell L_\ell S\, 0\, 0 J_\ell J_\ell) = (2L_\ell + 1)\, B(\beta_\ell L_\ell S \to \beta_u L_u S) \\ &\quad \times \sqrt{3(2J_\ell+1)(2J_u+1)(2J'_u+1)}\; \begin{Bmatrix} 1 & 1 & K \\ J_u & J'_u & J_\ell \end{Bmatrix} \begin{Bmatrix} L_u & L_\ell & 1 \\ J_\ell & J_u & S \end{Bmatrix} \begin{Bmatrix} L_u & L_\ell & 1 \\ J_\ell & J'_u & S \end{Bmatrix} \\ &\quad \times (-1)^{1+J_\ell+J_u+Q}\; J^K_{-Q}(\nu_{\beta_u L_u S, \beta_\ell L_\ell S})\;. \end{aligned} \tag{10.124}$$

In the following sections we will analyze the consequences of Eq. (10.123) both in the non-magnetic and in the magnetic regime.

10.16. The Two-Term Atom: Resonance Polarization

(*unpolarized lower term - no magnetic field*)

To describe resonance polarization, we neglect in Eq. (10.123) the contribution of the magnetic field. Setting $\nu_{\rm L} = 0$ in Eq. (7.41), the kernel N takes the simpler form

$$N_{\beta_u L_u S}(KQJ_uJ'_u, K'Q'J''_uJ'''_u) = \delta_{KK'}\,\delta_{QQ'}\,\delta_{J_uJ''_u}\,\delta_{J'_uJ'''_u} \times \nu_{\beta_u L_u S J_u,\,\beta_u L_u S J'_u}\,, \tag{10.125}$$

where the Bohr frequency $\nu_{\beta_u L_u S J_u,\,\beta_u L_u S J'_u}$ is given by Eq. (7.43). Equation (10.123) can now be solved for the statistical tensors of the upper term. Substitution of Eqs. (10.124) and (10.125) yields

$$\begin{aligned}{}^{\beta_u L_u S}\rho^K_Q(J_u, J'_u) = {}& \frac{\mathbb{N}_\ell}{\mathcal{N}}\,\frac{\sqrt{3(2J_u+1)(2J'_u+1)}}{2S+1} \\ & \times \frac{B(\beta_\ell L_\ell S \to \beta_u L_u S)}{A(\beta_u L_u S \to \beta_\ell L_\ell S) + 2\pi\mathrm{i}\,\nu_{\beta_u L_u S J_u,\,\beta_u L_u S J'_u}} \\ & \times \sum_{J_\ell} (-1)^{1+J_\ell+J_u+Q}\,(2J_\ell+1) \\ & \times \begin{Bmatrix} 1 & 1 & K \\ J_u & J'_u & J_\ell \end{Bmatrix} \begin{Bmatrix} L_u & L_\ell & 1 \\ J_\ell & J_u & S \end{Bmatrix} \begin{Bmatrix} L_u & L_\ell & 1 \\ J_\ell & J'_u & S \end{Bmatrix} J^K_{-Q}\big(\nu_{\beta_u L_u S,\,\beta_\ell L_\ell S}\big)\,, \end{aligned}$$

or, performing the summation over J_ℓ via Eq. (2.41)

$$\begin{aligned}{}^{\beta_u L_u S}\rho^K_Q(J_u, J'_u) = {}& \frac{\mathbb{N}_\ell}{\mathcal{N}}\,\frac{\sqrt{3(2J_u+1)(2J'_u+1)}}{2S+1} \\ & \times \frac{B(\beta_\ell L_\ell S \to \beta_u L_u S)}{A(\beta_u L_u S \to \beta_\ell L_\ell S) + 2\pi\mathrm{i}\,\nu_{\beta_u L_u S J_u,\,\beta_u L_u S J'_u}}\,(-1)^{1-L_\ell+S+J'_u+K+Q} \\ & \times \begin{Bmatrix} 1 & 1 & K \\ L_u & L_u & L_\ell \end{Bmatrix} \begin{Bmatrix} L_u & L_u & K \\ J_u & J'_u & S \end{Bmatrix} J^K_{-Q}\big(\nu_{\beta_u L_u S,\,\beta_\ell L_\ell S}\big)\,. \end{aligned} \tag{10.126}$$

To obtain the radiation emitted by the atom along a given direction $\vec{\Omega}$, we have to substitute Eq. (10.126) into the expression of the emission coefficient for the multi-term atom. This is given by Eq. (7.47e) for the general case where a magnetic field is present. In the non-magnetic case it becomes much simpler, since the following substitutions are to be performed

$$C^j_J(\beta LS, M) \to \delta_{jJ}\,, \qquad \Phi(\nu_{\beta_u L_u S j_u M_u,\,\beta_\ell L_\ell S j_\ell M_\ell} - \nu) \to \Phi(\nu_{\beta_u L_u S J_u,\,\beta_\ell L_\ell S J_\ell} - \nu)\,,$$

where

$$\nu_{\beta_u L_u S J_u,\, \beta_\ell L_\ell S J_\ell} = \frac{E_{\beta_u L_u S}(J_u) - E_{\beta_\ell L_\ell S}(J_\ell)}{h} \,,$$

with $E_{\beta LS}(J)$ the eigenvalue of the spin-orbit Hamiltonian corresponding to the eigenvector $|\beta LSJM\rangle$ (see Eq. (3.61a)). With the help of Eqs. (2.34), (3.100) and (5.158) we obtain[1]

$$\begin{aligned}
\varepsilon_i(\nu,\vec{\Omega}) &= \frac{h^2\nu^4}{2\pi c^2}\,\mathcal{N}\,(2L_u+1)\,B(\beta_u L_u S \to \beta_\ell L_\ell S) \\
&\times \sum_{KQ}\sum_{J_u J'_u J_\ell} (-1)^{1+J_\ell+J'_u}\,(2J_\ell+1)\,\sqrt{3(2J_u+1)(2J'_u+1)} \\
&\qquad \times \left\{ \begin{array}{ccc} L_u & L_\ell & 1 \\ J_\ell & J_u & S \end{array} \right\} \left\{ \begin{array}{ccc} L_u & L_\ell & 1 \\ J_\ell & J'_u & S \end{array} \right\} \left\{ \begin{array}{ccc} 1 & 1 & K \\ J_u & J'_u & J_\ell \end{array} \right\} \\
&\qquad \times \mathcal{T}^K_Q(i,\vec{\Omega})\;\; {}^{\beta_u L_u S}\rho^K_Q(J'_u, J_u) \\
&\qquad \times \frac{1}{2}\left[\Phi(\nu_{\beta_u L_u S J_u,\, \beta_\ell L_\ell S J_\ell} - \nu) + \Phi(\nu_{\beta_u L_u S J'_u,\, \beta_\ell L_\ell S J_\ell} - \nu)^* \right] . \qquad (10.127)
\end{aligned}$$

Now we substitute in this expression the upper-term statistical tensors given by Eq. (10.126). Bearing in mind the relations between the Einstein coefficients (Eqs. (7.33)), and introducing the frequency-integrated absorption coefficient in the multiplet[2]

$$k^{\mathrm{A}}_{\mathrm{M}} = \frac{h\,\nu_{\beta_u L_u S,\, \beta_\ell L_\ell S}}{4\pi}\;\mathbb{N}_\ell\;B(\beta_\ell L_\ell S \to \beta_u L_u S)\,, \qquad (10.128)$$

we obtain

$$\begin{aligned}
\varepsilon_i(\nu,\vec{\Omega}) &= k^{\mathrm{A}}_{\mathrm{M}}\;\frac{2L_u+1}{2S+1}\sum_{KQ}\sum_{J_u J'_u J_\ell} (-1)^{S-L_\ell+J_u+J'_u+J_\ell+K+Q} \\
&\times 3(2J_u+1)(2J'_u+1)(2J_\ell+1) \left\{ \begin{array}{ccc} L_u & L_\ell & 1 \\ J_\ell & J_u & S \end{array} \right\} \left\{ \begin{array}{ccc} L_u & L_\ell & 1 \\ J_\ell & J'_u & S \end{array} \right\} \\
&\times \left\{ \begin{array}{ccc} 1 & 1 & K \\ J_u & J'_u & J_\ell \end{array} \right\} \left\{ \begin{array}{ccc} 1 & 1 & K \\ L_u & L_u & L_\ell \end{array} \right\} \left\{ \begin{array}{ccc} L_u & L_u & K \\ J_u & J'_u & S \end{array} \right\} \mathcal{T}^K_Q(i,\vec{\Omega})\; J^K_{-Q}(\nu_{\beta_u L_u S,\, \beta_\ell L_\ell S}) \\
&\times \frac{1}{2}\frac{\Phi(\nu_{\beta_u L_u S J_u,\, \beta_\ell L_\ell S J_\ell} - \nu) + \Phi(\nu_{\beta_u L_u S J'_u,\, \beta_\ell L_\ell S J_\ell} - \nu)^*}{1 + 2\pi\mathrm{i}\,\nu_{\beta_u L_u S J'_u,\, \beta_u L_u S J_u} \,/\, A(\beta_u L_u S \to \beta_\ell L_\ell S)} \,. \qquad (10.129)
\end{aligned}$$

---

1 Similar calculations have been performed to derive Eq. (7.48g) from Eq. (7.47e).

2 The quantity $k^{\mathrm{A}}_{\mathrm{M}}$ – the analogue of $k^{\mathrm{A}}_{\mathrm{L}}$ of Eq. (9.5) for a multiplet – is defined as the integral over frequency of the absorption coefficient $\eta^{\mathrm{A}}_0(\nu,\vec{\Omega})$ for a two-term atom with unpolarized lower term. The integral is easily evaluated using Eq. (7.47a) – or equivalently Eq. (7.48b) – and taking into account Eqs. (10.121) and (10.122). The expression in Eq. (10.128) implies the approximation $\nu \approx \nu_{\beta_u L_u S,\, \beta_\ell L_\ell S}$.

The frequency dependence of $\varepsilon_i(\nu,\vec{\Omega})$, contained in the last term of Eq. (10.129), will be analyzed in the next section. Here we restrict attention to the frequency-integrated emission coefficient, $\tilde{\varepsilon}_i(\vec{\Omega})$, defined by

$$\tilde{\varepsilon}_i(\vec{\Omega}) = \int_{\Delta\nu} \varepsilon_i(\nu,\vec{\Omega})\,\mathrm{d}\nu\ , \tag{10.130}$$

where the interval $\Delta\nu$ is sufficiently broad to fully cover all the lines of the multiplet. Since the Φ profiles are normalized to unity in frequency (Eqs. (6.59a-c)), we can perform the summation over J_ℓ via Eq. (2.41). Writing the radiation field tensor in terms of the Stokes parameters via Eqs. (5.157), we obtain the expression (see the analogous Eq. (10.19) valid for the two-level atom with unpolarized lower level)

$$\tilde{\varepsilon}_i(\vec{\Omega}) = k_{\mathrm{M}}^{\mathrm{A}} \oint \frac{\mathrm{d}\Omega'}{4\pi} \sum_{j=0}^{3} \left[P_{ij}(\vec{\Omega},\vec{\Omega}')\right]_{\mathrm{fs}} I_j(\nu_{\beta_u L_u S,\,\beta_\ell L_\ell S},\vec{\Omega}')\ , \tag{10.131}$$

where $[P_{ij}(\vec{\Omega},\vec{\Omega}')]_{\mathrm{fs}}$, the fine-structure scattering phase matrix, is given by

$$\left[P_{ij}(\vec{\Omega},\vec{\Omega}')\right]_{\mathrm{fs}} = \sum_{KQ} \left[W_K(\beta_\ell L_\ell S \beta_u L_u)\right]_{\mathrm{fs}}\ (-1)^Q\, \mathcal{T}^K_Q(i,\vec{\Omega})\, \mathcal{T}^K_{-Q}(j,\vec{\Omega}')\ , \tag{10.132}$$

with

$$\begin{aligned}\left[W_K(\beta_\ell L_\ell S \beta_u L_u)\right]_{\mathrm{fs}} &= \frac{3(2L_u+1)}{2S+1} \\ &\times \sum_{J_u J'_u} (2J_u+1)(2J'_u+1) \left\{ \begin{array}{ccc} 1 & 1 & K \\ L_u & L_u & L_\ell \end{array} \right\}^2 \left\{ \begin{array}{ccc} L_u & L_u & K \\ J_u & J'_u & S \end{array} \right\}^2 \\ &\times \frac{1}{1 + 2\pi\mathrm{i}\,\nu_{\beta_u L_u S J'_u,\,\beta_u L_u S J_u} \,/\, A(\beta_u L_u S \rightarrow \beta_\ell L_\ell S)}\ . \end{aligned} \tag{10.133}$$

Comparison of Eqs. (10.132) and (10.20) shows that the new coefficient is the direct equivalent, for fine-structure multiplets, of the coefficient $W_K(J_\ell,J_u)$ introduced for the two-level atom. It can easily be proved that, like $W_K(J_\ell,J_u)$, it is real

$$\left[W_K(\beta_\ell L_\ell S \beta_u L_u)\right]^*_{\mathrm{fs}} = \left[W_K(\beta_\ell L_\ell S \beta_u L_u)\right]_{\mathrm{fs}}\ , \tag{10.134}$$

and satisfies (see Eq. (2.36a))

$$\left[W_0(\beta_\ell L_\ell S \beta_u L_u)\right]_{\mathrm{fs}} = 1\ .$$

Equation (10.133) can be cast in a more significant form. Recalling Eq. (10.17) one has

$$\left[W_K(\beta_\ell L_\ell S \beta_u L_u)\right]_{\mathrm{fs}} = W_K(L_\ell,L_u)\ \left[D_K(\beta_u L_u S)\right]_{\mathrm{fs}}\ , \tag{10.135}$$

where $[D_K(\beta LS)]_{\rm fs}$, the depolarizing factor due to fine structure,[1] is given by

$$\left[D_K(\beta LS)\right]_{\rm fs} = \frac{1}{2S+1} \sum_{JJ'} (2J+1)(2J'+1) \left\{ \begin{matrix} L & L & K \\ J & J' & S \end{matrix} \right\}^2 \times \frac{1}{1 + 2\pi {\rm i}\, \nu_{\beta LSJ',\, \beta LSJ} \big/ A(\beta LS \rightarrow \beta_\ell L_\ell S)} \,. \quad (10.136)$$

The depolarizing factor satisfies some important properties:

a) When the fine-structure intervals of the term are negligible in comparison with the de-excitation Einstein coefficient, the last factor in Eq. (10.136) reduces to unity and one obtains, with the use of Eq. (2.39)

$$\left[D_K(\beta LS)\right]_{\rm fs} = 1 \,. \quad (10.137)$$

In this case Eq. (10.135) becomes

$$\left[W_K(\beta_\ell L_\ell S \beta_u L_u)\right]_{\rm fs} = W_K(L_\ell, L_u) \,, \quad (10.138)$$

which shows that the two-term atom behaves as a two-level atom having $J_\ell = L_\ell$, $J_u = L_u$. This is an obvious manifestation of the principle of spectroscopic stability: if the spin induces negligible splittings, it can just be disregarded.

b) In the opposite case where the fine-structure intervals are much larger than the Einstein coefficient, all the terms with $J \neq J'$ make a negligible contribution to the double summation in Eq. (10.136), so that

$$\left[D_K(\beta LS)\right]_{\rm fs} = \left[D_K^\infty(LS)\right]_{\rm fs} = \frac{1}{2S+1} \sum_J (2J+1)^2 \left\{ \begin{matrix} L & L & K \\ J & J & S \end{matrix} \right\}^2 . \quad (10.139)$$

Values of D_K^∞ are collected in Table 10.6 for $K = 1, 2$ [2] and for all terms having $S \leq 9/2$, $L \leq 7$. Terms with $S = 0$ or $L = 0$ are not included since for such terms the definition of D_K^∞ is meaningless.

c) When the J-levels satisfy the Landé interval rule (see Eq. (3.60)), one has

$$\nu_{\beta LSJ',\, \beta LSJ} = \frac{1}{2h}\, \zeta(\beta LS) \left[J'(J'+1) - J(J+1) \right] , \quad (10.140)$$

and the depolarizing factor can be written in the form

$$\left[D_K(\beta LS)\right]_{\rm fs} = \frac{1}{2S+1} \sum_{JJ'} (2J+1)(2J'+1) \left\{ \begin{matrix} L & L & K \\ J & J' & S \end{matrix} \right\}^2 \times \frac{1}{1 + x^2 \left[J'(J'+1) - J(J+1) \right]^2} \,, \quad (10.141)$$

[1] It is important to note that the depolarizing factor depends only on the fine-structure properties and on the Einstein coefficient for spontaneous de-excitation of the term.

[2] Use of Eq. (2.36a) shows that $[D_0^\infty(LS)]_{\rm fs} = [D_0(\beta LS)]_{\rm fs} = 1$.

TABLE 10.6

Values of the depolarizing factors $[D_K^\infty(LS)]_{\rm fs}$ for different terms

Term	D_1^∞	D_2^∞	Term	D_1^∞	D_2^∞	Term	D_1^∞	D_2^∞
^{2}P	0.778	0.333	^{5}P	0.389	0.231	^{8}P	0.354	0.212
^{2}D	0.92	0.76	^{5}D	0.5	0.265	^{8}D	0.391	0.227
^{2}F	0.959	0.878	^{5}F	0.705	0.349	^{8}F	0.453	0.248
^{2}G	0.975	0.926	^{5}G	0.813	0.529	^{8}G	0.573	0.255
^{2}H	0.983	0.950	^{5}H	0.873	0.658	^{8}H	0.691	0.342
^{2}I	0.988	0.964	^{5}I	0.908	0.744	^{8}I	0.770	0.456
^{2}K	0.991	0.973	^{5}K	0.930	0.803	^{8}K	0.824	0.555
^{3}P	0.5	0.278	^{6}P	0.371	0.222	^{9}P	0.35	0.210
^{3}D	0.796	0.473	^{6}D	0.441	0.247	^{9}D	0.378	0.221
^{3}F	0.894	0.702	^{6}F	0.597	0.261	^{9}F	0.425	0.238
^{3}G	0.935	0.813	^{6}G	0.737	0.399	^{9}G	0.5	0.257
^{3}H	0.956	0.872	^{6}H	0.818	0.541	^{9}H	0.623	0.280
^{3}I	0.969	0.908	^{6}I	0.867	0.648	^{9}I	0.716	0.374
^{3}K	0.976	0.930	^{6}K	0.899	0.724	^{9}K	0.780	0.474
^{4}P	0.422	0.247	^{7}P	0.361	0.216	^{10}P	0.347	0.208
^{4}D	0.646	0.276	^{7}D	0.41	0.235	^{10}D	0.369	0.217
^{4}F	0.807	0.510	^{7}F	0.5	0.260	^{10}F	0.406	0.231
^{4}G	0.880	0.674	^{7}G	0.655	0.302	^{10}G	0.461	0.248
^{4}H	0.919	0.772	^{7}H	0.757	0.432	^{10}H	0.558	0.253
^{4}I	0.942	0.833	^{7}I	0.821	0.549	^{10}I	0.659	0.310
^{4}K	0.956	0.872	^{7}K	0.864	0.640	^{10}K	0.734	0.400

where

$$x = \frac{\pi\,\zeta(\beta LS)}{h\,A(\beta LS \to \beta_\ell L_\ell S)}\,. \tag{10.142}$$

The dimensionless parameter x represents the ratio between a typical fine-structure splitting of the J-levels of the term and the natural width of the same levels. Obviously, Eq. (10.141) reduces to Eq. (10.137) for $x = 0$, and to Eq. (10.139) for $x \to \infty$. As an illustration of Eq. (10.141) we plot in Fig. 10.16, as functions of x, the depolarizing factors $[D_1]_{\rm fs}$ and $[D_2]_{\rm fs}$ for the term ^{3}P.

Consider now the polarization of the radiation emitted in a scattering process. Because of the close similarity of Eqs. (10.131) and (10.19), the phase matrix corresponding to the geometry of Fig. 10.1 is given by Eq. (10.24) with the factor $[W_K(\beta_\ell L_\ell S \beta_u L_u)]_{\rm fs}$ in the place of $W_K(J_\ell, J_u)$. For the 90° scattering of an unpolarized radiation beam, the fractional frequency-integrated polarization is therefore given by (cf. Eqs. (10.25))

$$\tilde{p}_Q = \frac{3\,W_2(L_\ell, L_u)\left[D_2(\beta_u L_u S)\right]_{\rm fs}}{4 - W_2(L_\ell, L_u)\left[D_2(\beta_u L_u S)\right]_{\rm fs}}$$

$$\tilde{p}_U = 0\,. \tag{10.143}$$

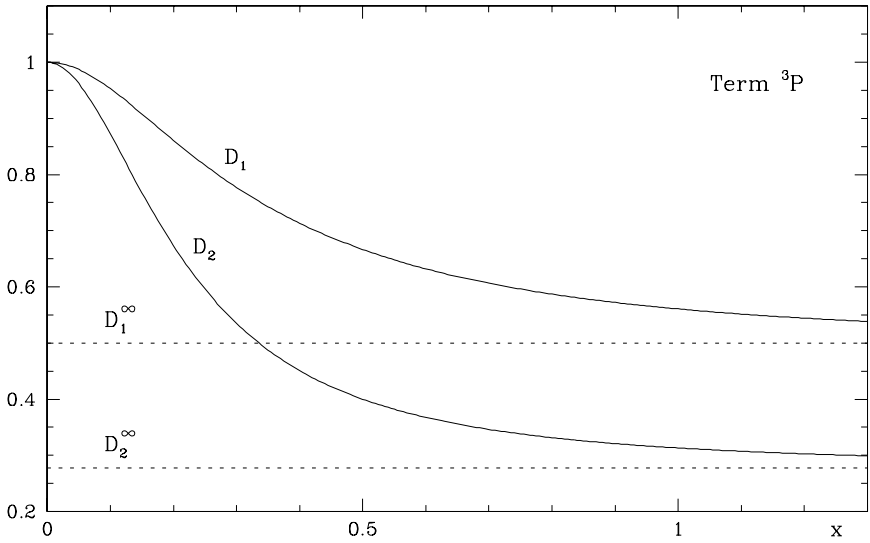

Fig.10.16. The depolarizing factors $[D_1(\beta LS)]_{\rm fs}$ and $[D_2(\beta LS)]_{\rm fs}$ for the term ^{3}P against the parameter x defined in Eq.(10.142). The asymptotic values for $x \to \infty$ (0.5 for D_1 and 0.278 for D_2) are also shown.

If we consider, for instance, the transition $^3{\rm S} - ^3{\rm P}$ ($L_\ell = 0$, $L_u = 1$, $S = 1$) and suppose the upper term to be described by the Landé interval rule, the polarization varies from $\tilde{p}_Q = 1$ for $x = 0$ to $\tilde{p}_Q = 0.224$ for $x \to \infty$.[1] This example clearly shows the *depolarizing effect of fine structure in scattering processes*. Such effect is the larger, the smaller the value of the Einstein A coefficient.

10.17. The Two-Term Atom: Spectral Details of Resonance Polarization

(*unpolarized lower term - no magnetic field*)

The frequency dependence of resonance polarization in a two-term atom with unpolarized lower term is fully described by Eq. (10.129).[2] That expression is very complicated and we will try to illustrate its consequences by studying a number of special cases. In the previous section we have already pointed out the depolarizing effect of fine structure on the frequency-integrated emission coefficient.

The frequency dependence of $\varepsilon_i(\nu, \vec{\Omega})$ is contained in the last factor of the right-hand side of Eq. (10.129). If the width of the J-levels of the lower term is much smaller than the width of the J-levels of the upper term, this factor can be cast into a simpler form (cf. the derivation of Eq. (10.42)). From Eqs. (6.59a,b) we

[1] We recall that a positive value for $\tilde{p}_Q$ means that the polarization direction is perpendicular to the scattering plane.

[2] Note, however, that Eq. (10.129) is valid under the flat-spectrum approximation.

have, neglecting frequency shifts

$$\Phi(\nu_{\beta_u L_u S J_u, \beta_\ell L_\ell S J_\ell} - \nu) = \frac{1}{\pi} \, \frac{1}{\Gamma - \mathrm{i}\left(\nu_{\beta_u L_u S J_u, \beta_\ell L_\ell S J_\ell} - \nu\right)} \, ,$$

where (see footnote 2 on p. 520 and footnote 2 on p. 314)

$$\Gamma = \frac{1}{4\pi} \sum_{J_\ell} A(\beta_u L_u S J_u \rightarrow \beta_\ell L_\ell S J_\ell) = \frac{A(\beta_u L_u S \rightarrow \beta_\ell L_\ell S)}{4\pi} \, .$$

Recalling Eq. (7.43), we easily obtain

$$\begin{aligned} &\frac{1}{2} \, \frac{\Phi(\nu_{\beta_u L_u S J_u, \beta_\ell L_\ell S J_\ell} - \nu) + \Phi(\nu_{\beta_u L_u S J'_u, \beta_\ell L_\ell S J_\ell} - \nu)^*}{1 + 2\pi\mathrm{i}\, \nu_{\beta_u L_u S J'_u, \beta_u L_u S J_u} \,/\, A(\beta_u L_u S \rightarrow \beta_\ell L_\ell S)} = \\ &= \frac{1}{\pi} \, \frac{\Gamma}{\left[\Gamma - \mathrm{i}\left(\nu_{\beta_u L_u S J_u, \beta_\ell L_\ell S J_\ell} - \nu\right)\right] \left[\Gamma + \mathrm{i}\left(\nu_{\beta_u L_u S J'_u, \beta_\ell L_\ell S J_\ell} - \nu\right)\right]} \, . \end{aligned} \tag{10.144}$$

In most fine-structure multiplets the different lines are well-separated in frequency, lying at distances that are much larger than their natural width.[1] To make an example, consider the H and K lines of the CaII doublet at 3950 Å. The frequency interval between the two lines is about 6.7×10^{12} s^{-1}, while the Einstein A coefficient is about 1.5×10^8 s^{-1}, i.e., 4×10^4 times smaller. For such multiplets, the emission coefficient in the neighborhood of a single line – say the line corresponding to $J_u = \bar{J}_u$ and $J_\ell = \bar{J}_\ell$ – can therefore be evaluated by restricting the summation over J_u, J'_u and J_ℓ in Eq. (10.129) to the values

$$J_u = J'_u = \bar{J}_u \, , \qquad J_\ell = \bar{J}_\ell \, .$$

Hence we can write, in the vicinity of $\nu_{\beta_u L_u S J_u, \beta_\ell L_\ell S J_\ell}$

$$\begin{aligned} \varepsilon_i(\nu, \vec{\Omega}) \approx k_{\mathrm{M}}^{\mathrm{A}} \, \frac{2L_u + 1}{2S + 1} \, 3(2J_u + 1)^2 \, (2J_\ell + 1) \left\{ \begin{array}{ccc} L_u & L_\ell & 1 \\ J_\ell & J_u & S \end{array} \right\}^2 \\ \times \sum_{KQ} (-1)^{S - L_\ell - J_\ell + K + Q} \left\{ \begin{array}{ccc} 1 & 1 & K \\ J_u & J_u & J_\ell \end{array} \right\} \left\{ \begin{array}{ccc} 1 & 1 & K \\ L_u & L_u & L_\ell \end{array} \right\} \left\{ \begin{array}{ccc} L_u & L_u & K \\ J_u & J_u & S \end{array} \right\} \\ \times \mathcal{T}_Q^K(i, \vec{\Omega}) \, J_{-Q}^K(\nu_{\beta_u L_u S, \beta_\ell L_\ell S}) \;\; \phi(\nu_{\beta_u L_u S J_u, \beta_\ell L_\ell S J_\ell} - \nu) \, , \end{aligned} \tag{10.145}$$

where

$$\phi(\nu_{\beta_u L_u S J_u, \beta_\ell L_\ell S J_\ell} - \nu) = \frac{1}{\pi} \, \frac{\Gamma}{\Gamma^2 + (\nu_{\beta_u L_u S J_u, \beta_\ell L_\ell S J_\ell} - \nu)^2} \, .$$

[1] This is no longer true for hyperfine-structure multiplets. See Sect. 10.22.

If we introduce the relative strengths of the lines in the multiplet defined in Eq. (3.65) – see also footnote 1 on p. 314 – we can rewrite Eq. (10.145) in the form

$$\varepsilon_i(\nu,\vec{\Omega}) \approx k_{\rm M}^{\rm A}\ S^{J_\ell,J_u}\ \phi(\nu_{\beta_u L_u S J_u,\beta_\ell L_\ell S J_\ell}-\nu) \times \sum_{KQ} W_K(L_\ell L_u S, J_\ell J_u)\ (-1)^Q\, \mathcal{T}^K_Q(i,\vec{\Omega})\, J^K_{-Q}(\nu_{\beta_u L_u S,\beta_\ell L_\ell S})\ , \quad (10.146)$$

where the symbol $W_K(L_\ell L_u S, J_\ell J_u)$ is given by

$$W_K(L_\ell L_u S, J_\ell J_u) = (-1)^{S-L_\ell-J_\ell+K}\ 3(2L_u+1)(2J_u+1) \times \begin{Bmatrix} 1 & 1 & K \\ J_u & J_u & J_\ell \end{Bmatrix} \begin{Bmatrix} 1 & 1 & K \\ L_u & L_u & L_\ell \end{Bmatrix} \begin{Bmatrix} L_u & L_u & K \\ J_u & J_u & S \end{Bmatrix} ,$$

or, using Eq. (2.36a)

$$W_K(L_\ell L_u S, J_\ell J_u) = (-1)^K \frac{\begin{Bmatrix} 1 & 1 & K \\ J_u & J_u & J_\ell \end{Bmatrix} \begin{Bmatrix} 1 & 1 & K \\ L_u & L_u & L_\ell \end{Bmatrix} \begin{Bmatrix} L_u & L_u & K \\ J_u & J_u & S \end{Bmatrix}}{\begin{Bmatrix} 1 & 1 & 0 \\ J_u & J_u & J_\ell \end{Bmatrix} \begin{Bmatrix} 1 & 1 & 0 \\ L_u & L_u & L_\ell \end{Bmatrix} \begin{Bmatrix} L_u & L_u & 0 \\ J_u & J_u & S \end{Bmatrix}} . \quad (10.147)$$

Equation (10.146), when compared with Eq. (10.16), shows that a line belonging to a multiplet behaves in resonance scattering as an isolated line, with the only difference that the symbol $W_K(J_\ell, J_u)$ defined in Eq. (10.17) is replaced by the more general symbol $W_K(L_\ell L_u S, J_\ell J_u)$ defined above. This new symbol satisfies several important properties:

a) When $S = 0$ the multiplet reduces to a single line. This implies $L_u = J_u$ and $L_\ell = J_\ell$. Using Eq. (2.36a) one obtains the obvious result

$$W_K(J_\ell J_u\, 0, J_\ell J_u) = W_K(J_\ell, J_u)\ .$$

b) For $K = 0$, we have from Eq. (10.147)

$$W_0(L_\ell L_u S, J_\ell J_u) = 1\ .$$

c) Apart from the trivial case $S = 0$, the only multiplet for which the symbols $W_K(L_\ell L_u S, J_\ell J_u)$ and $W_K(J_\ell, J_u)$ coincide is the simplest of the multiplets, namely $^2\mathrm{S} - {}^2\mathrm{P}$ ($L_\ell = 0$, $L_u = 1$, $S = 1/2$). Using Eq. (2.36a) we have in fact

$$W_K\big(0\ 1\ \tfrac{1}{2}\ ,\tfrac{1}{2}\ J_u\big) = W_K\big(\tfrac{1}{2}\ , J_u\big)\ .$$

d) Owing to the properties of the 6-j symbols, all lines originating from an S upper term ($L_u = 0$) have W_1 and W_2 symbols equal to zero. The same holds for all lines having $J_u = 0$, whereas all lines with $J_u = 1/2$ have $W_2 = 0$, but $W_1 \neq 0$.

e) For several lines the value of W_2 is negative, which means that the direction of the scattered linear polarization produced by an unpolarized radiation beam is parallel to the scattering plane (see comments about Eq. (10.143)).

Table 10.7 collects the numerical values of $W_K(L_\ell L_u S, J_\ell J_u)$ for all multiplets (except singlets) satisfying the electric-dipole selection rules (cf. Sect. 7.11), up to $S = 5/2$, $L = 2$.

For frequencies that are not in the neighborhood of single spectral lines, the approximation of restricting the summation over J_u, J'_u and J_ℓ in Eq. (10.129) to specific values is not justified. All the terms contribute, and the influence of the 'off-diagonal' terms (those having $J_u \neq J'_u$) is fundamental.

Let us consider a frequency ν which is well outside the frequency range of the multiplet. The last term in Eq. (10.129) can approximately be written in the form (see Eq. (10.144))

$$\phi(\nu_0 - \nu) \approx \frac{1}{\pi} \frac{\Gamma}{(\nu_0 - \nu)^2} ,$$

where ν_0 is a sort of center of gravity of the whole multiplet. As this term does not depend on the quantum numbers J_u, J'_u, J_ℓ, the summation over these numbers can be performed via Eqs. (2.41) and (2.39). One gets

$$\varepsilon_i(\nu, \vec{\Omega}) \approx k_{\rm M}^{\rm A} \ \phi(\nu_0 - \nu) \times \sum_{KQ} W_K(L_\ell, L_u) \ (-1)^Q \mathcal{T}^K_Q(i, \vec{\Omega}) \, J^K_{-Q}(\nu_{\beta_u L_u S, \beta_\ell L_\ell S}) , \qquad (10.148)$$

where $W_K(L_\ell, L_u)$ is the symbol introduced for the two-level atom (Eq. (10.17)). This is an interesting result: at large distance from the 'center of gravity', the multiplet behaves in resonance scattering as a simple transition between two spinless levels L_ℓ and L_u.

To find the frequency dependence of the scattered radiation outside the limited ranges considered above (neighborhood of single lines, 'far wings' of the multiplet) one should resort to numerical calculations, by specifying the full set of physical parameters entering Eq. (10.129). These include – in addition to the scattering geometry – the quantum numbers of the lower and upper term, the energies of the different J-levels, and the value of the Einstein A coefficient.

Two examples are shown in Figs. 10.17 and 10.18, where the fractional linear polarization $p_Q = \varepsilon_Q/\varepsilon_I$ resulting from the 90° scattering of an unpolarized radiation beam is plotted as a function of wavelength for two different multiplets, multiplet n. 1 of CaII (^{2}S $-^2$P) and multiplet UV n. 1 of FeII (^{6}D $-^6$D). The curves have been computed from Eq. (10.129) by neglecting the width of the lower levels, so that the frequency-dependent term is given by Eq. (10.144). Both figures refer to the scattering geometry of Fig. 10.1 (with $\Theta = 90°$),[1] therefore a positive value for

[1] We recall that, for the scattering conditions specified above, the only non-zero components of the radiation field tensor are J^0_0 and $J^2_0 = J^0_0/\sqrt{2}$ (cf. Eqs. (5.164)), and that the components of the tensor $\mathcal{T}^K_Q$ are obtained from Table 5.6 setting $\theta = \gamma = 90°$.

TABLE 10.7

Values of the quantities $W_K(L_\ell L_u S, J_\ell J_u)$ for different multiplets

ℓ Term	uTerm	J_ℓ	J_u	W_1	W_2
^{2}S	^{2}P	1/2	1/2	0.667	0.
		1/2	3/2	0.833	0.5
^{2}P	^{2}S	1/2	1/2	0.	0.
		3/2	1/2	0.	0.
^{2}P	^{2}P	1/2	1/2	0.333	0.
		1/2	3/2	0.417	−0.25
		3/2	1/2	−0.167	0.
		3/2	3/2	0.167	0.2
^{2}P	^{2}D	1/2	3/2	0.75	0.35
		3/2	3/2	0.3	−0.28
		3/2	5/2	0.7	0.28
^{2}D	^{2}P	3/2	1/2	0.167	0.
		3/2	3/2	−0.167	−0.04
		5/2	3/2	0.25	0.01
^{2}D	^{2}D	3/2	3/2	0.1	0.28
		3/2	5/2	0.233	−0.28
		5/2	3/2	−0.15	−0.07
		5/2	5/2	0.067	0.32
^{3}S	^{3}P	1	0	0.	0.
		1	1	0.25	0.25
		1	2	0.75	0.35
^{3}P	^{3}S	0	1	0.	0.
		1	1	0.	0.
		2	1	0.	0.
^{3}P	^{3}P	0	1	0.25	0.25
		1	0	0.	0.
		1	1	0.125	−0.125
		1	2	0.375	−0.175
		2	1	−0.125	0.025
		2	2	0.125	0.175
^{3}P	^{3}D	0	1	0.75	0.35
		1	1	0.375	−0.175
		1	2	0.625	0.175
		2	1	−0.375	0.035
		2	2	0.208	−0.175
		2	3	0.667	0.24
^{3}D	^{3}P	1	0	0.	0.
		1	1	−0.125	0.025
		1	2	−0.375	0.035
		2	1	0.125	−0.005
		2	2	−0.125	−0.035
		3	2	0.25	0.01
^{3}D	^{3}D	1	1	0.125	0.175
		1	2	0.208	−0.175
		2	1	−0.125	−0.035
		2	2	0.069	0.175
		2	3	0.222	−0.24
		3	2	−0.139	−0.05
		3	3	0.056	0.3
^{4}S	^{4}P	3/2	1/2	0.167	0.
		3/2	3/2	0.133	0.32
		3/2	5/2	0.7	0.28
^{4}P	^{4}S	1/2	3/2	0.	0.
		3/2	3/2	0.	0.
		5/2	3/2	0.	0.
^{4}P	^{4}P	1/2	1/2	−0.167	0.
		1/2	3/2	0.167	0.2
		3/2	1/2	0.083	0.
		3/2	3/2	0.067	−0.16
		3/2	5/2	0.35	−0.14
		5/2	3/2	−0.1	0.04
		5/2	5/2	0.1	0.16

TABLE 10.7

(continued)

ℓ Term	uTerm	J_ℓ	J_u	W_1	W_2	ℓ Term	uTerm	J_ℓ	J_u	W_1	W_2
^{4}P	^{4}D	1/2	1/2	0.5	0.	^{5}P	^{5}S	1	2	0.	0.
		1/2	3/2	0.5	0.			2	2	0.	0.
		3/2	1/2	−0.25	0.			3	2	0.	0.
		3/2	3/2	0.2	0.	^{5}P	^{5}P	1	1	−0.125	0.025
		3/2	5/2	0.55	0.1			1	2	0.125	0.175
		5/2	3/2	−0.3	0.			2	1	0.125	−0.005
		5/2	5/2	0.157	−0.114			2	2	0.042	−0.175
		5/2	7/2	0.643	0.214			2	3	0.333	−0.12
^{4}D	^{4}P	1/2	1/2	0.167	0.			3	2	−0.083	0.05
		1/2	3/2	−0.167	−0.04			3	3	0.083	0.15
		3/2	1/2	−0.083	0.	^{5}P	^{5}D	1	0	0.	0.
		3/2	3/2	−0.067	0.032			1	1	0.125	0.175
		3/2	5/2	−0.35	0.028			1	2	0.375	−0.075
		5/2	3/2	0.1	−0.008			2	1	−0.125	−0.035
		5/2	5/2	−0.1	−0.032			2	2	0.125	0.075
		7/2	5/2	0.25	0.01			2	3	0.5	0.06
^{4}D	^{4}D	1/2	1/2	0.167	0.			3	2	−0.25	−0.021
		1/2	3/2	0.167	0.			3	3	0.125	−0.075
		3/2	1/2	−0.083	0.			3	4	0.625	0.196
		3/2	3/2	0.067	0.	^{5}D	^{5}P	0	1	0.25	0.01
		3/2	5/2	0.183	−0.1			1	1	0.125	−0.005
		5/2	3/2	−0.1	0.			1	2	−0.125	−0.035
		5/2	5/2	0.052	0.114			2	1	−0.125	0.001
		5/2	7/2	0.214	−0.214			2	2	−0.042	0.035
		7/2	5/2	−0.131	−0.036			2	3	−0.333	0.024
		7/2	7/2	0.048	0.286			3	2	0.083	−0.01
^{5}S	^{5}P	2	1	0.25	0.01			3	3	−0.083	−0.03
		2	2	0.083	0.35			4	3	0.25	0.01
		2	3	0.667	0.24						

TABLE 10.7

(continued)

ℓ Term	uTerm	J_ℓ	J_u	W_1	W_2
^{5}D	^{5}D	0	1	0.083	0.35
		1	0	0.	0.
		1	1	0.042	−0.175
		1	2	0.125	0.075
		2	1	−0.042	0.035
		2	2	0.042	−0.075
		2	3	0.167	−0.06
		3	2	−0.083	0.021
		3	3	0.042	0.075
		3	4	0.208	−0.196
		4	3	−0.125	−0.025
		4	4	0.042	0.275
^{6}S	^{6}P	5/2	3/2	0.3	0.02
		5/2	5/2	0.057	0.366
		5/2	7/2	0.643	0.214
^{6}P	^{6}S	3/2	5/2	0.	0.
		5/2	5/2	0.	0.
		7/2	5/2	0.	0.
^{6}P	^{6}P	3/2	3/2	−0.1	0.04
		3/2	5/2	0.1	0.16
		5/2	3/2	0.15	−0.01
		5/2	5/2	0.029	−0.183
		5/2	7/2	0.321	−0.107
		7/2	5/2	−0.071	0.057
		7/2	7/2	0.071	0.143
^{6}P	^{6}D	3/2	1/2	0.167	0.
		3/2	3/2	0.033	0.2
		3/2	5/2	0.3	−0.1
		5/2	3/2	−0.05	−0.05
		5/2	5/2	0.086	0.114
		5/2	7/2	0.464	0.036
		7/2	5/2	−0.214	−0.036
		7/2	7/2	0.103	−0.048
		7/2	9/2	0.611	0.183
^{6}D	^{6}P	1/2	3/2	0.25	0.01
		3/2	3/2	0.1	−0.008
		3/2	5/2	−0.1	−0.032
		5/2	3/2	−0.15	0.002
		5/2	5/2	−0.029	0.037
		5/2	7/2	−0.321	0.021
		7/2	5/2	0.071	−0.011
		7/2	7/2	−0.071	−0.029
		9/2	7/2	0.25	0.01
^{6}D	^{6}D	1/2	1/2	−0.111	0.
		1/2	3/2	0.028	0.25
		3/2	1/2	0.056	0.
		3/2	3/2	0.011	−0.2
		3/2	5/2	0.1	0.1
		5/2	3/2	−0.017	0.05
		5/2	5/2	0.029	−0.114
		5/2	7/2	0.155	−0.036
		7/2	5/2	−0.071	0.036
		7/2	7/2	0.034	0.048
		7/2	9/2	0.204	−0.183
		9/2	7/2	−0.120	−0.017
		9/2	9/2	0.037	0.267

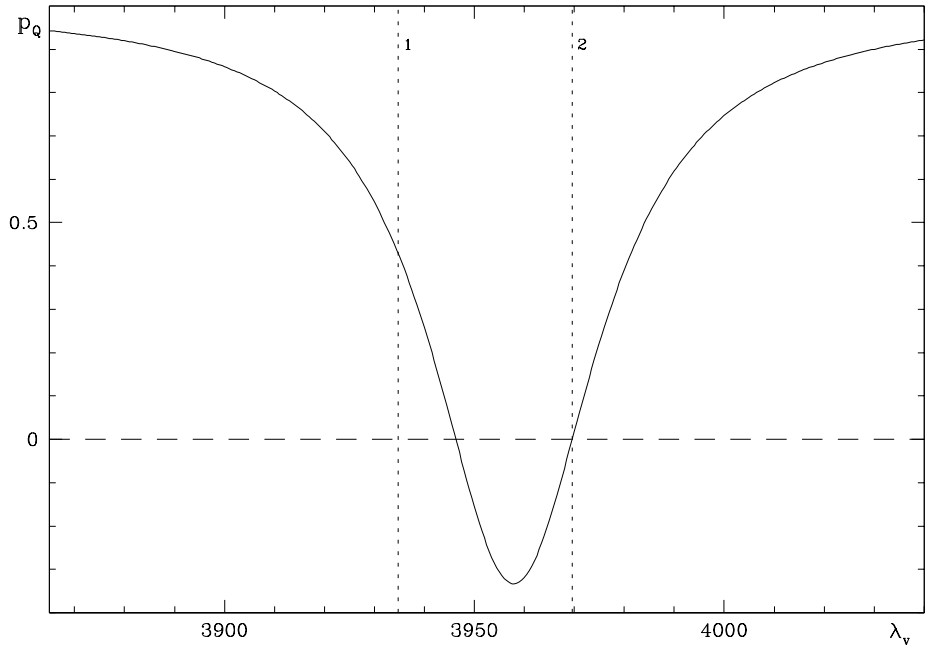

Fig.10.17. Fractional polarization p_Q against vacuum wavelength λ_v (in Å) in the 90° scattering of an unpolarized radiation beam, for multiplet n.1 of CaII. The vertical lines mark the wavelength positions of the two lines of the multiplet according to the code: 1) $J_\ell = 1/2$, $J_u = 3/2$ (K line); 2) $J_\ell = 1/2$, $J_u = 1/2$ (H line). Atomic data are from Moore (1949). The value of the Einstein coefficient is $A = 1.48 \times 10^8$ s^{-1}.

p_Q means that the polarization direction is perpendicular to the scattering plane: note that p_Q is negative (polarization direction parallel to the scattering plane) within certain frequency intervals.

The value of p_Q at the wavelengths of the individual lines, as well as its asymptotic value in the far wings, are easily understood in the light of our preceding results. Consider for instance the line marked with number 3 in Fig. 10.18 ($\lambda = 2600.2$ Å, $J_\ell = J_u = 9/2$). From Eq. (10.146) we obtain, with the use of Table 10.7

$$p_Q = \frac{3\,W_2\big(2\ 2\ \frac{5}{2}\,,\,\frac{9}{2}\ \frac{9}{2}\big)}{4 - W_2\big(2\ 2\ \frac{5}{2}\,,\,\frac{9}{2}\ \frac{9}{2}\big)} \simeq 0.214\ .$$

On the other hand, the asymptotic value for the multiplet of Fig. 10.18 can be derived from Eq. (10.148) with the use of Table 10.1,

$$p_Q = \frac{3\,W_2(2,2)}{4 - W_2(2,2)} \simeq 0.288\ .$$

It should be realized that the ε_I profile, as given by Eq. (10.129), basically consists of a set of *extremely narrow* ($\Delta\lambda < 0.1$ mÅ) Lorentzian profiles centered at the wavelengths of the individual lines (J_ℓ, J_u). The effect of interferences on the ratio

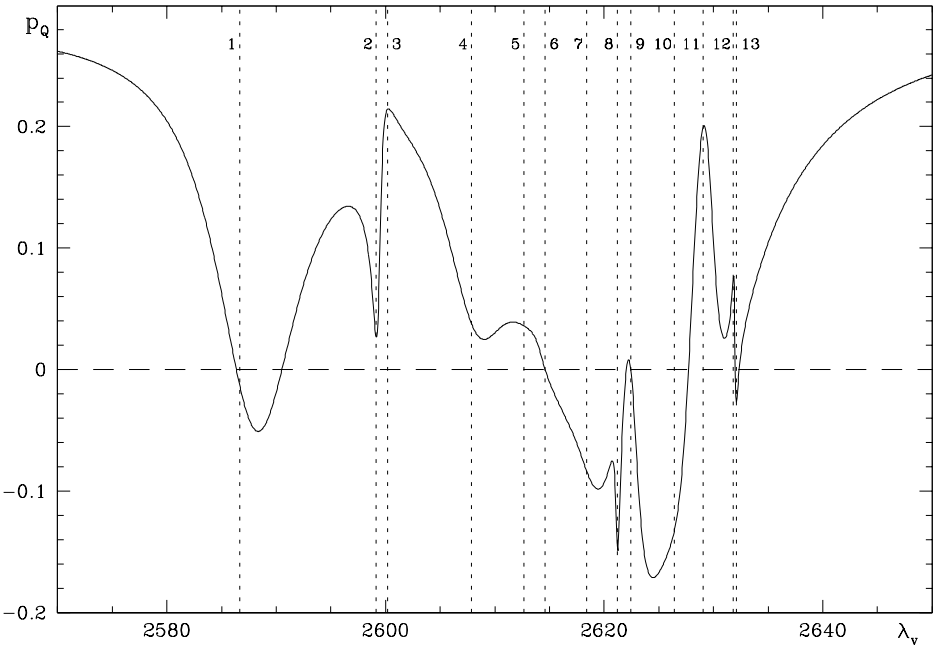

Fig.10.18. Same as Fig.10.17 for multiplet UV n.1 of FeII. The J_ℓ, J_u values of the lines are the following: 1) $9/2, 7/2$; 2) $7/2, 5/2$; 3) $9/2, 9/2$; 4) $5/2, 3/2$; 5) $7/2, 7/2$; 6) $3/2, 1/2$; 7) $5/2, 5/2$; 8) $3/2, 3/2$; 9) $1/2, 1/2$; 10) $7/2, 9/2$; 11) $1/2, 3/2$; 12) $3/2, 5/2$; 13) $5/2, 7/2$. Atomic data are from Moore (1952). The value of the Einstein coefficient is $A = 3.1 \times 10^8$ s^{-1}.

p_Q shows up just across those wavelength intervals where the emissivity is *extremely weak*. This is the reason why it is difficult to detect such interference phenomena in laboratory experiments. The situation may drastically change in astrophysical plasmas, where optical thickness effects can compensate for the low emissivity. These phenomena have indeed been observed, for the first time, in the radiation scattered by the CaII doublet at the extreme limb of the sun (Stenflo, 1980).

The 'fragile' nature of interference phenomena can also be realized by assuming that the plasma, in addition to the resonantly scattered radiation in a given multiplet, also emits a certain amount of continuum radiation (which, for the sake of simplicity, we suppose to be unpolarized). Denoting by $\varepsilon^{(\mathrm{c})}$ the continuum emissivity, the total emission coefficient is given by

$$\varepsilon_i(\nu, \vec{\Omega}) = \varepsilon_i^{(\mathrm{M})}(\nu, \vec{\Omega}) + \varepsilon^{(\mathrm{c})}\, \delta_{i0}\ , \tag{10.149}$$

where $\varepsilon_i^{(\mathrm{M})}(\nu, \vec{\Omega})$, the emissivity in the multiplet, is still given by Eq. (10.129). Figure 10.19 illustrates, in a specific case, the strong reduction of interference effects due to the presence of some continuum emissivity.

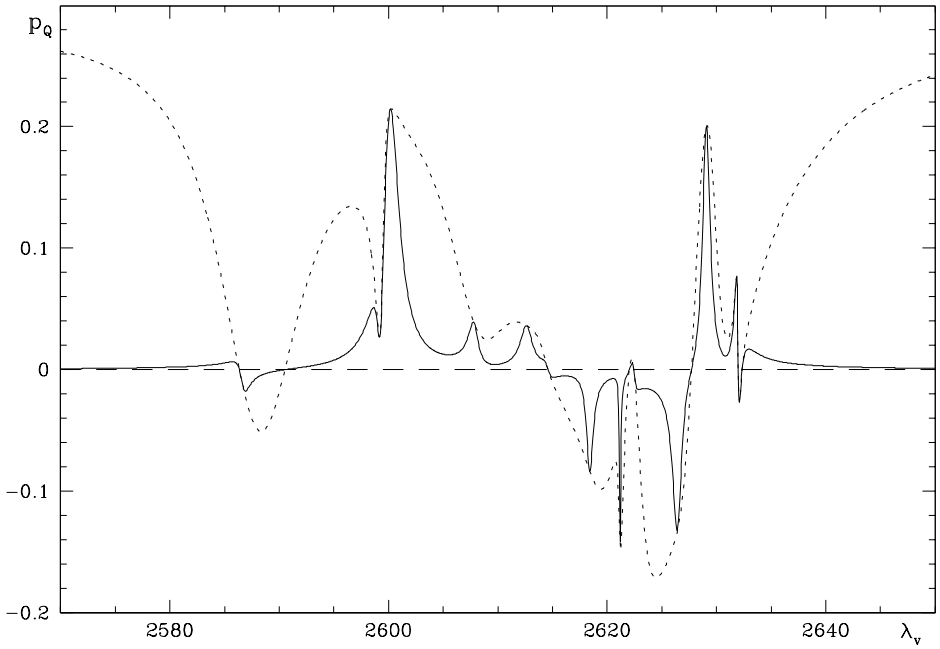

Fig.10.19. Solid line: same as Fig.10.18 in the presence of a given amount of continuum, unpolarized radiation (see Eq.(10.149)). The value of $\varepsilon^{(c)}$ is 3×10^{-9} times the maximum emissivity in the multiplet (at the center of line 3 of Fig.10.18). The dotted curve (identical with the curve of Fig.10.18) corresponds to $\varepsilon^{(c)} = 0$.

10.18. The Two-Term Atom: the Hanle Effect

(*unpolarized lower term*)

In this section we study the effect of a magnetic field of arbitrary strength[1] on the atomic polarization of a two-term atom, by keeping the assumption that the lower term is unpolarized. Obviously, the flat-spectrum approximation requires the incident radiation to be frequency-independent across a range which encompasses all the multiplet components connecting the magnetic sublevels in the Paschen-Back effect regime.

The set of equations for the statistical tensors of the upper term, ${}^{\beta_u L_u S}\rho^K_Q(J_u, J'_u)$, has already been deduced (Eq. (10.123)). However, while adequate to derive a numerical solution, this set is not suitable to obtain an analytical solution, because of the presence of the kernel N which mixes up different statistical tensors. Such difficulty is intrinsic to the two-term atom: in the two-level atom the magnetic term is 'diagonal', which immediately yields (under the unpolarized lower level assumption) the solution to the statistical equilibrium equations (Eq. (10.8)). By contrast, in the present case one is faced with a large algebraic system even for the simplest terms (see Eq. (10.117)).

1 See, however, the discussion following Eq. (3.2).

A closed expression for the statistical tensors of the upper term can be found by solving (in stationary situations) the statistical equilibrium equations in the energy-eigenvector representation, so to obtain the density-matrix elements of the upper term; these can then be combined, by the appropriate transformation, in order to get the statistical tensors. This procedure does not avoid the need for numerical calculations: the problem of solving a linear algebraic system is changed into the problem of diagonalizing the spin-orbit plus magnetic Hamiltonian (see Sect. 3.4), which in most cases must be performed numerically. However, the latter is a much easier task, because the matrix involved is of lower rank and block-diagonal.

The statistical equilibrium equations in the energy-eigenvector representation are given by Eq. (7.29). We are interested in the statistical tensors of the upper term of a two-term atom whose lower term is, by assumption, unpolarized. Using Eqs. (7.34e), (10.120) and (10.122), and neglecting stimulated emission, we obtain, in stationary situations

$$\rho_{\beta_u L_u S}(j_u M_u, j'_u M'_u) = \frac{\mathbb{N}_\ell}{\mathcal{N}} \frac{1}{(2S+1)(2L_\ell+1)} \times \sum_{j_\ell M_\ell} \frac{T_{\mathrm{A}}(\beta_u L_u S j_u M_u\, j'_u M'_u, \beta_\ell L_\ell S j_\ell M_\ell\, j_\ell M_\ell)}{A(\beta_u L_u S \to \beta_\ell L_\ell S) + 2\pi \mathrm{i}\, \nu_{\beta_u L_u S}(j_u M_u, j'_u M'_u)} ,$$

where the rate T_{A} is given by Eq. (7.34a) and the Bohr frequency $\nu_{\beta_u L_u S}$ by Eq. (7.30). The statistical tensors of the upper term can now be obtained by applying the transformation (7.37). Via a long but direct calculation involving the use of Eqs. (3.62b), (5.156), (2.42), and (2.41), one obtains

$$\begin{aligned} {}^{\beta_u L_u S}\rho^K_Q(J_u, J'_u) = \frac{\mathbb{N}_\ell}{\mathcal{N}} \sum_{J''_u J'''_u K'} & \frac{\sqrt{3(2J''_u+1)(2J'''_u+1)}}{2S+1}\ \mathcal{K} \\ & \times (-1)^{1+L_\ell-S+J_u+J''_u+J'''_u+K'+Q} \begin{Bmatrix} 1 & 1 & K' \\ L_u & L_u & L_\ell \end{Bmatrix} \begin{Bmatrix} L_u & L_u & K' \\ J''_u & J'''_u & S \end{Bmatrix} \\ & \times J^{K'}_{-Q}(\nu_{\beta_u L_u S, \beta_\ell L_\ell S}) , \end{aligned} \tag{10.150}$$

where the kernel $\mathcal{K}$ is given by

$$\begin{aligned} \mathcal{K} = \sum_{M_u M'_u} & \sqrt{(2K+1)(2K'+1)} \begin{pmatrix} J_u & J'_u & K \\ M_u & -M'_u & -Q \end{pmatrix} \begin{pmatrix} J''_u & J'''_u & K' \\ M_u & -M'_u & -Q \end{pmatrix} \\ & \times \sum_{j_u j'_u} C^{j_u}_{J_u}(\beta_u L_u S, M_u)\, C^{j_u}_{J''_u}(\beta_u L_u S, M_u)\, C^{j'_u}_{J'_u}(\beta_u L_u S, M'_u)\, C^{j'_u}_{J'''_u}(\beta_u L_u S, M'_u) \\ & \times \frac{B(\beta_\ell L_\ell S \to \beta_u L_u S)}{A(\beta_u L_u S \to \beta_\ell L_\ell S) + 2\pi \mathrm{i}\, \nu_{\beta_u L_u S}(j_u M_u, j'_u M'_u)} . \end{aligned}$$

Obviously, for zero magnetic field we get back previous results. For $B = 0$ we have in fact

$$C^{j_u}_{J_u} \to \delta_{j_u J_u} , \qquad \nu_{\beta_u L_u S}(j_u M_u, j'_u M'_u) \to \nu_{\beta_u L_u S J_u, \beta_u L_u S J'_u} ,$$

where the last Bohr frequency is given by Eq. (7.43). Use of Eq. (2.23a) yields

$$\lim_{B\to 0} \mathcal{K} = \delta_{KK'}\ \delta_{J_u J_u''}\ \delta_{J_u' J_u'''}\ \frac{B(\beta_\ell L_\ell S \to \beta_u L_u S)}{A(\beta_u L_u S \to \beta_\ell L_\ell S) + 2\pi \mathrm{i}\, \nu_{\beta_u L_u S J_u,\, \beta_u L_u S J_u'}} ,$$

hence Eq. (10.150) reduces to Eq. (10.126).

To obtain the radiation emitted by the atom along a given direction $\vec{\Omega}$, we have to substitute Eq. (10.150) into Eq. (7.47e). The resulting expression is very complicated, and will not be written down explicitly. We rather restrict attention to the frequency-integrated emission coefficient, $\tilde{\varepsilon}_i(\vec{\Omega})$, defined in Eq. (10.130). Since the profiles $\Phi(\nu_{\beta_u L_u S j_u M_u,\, \beta_\ell L_\ell S j_\ell M_\ell} - \nu)$ are normalized to unity in frequency, the expression for $\tilde{\varepsilon}_i(\vec{\Omega})$ turns out to be identical to Eq. (7.48g) except for the disappearance of the profile $\phi(\nu_{\beta_u L_u S,\, \beta_\ell L_\ell S} - \nu)$. Substitution of Eq. (10.150) in this expression yields, with the use of Eqs. (5.157), (7.33) and (10.128)

$$\tilde{\varepsilon}_i(\vec{\Omega}) = k_{\mathrm{M}}^{\mathrm{A}} \oint \frac{\mathrm{d}\Omega'}{4\pi} \sum_{j=0}^{3} \left[P_{ij}(\vec{\Omega}, \vec{\Omega}'; \vec{B})\right]_{\mathrm{fs}}\ I_j(\nu_{\beta_u L_u S,\, \beta_\ell L_\ell S}, \vec{\Omega}') , \qquad (10.151)$$

where $[P_{ij}(\vec{\Omega}, \vec{\Omega}'; \vec{B})]_{\mathrm{fs}}$, the scattering phase matrix for a fine-structure multiplet in the presence of a magnetic field, is given by[1]

$$\left[P_{ij}(\vec{\Omega}, \vec{\Omega}'; \vec{B})\right]_{\mathrm{fs}} = \sum_{KK'Q} \left[W_{KK'Q}(\beta_\ell L_\ell S \beta_u L_u; B)\right]_{\mathrm{fs}} \times (-1)^Q\ \mathcal{T}_Q^K(i, \vec{\Omega})\, \mathcal{T}_{-Q}^{K'}(j, \vec{\Omega}') , \qquad (10.152)$$

with

$$\begin{aligned}
\left[W_{KK'Q}(\beta_\ell L_\ell S \beta_u L_u; B)\right]_{\mathrm{fs}} &= \frac{3(2L_u+1)}{2S+1} \begin{Bmatrix} 1 & 1 & K \\ L_u & L_u & L_\ell \end{Bmatrix} \begin{Bmatrix} 1 & 1 & K' \\ L_u & L_u & L_\ell \end{Bmatrix} \\
&\times \sum_{J_u J_u' J_u'' J_u''' M_u M_u'} \sqrt{(2K+1)(2K'+1)(2J_u+1)(2J_u'+1)(2J_u''+1)(2J_u'''+1)} \\
&\times \begin{Bmatrix} L_u & L_u & K \\ J_u & J_u' & S \end{Bmatrix} \begin{Bmatrix} L_u & L_u & K' \\ J_u'' & J_u''' & S \end{Bmatrix} \begin{pmatrix} J_u & J_u' & K \\ -M_u & M_u' & -Q \end{pmatrix} \begin{pmatrix} J_u'' & J_u''' & K' \\ -M_u & M_u' & -Q \end{pmatrix} \\
&\times \sum_{j_u j_u'} C_{J_u}^{j_u}(\beta_u L_u S, M_u)\, C_{J_u''}^{j_u}(\beta_u L_u S, M_u)\, C_{J_u'}^{j_u'}(\beta_u L_u S, M_u')\, C_{J_u'''}^{j_u'}(\beta_u L_u S, M_u') \\
&\quad \times \frac{1}{1 + 2\pi \mathrm{i}\, \nu_{\beta_u L_u S}(j_u' M_u', j_u M_u) \,/\, A(\beta_u L_u S \to \beta_\ell L_\ell S)} . \qquad (10.153)
\end{aligned}$$

The symbol now introduced depends on the quantum numbers specifying the multiplet (L_ℓ, L_u, S), on the fine-structure intervals of the upper term, on the Einstein

[1] The following expression was first derived by Landi Degl'Innocenti (1990).

coefficient $A(\beta_u L_u S \rightarrow \beta_\ell L_\ell S)$, and on the magnetic field modulus B. Its main properties are collected in App. 14.

In the following we apply Eq. (10.151) to a particularly simple case, i.e., the transition ${}^3\mathrm{S} - {}^3\mathrm{P}$ ($L_\ell = 0$, $L_u = 1$, $S = 1$). We assume that the upper term satisfies the Landé interval rule, so that it can be fully characterized by the quantity $\zeta(\beta_u L_u S)$ – see Eqs. (3.60), (10.140). Bearing in mind Eqs. (10.153) and (3.61), it is immediately seen that the Stokes parameters of the scattered radiation depend on $A(\beta_u L_u S \rightarrow \beta_\ell L_\ell S)$, $\zeta(\beta_u L_u S)$ and B via the two ratios

$$\frac{\zeta(\beta_u L_u S)}{A(\beta_u L_u S \rightarrow \beta_\ell L_\ell S)} \qquad \text{and} \qquad \frac{\mu_0 B}{A(\beta_u L_u S \rightarrow \beta_\ell L_\ell S)} \; .$$

Equivalently, we can use the dimensionless parameters

$$x = \frac{\pi \, \zeta(\beta_u L_u S)}{h \; A(\beta_u L_u S \rightarrow \beta_\ell L_\ell S)} \; , \qquad \gamma = \frac{\mu_0 B}{\zeta(\beta_u L_u S)} \; , \tag{10.154}$$

already introduced in Eqs. (10.142) and (3.63), respectively.

Let us assume that the incident radiation is a unidirectional, unpolarized beam, and let us refer – as in previous sections of this chapter – to the scattering geometry of Fig. 5.11. The relevant components of the tensors $\mathcal{T}^K_Q$ for the incident and scattered radiation can be derived from Table 5.6 (the simplest choice is $\theta' = 90°$, $\chi' = 0°$; $\theta = \beta$, $\chi = 90°$, $\gamma = 0°$). The frequency-integrated fractional polarization of the scattered radiation can be derived from Eqs. (10.151)-(10.152). Taking into account the properties of the symbol $W_{KK'Q}$ given in App. 14, we obtain

$$\tilde{p}_Q = \frac{3 \left[\sin^2\beta \; W_{220} + (1 + \cos^2\beta) \; \mathrm{Re}(W_{222}) \right]}{8 + (1 - 3\cos^2\beta) \, W_{220} - 3 \sin^2\beta \; \mathrm{Re}(W_{222})}$$

$$\tilde{p}_U = \frac{-6 \cos\beta \; \mathrm{Im}(W_{222})}{8 + (1 - 3\cos^2\beta) \, W_{220} - 3 \sin^2\beta \; \mathrm{Re}(W_{222})}$$

$$\tilde{p}_V = \frac{-2\sqrt{3} \; \cos\beta \; W_{120}}{8 + (1 - 3\cos^2\beta) \, W_{220} - 3 \sin^2\beta \; \mathrm{Re}(W_{222})} \; . \tag{10.155}$$

The last expression shows that the scattered radiation contains, in general, a definite amount of circular polarization. This phenomenon is closely associated with the existence of fine structure (it has no counterpart in the multi-level atom) and will be discussed extensively in Sect. 10.20. The expressions for the linear polarization still bear a clear resemblance to the corresponding expressions for the two-level atom (Eqs. (10.37)). For zero magnetic field the circular polarization vanishes and the expressions for the linear polarization reduce to Eqs. (10.143) – see Eqs. (A14.6), (10.134) and (10.135).

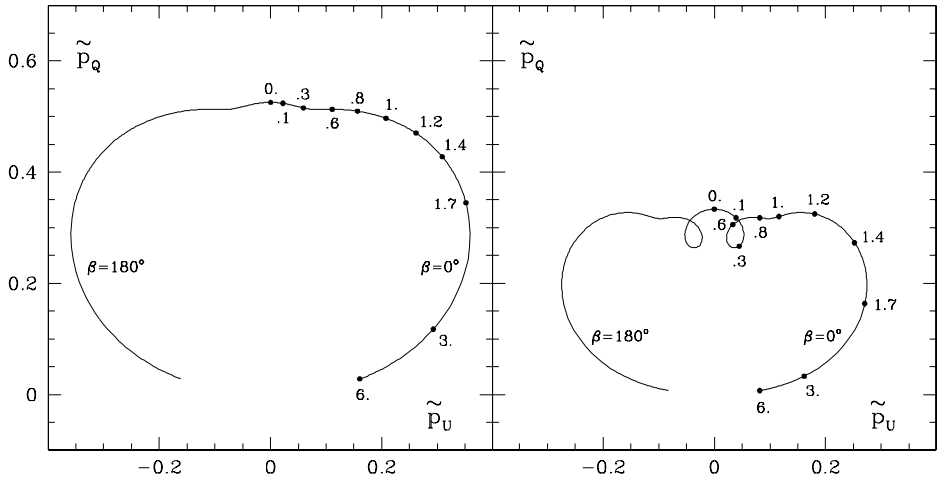

Fig.10.20. Polarization (or Hanle) diagrams for the transition between the lower term ^{3}S and the upper term ^{3}P, corresponding to the scattering geometry of Fig.5.11 (only the curves for $\beta = 0°$ and $\beta = 180°$ are shown). The left panel is obtained for $x = 0.25$, the right panel for $x = 0.5$. The curve $\beta = 0°$ is labelled by the values of γ.

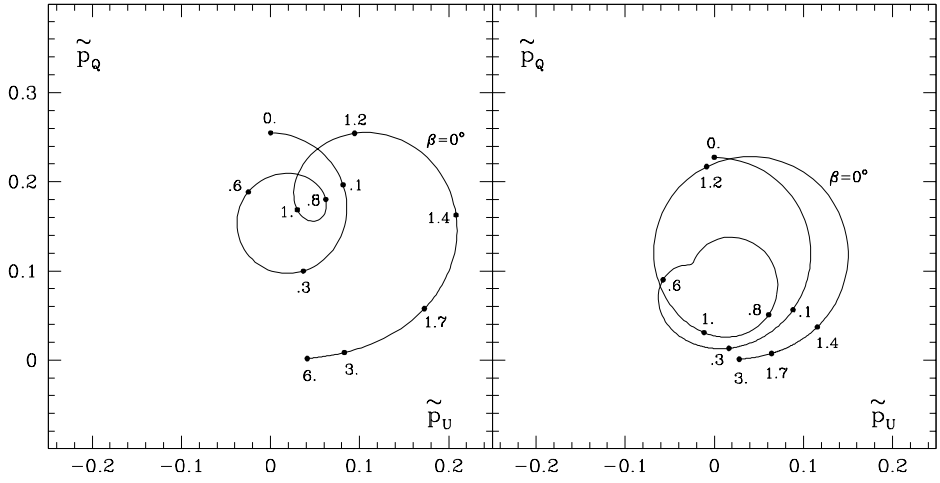

Fig.10.21. Same as Fig.10.20 for $x = 1$ (left panel) and $x = 3$ (right panel). The curve corresponding to $\beta = 180°$ (symmetrical to the curve $\beta = 0°$ about the line $\tilde{p}_U = 0$) is not drawn. Note the scale difference with Fig.10.20.

Figures 10.20-10.21 show the Hanle diagrams obtained from Eqs. (10.155)[1] by assigning different values to the parameter x. The first thing to notice is the overall

[1] Note that the evaluation of the symbols $W_{KK'Q}$ requires the numerical calculation, for each value of x and γ, of the eigenvalues and eigenvectors of the matrix defined in Eqs. (3.61). Alternatively, one can determine (for each value of x and γ) the upper-level statistical tensors by solving numerically Eqs. (10.123); the frequency-integrated scattered polarization is then obtained from Eq. (7.48g) – with the profile ϕ replaced by unity.

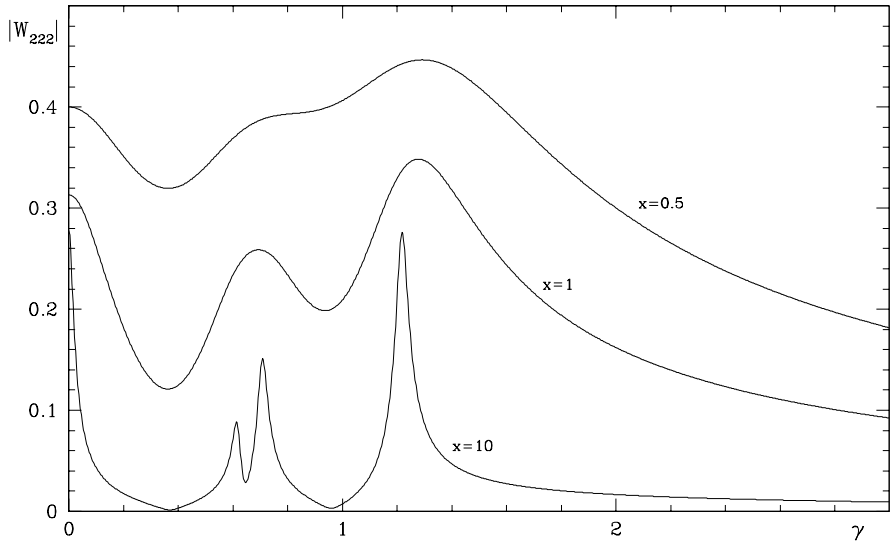

Fig.10.22. Absolute value of the quantity W_{222} for the transition $^3\mathrm{S} - {}^3\mathrm{P}$ as a function of the magnetic field strength (parameterized through γ), for different values of x. Note the appearance of sharp peaks around the critical γ values 0.616, 0.707, and 1.217 for large x values.

decrease of the scattered polarization with increasing x (i.e., with decreasing the Einstein A coefficient): this effect has already been pointed out in our discussion of resonance polarization in the absence of magnetic fields (see Sect. 10.16).

The second phenomenon is the appearance of characteristic curly shapes which become more and more prominent as x is increased. This phenomenon is due to *level-crossing interferences* (see Bommier, 1980), and is associated with the overlapping of different M-sublevels in the (incomplete) Paschen-Back effect – see Sect. 3.4, and in particular Fig. 3.8 which refers to the term ^{3}P. Whereas in the Zeeman effect of an 'isolated' J-level the M-sublevels spread out linearly in energy with increasing magnetic field – with a monotonic decrease of the corresponding coherences – the M-sublevels of a given term may get closer, or even overlap, as the field is increased. Table 3.5 shows that for $\gamma = 0.616$, 0.707, and 1.217 there are overlappings between pairs of M-sublevels of the term ^{3}P corresponding to $\Delta M = 2$ (these are the only overlappings that affect scattering polarization in the particular geometry considered). Around such critical γ values the coherence between the two overlapping sublevels gets larger (in absolute value) and the scattering polarization approaches its zero-field value, which explains the presence of curls in the diagrams.

On the other hand, the Einstein A coefficient controls the natural width of the sublevels. Thus the larger is A, the larger is the γ-interval (around each critical value) in which the sublevels effectively overlap. This explains why the curls in the diagrams clearly show up for small values of A (large values of x) while they practically disappear for larger values of A (smaller values of x).

As a further illustration of these concepts, we plot in Fig. 10.22 the absolute value of W_{222} as a function of γ for three different values of x. It is clearly seen that the

three peaks are almost 'unresolved' for small x values, while they get sharper and sharper as x is increased.

Apart from the loopy structure of the diagrams, the Hanle effect in two-term atoms involves another interesting phenomenon which shows up most clearly when the magnetic field is perpendicular to the scattering plane. For $\beta = 90°$ or $270°$, Eqs. (10.155) yield

$$\tilde{p}_Q = \frac{3\left[W_{220} + \mathrm{Re}(W_{222})\right]}{8 + W_{220} - 3\,\mathrm{Re}(W_{222})}$$

$$\tilde{p}_U = \tilde{p}_V = 0 \; .$$

Let us compare the values of $\tilde{p}_Q$ corresponding to zero magnetic field and to very strong magnetic field (in the sense specified in App. 14). From Eqs. (A14.6), (10.135), and (A14.8) we have

$$\lim_{B\to 0} \tilde{p}_Q = \frac{3\,W_2(L_\ell, L_u)\,\left[D_2(\beta_u L_u S)\right]_{\rm fs}}{4 - W_2(L_\ell, L_u)\,\left[D_2(\beta_u L_u S)\right]_{\rm fs}}$$

$$\lim_{B\to \infty} \tilde{p}_Q = \frac{3\,W_2(L_\ell, L_u)}{8 + W_2(L_\ell, L_u)} \; ,$$

and it may well happen that the second value is larger than the first. Consider for instance the transition ${}^3\mathrm{S} - {}^3\mathrm{P}$. If the fine-structure separations of the upper term are much larger than the Einstein A coefficient ($x \to \infty$), one obtains from Tables 10.1 and 10.6

$$\lim_{B\to 0} \tilde{p}_Q \simeq 0.224 \; , \qquad \lim_{B\to \infty} \tilde{p}_Q \simeq 0.333 \; .$$

This is an extreme example of a phenomenon that can be called the *anti-level-crossing effect*.[1] It is due to the growth of the element W_{220} with increasing magnetic field. As shown in point g) of App. 14, the phenomenon is related to the basis transformation of the energy eigenstates which takes place in the regime of complete Paschen-Back effect.

Finally, it is interesting to evaluate the average of the Hanle phase matrix for two-term atoms over an isotropic distribution of magnetic fields. Along the same lines of Sect. 5.12 (see also Sect. 10.3), we obtain from Eq. (10.152)

$$\left\langle \left[P_{ij}(\vec{\Omega}, \vec{\Omega}'; \vec{B})\right]_{\rm fs} \right\rangle = \sum_K \left[M_K(B)\right]_{\rm fs} \; R_{ij}^{(\mathrm{K})}(\vec{\Omega}, \vec{\Omega}'; 0) \; , \tag{10.156a}$$

where

$$\left[M_K(B)\right]_{\rm fs} = \frac{1}{2K+1} \sum_Q \left[W_{KKQ}(\beta_\ell L_\ell S \beta_u L_u; B)\right]_{\rm fs} \; . \tag{10.156b}$$

[1] This name has been suggested by Bommier (1980) who discusses the importance of the effect on the polarization of the HeI D_3 line at 5876 Å.

The quantity $[M_K(B)]_{\rm fs}$ generally decreases with increasing magnetic field. In particular we have, using Eqs. (A14.6), (10.135), and (A14.8)

$$\frac{\left[M_K(B\to\infty)\right]_{\rm fs}}{\left[M_K(B=0)\right]_{\rm fs}} = \frac{1}{(2K+1)\,\left[D_K(\beta_u L_u S)\right]_{\rm fs}}\,.$$

If the fine-structure intervals of the upper term are much smaller than the Einstein A coefficient, the depolarizing factor is unity (see Eq. (10.137)), thus the above ratio is $1/3$ for $K=1$ and $1/5$ for $K=2$. This is the classical result predicted by Eqs. (5.173). On the other hand, if the fine-structure intervals are comparable with A, the depolarizing factor is less than unity, hence the above ratio is larger than $1/3$ and $1/5$, respectively. For instance, for an upper term ^{3}P in the limit of very large fine-structure intervals ($x\to\infty$), one gets from Table 10.6

$$\frac{\left[M_1(B\to\infty)\right]_{\rm fs}}{\left[M_1(B=0)\right]_{\rm fs}} \simeq 0.667\,, \qquad \frac{\left[M_2(B\to\infty)\right]_{\rm fs}}{\left[M_2(B=0)\right]_{\rm fs}} \simeq 0.719\,.$$

This is a further manifestation of the anti-level-crossing effect discussed above.

10.19. The Two-Term Atom: the Franken Effect

(*unpolarized lower term*)

Besides the characteristic 'curls' in the Hanle diagram, level-crossing interferences also produce, in many cases, sharp variations of the intensity of the scattered radiation: this phenomenon can be used in laboratory spectroscopy to measure the fine-structure (and hyperfine-structure)[1] energy separations of excited atomic terms. The technique consists in pumping the excited term by a spectroscopic lamp and in recording the intensity variation of the resonantly scattered radiation as a function of the magnetic field strength. The knowledge of the magnetic field values corresponding to the intensity peaks allows one to recover the value of the fine-structure constants of the excited term.

Many different geometries can be envisaged to perform the experiment and, in some cases, it can be convenient to introduce polarizers in the path of either the incoming or the outgoing beam. The simplest geometry is that of forward scattering, schematically depicted in Fig. 10.23.

The signal $S_{\rm D}$ recorded by the detector can be easily obtained from Eqs. (10.151)-(10.152), using the values of the tensors $\mathcal{T}^K_Q$ given in Table 5.6 (with $\theta=\delta$, $\chi=0°$, $\gamma=0°$ both for the incident and for the scattered beam). Bearing in mind the properties of the symbol $W_{KK'Q}$ (see App. 14), we get

$$S_{\rm D} = k\left[1+\frac{1}{8}\left(3\cos^2\delta-1\right)^2 W_{220} + \frac{3}{2}\,\sin^2\delta\cos^2\delta\;\mathrm{Re}(W_{221}) + \frac{3}{8}\,\sin^4\delta\;\mathrm{Re}(W_{222})\right], \tag{10.157}$$

[1] Hyperfine structure is discussed in Sect. 10.22.

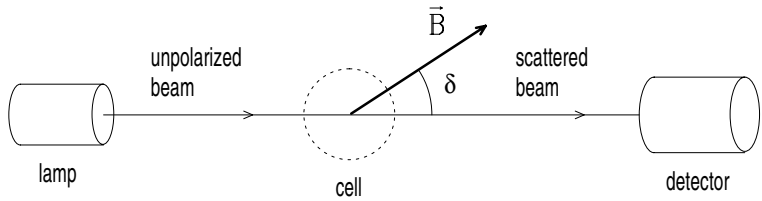

Fig.10.23. Schematic experimental set-up for measuring fine-structure constants via level-crossing interferences (Franken effect). The cell contains a vapor of the atomic species to be investigated. In practice, it is necessary to introduce a small tilt angle between the scattered and the incident beam to avoid contamination of the signal by direct incoming light.

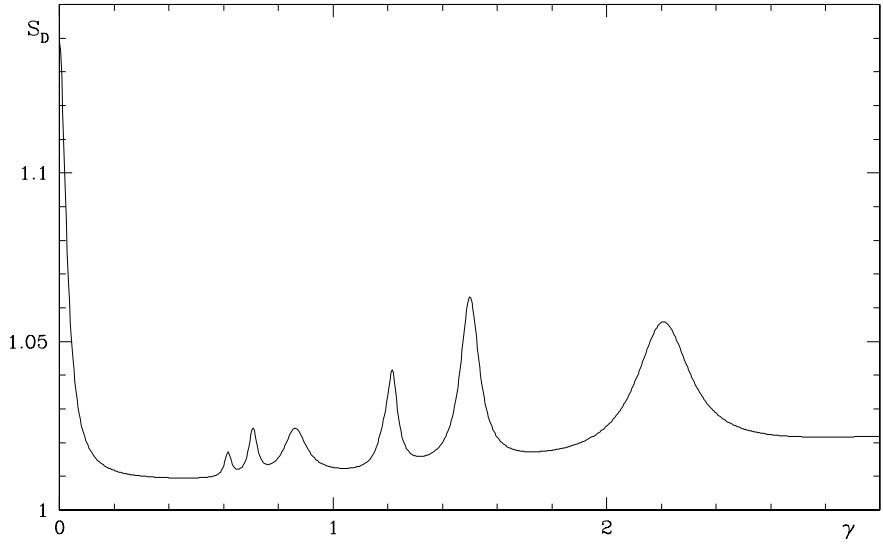

Fig.10.24. The signal $S_{\rm D}$ at the photodetector (in units of k) as a function of the magnetic field strength, for the scattering geometry of Fig.10.23. The resonant transition is $^3{\rm S}-{}^3{\rm P}$. The relevant parameters are $x = 10$, $\delta = 45°$.

where k is a constant proportional to the intensity of the incident radiation.

As an illustration, we show in Fig. 10.24 the signal $S_{\rm D}$ as a function of the magnetic field strength for the transition $^3{\rm S}-{}^3{\rm P}$ already considered in the previous section. The field strength is expressed in terms of γ, the parameter x is set to 10 (see Eqs. (10.154)), and the angle δ to 45° (or 135°). According to Eq. (10.157), both the interferences between sublevels with $\Delta M = 1$ (contained in W_{221}) and those between sublevels with $\Delta M = 2$ (contained in W_{222}) play a role.

Figure 10.24 shows the appearance of six distinct peaks (in addition to the 'standard' peak at $\gamma = 0$). Each of them corresponds to the crossing of a specific pair of M-sublevels with $\Delta M = 1$ or $\Delta M = 2$, in strict agreement with the results of Table 3.5. Notice that there is no peak at $\gamma = 0.45$ (at this γ value there is a crossing of two sublevels with $\Delta M = 3$), and that the peak at $\gamma \simeq 1.2$ corresponds in fact to two distinct crossings (with $\Delta M = 1$ and $\Delta M = 2$, respectively).

It is important to remark that the determination of fine-structure constants by the method described above requires that the intensity peaks corresponding to level crossings can be easily identified on a plot like that of Fig. 10.24. This means that the Einstein A coefficient of the transition must be sufficiently small compared to the fine-structure intervals ($h\,A \ll \zeta$, or $x \gg 1$, for a term satisfying the Landé interval rule).

The first application of this method dates back to 1959 (Colegrove et al., 1959) and led to the measurement of the fine structure of the term $2\,^3$P of HeI. In laboratory spectroscopy, the modulation of resonantly scattered radiation by level-crossing interferences is referred to as the *Franken effect* (Franken, 1961).

10.20. The Two-Term Atom: the Alignment-to-Orientation Conversion Mechanism

(*unpolarized lower term*)

The Hanle phase matrix for the two-term atom (Eq. (10.152)) differs radically from the corresponding matrix for the two-level atom (Eq. (10.33)) because of the double summation over K and K'. The presence of this double summation, together with the fact that the only non-zero components of the tensor $\mathcal{T}^K_Q(3,\vec{\Omega})$ are those with $K = 1$ (see Table 5.6), has important consequences on the circular polarization of the scattered radiation.

In a two-level atom, the only way to get frequency-integrated, circularly polarized scattered radiation is to irradiate the atom with circularly polarized light. This property is already contained in the classical expression of the scattering phase matrix (Eqs. (5.99)) and passes directly to the quantum-mechanical expression (Eq. (10.34)). It can be understood by observing that frequency-integrated circular polarization can be emitted in a given transition only if some *orientation* is present in the upper level (see Eq. (10.31)); on the other hand, orientation in the upper level of a two-level atom can only be produced by illuminating the atom with circularly polarized radiation.[1]

These properties are no longer valid for the two-term atom. Equation (10.150) shows, because of the presence of the summation over K', that orientation can be produced in the upper term even if no circular polarization is present in the incident radiation. This phenomenon has properly been called the *alignment-to-orientation conversion mechanism*[2] since the upper term has, so to say, the possibility of converting some 'alignment' present in the radiation field (the $K = 2$ components of the radiation field tensor) into atomic orientation (the $K = 1$ components of the statistical tensors).[3]

---

[1] An exception to this rule occurs in the presence of strong magnetic fields, provided the spectrum of the incident radiation satisfies suitable conditions (see Sect. 10.5 and Landi Degl'Innocenti, 1985b). Such peculiar situation is not considered in this section.

[2] This name was proposed by Kemp et al. (1984).

[3] Obviously, the component J^0_0 makes no contribution to the atomic orientation of the upper

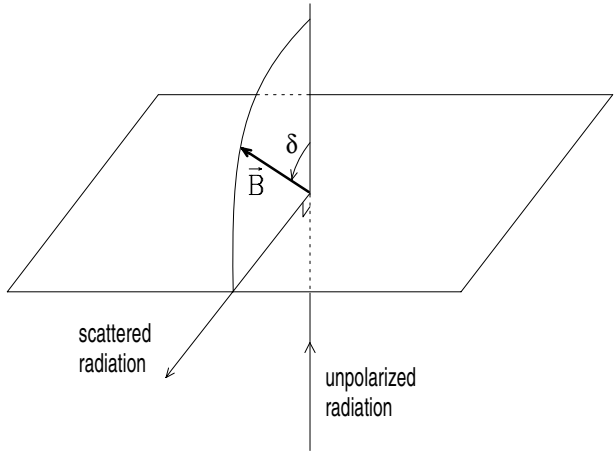

Fig.10.25. Scattering geometry for illustrating the alignment-to-orientation conversion mechanism. The magnetic field vector lies in the scattering plane.

In order to illustrate the phenomenon in a specific case, we consider the scattering of an unpolarized radiation beam for the transition $^3\mathrm{S} - {}^3\mathrm{P}$ (already used in the former sections) and the geometry of Fig. 10.25.[1] The frequency-integrated fractional circular polarization can be obtained from Eqs. (10.151)-(10.152) by substituting the values of the tensors $\mathcal{T}^K_Q$ given in Table 5.6 (with $\theta' = \delta$, $\chi' = 180°$, $\gamma' = 0°$; $\theta = 90° - \delta$, $\chi = \gamma = 0°$) and by using the properties of the symbols $W_{KK'Q}$ (see App. 14). We get

$$\tilde{p}_V = \frac{2\sin\delta\,\left[\sqrt{3}\,(3\cos^2\delta - 1)\,W_{120} - 6\cos^2\delta\ \mathrm{Re}(W_{121})\right]}{8 + (3\sin^2\delta - 1)(3\cos^2\delta - 1)\,W_{220} - 3\sin^2\delta\cos^2\delta\,\left[4\,\mathrm{Re}(W_{221}) - \mathrm{Re}(W_{222})\right]}.$$

Figure 10.26 shows $\tilde{p}_V$ as a function of γ, for $x = 10$ (see Eqs. (10.154)) and $\delta = 40°$. It is clear from the figure that the conversion mechanism is quite efficient especially at those magnetic field values corresponding to level crossings between pairs of M-sublevels with $\Delta M = 1$ (cf. Table 3.5).

The importance of this mechanism for broad-band circular polarization in stellar atmospheres has been discussed by Kemp et al. (1984). According to these authors, Lehmann (1964) was apparently the first to realize that excitation of atoms in a magnetic field by non-circularly polarized light could lead to atomic orientation. Some circular polarization *profiles* observed in the radiation from solar prominences have been interpreted by Landi Degl'Innocenti (1982b) on the basis of this mechanism (to obtain the line profile of the scattered radiation in the four

term (see Eq. (A14.5)).

[1] The scattered circular polarization $\tilde{p}_V$ for this transition has already been calculated for a slightly different geometry (see Eqs. (10.155)). The geometry of Fig. 10.25, with the magnetic field vector lying in the scattering plane, is more appropriate to illustrate the variation of $\tilde{p}_V$ with the field strength, since level crossings with $\Delta M = 1$ (contained in the factors $W_{KK'1}$) also come into play.

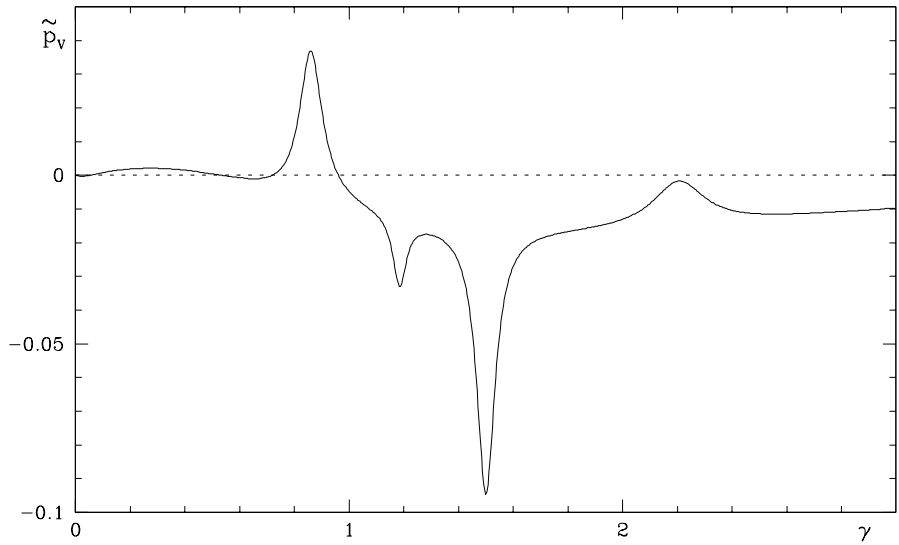

Fig.10.26. The frequency-integrated fractional circular polarization for the transition ${}^3\mathrm{S} - {}^3\mathrm{P}$ (with $x = 10$) and the scattering geometry of Fig.10.25 is plotted as a function of the magnetic field strength. The value of the angle δ is 40°.

Stokes parameters one should substitute the statistical tensors of Eq. (10.150) into the frequency-dependent expression of the emission coefficient, Eq. (7.47e)).

It should be remarked that the 'opposite' of the alignment-to-orientation conversion mechanism exists as well. Such mechanism, that can be named *orientation-to-alignment conversion*, is responsible for the appearance of an additional contribution to the linear polarization of scattered radiation when the atom is irradiated by circularly polarized light.

10.21. The Two-Term Atom: the Role of Lower-Term Polarization

(*cylindrical symmetry - no magnetic field - no stimulated emission*)

The results obtained in Sects. 10.16-10.20 are based on the hypothesis that no atomic polarization is present in the lower term. If we want to release this hypothesis, we have to go back to the statistical equilibrium equations (10.115) and (10.116) established in Sect. 10.15. In the general case (arbitrary radiation field, presence of a magnetic field) these equations are rather involved. In this section we confine attention to a particularly simple, yet illuminating case.

Similarly to Sect. 10.7, we assume that the incident radiation field – besides satisfying the flat-spectrum approximation, see Sect. 10.15 – is unpolarized and cylindrically symmetrical about a fixed direction, which we take as the z-axis of our reference system: this means that the only non-zero components of the radiation field tensor are $J^0_0(\nu_{\beta_u L_u S, \beta_\ell L_\ell S})$ and $J^2_0(\nu_{\beta_u L_u S, \beta_\ell L_\ell S})$. We also assume that the

magnetic field is zero and that stimulation effects are negligible.

The first two assumptions (concerning the incident radiation and the magnetic field) lead to the considerable simplification that, in stationary situations, the only non-vanishing statistical tensors $\rho^K_Q(J,J')$ are those with K even and $Q=0$. The proof of this property is quite similar to that given in Sect. 10.7, because the spontaneous emission rates $\mathbb{T}_{\rm E}$, $\mathbb{R}_{\rm E}$ (Eqs. (7.45b) and (7.46b)) are proportional to $\delta_{KK'}\,\delta_{QQ'}$, and the expressions of the absorption rates $\mathbb{T}_{\rm A}$, $\mathbb{R}_{\rm A}$ (Eqs. (7.45a) and (7.46a)) contain a 3-j symbol of the form (10.58); on the other hand, the kernel N defined in Eq. (7.41) is also proportional to $\delta_{KK'}\,\delta_{QQ'}$ for zero magnetic field.

An obvious consequence of this property is that the number of equations (and of unknowns) is largely reduced. Such number is given by[1]

$$N_{\rm eq} = n(L_u,S) + n(L_\ell,S)\;, \tag{10.158}$$

where $n(L,S)$, the number of statistical tensors of the form ${}^{\beta LS}\rho^K_Q(J,J')$ with K even and $Q=0$, can be written in the form

$$n(L,S) = \frac{1}{6}\big(J_> - J_<\big)\big(2J_>^2 + 2J_>J_< - 4J_<^2 + 6J_> + 6J_< + 1\big) + J_> + \xi\;,$$

where

$$J_> = L+S\;, \qquad J_< = |L-S|\;, \qquad \xi = \begin{cases} 1 & \text{if } S \text{ is an integer} \\ \frac{1}{2} & \text{if } S \text{ is a half-integer}\;. \end{cases}$$

Under the above assumptions, the statistical equilibrium equations (10.115) and (10.116) reduce to the following (see Eqs. (7.41), (7.45b) and (7.46b))

$$\begin{aligned}
\frac{\rm d}{{\rm d}t}\,{}^{\beta_u L_u S}\rho^K_0(J_u,J'_u) &= -\Big[A(\beta_u L_u S \to \beta_\ell L_\ell S) + 2\pi{\rm i}\,\nu_{\beta_u L_u S J_u,\,\beta_u L_u S J'_u}\Big]\,{}^{\beta_u L_u S}\rho^K_0(J_u,J'_u) \\
&\quad + \sum_{K'\,\text{even}}\;\sum_{J_\ell J'_\ell} \mathbb{T}_{\rm A}(\beta_u L_u S K 0 J_u J'_u, \beta_\ell L_\ell S K' 0 J_\ell J'_\ell)\,{}^{\beta_\ell L_\ell S}\rho^{K'}_0(J_\ell,J'_\ell) \\
\frac{\rm d}{{\rm d}t}\,{}^{\beta_\ell L_\ell S}\rho^K_0(J_\ell,J'_\ell) &= -2\pi{\rm i}\,\nu_{\beta_\ell L_\ell S J_\ell,\,\beta_\ell L_\ell S J'_\ell}\;{}^{\beta_\ell L_\ell S}\rho^K_0(J_\ell,J'_\ell) \\
&\quad + \sum_{J_u J'_u} \mathbb{T}_{\rm E}(\beta_\ell L_\ell S K 0 J_\ell J'_\ell, \beta_u L_u S K 0 J_u J'_u)\,{}^{\beta_u L_u S}\rho^K_0(J_u,J'_u) \\
&\quad - \sum_{K'\,\text{even}}\;\sum_{J''_\ell J'''_\ell} \mathbb{R}_{\rm A}(\beta_\ell L_\ell S K 0 J_\ell J'_\ell K' 0 J''_\ell J'''_\ell)\,{}^{\beta_\ell L_\ell S}\rho^{K'}_0(J''_\ell,J'''_\ell)\;,
\end{aligned} \tag{10.159}$$

where K is even and the Bohr frequencies are defined in Eq. (7.43). The expressions of the rates $\mathbb{T}_{\rm A}$, $\mathbb{T}_{\rm E}$, $\mathbb{R}_{\rm A}$ are easily derived from Eqs. (7.45a,b) and (7.46a) with the

[1] Because of the conjugation property (3.100), $N_{\rm eq}$ also represents the number of *real* unknowns of the algebraic system.

help of Eqs. (2.26a), (2.36a) and (2.49)

$$\mathbb{T}_{\rm A}(\beta_u L_u S K 0 J_u J'_u, \beta_\ell L_\ell S K' 0 J_\ell J'_\ell) = (2L_\ell + 1)\, B(\beta_\ell L_\ell S \to \beta_u L_u S)$$
$$\times \sqrt{(2J_u+1)(2J'_u+1)(2J_\ell+1)(2J'_\ell+1)} \begin{Bmatrix} L_u & L_\ell & 1 \\ J_\ell & J_u & S \end{Bmatrix} \begin{Bmatrix} L_u & L_\ell & 1 \\ J'_\ell & J'_u & S \end{Bmatrix}$$
$$\times \Bigg[\delta_{KK'}\, (-1)^{1+J'_\ell+J'_u} \begin{Bmatrix} J_u & J'_u & K \\ J'_\ell & J_\ell & 1 \end{Bmatrix} J_0^0(\nu_{\beta_u L_u S, \beta_\ell L_\ell S})$$
$$+ \sqrt{15(2K+1)(2K'+1)}\ (-1)^{J'_\ell - J_\ell} \begin{Bmatrix} J_u & J_\ell & 1 \\ J'_u & J'_\ell & 1 \\ K & K' & 2 \end{Bmatrix} \begin{pmatrix} K & K' & 2 \\ 0 & 0 & 0 \end{pmatrix}$$
$$\times J_0^2(\nu_{\beta_u L_u S, \beta_\ell L_\ell S}) \Bigg]$$

$$\mathbb{T}_{\rm E}(\beta_\ell L_\ell S K 0 J_\ell J'_\ell, \beta_u L_u S K 0 J_u J'_u) = (2L_u + 1)\, A(\beta_u L_u S \to \beta_\ell L_\ell S)$$
$$\times \sqrt{(2J_\ell+1)(2J'_\ell+1)(2J_u+1)(2J'_u+1)}\ (-1)^{1+J'_\ell+J'_u}$$
$$\times \begin{Bmatrix} J_\ell & J'_\ell & K \\ J'_u & J_u & 1 \end{Bmatrix} \begin{Bmatrix} L_u & L_\ell & 1 \\ J_\ell & J_u & S \end{Bmatrix} \begin{Bmatrix} L_u & L_\ell & 1 \\ J'_\ell & J'_u & S \end{Bmatrix}$$

$$\mathbb{R}_{\rm A}(\beta_\ell L_\ell S K 0 J_\ell J'_\ell K' 0 J''_\ell J'''_\ell) = (2L_\ell + 1)\, B(\beta_\ell L_\ell S \to \beta_u L_u S)$$
$$\times \Bigg\{ \delta_{KK'}\, \delta_{J_\ell J''_\ell}\, \delta_{J'_\ell J'''_\ell}\, \frac{1}{2L_\ell + 1}\, J_0^0(\nu_{\beta_u L_u S, \beta_\ell L_\ell S})$$
$$+ \sqrt{15(2K+1)(2K'+1)}\ (-1)^{1+L_u-S+J_\ell} \begin{Bmatrix} L_\ell & L_\ell & 2 \\ 1 & 1 & L_u \end{Bmatrix} \begin{pmatrix} K & K' & 2 \\ 0 & 0 & 0 \end{pmatrix}$$
$$\times \frac{1}{2} \Bigg[\delta_{J_\ell J''_\ell} \sqrt{(2J'_\ell+1)(2J'''_\ell+1)} \begin{Bmatrix} L_\ell & L_\ell & 2 \\ J'''_\ell & J'_\ell & S \end{Bmatrix} \begin{Bmatrix} K & K' & 2 \\ J'''_\ell & J'_\ell & J_\ell \end{Bmatrix}$$
$$+ \delta_{J'_\ell J'''_\ell} \sqrt{(2J_\ell+1)(2J''_\ell+1)}\, (-1)^{J''_\ell - J'_\ell} \begin{Bmatrix} L_\ell & L_\ell & 2 \\ J''_\ell & J_\ell & S \end{Bmatrix} \begin{Bmatrix} K & K' & 2 \\ J''_\ell & J_\ell & J'_\ell \end{Bmatrix} \Bigg]$$
$$\times J_0^2(\nu_{\beta_u L_u S, \beta_\ell L_\ell S}) \Bigg\}\,.$$

Equation (10.159) can be cast in dimensionless form by dividing both sides by the Einstein coefficient $A(\beta_u L_u S \to \beta_\ell L_\ell S)$ and by introducing the parameters

$$\frac{(2L_\ell + 1)\, B(\beta_\ell L_\ell S \to \beta_u L_u S)}{(2L_u + 1)\, A(\beta_u L_u S \to \beta_\ell L_\ell S)}\, J_0^0(\nu_{\beta_u L_u S, \beta_\ell L_\ell S}) =$$
$$= \frac{c^2}{2h\, \nu^3_{\beta_u L_u S, \beta_\ell L_\ell S}}\, J_0^0(\nu_{\beta_u L_u S, \beta_\ell L_\ell S}) = \bar{n}\,,$$

$$\frac{J^2_0(\nu_{\beta_u L_u S,\,\beta_\ell L_\ell S})}{J^0_0(\nu_{\beta_u L_u S,\,\beta_\ell L_\ell S})} = \frac{w}{\sqrt{2}} \tag{10.160}$$

(Eqs. (7.33) have been used in the first relation). The quantities $\bar{n}$ and w – already introduced in Sect. 10.7 – represent the solid-angle average of the number of photons per mode and the anisotropy factor at the transition frequency, respectively. If both the upper and lower term satisfy the Landé interval rule (Eq. (10.140)), we can also introduce the parameters

$$\frac{\pi\,\zeta(\beta_u L_u S)}{h\,A(\beta_u L_u S \to \beta_\ell L_\ell S)} = x_u \ ,$$

$$\frac{\pi\,\zeta(\beta_\ell L_\ell S)}{h\,B(\beta_\ell L_\ell S \to \beta_u L_u S)\;J^0_0(\nu_{\beta_u L_u S,\,\beta_\ell L_\ell S})} =$$
$$= \frac{2L_\ell + 1}{2L_u + 1}\;\frac{\pi\,\zeta(\beta_\ell L_\ell S)}{h\,\bar{n}\;A(\beta_u L_u S \to \beta_\ell L_\ell S)} = x_\ell \ , \tag{10.161}$$

which represent the ratios of the typical fine-structure splitting of the upper and lower term, respectively, to the corresponding inverse lifetime. The parameter x_u has already been used in former sections (see Eq. (10.142)).

Let us apply Eqs. (10.159) to the simplest transition where lower-term atomic polarization (including coherences between different J-levels) plays a role: this is the transition between a lower term ^{2}P and an upper term ^{2}S. The statistical tensors involved are six; introducing shorthand notations, they can be written in the form

$$^{u}\rho^0_0\Big(\frac{1}{2},\frac{1}{2}\Big) = \mathtt{x} \qquad {}^{\ell}\rho^0_0\Big(\frac{3}{2},\frac{3}{2}\Big) = \mathtt{z} \qquad {}^{\ell}\rho^2_0\Big(\frac{1}{2},\frac{3}{2}\Big) = \mathtt{u} + \mathrm{i}\,\mathtt{v}$$
$$^{\ell}\rho^0_0\Big(\frac{1}{2},\frac{1}{2}\Big) = \mathtt{y} \qquad {}^{\ell}\rho^2_0\Big(\frac{3}{2},\frac{3}{2}\Big) = \mathtt{t} \qquad {}^{\ell}\rho^2_0\Big(\frac{3}{2},\frac{1}{2}\Big) = -\mathtt{u} + \mathrm{i}\,\mathtt{v} \ ,$$

where $\mathtt{x}$, $\mathtt{y}$, $\mathtt{z}$, $\mathtt{t}$, $\mathtt{u}$, $\mathtt{v}$ are real. We assume that the lower term satisfies the Landé interval rule, so that the quantity x_ℓ defined in Eq. (10.161) can be used. After some calculations, involving the numerical evaluation of several 3-j, 6-j, and 9-j symbols, we obtain the set of equations

$$\frac{1}{A(u \to \ell)}\;\frac{\mathrm{d}}{\mathrm{d}t}\,\mathtt{x} = -\mathtt{x} + \frac{1}{3}\,\bar{n}\,\mathtt{y} + \frac{\sqrt{2}}{3}\,\bar{n}\,\mathtt{z} + \frac{\sqrt{2}}{6}\,\bar{n}w\,\mathtt{t} - \frac{\sqrt{2}}{3}\,\bar{n}w\,\mathtt{u}$$

$$\frac{1}{A(u \to \ell)}\;\frac{\mathrm{d}}{\mathrm{d}t}\,\mathtt{y} = \frac{1}{3}\,\mathtt{x} - \frac{1}{3}\,\bar{n}\,\mathtt{y} + \frac{\sqrt{2}}{6}\,\bar{n}w\,\mathtt{u}$$

$$\frac{1}{A(u \to \ell)}\;\frac{\mathrm{d}}{\mathrm{d}t}\,\mathtt{z} = \frac{\sqrt{2}}{3}\,\mathtt{x} - \frac{1}{3}\,\bar{n}\,\mathtt{z} - \frac{1}{6}\,\bar{n}w\,\mathtt{t} + \frac{1}{6}\,\bar{n}w\,\mathtt{u}$$

$$\frac{1}{A(u \to \ell)}\;\frac{\mathrm{d}}{\mathrm{d}t}\,\mathtt{t} = -\frac{1}{6}\,\bar{n}w\,\mathtt{z} - \frac{1}{3}\,\bar{n}\,\mathtt{t} - \frac{1}{6}\,\bar{n}w\,\mathtt{u}$$

$$\frac{1}{A(u\to\ell)}\,\frac{\mathrm{d}}{\mathrm{d}t}\,\mathtt{u}=\frac{\sqrt{2}}{12}\,\bar{n}w\,\mathtt{y}+\frac{1}{12}\,\bar{n}w\,\mathtt{z}-\frac{1}{12}\,\bar{n}w\,\mathtt{t}-\frac{1}{12}\,\bar{n}(4-w)\,\mathtt{u}-\bar{n}\,x_\ell\,\mathtt{v}$$

$$\frac{1}{A(u\to\ell)}\,\frac{\mathrm{d}}{\mathrm{d}t}\,\mathtt{v}=\bar{n}\,x_\ell\,\mathtt{u}-\frac{1}{12}\,\bar{n}(4-w)\,\mathtt{v}\;, \tag{10.162}$$

and the trace equation (see Eq. (10.118))

$$\sqrt{2}\,\mathtt{x}+\sqrt{2}\,\mathtt{y}+2\,\mathtt{z}=1\;.$$

The expressions of the statistical tensors corresponding to the stationary situation are found to be[1]

$${}^{\ell}\rho_0^0\Big(\frac{1}{2},\frac{1}{2}\Big)=\frac{1}{\sqrt{2}}\,(4-w^2)\Big[(4-w)^2+144\,x_\ell^2\Big]\,/\Delta$$

$${}^{\ell}\rho_0^0\Big(\frac{3}{2},\frac{3}{2}\Big)=\Big[(4-w)^2\,(4-w^2)+576\,x_\ell^2\Big]\,/\Delta$$

$${}^{\ell}\rho_0^2\Big(\frac{3}{2},\frac{3}{2}\Big)=-w\Big[(4-w)^2\,(2+w)+288\,x_\ell^2\Big]\,/\Delta$$

$${}^{\ell}\rho_0^2\Big(\frac{1}{2},\frac{3}{2}\Big)=w(4-w)(2+w)\Big[4-w+12\,\mathrm{i}\,x_\ell\Big]\,/\Delta$$

$${}^{u}\rho_0^0\Big(\frac{1}{2},\frac{1}{2}\Big)=\frac{1}{\sqrt{2}}\,\bar{n}(2+w)\Big[(4-w)^2\,(2+w)(1-w)+144(2-w)\,x_\ell^2\Big]\,/\Delta\;, \tag{10.163}$$

where

$$\Delta=(4-w)^2\,(2+w)\Big[3(2-w)+\bar{n}(1-w)(2+w)\Big]$$
$$+144\Big[12-w^2+\bar{n}(4-w^2)\Big]\,x_\ell^2\;.$$

These equations show that the interference term, ${}^{\ell}\rho_0^2(1/2,3/2)$, decreases with increasing x_ℓ and tends to zero for $x_\ell\to\infty$. Under this limit, the two-term atom considered here reduces to a special case of the three-level atom examined in Sect. 10.12 (two lower 'uncorrelated' levels with $J=1/2$ and $J=3/2$ respectively, one upper level with $J=1/2$). It can be easily seen that the results there obtained (Eqs. (10.89a-c)), once adapted to the present case by the substitutions

$$\bar{n}_{\mathrm{ca}}\to\bar{n}\;,\qquad \bar{n}_{\mathrm{cb}}\to\bar{n}\;,\qquad w_{\mathrm{cb}}\to w\;,\qquad \delta_{\mathrm{b}}^{(2)}\to 0\;,$$

coincide with those derived from Eqs. (10.163) for $x_\ell\to\infty$.

[1] It can easily be shown that the determinant of the (algebraic) system (10.162) is zero – cf. footnote on p.582.

On the other hand, for $x_\ell \to 0$ the interference term is comparable with the other statistical tensors. Under this limit, the J-levels of the lower term are degenerate and one can apply the principle of spectroscopic stability (see Sect. 7.10). The statistical tensors of the lower and upper term (now considered as spinless terms) can be derived from Eq. (3.105). Bearing in mind Eq. (3.100), we obtain

$$
{}^{\ell}\rho^0_0(L=1) = \frac{\sqrt{3}\,(2-w)}{3(2-w)+\bar{n}(1-w)(2+w)}
$$

$$
{}^{\ell}\rho^2_0(L=1) = -\frac{\sqrt{6}\,w}{3(2-w)+\bar{n}(1-w)(2+w)}
$$

$$
{}^{u}\rho^0_0(L=0) = \frac{\bar{n}(1-w)(2+w)}{3(2-w)+\bar{n}(1-w)(2+w)}\ .
$$

These results are in agreement with those obtained in Sect. 10.7 for the two-level atom with $J_\ell = 1$, $J_u = 0$ (cf. Eqs. (10.64) with $\delta^{(2)}_\ell = 0$).

Equations (10.163) show that the statistical tensors of both the lower and the upper term are strongly sensitive to the value of x_ℓ. It should be remarked, however, that the quantity x_ℓ is fairly large for most fine-structure multiplets under typical astrophysical or laboratory conditions (where the radiation field is very diluted, $\bar{n} \ll 1$). As an example, we can consider the MgI triplet at $\lambda \simeq 5170\,\text{Å}$. The lower term is a ^{3}P whereas the upper term is a ^{3}S. The three lines of the multiplet – named b_1, b_2, and b_4, respectively – lie at 5183.6 Å ($J_\ell = 2, J_u = 1$), 5172.7 Å ($J_\ell = 1, J_u = 1$), and 5167.3 Å ($J_\ell = 0, J_u = 1$). The quantity ζ/h for the lower term is approximately $6 \times 10^{11}\,\text{s}^{-1}$ (see Eq. (10.140)), and the Einstein A coefficient is $1.04 \times 10^8\,\text{s}^{-1}$. Assuming $\bar{n} \simeq 10^{-2}$ (typical of the solar atmosphere), we get $x_\ell \simeq 5 \times 10^6$, which means that coherences between different J-levels of the lower term are 6 to 7 orders of magnitude smaller than the 'diagonal' statistical tensors. In particular, the atomic polarization of the upper term (hence scattering polarization) is practically unaffected by lower-term interferences.

The simple transition $^2\text{P}-^2\text{S}$ discussed above requires the solution of an algebraic system of 6 equations. For more complicated transitions, it is almost mandatory to resort to a numerical solution of the statistical equilibrium equations (10.159). The Stokes parameters of the scattered radiation can then be obtained by substituting the values of the statistical tensors of the upper term into Eq. (10.127).

In the following we illustrate the results of such numerical calculations for two different multiplets, multiplet UV n. 1 of FeII ($^6\text{D} - {}^6\text{D}$) – already considered in Sect. 10.17 – and multiplet n. 2 of MgI ($^3\text{P} - {}^3\text{S}$). According to Eq. (10.158), the corresponding algebraic systems contain 110 and 12 equations, respectively. In both cases we refer to the 90° scattering of an unpolarized radiation beam (Fig. 10.1 with $\Theta = 90°$): the anisotropy factor w is unity, and the fractional polarization of the scattered radiation is independent of the average number of photons $\bar{n}$ provided $\bar{n} \ll 1$ (which is implicit in Eqs. (10.159) since stimulated emission is neglected).[1]

[1] In fact it can be shown, bearing in mind the structure of Eqs. (10.159) and the expressions of

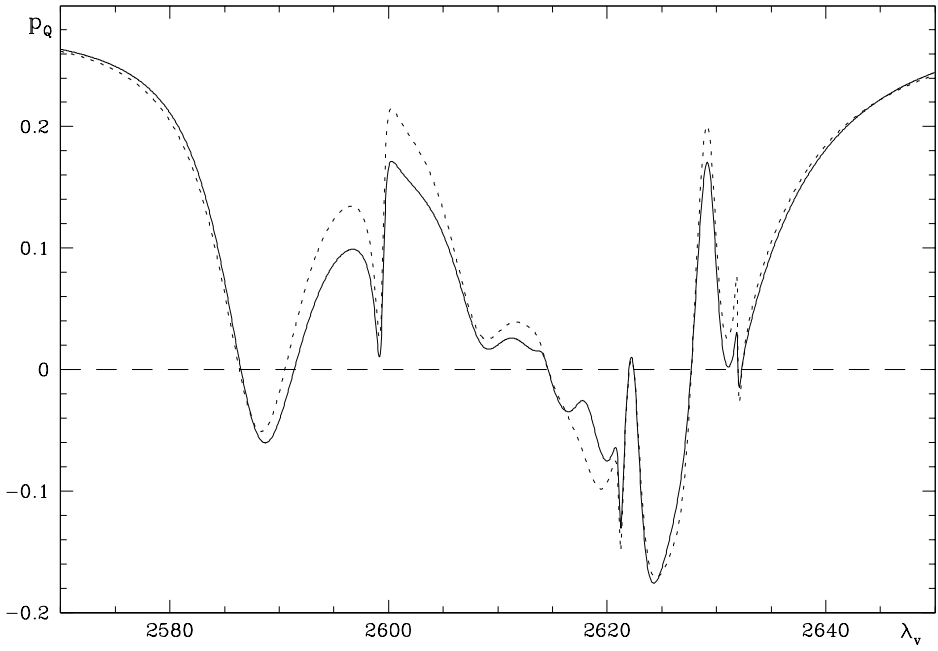

Fig.10.27. Fractional polarization p_Q against vacuum wavelength λ_v (in Å) in the 90° scattering of an unpolarized radiation beam, for multiplet UV n.1 of FeII. The reference direction for linear polarization is the perpendicular to the scattering plane. The solid line is obtained by taking lower-term atomic polarization into account, the dashed line (identical to the curve in Fig.10.18) by neglecting it.

Figures 10.27 and 10.28 show the fractional linear polarization p_Q as a function of wavelength in the two multiplets. For the multiplet of FeII the results are not very different from those obtained in the absence of lower-term polarization. On the contrary, there is a dramatic effect for the multiplet of MgI. The fractional polarization has a complicated wavelength dependence, with a peak value of almost 40% (in absolute value): if lower-term atomic polarization were neglected, p_Q would be zero at all wavelengths.[1]

the radiative rates, that the statistical tensors of the upper term are proportional to $\bar{n}$ provided $\bar{n}$ is much smaller than the ratio between the typical fine-structure splitting of the lower term and the Einstein A coefficient.

[1] This is easily verified from Eq. (10.129). The only non-zero components of the tensor $\mathcal{T}^K_Q(1,\vec{\Omega})$ have $K=2$ (see Table 5.6), and the 6-j symbol

$$\left\{ \begin{array}{ccc} 1 & 1 & K \\ L_u & L_u & L_\ell \end{array} \right\}$$

is zero for $L_u = 0$ and $K = 2$. Note that the same symbol appears in Eq. (10.126), which means that there is no atomic polarization in the upper term ^{3}S.

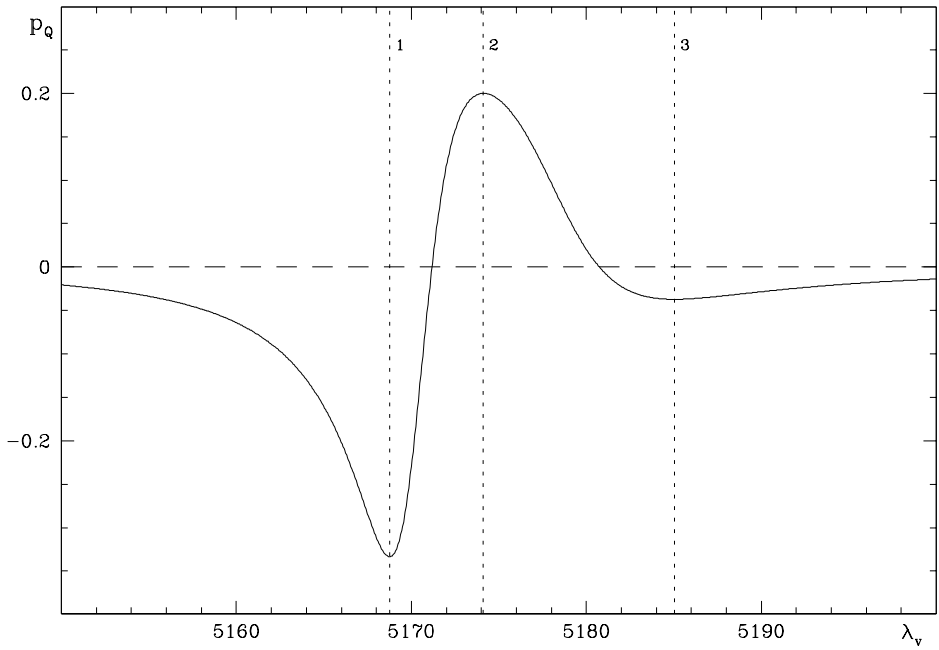

Fig.10.28. Same as Fig.10.27 for multiplet n.2 of MgI. The vertical lines mark the wavelength positions of the three lines of the multiplet according to the code: 1) $J_\ell = 0, J_u = 1$ (b_4 line); 2) $J_\ell = 1, J_u = 1$ (b_2 line); 3) $J_\ell = 2, J_u = 1$ (b_1 line). Atomic data are from Moore (1949). The value of the Einstein A coefficient is $1.04 \times 10^8\ \mathrm{s}^{-1}$.

10.22. The Two-Level Atom with Hyperfine Structure

As remarked in Sect. 7.9, the statistical equilibrium equations for the multi-level atom with hyperfine structure bear a very strong resemblance to the corresponding equations for the multi-term atom, and the same holds for the expressions of the radiative transfer coefficients. Most of the results obtained in this chapter for the two-term atom can thus be extended to the two-level atom with hyperfine structure by means of simple, formal transformations.

Let us consider a simplified atomic model consisting of two levels, a lower level having quantum numbers (α_ℓ, J_ℓ) and an upper level having quantum numbers (α_u, J_u). If the atom has nuclear spin I, both levels are split into a collection of hyperfine components characterized by the total angular momentum F_ℓ (for the lower level) and F_u (for the upper level). When a magnetic field is present, the F-levels are further split into their magnetic components as fully explained in Sect. 3.5.

For this model atom, we can study the problem of resonance scattering under the flat-spectrum approximation and the unpolarized lower level assumption. The relevant equations are readily obtained by carrying out the formal substitutions

$$\begin{array}{lll} \beta_\ell \to \alpha_\ell & \beta_u \to \alpha_u & S \to I \\ L_\ell \to J_\ell & L_u \to J_u & \\ J_\ell \to F_\ell & J_u \to F_u & \end{array} \tag{10.164}$$

on the corresponding equations of Sect. 10.16.

Consider for instance the expression of the frequency-integrated absorption coefficient. According to Eqs. (10.164), the quantity $k^{\rm A}_{\rm M}$ defined in Eq. (10.128) transforms into[1]

$$\frac{h\,\nu_{\alpha_u J_u,\,\alpha_\ell J_\ell}}{4\pi}\,\mathcal{N}_\ell\,B(\alpha_\ell J_\ell \to \alpha_u J_u)\;,$$

which is just the frequency-integrated absorption coefficient in the line, $k^{\rm A}_{\rm L}$, defined in Eq. (9.5).

Similarly, from Eqs. (10.131)-(10.133) we obtain the expression of the frequency-integrated emission coefficient

$$\tilde{\varepsilon}_i(\vec{\Omega}) = k^{\rm A}_{\rm L} \oint \frac{{\rm d}\Omega'}{4\pi} \sum_{j=0}^{3} \left[P_{ij}(\vec{\Omega},\vec{\Omega}')\right]_{\rm hfs}\; I_j(\nu_{\alpha_u J_u,\,\alpha_\ell J_\ell},\vec{\Omega}')\;,$$

where $[P_{ij}(\vec{\Omega},\vec{\Omega}')]_{\rm hfs}$, the hyperfine-structure scattering matrix, is given by

$$\left[P_{ij}(\vec{\Omega},\vec{\Omega}')\right]_{\rm hfs} = \sum_{KQ} \left[W_K(\alpha_\ell J_\ell I \alpha_u J_u)\right]_{\rm hfs}\; (-1)^Q\, \mathcal{T}^K_Q(i,\vec{\Omega})\, \mathcal{T}^K_{-Q}(j,\vec{\Omega}')\;,$$

with

$$\begin{aligned} \left[W_K(\alpha_\ell J_\ell I \alpha_u J_u)\right]_{\rm hfs} &= \frac{3(2J_u+1)}{2I+1} \\ &\times \sum_{F_u F'_u} (2F_u+1)(2F'_u+1) \left\{ \begin{array}{ccc} 1 & 1 & K \\ J_u & J_u & J_\ell \end{array} \right\}^2 \left\{ \begin{array}{ccc} J_u & J_u & K \\ F_u & F'_u & I \end{array} \right\}^2 \\ &\times \frac{1}{1 + 2\pi{\rm i}\,\nu_{\alpha_u J_u I F'_u,\,\alpha_u J_u I F_u} \,/\, A(\alpha_u J_u \to \alpha_\ell J_\ell)}\;, \end{aligned}$$

where the Bohr frequency $\nu_{\alpha_u J_u I F'_u,\,\alpha_u J_u I F_u}$ is given by Eq. (7.67).

It is also possible to define the depolarizing factors due to hyperfine structure. From Eqs. (10.135)-(10.136) we have

$$\left[W_K(\alpha_\ell J_\ell I \alpha_u J_u)\right]_{\rm hfs} = W_K(J_\ell, J_u)\; \left[D_K(\alpha_u J_u I)\right]_{\rm hfs}\;,$$

[1] Following the formalism of Sect. 7.9, we omit the index I when inessential.

where

$$\left[D_K(\alpha JI)\right]_{\rm hfs} = \frac{1}{2I+1}\sum_{FF'}(2F+1)(2F'+1)\left\{\begin{array}{ccc} J & J & K \\ F & F' & I \end{array}\right\}^2 \times \frac{1}{1+2\pi{\rm i}\,\nu_{\alpha JIF',\,\alpha JIF}\,/\,A(\alpha J\rightarrow\alpha_\ell J_\ell)}\,.$$

The properties of the depolarizing factors are strictly similar to those of their fine-structure analogues (cf. Eqs. (10.137)-(10.142)):

a) If the hyperfine-structure intervals of the upper level are much smaller than the Einstein A coefficient, the depolarizing factors reduce to unity.

b) If such intervals are much larger than A, they tend to the asymptotic values

$$\left[D_K^\infty(JI)\right]_{\rm hfs} = \frac{1}{2I+1}\sum_{F}(2F+1)^2\left\{\begin{array}{ccc} J & J & K \\ F & F & I \end{array}\right\}^2\,.$$

Numerical values of $[D_1^\infty]_{\rm hfs}$ and $[D_2^\infty]_{\rm hfs}$ for half-integral values of J are given in Table 10.8 (the table is restricted to $I \leq 9/2$, $J \leq 15/2$). For integral values of J one can directly use Table 10.6, taking into account the formal identity of $[D_K^\infty(JI)]_{\rm hfs}$ and $[D_K^\infty(LS)]_{\rm fs}$ under the substitution $J \rightarrow L$, $I \rightarrow S$.

c) If the hyperfine-structure intervals of the upper level are simply described by the magnetic-dipole term, one has (see Eqs. (3.70))

$$\nu_{\alpha JIF',\,\alpha JIF} = \frac{1}{2h}\,\mathcal{A}(\alpha,J,I)\,\left[F'(F'+1)-F(F+1)\right]\,,$$

and the depolarizing factor can be written in the form

$$\left[D_K(\alpha JI)\right]_{\rm hfs} = \frac{1}{2I+1}\sum_{FF'}(2F+1)(2F'+1)\left\{\begin{array}{ccc} J & J & K \\ F & F' & I \end{array}\right\}^2 \times \frac{1}{1+x^2\left[F'(F'+1)-F(F+1)\right]^2}\,,$$

where x is given by

$$x = \frac{\pi\,\mathcal{A}(\alpha,J,I)}{h\,A(\alpha J\rightarrow\alpha_\ell J_\ell)}\,. \qquad (10.165)$$

The full frequency-dependent emission coefficient is given by the following expression, obtained by carrying out the formal transformations (10.164) on Eq. (10.129)

TABLE 10.8

Values of the depolarizing factors $[D_K^\infty(JI)]_{\rm hfs}$ for levels with half-integral J quantum number

I	J	D_1^∞	D_2^∞	I	J	D_1^∞	D_2^∞	I	J	D_1^∞	D_2^∞
1/2	1/2	0.5	0.	2	1/2	0.36	0.	7/2	1/2	0.344	0.
	3/2	0.875	0.625		3/2	0.433	0.247		3/2	0.37	0.219
	5/2	0.944	0.833		5/2	0.617	0.266		5/2	0.418	0.237
	7/2	0.969	0.906		7/2	0.768	0.444		7/2	0.5	0.258
	9/2	0.98	0.94		9/2	0.847	0.600		9/2	0.637	0.290
	11/2	0.986	0.958		11/2	0.892	0.705		11/2	0.735	0.399
	13/2	0.990	0.969		13/2	0.920	0.776		13/2	0.800	0.508
	15/2	0.992	0.977		15/2	0.939	0.825		15/2	0.844	0.597
1	1/2	0.407	0.	5/2	1/2	0.352	0.	4	1/2	0.342	0.
	3/2	0.692	0.293		3/2	0.400	0.233		3/2	0.362	0.215
	5/2	0.856	0.609		5/2	0.5	0.262		5/2	0.399	0.229
	7/2	0.918	0.766		7/2	0.677	0.321		7/2	0.457	0.248
	9/2	0.947	0.847		9/2	0.783	0.474		9/2	0.564	0.254
	11/2	0.963	0.892		11/2	0.846	0.599		11/2	0.674	0.324
	13/2	0.973	0.920		13/2	0.885	0.689		13/2	0.751	0.425
	15/2	0.979	0.938		15/2	0.911	0.754		15/2	0.805	0.519
3/2	1/2	0.375	0.	3	1/2	0.347	0.	9/2	1/2	0.34	0.
	3/2	0.5	0.27		3/2	0.382	0.224		3/2	0.356	0.212
	5/2	0.743	0.395		5/2	0.448	0.247		5/2	0.385	0.224
	7/2	0.85	0.603		7/2	0.583	0.258		7/2	0.430	0.239
	9/2	0.902	0.729		9/2	0.712	0.366		9/2	0.5	0.256
	11/2	0.932	0.806		11/2	0.793	0.494		11/2	0.612	0.274
	13/2	0.950	0.854		13/2	0.845	0.598		13/2	0.700	0.354
	15/2	0.961	0.887		15/2	0.880	0.677		15/2	0.763	0.445

$$
\begin{aligned}
\varepsilon_i(\nu,\vec{\Omega}) = k_{\rm L}^{\rm A}\,\frac{2J_u+1}{2I+1}\sum_{KQ}\sum_{F_uF_u'F_\ell}(-1)^{I-J_\ell+F_u+F_u'+F_\ell+K+Q}\\
\times 3(2F_u+1)(2F_u'+1)(2F_\ell+1)\begin{Bmatrix} J_u & J_\ell & 1\\ F_\ell & F_u & I\end{Bmatrix}\begin{Bmatrix} J_u & J_\ell & 1\\ F_\ell & F_u' & I\end{Bmatrix}\\
\times\begin{Bmatrix} 1 & 1 & K\\ F_u & F_u' & F_\ell\end{Bmatrix}\begin{Bmatrix} 1 & 1 & K\\ J_u & J_u & J_\ell\end{Bmatrix}\begin{Bmatrix} J_u & J_u & K\\ F_u & F_u' & I\end{Bmatrix}\mathcal{T}_Q^K(i,\vec{\Omega})\;J_{-Q}^K(\nu_{\alpha_uJ_u,\,\alpha_\ell J_\ell})\\
\times\frac{1}{2}\frac{\Phi(\nu_{\alpha_uJ_uIF_u,\,\alpha_\ell J_\ell IF_\ell}-\nu)+\Phi(\nu_{\alpha_uJ_uIF_u',\,\alpha_\ell J_\ell IF_\ell}-\nu)^*}{1+2\pi{\rm i}\,\nu_{\alpha_uJ_uIF_u',\,\alpha_uJ_uIF_u}/A(\alpha_uJ_u\to\alpha_\ell J_\ell)}\,. \qquad (10.166)
\end{aligned}
$$

If the width of the F-sublevels of the lower level is negligible compared to the width of the F-sublevels of the upper level, the last term can be written in the simpler

form (cf. Eq. (10.144))

$$\frac{1}{\pi}\,\frac{\mathit{\Gamma}}{\left[\mathit{\Gamma}-\mathrm{i}\,(\nu_{\alpha_u J_u I F_u,\,\alpha_\ell J_\ell I F_\ell}-\nu)\right]\left[\mathit{\Gamma}+\mathrm{i}\,(\nu_{\alpha_u J_u I F'_u,\,\alpha_\ell J_\ell I F_\ell}-\nu)\right]}\,,$$

where

$$\mathit{\Gamma}=\frac{A(\alpha_u J_u\to\alpha_\ell J_\ell)}{4\pi}\,.$$

It should be remarked that the frequency distance between the individual lines of a hyperfine-structure multiplet is usually comparable with their natural width. Therefore, the value of the emission coefficient at the frequency of a specific line $(\bar{F}_u,\bar{F}_\ell)$ *cannot* be deduced by restricting the summation in Eq. (10.166) to the values $F_u=F'_u=\bar{F}_u$, $F_\ell=\bar{F}_\ell$: in other words, the analogue of Eq. (10.145) for hyperfine-structure multiplets is not valid. On the contrary, the asymptotic expression given in Eq. (10.148) has its direct hyperfine-structure counterpart. At large distance from the single lines we have

$$\varepsilon_i(\nu,\vec{\Omega})\approx k_{\mathrm{L}}^{\mathrm{A}}\,\frac{1}{\pi}\,\frac{\mathit{\Gamma}}{(\nu_0-\nu)^2}\,\sum_{KQ}\,W_K(J_\ell,J_u)\;(-1)^Q\,\mathcal{T}^K_Q(i,\vec{\Omega})\,J^K_{-Q}(\nu_{\alpha_u J_u,\,\alpha_\ell J_\ell})\,,$$

where ν_0 is the 'center of gravity' of the multiplet.

To make an example, let us consider the NaI D_2 line at 5890 Å ($^2\mathrm{S}_{1/2}-{}^2\mathrm{P}_{3/2}$). The nuclear spin is $I=3/2$, the Einstein coefficient $A=6.3\times10^7\,\mathrm{s}^{-1}$, and the hyperfine-structure constant for the upper level is approximately $\mathcal{A}/h=1.6\times10^7\,\mathrm{s}^{-1}$. From Eq. (10.165) we obtain $x=0.80$, and the depolarizing factors $[D_1]_{\mathrm{hfs}}$ and $[D_2]_{\mathrm{hfs}}$ turn out to be 0.56 and 0.30, respectively. The line consists of 6 components, with a natural width of the order of 1 mÅ. Owing to the large hyperfine splitting of the lower level, they are divided in two groups of 3 components each. The typical wavelength distance between the components of either group is 1 mÅ (comparable with the natural width), whereas the separation between the two groups is about 20 mÅ.

Figure 10.29 shows the fractional linear polarization to be expected in the 90° scattering of an unpolarized radiation beam for this line. One can notice the strong depolarizing effect of hyperfine structure and the rapid approach of p_Q to its asymptotic value ($p_Q=3/7$, typical of the transition $(J_\ell=1/2, J_u=3/2)$) at a distance of a few mÅ from either group of components. This 'spiky' behavior of the fractional polarization with wavelength is due to the fact that the hyperfine-structure intervals of the upper level are of the same order as the Einstein A coefficient.

The Hanle effect in hyperfine-structured lines can be deduced by applying transformations (10.164) to the relevant equations derived in Sect. 10.18. In this case, however, one has to apply the additional formal substitutions (see Eqs. (7.64))

$$j_u\to i_u\,,\qquad M_u\to f_u\,,$$

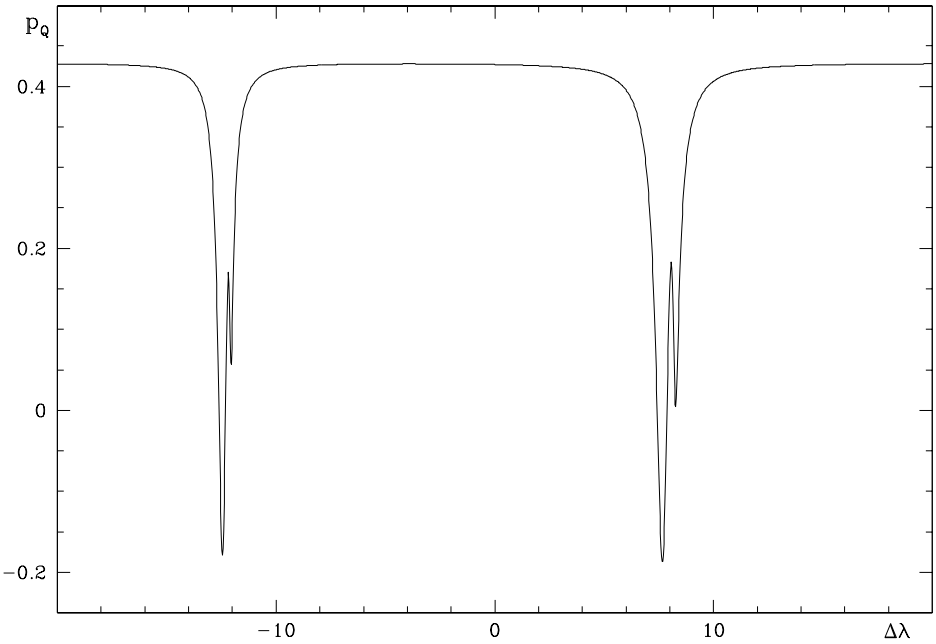

Fig.10.29. Fractional polarization p_Q against wavelength distance from line center (in mÅ) in the 90° scattering of an unpolarized radiation beam, for the NaI D_2 line. Hyperfine-structure constants are from Fuller and Cohen (1969), Hartmann (1970), Figger and Walther (1974).

connected with the presence of the magnetic field. Neglecting stimulation effects, we can write the frequency-integrated emission coefficient in the form (cf. Eqs. (10.151)-(10.153))

$$\tilde{\varepsilon}_i(\vec{\Omega}) = k_{\rm L}^{\rm A} \oint \frac{{\rm d}\Omega'}{4\pi} \sum_{j=0}^{3} \left[P_{ij}(\vec{\Omega},\vec{\Omega}';\vec{B})\right]_{\rm hfs} \; I_j(\nu_{\alpha_u J_u,\,\alpha_\ell J_\ell},\vec{\Omega}') \;,$$

where $[P_{ij}(\vec{\Omega},\vec{\Omega}';\vec{B})]_{\rm hfs}$, the Hanle phase matrix for a hyperfine-structure multiplet, is given by

$$\left[P_{ij}(\vec{\Omega},\vec{\Omega}';\vec{B})\right]_{\rm hfs} = \sum_{KK'Q} \left[W_{KK'Q}(\alpha_\ell J_\ell I \alpha_u J_u;B)\right]_{\rm hfs} \; (-1)^Q \, \mathcal{T}^K_Q(i,\vec{\Omega}) \, \mathcal{T}^{K'}_{-Q}(j,\vec{\Omega}') \;,$$

with

$$\left[W_{KK'Q}(\alpha_\ell J_\ell I \alpha_u J_u;B)\right]_{\rm hfs} = \frac{3(2J_u+1)}{2I+1} \left\{ \begin{array}{ccc} 1 & 1 & K \\ J_u & J_u & J_\ell \end{array} \right\} \left\{ \begin{array}{ccc} 1 & 1 & K' \\ J_u & J_u & J_\ell \end{array} \right\}$$

$$\times \sum_{F_u F'_u F''_u F'''_u f_u f'_u} \sqrt{(2K+1)(2K'+1)(2F_u+1)(2F'_u+1)(2F''_u+1)(2F'''_u+1)}$$

$$\times \left\{ \begin{array}{ccc} J_u & J_u & K \\ F_u & F'_u & I \end{array} \right\} \left\{ \begin{array}{ccc} J_u & J_u & K' \\ F''_u & F'''_u & I \end{array} \right\} \left(\begin{array}{ccc} F_u & F'_u & K \\ -f_u & f'_u & -Q \end{array} \right) \left(\begin{array}{ccc} F''_u & F'''_u & K' \\ -f_u & f'_u & -Q \end{array} \right) \;\times$$

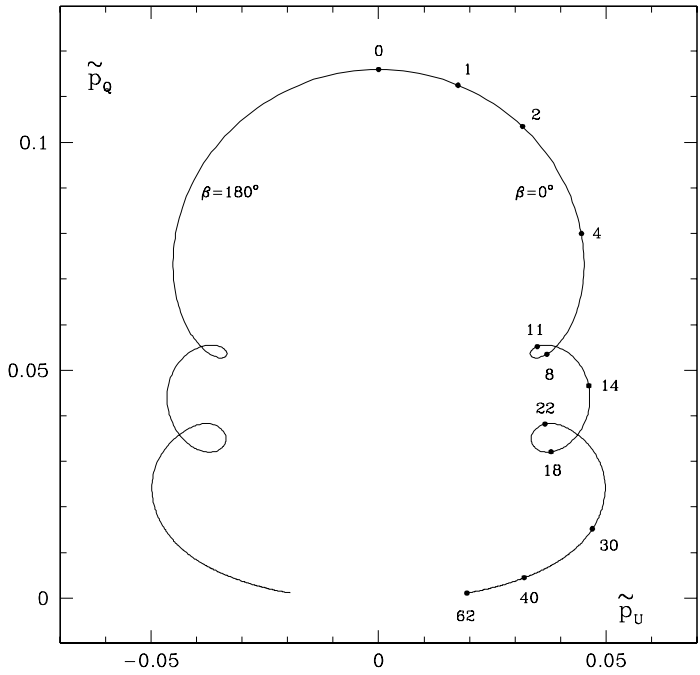

Fig.10.30. Polarization (or Hanle) diagram for the D_2 line of NaI, corresponding to the scattering process illustrated in Fig.5.11. The curve $\beta = 0°$ is labelled by the field intensity in G.

$$\times \sum_{i_u i'_u} C^{i_u}_{F_u}(\alpha_u J_u I, f_u)\, C^{i_u}_{F''_u}(\alpha_u J_u I, f_u)\, C^{i'_u}_{F'_u}(\alpha_u J_u I, f'_u)\, C^{i'_u}_{F'''_u}(\alpha_u J_u I, f'_u)$$
$$\times \frac{1}{1 + 2\pi \mathrm{i}\, \nu_{\alpha_u J_u I}(i'_u f'_u, i_u f_u) \,/\, A(\alpha_u J_u \to \alpha_\ell J_\ell)} \,. \qquad (10.167)$$

The Bohr frequency occurring in the last term is defined by (cf. the analogous definition (7.30) for fine structure)

$$\nu_{\alpha JI}(if, i'f') = \frac{\lambda_i(\alpha JI, f) - \lambda_{i'}(\alpha JI, f')}{h} \,.$$

The eigenvalues $\lambda_i(\alpha JI, f)$ and the coefficients $C^i_F(\alpha JI, f)$ are obtained by diagonalization of the hyperfine-structure and magnetic Hamiltonians, as described in Sect. 3.5.

Figure 10.30 shows the Hanle diagram for the NaI D_2 line and the scattering geometry of Fig. 5.11, with evident loops due to level-crossing interferences. In the geometry considered, only crossings between levels with $\Delta f = 2$ are effective. From Fig. 3.11 one can readily see that four such crossings occur, for B values of the order of 12, 22, 25, and 43 G, respectively. This is consistent with the curves in Fig. 10.30.

Finally, it should be remarked that the phenomena due to the anti-level-crossing effect, the Franken effect, and the alignment-to-orientation conversion mechanism

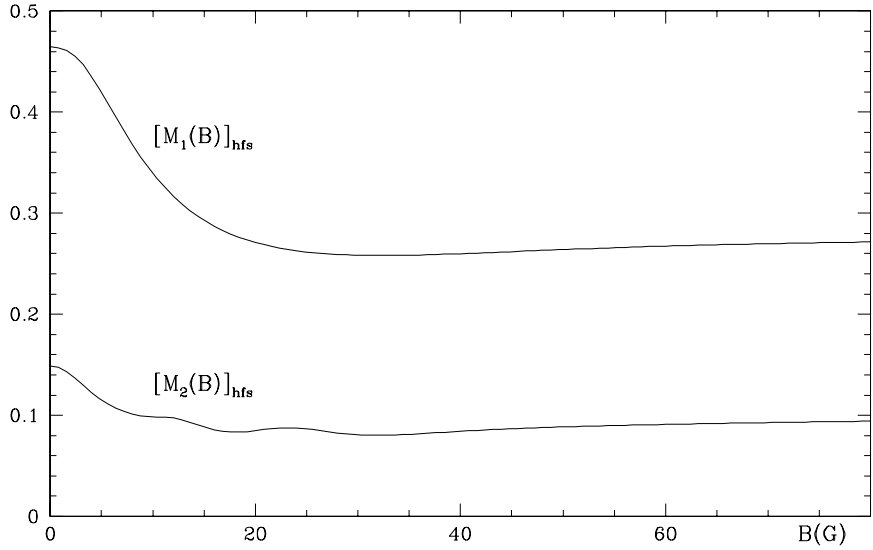

Fig.10.31. Depolarizing effect due to an isotropic distribution of magnetic fields on the NaI D_2 line. The quantities $[M_K(B)]_{\rm hfs}$ are defined in Eq.(10.168).

– described in Sects. 10.18, 10.19 and 10.20, respectively – also take place in hyperfine-structure multiplets. All these phenomena are conveniently described in terms of the symbol $W_{KK'Q}$ defined in Eq. (10.167). For instance, the Hanle phase matrix averaged over an isotropic distribution of magnetic fields is given by (cf. Eqs. (10.156a,b))

$$\left\langle \left[P_{ij}(\vec{\Omega},\vec{\Omega}';\vec{B})\right]_{\rm hfs}\right\rangle = \sum_K \left[M_K(B)\right]_{\rm hfs} R^{(\rm K)}_{ij}(\vec{\Omega},\vec{\Omega}';0)\ ,$$

with

$$\left[M_K(B)\right]_{\rm hfs} = \frac{1}{2K+1}\ \sum_Q\ \left[W_{KKQ}(\alpha_\ell J_\ell I \alpha_u J_u;B)\right]_{\rm hfs}\ . \qquad (10.168)$$

Figure 10.31 shows the behavior of the quantities $[M_K(B)]_{\rm hfs}$ with magnetic field intensity for the NaI D_2 line. Note the conspicuous anti-level-crossing effect on this particular line. The ratio $[M_K(B\to\infty)]_{\rm hfs}/[M_K(B=0)]_{\rm hfs}$ is found to be 0.60 for $K=1$ and 0.67 for $K=2$, rather than 1/3 and 1/5, respectively, as it would if hyperfine separations were negligible compared to the Einstein A coefficient.

This page intentionally left blank

CHAPTER 11

ASTROPHYSICAL APPLICATIONS: SOLAR MAGNETOMETRY

Solar magnetometry, or the 'art' of measuring magnetic fields in the solar atmosphere, started almost one century ago with the first application of polarimetry to astrophysical research. By means of a Fresnel prism (acting as a quarter-wave plate) and a Nicol prism (acting as a polarizer), in 1908 Hale succeeded in taking two separate spectra of a sunspot in right and left circular polarization. The line shifts between the two spectra, due to the Zeeman effect, led to the first measurement of a solar magnetic field (Hale, 1908).

Solar magnetometry has enormously evolved since the pioneering work of Hale and has now become a mature science which employs sophisticated technologies and modern astronomical instrumentation. The photographic plate used by Hale has been replaced, during the years, by photomultipliers, diode arrays, and CCD cameras. At the same time, new polarimeters have been conceived, capable of attaining higher and higher polarimetric accuracy. The advent of techniques of image stabilization and the construction of new instruments in proper sites (or operating from space) has also opened the possibility of observing the sun at higher and higher spatial and temporal resolution.

All these technological improvements have led to a better understanding of solar magnetism but, at the same time, have opened new questions about the meaning itself of the process of measuring magnetic fields in a highly structured plasma such as the solar atmosphere. There is today strong evidence that the solar magnetic field outside sunspots is often concentrated in structures whose lateral dimensions are at the limit of the resolving power that can be attained with present instrumentation, which is of the order of a few tenths of arcsec[1] (see for instance Stenflo, 1994). Even more complex is the picture emerging from some recent ideas, which point to the existence of magnetic fields organized in fibrils of some few km in diameter (the MISMA hypothesis, Sánchez Almeida et al., 1996), and of 'turbulent' fields of a few G permeating the full solar atmosphere outside active regions (Stenflo, 1994). Although these ideas have not yet been fully confirmed by observations, they clearly suggest the difficulties inherent in the measurement of a quantity, the magnetic field, that may show sharp variations over length-scales smaller than the resolution element of the instrument.

Most of the methods and the techniques that have been developed for solar magnetometry ignore, however, this kind of difficulties, and are based on the simple assumption that the magnetic field is uniform across the resolution element. In some cases a less restrictive assumption is made, i.e., that the magnetic field is uniform but covers only a fraction f – the so-called filling factor – of the observed

[1] One arcsec corresponds to about 730 km on the solar surface.

solar area, while the remaining fraction $(1 - f)$ is field-free or non-magnetic. In recent times, more sophisticated methods which allow for line-of-sight gradients or for more complicated structuring of the magnetic field have also been developed. In this chapter we will describe in some detail only the most traditional methods, whereas the other ones will be briefly reviewed in a single section (Sect. 11.6).

A particular problem of solar magnetometry is the ambiguity of the azimuth of the magnetic field vector, which is related to a symmetry property of the solution to the transfer equation (see Eq. (9.57)). To solve this problem, some specific 'disambiguation' techniques have been developed. These are described in Sect. 11.7.

11.1. The Longitudinal Magnetograph

First introduced in solar research in the early 1950s (Babcock, 1953), the longitudinal magnetograph is probably the most renowned and certainly the most widespread instrument for the study of solar magnetism.

A typical longitudinal magnetograph performs a polarimetric and spectral analysis of the solar radiation and records, for each resolution element, a signal S_V given by

$$S_V = \frac{\int V(\lambda)\, p(\lambda)\, \mathrm{d}\lambda}{\int I(\lambda)\, p(\lambda)\, \mathrm{d}\lambda}\,, \tag{11.1}$$

where $I(\lambda)$, $V(\lambda)$ are the Stokes parameters and $p(\lambda)$ is a narrow profile centered over one of the wings (the blue or the red) of a magnetically sensitive line. The signal is then encoded on a grey-scale to produce a map of the full sun or of an active region called a *magnetogram*.

The spectral analysis can be performed by a Lyot-type birefringent filter or by an interference filter or by a combination of both. In this case $p(\lambda)$ is nothing but the filter profile. Alternatively, one can use a spectrograph and feed the detector by means of a slit in its focal plane. In this case $p(\lambda)$ is (nominally) a rectangle function that differs from zero in the wavelength interval corresponding to the slit. The polarimetric analysis, which must take place before the spectral analysis, can be carried out in a variety of different ways. In the original Babcock's magnetograph, for instance, it was performed by the combination of an ADP crystal (see Sect. 1.5) and a polarizer. In some magnetographs two signals are recorded, one in the blue wing and the other (of opposite sign) in the red wing. The two individual signals are then combined to obtain a composite signal with less noise.

The signal S_V can be related in a simple way to the longitudinal component of the magnetic field vector in the observed area under a number of assumptions, the most important of which is the weak field approximation. We have seen in Sect. 9.6 that, under this approximation, the V Stokes parameter is given by the expression[1]

[1] We recall here that the only condition for this formula to hold – besides the weak field

(Eq. (9.80))

$$V(\lambda) = -\Delta\lambda_B \, \bar{g} \, \cos\theta \, \frac{\partial I(\lambda)}{\partial \lambda} \, , \tag{11.2}$$

where $\Delta\lambda_B$ is the Zeeman splitting defined in Eq. (3.13), $\bar{g}$ is the effective Landé factor of the selected line (defined in Eq. (3.44)), θ is the angle between the magnetic field direction and the line of sight (see Fig. 9.1), and $I(\lambda)$ is the intensity profile. Since $V(\lambda)$ is linear in the product $B\cos\theta$ and $I(\lambda)$ is unaffected by the magnetic field to lowest order, under the weak field approximation we have

$$S_V = C_{\parallel} \, B_{\parallel} \, , \tag{11.3}$$

where $B_{\parallel} = B\cos\theta$ is the longitudinal component of the magnetic field and where $C_{\parallel}$ is the so-called *calibration constant* of the longitudinal magnetograph, that can be deduced via more or less complicated procedures involving the knowledge of the filter profile $p(\lambda)$ and of the line profile $I(\lambda)$.

As a first-order approximation, one can assume that the line profile has a Gaussian shape of the form (cf. Eq. (9.86))

$$I(\lambda) = I_{\rm c} \left[1 - d_{\rm c} \, {\rm e}^{-\left(\frac{\lambda-\lambda_0}{\Delta\lambda_{\rm p}}\right)^2} \right] , \tag{11.4}$$

where $I_{\rm c}$ is the continuum intensity, $d_{\rm c}$ is the line central depression in units of $I_{\rm c}$, λ_0 is the line center wavelength, and $\Delta\lambda_{\rm p}$ is a quantity proportional to the line width.[1] If the filter profile has also a Gaussian shape, which is typical of filter-type magnetographs, the integrals in Eq. (11.1) can be performed analytically and the calibration constant can readily be recovered. Let us set

$$p(\lambda) = k \, {\rm e}^{-\left(\frac{\lambda-\lambda_{\rm F}}{\Delta\lambda_{\rm F}}\right)^2} \, , \tag{11.5}$$

where k is an arbitrary constant, $\lambda_{\rm F}$ is the central wavelength of the filter, and $\Delta\lambda_{\rm F}$ is a quantity proportional to its width. Evaluation of elementary integrals yields

$$S_V = -\Delta\lambda_B \, \bar{g} \, \cos\theta \, X \, ,$$

where

$$X = \frac{2\, d_{\rm c} \, \frac{(\lambda_{\rm F}-\lambda_0)\,\Delta\lambda_{\rm p}}{\sqrt{(\Delta\lambda_{\rm p}^2+\Delta\lambda_{\rm F}^2)^3}} \, {\rm e}^{-\frac{(\lambda_{\rm F}-\lambda_0)^2}{\Delta\lambda_{\rm p}^2+\Delta\lambda_{\rm F}^2}}}{1 - d_{\rm c} \, \frac{\Delta\lambda_{\rm p}}{\sqrt{\Delta\lambda_{\rm p}^2+\Delta\lambda_{\rm F}^2}} \, {\rm e}^{-\frac{(\lambda_{\rm F}-\lambda_0)^2}{\Delta\lambda_{\rm p}^2+\Delta\lambda_{\rm F}^2}}} \, .$$

assumption – is the constancy with depth of the longitudinal component of the magnetic field; see Table 9.1.

[1] In a profile of the form ${\rm e}^{-(x/a)^2}$, the quantity a is connected with the full width at half maximum, Δx, by the relation $\Delta x = 2\sqrt{\ln 2}\, a \simeq 1.665\, a$.

Recalling Eqs. (11.3) and (3.14), the calibration constant of the longitudinal magnetograph can thus be written in the form

$$C_{\parallel} = -4.67 \times 10^{-10}\ \lambda_0^2\ \bar{g}\ X\ ,$$

where $C_{\parallel}$ is in G^{-1}, λ_0 in Å and X in $\mathrm{m\AA}^{-1}$.

It is often in the observer's interest to increase the signal S_V (for an assigned line and a given magnetic field) as much as possible. This can be obtained by carefully selecting the filter position λ_{F} so as to maximize the absolute value of the quantity X. As an example, consider the FeI line $\lambda\,6302.5$, a Zeeman triplet having $\bar{g} = 2.5$.[1] From the atlas of the solar spectrum by Delbouille et al. (1973) one can estimate the quantities d_{c} and $\Delta\lambda_{\mathrm{p}}$ of Eq. (11.4). Their values, which refer to disk center, are found to be $d_{\mathrm{c}} \simeq 0.66$ and $\Delta\lambda_{\mathrm{p}} \simeq 60\,\mathrm{m\AA}$. If the filter passband is $\Delta\lambda_{\mathrm{F}} = 75\,\mathrm{m\AA}$ (a typical value for filter-type magnetographs), the extrema of X are located at $(\lambda_{\mathrm{F}} - \lambda_0) = \pm\,57.3\,\mathrm{m\AA}$, where $X = \pm\,5.05 \times 10^{-3}\,\mathrm{m\AA}^{-1}$. The corresponding value of the calibration constant (when the filter is positioned in the blue wing) is

$$C_{\parallel} = 2.3 \times 10^{-4}\ \mathrm{G}^{-1}\ .$$

The linear relationship between polarization signal and longitudinal component of the magnetic field is indeed valid only in the limit of weak field. When the field intensity increases, the signal S_V turns out to be much smaller than what expected from the linear relationship and the magnetograph is said to enter the *saturation regime*.

To analyze this phenomenon in some detail, let us assume the process of line formation in the solar atmosphere to be described by the Milne-Eddington model. The Stokes profiles of the emergent radiation are then given by the Unno-Rachkovsky solution (Eqs. (9.110)). Once the atmospheric and line parameters, and the width and position of the filter are specified, the magnetograph signal S_V can be computed from Eq. (11.1). Figure 11.1 shows the behavior of S_V as a function of $B_{\parallel}$ for a collection of parameters' values simulating the $\lambda\,6302.5$ FeI line, namely $\kappa_{\mathrm{L}} = 6.75$, $\Delta\lambda_{\mathrm{D}} = 40\,\mathrm{m\AA}$, $a = 0.04$, $\beta\mu = 5$. The signal S_V was computed by taking for $p(\lambda)$ a Gaussian function centered in the blue wing of the line at 60 mÅ from line center and having a full width at half maximum of 125 mÅ ($\Delta\lambda_{\mathrm{F}} = 75\,\mathrm{m\AA}$ in Eq. (11.5)).

Apart from saturation, the longitudinal magnetograph suffers from other causes of inaccuracy that are due to the calibration procedure. In practice the calibration is performed by selecting a fixed intensity profile $I(\lambda)$ to be substituted into Eqs. (11.1) and (11.2), whereas such profile generally shows non-negligible variations over the solar disk. These may be due either to limb-darkening effects, or to

[1] Owing to its high sensitivity to magnetic fields (see Tables 9.2 and 9.3), this line is widely used for solar magnetometry, notwithstanding the presence of a blend due to a telluric O_2 line in its red wing. The presence of the blend is often rather useful in observations because it provides an absolute reference wavelength for measuring Doppler shifts.

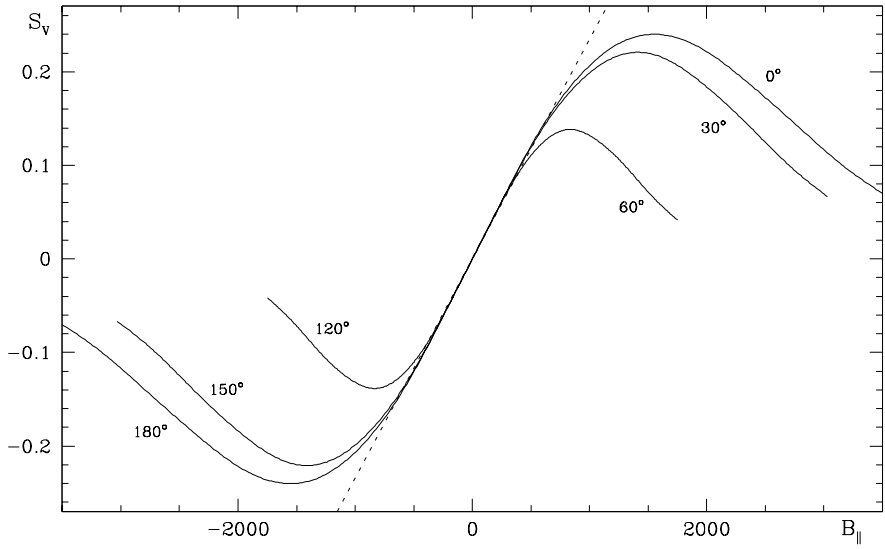

Fig.11.1. The magnetograph signal S_V as a function of the longitudinal component of the magnetic field $B_\parallel$ for a specific line – a Zeeman triplet with $\bar{g} = 2.5$ – formed in a Milne-Eddington atmosphere (see text for details). The curves are labelled by the value of the inclination angle θ defined in Fig.9.1, and are drawn up to a field intensity of 3500 G. The dotted line represents the linear relation implicit in the magnetograph calibration.

velocity fields, or to differences – with respect to the average sun – of the thermodynamic parameters characterizing the various structures of the solar atmosphere (granules, intergranular lanes, faculae, pores, sunspots' umbrae and penumbrae, etc.).

The saturation effect and the inaccuracies just mentioned are important limitations which prevent one from regarding the longitudinal magnetograph as a fully quantitative instrument for the measurement of solar magnetic fields. Yet its importance in solar research can hardly be overestimated. It is just through magnetographs that the general properties of solar magnetism have been determined (large-scale topology, fine structure, cyclic variations, etc.) and that several correlations between magnetic fields and other indicators of solar activity have been established. It is also important to mention that the results obtained by magnetographs are currently used for the reconstruction of coronal magnetic fields by means of suitable numerical techniques.

11.2. The Vector Magnetograph

The vector magnetograph is a natural generalization of the longitudinal magnetograph. Besides the circular polarization signal S_V of Eq. (11.1), two more signals related to linear polarization are recorded

$$S_Q = \frac{\int Q(\lambda)\, p'(\lambda)\, \mathrm{d}\lambda}{\int I(\lambda)\, p'(\lambda)\, \mathrm{d}\lambda}\,, \qquad S_U = \frac{\int U(\lambda)\, p'(\lambda)\, \mathrm{d}\lambda}{\int I(\lambda)\, p'(\lambda)\, \mathrm{d}\lambda}\,, \tag{11.6}$$

where $p'(\lambda)$ is a profile that may differ from $p(\lambda)$. The three signals S_Q, S_U, S_V may be recorded either simultaneously or sequentially. The first alternative implies the use of a sophisticated polarimeter, capable of measuring the four Stokes parameters at the same time. In this case, the spectral analysis is the same for the various Stokes parameters and $p'(\lambda)$ is identical with $p(\lambda)$. In the second alternative it is convenient to use different profiles in order to maximize the signals. Since the extrema of Q and U do not occur at the same wavelength positions as those of V, one can adapt the spectral analysis to the observed Stokes parameter by tuning the filter (in filter-type magnetographs) or by moving the slit (in spectrograph-type magnetographs).

Similarly to the preceding section, one can easily relate the polarization signals S_Q, S_U to the modulus of the transverse component of the magnetic field and to its orientation in the plane perpendicular to the line of sight provided a number of conditions – basically the weak field approximation – are met. We found in Sect. 9.6 that, under this approximation, the U Stokes parameter defined in the preferred frame is given by $\tilde{U}(\lambda) = 0$, which implies

$$S_{\tilde{U}} = \frac{\int \tilde{U}(\lambda)\, p'(\lambda)\, \mathrm{d}\lambda}{\int I(\lambda)\, p'(\lambda)\, \mathrm{d}\lambda} = 0\,, \tag{11.7}$$

whereas for the Q Stokes parameter, defined in the same frame, we obtained various expressions (see Eqs. (9.83), (9.84) and (9.85)) each valid in different wavelength intervals and under different assumptions on the depth dependence of the physical parameters (see Table 9.1).[1] For our purposes it is convenient to use Eq. (9.84)

$$\tilde{Q}(\lambda) = -\frac{1}{4}\, \Delta\lambda_B^2\ \bar{G}\, \sin^2\theta\ \frac{\eta''}{\eta'}\ \frac{\partial I(\lambda)}{\partial \lambda}\,, \tag{11.8}$$

which is valid at any λ, even if it implies rather restrictive assumptions on the process of line formation. The meaning of the symbols $\Delta\lambda_B$, θ, and $I(\lambda)$ has already been recalled after Eq. (11.2). $\bar{G}$ is defined in Eq. (9.76), while η' and η'' are defined in Eqs. (9.65) and (9.70).

Since $\tilde{Q}(\lambda)$ is proportional to the product $B^2 \sin^2\theta$, and $I(\lambda)$ is unaffected by the magnetic field to lowest order, under the weak field approximation we have

$$S_{\tilde{Q}} = \frac{\int \tilde{Q}(\lambda)\, p'(\lambda)\, \mathrm{d}\lambda}{\int I(\lambda)\, p'(\lambda)\, \mathrm{d}\lambda} = C_\perp\, B_\perp^2\,, \tag{11.9}$$

[1] A common assumption is the constancy with depth of the azimuth of the magnetic field vector, which enables a preferred frame to be defined.

where $B_\perp^2 = B^2 \sin^2\theta$ is the square modulus of the transverse component of the magnetic field vector and $C_\perp$ is the *second calibration constant* of the vector magnetograph. To derive an expression for $C_\perp$, we follow a procedure quite similar to that followed for $C_\parallel$ in the previous section. Using Eqs. (11.4) and (11.5) for the line and filter profile, respectively, and assuming that the profile of the line absorption coefficient for zero magnetic field, η, has also a Gaussian shape

$$\eta(\lambda) = \frac{1}{\sqrt{\pi}}\ \mathrm{e}^{-\left(\frac{\lambda-\lambda_0}{\Delta\lambda_\mathrm{D}}\right)^2}\ ,$$

one finds, by evaluating elementary integrals

$$S_{\bar{Q}} = -\frac{1}{4}\,\Delta\lambda_B^2\ \bar{G}\,\sin^2\theta\ Y\ ,$$

where

$$Y = \frac{2\,d_\mathrm{c}\,\frac{1}{\Delta\lambda_\mathrm{p}\sqrt{\Delta\lambda_\mathrm{p}^2+\Delta\lambda_\mathrm{F}^2}}\ \mathrm{e}^{-\frac{(\lambda_\mathrm{F}-\lambda_0)^2}{\Delta\lambda_\mathrm{p}^2+\Delta\lambda_\mathrm{F}^2}}\left[1-\frac{\Delta\lambda_\mathrm{p}^2\,\Delta\lambda_\mathrm{F}^2}{(\Delta\lambda_\mathrm{p}^2+\Delta\lambda_\mathrm{F}^2)\,\Delta\lambda_\mathrm{D}^2}-2\,\frac{(\lambda_\mathrm{F}-\lambda_0)^2\,\Delta\lambda_\mathrm{p}^4}{(\Delta\lambda_\mathrm{p}^2+\Delta\lambda_\mathrm{F}^2)^2\,\Delta\lambda_\mathrm{D}^2}\right]}{1-d_\mathrm{c}\,\frac{\Delta\lambda_\mathrm{p}}{\sqrt{\Delta\lambda_\mathrm{p}^2+\Delta\lambda_\mathrm{F}^2}}\ \mathrm{e}^{-\frac{(\lambda_\mathrm{F}-\lambda_0)^2}{\Delta\lambda_\mathrm{p}^2+\Delta\lambda_\mathrm{F}^2}}}.$$

From Eqs. (11.9) and (3.14), the second calibration constant of the vector magnetograph can thus be written in the form

$$C_\perp = -5.45\times10^{-20}\ \lambda_0^4\ \bar{G}\ Y\ , \tag{11.10}$$

where $C_\perp$ is in G^{-2}, λ_0 in Å and Y in $\mathrm{m\AA}^{-2}$.

To give an example, let us refer to the line FeI $\lambda\,6302.5$, already considered in the former section, with $\Delta\lambda_\mathrm{p} = 60\,\mathrm{m\AA}$, $d_\mathrm{c} = 0.66$, $\Delta\lambda_\mathrm{D} = 40\,\mathrm{m\AA}$, and $\Delta\lambda_\mathrm{F} = 75\,\mathrm{m\AA}$. It can easily be seen that the quantity Y is negative for all values of $(\lambda_\mathrm{F}-\lambda_0)$, and that its extrema are located at $(\lambda_\mathrm{F}-\lambda_0) = \pm\,71.3\,\mathrm{m\AA}$, where $Y = -2.32\times10^{-4}\,\mathrm{m\AA}^{-2}$.This would be the optimum filter position for measuring weak transverse fields. However, in actual measurements, it is convenient to shift the filter position to larger distances from line center in order to avoid, as much as possible, the contamination due to magneto-optical effects (that will be analyzed below),[1] whose importance strongly decreases in the line wings (see Sect. 9.22 and, in particular, Fig. 9.17). In the present example, a good compromise is to position the filter at $(\lambda_\mathrm{F}-\lambda_0) = \pm\,120\,\mathrm{m\AA}$ (three Doppler widths), where the quantity Y is $-1.64\times10^{-4}\,\mathrm{m\AA}^{-2}$, which corresponds to a reduction of sensitivity of only 30%

[1] Note that Eq. (11.8), which is obtained from an expansion of the radiative transfer equations to the second order in $\Delta\lambda_B/\Delta\lambda_\mathrm{D}$, does not contain terms related to magneto-optical effects. Such terms appear in the expansion from the third order on (see Sect. 9.6).

relative to its maximum value. Since for the FeI $\lambda\,6302.5$ line is $\bar{G} = 6.25$ (see Table 9.3), we obtain from Eq. (11.10)

$$C_\perp = 8.8 \times 10^{-8}\ \ \mathrm{G}^{-2}\ .$$

The calibration procedure described so far is obviously incomplete, as Eqs. (11.7) and (11.9) are valid in the preferred reference frame which in real observations is a priori unknown. The quantities actually available to the observer are the signals S_Q and S_U of Eq. (11.6), where $Q(\lambda)$ and $U(\lambda)$ refer to the observer's reference frame. This frame is determined by the experimental set-up of the instrument, and defines a physical direction on the solar disk which may be used as the zero for reckoning the azimuth χ of the magnetic field vector (see Fig. 9.1). The value of χ – undetermined up to multiples of π because of an intrinsic symmetry of the process of LTE line formation in a magnetic field, see Sect. 9.5 – can be recovered via the following line of reasoning. Performing a rotation through an angle $\alpha = \chi$ of the reference direction as in Fig. 1.10, the observer's frame is changed into the preferred frame. From Eqs. (1.45) one has

$$\begin{aligned} S_{\tilde{Q}} &= \cos 2\chi\ S_Q + \sin 2\chi\ S_U \\ S_{\tilde{U}} &= -\sin 2\chi\ S_Q + \cos 2\chi\ S_U\ . \end{aligned} \tag{11.11}$$

On the other hand, Eq. (11.7) yields $S_{\tilde{U}} = 0$. Assuming $S_{\tilde{Q}} > 0$,[1] the angle χ, defined in the interval $(-\pi/2, \pi/2)$, can be found from the following expressions (cf. Eqs. (1.8)): for $S_Q \neq 0$

$$\chi = \frac{1}{2}\arctan\left(\frac{S_U}{S_Q}\right) + \chi_0 \tag{11.12a}$$

where

$$\chi_0 = \begin{cases} 0 & \text{if } S_Q > 0 \\ \frac{\pi}{2} & \text{if } S_Q < 0 \text{ and } S_U > 0 \\ -\frac{\pi}{2} & \text{if } S_Q < 0 \text{ and } S_U < 0\ , \end{cases} \tag{11.12b}$$

and for $S_Q = 0$

$$\chi = \begin{cases} \frac{1}{4}\pi & \text{if } S_U > 0 \\ -\frac{1}{4}\pi & \text{if } S_U < 0\ . \end{cases} \tag{11.12c}$$

Finally, since from Eqs. (11.11) we have $S_{\tilde{Q}} = \sqrt{S_Q^2 + S_U^2}$, Eq. (11.9) can be rewritten in the form

$$S_{\mathrm{L}} \equiv \sqrt{S_Q^2 + S_U^2} = C_\perp\, B_\perp^2\ . \tag{11.13}$$

[1] This is the case for the example just mentioned of the FeI $\lambda\,6302.5$ line, where the calibration constant $C_\perp$ was found to be positive. In the (less frequent) opposite case, all the $>$ signs in Eqs. (11.12) should be changed into $<$ signs, and vice versa.

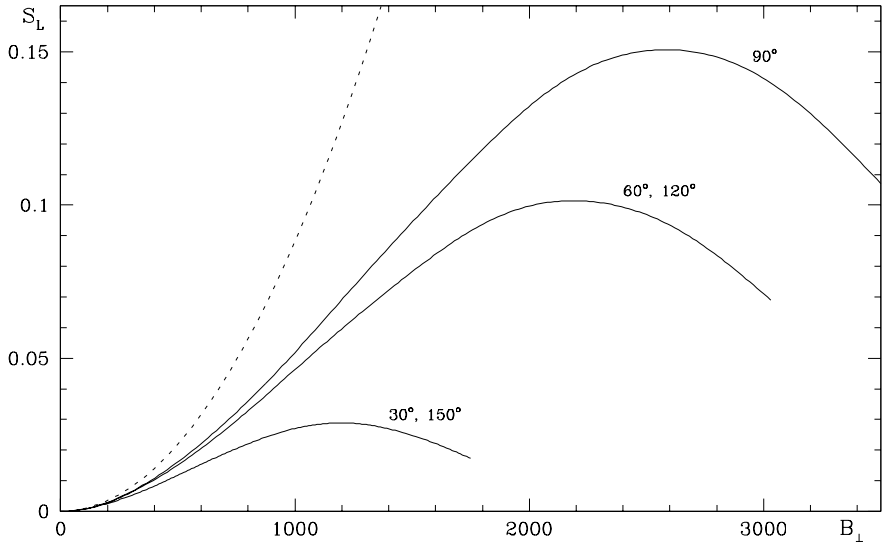

Fig.11.2. The magnetograph signal $S_{\rm L}$ as a function of the transverse component of the magnetic field $B_\perp$ for the same line and atmospheric parameters as in Fig.11.1. The curves are labelled by the value of the inclination angle θ defined in Fig.9.1, and are drawn up to a field intensity of 3500 G. The dotted line represents the quadratic relation implicit in the magnetograph calibration.

The expressions just derived allow one to recover the direction and the modulus of the transverse component of the magnetic field vector from the linear polarization signals S_Q and S_U. Such expressions are however valid only in the limit of weak magnetic fields. When the field intensity increases, saturation effects come into play, similarly to the case of the longitudinal magnetograph discussed in the previous section.

For linear polarization there are two distinct effects due to saturation: on the one hand, the signal $S_{\rm L}$ turns out to be much smaller than what predicted by the quadratic relationship of Eq. (11.13); on the other hand, the azimuth χ is found to be affected by an 'error', $\Delta\chi$, due to magneto-optical effects.

To give a quantitative idea of these two effects, we assume – as in the former section – the process of line formation in the solar atmosphere to be described by the Milne-Eddington model. Once the atmospheric and line parameters, and the width and position of the filter are specified, the magnetograph signals S_Q and S_U can be computed from Eqs. (11.6) using the Unno-Rachkovsky expressions (9.110) for $I(\lambda)$, $Q(\lambda)$ and $U(\lambda)$. The behavior of $S_{\rm L}$ and $\Delta\chi$ against $B_\perp$ for a set of parameters (the same as in Fig. 11.1) simulating the $\lambda\,6302.5$ FeI line is shown in Figs. 11.2 and 11.3, respectively. The profile $p'(\lambda)$ in Eqs. (11.6) was assumed to be a Gaussian function centered at 120 mÅ from line center and having $\Delta\lambda_{\rm F} = 75$ mÅ. The sign convention for $\Delta\chi$ in Fig. 11.3 is such that it has to be *added* to the χ value of Eqs. (11.12) in order to retrieve the true azimuth of the magnetic field vector.

Apart from saturation effects, the vector magnetograph is subjected to the same

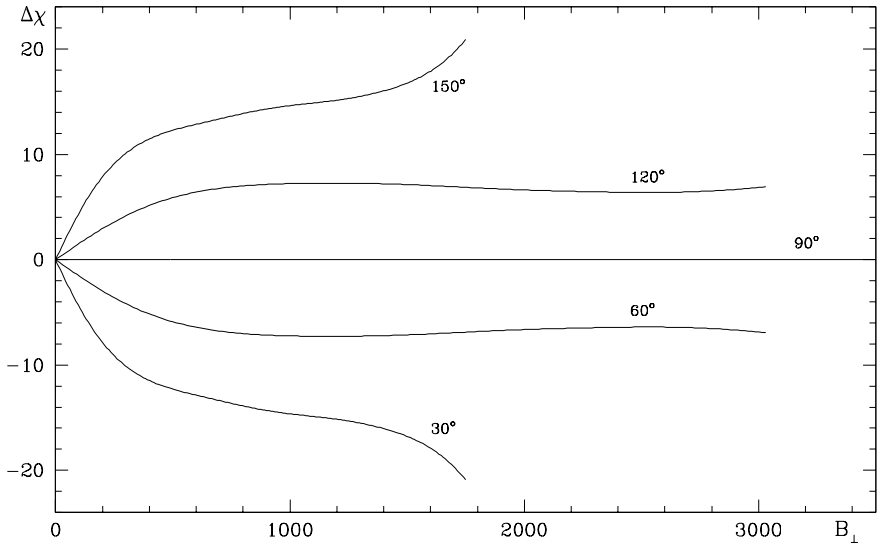

Fig.11.3. The 'error' angle $\Delta\chi$ due to magneto-optical effects is plotted against $B_\perp$ for the same line and atmospheric parameters as in Figs.11.1 and 11.2 and the same filter profile as in Fig.11.2. The curves are labelled by the values of θ. For the sign convention of $\Delta\chi$ refer to the text.

limitations pointed out for the longitudinal magnetograph at the end of Sect. 11.1. Notwithstanding such limitations, this instrument remains one of the main tools of solar physics. A particularly long lasting and successful example is the tower vector magnetograph of the University of Alabama in Huntsville and of the Marshall Space Flight Center that has been operating since the mid-1970s (Hagyard et al., 1982) and that has provided important results on the shear of magnetic fields in flare sites. It has to be remarked that in the early period of operation of this instrument, the error $\Delta\chi$ introduced by saturation and magneto-optical effects was not taken into account in the data-reduction analysis, which led Hagyard et al. (1977) to interpret their observations of isolated sunspots in terms of a twisted magnetic field. It was shown later (Landi Degl'Innocenti, 1979a) that such observations were fully consistent with a pure radial magnetic configuration once the $\Delta\chi$ correction was properly included.

11.3. The Unno-fit Technique

To overcome the limitations of magnetographs, it was early realized that the measurement of solar magnetic fields could be substantially improved by recording the *full profiles* of the four Stokes parameters across a wavelength interval encompassing one or more suitable spectral lines. An instrument capable of such recordings is currently called a *Stokesmeter*, though the name of *spectropolarimeter* is used as well. The data obtained with a Stokesmeter contain a wealth of information, whereas a typical vector magnetograph 'compresses' all this information into just

three quantities (the signals S_V, S_Q, and S_U defined in Eqs. (11.1) and (11.6)). Hence the obvious superiority of Stokesmeters over magnetographs.[1]

Several techniques have been developed in the past for recovering the magnetic field vector from the Stokes parameters' profiles recorded, as a function of wavelength, by a Stokesmeter. In this section we describe in some detail one of such techniques, the so-called Unno-fit technique. Pioneered by Harvey et al. (1972) and Auer et al. (1977b), and improved by Landolfi and Landi Degl'Innocenti (1982) and Landolfi et al. (1984) to allow for magneto-optical and damping effects, this technique has been brought to a high level of sophistication by the group of the High Altitude Observatory working on the Advanced Stokes Polarimeter data (see for instance Skumanich and Lites, 1987; Lites and Skumanich, 1990).

The technique consists in comparing the observed Stokes profiles with the Unno-Rachkovsky solution to the radiative transfer equation for polarized radiation (see Sect. 9.8) and in varying the set of parameters on which such solution depends until a best fit is obtained. In practice, a kind of 'merit function' is constructed, typically of the form

$$M\big(\{\zeta_i\}\big) = \sum_{j=0}^{3} \sum_{\alpha=1}^{N} W_{j\alpha} \left[I_{j\alpha}^{(\mathrm{obs})} - I_{j\alpha}^{(\mathrm{thr})}\big(\{\zeta_i\}\big) \right]^2 , \tag{11.14}$$

where $I_{j\alpha}^{(\mathrm{obs})}$ is the j-th Stokes parameter measured at wavelength λ_α,[2] $I_{j\alpha}^{(\mathrm{thr})}$ is the corresponding theoretical value dependent on a set $\{\zeta_i\}$ of physical parameters ($i = 1, 2, \ldots, p$), and $W_{j\alpha}$ is a matrix of weights. The quantities $I_{j\alpha}^{(\mathrm{thr})}$ can be computed from Eq. (9.109) by taking into account the spectral smearing profile of the instrument, which depends on the resolving power of the spectrograph, on the geometrical width of the entrance slit, on the pixel width and, in many cases, on the data reduction procedure. If $P(\Delta\lambda)$ is such a profile (normalized to unity in wavelength), one has from Eq. (9.109)

$$I_{j\alpha}^{(\mathrm{thr})} = B_0 \left\{ \delta_{j0} + \beta' \int \left[(C^{-1})_{j0} \right]_{\lambda=\lambda_\alpha-\Delta\lambda} P(\Delta\lambda)\, \mathrm{d}(\Delta\lambda) \right\} , \tag{11.15}$$

where $\boldsymbol{C}$ is the matrix defined in Eq. (9.91) and $\beta' = \beta\mu$ is the slope of the Planck function along the propagation direction in the solar atmosphere.

The dependence of $I_{j\alpha}^{(\mathrm{thr})}$ on the two physical parameters B_0 and β' is explicitly expressed in Eq. (11.15). The dependence on the other seven physical parameters (κ_L, B, θ, χ, $\Delta\lambda_\mathrm{D}$, Γ', w_A – see Sect. 9.5 for their definition) is implicitly contained in the matrix $\boldsymbol{C}$. The merit function $M(\{\zeta_i\})$ thus depends, in total, on

[1] It should not be forgotten that magnetographs may be preferred to Stokesmeters for scientific purposes which do not require high precision magnetometry. Just because they involve a much smaller number of observational data, magnetographs are generally faster and more agile than Stokesmeters. For this reason they are often preferred in space research.

[2] We assume that the Stokes parameters are sampled at different wavelength points (pixels) along the dispersion axis, as typical of modern observations. N represents the number of pixels covered by the observation.

nine physical parameters which, for later reference, can be conveniently divided into *magnetic parameters* (B, θ, χ), *velocity parameter* ($w_{\rm A}$), and *thermodynamic parameters* (B_0, β', $\kappa_{\rm L}$, $\Delta\lambda_{\rm D}$, Γ').[1] As to the weights $W_{j\alpha}$, they can be used for two different purposes. On one side they allow one to remove from the fit – by setting to zero the corresponding weight – certain wavelength intervals where the observed Stokes profiles are contaminated either by experimental errors or by the presence of a blending line (like, for instance, the telluric line in the red wing of FeI $\lambda\,6302.5$, see footnote on p. 628). On the other side, they can be used to increase the importance of the fit to one (or more) Stokes parameter(s) relative to the remaining ones. In many cases, for instance, the intensity profile is one to two orders of magnitude larger (in absolute value) than the other Stokes profiles. A fit with equal weights will eventually favor just that profile which is less sensitive to the magnetic parameters. Since in general the intensity profile is also affected by other sources of contamination – like stray light in the spectrograph – it turns out that a good choice is to assign weight unity to the Stokes profiles Q, U, and V and a weight ranging from 0.01 to 0.1 to the I profile.[2]

In order to obtain the best fit to the observed data, one needs to find the absolute minimum of the merit function in the hyperspace of the parameters ζ_i. This is not a trivial problem because the dependence of the merit function on the parameters is non-linear and because the merit function has, in general, several secondary minima. An appropriate mathematical procedure that can be followed in such cases is due to Marquardt (1963) and is fully described in Bevington (1969). Starting from some 'guess values' of the parameters ζ_i, the Marquardt algorithm looks for the minima of the merit function by following a path in the parameters' hyperspace. The path consists in a succession of steps whose length and direction is determined by evaluating the quantities β_k $(k = 1, \ldots, p)$ and α_{km} $(k, m = 1, \ldots, p)$ defined by

$$\beta_k = \frac{\partial M\big(\{\zeta_i\}\big)}{\partial \zeta_k}\,, \qquad \alpha_{km} = \frac{\partial^2 M\big(\{\zeta_i\}\big)}{\partial \zeta_k\,\partial \zeta_m} = \frac{\partial \beta_k}{\partial \zeta_m} = \frac{\partial \beta_m}{\partial \zeta_k}\,.$$

From Eq. (11.14) one has

$$\beta_k = -2 \sum_{j=0}^{3} \sum_{\alpha=1}^{N} W_{j\alpha} \left[I_{j\alpha}^{(\rm obs)} - I_{j\alpha}^{(\rm thr)} \right] \frac{\partial I_{j\alpha}^{(\rm thr)}}{\partial \zeta_k}$$

$$\alpha_{km} = 2 \sum_{j=0}^{3} \sum_{\alpha=1}^{N} W_{j\alpha} \left\{ \frac{\partial I_{j\alpha}^{(\rm thr)}}{\partial \zeta_k} \frac{\partial I_{j\alpha}^{(\rm thr)}}{\partial \zeta_m} - \left[I_{j\alpha}^{(\rm obs)} - I_{j\alpha}^{(\rm thr)} \right] \frac{\partial^2 I_{j\alpha}^{(\rm thr)}}{\partial \zeta_k\,\partial \zeta_m} \right\},$$

[1] The number of parameters can be reduced to 8 by defining the merit function in terms of the Stokes parameters normalized as in Eqs. (9.112). By so doing, the dependence on B_0 disappears and β' is replaced by $\beta'/(1+\beta')$.

[2] This statement is based on the experience gathered mostly with the data of the Advanced Stokes Polarimeter of the High Altitude Observatory. For an ideal Stokesmeter, with observed Stokes profiles affected by Gaussian errors with variance $\sigma_{j\alpha}$, the weights should indeed be given by $W_{j\alpha} = 1/\sigma_{j\alpha}$. In that case the merit function of Eq. (11.14) would reduce to a standard chi-square function (see e.g. Bevington, 1969).

the last expression being usually approximated by neglecting the second term in braces which gets much smaller that the first when approaching the minimum of the merit function. The Marquardt algorithm thus requires the evaluation of derivatives of the form $\partial I_{j\alpha}^{(\mathrm{thr})}/\partial\zeta_k$. As apparent from Eq. (11.15), the derivatives with respect to B_0 and β' are trivial. The derivatives with respect to the other parameters (implicitly contained in the matrix $\boldsymbol{C}$) can be obtained with the help of Eq. (9.204). One has

$$\frac{\partial I_{j\alpha}^{(\mathrm{thr})}}{\partial\zeta_k} = -B_0\,\beta' \int \left[\left(\boldsymbol{C}^{-1}\,\frac{\partial \boldsymbol{C}}{\partial\zeta_k}\,\boldsymbol{C}^{-1}\right)_{j0}\right]_{\lambda=\lambda_\alpha-\Delta\lambda} P(\Delta\lambda)\;\mathrm{d}(\Delta\lambda)\;,$$

and the derivatives of the matrix $\boldsymbol{C}$ with respect to the various parameters are easily evaluated using Eqs. (9.91), (9.39), (9.32), (9.29), (9.27), (9.26) and (5.58).

As stated above, the Marquardt algorithm eventually finds a minimum of the merit function in the hyperspace of the parameters, but there is no guarantee that this is the absolute minimum. To overcome such problem, one is forced to iterate the procedure starting from a different set of guess values of the parameters, and only after a sufficient number of iterations one can be reasonably confident that the absolute minimum has indeed been reached. To make the search easier, it is advisable to start the Marquardt algorithm with 'plausible' initial values (as close as possible to those corresponding to the absolute minimum).[1] By so doing, the possibility of finding a secondary minimum is largely reduced. In the case of raster-type observations, the best fit values of the parameters found for a given point of the solar surface can serve as initial values for the surrounding points.

When applied to data showing a reasonable amount of polarization (roughly speaking, when the maximum value of $\sqrt{Q^2+U^2+V^2}\,/\,I$ across the line profile is larger than 1%), the Unno-fit technique provides reliable values of the magnetic parameters. Such values are practically independent of the weights $W_{j\alpha}$ introduced in Eq. (11.14). The same is true for the velocity parameter, whereas the thermodynamic parameters may show larger variations when varying the weights and, in some cases, even somewhat unrealistic values may be found for them. This is due to the fact that there is a strong 'trade-off' in the Unno-Rachkovsky solutions among the parameters B_0, β', κ_{L}, $\Delta\lambda_{\mathrm{D}}$, and Γ', in the sense that a given set of Stokes profiles can be reproduced, approximately with the same accuracy, by several different combinations of these parameters. However, this drawback of the Unno-fit technique does not represent a serious limitation for the measurement of the magnetic field – which is the main object of the method.

Two examples of the application of the Unno-fit technique are shown in Figs. 11.4 and 11.5. The data were collected at the Advanced Stokes Polarimeter on June 19, 1992 in the penumbra of the large round sunspot of Active Region NOAA 7201 (see Skumanich et al., 1997, for a description of the observations). One can notice

[1] The thermodynamic parameters of a line are known fairly well and do not show very large variations over the solar surface. The velocity parameter can be simply set to zero. The real problem is with the magnetic parameters. Suitable first-guess values can be obtained, for instance, from a preliminary data analysis based on the weak field approximation.

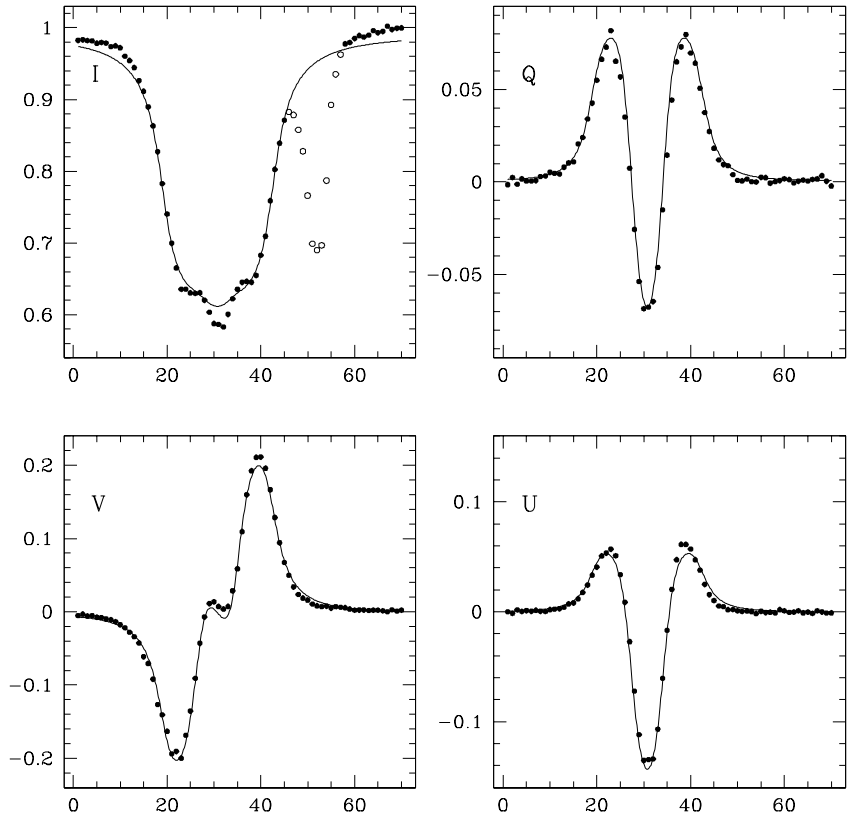

Fig.11.4. Unno-fit to ASP data for the FeI $\lambda\,6302.5$ line observed in the penumbra of a sunspot. The Stokes parameters are normalized to the continuum intensity and are plotted against pixel number. The dispersion is 12.74 mÅ/pixel. The data points drawn as open circles are due to a telluric line and were excluded from the fit. Note the reversal in the V profile due to magneto-optical effects (see Sect. 9.22). The magnetic parameters are $B = 2130\,\mathrm{G}$, $\theta = 128°$, $\chi = 22°$ (see Fig.9.1 for the definitions of θ and χ).

the quite remarkable fit to the observed Q, U, and V profiles in Fig. 11.4 (the fit to the intensity profile is worse because, in these illustrative examples, we have not taken into account the spectral smearing profile of the instrument, $P(\Delta\lambda)$). On the contrary, the observed polarization profiles shown in Fig. 11.5 are reproduced only marginally by the fit. This is probably due to the presence of strong velocity gradients (Evershed flow) which introduce considerable asymmetries in the profiles (note, for instance, the presence of three distinct lobes in the V profile). Obviously, such asymmetries cannot be reproduced by the fit, based on a model which does not allow for any depth dependence of the physical parameters.

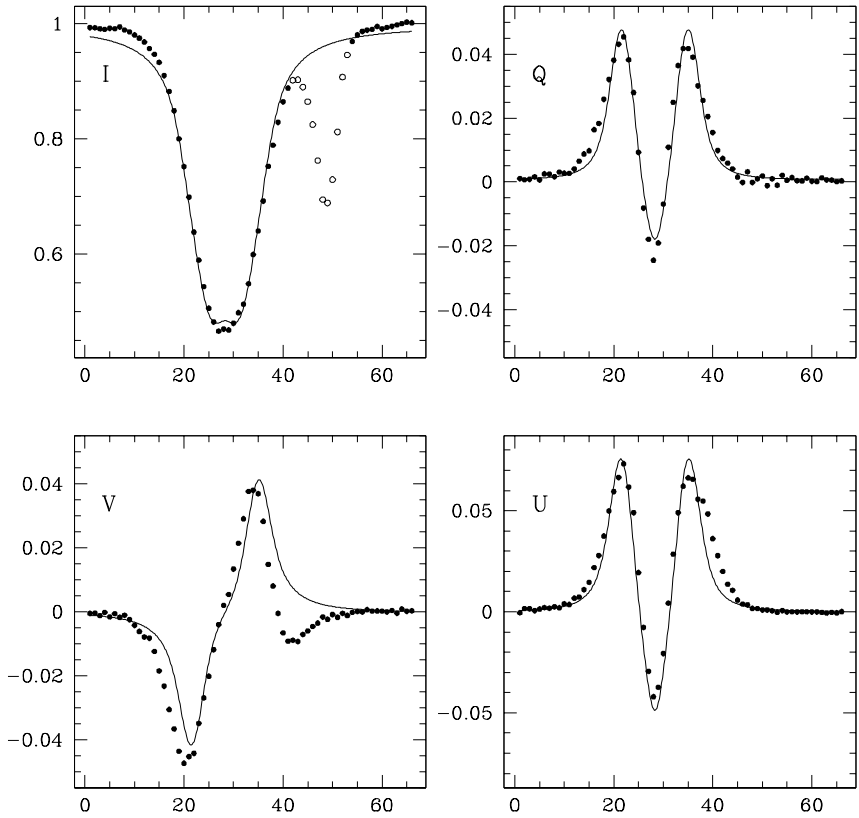

Fig.11.5. Same as Fig.11.4 for a different region of the sunspot. The magnetic parameters are $B = 1070\,\mathrm{G}$, $\theta = 100°$, $\chi = 31°$. Note that the quality of the fit is much worse than in Fig.11.4. This is probably due to the Evershed effect (see text).

11.4. The Bisector and the Center-of-Gravity Techniques

The bisector technique and the center-of-gravity technique were proposed in the late 1960s to overcome the saturation problems inherent in the magnetographic measurements of the longitudinal component of the magnetic field vector. The two techniques were developed almost simultaneously by Rayrole (1967) and Semel (1967), respectively.

Both techniques are based on the observation of the right and left (positive and negative) circular polarization in a magnetically sensitive spectral line. Such quantities are connected with the Stokes parameters I and V by the simple relation

$$I_{\pm}(\lambda) = \frac{1}{2}\left[I(\lambda) \pm V(\lambda)\right] . \tag{11.16}$$

In the bisector technique the two profiles $I_+(\lambda)$ and $I_-(\lambda)$ are observed simultaneously, and their 'central' wavelengths or *bisectors*, $\lambda_+^{(\mathrm{b})}$ and $\lambda_-^{(\mathrm{b})}$ respectively, are

recovered via a procedure described in more detail below. The longitudinal component of the magnetic field is then obtained from the equation (see Eq. (3.13) for the definition of $\Delta\lambda_B$)

$$\lambda_+^{(\mathrm{b})} - \lambda_-^{(\mathrm{b})} = 2\,\bar{g}\,\Delta\lambda_B \cos\theta = \frac{\bar{g}\,\lambda_0^2\,e_0}{2\pi\,mc^2}\;B\cos\theta\;, \tag{11.17}$$

where $\bar{g}$ is the effective Landé factor of the line. Numerically one gets

$$B_\parallel = B\cos\theta = \frac{1.071\times10^9}{\bar{g}\,\lambda_0^2}\left(\lambda_+^{(\mathrm{b})} - \lambda_-^{(\mathrm{b})}\right)\;, \tag{11.18}$$

where λ_0 is in Å, $(\lambda_+^{(\mathrm{b})} - \lambda_-^{(\mathrm{b})})$ in mÅ, and $B_\parallel$ in G.

The center-of-gravity technique is based, rather than on the profiles $I_\pm(\lambda)$, on the direct measurement of their first-order moments defined by[1]

$$\lambda_\pm^{(\mathrm{g})} = \frac{\displaystyle\int\Big[\,\frac{1}{2}\,I_\mathrm{c} - I_\pm(\lambda)\,\Big]\lambda\;\mathrm{d}\lambda}{\displaystyle\int\Big[\,\frac{1}{2}\,I_\mathrm{c} - I_\pm(\lambda)\,\Big]\;\mathrm{d}\lambda}\;, \tag{11.19}$$

where I_c is the intensity of the continuum (assumed unpolarized), and where the integrals are extended to the full line profile. The longitudinal component of the magnetic field vector is obtained from equations strictly similar to Eqs. (11.17)-(11.18)

$$\lambda_+^{(\mathrm{g})} - \lambda_-^{(\mathrm{g})} = 2\,\bar{g}\,\Delta\lambda_B\cos\theta\;, \tag{11.20}$$

or, numerically

$$B_\parallel = B\cos\theta = \frac{1.071\times10^9}{\bar{g}\,\lambda_0^2}\left(\lambda_+^{(\mathrm{g})} - \lambda_-^{(\mathrm{g})}\right)\;. \tag{11.21}$$

Equations (11.17) and (11.20) are indeed exact for any Zeeman triplet (normal or anomalous) formed in an arbitrary atmosphere with a constant magnetic field parallel or antiparallel to the line of sight ($\theta = 0°$ or $180°$ referring to the geometry of Fig. 9.1). This particular case has been analyzed in Sect. 9.10. From Eqs. (9.126) we have, for $\theta = 0°$

$$I_\pm(\lambda) = \frac{1}{2}\,\bar{I}(\lambda \mp g\,\Delta\lambda_B)\;,$$

where $\bar{I}(\lambda)$ is the intensity that would be observed if the magnetic field were switched off leaving all the other physical parameters (including the source functions) unchanged. This equation shows that the profiles $I_+(\lambda)$ and $I_-(\lambda)$ have *exactly the same shape*, and are just shifted in wavelength by $2g\Delta\lambda_B$. It follows that, irrespective of the procedure followed to deduce $\lambda_+^{(\mathrm{b})}$ and $\lambda_-^{(\mathrm{b})}$ from the profiles

[1] An instrumental set-up for measuring the quantities $\lambda_\pm^{(\mathrm{g})}$, sometimes called a *lambdameter*, is described in Semel (1967).

$$\lambda_+^{(\mathrm{b})} - \lambda_-^{(\mathrm{b})} = \lambda_+^{(\mathrm{g})} - \lambda_-^{(\mathrm{g})} = 2\, g\, \Delta\lambda_B \,. \tag{11.22}$$

This equation coincides with Eqs. (11.17) and (11.20) evaluated for $\theta = 0°$ and for a Zeeman triplet ($\bar{g} = g$). The case $\theta = 180°$ can be treated in a strictly similar way and shows again the correctness of Eqs. (11.17) and (11.20). Moreover, the same line of reasoning leads to the conclusion that the restriction about the Zeeman pattern can be partly released. Still under the assumption of a constant magnetic field with $\theta = 0°$ or 180°, the two equations are also valid for Zeeman patterns classified as Type III in Sect. 3.3 (σ components symmetrical about their center of gravity).

On the other hand, Eqs. (11.17) and (11.20) are correct for *any* value of θ and *any* Zeeman pattern provided the magnetic field is weak and its longitudinal component is independent of depth. In this case we have from Eq. (9.80) – see also Table 9.1

$$V(\lambda) = -\,\bar{g}\; \Delta\lambda_B \cos\theta\; \frac{\partial I}{\partial \lambda} \,,$$

so that Eq. (11.16) becomes

$$I_\pm(\lambda) = \frac{1}{2}\left[I(\lambda) \mp \bar{g}\, \Delta\lambda_B \cos\theta\; \frac{\partial I}{\partial \lambda} \right] \approx \frac{1}{2}\, I(\lambda \mp \bar{g}\, \Delta\lambda_B \cos\theta) \,.$$

This expression shows that the right and left circular polarization profiles are again the same except for an overall shift, hence[1]

$$\lambda_+^{(\mathrm{b})} - \lambda_-^{(\mathrm{b})} = \lambda_+^{(\mathrm{g})} - \lambda_-^{(\mathrm{g})} = 2\, \bar{g}\, \Delta\lambda_B \cos\theta \,,$$

which coincides with Eqs. (11.17) and (11.20).

Apart from the special cases analyzed above, it is expected that Eqs. (11.17) and (11.20) are only approximately valid. However, to put this statement on a more quantitative basis, it is necessary to specify the procedure for deriving the quantities $\lambda_\pm^{(\mathrm{b})}$ from the observed right and left circular polarization profiles (this is unnecessary for the quantities $\lambda_\pm^{(\mathrm{g})}$ because Eq. (11.19) is itself an operational definition). As suggested by Rayrole (1967), the profiles $I_\pm(\lambda)$ have first to be convolved with a rectangle function having width $\Delta\lambda_\mathrm{R}$. This yields the new profiles $I'_\pm(\lambda)$ defined by

$$I'_\pm(\lambda) = \frac{1}{\Delta\lambda_\mathrm{R}} \int_{-\Delta\lambda_\mathrm{R}/2}^{\Delta\lambda_\mathrm{R}/2} I_\pm(\lambda - \lambda')\, \mathrm{d}\lambda' \,.$$

Such convolution has the double purpose of reducing the noise contained in the data and of transforming the original profiles $I_\pm(\lambda)$, often characterized by two or

[1] Note that this result is independent of the actual shape of the profile and is also independent of the procedure followed to deduce $\lambda_+^{(\mathrm{b})}$ and $\lambda_-^{(\mathrm{b})}$ from the profile itself.

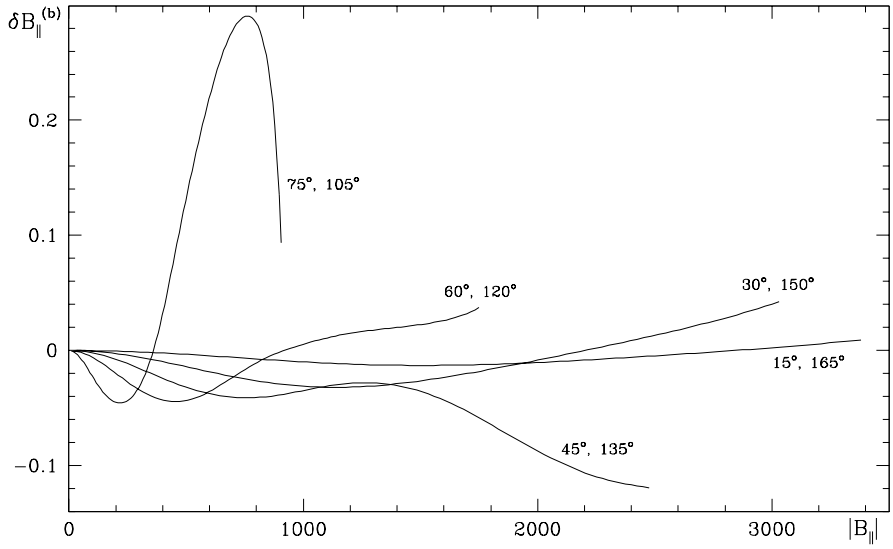

Fig.11.6. The relative error introduced in the measurement of $B_{\parallel}$ by the bisector technique is plotted as a function of $|B_{\parallel}|$ for different values of the inclination angle θ, defined as in Fig.9.1. The curves are drawn up to a field strength of 3500 G. The figure refers to the line FeI $\lambda\,5250.21$ formed in a Milne-Eddington atmosphere (see text for further details).

three minima,[1] into profiles having just one minimum. Referring to one of the two profiles, for instance $I'_{+}(\lambda)$, one then looks for the two solutions, λ_1 and λ_2, of the equation

$$I'_{+}(\lambda) = I_{\rm m} + r\left(I_{\rm w} - I_{\rm m}\right) ,$$

where $I_{\rm m}$ is the value of I'_{+} corresponding to the minimum of the profile, $I_{\rm w}$ is its value in the far wings, and r is a parameter ranging from 0 to 1. From λ_1 and λ_2 one finally obtains the bisector $\lambda_{+}^{(\rm b)}$ as $(\lambda_1 + \lambda_2)/2$. The bisector $\lambda_{-}^{(\rm b)}$ is obtained by applying the same procedure to the profile $I'_{-}(\lambda)$. Obviously, the two parameters $\Delta\lambda_{\rm R}$ and r are in principle arbitrary, and the value of $B_{\parallel}$ derived from Eq. (11.18) depends on them. This dependence is weak if the magnetic field is only mildly inclined with respect to the line of sight but can drastically increase for large inclinations.

We have checked the reliability of Eqs. (11.18) and (11.21) by selecting a specific spectral line and by varying the modulus and inclination of the magnetic field. The line is FeI $\lambda\,5250.21$, a Zeeman triplet having $\bar{g} = 3$ that is currently used in solar magnetometry for its high sensitivity (see Tables 9.2 and 9.3). In our simulation the line is formed in a Milne-Eddington model atmosphere with a suitable choice of atmospheric and line parameters ($\kappa_{\rm L} = 6.1$, $\Delta\lambda_{\rm D} = 32\,$mÅ, $a = 0.04$, $\beta\mu = 12$). Figure 11.6 shows the relative error, $\delta B_{\parallel}^{(\rm b)}$, introduced by the bisector technique

[1] When the magnetic field is sufficiently large and inclined with respect to the line of sight, the profiles $I_{\pm}(\lambda)$ show three minima, corresponding to the Zeeman components $\sigma_{\rm b}$, π, and $\sigma_{\rm r}$.

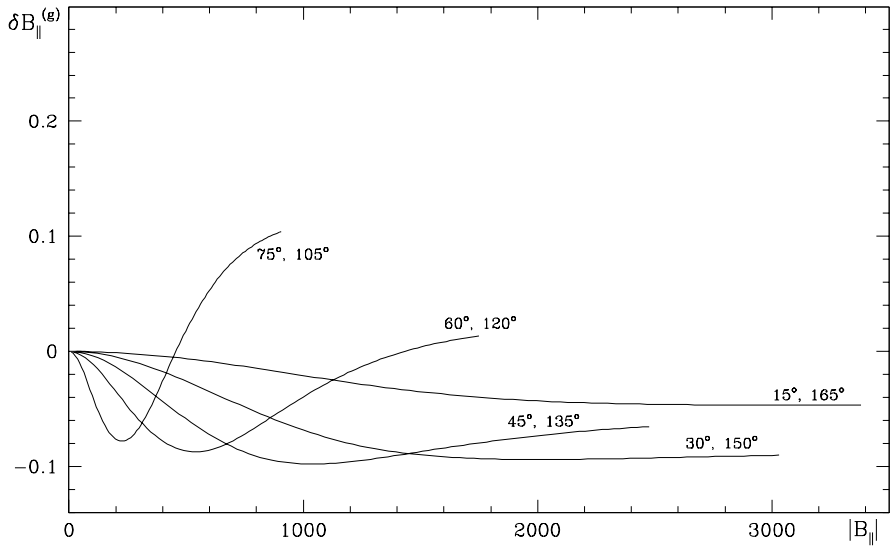

Fig.11.7. Same as Fig.11.6 for the relative error introduced in the measurement of $B_{\parallel}$ by the center-of-gravity technique.

when the two parameters $\Delta\lambda_{\rm R}$ and r are set to 140 mÅ and 0.65, respectively. The error $\delta B_{\parallel}^{(\rm b)}$ is defined by

$$\delta B_{\parallel}^{(\rm b)} = \frac{B_{\parallel}^{(\rm b)} - B_{\parallel}}{B_{\parallel}} \,,$$

where $B_{\parallel}^{(\rm b)}$ is evaluated via Eq. (11.18) and $B_{\parallel}$ is the value of the longitudinal magnetic field employed in the simulation. The figure shows that the relative error is always less than about 10% for magnetic field's inclinations smaller than 60°. Similarly, Fig. 11.7 gives the relative error $\delta B_{\parallel}^{(\rm g)}$ introduced by the center-of-gravity technique

$$\delta B_{\parallel}^{(\rm g)} = \frac{B_{\parallel}^{(\rm g)} - B_{\parallel}}{B_{\parallel}} \,,$$

where $B_{\parallel}^{(\rm g)}$ is obtained from Eq. (11.21). In this case the relative error is always less than about 10%, with a definite tendency to underestimate the actual value of $B_{\parallel}$.

The bisector technique and the center-of-gravity technique provide only the longitudinal component of the magnetic field. They have to be complemented with other techniques in order to obtain the full measurement of the magnetic field vector (see e.g. Rayrole, 1967, for the possibility of recovering the transverse component from the maximum amplitude of the V Stokes parameter). Moreover, both techniques are limited by systematic errors which, however, can be fairly well estimated by means of correction tables adapted to the specific observation, and constructed via procedures similar to that followed above for obtaining Figs. 11.6

and 11.7. The main advantage of these techniques is the possibility of obtaining a fairly accurate estimate of the longitudinal component of the magnetic field (not affected by saturation effects) either by a simple procedure of data handling on the profiles $I_{\pm}(\lambda)$ (bisector technique) or by a direct measurement of the quantities $\lambda_{\pm}^{(g)}$ (center-of-gravity technique).

11.5. Unresolved Fields

One of the major problems of solar magnetometry is the fact that, in many cases, the magnetic field is not uniform across the resolution element of the instrument employed in the observations. A second problem, intimately related to the first, is the fact that the local values of the thermodynamic parameters of the solar atmosphere, being strongly correlated with the amplitude and direction of the magnetic field vector, may also show large spatial variations over the same area. In this situation, any method or technique that can be envisaged to deduce the magnetic field vector – or one of its components – from observations is obviously bound to yield a sort of ill-defined 'average' value.

In this section we will analyze in some detail this particular aspect of solar magnetometry, by illustrating how the different techniques that have been described in the previous sections are affected by the lack of resolution in the observations.

11.5.a Longitudinal and Vector Magnetographs

Denoting by $I(\lambda;\mathrm{P})$ the intensity profile emerging from an element of the solar surface $\mathrm{d}S$ centered at the point P, and introducing similar notations for the other Stokes parameters, the signal of a longitudinal magnetograph is given by (cf. Eq. (11.1))

$$\left(S_V\right)_{\Sigma} = \frac{\displaystyle\int_{\Sigma} \mathrm{d}S \int V(\lambda;\mathrm{P})\, p(\lambda)\, \mathrm{d}\lambda}{\displaystyle\int_{\Sigma} \mathrm{d}S \int I(\lambda;\mathrm{P})\, p(\lambda)\, \mathrm{d}\lambda} \,, \tag{11.23}$$

where the integrals in $\mathrm{d}S$ are extended to the solar region Σ covered by the instrument. A more significant expression can be obtained by introducing the local value of the magnetograph signal, $S_V(\mathrm{P})$, defined by

$$S_V(\mathrm{P}) = \frac{\displaystyle\int V(\lambda;\mathrm{P})\, p(\lambda)\, \mathrm{d}\lambda}{\displaystyle\int I(\lambda;\mathrm{P})\, p(\lambda)\, \mathrm{d}\lambda} \,,$$

and the local value of the *filtered intensity*

$$\mathcal{I}(\mathrm{P}) = \int I(\lambda;\mathrm{P})\, p(\lambda)\, \mathrm{d}\lambda \,.$$

With these notations Eq. (11.23) can be rewritten in the form

$$\big(S_V\big)_{\Sigma} = \frac{\displaystyle\int_{\Sigma} S_V(\mathrm{P})\, \mathcal{I}(\mathrm{P})\, \mathrm{d}S}{\displaystyle\int_{\Sigma} \mathcal{I}(\mathrm{P})\, \mathrm{d}S} \,,$$

which shows that the 'unresolved' magnetograph signal $(S_V)_{\Sigma}$ is an average over the observed area of the 'resolved' magnetograph signal $S_V(\mathrm{P})$ weighted by the filtered intensity.

As shown in Sect. 11.1, the magnetograph signal is proportional to the longitudinal component of the magnetic field vector under the weak field approximation. Therefore, if the magnetic field is everywhere weak across the surface Σ, one has, recalling Eq. (11.3)

$$\big(S_V\big)_{\Sigma} = \frac{\displaystyle\int_{\Sigma} C_{\parallel}(\mathrm{P})\, B_{\parallel}(\mathrm{P})\ \mathcal{I}(\mathrm{P})\, \mathrm{d}S}{\displaystyle\int_{\Sigma} \mathcal{I}(\mathrm{P})\, \mathrm{d}S} \,,$$

where $C_{\parallel}(\mathrm{P})$ is the calibration constant corresponding to the intensity profile emerging from point P. On the other hand, the magnetograph is calibrated with a fixed intensity profile, usually the profile corresponding to the quiet (or non-magnetic) average photosphere (see Sect. 11.1). Let us denote by $(C_{\parallel})_{\mathrm{q}}$ the actual calibration constant. When the magnetograph signal is interpreted in terms of a linear relation of the form of Eq. (11.3), what is in fact obtained is an apparent longitudinal component given by

$$(B_{\parallel})_{\mathrm{app}} = \frac{\displaystyle\int_{\Sigma} C_{\parallel}(\mathrm{P})\, B_{\parallel}(\mathrm{P})\ \mathcal{I}(\mathrm{P})\, \mathrm{d}S}{(C_{\parallel})_{\mathrm{q}} \displaystyle\int_{\Sigma} \mathcal{I}(\mathrm{P})\, \mathrm{d}S} \,. \tag{11.24}$$

Two special cases of this equation deserve some attention. The first is the case where the intensity profile $I(\lambda;\mathrm{P})$ is the same as the profile corresponding to the quiet photosphere. This implies that the quantity $\mathcal{I}(\mathrm{P})$ is independent of P and that $C_{\parallel}(\mathrm{P}) = (C_{\parallel})_{\mathrm{q}}$, thus Eq. (11.24) reduces to

$$(B_{\parallel})_{\mathrm{app}} = \big\langle B_{\parallel} \big\rangle = \frac{1}{A} \int_{\Sigma} B_{\parallel}(\mathrm{P})\, \mathrm{d}S \,, \tag{11.25}$$

where A is the area of the surface Σ. This result is at the basis of the statement – often quoted in solar magnetometry – according to which the longitudinal magnetograph measures the flux of the magnetic field vector across the observed area. Apart from an obvious dimensional factor (needed to transform the average longitudinal field into the magnetic flux), and from an equally obvious geometrical

distinction (the longitudinal component coincides with the vertical component only at disk center), the above derivation shows that this statement is only valid under a heavy set of assumptions (field everywhere weak, intensity profile independent of point P and coincident with the average photospheric profile).

The second special case of Eq. (11.24) occurs when one assumes that a fraction f of the observed area is covered by a uniform magnetic field having longitudinal component $(B_\parallel)_\mathrm{m}$, whereas the remaining fraction $(1-f)$ is just the quiet (non-magnetic) solar atmosphere. The quantity f is often referred to as the *filling factor*. The intensity profile is assumed to be constant throughout the 'magnetic fraction' of the observed area and may differ from the profile corresponding to the quiet atmosphere. This implies different values for the filtered intensities of the 'magnetic' and 'quiet' fractions ($\mathcal{I}_\mathrm{m}$ and $\mathcal{I}_\mathrm{q}$, respectively) as well as different values for the calibration constants $(C_\parallel)_\mathrm{m}$ and $(C_\parallel)_\mathrm{q}$. Under these assumptions we obtain from Eq. (11.24)

$$(B_\parallel)_\mathrm{app} = \frac{f\,(C_\parallel)_\mathrm{m}\,\mathcal{I}_\mathrm{m}}{(C_\parallel)_\mathrm{q}\left[(1-f)\,\mathcal{I}_\mathrm{q} + f\,\mathcal{I}_\mathrm{m}\right]}\;(B_\parallel)_\mathrm{m}\;. \tag{11.26}$$

If, for instance, the intensity profile in the magnetic region is simply scaled by a factor Θ (a sort of thermodynamic parameter) with respect to the profile corresponding to the quiet atmosphere, one has

$$\mathcal{I}_\mathrm{m} = \Theta\,\mathcal{I}_\mathrm{q}\;, \qquad (C_\parallel)_\mathrm{m} = (C_\parallel)_\mathrm{q}\;, \tag{11.27}$$

so that

$$(B_\parallel)_\mathrm{app} = \frac{f\,\Theta}{1-f+f\,\Theta}\;(B_\parallel)_\mathrm{m}\;. \tag{11.28}$$

Equations (11.26) and (11.28), though valid under a number of simplifying assumptions, are able to account for a phenomenon known since a long time in solar magnetometry, namely the differences that are commonly found when comparing the values of $B_\parallel$ derived from longitudinal magnetographs operating simultaneously on different spectral lines (Harvey and Livingston, 1969). Such differences cannot be interpreted as due only to magnetic saturation effects (see Sect. 11.1) and imply that each spectral line has its own peculiar behavior in magnetic regions (its own Θ value, for instance, in the simplified model leading to Eq. (11.28)). In other words, since the thermodynamic structure of magnetic regions is different from that of the quiet atmosphere, each line is characterized by a different amount of weakening (or strengthening) which eventually affects the apparent value of $B_\parallel$ measured by a longitudinal magnetograph.

In order to analyze the influence of unresolved fields on the results obtained by vector magnetographs, Eq. (11.23) has to be complemented with the corresponding equations for the Stokes parameters Q and U (see Eqs. (11.6))

$$\left(S_Q\right)_\Sigma = \frac{\displaystyle\int_\Sigma \mathrm{d}S \int Q(\lambda;\mathrm{P})\,p'(\lambda)\,\mathrm{d}\lambda}{\displaystyle\int_\Sigma \mathrm{d}S \int I(\lambda;\mathrm{P})\,p'(\lambda)\,\mathrm{d}\lambda}$$

$$\big(S_U\big)_{\Sigma} = \frac{\displaystyle\int_{\Sigma} \mathrm{d}S \int U(\lambda;\mathrm{P})\, p'(\lambda)\, \mathrm{d}\lambda}{\displaystyle\int_{\Sigma} \mathrm{d}S \int I(\lambda;\mathrm{P})\, p'(\lambda)\, \mathrm{d}\lambda} \,. \tag{11.29}$$

Similarly to the case of the longitudinal magnetograph, these expressions can be cast into a more significant form by introducing the local values of the linear polarization signals (defined in the preferred frame)

$$S_{\tilde{Q}}(\mathrm{P}) = \frac{\displaystyle\int \tilde{Q}(\lambda;\mathrm{P})\, p'(\lambda)\, \mathrm{d}\lambda}{\displaystyle\int I(\lambda;\mathrm{P})\, p'(\lambda)\, \mathrm{d}\lambda} \,, \qquad S_{\tilde{U}}(\mathrm{P}) = \frac{\displaystyle\int \tilde{U}(\lambda;\mathrm{P})\, p'(\lambda)\, \mathrm{d}\lambda}{\displaystyle\int I(\lambda;\mathrm{P})\, p'(\lambda)\, \mathrm{d}\lambda} \,,$$

and the local value of the filtered intensity

$$\mathcal{I}'(\mathrm{P}) = \int I(\lambda;\mathrm{P})\, p'(\lambda)\, \mathrm{d}\lambda \,.$$

Denoting by $\chi(\mathrm{P})$ the azimuth of the magnetic field at point P reckoned in the observer's frame, Eqs. (11.29) can be rewritten in the following form (cf. Eqs. (11.11))

$$\big(S_Q\big)_{\Sigma} = \frac{\displaystyle\int_{\Sigma} \Big[S_{\tilde{Q}}(\mathrm{P})\, \cos 2\chi(\mathrm{P}) - S_{\tilde{U}}(\mathrm{P})\, \sin 2\chi(\mathrm{P})\Big]\, \mathcal{I}'(\mathrm{P})\, \mathrm{d}S}{\displaystyle\int_{\Sigma} \mathcal{I}'(\mathrm{P})\, \mathrm{d}S}$$

$$\big(S_U\big)_{\Sigma} = \frac{\displaystyle\int_{\Sigma} \Big[S_{\tilde{Q}}(\mathrm{P})\, \sin 2\chi(\mathrm{P}) + S_{\tilde{U}}(\mathrm{P})\, \cos 2\chi(\mathrm{P})\Big]\, \mathcal{I}'(\mathrm{P})\, \mathrm{d}S}{\displaystyle\int_{\Sigma} \mathcal{I}'(\mathrm{P})\, \mathrm{d}S} \,.$$

As shown in Sect. 11.2, when the magnetic field is weak, the signal $S_{\tilde{U}}$ is zero (Eq. (11.7)), whereas the signal $S_{\tilde{Q}}$ is proportional to the square of the transverse component of the magnetic field vector (Eq. (11.9)). Thus, if the magnetic field is everywhere weak across the surface Σ, one has

$$\big(S_Q\big)_{\Sigma} = \frac{\displaystyle\int_{\Sigma} C_{\perp}(\mathrm{P})\, \big[B_{\perp}(\mathrm{P})\big]^2 \cos 2\chi(\mathrm{P})\;\; \mathcal{I}'(\mathrm{P})\, \mathrm{d}S}{\displaystyle\int_{\Sigma} \mathcal{I}'(\mathrm{P})\, \mathrm{d}S}$$

$$\big(S_U\big)_{\Sigma} = \frac{\displaystyle\int_{\Sigma} C_{\perp}(\mathrm{P})\, \big[B_{\perp}(\mathrm{P})\big]^2 \sin 2\chi(\mathrm{P})\;\; \mathcal{I}'(\mathrm{P})\, \mathrm{d}S}{\displaystyle\int_{\Sigma} \mathcal{I}'(\mathrm{P})\, \mathrm{d}S} \,, \tag{11.30}$$

where $C_{\perp}(\mathrm{P})$ is the calibration constant corresponding to the intensity profile emerging from point P. Denoting by $(C_{\perp})_{\mathrm{q}}$ the calibration constant corresponding to the intensity profile of the quiet solar atmosphere, the signals of Eqs. (11.30)

will then be interpreted in terms of 'apparent' quantities: the apparent azimuth $\chi_{\rm app}$ implicitly defined by[1]

$$\int_{\Sigma} C_{\perp}(\mathrm{P}) \left[B_{\perp}(\mathrm{P})\right]^2 \sin 2\big[\chi(\mathrm{P}) - \chi_{\rm app}\big] \; \mathcal{I}'(\mathrm{P}) \, \mathrm{d}S = 0 \; , \tag{11.31}$$

and the apparent transverse component

$$(B_{\perp})_{\rm app} = \sqrt{\frac{\displaystyle\int_{\Sigma} C_{\perp}(\mathrm{P}) \left[B_{\perp}(\mathrm{P})\right]^2 \cos 2\big[\chi(\mathrm{P}) - \chi_{\rm app}\big] \; \mathcal{I}'(\mathrm{P}) \, \mathrm{d}S}{(C_{\perp})_{\rm q} \displaystyle\int_{\Sigma} \mathcal{I}'(\mathrm{P}) \, \mathrm{d}S}} \; . \tag{11.32}$$

Similarly to the former discussion concerning the longitudinal magnetograph, we consider two special cases. The first is the case where the intensity profile does not depend on point P and can be considered the same as the profile of the quiet atmosphere. Here the angle $\chi_{\rm app}$ is implicitly defined by

$$\big\langle \left[B_{\perp}(\mathrm{P})\right]^2 \sin 2\big[\chi(\mathrm{P}) - \chi_{\rm app}\big] \big\rangle = 0 \; ,$$

where the symbol $\langle \cdots \rangle$ means an average over the surface Σ as in Eq. (11.25), and the apparent transverse component is given by

$$(B_{\perp})_{\rm app} = \sqrt{\big\langle \left[B_{\perp}(\mathrm{P})\right]^2 \cos 2\big[\chi(\mathrm{P}) - \chi_{\rm app}\big] \big\rangle} \; .$$

The second is the case of the filling factor hypothesis. Here, denoting by the index 'm' all quantities referring to the magnetic region, and by the index 'q' all quantities referring to the quiet atmosphere, one has

$$\chi_{\rm app} = \chi_{\rm m}$$

and

$$(B_{\perp})_{\rm app} = \sqrt{\frac{f \, (C_{\perp})_{\rm m} \, \mathcal{I}'_{\rm m}}{(C_{\perp})_{\rm q} \left[(1-f) \, \mathcal{I}'_{\rm q} + f \, \mathcal{I}'_{\rm m}\right]}} \; (B_{\perp})_{\rm m} \; , \tag{11.33}$$

or, introducing the scale factor Θ as in Eqs. (11.27)

$$(B_{\perp})_{\rm app} = \sqrt{\frac{f \, \Theta}{1 - f + f \, \Theta}} \; (B_{\perp})_{\rm m} \; . \tag{11.34}$$

It is also interesting to combine these last expressions with Eqs. (11.26) or (11.28) in order to find the influence of the lack of resolution on the inclination angle θ of

[1] Note that Eq. (11.31) leaves an ambiguity of 90° in the value of $\chi_{\rm app}$. This ambiguity can be removed by requiring that the argument of the square root in Eq. (11.32) be positive.

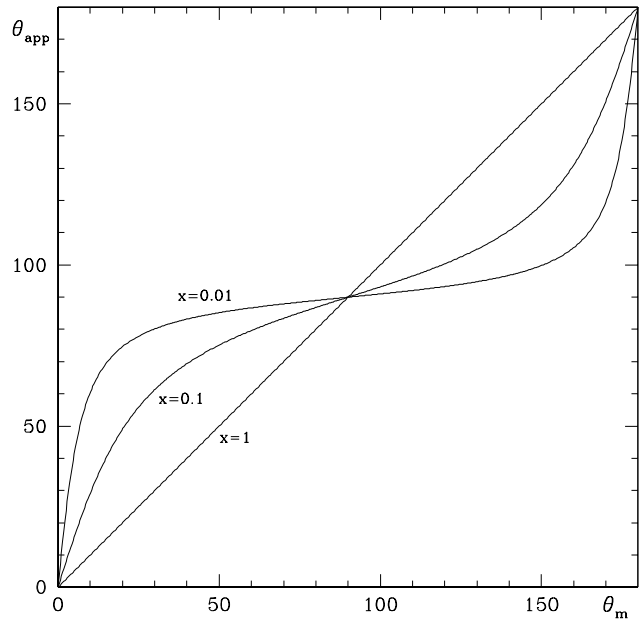

Fig.11.8. The 'apparent' inclination of the magnetic field vector is plotted as a function of the true inclination angle of the field in an unresolved magnetic region. The parameter x is, as an order of magnitude, equal to the filling factor f (see text).

the magnetic field vector with respect to the line of sight. The 'apparent' value of the inclination angle, $\theta_{\rm app}$, is connected with the value in the unresolved magnetic region, $\theta_{\rm m}$, by the relation

$$\tan\theta_{\rm app} = \frac{(B_\perp)_{\rm app}}{(B_\parallel)_{\rm app}} = \frac{\tan\theta_{\rm m}}{\sqrt{x}} \ ,$$

where[1]

$$x = \frac{f\,\Theta}{1-f+f\,\Theta} \ .$$

The relation between $\theta_{\rm app}$ and $\theta_{\rm m}$ is shown in Fig. 11.8 for different values of the parameter x. The figure clearly shows that when the filling factor f is very small (hence x is also very small), the magnetic field recovered by a vector magnetograph tends to appear as a highly inclined field (θ close to 90°), no matter what the true inclination of the field in the unresolved region is.

Up to now we have basically restricted our discussion to weak fields. When strong, unresolved fields are present, things get more complicated because saturation effects come into play and it is difficult, in general, to disentangle such effects from those

[1] This expression for x is obtained by combining Eqs. (11.28) and (11.34). The combination of Eqs. (11.26) and (11.33) leads to a more complicated expression for x which, however, is still proportional to the filling factor f under the limit $f \to 0$.

due to the lack of resolution. Exceptions can however be found, as demonstrated by a diagnostic technique which is just based on saturation phenomena and is known under the name of *line-ratio technique* (Stenflo, 1973).

The line-ratio technique is based on the comparison of the (longitudinal) magnetograph signals observed simultaneously in two spectral lines having the same behavior with respect to the thermodynamic parameters but different Landé factors. Denoting the two lines by the indices 1 and 2, respectively, and introducing the filling factor hypothesis, the magnetograph signal in either line is given by

$$\left(S_V\right)_i = \frac{f \int V_{\rm m}^{(i)}(\lambda)\, p_i(\lambda)\, {\rm d}\lambda}{\int \left[(1-f)\, I_{\rm q}^{(i)}(\lambda) + f\, I_{\rm m}^{(i)}(\lambda)\right] p_i(\lambda)\, {\rm d}\lambda} \qquad (i = 1, 2)\,, \tag{11.35}$$

where $I_{\rm q}^{(i)}(\lambda)$ is the intensity of the solar radiation coming from the quiet atmosphere, $I_{\rm m}^{(i)}(\lambda)$ and $V_{\rm m}^{(i)}(\lambda)$ are the intensity and circular polarization emerging from the magnetic region, and $p_1(\lambda)$, $p_2(\lambda)$ are two identical profiles, the first centered in a wing of line 1 and the second in the corresponding wing of line 2, at the same distance from line center. If the two lines are identical from the point of view of their thermodynamic behavior, this implies that

$$\int I_{\rm q}^{(1)}(\lambda)\, p_1(\lambda)\, {\rm d}\lambda = \int I_{\rm q}^{(2)}(\lambda)\, p_2(\lambda)\, {\rm d}\lambda\,, \tag{11.36}$$

and if the magnetic field in the magnetic region is weak we also have

$$\int I_{\rm m}^{(1)}(\lambda)\, p_1(\lambda)\, {\rm d}\lambda = \int I_{\rm m}^{(2)}(\lambda)\, p_2(\lambda)\, {\rm d}\lambda$$

and, from Eq. (11.2)

$$\int V_{\rm m}^{(1)}(\lambda)\, p_1(\lambda)\, {\rm d}\lambda = \frac{\bar{g}_1}{\bar{g}_2} \int V_{\rm m}^{(2)}(\lambda)\, p_2(\lambda)\, {\rm d}\lambda\,,$$

where $\bar{g}_1$ and $\bar{g}_2$ are the effective Landé factors of the two lines. Substituting these relations into Eq. (11.35) and evaluating the ratio R of the two signals one has, irrespective of the filling factor and of any possible weakening (or enhancement) of the lines in the magnetic region

$$R = \frac{\left(S_V\right)_1}{\left(S_V\right)_2} = \frac{\bar{g}_1}{\bar{g}_2}\,.$$

If, on the contrary, the magnetic field falls outside the weak field regime, it can be expected that the line having the larger Landé factor (line 1, say) saturates more than the other, so that

$$R < \frac{\bar{g}_1}{\bar{g}_2}\,.$$

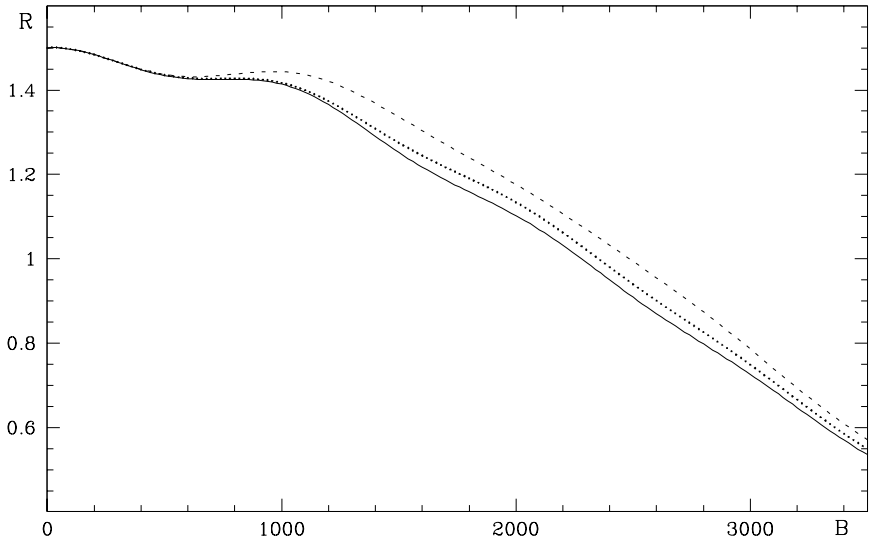

Fig.11.9. A simulation of the ratio R of the circular polarization signals observed by a longitudinal magnetograph in the two lines $\lambda\,5250.21$ and $\lambda\,5247.05$, plotted as a function of the magnetic field intensity for different values of the inclination angle θ (full line: $\theta = 0^\circ$ or 180°; dotted line: $\theta = 30^\circ$ or 150°; dashed line: $\theta = 60^\circ$ or 120°).

Since the ratio R is a function of the magnetic field vector that can be evaluated through model calculations, it follows that from the observed value of R it is possible to obtain an order-of-magnitude estimate of the magnetic field intensity in the unresolved structure.

By a fortunate coincidence, the solar spectrum does indeed present a pair of lines particularly suitable for the application of the line-ratio technique. These are the two FeI lines at 5250.21 Å (line 1) and 5247.05 Å (line 2). Both lines belong to multiplet n. 1 of FeI [1] and happen to have practically the same value for the quantity $\tilde{g}_\ell\, f(\alpha_\ell J_\ell \rightarrow \alpha_u J_u)$, $\tilde{g}_\ell$ being the degeneracy of the lower level of the transition and $f(\alpha_\ell J_\ell \rightarrow \alpha_u J_u)$ the oscillator strength defined in Eq. (9.20). Laboratory measurements by Blackwell et al. (1979) give in fact

$$\left[\mathrm{Log}(\tilde{g}f)\right]_{\mathrm{line\,1}} = -4.938\,, \qquad \left[\mathrm{Log}(\tilde{g}f)\right]_{\mathrm{line\,2}} = -4.946\,,$$

with a relative difference less than 2%. This property, together with the fact that the lower levels of the two lines are very close in energy (the difference is 0.034 eV) and with the further property of the closeness in the spectrum (which implies the same Doppler broadening) assures that the two lines have, to a very good approximation, the same absorption coefficient and hence the same behavior for any stratification of the thermodynamic parameters with depth.

Figure 11.9 shows the behavior of the ratio R for the two lines mentioned as a function of the magnetic field intensity, for different field inclinations. R was

[1] Line 1 corresponds to the transition $a^5\mathrm{D}_0 - z^7\mathrm{D}^\mathrm{o}_1$. It is a normal Zeeman triplet having $\bar{g} = 3$. Line 2 corresponds to the transition $a^5\mathrm{D}_2 - z^7\mathrm{D}^\mathrm{o}_3$. It is a Zeeman multiplet with $\bar{g} = 2$.

computed under the limit of very small filling factor which yields, taking into account Eqs. (11.35) and (11.36)

$$R = \frac{\int V_{\rm m}^{(1)}(\lambda)\, p_1(\lambda)\, {\rm d}\lambda}{\int V_{\rm m}^{(2)}(\lambda)\, p_2(\lambda)\, {\rm d}\lambda} \,.$$

The V Stokes profiles were computed assuming the two lines to be formed in a Milne-Eddington atmosphere with the same set of atmospheric and line parameters (the same values as in Fig. 11.6 – which refers to the $\lambda\,5250.21$ line – were used, namely $\kappa_{\rm L} = 6.1$, $\Delta\lambda_{\rm D} = 32\,{\rm m\AA}$, $a = 0.04$, $\beta\mu = 12$). The profiles $p_1(\lambda)$ and $p_2(\lambda)$ were supposed to have a Gaussian shape as in Eq. (11.5) with $\Delta\lambda_{\rm F} = 75\,{\rm m\AA}$, and to be positioned at $60\,{\rm m\AA}$ from line center for both lines. As expected from our previous discussion, the ratio R approaches asymptotically the value 1.5 ($= \bar{g}_1/\bar{g}_2$) under the limit $B \to 0$, and decreases monotonically with increasing B.

Through the line-ratio technique applied to this specific pair of lines it has been possible to give a quantitative estimate of the dimensions and of the intrinsic field intensity of magnetic regions observed at low spatial resolution by magnetographic techniques (Howard and Stenflo, 1972; Frazier and Stenflo, 1972; Stenflo, 1973). The magnetic field outside sunspots was found to be concentrated in small areas, with typical dimensions of the order of 100-300 km, mostly located in the supergranular network and having intrinsic magnetic field intensities in the kG range.

It should be remarked, however, that in low resolution observations weak fields tend to be substantially underestimated, because they have a larger probability of reconnecting at short distances, i.e., within the resolution element of the instrument. This implies that the contribution of weak fields to both the observed signals $(S_V)_1$ and $(S_V)_2$, and hence to their ratio R, is likely to cancel out in many cases.

11.5.b Unno-fit Technique

The Unno-fit technique described in Sect. 11.3 can be suitably adapted to measure the intensity and direction of the magnetic field vector in an unresolved magnetic structure under the 'filling factor' approximation. To this aim, the theoretical Stokes profiles entering the merit function of Eq. (11.14) are modified according to the transformation

$$I_{j\alpha}^{(\rm thr)} \to f\, I_{j\alpha}^{(\rm thr)} + (1-f)\, \delta_{j0}\, (I_\alpha)_{\rm q} \,,$$

where $I_{j\alpha}^{(\rm thr)}$ (in the right-hand side) is defined in Eq. (11.15) and where $(I_\alpha)_{\rm q}$, the intensity of the quiet atmosphere at wavelength point α, is assumed to be known a priori.[1] The filling factor f can now be considered as an additional parameter that can be deduced, together with the other ones, from the observational data.

[1] In raster-type observations, $(I_\alpha)_{\rm q}$ can be obtained by taking the average of the intensity spectra over all the points of the raster (excluding sunspots and active regions, if necessary).

This procedure, when applied to active region observations, generally shows that the filling factor f recovered from the fit is much less than unity outside sunspots, a further indication of the existence of unresolved fields (Lites and Skumanich, 1990).

11.5.c Center-of-Gravity Technique

In this subsection we analyze the results of the application of the center-of-gravity technique to observations involving unresolved fields. The corresponding analysis on the bisector technique is omitted because too complicated and dependent on too many parameters.

Using notations similar to those of Eq. (11.23), the first-order moments of the right and left circular polarization profiles are given by (cf. Eq. (11.19))

$$\left(\lambda_{\pm}^{(\mathrm{g})}\right)_{\Sigma} = \frac{\displaystyle\int_{\Sigma} \mathrm{d}S \int \Big[\, \frac{1}{2}\, I_{\mathrm{c}}(\mathrm{P}) - I_{\pm}(\lambda;\mathrm{P}) \,\Big] \lambda \, \mathrm{d}\lambda}{\displaystyle\int_{\Sigma} \mathrm{d}S \int \Big[\, \frac{1}{2}\, I_{\mathrm{c}}(\mathrm{P}) - I_{\pm}(\lambda;\mathrm{P}) \,\Big] \, \mathrm{d}\lambda} \,, \tag{11.37}$$

where the integrals in $\mathrm{d}S$ are extended to the solar region Σ covered by the instrument. It is convenient to introduce the local value of the moments, $\lambda_{\pm}^{(\mathrm{g})}(\mathrm{P})$, defined by

$$\lambda_{\pm}^{(\mathrm{g})}(\mathrm{P}) = \frac{\displaystyle\int \Big[\, \frac{1}{2}\, I_{\mathrm{c}}(\mathrm{P}) - I_{\pm}(\lambda;\mathrm{P}) \,\Big] \lambda \, \mathrm{d}\lambda}{\displaystyle\int \Big[\, \frac{1}{2}\, I_{\mathrm{c}}(\mathrm{P}) - I_{\pm}(\lambda;\mathrm{P}) \,\Big] \, \mathrm{d}\lambda} \,,$$

and the local value of the *integrated line depression*

$$\mathcal{J}_{\pm}(\mathrm{P}) = \int \Big[\, \frac{1}{2}\, I_{\mathrm{c}}(\mathrm{P}) - I_{\pm}(\lambda;\mathrm{P}) \,\Big] \, \mathrm{d}\lambda \,.$$

With these notations, Eq. (11.37) reads

$$\left(\lambda_{\pm}^{(\mathrm{g})}\right)_{\Sigma} = \frac{\displaystyle\int_{\Sigma} \lambda_{\pm}^{(\mathrm{g})}(\mathrm{P}) \;\, \mathcal{J}_{\pm}(\mathrm{P}) \, \mathrm{d}S}{\displaystyle\int_{\Sigma} \mathcal{J}_{\pm}(\mathrm{P}) \, \mathrm{d}S} \,,$$

which shows that the 'unresolved' center of gravity of the right (left) circular polarization profile is an average over the observed region of the 'resolved' center of gravity of the same profile weighted by the corresponding integrated line depression.

As shown in Sect. 11.4, for any Zeeman triplet formed in a constant magnetic field parallel to the line of sight ($\theta = 0^{\circ}$ in the geometry of Fig. 9.1), one has (see Eq. (11.22))

$$\lambda_{+}^{(\mathrm{g})}(\mathrm{P}) - \lambda_{-}^{(\mathrm{g})}(\mathrm{P}) = 2\, g\, \Delta\lambda_B(\mathrm{P})$$

and

$$\mathcal{J}_{+}(\mathrm{P}) = \mathcal{J}_{-}(\mathrm{P}) = \mathcal{J}(\mathrm{P}) \,,$$

so that one obtains, in terms of apparent fields[1]

$$(B_\parallel)_{\rm app} = \frac{\displaystyle\int_\Sigma B_\parallel({\rm P})\, \mathcal{J}({\rm P})\, {\rm d}S}{\displaystyle\int_\Sigma \mathcal{J}({\rm P})\, {\rm d}S} \ . \tag{11.38}$$

This expression bears a strong resemblance to the corresponding expression derived for the longitudinal magnetograph (Eq. (11.24)). By analogy, we consider two particular cases. The first is the case where the right and left circular polarization profiles are independent of the point P (apart from the shift due to the magnetic field), and the continuum intensity is also independent of P. In this case the integrated line depression $\mathcal{J}$ is independent of P and one obtains

$$(B_\parallel)_{\rm app} = \langle B_\parallel \rangle = \frac{1}{A} \int_\Sigma B_\parallel({\rm P})\, {\rm d}S \ ,$$

where A is the area of the surface Σ. This equation shows that, in the case of unresolved fields, the center-of-gravity technique measures the flux (see comments after Eq. (11.25)) of the magnetic field vector across the observed area, though it should be stressed that this statement is only valid under the restrictive set of assumptions specified above (Zeeman triplet, field parallel or antiparallel to the line of sight, integrated line depression independent of P).

The second particular case is that of the filling factor hypothesis; one gets (cf. del Toro Iniesta et al., 1990)

$$(B_\parallel)_{\rm app} = \frac{f\, \mathcal{J}_{\rm m}}{(1-f)\, \mathcal{J}_{\rm q} + f\, \mathcal{J}_{\rm m}}\ (B_\parallel)_{\rm m} \ ,$$

where the indices 'q' and 'm' refer to the quiet atmosphere and to the magnetic atmosphere, respectively.

11.6. Other Inversion Techniques

In the previous sections of this chapter we have analyzed in some detail the most traditional inversion techniques of solar magnetometry, with the aim of providing the reader with a firm background on the physical phenomena that underlie the problem of measuring magnetic fields in the solar atmosphere. In this section we give a brief review and some bibliographical references on more recent techniques, without however pretending to be exhaustive. It should be realized that the amount

[1] The same line of reasoning can be applied to $\theta = 180°$ and leads to the same expression for $(B_\parallel)_{\rm app}$. Equation (11.38) is thus valid for an arbitrary mixture of fields parallel or antiparallel to the line of sight.

of work carried out on this subject during almost one century is very large, and a full treatment is outside the aims of this book.

11.6.a Stokes Inversion based on Response Functions (SIR)

One of the most sophisticated methods that have been developed in the last few years for recovering the magnetic field vector from Stokes profiles (observed in a wavelength range covering one or more spectral lines) is the so-called SIR ('Stokes Inversion based on Response functions': Ruiz Cobo and del Toro Iniesta, 1992). This method can be considered as the natural evolution of two distinct techniques: on one side, the Unno-fit technique (described in Sect. 11.3); on the other side, an empirical approach which consists in fitting numerical solutions of the radiative transfer equation based on detailed atmospheric models (quiet atmosphere, sunspot, plage, etc.) to the observed Stokes profiles. The Unno-fit technique suffers from the disadvantage of being based on a rather crude approximation (the Milne-Eddington model atmosphere, described in Sect. 9.8), which does not allow for the depth dependence of important physical parameters such as the absorption coefficients, the slope of the source function, the line Doppler width, etc. On the other hand, in the empirical approach outlined above the description of the depth dependence of the thermodynamic parameters is certainly more accurate, but the fit to the observed data is obtained by a trial-and-error procedure which suffers from all the limitations typical of its kind.[1]

In the SIR method one constructs a merit function similar to that introduced for the Unno-fit technique (see Eq. (11.14)), with the difference that the theoretical Stokes profiles are now obtained via a numerical solution to the radiative transfer equation for polarized radiation. The set of parameters $\{\zeta_i\}$ includes the magnetic field (intensity, inclination and azimuth), the line-of-sight velocity of the atmospheric plasma, and the thermodynamic parameters like temperature, gas pressure and microturbulent velocity, all these quantities being parameterized at a few depth points in the atmosphere. The procedure to find the best fit is still based on the Marquardt algorithm and makes a heavy use of response functions and of generalized response functions (see Sect. 9.16) in order to calculate the derivatives of the theoretical Stokes profiles with respect to the different parameters ζ_i.

The SIR technique was developed for the interpretation of spectral lines formed under LTE conditions in plane-parallel atmospheres. The method has been successfully applied to solar spectropolarimetric observations in photospheric lines, e.g., for recovering the depth dependence of the atmospheric parameters in sunspots (Westendorp Plaza et al., 1997) and the magnetic and thermodynamic parameters of unresolved magnetic structures embedded in the quiet solar photosphere (Bellot Rubio et al., 1997). More recently, the combination of efficient iterative methods for the solution of multilevel transfer problems (Trujillo Bueno and Fabiani Bendicho, 1995; Socas Navarro and Trujillo Bueno, 1997) with the SIR method has allowed the development of a non-LTE inversion technique of Stokes profiles (Socas

[1] The most important limitation is the 'cultural bias' introduced by the operator in determining which of the parameters has to be varied to obtain a better fit.

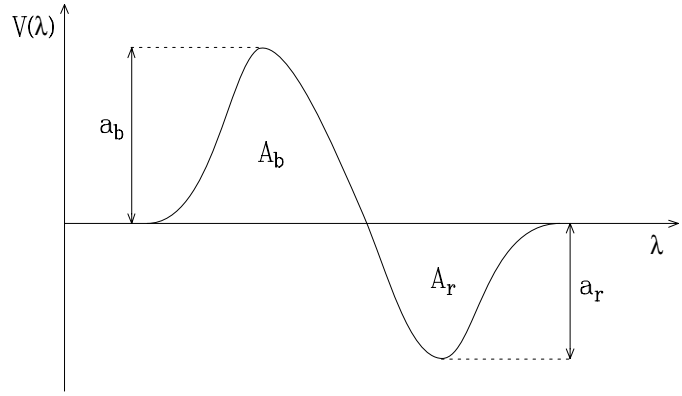

Fig.11.10. The peak asymmetry and the area asymmetry are defined in terms of the quantities $a_{\rm b}$, $a_{\rm r}$, $A_{\rm b}$, and $A_{\rm r}$ (see Eqs.(11.39)). $A_{\rm b}$ and $A_{\rm r}$ (where b and r stand, as customary, for 'blue' and 'red') are the absolute values of the areas contained between the V profile and the wavelength axis, $a_{\rm b}$ and $a_{\rm r}$ the absolute values of the peak heights. The figure refers to a positive polarity observation. For negative polarity it would be reversed about the wavelength axis.

Navarro et al., 2000).

11.6.b Inversion of FTS Data

The use of the Fourier Transform Spectrometer at the McMath-Pierce solar facility of the National Solar Observatory (Kitt Peak) made possible, in the late 1970s, the observation of the full solar spectrum in two directions of polarization (typically $I+V$ and $I-V$) with unprecedented spectral resolution though with very low spatial resolution (Stenflo et al., 1983a, 1983b, 1984). Such observations, usually performed on facular regions, revealed a number of interesting phenomena and, in particular, pointed out the existence of prominent asymmetries in the V profiles of most spectral lines.[1] These asymmetries have been characterized by Solanki and Stenflo (1985) by means of two parameters: the *peak asymmetry* and the *area asymmetry* defined, respectively, as

$$\delta_a = \frac{a_{\rm b} - a_{\rm r}}{a_{\rm b} + a_{\rm r}} \,, \qquad \delta_A = \frac{A_{\rm b} - A_{\rm r}}{A_{\rm b} + A_{\rm r}} \,, \tag{11.39}$$

where the meaning of the different symbols is specified in Fig. 11.10. It turns out that both the peak asymmetry and the area asymmetry are generally positive (irrespective of the prevailing polarity of the observed active region), and widely vary from line to line. Typical values at disk center are of the order of 10% for the peak asymmetry and 5% for the area asymmetry. Such values generally decrease with increasing distance from disk center and become negative for many lines at the extreme limb.

[1] Stokes profiles asymmetries had already been observed by the so-called Stokes-I and Stokes-II polarimeters of the High Altitude Observatory (Baur et al., 1981).

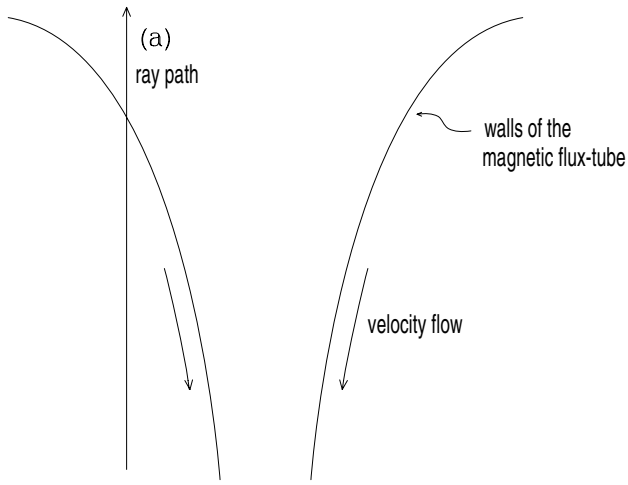

Fig.11.11. In a funnel-shaped magnetic flux-tube a ray path like (a) gives rise to a V profile with positive peak asymmetry and positive area asymmetry.

The interpretation of these results has basically been given in terms of the filling factor hypothesis, by supposing that the polarization signal contained in the observations (the spectrum of V, or of Q and U) is due to a collection of unresolved and ubiquitous magnetic structures, the so-called flux-tubes. In an extensive series of papers, the geometrical and thermodynamic properties of a kind of 'average' flux-tube have been established by comparing the observed polarization profiles with numerical solutions to the radiative transfer equations for polarized radiation (see Solanki, 1993, for a detailed review of the subject). The model that has emerged from these investigations is that of a slender, funnel-shaped, static magnetic tube having typical horizontal dimensions of a few hundreds of km, in hydrostatic equilibrium with the surrounding unperturbed atmosphere. The asymmetries of the V profiles are interpreted in this model as due to the presence of a macroscopic flow of material directed downward in the non-magnetic atmosphere surrounding the tube (Grossman-Doerth et al., 1988b). It can be proved that the ray paths crossing the walls of the flux-tube, such as that schematized in Fig. 11.11, lead to positive values for the peak and area asymmetries defined in Eqs. (11.39).[1] It should be remarked that the empirical flux-tube model described above is consistent with a dynamical model obtained by two-dimensional magnetohydrodynamic simulations of a collapsing magnetic structure (Knölker et al., 1988).

Notwithstanding the success obtained by the flux-tube hypothesis in explaining the FTS data, the intrinsic lack of spatial resolution of the data themselves inevitably raises some doubts on whether the model described above may indeed

[1] The positive sign of the area asymmetry is in fact predicted by the simple slab-model developed as *Case iii* of Sect. 9.21. That model can be adapted to the present case by setting $\Delta\lambda_{\rm A}^{(\rm s)} < 0$ and $(\Delta\lambda_B - \Delta\lambda_B^{(\rm s)}) < 0$. For a line with $g > 0$, Eqs. (9.256) and (9.257) yield $\mathfrak{v} > 0$ for $\theta = 0^\circ$ and $\mathfrak{v} < 0$ for $\theta = 180^\circ$, which are consistent with a positive area asymmetry (cf. Eq. (9.238)).

give a faithful representation of the physical reality. A definite breakthrough on this subject may only be obtained when high spatial resolution observations, of the same spectral quality as the FTS data, will be available.

11.6.c Infrared Lines

Infrared lines are of great importance in solar magnetometry. This is due to the fact that, with increasing the wavelength λ, the Zeeman splitting of spectral lines increases as λ^2 (see Eq. (3.14)), whereas the typical line width, due essentially to the Doppler effect, increases as λ (see Eq. (5.46)). As a consequence, when moving towards the infrared, the different Zeeman components are more and more spaced in wavelength for a given value of the magnetic field intensity. To give an example, a magnetic field of 300 G is sufficient to produce a splitting as large as three Doppler widths in a Zeeman triplet at $12\,\mu$m formed in the solar atmosphere.[1] Although this looks very promising, it should be taken into account that the resolving power of a telescope scales as λ^{-1}, which is a rather serious drawback in solar magnetometry. A 1m-aperture telescope, for instance, has a theoretical spatial resolution of approximately $0''.1$ at optical wavelengths, but the resolution degrades to $2''.5$ at $12\,\mu$m.

In spite of these limitations, infrared solar magnetometry is a field which is rapidly evolving both on the instrumental and the theoretical side. Lists of infrared lines especially suitable for solar magnetometry can be found in Solanki et al. (1990), Ramsauer et al. (1995), Rüedi et al. (1995).

In general, any of the techniques described earlier in this chapter – like the Unno-fit or the center-of-gravity technique – can be applied to recover the magnetic field from infrared observations. There is however a particular case which deserves special attention, because it leads to a very simple inversion method. This is the case where the magnetic field is sufficiently strong to separate completely the different Zeeman components, a case discussed in detail in Sect. 9.12. It was shown there that the solutions to the radiative transfer equation can be written in the form of Eqs. (9.144). Here we restrict attention to the case of a normal Zeeman triplet and we also assume the magnetic field vector to be constant and the atmosphere to be static.[2] Under these approximations the emerging Stokes parameters can be cast into the form:

- in the $\sigma_{\rm b}$ component

$$I(\lambda) = I_{\rm c}\left[1 - p_{\rm b}(\lambda)\right]$$

$$Q(\lambda) = I_{\rm c}\, p_{\rm b}(\lambda)\, \frac{\sin^2\theta \cos 2\chi}{1 + \cos^2\theta}$$

[1] This result is obtained from Eq. (5.49) with $T = 5800\,\mathrm{K}$, $\xi = 1\,\mathrm{km\,s^{-1}}$, $\mu = 55.8$ (atomic weight of iron).

[2] It should be recalled that Eqs. (9.144) are valid under the restriction of a constant magnetic field *direction*. Gradients of the magnetic field intensity and of the line-of-sight velocity are in principle allowed, provided that no overlapping of the different Zeeman components occurs (cf. Eqs. (9.138)).

$$U(\lambda) = I_{\rm c}\, p_{\rm b}(\lambda)\, \frac{\sin^2\theta \sin 2\chi}{1+\cos^2\theta}$$

$$V(\lambda) = 2I_{\rm c}\, p_{\rm b}(\lambda)\, \frac{\cos\theta}{1+\cos^2\theta}\ , \qquad (11.40)$$

- in the π component

$$I(\lambda) = I_{\rm c}\left[1 - p_{\rm p}(\lambda)\right]$$

$$Q(\lambda) = -I_{\rm c}\, p_{\rm p}(\lambda)\, \cos 2\chi$$

$$U(\lambda) = -I_{\rm c}\, p_{\rm p}(\lambda)\, \sin 2\chi$$

$$V(\lambda) = 0\ , \qquad (11.41)$$

- in the $\sigma_{\rm r}$ component

$$I(\lambda) = I_{\rm c}\left[1 - p_{\rm r}(\lambda)\right]$$

$$Q(\lambda) = I_{\rm c}\, p_{\rm r}(\lambda)\, \frac{\sin^2\theta \cos 2\chi}{1+\cos^2\theta}$$

$$U(\lambda) = I_{\rm c}\, p_{\rm r}(\lambda)\, \frac{\sin^2\theta \sin 2\chi}{1+\cos^2\theta}$$

$$V(\lambda) = -2I_{\rm c}\, p_{\rm r}(\lambda)\, \frac{\cos\theta}{1+\cos^2\theta}\ , \qquad (11.42)$$

where $I_{\rm c}$ is the continuum intensity, θ and χ are the inclination and azimuth angles defined in Fig. 9.1, and $p_{\rm b}(\lambda)$, $p_{\rm p}(\lambda)$, $p_{\rm r}(\lambda)$ are three profiles centered at the wavelengths $(\lambda_0 - g\,\Delta\lambda_B)$, λ_0, and $(\lambda_0 + g\,\Delta\lambda_B)$ respectively, g being the Landé factor and $\Delta\lambda_B$ the Zeeman splitting defined in Eq. (3.14). The two profiles $p_{\rm b}(\lambda)$ and $p_{\rm r}(\lambda)$ have the same shape and coincide with the profile of a fictitious, non-magnetic line formed in the same atmosphere and having a ratio between line and continuum absorption coefficient given by

$$\kappa = \frac{1}{2}\left(1+\cos^2\theta\right)\kappa_{\rm L}\ ,$$

where $\kappa_{\rm L}$ is the corresponding quantity for the full line. The profile $p_{\rm p}(\lambda)$ has a different shape and coincides with the profile of a fictitious, non-magnetic line having

$$\kappa = \sin^2\theta\ \kappa_{\rm L}\ .$$

Equations (11.40)-(11.42) can be used to derive the magnetic field vector from the observed Stokes profiles of an infrared triplet with well-separated σ and π components. The field intensity is directly obtained by measuring the wavelength separation between any two components (σ or π) in any of the four Stokes parameters and by using Eq. (3.14).[1] The azimuth χ is obtained by considering the ratio

[1] Note that to perform this operation there is no need for polarimetric observations, it

between Q and U in any of the components, σ or π. One has

$$\tan 2\chi = \frac{U(\lambda)}{Q(\lambda)} \, .$$

Finally, the inclination θ is obtained from the ratio between V and $\sqrt{Q^2 + U^2}$ in either the $\sigma_{\rm b}$ or the $\sigma_{\rm r}$ component. For instance, in the $\sigma_{\rm b}$ component

$$\frac{2\cos\theta}{\sin^2\theta} = \frac{V(\lambda)}{\sqrt{Q^2(\lambda) + U^2(\lambda)}} \, ,$$

whence

$$\theta = \arccos\left[\frac{\sqrt{1+x^2}-1}{x}\right] ,$$

where

$$x = \frac{V(\lambda)}{\sqrt{Q^2(\lambda) + U^2(\lambda)}} \, .$$

Obviously, in the case of noisy data this simple procedure can be replaced by a more sophisticated one involving the minimization of an appropriate merit function, similarly to what discussed in Sect. 11.3 about the Unno-fit technique.

11.6.d The Inversion Technique under the MISMA Hypothesis

As illustrated in Subsect. 11.6.b, the Stokes profiles asymmetries observed in facular regions with the Fourier Transform Spectrometer have been interpreted in terms of flux-tube models. An alternative explanation of such asymmetries and of similar phenomena observed in the penumbrae of sunspots (Sánchez Almeida and Lites, 1992) and in the quiet sun (Lites et al., 1996) is based on the MISMA model, where the acronym stands for 'Micro-Structured Magnetic Atmosphere' (Sánchez Almeida et al., 1996). This model is based on the idea that the magnetic structures pervading the solar atmosphere have typical sizes smaller than the mean free path of a photon. In such an environment, the most natural way to treat the process of line formation is the one that we have analyzed in detail in Sect. 9.24 by introducing a stochastic approach. We found there that, under the so-called microturbulent limit (corresponding to the case where the dimensions of the magnetic structures are much smaller than the photon's mean free path), one obtains for the Stokes parameters emerging from a Milne-Eddington model atmosphere (cf. Eq. (9.276))

$$\boldsymbol{I} = B_0 \left[\boldsymbol{1} + \beta' \left\langle \boldsymbol{A} \right\rangle^{-1}\right] \boldsymbol{U} \, , \tag{11.43}$$

is sufficient to have the intensity spectrum. Moreover, this operation is so simple as to justify the statement, often heard about infrared lines, 'A ruler is all that is needed to measure the magnetic field'. However, Eqs. (11.40)-(11.42) show that the intensity spectrum carries very little information about θ and no information at all about χ.

where B_0 and β' are the parameters specifying the source function, $\boldsymbol{A}$ is the propagation matrix defined in Eqs. (9.164), and where the meaning of the symbol $\langle \cdots \rangle$ is defined in Eq. (9.271).

In the MISMA hypothesis, the stochastic average of the propagation matrix, $\langle \boldsymbol{A} \rangle$, is assumed to be represented by an expression of the form

$$\left\langle \, \boldsymbol{A} \, \right\rangle = \sum_{i=1}^{n} \, f_i \, \boldsymbol{A}_i \, . \tag{11.44}$$

This is a special case of Eq. (9.271) corresponding to the assumption that the atmosphere consists of n independent components, each one characterized by its own propagation matrix, $\boldsymbol{A}_i$, and its own probability (or occupation fraction), f_i. By means of Eqs. (11.43) and (11.44) it is possible to reproduce rather well the typical asymmetries of the Stokes profiles observed either in sunspots, or in facular regions or on the quiet sun, even if this requires, in some cases, the introduction of up to three components (Sánchez Almeida et al., 1996). For explaining facular observations, for instance, one needs one prevailing, non-magnetic component with an inclined flow, a static magnetic component with a field slightly inclined with respect to the vertical, and a supplementary magnetic component having a field again slightly inclined with respect to the vertical and a flow of material antiparallel to the magnetic field.

The MISMA hypothesis has also been generalized to allow for a depth dependence of the matrices $\boldsymbol{A}_i$ of Eq. (11.44) and an arbitrary behavior with depth of the source function $B_{\rm P}$. An inversion technique for this case has been proposed by Sánchez Almeida (1997). Broadly speaking, this technique resembles, in its mathematical details, the one that we have already described in Subsect. 11.6.a, with the difference that the radiative transfer equation that is solved to find a fit to the observations is the 'stochastic' equation in the microturbulent limit, namely

$$\frac{\mathrm{d}\, \boldsymbol{I}}{\mathrm{d}\tau} = \left\langle \, \boldsymbol{A} \, \right\rangle \left(\, \boldsymbol{I} - B_{\rm P} \boldsymbol{U} \, \right) \, ,$$

where the matrix $\langle \boldsymbol{A} \rangle$ is given by Eq. (11.44) and $B_{\rm P}$ is the local value of the Planck function. This generalized version of the MISMA hypothesis can lead to a very large number of degrees of freedom. To narrow down the number of possibilities, the inversion code uses several restrictive assumptions based on magnetohydrodynamic considerations. This inversion procedure seems very promising and has proved particularly successful for interpreting the asymmetries observed in the V profile in quiet sun observations (Sánchez Almeida and Lites, 2000).

11.7. Disambiguation

We have already remarked in Sect. 9.5 that the radiative transfer equation for polarized radiation is invariant under a rotation of 180° of the magnetic field vector

about the line of sight, provided atomic polarization phenomena are neglected (see the introduction to Chap. 9). In most of the spectral lines that are commonly employed in solar magnetometry, atomic polarization is believed to play an insignificant role. It follows that the magnetic field vector recovered from standard observations suffers from an intrinsic 180° ambiguity in its azimuth. This raises the fundamental problem – often referred to as the *disambiguation* problem – of finding the true orientation of the transverse component of the magnetic field vector between the two alternatives which are left undecided by the observations.

In the case of an isolated observation the problem cannot be solved. On the contrary, in the case of raster-type observations, several different strategies can be followed. Important contributions to this matter have been given by Cuperman et al. (1990), Canfield et al. (1993), Lites et al. (1995), and Semel and Skumanich (1998). Just to give an example, we describe in some detail the procedure followed by Lites et al. (1995): one starts by considering the sunspots as 'azimuth centers' from which the transverse component of the magnetic field must diverge for positive polarity or to which must converge for negative polarity. This criterion solves the ambiguity for the regions surrounding the sunspots. In plage areas, and away from regions of newly emerging flux, one selects the azimuth which gives a field direction closer to the local vertical.[1] Finally, when the previous criteria are not effective, the selection is made by minimizing the point-by-point discontinuity of the azimuth in the observer's frame. By so doing, a 'map' of the magnetic field is recovered and this also allows one to determine one component of the electric current density j_z (with z the vertical axis) through the equation

$$4\pi\, j_z = \frac{\partial B_y}{\partial x} - \frac{\partial B_x}{\partial y}\ .$$

It should be remarked that a purely spectroscopic disambiguation method has also been devised (Landi Degl'Innocenti and Bommier, 1993). The method is based on the observation of the Stokes parameters profiles in resonance lines originating from transitions between *polarized* atomic levels. In this case, the vertical to the solar atmosphere introduces a 'symmetry breaking' in the physical scenario which allows one, in many cases, to recover the magnetic field vector without ambiguity.

[1] This criterion is based on the idea that in such regions the magnetic field is nearly always oriented close to the vertical direction. Obviously, the criterion does not work for observations performed at disk center.

CHAPTER 12

ASTROPHYSICAL APPLICATIONS: RADIATION ANISOTROPY IN STELLAR ATMOSPHERES

As shown in Chaps. 5, 7, and 10, the anisotropy of the radiation field, suitably described by the irreducible tensor $J^K_Q(\nu)$ defined in Eqs. (5.157), is the basic physical quantity controlling the amount of atomic polarization in atomic energy levels. Referring for instance to the idealized case of a two-level atom with unpolarized lower level, Eq. (10.10) shows that in the non-magnetic, collisionless regime, the statistical tensors of the upper level are proportional to the corresponding components of the radiation field tensor. In the following chapters we will discuss the phenomena of resonance polarization and the Hanle effect – which are intimately connected with the presence of atomic polarization – in the astrophysical context. In view of this analysis, it is useful to study in some detail the properties of the radiation field anisotropy in some of the most common astrophysical scenarios, like the interior or the outer layers of a 'classical' stellar atmosphere.[1]

The study presented in this chapter is restricted to schematic situations where the atmospheric structure is described by analytical, plane-parallel models. In particular, we will consider the Milne-Eddington and the grey model atmospheres, and we will find the behavior of the radiation field anisotropy both 'inside' the atmosphere (as a function of optical depth) and 'outside' the atmosphere (as a function of height over the stellar surface).

It should be remarked from the very beginning that a plane-parallel atmosphere is a cylindrically symmetrical environment, the symmetry axis being the vertical to the atmosphere itself. It is readily seen from Eqs. (5.157) and Table 5.6 that, in such an environment, the only non-zero components of the irreducible radiation field tensor (in a reference system with the z-axis directed as the vertical) are J^0_0 and J^2_0. A single parameter is therefore sufficient to fully characterize the anisotropy of the radiation field. This parameter is the so-called anisotropy factor, already defined in Chap. 10 (cf. Eqs. (10.62) and (10.160))

$$w_\nu = \sqrt{2}\ \frac{J^2_0(\nu)}{J^0_0(\nu)}\ , \tag{12.1}$$

where the expressions of $J^0_0(\nu)$ and $J^2_0(\nu)$ are given by Eqs. (5.164) and the factor $\sqrt{2}$ is introduced for convenience. We remind the reader (cf. Sect. 10.7) that the value of the anisotropy factor is always contained in the range $(-1/2, 1)$, being 0 for an isotropic radiation field, 1 for an infinitely sharp beam parallel or antiparallel to the z-axis, and $-1/2$ for an azimuth-independent radiation field in the x-y plane.

[1] By 'classical' we mean an atmosphere where the radiation field is unpolarized and therefore described by the only intensity.

The main body of this chapter is devoted to the analysis of the anisotropy factor in stellar atmospheres. In Sect. 12.4 we will consider some typical phenomena of 'symmetry breaking' which entail the appearance of further components of the tensor $J^K_Q(\nu)$.

12.1. The Milne-Eddington Model Atmosphere

We consider a plane-parallel atmosphere such as the one schematized in Fig. 9.2 and we denote by t_ν the optical depth at frequency ν measured along the z-axis in the inward direction

$$\mathrm{d}t_\nu = -k_\nu \, \mathrm{d}z \ ,$$

where k_ν is the absorption coefficient (corrected for stimulated emission) at frequency ν.[1] The transfer equation for the specific intensity $I_\nu(t_\nu, \mu)$ of the radiation propagating at optical depth t_ν along a direction forming an angle θ with the vertical is

$$\mu \frac{\mathrm{d}}{\mathrm{d}t_\nu} I_\nu(t_\nu, \mu) = I_\nu(t_\nu, \mu) - S_\nu(t_\nu) \ , \tag{12.2}$$

where $\mu = \cos\theta$ and S_ν, the source function at frequency ν, is the ratio between the emission and the absorption coefficient ($S_\nu = \varepsilon_\nu / k_\nu$).

Equation (12.2) can easily be solved to give, for the radiation propagating outwards

$$I_\nu(t_\nu, \mu) = \int_{t_\nu}^{\infty} S_\nu(t'_\nu) \ \mathrm{e}^{-\frac{t'_\nu - t_\nu}{\mu}} \ \frac{\mathrm{d}t'_\nu}{\mu} \qquad (\mu > 0) \ , \tag{12.3}$$

and, for the radiation propagating inwards

$$I_\nu(t_\nu, \mu) = \int_{0}^{t_\nu} S_\nu(t'_\nu) \ \mathrm{e}^{-\frac{t_\nu - t'_\nu}{|\mu|}} \ \frac{\mathrm{d}t'_\nu}{|\mu|} \qquad (\mu < 0) \ , \tag{12.4}$$

where we have assumed that the atmosphere is not irradiated by any external source.

We now evaluate the *moments* of the intensity, defined by (cf. Chandrasekhar, 1950)

$$J_\nu(t_\nu) = \frac{1}{2} \int_{-1}^{1} I_\nu(t_\nu, \mu) \, \mathrm{d}\mu$$

[1] The absorption coefficient considered here is the 'scalar' absorption coefficient of the traditional (non polarized) theory of stellar atmospheres. For our purposes it is not necessary to specify the physical processes contributing to k_ν.

$$F_\nu(t_\nu) = 2 \int_{-1}^{1} I_\nu(t_\nu, \mu)\ \mu\ \mathrm{d}\mu$$

$$K_\nu(t_\nu) = \frac{1}{2} \int_{-1}^{1} I_\nu(t_\nu, \mu)\ \mu^2\ \mathrm{d}\mu\ . \tag{12.5}$$

J_ν is the solid-angle average of the specific intensity, F_ν is (apart from a factor π) the specific flux,[1] and K_ν is the so-called *K-integral*. Substituting Eqs. (12.3)-(12.4) into Eqs. (12.5), and recalling the definition of the exponential integrals

$$E_n(x) = \int_1^\infty \frac{\mathrm{e}^{-xy}}{y^n}\ \mathrm{d}y = \int_0^1 \mathrm{e}^{-\frac{x}{\mu}}\ \mu^{n-2}\ \mathrm{d}\mu \qquad (x > 0\,;\ n = 0, 1, 2, \ldots)\ , \tag{12.6}$$

one obtains with some easy algebra

$$J_\nu(t_\nu) = \frac{1}{2} \int_0^\infty E_1\big(|t'_\nu - t_\nu|\big)\ S_\nu(t'_\nu)\ \mathrm{d}t'_\nu \tag{12.7a}$$

$$F_\nu(t_\nu) = 2 \int_0^\infty E_2\big(|t'_\nu - t_\nu|\big)\ \sigma(t'_\nu - t_\nu)\ S_\nu(t'_\nu)\ \mathrm{d}t'_\nu \tag{12.7b}$$

$$K_\nu(t_\nu) = \frac{1}{2} \int_0^\infty E_3\big(|t'_\nu - t_\nu|\big)\ S_\nu(t'_\nu)\ \mathrm{d}t'_\nu\ , \tag{12.7c}$$

where

$$\sigma(t'_\nu - t_\nu) = \mathrm{sign}\,(t'_\nu - t_\nu) = \frac{t'_\nu - t_\nu}{|t'_\nu - t_\nu|}\ . \tag{12.8}$$

The anisotropy factor at optical depth t_ν can be expressed in terms of the moments $J_\nu(t_\nu)$ and $K_\nu(t_\nu)$. From Eqs. (12.1), (5.164) and (12.5) we have

$$w_\nu(t_\nu) = \frac{3K_\nu(t_\nu) - J_\nu(t_\nu)}{2\,J_\nu(t_\nu)}\ , \tag{12.9}$$

or, using Eqs. (12.7a,c)

$$w_\nu(t_\nu) = \frac{\displaystyle\int_0^\infty \Big[3E_3\big(|t'_\nu - t_\nu|\big) - E_1\big(|t'_\nu - t_\nu|\big)\Big] S_\nu(t'_\nu)\ \mathrm{d}t'_\nu}{\displaystyle 2 \int_0^\infty E_1\big(|t'_\nu - t_\nu|\big)\ S_\nu(t'_\nu)\ \mathrm{d}t'_\nu}\ . \tag{12.10}$$

[1] The flux is indeed $\pi\, F_\nu$.

This expression is valid under the only assumption that the atmosphere is plane-parallel (hence cylindrically symmetrical).

Now we consider the special case of the Milne-Eddington model, which implies that the source function coincides with the local Planck function (LTE hypothesis) and that the latter varies linearly with the optical depth t_ν ,[1]

$$S_\nu(t_\nu) \equiv B_{\rm P}(\nu, t_\nu) = B_0(1 + \beta_\nu t_\nu) \; . \tag{12.11}$$

Substituting into Eq. (12.10), and performing elementary integrals,[2] one finds the following expression

$$w_\nu(t_\nu) = \frac{1}{2} \; \frac{E_2(t_\nu) - \beta_\nu E_3(t_\nu) - 3E_4(t_\nu) + 3\beta_\nu E_5(t_\nu)}{2 + 2\beta_\nu t_\nu - E_2(t_\nu) + \beta_\nu E_3(t_\nu)} \; . \tag{12.12}$$

The surface value of the anisotropy factor is

$$w_\nu(0) = \frac{1}{4} \; \frac{\beta_\nu}{\beta_\nu + 2} \; . \tag{12.13}$$

In the special case of an isothermal atmosphere ($\beta_\nu = 0$) one has

$$\big[w_\nu(t_\nu)\big]_{\rm isoth} = \frac{1}{2} \; \frac{E_2(t_\nu) - 3E_4(t_\nu)}{2 - E_2(t_\nu)} \; .$$

Figure 12.1 shows the behavior of the anisotropy factor with optical depth as derived from Eq. (12.12), for several values of β_ν (only positive values are considered, which implies a source function increasing with optical depth). Such behavior can be understood via the following arguments. First of all it should be noticed that, as apparent from Eqs. (5.164), the component $J^2_0(\nu)$ – hence the anisotropy factor – tends to be positive when the radiation flowing 'almost vertically' ($\theta \simeq 0°$ or $\theta \simeq 180°$) is more intense than the radiation flowing 'almost horizontally' ($\theta \simeq 90°$), and negative in the opposite case.[3] Next we write down the expressions of the intensity $I_\nu(t_\nu, \mu)$ for the Milne-Eddington model atmosphere. From Eqs. (12.3)-(12.4) we obtain, using Eq. (12.11)[4]

---

[1] Apart from slightly different notations, these assumptions are the same as those introduced in Sect. 9.8 when discussing the Unno-Rachkovsky solution.

[2] It is useful to recall that the exponential integrals satisfy the relations

$$\frac{\rm d}{{\rm d}x} \, E_n(x) = -E_{n-1}(x) \qquad (n > 0) \; , \qquad\qquad E_n(0) = \frac{1}{n-1} \qquad (n > 1) \; .$$

[3] The boundary between the two cases involves the Van Vleck angle $\theta_{\rm V} = \arccos(1/\sqrt{3})$, cf. Eq. (5.100).

[4] Equations (12.14) can also be derived as a special case of the Unno-Rachkovsky solutions (Eqs. (9.108)) corresponding to no magnetic field. It should be kept in mind, however, that $t_{\rm c}$ is the continuum optical depth, while t_ν is the total (line plus continuum) optical depth.

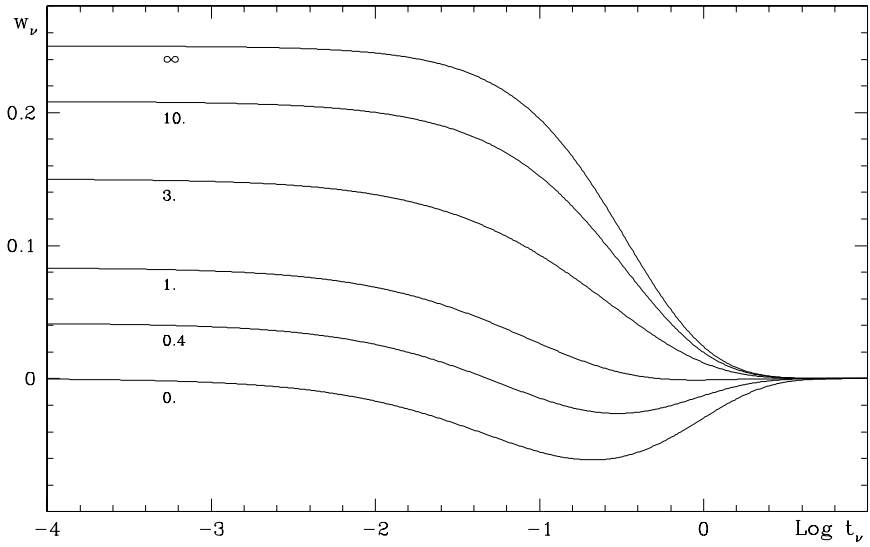

Fig.12.1. The anisotropy factor in a Milne-Eddington model atmosphere is plotted as a function of optical depth for different values of the parameter β_ν defined in Eq.(12.11).

$$I_\nu(t_\nu,\mu) = B_0\Big[1+\beta_\nu\mu+\beta_\nu t_\nu\Big] \qquad (\mu>0)$$

$$I_\nu(t_\nu,\mu) = B_0\Big[1+\beta_\nu t_\nu - \mathrm{e}^{-\frac{t_\nu}{|\mu|}} - \beta_\nu|\mu|\Big(1-\mathrm{e}^{-\frac{t_\nu}{|\mu|}}\Big)\Big] \qquad (\mu<0)\,. \qquad (12.14)$$

These expressions show that, for the outward-directed radiation ($\mu > 0$), the intensity increases – provided $\beta_\nu > 0$ – with increasing μ, whatever the value of t_ν. The opposite occurs for the radiation flowing inward ($\mu < 0$): at any given t_ν, the intensity decreases as $|\mu|$ is increased.

The former effect is responsible for limb darkening and will be referred to as the *source-function gradient effect*: it gives a positive contribution to the anisotropy factor. The latter, which may be called the *surface effect*, gives a negative contribution to the anisotropy factor. For $\beta_\nu = 0$ the radiation flowing outward is isotropic, thus only the surface effect is at work and, as shown in Fig. 12.1, the anisotropy factor is always negative. By contrast, for large values of β_ν the source-function gradient effect takes over and the anisotropy factor is always positive. For intermediate values of β_ν, the anisotropy factor is positive at $t_\nu = 0$ (as shown by Eq. (12.13)) and then decreases with increasing t_ν. If β_ν is smaller than a threshold value (that is numerically found to be 1.1098) the anisotropy factor becomes negative beyond a certain value of t_ν, otherwise it remains positive at any t_ν. In any case, the anisotropy factor tends to zero for $t_\nu \to \infty$, because both the outward and the inward-directed radiation become isotropic.

The maximum value of the anisotropy factor in the Milne-Eddington model atmosphere is 0.25. Such value is found at $t_\nu = 0$ in a high-gradient atmosphere

($\beta_\nu \to \infty$). The minimum value is -0.0611, found at $t_\nu = 0.2097$ in an isothermal atmosphere ($\beta_\nu = 0$).

12.2. The Grey Atmosphere

A plane-parallel atmosphere in local thermodynamic equilibrium and in radiative equilibrium, and having a frequency-independent absorption coefficient, is referred to as a *grey atmosphere*. This model atmosphere has been extensively studied in the past and its main properties have been fully established by means of very elegant analytical and numerical techniques (Chandrasekhar, 1950).

As the absorption coefficient is ν-independent, the grey atmosphere allows a 'unique' optical depth t to be defined. Bearing in mind the LTE assumption, the transfer equation for the specific intensity at frequency ν reads

$$\mu \frac{\mathrm{d}}{\mathrm{d}t} I_\nu(t,\mu) = I_\nu(t,\mu) - B_\mathrm{P}\big(\nu, T(t)\big) \,, \tag{12.15}$$

where $B_\mathrm{P}\big(\nu, T(t)\big)$ is the Planck function at temperature $T(t)$ and frequency ν. The formal solution for $I_\nu(t,\mu)$, as well as the expressions for the moments and for the anisotropy factor, are readily obtained from Eqs. (12.3)-(12.9) by performing the substitutions

$$t_\nu \to t \,, \qquad\qquad S_\nu(t_\nu) \to B_\mathrm{P}\big(\nu, T(t)\big) \,. \tag{12.16}$$

The radiative equilibrium assumption means that the frequency-integrated flux is independent of optical depth. It is therefore convenient to introduce the frequency-integrated intensity

$$I(t,\mu) = \int_0^\infty I_\nu(t,\mu)\, \mathrm{d}\nu \,,$$

and its moments (cf. Eqs. (12.5))

$$\begin{aligned} J(t) &= \frac{1}{2} \int_{-1}^{1} I(t,\mu)\, \mathrm{d}\mu \\ F(t) &= 2 \int_{-1}^{1} I(t,\mu)\, \mu\, \mathrm{d}\mu \\ K(t) &= \frac{1}{2} \int_{-1}^{1} I(t,\mu)\, \mu^2\, \mathrm{d}\mu \,. \end{aligned} \tag{12.17}$$

Integration of Eq. (12.15) over frequency yields the transfer equation for $I(t,\mu)$

$$\mu \frac{\mathrm{d}}{\mathrm{d}t} I(t,\mu) = I(t,\mu) - B_\mathrm{P}(t) \,, \tag{12.18}$$

where

$$B_{\rm P}(t) = \int_0^\infty B_{\rm P}\big(\nu, T(t)\big)\,{\rm d}\nu = \frac{\sigma}{\pi}\,\big[T(t)\big]^4\,, \tag{12.19}$$

with σ the Stefan-Boltzmann constant and T the local temperature. By averaging over the solid angle Eq. (12.18), and the same equation multiplied by μ, one obtains

$$\frac{1}{4}\,\frac{\rm d}{{\rm d}t}\,F(t) = J(t) - B_{\rm P}(t)$$
$$\frac{\rm d}{{\rm d}t}\,K(t) = \frac{1}{4}\,F(t)\,,$$

where Eqs. (12.17) have been used. The assumption of radiative equilibrium gives

$$J(t) = B_{\rm P}(t) \tag{12.20a}$$

$$F(t) = F_0 \tag{12.20b}$$

$$K(t) = \frac{1}{4}\,F_0\,\big(t+Q\big)\,, \tag{12.20c}$$

where Q is an integration constant. Equations (12.20a) and (12.18) allow us to write the zero-order moment of the frequency-integrated intensity in the form (cf. Eq. (12.7a))

$$J(t) = \frac{1}{2}\int_0^\infty E_1\big(|t'-t|\big)\;J(t')\;{\rm d}t'\,, \tag{12.21}$$

while for the first-order moment we have, considering the flux at the surface (cf. Eq. (12.7b))

$$F_0 = 2\int_0^\infty E_2(t)\;J(t)\;{\rm d}t\,. \tag{12.22}$$

In order to solve the grey-atmosphere problem, we need to find the dependence on optical depth of the temperature T, or equivalently – because of Eq. (12.20a) – of the mean intensity J. The latter obeys the homogeneous integral equation (12.21) and the normalization required by the boundary condition at the stellar surface (Eq. (12.22)).

Consideration of the boundary conditions in the deep interior of the atmosphere suggests a convenient algebraic manipulation to be performed on Eq. (12.21). Since under the limit $t \to \infty$ the radiation field eventually becomes isotropic, and since for an isotropic field one has (see Eqs. (12.17))

$$J(t) = 3\,K(t)\,,$$

it follows from Eq. (12.20c) that for $t \gg 1$

$$J(t) \approx \frac{3}{4}\,F_0\,\big(t+Q\big)\,.$$

Following Hopf (1934), the function $J(t)$ is written, for an arbitrary value of t, in the form

$$J(t) = \frac{3}{4} F_0 \left[t + q(t) \right] , \tag{12.23}$$

where $q(t)$ is the so-called *Hopf function* which obviously satisfies the property

$$\lim_{t \to \infty} q(t) = Q .$$

Substitution of Eq. (12.23) into Eq. (12.21), and evaluation of elementary integrals,[1] leads to the following non-homogeneous integral equation for $q(t)$

$$q(t) = \frac{1}{2} E_3(t) + \frac{1}{2} \int_0^\infty E_1\big(|t' - t|\big)\, q(t')\, \mathrm{d}t' . \tag{12.24}$$

On the other hand, substitution of Eq. (12.23) into Eq. (12.22) shows that the Hopf function obeys the relation

$$\int_0^\infty E_2(t)\, q(t)\, \mathrm{d}t = \frac{1}{3} . \tag{12.25}$$

The Hopf function has been widely studied by means of analytical, as well as numerical techniques (Chandrasekhar, 1950; Kourganoff and Busbridge, 1952). In particular, it can be proved that $q(0)$, the surface value of the Hopf function, is given by (see App. 15)

$$q(0) = \frac{1}{\sqrt{3}} . \tag{12.26}$$

With modern computing techniques, the evaluation of the Hopf function is rather straightforward. A simple numerical algorithm is described in App. 16, and a graph of $q(t)$ is given in Fig. 12.2. The figure shows that $q(t)$ is a monotonic function which grows from the surface value $1/\sqrt{3} = 0.57735$ to the boundary value at $t \to \infty$, $Q = 0.71044$.

The anisotropy factor for the frequency-integrated intensity in a grey atmosphere can easily be expressed in terms of the Hopf function. Considering the grey analogue of Eq. (12.9) one obtains, with the use of Eqs. (12.20c) and (12.23)

$$w(t) = \frac{3K(t) - J(t)}{2\, J(t)} = \frac{Q - q(t)}{2 \left[t + q(t) \right]} . \tag{12.27}$$

In particular, for $t = 0$ one has

$$w(0) = \frac{\sqrt{3}\, Q - 1}{2} = 0.11526 .$$

[1] See footnote 2 on p.666.

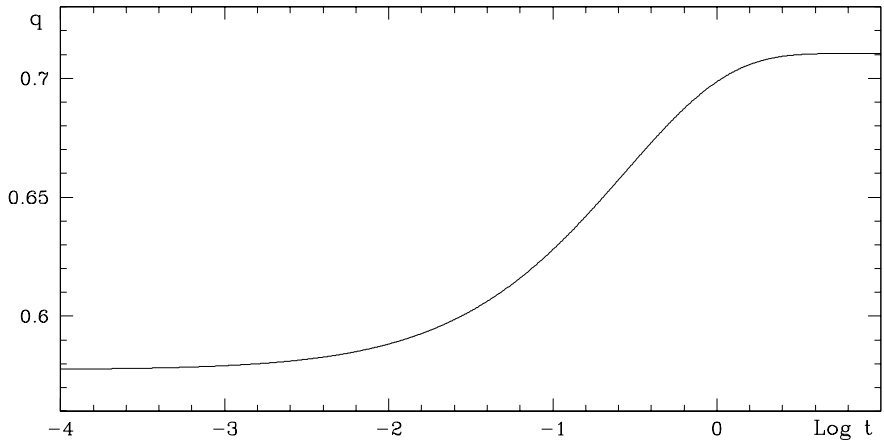

Fig.12.2. The Hopf function, solution of the integral equation (12.24), is plotted against optical depth.

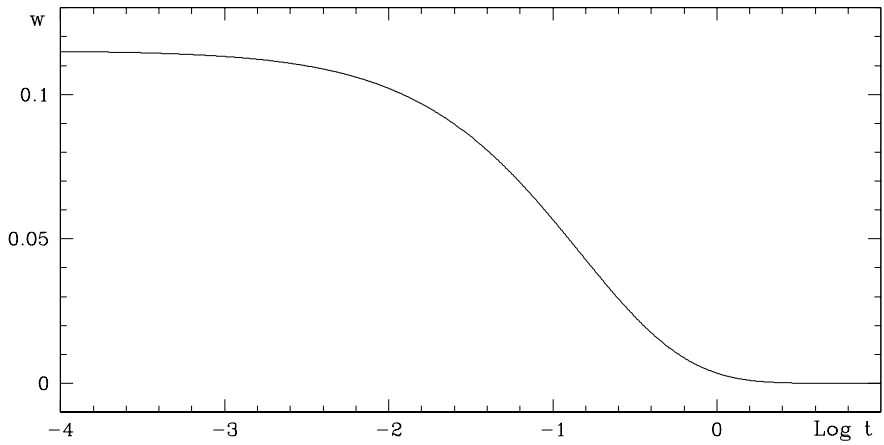

Fig.12.3. The anisotropy factor for the frequency-integrated intensity in the grey model atmosphere is plotted as a function of optical depth. Its surface value is 0.11526.

Figure 12.3 shows a graph of the anisotropy factor w versus $\mathrm{Log}\, t$. The function $w(t)$ decreases monotonically with increasing t – as obvious from Eq. (12.27). According to the discussion presented at the end of the former section this means that, in the grey model atmosphere, the source-function gradient effect prevails over the surface effect at all optical depths.

In the grey atmosphere it is also possible to find the behavior with optical depth of the anisotropy factor at a specific frequency (or wavelength). The expression of the 'monochromatic' anisotropy factor, $w_\nu(t)$, is obtained from Eqs. (12.9), (12.7a) and (12.7c) by performing the substitutions in Eq. (12.16). It is therefore necessary to determine the dependence of the temperature T on optical depth, and then to evaluate numerically the integrals in Eqs. (12.7a,c). Introducing the effective

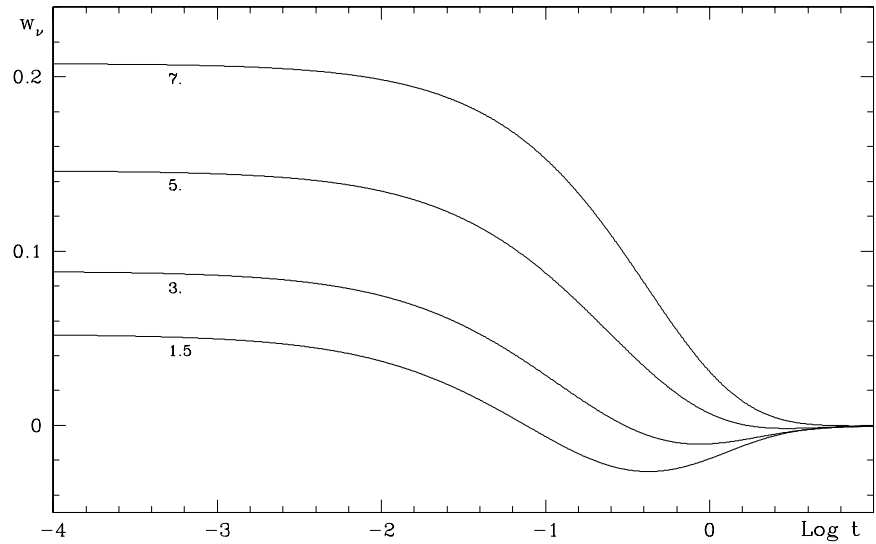

Fig.12.4. The frequency-dependent anisotropy factor of a grey atmosphere is plotted against optical depth for different frequencies. The curves are labelled by the value of the normalized frequency x defined in Eq.(12.28).

temperature $T_{\rm eff}$ via the definition

$$F_0 = \frac{\sigma}{\pi}\, T_{\rm eff}^4 \,,$$

we obtain, with the use of Eqs. (12.19), (12.20a) and (12.23)

$$T(t) = T_{\rm eff}\, \sqrt[4]{\frac{3}{4}\Big[t + q(t)\Big]} \;\;,$$

thus the source function can be written in the form

$$S_\nu(t) = B_{\rm P}\big(\nu, T(t)\big) = \frac{2h\nu^3}{c^2}\, \left[\, \exp\!\left(x \,\Big/\, \sqrt[4]{\frac{3}{4}\Big[t + q(t)\Big]} \right) - 1 \right]^{-1} \,,$$

where

$$x = \frac{h\,\nu}{k_{\rm B}\, T_{\rm eff}} \,. \tag{12.28}$$

Figure 12.4 shows the anisotropy factor w_ν as a function of $\mathrm{Log}\, t$ for four different x values. For the solar case ($T_{\rm eff} = 5800\,\mathrm{K}$) the four curves correspond approximately to the wavelengths (from top to bottom) 3500, 5000, 8000, and 16000 Å, respectively. The increase of the anisotropy factor with increasing frequency is simply understood in terms of the source-function gradient effect illustrated in the previous section. The relative gradient of the source function is given by

$$\beta_\nu = \frac{1}{S_\nu(t)}\, \frac{\mathrm{d}S_\nu(t)}{\mathrm{d}t} = \frac{\mathrm{d}}{\mathrm{d}t}\, \ln\big[S_\nu(t)\big] \,,$$

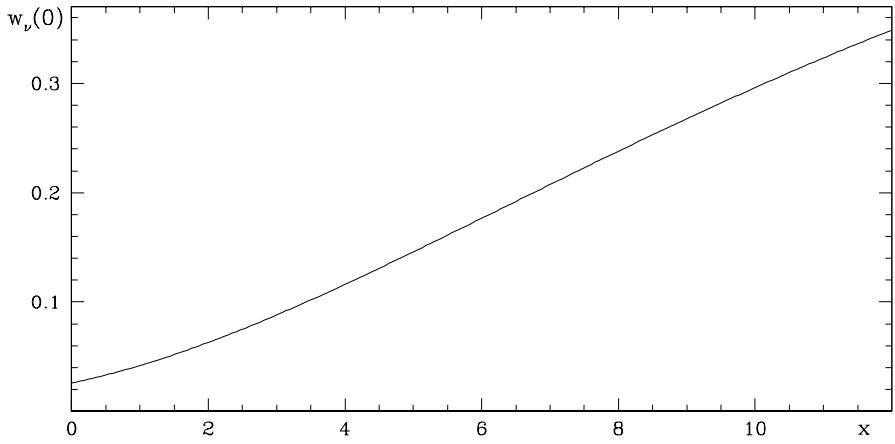

Fig.12.5. The surface value of the anisotropy factor of a grey atmosphere is plotted as a function of the normalized frequency x.

and, for the LTE case,

$$\beta_\nu = \frac{\mathrm{d}}{\mathrm{d}t}\,\ln\bigl[B_{\mathrm{P}}\bigl(\nu,T(t)\bigr)\bigr] = \Bigl[1-\,\mathrm{e}^{-\frac{h\nu}{k_{\mathrm{B}}T}}\Bigr]^{-1}\;\frac{h\,\nu}{k_{\mathrm{B}}T^2}\;\frac{\mathrm{d}T}{\mathrm{d}t}\;,$$

which, at any optical depth, is a monotonically increasing function of frequency. As a further illustration of the same effect, we plot in Fig. 12.5 the surface value of the anisotropy factor w_ν as a function of x. The limiting value in the far infrared ($x \to 0$) is 0.02571.

12.3. Outer Atmospheres

In the previous sections we have analyzed the anisotropy factor in the interior of a stellar atmosphere. Here we extend such analysis to the 'outer' environment of a star. Referring to Fig. 12.6, let us consider a point P located at a height h over the stellar surface. Neglecting the possible presence of starspots over the spherical cap seen from point P, the radiation field is cylindrically symmetrical about the vertical direction, and its properties are fully described by the two components $J^0_0(\nu)$ and $J^2_0(\nu)$ of the radiation field tensor or, alternatively, by $J^0_0(\nu)$ and the anisotropy factor w_ν .

Similarly to Sect. 12.1, we introduce the two integrals

$$J_\nu = \frac{1}{2}\int_{-1}^{1} I_\nu(\mu)\;\mathrm{d}\mu\;, \qquad K_\nu = \frac{1}{2}\int_{-1}^{1} I_\nu(\mu)\;\mu^2\;\mathrm{d}\mu\;, \tag{12.29}$$

where $I_\nu(\mu)$ is the specific intensity of the radiation propagating through point P along the direction specified by the angle θ, with $\mu = \cos\theta$. The anisotropy factor

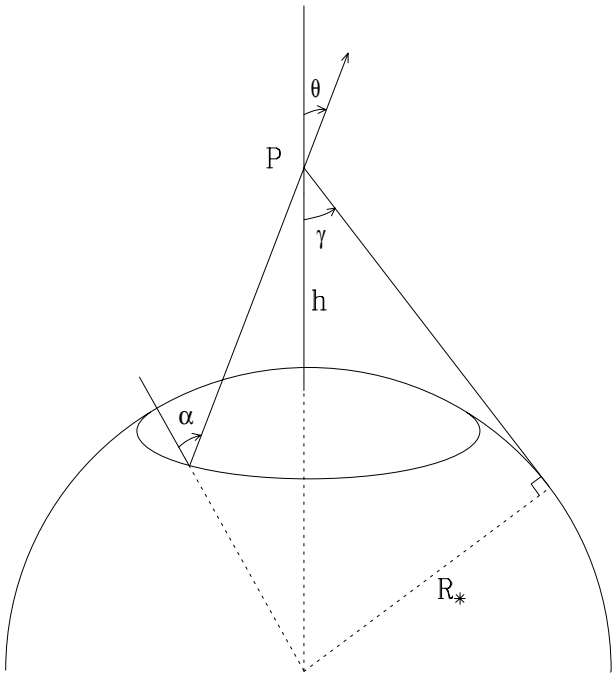

Fig.12.6. Geometry for the calculation of the anisotropy factor in the outer layers of a star. R_* is the stellar radius.

at point P is given by Eq. (12.9),

$$w_\nu = \frac{3K_\nu - J_\nu}{2\,J_\nu}\ . \tag{12.30}$$

Obviously the anisotropy factor is affected by the limb-darkening law, which is usually given by an expression of the form

$$I_\nu(\alpha) = I_\nu(0)\left[1 - \sum_{i=1}^{N} u_i(\nu)\ \left(1 - \cos^i\alpha\right)\right]\ , \tag{12.31}$$

where α is the angle between the propagation direction of the radiation and the vertical to the atmosphere, and where $u_i(\nu)$ are empirically determined coefficients.[1] As apparent from Fig. 12.6, the angle α is related to the angle θ. Since

$$\sin\gamma = \frac{R_*}{R_* + h}\ , \tag{12.32}$$

[1] The direct determination of these coefficients from observations is possible only for the sun. In the stellar case, they can be determined from a fit to theoretical results based on model atmospheres.

one obtains from the sine-formula

$$\sin\alpha = \sin\theta \ \frac{R_* + h}{R_*} = \frac{\sin\theta}{\sin\gamma} \ ,$$

whence

$$\cos\alpha = \frac{\sqrt{\cos^2\theta - \cos^2\gamma}}{\sin\gamma} \ . \tag{12.33}$$

Substituting Eq. (12.31) into Eq. (12.29), and taking into account Eq. (12.33), one gets

$$J_\nu = \frac{1}{2}\, I_\nu(0) \int\limits_{\cos\gamma}^{1} \left[\, u_0(\nu) + \sum_{i=1}^{N} \, u_i(\nu) \, \frac{\sqrt{(\mu^2 - \cos^2\gamma)^i}}{\sin^i\gamma} \, \right] \mathrm{d}\mu$$

$$K_\nu = \frac{1}{2}\, I_\nu(0) \int\limits_{\cos\gamma}^{1} \left[\, u_0(\nu) + \sum_{i=1}^{N} \, u_i(\nu) \, \frac{\sqrt{(\mu^2 - \cos^2\gamma)^i}}{\sin^i\gamma} \, \right] \mu^2 \, \mathrm{d}\mu \ ,$$

where

$$u_0(\nu) = 1 - \sum_{i=1}^{N} \, u_i(\nu) \ .$$

We now restrict our analysis to the case of a quadratic expansion of the limb-darkening law ($N = 2$ in Eq. (12.31)). After some algebra, which involves the evaluation of elementary integrals, one gets

$$\begin{aligned} J_\nu &= \frac{1}{2}\, I_\nu(0) \left[\, a_0 \, + \, a_1 \, u_1(\nu) \, + \, a_2 \, u_2(\nu) \, \right] \\ K_\nu &= \frac{1}{2}\, I_\nu(0) \left[\, b_0 \, + \, b_1 \, u_1(\nu) \, + \, b_2 \, u_2(\nu) \, \right] , \end{aligned} \tag{12.34}$$

where

$$\begin{aligned} a_0 &= 1 - C_\gamma \\ a_1 &= C_\gamma - \frac{1}{2} - \frac{1}{2}\, \frac{C_\gamma^2}{S_\gamma} \, \ln\!\left(\frac{1 + S_\gamma}{C_\gamma} \right) \\ a_2 &= \frac{(C_\gamma + 2)(C_\gamma - 1)}{3(C_\gamma + 1)} \end{aligned} \tag{12.35}$$

and

$$\begin{aligned} b_0 &= \frac{1}{3} \left(1 - C_\gamma^3 \right) \\ b_1 &= \frac{1}{24} \left(8C_\gamma^3 - 3C_\gamma^2 - 2 \right) - \frac{1}{8}\, \frac{C_\gamma^4}{S_\gamma} \, \ln\!\left(\frac{1 + S_\gamma}{C_\gamma} \right) \\ b_2 &= \frac{(C_\gamma - 1)(3C_\gamma^3 + 6C_\gamma^2 + 4C_\gamma + 2)}{15(C_\gamma + 1)} \ , \end{aligned}$$

with

$$C_\gamma = \cos\gamma\,, \qquad S_\gamma = \sin\gamma\,.$$

Substitution into Eq. (12.30) yields

$$w_\nu = \frac{1}{2}\,\frac{c_0 \,+\, c_1\,u_1(\nu) \,+\, c_2\,u_2(\nu)}{a_0 \,+\, a_1\,u_1(\nu) \,+\, a_2\,u_2(\nu)}\,, \tag{12.36}$$

where

$$\begin{aligned}
c_0 &= 3b_0 - a_0 = C_\gamma S_\gamma^2 \\
c_1 &= 3b_1 - a_1 = \frac{1}{8}\left[8C_\gamma^3 - 3C_\gamma^2 - 8C_\gamma + 2 + (4 - 3C_\gamma^2)\,\frac{C_\gamma^2}{S_\gamma}\,\ln\!\left(\frac{1+S_\gamma}{C_\gamma}\right)\right] \\
c_2 &= 3b_2 - a_2 = \frac{C_\gamma - 1}{15(C_\gamma + 1)}\left[9C_\gamma^3 + 18C_\gamma^2 + 7C_\gamma - 4\right]\,.
\end{aligned} \tag{12.37}$$

It is instructive to consider some limiting cases of Eq. (12.36). The first is the case of a star without limb darkening. Setting $u_1(\nu) = u_2(\nu) = 0$, Eq. (12.36) reduces to

$$w_\nu = \frac{1}{2}\,\frac{c_0}{a_0} = \frac{1}{2}\,C_\gamma\,(1 + C_\gamma)\,.$$

The anisotropy factor is independent of frequency and is simply due to geometrical effects. Recalling Eq. (12.32), w_ν can explicitly be expressed in terms of the height h. We have

$$w_\nu = \frac{2x + x^2 + (1+x)\sqrt{2x + x^2}}{2(1+x)^2}\,,$$

where

$$x = \frac{h}{R_*}\,.$$

In particular, for small heights ($h \ll R_*$) we obtain the asymptotic behavior

$$w_\nu \approx \sqrt{\frac{x}{2}} \;=\; \sqrt{\frac{h}{2R_*}}\,,$$

while for large heights we find the obvious result (see comments after Eq. (12.1))

$$\lim_{h\to\infty} w_\nu = 1\,.$$

Next we consider the behavior of w_ν for small and large values of h/R_* in the general case where $u_1(\nu)$ and $u_2(\nu)$ are non-zero. For $h \to 0$ (or $\gamma \to \pi/2$) one obtains from Eq. (12.36), with the help of Eqs. (12.35) and (12.37)

$$\lim_{h\to 0} w_\nu = \big[w_\nu\big]_0 = \frac{1}{20}\,\frac{15\,u_1(\nu) + 16\,u_2(\nu)}{6 - 3\,u_1(\nu) - 4\,u_2(\nu)}\,.$$

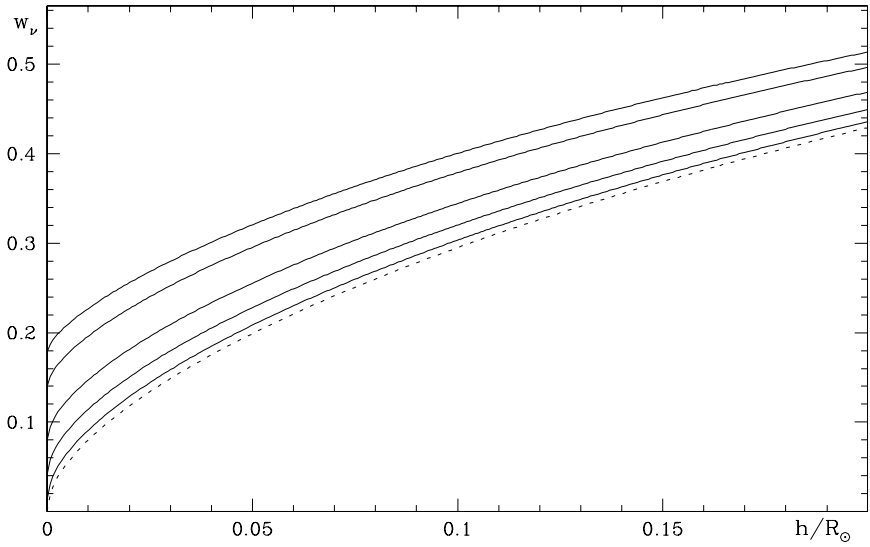

Fig.12.7. The anisotropy factor in the outer layers of the solar atmosphere is plotted against the height h normalized to the solar radius $R_\odot$. The full lines correspond, from top to bottom, to the wavelengths 0.37, 0.50, 0.80, 2.0, and 10.0 μm, respectively. The dashed line is obtained by neglecting limb darkening. Data for limb darkening are from Allen (1973).

By means of a series expansion it can also be proved that for $h \ll R_*$ one has

$$w_\nu \approx \left[w_\nu\right]_0 + \frac{9}{5}\,\frac{\left[1-u_1(\nu)-u_2(\nu)\right]\left[20-5\,u_1(\nu)-8\,u_2(\nu)\right]}{\left[6-3\,u_1(\nu)-4\,u_2(\nu)\right]^2}\,\sqrt{\frac{h}{2R_*}}\,.$$

Finally, it can be proved by series expansion that for large values of h ($h \gg R_*$) one gets the asymptotic behavior

$$w_\nu \approx 1 - \frac{3}{10}\,\frac{15-7\,u_1(\nu)-10\,u_2(\nu)}{6-2\,u_1(\nu)-3\,u_2(\nu)}\,\frac{1}{(1+h/R_*)^2}\,.$$

For the solar case, the quantities $u_1(\nu)$ and $u_2(\nu)$ are tabulated by Allen (1973), and the anisotropy factor can be computed via Eq. (12.36). Figure 12.7 shows the behavior of w_ν as a function of height over the solar surface expressed in solar radii. For a given height, the anisotropy factor is larger in the ultraviolet, consistently with the results obtained in the previous section (cf. Fig. 12.4).

12.4. Symmetry-Breaking Effects

In the former sections of this chapter we have considered the idealized situation of a plane-parallel, cylindrically symmetrical stellar atmosphere. The assumption of cylindrical symmetry implies that the only non-zero components of the radiation

field tensor are $J^0_0(\nu)$ and $J^2_0(\nu)$. However, such assumption is only approximately satisfied in real stellar atmospheres, and there are many different phenomena that may be responsible for symmetry breaking. In these cases, the radiation field can no longer be described in terms of the mean intensity and anisotropy factor alone. Further components of the radiation field tensor come into play, as obvious from Eqs. (5.157) and Table 5.6. Restricting our analysis to 'classical' (or unpolarized, see footnote on p. 663) atmospheres, the non-zero components of the radiation field tensor are given by

$$J^K_Q(\nu) = \oint \frac{\mathrm{d}\Omega}{4\pi}\, \mathcal{T}^K_Q(0,\vec{\Omega})\, I(\nu,\vec{\Omega}) \ ,$$

or, more explicitly, by

$$\begin{aligned}
J^0_0(\nu) &= \oint \frac{\mathrm{d}\Omega}{4\pi}\, I(\nu,\vec{\Omega}) \\
J^2_0(\nu) &= \frac{1}{2\sqrt{2}} \oint \frac{\mathrm{d}\Omega}{4\pi}\, (3\cos^2\theta - 1)\, I(\nu,\vec{\Omega}) \\
J^2_{\pm 1}(\nu) &= \mp \frac{\sqrt{3}}{2} \oint \frac{\mathrm{d}\Omega}{4\pi}\, \sin\theta\cos\theta\ \ \mathrm{e}^{\,\pm\,\mathrm{i}\chi}\, I(\nu,\vec{\Omega}) \\
J^2_{\pm 2}(\nu) &= \frac{\sqrt{3}}{4} \oint \frac{\mathrm{d}\Omega}{4\pi}\, \sin^2\theta\ \ \mathrm{e}^{\,\pm\,2\mathrm{i}\chi}\, I(\nu,\vec{\Omega}) \ .
\end{aligned}$$

Consider for instance the solar atmosphere. The phenomena of granulation and supergranulation, or the presence of any structure typical of solar activity, such as sunspots, faculae, etc.,[1] introduce local symmetry breakings. Obviously, the quantitative evaluation of the radiation field tensor cannot be carried out without a detailed three-dimensional model of the structure considered and of its interface with the surrounding atmosphere.

It is possible, however, to write down simple expressions for the radiation field tensor at a given point P of the outer atmosphere under the assumption of a 'point-like' structure. Let us refer to Fig. 12.8, where the z-axis of the right-handed, orthogonal frame (xyz) is directed along the vertical through P and the x-axis points in an arbitrary direction. We suppose the spot to be centered at a point of the solar surface characterized by the colatitude δ and the longitude φ in the spherical coordinate system illustrated in the same figure. We also suppose that the spot is seen under a small solid angle $\Delta\Omega$ from point P and that ΔI_ν is the contrast, as seen from point P, of its intensity with respect to the unperturbed atmosphere. Under these assumptions, the radiation field tensor at point P is given by[2]

[1] We recall again that we are concerned here with 'classical' atmospheres. In this context typical symmetry-breaking agents, like magnetic fields, have no direct effect. An 'active region' is simply characterized by an intensity contrast with respect to the nearby regions.

[2] Equations (12.38) are valid provided the spot is visible from point P, which implies $\delta < \arccos\left[R_\odot/(h+R_\odot)\right]$.

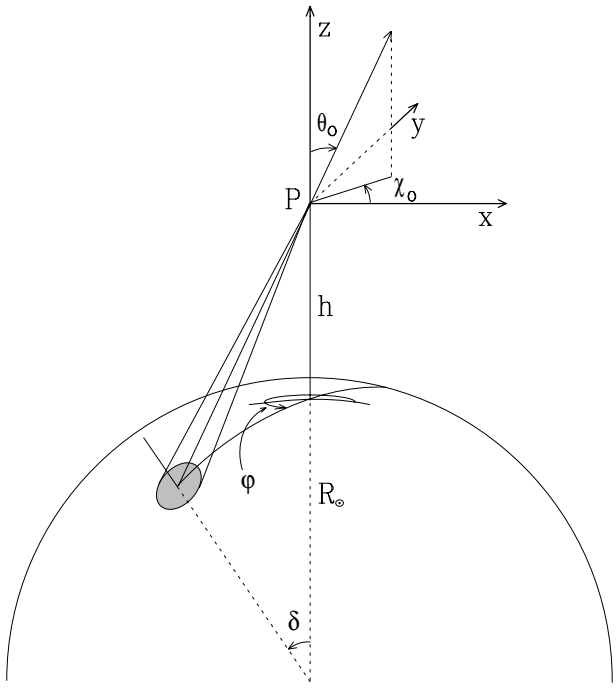

Fig.12.8. Geometry for the evaluation of the radiation field tensor at point P in the presence of a spot over the solar surface.

$$
\begin{aligned}
J^0_0(\nu) &= \left[J^0_0(\nu)\right]_{\text{cyl.s.}} + \frac{\Delta\Omega}{4\pi}\,\Delta I_\nu \\
J^2_0(\nu) &= \left[J^2_0(\nu)\right]_{\text{cyl.s.}} + \frac{1}{2\sqrt{2}}\,(3\cos^2\theta_0 - 1)\,\frac{\Delta\Omega}{4\pi}\,\Delta I_\nu \\
J^2_{\pm1}(\nu) &= \mp\,\frac{\sqrt{3}}{2}\,\sin\theta_0\cos\theta_0\;\, \mathrm{e}^{\,\pm\,\mathrm{i}\chi_0}\;\,\frac{\Delta\Omega}{4\pi}\,\Delta I_\nu \\
J^2_{\pm2}(\nu) &= \frac{\sqrt{3}}{4}\,\sin^2\theta_0\;\, \mathrm{e}^{\,\pm\,2\mathrm{i}\chi_0}\;\,\frac{\Delta\Omega}{4\pi}\,\Delta I_\nu\ ,
\end{aligned}
\tag{12.38}
$$

where $[J^0_0(\nu)]_{\text{cyl.s.}}$ and $[J^2_0(\nu)]_{\text{cyl.s.}}$ are the components of the radiation field tensor as computed in the cylindrically symmetrical case (see former sections), and where the angles θ_0 and χ_0 are connected with the spot's coordinates by the simple relations

$$
\chi_0 = \varphi - \pi\ , \qquad\qquad \theta_0 = \arctan\left[\frac{\sin\delta}{1-\cos\delta + h/R_\odot}\right]\ .
$$

Equations (12.38) can easily be generalized to the case where several structures are present over the solar surface, and clearly show the role played by activity in determining the radiation field tensor in the outer solar atmosphere.

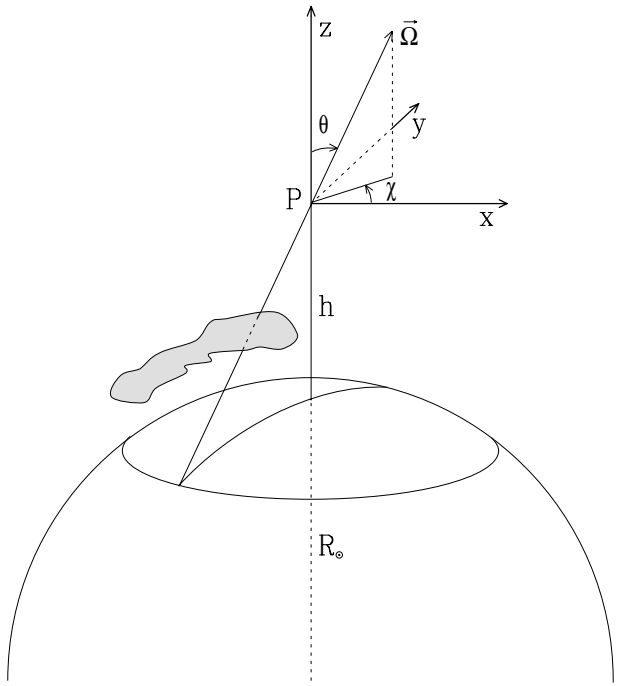

Fig.12.9. Schematic illustration of the radiation field symmetry breaking at point P due to the presence of a prominence between P and the solar surface.

Another cause of symmetry breaking may be the presence of absorbing material, like for instance a prominence, between the solar surface and the point P where the radiation field tensor is to be evaluated. This physical situation is schematically illustrated in Fig. 12.9. The intensity $I(\nu, \vec{\Omega})$ of the radiation propagating through point P along the direction $\vec{\Omega}$ is obviously modified by the presence of the interposed material, but the quantitative evaluation of the radiation field tensor requires a detailed physical and geometrical model of the material itself. An example of how such calculation can be carried out when the absorbing material (the prominence) is schematized as a homogeneous vertical slab of finite thickness can be found in Landi Degl'Innocenti et al. (1987).

All the above-mentioned phenomena produce a loss of the symmetry characteristics of the radiation field at a given point of the outer stellar atmosphere. Besides them, there is an important symmetry-breaking phenomenon which is of a completely different nature, being connected with the Doppler effect. We go back to the case of a cylindrically symmetrical stellar atmosphere, but we now consider the radiation field as seen in a reference frame located at a point P of the outer atmosphere and moving with velocity $\vec{v}$ with respect to the star. Such frame will be referred to in the following as the *comoving frame*. Since the radiation coming from different points of the stellar surface is differently affected by the Doppler effect, if the spectrum presents an absorption (or emission) line there is an obvious

symmetry-breaking effect on the radiation field tensor. In quantitative terms, if $I(\nu', \vec{\Omega})$ is the intensity of the radiation propagating through point P along the direction $\vec{\Omega}$, as seen in a reference frame at rest with respect to the star, an observer moving with velocity $\vec{v}$ will experience an intensity $I(\nu, \vec{\Omega})$, where, to first order in v/c [1]

$$\nu = \nu' \left(1 - \frac{\vec{v} \cdot \vec{\Omega}}{c}\right), \qquad \nu' = \nu \left(1 + \frac{\vec{v} \cdot \vec{\Omega}}{c}\right). \tag{12.39}$$

The radiation field tensor in the comoving frame is thus given by

$$\begin{aligned} J^K_Q(\nu) &= \oint \frac{\mathrm{d}\Omega}{4\pi} \mathcal{T}^K_Q(0, \vec{\Omega})\, I(\nu', \vec{\Omega}) \\ &= \oint \frac{\mathrm{d}\Omega}{4\pi} \mathcal{T}^K_Q(0, \vec{\Omega})\, I\left(\nu\left(1 + \frac{\vec{v} \cdot \vec{\Omega}}{c}\right), \vec{\Omega}\right). \end{aligned} \tag{12.40}$$

Its symmetry properties are summarized in App. 17.

As an application of Eq. (12.40), we consider the case where the radiation coming from the star is cylindrically symmetrical about the vertical and the stellar spectrum presents an absorption (or emission) line with a Gaussian profile. For the sake of simplicity we also suppose that limb darkening is frequency-independent and described by a linear function ($N = 1$ in Eq. (12.31)). Under these assumptions, the intensity entering the integral in Eq. (12.40) can be written in the form

$$I(\nu', \vec{\Omega}) = I^{(0)}_{\mathrm{c}} \left[1 - d_{\mathrm{c}}\, \mathrm{e}^{-\left(\frac{\nu' - \nu_0}{\Delta\nu_{\mathrm{p}}}\right)^2}\right] \Big[1 - u_1(1 - \cos\alpha)\Big], \tag{12.41}$$

where $I^{(0)}_{\mathrm{c}}$ is the continuum intensity at disk center, d_{c} is the central depression of the line ($d_{\mathrm{c}} < 1$), ν_0 and $\Delta\nu_{\mathrm{p}}$ are the line central frequency and width, respectively, u_1 is the limb-darkening coefficient, and α is the angle between the direction $\vec{\Omega}$ and the vertical to the atmosphere. The geometry is illustrated in Fig. 12.10: (xyz) is the reference system (the comoving frame) which is moving with velocity $\vec{v}$ with respect to the star; the velocity direction is specified by the angles θ_v and χ_v, the direction $\vec{\Omega}$ by the angles θ and χ; the angle α is related to θ and to the relative height h/R_* of point P by Eqs. (12.33) and (12.32). Introducing these notations, and recalling Eq. (12.39), the argument of the exponential in Eq. (12.41) takes the form

[1] The transformation between the two reference systems entails indeed further effects of order v/c. One is aberration, which implies that a ray propagating along the direction $\vec{\Omega}'$ in the star's frame propagates, in the comoving frame, along a direction $\vec{\Omega}$ given by $\vec{\Omega}'(1 + \vec{v} \cdot \vec{\Omega}'/c) - \vec{v}/c$ (to first order in v/c). The second is the fact that the intensity is multiplied by the factor $(\nu/\nu')^3 \approx 1 - 3(\vec{v} \cdot \vec{\Omega})/c$ when passing from the first to the second frame. Both effects are however rather small, and negligible in most applications. Even considering a velocity $v \simeq 100\,\mathrm{km\,s^{-1}}$, aberration implies an angular distance between $\vec{\Omega}$ and $\vec{\Omega}'$ of the order of 1 arcmin, whereas the second effect implies a correction to the intensity of order 10^{-3}.

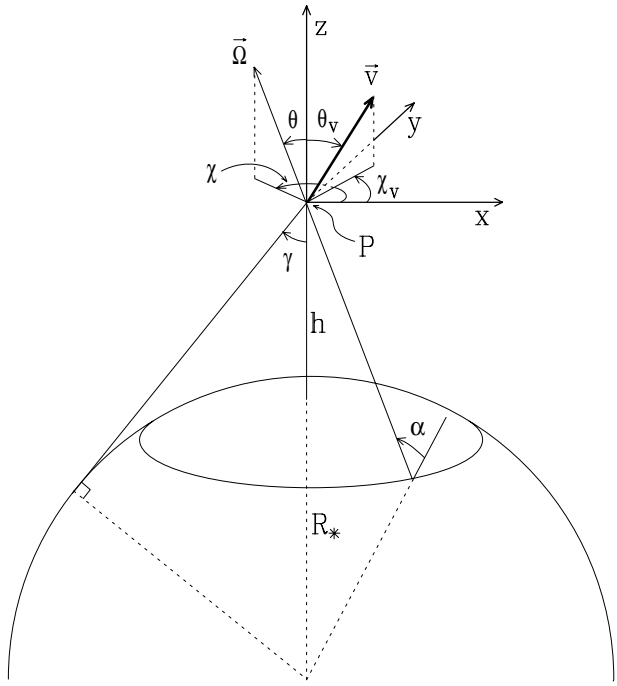

Fig.12.10. Geometry for the evaluation of the comoving-frame radiation field tensor at point P. The reference system (xyz) – the comoving frame – moves with velocity $\vec{v}$ relative to the star. The direction of $\vec{v}$ is specified by the angles θ_v and χ_v.

$$-\left(\frac{\nu' - \nu_0}{\Delta\nu_{\rm p}}\right)^2 = -\left(\frac{\nu - \nu_0 + \nu\,(v/c)\cos\Theta}{\Delta\nu_{\rm p}}\right)^2 , \tag{12.42}$$

where, via the cosine theorem

$$\cos\Theta = \frac{\vec{v}\cdot\vec{\Omega}}{v} = \cos\theta\cos\theta_v + \sin\theta\sin\theta_v\cos(\chi - \chi_v) . \tag{12.43}$$

Substitution of Eqs. (12.41) and (12.42) into Eq. (12.40) leads to the following expression for the comoving-frame radiation field tensor at frequency ν_0

$$J^K_Q(\nu_0) = \frac{I^{(0)}_{\rm c}}{4\pi}\int_0^{2\pi}{\rm d}\chi\int_0^{\gamma}{\rm d}\theta\ \ \sin\theta\ \ \mathcal{T}^K_Q(0,\vec{\Omega})\left[1 - d_{\rm c}\,{\rm e}^{-\omega^2\cos^2\Theta}\right] \times\left[1 - u_1(1-\cos\alpha)\right] , \tag{12.44}$$

where

$$\omega = \frac{\nu_0\, v}{\Delta\nu_{\rm p}\, c} \tag{12.45}$$

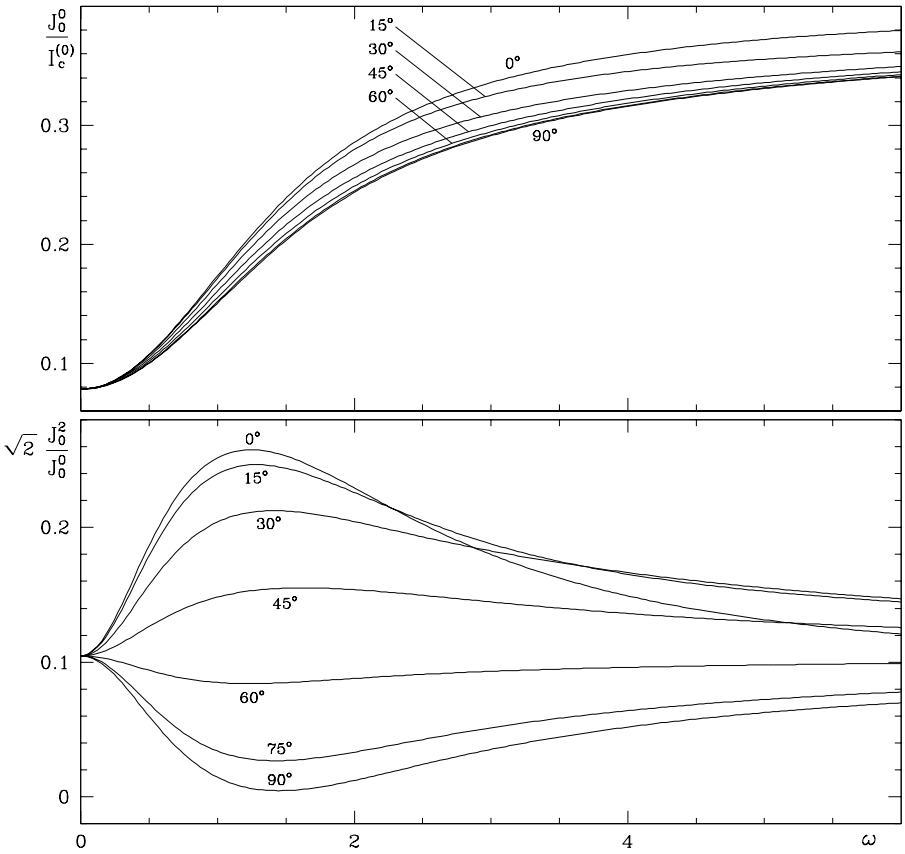

Fig.12.11. The radiation field tensor in the comoving frame, computed according to Eq.(12.44), is plotted against the parameter ω defined in Eq.(12.45). Curves are labelled by the value of θ_v, while χ_v is set to 0°. The average intensity $J_0^0(\nu_0)$ – upper panel – is normalized to the continuum intensity at disk center, while $J_0^2(\nu_0)$ – lower panel – is normalized to $J_0^0(\nu_0)/\sqrt{2}$. The relevant parameters are: $d_c = +0.8$ (absorption line), $u_1 = 0.2$, $h = 0.01\,R_*$. Note in the upper panel the Doppler brightening effect.

is the ratio between the Doppler shift induced by the velocity v and the width of the spectral line (both expressed in frequency units).

It should be borne in mind that the key parameter in the Doppler effect is the component of the velocity $\vec{v}$ along the propagation direction $\vec{\Omega}$, $\vec{v}\cdot\vec{\Omega} = v\cos\Theta$. For an assigned $\vec{v}$, the angle Θ obviously depends *both* on θ *and* on χ (see Fig. 12.10 or Eq. (12.43)), and this entails the symmetry breaking: the radiation field at point P is cylindrically symmetrical (χ-independent) in the star's frame, but not in the comoving frame. At the same time, Eqs. (12.44)-(12.45) show that this effect vanishes for $v \to \infty$: under this limit the radiation field becomes cylindrically symmetrical also in the comoving frame.

The integral in Eq. (12.44) can be evaluated numerically. Figures 12.11 and 12.12 show the various components of the radiation field tensor as functions of the

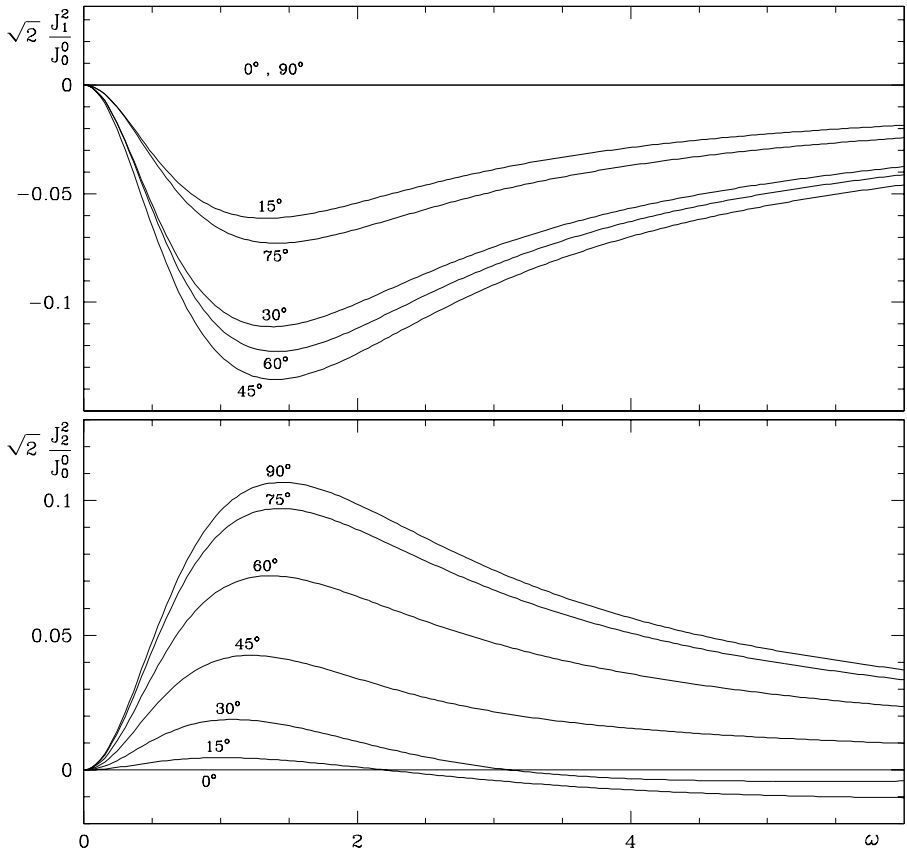

Fig.12.12. Same as Fig.12.11 for the components $J^2_1(\nu_0)$ and $J^2_2(\nu_0)$. The remaining components are obtained from $J^2_{-Q}(\nu_0) = (-1)^Q\, J^2_Q(\nu_0)$.

parameter ω for $\chi_v = 0°$ and for different values of θ_v (with $0° \leq \theta_v \leq 90°$). The components of the radiation field tensor corresponding to $\chi_v \neq 0°$ and/or $\theta_v > 90°$ can easily be deduced from the symmetry properties proved in App. 17. Figures 12.11 and 12.12 are obtained by assuming for the central depression of the line the value $d_c = 0.8$, for the limb-darkening coefficient the value $u_1 = 0.2$, and for the height of point P over the stellar surface the value $h = 0.01\, R_*$. In the solar case, these values are representative of a strong absorption line in the visible and a point P at a height of approximately 10 arcsec over the solar limb. The two figures show the strong sensitivity of the comoving-frame radiation field tensor to the velocity $\vec{v}$. Hereafter we briefly comment on the main features of the various curves.

The upper panel of Fig. 12.11 shows that the average intensity, $J^0_0(\nu_0)$, increases monotonically with increasing velocity. This is the well-known phenomenon of *Doppler brightening*, which is an obvious consequence of the presence of an absorption line in the star's spectrum: an observer moving with sufficiently large velocity 'sees', at frequency ν_0, the radiation emitted by the star in the far wings of the

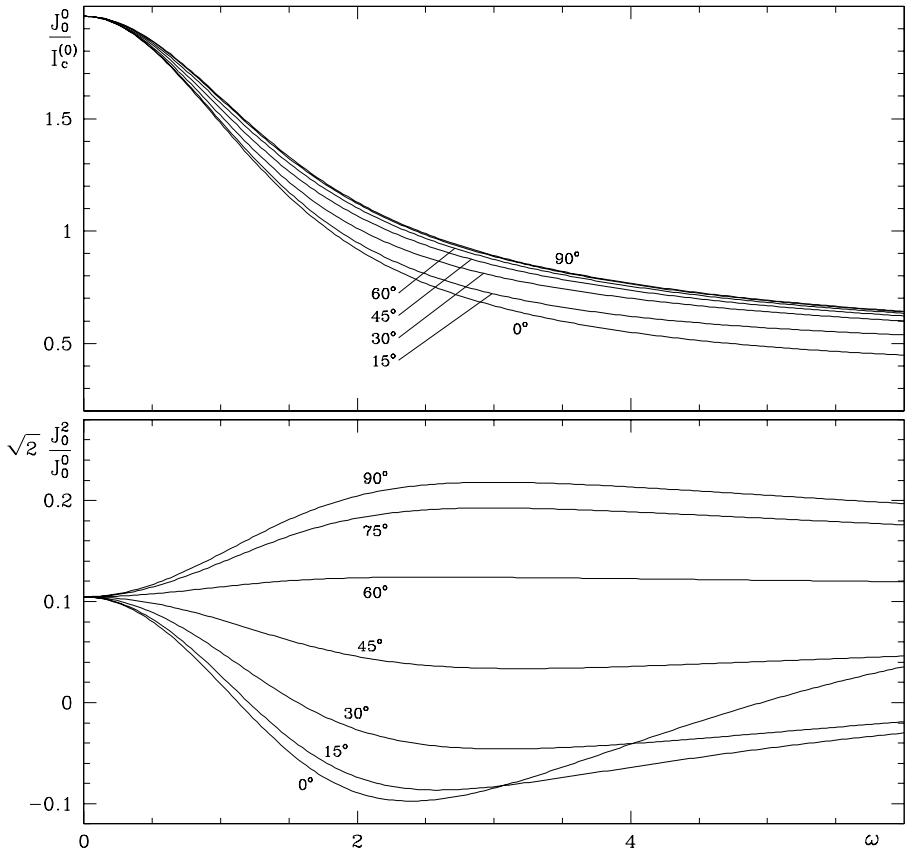

Fig.12.13. Same as Fig.12.11 except for the line depression d_c, which is set to -4 (emission line). Note in the upper panel the Doppler dimming effect.

line, where the intensity is larger than in the line core.

The interpretation of the lower panel of Fig. 12.11, showing the behavior of the anisotropy factor (see Eq. (12.1)), follows from similar arguments. Consider first an observer moving in the upward direction ($\theta_v = 0°$). The radiation coming from 'below' ($\theta \simeq 0°$) is redshifted and therefore enhanced, while the same effect is weaker for the radiation coming from the sides ($\theta \simeq \gamma$). Thus the Doppler effect acts *in the same sense* as geometrical and limb-darkening effects (see the former sections). As a result, the anisotropy factor increases when v is increased. On the contrary, for an observer moving horizontally ($\theta_v = 90°$) the maximum Doppler shift (hence the maximum intensity enhancement) occurs for the radiation coming from the sides – especially from the directions ($\theta \approx \gamma, \chi \approx \chi_v$) and ($\theta \approx \gamma$, $\chi \approx \chi_v + 180°$).[1] Now the roles of the Doppler effect and of geometrical/limb-darkening effects are opposite, and the anisotropy factor is reduced compared to

[1] Obviously, there is a blueshift for the former direction and a redshift for the latter, but this makes no difference in the present context.

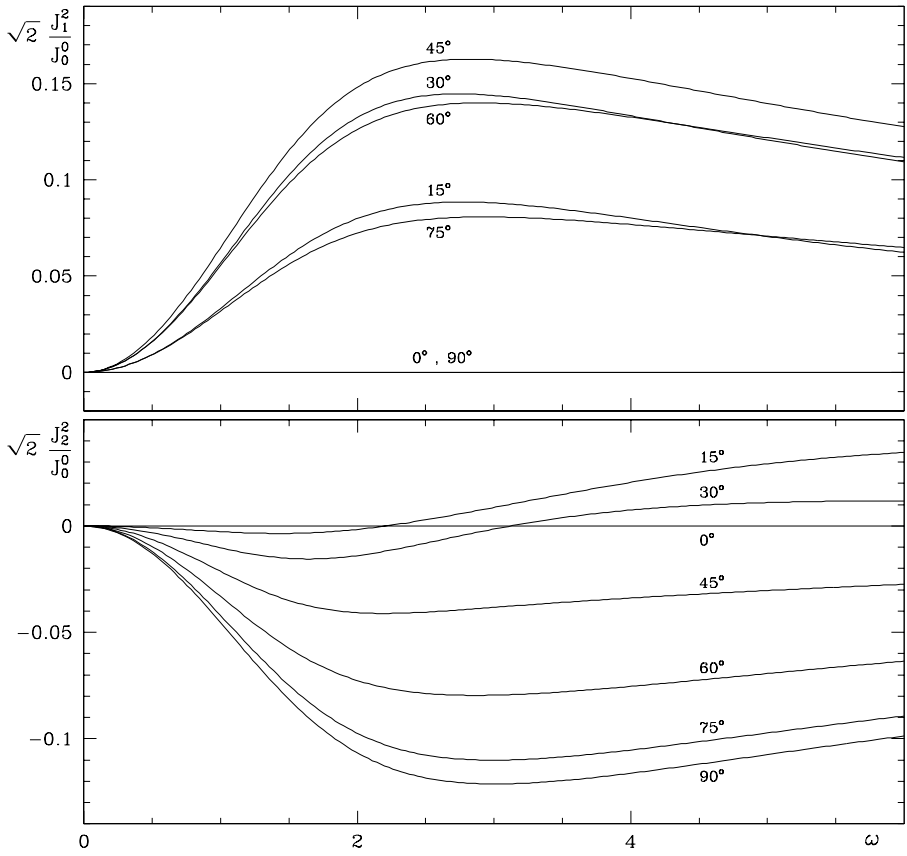

Fig.12.14. Same as Fig.12.12 for an emission line with $d_c = -4$.

the zero-velocity case. As expected, the Doppler effect becomes ineffective for very large velocity, since in that case the observer sees, at frequency ν_0, the radiation emitted by the star in the far wings of the line irrespective of the velocity direction. Thus for $\omega \to \infty$ the anisotropy factor tends to its $\omega = 0$ value,[1] and this implies that the curves in the lower panel of Fig. 12.11 have to go through a maximum or a minimum. Actually, such extrema are found at ω values of about 1.5 or slightly less.

Figure 12.12 shows the behavior of the other non-vanishing components of the comoving-frame radiation field tensor. The interpretation of the different curves follows from arguments similar to those developed above. In particular, it should be remarked that J^2_1 and J^2_2 are zero both for $\omega = 0$ and for $\omega \to \infty$, because in either case the radiation field in the comoving frame is cylindrically symmetrical.

The situation is completely reversed for an emission line, as shown in Figs. 12.13

[1] The coincidence of these two values is a consequence of the assumption of a frequency-independent limb-darkening coefficient.

and 12.14. In this case one speaks of *Doppler dimming* effect (upper panel of Fig. 12.13). The anisotropy factor turns out to be lowered – relative to its zero-velocity value – for radial velocities ($\theta_v \simeq 0^\circ$), and enhanced for transversal velocities ($\theta_v \simeq 90^\circ$). Similarly, there is a sign switch for the components J^2_1 andJ^2_2 in comparison with the absorption line case.

This page intentionally left blank

CHAPTER 13

ASTROPHYSICAL APPLICATIONS: THE OUTER LAYERS OF STELLAR ATMOSPHERES

The theoretical results on atomic polarization derived in Chap. 10, and the study performed in Chap. 12 on the properties of the radiation field flowing from a stellar atmosphere allow one to deduce in a rather straightforward way the polarization signatures of spectral lines formed in an optically thin plasma (like a prominence or a coronal condensation) located at a certain height over the stellar surface. In this chapter we present a number of applications of such results with the purpose, on one side, of discussing the limits of applicability of the theory developed in this book, and, on the other side, of showing the important role often played by the Doppler effect in determining the shape of polarimetric profiles. The methods illustrated in this chapter can be considered as the basic tools for the interpretation of spectropolarimetric observations in solar prominences or in the solar corona – as long as the hypothesis of optical thinness is verified – and for the diagnostics of prominence and/or coronal magnetic fields.

13.1. The Flat-Spectrum Approximation

The flat-spectrum approximation has been introduced and widely discussed in Chap. 6. This approximation is at the basis of the statistical equilibrium equations that have been derived in Chap. 7 and solved in Chap. 10 for atomic systems of increasing complexity. The astrophysical applications that we are going to perform in the present chapter heavily rely on the results obtained in Chaps. 7 and 10, so that it is now necessary to discuss in some detail the limitations imposed by the flat-spectrum approximation on the description of resonance polarization and the Hanle effect.

Suppose we wish to investigate the polarization properties of a spectral line of a given atom, located at a point P in the outer atmosphere of a star and moving with velocity $\vec{v}$ with respect to the star. The spectral line can be a resonance line, originating from the transition between the ground level and an excited level, or, more generally, a subordinate line due to the transition between two excited levels. The atom is illuminated by the radiation field flowing from the stellar atmosphere which affects, together with collisions and with a magnetic field, possibly present at point P, its physical state. Such state can be determined by introducing a suitable model, capable of describing the atomic structure and the radiative and collisional connections among the various atomic levels, and by solving the statistical equilibrium equations for the different levels (or terms). The model involves a number of electric-dipole transitions between the various levels and, for each transition, the

flat-spectrum approximation has to be satisfied.

As far as the radiation field is concerned, there are two possibilities: either the stellar spectrum presents an absorption (or emission) line at (or in the immediate neighborhood of) the transition frequency, or such frequency falls into a continuum window of the stellar spectrum. In the former case, denoting by $\Delta\nu_{\rm p}$ the line width, the spectrum can be considered flat only within a frequency interval $\Delta\nu \ll \Delta\nu_{\rm p}$. In the latter, if $\Delta\nu_{\rm w}$ is the width of the continuum window, the spectrum is actually flat within an interval $\Delta\nu \leq \Delta\nu_{\rm w}$. In order for the flat-spectrum approximation to hold, the interval $\Delta\nu$ must be larger than the natural width of the levels, and, when coherences between non-degenerate levels are involved, it must be larger than the corresponding Bohr frequencies (cf. Chap. 6).

As to the natural width requirement, it should be remarked that stellar spectra have, as a rule, rather broad absorption (or emission) lines, the typical widths being two or more orders of magnitude larger than the typical natural width of a level. To make an example, a medium-strength line of the solar spectrum at 5000 Å has a typical full width at half maximum of the order of 100 mÅ, which corresponds to $\Delta\nu_{\rm p} \simeq 1.2 \times 10^{10}\ {\rm s}^{-1}$. This is to be compared to a characteristic natural width, which is of the order or less than $10^8\,{\rm s}^{-1}$.

The only limitation to the applicability of the flat-spectrum approximation thus comes from coherences between non-degenerate levels, whose Bohr frequencies have to be sufficiently small. In the case of a multi-level atom without hyperfine structure, such coherences are those between magnetic sublevels split by a magnetic field. Since the frequency separation between two different sublevels is of the order of $\nu_{\rm L}$, the flat-spectrum approximation is verified when $\nu_{\rm L} \ll \Delta\nu_{\rm p}$ in the first of the two cases outlined above (presence of an absorption or emission line), and when $\nu_{\rm L} \ll \Delta\nu_{\rm w}$ in the second case (transition falling into a continuum window). Referring to the previous example of a line with $\Delta\nu_{\rm p} \simeq 1.2 \times 10^{10}\,{\rm s}^{-1}$, and recalling the definition of $\nu_{\rm L}$ (see Eq. (3.11)), it follows that the magnetic field has to satisfy the condition $B \ll 0.9 \times 10^4\,{\rm G}$; such value can be much larger in the second case.

Similar limitations apply to fine-structured or hyperfine-structured atomic systems. In these cases coherences may be present between J-levels belonging to the same term, or between F-levels belonging to the same level, respectively. Recalling the definitions of the quantities ζ and $\mathcal{A}$ given in Eqs. (3.59) and (3.70), respectively, we see that the following inequalities must be satisfied in order for the flat-spectrum approximation to hold

$$\frac{\zeta}{h} \ll \Delta\nu_{\rm p}\ , \qquad \frac{\mathcal{A}}{h} \ll \Delta\nu_{\rm p} \tag{13.1}$$

in the case of an absorption or emission line, and

$$\frac{\zeta}{h} \ll \Delta\nu_{\rm w}\ , \qquad \frac{\mathcal{A}}{h} \ll \Delta\nu_{\rm w} \tag{13.2}$$

in the case of a continuum window.

It should also be considered that, because of a general property of the statistical equilibrium equations (see the introduction to Chap. 7), coherences between non-degenerate levels are the smaller, the larger the energy separation between the

levels. The ratio of such coherences to level populations is roughly the same as the ratio of the natural width of the level to the Bohr frequency of the coherence. Therefore, if the Bohr frequency of one of the coherences is 'large' (comparable with $\Delta\nu_{\rm p}$ or $\Delta\nu_{\rm w}$, so that the flat-spectrum approximation is not valid), the coherence itself is expected to be much smaller that the diagonal elements of the density matrix (by two orders of magnitude in the example above). Moreover, as illustrated in Sect. 10.17, such coherences are important in affecting the polarization properties of the emissivity only in the far wings of the spectral line, where the emissivity itself is very low in all four Stokes parameters and is often masked by other processes, like, e.g., the continuum emissivity. These arguments show that, if we exclude some few special cases involving particularly strong lines with well-developed damping wings formed in optically thick media, it is usually justified to consider a simplified atomic model where such coherences are set to zero ab initio. This approximation is particularly suited for the applications that we are going to develop in this chapter, which refer to optically thin plasmas.

To conclude, we want to stress that the flat-spectrum approximation in polarized radiative transfer is analogous to the complete redistribution approximation (in the atomic frame) in standard radiative transfer. In the latter, only few lines need to be treated with the more sophisticated theory of partial redistribution; similarly, in polarized radiative transfer most of the applications to concrete problems can be handled with the simple approach of the flat-spectrum approximation. Only in few cases more sophisticated (and more complicated) formalisms have to be invoked (Bommier, 1997a,b; Landi Degl'Innocenti et al., 1997).

13.2. Velocity/Density-Matrix Correlations and the Approximation of Complete Redistribution on Velocities

As shown in Sect. 12.4, the radiation field tensor experienced by an observer moving with velocity $\vec{v}$ in the outer layers of a stellar atmosphere may strongly depend, because of the Doppler effect, on $\vec{v}$. As a consequence, it has to be expected that the density matrix of an atomic system moving in the same environment may be strongly correlated with its velocity.

Given this situation, a statistical description of the atomic system has to be given in terms of the product of two functions: the velocity distribution function $f(\vec{v})$, defined such that $f(\vec{v})\,{\rm d}^3\vec{v}$, with

$$\int f(\vec{v})\,{\rm d}^3\vec{v} = 1\,, \tag{13.3}$$

is the probability of finding an atom of the given species with velocity contained in the infinitesimal volume ${\rm d}^3\vec{v}$ of the velocity space, times $\rho_{nm}(\vec{v})$, the $\vec{v}$-dependent density matrix, here defined on the basis of the energy eigenvectors. With these notations, the quantity

$$dP = f(\vec{v})\,\rho_{nn}(\vec{v})\,{\rm d}^3\vec{v}$$

gives, for instance, the probability of finding the atom with velocity $\vec{v}$ *and* in the internal state specified by the eigenvector $|\, n \rangle$. In the following, we will refer to products of the form $f(\vec{v})\, \rho_{nm}(\vec{v})$, or – when using the spherical tensor representation – $f(\vec{v})\, \rho^K_Q(\alpha J; \vec{v})$ or $f(\vec{v})\ {}^{\beta LS}\rho^K_Q(J, J'; \vec{v})$, with the name of *velocity-space density matrix*.

We will now derive a statistical equilibrium equation for the velocity-space density matrix. To this aim, it should be taken into account that all the processes that we have considered so far in establishing the time evolution of the density matrix, such as absorption and emission of photons, inelastic and superelastic collisions with electrons, and depolarizing collisions with perturbers (mainly neutral hydrogen atoms), are practically ineffective in changing the velocity of the atom. Consider, for instance, the emission or the absorption of a photon of visible wavelength by an atom which is moving with velocity $\vec{v}$. The conservation of momentum implies that the atom experiences a recoil corresponding to a velocity variation Δv given by

$$\Delta v \approx \frac{h}{\lambda\, \mu\, m_{\mathrm{H}}} \,,$$

where λ is the photon's wavelength and μ is the atomic weight of the atom. For example, assuming $\lambda = 5000\,\text{Å}$ and $\mu = 56$ (the atomic weight of iron), one gets

$$\Delta v \simeq 1.4 \ \mathrm{cm\ s^{-1}} \,,$$

which should be compared with velocities of the order of some km s^{-1} that are typically found in stellar atmospheres. Somewhat more efficient from this point of view are collisions with thermal electrons, either elastic, inelastic, or superelastic. If v_{e} is the typical velocity of an electron, the recoil suffered by the atom is given, in terms of velocity variation, by

$$\Delta v \approx \frac{m\, v_{\mathrm{e}}}{\mu\, m_{\mathrm{H}}} \,.$$

Assuming for v and v_{e} the r.m.s. values corresponding to the same temperature, one has

$$\frac{v_{\mathrm{e}}}{v} = \sqrt{\frac{\mu\, m_{\mathrm{H}}}{m}} \,,$$

so that

$$\frac{\Delta v}{v} \approx \sqrt{\frac{m}{\mu\, m_{\mathrm{H}}}} \,.$$

For $\mu = 56$ one gets, for instance

$$\frac{\Delta v}{v} \simeq 3.1 \times 10^{-3} \,.$$

Finally, depolarizing collisions are elastic collisions due to long-range interactions, and they are also ineffective in changing appreciably the velocity of the atom.

The only processes that are important, under this point of view, are close collisions with atoms. Such collisions, that can be referred to as *velocity-changing* collisions, are characterized by very small impact parameters and by a relatively large exchange of kinetic energy between the colliding atoms. It has then to be expected that such collisions will also induce transitions between the energy levels (or sublevels) of the atom, thus affecting its density matrix.

Referring for simplicity to the case of a multi-level atom in the statistical tensor representation, and taking into account the foregoing considerations, we can write the statistical equilibrium equation for the velocity-space density matrix in the form

$$\frac{\mathrm{d}}{\mathrm{d}t}\Big[f(\vec{v})\,\rho^K_Q(\alpha J;\vec{v})\Big] = f(\vec{v})\left(\frac{\mathrm{d}}{\mathrm{d}t}\,\rho^K_Q(\alpha J;\vec{v})\right)_0 + \left(\frac{\delta}{\delta t}\Big[f(\vec{v})\,\rho^K_Q(\alpha J;\vec{v})\Big]\right)_{\text{v.c.c.}} . \quad (13.4)$$

The first term in the right-hand side is due to the 'ordinary' processes mentioned above – which are ineffective, to a very good approximation, in changing the velocity of the atom. In particular, the quantity

$$\left(\frac{\mathrm{d}}{\mathrm{d}t}\,\rho^K_Q(\alpha J;\vec{v})\right)_0$$

is the sum of the right-hand side of Eq. (7.11) – radiative processes – and the right-hand side of Eq. (7.101) – collisional processes. It should be remarked that the radiative rates $\mathbb{T}_{\mathrm{A}}$, $\mathbb{T}_{\mathrm{S}}$, $\mathbb{R}_{\mathrm{A}}$, and $\mathbb{R}_{\mathrm{S}}$ (which are proportional to the radiation field tensor) depend in general on the velocity $\vec{v}$.

The second term in the right-hand side of Eq. (13.4) is due to velocity-changing collisions, and can be regarded as a generalization of the Boltzmann term which is met in the usual kinetic theory of gases (see e.g. Oxenius, 1986). Neglecting the internal state of the colliders, such term – that will be referred to in the following as the *generalized Boltzmann term* – can be written in the form

$$\begin{aligned}
&\left(\frac{\delta}{\delta t}\Big[f(\vec{v})\,\rho^K_Q(\alpha J;\vec{v})\Big]\right)_{\text{v.c.c.}} = \\
&= \sum_i \sum_{\alpha' J' K' Q'} \int f(\vec{v}\,')\,\rho^{K'}_{Q'}(\alpha' J';\vec{v}\,')\,F_i(\vec{u}\,') \\
&\qquad\qquad \times q_i(\vec{v}\,',\vec{u}\,' \to \vec{v},\vec{u}\,;\alpha' J' K' Q' \to \alpha J K Q)\; w'\;\mathrm{d}^3\vec{u}\,' \\
&\quad - f(\vec{v})\,\rho^K_Q(\alpha J;\vec{v}) \\
&\qquad \times \sum_i \sum_{\alpha' J' K' Q'} \int F_i(\vec{u})\; q_i(\vec{v},\vec{u} \to \vec{v}\,',\vec{u}\,';\alpha J K Q \to \alpha' J' K' Q')\; w\;\mathrm{d}^3\vec{u}\,. \quad (13.5)
\end{aligned}$$

In this equation, $F_i(\vec{u})$ is the distribution function of particles of species i, normalized to the number density n_i of the same particles,

$$n_i = \int F_i(\vec{u})\;\mathrm{d}^3\vec{u}\,;$$

$q_i(\vec{v}, \vec{u} \to \vec{v}', \vec{u}'; \alpha JKQ \to \alpha' J' K' Q')$ is the cross section for the collision in which the atom goes from velocity $\vec{v}$ to velocity $\vec{v}'$ (changing at the same time its internal state from level αJ to level $\alpha' J'$ and from multipole KQ to multipole $K'Q'$) whereas the collider – of species i – goes from velocity $\vec{u}$ to velocity $\vec{u}'$; w and w' are the moduli of the relative velocities defined by $\vec{w} = \vec{v} - \vec{u}$, $\vec{w}\,' = \vec{v}\,' - \vec{u}\,'$.[1]

Owing to the presence of the generalized Boltzmann term, Eq. (13.4) is in fact extremely complicated. Moreover, little is known, both from the experimental and from the theoretical side, on the cross sections q_i entering Eq. (13.5). For these reasons, two different approximations (or working hypotheses) are generally introduced to bring back the problem to a more tractable form.

The first one, that can be referred to as the *velocity-coherence* approximation, consists in simply neglecting the generalized Boltzmann term in Eq. (13.4). This is justified only when the number density of perturbers (typically hydrogen atoms or ions) is sufficiently low, say, less than a critical value $n_{\rm c}$ whose order of magnitude can be estimated through the following considerations.

The order of magnitude of the rates for velocity-changing collisions is given by $n\,q\,v$, where n is the number density of perturbers, q is the cross section for velocity-changing collisions, and v is the average velocity of perturbers relative to the atom. Such a rate has to be compared with the other rates appearing in the first term of the right-hand side of Eq. (13.4), and, more specifically,[2] with the Einstein coefficient for spontaneous de-excitation, A. This leads to the following equation for the critical density

$$n_{\rm c}\, q\, v \approx A\ .$$

Let us take for v the average relative velocity of hydrogen atoms corresponding to a Maxwellian distribution at temperature T,

$$v \;=\; \sqrt{\frac{8k_{\rm B}T}{\pi\, m_{\rm H}}\left(1+\frac{1}{\mu}\right)}\ .$$

Neglecting the factor $1/\mu$, and expressing q in units of πa_0^2 (a_0 being the Bohr radius), A in units of $10^7\ {\rm s}^{-1}$, and T in units of $10^4\ {\rm K}$, one gets, numerically

$$n_{\rm c} \simeq 7.8\times 10^{16}\ \frac{A}{q\,\sqrt{T}}\ \ {\rm cm}^{-3}\ . \tag{13.6}$$

This expression, joined with the fact that values of q (in units of πa_0^2) are rarely larger that 10^1-10^2, leads to the conclusion that in the outer layers of stellar atmospheres the approximation of neglecting the generalized Boltzmann term in Eq. (13.4) is fully justified.[3]

---

[1] Equation (13.5) is a heuristic equation based on the possibility of defining a cross section such as $q_i(\vec{v}, \vec{u} \to \vec{v}', \vec{u}'; \alpha JKQ \to \alpha' J' K' Q')$.

[2] Excluding particular cases involving anisotropic velocity distributions, velocity-changing collisions are responsible for a relaxation mechanism of the density matrix. For this reason, the comparison has to be made with the largest of the relaxation rates, which, in many cases, is the spontaneous de-excitation rate.

[3] In solar prominences, for instance, the typical number density of hydrogen is of the order of $10^{11}\ {\rm cm}^{-3}$.

Under this approximation, Eq. (13.4) reduces to

$$\frac{\mathrm{d}}{\mathrm{d}t}\Big[f(\vec{v})\,\rho^K_Q(\alpha J;\vec{v})\Big] = f(\vec{v})\left(\frac{\mathrm{d}}{\mathrm{d}t}\,\rho^K_Q(\alpha J;\vec{v})\right)_0 ,$$

which is solved by

$$\frac{\mathrm{d}}{\mathrm{d}t}\,f(v) = 0$$
$$\frac{\mathrm{d}}{\mathrm{d}t}\,\rho^K_Q(\alpha J;\vec{v}) = \left(\frac{\mathrm{d}}{\mathrm{d}t}\,\rho^K_Q(\alpha J;\vec{v})\right)_0 .$$

These equations show that the density matrix of an atom moving with velocity $\vec{v}$ is completely decoupled from the density matrix of atoms moving with different velocities, and that its value can be found by solving the statistical equilibrium equations of Chap. 7: obviously, the Doppler effect must be taken into account in the expressions for the radiative rates involving the radiation field tensor. On the other hand, the velocity distribution $f(\vec{v})$ remains undetermined, and can only be established by means of different physical considerations. In many cases, $f(\vec{v})$ can be simply assumed to be a Maxwellian distribution, possibly centered at a non-zero velocity, like in the case of the solar wind.[1]

It should be remarked that, when the velocity-coherence approximation is valid, the $\vec{v}$-dependence of the density matrix is only due to the fact that atoms moving with different velocities may experience, because of the Doppler effect, different values of the radiation field tensor. Obviously, when the incident radiation field presents no spectral structure across each of the frequency intervals centered at the transition frequencies of the model atom and sufficiently wide to encompass all possible Doppler shifts, the $\vec{v}$-dependence of the density matrix disappears and one is left with a 'unique' density matrix $\rho^K_Q(\alpha J)$.

The second approximation that can be introduced to bring back Eq. (13.4) to a more tractable form is the so-called approximation of *complete redistribution on velocities*. Here one assumes a priori that velocity-changing collisions are so efficient in reshuffling the atomic velocities that any velocity/density-matrix correlation is lost. This implies that the velocity-space density matrix can be written as $f(\vec{v})\,\rho^K_Q(\alpha J)$, the second factor being independent of $\vec{v}$, which in turn implies that the term

$$\left(\frac{\mathrm{d}}{\mathrm{d}t}\,\rho^K_Q(\alpha J;\vec{v})\right)_0$$

appearing in Eq. (13.4) reduces to the sum of products of velocity-dependent rates times velocity-independent density-matrix elements. It is then convenient to integrate Eq. (13.4) in $\mathrm{d}^3\vec{v}$. Disregarding, for the time being, the generalized Boltzmann term, and recalling the normalization of the velocity distribution (see Eq. (13.3)), one finds for $\rho^K_Q(\alpha J)$ the 'ordinary' statistical equilibrium equation

[1] In certain situations, bi-modal or three-modal distributions can be more appropriate.

with the velocity-dependent rates replaced by their averages over the velocity distribution $f(\vec{v})$. Synthetically,

$$\text{Rate}\,(\vec{v}\,) \;\to \int f(\vec{v}\,)\;\text{Rate}\,(\vec{v}\,)\;\mathrm{d}^3\vec{v}\,. \tag{13.7}$$

Since the rates depend on $\vec{v}$ only through the radiation field tensor, it is easily seen, recalling Eqs. (5.157) and the formulae for the non-relativistic Doppler effect, that substitution (13.7) is equivalent to

$$J^K_Q(\nu) \to \bar{J}^K_Q(\nu) = \int \mathrm{d}^3\vec{v}\;\, f(\vec{v}\,)\,\big[J^K_Q(\nu)\big]_{\vec{v}}\,, \tag{13.8}$$

where $[J^K_Q(\nu)]_{\vec{v}}$, the radiation field tensor in the comoving frame, is given by (cf. Eq. (12.40))

$$\big[J^K_Q(\nu)\big]_{\vec{v}} = \oint \frac{\mathrm{d}\Omega}{4\pi} \sum_{i=0}^{3} \mathcal{T}^K_Q(i,\vec{\Omega})\; I_i\Big(\nu\Big(1+\frac{\vec{v}\cdot\vec{\Omega}}{c}\Big),\vec{\Omega}\Big)\,. \tag{13.9}$$

In particular, for an isotropic distribution of velocities, denoting by $f_{\mathrm{c}}(v)$ the distribution (normalized to unity) of the component of the velocity along an arbitrary direction, one has

$$\bar{J}^K_Q(\nu) = \int_{-\infty}^{\infty} \mathrm{d}v\; f_{\mathrm{c}}(v) \oint \frac{\mathrm{d}\Omega}{4\pi} \sum_{i=0}^{3} \mathcal{T}^K_Q(i,\vec{\Omega})\; I_i\Big(\nu\Big(1+\frac{v}{c}\Big),\vec{\Omega}\Big)\,,$$

or, via the new variable $\nu' = \nu\,(1+v/c)$,

$$\begin{aligned}\bar{J}^K_Q(\nu) &= \int_{-\infty}^{\infty} \mathrm{d}\nu'\;\, \frac{c}{\nu}\; f_{\mathrm{c}}\Big(c\,\frac{\nu'-\nu}{\nu}\Big) \oint \frac{\mathrm{d}\Omega}{4\pi} \sum_{i=0}^{3} \mathcal{T}^K_Q(i,\vec{\Omega})\; I_i(\nu',\vec{\Omega}) \\ &= \int_{-\infty}^{\infty} \mathrm{d}\nu'\;\, p(\nu'-\nu)\; J^K_Q(\nu')\,,\end{aligned} \tag{13.10}$$

where

$$p(\nu'-\nu) = \frac{c}{\nu}\; f_{\mathrm{c}}\Big(c\,\frac{\nu'-\nu}{\nu}\Big)\,.$$

For an isotropic distribution of velocities, substitution (13.7) is thus equivalent to the substitution of the radiation field tensor with a suitable convolution over frequencies. In the case of a Maxwellian distribution, where $f_{\mathrm{c}}(v)$ is given by (cf. Eq. (5.42))

$$f_{\mathrm{c}}(v) = \frac{1}{\sqrt{\pi}}\,\frac{1}{v_{\mathrm{T}}}\;\, \mathrm{e}^{-\left(\frac{v}{v_{\mathrm{T}}}\right)^2}\,,$$

with v_{T} the thermal velocity, the convolution profile is given by

$$p(\nu' - \nu) = \frac{1}{\sqrt{\pi}} \frac{1}{\Delta\nu_{\mathrm{D}}} \ \mathrm{e}^{-\left(\frac{\nu' - \nu}{\Delta\nu_{\mathrm{D}}}\right)^2} \ , \tag{13.11}$$

where

$$\Delta\nu_{\mathrm{D}} = \nu \, \frac{v_{\mathrm{T}}}{c} \ .$$

Up to now, the integral in $\mathrm{d}^3\vec{v}$ of the generalized Boltzmann term has been disregarded. An inspection of the right-hand side of Eq. (13.5), joined with the hypothesis of the velocity independence of the density matrix, shows that such term leads to the appearance in the statistical equilibrium equations of two additional contributions that can be written in the form

$$\begin{aligned} &+ \sum_{\alpha' J' K' Q'} \mathcal{B}_{\mathbb{T}}(\alpha' J' K' Q' \to \alpha J K Q) \ \rho^{K'}_{Q'}(\alpha' J') \\ &- \left[\sum_{\alpha' J' K' Q'} \mathcal{B}_{\mathbb{R}}(\alpha J K Q \to \alpha' J' K' Q') \right] \rho^{K}_{Q}(\alpha J) \ , \end{aligned} \tag{13.12}$$

where

$$\begin{aligned} &\mathcal{B}_{\mathbb{T}}(\alpha' J' K' Q' \to \alpha J K Q) = \\ &= \sum_i \int \mathrm{d}^3\vec{v} \int \mathrm{d}^3\vec{u}\,' \ f(\vec{v}\,') \ F_i(\vec{u}\,') \ q_i(\vec{v}\,', \vec{u}\,' \to \vec{v}, \vec{u}\,; \alpha' J' K' Q' \to \alpha J K Q) \ w' \\ &\mathcal{B}_{\mathbb{R}}(\alpha J K Q \to \alpha' J' K' Q') = \\ &= \sum_i \int \mathrm{d}^3\vec{v} \int \mathrm{d}^3\vec{u} \ f(\vec{v}\,) \ F_i(\vec{u}\,) \ q_i(\vec{v}, \vec{u} \to \vec{v}\,', \vec{u}\,'; \alpha J K Q \to \alpha' J' K' Q') \ w \ . \end{aligned}$$

In particular, when the velocity distribution of each species of colliders is isotropic, the considerations developed in Sect. 7.13 can be applied to these terms, so that the contribution of Eq. (13.12) can be cast into a form similar to the right-hand side of Eq. (7.101).

It should be pointed out that the approximation of complete redistribution on velocities can in principle be applied only when the generalized Boltzmann term predominates over the other terms appearing in Eq. (13.4), or, in other words, when the number density of colliders is much larger that the critical value n_{c} defined in Eq. (13.6). A large number density of colliders implies, however, large depolarizing rates, due both to long-range interactions and to velocity-changing collisions: as a consequence, when the approximation of complete redistribution on velocities is fully justified, polarization phenomena turn out, in general, to be of marginal importance. Actually, an 'intermediate' approach is often used where the generalized Boltzmann term is neglected, still assuming a velocity-independent density matrix and using averaged rates according to Eq. (13.7). This obviously leads to

major simplifications, because the atomic system is described by a 'unique' density matrix and because the poorly known cross sections appearing in the generalized Boltzmann term are no longer involved. Such approach, though incorrect in principle, is adopted in order to get an approximate solution to a problem that would otherwise be insoluble in practice. Hence its importance in radiative transfer for polarized radiation, particularly for the solution of non-LTE problems.

13.3. Resonance Polarization and the Hanle Effect in the Absence of Velocity/Density-Matrix Correlations

As shown in the former section, there is a special case where the density matrix does not depend on the velocity of the atom. This happens when the radiation field impinging on the atom is spectrally unstructured at all the transition frequencies that contribute to establish its statistical equilibrium.

Whereas this situation is common in laboratory experiments, it is much less frequent in astrophysical plasmas. However, some of the spectral lines that are currently used for the diagnostics of the outer layers of the solar atmosphere fall within this category. A typical example is the so-called coronal green line of FeXIV at 5304 Å. The solar spectrum shows no prominent lines in the neighborhood of this wavelength, which implies that the excitation of the ions is due to the solar continuum and is practically independent of the Doppler effect.

In this section we illustrate the main features of the phenomena of resonance polarization and the Hanle effect for this simple case where it is fully justified to neglect velocity/density-matrix correlations, so that a unique, velocity-independent density matrix can be defined.

Referring to Fig. 13.1, we consider an atom (described by a suitable model as outlined in Sect. 13.1) located at point P in the outer solar atmosphere. We assume the incident radiation field at P to be unpolarized, cylindrically symmetrical about the vertical through P, and spectrally unstructured in the neighborhood of each of the frequencies ν_i corresponding to the transitions involved in the model atom. The observer, receiving the radiation along the direction $\vec{\Omega}_0$, sees the atom at an apparent height h' over the solar limb, the true height h over the solar surface being related to h' and to the aspect angle[1] δ by the simple equation

$$(h + R_\odot) \cos\delta = h' + R_\odot \ ,$$

where $R_\odot$ is the solar radius. From the knowledge of h and of the limb-darkening coefficients of the solar spectrum, the radiation field tensor can easily be derived at each of the frequencies ν_i. Assuming a quadratic limb-darkening law, and drawing on the results derived in Sect. 12.3, we can write the non-zero components of

[1] The determination of the angle δ is often non-trivial and, in some cases, even impossible. For prominences, one can obtain an estimate of δ by measuring the position of the corresponding filament over the disk during the few days preceding (or following) the observation.

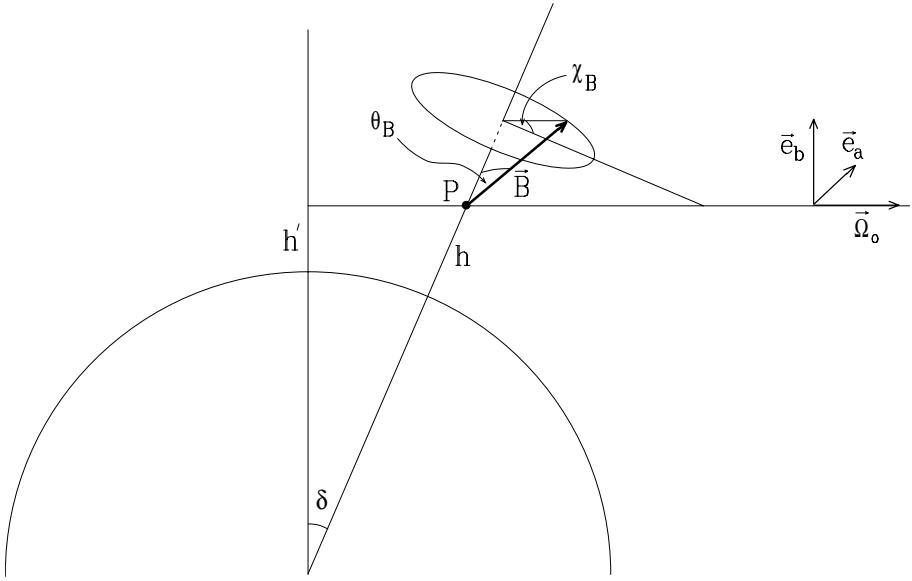

Fig.13.1. Geometry of a scattering process in the outer layers of the solar atmosphere. The direction $\vec{\Omega}_0$ points to the observer, while the direction $\vec{e}_a$ – the reference direction for positive Q – is parallel to the solar limb (as seen by the observer). θ_B and χ_B are the polar angles of the magnetic field vector relative to the local vertical.

the radiation field tensor in a reference system with the z-axis directed along the vertical through P in the form

$$J^0_0(\nu_i) = J_{\nu_i} \,, \qquad J^2_0(\nu_i) = \frac{1}{\sqrt{2}}\; w_{\nu_i}\, J_{\nu_i} \,, \tag{13.13}$$

where J_{ν_i} and w_{ν_i} are given in Eqs. (12.34) and (12.36), respectively.

The radiation field tensor is just one of the factors that have to be specified to find the density-matrix components of the atom and, ultimately, the Stokes parameters of the radiation emitted along the direction $\vec{\Omega}_0$. The remaining factors are the magnetic field, that can be parameterized through its modulus, B, and the angles θ_B and χ_B as in Fig. 13.1, and the collisional cross sections. Here we are mainly interested in the basic features of resonance polarization and the Hanle effect in the outer layers of the solar atmosphere, so we will just suppose that, owing to the low density of the plasma, collisions can be neglected. Obviously, when using a specific spectral line as a diagnostic tool for inferring – for instance – the value of the magnetic field, this approximation has to be carefully tested, case by case. For example, detailed analyses have shown that such approximation is justified for the HeI $\lambda\,10830$ and $\lambda\,5876$ lines, whereas it is not for the hydrogen lines of the Balmer series and for the magnetic-dipole forbidden lines that are commonly used for the diagnostics of coronal fields (FeXIV $\lambda\,5304$, FeXIII $\lambda\,10747$ and $\lambda\,10798$, FeX $\lambda\,6374$).[1]

[1] For the hydrogen lines, collisions with electrons (and protons) turn out to be important

Having specified all the geometrical and physical parameters, one can turn to the problem of finding the density matrix of the radiating atom. This is obtained by solving (for stationary situations) the statistical equilibrium equations that have been derived in Chap. 7. The relevant equations are Eq. (7.11) for the case of a multi-level atom, Eq. (7.38) for a multi-term atom, or Eq. (7.65) for a multi-level atom with hyperfine structure. It should be remarked that all three equations are valid in a reference system with the z-axis directed along the magnetic field. The radiative rates appearing in these equations obviously contain the radiation field tensor evaluated in that reference system, while Eqs. (13.13) refer to a system with the z-axis in the vertical direction. The two systems are related by a suitable rotation. Taking into account Eq. (2.78) one has, with evident notations[1]

$$\left[J^K_Q(\nu_i)\right]_{\text{mag.field}} = \mathcal{D}^K_{0Q}(R)\left[J^K_0(\nu_i)\right]_{\text{vert.}} , \tag{13.14}$$

where (cf. Fig. 13.1)

$$R \equiv \left(\chi_B, \theta_B, \gamma_B\right) . \tag{13.15}$$

Equation (13.14) shows that the radiation field tensor in the magnetic frame is unaffected by the angle χ_B: this is due to the assumption of an unpolarized and cylindrically symmetrical radiation field. The angle γ_B can be chosen arbitrarily, in the sense that all the reference frames corresponding to different γ_B values have the z-axis in the magnetic field direction. However, by fixing a γ_B value, a specific frame is chosen, so that the atomic density matrix is defined in that frame. This should be kept in mind when expressing the emissivity in the observer's frame (see later). In any case, the polarization of the emitted radiation is independent of γ_B.

The solution to the statistical equilibrium equations yields the statistical tensors of all the levels (or terms) involved in the model atom considered, and, in particular, those of the upper level (or term) of the transition under study. This allows one to evaluate the emission coefficient, $\varepsilon_i(\nu, \vec{\Omega}_0)$, which is given by Eq. (7.15e) – or Eq. (10.39) – for the multi-level atom, by Eq. (7.47e) for the multi-term atom, or by Eq. (7.70e) for the multi-level atom with hyperfine structure.[2] It should be recalled, however, that such expressions are valid in the rest frame of the atom. For a collection of atoms having a velocity distribution $f(\vec{v})$, the expression for $\varepsilon_i(\nu, \vec{\Omega}_0)$ must be transformed to take the Doppler effect into account. This is easily done by substituting each of the complex profiles of the form $\Phi(\nu_0 - \nu)$ with the convolution

$$\Phi(\nu_0 - \nu) \rightarrow \hat{\Phi}(\nu_0 - \nu) = \int \mathrm{d}^3\vec{v}\ f(\vec{v})\ \Phi\left(\nu_0\left(1 + \frac{\vec{v}\cdot\vec{\Omega}_0}{c}\right) - \nu\right) , \tag{13.16}$$

because of the quasi-degeneracy of the energy levels with respect to the quantum number l. For coronal lines, collisional rates are comparable to radiative rates because of the low values of the Einstein coefficients ($A \simeq 10^1$-10^2 s^{-1}).

[1] Alternatively, one can use the equations written in the vertical frame, with the difference that the magnetic term takes a more complicated form, as explained in Sect. 7.12.

[2] Note that this last equation is valid under the limit where all the hyperfine components can be considered coincident.

which, in the case of a Maxwellian distribution of velocities, implies the appearance of Voigt functions and of the associated dispersion profiles (or Faraday-Voigt functions; cf. Sect. 5.4).

Next, we have to evaluate the geometrical tensor $\mathcal{T}^K_Q(i,\vec{\Omega}_0)$ appearing in the expression of the emission coefficient for the geometry of Fig. 13.1. Recalling Eq. (5.159), one has

$$\mathcal{T}^K_Q(i,\vec{\Omega}_0) = \sum_P t^K_P(i)\, \mathcal{D}^K_{PQ}(R)\ , \tag{13.17}$$

where R, the rotation carrying the reference system $(\vec{e}_a, \vec{e}_b, \vec{\Omega}_0)$ into the system having the z-axis directed along the magnetic field, is given by

$$R \equiv \left(-90^\circ, -90^\circ + \delta\,, 0^\circ\right) \times \left(\chi_B, \theta_B, \gamma_B\right)\ , \tag{13.18}$$

where the value of the angle γ_B is the same as in Eq. (13.15). We recall that the rotation matrix $\mathcal{D}^K_{PQ}(R)$ for the composite rotation of Eq. (13.18) can be computed with the help of Eq. (2.74).

The Stokes parameters of the radiation flowing along the direction $\vec{\Omega}_0$ can be finally obtained by integration of the radiative transfer equations. Under the hypothesis of an optically thin plasma, one has

$$I_i(\nu,\vec{\Omega}_0) = \int \varepsilon_i(\nu,\vec{\Omega}_0)\ \mathrm{d}s\ , \tag{13.19}$$

where s is the coordinate measured along the direction $\vec{\Omega}_0$.

The procedure that we have outlined above can be followed for any model atom, provided the flat-spectrum approximation is verified. According to our discussion of Sect. 13.1, since we are considering the case where all the transition frequencies of the model atom fall within windows of the continuous solar spectrum, the only limitations are those imposed by inequalities (13.2). Obviously, the validity of such conditions has to be carefully checked before applying the present theory to specific model atoms.

We will now illustrate the basic features of resonance polarization and the Hanle effect in the outer solar atmosphere for a particularly simple model atom, i.e., a two-level atom with $J_\ell = 0$, $J_u = 1$. This simple model avoids the need of finding a numerical solution to the statistical equilibrium equations since the lower level is, by definition, unpolarized. We will also neglect stimulated emission, which is a good approximation for lines at optical wavelengths. The general problem of resonance scattering and the Hanle effect for two-level atoms has already been considered in Sects. 10.2-10.4, so we have just to adapt the equations there obtained to the case of the solar atmosphere. In particular, we can draw the expression for the emission coefficient directly from Eq. (10.41), that we can here rewrite, via Eqs. (5.157), in the form[1]

[1] Note that the contribution to Eq. (13.20) from $K = 1$ is zero (see Eqs. (13.13)-(13.14)), and that $w^{(0)}_{10} = w^{(2)}_{10} = 1$ (see Eq. (10.14) and Table 10.1).

$$\varepsilon_i(\nu,\vec{\Omega}_0) = k_{\rm L}^{\rm A} \sum_{KK'Q} \hat{\Phi}_Q^{KK'}(J_\ell = 0, J_u = 1\,;\nu) \times (-1)^Q\, \mathcal{T}_Q^{K'}(i,\vec{\Omega}_0)\, \frac{1}{1+{\rm i}\,Q H_u}\, J_{-Q}^K(\nu_0)\;, \tag{13.20}$$

where $k_{\rm L}^{\rm A}$ is the frequency-integrated line absorption coefficient defined in Eq. (9.5), $\hat{\Phi}_Q^{KK'}$ is the generalized profile defined in Eq. (10.40)[1] – with the individual profiles $\Phi(\nu_i - \nu)$ replaced by their Doppler convolutions as in Eq. (13.16) – , H_u is given by Eq. (10.29), $\mathcal{T}_Q^K(i,\vec{\Omega}_0)$ by Eq. (13.17), and $J_Q^K(\nu_0)$, the radiation field tensor at the transition frequency ν_0 defined in the magnetic field frame, is given by Eq. (13.14). Similarly, for the frequency-integrated emission coefficient one can rewrite Eq. (10.32) in the form

$$\tilde{\varepsilon}_i(\vec{\Omega}_0) = k_{\rm L}^{\rm A} \sum_{KQ} (-1)^Q\, \mathcal{T}_Q^K(i,\vec{\Omega}_0)\, \frac{1}{1+{\rm i}\,Q H_u}\, J_{-Q}^K(\nu_0)\;. \tag{13.21}$$

Substituting Eq. (13.20) into Eq. (13.19), and assuming a small-size coronal condensation permeated by a uniform magnetic field, one obtains for the Stokes parameters of the radiation reaching the observer the same expression as the right-hand side of Eq. (13.20) with the quantity $k_{\rm L}^{\rm A}$ replaced by the frequency-integrated optical thickness $\tau_{\rm L}$ defined by

$$\tau_{\rm L} = \int k_{\rm L}^{\rm A}\; {\rm d}s\;. \tag{13.22}$$

Similarly, for the frequency-integrated Stokes parameters one obtains the same expression as the right-hand side of Eq. (13.21) with $k_{\rm L}^{\rm A}$ replaced by $\tau_{\rm L}$.

In spite of the simplicity of the model atom considered, the expressions just derived implicitly depend on several parameters (limb-darkening coefficients of the continuous solar radiation, height and aspect angle of the coronal condensation, intensity and direction of the magnetic field, Einstein coefficient of the line, velocity distribution of the scattering atoms). A full analysis of the interplay of the different parameters is well outside the purposes of this book. In the following we limit ourselves to present a number of illustrative results for a few special cases.

a) *Resonance polarization*

In the absence of magnetic fields, the expressions of the emitted Stokes parameters considerably simplify, since $H_u = 0$ and it is not necessary to perform the rotation (13.15) to change the reference system. On the other hand, the generalized profiles simplify according to Eq. (A13.5). With the help of Table 5.6 one obtains for the non-zero Stokes parameters

$$\begin{aligned} I(\nu,\vec{\Omega}_0) &= \tau_{\rm L}\left[J_0^0(\nu_0) + \frac{1}{2\sqrt{2}}\left(3\sin^2\delta - 1\right) J_0^2(\nu_0)\right]\hat{\phi}(\nu) \\ Q(\nu,\vec{\Omega}_0) &= \tau_{\rm L}\,\frac{3}{2\sqrt{2}}\,\cos^2\delta\;\; J_0^2(\nu_0)\;\;\hat{\phi}(\nu)\;, \end{aligned} \tag{13.23}$$

[1] The generalized profiles for the special case $J_\ell = 0$, $J_u = 1$ are explicitly given in App. 13 (see Eqs. (A13.11)).

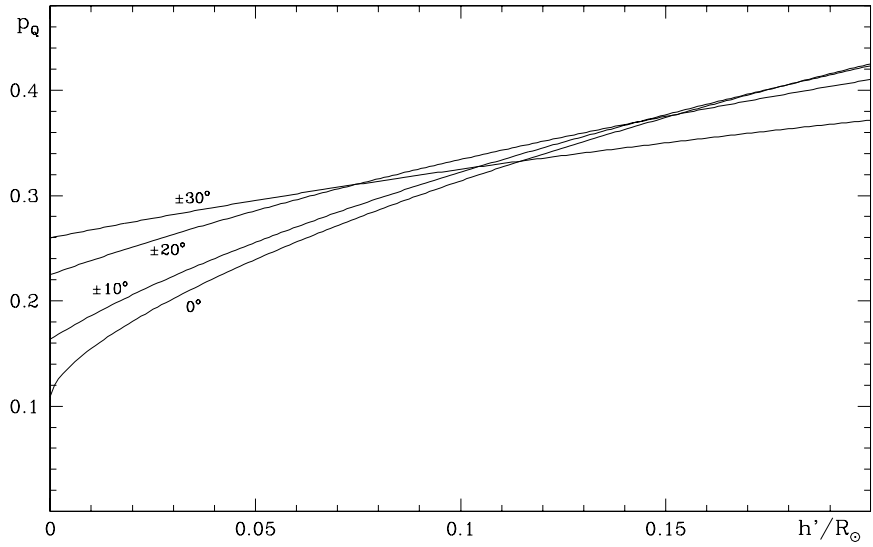

Fig.13.2. The fractional linear polarization $p_Q(\vec{\Omega}_0)$ is plotted as a function of the projected height h' (normalized to the solar radius) for different values of the angle δ in the geometry of Fig.13.1. The figure refers to a two-level atom ($J_\ell = 0, J_u = 1$) illuminated by the continuous solar radiation at 5000 Å in the absence of magnetic fields.

where the tensor $J^K_Q(\nu_0)$ is evaluated in the vertical frame, and where the real profile $\hat{\phi}(\nu)$, which takes the Doppler effect due to the velocity distribution of atoms into account, is given by

$$\hat{\phi}(\nu) = \int \mathrm{d}^3\vec{v}\ \ f(\vec{v})\ \ \phi\left(\nu_0\left(1 + \frac{\vec{v}\cdot\vec{\Omega}_0}{c}\right) - \nu\right) . \tag{13.24}$$

Equations (13.23) show that the ratio $p_Q = Q(\nu, \vec{\Omega}_0)/I(\nu, \vec{\Omega}_0)$ is frequency-independent and equal to the ratio between the frequency-integrated Stokes profiles.

Figure 13.2 shows the behavior of p_Q as a function of the projected height h' for several values of δ. The limb-darkening coefficients are assumed to be $u_1(\nu_0) = 0.95$, $u_2(\nu_0) = -0.20$, corresponding to the wavelength $\lambda = 5000$ Å (Allen, 1973). Such curves, when computed for realistic model atoms, can be very useful for inferring, by comparison with the observed fractional linear polarization, the possible presence of depolarizing mechanisms and, in particular, the presence of magnetic fields (a typical example, referring to the D_3 line of HeI, can be found in Leroy et al., 1977).

b) *The Hanle effect (polarization diagrams)*

In the presence of a magnetic field, the polarization of the radiation scattered along the direction $\vec{\Omega}_0$ is deeply modified by the Hanle effect. This phenomenon can be illustrated by drawing suitable polarization diagrams for the quantities $\tilde{p}_Q$ and $\tilde{p}_U$

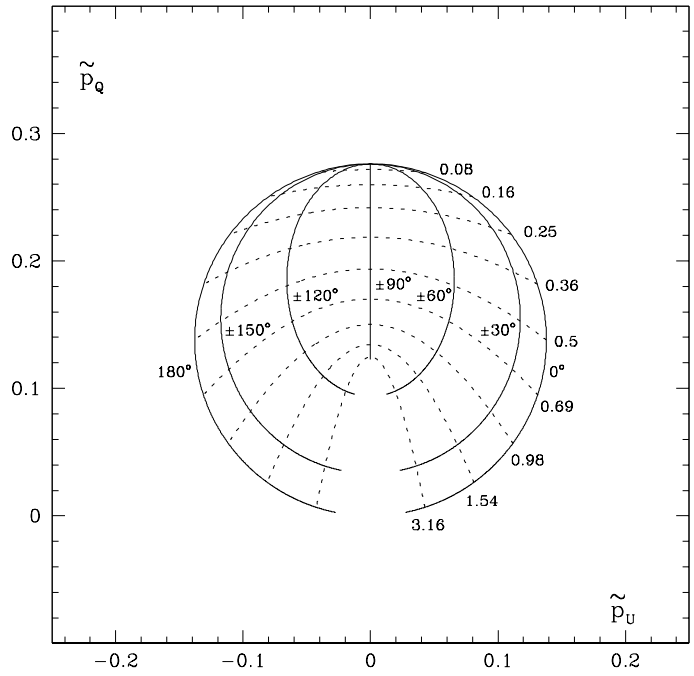

Fig.13.3. Polarization diagram for the radiation emitted along the direction $\vec{\Omega}_0$ in the geometry of Fig.13.1. The graph refers to a two-level atom ($J_\ell = 0, J_u = 1$) located in the plane of the sky ($\delta = 0°$) and illuminated by the continuous solar radiation at 5000 Å in the presence of a horizontal magnetic field ($\theta_B = 90°$). Full lines correspond to $\chi_B = $ const., while broken lines correspond to constant magnetic field strength, parameterized through the quantity H_u (see Eq.(10.29)).

defined by

$$\tilde{p}_Q = \frac{\int Q(\nu, \vec{\Omega}_0)\, \mathrm{d}\nu}{\int I(\nu, \vec{\Omega}_0)\, \mathrm{d}\nu}\,, \qquad \tilde{p}_U = \frac{\int U(\nu, \vec{\Omega}_0)\, \mathrm{d}\nu}{\int I(\nu, \vec{\Omega}_0)\, \mathrm{d}\nu}\,.$$

As apparent from Eq. (13.21), the corresponding quantity $\tilde{p}_V$ vanishes identically, because the only non-zero components of $J^K_Q(\nu_0)$ are those with $K = 0$ or $K = 2$, and the components $\mathcal{T}^0_0(3, \vec{\Omega}_0)$ and $\mathcal{T}^2_Q(3, \vec{\Omega}_0)$ are zero (see Table 5.6).

Traditionally, such polarization diagrams are obtained by fixing the value of θ_B to 90° and by drawing in the plane $\tilde{p}_U$ - $\tilde{p}_Q$ the curves corresponding to $\chi_B = $ const. (for variable H_u) and to $H_u = $ const. (for variable χ_B).[1] Two examples (drawn on the same scale) are shown in Figs. 13.3 and 13.4. Both figures are obtained for a projected height $h'/R_\odot = 0.073$ (corresponding to about 70 arcsec) and for the same limb-darkening coefficients as in point a). The diagram of Fig. 13.3, which

[1] It should be recalled that such diagrams have been introduced for the diagnostics of magnetic fields in prominences (Bommier, 1977), and that it is generally believed that in these objects the magnetic field is horizontal in order to sustain the prominence material against gravity.

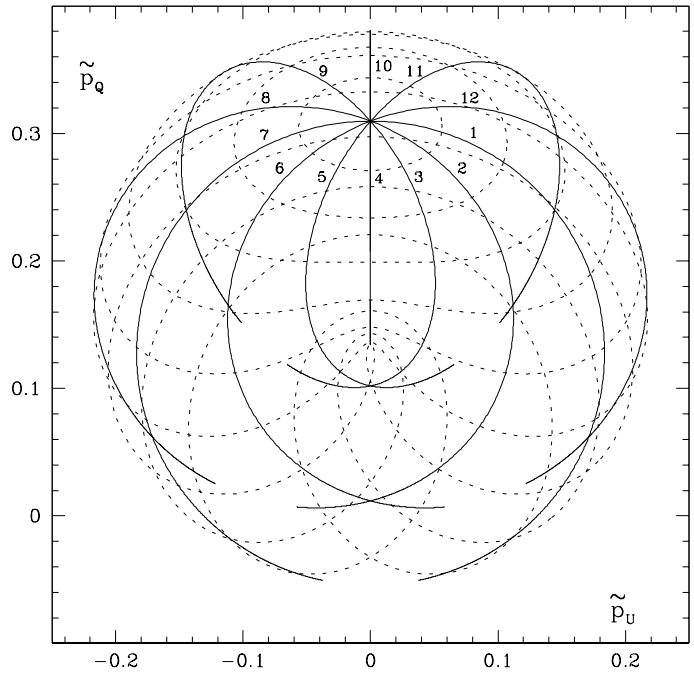

Fig.13.4. Same as Fig.13.3 for a different aspect angle ($\delta = 30°$). The solid lines labelled with 1, 2, ..., 12 correspond to $\chi_B = 0°$, 30°, ..., 330°, respectively. The broken lines correspond to the same H_u values as in Fig.13.3.

refers to a coronal condensation observed in the plane of the sky ($\delta = 0°$), shows an obvious symmetry. A given point in the diagram corresponds to a single value of the magnetic field intensity and to two opposite values of the angle χ_B, whose sign is left undetermined. This simple symmetry is clearly lost in the diagram of Fig. 13.4, obtained for an aspect angle $\delta = 30°$. Again, a single point of the diagram generally corresponds to two determinations of the parameters (H_u, χ_B), but the connection between the two sets cannot be expressed in simple terms. Note also in Fig. 13.4, that the maximum fractional polarization $\tilde{p}_Q$ is *not* obtained for zero magnetic field but for the set $(H_u \simeq 0.3, \chi_B = -90°)$ – which means that the Hanle effect acts, in this case, as a *polarizing* (instead of depolarizing) mechanism – and that for large values of H_u, $\tilde{p}_Q$ can even become negative.

If the angle θ_B is allowed to differ from 90°, the polarization diagrams take different forms. As an example, we show in Fig. 13.5 the polarization diagram obtained for $\theta_B = 45°$, $\delta = 30°$.

c) *The Hanle effect (polarization profiles)*

The Stokes parameters profiles of the radiation directed along $\vec{\Omega}_0$ can be computed from Eq. (13.20) once the velocity distribution $f(\vec{v})$ of the scattering atoms is specified. For our illustrative purposes, we can simply assume that the velocity distribution is Maxwellian and is characterized by the thermal velocity $v_{\rm T}$, which

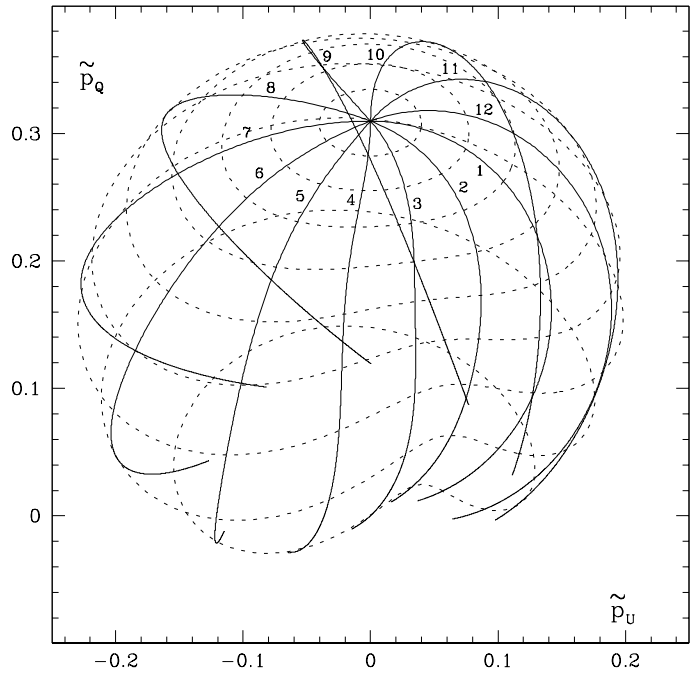

Fig.13.5. Same as Fig.13.3 for $\theta_B = 45°$ and $\delta = 30°$. The labelling of the curves is the same as in Fig.13.4.

implies on the profiles a Doppler broadening in frequency units, $\Delta\nu_{\rm D}$, given by $\Delta\nu_{\rm D} = \nu_0\, v_{\rm T}/c$, ν_0 being the line frequency.

Figure 13.6 shows the Stokes profiles computed for a line at 5000 Å having Einstein coefficient $A = 5 \times 10^7\,{\rm s}^{-1}$. The limb-darkening coefficients are the same as in points a) and b), while the projected height and aspect angle are the same as in Fig. 13.3 ($h' = 0.073\,R_\odot$, $\delta = 0°$). The magnetic field points to the observer ($\theta_B = 90°$, $\chi_B = 0°$) and is characterized by $H_u = 1$ (which implies $B = 5.69$ G for a line with $g_{\alpha_u J_u} = 1$; see Eq. (10.29)). Finally, the Doppler broadening is $\Delta\nu_{\rm D} = 4 \times 10^9\ {\rm s}^{-1}$ (corresponding to $v_{\rm T} = 2$ km s^{-1}), and the damping constant is $\Gamma = A/(4\pi)$ – see Eq. (10.43). The Stokes parameters turn out to be proportional to the combination of parameters $\tau_{\rm L}\, I_{\nu_0}(0)/(\sqrt{\pi}\,\Delta\nu_{\rm D})$, where $\tau_{\rm L}$ is defined in Eq. (13.22) and $I_{\nu_0}(0)$ is the disk-center intensity of the continuous solar radiation at the frequency ν_0. In Fig. 13.6 the Stokes parameters are normalized to this quantity.

In practice, the Stokes parameters $I(\nu,\vec{\Omega}_0)$, $Q(\nu,\vec{\Omega}_0)$, and $U(\nu,\vec{\Omega}_0)$ show almost pure Gaussian profiles characterized by a common width $\Delta\nu_{\rm D}$, whereas $V(\nu,\vec{\Omega}_0)$ shows a typical antisymmetrical profile of very small amplitude.[1] Considering

[1] Were not for the presence of atomic polarization, the V profile would be well-represented by Eq. (11.2), because the magnetic field is very weak ($\nu_{\rm L}/\Delta\nu_{\rm D} \simeq 2 \times 10^{-3}$). Since, in the case considered, atomic polarization is about 10% (as shown by the values of Q/I and U/I in

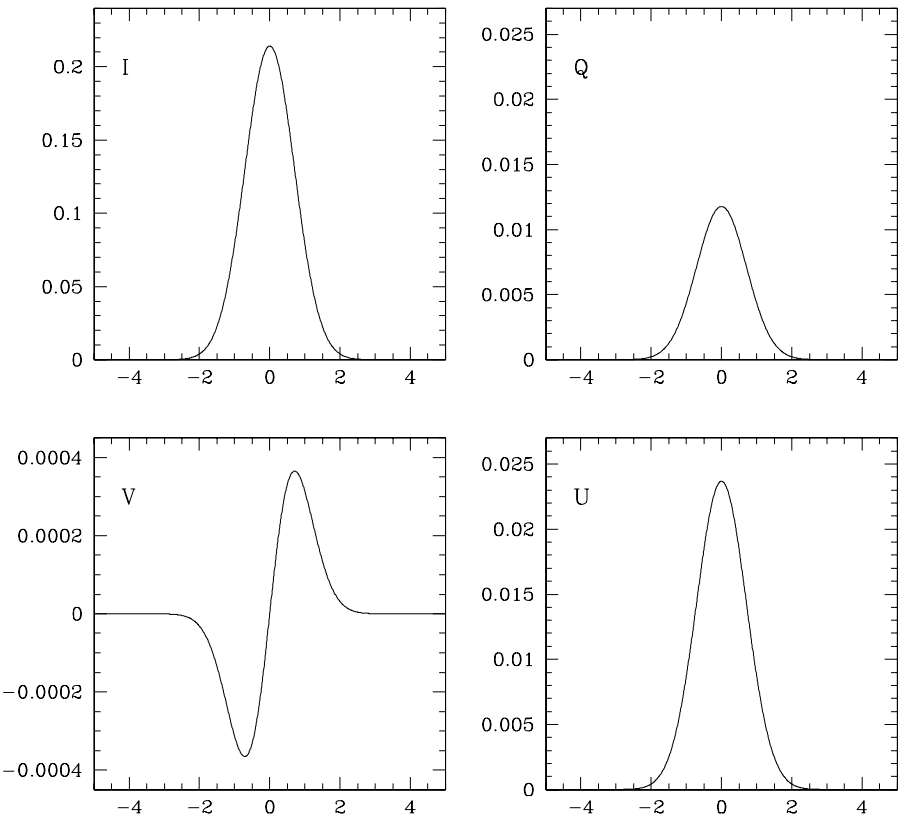

Fig.13.6. The Stokes parameters, computed from Eq.(13.20) for the geometry of Fig.13.1, are plotted against the reduced frequency $(\nu_0 - \nu)/\Delta\nu_{\rm D}$. The main geometrical parameters are: $\delta = 0°$, $\theta_B = 90°$, $\chi_B = 0°$. The remaining parameters, as well as the normalization of the Stokes parameters, are specified in the text. Note the different scale of the panels.

however the ratios p_Q, p_U, and p_V, defined by

$$p_Q(\nu, \vec{\Omega}_0) = \frac{Q(\nu, \vec{\Omega}_0)}{I(\nu, \vec{\Omega}_0)} \,, \qquad p_U(\nu, \vec{\Omega}_0) = \frac{U(\nu, \vec{\Omega}_0)}{I(\nu, \vec{\Omega}_0)} \,, \qquad p_V(\nu, \vec{\Omega}_0) = \frac{V(\nu, \vec{\Omega}_0)}{I(\nu, \vec{\Omega}_0)} \,,$$

some departures from this idealized situation clearly appear (see Fig. 13.7). In the line core, up to a distance of approximately two Doppler widths from line center, p_Q and p_U are practically constant and equal, with very good approximation, to the corresponding values $\tilde{p}_Q$ and $\tilde{p}_U$ relative to the integrated profiles. Beyond two Doppler widths the Hanle effect disappears – consistently with our discussion of Sect. 10.4 – so that p_U goes asymptotically to zero, whereas p_Q approaches the limiting value corresponding to resonance polarization in the absence of magnetic

Fig. 13.6), it has to be expected that Eq. (11.2) represents the V profile with a precision of the same order.

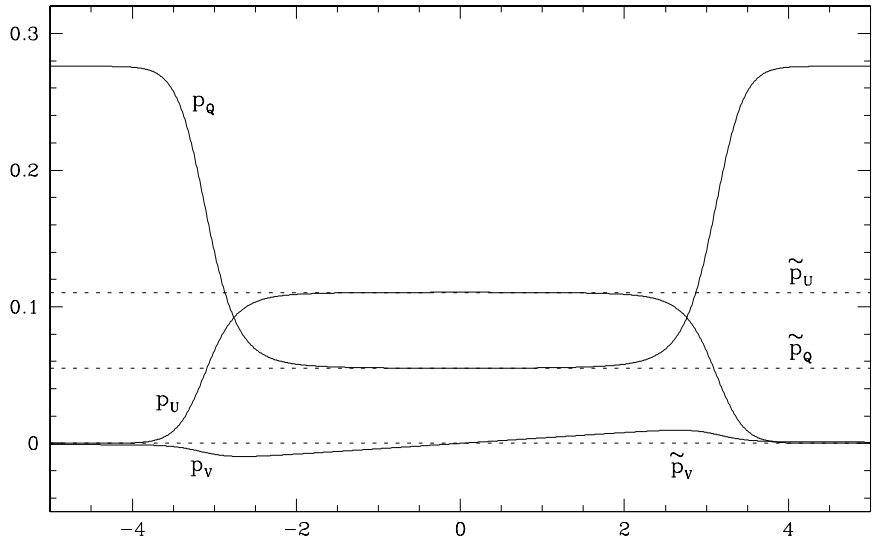

Fig.13.7. The fractional polarization in the three Stokes parameters Q, U, and V of Fig.13.6 is plotted against the reduced frequency $(\nu_0 - \nu)/\Delta\nu_{\rm D}$ (solid lines). The dashed lines represent the values obtained from frequency-integrated profiles.

fields ($p_Q \simeq 0.28$, cf. Fig. 13.3). It should be remarked that the frequency distance from line center where the curves p_Q and p_U start to inflect (about two Doppler widths in the example of Fig. 13.7) is a function of the reduced damping constant,

$$a = \frac{\Gamma}{\Delta\nu_{\rm D}} = \frac{A}{4\pi\,\Delta\nu_{\rm D}} \ ,$$

and that such distance increases for decreasing a, and vice versa. It should also be remarked that the behavior illustrated in Fig. 13.7 may substantially be altered by any source of (unpolarized) continuous emission that may add to the line emission. As apparent from Fig. 13.6, at two Doppler widths from line center the intensity is reduced by a factor 10^2 with respect to its peak value.

It is interesting to compare the Stokes profiles in Fig. 13.6 with those in Fig. 10.3. The two figures refer to the same transition ($J_\ell = 0, J_u = 1$) and to the same geometry (a 90° scattering with the magnetic field pointing to the observer); the Einstein coefficient A, the Landé factor, and the magnetic field intensity are the same; stimulated emission is neglected in both cases. The main difference is that Fig. 10.3 refers to the rest frame of the atom, while Fig. 13.6 refers to the observer's frame, the emitting atoms being characterized by an assigned velocity distribution. The second difference concerns the anisotropy of the incident radiation field, which is much smaller in the case of Fig. 13.6 (in Fig. 10.3 we had a radiation beam). The profiles in Fig. 13.6 are convolutions of profiles like those in Fig. 10.3 with the velocity distribution of atoms. As a result, the 'structure' visible in Fig. 10.3 – characterized by typical widths of order $\Gamma = A/(4\pi)$ – is completely lost in Fig. 13.6, where the typical width is the Doppler broadening $\Delta\nu_{\rm D}$ (numerically,

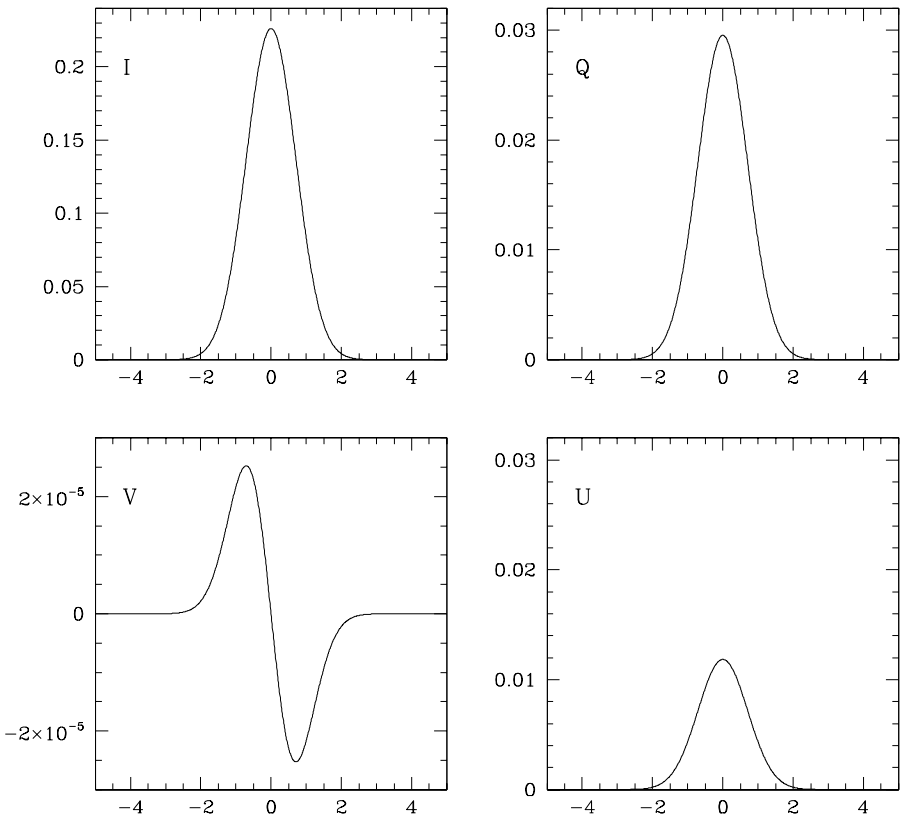

Fig.13.8. Same as Fig.13.6 for a magnetic field lying in the plane of the sky ($\delta = 0°$, $\theta_B = 45°$, $\chi_B = -90°$). Note the presence of a weak circular polarization signal.

$\Delta\nu_{\rm D} \simeq 10^3 \times \Gamma$). In Fig. 13.6 the polarization in the far wings is reduced because of the smaller anisotropy ($p_Q \simeq 0.28$, to be compared with $p_Q = 1$). Moreover, as shown by Fig. 13.7, the polarization within the line is further reduced by the Doppler effect (in Fig. 10.3 the radiation is totally polarized at every single frequency).

The polarization profiles in the Hanle effect regime may show, in some cases, rather peculiar features. A striking example is given in Fig. 13.8, which corresponds to the same set of parameters as Fig. 13.6 except for the magnetic field's direction, which is now characterized by the angles $\theta_B = 45°$, $\chi_B = -90°$. In spite of the fact that the magnetic field is now lying in the plane of the sky, and is thus perpendicular to the line of sight, the V Stokes parameter shows a typical antisymmetrical profile that might erroneously be interpreted (according to Eq. (11.2)) as due to a very weak magnetic field having a non-zero component along the line of sight. In fact, this circular polarization profile originates from the terms with $K' = 1$, $K = 2$, $Q = \pm 1$ in Eq. (13.20), whose contribution does not vanish, in general, even for magnetic fields perpendicular to the line of sight.

13.4. Diagnostics of Magnetic Fields in Solar Prominences

It is nowadays believed (on the basis of several observations) that magnetic fields in solar prominences typically range from 0 to 100 G, with most of reliable measurements falling in a more restricted interval centered at about 20 G. On the other hand, as we have seen on several examples developed in this book (cf. Sects. 5.9, 10.3, and 13.3), the Hanle effect, as observed in a given spectral line, turns out to be particularly sensitive to magnetic field values such that the dimensionless parameter H_u, defined in Eq. (10.29), is contained in an interval that we can – somewhat arbitrarily – set to (0.1–10). As shown by Eq. (10.29), the range of sensitivity of the Hanle effect in terms of magnetic field's intensity depends on the Einstein coefficient of the line and on the Landé factor of the upper level involved in the transition. Assuming for these quantities the typical values $A = 5 \times 10^7$ s^{-1} and $g_{\alpha_u J_u} = 1$, we obtain a range that extends between 0.6 G and 60 G. Therefore, the Hanle effect turns out to be a particularly suitable diagnostic tool for the magnetic fields typically found in solar prominences.[1]

Among the many spectral lines that are observed in solar prominences, one may ask which would be the most suitable for this type of diagnostics. The answer is that the 'ideal' spectral line should have the following properties:

a) It should be sufficiently bright in the prominence spectrum to allow high precision polarimetric measurements. Typically, an error less than at least 10^{-3} in the observed quantities $\tilde{p}_Q$ and $\tilde{p}_U$ is required.

b) The spectral line itself, and all the other lines involved in the model atom needed to treat the problem, should be optically thin. When this requirement is fulfilled, the radiation field tensor $J^K_Q(\nu_i)$ of Eqs. (13.13) can be simply computed from the photospheric intensity, whose spectral and center-to-limb properties are well-known. For optically thick lines, the tensor $J^K_Q(\nu_i)$ can only be computed by introducing a model for the thermodynamic structure of the prominence and its geometry (vertical slab, horizontal slab, cylinder, arch, etc.). This obviously leads to a strongly model-dependent diagnostics (for an example, see Landi Degl'Innocenti et al., 1987).

c) Since high velocities are often observed in prominences,[2] all the lines involved in the model atom should fall within continuum windows of the photospheric solar spectrum, in order to avoid possible contaminations of the radiation field tensor $J^K_Q(\nu_i)$ due to the Doppler effect. If this is not the case, the theory presented in the former section – which implies the absence of velocity/density-matrix correlations – cannot be applied, and one has to resort to a more complicated formalism (see Sect. 13.7). It should be noticed that this is a rather severe requirement because

[1] Early suggestions for using the Hanle effect for the measurement of magnetic fields in prominences were given by Öhman (1929).

[2] According to Tandberg-Hanssen (1995), non-thermal velocities up to 10 km s^{-1} are often observed in the outer edges of quiescent prominences. In active prominences velocities can be even higher.

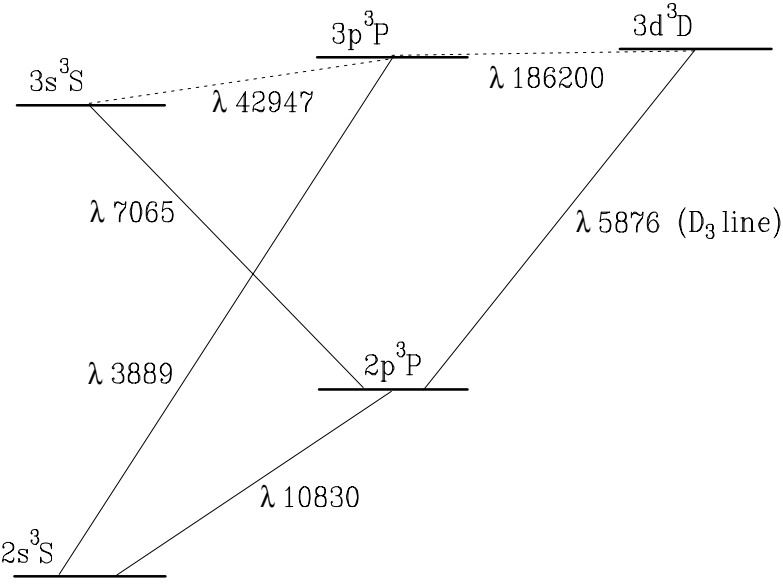

Fig.13.9. The model atom of the triplet system of HeI (orthohelium) used for the diagnostics of magnetic fields in prominences. The dashed lines refer to two infrared transitions that can be omitted in the theoretical calculations. Note that each of the terms ^{3}P and ^{3}D is actually composed of three different J-levels.

it implies that all the lines involved in the model atom are not present in the photospheric spectrum.

d) Since depolarizing collisions are often poorly known, it may be convenient to avoid lines whose interpretation requires atomic models involving transitions with low values of the A Einstein coefficient. By so doing, one can avoid the introduction of depolarizing rates into the statistical equilibrium equations and the ensuing dependence of the results on a further parameter (the number density of particles). On the other hand, when the cross sections for depolarizing collisions are accurately known (either from laboratory experiments or from theoretical calculations), observations of linear polarization may also be used as a diagnostic tool for inferring the particle density – although the disentangling process generally requires the use of simultaneous observations in several lines. An example of such procedure has been given by Bommier et al. (1986a,b).

One line which meets to a large extent the above requirements is the D_3 line of HeI at 5876 Å. According to Bommier (1977), the polarization characteristics of this line can be described by means of the atomic model of Fig. 13.9. The model involves 5 terms (11 levels) and 6 transitions, though the two infrared transitions drawn in broken lines in the figure can safely be omitted. The two visible lines at 5875.6 Å and 7065.3 Å fall into broad continuum windows. The infrared line at 10830 Å presents in the photospheric spectrum a very shallow depression (of the order of 5% of the continuum) that can safely be neglected. The only problem is

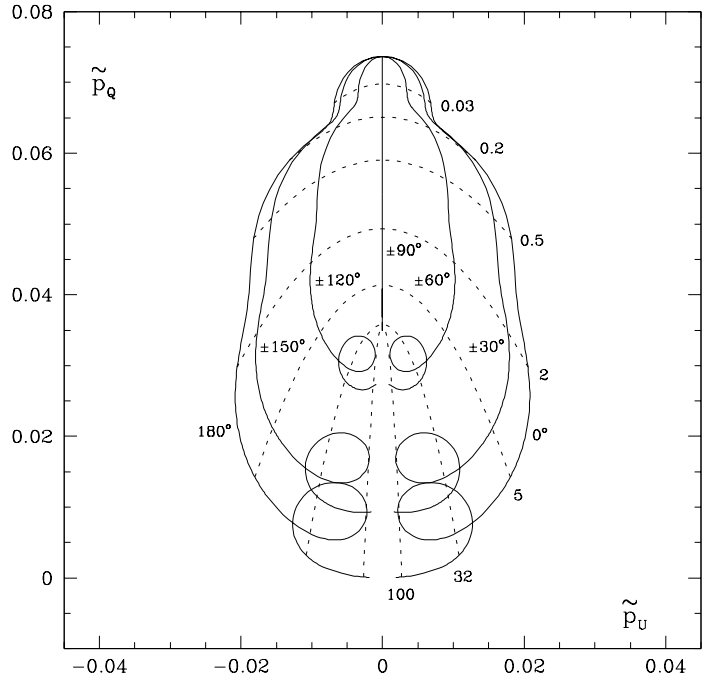

Fig.13.10. Theoretical polarization diagram of the frequency-integrated linear polarization Stokes parameters of the D_3 line observed in a solar prominence. The diagram refers to a point located in the plane of the sky at a height of $70''$. The magnetic field is assumed to be horizontal ($\theta_B = 90°$, see Fig.13.1). Full lines correspond to χ_B = const., while broken lines correspond to constant field intensity (expressed in G).

caused by the UV line at 3888.6 Å, which falls into a complicated region of the spectrum covered by several absorption lines of FeI. Since, however, this is a line of secondary importance in establishing the statistical equilibrium of the atomic model, it is reasonable to neglect the exact wavelength dependence of the solar spectrum in the neighborhood of this line and to smooth it through a convolution with a rectangular profile having a width of the order of 1 Å.

Concerning optical thickness, it can be stated with a good degree of confidence that the four lines involved in the calculations are indeed optically thin in quiescent prominences, except for the infrared line $\lambda\,10830$ which, in some cases, may reach non-negligible values of optical thickness.[1]

Taking into account these remarks, and considering that the four lines involved in the model have pretty large values of the A Einstein coefficient (so that collisions can be neglected), one can apply to this model atom the theory developed in the former section.

Figure 13.10 shows the polarization diagram for the frequency-integrated radia-

[1] Polarimetric observations of this line, performed by Lin et al. (1998) on filaments over the disk, provide a clear indication of non-negligible optical thickness along the vertical direction in the observed objects.

tion emitted in the D_3 line. The diagram refers to a prominence observed in the plane of the sky ($\delta = 0°$) at a height $h = 0.073\,R_\odot$ (corresponding to 70 arcsec). The atomic data for the fine-structure intervals of the terms ^{3}P and ^{3}D of the model atom are from Wieder and Lamb (1957), Pichanik et al. (1968), Kponou et al. (1971), and Tam (1975), whereas the Einstein coefficients of the transitions are from Wiese et al. (1966). The limb-darkening coefficients and the intensities of the continuum radiation (needed to compute the radiation field tensor components J^0_0 and J^2_0 at the frequencies of the transitions) were obtained from the tables of Allen (1973) by interpolation. For the UV line at 3888.6 Å, the continuum intensity is reduced by a factor 5 (see our previous discussion).

The shape of the diagram presents many of the features illustrated on simpler model atoms in Chap. 10. In particular, the feature present in the upper part of the diagram is due to the partial relaxation of coherences in the levels $2s\ ^3$S and $2p\ ^3$P (lower-level Hanle effect, cf. Sects. 10.8-10.9), while the loops appearing for field intensities $\simeq 10$ G are due to level-crossing interferences in the upper term of the D_3 line $3d\ ^3$D (cf. Sect. 10.18).

Diagrams like that of Fig. 13.10 have been extensively used by Bommier and collaborators for the diagnostics of magnetic fields in prominences (Bommier et al., 1994). It should be remarked that the intrinsic symmetry of the diagram leaves a fundamental ambiguity in the determination of the magnetic field vector. Such ambiguity can be removed either with the help of simultaneous measurements in optically thick lines or by taking advantage of the rotation of the sun under the hypothesis of a rigid or quasi-rigid rotation of the prominence (Bommier et al., 1981, 1994).

The diagnostics of prominence magnetic fields can also be performed by interpreting directly the Stokes parameters profiles observed in the D_3 line. This line is in fact composed of six fine-structure components, five of which are very close in wavelength while the sixth, originating from the transition $2p\ ^3\mathrm{P}_0 - 3d\ ^3\mathrm{D}_1$, is well-separated, lying at a distance of approximately 350 mÅ to the red from the center of gravity of the others. In practice, it is like observing two distinct lines for which two separate polarization diagrams can be drawn.[1] Full theoretical details of this diagnostic procedure are given in Landi Degl'Innocenti (1982b). Its applications to the interpretation of Stokes profiles from prominences can be found in Athay et al. (1983) and Querfeld et al. (1985).

An interesting feature of the D_3 line is the appearance of a complicated circular polarization profile. This is because the usual Zeeman effect mixes with the effect of atomic orientation due to the alignment-to-orientation conversion mechanism discussed in Sect. 10.20. Figures 13.11 and 13.12 show the Stokes profiles computed according to Eq. (7.47e). One can notice that the signature of the Zeeman effect is largely masked by the presence of atomic orientation which produces the prominent negative lobe.

[1] The polarization diagrams for the frequency-integrated radiation in the two components can be computed from Eqs. (7.48g) and (7.48c). In the latter, one should omit the profile ϕ and restrict the summation over J_ℓ to the values $J_\ell = 1, 2$ for the blue component and $J_\ell = 0$ for the red component.

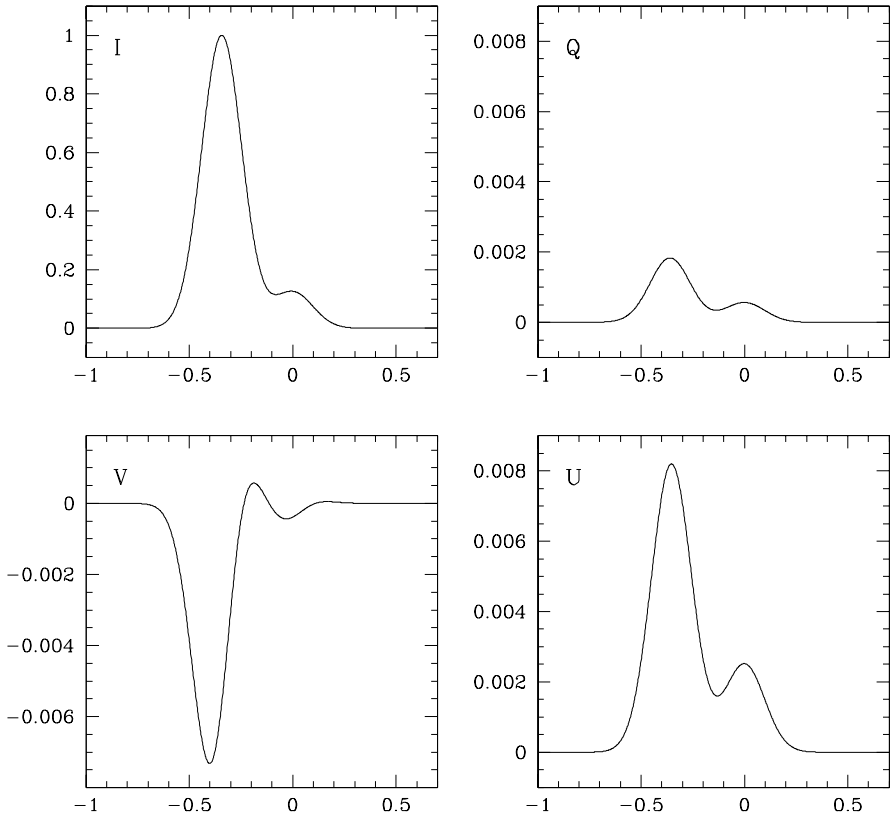

Fig.13.11. The theoretical Stokes profiles of the D_3 line, normalized to the maximum intensity, are plotted as a function of the wavelength distance from the center of the red component (expressed in Å). The profiles refer to a point located in the plane of the sky at a height of $70''$. The magnetic field vector is specified by $B = 35$ G, $\theta_B = 90°$, $\chi_B = 0°$. The Doppler width is $\Delta\lambda_D = 137$ mÅ, corresponding to a thermal velocity of 7 km s^{-1}.

Apart from the Hanle effect, the diagnostics of magnetic fields in prominences can also be carried out with the traditional technique of the longitudinal magnetograph.[1] As discussed in Sect. 11.1, such technique is based on Eq. (11.2), which implies both the weak field approximation and the absence of atomic polarization in the levels involved in the transition. Whereas the weak field approximation is definitely justified in prominences, the existence of atomic polarization implies that the magnetograph technique fails in general to give reliable measurements of $B_{\|}$ in these objects. This is especially true for fine-structured and hyperfine-structured lines, whose circular polarization profiles are deeply contaminated by the presence of a 'spurious' signal due to the atomic orientation induced in the upper level by the alignment-to-orientation conversion mechanism. A typical example is the V pro-

[1] Early measurements of the longitudinal component of the magnetic field in prominences were reported by Zirin and Severny (1961) and by Rust (1966).

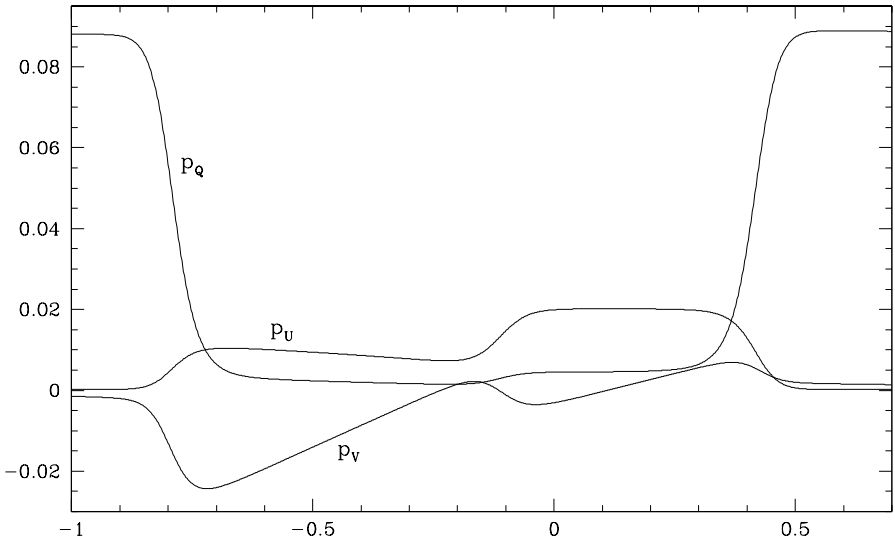

Fig.13.12. Same as Fig.13.11 for the fractional polarization in the three Stokes parameters Q, U, and V. Note the disappearance of the Hanle effect in the far wings.

file of the D_3 line shown in Fig. 13.11. There is no doubt that the magnetograph technique applied to that profile would produce an erroneous result.

For 'spectroscopically simple' lines, on the other hand, Eq. (11.2) gives indeed a zero-order approximation, that might be improved by solving the statistical equilibrium equations and by computing, via Eqs. (10.39) and (A13.6), the first-order correction to the V Stokes parameter due to the presence of atomic polarization. In general, this correction is expected to be rather small (typically of the order of 10%–20%), so that Eq. (11.2) should give a fairly good representation of the V profile.[1] Unfortunately, among the many lines that have extensively been used for the diagnostics of magnetic fields in prominences through the magnetograph technique (Hα, Hβ, HeI λ4771, HeI D_3, NaI D_1 and D_2, Mg b), only the magnesium lines fall into this category.

13.5. Diagnostics of Magnetic Fields from Coronal Forbidden Lines

The procedure that has been outlined in Sect. 13.3 for deducing the density matrix of an atom (or ion) located in the outer layers of a stellar atmosphere, and hence the polarization properties of the radiation emitted in one of its spectral lines, can be directly applied to the interpretation of coronal observations in the well-known forbidden lines of iron. These are the so-called green line of FeXIV at 5304 Å, the

[1] Note, however, that the zero-order approximation predicts $V = 0$ when the magnetic field is perpendicular to the line of sight. In that case, the only contribution to the circular polarization profile comes from the first-order correction, and Eq. (11.2) cannot be applied (see Fig. 13.8).

so-called red line of FeX at 6374 Å, and the two infrared lines of FeXIII at 10747 Å and 10798 Å. All the transitions involved in the model atoms needed to interpret these lines do not match significant features of the solar spectrum, so that the flat-spectrum approximation is well-justified and velocity/density-matrix correlations can be neglected.[1]

Notwithstanding the similarities of the theoretical approach, the interpretation of polarimetric observations in coronal forbidden lines involves some differences with respect to the 'prominence case' that have to be discussed in some detail.

The first difference concerns the atomic models. Because of the large ionization degree of the iron ions, fine-structure intervals turn out to be very large, which entails that such ions can be treated as multi-level atoms, rather than multi-term atoms.

The second difference arises from the small values of the Einstein coefficient. The four lines mentioned above, as well as the other lines involved in the model atoms, are magnetic-dipole forbidden lines with values of $A(\alpha_u J_u \rightarrow \alpha_\ell J_\ell)$ ranging from $10\ \mathrm{s}^{-1}$ to $10^2\ \mathrm{s}^{-1}$. This means a difference of the order of 10^6 with respect to the Einstein coefficient of typical prominence lines, and implies that collisional rates have to be included in the statistical equilibrium equations, as they are in fact comparable to the radiative rates, or even larger (Sahal-Bréchot, 1974a,b; 1977). This is a serious drawback because collisional cross sections are, in general, rather poorly known; a major effort is still needed on this point in order to attain fully reliable diagnostic techniques.

The third difference is due to the magnetic-dipole character of the transitions. As shown in Sect. 6.8, this implies the following transformation on the geometrical tensor $\mathcal{T}^K_Q(i,\vec{\Omega})$ – see Eq. (5.155)

$$\mathcal{T}^K_Q(i,\vec{\Omega}) \rightarrow \gamma_i\, \mathcal{T}^K_Q(i,\vec{\Omega})\ , \tag{13.25}$$

where γ_i $(i = 0,\ldots,3)$ is the formal vector defined by

$$\gamma_i \equiv (1,-1,-1,1)\ . \tag{13.26}$$

For the case we are considering here, transformation (13.25) has no effect on the statistical equilibrium equations because the radiation field tensor $J^K_Q(\nu_i)$ appearing in the radiative rates involves only the unpolarized solar radiation (cf. Eqs. (5.157)). On the contrary, such transformation is fundamental in determining the Stokes parameters of the radiation emitted in a magnetic-dipole transition: it entails a sign switch of the emission coefficients ε_Q and ε_U with respect to the usual electric-dipole case.

The fourth difference is also connected with the low values of the Einstein coefficient: even for magnetic fields as weak as 10^{-4} G, the parameter H_u defined in

[1] The only exceptions may be provided by some UV transitions needed for the interpretation of the green line. However, such transitions are dominated by collisional rates, thus the solar UV spectrum plays no significant role in the statistical equilibrium equations (Casini and Judge, 1999).

Eq. (10.29) turns out to be much larger than unity. This means that, in the reference system of the magnetic field, all the density-matrix elements $\rho^K_Q(\alpha J)$ with $Q \neq 0$ can simply be set to zero. From the diagnostic point of view, this also implies that there is no possibility of measuring the magnetic field intensity from linear polarization observations in these lines.

Finally, the fifth difference is related to the fact that the corona, as observed in the forbidden lines mentioned above, does not present, in general, remarkable condensations. Therefore, the diagnostic content of observations in these lines is non-local, and one must ultimately rely either on coronal models of the density and magnetic field, or on tomographic techniques based on the hypothesis of a rigid or quasi-rigid rotation.

The peculiarities outlined above have some consequences that are worth to be discussed in detail. The first thing to notice is that the statistical equilibrium equations for the density matrix take, in this case, a relatively simple form. Writing these equations in the reference system of the magnetic field, it turns out that the only non-vanishing statistical tensors are those of the form $\rho^K_Q(\alpha J)$ with K even and $Q = 0$. The condition on Q has been discussed above, whereas the condition on K follows from arguments similar to those presented in Sect. 10.7,[1] which remain valid even considering the presence of collisions and/or stimulation effects. It follows that for an atomic model composed of N levels with quantum numbers $(\alpha_i J_i)$, with $i = 1, \ldots, N$, the total number of equations (and unknowns) is

$$N_{\rm eq} = \begin{cases} \sum_{i=1}^{N} (J_i + 1) & \text{for } J_i \text{ integers} \\ \sum_{i=1}^{N} (J_i + \frac{1}{2}) & \text{for } J_i \text{ half-integers} . \end{cases}$$

Next we observe that the emission coefficient in a magnetic-dipole forbidden line is given by Eq. (10.39) with the tensor $\mathcal{T}^K_Q$ transformed according to Eq. (13.25). For the radiation emitted along the direction $\vec{\Omega}_0$ one has

$$\varepsilon_i(\nu, \vec{\Omega}_0) = \frac{h\nu}{4\pi} \mathcal{N} \sqrt{2J_u + 1}\ A(\alpha_u J_u \rightarrow \alpha_\ell J_\ell) \times \sum_{K\,\text{even}} \sum_{K'} \gamma_i\, \mathcal{T}^{K'}_0(i, \vec{\Omega}_0)\ \rho^K_0(\alpha_u J_u)\ \hat{\Phi}^{KK'}_0(J_\ell, J_u; \nu) ,$$

where γ_i is defined in Eq. (13.26), the tensor ρ^K_0 is defined in the magnetic frame, and the symbol $\hat{\Phi}^{KK'}_Q(J_\ell, J_u; \nu)$ has been introduced in Eq. (13.20). This expression considerably simplifies by introducing the angle Θ between the magnetic field vector and the direction $\vec{\Omega}_0$, and by defining the reference direction for the Stokes parameters in such a way that the positive Q direction coincides with the projection of $\vec{B}$ onto the plane perpendicular to $\vec{\Omega}_0$. By so doing, the components of the

[1] Note that, since the only non-zero components of J^K_Q in the vertical frame are by assumption J^0_0 and J^2_0, the components J^1_Q in the magnetic frame are zero (see Eq. (13.14)).

tensor $\mathcal{T}_0^{K'}$ can be simply deduced from Table 5.6 with the substitutions $\theta = \Theta$, $\gamma = 0$, which imply, in particular, that all the components $\mathcal{T}_0^{K'}(2, \vec{\Omega}_0)$ vanish. As a consequence, the emission coefficient in the U Stokes parameter is zero, so that the linear polarization of the radiation emitted along $\vec{\Omega}_0$ is either parallel or perpendicular to the projection of the magnetic field vector onto the plane perpendicular to $\vec{\Omega}_0$.[1]

An analytical expression for the non-vanishing Stokes parameters can be found with the help of Eq. (A13.6), which is well-verified in the corona given the weak intensity of the magnetic field. After some Racah algebra we obtain for the emission coefficient in the four Stokes parameters

$$\begin{aligned}
\varepsilon_0(\nu, \vec{\Omega}_0) &= C \left[\rho_0^0(\alpha_u J_u) + \frac{1}{2\sqrt{2}} \left(3\cos^2\Theta - 1\right) \, w^{(2)}_{J_u J_\ell} \, \rho_0^2(\alpha_u J_u) \right] \hat{\phi}(\nu) \\
\varepsilon_1(\nu, \vec{\Omega}_0) &= C \, \frac{3}{2\sqrt{2}} \, \sin^2\Theta \, w^{(2)}_{J_u J_\ell} \, \rho_0^2(\alpha_u J_u) \, \hat{\phi}(\nu) \\
\varepsilon_2(\nu, \vec{\Omega}_0) &= 0 \\
\varepsilon_3(\nu, \vec{\Omega}_0) &= C \, \cos\Theta \, \nu_{\rm L} \left[\bar{g} \, \rho_0^0(\alpha_u J_u) + \Delta \, \rho_0^2(\alpha_u J_u) \right] \frac{\partial \hat{\phi}(\nu)}{\partial \nu} \, ,
\end{aligned} \tag{13.27}$$

where

$$C = \frac{h\nu}{4\pi} \, \mathcal{N} \, \sqrt{2J_u + 1} \; A(\alpha_u J_u \rightarrow \alpha_\ell J_\ell) \, ,$$

and where $w^{(2)}_{J_u J_\ell}$ is the symbol defined in Eq. (10.12) – see also Table 10.1 – , $\hat{\phi}(\nu)$ is given by Eq. (13.24), $\nu_{\rm L}$ is the Larmor frequency given by Eq. (3.10), $\bar{g}$ is the effective Landé factor of Eq. (3.44), and Δ is given by

$$\begin{aligned}
\Delta = -3 \sqrt{2J_u + 1} \Bigg[& g_{\alpha_u J_u} \, (-1)^{1 + J_\ell - J_u} \, \sqrt{J_u(J_u+1)(2J_u+1)} \\
& \times \left\{ \begin{array}{ccc} 2 & 1 & 1 \\ J_u & J_u & J_u \end{array} \right\} \left\{ \begin{array}{ccc} 1 & 1 & 1 \\ J_\ell & J_u & J_u \end{array} \right\} \\
& + \; g_{\alpha_\ell J_\ell} \, \sqrt{J_\ell(J_\ell+1)(2J_\ell+1)} \, \left\{ \begin{array}{ccc} J_\ell & J_u & 1 \\ J_\ell & J_u & 1 \\ 1 & 2 & 1 \end{array} \right\} \Bigg] \, .
\end{aligned} \tag{13.28}$$

The sign of $\varepsilon_1(\nu, \vec{\Omega}_0)$ determines whether the linear polarization is parallel or perpendicular to the projection of $\vec{B}$. In general, this can only be established through the solution of the statistical equilibrium equations, which determines the sign of $\rho_0^2(\alpha_u J_u)$. For a two-level atom with unpolarized lower level, however, the

[1] Note that this property is valid locally; line-of-sight integration of the emission coefficient can obviously invalidate this statement.

value of $\rho^2_0(\alpha_u J_u)$ can be obtained from Eq. (10.50). One has

$$\rho^2_0(\alpha_u J_u) = \sqrt{\frac{2J_\ell+1}{2J_u+1}}\ \frac{B(\alpha_\ell J_\ell \rightarrow \alpha_u J_u)}{A(\alpha_u J_u \rightarrow \alpha_\ell J_\ell)}\ \frac{w^{(2)}_{J_u J_\ell}\ J^2_0(\nu_0)}{1+\epsilon+\delta^{(2)}_u}\ \rho^0_0(\alpha_\ell J_\ell)\ , \qquad (13.29)$$

where the quantities ϵ and $\delta^{(2)}_u$ are defined in Eq. (10.51), and where $J^2_0(\nu_0)$ is the radiation field tensor evaluated in the magnetic frame. Taking into account Eqs. (13.14)-(13.15) and the expression of the rotation matrix $\mathcal{D}^2_{00}$ (see Table 2.1), it is easily found, by substitution of Eq. (13.29) into Eq. (13.27), that the sign of $\varepsilon_1(\nu, \vec{\Omega}_0)$ is the same as the sign of the quantity $(3\cos^2\theta_B - 1)$, where θ_B is the angle between the magnetic field vector and the vertical. Bearing in mind the definition of the Van Vleck angle $\theta_{\rm V}$ (see Eq. (5.100)), one has[1]

$$\varepsilon_1(\nu, \vec{\Omega}_0) > 0 \quad \text{(linear polarization parallel to } \vec{B}\,) \qquad \begin{array}{ll} \text{for} & 0 < \theta_B < \theta_{\rm V} \\ \text{or} & \pi - \theta_{\rm V} < \theta_B < \pi \end{array}$$

$$\varepsilon_1(\nu, \vec{\Omega}_0) < 0 \quad \text{(linear polarization perpendicular to } \vec{B}\,) \quad \text{for} \quad \theta_{\rm V} < \theta_B < \pi - \theta_{\rm V}\ .$$

It should be mentioned that the diagnostics of coronal magnetic fields based on observations of linear polarization in forbidden lines was first suggested by Charvin (1965), and that important theoretical contributions where brought by House (1970a,b; 1971), Sahal-Bréchot (1974a,b; 1977) and, more recently, by Casini and Judge (1999). From the observational side, successful results were obtained by Mickey (1973), Arnaud (1982), Querfeld and Smartt (1984), and Arnaud and Newkirk (1987).

Obviously, the diagnostics of magnetic fields in the corona can also be performed via the more traditional techniques based on circular polarization. For such observations, the magnetograph relation (Eq. (11.2)) is still valid, although the effective Landé factor, $\bar{g}$, should be corrected to allow for atomic polarization. From Eqs. (13.27) we easily obtain

$$V(\lambda) = -\Delta\lambda_B\ \bar{g}\ \kappa\ \cos\Theta\ \frac{\partial I}{\partial \lambda}\ ,$$

where the 'correction factor' κ is given by (cf. Casini and Judge, 1999)

$$\kappa = \frac{1\ +\ \frac{\Delta}{\bar{g}}\ \sigma^2_0(\alpha_u J_u)}{1\ +\ \frac{1}{2\sqrt{2}}\,(3\cos^2\Theta - 1)\ w^{(2)}_{J_u J_\ell}\ \sigma^2_0(\alpha_u J_u)}\ ,$$

with Δ given by Eq. (13.28) and $\sigma^2_0(\alpha_u J_u) = \rho^2_0(\alpha_u J_u)/\rho^0_0(\alpha_u J_u)$.

Early attempts of measuring the longitudinal component of the coronal magnetic field through this technique were made by Harvey (1969), who could only give

[1] Note that this conclusion is just the opposite of that obtained in Sect. 5.8 for the resonance scattering of a classical oscillator. The difference is due to the fact that now we are dealing with a magnetic-dipole transition.

an upper limit of about 40 G. Recently Lin et al. (2000) have detected clear antisymmetrical circular polarization signals in the FeXIII $\lambda\,10747$ line from a coronal condensation located over an active region. Two observations, interpreted according to Eq. (11.2), give magnetic field components of 33 G at $0.15\,R_\odot$, and 10 G at $0.12\,R_\odot$, respectively.

13.6. Resonance Polarization in the Presence of Velocity/Density-Matrix Correlations

We will now consider a physical situation more complicated than that of Sects. 13.3-13.5. We still assume that the particle density is much smaller than the critical value $n_{\rm c}$ of Eq. (13.6), so that the generalized Boltzmann term can be neglected; but we suppose that the transition frequencies involved in the model atom may correspond to significant spectral features of the incident radiation field, so that – contrary to the previous sections – the density matrix of atoms moving with velocity $\vec{v}$ will depend on $\vec{v}$. Under such circumstances, the density matrices of atoms moving with different velocities are completely decoupled (see Sect. 13.2). The $\vec{v}$-dependent density matrix can be determined by solving the 'ordinary' statistical equilibrium equations, which are written in the atomic rest frame (the comoving frame introduced in Sect. 12.4). Once the equations are solved, the emissivity in that frame can be calculated from the expressions derived in Chap. 7. To obtain the emissivity in the observer's frame, we must take into account the Doppler shifts corresponding to the velocities of the individual atoms and integrate over the velocity distribution.

In this section we illustrate these concepts by referring to a simple case where an approximate analytical expression can be found for the $\vec{v}$-dependent density matrix. The problem that we are going to address consists in finding the radiation scattered by a collection of two-level atoms (with unpolarized lower level) having an arbitrary distribution of velocities and illuminated by an anisotropic and frequency-dependent radiation field. The basic features of this problem have already been analyzed by Sahal-Bréchot et al. (1998), who also carried out an application to the OVI coronal line at 1032 Å, and by de Kertanguy (1998) who studied the polarization of Hα in solar spicules.

Let us consider an atom located at a point P in the outer layers of a stellar atmosphere. The two-level model atom with unpolarized lower level has been analyzed in Sects. 10.1-10.2, where it was found that, neglecting the effects of magnetic fields and collisions, the upper-level statistical tensors are given by Eq. (10.13). That expression is valid in the comoving frame. In the observer's frame, the upper-level statistical tensors can be written in the form

$$\rho^K_Q(\alpha_u J_u;\vec{v}\,) = \sqrt{\frac{2J_\ell+1}{2J_u+1}}\;\frac{B(\alpha_\ell J_\ell \to \alpha_u J_u)}{A(\alpha_u J_u \to \alpha_\ell J_\ell)}\;\; w^{(K)}_{J_u J_\ell}\;\; (-1)^Q\;\left[J^K_{-Q}(\nu_0)\right]_{\vec{v}} \times\; \rho^0_0(\alpha_\ell J_\ell)\;, \tag{13.30}$$

where $[J^K_Q(\nu_0)]_{\vec{v}}$ is given by Eq. (13.9),

$$\left[J^K_Q(\nu_0)\right]_{\vec{v}} = \oint \frac{\mathrm{d}\Omega}{4\pi} \sum_{i=0}^{3} \mathcal{T}^K_Q(i,\vec{\Omega})\ I_i\left(\nu_0\left(1+\frac{\vec{v}\cdot\vec{\Omega}}{c}\right),\vec{\Omega}\right). \tag{13.31}$$

In Eq. (13.30) we have introduced the approximation of neglecting the $\vec{v}$-dependence of $\rho^0_0(\alpha_\ell J_\ell)$: since the incident radiation field is weak (as implied by the unpolarized lower level approximation – see the introduction to Chap. 10), the population of the lower level is always very large compared to the statistical tensors of the upper level.

On the other side, we have to remind that Eq. (10.13) is valid under the flat-spectrum approximation, which is not rigorously verified for the problem we are considering here because, by assumption, the incident radiation field has a spectral structure around the transition frequency ν_0 – typically, an absorption (or emission) line characterized by a width $\Delta\nu_{\mathrm{p}}$. It has then to be expected that Eq. (13.30) is only approximately valid, the error related to the flat-spectrum approximation being of the order of $\Gamma/\Delta\nu_{\mathrm{p}}$, where Γ is the natural width of the upper level. We assume $\Gamma/\Delta\nu_{\mathrm{p}} \ll 1$, a condition that is satisfied in many cases of interest (see Sect. 13.1).[1]

The emission coefficient of the atom is given by Eq. (10.15) – but, again, we have to remind that such expression is valid in the comoving frame; in the observer's frame, the frequency ν_0 must be replaced by $\nu_0(1+\vec{v}\cdot\vec{\Omega}/c)$. Moreover, the width of the emission profile corresponding to any realistic velocity distribution is much larger than Γ, the width of the ϕ profile appearing in Eq. (10.15), so that such profile may in practice be replaced by a Dirac delta-function.[2] It follows that the emission coefficient for an ensemble of atoms having a velocity distribution $f(\vec{v})$ can be written in the form

$$\varepsilon_i(\nu,\vec{\Omega}) = \int \mathrm{d}^3\vec{v}\ f(\vec{v})\ \frac{h\nu}{4\pi}\mathcal{N}\sqrt{2J_u+1}\ A(\alpha_u J_u \to \alpha_\ell J_\ell)$$
$$\times \sum_{KQ} w^{(K)}_{J_u J_\ell}\ \mathcal{T}^K_Q(i,\vec{\Omega})\ \rho^K_Q(\alpha_u J_u;\vec{v})\ \delta\left(\nu_0\left(1+\frac{\vec{v}\cdot\vec{\Omega}}{c}\right)-\nu\right). \tag{13.32}$$

Substitution of Eq. (13.30) into Eq. (13.32) leads, with the help of Eqs. (10.6), (9.5), and (10.17), to the expression

$$\varepsilon_i(\nu,\vec{\Omega}) = k^{\mathrm{A}}_{\mathrm{L}} \sum_{KQ} W_K(J_\ell,J_u)\ (-1)^Q\ \mathcal{T}^K_Q(i,\vec{\Omega})$$
$$\times \int \mathrm{d}^3\vec{v}\ f(\vec{v})\ \delta\left(\nu_0\left(1+\frac{\vec{v}\cdot\vec{\Omega}}{c}\right)-\nu\right)\ \left[J^K_{-Q}(\nu_0)\right]_{\vec{v}}. \tag{13.33}$$

[1] A rigorous treatment of this problem requires more sophisticated theories of frequency-redistribution effects.

[2] This substitution, joined with the approximation contained in Eq. (13.30), is often referred to as the *coherent-scattering* approximation. It introduces an error of the order of $\Gamma/\Delta\nu_{\mathrm{e}}$, where $\Delta\nu_{\mathrm{e}}$ is the width of the emission profile.

This expression can be rewritten in a compact form by introducing a suitable redistribution function. Substituting Eq. (13.31) and recalling the definition of the quantum-mechanical scattering phase matrix $P_{ij}(\vec{\Omega},\vec{\Omega}')$ – see Eq. (10.20) – , one obtains

$$\varepsilon_i(\nu,\vec{\Omega}) = k_{\rm L}^{\rm A} \oint \frac{{\rm d}\Omega'}{4\pi} \sum_{j=0}^{3} P_{ij}(\vec{\Omega},\vec{\Omega}') \times \int {\rm d}^3\vec{v}\ f(\vec{v})\ \delta\Big(\nu_0\Big(1+\frac{\vec{v}\cdot\vec{\Omega}}{c}\Big)-\nu\Big)\ I_j\Big(\nu_0\Big(1+\frac{\vec{v}\cdot\vec{\Omega}'}{c}\Big),\vec{\Omega}'\Big)\ ,$$

or

$$\varepsilon_i(\nu,\vec{\Omega}) = k_{\rm L}^{\rm A} \oint \frac{{\rm d}\Omega'}{4\pi} \int {\rm d}\nu' \sum_{j=0}^{3} R_{ij}(\nu,\vec{\Omega}\,;\nu',\vec{\Omega}')\ I_j(\nu',\vec{\Omega}')\ , \qquad (13.34)$$

where the redistribution function $R_{ij}(\nu,\vec{\Omega}\,;\nu',\vec{\Omega}')$ is given by[1]

$$R_{ij}(\nu,\vec{\Omega}\,;\nu',\vec{\Omega}') = \\ = P_{ij}(\vec{\Omega},\vec{\Omega}') \int {\rm d}^3\vec{v}\ f(\vec{v})\ \delta\Big(\nu'-\nu_0-\nu_0\frac{\vec{v}\cdot\vec{\Omega}'}{c}\Big)\ \delta\Big(\nu_0-\nu+\nu_0\frac{\vec{v}\cdot\vec{\Omega}}{c}\Big)\ . \qquad (13.35)$$

An expression for $R_{ij}(\nu,\vec{\Omega}\,;\nu',\vec{\Omega}')$ valid for a Maxwellian distribution of velocities is given in App. 18.

It is interesting to compare Eq. (13.33) with the expression that would be deduced for the emission coefficient under the hypothesis of complete redistribution on velocities. Following the discussion of Sect. 13.2 one obtains

$$\big[\varepsilon_i(\nu,\vec{\Omega})\big]_{\rm c.r.v.} = k_{\rm L}^{\rm A} \sum_{KQ} W_K(J_\ell,J_u)\ (-1)^Q\ \mathcal{T}_Q^K(i,\vec{\Omega}) \times \left[\int {\rm d}^3\vec{v}\ f(\vec{v})\ \delta\Big(\nu_0\Big(1+\frac{\vec{v}\cdot\vec{\Omega}}{c}\Big)-\nu\Big)\right] \bar{J}^K_{-Q}(\nu_0)\ , \qquad (13.36)$$

where $\bar{J}^K_Q(\nu_0)$ is given by Eq. (13.8).

Equations (13.33) and (13.36) are deeply different. The former involves a single integral over the velocity space, while the latter involves the product of two independent integrals. Only when the radiation field presents no variation across a spectral interval centered at ν_0 and encompassing all the possible Doppler shifts induced by the velocity distribution $f(\vec{v})$, do the two equations coincide – because, in that case, $[J^K_{-Q}(\nu_0)]_{\vec{v}}$ is independent of $\vec{v}$ and equal to $\bar{J}^K_{-Q}(\nu_0)$. Obviously, it

[1] The notation employed here for the redistribution function differs from that employed in the classical book of Mihalas (1978). Apart from the obvious difference that we have here a 4×4 matrix-type redistribution function instead of a scalar one, there is an ordering inversion in the arguments. What we write as $R_{00}(\nu,\vec{\Omega}\,;\nu',\vec{\Omega}')$ is written by Mihalas as $R(\nu',\vec{n}';\nu,\vec{n})$.

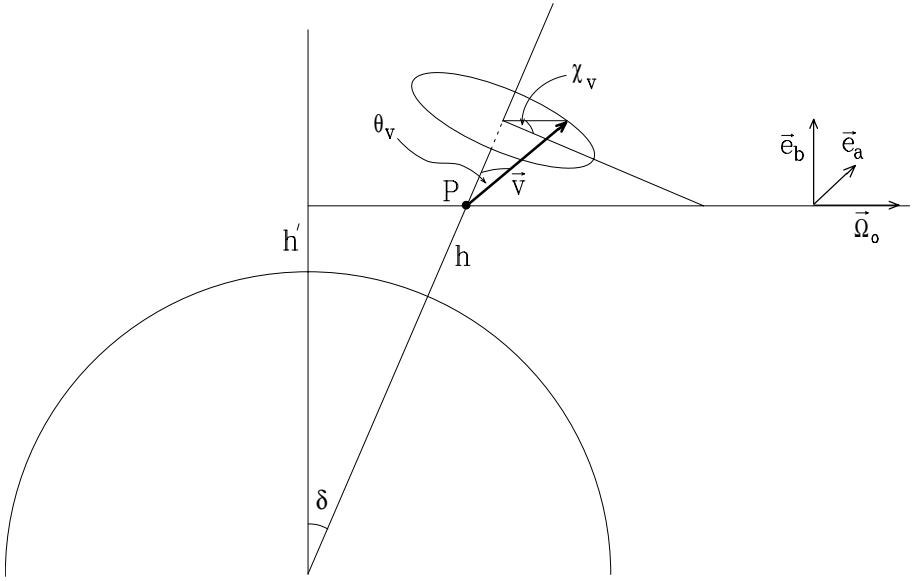

Fig.13.13. Geometry of a scattering process in the outer layers of the solar atmosphere, in the presence of a velocity distribution. The observer's frame $(\vec{e}_a, \vec{e}_b, \vec{\Omega}_0)$ is the same as in Fig.13.1. The direction of the atomic velocity $\vec{v}$ is specified by the angles θ_v and χ_v.

is Eq. (13.33) that gives, in general, the correct physical description of scattering phenomena in very diluted plasmas.

It is also interesting to observe that the two equations give the same result for the frequency-integrated emission coefficient. Bearing in mind Eq. (13.3), one gets

$$\tilde{\varepsilon}_i(\vec{\Omega}) \equiv \int \mathrm{d}\nu \ \varepsilon_i(\nu, \vec{\Omega}) = \left[\tilde{\varepsilon}_i(\vec{\Omega})\right]_{\mathrm{c.r.v.}} \equiv \int \mathrm{d}\nu \ \left[\varepsilon_i(\nu, \vec{\Omega})\right]_{\mathrm{c.r.v.}} =$$

$$= k_{\mathrm{L}}^{\mathrm{A}} \sum_{KQ} W_K(J_\ell, J_u) \ (-1)^Q \ \mathcal{T}^K_Q(i, \vec{\Omega}) \ \bar{J}^K_{-Q}(\nu_0) \ . \qquad (13.37)$$

This means that velocity/density-matrix correlations act, in resonance scattering, as a redistribution mechanism within each Stokes profile. The profiles are altered, but their frequency-integrals are the same as those resulting from the approximation of complete redistribution on velocities.

As an application of the results just obtained, we refer to the geometry of Fig. 13.13 and we study the polarization properties of the radiation scattered along the direction $\vec{\Omega}_0$ by a collection of two-level atoms located at the point P and having a velocity distribution $f(\vec{v})$. We assume that the radiation field illuminating the atoms, due to the star, is unpolarized and cylindrically symmetrical around the vertical, and that its spectrum contains an absorption (or emission) line with Gaussian shape centered at the transition frequency ν_0. As in Sect. 12.4, we denote by $I_{\mathrm{c}}^{(0)}$ the continuum intensity at disk center, by d_{c} the central depression of the spectral line, by $\Delta\nu_{\mathrm{D}}$ its width in frequency units, and by u_1 the limb-darkening

coefficient (supposed independent of frequency). Under these assumptions, the radiation field tensor in the comoving frame is given by Eq. (12.44).

Let us apply Eq. (13.33) to the case of a coronal condensation lying in the plane of the sky ($\delta = 0°$ in Fig. 13.13). The components of the tensor $\mathcal{T}^K_Q(i, \vec{\Omega}_0)$ can be obtained from Table 5.6 by setting $\chi = 0°$, $\theta = 90°$, $\gamma = 90°$. Taking into account properties (A17.1) and (A17.6), one obtains

$$\varepsilon_i(\nu, \vec{\Omega}_0) = k_{\rm L}^{\rm A} \int {\rm d}^3\vec{v} \;\; f(\vec{v}) \;\; \delta\!\left(\nu_0 - \nu + \nu_0 \, \frac{v_x}{c}\right) \mathcal{L}_i(\vec{v}) \, , \tag{13.38}$$

where

$$v_x = v \, \sin\theta_v \cos\chi_v \, ,$$

and where

$$\begin{aligned}
\mathcal{L}_0(\vec{v}) &= J^0_0(\nu_0; v, \theta_v, 0) - \frac{1}{2\sqrt{2}} \, W_2 \, J^2_0(\nu_0; v, \theta_v, 0) + \frac{\sqrt{3}}{2} \, W_2 \, \cos 2\chi_v \, J^2_2(\nu_0; v, \theta_v, 0) \\
\mathcal{L}_1(\vec{v}) &= \frac{3}{2\sqrt{2}} \, W_2 \, J^2_0(\nu_0; v, \theta_v, 0) + \frac{\sqrt{3}}{2} \, W_2 \, \cos 2\chi_v \, J^2_2(\nu_0; v, \theta_v, 0) \\
\mathcal{L}_2(\vec{v}) &= \sqrt{3} \;\; W_2 \;\; \sin\chi_v \;\; J^2_1(\nu_0; v, \theta_v, 0) \\
\mathcal{L}_3(\vec{v}) &= 0 \, .
\end{aligned} \tag{13.39}$$

In particular, for the frequency-integrated Stokes parameters one simply has

$$\tilde{\varepsilon}_i(\vec{\Omega}_0) = k_{\rm L}^{\rm A} \int {\rm d}^3\vec{v} \;\; f(\vec{v}) \;\; \mathcal{L}_i(\vec{v}) \, . \tag{13.40}$$

The expressions just derived show the existence of an important physical phenomenon induced by velocity on the polarization of the scattered radiation. As shown in Sect. 12.4, the component $J^2_1(\nu_0; v, \theta_v, 0)$ of the comoving frame radiation field tensor is generally non-zero. Therefore, as apparent from Eqs. (13.40) and (13.39), the frequency-integrated U Stokes parameter of the scattered radiation does not vanish in general (unless the velocity distribution is isotropic or at least symmetrical about the vertical). This implies a rotation of the polarization direction with respect to the tangent to the solar limb. From this point of view, an anisotropic distribution of velocities acts similarly to a magnetic field, and much care has to be taken, when interpreting observations, to disentangle the rotation induced by velocities from that due to the Hanle effect.

As an application of Eq. (13.40) to the diagnostics of velocities, we consider a stream of atoms moving with a bulk velocity $\vec{w}$ and we suppose, for the sake of simplicity, that there is no dispersion around this value, so that the function $f(\vec{v})$ is given by

$$f(\vec{v}) = \delta^{(3)}(\vec{v} - \vec{w}) \, .$$

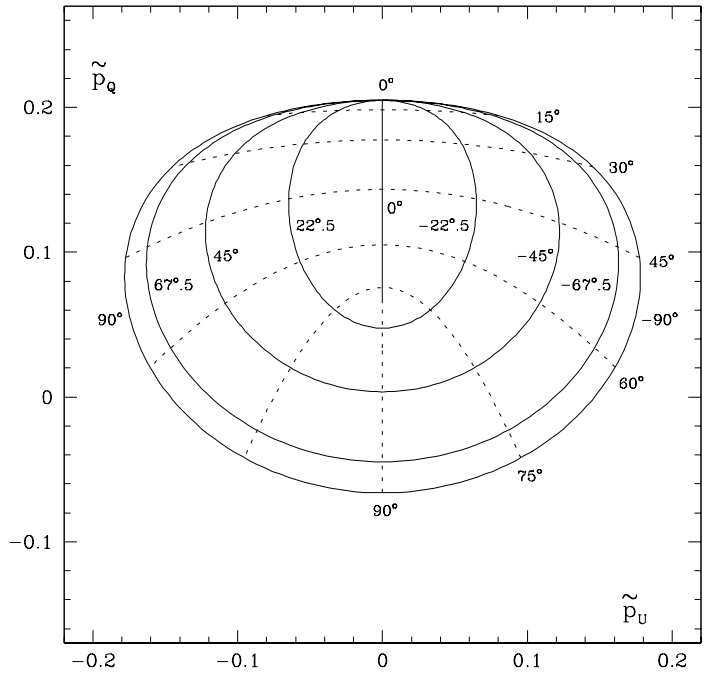

Fig.13.14. Velocity diagram for the scattering by a two-level atom in the geometry of Fig.13.13. The scattering point is characterized by $\delta = 0°$ and $h = 0.01$ stellar radii. The stellar spectrum presents an absorption line, characterized by $d_c = 0.8$ and $u_1 = 0.2$ (see Eq.(12.41)), at the transition frequency. The atom moves relative to the star with a velocity $\vec{w}$ of fixed modulus. The ratio between the Doppler shift induced by w and the width of the absorption line is $\omega = 1.4$ (see Eq.(12.45)). Full lines correspond to $\chi_w = \text{const.}$, broken lines to $\theta_w = \text{const}$. The parameter W_2 in Eqs.(13.39) is set to unity, corresponding to the transition $(J_\ell = 0, J_u = 1)$.

In this case, one simply has

$$\tilde{\varepsilon}_i(\vec{\Omega}_0) = k_{\rm L}^{\rm A}\ \mathcal{L}_i(\vec{w})\ ,$$

where $\mathcal{L}_i(\vec{w})$ is given by Eqs. (13.39) with the substitutions $v \to w$, $\theta_v \to \theta_w$, $\chi_v \to \chi_w$, θ_w and χ_w being the polar and azimuth angles of $\vec{w}$ defined according to Fig. 13.13.

Figure 13.14 shows a typical 'velocity diagram', obtained by fixing the velocity modulus w and by plotting the fractional polarization parameters

$$\tilde{p}_Q = \frac{\tilde{\varepsilon}_Q(\vec{\Omega}_0)}{\tilde{\varepsilon}_I(\vec{\Omega}_0)}\ , \qquad \tilde{p}_U = \frac{\tilde{\varepsilon}_U(\vec{\Omega}_0)}{\tilde{\varepsilon}_I(\vec{\Omega}_0)}$$

against each other, while allowing the angles θ_w and χ_w to vary in the intervals $0° \le \theta_w \le 90°$, $-90° \le \chi_w \le 90°$.

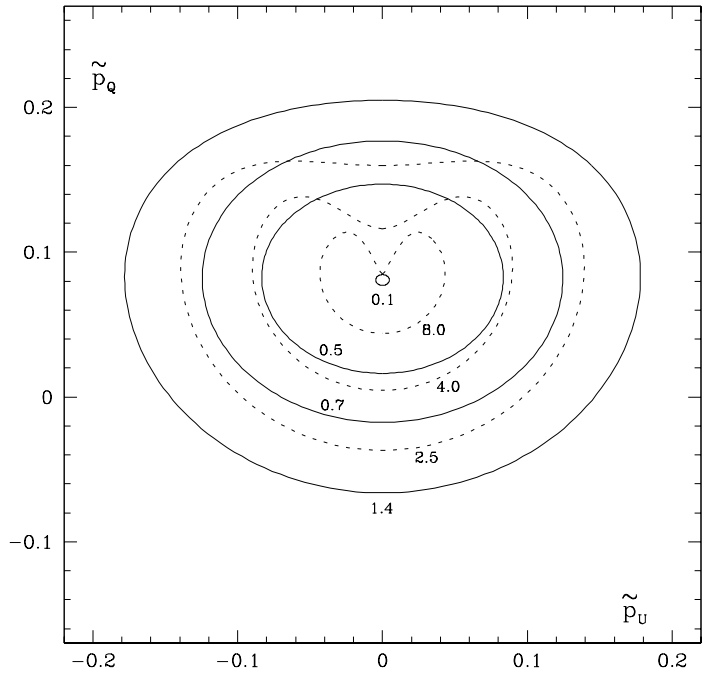

Fig.13.15. Velocity diagram for the same physical situation considered in Fig.13.14, obtained by varying the velocity modulus. Only the 'external borders', corresponding to $\chi_w = -90°$ and $+90°$ (right and left side respectively, cf. Fig.13.14) are shown. Curves are labelled by the value of ω (see Eq.(12.45)).

The velocity diagram of Fig. 13.14 presents a high degree of degeneracy. From Eqs. (13.39), and from the properties of the comoving-frame radiation field tensor,[1] it can easily be seen that both the transformation $\chi_w \to \pi - \chi_w$ and the transformation $\vec{w} \to -\vec{w}$ (i.e., $\theta_w \to \pi - \theta_w$, $\chi_w \to \pi + \chi_w$) leave the quantities $\tilde{p}_Q$ and $\tilde{p}_U$ unchanged. Therefore, each point of the diagram corresponds to four possible determinations: the nominal values (θ_w, χ_w) and the combinations $(\theta_w, \pi - \chi_w)$, $(\pi - \theta_w, \pi + \chi_w)$, $(\pi - \theta_w, -\chi_w)$. A further reason of degeneracy is the velocity modulus, kept fixed to a specific value in the diagram. Obviously, for $w = 0$ the diagram reduces to a single point, representing the fractional linear polarization due to the scattering on a static atom. When w is increased the diagram grows, reaching its maximum dimensions for a definite w value, and then decreases, as illustrated in Fig. 13.15. It can be shown that for $w \to \infty$ the diagram reduces again to a single point, which coincides with the point corresponding to $w = 0$ because of the assumption of a frequency-independent limb-darkening coefficient.

[1] Note that Eqs. (A17.1) and (A17.9) yield the relation

$$J^K_Q(\nu_0; v, \pi - \theta_v, 0) = \mathrm{e}^{\,\mathrm{i}Q\pi}\, J^K_Q(\nu_0; v, \theta_v, 0)\ .$$

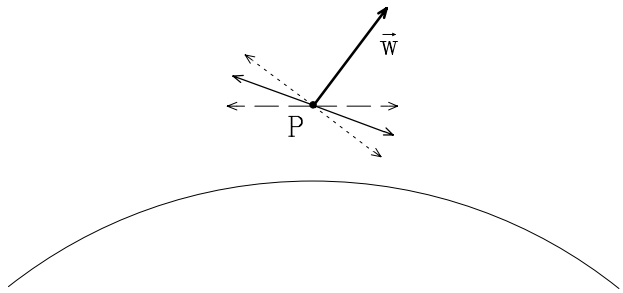

Fig.13.16. Observer's view of resonance polarization due to an atom moving with velocity $\vec{w}$ off the solar limb. The velocity vector lies in the plane of the sky. The direction of linear polarization (solid line) is intermediate between the parallel to the solar limb (dashed line) and the perpendicular to the velocity (dotted line).

The degeneracy contained in the velocity diagram can be considerably reduced by means of the further information coming from the frequency position of the scattered line. According to Eq. (13.38), this line is centered at the frequency $\nu = \nu_0 + \nu_0 \, w_x/c$, which allows one to retrieve the combination of parameters $w \sin\theta_w \cos\chi_w$ directly from observations. In particular, the four-fold degeneracy in the plane θ_w-χ_w of Fig. 13.14 is reduced to a two-fold degeneracy: (θ_w, χ_w), $(\pi - \theta_w, -\chi_w)$ when $w_x > 0$, or $(\theta_w, \pi - \chi_w)$, $(\pi - \theta_w, \pi + \chi_w)$ when $w_x < 0$.

The shape of the diagram of Fig. 13.14 can be qualitatively understood via arguments similar to those presented in Sect. 12.4. An illustration is given in Fig. 13.16, which is a 'front view' of the scattering geometry of Fig. 13.13 with $\delta = 0°$ ($\vec{e}_a$ points to the right, $\vec{e}_b$ upward; the velocity $\vec{w}$ is characterized by $\theta_w \simeq 40°$, $\chi_w = +90°$). Owing to limb-darkening and geometrical effects, the radiation scattered by a static atom would be linearly polarized along the parallel to the solar limb (dashed line: $\tilde{p}_Q > 0$, $\tilde{p}_U = 0$). The presence of an absorption line in the solar spectrum, combined with the motion of the scattering atom, induces the phenomenon of Doppler brightening: the radiation flowing 'almost parallel' to the velocity $\vec{w}$ is more redshifted (hence more intense) than the radiation coming 'from the sides', so that, if limb-darkening and geometrical effects were absent, the radiation scattered by the moving atom would be linearly polarized perpendicularly to $\vec{w}$ (dotted line). The combined result of the two effects is a skewed polarization represented by the solid line in the figure. Note that this implies a clockwise rotation of the polarization direction relative to the horizontal direction, thus $\tilde{p}_U < 0$ (left side of the diagram of Fig. 13.14).

As expected on general physical grounds, the velocity diagram depends critically both on the spectral characteristics of the stellar radiation and on the location of the observed point over the stellar surface (height h, aspect angle δ). As an example of the former effect, we show in Fig. 13.17 the velocity diagram corresponding to an emission line. Comparison of Figs. 13.14 and 13.17 shows that the velocity diagrams for absorption and emission lines are completely reversed; this is consistent with the results of Sect. 12.4 and with the intuitive considerations illustrated in Fig. 13.16. For an emission line, the phenomenon of Doppler dimming leads

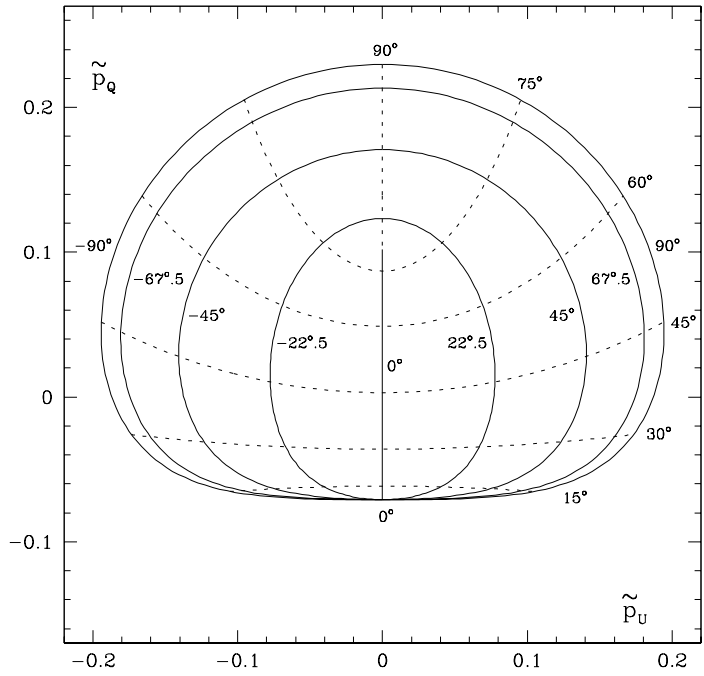

Fig.13.17. Velocity diagram for an emission line. All the parameters are the same as in Fig.13.14 except for d_c and ω, now set to -4 and 2.5, respectively.

to the opposite orientation (parallel to $\vec{w}$) of the dotted line in Fig. 13.16. The resulting polarization will thus be rotated in the counterclockwise direction with respect to the parallel to the solar limb.

Consider now the effect of velocity/density-matrix correlations on the polarization profiles of the scattered radiation. The frequency-dependent emission coefficient is given by Eq. (13.38), and strongly depends on the velocity distribution $f(\vec{v})$ of the atoms. We consider here the case of a displaced Maxwellian, namely

$$f(\vec{v}) = \frac{1}{\pi^{3/2}\, v_{\rm T}^3}\ \mathrm{e}^{-\left(\frac{v_x - w_x}{v_{\rm T}}\right)^2}\ \mathrm{e}^{-\left(\frac{v_y - w_y}{v_{\rm T}}\right)^2}\ \mathrm{e}^{-\left(\frac{v_z - w_z}{v_{\rm T}}\right)^2}\ , \tag{13.41}$$

where $v_{\rm T}$ is the thermal velocity and $\vec{w} \equiv (w_x, w_y, w_z)$ is the bulk velocity of the ensemble of atoms. Substituting Eq. (13.41) into Eq. (13.38), the integral in $\mathrm{d}v_x$ is immediately performed owing to the presence of the Dirac's delta. The integrals in $\mathrm{d}v_y$ and $\mathrm{d}v_z$ can then be performed numerically by means of Hermite integrations. The emission profiles depend on a large number of parameters, and a detailed investigation of their shapes is well outside the aims of this book. As an example, we show in Fig. 13.18 the profiles obtained for a specific combination of the parameters. Such profiles (solid line) are plotted together with those resulting from the approximation of complete redistribution on velocities (broken line). Whereas the latter peak all at the same distance from line center (the distance corresponding

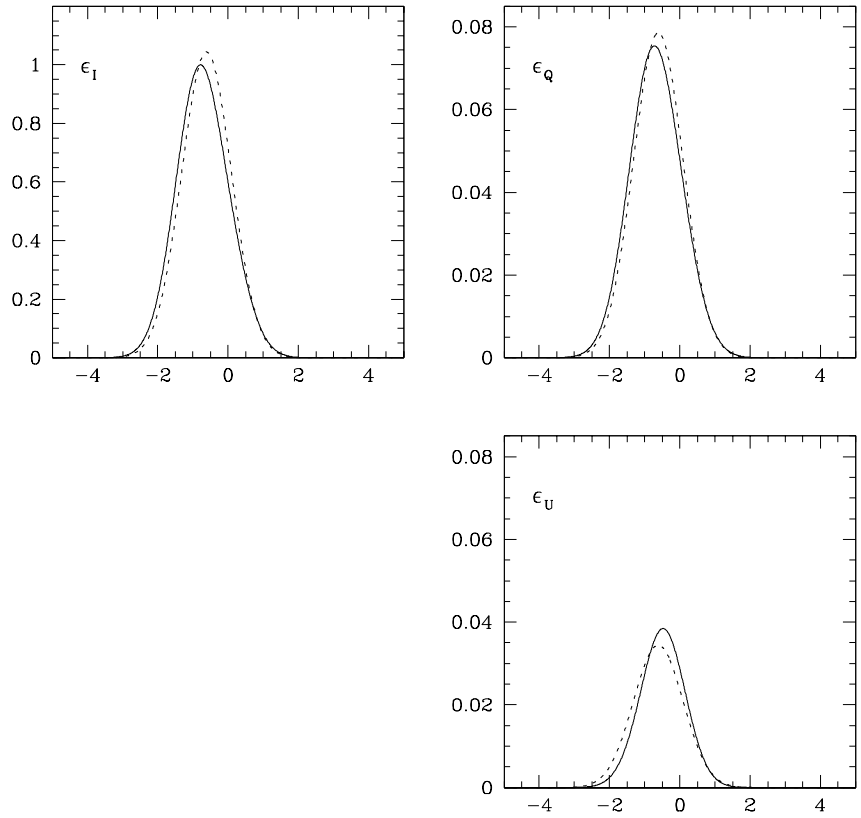

Fig.13.18. Stokes profiles of the radiation scattered in the direction $\vec{\Omega}_0$ (Fig.13.13 with $\delta = 0°$) by an ensemble of atoms characterized by the velocity distribution of Eq.(13.41). The profiles are normalized to the maximum intensity and are plotted against the reduced frequency $(\nu_0 - \nu)/\Delta\nu_{\rm D}$. The solid line is obtained by taking velocity/density-matrix correlations into account, the broken line corresponds to complete redistribution on velocities. The combination of parameters is: $d_{\rm c} = 0.8$, $u_1 = 0.2$, $h = 0.01\, R_\odot$, $\omega = 1$, $w = v_{\rm T}$, $\theta_w = 60°$, $\chi_w = -45°$, $W_2 = 1$ (see text for explanation of the symbols). Note the blue-shift due to the negative component of the bulk velocity $\vec{w}$ along the line of sight.

to the Doppler shift due to the bulk velocity $\vec{w}$), the maxima of $\varepsilon_I(\nu, \vec{\Omega}_0)$ and $\varepsilon_Q(\nu, \vec{\Omega}_0)$ for the former case are shifted to the blue, and the maximum of $\varepsilon_U(\nu, \vec{\Omega}_0)$ is shifted to the red. The profile of $\varepsilon_U(\nu, \vec{\Omega}_0)$ seems to be the most affected by velocity/density-matrix correlations. This is better illustrated in Fig. 13.19, where the fractional Stokes parameters

$$p_Q(\nu, \vec{\Omega}_0) = \frac{\varepsilon_Q(\nu, \vec{\Omega}_0)}{\varepsilon_I(\nu, \vec{\Omega}_0)}\,, \qquad p_U(\nu, \vec{\Omega}_0) = \frac{\varepsilon_U(\nu, \vec{\Omega}_0)}{\varepsilon_I(\nu, \vec{\Omega}_0)}$$

are compared with the corresponding quantities obtained under the assumption of complete redistribution on velocities. The figure clearly shows the exact symmetry

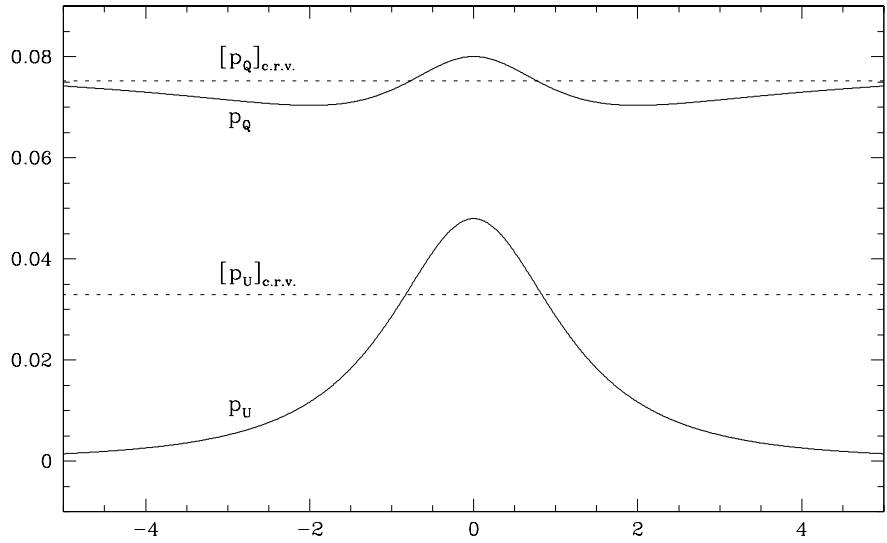

Fig.13.19. Same as Fig.13.18 for the fractional Stokes parameters.

of these profiles about line center (which reflects the symmetry of the intensity profile of the photospheric absorption line) and the substantial decrease of $p_U(\nu, \vec{\Omega}_0)$ in the wings. This is a further similarity between the Hanle effect and the effects of a velocity distribution on resonance polarization.

13.7. The Hanle Effect in the Presence of Velocity/Density-Matrix Correlations

The results obtained in the former section can be easily generalized to the case where a weak magnetic field is present. By 'weak' we mean here a field such that

$$\nu_{\rm L} \ll \Delta\nu_{\rm p} \ ,$$

so that the flat-spectrum approximation is well-verified (see Sect. 13.1) and the splittings between the different Zeeman components of the transition can be neglected. The results obtained by this approach are obviously in error by a quantity of order $\nu_{\rm L}/\Delta\nu_{\rm p}$ – or $\Gamma/\Delta\nu_{\rm p}$, where Γ is the natural width in frequency units of the upper level of the transition, if this ratio is larger than the former. We recall again that more sophisticated theories of frequency redistribution are needed to overcome such limitation.

The generalization of the equations of the former section to the case of the Hanle effect is obtained starting from the expression of the upper-level statistical tensors in the presence of a magnetic field (i.e., from Eq. (10.27) instead of Eq. (10.13)).

Equation (13.30) is therefore replaced by the following

$$\rho^K_Q(\alpha_u J_u;\vec{v}) = \sqrt{\frac{2J_\ell+1}{2J_u+1}}\,\frac{B(\alpha_\ell J_\ell \rightarrow \alpha_u J_u)}{A(\alpha_u J_u \rightarrow \alpha_\ell J_\ell) + 2\pi \mathrm{i}\,\nu_{\mathrm{L}}\, g_{\alpha_u J_u}\, Q}\; w^{(K)}_{J_u J_\ell}\; (-1)^Q \left[J^K_{-Q}(\nu_0)\right]_{\vec{v}}$$
$$\times\; \rho^0_0(\alpha_\ell J_\ell)\;, \qquad (13.42)$$

where all the tensorial quantities are defined in a reference system having the z-axis in the magnetic field direction.[1] On the other hand, the expression for the emission coefficient given in Eq. (13.32) is still valid. Substitution of Eq. (13.42) yields

$$\varepsilon_i(\nu,\vec{\Omega}) = k^{\mathrm{A}}_{\mathrm{L}} \sum_{KQ} W_K(J_\ell,J_u)\;\; (-1)^Q\; \mathcal{T}^K_Q(i,\vec{\Omega})\; \frac{1}{1+\mathrm{i}\,QH_u}$$
$$\times \int \mathrm{d}^3\vec{v}\;\; f(\vec{v})\;\; \delta\!\left(\nu_0\!\left(1+\frac{\vec{v}\cdot\vec{\Omega}}{c}\right)-\nu\right)\left[J^K_{-Q}(\nu_0)\right]_{\vec{v}}\,, \qquad (13.43)$$

where H_u is given by Eq. (10.28), or, similarly to Eq. (13.34)

$$\varepsilon_i(\nu,\vec{\Omega}) = k^{\mathrm{A}}_{\mathrm{L}} \oint \frac{\mathrm{d}\Omega'}{4\pi} \int \mathrm{d}\nu' \sum_{j=0}^{3} R_{ij}(\nu,\vec{\Omega};\nu',\vec{\Omega}';\vec{B})\; I_j(\nu',\vec{\Omega}')\,,$$

where

$$R_{ij}(\nu,\vec{\Omega};\,\nu',\vec{\Omega}';\vec{B}) = P_{ij}(\vec{\Omega},\vec{\Omega}';\vec{B})$$
$$\times \int \mathrm{d}^3\vec{v}\;\; f(\vec{v})\;\; \delta\!\left(\nu'-\nu_0-\nu_0\frac{\vec{v}\cdot\vec{\Omega}'}{c}\right)\delta\!\left(\nu_0-\nu+\nu_0\frac{\vec{v}\cdot\vec{\Omega}}{c}\right), \qquad (13.44)$$

$P_{ij}(\vec{\Omega},\vec{\Omega}';\vec{B})$ being the quantum-mechanical scattering phase matrix in the presence of a magnetic field of Eq. (10.33). It is easily seen that Eq. (13.36) generalizes into

$$\left[\varepsilon_i(\nu,\vec{\Omega})\right]_{\mathrm{c.r.v.}} = k^{\mathrm{A}}_{\mathrm{L}} \sum_{KQ} W_K(J_\ell,J_u)\;\; (-1)^Q\; \mathcal{T}^K_Q(i,\vec{\Omega})\;\; \frac{1}{1+\mathrm{i}\,QH_u}$$
$$\times \left[\int \mathrm{d}^3\vec{v}\;\; f(\vec{v})\;\; \delta\!\left(\nu_0\!\left(1+\frac{\vec{v}\cdot\vec{\Omega}}{c}\right)-\nu\right)\right] \bar{J}^K_{-Q}(\nu_0)\,, \qquad (13.45)$$

[1] Note that the radiation field tensor $[J^K_Q(\nu_0)]_{\vec{v}}$ appearing in Eq. (13.42) is defined in a reference frame which *moves* with velocity $\vec{v}$ and has its z-axis directed *along* $\vec{B}$. Effects of order v/c on $\vec{B}$ implied by the Lorentz transformations are neglected.

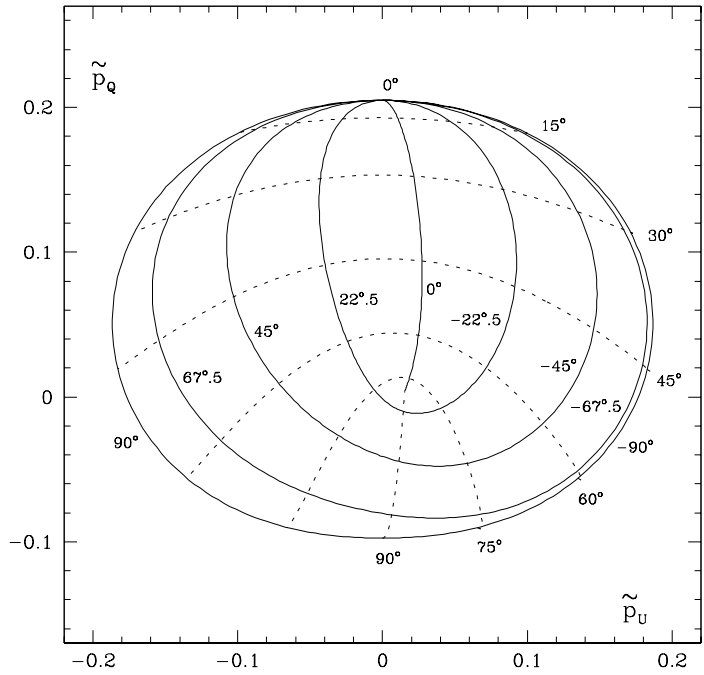

Fig.13.20. Velocity-Hanle diagram corresponding to the physical situation of Fig. 13.14 with the additional presence of a magnetic field of constant modulus ($H_u = 2$) parallel to $\vec{w}$. All the remaining parameters have the same values as in Fig.13.14.

and Eq. (13.37) into

$$\tilde{\varepsilon}_i(\vec{\Omega}) = \left[\tilde{\varepsilon}_i(\vec{\Omega})\right]_{\text{c.r.v.}} =$$

$$= k_{\text{L}}^{\text{A}} \sum_{KQ} W_K(J_\ell, J_u)\ (-1)^Q\, \mathcal{T}_Q^K(i, \vec{\Omega})\ \frac{1}{1 + \mathrm{i}\, Q H_u}\ \bar{J}_{-Q}^K(\nu_0)\ . \qquad (13.46)$$

The expressions now derived depend on a very large number of parameters. A few applications are described in the following.

First of all, we will examine how the frequency-integrated linear polarization of the scattered radiation is affected by the simultaneous presence of a velocity distribution and a magnetic field. To make an example, we consider the physical situation of Fig. 13.14, where the atoms move with a unimodal velocity $\vec{w}$ and the incident radiation presents an absorption line at the transition frequency, and we 'add' a magnetic field $\vec{B}$ of constant modulus parallel to $\vec{w}$. The resulting 'velocity-Hanle diagram' is shown in Fig. 13.20. The mirror-like diagram of Fig. 13.21 refers to the same situation with $\vec{B}$ antiparallel to $\vec{w}$.

Comparison of Figs. 13.20-13.21 with Fig. 13.14 shows that the magnetic field has an important effect on the frequency-integrated fractional polarization, especially for large inclinations with respect to the vertical. Another obvious effect of the

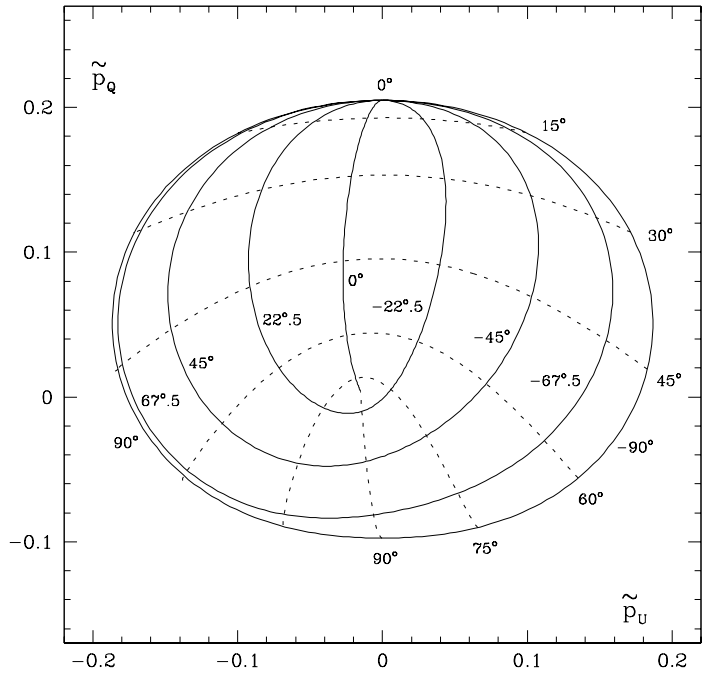

Fig.13.21. Same as Fig.13.20 with the magnetic field antiparallel to $\vec{w}$.

magnetic field is the symmetry breaking of the diagram. Whereas in the zero-field case the transformation

$$\chi_w \rightarrow -\chi_w$$

produces a sign switch in $\tilde{p}_U$ (leading to a diagram symmetrical about the vertical axis), this symmetry is lost in the magnetic case and is replaced by a more general one,

$$\begin{cases} \tilde{p}_Q \rightarrow \tilde{p}_Q \\ \tilde{p}_U \rightarrow -\tilde{p}_U \end{cases} \qquad \text{for} \qquad \chi_w \rightarrow -\chi_w \quad \textit{and} \quad \vec{B} \rightarrow -\vec{B}\,,$$

where $\vec{B} \rightarrow -\vec{B}$ has to be understood in the sense that the magnetic field vector changes from parallel to antiparallel to the velocity vector $\vec{w}$.

Similarly to the non-magnetic case discussed in Sect. 13.6, the velocity-Hanle diagrams of Figs. 13.20-13.21 present a high degree of degeneracy. It can indeed be shown from Eq. (13.46), using the properties of the comoving-frame radiation field tensor and those of the rotation matrices, that a single point in the diagram of Fig. 13.20 corresponds to four determinations: the nominal set of parameters

$$\theta_w\,,\ \chi_w\,,\ \xi = +1$$

and the further combinations

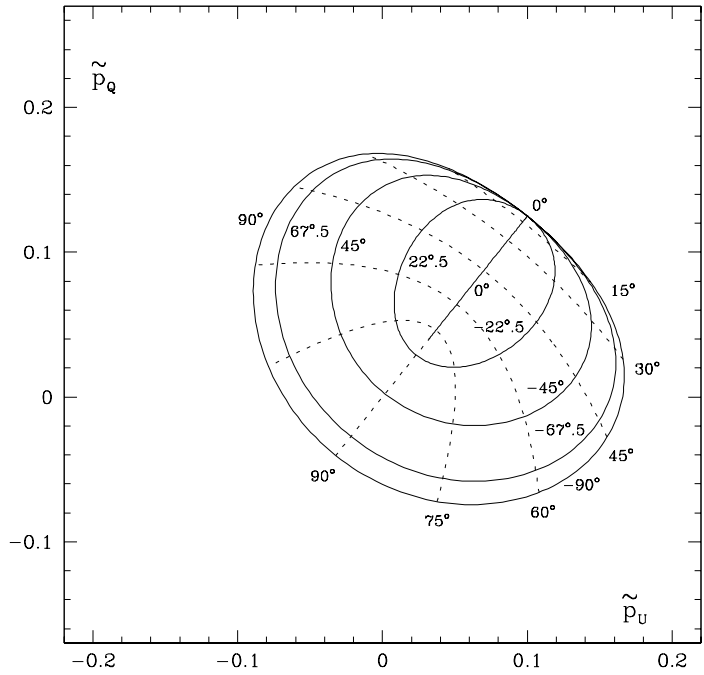

Fig.13.22. Velocity-Hanle diagram for a magnetic field of constant modulus ($H_u = 0.4$) and direction (pointing to the observer). The other parameters have the same values as in Fig.13.14.

$$\theta_w\,,\ \pi-\chi_w\,,\ \xi=-1$$
$$\pi-\theta_w\,,\ \pi+\chi_w\,,\ \xi=-1$$
$$\pi-\theta_w\,,\ -\chi_w\,,\ \xi=+1\,,$$

where $\xi = +1$ or -1 according as $\vec{B}$ and $\vec{w}$ are parallel or antiparallel, respectively. Further degeneracies are related to the velocity modulus (cf. Fig. 13.15) and to the magnetic field modulus. Obviously, the degeneracy can be partly removed if spectroscopic observations are available, as already discussed in Sect. 13.6.

A different kind of velocity-Hanle diagram is presented in Fig. 13.22. Here, the combination of parameters is the same as in Fig. 13.20 except for the magnetic field direction, which is kept fixed and parallel to the line of sight.

Consider now the combined effect of a magnetic field and a velocity distribution on the Stokes profiles of the scattered radiation. We refer to the physical situation of Fig. 13.18 with the following differences: the bulk velocity of the atoms (characterizing the 'displaced' Maxwellian distribution of Eq. (13.41)) points in the vertical direction, and a magnetic field specified by $H_u = 2$ and pointing in the same direction is present at the scattering point. The resulting profiles are shown in Fig. 13.23. It is interesting to notice the presence of a purely antisymmetrical U profile, a surprising result which is one of the most remarkable consequences of

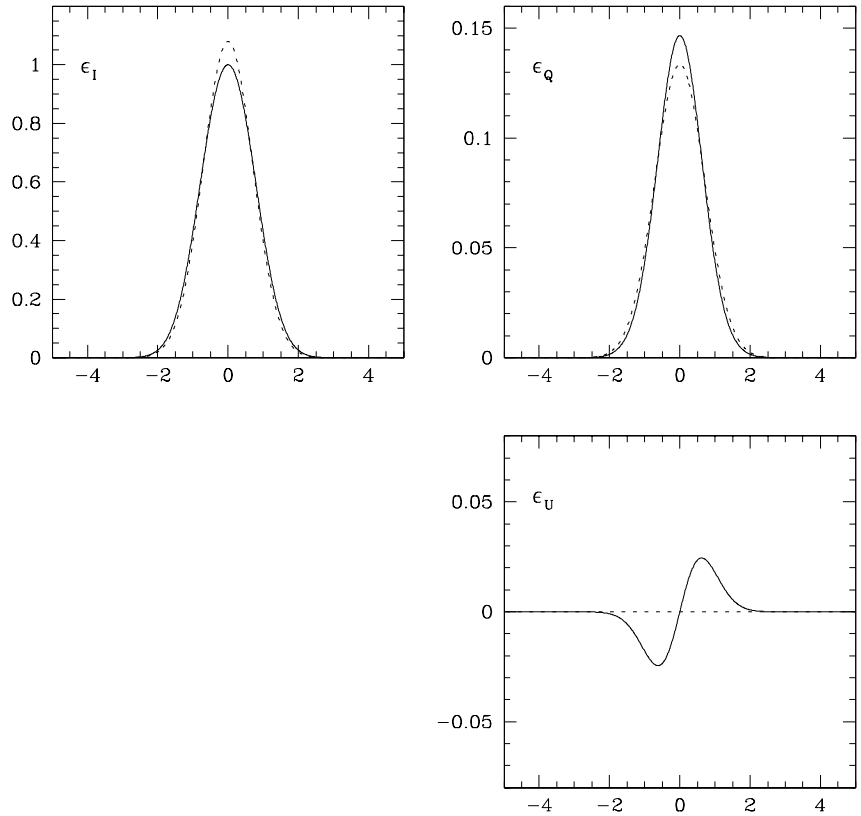

Fig.13.23. Same as Fig.13.18 except for the direction of the bulk velocity $\vec{w}$, here parallel to the local vertical ($\theta_w = 0°$), and for the presence of a magnetic field pointing in the same direction ($\theta_B = 0°$, $H_u = 2$). Full line: taking velocity/density-matrix correlations into account (Eq.(13.43)). Dashed line: assuming complete redistribution on velocities (Eq.(13.45)).

velocity/density-matrix correlations. The sign of U is positive in the red wing and negative in the blue wing. It can be shown that the inversion of either $\vec{w}$ or $\vec{B}$ produces a sign switch, so that, when $\vec{w}$ and $\vec{B}$ are antiparallel, the U profile is negative in the red wing and positive in the blue wing.

This page intentionally left blank

CHAPTER 14

ASTROPHYSICAL APPLICATIONS: STELLAR ATMOSPHERES

In the previous chapter we studied the polarization characteristics of spectral lines formed in an optically thin plasma, where transfer effects are negligible. Here we tackle the much more difficult subject of line formation in a (possibly magnetized) optically thick plasma – e.g., a stellar atmosphere. This requires the simultaneous consideration of the statistical equilibrium and the radiative transfer equations, so that the theoretical framework of this chapter represents an extension to the 'polarized case' of the non-equilibrium theory usually referred to as *non-LTE theory of stellar atmospheres*. The methods discussed in the following are the basic tools for the interpretation of spectropolarimetric observations performed over the solar disk. Special emphasis is devoted to resonance polarization in observations performed close to the solar limb, both in the absence and in the presence of a magnetic field.

14.1. The Non-LTE Problem

We have already analyzed some of the non-equilibrium phenomena that naturally arise under laboratory conditions or in astrophysical plasmas when an atomic system interacts with the radiation field. Both in the systematic investigation performed in Chap. 10 and in the applications described in Chap. 13 we assumed that the radiation field impinging on the atomic system is a *known function* of frequency and direction. Obviously, this approach becomes totally inappropriate when one aims at understanding the spectropolarimetric profiles of lines that are formed in an optically thick plasma such as a stellar atmosphere. In this case one is forced, in general, to look for a self-consistent solution of the statistical equilibrium equations and of the radiative transfer equations, starting from a model – either theoretical or empirical – of the medium where the process of line formation takes place.

Historically, it was in the late 1960s that solar physicists realized that the interpretation of the intensity profiles of many lines of the solar spectrum required this more sophisticated approach, for which the name of *non-LTE* was soon adopted.[1] This first non-LTE theory, fully described in the classical monograph by Mihalas (1978), considerably improved our understanding of spectral line profiles. However, this theory has the intrinsic limitation of leaving aside polarization phenomena: the atomic system is described in terms of the only level populations, and the radiation

[1] The name 'non-LTE' reminds the upgrading of the older and simpler theory based on the hypothesis of Local Thermodynamic Equilibrium (LTE).

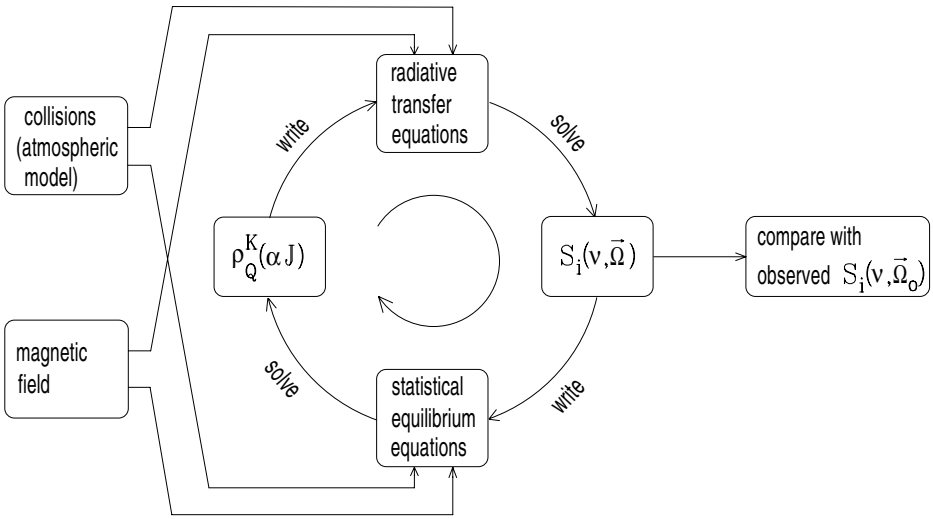

Fig.14.1. Schematic representation of the non-LTE problem of the 2nd kind. In principle, the problem is solved by iterating the operations indicated in the loop until self-consistency is reached.

field in terms of the only intensity.

In the following we will refer to the 'old' non-LTE theory as *non-LTE of the 1st kind*, and we will use the expression *non-LTE of the 2nd kind* for the more general theory which takes polarization phenomena (both in the atomic system and in the radiation field) into account. Needless to say that the two theories have to coincide under the limit where polarization phenomena are neglected.

The physical scenario underlying the theory of non-LTE of the 2nd kind can be synthetically described by a block diagram such as that of Fig. 14.1. The diagram refers to the case of a collection of multi-level atoms having a local distribution of velocities $f(\vec{v})$. It is assumed that velocity/density-matrix correlations can be neglected, so that a unique, velocity-independent density matrix can be defined (this is the approximation of complete redistribution on velocities discussed in Sect. 13.2). It is understood that the flat-spectrum approximation, which is at the basis of our theoretical development, is also satisfied (the limitations on non-LTE theory implied by this approximation will be discussed at the end of this section).

Referring to Fig. 14.1, let us suppose that, for each level (αJ) of the model atom considered, the statistical tensors $\rho^K_Q(\alpha J)$ are known at each point of the medium. The transfer coefficients $\eta^{\rm A}_i(\nu,\vec{\Omega})$, $\rho^{\rm A}_i(\nu,\vec{\Omega})$, $\eta^{\rm S}_i(\nu,\vec{\Omega})$, $\rho^{\rm S}_i(\nu,\vec{\Omega})$, and $\varepsilon_i(\nu,\vec{\Omega})$ are given – in the atomic rest frame – by Eqs. (7.15). Since the atoms are moving with a local velocity distribution $f(\vec{v})$, the Φ profiles in Eqs. (7.15) should be changed according to (cf. Eq. (13.16))[1]

[1] This substitution depends, in general, on the direction $\vec{\Omega}$ for which the transfer coefficients are computed. However, this is not true in the important case where the velocity distribution is Maxwellian. In that case the real and imaginary parts of the $\hat{\Phi}$ profile reduce, respectively, to the (suitably normalized) Voigt function and the associated dispersion profile (see Sect. 5.4).

$$\Phi(\nu_{\alpha_u J_u M_u,\,\alpha_\ell J_\ell M_\ell} - \nu) \to \hat{\Phi}(\nu_{\alpha_u J_u M_u,\,\alpha_\ell J_\ell M_\ell} - \nu) =$$

$$= \int \mathrm{d}^3\vec{v}\ f(\vec{v})\ \Phi\left(\nu_{\alpha_u J_u M_u,\,\alpha_\ell J_\ell M_\ell}\left(1 + \frac{\vec{v}\cdot\vec{\Omega}}{c}\right) - \nu\right). \qquad (14.1)$$

Substituting the values of $\rho^K_Q(\alpha J)$ at a given point into Eqs. (7.15), we can compute the transfer coefficients at that point for any direction and frequency.

On the other hand, the knowledge of the transfer coefficients at each point of the medium allows one to solve, via the methods developed in Chap. 8, the transfer equation for the (polarized) radiation travelling along any given direction. In other words, we can compute the Stokes parameters $I(\nu,\vec{\Omega})$, $Q(\nu,\vec{\Omega})$, $U(\nu,\vec{\Omega})$, and $V(\nu,\vec{\Omega})$ at any point.

This allows one to compute the radiation field tensor $\bar{J}^K_Q(\nu)$ of Eq. (13.8) at each point, and then the radiative rates appearing in the statistical equilibrium equations via Eqs. (7.14).[1] Adding the collisional rates of Sect. 7.13 (see Eq. (7.101)), and solving the statistical equilibrium equations, we obtain new values for the statistical tensors $\rho^K_Q(\alpha J)$.[2]

The loop of Fig. 14.1 is thus closed, and – at least in principle – it is sufficient to repeat it as many times as needed until a self-consistent solution for the statistical tensors and the radiation field is reached, which solves the non-LTE problem of the 2^{nd} kind.

In the following sections we will present some practical applications of the scheme just described. However, before proceeding, we feel necessary to add some general remarks and considerations which may help to clarify the physical and mathematical aspects of the problem.

a) Under the limit of very large depolarizing rates, or, in other words, when the quantities $D^{(K)}(\alpha J)$ defined in Eq. (7.102) are such that

$$D^{(K)}(\alpha J) \to \infty \qquad (K \geq 1)$$

for each (αJ)-level of the atomic model, all the statistical tensors – except those of rank 0 – vanish. In this case there is no atomic polarization, and the physical state of the atom is completely specified by the level populations (or the statistical tensors $\rho^0_0(\alpha J)$). If, in addition, the magnetic field is zero throughout the medium, the radiation field is unpolarized, so it is fully specified by its intensity (the Stokes parameter $I(\nu,\vec{\Omega})$). As a result, the non-LTE problem of the 2^{nd} kind reduces to the non-LTE problem of the 1^{st} kind. The latter is thus a special case of the former, corresponding to the two conditions just specified.

---

1 The replacement of $J^K_Q(\nu)$ with $\bar{J}^K_Q(\nu)$ in Eqs. (7.14) is the obvious counterpart of the substitution in Eq. (14.1).

2 In this chapter we adopt the assumption of complete redistribution on velocities in its more restrictive meaning, where the generalized Boltzmann term is neglected (see comments at the end of Sect. 13.2). Accordingly, the contributions of Eq. (13.12) are disregarded.

This argument also shows that it is possible to envisage a kind of intermediate non-LTE regime, that may be called *non-LTE of order 1.5*, where the atomic system is unpolarized whereas the radiation field, owing to the presence of a magnetic field, is polarized. This intermediate regime, which also can be regarded as a special case of non-LTE of the 2nd kind, has received considerable attention in the literature because it is considered appropriate to describe line formation in sunspots. Its discussion is deferred until Sect. 14.4.

b) The second remark concerns the general role of the magnetic field and of collisions in non-LTE of the 2nd kind. As pointed out in Fig. 14.1, the magnetic field has a double effect: on the one side, it affects the radiative transfer coefficients by splitting up the lines into several components; on the other side, it affects the statistical equilibrium equations via a term (or a kernel) which controls the relaxation of coherences between different magnetic sublevels. Roughly speaking, one can ascribe the first action to the Zeeman effect, and the second to the Hanle effect.

Collisions play also a double role: they affect the radiative transfer coefficients by increasing the width of the individual profiles, and the statistical equilibrium equations through different kinds of rates (depolarizing, inelastic, superelastic).

c) The third remark concerns the model atom that we have used as a prototype to introduce the non-LTE problem. We referred to a multi-level atom described in the statistical tensor representation, but the theoretical scheme is obviously more general: it can be applied both to the multi-level atom described in different representations (like the standard representation $\rho_{\alpha J}(M, M')$) and to different atomic models (like the multi-term atom, or the multi-level atom with hyperfine structure: these models can in their turn be described in different representations). Each atomic model and each representation obviously implies the use of the relevant equations. For instance, to deal with the multi-term model atom in the statistical tensor representation one should use the statistical equilibrium equations of Eq. (7.38) and the radiative transfer coefficients of Eqs. (7.47).

d) A fourth remark concerns the self-consistent solution of the non-LTE loop of Fig. 14.1. The procedure implied in the figure, often referred to as *Picard's* or *Λ-iteration method*, has, in general, an extremely slow convergence rate under typical non-LTE conditions. For this reason, much effort has been devoted since the earliest years of the non-LTE theory to develop faster and faster numerical methods for solving the coupled set of radiative transfer and statistical equilibrium equations. The currently used techniques are based on accelerated iterative schemes that evolved from earlier techniques developed for the non-LTE problem of the 1st kind. A full discussion of this subject is well outside the purposes of this book. We just refer the reader to a few papers by Trujillo Bueno and collaborators (Trujillo Bueno and Manso Sainz, 1999; Trujillo Bueno, 1999) where the state-of-the-art techniques are described in detail.

e) A further remark concerns the possibility of 'cutting', under particular physical circumstances, the block diagram of Fig. 14.1, thus avoiding the need to solve the coupled set of statistical equilibrium and radiative transfer equations.

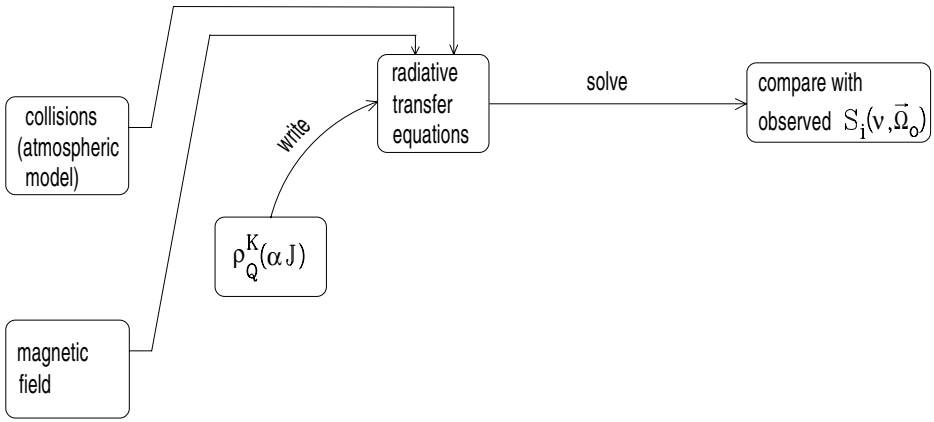

Fig.14.2. The self-consistency loop of Fig.14.1 is 'broken off' by the LTE assumption, which sets the density-matrix elements to fixed values, independent of the radiation field.

A possibility is provided by the LTE hypothesis, which implies that the statistical tensors at any point of the medium are univocally determined by the local values of the thermodynamic parameters. The statistical equilibrium equations are in this case 'implicitly solved', so that – as schematically illustrated in Fig. 14.2 – to obtain the Stokes parameters of the radiation travelling along any direction in the medium one only needs to solve the radiative transfer equations. Most of the results obtained in Chaps. 9 and 11 are based on this approach.

The second possibility takes place when the medium is optically thin at each of the wavelengths corresponding to the different transitions involved in the model atom considered, so that the radiation field impinging on the atom is fixed by the boundary conditions. Knowing the radiation field and the thermodynamic parameters of the medium, one can write down the statistical equilibrium equations. Their solution provides the values of the statistical tensors, which allow one to determine the emissivity and absorptivity properties of the medium and, consequently, the spectropolarimetric profiles of the emerging radiation. This second possibility is illustrated in Fig. 14.3. The results obtained in Chaps. 10 and 13 follow from an approach of this kind.

f) The final remark concerns the limitations related to the flat-spectrum approximation and to the approximation of complete redistribution on velocities. The problems raised by the flat-spectrum approximation have already been discussed, though in a different context, in Sect. 13.1. The conclusions that have been reached there can be easily transferred to the non-LTE problem of the 2$^{\rm nd}$ kind. In particular, one has to be especially careful with the limitations on the magnetic field's intensity ($\nu_{\rm L} \ll \Delta\nu_{\rm p}$) when dealing with the multi-level atom, and with the limitations of Eq. (13.1) when dealing with the multi-term atom or the multi-level atom with hyperfine structure. If such limitations are not satisfied, one can still treat the non-LTE problem of the 2$^{\rm nd}$ kind under the flat-spectrum approximation provided the interferences which violate the limitations themselves are set to zero

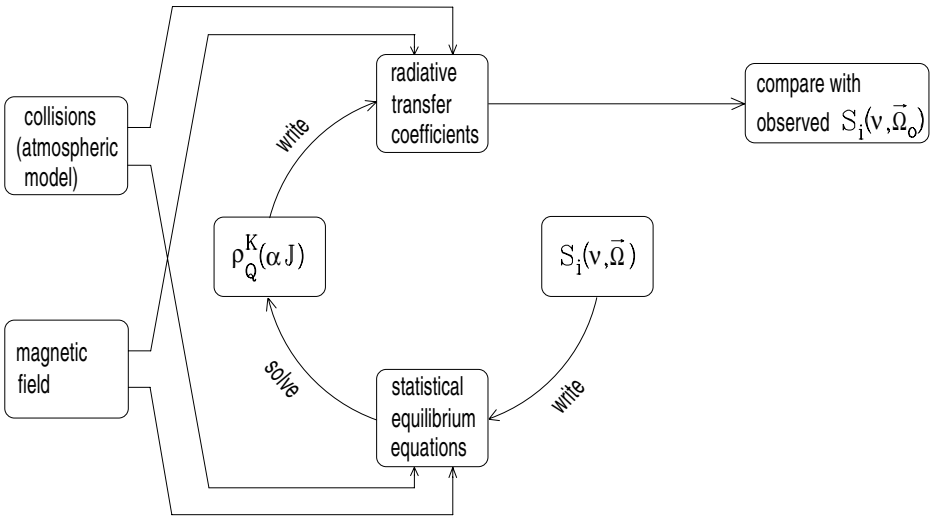

Fig.14.3. In an optically thin plasma – for instance in a solar prominence – the radiation field illuminating the atomic system is known a priori. This again 'breaks off' the self-consistency loop of Fig.14.1.

ab initio. This approach fails to give an accurate description of the far wings of the lines, but this is usually a minor drawback since the diagnostic content of such spectral intervals is often limited. As remarked in Sect. 13.1, only for particularly strong spectral lines this approach proves to be inadequate, and a theory including partial frequency redistribution effects is required.

As far as the approximation of complete redistribution on velocities is concerned, the situation is quite different. In principle, this approximation might be dropped by introducing – as in Sect. 13.2 – velocity/density-matrix correlations, thus describing the atomic system in terms of velocity-dependent statistical tensors. This implies, however, a dramatic increase in the number of unknowns, which has so far discouraged any attempt to tackle the non-LTE problem of the 2nd kind in these more general terms. Yet, the results on resonance scattering and the Hanle effect obtained in Chap. 13 clearly show that the introduction of velocity/density-matrix correlations into the non-LTE theory may be important for the correct interpretation of spectropolarimetric profiles. For the time being, the approximation of complete redistribution on velocities can simply be considered as an artifice used to bring an extremely complex problem to a tractable form.

14.2. The Two-Level Atom: Non-LTE Theory for Weak Magnetic Fields (Hanle Effect Regime)

As an application of the general non-LTE problem of the 2nd kind outlined in Sect. 14.1, we consider – following Landi Degl'Innocenti et al., 1990 – the simplest

possible atomic model, namely a two-level atom without hyperfine structure and with unpolarized lower level. Consistently with the last assumption, we suppose that the radiation field impinging on the atom is weak, in the sense that the average number of photons per mode, $\bar{n}$, is much smaller than unity, which allows one to neglect stimulated emission.

We suppose that a collection of such atoms is distributed within a static medium of arbitrary shape. In this medium the atoms interact with a magnetic field, $\vec{B}$, and with a population of colliding particles having a Maxwellian distribution of velocities characterized by the temperature T. The atoms have also a Maxwellian distribution of velocities, such that the corresponding Doppler width of the absorption profile is $\Delta\nu_{\rm D}$ (in frequency units).

No restriction is made on the spatial variation of the temperature T of the colliders and of the magnetic field vector $\vec{B}$, as well as on the densities of the atoms and of the colliders. However, we suppose for simplicity the Doppler width $\Delta\nu_{\rm D}$ to be constant throughout the medium.

Furthermore, we suppose that the magnetic field is weak (in the sense that the associated Larmor frequency $\nu_{\rm L}$ is much smaller than $\Delta\nu_{\rm D}$) and that the inverse lifetime of the upper level, γ_u, is also much smaller than $\Delta\nu_{\rm D}$, so that the flat-spectrum approximation is satisfied.[1] Finally, we adopt the approximation of complete redistribution on velocities, which implies that at any point P of the medium the atom can be described by a unique, velocity-independent density matrix that we denote by

$$\left[\rho^K_Q(\alpha J)\right]_{\vec{x}}\,,$$

with $(\alpha J) = (\alpha_u J_u)$ for the upper level and $(\alpha J) = (\alpha_\ell J_\ell)$ for the lower level, where $\vec{x}$ is the coordinate of point P.

Now we write the statistical equilibrium equation for the multipole moments of the upper level. Such equation has already been written down explicitly in Chap. 10 (see Eq. (10.1)): however, Eq. (10.1) holds in a reference system with the z-axis parallel to the magnetic field. Since in the present case the magnetic field vector is allowed to vary in the medium, it is convenient to introduce a fixed reference system Σ and to characterize the direction of the field at each point through the angles θ_B and χ_B defined in Fig. 14.4. Then we have to transform Eq. (10.1) as explained in Sect. 7.12. This leads to the following equation[2]

$$\frac{\mathrm{d}}{\mathrm{d}t}\left[\rho^K_Q(\alpha_u J_u)\right]_{\vec{x}} = -2\pi\mathrm{i}\,\nu_{\rm L}\,g_{\alpha_u J_u}\sum_{Q'}\mathcal{K}^K_{QQ'}\left[\rho^K_{Q'}(\alpha_u J_u)\right]_{\vec{x}}$$

$$+\sum_{K'Q'}\mathbb{T}_{\rm A}(\alpha_u J_u K Q, \alpha_\ell J_\ell K' Q')\left[\rho^{K'}_{Q'}(\alpha_\ell J_\ell)\right]_{\vec{x}} +$$

[1] The applicability of the flat-spectrum approximation follows from the two inequalities $\gamma_u \ll \Delta\nu_{\rm D}$ and $\nu_{\rm L} \ll \Delta\nu_{\rm D}$. The latter obviously implies an upper limit on the magnetic field intensities that can be handled by this formalism.

[2] Note that the last two lines of Eq. (10.1) are not affected by a rotation of the reference system because of the assumed isotropy of collisions.

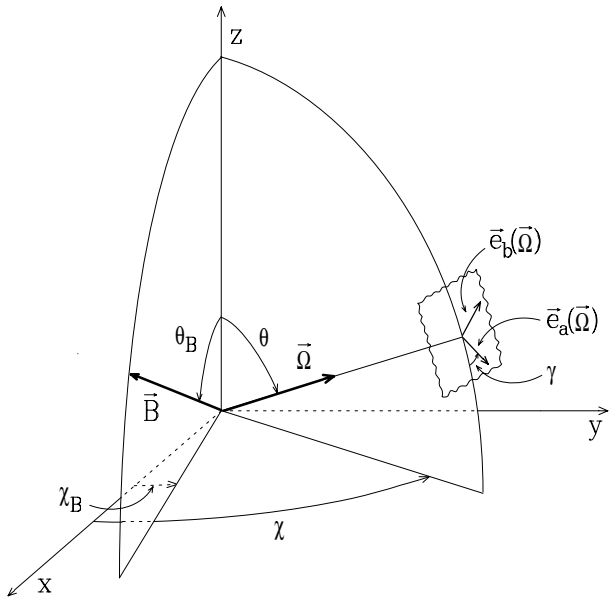

Fig.14.4. The fixed reference system $\Sigma \equiv (xyz)$ used for the calculations of this section. At each point P of the medium, the magnetic field vector is specified by the angles θ_B and χ_B. $\vec{e}_a(\vec{\Omega})$ and $\vec{e}_b(\vec{\Omega})$ are the polarization unit vectors for the radiation flowing through P in the direction $\vec{\Omega} \equiv (\theta, \chi)$.

$$
\begin{aligned}
&- \sum_{K'Q'} \Big[\mathbb{R}_{\rm E}(\alpha_u J_u K Q K' Q') + \mathbb{R}_{\rm S}(\alpha_u J_u K Q K' Q') \Big] \big[\rho^{K'}_{Q'}(\alpha_u J_u)\big]_{\vec{x}} \\
&+ \sqrt{\frac{2J_\ell + 1}{2J_u + 1}}\ C^{(K)}_{\rm I}(\alpha_u J_u, \alpha_\ell J_\ell)\ \big[\rho^{K}_{Q}(\alpha_\ell J_\ell)\big]_{\vec{x}} \\
&- \Big[C^{(0)}_{\rm S}(\alpha_\ell J_\ell, \alpha_u J_u) \ + \ D^{(K)}(\alpha_u J_u) \Big] \big[\rho^{K}_{Q}(\alpha_u J_u)\big]_{\vec{x}} \, ,
\end{aligned}
\tag{14.2}
$$

where all the rates are evaluated at point $\vec{x}$, $\nu_{\rm L}$ is the Larmor frequency at the same point, and the kernel $\mathcal{K}^K_{QQ'}$ is explicitly given by Eq. (7.79),

$$
\mathcal{K}^K_{QQ'} = \sum_{Q''} \mathcal{D}^K_{Q''Q}(R_B)^* \ Q'' \ \mathcal{D}^K_{Q''Q'}(R_B) \, , \tag{14.3}
$$

R_B being the rotation that carries the local 'magnetic' reference system (having the z-axis aligned with the magnetic field) into the fixed reference system Σ. In terms of Euler angles one simply has

$$
R_B \equiv (-\gamma_B, -\theta_B, -\chi_B) \, , \tag{14.4}
$$

where γ_B is an arbitrary angle that can be set to zero. The main properties and the explicit expressions of the components of $\mathcal{K}^K_{QQ'}$ are given in App. 19.

The assumptions made at the beginning of this section yield two basic simplifications in Eq. (14.2):
- because stimulation effects are neglected, the relaxation rate $\mathbb{R}_{\rm S}$ is zero;
- because lower-level polarization is neglected, the statistical tensors of the lower level reduce to $\rho^K_Q(\alpha_\ell J_\ell) = \rho^0_0(\alpha_\ell J_\ell)\,\delta_{K0}\,\delta_{Q0}$. This implies that the only radiative rate $\mathbb{T}_{\rm A}$ needed in Eq. (14.2) is $\mathbb{T}_{\rm A}(\alpha_u J_u K Q, \alpha_\ell J_\ell\, 0\, 0)$. Such rate is explicitly given – in the atomic rest frame – by Eq. (10.9). Because of the assumption of complete redistribution on velocities, the radiation field tensor $J^K_Q(\nu_0)$ in Eq. (10.9) has to be replaced with the 'average' radiation field tensor $\bar{J}^K_Q(\nu_0)$ given by Eq. (13.8). And since the velocity distribution of the atoms is assumed to be Maxwellian, $\bar{J}^K_Q(\nu_0)$ is given by (cf. Eqs. (13.10) and (13.11))

$$\bar{J}^K_Q(\nu_0) = \int_{-\infty}^{\infty} {\rm d}\nu\ p(\nu_0-\nu)\ J^K_Q(\nu)\ , \tag{14.5}$$

with

$$p(\nu_0-\nu) = \frac{1}{\sqrt{\pi}}\,\frac{1}{\Delta\nu_{\rm D}}\ {\rm e}^{-\left(\frac{\nu_0-\nu}{\Delta\nu_{\rm D}}\right)^2}\ . \tag{14.6}$$

Recalling the expression of the radiative rate $\mathbb{R}_{\rm E}$ (Eq. (7.14e)), we can rewrite Eq. (14.2) in the form

$$\begin{aligned}
\frac{\rm d}{{\rm d}t}\left[\rho^K_Q(\alpha_u J_u)\right]_{\vec{x}} &= -2\pi{\rm i}\,\nu_{\rm L}\,g_{\alpha_u J_u}\sum_{Q'}\mathcal{K}^K_{QQ'}\left[\rho^K_{Q'}(\alpha_u J_u)\right]_{\vec{x}} \\
&\quad - \left[A(\alpha_u J_u\to\alpha_\ell J_\ell) + C^{(0)}_{\rm S}(\alpha_\ell J_\ell,\alpha_u J_u) + D^{(K)}(\alpha_u J_u)\right]\left[\rho^K_Q(\alpha_u J_u)\right]_{\vec{x}} \\
&\quad + \sqrt{\frac{2J_\ell+1}{2J_u+1}}\,\Big[B(\alpha_\ell J_\ell\to\alpha_u J_u)\,w^{(K)}_{J_u J_\ell}\,(-1)^Q\,\bar{J}^K_{-Q}(\nu_0) \\
&\qquad\qquad + \delta_{K0}\,\delta_{Q0}\,C^{(0)}_{\rm I}(\alpha_u J_u,\alpha_\ell J_\ell)\Big]\left[\rho^0_0(\alpha_\ell J_\ell)\right]_{\vec{x}}\ ,
\end{aligned}$$

where the symbol $w^{(K)}_{J_u J_\ell}$ is given by Eq. (10.11).

Since the colliding particles have also a Maxwellian distribution of velocities, we can apply the Einstein-Milne relation (Eq. (10.49)). Next we divide both members by $A(\alpha_u J_u\to\alpha_\ell J_\ell)$ and introduce the usual notations (cf. Eqs. (10.51), (10.28))

$$\epsilon = \frac{C^{(0)}_{\rm S}(\alpha_\ell J_\ell,\alpha_u J_u)}{A(\alpha_u J_u\to\alpha_\ell J_\ell)}\,,\quad \delta^{(K)}_u = \frac{D^{(K)}(\alpha_u J_u)}{A(\alpha_u J_u\to\alpha_\ell J_\ell)}\,,\quad H_u = \frac{2\pi\nu_{\rm L}\,g_{\alpha_u J_u}}{A(\alpha_u J_u\to\alpha_\ell J_\ell)}\,. \tag{14.7}$$

Recalling Eqs. (7.8) we obtain, for stationary situations

$$\begin{aligned}
&\left[1+\epsilon+\delta^{(K)}_u\right]\left[\rho^K_Q(\alpha_u J_u)\right]_{\vec{x}} + {\rm i}H_u\sum_{Q'}\mathcal{K}^K_{QQ'}\left[\rho^K_{Q'}(\alpha_u J_u)\right]_{\vec{x}} = \\
&= \frac{c^2}{2h\nu_0^3}\sqrt{\frac{2J_u+1}{2J_\ell+1}}\,\left[w^{(K)}_{J_u J_\ell}\,(-1)^Q\,\bar{J}^K_{-Q}(\nu_0) + \delta_{K0}\,\delta_{Q0}\,\epsilon\,B_{\rm P}(T)\right]\left[\rho^0_0(\alpha_\ell J_\ell)\right]_{\vec{x}}\ ,
\end{aligned} \tag{14.8}$$

where

$$B_{\rm P}(T) = \frac{2h\nu_0^3}{c^2}\ \mathrm{e}^{-\frac{h\nu_0}{k_{\rm B}T}} \tag{14.9}$$

is the Planck function in the Wien limit (where stimulation effects are neglected).

In view of the following applications, it is convenient to rewrite Eq. (14.8) in a more compact form by introducing suitable 'source functions' for the different statistical tensors. Defining

$$S_Q^K(\vec{x}\,) = \frac{2h\nu_0^3}{c^2}\sqrt{\frac{2J_\ell+1}{2J_u+1}}\ \frac{\left[\rho_Q^K(\alpha_u J_u)\right]_{\vec{x}}}{\left[\rho_0^0(\alpha_\ell J_\ell)\right]_{\vec{x}}}\ , \tag{14.10}$$

Eq. (14.8) becomes

$$\left[1+\epsilon+\delta_u^{(K)}\right] S_Q^K(\vec{x}\,) + \mathrm{i}H_u \sum_{Q'} \mathcal{K}_{QQ'}^K\, S_{Q'}^K(\vec{x}\,) =$$

$$= w_{J_u J_\ell}^{(K)}\ (-1)^Q \bar{J}_{-Q}^K(\nu_0) + \delta_{K0}\,\delta_{Q0}\,\epsilon\, B_{\rm P}(T)\ . \tag{14.11}$$

The quantities $S_Q^K(\vec{x}\,)$ can be referred to as the *irreducible components of the two-level source function*. They represent the obvious extension of the usual concept of source function to the 'polarized case', as it is easily seen by considering the $(K=0, Q=0)$ component

$$S_0^0(\vec{x}\,) = \frac{2h\nu_0^3}{c^2}\sqrt{\frac{2J_\ell+1}{2J_u+1}}\ \frac{\left[\rho_0^0(\alpha_u J_u)\right]_{\vec{x}}}{\left[\rho_0^0(\alpha_\ell J_\ell)\right]_{\vec{x}}}\ ,$$

which, recalling Eq. (3.108), can be written as

$$S_0^0(\vec{x}\,) = \frac{2h\nu_0^3}{c^2}\ \frac{2J_\ell+1}{2J_u+1}\ \frac{n_{\alpha_u J_u}}{n_{\alpha_\ell J_\ell}}\ , \tag{14.12}$$

where $n_{\alpha_u J_u}$ and $n_{\alpha_\ell J_\ell}$ are the overall populations at point $\vec{x}$ of the upper and lower level, respectively. The last expression shows that $S_0^0(\vec{x}\,)$ is nothing but the 'classical' source function for a two-level atom under the limit of negligible stimulation effects. It should also be noticed that, according to Eq. (14.11), $S_0^0(\vec{x}\,)$ obeys the equation (see Eqs. (7.102), (14.7), (10.14) and (A19.2))

$$(1+\epsilon)\, S_0^0(\vec{x}\,) = \bar{J}_0^0(\nu_0) + \epsilon\, B_{\rm P}(T)\ ,$$

or

$$S_0^0(\vec{x}\,) = (1-\epsilon')\, \bar{J}_0^0(\nu_0) + \epsilon'\, B_{\rm P}(T)\ , \tag{14.13}$$

where

$$\epsilon' = \frac{\epsilon}{1+\epsilon} = \frac{C_{\rm S}^{(0)}(\alpha_\ell J_\ell, \alpha_u J_u)}{A(\alpha_u J_u \to \alpha_\ell J_\ell) + C_{\rm S}^{(0)}(\alpha_\ell J_\ell, \alpha_u J_u)}\ .$$

Equation (14.13) is the 'classical' expression relating the source function to the angle and frequency averaged radiation field and to the Planck function.

We point out that the preceding equations (particularly Eqs. (14.8) and (14.13)) are basically the same as those derived in Sect. 10.6 (see Eqs. (10.50) and (10.52), respectively). The only difference is that Eq. (10.50) holds in a reference system where the atom is at rest and with the z-axis parallel to the magnetic field, whereas Eq. (14.8) holds in the fixed reference system Σ of Fig. 14.4, the atoms being characterized by an assigned velocity distribution and the magnetic field's direction by the angles θ_B, χ_B. This implies the appearance in Eq. (14.8) of the kernel $\mathcal{K}^K_{QQ'}$ and – because of the assumption of complete redistribution on velocities – of the tensor $\bar{J}^K_Q(\nu_0)$ in the place of $J^K_Q(\nu_0)$.

Consider now the radiative transfer equation. From Eq. (6.83) we have, neglecting stimulated emission

$$\frac{\mathrm{d}}{\mathrm{d}s} I_i(\nu, \vec{\Omega}) = -\sum_{j=0}^{3} K^{\mathrm{A}}_{ij}\, I_j(\nu, \vec{\Omega}) + \varepsilon_i \qquad (i = 0, \ldots, 3)\,, \tag{14.14}$$

where $I_i(\nu, \vec{\Omega})$ are the Stokes parameters of the radiation flowing through point $\vec{x}$ in the direction $\vec{\Omega}$, defined with respect to the unit vectors $\vec{e}_a(\vec{\Omega})$, $\vec{e}_b(\vec{\Omega})$ of Fig. 14.4. The radiative transfer coefficients are given by Eqs. (6.86) and (6.87). Their explicit expressions for the case we are concerned with can be derived from Eqs. (7.15) by modifying the Φ profiles according to Eq. (14.1). However, since we have assumed that the magnetic field is weak ($\nu_{\mathrm{L}} \ll \Delta\nu_{\mathrm{D}}$), we can use Eqs. (7.16) in the place of Eqs. (7.15). The ϕ profile in the expressions of η^{A}_i and ε_i is a Voigt profile centered at the transition frequency ν_0, because the velocity distribution of the atoms has been assumed to be Maxwellian. But since the inverse lifetime of the upper level has also been supposed much smaller than $\Delta\nu_{\mathrm{D}}$, the Voigt profile can be approximated by the Gaussian profile $p(\nu_0 - \nu)$ of Eq. (14.6).[1] On the other hand, the assumption of unpolarized lower level implies that the summation over K and Q in Eq. (7.16a) is restricted to $K = Q = 0$. And since $\mathcal{T}^0_0(i, \vec{\Omega}) = \delta_{i0}$ (see Table 5.6), we obtain

$$\begin{aligned}\eta^{\mathrm{A}}_i = {} & \frac{h\nu}{4\pi}\, \mathcal{N}\, (2J_\ell + 1)\, B(\alpha_\ell J_\ell \rightarrow \alpha_u J_u) \\ & \times \sqrt{3}\ (-1)^{1+J_\ell+J_u} \begin{Bmatrix} 1 & 1 & 0 \\ J_\ell & J_\ell & J_u \end{Bmatrix} \rho^0_0(\alpha_\ell J_\ell)\ p(\nu_0 - \nu)\ \delta_{i0}\,,\end{aligned}$$

or, using Eqs. (2.36a), (10.6) and (9.5)

$$\eta^{\mathrm{A}}_i = k^{\mathrm{A}}_{\mathrm{L}}\ p(\nu_0 - \nu)\ \delta_{i0}\,,$$

[1] It should be remarked that such substitution, based on the assumptions $\nu_{\mathrm{L}} \ll \Delta\nu_{\mathrm{D}}$ and $\gamma_u \ll \Delta\nu_{\mathrm{D}}$, implies the same order of approximation as the flat-spectrum approximation that we have used to derive the statistical equilibrium equation.

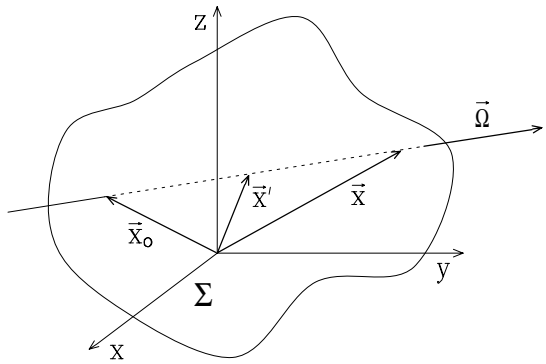

Fig.14.5. A ray with direction $\vec{\Omega}$ enters the medium at point $\vec{x}_0$, where its Stokes parameters are $I_i^{(\mathrm{b})}(\nu, \vec{\Omega})$. At point $\vec{x}$, the Stokes parameters are given by Eq.(14.16).

where $k_{\mathrm{L}}^{\mathrm{A}}$ is the frequency-integrated absorption coefficient in the line,

$$k_{\mathrm{L}}^{\mathrm{A}} = \frac{h\nu}{4\pi} \mathcal{N}_\ell \; B(\alpha_\ell J_\ell \rightarrow \alpha_u J_u) \; , \tag{14.15}$$

$\mathcal{N}_\ell$ being the number density of atoms in the lower level. It can easily be seen that the unpolarized lower level assumption also implies that the coefficients ρ_i^{A} are identically zero. It follows that the propagation matrix is diagonal,

$$K_{ij}^{\mathrm{A}} = k_{\mathrm{L}}^{\mathrm{A}} \; p(\nu_0 - \nu) \; \delta_{ij} \; .$$

By similar arguments we obtain

$$\varepsilon_i = k_{\mathrm{L}}^{\mathrm{A}} \; p(\nu_0 - \nu) \sum_{KQ} w_{J_u J_\ell}^{(K)} \; \mathcal{T}_Q^K(i, \vec{\Omega}) \; S_Q^K(\vec{x}) \; ,$$

where the quantities $w_{J_u J_\ell}^{(K)}$ and $S_Q^K(\vec{x})$ are defined by Eqs. (10.11) and (14.10), respectively.

Obviously, the preceding expressions imply that the only contribution to the opacity and the emissivity of the medium comes from transitions between the two levels of the model atom. The case where a source of continuum opacity (and emissivity) is also present is formally more complicated and will not be treated here.

Since the propagation matrix is diagonal, Eq. (14.14) reduces to a system of four uncoupled equations whose solution can be expressed in terms of the scalar attenuation operator of Eq. (8.16). Using Eq. (8.18) and referring to Fig. 14.5, we can write the Stokes parameters at point $\vec{x}$ of the radiation at frequency ν flowing along the direction $\vec{\Omega}$ in the form

$$\begin{aligned} I_i(\nu, \vec{\Omega}) = \int_{\vec{x}_0}^{\vec{x}} & p(\nu_0 - \nu) \; k_{\mathrm{L}}^{\mathrm{A}}(\vec{x}\,') \; \mathrm{e}^{-\tau_\nu(\vec{x}, \vec{x}')} \sum_{KQ} w_{J_u J_\ell}^{(K)} \; \mathcal{T}_Q^K(i, \vec{\Omega}) \; S_Q^K(\vec{x}\,') \; \mathrm{d}s' \\ & + \mathrm{e}^{-\tau_\nu(\vec{x}, \vec{x}_0)} \; I_i^{(\mathrm{b})}(\nu, \vec{\Omega}) \; , \end{aligned} \tag{14.16}$$

where $I_i^{(\mathrm{b})}(\nu,\vec{\Omega})$ is the Stokes vector of the radiation entering the medium at point $\vec{x}_0$ along the direction $\vec{\Omega}$, s' is the coordinate of $\vec{x}'$ reckoned along $\vec{\Omega}$ ($s'=|\vec{x}'-\vec{x}_0|$), and $\tau_\nu(\vec{x},\vec{x}')$ is the optical depth at frequency ν between points $\vec{x}$ and $\vec{x}'$,

$$\tau_\nu(\vec{x},\vec{x}') = \int_{\vec{x}'}^{\vec{x}} p(\nu_0-\nu)\; k_{\mathrm{L}}^{\mathrm{A}}(\vec{x}'')\;\mathrm{d}s'' \;. \tag{14.17}$$

From Eq. (14.16) it is now possible to find the expression for the radiation field tensor at point $\vec{x}$. Using Eqs. (14.5) and (5.157) we obtain two contributions, arising from the two terms in the right-hand side of Eq. (14.16). We can write

$$\bar{J}_Q^K(\nu_0) = \left[\bar{J}_Q^K(\nu_0)\right]_{\mathrm{I}} + \left[\bar{J}_Q^K(\nu_0)\right]_{\mathrm{E}} , \tag{14.18}$$

where the 'internal' part $[\bar{J}_Q^K(\nu_0)]_{\mathrm{I}}$ is given by

$$\begin{aligned}\left[\bar{J}_Q^K(\nu_0)\right]_{\mathrm{I}} = \int_{-\infty}^{\infty}\mathrm{d}\nu\; p(\nu_0-\nu)\oint\frac{\mathrm{d}\Omega}{4\pi}\sum_{i=0}^{3}\mathcal{T}_Q^K(i,\vec{\Omega})\int_{\vec{x}_0}^{\vec{x}}\mathrm{d}s'\,p(\nu_0-\nu)\\ \times k_{\mathrm{L}}^{\mathrm{A}}(\vec{x}')\;\mathrm{e}^{-\tau_\nu(\vec{x},\vec{x}')}\sum_{K'Q'} w^{(K')}_{J_u J_\ell}\;\mathcal{T}_{Q'}^{K'}(i,\vec{\Omega})\;S_{Q'}^{K'}(\vec{x}')\;,\end{aligned} \tag{14.19}$$

and the 'external' part $[\bar{J}_Q^K(\nu_0)]_{\mathrm{E}}$, originating from the boundary conditions, by

$$\left[\bar{J}_Q^K(\nu_0)\right]_{\mathrm{E}} = \int_{-\infty}^{\infty}\mathrm{d}\nu\; p(\nu_0-\nu)\oint\frac{\mathrm{d}\Omega}{4\pi}\sum_{i=0}^{3}\mathcal{T}_Q^K(i,\vec{\Omega})\;\mathrm{e}^{-\tau_\nu(\vec{x},\vec{x}_0)}\;I_i^{(\mathrm{b})}(\nu,\vec{\Omega})\;. \tag{14.20}$$

Equation (14.19) can be cast in a simpler form by changing the double integral in $\mathrm{d}\Omega$ and $\mathrm{d}s'$ into a volume integral. Since

$$\mathrm{d}^3\vec{x}' = (\vec{x}-\vec{x}')^2\;\mathrm{d}\Omega\,\mathrm{d}s' \;, \tag{14.21}$$

we get

$$\begin{aligned}\left[\bar{J}_Q^K(\nu_0)\right]_{\mathrm{I}} = \int_{-\infty}^{\infty}\mathrm{d}\nu\;[p(\nu_0-\nu)]^2\int\mathrm{d}^3\vec{x}'\;\frac{k_{\mathrm{L}}^{\mathrm{A}}(\vec{x}')\;\mathrm{e}^{-\tau_\nu(\vec{x},\vec{x}')}}{4\pi(\vec{x}-\vec{x}')^2}\\ \times\sum_{i=0}^{3}\mathcal{T}_Q^K(i,\vec{\Omega})\sum_{K'Q'} w^{(K')}_{J_u J_\ell}\;\mathcal{T}_{Q'}^{K'}(i,\vec{\Omega})\;S_{Q'}^{K'}(\vec{x}')\;.\end{aligned} \tag{14.22}$$

Finally, we can substitute the expression of the radiation field tensor at point $\vec{x}$ into the statistical equilibrium equation. From Eqs. (14.11), (14.18), and (14.22)

we obtain

$$\Big[1+\epsilon+\delta_u^{(K)}\Big]S_Q^K(\vec{x}\,) \,+\, \mathrm{i}H_u \sum_{Q'} \mathcal{K}_{QQ'}^K\, S_{Q'}^K(\vec{x}\,) =$$

$$= \,\delta_{K0}\,\delta_{Q0}\,\epsilon\, B_{\mathrm{P}}(T) \,+\, w_{J_u J_\ell}^{(K)}\,(-1)^Q\big[\bar{J}_{-Q}^K(\nu_0)\big]_{\mathrm{E}}$$

$$+\int \mathrm{d}^3\vec{x}\,'\;\frac{k_{\mathrm{L}}^{\mathrm{A}}(\vec{x}\,')}{4\pi(\vec{x}-\vec{x}\,')^2}\;\sum_{K'Q'}\,G_{KQ,K'Q'}(\vec{x},\vec{x}\,')\;S_{Q'}^{K'}(\vec{x}\,')\;, \qquad (14.23)$$

where

$$G_{KQ,K'Q'}(\vec{x},\vec{x}\,') = \int_{-\infty}^{\infty}\mathrm{d}\nu\;\big[p(\nu_0-\nu)\big]^2\;\mathrm{e}^{-\tau_\nu(\vec{x},\vec{x}')}$$

$$\times\, w_{J_u J_\ell}^{(K)}\; w_{J_u J_\ell}^{(K')}\;\sum_{i=0}^{3}\,(-1)^Q\;\mathcal{T}_{-Q}^K(i,\vec{\Omega})\,\mathcal{T}_{Q'}^{K'}(i,\vec{\Omega})\;. \qquad (14.24)$$

The quantities $G_{KQ,K'Q'}(\vec{x},\vec{x}\,')$ appearing in this equation can be expressed in terms of Wigner symbols and of rotation matrices. Details are given in App. 20. From the physical point of view, they represent a numerical factor which weights the amount of coupling between the statistical tensor ρ_Q^K at point $\vec{x}$ and the statistical tensor $\rho_{Q'}^{K'}$ at point $\vec{x}\,'$. For this reason, they can be referred to as *multipole coupling coefficients*.

Equation (14.23) is a system of linear, non-homogeneous, integral equations in the unknowns $S_Q^K(\vec{x}\,)$, the irreducible components of the source function, which can in principle be solved once the properties of the medium and the boundary conditions are specified. When the values of these components are known at each point, the Stokes parameters of the radiation emerging from the medium can be computed by applying Eq. (14.16). It should be remarked that, owing to property (A20.8) of the multipole coupling coefficients, Eq. (14.23) decouples in two different sets of equations involving, respectively, the components with $K = 0, 2$ and those with $K = 1$. In the latter set, the only source term is $[\bar{J}_{-Q}^1(\nu_0)]_{\mathrm{E}}$, which vanishes unless the boundary radiation field, once integrated in frequency according to Eq. (14.20), has some contribution from circular polarization. Excluding this case of limited interest, all the components $S_Q^1(\vec{x}\,)$ are everywhere zero in the medium.

It is especially interesting to study Eq. (14.23) in the particular case of a plane-parallel, semi-infinite stellar atmosphere. In this case all the physical quantities of the medium depend on a single coordinate, the height in the atmosphere, that we assume as the z-axis of our reference system Σ. As a consequence, the irreducible components of the source function depend only on the height z. Introducing the line optical depth t_{L} through the equation (cf. Eqs. (9.34))

$$\mathrm{d}t_{\mathrm{L}} = -\frac{k_{\mathrm{L}}^{\mathrm{A}}}{\Delta\nu_{\mathrm{D}}}\,\mathrm{d}z\;, \qquad (14.25)$$

and assuming that the stellar atmosphere is not illuminated by external sources of radiation, Eq. (14.23) takes the form

$$\Big[1+\epsilon+\delta_u^{(K)}\Big]S_Q^K(t_{\rm L}) \,+\, {\rm i}H_u \sum_{Q'} \mathcal{K}^K_{QQ'}\, S^K_{Q'}(t_{\rm L}) = \,\delta_{K0}\,\delta_{Q0}\,\epsilon\, B_{\rm P}(T)$$

$$+\int_0^\infty {\rm d}t'_{\rm L} \int_{-\infty}^{\infty}{\rm d}x' \int_{-\infty}^{\infty}{\rm d}y' \,\frac{\Delta\nu_{\rm D}}{4\pi(\vec{x}-\vec{x}')^2} \sum_{K'=0,2}\,\sum_{Q'} G_{KQ,K'Q'}(\vec{x},\vec{x}')\; S^{K'}_{Q'}(t'_{\rm L})\,, \qquad (14.26)$$

where the indices K and K' are restricted to the values 0 and 2. The integral over x' and y' can be performed by introducing cylindrical coordinates. These calculations, that are developed in detail in App. 21, restrict the summation over Q' in the last term of Eq. (14.26) to the single value $Q' = Q$ and lead to the following equation

$$\Big[1+\epsilon+\delta_u^{(K)}\Big]S_Q^K(t_{\rm L}) \,+\, {\rm i}H_u \sum_{Q'} \mathcal{K}^K_{QQ'}\, S^K_{Q'}(t_{\rm L}) =$$

$$= \,\delta_{K0}\,\delta_{Q0}\,\epsilon\, B_{\rm P}(T) \,+\, \sum_{K'=0,2} \int_0^\infty \mathcal{G}_{KQ,K'Q}\big(|t'_{\rm L}-t_{\rm L}|\big)\; S^{K'}_{Q}(t'_{\rm L})\;{\rm d}t'_{\rm L}\,, \qquad (14.27)$$

where we have introduced the *multipolar kernels* $\mathcal{G}_{KQ,K'Q}$ defined by

$$\mathcal{G}_{KQ,K'Q}\big(|t'_{\rm L}-t_{\rm L}|\big) = \int_{-\infty}^{\infty}{\rm d}x' \int_{-\infty}^{\infty}{\rm d}y' \,\frac{\Delta\nu_{\rm D}}{4\pi(\vec{x}-\vec{x}')^2}\; G_{KQ,K'Q}(\vec{x},\vec{x}')\,. \qquad (14.28)$$

These quantities are real and satisfy the symmetry properties (cf. Eqs. (A20.5) and (A20.6))

$$\mathcal{G}_{K'Q,KQ}(x) = \mathcal{G}_{K\,-Q,K'\,-Q}(x) = \mathcal{G}_{KQ,K'Q}(x)\,. \qquad (14.29)$$

The explicit expressions of the multipolar kernels appearing in Eq. (14.27) can be derived from Eqs. (A21.8), (A21.7) and (A20.11). We obtain

$$\mathcal{G}_{00,00}(x) = \frac{1}{2}\int_{-\infty}^{\infty}{\rm d}v\;\big[\varphi(v)\big]^2\,E_1\big(x\,\varphi(v)\big)$$

$$\mathcal{G}_{00,20}(x) = \frac{1}{4\sqrt{2}}\;w^{(2)}_{J_u J_\ell}\int_{-\infty}^{\infty}{\rm d}v\;\big[\varphi(v)\big]^2\Big[3E_3\big(x\,\varphi(v)\big)-E_1\big(x\,\varphi(v)\big)\Big]$$

$$\mathcal{G}_{20,20}(x) = \frac{1}{8}\,W_2(J_\ell,J_u)\int_{-\infty}^{\infty}{\rm d}v\;\big[\varphi(v)\big]^2\Big[5E_1\big(x\,\varphi(v)\big)-12E_3\big(x\,\varphi(v)\big)+9E_5\big(x\,\varphi(v)\big)\Big]$$

$$\mathcal{G}_{21,21}(x) = \frac{3}{8}\,W_2(J_\ell,J_u)\int_{-\infty}^{\infty}{\rm d}v\;\big[\varphi(v)\big]^2\Big[E_1\big(x\,\varphi(v)\big)+E_3\big(x\,\varphi(v)\big)-2E_5\big(x\,\varphi(v)\big)\Big]$$

$$\mathcal{G}_{22,22}(x) = \frac{3}{16}\, W_2(J_\ell, J_u) \int\limits_{-\infty}^{\infty} \mathrm{d}v\, \left[\varphi(v)\right]^2 \Big[E_1\big(x\,\varphi(v)\big) + 2E_3\big(x\,\varphi(v)\big) + E_5\big(x\,\varphi(v)\big)\Big] \,. \tag{14.30}$$

The remaining components can be deduced from Eqs. (14.29). In these expressions, E_n is the n^{th} exponential integral defined in Eq. (12.6), the symbol $W_2(J_\ell, J_u)$ is defined in Eq. (10.17), v and $\varphi(v)$ are the reduced frequency and the Gaussian profile of Eq. (A21.5),

$$v = \frac{\nu_0 - \nu}{\Delta\nu_{\mathrm{D}}} \,, \qquad \varphi(v) = \frac{1}{\sqrt{\pi}}\ \mathrm{e}^{-v^2} \,. \tag{14.31}$$

Recalling that

$$\int\limits_0^{\infty} E_n(x)\ \mathrm{d}x = \frac{1}{n} \qquad (n = 1, 2, \ldots) \,,$$

and that

$$\int\limits_{-\infty}^{\infty} \varphi(v)\ \mathrm{d}v = 1 \,,$$

we obtain the integral properties

$$\int\limits_0^{\infty} \mathcal{G}_{00,00}(x)\ \mathrm{d}x = \frac{1}{2} \,, \qquad \int\limits_0^{\infty} \mathcal{G}_{00,20}(x)\ \mathrm{d}x = 0 \,,$$

$$\int\limits_0^{\infty} \mathcal{G}_{2Q,2Q}(x)\ \mathrm{d}x = \frac{7}{20}\, W_2(J_\ell, J_u) \qquad (Q = 0, \pm 1, \pm 2) \,. \tag{14.32}$$

The multipolar kernels can be evaluated from Eqs. (14.30) via numerical computations. Figure 14.6 shows a plot of these quantities obtained by Gauss-Hermite integration. The plot refers to the transition $(J_\ell = 0, J_u = 1)$ which implies $w^{(2)}_{J_u J_\ell} = 1$ and $W_2(J_\ell, J_u) = 1$.

Equation (14.27) can be solved by means of different numerical techniques. A possible algorithm is similar to the one described in App. 16 for the solution of the Hopf equation and is based on a discretization grid on t_{L} and the transformation of the system of integral equations into a linear system of algebraic equations. Details can be found in Bommier et al. (1991). Other methods have also been devised, among which we wish to quote, for their speed and accuracy, the operator-splitting, iterative methods described by Trujillo Bueno and Manso Sainz (1999).

Once the irreducible components of the source function are known, the Stokes parameters profiles of the radiation emerging from the atmosphere can be deduced

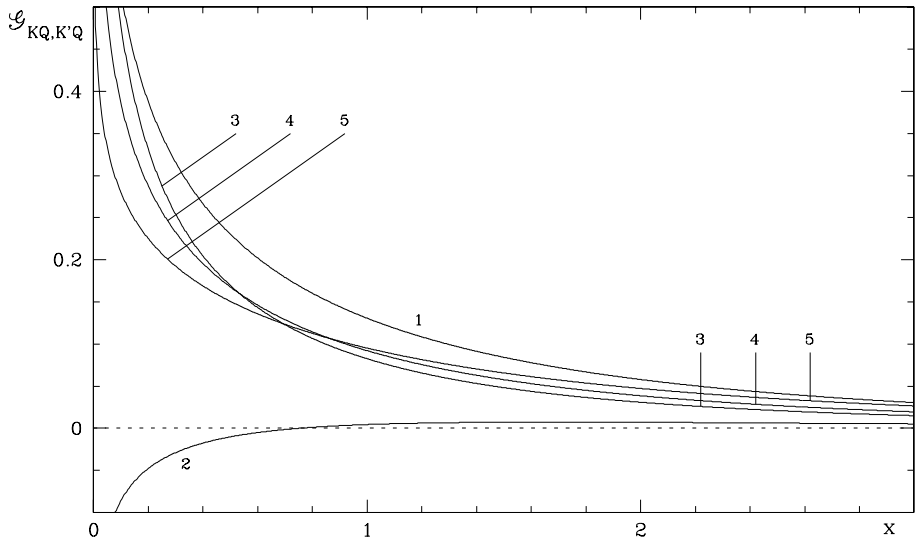

Fig.14.6. The multipolar kernels defined in Eqs.(14.30) are plotted as a function of x for the transition $(J_\ell = 0, J_u = 1)$. The curves are labelled according to the following code: 1) $\mathcal{G}_{00,00}$; 2) $\mathcal{G}_{00,20}$; 3) $\mathcal{G}_{20,20}$; 4) $\mathcal{G}_{21,21}$; 5) $\mathcal{G}_{22,22}$. Note the sign change of curve 2 which occurs at $x = 0.75125$.

by applying Eq. (14.16) to the case of a plane-parallel atmosphere. This gives, setting $\mu = \cos\theta$

$$I_i(\nu,\vec{\Omega}) = \int_0^\infty \varphi(v)\ \mathrm{e}^{-\frac{t_\mathrm{L}\,\varphi(v)}{\mu}} \sum_{K=0,2}\sum_{Q} w^{(K)}_{J_u J_\ell}\ \mathcal{T}^K_Q(i,\vec{\Omega})\ S^K_Q(t_\mathrm{L})\ \frac{\mathrm{d}t_\mathrm{L}}{\mu}\ ,$$

or, introducing the variable $\tau_\nu = t_\mathrm{L}\,\varphi(v)/\mu$

$$I_i(\nu,\vec{\Omega}) = \sum_{K=0,2}\sum_{Q} w^{(K)}_{J_u J_\ell}\ \mathcal{T}^K_Q(i,\vec{\Omega}) \int_0^\infty \mathrm{e}^{-\tau_\nu}\ S^K_Q\Big(\frac{\mu\,\tau_\nu}{\varphi(v)}\Big)\ \mathrm{d}\tau_\nu\ . \tag{14.33}$$

In particular, for the radiation emerging along a direction $\vec{\Omega}_\parallel$ parallel to the stellar surface one has, by considering the limit $\mu \to 0$

$$I_i(\nu,\vec{\Omega}_\parallel) = \sum_{K=0,2}\sum_{Q} w^{(K)}_{J_u J_\ell}\ \mathcal{T}^K_Q(i,\vec{\Omega}_\parallel)\ S^K_Q(0)\ . \tag{14.34}$$

Since under this limit the irreducible components of the source function appearing in Eq. (14.33) become independent of optical depth, the Stokes parameters of the emerging radiation turn out to be independent of frequency. This is not the case when continuum opacity is taken into account (see Sect. 14.7).

Particularly important for the theory of radiative transfer of polarized radiation is the special case of Eq. (14.27) which is obtained by setting $H_u = \delta^{(K)}_u = 0$ and by

assuming ϵ and $B_{\rm P}(T)$ independent of $t_{\rm L}$. One is here faced with a homogeneous, isothermal, non-magnetic, non-depolarizing atmosphere, and Eq. (14.27) takes the form[1]

$$\begin{aligned}(1+\epsilon)\, S^0_0(t_{\rm L}) &= \epsilon\, B_{\rm P} + \int_0^\infty \mathcal{G}_{00,00}\big(|t'_{\rm L}-t_{\rm L}|\big)\, S^0_0(t'_{\rm L})\, {\rm d}t'_{\rm L} \\ &\quad + \int_0^\infty \mathcal{G}_{00,20}\big(|t'_{\rm L}-t_{\rm L}|\big)\, S^2_0(t'_{\rm L})\, {\rm d}t'_{\rm L} \\ (1+\epsilon)\, S^2_0(t_{\rm L}) &= \int_0^\infty \mathcal{G}_{20,00}\big(|t'_{\rm L}-t_{\rm L}|\big)\, S^0_0(t'_{\rm L})\, {\rm d}t'_{\rm L} \\ &\quad + \int_0^\infty \mathcal{G}_{20,20}\big(|t'_{\rm L}-t_{\rm L}|\big)\, S^2_0(t'_{\rm L})\, {\rm d}t'_{\rm L}\ . \end{aligned} \tag{14.35}$$

This system of equations was established – though with different notations – by Stenflo and Stenholm (1976) and by Rees (1978). It can be considered a typical bench-mark problem in radiative transfer for polarized radiation because, as proved in App. 22 (see Eq. (A22.13) with $\delta^{(2)}_u = 0$), the irreducible components of the source function at the surface of the atmosphere obey the following relation, originally due to Ivanov (1990) and often referred to as the *generalized* $\sqrt{\epsilon}$ *- law*[2]

$$\sqrt{\big[S^0_0(0)\big]^2 + \big[S^2_0(0)\big]^2} \;=\; \sqrt{\frac{\epsilon}{1+\epsilon}}\, B_{\rm P} \;=\; \sqrt{\epsilon'}\, B_{\rm P}\ ,$$

which can conveniently be used to test the accuracy of the numerical method employed for solving the system.

Numerical results on the integration of the system of Eqs. (14.35) and on the ensuing spectropolarimetric profiles have been published by different authors (Rees, 1978; Faurobert-Scholl and Frisch, 1989; Ivanov, 1990; Bommier et al., 1991; Bommier and Landi Degl'Innocenti, 1996; Ivanov et al., 1997; Trujillo Bueno and Manso Sainz, 1999). Other numerical results on the profiles have been obtained as particular cases of more general approaches involving partial redistribution effects (see Sect. 14.8 and references therein). In Figs. 14.7-14.9 we show some examples for the transition ($J_\ell = 0, J_u = 1$).

A particularly significant numerical result is the surface value of the ratio of the two components of the source function, $\sigma = S^2_0(0)/S^0_0(0)$. This ratio is related

[1] In the system of Eq. (14.27) with $H_u = 0$, the equations involving the components S^2_Q with $Q \neq 0$ are decoupled from the equation containing the source term $\epsilon\, B_{\rm P}(T)$. As a consequence, such components are zero.

[2] In our notations, this law should better be referred to as the *generalized* $\sqrt{\epsilon'}$ *- law*.

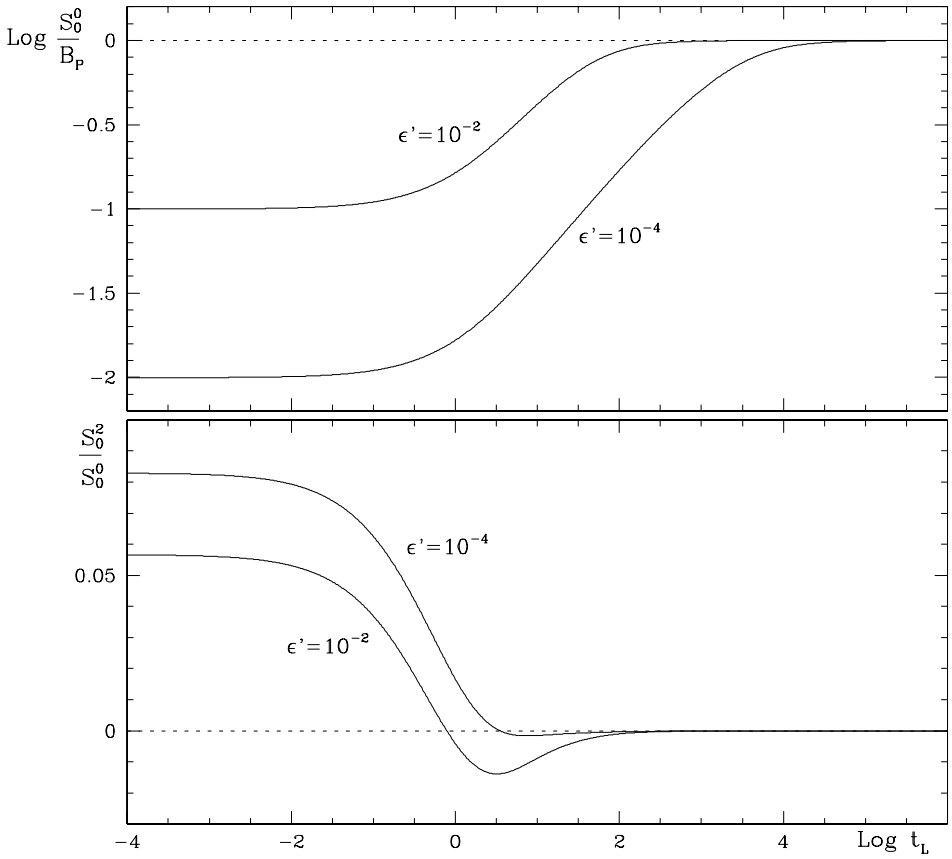

Fig.14.7. The logarithm of the component $S_0^0(t_{\rm L})$ of the source function (normalized to $B_{\rm P}$), and the ratio $S_0^2(t_{\rm L})/S_0^0(t_{\rm L})$ – upper and lower panel, respectively – are plotted against the logarithm of optical depth. The curves are obtained by solving Eqs.(14.35) – homogeneous, isothermal, non-magnetic, non-depolarizing atmosphere – for the transition ($J_\ell = 0, J_u = 1$) and for two different values of ϵ'.

to the fractional linear polarization observed in the tangential direction by the relation, easily obtained from Eq. (14.34)[1]

$$p_{\parallel} \equiv \frac{Q(\nu, \vec{\Omega}_{\parallel})}{I(\nu, \vec{\Omega}_{\parallel})} = \frac{3\, w^{(2)}_{J_u J_\ell}\, \sigma}{2\sqrt{2} - w^{(2)}_{J_u J_\ell}\, \sigma} \,. \tag{14.36}$$

For the transition ($J_\ell = 0, J_u = 1$) – which implies $w^{(2)}_{J_u J_\ell} = 1$ – and for $\epsilon' = 10^{-4}$, the published values of σ are 0.08294 (Bommier and Landi Degl'Innocenti, 1996) and 0.08292 (Trujillo Bueno and Manso Sainz, 1999), corresponding to the $p_{\parallel}$ values

[1] In Eq. (14.36), the reference direction for positive Q is parallel to the stellar surface ($\theta = 90°$, $\gamma = 90°$ in Table 5.6).

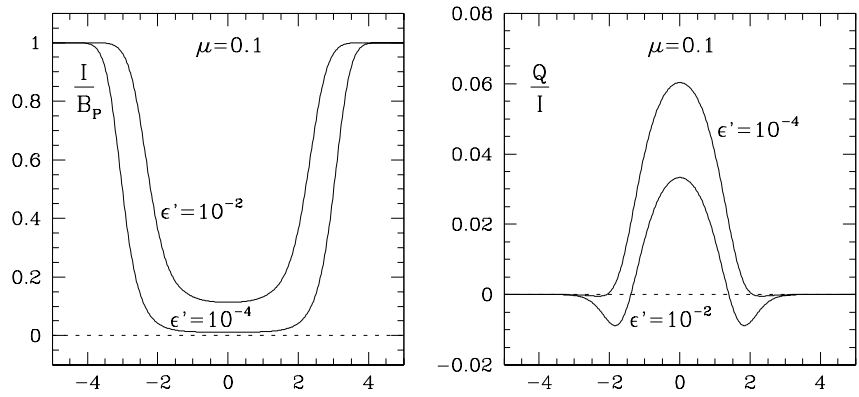

Fig.14.8. The emerging profiles of the intensity (normalized to $B_{\rm P}$) and of the ratio Q/I – left and right panel, respectively – corresponding to the irreducible components of the source function shown in Fig.14.7. The profiles, obtained from Eq.(14.33) for a heliocentric angle $\theta = 84°.3$ ($\mu = 0.1$), are plotted against the reduced frequency $(\nu_0 - \nu)/\Delta\nu_{\rm D}$. The positive Q direction is parallel to the stellar surface.

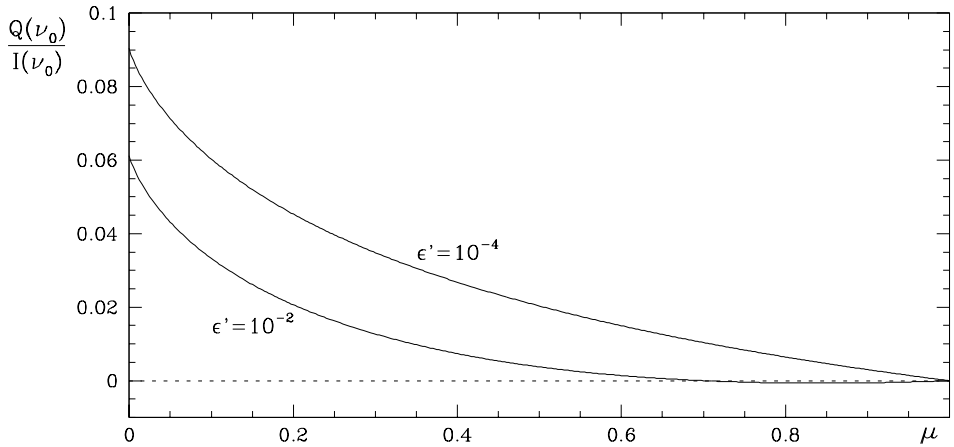

Fig.14.9. Limb-darkening curve for the fractional polarization at line center, corresponding to the irreducible components of the source function of Fig.14.7.

0.09063 and 0.09061, respectively. These values are in agreement with the result of Ivanov et al. (1997), who give for $p_{\|}$ the asymptotic expression

$$p_{\|} = 0.09443 - 0.3805\,\sqrt{\epsilon'}\ .$$

Apart from the special case of Eqs. (14.35), it is important to remark that Eq. (14.27) holds without any limitation on the optical depth variation of the different parameters. The quantities ϵ, $\delta_u^{(K)}$, H_u, $B_{\rm P}(T)$, θ_B, and χ_B, which appear either explicitly or implicitly (through the kernel $\mathcal{K}^K_{QQ'}$) in this equation, can be arbitrary functions of optical depth. A full analysis of the solution of Eq. (14.27) for different atomic transitions and for different values (and depth dependence) of the

above-mentioned parameters is well outside the purposes of this book. Some results can be found in Bommier et al. (1991) and in Bommier and Landi Degl'Innocenti (1996).

For further applications involving turbulent magnetic fields, it is convenient to rewrite Eq. (14.27) by introducing as unknowns the irreducible components of the source function expressed in the local magnetic frame.[1] Such components will be denoted by the symbol $[S^K_Q(t_{\rm L})]_{\rm M}$ and are still given by Eq. (14.10), the statistical tensors in the right-hand side being now defined in the local magnetic frame. Referring to the geometry of Fig. 14.4, and denoting by R_B the rotation that carries the magnetic frame at $t_{\rm L}$ into the fixed reference frame Σ (see Eq. (14.4)), we have from Eqs. (7.76) and (7.77)

$$S^K_Q(t_{\rm L}) = \sum_{Q'} \left[S^K_{Q'}(t_{\rm L})\right]_{\rm M} \mathcal{D}^K_{Q'Q}(R_B)^* \tag{14.37}$$

$$\left[S^K_Q(t_{\rm L})\right]_{\rm M} = \sum_{Q'} S^K_{Q'}(t_{\rm L})\, \mathcal{D}^K_{QQ'}(R_B)\ . \tag{14.38}$$

Multiplication of Eq. (14.27) by $\mathcal{D}^K_{Q''Q}(R_B)$ and summation over Q yields, with the use of Eqs. (14.37), (14.38), (14.3), and (2.72)

$$\begin{aligned}\left[1+\epsilon+\delta^{(K)}_u + {\rm i}H_u Q\right]\left[S^K_Q(t_{\rm L})\right]_{\rm M} = {}& \delta_{K0}\,\delta_{Q0}\,\epsilon\, B_{\rm P}(T) \\ & + \sum_{K'=0,2}\sum_{Q'}\int_0^\infty \hat{\mathcal{G}}_{KQ,K'Q'}\left(|t'_{\rm L}-t_{\rm L}|\right)\left[S^{K'}_{Q'}(t'_{\rm L})\right]_{\rm M}\,{\rm d}t'_{\rm L}\ ,\end{aligned} \tag{14.39}$$

where

$$\begin{aligned}&\hat{\mathcal{G}}_{KQ,K'Q'}\left(|t'_{\rm L}-t_{\rm L}|\right) = \\ &= \sum_{Q''} \mathcal{D}^K_{QQ''}(R_B)\ \mathcal{G}_{KQ'',K'Q''}\left(|t'_{\rm L}-t_{\rm L}|\right)\mathcal{D}^{K'}_{Q'Q''}(R'_B)^*\ ,\end{aligned} \tag{14.40}$$

R'_B being the rotation that carries the magnetic frame at $t'_{\rm L}$ into the frame Σ.

The kernels $\hat{\mathcal{G}}_{KQ,K'Q'}$ are a generalization of the multipolar kernels $\mathcal{G}_{KQ,K'Q}$ introduced in Eq. (14.28). Since these quantities depend on the magnetic field's direction at different optical depths, in general they do not satisfy specific symmetry properties. However, if the magnetic field's direction is independent of optical depth, and if the x-axis of the magnetic frame is chosen to lie in the plane containing the vertical to the atmosphere and the magnetic field vector itself ($\gamma_B = 0$ in Eq. (14.4)), it can be shown, using Eqs. (14.29) and (2.68), that the kernels $\hat{\mathcal{G}}_{KQ,K'Q'}$ are real and obey the symmetry property

$$\hat{\mathcal{G}}_{K'Q',KQ}(x) = \hat{\mathcal{G}}_{KQ,K'Q'}(x)\ . \tag{14.41}$$

[1] The local magnetic frame has the z-axis directed along the local magnetic field.

Moreover, they obey the integral properties

$$\int_0^\infty \hat{\mathcal{G}}_{00,00}(x)\,\mathrm{d}x = \frac{1}{2}\,, \qquad \int_0^\infty \hat{\mathcal{G}}_{00,2Q}(x)\,\mathrm{d}x = 0\,,$$
$$\int_0^\infty \hat{\mathcal{G}}_{2Q,2Q'}(x)\,\mathrm{d}x = \delta_{QQ'}\,\frac{7}{20}\,W_2(J_\ell, J_u)\,, \tag{14.42}$$

which follow from Eqs. (14.32) and (2.72).[1] As shown in App. 22, these properties allow one to prove a further generalization of the $\sqrt{\epsilon}$-law (see Eq. (A22.14)), holding in the case of a homogeneous, isothermal atmosphere permeated by a depth-independent magnetic field.

An important application of Eq. (14.39) concerns the case of an atmosphere embedded in a turbulent magnetic field. To deal with this case, it is convenient to cast the equation in the equivalent form

$$\big[S_Q^K(t_\mathrm{L})\big]_\mathrm{M} = \delta_{K0}\,\delta_{Q0}\,\epsilon'\,B_\mathrm{P}(T) + \sum_{K'=0,2}\sum_{Q'}\int_0^\infty \frac{\hat{\mathcal{G}}_{KQ,K'Q'}\big(|t'_\mathrm{L}-t_\mathrm{L}|\big)}{1+\epsilon+\delta_u^{(K)}+\mathrm{i}H_uQ}\,\big[S_{Q'}^{K'}(t'_\mathrm{L})\big]_\mathrm{M}\,\mathrm{d}t'_\mathrm{L}\,,$$

and then to return to the fixed reference system Σ through Eqs. (14.37) and (14.38). As a result of this back-transformation we obtain the further equivalent equation

$$S_Q^K(t_\mathrm{L}) = \delta_{K0}\,\delta_{Q0}\,\epsilon'\,B_\mathrm{P}(T) + \sum_{K'=0,2}\sum_{Q'} M_{QQ'}^K(t_\mathrm{L})\int_0^\infty \mathcal{G}_{KQ',K'Q'}\big(|t'_\mathrm{L}-t_\mathrm{L}|\big)\,S_{Q'}^{K'}(t'_\mathrm{L})\,\mathrm{d}t'_\mathrm{L}\,, \tag{14.43}$$

where

$$M_{QQ'}^K(t_\mathrm{L}) = \sum_{Q''}\mathcal{D}_{Q''Q}^K(R_B)^*\,\mathcal{D}_{Q''Q'}^K(R_B)\,\frac{1}{1+\epsilon+\delta_u^{(K)}+\mathrm{i}\,Q''H_u}\,.$$

The quantity $M_{QQ'}^K(t_\mathrm{L})$ now introduced bears a strong resemblance with the magnetic kernel $\mathcal{M}_{QQ'}^K(\vec{B})$ defined in Eq. (5.166). Indeed, from Eqs. (14.4) and (2.71) we have

$$M_{QQ'}^K(t_\mathrm{L}) = \sum_{Q''}\mathcal{D}_{QQ''}^K(\chi_B\theta_B\gamma_B)\,\mathcal{D}_{Q''Q'}^K(-\gamma_B-\theta_B-\chi_B)\,\frac{1}{1+\epsilon+\delta_u^{(K)}+\mathrm{i}\,Q''H_u}\,,$$

[1] Equations (14.42) are valid (provided the magnetic field's direction is depth-independent) irrespective of the value of γ_B.

which is the same as Eq. (5.166) except for a slight difference in the denominator of the last factor.

Equation (14.43) can conveniently be used to handle the case of an atmosphere pervaded by a microturbulent magnetic field. By 'microturbulent' we mean here that, at any optical depth, the magnetic field has an isotropic distribution of directions and that the direction at optical depth $t_{\rm L}$ is uncorrelated with the direction at optical depth $t'_{\rm L}$, no matter how close the two points are in space. Under this hypothesis, and under the further assumption that the quantities ϵ, $\delta_u^{(K)}$, $B_{\rm P}$, and H_u are deterministic, one obtains, averaging over the distribution of magnetic fields at each depth

$$\begin{aligned}\left\langle S_Q^K(t_{\rm L})\right\rangle = {} & \delta_{K0}\,\delta_{Q0}\,\epsilon'\,B_{\rm P}(T) \\ & + \sum_{K'=0,2}\ \sum_{Q'} \left\langle M_{QQ'}^K(t_{\rm L})\right\rangle \int_0^\infty \mathcal{G}_{KQ',K'Q'}\big(|t'_{\rm L}-t_{\rm L}|\big)\left\langle S_{Q'}^{K'}(t'_{\rm L})\right\rangle {\rm d}t'_{\rm L}\,. \qquad (14.44)\end{aligned}$$

The components of the averaged magnetic kernel $\langle M_{QQ'}^K(t_{\rm L})\rangle$ are easily obtained by comparison with Eqs. (5.170)-(5.173). One gets

$$\left\langle M_{00}^0(t_{\rm L})\right\rangle = \frac{1}{1+\epsilon}\,, \qquad \left\langle M_{QQ'}^2(t_{\rm L})\right\rangle = \delta_{QQ'}\,\frac{1}{1+\epsilon+\delta_u^{(2)}}\,\mu_2(t_{\rm L})\,, \qquad (14.45)$$

where

$$\mu_2(t_{\rm L}) = \frac{1}{5}\left[1+\frac{2}{1+(H'_u)^2}+\frac{2}{1+4(H'_u)^2}\right],$$

with

$$H'_u = \frac{H_u}{1+\epsilon+\delta_u^{(2)}}\,.$$

Using Eqs. (14.45) and (14.30), it is easily seen that Eq. (14.44) reduces to a system of coupled integral equations involving only the two quantities $\langle S_0^0(t_{\rm L})\rangle$ and $\langle S_0^2(t_{\rm L})\rangle$, namely

$$\begin{aligned}(1+\epsilon)\left\langle S_0^0(t_{\rm L})\right\rangle = {} & \epsilon\,B_{\rm P}(T) + \int_0^\infty \mathcal{G}_{00,00}\big(|t'_{\rm L}-t_{\rm L}|\big)\left\langle S_0^0(t'_{\rm L})\right\rangle {\rm d}t'_{\rm L} \\ & + \int_0^\infty \mathcal{G}_{00,20}\big(|t'_{\rm L}-t_{\rm L}|\big)\left\langle S_0^2(t'_{\rm L})\right\rangle {\rm d}t'_{\rm L}\end{aligned}$$

$$\begin{aligned}(1+\epsilon+\delta_u^{(2)})\left\langle S_0^2(t_{\rm L})\right\rangle = \mu_2(t_{\rm L})\Bigg[& \int_0^\infty \mathcal{G}_{20,00}\big(|t'_{\rm L}-t_{\rm L}|\big)\left\langle S_0^0(t'_{\rm L})\right\rangle {\rm d}t'_{\rm L} \\ & + \int_0^\infty \mathcal{G}_{20,20}\big(|t'_{\rm L}-t_{\rm L}|\big)\left\langle S_0^2(t'_{\rm L})\right\rangle {\rm d}t'_{\rm L}\Bigg]. \qquad (14.46)\end{aligned}$$

Apart from the presence of the factor $\mu_2(t_{\rm L})$ in the right-hand side of the second equation, this is the same as the system holding for $S^0_0(t_{\rm L})$ and $S^2_0(t_{\rm L})$ in a non-magnetic atmosphere (cf. Eqs. (14.35)),[1] and obviously reduces to it under the limit $H'_u \to 0$. Formally, one can pass from the non-magnetic to the 'turbulent' atmosphere by the simple transformations

$$\mathcal{G}_{20,00}\big(|t'_{\rm L} - t_{\rm L}|\big) \to \mu_2(t_{\rm L})\, \mathcal{G}_{20,00}\big(|t'_{\rm L} - t_{\rm L}|\big)$$

$$\mathcal{G}_{20,20}\big(|t'_{\rm L} - t_{\rm L}|\big) \to \mu_2(t_{\rm L})\, \mathcal{G}_{20,20}\big(|t'_{\rm L} - t_{\rm L}|\big)\ .$$

It is important to remark that, even in the case of a depth-independent turbulent field ($\mu_2(t_{\rm L}) = $ const.), these transformations imply $\mathcal{G}_{00,20}(x) \neq \mathcal{G}_{20,00}(x)$. As a consequence, the generalized $\sqrt{\epsilon}$ - law does not hold for the turbulent-field atmosphere.

One can also consider the case of a horizontal magnetic field with random azimuth distribution. Following the same line of reasoning, one still gets Eqs. (14.46) with the depolarizing factor $\mu_2(t_{\rm L})$ replaced by

$$\mu'_2(t_{\rm L}) = \frac{1}{4}\left[1 + \frac{3}{1 + 4(H'_u)^2}\right]\ .$$

14.3. The Two-Level Atom: Non-LTE Theory for Strong Magnetic Fields

The results obtained in the former section are restricted to a physical regime where the magnetic field is either zero or, if present, is so weak that the Larmor frequency $\nu_{\rm L}$ is much smaller than the Doppler broadening $\Delta\nu_{\rm D}$. When this inequality is not satisfied, one enters a different regime that can be simply referred to as the 'strong field regime'.[2] From one side, the Larmor frequency is much larger than the inverse lifetime of the upper level γ_u, and from the other side it is comparable with or even larger than $\Delta\nu_{\rm D}$. As explained in Sect. 13.1, the formalism developed in this book – based on the flat-spectrum assumption – can still be applied in this physical regime provided all interferences between different Zeeman sublevels are neglected a priori. Under this approximation, the atom is described only in terms of populations of Zeeman sublevels, i.e., only by the diagonal elements of the density matrix $\rho_{\alpha J}(M, M)$ in the standard representation, or only by the components $\rho^K_0(\alpha J)$ in the statistical tensor representation.

---

[1] In Eqs. (14.35), $\delta^{(2)}_u$ was set to zero. Moreover, ϵ and $B_{\rm P}(T)$ were assumed to be depth-independent, but this does not change the structure of the equations.

[2] According to the classification proposed in Sect. 5.16, we deal here with regimes III, IV and V of panel (a) in Fig. 5.18.

In this section we present another example of the general non-LTE problem of the 2nd kind by considering, similarly to the previous section, a two-level atom without hyperfine structure and with unpolarized lower level. We suppose again that a collection of such atoms is distributed within a static medium of arbitrary shape, where it interacts with a strong magnetic field and with a population of colliding particles having a Maxwellian distribution of velocities. We assume, as in the former section, that the atoms themselves have a Maxwellian distribution of velocities characterized by the parameter $\Delta\nu_{\rm D}$, and that the radiation field is weak so that stimulated emission can be neglected. Finally, we adopt again the approximation of complete redistribution on velocities and, to avoid the introduction of a too heavy formalism, we suppose that the Doppler broadening $\Delta\nu_{\rm D}$ and the magnetic field vector are constant throughout the medium, whereas we do not impose any restriction on the spatial variation of the other physical parameters. The derivation presented below follows closely the line of reasoning of the former section. A similar derivation has been given by Landi Degl'Innocenti et al. (1991).

At a point P of the medium, having coordinate $\vec{x}$, we write the statistical equilibrium equation for the multipole moments of the density matrix, defined in the reference system of the magnetic field. To this aim, we use for the radiative rates the expressions developed in Sect. 7.4 and, in particular, Eqs. (7.20a) and (7.20e), whereas for the collisional rates we adopt the same expressions as those of the former section (see Sect. 7.13.d). Recalling the hypothesis of the unpolarized lower level, neglecting stimulated emission, taking into account the approximation of complete redistribution on velocities through the 'recipe' of Eq. (13.8), and performing some algebra along the lines of the former section, one obtains, in stationary situations, the following equation

$$\left[1+\epsilon+\delta_u^{(K)}\right]\left[\rho_0^K(\alpha_u J_u)\right]_{\vec{x}} = \frac{c^2}{2h\nu_0^3}\sqrt{\frac{2J_u+1}{2J_\ell+1}}$$

$$\times\Bigg\{\sum_{K'}\Bigg[\sqrt{3(2J_u+1)(2K+1)(2K'+1)}\sum_{M_u M_\ell q}(-1)^{1+J_u-M_\ell}$$

$$\times\begin{pmatrix} J_u & J_\ell & 1\\ -M_u & M_\ell & -q\end{pmatrix}^2\begin{pmatrix} J_u & J_u & K\\ M_u & -M_u & 0\end{pmatrix}\begin{pmatrix} 1 & 1 & K'\\ q & -q & 0\end{pmatrix}$$

$$\times\ \bar{J}_0^{K'}(\nu_{\alpha_u J_u M_u,\,\alpha_\ell J_\ell M_\ell})\Bigg] \ +\ \delta_{K0}\,\epsilon\,B_{\rm P}(T)\Bigg\}\left[\rho_0^0(\alpha_\ell J_\ell)\right]_{\vec{x}}\,, \qquad (14.47)$$

with $\bar{J}_0^{K'}(\nu_{\alpha_u J_u M_u,\,\alpha_\ell J_\ell M_\ell})$ defined according to Eqs. (14.5) and (14.6).

The quantity in square brackets in the right-hand side of Eq. (14.47) can be expressed in terms of the convolution of the generalized profiles defined in Eq. (10.40) with the velocity distribution of atoms. Such convolution has already been introduced in Chap. 13 and denoted by the symbol $\hat{\Phi}_Q^{KK'}(J_\ell, J_u\,;\nu)$ – see Eq. (13.20). Here we define a slightly different quantity by setting, for $Q=0$

$$\tilde{\Phi}_0^{KK'}(J_\ell, J_u\,;\nu) = \sqrt{3(2J_u+1)(2K+1)(2K'+1)}$$
$$\times \sum_{M_u M_\ell q} (-1)^{1+J_u-M_u+q} \begin{pmatrix} J_u & J_\ell & 1 \\ -M_u & M_\ell & -q \end{pmatrix}^2 \begin{pmatrix} J_u & J_u & K \\ M_u & -M_u & 0 \end{pmatrix}$$
$$\times \begin{pmatrix} 1 & 1 & K' \\ q & -q & 0 \end{pmatrix} p(\nu_{\alpha_u J_u M_u,\, \alpha_\ell J_\ell M_\ell} - \nu)\,, \tag{14.48}$$

where the profile p is given by Eq. (14.6).[1] With this position, Eq. (14.47) takes the form

$$\left[1+\epsilon+\delta_u^{(K)}\right]\left[\rho_0^K(\alpha_u J_u)\right]_{\vec{x}} = \frac{c^2}{2h\nu_0^3}\sqrt{\frac{2J_u+1}{2J_\ell+1}}$$
$$\times \left\{ \sum_{K'} \int_{-\infty}^{\infty} \mathrm{d}\nu\ \tilde{\Phi}_0^{KK'}(J_\ell, J_u\,;\nu)\, J_0^{K'}(\nu) \;+\; \delta_{K0}\,\epsilon\, B_{\mathrm{P}}(T) \right\} \left[\rho_0^0(\alpha_\ell J_\ell)\right]_{\vec{x}}\,,$$

or, introducing the irreducible components of the two-level source function defined in Eq. (14.10)[2]

$$\left[1+\epsilon+\delta_u^{(K)}\right]\left[S_0^K(\vec{x}\,)\right]_{\mathrm{M}} = \delta_{K0}\,\epsilon\, B_{\mathrm{P}}(T)$$
$$+ \sum_{K'} \int_{-\infty}^{\infty} \mathrm{d}\nu\ \tilde{\Phi}_0^{KK'}(J_\ell, J_u\,;\nu)\, J_0^{K'}(\nu)\,. \tag{14.49}$$

Next we turn to the radiative transfer equation. Neglecting stimulated emission, the Stokes parameters of the radiation propagating through point P along the direction $\vec{\Omega}$ (defined according to the reference direction $\vec{e}_a(\vec{\Omega})$ of Fig. 14.4) obey the transfer equation (14.14), with the propagation matrix $\boldsymbol{K}^{\mathrm{A}}$ explicitly given by (see Eqs. (6.86), (6.87))

$$\boldsymbol{K}^{\mathrm{A}} = \begin{pmatrix} \eta_0^{\mathrm{A}}(\nu,\vec{\Omega}) & \eta_1^{\mathrm{A}}(\nu,\vec{\Omega}) & \eta_2^{\mathrm{A}}(\nu,\vec{\Omega}) & \eta_3^{\mathrm{A}}(\nu,\vec{\Omega}) \\ \eta_1^{\mathrm{A}}(\nu,\vec{\Omega}) & \eta_0^{\mathrm{A}}(\nu,\vec{\Omega}) & \rho_3^{\mathrm{A}}(\nu,\vec{\Omega}) & -\rho_2^{\mathrm{A}}(\nu,\vec{\Omega}) \\ \eta_2^{\mathrm{A}}(\nu,\vec{\Omega}) & -\rho_3^{\mathrm{A}}(\nu,\vec{\Omega}) & \eta_0^{\mathrm{A}}(\nu,\vec{\Omega}) & \rho_1^{\mathrm{A}}(\nu,\vec{\Omega}) \\ \eta_3^{\mathrm{A}}(\nu,\vec{\Omega}) & \rho_2^{\mathrm{A}}(\nu,\vec{\Omega}) & -\rho_1^{\mathrm{A}}(\nu,\vec{\Omega}) & \eta_0^{\mathrm{A}}(\nu,\vec{\Omega}) \end{pmatrix}\,. \tag{14.50}$$

[1] The two quantities $\hat{\Phi}_0^{KK'}$ and $\tilde{\Phi}_0^{KK'}$ just differ in the fact that the first is a weighted sum of Voigt profiles centered at the individual frequencies of the Zeeman components of the transition, while in the second the Voigt profiles are replaced by Gaussian profiles.

[2] Consistently with the notations employed in the former section, we use the symbol $[S_Q^K(\vec{x})]_{\mathrm{M}}$ to recall that the irreducible components of the source function are defined in the magnetic reference system.

The radiative transfer coefficients η_i^{A}, ρ_i^{A}, and ε_i can be found from Eqs. (7.21). Taking into account the hypothesis of complete redistribution on velocities, neglecting for consistency the finite width of the levels, and recalling the definition of the symbol $\tilde{\Phi}_0^{KK'}$ of Eq. (14.48), one has (see Eq. (A13.9))

$$\eta_i^{\mathrm{A}}(\nu,\vec{\Omega}) = k_{\mathrm{L}}^{\mathrm{A}} \sum_K \mathcal{T}_0^K(i,\vec{\Omega})\, \tilde{\Phi}_0^{0K}(J_\ell, J_u\,;\nu)\ , \tag{14.51}$$

where $k_{\mathrm{L}}^{\mathrm{A}}$ is given by Eq. (14.15). Similarly (see Eq. (A13.14))

$$\rho_i^{\mathrm{A}}(\nu,\vec{\Omega}) = k_{\mathrm{L}}^{\mathrm{A}} \sum_K \mathcal{T}_0^K(i,\vec{\Omega})\, \tilde{\Psi}_0^{0K}(J_\ell, J_u\,;\nu)\ , \tag{14.52}$$

where $\tilde{\Psi}_0^{0K}(J_\ell, J_u\,;\nu)$ is the same as $\tilde{\Phi}_0^{0K}(J_\ell, J_u\,;\nu)$ except for the replacement of the Gaussian profile $p(\nu_0-\nu)$ with the associated dispersion profile $q(\nu_0-\nu)$ given by (see Eqs. (5.44) and (5.55))

$$q(\nu_0-\nu) = \frac{2}{\pi\,\Delta\nu_{\mathrm{D}}}\, D\!\left(\frac{\nu_0-\nu}{\Delta\nu_{\mathrm{D}}}\right)\ , \tag{14.53}$$

where D is the Dawson function defined in Eq. (5.56). Finally (see Eqs. (A13.8), (7.8), (14.10), (10.6), and (14.15))

$$\varepsilon_i(\nu,\vec{\Omega}) = k_{\mathrm{L}}^{\mathrm{A}} \sum_{KK'} \mathcal{T}_0^{K'}(i,\vec{\Omega})\, \left[S_0^K(\vec{x})\right]_{\mathrm{M}}\, \tilde{\Phi}_0^{KK'}(J_\ell, J_u\,;\nu)\ . \tag{14.54}$$

The radiative transfer equation can be solved by the methods developed in Chap. 8. Substituting Eq. (14.54) into Eq. (8.14) and referring to Fig. 14.5, one obtains, for the Stokes parameters of the radiation propagating through point P along the direction $\vec{\Omega}$

$$\begin{aligned} I_i(\nu,\vec{\Omega}) = &\int_{\vec{x}_0}^{\vec{x}} \sum_{j=0}^{3} O_{ij}(\vec{x},\vec{x}\,';\nu)\, k_{\mathrm{L}}^{\mathrm{A}}(\vec{x}\,') \sum_{KK'} \mathcal{T}_0^{K'}(j,\vec{\Omega})\, \left[S_0^K(\vec{x}\,')\right]_{\mathrm{M}}\, \tilde{\Phi}_0^{KK'}(J_\ell, J_u\,;\nu)\, \mathrm{d}s' \\ &+ \sum_{j=0}^{3} O_{ij}(\vec{x},\vec{x}_0;\nu)\, I_j^{(\mathrm{b})}(\nu,\vec{\Omega})\ , \end{aligned} \tag{14.55}$$

where $O_{ij}(\vec{x},\vec{x}\,';\nu)$ is the evolution operator between points $\vec{x}\,'$ and $\vec{x}$, s' is the coordinate of $\vec{x}\,'$ reckoned along the direction $\vec{\Omega}$, and $I_j^{(\mathrm{b})}(\nu,\vec{\Omega})$ are the Stokes parameters of the radiation entering the medium at point $\vec{x}_0$ and directed along $\vec{\Omega}$. Because of the assumption of constant magnetic field and Doppler broadening, the propagation matrix $\boldsymbol{K}^{\mathrm{A}}$ of Eq. (14.50) can be written, according to Eqs. (14.51) and (14.52), in the form

$$\boldsymbol{K}^{\mathrm{A}} = k_{\mathrm{L}}^{\mathrm{A}}\, \boldsymbol{H}(\nu,\vec{\Omega})\ , \tag{14.56}$$

where $k_{\rm L}^{\rm A}$ depends on $\vec{x}$, while the matrix $\boldsymbol{H}$ depends on frequency and direction but is independent of $\vec{x}$. It follows that the evolution operator has the form of Eq. (8.22),

$$O_{ij}(\vec{x},\vec{x}\,';\nu) = \left[\mathrm{e}^{-\tau(\vec{x},\vec{x}\,')\,\boldsymbol{H}(\nu,\vec{\Omega})}\right]_{ij} , \tag{14.57}$$

where

$$\tau(\vec{x},\vec{x}\,') = \int_{\vec{x}\,'}^{\vec{x}} k_{\rm L}^{\rm A}(\vec{x}\,'')\;\mathrm{d}s'' .$$

Using Eq. (14.55), it is now possible to find an expression for the radiation field tensor $J_0^K(\nu)$ to be substituted into the statistical equilibrium equation (14.49). From the definition in Eqs. (5.157) one gets

$$J_0^K(\nu) = \left[J_0^K(\nu)\right]_{\rm I} + \left[J_0^K(\nu)\right]_{\rm E} , \tag{14.58}$$

where the 'internal' part $[J_0^K(\nu)]_{\rm I}$ is given by

$$\left[J_0^K(\nu)\right]_{\rm I} = \oint \frac{\mathrm{d}\Omega}{4\pi} \sum_{i=0}^{3} \mathcal{T}_0^K(i,\vec{\Omega}) \int_{\vec{x}_0}^{\vec{x}} \mathrm{d}s' \sum_{j=0}^{3} O_{ij}(\vec{x},\vec{x}\,';\nu)\; k_{\rm L}^{\rm A}(\vec{x}\,')$$

$$\times \sum_{K'K''} \mathcal{T}_0^{K''}(j,\vec{\Omega}) \left[S_0^{K'}(\vec{x}\,')\right]_{\rm M} \tilde{\Phi}_0^{K'K''}(J_\ell, J_u;\nu) ,$$

and the 'external' part $[J_0^K(\nu)]_{\rm E}$ by

$$\left[J_0^K(\nu)\right]_{\rm E} = \oint \frac{\mathrm{d}\Omega}{4\pi} \sum_{i=0}^{3} \mathcal{T}_0^K(i,\vec{\Omega}) \sum_{j=0}^{3} O_{ij}(\vec{x},\vec{x}_0\,;\nu)\; I_j^{(\rm b)}(\nu,\vec{\Omega}) .$$

Now we substitute Eq. (14.58) into Eq. (14.49) and transform the double integral over $\mathrm{d}\Omega$ and $\mathrm{d}s'$ into an integral in $\mathrm{d}^3\vec{x}\,'$ (see Eq. (14.21)). This leads to the following equation

$$\left[1+\epsilon+\delta_u^{(K)}\right]\left[S_0^K(\vec{x})\right]_{\rm M} = \delta_{K0}\,\epsilon\,B_{\rm P}(T) + \sum_{K'} \int_{-\infty}^{\infty} \mathrm{d}\nu\;\tilde{\Phi}_0^{KK'}(J_\ell, J_u\,;\nu) \left[J_0^{K'}(\nu)\right]_{\rm E}$$

$$+ \sum_{K'} \int \mathrm{d}^3\vec{x}\,' \;\frac{k_{\rm L}^{\rm A}(\vec{x}\,')}{4\pi(\vec{x}-\vec{x}\,')^2}\;\tilde{G}_{K0,K'0}(\vec{x},\vec{x}\,') \left[S_0^{K'}(\vec{x}\,')\right]_{\rm M} , \tag{14.59}$$

where

$$\tilde{G}_{K0,K'0}(\vec{x},\vec{x}') = \sum_{K''K'''} \int_{-\infty}^{\infty} \mathrm{d}\nu \;\; \tilde{\Phi}_0^{KK''}(J_\ell, J_u\,;\nu)\; \tilde{\Phi}_0^{K'K'''}(J_\ell, J_u\,;\nu) \times \sum_{i=0}^{3}\sum_{j=0}^{3} \mathcal{T}_0^{K''}(i,\vec{\Omega})\; O_{ij}(\vec{x},\vec{x}';\nu)\; \mathcal{T}_0^{K'''}(j,\vec{\Omega})\;. \qquad (14.60)$$

The quantities $\tilde{G}_{K0,K'0}$ are a natural generalization (though restricted to the values $Q = Q' = 0$) of the multipole coupling coefficients $G_{KQ,K'Q'}$ defined in Eq. (14.24). Their main properties are collected in App. 23.

Equation (14.59) is a system of linear, non-homogeneous, integral equations in the unknowns $[S_0^K(\vec{x})]_{\mathrm{M}}$. When the local properties of the medium and the boundary conditions are specified, the system can be solved, and the Stokes parameters of the radiation emerging from the medium can be computed by means of Eq. (14.55). Owing to property (A23.6), Eq. (14.59) decouples in two distinct sets of equations, involving the irreducible components of the source function of even rank ($K = 0, 2, \ldots$) and of odd rank ($K = 1, 3, \ldots$), respectively. In the latter, the only source terms may be provided by the radiation entering the medium through the boundary, and it can be shown, using property (A13.4) of the generalized profiles, that such terms are zero unless the boundary radiation field either contains some net circular polarization, or is characterized by I, Q, and U Stokes parameters that are not symmetrical about line center. Excluding these cases, all the components $[S_0^K(\vec{x})]_{\mathrm{M}}$ with K odd are everywhere zero in the medium, and one is left with the unknowns $[S_0^0(\vec{x})]_{\mathrm{M}}$, $[S_0^2(\vec{x})]_{\mathrm{M}}$, $\ldots$, $[S_0^{K_{\max}}(\vec{x})]_{\mathrm{M}}$, where

$$K_{\max} = \begin{cases} 2J_u & \text{if } J_u \text{ is integer} \\ 2J_u - 1 & \text{if } J_u \text{ is half-integer}\,. \end{cases} \qquad (14.61)$$

Similarly to the previous section, we can apply Eq. (14.59) to the special case of a plane-parallel, semi-infinite stellar atmosphere. Introducing the line optical depth of Eq. (14.25), and assuming that the atmosphere is not illuminated by external sources of radiation, we obtain

$$\Big[1 + \epsilon + \delta_u^{(K)}\Big]\big[S_0^K(t_{\mathrm{L}})\big]_{\mathrm{M}} = \delta_{K0}\,\epsilon\, B_{\mathrm{P}}(T) + \sum_{K'=0,2,\ldots,K_{\max}} \int_0^{\infty} \tilde{\mathcal{G}}_{K0,K'0}\big(|t'_{\mathrm{L}} - t_{\mathrm{L}}|\big)\,\big[S_0^{K'}(t'_{\mathrm{L}})\big]_{\mathrm{M}}\,\mathrm{d}t'_{\mathrm{L}}\;, \qquad (14.62)$$

where the kernels $\tilde{\mathcal{G}}_{K0,K'0}$ are given by (cf. Eq. (14.28))

$$\tilde{\mathcal{G}}_{K0,K'0}\big(|t'_{\mathrm{L}} - t_{\mathrm{L}}|\big) = \int_{-\infty}^{\infty}\mathrm{d}x' \int_{-\infty}^{\infty}\mathrm{d}y' \;\frac{\Delta\nu_{\mathrm{D}}}{4\pi(\vec{x}-\vec{x}')^2}\;\tilde{G}_{K0,K'0}(\vec{x},\vec{x}')\;. \qquad (14.63)$$

Performing some algebra similar to that developed in App. 21, Eq. (14.63) can be cast in the form

$$\tilde{\mathcal{G}}_{K0,K'0}(x) = \frac{\Delta\nu_{\rm D}}{4\pi} \int_0^{\pi/2} {\rm d}\theta \ \tan\theta \int_0^{2\pi} {\rm d}\chi \\ \times \sum_{i=0}^{3} \sum_{j=0}^{3} \sum_{K''K'''} \int_{-\infty}^{\infty} {\rm d}\nu \ \tilde{\Phi}_0^{KK''}(J_\ell, J_u\,;\nu)\, \tilde{\Phi}_0^{K'K'''}(J_\ell, J_u\,;\nu) \\ \times \mathcal{T}_0^{K''}(i,\vec{\Omega}) \left[{\rm e}^{-\frac{x\,\Delta\nu_{\rm D}}{\cos\theta}\,\boldsymbol{H}(\nu,\vec{\Omega})} \right]_{ij} \mathcal{T}_0^{K'''}(j,\vec{\Omega}) \ . \tag{14.64}$$

The kernels $\tilde{\mathcal{G}}_{K0,K'0}(x)$ obey some important properties. The first is the symmetry property

$$\tilde{\mathcal{G}}_{K'0,K0}(x) = \tilde{\mathcal{G}}_{K0,K'0}(x) \ , \tag{14.65}$$

which follows directly from the analogous property of the generalized multipole coupling coefficients (Eq. (A23.7)).

A second property concerns the integrals of some of the kernels $\tilde{\mathcal{G}}_{K0,K'0}$. One has

$$\int_0^{\infty} \tilde{\mathcal{G}}_{00,00}(x)\ {\rm d}x = \frac{1}{2} \ , \qquad\qquad \int_0^{\infty} \tilde{\mathcal{G}}_{00,20}(x)\ {\rm d}x = 0 \ . \tag{14.66}$$

To prove these properties, we observe that, using Eq. (9.106)

$$\int_0^{\infty} \left[{\rm e}^{-\frac{x\,\Delta\nu_{\rm D}}{\cos\theta}\,\boldsymbol{H}(\nu,\vec{\Omega})} \right]_{ij} {\rm d}x \ = \ \frac{\cos\theta}{\Delta\nu_{\rm D}} \left[\boldsymbol{H}^{-1}(\nu,\vec{\Omega})\right]_{ij} \ ,$$

where $\boldsymbol{H}^{-1}$ is the inverse of the matrix $\boldsymbol{H}$. On the other hand, from Eqs. (14.50), (14.51), and (14.56), we have

$$\sum_{K''} \tilde{\Phi}_0^{0K''}(J_\ell, J_u\,;\nu)\, \mathcal{T}_0^{K''}(i,\vec{\Omega}) = \left[\boldsymbol{H}(\nu,\vec{\Omega})\right]_{0i} \ , \tag{14.67}$$

so that

$$\int_0^{\infty} \tilde{\mathcal{G}}_{00,K'0}(x)\ {\rm d}x = \frac{1}{4\pi} \int_0^{\pi/2} {\rm d}\theta \ \sin\theta \int_0^{2\pi} {\rm d}\chi \ \sum_{K'''} \int_{-\infty}^{\infty} {\rm d}\nu \ \tilde{\Phi}_0^{K'K'''}(J_\ell, J_u\,;\nu)\, \mathcal{T}_0^{K'''}(0,\vec{\Omega}) \ .$$

Taking finally into account Eq. (A13.3), and considering that (see Table 5.6)

$$\frac{1}{4\pi} \int_0^{\pi/2} {\rm d}\theta \ \sin\theta \int_0^{2\pi} {\rm d}\chi \ \mathcal{T}_0^0(0,\vec{\Omega}) = \frac{1}{2} \ , \qquad \frac{1}{4\pi} \int_0^{\pi/2} {\rm d}\theta \ \sin\theta \int_0^{2\pi} {\rm d}\chi \ \mathcal{T}_0^2(0,\vec{\Omega}) = 0 \ ,$$

we obtain the results in Eq. (14.66).

The properties expressed by Eqs. (14.65) and (14.66) are particularly important because they allow one to prove that, for a homogeneous and isothermal atmosphere, the $\sqrt{\epsilon}$-law can be extended to the strong field regime analyzed in this section. Such generalized $\sqrt{\epsilon}$-law is given by Eq. (A22.15).

It should be remarked that Eq. (14.62) holds without any limitation on the variation of the different parameters with optical depth. The quantities ϵ, $\delta_u^{(K)}$ and $B_{\rm P}$ appearing in the equation can be arbitrary functions of optical depth (contrary to the magnetic field vector which is assumed to be constant). A full analysis of the solution of Eq. (14.62) for different atomic transitions, different values and/or depth dependence of the above-mentioned parameters, and different inclinations and strengths of the magnetic field vector is well outside the aims of this book. Some numerical results can be found in Bommier and Landi Degl'Innocenti (1996). It should also be mentioned that integral equations similar to Eq. (14.62) and containing the basic physical aspects of the problem of line formation in a (strong) magnetic field with population unbalances among Zeeman sublevels were derived, using more standard formalisms, by Domke (1969, 1971) and by Landi Degl'Innocenti (1978b).

14.4. The Non-LTE Regime of Order 1.5

The formalism developed in the former section is suitable to discuss in some detail the special case of the non-LTE problem that has been classified in Sect. 14.1 as non-LTE of order 1.5. This is an intermediate non-LTE regime where it is assumed that the atomic system is not polarized whereas the radiation field, because of the presence of a magnetic field, is polarized. As mentioned in Sect. 14.1, this physical situation has received considerable attention in the literature because it is considered appropriate to describe the process of formation of weak or medium-strong spectral lines in relatively dense and strongly magnetized plasmas, like sunspots or the atmospheres of magnetic stars. Owing to the relatively high density of the plasma, it is believed that depolarizing collisions are so efficient to completely destroy atomic polarization, which considerably simplifies the description of the atomic system.

Restricting our analysis to a two-level atom, the non-LTE problem of order 1.5 reduces to the solution of the following equation (obtained from Eq. (14.62) under the limit $\delta_u^{(K)} \to \infty$ for $K = 2, 4, \ldots, K_{\max}$, with $K_{\max}$ given by Eq. (14.61))[1]

$$(1+\epsilon)\, S_0^0(t_{\rm L}) = \epsilon\, B_{\rm P}(T) + \int_0^\infty \tilde{\mathcal{G}}_{00,00}\big(|t'_{\rm L} - t_{\rm L}|\big)\, S_0^0(t'_{\rm L})\, {\rm d}t'_{\rm L}\ , \tag{14.68}$$

where we have omitted the bracket $[\ldots]_{\rm M}$ around the symbol $S_0^0(t_{\rm L})$ because this

[1] Equation (14.62) holds for a two-level atom with unpolarized lower level. In the present regime, both levels are unpolarized by definition.

component of the source function does not depend on the reference system (see Eq. (14.38)).

The explicit expression of the kernel can be obtained from Eq. (14.64) with the help of Eq. (14.67). One gets

$$\tilde{\mathcal{G}}_{00,00}(x) = \frac{\Delta\nu_{\rm D}}{4\pi} \int_0^{\pi/2} {\rm d}\theta \ \tan\theta \int_0^{2\pi} {\rm d}\chi \int_{-\infty}^{\infty} {\rm d}\nu \ \mathcal{H} \ , \tag{14.69}$$

where the quantity $\mathcal{H}$ is defined by

$$\mathcal{H} = \Big[\boldsymbol{H}(\nu,\vec{\Omega}) \ {\rm e}^{-\frac{x\,\Delta\nu_{\rm D}}{\cos\theta}\,\boldsymbol{H}(\nu,\vec{\Omega})} \ \boldsymbol{H}(\nu,\vec{\Omega}) \Big]_{00} \ . \tag{14.70}$$

In order to simplify Eq. (14.68), two different approximations have been proposed in the literature, referred to as the *field-free* and the *polarization-free* approximation, respectively. The former (Rees, 1969) is based on the substitution of the quantity $\mathcal{H}$ with its limiting value obtained by setting to zero the magnetic field. In other words, with evident notations

$$\mathcal{H}_{\rm f.f.} = \lim_{\vec{B}\to 0} \ \mathcal{H} \ .$$

From Eqs. (14.51)-(14.52), using Eqs. (A23.2) and (A23.3), it can easily be seen that under this limit the matrix $\boldsymbol{H}$ reduces to

$$\big[\boldsymbol{H}(\nu,\vec{\Omega})\big]_{ij} = \ \delta_{ij} \ p(\nu_0 - \nu) \ ,$$

where $p(\nu_0 - \nu)$ is the profile defined in Eq. (14.6). Substitution into Eq. (14.70) shows that the kernel $\tilde{\mathcal{G}}_{00,00}$ takes the form

$$\Big[\tilde{\mathcal{G}}_{00,00}(x)\Big]_{\rm f.f.} = \frac{1}{2} \int_{-\infty}^{\infty} {\rm d}v \ \big[\varphi(v)\big]^2 \, E_1\big(x\varphi(v)\big) \ ,$$

where v and $\varphi(v)$ are defined in Eq. (14.31), and where E_1 is the first exponential integral defined in Eq. (12.6). Obviously, under this approximation Eq. (14.68) reduces to the standard equation of the non-LTE problem of the 1$^{\rm st}$ kind, and $S_0^0(t_{\rm L})$ is just the corresponding source function.

The polarization-free approximation (Trujillo Bueno and Landi Degl'Innocenti, 1996) is in principle less restrictive. It consists in retaining the diagonal elements of the matrix $\boldsymbol{H}(\nu,\vec{\Omega})$ while setting to zero the off-diagonal ones. In this approximation one has

$$\big[\boldsymbol{H}(\nu,\vec{\Omega})\big]_{ij} = \ \delta_{ij} \ h_0(\nu,\vec{\Omega}) \ ,$$

where $h_0(\nu,\vec{\Omega})$ is given by (cf. Eqs. (14.51) and (14.56))

$$h_0(\nu,\vec{\Omega}) = \frac{\eta_0^{\mathrm{A}}(\nu,\vec{\Omega})}{k_{\mathrm{L}}^{\mathrm{A}}} = \sum_K \mathcal{T}_0^K(0,\vec{\Omega})\,\tilde{\Phi}_0^{0K}(J_\ell, J_u\,;\nu)\ .$$

One then gets, substituting into Eqs. (14.69)-(14.70) and performing the integration over χ

$$\left[\tilde{\mathcal{G}}_{00,00}(x)\right]_{\mathrm{p.f.}} = \frac{\Delta\nu_{\mathrm{D}}}{2}\int_0^{\pi/2} \mathrm{d}\theta\ \tan\theta \int_{-\infty}^{\infty} \mathrm{d}\nu\ \left[h_0(\nu,\vec{\Omega})\right]^2\ \mathrm{e}^{-\frac{x\,\Delta\nu_{\mathrm{D}}}{\cos\theta}\,h_0(\nu,\vec{\Omega})}\ .$$

It should be remarked that, although the field-free and the polarization-free approximations have been discussed here in the special case of a two-level atom, they are indeed more general and can be applied to multi-level atoms as well. Given a model atmosphere, the field-free approximation, for instance, tackles the non-LTE problem of order 1.5 through the following strategy: a) the statistical equilibrium equations for the level populations are solved as if the magnetic field were not present; b) from such values, and from the value of the magnetic field vector, one finds the expressions of the radiative transfer coefficients; c) the radiative transfer equation is finally solved for any desired line of sight. This procedure implies the use of a standard non-LTE numerical code for the solution of the statistical equilibrium equations (point a). The complications arising from the presence of the magnetic field and from polarization only intervene at points b) and c), when the self-consistency loop has already been solved. Given its simplicity, the field-free approximation has been widely used in the past, especially to compute theoretical Stokes profiles of weak or medium-strong spectral lines originating from magnetized atmospheres of relatively high density, such as sunspots or Ap stars.

14.5. The Non-LTE Problem for More Complicated Atomic Models

In Sects. 14.2 and 14.3 we have analyzed the non-LTE problem of the 2$^{\mathrm{nd}}$ kind for a two-level atom with unpolarized lower level. The hypothesis of the absence of atomic polarization in the lower level, joined with the further hypothesis of neglecting stimulated emission, has allowed us to reduce the general non-LTE problem (summarized by the self-consistency loop of Fig. 14.1) to the solution of a linear system of integral equations. However, this linearity property is strictly confined to the particular case just mentioned. It is no longer valid both when a model atom with more than two levels is considered and, even for a two-level model atom, when either the approximation of the unpolarized lower level or the approximation of neglecting stimulated emission cannot be applied. In such cases, the solution of the self-consistency loop has to be performed by means of numerical algorithms, and it is usually impossible to establish general analytical results.

As an illustration of the problems involved, we consider in this section the simplest possible atomic model leading to a non-linear set of equations, namely a

two-level atom having $J_\ell = 1$ and $J_u = 0$. Following Trujillo Bueno and Landi Degl'Innocenti (1997), we introduce the same hypotheses as those specified at the beginning of Sect. 14.2[1] for treating the case of the two-level atom with unpolarized lower level. In addition, we assume that there is no magnetic field, and that the medium is cylindrically symmetrical about an axis (that we take as the z-axis of our reference system) and is not illuminated from the boundary by circularly polarized radiation. Under these conditions, the only non-zero components of the radiation field tensor are J^0_0 and J^2_0, and the only non-zero statistical tensors are $\rho^0_0(\alpha_\ell J_\ell)$, $\rho^2_0(\alpha_\ell J_\ell)$, and $\rho^0_0(\alpha_u J_u)$ – cf. Sect. 10.7.

The statistical equilibrium equations can be derived from Eqs. (10.1) and (10.2) by setting $\nu_{\rm L} = 0$ and by evaluating the rates for the transition $(J_\ell = 1, J_u = 0)$. Taking into account Eqs. (7.14a), (7.14b), (7.14d) and (7.14e), and performing on the radiation field tensor the substitution of Eq. (13.8) implied by the approximation of complete redistribution on velocities, one obtains, for the statistical tensors at point $\vec{x}$

$$\begin{aligned}
\frac{\mathrm{d}}{\mathrm{d}t}\left[\rho^0_0(\alpha_u J_u)\right]_{\vec{x}} &= -\Big[A(\alpha_u J_u \rightarrow \alpha_\ell J_\ell) + C^{(0)}_{\rm S}(\alpha_\ell J_\ell, \alpha_u J_u)\Big]\left[\rho^0_0(\alpha_u J_u)\right]_{\vec{x}} \\
&\quad + \sqrt{3}\, B(\alpha_\ell J_\ell \rightarrow \alpha_u J_u)\left\{\bar{J}^0_0(\nu_0)\left[\rho^0_0(\alpha_\ell J_\ell)\right]_{\vec{x}} + \bar{J}^2_0(\nu_0)\left[\rho^2_0(\alpha_\ell J_\ell)\right]_{\vec{x}}\right\} \\
&\quad + \sqrt{3}\, C^{(0)}_{\rm I}(\alpha_u J_u, \alpha_\ell J_\ell)\, \left[\rho^0_0(\alpha_\ell J_\ell)\right]_{\vec{x}}
\end{aligned}$$

$$\begin{aligned}
\frac{\mathrm{d}}{\mathrm{d}t}\left[\rho^2_0(\alpha_\ell J_\ell)\right]_{\vec{x}} &= -B(\alpha_\ell J_\ell \rightarrow \alpha_u J_u) \\
&\quad \times \left\{\bar{J}^2_0(\nu_0)\left[\rho^0_0(\alpha_\ell J_\ell)\right]_{\vec{x}} + \bar{J}^0_0(\nu_0)\left[\rho^2_0(\alpha_\ell J_\ell)\right]_{\vec{x}} - \frac{1}{\sqrt{2}}\,\bar{J}^2_0(\nu_0)\left[\rho^2_0(\alpha_\ell J_\ell)\right]_{\vec{x}}\right\} \\
&\quad - \Big[C^{(0)}_{\rm I}(\alpha_u J_u, \alpha_\ell J_\ell) + D^{(2)}(\alpha_\ell J_\ell)\Big]\left[\rho^2_0(\alpha_\ell J_\ell)\right]_{\vec{x}}\,,
\end{aligned}$$

where $\bar{J}^K_Q(\nu_0)$ is given by Eq. (14.5).

These two equations can be cast in a simpler form by introducing a scalar source function, $S(\vec{x}\,)$, defined by (cf. Eq. (14.10))

$$S(\vec{x}\,) = \frac{2h\nu_0^3}{c^2}\,\sqrt{3}\,\frac{\left[\rho^0_0(\alpha_u J_u)\right]_{\vec{x}}}{\left[\rho^0_0(\alpha_\ell J_\ell)\right]_{\vec{x}}}\,, \tag{14.71}$$

and a parameter, $\sigma(\vec{x}\,)$, describing the amount of alignment in the lower level

$$\sigma(\vec{x}\,) = \frac{\left[\rho^2_0(\alpha_\ell J_\ell)\right]_{\vec{x}}}{\left[\rho^0_0(\alpha_\ell J_\ell)\right]_{\vec{x}}}\,. \tag{14.72}$$

[1] The hypotheses are the following: static medium, atoms and colliding particles with Maxwellian velocity distributions, constant Doppler broadening, weak radiation field (negligible stimulated emission), flat-spectrum approximation, approximation of complete redistribution on velocities, negligible continuum opacity.

Use of Eqs. (10.49) and (7.8) allows one to rewrite the two equations, for stationary situations, in the form

$$(1+\epsilon)\, S(\vec{x}\,) = \bar{J}^0_0(\nu_0)\left[1 + \frac{1}{\sqrt{2}}\,\bar{w}\,\sigma(\vec{x}\,)\right] + \epsilon\, B_{\rm P}(T)$$

$$\sigma(\vec{x}\,) = -\frac{1}{\sqrt{2}}\,\frac{\bar{w}}{1 - \frac{1}{2}\,\bar{w} + \epsilon\beta + \delta_\ell}\,, \tag{14.73}$$

where $\bar{w}$ is the average anisotropy factor (cf. Eqs. (10.62))

$$\bar{w} = \sqrt{2}\,\frac{\bar{J}^2_0(\nu_0)}{\bar{J}^0_0(\nu_0)}\,,$$

ϵ is defined in Eqs. (14.7), $B_{\rm P}(T)$ is the Planck function in the Wien limit (see Eq. (14.9)), and where the quantities β and δ_ℓ are given by

$$\beta = \frac{B_{\rm P}(T)}{\bar{J}^0_0(\nu_0)}\,, \qquad\qquad \delta_\ell = \frac{D^{(2)}(\alpha_\ell J_\ell)}{B(\alpha_\ell J_\ell \to \alpha_u J_u)\,\bar{J}^0_0(\nu_0)}\,.$$

Equations (14.73) depend, either explicitly or implicitly through the parameters $\bar{w}$, β, and δ_ℓ, on the components of the radiation field tensor, $\bar{J}^0_0(\nu_0)$ and $\bar{J}^2_0(\nu_0)$, expressed at point $\vec{x}$. These quantities can be evaluated by solving the radiative transfer equation which, owing to the cylindrical symmetry of the medium, takes a particularly simple form. Defining the reference direction $\vec{e}_a(\vec{\Omega})$ to lie in the plane containing the z-axis and the direction $\vec{\Omega}$ (see Fig. 14.4 with $\gamma = 0$), and taking into account Eqs. (7.16a) and (7.16e) and the hypothesis of complete redistribution on velocities, one obtains

$$\frac{\mathrm{d}}{\mathrm{d}s}\begin{pmatrix} I(\nu,\vec{\Omega}) \\ Q(\nu,\vec{\Omega}) \end{pmatrix} = -k^{\rm A}_{\rm L}\; p(\nu_0 - \nu)\left[\begin{pmatrix} h_0 & h_1 \\ h_1 & h_0 \end{pmatrix}\begin{pmatrix} I(\nu,\vec{\Omega}) \\ Q(\nu,\vec{\Omega}) \end{pmatrix} - \begin{pmatrix} \varepsilon_0 \\ 0 \end{pmatrix}\right]\,, \tag{14.74}$$

where $k^{\rm A}_{\rm L}$ and $p(\nu_0 - \nu)$ are defined, respectively, in Eqs. (14.15) and (14.6), and where h_0, h_1, and ε_0 are given by

$$h_0 = 1 + \frac{1}{2\sqrt{2}}\left(3\cos^2\theta - 1\right)\sigma(\vec{x}\,)$$

$$h_1 = -\frac{3}{2\sqrt{2}}\,\sin^2\theta\;\sigma(\vec{x}\,)$$

$$\varepsilon_0 = S(\vec{x}\,)\,,$$

θ being the angle between the z-axis and the direction $\vec{\Omega}$ (see Fig. 14.4).

The radiative transfer equation can be solved through the methods outlined in Chap. 8 (see Eq. (8.28)). For a plane-parallel, semi-infinite atmosphere, introducing

the optical depth $t_{\rm L}$ of Eq. (14.25) and setting $\mu = \cos\theta$, one has, for the radiation at optical depth $t_{\rm L}$ propagating outward ($\mu > 0$)

$$I(\nu,\vec{\Omega}) = \frac{1}{2}\int\limits_{t_{\rm L}}^{\infty} \varphi(v)\, S(t'_{\rm L}) \left[\, {\rm e}^{-\frac{\varphi(v)\, H_+(t_{\rm L},t'_{\rm L})}{\mu}} + {\rm e}^{-\frac{\varphi(v)\, H_-(t_{\rm L},t'_{\rm L})}{\mu}} \,\right] \frac{{\rm d}t'_{\rm L}}{\mu}$$

$$Q(\nu,\vec{\Omega}) = \frac{1}{2}\int\limits_{t_{\rm L}}^{\infty} \varphi(v)\, S(t'_{\rm L}) \left[\, {\rm e}^{-\frac{\varphi(v)\, H_+(t_{\rm L},t'_{\rm L})}{\mu}} - {\rm e}^{-\frac{\varphi(v)\, H_-(t_{\rm L},t'_{\rm L})}{\mu}} \,\right] \frac{{\rm d}t'_{\rm L}}{\mu}\,, \qquad (14.75)$$

where v and $\varphi(v)$ are the reduced frequency and the Gaussian profile of Eq. (14.31), and where

$$H_+(t_{\rm L},t'_{\rm L}) = \int\limits_{t_{\rm L}}^{t'_{\rm L}} \left[1 + \frac{1}{\sqrt{2}}\left(3\mu^2 - 2\right)\sigma(t''_{\rm L})\right] {\rm d}t''_{\rm L}$$

$$H_-(t_{\rm L},t'_{\rm L}) = \int\limits_{t_{\rm L}}^{t'_{\rm L}} \left[1 + \frac{1}{\sqrt{2}}\,\sigma(t''_{\rm L})\right] {\rm d}t''_{\rm L}\,.$$

Similarly, for the radiation propagating inward ($\mu < 0$) one has

$$I(\nu,\vec{\Omega}) = \frac{1}{2}\int\limits_{0}^{t_{\rm L}} \varphi(v)\, S(t'_{\rm L}) \left[\, {\rm e}^{-\frac{\varphi(v)\, H_+(t'_{\rm L},t_{\rm L})}{|\mu|}} + {\rm e}^{-\frac{\varphi(v)\, H_-(t'_{\rm L},t_{\rm L})}{|\mu|}} \,\right] \frac{{\rm d}t'_{\rm L}}{|\mu|}$$

$$Q(\nu,\vec{\Omega}) = \frac{1}{2}\int\limits_{0}^{t_{\rm L}} \varphi(v)\, S(t'_{\rm L}) \left[\, {\rm e}^{-\frac{\varphi(v)\, H_+(t'_{\rm L},t_{\rm L})}{|\mu|}} - {\rm e}^{-\frac{\varphi(v)\, H_-(t'_{\rm L},t_{\rm L})}{|\mu|}} \,\right] \frac{{\rm d}t'_{\rm L}}{|\mu|}\,. \qquad (14.76)$$

Equations (14.75) and (14.76) can be used to obtain the two components of the radiation field tensor, $\bar{J}^0_0$ and $\bar{J}^2_0$, through the usual expressions (see Eqs. (5.157) and (14.5))

$$\bar{J}^0_0(\nu_0) = \frac{1}{2}\int\limits_{-\infty}^{\infty} {\rm d}v\, \varphi(v) \int\limits_{-1}^{1} {\rm d}\mu\, I(\nu,\vec{\Omega})$$

$$\bar{J}^2_0(\nu_0) = \frac{1}{4\sqrt{2}}\int\limits_{-\infty}^{\infty} {\rm d}v\, \varphi(v) \int\limits_{-1}^{1} {\rm d}\mu \left[\left(3\mu^2 - 1\right) I(\nu,\vec{\Omega}) + 3\left(\mu^2 - 1\right) Q(\nu,\vec{\Omega})\right].$$

Substitution of these expressions into Eqs. (14.73) closes the non-LTE loop of the 2$^{\rm nd}$ kind, which – as anticipated – shows a complicated non-linear character.

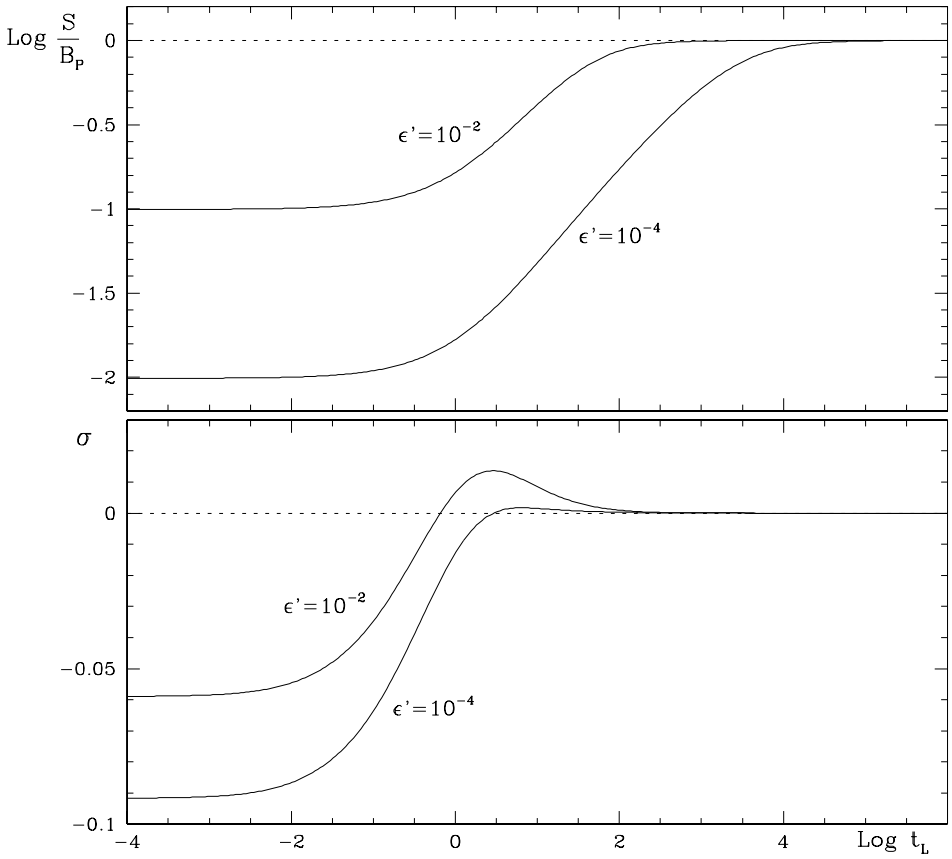

Fig.14.10. The logarithm of the source function S of Eq.(14.71) normalized to $B_{\rm P}$, and the reduced statistical tensor σ of Eq.(14.72) – upper and lower panel, respectively – are plotted against the logarithm of optical depth for two different values of ϵ'. The plots refer to a homogeneous, isothermal, non-magnetic, non-depolarizing atmosphere and to the transition ($J_\ell = 1, J_u = 0$).

As pointed out in Sect. 14.1, a solution of the non-LTE loop can be found only via sophisticated numerical methods. Some results, obtained through accelerated iterative schemes, are presented in Figs. 14.10 and 14.11. We point out that the surface value of lower-level atomic polarization, $\sigma(0)$, obtained for a homogeneous, isothermal, non-depolarizing atmosphere with $\epsilon' = 10^{-4}$, turns out to be equal to -0.09171. This ratio is related to the fractional linear polarization observed in the tangential direction by the expression, easily derived from Eq. (14.74)[1]

$$p_\parallel \equiv \frac{Q(\nu, \vec{\Omega}_\parallel)}{I(\nu, \vec{\Omega}_\parallel)} = -\frac{3\,\sigma(0)}{2\sqrt{2} - \sigma(0)}\ , \qquad (14.77)$$

[1] Equation (14.77) can be obtained by observing that $\mathrm{d}Q(\nu, \vec{\Omega}_\parallel)/\mathrm{d}s = 0$ because of the translational invariance of the atmosphere under lateral displacements. Moreover, the reference direction for positive Q in Eq. (14.77) is parallel to the stellar surface (while in Eq. (14.74) it is perpendicular to the stellar surface).

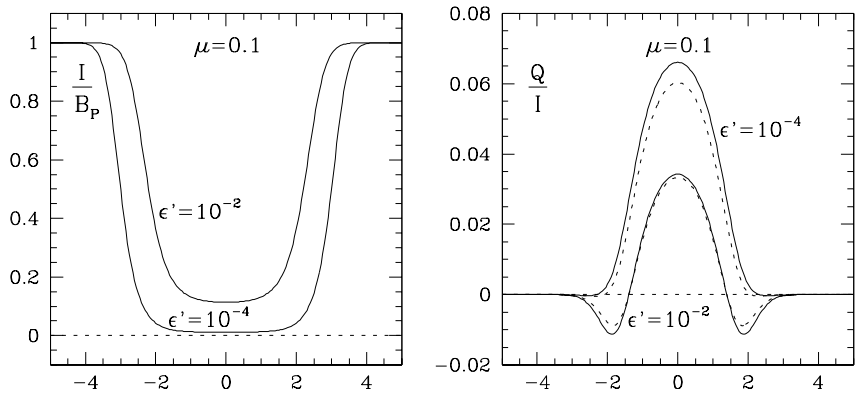

Fig.14.11. The emerging profiles of the intensity (normalized to $B_{\rm P}$) and of the ratio Q/I corresponding to the functions $S(t_{\rm L})$ and $\sigma(t_{\rm L})$ of Fig.14.10 are plotted against the reduced frequency $(\nu_0 - \nu)/\Delta\nu_{\rm D}$ (solid line). The plots refer to a heliocentric angle $\theta = 84°.3$ ($\mu = 0.1$). The positive Q direction is parallel to the stellar surface. The dotted curves in the right panel show, for comparison, the Q/I profiles corresponding to the 'reversed' transition ($J_\ell = 0, J_u = 1$) – cf. Fig.14.8.

which, for the $\sigma(0)$ value quoted above, yields $p_\parallel = 0.09422$. Note that both $|\sigma(0)|$ and $p_\parallel$ turn out to be larger than the corresponding values obtained for the 'inverted' transition ($J_\ell = 0, J_u = 1$) – see the discussion following Eq. (14.36). This result shows that, in the absence of depolarizing collisions, dichroism is a very efficient mechanism for introducing linear polarization in spectral lines.

It should be remarked that in recent times the non-LTE problem of the 2$^{\rm nd}$ kind has been solved for a variety of two-level model atoms with different values of J_ℓ and J_u, and also for more complicated atomic models involving up to 5 different levels (Trujillo Bueno, 1999; Manso Sainz and Trujillo Bueno, 2001; Manso Sainz, 2002).

14.6. Applications to Realistic Atmospheres: Polarization in the Continuum Spectrum

In the former sections we have shown how the self-consistency loop underlying the non-LTE problem of the 2$^{\rm nd}$ kind can be solved in some rather schematic physical situations involving simple atomic models and highly idealized, unidimensional (or plane-parallel) atmospheres. However, when trying to interpret real observations from stellar atmospheres, and particularly solar observations, one has to be aware of the presence of additional facts which tend to complicate, to some extent, the physical scenario.

First of all, it should be kept in mind that the solar atmosphere is highly structured. Even considering the so-called 'quiet' atmosphere, the presence of convective motions which manifest themselves through the well-known phenomena of granulation and supergranulation raises serious doubts about the reliability of the

plane-parallel approximation, especially when one tries to interpret polarimetric observations at high heliocentric angles. Under this respect, it is important to remind that even the interpretation of the usual solar spectrum at high heliocentric angles has raised several problems, which still remain partially unsolved (see Pecker, 1999, for a historical perspective of this subject).

Another problem is the polarization of the continuum spectrum and its interaction with the line spectrum polarization. This is an important subject that we are going to analyze here in some detail.

Historically, the continuum solar spectrum was discovered to be linearly polarized by Lyot (1948). According to his observations, the polarization is perpendicular to the solar radius and increases with decreasing limb distance. More recently, Kemp et al. (1983) have shown that the same phenomenon is present in the eclipsing variable Algol.[1]

Polarization is introduced in the continuum stellar spectrum by two different kinds of mechanism: dichroism and scattering. The role of dichroism as a source of continuum polarization has generally been neglected in the past. It is nevertheless obvious that a photoionization process taking place from a *polarized* atomic level has a cross section which depends on the polarization of the incident radiation. This implies that the continuum absorption coefficient depends on polarization, or, in other words, that the stellar atmosphere behaves as a dichroic medium.

Referring more specifically to the solar case, the major contribution to the continuum absorption coefficient at visible and near-infrared wavelengths comes from the photoionization of the H^- ion. Since this ion has a single bound state $1s^2\,{}^1S_0$, and since this state cannot harbor atomic polarization – being a $J = 0$ state – it follows that dichroism phenomena are of marginal importance in this spectral range. However, at short wavelengths in the visible and especially in the near UV, the major contributors to the continuum absorption coefficient are different atoms, such as neutral hydrogen, silicon, carbon, magnesium, aluminum, and iron. Since the levels of these atoms from which photoionization processes can take place *may* be polarized, it follows that dichroism has to be taken into account at these wavelengths.

The formalism to describe this phenomenon does not need to be derived through ab initio calculations. We can just adapt the results derived in Sect. 7.2, in particular Eq. (7.16a), to the case of a transition where the upper level is a level of the continuum. Denoting by α and J the quantum numbers of the atomic level from which photoionization takes place, by α_+ and J_+ the quantum numbers of the level in which the ion is left after photoionization, with ϵ, ℓ and j the energy and quantum numbers of the electron released by photoionization, and finally with J' the total angular momentum of the final state ($\vec{J}' = \vec{J}_+ + \vec{j}$), one obtains from

[1] For obvious symmetry reasons, it is impossible to detect this phenomenon in an isolated star, because of the lack of spatial resolution. On the contrary, the phenomenon can show up with a typical time-dependent signal when the star is eclipsed by a dark companion (see Landi Degl'Innocenti et al., 1988, for an analysis of the time variability of the polarization signal during the eclipse).

Eq. (7.16a)[1]

$$\left[\eta_i^{\rm A}(\nu,\vec{\Omega})\right]_{\rm ph} = \frac{h\nu}{4\pi}\mathcal{N}\, h\, n(\epsilon) \sum_{\ell j J'} (2J+1)\, B(\alpha J \rightarrow \alpha_+ J_+, \epsilon\ell j, J') \times \sum_{KQ} \sqrt{3}\ (-1)^{1+J+J'+K} \left\{ \begin{array}{ccc} 1 & 1 & K \\ J & J & J' \end{array} \right\} \mathcal{T}_Q^K(i,\vec{\Omega})\, \rho_Q^K(\alpha J)\,. \quad (14.78)$$

In this equation, $\mathcal{N}$ is the number density of atoms, $\rho_Q^K(\alpha J)$ is the statistical tensor of the photoionized level, ν is the frequency of the absorbed photon, which is connected to the energy ϵ of the free electron by the relation

$$\nu = \frac{1}{h}\left(E_{\alpha_+ J_+} + \epsilon - E_{\alpha J}\right),$$

$n(\epsilon)\,{\rm d}\epsilon$ is the number of quantum states of the free electron with energy contained in the interval $(\epsilon, \epsilon + {\rm d}\epsilon)$, and, finally

$$B(\alpha J \rightarrow \alpha_+ J_+, \epsilon\ell j, J') = \frac{32\pi^4}{3h^2 c}\, |\langle \alpha J \| \vec{d}\, \| \alpha_+ J_+, \epsilon\ell j, J' \rangle|^2\,. \quad (14.79)$$

Substitution of Eq. (14.79) into Eq. (14.78) yields

$$\left[\eta_i^{\rm A}(\nu,\vec{\Omega})\right]_{\rm ph} = \frac{8\pi^3\nu}{3c}\mathcal{N}\, n(\epsilon) \sum_{\ell j J'} (2J+1)\, |\langle \alpha J \| \vec{d}\, \| \alpha_+ J_+, \epsilon\ell j, J' \rangle|^2 \times \sum_{KQ} \sqrt{3}\ (-1)^{1+J+J'+K} \left\{ \begin{array}{ccc} 1 & 1 & K \\ J & J & J' \end{array} \right\} \mathcal{T}_Q^K(i,\vec{\Omega})\, \rho_Q^K(\alpha J)\,. \quad (14.80)$$

It is interesting to connect this expression with the 'classical' expression (see e.g. Mihalas, 1978) for the absorption coefficient due to photoionization. Such coefficient, denoted by $k_{\rm ph}(\nu)$, is generally expressed in the form

$$k_{\rm ph}(\nu) = \mathcal{N}_{\alpha J}\left[\sigma_{\rm ph}(\nu)\right]_{\alpha J}, \quad (14.81)$$

where $\mathcal{N}_{\alpha J}$ is the number density of atoms in the photoionized level and $[\sigma_{\rm ph}(\nu)]_{\alpha J}$ is the photoionization cross section for the same level. From Eq. (14.80), assuming the level (αJ) to be unpolarized ($\rho_Q^K(\alpha J) = \delta_{K0}\,\delta_{Q0}\ \rho_0^0(\alpha J)$), and taking into account that

$$\mathcal{N}_{\alpha J} = \sqrt{2J+1}\ \rho_0^0(\alpha J)\,\mathcal{N}\,, \qquad \mathcal{T}_0^0(0,\vec{\Omega}) = 1\,,$$

[1] Equation (14.78) refers to a *single* photoionization process from a given level (αJ) to a given level $(\alpha_+ J_+)$. Moreover, the sum over the final states also implies an integral over the energy ϵ of the free electron. This integral is easily performed taking into account that the profile ϕ contained in Eq. (7.16a) is practically a Dirac delta-function.

and that

$$\left\{ \begin{array}{ccc} 1 & 1 & 0 \\ J & J & J' \end{array} \right\} = (-1)^{1+J+J'} \, \frac{1}{\sqrt{3(2J+1)}} \, ,$$

one gets, by comparison with Eq. (14.81)

$$\left[\sigma_{\rm ph}(\nu)\right]_{\alpha J} = \frac{8\pi^3 \nu}{3c} \, n(\epsilon) \sum_{\ell j J'} \, |\langle \alpha J \| \, \vec{d} \, \| \alpha_+ J_+, \epsilon \ell j, J' \rangle|^2 \, .$$

Recalling Eq. (10.11), this allows one to cast Eq. (14.80) in the more significant form

$$\left[\eta_i^{\rm A}(\nu, \vec{\Omega})\right]_{\rm ph} = \mathcal{N}_{\alpha J} \left[\sigma_{\rm ph}(\nu)\right]_{\alpha J} \sum_{KQ} (-1)^K \, \mathcal{W}_{\alpha J}^{(K)}(\epsilon) \; \mathcal{T}_Q^K(i, \vec{\Omega}) \, \sigma_Q^K(\alpha J) \, , \qquad (14.82)$$

where $\sigma_Q^K(\alpha J) = \rho_Q^K(\alpha J)/\rho_0^0(\alpha J)$ and where the symbol $\mathcal{W}_{\alpha J}^{(K)}(\epsilon)$, which represents an extension of the symbol $w_{JJ'}^{(K)}$ of Eq. (10.11) to photoionization, is defined by

$$\mathcal{W}_{\alpha J}^{(K)}(\epsilon) = \frac{\sum_{\ell j J'} \; w_{JJ'}^{(K)} \; |\langle \alpha J \| \, \vec{d} \, \| \alpha_+ J_+, \epsilon \ell j, J' \rangle|^2}{\sum_{\ell j J'} \; |\langle \alpha J \| \, \vec{d} \, \| \alpha_+ J_+, \epsilon \ell j, J' \rangle|^2} \, . \qquad (14.83)$$

The explicit evaluation of the reduced matrix elements appearing in Eq. (14.83) is, in general, quite involved. In App. 24 we consider a particularly simple case where the atomic states can be described in the L-S coupling scheme and where the photoionized electron belongs, before photoionization, to an open shell.

We now turn to discuss scattering phenomena in the continuum, namely Thomson scattering on free electrons and Rayleigh scattering on atoms or molecules. These phenomena have been analyzed in great detail by Chandrasekhar (1950). Here we just recall his conclusions and adapt his results to the formalism used in this book.

In the non-relativistic limit, i.e., at frequencies ν such that $h\nu \ll mc^2$, m being the electron mass, Thomson scattering is characterized by a frequency-independent, non-dichroic cross section given by

$$\sigma_{\rm T} = \frac{8\pi}{3} \, \frac{e_0^4}{m^2 c^4}$$

(where e_0 is the electron charge and c the speed of light), and by a scattering phase matrix which, in our notations, has been denoted by the symbol $R_{ij}(\vec{\Omega}, \vec{\Omega}')$ – or $R_{ij}(\vec{\Omega}, \vec{\Omega}'; 0)$ – and which is given by (cf. Eqs. (5.137), (5.138), and (10.21))

$$R_{ij}(\vec{\Omega}, \vec{\Omega}') = \sum_{KQ} (-1)^Q \, \mathcal{T}_Q^K(i, \vec{\Omega}) \, \mathcal{T}_{-Q}^K(j, \vec{\Omega}') \, . \qquad (14.84)$$

Moreover, it has to be taken into account that scattering is coherent in the reference frame of the electron.

From the point of view of radiative transfer, Thomson scattering is therefore characterized by an absorption coefficient of the form

$$\left[\eta_i(\nu,\vec{\Omega})\right]_{\rm T.sc} = N_{\rm e}\,\sigma_{\rm T}\,\delta_{i0}\;, \tag{14.85}$$

$N_{\rm e}$ being the number density of electrons, and by an emission coefficient $\varepsilon_i(\nu,\vec{\Omega})$ which, taking into account the Doppler effect due to the motion of the electrons, is given by[1]

$$\begin{aligned}\left[\varepsilon_i(\nu,\vec{\Omega})\right]_{\rm T.sc} = N_{\rm e}\,\sigma_{\rm T}\oint\frac{{\rm d}\Omega'}{4\pi}\,\sum_{j=0}^{3}R_{ij}(\vec{\Omega},\vec{\Omega}')\int{\rm d}\nu'\int{\rm d}^3\vec{v}\;f(\vec{v})\\ \times\,\delta\!\left(\nu-\nu\frac{\vec{v}\cdot\vec{\Omega}}{c}+\nu\frac{\vec{v}\cdot\vec{\Omega}'}{c}-\nu'\right)I_j(\nu',\vec{\Omega}')\;,\end{aligned} \tag{14.86}$$

where $f(\vec{v})$ is the normalized velocity distribution of the electrons. In particular, for the case of a Maxwellian distribution of velocities, the integral in ${\rm d}^3\vec{v}$ can be performed to give (see the analogous calculation carried out in App. 18)

$$\begin{aligned}\left[\varepsilon_i(\nu,\vec{\Omega})\right]_{\rm T.sc} = N_{\rm e}\,\sigma_{\rm T}\oint\frac{{\rm d}\Omega'}{4\pi}\,\sum_{j=0}^{3}R_{ij}(\vec{\Omega},\vec{\Omega}')\int{\rm d}\nu'\\ \times\,\frac{1}{\sqrt{2\pi(1-\cos\Theta)}\;\Delta\nu_{\rm e}}\;{\rm e}^{-\frac{(\nu-\nu')^2}{2(1-\cos\Theta)\,\Delta\nu_{\rm e}^2}}\;I_j(\nu',\vec{\Omega}')\;,\end{aligned} \tag{14.87}$$

where Θ is the angle between the directions $\vec{\Omega}$ and $\vec{\Omega}'$, and where $\Delta\nu_{\rm e}$ is the Doppler broadening (in frequency units) corresponding to the thermal velocity of the electrons,

$$\Delta\nu_{\rm e} = \frac{\nu}{c}\sqrt{\frac{2k_{\rm B}T_{\rm e}}{m}}\;, \tag{14.88}$$

with $k_{\rm B}$ the Boltzmann constant and $T_{\rm e}$ the electronic temperature.

Equation (14.86) can be cast in a different form recalling Eq. (14.84) and the definition of the radiation field tensor in the comoving frame. With easy transformations one gets

$$\begin{aligned}\left[\varepsilon_i(\nu,\vec{\Omega})\right]_{\rm T.sc} = N_{\rm e}\,\sigma_{\rm T}\sum_{KQ}(-1)^Q\,\mathcal{T}^K_Q(i,\vec{\Omega})\\ \times\int{\rm d}^3\vec{v}\;f(\vec{v})\left[J^K_{-Q}\!\left(\nu-\nu\frac{\vec{v}\cdot\vec{\Omega}}{c}\right)\right]_{\vec{v}}\;,\end{aligned} \tag{14.89}$$

where the radiation field tensor in the comoving frame is given by Eq. (13.31).

[1] In this formula, as well as in Eqs. (14.87) and (14.89), we suppose $v/c \ll 1$.

The preceding results on Thomson scattering can be simply modified to handle Rayleigh scattering. Obviously, Rayleigh scattering may occur on any atom (or molecule), but in the solar atmosphere it is generally sufficient to take into account the contributions of neutral hydrogen and neutral helium. Neglecting atomic polarization,[1] Rayleigh scattering on hydrogen atoms is still described by Eqs. (14.85)-(14.89) provided the following formal transformations are performed

$$N_{\rm e} \rightarrow N_{\rm H} \ , \qquad \sigma_{\rm T} \rightarrow \sigma_{\rm R}^{\rm (H)} \ , \qquad \Delta\nu_{\rm e} \rightarrow \Delta\nu_{\rm H} \ ,$$

where $N_{\rm H}$ is the number density of hydrogen atoms, $\sigma_{\rm R}^{\rm (H)}$ is the frequency-dependent Rayleigh scattering cross section, and $\Delta\nu_{\rm H}$ is the Doppler broadening (in frequency units) corresponding to the thermal velocity of the hydrogen atoms. The explicit expression for $\sigma_{\rm R}^{\rm (H)}$ is quite involved (Kramers, 1924), but a good approximation at optical wavelengths is provided by the formula

$$\sigma_{\rm R}^{\rm (H)} = \sigma_{\rm T} \, \frac{\nu^4}{(\nu^2 - \nu_0^2)^2} \ , \tag{14.90}$$

where ν_0 is the frequency of Lyman α ($\nu_0 = 2.466 \times 10^{15} \, {\rm s}^{-1}$).

Similar expressions hold for Rayleigh scattering on helium atoms. The main difference from the hydrogen case, apart from the Doppler broadening which is now smaller by a factor 2 ($\Delta\nu_{\rm He} \simeq 0.5 \, \Delta\nu_{\rm H}$), comes from the cross section – denoted in the following by $\sigma_{\rm R}^{\rm (He)}$ – which can still be approximated as in Eq. (14.90) with ν_0 the frequency of the first resonance line of HeI, $1s^2 \ {}^1{\rm S}_0 \rightarrow 1s\,2p \ {}^1{\rm P}_1$ ($\nu_0 = 5.130 \times 10^{15} \, {\rm s}^{-1}$).

An important remark about Eq. (14.86) is that the integral over the distribution of velocities can be trivially performed whenever the Stokes parameters $I_j(\nu', \vec{\Omega}')$ are constant over a frequency interval centered at the frequency ν and having a width of the order of $\Delta\nu_{\rm e}$ for the case of Thomson scattering or $\Delta\nu_{\rm H}$ ($\Delta\nu_{\rm He}$) for the case of Rayleigh scattering on hydrogen (helium) atoms. In such case, irrespective of the velocity distribution $f(\vec{v})$, one gets, for Thomson scattering

$$\begin{aligned} \left[\varepsilon_i(\nu, \vec{\Omega})\right]_{\rm T.sc} &= N_{\rm e} \, \sigma_{\rm T} \oint \frac{{\rm d}\Omega'}{4\pi} \sum_{j=0}^{3} R_{ij}(\vec{\Omega}, \vec{\Omega}') \, I_j(\nu, \vec{\Omega}') \\ &= N_{\rm e} \, \sigma_{\rm T} \sum_{KQ} (-1)^Q \, \mathcal{T}_Q^K(i, \vec{\Omega}) \, J_{-Q}^K(\nu) \ , \end{aligned} \tag{14.91}$$

with similar expressions holding for Rayleigh scattering on hydrogen or helium atoms.

[1] This approximation must not be taken for granted and might prove to be unreliable to properly handle continuum polarization phenomena in the solar atmosphere. A consistent theoretical treatment of Rayleigh scattering on polarized atoms is still missing and is beyond the purposes of this book.

The expressions now derived allow one to deduce the polarization properties of the continuum spectrum of the solar atmosphere. In the plane-parallel approximation, owing to the cylindrical symmetry of the environment, the transfer of polarized radiation can be described by a simplified equation which, by a suitable choice of the reference direction,[1] only involves the two Stokes parameters $I(\nu,\vec{\Omega})$ and $Q(\nu,\vec{\Omega})$. This follows from the fact that the only non-zero components of the tensor $J^K_Q(\nu)$ – appearing in Eqs. (14.89) and (14.91) – and $\sigma^K_Q(\alpha J)$ – appearing in Eq. (14.82) – are those with $(K=0, Q=0)$ and $(K=2, Q=0)$.[2] Taking into account the expressions of the tensor $\mathcal{T}^K_Q(i,\vec{\Omega})$ – Table 5.6 – it can easily be seen that the only non-vanishing components of $[\varepsilon_i(\nu,\vec{\Omega})]_{\rm T.sc}$ and of $[\eta^{\rm A}_i(\nu,\vec{\Omega})]_{\rm ph}$ are those with $i=0,1$, so that the transfer equation has the form

$$\frac{\mathrm{d}}{\mathrm{d}s}\begin{pmatrix} I(\nu,\vec{\Omega}) \\ Q(\nu,\vec{\Omega}) \end{pmatrix} = -\begin{pmatrix} \eta_0(\nu,\vec{\Omega}) & \eta_1(\nu,\vec{\Omega}) \\ \eta_1(\nu,\vec{\Omega}) & \eta_0(\nu,\vec{\Omega}) \end{pmatrix}\begin{pmatrix} I(\nu,\vec{\Omega}) \\ Q(\nu,\vec{\Omega}) \end{pmatrix} + \begin{pmatrix} \varepsilon_0(\nu,\vec{\Omega}) \\ \varepsilon_1(\nu,\vec{\Omega}) \end{pmatrix}, \quad (14.92)$$

where the transfer coefficients η_0, η_1, ε_0, and ε_1 result from the sum of the contributions of all the processes responsible for absorption and emission in the continuum.

Since the degree of anisotropy in the solar atmosphere is everywhere weak, and since the major source of continuum opacity at visible wavelengths (the H^- ion) contributes neither to dichroism nor to emission of polarized radiation, it follows that

$$\eta_1(\nu,\vec{\Omega}) \ll \eta_0(\nu,\vec{\Omega}) , \qquad \varepsilon_1(\nu,\vec{\Omega}) \ll \varepsilon_0(\nu,\vec{\Omega}) ,$$

so that Eq. (14.92) can be solved by a perturbative approach. One thus gets the zero-order equation

$$\frac{\mathrm{d}}{\mathrm{d}s} I(\nu,\vec{\Omega}) = -\eta_0(\nu,\vec{\Omega})\, I(\nu,\vec{\Omega}) + \varepsilon_0(\nu,\vec{\Omega}) , \quad (14.93)$$

and the first-order equation

$$\frac{\mathrm{d}}{\mathrm{d}s} Q(\nu,\vec{\Omega}) = -\eta_0(\nu,\vec{\Omega})\, Q(\nu,\vec{\Omega}) + \left[\varepsilon_1(\nu,\vec{\Omega}) - \eta_1(\nu,\vec{\Omega})\, I(\nu,\vec{\Omega})\right] , \quad (14.94)$$

where, from Eqs. (14.82), (14.85), and (14.91)

---

[1] This choice is illustrated in Fig. 14.4, where z is the vertical to the atmosphere and where the angle γ has to be set to $\pi/2$ (or 0).

[2] The tensor components with $K=1$ can be excluded through general considerations involving the absence of circular polarization inside the atmosphere (see, for instance, the discussion following Eq. (14.23)). On the contrary, the presence of a magnetic field inclined with respect to the vertical may introduce non-vanishing $\sigma^2_Q(\alpha J)$ components with $Q \neq 0$. When dichroism phenomena are important, Eq. (14.92) is valid only in the absence of such fields.

$$\eta_0(\nu,\vec{\Omega}) = \sum_{\alpha J} \mathcal{N}_{\alpha J} \left[\sigma_{\rm ph}(\nu)\right]_{\alpha J} + N_{\rm e}\,\sigma_{\rm T} + N_{\rm H}\,\sigma_{\rm R}^{(\rm H)} + N_{\rm He}\,\sigma_{\rm R}^{(\rm He)}$$

$$\eta_1(\nu,\vec{\Omega}) = \sum_{\alpha J} \mathcal{N}_{\alpha J} \left[\sigma_{\rm ph}(\nu)\right]_{\alpha J} \mathcal{W}^{(2)}_{\alpha J}(\epsilon)\; \mathcal{T}^2_0(1,\vec{\Omega})\; \sigma^2_0(\alpha J)$$

$$\varepsilon_0(\nu,\vec{\Omega}) = B_{\rm P} \sum_{\alpha J} \mathcal{N}_{\alpha J} \left[\sigma_{\rm ph}(\nu)\right]_{\alpha J} + \left[N_{\rm e}\,\sigma_{\rm T} + N_{\rm H}\,\sigma_{\rm R}^{(\rm H)} + N_{\rm He}\,\sigma_{\rm R}^{(\rm He)}\right] J^0_0(\nu)$$

$$\varepsilon_1(\nu,\vec{\Omega}) = \left[N_{\rm e}\,\sigma_{\rm T} + N_{\rm H}\,\sigma_{\rm R}^{(\rm H)} + N_{\rm He}\,\sigma_{\rm R}^{(\rm He)}\right] \mathcal{T}^2_0(1,\vec{\Omega})\; J^2_0(\nu)\;. \tag{14.95}$$

The first term in the expression of $\varepsilon_0(\nu,\vec{\Omega})$, where $B_{\rm P}$ is the Planck function at the electronic temperature $T_{\rm e}$, describes radiative recombination (the process inverse to photoionization), which takes place under LTE conditions.

Equations (14.93)-(14.94) can be formally integrated by introducing the optical depth in the continuum, t_ν, defined by

$$\mathrm{d}t_\nu = -\eta_0(\nu,\vec{\Omega})\,\mathrm{d}z\;,$$

z being the vertical to the atmosphere (directed upwards), and the continuum source function

$$S_{\rm c}(\nu) = \frac{\varepsilon_0(\nu,\vec{\Omega})}{\eta_0(\nu,\vec{\Omega})}\;.$$

We easily obtain

$$S_{\rm c}(\nu) = (1-\beta)\,B_{\rm P} \;+\; \beta\,J^0_0(\nu)\;, \tag{14.96}$$

where β is the fraction of continuum opacity due to scattering processes,

$$\beta = \frac{N_{\rm e}\,\sigma_{\rm T} + N_{\rm H}\,\sigma_{\rm R}^{(\rm H)} + N_{\rm He}\,\sigma_{\rm R}^{(\rm He)}}{\sum_{\alpha J} \mathcal{N}_{\alpha J} \left[\sigma_{\rm ph}(\nu)\right]_{\alpha J} + N_{\rm e}\,\sigma_{\rm T} + N_{\rm H}\,\sigma_{\rm R}^{(\rm H)} + N_{\rm He}\,\sigma_{\rm R}^{(\rm He)}}\;. \tag{14.97}$$

Integration of Eq. (14.93) gives, for the intensity of the radiation emerging from the solar atmosphere

$$I(\nu,\vec{\Omega}) = \int_0^\infty S_{\rm c}(\nu)\;\; \mathrm{e}^{-\frac{t_\nu}{\mu}}\;\; \frac{\mathrm{d}t_\nu}{\mu}\;, \tag{14.98}$$

where $\mu = \cos\theta$ is the cosine of the heliocentric angle. Similarly, integration of Eq. (14.94) yields the Q Stokes parameter of the emerging radiation. Two contributions arise, one due to scattering processes and the other to dichroism phenomena. With self-evident notations

$$Q(\nu,\vec{\Omega}) = \left[Q(\nu,\vec{\Omega})\right]_{\rm sc} + \left[Q(\nu,\vec{\Omega})\right]_{\rm ph} ,$$

where, recalling Eqs. (14.95) and (14.98), and the expression of the tensor $\mathcal{T}^2_0(1,\vec{\Omega})$[1]

$$\left[Q(\nu,\vec{\Omega})\right]_{\rm sc} = \frac{3}{2\sqrt{2}}\left(1-\mu^2\right)\int_0^\infty \beta\, J^2_0(\nu)\ \ {\rm e}^{-\frac{t_\nu}{\mu}}\ \ \frac{{\rm d}t_\nu}{\mu}\ , \tag{14.99}$$

and

$$\left[Q(\nu,\vec{\Omega})\right]_{\rm ph} = -\frac{3}{2\sqrt{2}}\left(1-\mu^2\right)\int_0^\infty (1-\beta)\ \frac{\sum_{\alpha J}\ \mathcal{N}_{\alpha J}\left[\sigma_{\rm ph}(\nu)\right]_{\alpha J}\ \mathcal{W}^{(2)}_{\alpha J}(\epsilon)\ \ \sigma^2_0(\alpha J)}{\sum_{\alpha J}\ \mathcal{N}_{\alpha J}\left[\sigma_{\rm ph}(\nu)\right]_{\alpha J}}$$

$$\times\left[\ \int_{t_\nu}^\infty S_{\rm c}(\nu)\ \ {\rm e}^{-\frac{t'_\nu}{\mu}}\ \ \frac{{\rm d}t'_\nu}{\mu}\ \right]\ \frac{{\rm d}t_\nu}{\mu}\ . \tag{14.100}$$

The emerging intensity and the scattering contribution to the Q Stokes parameter can be computed by standard numerical techniques from a given model of the solar atmosphere. Since in the solar atmosphere the contribution of scattering processes to the continuum opacity is small ($\beta \ll 1$), one can simply set $S_{\rm c}(\nu) = B_{\rm P}(\nu)$ – see Eq. (14.96). The emerging intensity can then be evaluated using Eq. (14.98), and the tensor $J^2_0(\nu)$ at any optical depth can be obtained by a numerical quadrature. The scattering contribution to Q can finally be calculated from Eq. (14.99). Detailed theoretical results on the fractional polarization, obtained through numerical procedures similar to the one just described, can be found in Débarbat et al. (1970) and in Fluri and Stenflo (1999).[2]

On the contrary, the contribution to the continuum linear polarization arising from dichroism is more difficult to compute because of the presence in Eq. (14.100) of the atomic polarization factors, $\sigma^2_0(\alpha J)$, relative to all the atomic levels of different atomic species from which significant photoionization can take place. Obviously, the evaluation of the factors $\sigma^2_0(\alpha J)$ requires the solution of the non-LTE problem of the 2$^{\rm nd}$ kind for multi-level atoms, a difficult subject which is presently in a phase of development and upon which we will not dwell any longer in this book.

---

[1] The reference direction for the Stokes parameters is defined here as in Fig. 14.4 with $\gamma = \pi/2$. Positive Q means linear polarization parallel to the solar limb.

[2] Note that very little progress has been made in this field from the observational side. To the authors' knowledge, the most complete measurements of continuum linear polarization at the solar limb are still those by Leroy (1972). Such observations, however, were performed with broad-band filters and are therefore contaminated by the spurious signals due to spectral lines. Observations of the true continuum polarization in selected spectral windows have been presented by Mickey and Orrall (1974) and by Wiehr (1975, 1978).

14.7. Applications to Realistic Atmospheres: Approximate Results on the Polarization of the Fraunhofer Spectrum

Although a fully consistent description of the polarization properties of a spectral line formed in a stellar atmosphere has eventually to rely on the solution of the self-consistency loop schematized in Fig. 14.1, it is nevertheless possible to obtain some results by means of suitable approximations performed directly on the radiative transfer equation for polarized radiation. The approximate results that will be deduced in this section can be considered, to some extent, as the generalization to polarized transfer of the well-known Eddington-Barbier approximation extensively used in the usual transfer theory.

We refer to a plane-parallel, non-magnetic atmosphere and we consider an isolated (non-blended) spectral line originating from the transition between two levels of a given atomic species. The two levels, which we suppose devoid of hyperfine structure, are described by the sets of quantum numbers $(\alpha_\ell J_\ell)$ for the lower level and $(\alpha_u J_u)$ for the upper level. We assume the atoms to have a Maxwellian distribution of velocities characterized, at the frequency ν_0 of the transition, by the Doppler broadening $\Delta\nu_{\rm D}$, and we adopt the approximation of complete redistribution on velocities, which implies that the atomic polarization of the two levels is described by the (velocity-independent) statistical tensors $\rho^K_Q(\alpha_\ell J_\ell)$ and $\rho^K_Q(\alpha_u J_u)$, defined in a reference system with the z-axis directed along the vertical. We assume the atmosphere to be characterized by a non-dichroic continuum absorption coefficient and by an emission coefficient partly due to scattering phenomena. Finally, we neglect stimulated emission.

An analysis of the statistical equilibrium equations similar to that carried out in Sect. 14.2 shows that under the preceding hypotheses only the statistical tensors of even rank ($K = 0, 2, 4, \ldots$) and $Q = 0$ are different from zero. This remark, joined with the other hypotheses outlined above, allows one to write the radiative transfer equation for polarized radiation in the same form as Eq. (14.92),[1] where the radiative transfer coefficients, resulting from the contributions of continuum and line processes, are given by

$$\eta_0(\nu,\vec{\Omega}) = k^{(\rm c)}_\nu + k^{\rm A}_{\rm L}\left[1 + \frac{1}{2\sqrt{2}}\left(3\cos^2\theta - 1\right) w^{(2)}_{J_\ell J_u}\, \sigma^2_0(\alpha_\ell J_\ell)\right]\hat{\phi}(\nu_0 - \nu)$$

$$\eta_1(\nu,\vec{\Omega}) = k^{\rm A}_{\rm L}\,\frac{3}{2\sqrt{2}}\,\sin^2\theta\; w^{(2)}_{J_\ell J_u}\,\sigma^2_0(\alpha_\ell J_\ell)\;\hat{\phi}(\nu_0 - \nu)$$

$$\varepsilon_0(\nu,\vec{\Omega}) = k^{(\rm c)}_\nu\left\{(1-\beta)\,B_{\rm P} + \sum_{i=1}^{3}\,\beta_i \int {\rm d}^3\vec{v}_i\;\, f(\vec{v}_i)\left[J^0_0\Big(\nu - \nu\,\frac{\vec{v}_i\cdot\vec{\Omega}}{c}\Big)\right]_{\vec{v}_i}\; +\right.$$

[1] The reference direction for the definition of the Stokes parameters is the same as for Eq. (14.92), namely the direction $\vec{e}_a(\vec{\Omega})$ of Fig. 14.4 with $\gamma = \pi/2$.

$$+\frac{1}{2\sqrt{2}}\left(3\cos^2\theta-1\right)\sum_{i=1}^{3}\beta_i\int \mathrm{d}^3\vec{v}_i\;\; f(\vec{v}_i)\left[J_0^2\Big(\nu-\nu\,\frac{\vec{v}_i\cdot\vec{\Omega}}{c}\Big)\right]_{\vec{v}_i}\Bigg\}$$

$$+\,k_{\rm L}^{\rm A}\,S_{\rm L}\left[1+\frac{1}{2\sqrt{2}}\left(3\cos^2\theta-1\right)\,w^{(2)}_{J_uJ_\ell}\,\sigma_0^2(\alpha_uJ_u)\right]\hat{\phi}(\nu_0-\nu)$$

$$\varepsilon_1(\nu,\vec{\Omega})=\frac{3}{2\sqrt{2}}\;\sin^2\theta\left\{k_\nu^{(\rm c)}\sum_{i=1}^{3}\beta_i\int \mathrm{d}^3\vec{v}_i\;\; f(\vec{v}_i)\left[J_0^2\Big(\nu-\nu\,\frac{\vec{v}_i\cdot\vec{\Omega}}{c}\Big)\right]_{\vec{v}_i}\right.$$

$$\left.+\,k_{\rm L}^{\rm A}\,S_{\rm L}\;\,w^{(2)}_{J_uJ_\ell}\,\sigma_0^2(\alpha_uJ_u)\;\,\hat{\phi}(\nu_0-\nu)\right\}.$$

In these expressions, $k_\nu^{(\rm c)}$ is the continuum absorption coefficient due to photoionization and scattering processes, $k_{\rm L}^{\rm A}$ and $S_{\rm L}$ are the line opacity and the line source function defined, respectively, in Eqs. (14.15) and (14.12), $\sigma_0^2(\alpha_\ell J_\ell)$ and $\sigma_0^2(\alpha_u J_u)$ are the reduced statistical tensors defined by

$$\sigma_0^2(\alpha_\ell J_\ell)=\frac{\rho_0^2(\alpha_\ell J_\ell)}{\rho_0^0(\alpha_\ell J_\ell)}\,,\qquad \sigma_0^2(\alpha_u J_u)=\frac{\rho_0^2(\alpha_u J_u)}{\rho_0^0(\alpha_u J_u)}\,,$$

$w^{(2)}_{JJ'}$ is the symbol defined in Eq. (10.98), θ is the heliocentric angle defined as in Fig. 14.4 (z being the vertical to the solar atmosphere), the profile $\hat{\phi}(\nu_0-\nu)$ is defined according to Eq. (14.1), $B_{\rm P}(\nu)$ is the Planck function, and β_i ($i=1,2,3$) is the fractional contribution to the opacity coming from scattering by electrons, H atoms, and He atoms, respectively

$$\beta_1=\frac{N_{\rm e}\,\sigma_{\rm T}}{k_\nu^{(\rm c)}}\,,\qquad \beta_2=\frac{N_{\rm H}\,\sigma_{\rm R}^{(\rm H)}}{k_\nu^{(\rm c)}}\,,\qquad \beta_3=\frac{N_{\rm He}\,\sigma_{\rm R}^{(\rm He)}}{k_\nu^{(\rm c)}}\,;$$

finally (cf. Eq. (14.97))

$$\beta=\sum_{i=1}^{3}\beta_i\,.$$

In the solar atmosphere, the reduced statistical tensors of rank 2 are generally very small ($\sigma_0^2(\alpha_\ell J_\ell)$, $\sigma_0^2(\alpha_u J_u)\ll 1$), as well as the scattering contribution to the continuum opacity ($\beta\ll 1$).[1] This implies that the fractional linear polarization Q/I is also small, so that the radiative transfer equation can be solved by a perturbative approach, similarly to the previous section. For the intensity one obtains the zero-order equation

$$\frac{\mathrm{d}}{\mathrm{d}s}\,I(\nu,\vec{\Omega})=-\Big[k_\nu^{(\rm c)}+k_{\rm L}^{\rm A}\,\hat{\phi}(\nu_0-\nu)\Big]I(\nu,\vec{\Omega})\;+\;k_\nu^{(\rm c)}B_{\rm P}\;+\;k_{\rm L}^{\rm A}\,S_{\rm L}\,\hat{\phi}(\nu_0-\nu)\,,\quad(14.101)$$

[1] In the top layers of the atmosphere, and especially in the UV region of the spectrum, this inequality may well be violated, β attaining values close to unity. This happens, however, in a layer of very small optical thickness, that can be safely neglected for our considerations.

whereas for the Q Stokes parameter one gets the first-order equation

$$\frac{\mathrm{d}}{\mathrm{d}s}\,Q(\nu,\vec{\Omega}) = -\Big[k_\nu^{(\mathrm{c})} + k_\mathrm{L}^\mathrm{A}\,\hat{\phi}(\nu_0-\nu)\Big]Q(\nu,\vec{\Omega}) + \frac{3}{2\sqrt{2}}\,k_\mathrm{L}^\mathrm{A}\,\sin^2\theta\left[w^{(2)}_{J_u J_\ell}\,\sigma_0^2(\alpha_u J_u)\,S_\mathrm{L} - w^{(2)}_{J_\ell J_u}\,\sigma_0^2(\alpha_\ell J_\ell)\,I(\nu,\vec{\Omega})\right]\hat{\phi}(\nu_0-\nu) + \frac{3}{2\sqrt{2}}\,k_\nu^{(\mathrm{c})}\,\sin^2\theta\sum_{i=1}^{3}\beta_i\int \mathrm{d}^3\vec{v}_i\;f(\vec{v}_i)\left[J_0^2\Big(\nu-\nu\,\frac{\vec{v}_i\cdot\vec{\Omega}}{c}\Big)\right]_{\vec{v}_i}. \tag{14.102}$$

These equations can be formally solved for a direction, $\vec{\Omega}_\parallel$, parallel to the atmosphere. Taking into account the translational invariance of the atmosphere under lateral displacements, one has

$$\frac{\mathrm{d}}{\mathrm{d}s}\,I(\nu,\vec{\Omega}_\parallel) = \frac{\mathrm{d}}{\mathrm{d}s}\,Q(\nu,\vec{\Omega}_\parallel) = 0\,.$$

From Eq. (14.101) we thus obtain

$$I(\nu,\vec{\Omega}_\parallel) = \frac{k_\nu^{(\mathrm{c})}B_\mathrm{P} + k_\mathrm{L}^\mathrm{A}\,S_\mathrm{L}\,\hat{\phi}(\nu_0-\nu)}{k_\nu^{(\mathrm{c})} + k_\mathrm{L}^\mathrm{A}\,\hat{\phi}(\nu_0-\nu)}\,, \tag{14.103}$$

and from Eq. (14.102), using Eq. (14.103), we get

$$\frac{Q(\nu,\vec{\Omega}_\parallel)}{I(\nu,\vec{\Omega}_\parallel)} = \left[\frac{Q(\nu,\vec{\Omega}_\parallel)}{I(\nu,\vec{\Omega}_\parallel)}\right]_\mathrm{line} + \left[\frac{Q(\nu,\vec{\Omega}_\parallel)}{I(\nu,\vec{\Omega}_\parallel)}\right]_\mathrm{sc},$$

where the 'line contribution' is given by

$$\left[\frac{Q(\nu,\vec{\Omega}_\parallel)}{I(\nu,\vec{\Omega}_\parallel)}\right]_\mathrm{line} = \frac{3}{2\sqrt{2}}\,k_\mathrm{L}^\mathrm{A}\left[\frac{w^{(2)}_{J_u J_\ell}\,\sigma_0^2(\alpha_u J_u)\,S_\mathrm{L}}{k_\nu^{(\mathrm{c})}\,B_\mathrm{P} + k_\mathrm{L}^\mathrm{A}\,S_\mathrm{L}\,\hat{\phi}(\nu_0-\nu)} - \frac{w^{(2)}_{J_\ell J_u}\,\sigma_0^2(\alpha_\ell J_\ell)}{k_\nu^{(\mathrm{c})} + k_\mathrm{L}^\mathrm{A}\,\hat{\phi}(\nu_0-\nu)}\right]\hat{\phi}(\nu_0-\nu)\,, \tag{14.104}$$

and the 'scattering contribution' by

$$\left[\frac{Q(\nu,\vec{\Omega}_\parallel)}{I(\nu,\vec{\Omega}_\parallel)}\right]_\mathrm{sc} = \frac{3}{2\sqrt{2}}\,k_\nu^{(\mathrm{c})}\;\frac{\displaystyle\sum_{i=1}^{3}\beta_i\int \mathrm{d}^3\vec{v}_i\;f(\vec{v}_i)\left[J_0^2\Big(\nu-\nu\,\frac{\vec{v}_i\cdot\vec{\Omega}_\parallel}{c}\Big)\right]_{\vec{v}_i}}{k_\nu^{(\mathrm{c})}\,B_\mathrm{P} + k_\mathrm{L}^\mathrm{A}\,S_\mathrm{L}\,\hat{\phi}(\nu_0-\nu)}\,. \tag{14.105}$$

All the quantities in the right-hand sides of Eqs. (14.103), (14.104) and (14.105) have to be evaluated at the top layers of the atmosphere (formally at $\tau = 0$).

In the following we analyze separately the two contributions to the fractional polarization. As far as the line contribution is concerned, we observe that the polarization signal disappears in the line wings and that it is usually maximum (in absolute value) at line center. At this frequency we obtain the following expressions, valid in the limiting cases of strong and weak lines, respectively

a) strong line ($k_{\rm L}^{\rm A}\,\hat{\phi}(0) \gg k_\nu^{\rm (c)}$)

$$\left[\frac{Q(\nu_0,\vec{\Omega}_\parallel)}{I(\nu_0,\vec{\Omega}_\parallel)}\right]_{\rm line} = \frac{3}{2\sqrt{2}}\left[w^{(2)}_{J_u J_\ell}\;\sigma_0^2(\alpha_u J_u) - \;w^{(2)}_{J_\ell J_u}\;\sigma_0^2(\alpha_\ell J_\ell)\right], \tag{14.106}$$

b) weak line ($k_{\rm L}^{\rm A}\,\hat{\phi}(0) \ll k_\nu^{\rm (c)}$)

$$\left[\frac{Q(\nu_0,\vec{\Omega}_\parallel)}{I(\nu_0,\vec{\Omega}_\parallel)}\right]_{\rm line} = \frac{3}{2\sqrt{2}}\,\frac{k_{\rm L}^{\rm A}\,\hat{\phi}(0)}{k_\nu^{\rm (c)}}\left[w^{(2)}_{J_u J_\ell}\;\sigma_0^2(\alpha_u J_u)\,\frac{S_{\rm L}}{B_{\rm P}} - \;w^{(2)}_{J_\ell J_u}\;\sigma_0^2(\alpha_\ell J_\ell)\right]. \tag{14.107}$$

Equation (14.106) has been proposed by Trujillo Bueno (1999) to give an estimate of the polarization signal observed in spectral lines close to the solar limb, and to point out the importance of lower-level atomic polarization in the solar atmosphere. Considering a multiplet of lines sharing the same upper level, and neglecting lower-level polarization, we see from Eq. (14.106) that the observed fractional polarization in the different lines has to be proportional to the value of the corresponding symbol $w^{(2)}_{J_u J_\ell}$. Following Trujillo Bueno (1999), consider for instance the MgI triplet in the green region of the solar spectrum. The three lines at 5167.3 Å, 5172.7 Å, and 5183.6 Å correspond to the transition between a common upper level $3s\,4s\,{}^3{\rm S}_1$ and a lower level $3s\,3p\,{}^3{\rm P}^{\rm o}_J$ with $J = 0$, 1, and 2, respectively. In the absence of lower-level polarization, the fractional linear polarization should therefore be proportional to $w^{(2)}_{10}$, $w^{(2)}_{11}$, $w^{(2)}_{12}$ respectively, or, according to Table 10.1, to 1.0, −0.5, 0.1. Since the observed values of the limb fractional polarization in the three lines are very far from satisfying these relations, it follows that lower-level polarization must play a significant role.

It is also important to remark that, according both to Eq. (14.106) and to Eq. (14.107), the line contribution to the fractional polarization may be either positive or negative, because both expressions contain the difference between two terms that may themselves be positive or negative.

Turning to the scattering contribution given by Eq. (14.105), it is important to distinguish between Thomson scattering and Rayleigh scattering. In the first case, we should keep in mind that the thermal velocities of electrons are at least two orders of magnitude larger than the thermal velocities of most of the atoms contributing to the Fraunhofer spectrum. The ratio between the thermal velocity of an electron and that of a sodium atom, for instance, is 205, while for an iron atom such ratio is 319. It follows that the integral over the electron velocities contained in the numerator of the right-hand side of Eq. (14.105) completely washes out any spectral detail of the tensor $J^2_0(\nu)$, yielding an expression of the form

$$\left[\frac{Q(\nu,\vec{\Omega}_{\parallel})}{I(\nu,\vec{\Omega}_{\parallel})}\right]_{\rm T.sc} = \frac{3}{2\sqrt{2}}\ \frac{k_\nu^{(\rm c)}\,\beta_1\,\langle J_0^2\rangle_\nu}{k_\nu^{(\rm c)}B_{\rm P}\,+\,k_{\rm L}^{\rm A}\,S_{\rm L}\,\hat{\phi}(\nu_0-\nu)}\ , \tag{14.108}$$

where the quantity $\langle J_0^2\rangle_\nu$, defined by

$$\langle J_0^2\rangle_\nu = \int {\rm d}^3\vec{v}_1\ \ f(\vec{v}_1)\left[J_0^2\Big(\nu-\nu\,\frac{\vec{v}_1\cdot\vec{\Omega}_{\parallel}}{c}\Big)\right]_{\vec{v}_1}\ , \tag{14.109}$$

is in practice the average of $J_0^2(\nu)$ over a broad frequency interval centered at the frequency ν and having a width of the order of $2\Delta\nu_{\rm e}$ (cf. Eq. (14.87)), with $\Delta\nu_{\rm e}$ given by Eq. (14.88).[1] This phenomenon bears a strong resemblance with another phenomenon that solar physicists have known for a long time: the photospheric radiation scattered by electrons in the corona is indeed strongly polarized and has a featureless spectrum – whence the name of K (or continuum) corona.

As Eq. (14.108) clearly shows, the Thomson scattering contribution to fractional polarization is characterized by a frequency dependence typical of the absorption lines of the usual intensity spectrum, with a positive wing value[2] and a depression at line center. Such depression is totally independent of the intrinsic polarizability characteristics of the line, like atomic polarization or $w^{(2)}$ factors.

For the Rayleigh scattering contribution to fractional polarization similar arguments can be repeated, and an equation strictly similar to Eq. (14.108) holds. The only difference is that the factor β_1 has to be replaced by β_2 (for scattering on hydrogen atoms) or β_3 (for scattering on helium atoms), whereas the average $\langle J_0^2\rangle_\nu$ is still given by Eq. (14.109), the integral being performed on the hydrogen or helium atom velocities, respectively. Since the hydrogen atoms have thermal velocities that are several times (about 5 for sodium, 7 for iron, etc.) larger than the thermal velocities of most of the atoms contributing to the Fraunhofer spectrum, it follows that the frequency dependence of $J_0^2(\nu)$ will be substantially smoothed by the velocities of the hydrogen atoms but not totally destroyed. A qualitative sketch of the contribution to the fractional polarization arising from scattering processes is shown in Fig. 14.12.

We want to remark that the results derived in this section are strongly dependent on the approximation of plane-parallel atmosphere, thus they have to be used with much care when interpreting polarimetric observations of the solar limb spectrum.

14.8. Alternative Methods for the Solution of the Non-LTE Problem

The non-LTE theory that we have introduced in this chapter, schematically summarized in the self-consistency loop of Fig. 14.1 and usually referred to as 'non-LTE

[1] In terms of wavelength, and assuming an electronic temperature $T_{\rm e}$ of 6000 K, the width of the interval is about 10 Å at 5000 Å.

[2] $J_0^2(\nu)$ is generally positive in the top layers of a stellar atmosphere (see Chap. 12).

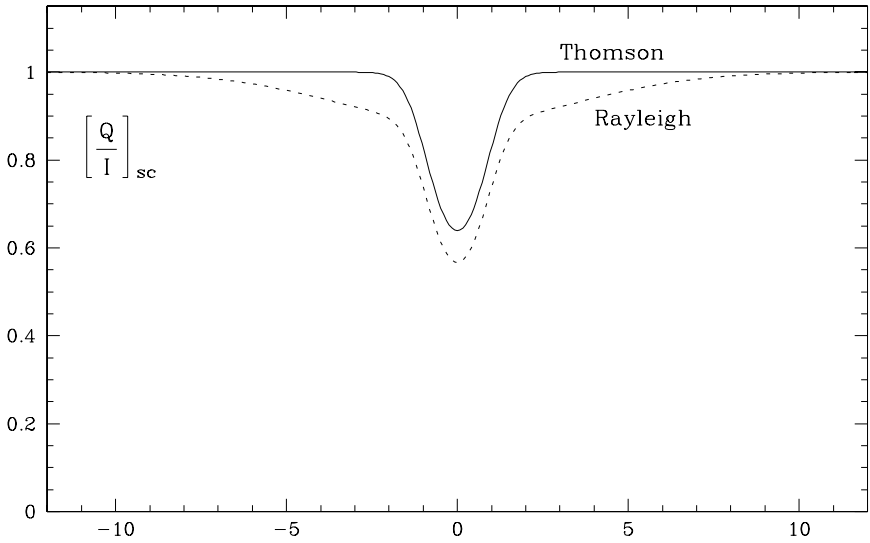

Fig.14.12. Schematic behavior, as a function of the reduced frequency $(\nu_0 - \nu)/\Delta\nu_D$, of the fractional polarization introduced by Thomson and Rayleigh scattering (full and dotted line, respectively) in the neighborhood of a spectral line of central frequency ν_0; $\Delta\nu_D$ is the Doppler width of the profile $\hat{\phi}(\nu_0 - \nu)$ of Eq.(14.108). The plot refers to the radiation propagating along the top layer of a plane-parallel atmosphere. The reference direction for positive Q is parallel to the atmosphere, and the fractional polarization is normalized to the value of the continuum spectrum.

of the 2nd kind', rests, as a foundation stone, on the concept of atomic density matrix. Such concept generalizes to polarized radiative transfer the usual concept of level populations employed in the non-LTE theory of the 1st kind, and appears to be well-suited to handle most transfer problems.

There are however some special cases where a different approach, not based on the density matrix, can be followed. These are the cases where the basic interaction process between radiation and atoms is a scattering process for which the emission coefficient vector can be expressed by a linear relation of the form

$$\varepsilon_i(\nu, \vec{\Omega}) = k_s \oint \frac{d\Omega'}{4\pi} \int_0^\infty d\nu' \sum_{j=0}^{3} R_{ij}(\nu, \vec{\Omega}\,; \nu', \vec{\Omega}')\, I_j(\nu', \vec{\Omega}') \,, \tag{14.110}$$

and the radiative transfer equation has the simple form

$$\frac{d}{ds} I_i(\nu, \vec{\Omega}) = -k_s\, I_i(\nu, \vec{\Omega}) + \varepsilon_i(\nu, \vec{\Omega}) \,. \tag{14.111}$$

In these equations, $I_i(\nu, \vec{\Omega})$ is the Stokes vector of the radiation at frequency ν propagating along the direction $\vec{\Omega}$, k_s is a scalar quantity proportional to the cross section of the scattering process and to the number density of scatterers, and $R_{ij}(\nu, \vec{\Omega}\,; \nu', \vec{\Omega}')$ is the so-called redistribution matrix.

As shown several times in this book, a linear equation similar to Eq. (14.110) can in fact be established under severe restrictive hypotheses which imply two-level (or two-terms) atomic models, the absence of atomic polarization in the lower level (or lower term), and negligible stimulated emission. Under these circumstances, the density matrix can be factored out and the non-LTE problem of the 2nd kind reduces to the self-consistent solution of Eqs. (14.110) and (14.111). In other words, there is no need to solve the statistical equilibrium equations for the density-matrix elements because such solution is implicitly contained in Eq. (14.110). Obviously, in these cases the theory provides explicit expressions for the coefficient $k_{\rm s}$ and for the redistribution matrix.

In general, an approach based on Eqs. (14.110) and (14.111), with suitable expressions for $k_{\rm s}$ and $R_{ij}(\nu,\vec{\Omega}\,;\nu',\vec{\Omega}')$, avoiding the introduction of the density matrix, can be more appropriate for the description of certain phenomena. An important example is the non-LTE problem concerning the interpretation of the extended wings of some particularly strong spectral lines formed in the solar atmosphere. Even the sophisticated redistribution matrices deduced in Chap. 13, which take velocity/density-matrix correlations into account (see Eqs. (13.35) and (A18.1)-(A18.2) for the non-magnetic case, and Eq. (13.44) for the magnetic case) are unable to explain such wings, and have to be replaced by redistribution matrices which include partial redistribution effects (in the atomic rest frame). The density-matrix theory developed in this book, being based on the Markov approximation, cannot account for such effects.

Much work has been devoted in the past to find the correct expression for the redistribution matrix capable of taking into account, at the same time, partial redistribution effects, depolarizing collisions, and the presence of a magnetic field. Important contributions to this subject have been given by Omont et al. (1972), Stenflo (1994), Bommier (1997a,b), and Landi Degl'Innocenti et al. (1997). Further efforts have been devoted to find numerical, self-consistent solutions to Eqs. (14.110)-(14.111) in plane-parallel atmospheres, either non-magnetized or magnetized, using various forms of the redistribution matrix and often introducing ad hoc approximations on the matrix itself.[1] Remarkable results on this subject have been obtained by Rees and Saliba (1982), Saliba (1986), Faurobert (1987, 1988), and Nagendra (1988, 1994) for the non-magnetic case, and by Faurobert-Scholl (1991, 1992) and Nagendra et al. (1998) for the case of the Hanle effect.

[1] From a historical point of view, it should be recalled that the first self-consistent solution of Eqs. (14.110)-(14.111) in a plane-parallel atmosphere has been given, through semi-analytical methods, by Chandrasekhar and Breen (1947). The problem solved by Chandrasekhar is that of an atmosphere composed of Thomson-scattering free electrons; in this case one has (see Eqs. (14.85) and (14.91)) $k_{\rm s} = N_{\rm e}\,\sigma_{\rm T}$, $R_{ij}(\nu,\vec{\Omega}\,;\nu'\vec{\Omega}') = R_{ij}(\vec{\Omega},\vec{\Omega}')\,\delta(\nu-\nu')$.

This page intentionally left blank

APPENDIX

A1. A Fortran Code for Computing 3-j, 6-j, and 9-j Symbols

The following code computes 3-j, 6-j, and 9-j symbols.[1] 3-j symbols are evaluated from Eqs. (2.19) and (2.22), 6-j symbols from Eq. (2.35), and 9-j symbols from Eq. (2.48). The variables appearing as dummy arguments of the three Fortran-functions W3JS, W6JS, W9JS are integers representing the values of the corresponding quantum numbers multiplied by 2. For instance

$$\begin{pmatrix} 2 & \frac{1}{2} & \frac{3}{2} \\ -1 & -\frac{1}{2} & \frac{3}{2} \end{pmatrix} = \mathrm{W3JS}\,(4,1,3,-2,-1,3)$$

$$\begin{Bmatrix} 1 & \frac{3}{2} & \frac{1}{2} \\ \frac{3}{2} & 1 & 2 \end{Bmatrix} = \mathrm{W6JS}\,(2,3,1,3,2,4)$$

$$\begin{Bmatrix} 2 & \frac{1}{2} & \frac{3}{2} \\ \frac{1}{2} & \frac{1}{2} & 1 \\ \frac{5}{2} & 1 & \frac{5}{2} \end{Bmatrix} = \mathrm{W9JS}\,(4,1,3,1,1,2,5,2,5)\,.$$

The various conditions that must be satisfied by the arguments of each symbol are explicitly checked within the code. If any of these conditions is not satisfied, the code returns the value 0 for the symbol. The instruction CALL FACTRL must appear in the main program before any of these Fortran-functions is used.

```
FUNCTION W3JS(J1,J2,J3,M1,M2,M3)
INTEGER Z,ZMIN,ZMAX
COMMON/FACT/FACT(0:301)
W3JS=0.0
IF(M1+M2+M3.NE.0) GOTO 1000
IA=J1+J2
IF(J3.GT.IA) GOTO 1000
IB=J1-J2
IF(J3.LT.IABS(IB)) GOTO 1000
JSUM=J3+IA
IC=J1-M1
ID=J2-M2
IF(MOD(JSUM,2).NE.0) GOTO 1000
IF(MOD(IC,2).NE.0) GOTO 1000
IF(MOD(ID,2).NE.0) GOTO 1000
IF(IABS(M1).GT.J1) GOTO 1000
IF(IABS(M2).GT.J2) GOTO 1000
IF(IABS(M3).GT.J3) GOTO 1000
IE=J3-J2+M1
IF=J3-J1-M2
```

[1] The code is due to Stephen Jackson, formerly at the National Center for Atmospheric Research, Boulder, Colorado.

```
      ZMIN=MAX0(0,-IE,-IF)
      IG=IA-J3
      IH=J2+M2
      ZMAX=MIN0(IG,IH,IC)
      CC=0.0
      DO 200 Z=ZMIN,ZMAX,2
      DENOM=FACT(Z/2)*FACT((IG-Z)/2)*FACT((IC-Z)/2)
     1        *FACT((IH-Z)/2)*FACT((IE+Z)/2)*FACT((IF+Z)/2)
      IF(MOD(Z,4).NE.0) DENOM=-DENOM
      CC=CC+1.0/DENOM
  200 CONTINUE
      CC1=FACT(IG/2)*FACT((J3+IB)/2)*FACT((J3-IB)/2)
     1        /FACT((JSUM+2)/2)
      CC2=FACT((J1+M1)/2)*FACT(IC/2)*FACT(IH/2)
     1        *FACT(ID/2)*FACT((J3-M3)/2)*FACT((J3+M3)/2)
      CC=CC*SQRT(CC1*CC2)
      IF(MOD(IB-M3,4).NE.0) CC=-CC
      W3JS=CC
 1000 RETURN
      END

      FUNCTION W6JS(J1,J2,J3,L1,L2,L3)
      INTEGER W,WMIN,WMAX
      INTEGER SUM1,SUM2,SUM3,SUM4
      COMMON/FACT/FACT(0:301)
      W6JS=0.0
      IA=J1+J2
      IF(IA.LT.J3) GOTO 1000
      IB=J1-J2
      IF(IABS(IB).GT.J3) GOTO 1000
      IC=J1+L2
      IF(IC.LT.L3) GOTO 1000
      ID=J1-L2
      IF(IABS(ID).GT.L3) GOTO 1000
      IE=L1+J2
      IF(IE.LT.L3) GOTO 1000
      IF=L1-J2
      IF(IABS(IF).GT.L3) GOTO 1000
      IG=L1+L2
      IF(IG.LT.J3) GOTO 1000
      IH=L1-L2
      IF(IABS(IH).GT.J3) GOTO 1000
      SUM1=IA+J3
      SUM2=IC+L3
      SUM3=IE+L3
      SUM4=IG+J3
      IF(MOD(SUM1,2).NE.0) GOTO 1000
      IF(MOD(SUM2,2).NE.0) GOTO 1000
      IF(MOD(SUM3,2).NE.0) GOTO 1000
      IF(MOD(SUM4,2).NE.0) GOTO 1000
      WMIN=MAX0(SUM1,SUM2,SUM3,SUM4)
      II=IA+IG
      IJ=J2+J3+L2+L3
      IK=J3+J1+L3+L1
```

```
      WMAX=MIN0(II,IJ,IK)
      OMEGA=0.0
      DO 200 W=WMIN,WMAX,2
      DENOM=FACT((W-SUM1)/2)*FACT((W-SUM2)/2)*FACT((W-SUM3)/2)
     1        *FACT((W-SUM4)/2)*FACT((II-W)/2)*FACT((IJ-W)/2)
     2        *FACT((IK-W)/2)
      IF(MOD(W,4).NE.0) DENOM=-DENOM
      OMEGA=OMEGA+FACT(W/2+1)/DENOM
  200 CONTINUE
      THETA1=FACT((IA-J3)/2)*FACT((J3+IB)/2)*FACT((J3-IB)/2)
     1        /FACT(SUM1/2+1)
      THETA2=FACT((IC-L3)/2)*FACT((L3+ID)/2)*FACT((L3-ID)/2)
     1        /FACT(SUM2/2+1)
      THETA3=FACT((IE-L3)/2)*FACT((L3+IF)/2)*FACT((L3-IF)/2)
     1        /FACT(SUM3/2+1)
      THETA4=FACT((IG-J3)/2)*FACT((J3+IH)/2)*FACT((J3-IH)/2)
     1        /FACT(SUM4/2+1)
      THETA=THETA1*THETA2*THETA3*THETA4
      W6JS=OMEGA*SQRT(THETA)
 1000 RETURN
      END

      FUNCTION W9JS(J1,J2,J3,J4,J5,J6,J7,J8,J9)
      KMIN=ABS(J1-J9)
      KMAX=J1+J9
      I=ABS(J4-J8)
      IF(I.GT.KMIN) KMIN=I
      I=J4+J8
      IF(I.LT.KMAX) KMAX=I
      I=ABS(J2-J6)
      IF(I.GT.KMIN) KMIN=I
      I=J2+J6
      IF(I.LT.KMAX) KMAX=I
      X=0.
      DO 1 K=KMIN,KMAX,2
      S=1.
      IF(MOD(K,2).NE.0) S=-1.
      X1=W6JS(J1,J9,K,J8,J4,J7)
      X2=W6JS(J2,J6,K,J4,J8,J5)
      X3=W6JS(J1,J9,K,J6,J2,J3)
      X=X+S*X1*X2*X3*FLOAT(K+1)
    1 CONTINUE
      W9JS=X
      RETURN
      END

      SUBROUTINE FACTRL
      COMMON/FACT/FACT(0:301)
      DATA NFAC/31/
      FACT(0)=1.0
      DO 10 I=1,NFAC
   10 FACT(I)=FACT(I-1)*FLOAT(I)
      RETURN
      END
```

A2. Sample Evaluation of a Quantity Involving the Contraction of 3-j Coefficients

Consider the quantity

$$S = \sum_{qq'MM'M''} (-1)^{J''+M''+2k-K+Q} \times \begin{pmatrix} J & J'' & k \\ -M & M'' & q \end{pmatrix} \begin{pmatrix} J'' & J' & k' \\ -M'' & M' & q' \end{pmatrix} \times \begin{pmatrix} k & k' & K \\ q & q' & -Q \end{pmatrix} \begin{pmatrix} J & J' & K \\ -M & M' & Q \end{pmatrix} . \tag{A2.1}$$

This is simply the contraction of four 3-j symbols over five angular momentum components, and closely resembles the right-hand side of Eq. (2.34) with $e' = e$, $\epsilon' = \epsilon$. In Eq. (2.34), the only component which is not a summation index (ϵ) appears in the first and fourth symbols, while the corresponding component (Q) in Eq. (A2.1) appears in the third and fourth symbols. Thus we start, for instance, from the third 3-j in Eq. (A2.1) and substitute $k = c$, $k' = d$, $K = e$, $q = \gamma$, $q' = -\delta$, $Q = -\epsilon$. By so doing, the third 3-j symbol in Eq. (A2.1) takes the same form as the first 3-j in Eq. (2.34).

Looking again at Eq. (2.34), we see that the second 3-j contains the column (d, δ) which appears also (apart from a sign) in the first 3-j. According to our previous substitution, d and δ correspond to k' and $-q'$, respectively, so that we must pick the second 3-j in Eq. (A2.1) and reshape it, using the symmetry properties of the 3-j symbols, in one of the two equivalent forms

$$\begin{pmatrix} J'' & J' & k' \\ -M'' & M' & q' \end{pmatrix} \to \begin{pmatrix} k' & J' & J'' \\ -q' & -M' & M'' \end{pmatrix} \to (-1)^{k'+J'+J''} \begin{pmatrix} k' & J'' & J' \\ -q' & M'' & -M' \end{pmatrix} . \tag{A2.2}$$

Of these two forms, it is the second one that brings the right-hand side of Eq. (A2.1) into a form equivalent to the right-hand side of Eq. (2.34). Indeed, choosing the second form, we substitute $J'' = b$, $J' = f$, $M'' = -\beta$, $M' = -\phi$, and we can now reshape the first 3-j in Eq. (A2.1) in the form

$$\begin{pmatrix} J & J'' & k \\ -M & M'' & q \end{pmatrix} \to (-1)^{k+J+J''} \begin{pmatrix} J'' & k & J \\ -M'' & -q & M \end{pmatrix}$$

to get, by the substitutions $J = a$, $M = \alpha$ and apart from a sign factor, the third 3-j in Eq. (2.34).[1]

[1] Note that if the first form were chosen for the 3-j in Eq. (A2.2) (implying the substitutions $J' = b$, $J'' = f$, $M' = \beta$, $M'' = \phi$), it would be impossible to arrange the first 3-j in Eq. (A2.1) in the form of either the third or the fourth 3-j in Eq. (2.34).

Finally, reshaping the fourth 3-j in the form

$$\begin{pmatrix} J & J' & K \\ -M & M' & Q \end{pmatrix} \rightarrow \begin{pmatrix} J' & J & K \\ -M' & M & -Q \end{pmatrix} ,$$

we obtain, by the substitutions given above, the correct 3-j appearing at the fourth place in Eq. (2.34).

Summarizing all the substitutions,

$$\begin{aligned} J &= a & M &= \alpha \\ J' &= f & M' &= -\phi \\ J'' &= b & M'' &= -\beta \\ k &= c & q &= \gamma \\ k' &= d & q' &= -\delta \\ K &= e & Q &= -\epsilon , \end{aligned} \tag{A2.3}$$

and recalling all the sign factors, we can write

$$S = \sum_{\alpha\beta\gamma\delta\phi} (-1)^{b-\beta+2c-e-\epsilon+d+f+b+c+a+b} \times \begin{pmatrix} c & d & e \\ \gamma & -\delta & \epsilon \end{pmatrix} \begin{pmatrix} d & b & f \\ \delta & -\beta & \phi \end{pmatrix} \begin{pmatrix} b & c & a \\ \beta & -\gamma & \alpha \end{pmatrix} \begin{pmatrix} f & a & e \\ \phi & \alpha & \epsilon \end{pmatrix} . \tag{A2.4}$$

Now we must work on the sign factor to cast it in a form such that Eq. (2.34) can be applied. In general, when performing this kind of calculations on sign factors appearing in Racah-algebra expressions, a number of rules can be applied. If Σ is an arbitrary linear combination of angular momentum and z-component quantum numbers, these rules can be summarized as follows

I)

$$(-1)^{a\pm\alpha+\Sigma} \begin{pmatrix} a & b & c \\ \alpha & \beta & \gamma \end{pmatrix} = (-1)^{-a\mp\alpha+\Sigma} \begin{pmatrix} a & b & c \\ \alpha & \beta & \gamma \end{pmatrix} ,$$

as $(a \pm \alpha)$ is an integer;

II)

$$(-1)^{\alpha+\beta+\gamma+\Sigma} \begin{pmatrix} a & b & c \\ \alpha & \beta & \gamma \end{pmatrix} = (-1)^{\Sigma} \begin{pmatrix} a & b & c \\ \alpha & \beta & \gamma \end{pmatrix} ,$$

as $(\alpha + \beta + \gamma) = 0$ because of the presence of the 3-j symbol;

III)

$$(-1)^{a\pm b\pm c+\Sigma} \begin{pmatrix} a & b & c \\ \alpha & \beta & \gamma \end{pmatrix} = (-1)^{-a\mp b\mp c+\Sigma} \begin{pmatrix} a & b & c \\ \alpha & \beta & \gamma \end{pmatrix} ,$$

as the quantity $(a \pm b \pm c)$ is an integer;

IV)

$$(-1)^{3a+\Sigma} = (-1)^{-a+\Sigma} , \qquad (-1)^{4a+\Sigma} = (-1)^{\Sigma} ,$$

as $4a$ is an even integer.

With the help of these rules, the sign factor appearing in Eq. (A2.4) can be transformed in the following way

$$(-1)^{a+3b+3c+d-e+f-\beta-\epsilon} =$$
$$= (-1)^{b+c+d+\beta+\gamma+\delta} (-1)^{a+3b+3c+d-e+f-\beta-\epsilon-b-c-d-\beta-\gamma-\delta} = S_1 S_2 .$$

S_1 is the correct sign factor appearing in Eq. (2.34), while S_2 can be transformed by replacing, according to Rule I, $(-b-\beta)$ by $(b+\beta)$ and $(-d-\delta)$ by $(d+\delta)$. Thus we obtain

$$S_2 = (-1)^{a+4b+2c+2d-e+f-\gamma+\delta-\epsilon} .$$

Now we can eliminate the terms $4b$ and $(-\gamma+\delta-\epsilon)$ according to Rules IV and II, respectively, and we get

$$S_2 = (-1)^{a+2c+2d-e+f} .$$

Finally, according to Rule III, we can substitute $(c+d-e)$ by $(-c-d+e)$ to obtain

$$S_2 = (-1)^{a+e+f} .$$

Since S_2 does not depend on the summation indices in Eq. (A2.4), we can apply Eq. (2.34) to get

$$S = (-1)^{a+e+f} \frac{1}{2e+1} \begin{Bmatrix} a & b & c \\ d & e & f \end{Bmatrix} ,$$

and recalling the substitutions (A2.3) we obtain the final result

$$S = (-1)^{J+J'+K} \frac{1}{2K+1} \begin{Bmatrix} J & J'' & k \\ k' & K & J' \end{Bmatrix} = (-1)^{J+J'+K} \frac{1}{2K+1} \begin{Bmatrix} J & J' & K \\ k' & k & J'' \end{Bmatrix} .$$

Obviously, the calculation scheme presented here is nothing but an example, and different procedures can be followed to obtain the same result.

A3. Momentum and Angular Momentum of the Electromagnetic Field

In classical physics, the momentum of the electromagnetic field is given by (see e.g. Jackson, 1962)

$$\vec{P} = \frac{1}{4\pi c} \int_V \vec{E} \times \vec{B} \, \mathrm{d}V .$$

Since $\vec{B} = \operatorname{curl} \vec{A}$, the j-th Cartesian component of $\vec{P}$ is

$$P_j = \frac{1}{4\pi c} \sum_m \int_V \left(E_m \frac{\partial A_m}{\partial x_j} - E_m \frac{\partial A_j}{\partial x_m} \right) \mathrm{d}V \ . \tag{A3.1}$$

Being in vacuum $\operatorname{div} \vec{E} = 0$, the second term in the right-hand side can be written in the form

$$\sum_m \int_V E_m \frac{\partial A_j}{\partial x_m} \, \mathrm{d}V = \sum_m \int_V \frac{\partial}{\partial x_m} (E_m A_j) \, \mathrm{d}V \ .$$

On the other hand, this integral can be transformed into a surface integral. Assuming that the fields vanish at infinity, Eq. (A3.1) reduces to

$$P_j = \frac{1}{4\pi c} \sum_m \int_V E_m \frac{\partial A_m}{\partial x_j} \, \mathrm{d}V \ . \tag{A3.2}$$

Similarly, writing the angular momentum of the electromagnetic field in the form

$$\vec{M} = \frac{1}{4\pi c} \int_V \vec{r} \times (\vec{E} \times \vec{B}) \, \mathrm{d}V \ ,$$

one obtains for the j-th component of $\vec{M}$

$$M_j = \frac{1}{4\pi c} \sum_{klm} \epsilon_{jkl} \int_V x_k \left(E_m \frac{\partial A_m}{\partial x_l} - E_m \frac{\partial A_l}{\partial x_m} \right) \mathrm{d}V \ .$$

For the second term we have

$$\sum_m \int_V x_k E_m \frac{\partial A_l}{\partial x_m} \, \mathrm{d}V = \sum_m \int_V \frac{\partial}{\partial x_m} (x_k E_m A_l) \, \mathrm{d}V - \int_V E_k A_l \, \mathrm{d}V \ ,$$

and observing that the first integral in the right-hand side is zero we obtain

$$M_j = \frac{1}{4\pi c} \sum_{klm} \epsilon_{jkl} \int_V x_k E_m \frac{\partial A_m}{\partial x_l} \, \mathrm{d}V + \frac{1}{4\pi c} \sum_{kl} \epsilon_{jkl} \int_V E_k A_l \, \mathrm{d}V \ . \tag{A3.3}$$

We now recall that in Quantum Mechanics the momentum operator $\hat{p}_j$ and the orbital angular momentum operator $\hat{l}_j$ are given by

$$\hat{p}_j = -\mathrm{i}\hbar \frac{\partial}{\partial x_j}$$

$$\hat{l}_j = -\mathrm{i}\hbar \sum_{kl} \epsilon_{jkl} \, x_k \, \frac{\partial}{\partial x_l} \ ,$$

therefore Eqs. (A3.2) and (A3.3) can be written in the form

$$P_j = \frac{\mathrm{i}}{4\pi\hbar c} \int_V \sum_m \left(E_m \, \hat{p}_j \, A_m\right) \mathrm{d}V$$

$$M_j = \frac{\mathrm{i}}{4\pi\hbar c} \int_V \sum_m \left(E_m \, \hat{l}_j \, A_m\right) \mathrm{d}V + \frac{1}{4\pi c} \int_V \left(\vec{E} \times \vec{A}\right)_j \mathrm{d}V \, . \qquad \text{(A3.4)}$$

These expressions suggest quite naturally that the first term in the right-hand side of Eq. (A3.4) can be regarded as the orbital angular momentum, and the second term as the intrinsic angular momentum (or spin) of the radiation.

Now we introduce the formalism of second quantization to derive the expressions of the operators $\hat{\vec{P}}$ and $\hat{\vec{M}}$ according to the Correspondence Principle. For the operator $\hat{\vec{P}}$ we start from Eq. (A3.2). Substituting for $\vec{A}$ and $\vec{E}$ the expressions of the corresponding operators given by Eqs. (4.30) and (4.33), and carrying out the volume integration along the same lines leading to Eq. (4.24), one obtains

$$\hat{\vec{P}} = \sum_{\nu\vec{\Omega}\lambda} \frac{h\nu}{2c} \, \vec{\Omega} \left[a(\nu, \vec{\Omega}, \lambda) \, a^\dagger(\nu, \vec{\Omega}, \lambda) + a^\dagger(\nu, \vec{\Omega}, \lambda) \, a(\nu, \vec{\Omega}, \lambda)\right] .$$

Owing to the commutation rule (4.32) this expression reduces to

$$\hat{\vec{P}} = \sum_{\nu\vec{\Omega}\lambda} \frac{h\nu}{c} \, \vec{\Omega} \, a^\dagger(\nu, \vec{\Omega}, \lambda) \, a(\nu, \vec{\Omega}, \lambda) \, ,$$

which, recalling the physical meaning of the operator $a^\dagger(\nu, \vec{\Omega}, \lambda) \, a(\nu, \vec{\Omega}, \lambda)$, shows that each photon of frequency ν and direction $\vec{\Omega}$ carries a momentum $h\nu \, \vec{\Omega}/c$.

For the operator $\hat{\vec{M}}$, we consider only the contribution of the intrinsic angular momentum. Therefore, we calculate the operator

$$\hat{\vec{M}}_{\mathrm{S}} = \frac{1}{4\pi c} \int_V \hat{\vec{E}} \times \hat{\vec{A}} \, \mathrm{d}V \, .$$

Evaluation of the volume integral via the same substitutions leads to

$$\hat{\vec{M}}_{\mathrm{S}} = \sum_{\nu\vec{\Omega}\lambda\lambda'} \frac{\mathrm{i}h}{4\pi} \Big[a(\nu, \vec{\Omega}, \lambda) \, a^\dagger(\nu, \vec{\Omega}, \lambda') \, \vec{e}_\lambda(\vec{\Omega}) \times \vec{e}_{\lambda'}(\vec{\Omega})^* - a^\dagger(\nu, \vec{\Omega}, \lambda) \, a(\nu, \vec{\Omega}, \lambda') \, \vec{e}_\lambda(\vec{\Omega})^* \times \vec{e}_{\lambda'}(\vec{\Omega})\Big] \, . \qquad \text{(A3.5)}$$

The expression in square bracket can be related to the Stokes parameter operator $\hat{V}(\nu, \vec{\Omega})$ defined in Sect. 4.4. Let us consider, for instance, the representation (4.38) for the unit vectors $\vec{e}_\lambda(\vec{\Omega})$. The cross products are

$$\vec{e}_{+1}(\vec{\Omega}) \times \vec{e}_{+1}(\vec{\Omega})^* = \mathrm{i} \, \vec{\Omega}$$

$$\vec{e}_{-1}(\vec{\Omega}) \times \vec{e}_{-1}(\vec{\Omega})^* = -\mathrm{i} \, \vec{\Omega}$$

$$\vec{e}_{+1}(\vec{\Omega}) \times \vec{e}_{-1}(\vec{\Omega})^* = \vec{e}_{-1}(\vec{\Omega}) \times \vec{e}_{+1}(\vec{\Omega})^* = 0 \, ,$$

thus Eq. (A3.5) becomes

$$\hat{\vec{M}}_{\rm S} = -\sum_{\nu\vec{\Omega}} \frac{h}{4\pi}\,\vec{\Omega}\left\{\left[a(\nu,\vec{\Omega},+1)\,a^{\dagger}(\nu,\vec{\Omega},+1) + a^{\dagger}(\nu,\vec{\Omega},+1)\,a(\nu,\vec{\Omega},+1)\right]\right.$$
$$\left. - \left[a(\nu,\vec{\Omega},-1)\,a^{\dagger}(\nu,\vec{\Omega},-1) + a^{\dagger}(\nu,\vec{\Omega},-1)\,a(\nu,\vec{\Omega},-1)\right]\right\},$$

or, using Eq. (4.32)

$$\hat{\vec{M}}_{\rm S} = -\sum_{\nu\vec{\Omega}} \frac{h}{2\pi}\,\vec{\Omega}\left[a^{\dagger}(\nu,\vec{\Omega},+1)\,a(\nu,\vec{\Omega},+1) - a^{\dagger}(\nu,\vec{\Omega},-1)\,a(\nu,\vec{\Omega},-1)\right]. \quad \text{(A3.6)}$$

Recalling Eqs. (4.37) and (4.39) we finally obtain

$$\hat{\vec{M}}_{\rm S} = -\sum_{\nu\vec{\Omega}} \frac{c^2}{2\pi\nu^3}\,\vec{\Omega}\,\hat{V}(\nu,\vec{\Omega})\,. \quad \text{(A3.7)}$$

Although this result has been obtained using the specific unit vectors of Eqs. (4.38), it can be shown directly that it holds also for the more general unit vectors defined in Eqs. (1.41).

Equations (A3.6) and (A3.7) have a simple physical interpretation. They show that each circularly polarized photon carries an intrinsic angular momentum of magnitude $\hbar$, parallel or antiparallel to the propagation direction $\vec{\Omega}$. It is also seen that a *positive* (or right-handed) circular polarization corresponds to a *negative* projection of the angular momentum on the propagation direction (negative *helicity*), and vice versa.

The inconsistency between the sign of circular polarization and the sign of helicity is obviously due to the convention adopted in this book for the sign of circular polarization. The reasons of our choice are mainly of practical nature and are explained in Sect. 1.2. In any case, it should be remarked that even the definition of positive helicity is purely conventional.

A4. Multipole Components of Collisional Rates

In Sect. 7.13.a we have seen that the hypothesis of isotropic collisions implies that the transfer collisional rates $C_{\rm I}(\alpha JMM', \alpha_\ell J_\ell M_\ell M'_\ell)$ must satisfy Eq. (7.84) for any arbitrary rotation R of the reference system. Instead of transforming the right-hand side of Eq. (7.84) via Eqs. (7.85), we can couple the rotation matrices in a different way, writing

$$\mathcal{D}^{J_\ell}_{N_\ell M_\ell}(R)\;\mathcal{D}^{J}_{NM}(R)^* =$$
$$= (-1)^{N-M}\sum_K (2K+1)\begin{pmatrix} J_\ell & J & K \\ N_\ell & -N & P\end{pmatrix}\begin{pmatrix} J_\ell & J & K \\ M_\ell & -M & Q\end{pmatrix}\mathcal{D}^{K}_{PQ}(R)^*\,,$$

$$\mathcal{D}^{J}_{N'M'}(R)\,\mathcal{D}^{J_\ell}_{N'_\ell M'_\ell}(R)^* =$$
$$= (-1)^{N'_\ell - M'_\ell} \sum_{K'} (2K'+1) \begin{pmatrix} J & J_\ell & K' \\ N' & -N'_\ell & P' \end{pmatrix} \begin{pmatrix} J & J_\ell & K' \\ M' & -M'_\ell & Q' \end{pmatrix} \mathcal{D}^{K'}_{P'Q'}(R)^* \,,$$

$$\mathcal{D}^{K}_{PQ}(R)^*\,\mathcal{D}^{K'}_{P'Q'}(R)^* =$$
$$= \sum_{K''} (2K''+1) \begin{pmatrix} K & K' & K'' \\ P & P' & P'' \end{pmatrix} \begin{pmatrix} K & K' & K'' \\ Q & Q' & Q'' \end{pmatrix} \mathcal{D}^{K''}_{P''Q''}(R) \,. \tag{A4.1}$$

Substitution into Eq. (7.84) gives

$$C_{\rm I}(\alpha J M M', \alpha_\ell J_\ell M_\ell M'_\ell) = \sum_{N N' N_\ell N'_\ell} C_{\rm I}(\alpha J N N', \alpha_\ell J_\ell N_\ell N'_\ell)$$
$$\times \sum_{K K' K''} (2K+1)(2K'+1)(2K''+1)\,(-1)^{N-M+N'_\ell - M'_\ell}$$
$$\times \begin{pmatrix} J_\ell & J & K \\ N_\ell & -N & P \end{pmatrix} \begin{pmatrix} J_\ell & J & K \\ M_\ell & -M & Q \end{pmatrix} \begin{pmatrix} J & J_\ell & K' \\ N' & -N'_\ell & P' \end{pmatrix}$$
$$\times \begin{pmatrix} J & J_\ell & K' \\ M' & -M'_\ell & Q' \end{pmatrix} \begin{pmatrix} K & K' & K'' \\ P & P' & P'' \end{pmatrix} \begin{pmatrix} K & K' & K'' \\ Q & Q' & Q'' \end{pmatrix} \mathcal{D}^{K''}_{P''Q''}(R) \,.$$

Since the right-hand side must be independent of the rotation R, the index K'' can only take the value $K''=0$. This implies $K=K'$, $P=-P'$, $Q=-Q'$. We thus obtain, using Eq. (2.26a)

$$C_{\rm I}(\alpha J M M', \alpha_\ell J_\ell M_\ell M'_\ell) = (-1)^{M'_\ell - M_\ell}\ (2J_\ell+1)$$
$$\times \sum_{K} \begin{pmatrix} J & J_\ell & K \\ -M & M_\ell & Q \end{pmatrix} \begin{pmatrix} J & J_\ell & K \\ -M' & M'_\ell & Q \end{pmatrix} \Gamma^{(K)}_{\rm I}(\alpha J, \alpha_\ell J_\ell) \,, \tag{A4.2}$$

where we have defined another set of multipole components of the collisional rates, given by

$$\Gamma^{(K)}_{\rm I}(\alpha J, \alpha_\ell J_\ell) = \frac{2K+1}{2J_\ell+1}$$
$$\times \sum_{N N' N_\ell N'_\ell P} (-1)^{N'_\ell - N_\ell} \begin{pmatrix} J & J_\ell & K \\ -N & N_\ell & P \end{pmatrix} \begin{pmatrix} J & J_\ell & K \\ -N' & N'_\ell & P \end{pmatrix}$$
$$\times C_{\rm I}(\alpha J N N', \alpha_\ell J_\ell N_\ell N'_\ell) \,.$$

The multipole components $\Gamma^{(K)}_{\rm I}$ are of course related to the multipole components $C^{(K)}_{\rm I}$ defined in Eq. (7.87). To find this relation we start from Eq. (7.87) and write

the product of the two 3-j symbols via Eq. (2.43)

$$\begin{pmatrix} J & J & K \\ N' & -N & P \end{pmatrix}\begin{pmatrix} J_\ell & J_\ell & K \\ N'_\ell & -N_\ell & P \end{pmatrix} = \begin{pmatrix} J & J & K \\ N' & -N & P \end{pmatrix}\begin{pmatrix} J_\ell & J_\ell & K \\ N_\ell & -N'_\ell & -P \end{pmatrix}$$

$$= \sum_{K'} (-1)^{2J+2J_\ell+K'-K-N'-N_\ell} \times (2K'+1) \begin{Bmatrix} J & J & K \\ J_\ell & J_\ell & K' \end{Bmatrix} \begin{pmatrix} J & J_\ell & K' \\ -N & N_\ell & P' \end{pmatrix}\begin{pmatrix} J & J_\ell & K' \\ -N' & N'_\ell & P' \end{pmatrix} .$$

We thus obtain, after some algebra

$$C_{\rm I}^{(K)}(\alpha J, \alpha_\ell J_\ell) = \sqrt{(2J+1)(2J_\ell+1)} \times \sum_{K'} (-1)^{J+J_\ell+K'-K} \begin{Bmatrix} J & J & K \\ J_\ell & J_\ell & K' \end{Bmatrix} \Gamma_{\rm I}^{(K')}(\alpha J, \alpha_\ell J_\ell) ,$$

with the inverse formula (that can be deduced with the help of Eq. (2.39))

$$\Gamma_{\rm I}^{(K)}(\alpha J, \alpha_\ell J_\ell) = \frac{2K+1}{\sqrt{(2J+1)(2J_\ell+1)}} \times \sum_{K'} (-1)^{J+J_\ell-K'+K} (2K'+1) \begin{Bmatrix} J & J & K' \\ J_\ell & J_\ell & K \end{Bmatrix} C_{\rm I}^{(K')}(\alpha J, \alpha_\ell J_\ell) .$$

In particular, using Eq. (2.36a) we obtain

$$C_{\rm I}^{(0)}(\alpha J, \alpha_\ell J_\ell) = \sum_K \Gamma_{\rm I}^{(K)}(\alpha J, \alpha_\ell J_\ell) .$$

The coupling of rotation matrices in Eqs. (A4.1) is particularly interesting because of the decomposition of the transfer collisional rate expressed by Eq. (A4.2). The structure of the 3-j symbols (cf. the expression of the transfer radiative rate $T_{\rm A}(\alpha JMM', \alpha_\ell J_\ell M_\ell M'_\ell)$ in Eq. (7.9a)) suggests for Eq. (A4.2) the following interpretation: the interaction between the atomic system and the collider is described by a sum of tensor operators of rank K acting on the state vectors of the atom. The summation over K represents the contribution to the rate of the various operators.

The important fact to be stressed here is that, in many cases, the interaction is suitably described by just one operator of rank $\tilde{K}$.[1] In such cases one has

$$C_{\rm I}^{(K)}(\alpha J, \alpha_\ell J_\ell) = \sqrt{(2J+1)(2J_\ell+1)} \times (-1)^{J+J_\ell+\tilde{K}-K} \begin{Bmatrix} J & J & K \\ J_\ell & J_\ell & \tilde{K} \end{Bmatrix} \Gamma_{\rm I}^{(\tilde{K})}(\alpha J, \alpha_\ell J_\ell) ,$$

[1] For instance, the electron-atom interaction can be treated under the Born approximation provided the energy of the colliding electrons is much larger than the threshold energy. In this case the interaction Hamiltonian depends on the dynamical variables of the atomic system only through the dipole operator (which is a tensor of rank 1), so that $\tilde{K} = 1$.

so that the multipole component of rank K is related to the multipole component of rank 0 by the equation

$$C_{\rm I}^{(K)}(\alpha J,\alpha_\ell J_\ell) = (-1)^K \frac{\left\{\begin{array}{ccc} J & J & K \\ J_\ell & J_\ell & \tilde{K}\end{array}\right\}}{\left\{\begin{array}{ccc} J & J & 0 \\ J_\ell & J_\ell & \tilde{K}\end{array}\right\}} C_{\rm I}^{(0)}(\alpha J,\alpha_\ell J_\ell)\ .$$

The same line of reasoning can be followed for the collisional rates due to superelastic and to elastic collisions (considered in Sects. 7.13.a and 7.13.b, respectively). As far as superelastic collisions are concerned, the expansion in multipole components of the form $\mathit{\Gamma}_{\rm S}^{(K)}$ is given by

$$C_{\rm S}(\alpha JMM',\alpha_u J_u M_u M_u') = (-1)^{M_u'-M_u}\ (2J_u+1) \times \sum_K \begin{pmatrix} J & J_u & K \\ -M & M_u & Q\end{pmatrix}\begin{pmatrix} J & J_u & K \\ -M' & M_u' & Q\end{pmatrix} \mathit{\Gamma}_{\rm S}^{(K)}(\alpha J,\alpha_u J_u)$$

with

$$\mathit{\Gamma}_{\rm S}^{(K)}(\alpha J,\alpha_u J_u) = \frac{2K+1}{2J_u+1} \times \sum_{NN'N_uN_u'P} (-1)^{N_u'-N_u}\begin{pmatrix} J & J_u & K \\ -N & N_u & P\end{pmatrix}\begin{pmatrix} J & J_u & K \\ -N' & N_u' & P\end{pmatrix} \times C_{\rm S}(\alpha JNN',\alpha_u J_u N_u N_u')\ .$$

The multipole components $C_{\rm S}^{(K)}$ defined in Eq. (7.89) are related to these new components by

$$C_{\rm S}^{(K)}(\alpha J,\alpha_u J_u) = \sqrt{(2J+1)(2J_u+1)} \times \sum_{K'} (-1)^{J+J_u+K'-K}\left\{\begin{array}{ccc} J & J & K \\ J_u & J_u & K'\end{array}\right\} \mathit{\Gamma}_{\rm S}^{(K')}(\alpha J,\alpha_u J_u)\ .$$

The corresponding expansion for elastic collisional rates is

$$C_{\rm E}(\alpha JMM',\alpha JM''M''') = (-1)^{M'''-M''}\ (2J+1) \times \sum_K \begin{pmatrix} J & J & K \\ -M & M'' & Q\end{pmatrix}\begin{pmatrix} J & J & K \\ -M' & M''' & Q\end{pmatrix} \mathit{\Gamma}_{\rm E}^{(K)}(\alpha J)$$

with

$$\mathit{\Gamma}_{\rm E}^{(K)}(\alpha J) = \frac{2K+1}{2J+1} \times \sum_{NN'N''N'''P} (-1)^{N'''-N''}\begin{pmatrix} J & J & K \\ -N & N'' & P\end{pmatrix}\begin{pmatrix} J & J & K \\ -N' & N''' & P\end{pmatrix} \times C_{\rm E}(\alpha JNN',\alpha JN''N''')\ ,$$

and the relation with the multipole components $C_{\rm E}^{(K)}$ defined in Eq. (7.100) is

$$C_{\rm E}^{(K)}(\alpha J) = (2J+1)\sum_{K'}(-1)^{2J+K'-K}\left\{\begin{array}{ccc} J & J & K \\ J & J & K' \end{array}\right\} \Gamma_{\rm E}^{(K')}(\alpha J)\,. \qquad \text{(A4.3)}$$

When the interaction between the atomic system and the collider is described by a single operator of rank $\tilde{K}$ we have

$$C_{\rm S}^{(K)}(\alpha J, \alpha_u J_u) = (-1)^K \frac{\left\{\begin{array}{ccc} J & J & K \\ J_u & J_u & \tilde{K} \end{array}\right\}}{\left\{\begin{array}{ccc} J & J & 0 \\ J_u & J_u & \tilde{K} \end{array}\right\}} C_{\rm S}^{(0)}(\alpha J, \alpha_u J_u)$$

and

$$C_{\rm E}^{(K)}(\alpha J) = (-1)^K \frac{\left\{\begin{array}{ccc} J & J & K \\ J & J & \tilde{K} \end{array}\right\}}{\left\{\begin{array}{ccc} J & J & 0 \\ J & J & \tilde{K} \end{array}\right\}} C_{\rm E}^{(0)}(\alpha J)\,.$$

A5. Explicit Expression for the Exponential of the Propagation Matrix

We want to calculate the expression

$$\mathrm{e}^{-x\,\boldsymbol{Z}}\,,$$

where x is a real variable and $\boldsymbol{Z}$ is a 4×4 real matrix of the form

$$\boldsymbol{Z} = \begin{pmatrix} w_0 & w_1 & w_2 & w_3 \\ w_1 & w_0 & y_3 & -y_2 \\ w_2 & -y_3 & w_0 & y_1 \\ w_3 & y_2 & -y_1 & w_0 \end{pmatrix}.$$

Let us introduce the formal vectors

$$\vec{w} = (w_1\,, w_2\,, w_3)\,, \qquad \vec{y} = (y_1\,, y_2\,, y_3)$$

and their complex linear combinations

$$\vec{a} = \frac{1}{2}\left(\vec{w} + \mathrm{i}\,\vec{y}\right) = \frac{1}{2}\left(w_1 + \mathrm{i}\,y_1\,, w_2 + \mathrm{i}\,y_2\,, w_3 + \mathrm{i}\,y_3\right)$$
$$\vec{b} = \vec{a}^{\,*} = \frac{1}{2}\left(\vec{w} - \mathrm{i}\,\vec{y}\right) = \frac{1}{2}\left(w_1 - \mathrm{i}\,y_1\,, w_2 - \mathrm{i}\,y_2\,, w_3 - \mathrm{i}\,y_3\right).$$

Introducing also the six 4×4 matrices

$$\vec{\boldsymbol{A}} = (\boldsymbol{A}_1\,, \boldsymbol{A}_2\,, \boldsymbol{A}_3\,)\,, \qquad \vec{\boldsymbol{B}} = (\boldsymbol{B}_1\,, \boldsymbol{B}_2\,, \boldsymbol{B}_3\,)$$

defined by

$$\boldsymbol{A}_1 = \boldsymbol{B}_1^* = \begin{pmatrix} 0 & 1 & 0 & 0 \\ 1 & 0 & 0 & 0 \\ 0 & 0 & 0 & -\,\mathrm{i} \\ 0 & 0 & \mathrm{i} & 0 \end{pmatrix} \tag{A5.1a}$$

$$\boldsymbol{A}_2 = \boldsymbol{B}_2^* = \begin{pmatrix} 0 & 0 & 1 & 0 \\ 0 & 0 & 0 & \mathrm{i} \\ 1 & 0 & 0 & 0 \\ 0 & -\,\mathrm{i} & 0 & 0 \end{pmatrix} \tag{A5.1b}$$

$$\boldsymbol{A}_3 = \boldsymbol{B}_3^* = \begin{pmatrix} 0 & 0 & 0 & 1 \\ 0 & 0 & -\,\mathrm{i} & 0 \\ 0 & \mathrm{i} & 0 & 0 \\ 1 & 0 & 0 & 0 \end{pmatrix}\,, \tag{A5.1c}$$

the matrix $\boldsymbol{Z}$ can be written in the form

$$\boldsymbol{Z} = w_0\, \boldsymbol{1} + \vec{a} \cdot \vec{\boldsymbol{A}} + \vec{b} \cdot \vec{\boldsymbol{B}}\,, \tag{A5.2}$$

where $\boldsymbol{1}$ is the 4×4 identity matrix.

The matrices $\vec{\boldsymbol{A}}$ and $\vec{\boldsymbol{B}}$ satisfy the following algebra

$$\big[\boldsymbol{A}_j\,, \boldsymbol{B}_k\big] = \boldsymbol{A}_j\, \boldsymbol{B}_k - \boldsymbol{B}_k\, \boldsymbol{A}_j = 0 \tag{A5.3}$$

$$\boldsymbol{A}_j\, \boldsymbol{A}_k = \delta_{jk}\, \boldsymbol{1} + \mathrm{i} \sum_l \epsilon_{jkl}\, \boldsymbol{A}_l \tag{A5.4}$$

$$\boldsymbol{B}_j\, \boldsymbol{B}_k = \delta_{jk}\, \boldsymbol{1} - \mathrm{i} \sum_l \epsilon_{jkl}\, \boldsymbol{B}_l\,, \tag{A5.5}$$

where δ_{jk} is the Kronecker symbol and ϵ_{jkl} is the antisymmetric tensor (defined on p. 7). Since by a well-known theorem on matrices[1]

$$\mathrm{e}^{\boldsymbol{M}_1 + \boldsymbol{M}_2} = \mathrm{e}^{\boldsymbol{M}_1}\, \mathrm{e}^{\boldsymbol{M}_2} \qquad \text{if} \qquad \big[\boldsymbol{M}_1\,, \boldsymbol{M}_2\big] = 0\,, \tag{A5.6}$$

we have from Eqs. (A5.2) and (A5.3)

$$\mathrm{e}^{-x\,\boldsymbol{Z}} = \mathrm{e}^{-x\,w_0\,\boldsymbol{1}}\, \mathrm{e}^{-x\,\vec{a}\cdot\vec{\boldsymbol{A}}}\, \mathrm{e}^{-x\,\vec{b}\cdot\vec{\boldsymbol{B}}}\,. \tag{A5.7}$$

[1] See e.g. Cohen-Tannoudji et al., 1977, p.170.

Now we turn to the evaluation of the single factors appearing in this equation. Recalling Eq. (8.21), and observing that $\boldsymbol{1}^n = \boldsymbol{1}$, we have

$$\mathrm{e}^{-x\,w_0\,\boldsymbol{1}} = \sum_{n=0}^{\infty} \frac{(-1)^n}{n!}\,(x w_0)^n\;\boldsymbol{1} = \mathrm{e}^{-x\,w_0}\;\boldsymbol{1}\;. \tag{A5.8}$$

On the other hand, using Eq. (A5.4) one gets

$$\begin{aligned}\bigl(\vec{a}\cdot\vec{\boldsymbol{A}}\bigr)^2 &= \sum_{jk} a_j\,\boldsymbol{A}_j\;a_k\,\boldsymbol{A}_k \\ &= \sum_{jk} a_j\,a_k\,\delta_{jk}\;\boldsymbol{1} + \mathrm{i}\sum_{jkl}\epsilon_{jkl}\;a_j\,a_k\,\boldsymbol{A}_l = a^2\,\boldsymbol{1}\;,\end{aligned}$$

where

$$a^2 = \vec{a}\cdot\vec{a} = \frac{1}{4}\bigl[\,w^2 - y^2 + 2\,\mathrm{i}\,\vec{w}\cdot\vec{y}\,\bigr] \tag{A5.9}$$

with

$$\begin{aligned} w^2 &= \vec{w}\cdot\vec{w} = w_1^2 + w_2^2 + w_3^2 \\ y^2 &= \vec{y}\cdot\vec{y} = y_1^2 + y_2^2 + y_3^2\;. \end{aligned}$$

Recalling again Eq. (8.21) we thus obtain

$$\mathrm{e}^{-x\,\vec{a}\cdot\vec{\boldsymbol{A}}} = \left[1 + \frac{x^2a^2}{2!} + \frac{x^4a^4}{4!} + \cdots\right]\boldsymbol{1} - \left[\frac{x}{1!} + \frac{x^3a^2}{3!} + \frac{x^5a^4}{5!} + \cdots\right]\vec{a}\cdot\vec{\boldsymbol{A}}\;,$$

which can also be written in the form[1]

$$\mathrm{e}^{-x\,\vec{a}\cdot\vec{\boldsymbol{A}}} = \cosh(xa)\;\boldsymbol{1} - \frac{\sinh(xa)}{a}\;\vec{a}\cdot\vec{\boldsymbol{A}}\;, \tag{A5.10}$$

where a is either of the two possible determinations of the square root of the complex number a^2 (note that Eq. (A5.10) is invariant under interchange of a and $-a$). In a similar way one gets

$$\mathrm{e}^{-x\,\vec{b}\cdot\vec{\boldsymbol{B}}} = \cosh(xb)\;\boldsymbol{1} - \frac{\sinh(xb)}{b}\;\vec{b}\cdot\vec{\boldsymbol{B}}\;, \tag{A5.11}$$

where

$$b^2 = \vec{b}\cdot\vec{b} = (a^2)^* = \frac{1}{4}\bigl[\,w^2 - y^2 - 2\,\mathrm{i}\,\vec{w}\cdot\vec{y}\,\bigr] \tag{A5.12}$$

and where b is either of the two possible determinations of the square root of b^2.

[1] The special case $a^2 = 0$ will be considered later.

Substitution of Eqs. (A5.8), (A5.10), and (A5.11) into Eq. (A5.7) gives

$$\begin{aligned} \mathrm{e}^{-x\,\boldsymbol{Z}} \;=\; & \mathrm{e}^{-x\,w_0}\left[\cosh(xa)\,\boldsymbol{1} - \frac{\sinh(xa)}{a}\;\vec{a}\cdot\vec{\boldsymbol{A}}\right] \\ & \times\left[\cosh(xb)\,\boldsymbol{1} - \frac{\sinh(xb)}{b}\;\vec{b}\cdot\vec{\boldsymbol{B}}\right]. \end{aligned} \tag{A5.13}$$

Now we choose the determination of a and b setting, in terms of the real numbers α and β

$$a = \frac{1}{2}\left(\alpha + \mathrm{i}\,\beta\right), \qquad b = a^* = \frac{1}{2}\left(\alpha - \mathrm{i}\,\beta\right), \tag{A5.14}$$

with the supplementary condition

$$\alpha \;\geq\; 0\,. \tag{A5.15}$$

Substituting Eqs. (A5.14) into Eq. (A5.13) we obtain

$$\begin{aligned} \mathrm{e}^{-x\,\boldsymbol{Z}} \;=\; & \mathrm{e}^{-x\,w_0}\left\{\frac{1}{2}\Big[\cosh(x\alpha)+\cos(x\beta)\Big]\,\boldsymbol{1}\right. \\ & - \Big[\sinh(x\alpha) + \mathrm{i}\,\sin(x\beta)\Big]\,\frac{\vec{a}\cdot\vec{\boldsymbol{A}}}{\alpha+\mathrm{i}\,\beta} \\ & - \Big[\sinh(x\alpha) - \mathrm{i}\,\sin(x\beta)\Big]\,\frac{\vec{b}\cdot\vec{\boldsymbol{B}}}{\alpha-\mathrm{i}\,\beta} \\ & \left. + 2\Big[\cosh(x\alpha)-\cos(x\beta)\Big]\,\frac{(\vec{a}\cdot\vec{\boldsymbol{A}})\,(\vec{b}\cdot\vec{\boldsymbol{B}})}{\alpha^2+\beta^2}\right\}. \end{aligned} \tag{A5.16}$$

The expressions for α and β can be found using Eqs. (A5.9) and (A5.14). One gets the equation

$$w^2 - y^2 + 2\,\mathrm{i}\,\vec{w}\cdot\vec{y} \;=\; \alpha^2 - \beta^2 + 2\,\mathrm{i}\,\alpha\beta\,,$$

which can be solved, adding the condition (A5.15), to give

$$\alpha = \Lambda_+(\vec{w},\vec{y}) \qquad \beta = \sigma\,\Lambda_-(\vec{w},\vec{y})\,, \tag{A5.17}$$

where[1]

$$\begin{aligned} \Lambda_+(\vec{w},\vec{y}) &= \sqrt{\sqrt{(w^2-y^2)^2/4 + (\vec{w}\cdot\vec{y})^2} + (w^2-y^2)/2} \\ \Lambda_-(\vec{w},\vec{y}) &= \sqrt{\sqrt{(w^2-y^2)^2/4 + (\vec{w}\cdot\vec{y})^2} - (w^2-y^2)/2} \end{aligned} \tag{A5.18}$$

$$\sigma \;=\; \mathrm{sign}\,(\vec{w}\cdot\vec{y}) = \frac{\vec{w}\cdot\vec{y}}{|\,\vec{w}\cdot\vec{y}\,|}\;. \tag{A5.19}$$

[1] Note that when $\vec{w}\cdot\vec{y}=0$, σ is undetermined. In this case, however, being $\Lambda_-(\vec{w},\vec{y})=0$, the final expression for $\exp(-x\boldsymbol{Z})$ is independent of σ (see Eqs. (A5.20)-(A5.21)).

Finally, substituting Eq. (A5.17) into Eq. (A5.16) and evaluating the matrices $\vec{a}\cdot\vec{\boldsymbol{A}}$, $\vec{b}\cdot\vec{\boldsymbol{B}}$, and their product, one gets the expression

$$\begin{aligned}
\mathrm{e}^{-x\,\boldsymbol{Z}} \;=\; & \mathrm{e}^{-x\,w_0} \\
& \times \Big\{ \frac{1}{2}\Big[\cosh\big[x\,\Lambda_+(\vec{w}\,,\vec{y}\,)\big] + \cos\big[x\,\Lambda_-(\vec{w}\,,\vec{y}\,)\big]\Big]\boldsymbol{M}_1(\vec{w}\,,\vec{y}\,) \\
& \quad - \sin\big[x\,\Lambda_-(\vec{w}\,,\vec{y}\,)\big]\,\boldsymbol{M}_2(\vec{w}\,,\vec{y}\,) \\
& \quad - \sinh\big[x\,\Lambda_+(\vec{w}\,,\vec{y}\,)\big]\,\boldsymbol{M}_3(\vec{w}\,,\vec{y}\,) \\
& \quad + \frac{1}{2}\Big[\cosh\big[x\,\Lambda_+(\vec{w}\,,\vec{y}\,)\big] - \cos\big[x\,\Lambda_-(\vec{w}\,,\vec{y}\,)\big]\Big]\boldsymbol{M}_4(\vec{w}\,,\vec{y}\,)\Big\}\,, \qquad \text{(A5.20)}
\end{aligned}$$

where the four matrices $\boldsymbol{M}_i(\vec{w}\,,\vec{y}\,)$ are given by

$$\boldsymbol{M}_1(\vec{w}\,,\vec{y}\,) = \boldsymbol{1} \qquad \text{(A5.21a)}$$

$$\boldsymbol{M}_2(\vec{w}\,,\vec{y}\,) = \qquad \text{(A5.21b)}$$

$$= \frac{1}{\Theta}\begin{pmatrix}
0 & \Lambda_- w_1 - \sigma\Lambda_+ y_1 & \Lambda_- w_2 - \sigma\Lambda_+ y_2 & \Lambda_- w_3 - \sigma\Lambda_+ y_3 \\
\Lambda_- w_1 - \sigma\Lambda_+ y_1 & 0 & \sigma\Lambda_+ w_3 + \Lambda_- y_3 & -\sigma\Lambda_+ w_2 - \Lambda_- y_2 \\
\Lambda_- w_2 - \sigma\Lambda_+ y_2 & -\sigma\Lambda_+ w_3 - \Lambda_- y_3 & 0 & \sigma\Lambda_+ w_1 + \Lambda_- y_1 \\
\Lambda_- w_3 - \sigma\Lambda_+ y_3 & \sigma\Lambda_+ w_2 + \Lambda_- y_2 & -\sigma\Lambda_+ w_1 - \Lambda_- y_1 & 0
\end{pmatrix}$$

$$\boldsymbol{M}_3(\vec{w}\,,\vec{y}\,) = \qquad \text{(A5.21c)}$$

$$= \frac{1}{\Theta}\begin{pmatrix}
0 & \Lambda_+ w_1 + \sigma\Lambda_- y_1 & \Lambda_+ w_2 + \sigma\Lambda_- y_2 & \Lambda_+ w_3 + \sigma\Lambda_- y_3 \\
\Lambda_+ w_1 + \sigma\Lambda_- y_1 & 0 & -\sigma\Lambda_- w_3 + \Lambda_+ y_3 & \sigma\Lambda_- w_2 - \Lambda_+ y_2 \\
\Lambda_+ w_2 + \sigma\Lambda_- y_2 & \sigma\Lambda_- w_3 - \Lambda_+ y_3 & 0 & -\sigma\Lambda_- w_1 + \Lambda_+ y_1 \\
\Lambda_+ w_3 + \sigma\Lambda_- y_3 & -\sigma\Lambda_- w_2 + \Lambda_+ y_2 & \sigma\Lambda_- w_1 - \Lambda_+ y_1 & 0
\end{pmatrix}$$

$$\boldsymbol{M}_4(\vec{w}\,,\vec{y}\,) =$$

$$= \frac{2}{\Theta}\begin{pmatrix}
t^2 & w_3 y_2 - w_2 y_3 & w_1 y_3 - w_3 y_1 & w_2 y_1 - w_1 y_2 \\
-w_3 y_2 + w_2 y_3 & w_1^2 + y_1^2 - t^2 & w_1 w_2 + y_1 y_2 & w_3 w_1 + y_3 y_1 \\
-w_1 y_3 + w_3 y_1 & w_1 w_2 + y_1 y_2 & w_2^2 + y_2^2 - t^2 & w_2 w_3 + y_2 y_3 \\
-w_2 y_1 + w_1 y_2 & w_3 w_1 + y_3 y_1 & w_2 w_3 + y_2 y_3 & w_3^2 + y_3^2 - t^2
\end{pmatrix} \qquad \text{(A5.21d)}$$

with $t^2 = (w^2 + y^2)/2$ and

$$\Theta = \alpha^2 + \beta^2 = \Lambda_+^2 + \Lambda_-^2 = 2\,\sqrt{(w^2 - y^2)^2/4 + (\vec{w}\cdot\vec{y}\,)^2}\,. \qquad \text{(A5.22)}$$

Equation (A5.20) can also be written in a different form, which involves only exponential factors (although complex)

$$\mathrm{e}^{-x\,\boldsymbol{Z}} = \mathrm{e}^{-x\,[\,w_0+\Lambda_+(\vec{w},\vec{y})\,]}\,\boldsymbol{N}_1(\vec{w},\vec{y}) + \mathrm{e}^{-x\,[\,w_0-\Lambda_+(\vec{w},\vec{y})\,]}\,\boldsymbol{N}_2(\vec{w},\vec{y}) + \mathrm{e}^{-x\,[\,w_0+\mathrm{i}\,\Lambda_-(\vec{w},\vec{y})\,]}\,\boldsymbol{N}_3(\vec{w},\vec{y}) + \mathrm{e}^{-x\,[\,w_0-\mathrm{i}\,\Lambda_-(\vec{w},\vec{y})\,]}\,\boldsymbol{N}_4(\vec{w},\vec{y})\,, \quad \text{(A5.23)}$$

where

$$\begin{aligned}
\boldsymbol{N}_1(\vec{w},\vec{y}) &= \frac{1}{4}\Big[\boldsymbol{M}_1(\vec{w},\vec{y}) + 2\,\boldsymbol{M}_3(\vec{w},\vec{y}) + \boldsymbol{M}_4(\vec{w},\vec{y})\Big]\\
\boldsymbol{N}_2(\vec{w},\vec{y}) &= \frac{1}{4}\Big[\boldsymbol{M}_1(\vec{w},\vec{y}) - 2\,\boldsymbol{M}_3(\vec{w},\vec{y}) + \boldsymbol{M}_4(\vec{w},\vec{y})\Big]\\
\boldsymbol{N}_3(\vec{w},\vec{y}) &= \frac{1}{4}\Big[\boldsymbol{M}_1(\vec{w},\vec{y}) - 2\,\mathrm{i}\,\boldsymbol{M}_2(\vec{w},\vec{y}) - \boldsymbol{M}_4(\vec{w},\vec{y})\Big]\\
\boldsymbol{N}_4(\vec{w},\vec{y}) &= \frac{1}{4}\Big[\boldsymbol{M}_1(\vec{w},\vec{y}) + 2\,\mathrm{i}\,\boldsymbol{M}_2(\vec{w},\vec{y}) - \boldsymbol{M}_4(\vec{w},\vec{y})\Big] = \boldsymbol{N}_3(\vec{w},\vec{y})^*\,. \quad \text{(A5.24)}
\end{aligned}$$

The explicit expressions of the matrices $\boldsymbol{N}_i$ are rather cumbersome and will not be given here.

It should be noticed that the matrices $\boldsymbol{M}_i(\vec{w},\vec{y})$ defined in Eqs. (A5.21b,c,d) – and hence the expression (A5.20) for $\exp(-x\boldsymbol{Z})$ – are ill-defined when $\Theta = 0$, that is

$$\Lambda_+(\vec{w},\vec{y}) = \Lambda_-(\vec{w},\vec{y}) = 0\,,$$

which implies (see Eq. (A5.22))

$$w^2 = y^2 \qquad \text{and} \qquad (\vec{w}\cdot\vec{y}) = 0\,.$$

Since in this case we have from Eqs. (A5.9) and (A5.12)

$$a^2 = b^2 = 0\,,$$

it is easily seen that expressions (A5.10) and (A5.11) reduce to

$$\mathrm{e}^{-x\,\vec{a}\cdot\vec{\boldsymbol{A}}} = \boldsymbol{1} - x\,\vec{a}\cdot\vec{\boldsymbol{A}}\,, \qquad \mathrm{e}^{-x\,\vec{b}\cdot\vec{\boldsymbol{B}}} = \boldsymbol{1} - x\,\vec{b}\cdot\vec{\boldsymbol{B}}\,.$$

Substituting into Eq. (A5.7) and applying the same procedure as before, one finds that Eq. (A5.20) must be replaced, in this particular case, by the expression

$$\mathrm{e}^{-x\,\boldsymbol{Z}} = \mathrm{e}^{-x\,w_0}\Big[\,\boldsymbol{1} - x\,\boldsymbol{G}(\vec{w},\vec{y}) + \frac{1}{2}\,x^2\,\boldsymbol{G}(\vec{w},\vec{y})^2\,\Big]\,,$$

where

$$\boldsymbol{G}(\vec{w},\vec{y}) = \begin{pmatrix} 0 & w_1 & w_2 & w_3\\ w_1 & 0 & y_3 & -y_2\\ w_2 & -y_3 & 0 & y_1\\ w_3 & y_2 & -y_1 & 0 \end{pmatrix}\,. \quad \text{(A5.25)}$$

This expression can also be obtained from Eqs. (A5.20)-(A5.21) performing the limit $\Lambda_+(\vec{w}\,,\vec{y}\,) \to 0$, $\Lambda_-(\vec{w}\,,\vec{y}\,) \to 0$.

A6. Diagonalization of the Propagation Matrix

We want to determine the matrices $\boldsymbol{X}$ and $\boldsymbol{X}^{-1}$ such that

$$\boldsymbol{X}^{-1}\,\boldsymbol{K}\,\boldsymbol{X} \;=\; \boldsymbol{K}'\,, \tag{A6.1}$$

where $\boldsymbol{K}$ is the propagation matrix defined in Eq. (8.3) and $\boldsymbol{K}'$ is the diagonal matrix

$$K'_{ij} = \lambda_i\,\delta_{ij} \qquad (i,j = 1,2,3,4)\,, \tag{A6.2}$$

λ_i being the eigenvalues of $\boldsymbol{K}$ (given by Eqs. (8.33)), that we assume to be distinct (see footnote on p. 358).

The matrices $\boldsymbol{X}$ and $\boldsymbol{X}^{-1}$ can be found as follows. First we determine the eigenvectors $\boldsymbol{u}^{(i)}$ of the matrix $\boldsymbol{K}$, defined by

$$\boldsymbol{K}\,\boldsymbol{u}^{(i)} = \lambda_i\,\boldsymbol{u}^{(i)} \qquad (i = 1,2,3,4)\,. \tag{A6.3}$$

Using these eigenvectors we construct a matrix $\boldsymbol{Z}$ whose columns are the four eigenvectors $\boldsymbol{u}^{(i)}$ each multiplied by an arbitrary constant c_i,

$$Z_{ij} = c_j\,u_i^{(j)}\,. \tag{A6.4}$$

From Eqs. (A6.2) and (A6.3) it follows that the matrix $\boldsymbol{Z}$ satisfies the equation

$$\boldsymbol{K}\,\boldsymbol{Z} = \boldsymbol{Z}\,\boldsymbol{K}'\,. \tag{A6.5}$$

Then we find the 'left' eigenvectors $\boldsymbol{v}^{(i)}$ of the matrix $\boldsymbol{K}$, defined by[1]

$$\big(\boldsymbol{v}^{(i)}\big)^\dagger\,\boldsymbol{K} = \lambda_i\,\big(\boldsymbol{v}^{(i)}\big)^\dagger\,, \tag{A6.6}$$

and construct a matrix $\boldsymbol{Y}$ whose rows are the four eigenvectors $(\boldsymbol{v}^{(i)})^\dagger$ each multiplied by an arbitrary constant d_i,

$$Y_{ij} = d_i\,v_j^{(i)}\,. \tag{A6.7}$$

The matrix $\boldsymbol{Y}$ satisfies the equation

$$\boldsymbol{Y}\,\boldsymbol{K} \;=\; \boldsymbol{K}'\,\boldsymbol{Y}\,. \tag{A6.8}$$

[1] It can be easily proved that the quantities λ_i in Eqs. (A6.6) and (A6.3) are the same.

If we now consider the product $\boldsymbol{Y}\,\boldsymbol{K}\,\boldsymbol{Z}$, we have from Eqs. (A6.5) and (A6.8)

$$\boldsymbol{Y}\,\boldsymbol{K}\,\boldsymbol{Z} = \boldsymbol{Y}\,\boldsymbol{Z}\,\boldsymbol{K}' = \boldsymbol{K}'\,\boldsymbol{Y}\,\boldsymbol{Z}\,,$$

which proves that the matrix $\boldsymbol{Y}\,\boldsymbol{Z}$ commutes with the diagonal matrix $\boldsymbol{K}'$. Since the four eigenvalues of $\boldsymbol{K}'$ have been assumed to be non-degenerate, it follows that $\boldsymbol{Y}\,\boldsymbol{Z}$ is also diagonal. On the other hand, the diagonal elements of $\boldsymbol{Y}\,\boldsymbol{Z}$ are given by

$$(YZ)_{ii} = \sum_{k=1}^{4} Y_{ik}\,Z_{ki} = c_i\,d_i \sum_{k=1}^{4} v_k^{(i)}\,u_k^{(i)} \qquad (i = 1, 2, 3, 4)\,.$$

Thus we get

$$\boldsymbol{Y}\,\boldsymbol{Z} = \boldsymbol{1}$$

if we choose the coefficients c_i, d_i in such a way that

$$c_i\,d_i = \frac{1}{\sum\limits_{k=1}^{4} v_k^{(i)}\,u_k^{(i)}}\,. \tag{A6.9}$$

It follows that a solution to Eq. (A6.1) is

$$\boldsymbol{X} = \boldsymbol{Z}\,, \qquad \boldsymbol{X}^{-1} = \boldsymbol{Y}\,,$$

with $\boldsymbol{Z}$ and $\boldsymbol{Y}$ given by Eqs. (A6.4) and (A6.7), respectively, and with the coefficients c_i and d_i satisfying Eq. (A6.9).

Let's now apply this method to find an explicit expression for the matrices $\boldsymbol{X}$ and $\boldsymbol{X}^{-1}$. The first step is to determine the eigenvectors of the propagation matrix $\boldsymbol{K}$. From Eq. (A6.3) we have

$$\begin{cases} (\eta_I - \lambda)\,u_1 + \eta_Q\,u_2 + \eta_U\,u_3 + \eta_V\,u_4 = 0 \\ \eta_Q\,u_1 + (\eta_I - \lambda)\,u_2 + \rho_V\,u_3 - \rho_U\,u_4 = 0 \\ \eta_U\,u_1 - \rho_V\,u_2 + (\eta_I - \lambda)\,u_3 + \rho_Q\,u_4 = 0 \\ \eta_V\,u_1 + \rho_U\,u_2 - \rho_Q\,u_3 + (\eta_I - \lambda)\,u_4 = 0\,, \end{cases} \tag{A6.10}$$

which is a system of four homogeneous, linear equations in the four unknowns u_1, u_2, u_3, u_4. Solutions other than the zero solution ($u_1 = u_2 = u_3 = u_4 = 0$) exist only if the determinant of the system vanishes: this leads to Eq. (8.30), whence the eigenvalues λ_i are obtained (see Eqs. (8.33)). Substituting one of the eigenvalues for λ, we can eliminate one of the equations and assign an arbitrary value to one of the unknowns. For instance, we can reject the first equation and write

$$\begin{cases} (\eta_I - \lambda_i)\,u_2^{(i)} + \rho_V\,u_3^{(i)} - \rho_U\,u_4^{(i)} = -\,\eta_Q\,u_1^{(i)} \\ -\rho_V\,u_2^{(i)} + (\eta_I - \lambda_i)\,u_3^{(i)} + \rho_Q\,u_4^{(i)} = -\,\eta_U\,u_1^{(i)} \\ \rho_U\,u_2^{(i)} - \rho_Q\,u_3^{(i)} + (\eta_I - \lambda_i)\,u_4^{(i)} = -\,\eta_V\,u_1^{(i)}\,, \end{cases} \tag{A6.11}$$

whose solution is[1]

$$
\begin{aligned}
u_1^{(i)} &= (\lambda_i - \eta_I)\left[(\lambda_i - \eta_I)^2 + \rho_Q^2 + \rho_U^2 + \rho_V^2\right] \\
u_2^{(i)} &= (\lambda_i - \eta_I)^2\,\eta_Q + (\lambda_i - \eta_I)(\eta_U\rho_V - \eta_V\rho_U) \\
&\quad + (\eta_Q\rho_Q + \eta_U\rho_U + \eta_V\rho_V)\,\rho_Q \\
u_3^{(i)} &= (\lambda_i - \eta_I)^2\,\eta_U + (\lambda_i - \eta_I)(\eta_V\rho_Q - \eta_Q\rho_V) \\
&\quad + (\eta_Q\rho_Q + \eta_U\rho_U + \eta_V\rho_V)\,\rho_U \\
u_4^{(i)} &= (\lambda_i - \eta_I)^2\,\eta_V + (\lambda_i - \eta_I)(\eta_Q\rho_U - \eta_U\rho_Q) \\
&\quad + (\eta_Q\rho_Q + \eta_U\rho_U + \eta_V\rho_V)\,\rho_V\ . \qquad \text{(A6.12)}
\end{aligned}
$$

The left eigenvectors are found in a strictly similar way; their expression is obtained by substituting $\rho_Q \to -\rho_Q$, $\rho_U \to -\rho_U$, $\rho_V \to -\rho_V$ in Eqs. (A6.12).

From the left eigenvectors we then construct the matrix $\boldsymbol{X}^{-1}$ without any multiplicative factor (the coefficients d_i in Eq. (A6.7) are set to 1). This is just the matrix given in Eq. (8.42a). To construct the matrix $\boldsymbol{X}$ we must first evaluate the coefficients c_i. Using the compact notations of Eqs. (8.31) and (8.41) we have

$$
\begin{aligned}
\sum_{k=1}^{4} u_k^{(i)}\, v_k^{(i)} &= (\lambda_i - \eta_I)^2\left[(\lambda_i - \eta_I)^2 + \rho^2\right]^2 + (\lambda_i - \eta_I)^4\,\eta^2 \\
&\quad - (\lambda_i - \eta_I)^2\,\zeta^2 + 2\,(\lambda_i - \eta_I)^2\,(\vec{\eta}\cdot\vec{\rho})^2 + (\vec{\eta}\cdot\vec{\rho})^2\,\rho^2\ ,
\end{aligned}
$$

and since from Eq. (8.32)

$$
(\lambda_i - \eta_I)^2\left[(\lambda_i - \eta_I)^2 + \rho^2\right] = (\lambda_i - \eta_I)^2\,\eta^2 + (\vec{\eta}\cdot\vec{\rho})^2
$$

and from Eq. (8.41)

$$
\eta^2\rho^2 - \zeta^2 = (\vec{\eta}\cdot\vec{\rho})^2\ ,
$$

we can write

$$
\sum_{k=1}^{4} u_k^{(i)}\, v_k^{(i)} = 2\left[\,(\lambda_i - \eta_I)^4\,\eta^2 + 2\,(\lambda_i - \eta_I)^2\,(\vec{\eta}\cdot\vec{\rho})^2 + (\vec{\eta}\cdot\vec{\rho})^2\,\rho^2\,\right]\ .
$$

The coefficients c_i then follow from Eq. (A6.9), and this leads to the matrix $\boldsymbol{X}$ as given in Eq. (8.42b).

It should be emphasized that the expressions for $\boldsymbol{X}$ and $\boldsymbol{X}^{-1}$ given in Eqs. (8.42) are valid provided two conditions are satisfied, namely: *i*) the four eigenvalues of

[1] Expressions (A6.12) are correct only if the determinant of the system (A6.11) is non-zero. However, the system (A6.10) can always be reduced – provided the four eigenvalues λ_i are distinct – to a system of three equations in three unknowns having a non-zero determinant. In other words, the matrix of the coefficients of the system (A6.10) is of rank 3.

the propagation matrix are distinct, and *ii*) the determinant of the system (A6.11) is non-zero. As apparent from Eqs. (8.33), the first condition means that both $\Lambda_+(\vec{\eta},\vec{\rho})$ and $\Lambda_-(\vec{\eta},\vec{\rho})$ must be non-zero, thus it is equivalent to (see Eqs. (A5.18))

$$\vec{\eta}\cdot\vec{\rho}\neq 0\,. \tag{A6.13}$$

The second condition leads to the further constraint

$$\rho^2-\Lambda_-(\vec{\eta},\vec{\rho})^2\neq 0\,,$$

or, using again Eqs. (A5.18)

$$\eta^2\rho^2\;\neq\;(\vec{\eta}\cdot\vec{\rho})^2\,. \tag{A6.14}$$

Expressions (8.42) are correct only if conditions (A6.13) and (A6.14) are satisfied.

A7. Formulae for the Calculation of the Evolution Operator

To shorten notations we write the coefficients $E^{(k)}(s,s')$, introduced in Eq. (8.76), in the form

$$E^{(k)}(s,s')=X_k+\mathrm{i}\,Y_k\qquad(k=0,1,2,3)\,, \tag{A7.1}$$

with X_k and Y_k real. Using Eqs. (8.62) and (8.63), the transfer equation (8.78) becomes

$$2\,\frac{\mathrm{d}}{\mathrm{d}s}\begin{pmatrix}X_0\\X_1\\X_2\\X_3\\Y_0\\Y_1\\Y_2\\Y_3\end{pmatrix}=-\begin{pmatrix}\eta_I&\eta_Q&\eta_U&\eta_V&0&-\rho_Q&-\rho_U&-\rho_V\\ \eta_Q&\eta_I&\rho_V&-\rho_U&-\rho_Q&0&\eta_V&-\eta_U\\ \eta_U&-\rho_V&\eta_I&\rho_Q&-\rho_U&-\eta_V&0&\eta_Q\\ \eta_V&\rho_U&-\rho_Q&\eta_I&-\rho_V&\eta_U&-\eta_Q&0\\ 0&\rho_Q&\rho_U&\rho_V&\eta_I&\eta_Q&\eta_U&\eta_V\\ \rho_Q&0&-\eta_V&\eta_U&\eta_Q&\eta_I&\rho_V&-\rho_U\\ \rho_U&\eta_V&0&-\eta_Q&\eta_U&-\rho_V&\eta_I&\rho_Q\\ \rho_V&-\eta_U&\eta_Q&0&\eta_V&\rho_U&-\rho_Q&\eta_I\end{pmatrix}\begin{pmatrix}X_0\\X_1\\X_2\\X_3\\Y_0\\Y_1\\Y_2\\Y_3\end{pmatrix}.$$

It is interesting to note that the 8×8 matrix can be written in the form

$$\begin{pmatrix}\boldsymbol{K}&-\boldsymbol{K}'\\ \boldsymbol{K}'&\boldsymbol{K}\end{pmatrix}\,,$$

where $\boldsymbol{K}$ is the propagation matrix (Eq. (8.3)) and $\boldsymbol{K}'$ is the matrix obtained from $\boldsymbol{K}$ setting $\eta_I=0$ and substituting

$$\begin{aligned}&\eta_Q\to\rho_Q\qquad&&\rho_Q\to-\eta_Q\\ &\eta_U\to\rho_U\qquad&&\rho_U\to-\eta_U\\ &\eta_V\to\rho_V\qquad&&\rho_V\to-\eta_V\,.\end{aligned}$$

As far as Eq. (8.77) is concerned, the trace of the product of four Pauli spin matrices is easily evaluated using Eqs. (8.56), (8.57), (8.62) and the relation

$$\sum_k \epsilon_{ijk}\, \epsilon_{lmk} \;=\; \delta_{il}\, \delta_{jm} \;-\; \delta_{im}\, \delta_{jl} \;\; .$$

We get

$$\mathrm{Tr}\left(\boldsymbol{\tau}_i\, \boldsymbol{\tau}_j\, \boldsymbol{\tau}_k\, \boldsymbol{\tau}_l\right) = \; 2\left(\delta_{ij}\, \delta_{kl} \;-\; \delta_{ik}\, \delta_{jl} \;+\; \delta_{il}\, \delta_{jk}\right) \qquad (i,j,k,l = 1,2,3)$$

(if one of the indices is zero, the trace is given directly from Eq. (8.62)). Substitution into Eq. (8.77) yields the expressions of the matrix elements O_{ij} in terms of the quantities $X_k\,,\; Y_k$ defined in Eq. (A7.1)

$$\begin{aligned}
O_{00} &= X_0^2 + X_1^2 + X_2^2 + X_3^2 + Y_0^2 + Y_1^2 + Y_2^2 + Y_3^2 \\
O_{11} &= X_0^2 + X_1^2 - X_2^2 - X_3^2 + Y_0^2 + Y_1^2 - Y_2^2 - Y_3^2 \\
O_{22} &= X_0^2 - X_1^2 + X_2^2 - X_3^2 + Y_0^2 - Y_1^2 + Y_2^2 - Y_3^2 \\
O_{33} &= X_0^2 - X_1^2 - X_2^2 + X_3^2 + Y_0^2 - Y_1^2 - Y_2^2 + Y_3^2 \\
O_{01} &= 2\,(X_0 X_1 + Y_0 Y_1 - X_2 Y_3 + X_3 Y_2) \\
O_{10} &= 2\,(X_0 X_1 + Y_0 Y_1 + X_2 Y_3 - X_3 Y_2) \\
O_{02} &= 2\,(X_0 X_2 + Y_0 Y_2 - X_3 Y_1 + X_1 Y_3) \\
O_{20} &= 2\,(X_0 X_2 + Y_0 Y_2 + X_3 Y_1 - X_1 Y_3) \\
O_{03} &= 2\,(X_0 X_3 + Y_0 Y_3 - X_1 Y_2 + X_2 Y_1) \\
O_{30} &= 2\,(X_0 X_3 + Y_0 Y_3 + X_1 Y_2 - X_2 Y_1) \\
O_{12} &= 2\,(X_1 X_2 + Y_1 Y_2 + X_0 Y_3 - X_3 Y_0) \\
O_{21} &= 2\,(X_1 X_2 + Y_1 Y_2 - X_0 Y_3 + X_3 Y_0) \\
O_{23} &= 2\,(X_2 X_3 + Y_2 Y_3 + X_0 Y_1 - X_1 Y_0) \\
O_{32} &= 2\,(X_2 X_3 + Y_2 Y_3 - X_0 Y_1 + X_1 Y_0) \\
O_{31} &= 2\,(X_1 X_3 + Y_1 Y_3 + X_0 Y_2 - X_2 Y_0) \\
O_{13} &= 2\,(X_1 X_3 + Y_1 Y_3 - X_0 Y_2 + X_2 Y_0)\;.
\end{aligned}$$

A8. The Feautrier Method: Numerical Details

To obtain a numerical solution of Eq. (9.183), subjected to the boundary conditions (9.185) and (9.186), we introduce a grid of N points $(\tau_1\,, \tau_2\,, \ldots, \tau_N)$ not necessarily evenly spaced.

Let us consider two adjacent intervals $(\tau_{k-1}\,,\tau_k)$ and $(\tau_k\,,\tau_{k+1})$, and their midpoints

$$\tilde{\tau}_{k-1} = \frac{\tau_{k-1} + \tau_k}{2}\,, \qquad \tilde{\tau}_k = \frac{\tau_k + \tau_{k+1}}{2} \qquad (k = 2, 3, \ldots, N-1)\,. \tag{A8.1}$$

Using a standard finite-differences formula we can write

$$\left[\boldsymbol{A}^{-1}\,\frac{\mathrm{d}\boldsymbol{G}}{\mathrm{d}\tau_{\mathrm{r}}}\right]_{\tau_{\mathrm{r}}=\tilde{\tau}_{k-1}} = \frac{\boldsymbol{A}_{k-1}^{-1} + \boldsymbol{A}_k^{-1}}{2}\;\frac{\boldsymbol{G}_k - \boldsymbol{G}_{k-1}}{\tau_k - \tau_{k-1}}$$

$$\left[\boldsymbol{A}^{-1}\,\frac{\mathrm{d}\boldsymbol{G}}{\mathrm{d}\tau_{\mathrm{r}}}\right]_{\tau_{\mathrm{r}}=\tilde{\tau}_{k}} = \frac{\boldsymbol{A}_{k}^{-1} + \boldsymbol{A}_{k+1}^{-1}}{2}\;\frac{\boldsymbol{G}_{k+1} - \boldsymbol{G}_k}{\tau_{k+1} - \tau_k}\,, \tag{A8.2}$$

where a subscript k means that the quantity is evaluated at $\tau_{\mathrm{r}} = \tau_k$. Similarly, we can replace Eq. (9.183) by the following

$$\frac{\left[\boldsymbol{A}^{-1}\,\dfrac{\mathrm{d}\boldsymbol{G}}{\mathrm{d}\tau_{\mathrm{r}}}\right]_{\tau_{\mathrm{r}}=\tilde{\tau}_{k}} - \left[\boldsymbol{A}^{-1}\,\dfrac{\mathrm{d}\boldsymbol{G}}{\mathrm{d}\tau_{\mathrm{r}}}\right]_{\tau_{\mathrm{r}}=\tilde{\tau}_{k-1}}}{\tilde{\tau}_k - \tilde{\tau}_{k-1}} = \boldsymbol{A}_k\,\boldsymbol{G}_k - \boldsymbol{b}_k\,. \tag{A8.3}$$

Substitution of Eqs. (A8.1) and (A8.2) into Eq. (A8.3) leads to the linear system

$$-\,\boldsymbol{x}^{(k)}\,\boldsymbol{G}_{k-1} + \boldsymbol{y}^{(k)}\,\boldsymbol{G}_k - \boldsymbol{z}^{(k)}\,\boldsymbol{G}_{k+1} = \boldsymbol{u}^{(k)} \qquad (k = 2, 3, \ldots, N-1)\,, \tag{A8.4}$$

where

$$\begin{aligned}
\boldsymbol{x}^{(k)} &= \frac{\boldsymbol{A}_{k-1}^{-1} + \boldsymbol{A}_k^{-1}}{(\tau_k - \tau_{k-1})\,(\tau_{k+1} - \tau_{k-1})}\\
\boldsymbol{z}^{(k)} &= \frac{\boldsymbol{A}_{k}^{-1} + \boldsymbol{A}_{k+1}^{-1}}{(\tau_{k+1} - \tau_{k})\,(\tau_{k+1} - \tau_{k-1})}\\
\boldsymbol{y}^{(k)} &= \boldsymbol{x}^{(k)} + \boldsymbol{z}^{(k)} + \boldsymbol{A}_k\\
\boldsymbol{u}^{(k)} &= \boldsymbol{b}_k\,.
\end{aligned} \tag{A8.5}$$

Boundary conditions can also be written in the form of difference equations. For the first interval we can write

$$\left[\boldsymbol{A}^{-1}\,\frac{\mathrm{d}\boldsymbol{G}}{\mathrm{d}\tau_{\mathrm{r}}}\right]_{\tau_{\mathrm{r}}=\tilde{\tau}_{1}} = \frac{\boldsymbol{A}_1^{-1} + \boldsymbol{A}_2^{-1}}{2}\;\frac{\boldsymbol{G}_2 - \boldsymbol{G}_1}{\tau_2 - \tau_1}\,.$$

On the other hand, following a method suggested by Auer (1967) for the scalar case, we have by a first-order expansion

$$\left[\boldsymbol{A}^{-1}\,\frac{\mathrm{d}\boldsymbol{G}}{\mathrm{d}\tau_{\mathrm{r}}}\right]_{\tau_{\mathrm{r}}=\tilde{\tau}_{1}} = \left[\boldsymbol{A}^{-1}\,\frac{\mathrm{d}\boldsymbol{G}}{\mathrm{d}\tau_{\mathrm{r}}}\right]_{\tau_{\mathrm{r}}=\tau_{1}} + \left\{\frac{\mathrm{d}}{\mathrm{d}\tau_{\mathrm{r}}}\left[\boldsymbol{A}^{-1}\,\frac{\mathrm{d}\boldsymbol{G}}{\mathrm{d}\tau_{\mathrm{r}}}\right]\right\}_{\tau_{\mathrm{r}}=\tau_{1}}\frac{\tau_2 - \tau_1}{2}\,.$$

Equating the expressions in the right-hand sides and applying the boundary condition (9.185) at $\tau_{\rm r} = \tau_1$ we obtain, with the help of Eq. (9.183)

$$\frac{\boldsymbol{A}_1^{-1} + \boldsymbol{A}_2^{-1}}{2} \, \frac{\boldsymbol{G}_2 - \boldsymbol{G}_1}{\tau_2 - \tau_1} = \boldsymbol{G}_1 + \left(\boldsymbol{A}_1 \boldsymbol{G}_1 - \boldsymbol{b}_1\right) \frac{\tau_2 - \tau_1}{2} \ ,$$

which can be cast into the form

$$\boldsymbol{y}^{(1)} \, \boldsymbol{G}_1 - \boldsymbol{z}^{(1)} \, \boldsymbol{G}_2 = \boldsymbol{u}^{(1)} \ , \tag{A8.6}$$

where

$$\begin{aligned} \boldsymbol{z}^{(1)} &= \frac{\boldsymbol{A}_1^{-1} + \boldsymbol{A}_2^{-1}}{2 \, (\tau_2 - \tau_1)^2} \\ \boldsymbol{y}^{(1)} &= \boldsymbol{z}^{(1)} + \frac{1}{\tau_2 - \tau_1} \, \boldsymbol{1} + \frac{1}{2} \, \boldsymbol{A}_1 \\ \boldsymbol{u}^{(1)} &= \frac{1}{2} \, \boldsymbol{b}_1 \ . \end{aligned} \tag{A8.7}$$

Performing analogous calculations at $\tau_{\rm r} = \tau_{\rm b} = \tau_N$, one obtains the equation

$$- \boldsymbol{x}^{(N)} \, \boldsymbol{G}_{N-1} + \boldsymbol{y}^{(N)} \, \boldsymbol{G}_N = \boldsymbol{u}^{(N)} \ , \tag{A8.8}$$

where

$$\begin{aligned} \boldsymbol{x}^{(N)} &= \frac{\boldsymbol{A}_{N-1}^{-1} + \boldsymbol{A}_N^{-1}}{2 \, (\tau_N - \tau_{N-1})^2} \\ \boldsymbol{y}^{(N)} &= \boldsymbol{x}^{(N)} + \frac{1}{\tau_N - \tau_{N-1}} \, \boldsymbol{1} + \frac{1}{2} \, \boldsymbol{A}_N \\ \boldsymbol{u}^{(N)} &= \frac{1}{2} \, \boldsymbol{b}_N + \frac{1}{\tau_N - \tau_{N-1}} \, \boldsymbol{I}^{(\rm b)} \ . \end{aligned} \tag{A8.9}$$

Collecting together Eqs. (A8.4), (A8.6), and (A8.8), we obtain a tridiagonal system of N equations (each being a vector equation of order 4). Such system can be solved via a recursive algorithm.

Left-multiplication of Eq. (A8.6) by $[\, \boldsymbol{y}^{(1)} \,]^{-1}$ gives

$$\boldsymbol{G}_1 = \boldsymbol{g}_1 + \boldsymbol{\Gamma}_1 \, \boldsymbol{G}_2 \ , \tag{A8.10}$$

where

$$\begin{aligned} \boldsymbol{g}_1 &= \left[\, \boldsymbol{y}^{(1)} \, \right]^{-1} \boldsymbol{u}^{(1)} \\ \boldsymbol{\Gamma}_1 &= \left[\, \boldsymbol{y}^{(1)} \, \right]^{-1} \boldsymbol{z}^{(1)} \ . \end{aligned} \tag{A8.11}$$

Substitution of Eq. (A8.10) into the first of Eqs. (A8.4) and left-multiplication by $[\,\boldsymbol{y}^{(2)} - \boldsymbol{x}^{(2)}\,\boldsymbol{\Gamma}_1\,]^{-1}$ gives $\boldsymbol{G}_2$ as a function of $\boldsymbol{G}_3$. Iteration of this procedure leads to the equations

$$\boldsymbol{G}_k = \boldsymbol{g}_k + \boldsymbol{\Gamma}_k\,\boldsymbol{G}_{k+1} \ , \tag{A8.12}$$

with

$$\begin{aligned} \boldsymbol{g}_k &= \left[\,\boldsymbol{y}^{(k)} - \boldsymbol{x}^{(k)}\,\boldsymbol{\Gamma}_{k-1}\,\right]^{-1} \left[\,\boldsymbol{u}^{(k)} + \boldsymbol{x}^{(k)}\,\boldsymbol{g}_{k-1}\,\right] \\ \boldsymbol{\Gamma}_k &= \left[\,\boldsymbol{y}^{(k)} - \boldsymbol{x}^{(k)}\,\boldsymbol{\Gamma}_{k-1}\,\right]^{-1} \boldsymbol{z}^{(k)} \ , \end{aligned} \tag{A8.13}$$

and with k ranging from 2 to $(N-1)$. For $k = 1$, Eq. (A8.10) is incorporated in Eq. (A8.12) if we define

$$\boldsymbol{g}_0 = \boldsymbol{\Gamma}_0 = 0 \ .$$

Finally, substitution of the expression for $\boldsymbol{G}_{N-1}$ given by Eq. (A8.12) into Eq. (A8.8) allows the vector $\boldsymbol{G}_N$ to be determined,

$$\boldsymbol{G}_N = \left[\,\boldsymbol{y}^{(N)} - \boldsymbol{x}^{(N)}\,\boldsymbol{\Gamma}_{N-1}\,\right]^{-1} \left[\,\boldsymbol{u}^{(N)} + \boldsymbol{x}^{(N)}\,\boldsymbol{g}_{N-1}\,\right] .$$

The vectors $\boldsymbol{G}_{N-1}\,,\,\boldsymbol{G}_{N-2}\,,\,\ldots\,,\,\boldsymbol{G}_1$ can then be recursively obtained from Eqs. (A8.12). In particular, $2\,\boldsymbol{G}_1$ is just the emerging Stokes vector (see Eqs. (9.181) and (9.184)).

The formulae now derived can be conveniently used to test the accuracy of the Feautrier solution. To this aim, let us consider the case of a purely absorbing atmosphere ($S_{\rm c} = S_{\rm L} = 0$). From Eqs. (9.164), (A8.5), (A8.7) and (A8.9) one has that all the vectors $\boldsymbol{u}^{(k)}$ are zero except $\boldsymbol{u}^{(N)}$. This implies, according to Eqs. (A8.11) and (A8.13), that all the $\boldsymbol{g}_k$ $(k = 1, 2, \ldots, N-1)$ are also zero. Therefore, Eq. (A8.12) reduces to

$$\boldsymbol{G}_k = \boldsymbol{\Gamma}_k\,\boldsymbol{G}_{k+1} \qquad (k = 1, 2, \ldots, N-1) \ . \tag{A8.14}$$

This formula gives a precise physical meaning to the matrix $\boldsymbol{\Gamma}_k$. For the particular atmosphere that we are considering, the emission vector $\boldsymbol{b}(\tau_{\rm r})$ is zero and – because of the boundary condition (9.184) – the vector $\tilde{\boldsymbol{I}}'$ is also zero at any optical depth. Therefore, at any optical depth we have from Eqs. (9.181) $\boldsymbol{G} = \boldsymbol{I}\,/\,2$, so that Eq. (A8.14) can be rewritten in the form

$$\boldsymbol{I}_k = \boldsymbol{\Gamma}_k\ \boldsymbol{I}_{k+1} \ .$$

Comparison with Eq. (9.165) – written for the case $\boldsymbol{b}(\tau_{\rm r}) = 0$ – shows that $\boldsymbol{\Gamma}_k$ gives a numerical representation of the evolution operator associated with the interval $(\tau_k\,,\tau_{k+1})$, a result that was pointed out by Rees et al. (1989),

$$\boldsymbol{\Gamma}_k \approx \boldsymbol{O}(\tau_k\,,\tau_{k+1}) \ .$$

Let's now assume, in addition to the pure absorption hypothesis, that the propagation matrix $\boldsymbol{A}$ is independent of optical depth. It follows from Eqs. (A8.7) and (A8.11) that

$$\boldsymbol{\Gamma}_1 = \left[\boldsymbol{A}^{-1} + \left(\tau_2 - \tau_1\right) \boldsymbol{1} + \frac{1}{2} \left(\tau_2 - \tau_1\right)^2 \boldsymbol{A} \right]^{-1} \boldsymbol{A}^{-1} ,$$

whence

$$\boldsymbol{\Gamma}_1{}^{-1} = \boldsymbol{1} + \left(\tau_2 - \tau_1\right) \boldsymbol{A} + \frac{1}{2} \left(\tau_2 - \tau_1\right)^2 \boldsymbol{A}^2 . \tag{A8.15}$$

Expansion of $\boldsymbol{\Gamma}_1$ into power series of $\boldsymbol{A}$

$$\boldsymbol{\Gamma}_1 = \sum_{\ell=0}^{\infty} c_\ell \, \boldsymbol{A}^\ell$$

and use of the relation $\boldsymbol{\Gamma}_1 \, \boldsymbol{\Gamma}_1{}^{-1} = \boldsymbol{1}$, with $\boldsymbol{\Gamma}_1{}^{-1}$ given by Eq. (A8.15), yields

$$\boldsymbol{\Gamma}_1 = \boldsymbol{1} - \left(\tau_2 - \tau_1\right) \boldsymbol{A} + \frac{1}{2} \left(\tau_2 - \tau_1\right)^2 \boldsymbol{A}^2 - \frac{1}{4} \left(\tau_2 - \tau_1\right)^4 \boldsymbol{A}^4 + \cdots \tag{A8.16}$$

On the other hand, the analytical expression of the evolution operator associated with the interval (τ_1 , τ_2) is (cf. Eq. (9.103))

$$\boldsymbol{O}(\tau_1 , \tau_2) = \mathrm{e}^{-(\tau_2 - \tau_1) \boldsymbol{A}} ,$$

thus the expression for $\boldsymbol{\Gamma}_1$ provided by the Feautrier method is correct up to second-order terms.

It can be shown by recursion that this statement is valid for all the matrices $\boldsymbol{\Gamma}_k$ $(k = 1, 2, \ldots, N-1)$. Considering for instance the matrix $\boldsymbol{\Gamma}_2$, we have from Eqs. (A8.5) and (A8.13), with easy algebra

$$\boldsymbol{\Gamma}_2{}^{-1} = \frac{\tau_3 - \tau_1}{\tau_2 - \tau_1} \, \boldsymbol{1} + \frac{1}{2} \left(\tau_3 - \tau_2\right)\left(\tau_3 - \tau_1\right) \boldsymbol{A}^2 - \frac{\tau_3 - \tau_2}{\tau_2 - \tau_1} \, \boldsymbol{\Gamma}_1 .$$

Substitution of Eq. (A8.16) and expansion of $\boldsymbol{\Gamma}_2$ into power series of $\boldsymbol{A}$ lead to the expression

$$\begin{aligned} \boldsymbol{\Gamma}_2 = \boldsymbol{1} &- \left(\tau_3 - \tau_2\right) \boldsymbol{A} + \frac{1}{2} \left(\tau_3 - \tau_2\right)^2 \boldsymbol{A}^2 \\ &- \frac{1}{4} \left(\tau_3 - \tau_2\right) \Big[\left(\tau_2 - \tau_1\right)^3 + \left(\tau_3 - \tau_2\right)^3 \Big] \boldsymbol{A}^4 + \cdots , \end{aligned}$$

which should be compared with the analytical result

$$\boldsymbol{O}(\tau_2 , \tau_3) = \mathrm{e}^{-(\tau_3 - \tau_2) \boldsymbol{A}} .$$

A9. The Diagonal Element Lambda-Operator (DELO) Method: Numerical Details

Starting at Eq. (9.189), we introduce an optical-depth scale y defined by

$$\mathrm{d}y = a_I(\tau_\mathrm{r})\,\mathrm{d}\tau_\mathrm{r}\ , \tag{A9.1}$$

so that

$$\frac{\mathrm{d}}{\mathrm{d}y}\,\boldsymbol{I}(y) = \boldsymbol{I}(y) - \boldsymbol{s}(y)\ . \tag{A9.2}$$

Let us introduce a grid of N points $(y_1\,, y_2\,, \ldots, y_N)$ not necessarily evenly spaced. Integration of Eq. (A9.2) in the interval $(y_k\,, y_{k+1})$ gives

$$\boldsymbol{I}(y_k) = \int_{y_k}^{y_{k+1}} \mathrm{e}^{-(y-y_k)}\ \boldsymbol{s}(y)\,\mathrm{d}y + \mathrm{e}^{-(y_{k+1}-y_k)}\ \boldsymbol{I}(y_{k+1})\ . \tag{A9.3}$$

Now we assume $\boldsymbol{s}(y)$ to be linear in y in the same interval,

$$\boldsymbol{s}(y) = \frac{(y_{k+1} - y)\,\boldsymbol{s}_k + (y - y_k)\,\boldsymbol{s}_{k+1}}{y_{k+1} - y_k}\ , \tag{A9.4}$$

with $\boldsymbol{s}_k = \boldsymbol{s}(y_k)$. Substituting Eq. (A9.4) into Eq. (A9.3) and evaluating analytically the integral, one gets, with the help of Eq. (9.190)

$$\boldsymbol{I}_k = \boldsymbol{p}_k + \boldsymbol{\Pi}_k\,\boldsymbol{I}_{k+1}\ , \tag{A9.5}$$

where $\boldsymbol{I}_k = \boldsymbol{I}(y_k)$ and

$$\begin{aligned}
\boldsymbol{p}_k &= \left(\boldsymbol{1} + m_k\,\boldsymbol{A}'_k\right)^{-1}\left(m_k\,\boldsymbol{b}'_k + n_k\,\boldsymbol{b}'_{k+1}\right)\\
\boldsymbol{\Pi}_k &= \left(\boldsymbol{1} + m_k\,\boldsymbol{A}'_k\right)^{-1}\left(\ell_k\,\boldsymbol{1} - n_k\,\boldsymbol{A}'_{k+1}\right)\ ,
\end{aligned} \tag{A9.6}$$

with

$$\begin{aligned}
\Delta_k &= y_{k+1} - y_k & m_k &= \frac{\Delta_k + \ell_k - 1}{\Delta_k}\\
\ell_k &= \mathrm{e}^{-\Delta_k} & n_k &= \frac{1 - \ell_k\,(\Delta_k + 1)}{\Delta_k}\ .
\end{aligned} \tag{A9.7}$$

Comparison of Eqs. (A9.5) and (9.165) shows that $\boldsymbol{\Pi}_k$ gives a numerical representation of the evolution operator associated with the interval $(y_k\,, y_{k+1})$,

$$\boldsymbol{\Pi}_k \approx \boldsymbol{O}(y_k\,, y_{k+1})\ .$$

Once the boundary condition $\boldsymbol{I}_N = \boldsymbol{I}^{(\mathrm{b})}$ is specified (see footnote 1 on p. 441), the emerging Stokes vector $\boldsymbol{I}_1$ can be determined by recursive application of Eq. (A9.5).

To test the accuracy of the DELO solution against the step length, we assume the matrix $\boldsymbol{A}'$ to be independent of y in the interval $(y_k\,, y_{k+1})$ and compare $\boldsymbol{\Pi}_k$ with the exact analytical expression of the evolution operator. From Eqs. (A9.6) we have

$$\boldsymbol{\Pi}_k = \left(\boldsymbol{1} + m_k\,\boldsymbol{A}'\right)^{-1} \left(\ell_k\,\boldsymbol{1} \,-\, n_k\,\boldsymbol{A}'\right) .$$

Expansion of the matrix $(\boldsymbol{1} + m_k\,\boldsymbol{A}')^{-1}$ into power series of $\boldsymbol{A}'$ yields

$$\left(\boldsymbol{1} + m_k\,\boldsymbol{A}'\right)^{-1} \,=\, \boldsymbol{1} \,+\, \sum_{r=1}^{\infty}\, (-1)^r\, m_k^r\, \boldsymbol{A}'^{\,r} \,,$$

whence

$$\boldsymbol{\Pi}_k = \ell_k \left[\, \boldsymbol{1} \,+\, \sum_{r=1}^{\infty}\, (-1)^r \left(m_k + \frac{n_k}{\ell_k}\right) m_k^{r-1}\, \boldsymbol{A}'^{\,r} \right] .$$

The quantities m_k and $(m_k + n_k\,/\,\ell_k)$ can be expanded into power series of Δ_k; up to third order we have

$$m_k = \frac{\Delta_k}{2} \,-\, \frac{\Delta_k^2}{6} \,+\, \frac{\Delta_k^3}{24} \,+\, \mathcal{O}(\Delta_k^4)$$

$$m_k + \frac{n_k}{\ell_k} = \frac{\mathrm{e}^{\,\Delta_k} \,+\, \mathrm{e}^{\,-\Delta_k} \,-\, 2}{\Delta_k} \,=\, \Delta_k + \frac{\Delta_k^3}{12} \,+\, \mathcal{O}(\Delta_k^5) \,,$$

so that, up to the same order of approximation, one gets

$$\boldsymbol{\Pi}_k = \ell_k \left[\, \boldsymbol{1} - \Delta_k\,\boldsymbol{A}' + \frac{1}{2}\,\Delta_k^2\,\boldsymbol{A}'^{\,2} \,-\, \frac{\Delta_k^3}{12}\left(\boldsymbol{A}' + 2\boldsymbol{A}'^{\,2} + 3\boldsymbol{A}'^{\,3}\right) + \mathcal{O}(\Delta_k^4) \right] . \quad \text{(A9.8)}$$

On the other hand, the analytical expression of the evolution operator is (see Eqs. (9.187), (9.104) and (A9.1))

$$\boldsymbol{O}(y_k\,, y_{k+1}) \,=\, \mathrm{e}^{\,-(y_{k+1} - y_k)}\; \mathrm{e}^{\,-(y_{k+1} - y_k)\,\boldsymbol{A}'} \,=\, \ell_k\; \mathrm{e}^{\,-\Delta_k\,\boldsymbol{A}'}$$

$$= \ell_k \left[\, \boldsymbol{1} - \Delta_k\,\boldsymbol{A}' + \frac{1}{2}\,\Delta_k^2\,\boldsymbol{A}'^{\,2} \,-\, \frac{1}{6}\,\Delta_k^3\,\boldsymbol{A}'^{\,3} \,+\, \mathcal{O}(\Delta_k^4) \right] .$$

Comparison with Eq. (A9.8) shows that the expression for $\boldsymbol{\Pi}_k$ resulting from the DELO method is correct up to second-order terms in $\Delta_k\,\boldsymbol{A}'$. The 'error' is

$$\boldsymbol{\mathcal{E}}_k = \boldsymbol{O}(y_k\,, y_{k+1}) \,-\, \boldsymbol{\Pi}_k \,=\, \mathrm{e}^{\,-\Delta_k} \left[\, \frac{\Delta_k^3}{12}\left(\boldsymbol{A}' + 2\boldsymbol{A}'^{\,2} + \boldsymbol{A}'^{\,3}\right) + \mathcal{O}(\Delta_k^4) \right] .$$

Since the series expansion in the right-hand side is meaningful only when $\Delta_k \ll 1$, we can replace the exponential by 1. The 'error' $\boldsymbol{\mathcal{E}}_k$ can be easily expressed in

terms of $\tau_{\rm r}$ and $\boldsymbol{A}$ rather than y and $\boldsymbol{A}'$. Denoting by $(\tau_1\,,\tau_2\,,\,\ldots\,,\tau_N)$ the $\tau_{\rm r}$ grid-points corresponding to $(y_1\,,y_2\,,\,\ldots\,,y_N)$, integration of Eq. (A9.1) in the interval $(\tau_k\,,\tau_{k+1})$ yields

$$y_{k+1} - y_k \,=\, a_I\,(\tau_{k+1} - \tau_k)\;,$$

where a_I is the mean value of $a_I(\tau_{\rm r})$ in the interval. Using Eqs. (A9.7) and (9.188) we have

$$\boldsymbol{\mathcal{E}}_k \approx \frac{\delta_k^3}{12}\left[\,a_I^2\,(\boldsymbol{A} - a_I\,\boldsymbol{1}) \,+\, 2a_I\,(\boldsymbol{A} - a_I\,\boldsymbol{1})^2 \,+\, (\boldsymbol{A} - a_I\,\boldsymbol{1})^3\,\right]\,, \tag{A9.9}$$

with

$$\delta_k = \,\tau_{k+1} - \tau_k\;\;.$$

Finally, it should be remarked that, for the particular case of the Milne-Eddington atmosphere, the DELO method provides the *exact* solution to the transfer equation for any *outward* propagation direction. This fact, which may look surprising at first sight, can be easily understood by the following argument. The basic assumptions of the Milne-Eddington model imply that the matrix $\boldsymbol{A}'$ and the vector $\boldsymbol{b}'$ in Eq. (9.187) are independent of $\tau_{\rm r}$ and linear in $\tau_{\rm r}$, respectively. On the other hand, the solution $\boldsymbol{I}(\tau_{\rm r})$ given by Eqs. (9.108) is also linear in $\tau_{\rm r}$, thus the 'modified source vector' $\boldsymbol{s}(\tau_{\rm r})$ defined in Eq. (9.190) is in turn linear in $\tau_{\rm r}$. Since the quantity a_I is also constant, it turns out that $\boldsymbol{s}$ is linear in y (cf. Eq. (A9.1)). Therefore, Eq. (A9.4) – which is the only assumption of the DELO method – is exactly satisfied under the Milne-Eddington approximations. It follows, incidentally, that it doesn't make sense to test the accuracy of the DELO method by comparing the numerical result with the Milne-Eddington analytical solution.

A10. Equivalent Width in the Presence of Depth-Dependent Line Shifts

Consider the transfer equation for the intensity of a non-magnetic spectral line formed in a static atmosphere in LTE. From Eqs. (9.29), (9.27), (9.32) and (9.35) we have, under the limit $\vec{B} = 0$

$$\frac{{\rm d}I}{{\rm d}\tau_{\rm c}} = (1+k)\,(I - B_{\rm P})\;, \tag{A10.1}$$

where

$$k = \,\kappa_{\rm L}\,\eta \,=\, \kappa_{\rm L}\,\frac{1}{\sqrt{\pi}}\;H(v,a)\;, \tag{A10.2}$$

with v the reduced wavelength

$$v = \frac{\lambda - \lambda_0}{\Delta\lambda_{\rm D}}\;\;. \tag{A10.3}$$

Following Sánchez Almeida et al. (1989), we assume that the absorption profile η is shifted from the wavelength λ_0 by a small amount $\delta\lambda$ which depends on optical depth, where small means

$$\delta\lambda(\tau_c) \ll \Delta\lambda_D \tag{A10.4}$$

for any τ_c. We want to evaluate the effect of this wavelength shift on the equivalent width of the line.

The variable v in Eq. (A10.2) becomes

$$v(\tau_c) = \frac{\lambda - \lambda_0 - \delta\lambda(\tau_c)}{\Delta\lambda_D} \ ,$$

and owing to assumption (A10.4) we can expand k in power series of $\delta\lambda(\tau_c)$. Up to the second order we have

$$k = \kappa_L \left[\eta - \eta' \, \delta\lambda(\tau_c) + \frac{1}{2} \, \eta'' \left[\delta\lambda(\tau_c) \right]^2 \right], \tag{A10.5}$$

where η is the unperturbed profile defined in Eq. (A10.2) and where primes denote derivatives with respect to λ.

Similarly to Sect. 9.6, we write I in the form

$$I = I_0 + I_1 + I_2 \ , \tag{A10.6}$$

where I_n is of order $\delta\lambda^n$. Substituting Eqs. (A10.5) and (A10.6) into Eq. (A10.1) and equating the terms of the same order, we obtain the following set of equations

$$\frac{dI_0}{d\tau_c} = (1 + \kappa_L \, \eta) \, (I_0 - B_P)$$

$$\frac{dI_1}{d\tau_c} = (1 + \kappa_L \, \eta) \, I_1 - \kappa_L \, \eta' \, \delta\lambda \ (I_0 - B_P)$$

$$\frac{dI_2}{d\tau_c} = (1 + \kappa_L \, \eta) \, I_2 - \kappa_L \, \eta' \, \delta\lambda \ I_1 + \frac{1}{2} \, \kappa_L \, \eta'' \, \delta\lambda^2 \ (I_0 - B_P) \ .$$

To solve these equations we make two further assumptions: i) the atmosphere is described by the Milne-Eddington model (see Sect. 9.8), and we consider vertical propagation ($\mu = 1, \ t_c = \tau_c$); ii) the wavelength shift $\delta\lambda$ varies linearly with optical depth,

$$\delta\lambda(\tau_c) = b \, \tau_c \ . \tag{A10.7}$$

A straightforward calculation shows that the contributions to the emerging intensity are

$$I_0(0) = B_0 \left[1 + \frac{\beta}{1 + \kappa_L \, \eta} \right]$$

$$I_1(0) = B_0 \, \beta \, b \, \frac{\kappa_L \, \eta'}{(1 + \kappa_L \, \eta)^3}$$

$$I_2(0) = - B_0 \, \beta \, b^2 \left[\frac{\kappa_L \, \eta''}{(1 + \kappa_L \, \eta)^4} - 3 \, \frac{\kappa_L^2 \, \eta'^2}{(1 + \kappa_L \, \eta)^5} \right] .$$

Using these expressions, we can calculate the equivalent width according to Eq. (9.219). We have

$$W = W_0 \, - \, \frac{1}{B_0 \, (1 + \beta)} \, \int\limits_{-\infty}^{\infty} \big[\, I_1(0) \, + \, I_2(0) \, \big] \, \mathrm{d}\lambda \, ,$$

where W_0 , the equivalent width corresponding to $\delta\lambda = 0$, is given by

$$W_0 \, = \, \Delta\lambda_{\mathrm{D}} \, \frac{\beta}{1 + \beta} \, \mathcal{I}_1(\kappa_{\mathrm{L}} \, , a) \, ,$$

with $\mathcal{I}_1$ defined in Eqs. (9.222). Since the profile η is symmetrical about λ_0 , the contribution of $I_1(0)$ to the equivalent width is zero. The contribution of $I_2(0)$ can be simplified by taking into account that

$$\int\limits_{-\infty}^{\infty} \frac{\kappa_{\mathrm{L}} \, \eta''}{(1 + \kappa_{\mathrm{L}} \, \eta)^4} \, \mathrm{d}\lambda \, = \, 4 \int\limits_{-\infty}^{\infty} \frac{\kappa_{\mathrm{L}}^2 \, \eta'^{\,2}}{(1 + \kappa_{\mathrm{L}} \, \eta)^5} \, \mathrm{d}\lambda \, .$$

The equivalent width can thus be written in the form

$$W = \, \Delta\lambda_{\mathrm{D}} \, \frac{\beta}{1 + \beta} \, \left[\, \mathcal{I}_1(\kappa_{\mathrm{L}} \, , a) \, + \, \left(\frac{b}{\Delta\lambda_{\mathrm{D}}} \right)^2 \, \mathcal{I}_6(\kappa_{\mathrm{L}} \, , a) \right] \, , \tag{A10.8}$$

where

$$\mathcal{I}_6(\kappa_{\mathrm{L}} \, , a) \, = \int\limits_{-\infty}^{\infty} \frac{\kappa_{\mathrm{L}}^2 \, \dot{\eta}^2}{(1 + \kappa_{\mathrm{L}} \, \eta)^5} \, \mathrm{d}v \, , \tag{A10.9}$$

with v the reduced wavelength defined in Eq. (A10.3) and $\dot{\eta} = \partial\eta \, / \, \partial v$.

A11. Net Circular Polarization in Blends

We consider the simplest case where the blend is formed by two independent, Zeeman-triplet spectral lines. We assume the atmosphere is plane-parallel and static and the magnetic field is in the vertical (outward or inward) direction, and we restrict attention to the radiation flowing in the vertical outward direction.

Use of Eqs. (9.216) and (9.32) allows us to write the net circular polarization parameter – defined in Eq. (9.235) – in the form (cf. Eq. (9.245))

$$\mathfrak{v} \, = \, \sigma \, \frac{W_{\mathrm{b}} \, - \, W_{\mathrm{r}}}{W_{\mathrm{b}} \, + \, W_{\mathrm{r}}} \, ,$$

where σ is the sign factor defined in Eq. (9.246) and where W_{b} and W_{r} are the equivalent widths of two 'fictitious' lines formed in the same atmosphere (without

magnetic field) and having absorption coefficients given by the blend of the $\sigma_{\rm b}$ and $\sigma_{\rm r}$ components of the two lines respectively, that is by

$$\kappa_{\rm L}^{(1)}\,\eta_{\rm b}^{(1)} + \kappa_{\rm L}^{(2)}\,\eta_{\rm b}^{(2)} \ , \qquad\qquad \kappa_{\rm L}^{(1)}\,\eta_{\rm r}^{(1)} + \kappa_{\rm L}^{(2)}\,\eta_{\rm r}^{(2)} \ .$$

Denoting by g_1 and g_2 the Landé factors of the two lines and by λ_1 and λ_2 their central wavelengths, the separation between the $\sigma_{\rm b}$ components is

$$|\,\lambda_2 - \lambda_1 - (g_2 - g_1)\,\Delta\lambda_B\,| \ ,$$

while the separation between the $\sigma_{\rm r}$ components is

$$|\,\lambda_2 - \lambda_1 + (g_2 - g_1)\,\Delta\lambda_B\,| \ .$$

We now observe that in 'standard' stellar atmospheres (where temperature is a monotonically increasing function of optical depth) the equivalent width of a spectral line formed by two components increases when the separation between the components is increased (cf. Sect. 9.21, Case ii). It follows that

$$\begin{cases} W_{\rm r} > W_{\rm b} & \text{if} \quad |\,\lambda_2 - \lambda_1 + (g_2 - g_1)\,\Delta\lambda_B\,| > |\,\lambda_2 - \lambda_1 - (g_2 - g_1)\,\Delta\lambda_B\,| \\ W_{\rm r} = W_{\rm b} & \text{if} \quad |\,\lambda_2 - \lambda_1 + (g_2 - g_1)\,\Delta\lambda_B\,| = |\,\lambda_2 - \lambda_1 - (g_2 - g_1)\,\Delta\lambda_B\,| \\ W_{\rm r} < W_{\rm b} & \text{if} \quad |\,\lambda_2 - \lambda_1 + (g_2 - g_1)\,\Delta\lambda_B\,| < |\,\lambda_2 - \lambda_1 - (g_2 - g_1)\,\Delta\lambda_B\,| \ . \end{cases}$$

The sign rule for $\mathfrak{v}$ is therefore

$$\text{sign}\,(\mathfrak{v}\,) \;=\; \text{sign}\left[\,\sigma\,(\lambda_2 - \lambda_1)\,(g_1 - g_2)\right] .$$

Obviously the net circular polarization is zero if $g_1 = g_2$. Bearing in mind Eq. (9.80), we can express the above relation in the following form: in a blend of two Zeeman triplets, the sign of the net circular polarization is the same as the sign of the V Stokes parameter in the external wing of the line having the larger Landé factor.[1]

It might be tempting to generalize this statement to more complicated physical situations (different orientations of the magnetic field, anomalous Zeeman patterns, etc.). Detailed numerical calculations show, however, that there are many exceptions to this simple rule. The exceptions occur mainly for large inclination angles of the magnetic field, for line pairs having close values of g, and for Type I and Type II anomalous Zeeman patterns.

One could wonder whether the simple mechanism described above (blends between magnetic lines) might produce a certain amount of net circular polarization in a broad spectral interval containing many blends. Although the net circular polarization in a single blend can be rather conspicuous (it is easy to find values of $\mathfrak{v}$

[1] 'External' means here 'at larger distance from the other line'. Note that the above statement is valid provided the larger of the two Landé factors is positive.

of the order or even larger than 0.2), there is indeed no reason why the blending line having the larger Landé factor should preferably lie on the red rather than on the blue side of the other line. A systematic effect could possibly exist for fine-structure or hyperfine-structure multiplets, but such investigation is beyond the aims of this book.

A12. Evolution Operator in Stochastic Media

We solve Eq. (9.285) considering the matrix $\boldsymbol{A}(\tau_{\mathrm{r}})$ as a Kubo-Anderson process; in other words, we suppose that its stochastic properties are described by assumptions b), c), and d) of Sect. 9.24.

The evolution operator is defined in Eq. (9.93),

$$\boldsymbol{I}(\tau_0) = \boldsymbol{O}(\tau_0\,,\tau)\;\boldsymbol{I}(\tau) \qquad (\tau_0 \le \tau)\;.$$

First of all we evaluate its expression for a particular realization of the jumping points $(\tau_1\,,\tau_2\,,\ldots,\tau_i\,,\ldots)$. If the number of such points in the interval $(\tau_0\,,\tau)$ is n, we have from Eqs. (9.95) and (9.103)

$$\boldsymbol{O}(\tau_0\,,\tau) = \mathrm{e}^{-(\tau_1-\tau_0)\,\boldsymbol{A}_1}\;\mathrm{e}^{-(\tau_2-\tau_1)\,\boldsymbol{A}_2}\;\cdots\;\mathrm{e}^{-(\tau_n-\tau_{n-1})\,\boldsymbol{A}_n} \times \mathrm{e}^{-(\tau-\tau_n)\,\boldsymbol{A}_{n+1}}\;, \tag{A12.1}$$

where $\boldsymbol{A}_1$ is the (constant) value of $\boldsymbol{A}(\tau_{\mathrm{r}})$ in the interval $(\tau_0\,,\tau_1)$, and so on.

Next we integrate over all possible realizations of the jumping points. The combined probability $\mathrm{d}Q_n$ that the jumping points in $(\tau_0\,,\tau)$ are n and that they lie in the intervals $(\tau_1\,,\tau_1+\mathrm{d}\tau_1)$, $(\tau_2\,,\tau_2+\mathrm{d}\tau_2)$, …, $(\tau_n\,,\tau_n+\mathrm{d}\tau_n)$, respectively, is given by

$$\mathrm{d}Q_n = \mathrm{e}^{-\frac{\tau_1-\tau_0}{\tau_{\mathrm{e}}}}\;\mathrm{e}^{-\frac{\tau_2-\tau_1}{\tau_{\mathrm{e}}}}\;\cdots\,\mathrm{e}^{-\frac{\tau_n-\tau_{n-1}}{\tau_{\mathrm{e}}}}\;\mathrm{e}^{-\frac{\tau-\tau_n}{\tau_{\mathrm{e}}}}\;\frac{\mathrm{d}\tau_1}{\tau_{\mathrm{e}}}\,\frac{\mathrm{d}\tau_2}{\tau_{\mathrm{e}}}\,\cdots\,\frac{\mathrm{d}\tau_n}{\tau_{\mathrm{e}}}\;, \tag{A12.2}$$

with

$$\sum_{n=0}^{\infty}\int \mathrm{d}Q_n = \sum_{n=0}^{\infty}\int_{\tau_0}^{\tau}\frac{\mathrm{d}\tau_1}{\tau_{\mathrm{e}}}\int_{\tau_1}^{\tau}\frac{\mathrm{d}\tau_2}{\tau_{\mathrm{e}}}\,\cdots \cdots\int_{\tau_{n-1}}^{\tau}\frac{\mathrm{d}\tau_n}{\tau_{\mathrm{e}}}\;\mathrm{e}^{-\frac{\tau_1-\tau_0}{\tau_{\mathrm{e}}}}\;\mathrm{e}^{-\frac{\tau_2-\tau_1}{\tau_{\mathrm{e}}}}\;\cdots\,\mathrm{e}^{-\frac{\tau_n-\tau_{n-1}}{\tau_{\mathrm{e}}}}\;\mathrm{e}^{-\frac{\tau-\tau_n}{\tau_{\mathrm{e}}}} \;=\; 1\;.$$

From Eqs. (A12.1) and (A12.2) we obtain

$$\sum_{n=0}^{\infty} \int \boldsymbol{O}(\tau_0\,,\tau)\;\mathrm{d}Q_n = \mathrm{e}^{-\frac{\tau-\tau_0}{\tau_\mathrm{e}}} \sum_{n=0}^{\infty} \int_{\tau_0}^{\tau} \frac{\mathrm{d}\tau_1}{\tau_\mathrm{e}} \int_{\tau_1}^{\tau} \frac{\mathrm{d}\tau_2}{\tau_\mathrm{e}} \cdots$$

$$\cdots \int_{\tau_{n-1}}^{\tau} \frac{\mathrm{d}\tau_n}{\tau_\mathrm{e}}\;\; \mathrm{e}^{-(\tau_1-\tau_0)\,\boldsymbol{A}_1}\; \mathrm{e}^{-(\tau_2-\tau_1)\,\boldsymbol{A}_2}\; \cdots\; \mathrm{e}^{-(\tau_n-\tau_{n-1})\,\boldsymbol{A}_n}\; \mathrm{e}^{-(\tau-\tau_n)\,\boldsymbol{A}_{n+1}}\;.$$

To perform this integral we expand the exponentials into power series. Using the formula[1]

$$\int_{\tau_0}^{\tau} \frac{\mathrm{d}\tau_1}{\tau_\mathrm{e}} \int_{\tau_1}^{\tau} \frac{\mathrm{d}\tau_2}{\tau_\mathrm{e}} \cdots \int_{\tau_{n-1}}^{\tau} \frac{\mathrm{d}\tau_n}{\tau_\mathrm{e}}\;\; (\tau_1-\tau_0)^{i_1}\,(\tau_2-\tau_1)^{i_2}\cdots(\tau_n-\tau_{n-1})^{i_n}\,(\tau-\tau_n)^{i_{n+1}} =$$

$$= \left(\frac{\tau-\tau_0}{\tau_\mathrm{e}}\right)^n (\tau-\tau_0)^{i_1+i_2+\cdots+i_n+i_{n+1}}\;\; \frac{i_1!\;i_2!\cdots i_n!\;i_{n+1}!}{(i_1+i_2+\cdots+i_n+i_{n+1}+n)\,!}\;,$$

we have

$$\sum_{n=0}^{\infty} \int \boldsymbol{O}(\tau_0\,,\tau)\;\mathrm{d}Q_n = \mathrm{e}^{-\frac{\tau-\tau_0}{\tau_\mathrm{e}}} \sum_{n=0}^{\infty} \left(\frac{\tau-\tau_0}{\tau_\mathrm{e}}\right)^n \sum_{i_1=0}^{\infty}\sum_{i_2=0}^{\infty} \cdots$$

$$\cdots \sum_{i_{n+1}=0}^{\infty} \frac{[-(\tau-\tau_0)\,]^{i_1+i_2+\cdots+i_{n+1}}}{(i_1+i_2+\cdots+i_{n+1}+n)\,!}\;\boldsymbol{A}_1^{i_1}\;\boldsymbol{A}_2^{i_2}\;\cdots\boldsymbol{A}_{n+1}^{i_{n+1}}\;.$$

Finally, we average over the distribution of the physical parameters and obtain the following expression for the statistical average of the evolution operator

$$\big[\,\boldsymbol{O}(\tau_0\,,\tau)\,\big]_\mathrm{av} = \mathrm{e}^{-\frac{\tau-\tau_0}{\tau_\mathrm{e}}} \sum_{n=0}^{\infty} \left(\frac{\tau-\tau_0}{\tau_\mathrm{e}}\right)^n \sum_{i_1=0}^{\infty}\sum_{i_2=0}^{\infty} \cdots$$

$$\cdots \sum_{i_{n+1}=0}^{\infty} \frac{[-(\tau-\tau_0)\,]^{i_1+i_2+\cdots+i_{n+1}}}{(i_1+i_2+\cdots+i_{n+1}+n)\,!}\;\big\langle \boldsymbol{A}^{i_1}\big\rangle\big\langle \boldsymbol{A}^{i_2}\big\rangle\cdots\big\langle \boldsymbol{A}^{i_{n+1}}\big\rangle\;.$$

This equation can be rewritten in a more convenient form by grouping together all the terms of the form

$$\big\langle \boldsymbol{A}^{j_1}\big\rangle\big\langle \boldsymbol{A}^{j_2}\big\rangle\cdots\big\langle \boldsymbol{A}^{j_m}\big\rangle$$

[1] See e.g. Gradshteyn and Ryzhik (1965), equation n. 4.634, p.620.

with $j_1 \geq 1,\ \ j_2 \geq 1, \ldots, j_m \geq 1$. With the help of some algebra, we obtain the expression

$$\big[\, \boldsymbol{O}(\tau_0\,,\tau) \,\big]_{\rm av} =$$

$$= \boldsymbol{1} + \sum_{k=1}^{\infty} (-1)^k\, \tau_{\rm e}^k \sum_{m=1}^{k} f_{km}\!\left(\frac{\tau-\tau_0}{\tau_{\rm e}}\right) \sum_{j_1 j_2 \cdots j_m} \big\langle \boldsymbol{A}^{j_1} \big\rangle \big\langle \boldsymbol{A}^{j_2} \big\rangle \cdots \big\langle \boldsymbol{A}^{j_m} \big\rangle\,, \quad \text{(A12.3)}$$

where $(j_1\,, j_2\,, \ldots, j_m)$ are all the different solutions of the equation

$$j_1 + j_2 + \cdots + j_m = k\,, \quad \text{(A12.4)}$$

and where the function $f_{km}(x)$, defined only for $k \geq 1$ and $1 \leq m \leq k$, is given by

$$f_{km}(x) = {\rm e}^{-x}\, x^k \sum_{n=m-1}^{\infty} \frac{x^n}{(n+k)\,!} \binom{n+1}{m}\,. \quad \text{(A12.5)}$$

The function $f_{km}(x)$ can be expressed in a variety of different forms. A tedious calculation, which is left as an exercise to the reader, allows one to transform the infinite sum into two finite sums. The result is the following[1]

$$f_{11}(x) = x$$

$$f_{km}(x) = (-1)^m \left\{ \sum_{n=0}^{m} (-1)^n\, \frac{x^n}{n!} \binom{k+m-2-n}{k-2} \right.$$

$$\left. - {\rm e}^{-x} \sum_{n=0}^{k-2} \frac{x^n}{n!} \binom{k+m-2-n}{m} \right\} \qquad (k \geq 2)\,. \quad \text{(A12.6)}$$

The solution to the homogeneous transfer equation (9.285) for a Kubo-Anderson process can thus be written in the form

$$\big[\, \boldsymbol{I}(\tau_0) \,\big]_{\rm av} = \big[\, \boldsymbol{O}(\tau_0\,,\tau) \,\big]_{\rm av}\ \boldsymbol{I}(\tau)\,,$$

with $\big[\, \boldsymbol{O}(\tau_0\,,\tau) \,\big]_{\rm av}$ given by Eqs. (A12.3) and (A12.6).

Equation (A12.3) contains, as particular cases, some interesting limits:

i) If the physical parameters are deterministic, the symbols $\langle \cdots \rangle$ can be removed. Since for a given k the number of different solutions of Eq. (A12.4) is $\binom{k-1}{m-1}$, we obtain

$$\big[\, \boldsymbol{O}(\tau_0\,,\tau) \,\big]_{\rm av} = \boldsymbol{1} + \sum_{k=1}^{\infty} (-1)^k\, \tau_{\rm e}^k\, \boldsymbol{A}^k \sum_{m=1}^{k} \binom{k-1}{m-1} f_{km}\!\left(\frac{\tau-\tau_0}{\tau_{\rm e}}\right).$$

[1] To obtain Eqs. (A12.6), use has been made of Eq. 45 on p.166 and Eq. 4 on p.705 in Prudnikov et al. (1986), and of Eq. 4 on p.8 and Eq. (ii) on p.1 in Riordan (1968). Equation 3 in the latter book is useful to prove Eq. (A12.7) using expression (A12.5).

The sum over m can be evaluated and yields

$$\frac{1}{k!}\left(\frac{\tau-\tau_0}{\tau_{\rm e}}\right)^k , \tag{A12.7}$$

so that

$$\left[\,\boldsymbol{O}(\tau_0\,,\tau)\,\right]_{\rm av} = \boldsymbol{1} + \sum_{k=1}^{\infty}(-1)^k\,\frac{(\tau-\tau_0)^k}{k!}\,\boldsymbol{A}^k = {\rm e}^{-(\tau-\tau_0)\,\boldsymbol{A}} ,$$

which is the correct expression for the evolution operator in the deterministic case.

ii) Microturbulent limit ($\tau_{\rm e} \to 0$). According to Eqs. (A12.6), the asymptotic expression of the function $f_{km}(x)$ for $x \to \infty$ is

$$f_{km}(x) \sim \frac{x^m}{m!} .$$

Substitution into Eq. (A12.3) shows that, for an assigned k, the only term in the summation over m which makes a non-zero contribution for $\tau_{\rm e} \to 0$ is the one corresponding to $m = k$. This implies $j_1 = j_2 = \cdots = j_m = 1$, hence Eq. (A12.3) reduces to

$$\left[\,\boldsymbol{O}(\tau_0\,,\tau)\,\right]_{\rm av} = \boldsymbol{1} + \sum_{k=1}^{\infty}(-1)^k\,\frac{(\tau-\tau_0)^k}{k!}\,\left\langle\boldsymbol{A}\right\rangle^k = {\rm e}^{-(\tau-\tau_0)\,\langle\boldsymbol{A}\rangle} . \tag{A12.8}$$

iii) Macroturbulent limit ($\tau_{\rm e} \to \infty$). According to Eq. (A12.5), the asymptotic expression of $f_{km}(x)$ for $x \to 0$ is

$$f_{km}(x) \sim \frac{x^{k+m-1}}{(k+m-1)\,!} .$$

For an assigned k, the only term in the summation over m in Eq. (A12.3) which makes a non-zero contribution for $\tau_{\rm e} \to \infty$ is the one with $m = 1$. This implies $j_1 = k$, so that Eq. (A12.3) yields

$$\begin{aligned}\left[\,\boldsymbol{O}(\tau_0\,,\tau)\,\right]_{\rm av} &= \boldsymbol{1} + \sum_{k=1}^{\infty}(-1)^k\,\frac{(\tau-\tau_0)^k}{k!}\,\left\langle\boldsymbol{A}^k\right\rangle \\ &= \left\langle\boldsymbol{1} + \sum_{k=1}^{\infty}(-1)^k\,\frac{(\tau-\tau_0)^k}{k!}\,\boldsymbol{A}^k\right\rangle = \left\langle{\rm e}^{-(\tau-\tau_0)\,\boldsymbol{A}}\right\rangle .\end{aligned}$$

iv) Scalar case. For non-magnetic media, $\boldsymbol{A}$ has the form $\boldsymbol{A} = \kappa\,\boldsymbol{1}$ (with κ given by Eq. (9.278)), thus all the matrices $\langle\boldsymbol{A}^{j_i}\rangle$ in Eq. (A12.3) commute. Equation

(A12.3) can be rewritten in the form

$$\big[\, \boldsymbol{O}(\tau_0\,,\tau)\,\big]_{\rm av} = \Big\{\, 1 + \sum_{k=1}^{\infty}\, (-1)^k\, \tau_{\rm e}^k\, \sum_{m=1}^{k}\, f_{km}\Big(\frac{\tau-\tau_0}{\tau_{\rm e}}\Big) \\ \times \sum_{p_1 p_2 \cdots p_m} N(p_1\,,p_2\,,\,\ldots\,,p_m)\, \big\langle \kappa^{\,p_1}\big\rangle \big\langle \kappa^{\,p_2}\big\rangle\, \cdots\, \big\langle \kappa^{\,p_m}\big\rangle \Big\}\, \boldsymbol{1}\ ,$$

where

$$p_1 + p_2 + \cdots + p_m = k\ , \qquad\qquad 1 \le p_1 \le p_2 \le\, \cdots\, \le p_m\ , \tag{A12.9}$$

and where $N(p_1\,,p_2\,,\,\ldots\,,p_m)$ is an integer defined in the following way. For each set $(p_1\,,p_2\,,\,\ldots\,,p_m)$ satisfying Eqs. (A12.9) we denote by ℓ the number of distinct p_i values contained in the set, and we divide the set into ℓ groups by collecting the p_i's with the same value into one group. If the number of elements in the i-th group is n_i, then

$$N(p_1\,,p_2\,,\,\ldots\,,p_m) \,=\, \frac{m!}{n_1!\ n_2!\ \cdots\ n_\ell!}\ .$$

As an example, let us consider the case $k=6$, $m=3$. The possible sets $(p_1\,,p_2\,,p_3)$ are $(1,1,4)$, $(1,2,3)$, and $(2,2,2)$. The corresponding values of $N(p_1\,,p_2\,,p_3)$ are 3, 6, and 1, respectively.[1]

v) Explicit expression up to $k=3$ terms. By evaluating the functions $f_{km}(x)$ one obtains

$$\begin{aligned}\big[\, \boldsymbol{O}(\tau_0\,,\tau)\,\big]_{\rm av} \,=\, & \boldsymbol{1} - \,(\tau-\tau_0)\,\big\langle \boldsymbol{A}\big\rangle \,+\, \tau_{\rm e}^2\,\Big[\,1 - \,x + \,\frac{x^2}{2}\, - \,{\rm e}^{\,-x}\Big]\big\langle \boldsymbol{A}\big\rangle^2 \\ & - \tau_{\rm e}^2\,\Big[\,1 - \,x - \,{\rm e}^{\,-x}\Big]\big\langle \boldsymbol{A}^2\big\rangle \\ & + \,\tau_{\rm e}^3\,\Big[\,4 - 3x + x^2 - \frac{x^3}{6} - \,(4+x)\,{\rm e}^{\,-x}\Big]\big\langle \boldsymbol{A}\big\rangle^3 \\ & - \tau_{\rm e}^3\,\Big[\,3 - 2x + \frac{x^2}{2} - \,(3+x)\,{\rm e}^{\,-x}\Big]\Big[\big\langle \boldsymbol{A}\big\rangle\,\big\langle \boldsymbol{A}^2\big\rangle + \big\langle \boldsymbol{A}^2\big\rangle\,\big\langle \boldsymbol{A}\big\rangle\Big] \\ & + \tau_{\rm e}^3\,\Big[\,2 - \,x - \,(2+x)\,{\rm e}^{\,-x}\Big]\big\langle \boldsymbol{A}^3\big\rangle\ ,\end{aligned}$$

where $x = \,(\tau-\tau_0)\,/\,\tau_{\rm e}\,.$

[1] Note that $\sum\, N(p_1\,,p_2\,,p_3) = 10 = \binom{5}{2}$. In general,

$$\sum\, N(p_1\,,p_2\,,\cdots,p_m) = \tbinom{k-1}{m-1}\,.$$

A13. Properties of the Generalized Profiles

a) *Definition*

The generalized profile is defined by Eq. (10.40)

$$\Phi_Q^{KK'}(J_\ell, J_u; \nu) = \sqrt{3(2J_u+1)(2K+1)(2K'+1)}$$
$$\times \sum_{M_u M'_u M_\ell q q'} (-1)^{1+J_u-M_u+q'} \begin{pmatrix} J_u & J_\ell & 1 \\ -M_u & M_\ell & -q \end{pmatrix} \begin{pmatrix} J_u & J_\ell & 1 \\ -M'_u & M_\ell & -q' \end{pmatrix}$$
$$\times \begin{pmatrix} J_u & J_u & K \\ M'_u & -M_u & -Q \end{pmatrix} \begin{pmatrix} 1 & 1 & K' \\ q & -q' & -Q \end{pmatrix}$$
$$\times \frac{1}{2}\left[\Phi(\nu_{\alpha_u J_u M_u, \alpha_\ell J_\ell M_\ell} - \nu) + \Phi(\nu_{\alpha_u J_u M'_u, \alpha_\ell J_\ell M_\ell} - \nu)^*\right], \qquad \text{(A13.1)}$$

where $\Phi(\nu_0 - \nu)$ is given by Eq. (6.59a). In general, it is a complex quantity.

b) *Limitation on indices*

Owing to the presence of the 3-j symbols, the indices are restricted to the range

$$K = 0, 1, \ldots, 2J_u$$
$$K' = 0, 1, 2$$
$$Q = 0, \pm 1, \pm 2 \qquad \text{with} \qquad |Q| \le K\,, \qquad |Q| \le K'\,.$$

Denoting by N_Q the number of different generalized profiles with given Q, we have

$$N_0 = 3(2J_u+1) \qquad N_2 = N_{-2} = \begin{cases} 0 & \text{if } J_u = 0 \\ 2J_u - 1 & \text{if } J_u \ne 0\,, \end{cases}$$
$$N_1 = N_{-1} = 4J_u\,,$$

so that the total number of generalized profiles is[1]

$$N = \sum_{Q=-2}^{2} N_Q = \begin{cases} 3 & \text{if } J_u = 0 \\ 18J_u + 1 & \text{if } J_u \ne 0\,. \end{cases}$$

c) *Conjugation*

Taking the complex conjugate of Eq. (A13.1) and interchanging the summation indices $M_u \rightleftarrows M'_u$ and $q \rightleftarrows q'$, one can easily prove, using the symmetry properties of the 3-j symbols (Eqs. (2.24), (2.25)), that

$$\Phi_Q^{KK'}(J_\ell, J_u; \nu)^* = \Phi_{-Q}^{KK'}(J_\ell, J_u; \nu)\,. \qquad \text{(A13.2)}$$

[1] Because of the conjugation property proved below (Eq. (A13.2)), N represents also the number of independent real quantities needed to fully specify all the complex generalized profiles.

d) *Integration over frequency*

$$\int_{-\infty}^{\infty} \Phi_Q^{KK'}(J_\ell, J_u; \nu)\, \mathrm{d}\nu = \delta_{KK'}\, w^{(K)}_{J_u J_\ell} \,, \tag{A13.3}$$

where $w^{(K)}_{J_u J_\ell}$ is the symbol defined in Eq. (10.11). This result can easily be proved with the help of Eqs. (6.59a-c), (2.42) and (2.23a).

e) *Inversion about line center*

Denoting by ν, ν' two frequencies symmetrical about the central frequency ν_0 of the line,

$$\nu' - \nu_0 = \nu_0 - \nu \,,$$

we have

$$\Phi_Q^{KK'}(J_\ell, J_u; \nu') = (-1)^{K+K'}\, \Phi_Q^{KK'}(J_\ell, J_u; \nu) \,; \tag{A13.4}$$

in other words, the generalized profile is symmetrical or antisymmetrical about line center according as the integer $(K + K')$ is even or odd, respectively. To prove this statement, we recall that from Eq. (7.3)

$$\nu_{\alpha_u J_u M_u, \alpha_\ell J_\ell M_\ell} = \nu_0 + \nu_{\mathrm{L}}\, (g_{\alpha_u J_u} M_u - g_{\alpha_\ell J_\ell} M_\ell) \,,$$

and that the profile $\Phi(\nu_0 - \nu)$ satisfies the conjugation property (cf. Eq. (6.59a))

$$\Phi(x) = \Phi(-x)^* \,,$$

thus

$$\begin{aligned} \Phi(\nu_{\alpha_u J_u M_u, \alpha_\ell J_\ell M_\ell} - \nu') &= \Phi(-\nu_0 + \nu_{\mathrm{L}}(g_{\alpha_u J_u} M_u - g_{\alpha_\ell J_\ell} M_\ell) + \nu) \\ &= \Phi(\nu_0 + \nu_{\mathrm{L}}\, [\, g_{\alpha_u J_u}(-M_u) - g_{\alpha_\ell J_\ell}(-M_\ell)] - \nu)^* \,. \end{aligned}$$

After some index renaming, Eq. (A13.4) is easily obtained from Eq. (A13.1) with the help of Eqs. (2.24) and (2.25).

f) *Limit for zero magnetic field*

Under this limit all the Zeeman splittings vanish, so that

$$\lim_{\nu_{\mathrm{L}} \to 0} \frac{1}{2} \left[\Phi(\nu_{\alpha_u J_u M_u, \alpha_\ell J_\ell M_\ell} - \nu) + \Phi(\nu_{\alpha_u J_u M'_u, \alpha_\ell J_\ell M_\ell} - \nu)^* \right] = \phi(\nu_0 - \nu) \,,$$

ϕ being the real part of the complex profile Φ (see Eq. (6.59a)). Substituting into Eq. (A13.1) and performing the same calculations as in point d), one obtains

$$\lim_{\nu_{\mathrm{L}} \to 0} \Phi_Q^{KK'}(J_\ell, J_u; \nu) = \delta_{KK'}\, w^{(K)}_{J_u J_\ell}\, \phi(\nu_0 - \nu) \,. \tag{A13.5}$$

g) *Expansion for weak field*

If the magnetic field is weak, the generalized profile can be expanded into power series of $\nu_{\rm L}$. To first order we can write

$$\begin{aligned}\Phi(\nu_{\alpha_u J_u M_u,\,\alpha_\ell J_\ell M_\ell}-\nu) &\approx \Phi(\nu_0-\nu)\\ &\quad+\nu_{\rm L}(g_{\alpha_u J_u}M_u-g_{\alpha_\ell J_\ell}M_\ell)\left[\frac{\partial\,\Phi(\nu_{\alpha_u J_u M_u,\,\alpha_\ell J_\ell M_\ell}-\nu)}{\partial\nu_{\rm L}}\right]_{\nu_{\rm L}=0}\\ &= \Phi(\nu_0-\nu)-\nu_{\rm L}(g_{\alpha_u J_u}M_u-g_{\alpha_\ell J_\ell}M_\ell)\,\frac{\partial\,\Phi(\nu_0-\nu)}{\partial\nu}\;.\end{aligned}$$

After substitution into Eq. (A13.1), we are left with a zero-order and a first-order contribution. The former has already been calculated (Eq. (A13.5)); the latter contains summations of the form

$$\sum_{M_u M_u' M_\ell q q'} M\;(-1)^{1+J_u-M_u+q'}\begin{pmatrix}J_u & J_\ell & 1\\ -M_u & M_\ell & -q\end{pmatrix}\begin{pmatrix}J_u & J_\ell & 1\\ -M_u' & M_\ell & -q'\end{pmatrix}$$
$$\times\begin{pmatrix}J_u & J_u & K\\ M_u' & -M_u & -Q\end{pmatrix}\begin{pmatrix}1 & 1 & K'\\ q & -q' & -Q\end{pmatrix},$$

where M is either M_u, or M_u', or M_ℓ. These can be performed by writing M in terms of a suitable 3-j symbol (as done, for instance, in Eqs. (3.42)). The summation involving M_u or M_u' can be evaluated by applying twice Eq. (2.42), while the summation involving M_ℓ can be evaluated via Eq. (2.52). The result is the following

$$\begin{aligned}\Phi_Q^{KK'}(J_\ell,J_u;\nu) &= \delta_{KK'}\,w^{(K)}_{J_u J_\ell}\,\phi(\nu_0-\nu)\\ &\quad-\nu_{\rm L}\sqrt{3(2J_u+1)(2K+1)(2K'+1)}\begin{pmatrix}K & K' & 1\\ Q & -Q & 0\end{pmatrix}\\ &\quad\times\Bigg[g_{\alpha_u J_u}\sqrt{J_u(J_u+1)(2J_u+1)}\;(-1)^{1+J_\ell-J_u+Q}\begin{Bmatrix}K & K' & 1\\ J_u & J_u & J_u\end{Bmatrix}\begin{Bmatrix}K' & 1 & 1\\ J_\ell & J_u & J_u\end{Bmatrix}\\ &\qquad\times\frac{1}{2}\left(\frac{\partial\,\Phi(\nu_0-\nu)}{\partial\nu}+(-1)^{1+K+K'}\,\frac{\partial\,\Phi(\nu_0-\nu)^*}{\partial\nu}\right)\\ &\qquad+g_{\alpha_\ell J_\ell}\sqrt{J_\ell(J_\ell+1)(2J_\ell+1)}\;(-1)^Q\begin{Bmatrix}J_\ell & J_u & 1\\ J_\ell & J_u & 1\\ 1 & K & K'\end{Bmatrix}\frac{\partial\phi(\nu_0-\nu)}{\partial\nu}\Bigg].\end{aligned}\tag{A13.6}$$

h) *Special case* $K=0$

For $K=0$ one gets, with the help of Eq. (2.26a)

$$\begin{aligned}\Phi_0^{0K'}(J_\ell,J_u;\nu) &= \sqrt{3(2K'+1)}\sum_{M_u M_\ell\,q}(-1)^{1+q}\begin{pmatrix}J_u & J_\ell & 1\\ -M_u & M_\ell & -q\end{pmatrix}^2\begin{pmatrix}1 & 1 & K'\\ q & -q & 0\end{pmatrix}\\ &\quad\times\phi(\nu_{\alpha_u J_u M_u,\,\alpha_\ell J_\ell M_\ell}-\nu)\;.\end{aligned}\tag{A13.7}$$

In particular, for $K' = 0$

$$\Phi_0^{00}(J_\ell, J_u; \nu) = \sum_{M_u M_\ell\, q} \begin{pmatrix} J_u & J_\ell & 1 \\ -M_u & M_\ell & q \end{pmatrix}^2 \phi(\nu_{\alpha_u J_u M_u, \alpha_\ell J_\ell M_\ell} - \nu) \, .$$

i) *Expression of the emission coefficient in terms of the generalized profile*

Consider the expression of the emission coefficient (Eq. (7.15e)), written for the two-level atom. Owing to the presence of the 3-j symbols, the indices Q and Q_u coincide. The last term can therefore be rewritten in the form

$$\begin{aligned} &\mathrm{Re}\left[\mathcal{T}_Q^K(i,\vec{\Omega})\, \rho_Q^{K_u}(\alpha_u J_u)\; \Phi(\nu_{\alpha_u J_u M_u, \alpha_\ell J_\ell M_\ell} - \nu)\right] = \\ &= \frac{1}{2}\Big[\mathcal{T}_Q^K(i,\vec{\Omega})\, \rho_Q^{K_u}(\alpha_u J_u)\; \Phi(\nu_{\alpha_u J_u M_u, \alpha_\ell J_\ell M_\ell} - \nu) \\ &\qquad + \mathcal{T}_{-Q}^K(i,\vec{\Omega})\, \rho_{-Q}^{K_u}(\alpha_u J_u)\; \Phi(\nu_{\alpha_u J_u M_u, \alpha_\ell J_\ell M_\ell} - \nu)^*\Big] \, , \end{aligned}$$

where Eqs. (3.102) and (5.158) have been used. Bearing in mind the properties of the 3-j symbols (Eqs. (2.24), (2.25)) and the relation between the Einstein coefficients (Eqs. (7.8)), one easily obtains after some index renaming

$$\begin{aligned} \varepsilon_i(\nu,\vec{\Omega}) = &\frac{h\nu}{4\pi}\, \mathcal{N}\, \sqrt{2J_u+1}\; A(\alpha_u J_u \to \alpha_\ell J_\ell) \\ &\times \sum_{K K' Q} \mathcal{T}_Q^{K'}(i,\vec{\Omega})\, \rho_Q^K(\alpha_u J_u)\, \Phi_Q^{K K'}(J_\ell, J_u; \nu) \, . \end{aligned} \tag{A13.8}$$

j) *Expression of the absorption coefficient in terms of the generalized profile*

We restrict attention to the two-level atom with unpolarized lower level. From Eq. (7.15a) we obtain, with the help of Eqs. (10.7), (10.6), (2.26a) and (5.158)

$$\begin{aligned} \eta_i^{\mathrm{A}}(\nu,\vec{\Omega}) = &\frac{h\nu}{4\pi}\, \mathcal{N}_\ell\; B(\alpha_\ell J_\ell \to \alpha_u J_u) \\ &\times \sum_K \sqrt{3(2K+1)} \sum_{M_u M_\ell\, q} (-1)^{1+q} \begin{pmatrix} J_u & J_\ell & 1 \\ -M_u & M_\ell & -q \end{pmatrix}^2 \begin{pmatrix} 1 & 1 & K \\ q & -q & 0 \end{pmatrix} \\ &\qquad \times \mathcal{T}_0^K(i,\vec{\Omega})\; \phi(\nu_{\alpha_u J_u M_u, \alpha_\ell J_\ell M_\ell} - \nu) \, , \end{aligned}$$

or, via Eq. (A13.7)

$$\eta_i^{\mathrm{A}}(\nu,\vec{\Omega}) = \frac{h\nu}{4\pi}\, \mathcal{N}_\ell\; B(\alpha_\ell J_\ell \to \alpha_u J_u) \sum_K \mathcal{T}_0^K(i,\vec{\Omega})\, \Phi_0^{0K}(J_\ell, J_u; \nu) \, , \tag{A13.9}$$

where $\mathcal{N}_\ell$ is the overall population of the lower level.

k) *Special case* $J_\ell = 0$, $J_u = 1$

Evaluating the relevant 3-j symbols via Eqs. (2.26), and introducing the compact notation (consistent with Eqs. (9.6) and (9.8))

$$\Phi_q = \phi_q + \mathrm{i}\,\psi_q = \Phi(\nu_{\alpha_u 1\,-q,\,\alpha_\ell 00} - \nu) \qquad (q = -1, 0, +1)\,, \tag{A13.10}$$

one obtains from Eq. (A13.1)

$$\begin{aligned}
\Phi_0^{00} &= \frac{1}{3}\Big[\phi_1 + \phi_0 + \phi_{-1}\Big] \\
\Phi_0^{01} &= -\Phi_0^{10} = \frac{1}{\sqrt{6}}\Big[\phi_1 - \phi_{-1}\Big] \\
\Phi_0^{02} &= \Phi_0^{20} = \frac{1}{3\sqrt{2}}\Big[\phi_1 - 2\phi_0 + \phi_{-1}\Big] \\
\Phi_0^{11} &= -\frac{1}{2}\Big[\phi_1 + \phi_{-1}\Big] \\
\Phi_1^{11} &= -\frac{1}{4}\Big[\phi_1 + \mathrm{i}\,\psi_1 + 2\phi_0 + \phi_{-1} - \mathrm{i}\,\psi_{-1}\Big] \\
\Phi_0^{12} &= -\Phi_0^{21} = -\frac{1}{2\sqrt{3}}\Big[\phi_1 - \phi_{-1}\Big] \\
\Phi_1^{12} &= -\Phi_1^{21} = -\frac{1}{4}\Big[\phi_1 + \mathrm{i}\,\psi_1 - 2\mathrm{i}\,\psi_0 - \phi_{-1} + \mathrm{i}\,\psi_{-1}\Big] \\
\Phi_0^{22} &= \frac{1}{6}\Big[\phi_1 + 4\phi_0 + \phi_{-1}\Big] \\
\Phi_1^{22} &= \frac{1}{4}\Big[\phi_1 + \mathrm{i}\,\psi_1 + 2\phi_0 + \phi_{-1} - \mathrm{i}\,\psi_{-1}\Big] \\
\Phi_2^{22} &= \frac{1}{2}\Big[\phi_1 + \mathrm{i}\,\psi_1 + \phi_{-1} - \mathrm{i}\,\psi_{-1}\Big]\,.
\end{aligned} \tag{A13.11}$$

The generalized profiles with negative Q are obtained from the expressions above via the conjugation property (A13.2).

As shown above – points i) and j) – the generalized profile $\Phi_Q^{KK'}(J_\ell, J_u; \nu)$ is useful to express the frequency dependence of the emission and absorption coefficients for the two-level atom in the presence of a magnetic field. Its direct counterpart, related to the anomalous dispersion coefficients $\rho_i^{\mathrm{A}}(\nu, \vec{\Omega})$ and $\rho_i^{\mathrm{S}}(\nu, \vec{\Omega})$, is the generalized dispersion profile $\Psi_Q^{KK'}(J_\ell, J_u; \nu)$, which is defined by an expression strictly similar to Eq. (A13.1)

$$\begin{aligned}
\mathrm{i}\,\Psi_Q^{KK'}(J_\ell, J_u; \nu) &= \sqrt{3(2J_u+1)(2K+1)(2K'+1)} \\
&\times \sum_{M_u M_u' M_\ell q q'} (-1)^{1+J_u-M_u+q'} \begin{pmatrix} J_u & J_\ell & 1 \\ -M_u & M_\ell & -q \end{pmatrix} \begin{pmatrix} J_u & J_\ell & 1 \\ -M_u' & M_\ell & -q' \end{pmatrix} \\
&\qquad \times \begin{pmatrix} J_u & J_u & K \\ M_u' & -M_u & -Q \end{pmatrix} \begin{pmatrix} 1 & 1 & K' \\ q & -q' & -Q \end{pmatrix} \\
&\qquad \times \frac{1}{2}\Big[\Phi(\nu_{\alpha_u J_u M_u,\,\alpha_\ell J_\ell M_\ell} - \nu) - \Phi(\nu_{\alpha_u J_u M_u',\,\alpha_\ell J_\ell M_\ell} - \nu)^*\Big]\,.
\end{aligned}$$

The expressions of $\Phi_Q^{KK'}$ and of $\mathrm{i}\,\Psi_Q^{KK'}$ are the same except for the opposite sign in the last square bracket. Because of this close resemblance, the following properties of the generalized dispersion profiles can be proved by strictly similar arguments.

b′) *Limitation on indices*

Same as b).

c′) *Conjugation*

$$\Psi_Q^{KK'}(J_\ell, J_u; \nu)^* = \Psi_{-Q}^{KK'}(J_\ell, J_u; \nu) \; .$$

d′) *Integration over frequency*

$$\int_{-\infty}^{\infty} \Psi_Q^{KK'}(J_\ell, J_u; \nu) \, \mathrm{d}\nu = 0 \; .$$

e′) *Inversion about line center*

$$\Psi_Q^{KK'}(J_\ell, J_u; \nu') = (-1)^{1+K+K'} \, \Psi_Q^{KK'}(J_\ell, J_u; \nu) \; , \tag{A13.12}$$

where the frequencies ν, ν' are symmetrical about the central frequency of the line.

f′) *Limit for zero magnetic field*

$$\lim_{\nu_\mathrm{L} \to 0} \Psi_Q^{KK'}(J_\ell, J_u; \nu) = \delta_{KK'} \, w^{(K)}_{J_u J_\ell} \, \psi(\nu_0 - \nu) \; , \tag{A13.13}$$

where ψ is the imaginary part of the profile Φ (see Eq. (6.59a)).

g′) *Expansion for weak field*

$$\begin{aligned}
\Psi_Q^{KK'}(J_\ell, J_u; \nu) &= \delta_{KK'} \, w^{(K)}_{J_u J_\ell} \, \psi(\nu_0 - \nu) \\
&\quad - \nu_\mathrm{L} \sqrt{3(2J_u+1)(2K+1)(2K'+1)} \begin{pmatrix} K & K' & 1 \\ Q & -Q & 0 \end{pmatrix} \\
&\quad \times \Bigg[g_{\alpha_u J_u} \sqrt{J_u(J_u+1)(2J_u+1)} \; (-1)^{1+J_\ell - J_u + Q} \begin{Bmatrix} K & K' & 1 \\ J_u & J_u & J_u \end{Bmatrix} \begin{Bmatrix} K' & 1 & 1 \\ J_\ell & J_u & J_u \end{Bmatrix} \\
&\qquad \times \frac{-\mathrm{i}}{2} \left(\frac{\partial \, \Phi(\nu_0 - \nu)}{\partial \nu} + (-1)^{K+K'} \, \frac{\partial \, \Phi(\nu_0 - \nu)^*}{\partial \nu} \right) \\
&\qquad + g_{\alpha_\ell J_\ell} \sqrt{J_\ell(J_\ell+1)(2J_\ell+1)} \; (-1)^Q \begin{Bmatrix} J_\ell & J_u & 1 \\ J_\ell & J_u & 1 \\ 1 & K & K' \end{Bmatrix} \frac{\partial \psi(\nu_0 - \nu)}{\partial \nu} \Bigg] \; .
\end{aligned}$$

h′) *Special case* $K = 0$

$$\Psi_0^{0K'}(J_\ell, J_u; \nu) = \sqrt{3(2K'+1)} \sum_{M_u M_\ell\, q} (-1)^{1+q} \begin{pmatrix} J_u & J_\ell & 1 \\ -M_u & M_\ell & -q \end{pmatrix}^2 \begin{pmatrix} 1 & 1 & K' \\ q & -q & 0 \end{pmatrix} \times \psi(\nu_{\alpha_u J_u M_u,\, \alpha_\ell J_\ell M_\ell} - \nu) \,,$$

and for $K' = 0$

$$\Psi_0^{00}(J_\ell, J_u; \nu) = \sum_{M_u M_\ell\, q} \begin{pmatrix} J_u & J_\ell & 1 \\ -M_u & M_\ell & q \end{pmatrix}^2 \psi(\nu_{\alpha_u J_u M_u,\, \alpha_\ell J_\ell M_\ell} - \nu) \,.$$

i′) *Expression of the anomalous dispersion coefficient* $\rho_i^{\mathrm{S}}(\nu, \vec{\Omega})$
For the two-level atom, Eq. (7.15d) can be written in the form

$$\rho_i^{\mathrm{S}}(\nu, \vec{\Omega}) = \frac{h\nu}{4\pi}\, \mathcal{N} \sqrt{2J_u + 1}\; B(\alpha_u J_u \to \alpha_\ell J_\ell) \times \sum_{KK'Q} \mathcal{T}_Q^{K'}(i, \vec{\Omega})\, \rho_Q^K(\alpha_u J_u)\, \Psi_Q^{KK'}(J_\ell, J_u; \nu) \,.$$

j′) *Expression of the anomalous dispersion coefficient* $\rho_i^{\mathrm{A}}(\nu, \vec{\Omega})$
For the two-level atom with unpolarized lower level, Eq. (7.15c) can be written in the form

$$\rho_i^{\mathrm{A}}(\nu, \vec{\Omega}) = \frac{h\nu}{4\pi}\, \mathcal{N}_\ell\; B(\alpha_\ell J_\ell \to \alpha_u J_u) \sum_K \mathcal{T}_0^K(i, \vec{\Omega})\, \Psi_0^{0K}(J_\ell, J_u; \nu) \,. \qquad \text{(A13.14)}$$

A14. Properties of the Symbol $\left[W_{KK'Q}(\beta_\ell L_\ell S \beta_u L_u; B)\right]_{\mathrm{fs}}$

a) *Definition*
The symbol, simply denoted by $W_{KK'Q}$ in this appendix, is defined by Eq. (10.153)

$$W_{KK'Q} = \frac{3(2L_u+1)}{2S+1} \begin{Bmatrix} 1 & 1 & K \\ L_u & L_u & L_\ell \end{Bmatrix} \begin{Bmatrix} 1 & 1 & K' \\ L_u & L_u & L_\ell \end{Bmatrix} \times \sum_{J_u J_u' J_u'' J_u''' M_u M_u'} \sqrt{(2K+1)(2K'+1)(2J_u+1)(2J_u'+1)(2J_u''+1)(2J_u'''+1)} \times \begin{Bmatrix} L_u & L_u & K \\ J_u & J_u' & S \end{Bmatrix} \begin{Bmatrix} L_u & L_u & K' \\ J_u'' & J_u''' & S \end{Bmatrix} \begin{pmatrix} J_u & J_u' & K \\ -M_u & M_u' & -Q \end{pmatrix} \begin{pmatrix} J_u'' & J_u''' & K' \\ -M_u & M_u' & -Q \end{pmatrix} \times \sum_{j_u j_u'} C^{j_u}_{J_u}(M_u)\, C^{j_u}_{J_u''}(M_u)\, C^{j_u'}_{J_u'}(M_u')\, C^{j_u'}_{J_u'''}(M_u') \frac{1}{1 + 2\pi \mathrm{i}\, \nu(j_u' M_u', j_u M_u)\,/\,A} \,, \quad \text{(A14.1)}$$

where we have used shorthand notations for the Bohr frequencies $\nu_{\beta LS}(jM, j'M')$ and the coefficients $C^j_J(\beta LS, M)$ defined in Eqs. (7.30) and (3.58), respectively, and for the Einstein coefficient $A(\beta_u L_u S \to \beta_\ell L_\ell S)$.

b) *Limitation on indices*

Owing to the presence of the 6-j and 3-j symbols, the indices are confined to the range

$$K, K' = \begin{cases} 0 & \text{if} \quad L_u = 0 \\ 0, 1, 2 & \text{if} \quad L_u \neq 0 \end{cases}$$

$$Q = 0, \pm 1, \pm 2 \qquad \text{with} \qquad |Q| \leq K, \quad |Q| \leq K' \,. \tag{A14.2}$$

c) *Symmetry*

Exchange of the dummy indices $J_u \rightleftarrows J''_u$, $J'_u \rightleftarrows J'''_u$ shows that

$$W_{KK'Q} = W_{K'KQ} \,. \tag{A14.3}$$

d) *Conjugation*

By exchanging the dummy indices $j_u \rightleftarrows j'_u$, $M_u \rightleftarrows M'_u$, $J_u \rightleftarrows J'_u$, $J''_u \rightleftarrows J'''_u$, and bearing in mind the reality of the C^j_J coefficients (Sect. 3.4), it can easily be proved, with the help of Eqs. (2.24) and (2.25), that

$$\left(W_{KK'Q}\right)^* = W_{KK'-Q} \,. \tag{A14.4}$$

e) *Special cases*

Use of Eqs. (2.26a), (2.36a), (3.62a,b) and (2.23a) shows that

$$W_{K00} = W_{0K0} = \delta_{K0} \,. \tag{A14.5}$$

From Eqs. (A14.2)-(A14.5) it follows that there are only 8 independent symbols, namely W_{000} $(= 1)$, W_{110}, W_{210}, W_{220}, W_{111}, W_{211}, W_{221}, W_{222}. The first four are real, the remaining are in general complex.

f) *Limit for zero magnetic field*

Under this limit we have

$$C^{j_u}_{J_u}(M_u) \to \delta_{j_u J_u} \,, \qquad \nu(j'_u M'_u, j_u M_u) \to \nu_{\beta_u L_u S J'_u, \beta_u L_u S J_u} \,,$$

the last quantity being defined in Eq. (7.43). Performing the summation over M_u and M'_u via Eq. (2.23a), one finds

$$\lim_{B \to 0} W_{KK'Q} = \delta_{KK'} \left[W_K(\beta_\ell L_\ell S \beta_u L_u)\right]_{\text{fs}} \,, \tag{A14.6}$$

where the symbol $[W_K(\beta_\ell L_\ell S \beta_u L_u)]_{\text{fs}}$ is defined in Eq. (10.133).

g) *Limit for strong magnetic field*

Let us assume that the field modulus B satisfies the inequalities

$$\mu_0 B \gg \zeta \,, \qquad \frac{\mu_0 B}{h} \gg A \,, \tag{A14.7}$$

or, equivalently

$$\gamma \gg 1 \,, \qquad \gamma\, x \gg 1 \,,$$

where γ and x are defined in Eqs. (10.154). It can be proved that under this limit

$$W_{KK'Q} = \delta_{KK'}\, \delta_{Q0}\; W_K(L_\ell, L_u) \,, \tag{A14.8}$$

where the symbol $W_K(L_\ell, L_u)$ is defined in Eq. (10.17). This property is at the basis of the anti-level-crossing effect described in Sect. 10.18.

The proof of Eq. (A14.8) is rather complicated. First of all, we notice that the first of inequalities (A14.7) implies that the upper term is in the complete Paschen-Back effect regime. It follows (see Sect. 3.4) that the energy eigenvectors of the upper term are of the form $|\beta_u L_u S M_{L_u} M_S\rangle$, hence the coefficients $C^{j_u}_{J_u}(M_u)$ defined in Eq. (3.58) reduce to Clebsh-Gordan coefficients. The magnetic quantum numbers are related by $M_{L_u} + M_S = M_u$, thus the index j_u can be identified with either M_{L_u} or M_S. Setting $j_u = M_S$ we can write, with the use of Eq. (2.22)

$$\begin{aligned} C^{j_u}_{J_u}(M_u) \equiv C^{M_S}_{J_u}(M_u) &= \langle L_u S J_u M_u | L_u S M_{L_u} M_S \rangle = \\ &= (-1)^{L_u - S + M_u} \sqrt{2J_u + 1} \begin{pmatrix} L_u & S & J_u \\ M_{L_u} & M_S & -M_u \end{pmatrix} . \end{aligned}$$

Substituting into Eq. (A14.1), and performing the summations over J_u and J''_u via Eq. (2.43), next the summations over J'_u and J'''_u via Eq. (2.23b), one obtains

$$\begin{aligned} W_{KK'Q} = \frac{3(2L_u+1)}{2S+1} \begin{Bmatrix} 1 & 1 & K \\ L_u & L_u & L_\ell \end{Bmatrix} \begin{Bmatrix} 1 & 1 & K' \\ L_u & L_u & L_\ell \end{Bmatrix} \sqrt{(2K+1)(2K'+1)} \\ \times (-1)^{K-K'} \sum_{M_u M'_u M_S} \begin{pmatrix} K & L_u & L_u \\ -Q & -M_{L_u} & M'_{L_u} \end{pmatrix} \begin{pmatrix} K' & L_u & L_u \\ -Q & -M_{L_u} & M'_{L_u} \end{pmatrix} \\ \times \frac{1}{1 + 2\pi \mathrm{i}\, \nu(M_S M'_u, M_S M_u)\,/\,A} \,, \end{aligned} \tag{A14.9}$$

where $M_{L_u} = M_u - M_S$, $M'_{L_u} = M'_u - M_S$.

On the other hand, in the complete Paschen-Back effect regime the Bohr frequency $\nu(M_S M'_u, M_S M_u)$ can be written in the form (see Sect. 3.4)

$$\nu(M_S M'_u, M_S M_u) = \frac{\mu_0 B}{h}(M'_u - M_u) + \epsilon(M_u, M'_u, M_S) \,,$$

where ϵ is a correction of order ζ/h due to fine structure. Taking into account inequalities (A14.7), it follows that

$$\frac{1}{1+2\pi\mathrm{i}\,\nu(M_S M'_u, M_S M_u)\,/\,A} \;=\; \delta_{M_u M'_u}\;,$$

which implies $M_{L_u} = M'_{L_u}$ and $Q = 0$. The triple summation in Eq. (A14.9) reduces to a double summation over M_u and M_S, or equivalently over M_{L_u} and M_S. The former can be performed via Eq. (2.23a), the latter yields a factor $(2S{+}1)$. Equation (A14.8) is thus proved.

A15. A Property of the Hopf Function

The Hopf function obeys the integral equation (cf. Eq. (12.24))

$$q(\tau) = \frac{1}{2}\,E_3(\tau) + \frac{1}{2}\int_0^\infty E_1\big(|t-\tau|\big)\;q(t)\;\mathrm{d}t\;, \tag{A15.1}$$

and satisfies the property (cf. Eq. (12.25))

$$\int_0^\infty E_2(\tau)\;q(\tau)\;\mathrm{d}\tau = \frac{1}{3}\;. \tag{A15.2}$$

Equation (A15.1) can be rewritten in the more explicit form

$$q(\tau) = \frac{1}{2}\,E_3(\tau) + \frac{1}{2}\int_0^\tau E_1(\tau-t)\;q(t)\;\mathrm{d}t \;+ \frac{1}{2}\int_\tau^\infty E_1(t-\tau)\;q(t)\;\mathrm{d}t\;,$$

or, performing the substitutions $(\tau - t) = u$ and $(t - \tau) = v$ in the first and second integral, respectively

$$q(\tau) = \frac{1}{2}\,E_3(\tau) + \frac{1}{2}\int_0^\tau E_1(u)\;q(\tau-u)\;\mathrm{d}u \;+ \frac{1}{2}\int_0^\infty E_1(v)\;q(\tau+v)\;\mathrm{d}v\;.$$

Let us consider the derivative of $q(\tau)$ with respect to τ. Recalling that

$$\frac{\mathrm{d}}{\mathrm{d}\tau}\,E_n(\tau) = -E_{n-1}(\tau)\;,$$

and denoting derivatives by apices, we have

$$\begin{aligned} q'(\tau) = &-\frac{1}{2}\,E_2(\tau) + \frac{1}{2}\,q(0)\,E_1(\tau) + \frac{1}{2}\int_0^\tau E_1(u)\;q'(\tau-u)\;\mathrm{d}u \\ &+ \frac{1}{2}\int_0^\infty E_1(v)\;q'(\tau+v)\;\mathrm{d}v\;, \end{aligned}$$

or, by means of the inverse transformations to those outlined above

$$q'(\tau) = -\frac{1}{2}\,E_2(\tau) + \frac{1}{2}\,q(0)\,E_1(\tau) + \frac{1}{2}\int_0^\infty E_1\big(|t-\tau|\big)\;q'(t)\;\mathrm{d}t\;. \tag{A15.3}$$

We now multiply both sides by $q(\tau)$ and integrate in $\mathrm{d}\tau$ between 0 and ∞,

$$\int_0^\infty q(\tau)\;q'(\tau)\;\mathrm{d}\tau = -\frac{1}{2}\,\mathcal{I}_1 \;+\; \frac{1}{2}\,q(0)\,\mathcal{I}_2 \;+\; \frac{1}{2}\,\mathcal{I}_3\;, \tag{A15.4}$$

where

$$\mathcal{I}_1 = \int_0^\infty E_2(\tau)\;q(\tau)\;\mathrm{d}\tau$$

$$\mathcal{I}_2 = \int_0^\infty E_1(\tau)\;q(\tau)\;\mathrm{d}\tau$$

$$\mathcal{I}_3 = \int_0^\infty \mathrm{d}\tau\;\;q(\tau)\;\int_0^\infty E_1\big(|t-\tau|\big)\;q'(t)\;\mathrm{d}t\;.$$

For the first integral we have from Eq. (A15.2)

$$\mathcal{I}_1 = \frac{1}{3}\;. \tag{A15.5}$$

For the second, evaluating Eq. (A15.1) at $\tau = 0$ and taking into account that $E_3(0) = 1/2$, we obtain

$$\mathcal{I}_2 = 2\,q(0) - \frac{1}{2}\;. \tag{A15.6}$$

For the third integral, reversing the order of the integrations we have

$$\mathcal{I}_3 = \int_0^\infty \mathrm{d}t\;\;q'(t)\;\int_0^\infty q(\tau)\;E_1\big(|t-\tau|\big)\;\mathrm{d}\tau = \int_0^\infty q'(t)\,\big[2q(t) - E_3(t)\big]\;\mathrm{d}t\;,$$

where Eq. (A15.1) has been used. On the other hand, using again Eq. (A15.2) we get

$$\int_0^\infty q'(t)\,E_3(t)\;\mathrm{d}t = -q(0)\,E_3(0) + \int_0^\infty q(t)\,E_2(t)\;\mathrm{d}t = -\frac{1}{2}\,q(0) + \frac{1}{3}\;,$$

thus

$$\mathcal{I}_3 = 2\int_0^\infty q(t)\,q'(t)\;\mathrm{d}t\;+\frac{1}{2}\,q(0) - \frac{1}{3}\;. \tag{A15.7}$$

Substitution of Eqs. (A15.5), (A15.6), and (A15.7) into Eq. (A15.4) yields

$$\int_0^\infty q(\tau)\, q'(\tau)\, \mathrm{d}\tau = \big[q(0)\big]^2 - \frac{1}{3} + \int_0^\infty q(\tau)\, q'(\tau)\, \mathrm{d}\tau \,,$$

whence

$$\big[q(0)\big]^2 = \frac{1}{3} \,.$$

Excluding the negative root which is physically meaningless (leading to a negative value for the surface source function, see Eqs. (12.20a) and (12.23)), one gets the final result

$$q(0) = \frac{1}{\sqrt{3}} \,.$$

A16. A Numerical Algorithm for the Solution of the Hopf Equation

Given the integral equation (see Eq. (12.24))

$$q(\tau) = \frac{1}{2}\, E_3(\tau) + \frac{1}{2} \int_0^\infty E_1\big(|t-\tau|\big)\, q(t)\, \mathrm{d}t \,,$$

we discretize it by selecting a grid of N τ-values τ_1, τ_2, …, τ_N, and we denote by q_1, q_2, …, q_N the unknown values taken by the function $q(\tau)$ at the various grid-points. We then calculate the integral appearing in the right-hand side by dividing the integration domain into $N+1$ intervals $(0, \tau_1)$, (τ_1, τ_2), …, (τ_{N-1}, τ_N), (τ_N, ∞), and by assuming the function $q(\tau)$ to be linear in τ in each interval, and to be constant ($= q_N$) in the last one. Taking into account the elementary formulae for the integration of the exponential integrals

$$\int_a^b E_n(\tau)\, \mathrm{d}\tau = E_{n+1}(a) - E_{n+1}(b)$$

$$\int_a^b E_n(\tau)\ \tau\, \mathrm{d}\tau = a\, E_{n+1}(a) - b\, E_{n+1}(b) + E_{n+2}(a) - E_{n+2}(b) \,,$$

we obtain after some algebra the following set of equations

$$\sum_{i=0}^{N-1} \frac{q_{i+1} - q_i}{\tau_{i+1} - \tau_i} \Big[E_3\big(|\tau_i - \tau_j|\big) - E_3\big(|\tau_{i+1} - \tau_j|\big) \Big] = q_0\, E_2(\tau_j) - E_3(\tau_j) \,,$$

where $j = 1, 2, \ldots, N$ and where (see Eq. (12.26))

$$\tau_0 = 0 \,, \qquad q_0 = \frac{1}{\sqrt{3}} \,.$$

This is a set of N linear equations in the N unknowns q_1, q_2, …, q_N that can be solved with standard numerical techniques – thus providing a numerical solution for the Hopf function $q(\tau)$.

The result presented in the text (Fig. 12.2) has been obtained with a grid of 1000 points equispaced in $\mathrm{Log}\,\tau$ between $\tau = 10^{-4}$ and $\tau = 10$.

A17. Symmetry Properties of the Comoving-Frame Radiation Field Tensor for a Cylindrically Symmetrical Atmosphere

For a given star, and for a given point P in its outer atmosphere, the radiation field tensor, defined in the comoving frame by Eq. (12.40), is a function of the velocity $\vec{v}$ of the frame itself. In this appendix we make a slight change of notations and explicitly attach such a functional dependence to the symbol J^K_Q, that is now written in the form

$$J^K_Q(\nu\,; v, \theta_v, \chi_v) \,,$$

where θ_v and χ_v are the angles defining the direction of $\vec{v}$ according to the geometry of Fig. 12.10.

If the radiation coming from the stellar surface is cylindrically symmetrical – in the star's frame – about the vertical axis through the point P, the radiation field tensor in the comoving frame satisfies a number of properties that are illustrated below.

a) The dependence on χ_v can be factored in the form

$$J^K_Q(\nu\,; v, \theta_v, \chi_v) = \mathrm{e}^{\,\mathrm{i}Q\chi_v}\; J^K_Q(\nu\,; v, \theta_v, 0) \,. \tag{A17.1}$$

This relation can be proved by considering the χ-dependence of the two factors $\mathcal{T}^K_Q(0, \vec{\Omega})$ and $I\big(\nu(1 + \vec{v}\cdot\vec{\Omega}/c), \vec{\Omega}\big)$ appearing in Eq. (12.40). From Table 5.6 it follows that

$$\mathcal{T}^K_Q(0, \vec{\Omega}) = f_{KQ}(\theta)\; \mathrm{e}^{\,\mathrm{i}Q\chi} \,, \tag{A17.2}$$

where f_{KQ} is a real function satisfying

$$f_{K,-Q}(\theta) = (-1)^Q\, f_{KQ}(\theta) \,. \tag{A17.3}$$

Moreover, because of the assumed cylindrical symmetry of the radiation field in the star's frame, we can write (see Eq. (12.43))

$$I\left(\nu\Big(1 + \frac{\vec{v}\cdot\vec{\Omega}}{c}\Big), \vec{\Omega}\right) = g\big(\nu, v, \theta, \theta_v, \cos(\chi - \chi_v)\big) \,, \tag{A17.4}$$

where g is another real function that doesn't need to be specified. Substitution of Eqs. (A17.2) and (A17.4) into Eq. (12.40) yields

$$J_Q^K(\nu\,;v,\theta_v,\chi_v) = \frac{1}{4\pi}\int_0^\gamma \mathrm{d}\theta\ \sin\theta\ f_{KQ}(\theta) \times \int_0^{2\pi} g\big(\nu,v,\theta,\theta_v,\cos(\chi-\chi_v)\big)\ \mathrm{e}^{\,\mathrm{i}Q\chi}\ \mathrm{d}\chi\ , \tag{A17.5}$$

where the angle γ is defined in Eq. (12.32). Performing in the last integral the substitution $(\chi-\chi_v)=\chi'$, one easily obtains the property in Eq. (A17.1).

b) All the components of the tensor $J_Q^K(\nu\,;v,\theta_v,0)$ are real, and satisfy the relation

$$J_{-Q}^K(\nu\,;v,\theta_v,0) = (-1)^Q\ J_Q^K(\nu\,;v,\theta_v,0)\ . \tag{A17.6}$$

In fact, Eq. (A17.5) shows that the imaginary components of $J_Q^K(\nu\,;v,\theta_v,0)$ are zero, because both f_{KQ} and g are real, and g is an even function of χ in the interval $(0,2\pi)$ whereas $\sin(Q\chi)$ is odd. The real components of $J_Q^K(\nu\,;v,\theta_v,0)$ have the form

$$J_Q^K(\nu\,;v,\theta_v,0) = \frac{1}{4\pi}\int_0^\gamma \mathrm{d}\theta\ \sin\theta\ f_{KQ}(\theta) \int_0^{2\pi} g(\nu,v,\theta,\theta_v,\cos\chi)\ \cos(Q\chi)\ \mathrm{d}\chi\ ,$$

which entails, because of Eq. (A17.3), the property in Eq. (A17.6).

c) If the spectrum of the radiation coming from the stellar surface is 'locally' symmetrical about a particular frequency ν_0 in the star's frame (as in the case of an absorption or emission line), namely if

$$I(\nu_0-\Delta\nu,\vec{\Omega}) = I(\nu_0+\Delta\nu,\vec{\Omega}) \tag{A17.7}$$

for any direction $\vec{\Omega}$, then

$$J_Q^K(\nu_0-\Delta\nu\,;v,\pi-\theta_v,\pi+\chi_v) = J_Q^K(\nu_0+\Delta\nu\,;v,\theta_v,\chi_v)\ , \tag{A17.8}$$

and, in particular

$$J_Q^K(\nu_0\,;v,\pi-\theta_v,\pi+\chi_v) = J_Q^K(\nu_0\,;v,\theta_v,\chi_v)\ . \tag{A17.9}$$

This property can easily be proved by observing that the transformation

$$\theta_v \to \pi-\theta_v\ , \qquad \chi_v \to \pi+\chi_v$$

implies $\vec{v} \to -\vec{v}$. From Eq. (12.40) one has

$$J_Q^K(\nu_0 - \Delta\nu\,; v, \pi - \theta_v, \pi + \chi_v) = \oint \frac{\mathrm{d}\Omega}{4\pi}\, \mathcal{T}_Q^K(0, \vec{\Omega})\; I\Big(\big(\nu_0 - \Delta\nu\big)\Big(1 - \frac{\vec{v}\cdot\vec{\Omega}}{c}\Big), \vec{\Omega}\Big)\ .$$

Neglecting the 'second-order' term $\Delta\nu\ (\vec{v}\cdot\vec{\Omega})/c$ and taking into account the assumption in Eq. (A17.7), the integrand can be transformed via the substitution

$$I\Big(\big(\nu_0 - \Delta\nu\big)\Big(1 - \frac{\vec{v}\cdot\vec{\Omega}}{c}\Big), \vec{\Omega}\Big) = I\Big(\big(\nu_0 + \Delta\nu\big)\Big(1 + \frac{\vec{v}\cdot\vec{\Omega}}{c}\Big), \vec{\Omega}\Big)\ ,$$

which shows, recalling again Eq. (12.40), the validity of Eq. (A17.8).

d) When the condition expressed by Eq. (A17.7) is satisfied, the comoving-frame radiation field tensor obeys the further relation

$$J_Q^K(\nu_0\,; v, \pi - \theta_v, \chi_v) = J_Q^K(\nu_0\,; v, \theta_v, \chi_v - \pi) = (-1)^Q\ J_Q^K(\nu_0\,; v, \theta_v, \chi_v)\ ,$$

which follows from Eqs. (A17.9) and (A17.1).

A18. Redistribution Matrix for a Maxwellian Distribution of Velocities

In Eq. (13.35) we suppose that the velocity distribution is Maxwellian, so that

$$f(\vec{v})\ \mathrm{d}^3\vec{v} = f_\mathrm{c}(v_x)\ f_\mathrm{c}(v_y)\ f_\mathrm{c}(v_z)\ \mathrm{d}v_x\ \mathrm{d}v_y\ \mathrm{d}v_z\ ,$$

where (xyz) is an arbitrary reference system and where

$$f_\mathrm{c}(v) = \frac{1}{\sqrt{\pi}}\ \frac{1}{v_\mathrm{T}}\ \mathrm{e}^{-\left(\frac{v}{v_\mathrm{T}}\right)^2}\ ,$$

v_T being the thermal velocity.

We now choose the reference system in such a way that the x-y plane coincides with the plane containing the two unit vectors $\vec{\Omega}$ and $\vec{\Omega}'$, with the x-axis directed along $\vec{\Omega}'$. If Θ is the angle between the two unit vectors, we have

$$\begin{aligned}\vec{v}\cdot\vec{\Omega}' &= v_x\\ \vec{v}\cdot\vec{\Omega} &= \cos\Theta\ v_x + \sin\Theta\ v_y\ .\end{aligned}$$

Substituting into Eq. (13.35), the integrals over v_z and v_x can be easily performed. Introducing the Doppler width in frequency units, $\Delta\nu_\mathrm{D} = \nu_0\, v_\mathrm{T}/c$ (see Eqs. (5.43)), one gets

$$R_{ij}(\nu,\vec{\Omega}\,;\nu',\vec{\Omega}') = P_{ij}(\vec{\Omega},\vec{\Omega}')\ \frac{1}{\pi\, v_{\rm T}\, \Delta\nu_{\rm D}}\ \mathrm{e}^{-\left(\frac{\nu'-\nu_0}{\Delta\nu_{\rm D}}\right)^2}$$

$$\times \int_{-\infty}^{\infty} \mathrm{d}v_y\ \mathrm{e}^{-\left(\frac{v_y}{v_{\rm T}}\right)^2}\ \delta\Big(\nu_0 - \nu + (\nu'-\nu_0)\cos\Theta + \frac{\nu_0}{c}\sin\Theta\ v_y\Big)\,,$$

whence it immediately follows, for $\Theta \neq 0$

$$R_{ij}(\nu,\vec{\Omega}\,;\nu',\vec{\Omega}') =$$

$$= P_{ij}(\vec{\Omega},\vec{\Omega}')\ \frac{1}{\pi\,\Delta\nu_{\rm D}^2\,\sin\Theta}\ \mathrm{e}^{-\left(\frac{\nu'-\nu_0}{\Delta\nu_{\rm D}}\right)^2}\ \mathrm{e}^{-\left[\frac{\nu-\nu_0}{\Delta\nu_{\rm D}\sin\Theta} - \frac{\nu'-\nu_0}{\Delta\nu_{\rm D}\tan\Theta}\right]^2}\,, \qquad \text{(A18.1)}$$

and for $\Theta = 0$

$$R_{ij}(\nu,\vec{\Omega}\,;\nu',\vec{\Omega}') = P_{ij}(\vec{\Omega},\vec{\Omega}')\ \frac{1}{\sqrt{\pi}}\ \frac{1}{\Delta\nu_{\rm D}}\ \mathrm{e}^{-\left(\frac{\nu'-\nu_0}{\Delta\nu_{\rm D}}\right)^2}\ \delta(\nu'-\nu)\,. \qquad \text{(A18.2)}$$

This redistribution function is nothing but the generalization to polarized radiation of the function $R_{\rm I}$ introduced by Hummer (1962).

A19. Properties of the Kernel $\mathcal{K}^K_{QQ'}(R_B)$

The kernel $\mathcal{K}^K_{QQ'}(R_B)$ is defined in Eq. (14.3),

$$\mathcal{K}^K_{QQ'}(R_B) = \sum_{Q''} \mathcal{D}^K_{Q''Q}(R_B)^*\ Q''\ \mathcal{D}^K_{Q''Q'}(R_B)\,, \qquad \text{(A19.1)}$$

where R_B is the rotation of Eq. (14.4)

$$R_B \equiv (-\gamma_B, -\theta_B, -\chi_B)\,.$$

Use of Eq. (2.68) shows that $\mathcal{K}^K_{QQ'}(R_B)$ is independent of the angle γ_B.

As proved in Sect. 10.8 (see Eq. (10.74)), Eq. (A19.1) can be rewritten in a simpler form, involving a single rotation matrix

$$\mathcal{K}^K_{QQ'}(R_B) = \sqrt{K(K+1)(2K+1)}\ (-1)^{K-Q'} \begin{pmatrix} K & K & 1 \\ Q & -Q' & q \end{pmatrix} \mathcal{D}^1_{0q}(R_B)\,. \qquad \text{(A19.2)}$$

This shows that the kernel $\mathcal{K}^0_{00}(R_B)$ is zero, and that the only non-zero components are those connecting Q-values such that $\Delta Q \equiv Q - Q' = 0, \pm 1$.

It can easily be seen, with the help of Eqs. (2.24), (2.25), and (2.73), that $\mathcal{K}^K_{QQ'}(R_B)$ satisfies the symmetry properties

$$\mathcal{K}^K_{Q'Q}(R_B) = \mathcal{K}^K_{QQ'}(R_B)^*$$

$$\mathcal{K}^K_{-Q-Q'}(R_B) = (-1)^{2K+1+Q+Q'}\, \mathcal{K}^K_{Q'Q}(R_B)\ .$$

Explicit expressions for the components with $K = 1$ and $K = 2$ can be obtained from Eq. (A19.2) using Eqs. (2.68), (2.70), (2.26), and the algebraic formulae for the reduced rotation matrices given in Table 2.1. The non-zero components are the following

$$\mathcal{K}^1_{-1-1} = -\mathcal{K}^1_{11} = -\cos\theta_B$$
$$\mathcal{K}^1_{-10} = (\mathcal{K}^1_{0-1})^* = (\mathcal{K}^1_{10})^* = \mathcal{K}^1_{01} = \frac{1}{\sqrt{2}}\ \sin\theta_B\ \mathrm{e}^{\mathrm{i}\chi_B}$$

$$\mathcal{K}^2_{-2-2} = -\mathcal{K}^2_{22} = -2\cos\theta_B$$
$$\mathcal{K}^2_{-2-1} = (\mathcal{K}^2_{-1-2})^* = (\mathcal{K}^2_{21})^* = \mathcal{K}^2_{12} = \sin\theta_B\ \mathrm{e}^{\mathrm{i}\chi_B}$$
$$\mathcal{K}^2_{-1-1} = -\mathcal{K}^2_{11} = -\cos\theta_B$$
$$\mathcal{K}^2_{-10} = (\mathcal{K}^2_{0-1})^* = (\mathcal{K}^2_{10})^* = \mathcal{K}^2_{01} = \sqrt{\frac{3}{2}}\ \sin\theta_B\ \mathrm{e}^{\mathrm{i}\chi_B}\ .$$

A20. The Multipole Coupling Coefficients

The multipole coupling coefficients are defined by Eq. (14.24),

$$G_{KQ,K'Q'}(\vec{x},\vec{x}') = \int_{-\infty}^{\infty} \mathrm{d}\nu\ \left[p(\nu_0-\nu)\right]^2\ \mathrm{e}^{-\tau_\nu(\vec{x},\vec{x}')}$$
$$\times\ w^{(K)}_{J_u J_\ell}\ w^{(K')}_{J_u J_\ell}\ \sum_{i=0}^{3}\ (-1)^Q\ \mathcal{T}^K_{-Q}(i,\vec{\Omega})\,\mathcal{T}^{K'}_{Q'}(i,\vec{\Omega})\ , \quad \text{(A20.1)}$$

where the symbol $w^{(K)}_{J_u J_\ell}$ is given by Eq. (10.11), the tensor $\mathcal{T}^K_Q(i,\vec{\Omega})$ – given by Eq. (5.134) – is defined in the system Σ of Fig. 14.4, the unit vector $\vec{\Omega}$ is given by $(\vec{x}-\vec{x}')/|\vec{x}-\vec{x}'|$, $p(\nu_0-\nu)$ is the Gaussian profile of Eq. (14.6), and $\tau_\nu(\vec{x},\vec{x}')$ is the optical thickness at frequency ν between points $\vec{x}$ and $\vec{x}'$ (see Eq. (14.17)).

Since $\mathcal{T}^K_Q(i,\vec{\Omega})$ is defined for $K = 0, 1, 2$ and, for a fixed K, for $Q = -K, \ldots, K$, it follows that there are in principle 81 different multipole coupling coefficients satisfying the limitations

$$\begin{cases} K = 0,1,2 \\ Q = -K,\ldots,K \end{cases} \qquad \begin{cases} K' = 0,1,2 \\ Q' = -K',\ldots,K'\ . \end{cases}$$

However, the number of non-zero, independent quantities is much smaller, as it will be shown in the following. Moreover, for special values of J_u this number can further decrease because of the presence of the symbol $w^{(K)}_{J_u J_\ell}$. For $J_u = 0$, for instance, only the symbol $G_{00,00}$ is non-zero, whereas for $J_u = 1/2$ the indices K and K' run only on the values 0 and 1.

To study the properties of the multipole coupling coefficients it is convenient to rewrite Eq. (A20.1) in the form

$$G_{KQ,K'Q'}(\vec{x},\vec{x}\,') = \int_{-\infty}^{\infty} \mathrm{d}\nu \, \left[p(\nu_0-\nu)\right]^2 \, \mathrm{e}^{-\tau_\nu(\vec{x},\vec{x}')} \times w^{(K)}_{J_u J_\ell} \, w^{(K')}_{J_u J_\ell} \, \mathit{\Gamma}_{KQ,K'Q'}(\vec{\Omega}) \, , \tag{A20.2}$$

where

$$\mathit{\Gamma}_{KQ,K'Q'}(\vec{\Omega}) = \sum_{i=0}^{3} \, (-1)^Q \, \mathcal{T}^K_{-Q}(i,\vec{\Omega}) \, \mathcal{T}^{K'}_{Q'}(i,\vec{\Omega}) \, .$$

From the conjugation property of the tensor $\mathcal{T}^K_Q(i,\vec{\Omega})$ – see Eqs. (5.158) – it follows

$$\mathit{\Gamma}_{K'Q',KQ}(\vec{\Omega}) = \mathit{\Gamma}_{KQ,K'Q'}(\vec{\Omega})^* \tag{A20.3}$$

and

$$\mathit{\Gamma}_{K-Q,K'-Q'}(\vec{\Omega}) = (-1)^{Q+Q'} \, \mathit{\Gamma}_{KQ,K'Q'}(\vec{\Omega})^* \, . \tag{A20.4}$$

Obviously, similar relations hold for the multipole coupling coefficients,

$$G_{K'Q',KQ}(\vec{x},\vec{x}\,') = G_{KQ,K'Q'}(\vec{x},\vec{x}\,')^* \tag{A20.5}$$

and

$$G_{K-Q,K'-Q'}(\vec{x},\vec{x}\,') = (-1)^{Q+Q'} \, G_{KQ,K'Q'}(\vec{x},\vec{x}\,')^* \, . \tag{A20.6}$$

The quantity $\mathit{\Gamma}_{KQ,K'Q'}(\vec{\Omega})$ can be expressed in terms of rotation matrices using Eq. (5.159)

$$\mathit{\Gamma}_{KQ,K'Q'}(\vec{\Omega}) = (-1)^Q \, \sum_{i=0}^{3} \sum_{PP'} \, t^K_P(i) \, \mathcal{D}^K_{P-Q}(R) \; t^{K'}_{P'}(i) \, \mathcal{D}^{K'}_{P'Q'}(R) \, , \tag{A20.7}$$

where $R \equiv (-\gamma,-\theta,-\chi)$ is the rotation carrying the system $(\vec{e}_a(\vec{\Omega}),\vec{e}_b(\vec{\Omega}),\vec{\Omega})$ into the system Σ where the multipole coupling coefficients are defined (see Fig. 14.4). On the other hand, Eqs. (5.162) and (5.161) yield

$$\sum_{i=0}^{3} \, t^K_P(i) \, t^{K'}_{P'}(i) = (-1)^{K+K'} \, \sum_{i=0}^{3} \, \xi_i^2 \, t^K_P(i) \, t^{K'}_{P'}(i) = (-1)^{K+K'} \, \sum_{i=0}^{3} \, t^K_P(i) \, t^{K'}_{P'}(i) \, ,$$

which implies

$$\mathit{\Gamma}_{KQ,K'Q'}(\vec{\Omega}) = (-1)^{K+K'}\mathit{\Gamma}_{KQ,K'Q'}(\vec{\Omega})$$

and

$$G_{KQ,K'Q'}(\vec{x},\vec{x}') = (-1)^{K+K'}\,G_{KQ,K'Q'}(\vec{x},\vec{x}')\,. \tag{A20.8}$$

As a consequence, the quantities $\mathit{\Gamma}_{KQ,K'Q'}(\vec{\Omega})$ and $G_{KQ,K'Q'}(\vec{x},\vec{x}')$ vanish unless K and K' are both even or both odd. This reduces the number of non-zero components from 81 to 45. Taking into account the symmetry properties (A20.3) and (A20.4), it can easily be seen that the number of non-zero, independent components is 17.

Equation (A20.7) can be simplified via the following transformations. First we express the coefficients $t_P^K(i)$ in terms of the Pauli spin matrices $\hat{\boldsymbol{\sigma}}_i$ defined in Eq. (5.128). Using Eq. (5.160) we have

$$\sum_{i=0}^{3} t_P^K(i)\,t_{P'}^{K'}(i) = \frac{3}{4}\sqrt{(2K+1)(2K'+1)} \times \sum_{i=0}^{3}\sum_{\alpha\beta\gamma\delta=\pm1} (\hat{\sigma}_i)_{\alpha\beta}\,(\hat{\sigma}_i)_{\gamma\delta} \begin{pmatrix} 1 & 1 & K \\ \beta & -\alpha & -P \end{pmatrix}\begin{pmatrix} 1 & 1 & K' \\ \delta & -\gamma & -P' \end{pmatrix},$$

where the rows and columns of $\hat{\boldsymbol{\sigma}}_i$ are labelled as in Eqs. (5.129). Using Eq. (8.64) we get[1]

$$\sum_{i=0}^{3} t_P^K(i)\,t_{P'}^{K'}(i) = \frac{3}{2}\sqrt{(2K+1)(2K'+1)} \times \sum_{\alpha\beta=\pm1} \begin{pmatrix} 1 & 1 & K \\ \beta & -\alpha & -P \end{pmatrix}\begin{pmatrix} 1 & 1 & K' \\ \alpha & -\beta & -P' \end{pmatrix}. \tag{A20.9}$$

This equation shows that $P' = -P$ and that the only allowed values for P and P' are 0 and ±2. Substitution of Eq. (A20.9) into Eq. (A20.7) and use of Eq. (2.75) yields

$$\mathit{\Gamma}_{KQ,K'Q'}(\vec{\Omega}) = (-1)^Q\ \frac{3}{2}\sqrt{(2K+1)(2K'+1)} \times \sum_{\alpha\beta=\pm1}\sum_{PP'}\sum_{K''} (2K''+1) \begin{pmatrix} 1 & 1 & K \\ \beta & -\alpha & -P \end{pmatrix}\begin{pmatrix} 1 & 1 & K' \\ \alpha & -\beta & -P' \end{pmatrix} \times \begin{pmatrix} K & K' & K'' \\ P & P' & S \end{pmatrix}\begin{pmatrix} K & K' & K'' \\ -Q & Q' & S' \end{pmatrix} \mathcal{D}_{SS'}^{K''}(R)^*\,.$$

The sums over α and β cannot be performed by standard sum rules of Racah algebra because the 'components' α and β run on the values ±1 but not on the

[1] We recall that Eq. (8.64) is valid for any representation of the Pauli spin matrices.

value 0. To overcome this difficulty, we multiply the right-hand side by the quantity $\alpha^2\beta^2$ which, using Eq. (3.52), can be written as

$$\alpha^2\beta^2 = (-1)^{\alpha-\beta}\ 36 \sum_{ff'} (2f+1)(2f'+1) \begin{Bmatrix} 1 & 1 & f \\ 1 & 1 & 1 \end{Bmatrix} \begin{Bmatrix} 1 & 1 & f' \\ 1 & 1 & 1 \end{Bmatrix} \times \begin{pmatrix} 1 & 1 & f \\ 0 & 0 & 0 \end{pmatrix} \begin{pmatrix} 1 & 1 & f' \\ 0 & 0 & 0 \end{pmatrix} \begin{pmatrix} 1 & 1 & f \\ \alpha & -\alpha & 0 \end{pmatrix} \begin{pmatrix} 1 & 1 & f' \\ \beta & -\beta & 0 \end{pmatrix}.$$

Now the sum can be extended to the values $\alpha = 0$ and $\beta = 0$, and the summation over the indices α, β, P, P' can be carried out with the help of Eq. (2.52). Changing the index K'' into f'', and using Eq. (2.73), we obtain the expression

$$\begin{aligned} \Gamma_{KQ,K'Q'}(\vec{\Omega}) = (-1)^{K'+Q'}\ & 54\sqrt{(2K+1)(2K'+1)} \\ & \times \sum_{ff'f''} (2f+1)(2f'+1)(2f''+1) \begin{pmatrix} 1 & 1 & f \\ 0 & 0 & 0 \end{pmatrix} \begin{pmatrix} 1 & 1 & f' \\ 0 & 0 & 0 \end{pmatrix} \\ & \times \begin{pmatrix} f & f' & f'' \\ 0 & 0 & 0 \end{pmatrix} \begin{pmatrix} K & K' & f'' \\ -Q & Q' & Q-Q' \end{pmatrix} \begin{Bmatrix} 1 & 1 & f \\ 1 & 1 & 1 \end{Bmatrix} \\ & \times \begin{Bmatrix} 1 & 1 & f' \\ 1 & 1 & 1 \end{Bmatrix} \begin{Bmatrix} f & f' & f'' \\ 1 & 1 & K \\ 1 & 1 & K' \end{Bmatrix} \mathcal{D}^{f''}_{0,Q'-Q}(R)\,. \end{aligned} \qquad \text{(A20.10)}$$

It should be noticed that, owing to the symmetry properties of the 3-j symbols, the sum over f, f', f'' is in fact restricted to even values, thus it contains 6 terms at most, corresponding respectively to the following triplets (f, f', f''): $(0,0,0)$, $(0,2,2)$, $(2,0,2)$, $(2,2,0)$, $(2,2,2)$, and $(2,2,4)$. According to the values of K and K', some of these terms can however be zero. If, for instance, K and K' are both zero, it follows that $f'' = 0$ and the sum contains only two terms.

The explicit expressions of the non-zero Γ's can be found from Eq. (A20.10) by evaluating the various 3-j, 6-j, and 9-j symbols and by using the analytical formulae for the rotation matrices (Eqs. (2.68) and Table 2.1). The results – that depend on the angles θ and χ specifying the direction $\vec{\Omega}$ but are obviously independent of the angle γ – are the following

$$\Gamma_{00,00}(\vec{\Omega}) = 1$$

$$\Gamma_{00,20}(\vec{\Omega}) = \tfrac{1}{2\sqrt{2}}\,(3\cos^2\theta - 1)$$

$$\Gamma_{00,21}(\vec{\Omega}) = -\tfrac{\sqrt{3}}{2}\,\sin\theta\cos\theta\,\mathrm{e}^{\,\mathrm{i}\chi}$$

$$\Gamma_{00,22}(\vec{\Omega}) = \tfrac{\sqrt{3}}{4}\,\sin^2\theta\,\mathrm{e}^{\,2\mathrm{i}\chi}$$

$$\Gamma_{20,20}(\vec{\Omega}) = \tfrac{1}{4}\,(5 - 12\cos^2\theta + 9\cos^4\theta)$$

$$\Gamma_{20,21}(\vec{\Omega}) = \tfrac{1}{2}\sqrt{\tfrac{3}{2}}\,\sin\theta\cos\theta\,(2 - 3\cos^2\theta)\,\mathrm{e}^{\,\mathrm{i}\chi}$$

$$\Gamma_{20,22}(\vec{\Omega}) = \tfrac{1}{4}\sqrt{\tfrac{3}{2}}\,\sin^2\theta\,(1 + 3\cos^2\theta)\,\mathrm{e}^{\,2\mathrm{i}\chi}$$

$$\Gamma_{21,2-2}(\vec{\Omega}) = -\tfrac{3}{4}\,\sin^3\theta\cos\theta\,\mathrm{e}^{\,-3\mathrm{i}\chi}$$

$$\Gamma_{21,2-1}(\vec{\Omega}) = \tfrac{3}{4}\,\sin^2\theta\,(1 - 2\cos^2\theta)\,\mathrm{e}^{\,-2\mathrm{i}\chi}$$

$$\Gamma_{10,10}(\vec{\Omega}) = \tfrac{3}{2}\,\cos^2\theta \qquad \Gamma_{21,21}(\vec{\Omega}) = \tfrac{3}{4}\,\sin^2\theta\,(1+2\cos^2\theta)$$

$$\Gamma_{10,11}(\vec{\Omega}) = -\tfrac{3}{2\sqrt{2}}\,\sin\theta\cos\theta\,\mathrm{e}^{\,\mathrm{i}\chi} \qquad \Gamma_{21,22}(\vec{\Omega}) = \tfrac{3}{4}\,\sin\theta\cos\theta\,(1+\cos^2\theta)\,\mathrm{e}^{\,\mathrm{i}\chi}$$

$$\Gamma_{11,1-1}(\vec{\Omega}) = -\tfrac{3}{4}\,\sin^2\theta\,\mathrm{e}^{-2\mathrm{i}\chi} \qquad \Gamma_{22,2-2}(\vec{\Omega}) = \tfrac{3}{8}\,\sin^4\theta\,\mathrm{e}^{-4\mathrm{i}\chi}$$

$$\Gamma_{11,11}(\vec{\Omega}) = \tfrac{3}{4}\,\sin^2\theta \qquad \Gamma_{22,22}(\vec{\Omega}) = \tfrac{3}{8}\,(1+\cos^2\theta)^2\ . \qquad \text{(A20.11)}$$

The remaining Γ's can easily be deduced from the symmetry properties (A20.3) and (A20.4). The multipole coupling coefficients for a given transition (J_ℓ, J_u) are then obtained from Eq. (A20.2).[1]

A remarkable property of the quantities $\Gamma_{KQ,K'Q'}(\vec{\Omega})$ is their invariance under inversion of the direction $\vec{\Omega}$,

$$\Gamma_{KQ,K'Q'}(-\vec{\Omega}) = \Gamma_{KQ,K'Q'}(\vec{\Omega})\ . \qquad \text{(A20.12)}$$

To prove this relation, we recall that the rotation appearing in Eq. (A20.10) carries the reference system $(\vec{e}_a(\vec{\Omega}), \vec{e}_b(\vec{\Omega}), \vec{\Omega})$ into the system Σ of Fig. 14.4,

$$R \equiv (-\gamma, -\theta, -\chi)\ .$$

The rotation carrying $(\vec{e}_a(-\vec{\Omega}), \vec{e}_b(-\vec{\Omega}), -\vec{\Omega})$ into Σ is

$$R' \equiv (-\gamma', -(\pi-\theta), -(\pi+\chi))\ ,$$

where the angle γ' specifies the direction of the unit vector $\vec{e}_a(-\vec{\Omega})$ in the plane perpendicular to $\vec{\Omega}$. Thus the rotation matrix appearing in the expression of $\Gamma_{KQ,K'Q'}(-\vec{\Omega})$ is

$$\mathcal{D}^{f''}_{0,Q'-Q}(R') \;=\; \mathrm{e}^{\,\mathrm{i}(\pi+\chi)(Q'-Q)}\; d^{f''}_{0,Q'-Q}(\theta-\pi) \;=\; (-1)^{f''}\,\mathcal{D}^{f''}_{0,Q'-Q}(R)\ ,$$

where Eqs. (2.68) and (2.70) have been used. But the summation in Eq. (A20.10) is limited to even values of the index f'', so Eq. (A20.12) is proved. In fact, it can easily be checked that the analytical expressions of Eqs. (A20.11) are invariant under the transformation $\theta \to \pi - \theta$, $\chi \to \pi + \chi$.

Since the optical thickness $\tau_\nu(\vec{x}, \vec{x}')$ is invariant under exchange of $\vec{x}$ and $\vec{x}'$,

$$\tau_\nu(\vec{x}', \vec{x}) = \tau_\nu(\vec{x}, \vec{x}')\ ,$$

it follows from Eqs. (A20.2) and (A20.12) that the multipole coupling coefficients satisfy the important relation

$$G_{KQ,K'Q'}(\vec{x}', \vec{x}) = G_{KQ,K'Q'}(\vec{x}, \vec{x}')\ .$$

[1] Note that Eq. (A20.10) implies that the components $\Gamma_{KQ,K'Q}(\vec{\Omega})$ and $G_{KQ,K'Q}(\vec{x}, \vec{x}')$ are real.

Finally, from Eq. (A20.10) one can easily evaluate the solid-angle average of the quantity $\Gamma_{KQ,K'Q'}(\vec{\Omega})$, defined by

$$\left\langle \Gamma_{KQ,K'Q'}(\vec{\Omega}) \right\rangle = \frac{1}{4\pi} \oint \mathrm{d}\Omega \ \Gamma_{KQ,K'Q'}(\vec{\Omega}) \ .$$

Since $\mathcal{D}^0_{00}(\alpha\beta\gamma) = 1$, we obtain from the Weyl theorem (Eq. (2.76))

$$\int_0^{2\pi} \mathrm{d}\gamma \int_0^{\pi} \mathrm{d}\beta \ \sin\beta \ \mathcal{D}^J_{0N}(\alpha\beta\gamma) = 4\pi \ \delta_{J0} \, \delta_{N0} \ ,$$

whence, using Eqs. (2.68) and (2.70)

$$\frac{1}{4\pi} \oint \mathrm{d}\Omega \ \mathcal{D}^{f''}_{0,Q'-Q}(-\gamma - \theta - \chi) = \delta_{f''0} \ \delta_{QQ'} \ .$$

Substitution into Eq. (A20.10) yields, with the help of Eqs. (2.26a) and (2.49)

$$\left\langle \Gamma_{KQ,K'Q'}(\vec{\Omega}) \right\rangle = \delta_{KK'} \, \delta_{QQ'} \ (-1)^K \ 54 \times \sum_{f=0,2} (2f+1) \begin{pmatrix} 1 & 1 & f \\ 0 & 0 & 0 \end{pmatrix}^2 \begin{Bmatrix} 1 & 1 & f \\ 1 & 1 & 1 \end{Bmatrix}^2 \begin{Bmatrix} 1 & 1 & K \\ 1 & 1 & f \end{Bmatrix} ,$$

and evaluating the relevant 3-j and 6-j symbols (Eqs. (2.26a,f), (2.36a,f))

$$\left\langle \Gamma_{KQ,K'Q'}(\vec{\Omega}) \right\rangle = \delta_{KK'} \, \delta_{QQ'} \left[\frac{2}{3} + (-1)^K \begin{Bmatrix} 1 & 1 & K \\ 1 & 1 & 2 \end{Bmatrix} \right] ,$$

or, explicitly (Eqs. (2.36a,d,h))

$$\left\langle \Gamma_{00,00}(\vec{\Omega}) \right\rangle = 1$$

$$\left\langle \Gamma_{1Q,1Q}(\vec{\Omega}) \right\rangle = \frac{1}{2} \qquad (Q = 0, \pm 1)$$

$$\left\langle \Gamma_{2Q,2Q}(\vec{\Omega}) \right\rangle = \frac{7}{10} \qquad (Q = 0, \pm 1, \pm 2) \ .$$

A21. The Calculation of a Double Integral

The integral to be calculated is the following (see Eq. (14.26))

$$\mathcal{I} = \int_{-\infty}^{\infty} \mathrm{d}x' \int_{-\infty}^{\infty} \mathrm{d}y' \ \frac{\Delta\nu_{\mathrm{D}}}{4\pi(\vec{x} - \vec{x}\,')^2} \ G_{KQ,K'Q'}(\vec{x}, \vec{x}\,') \ , \tag{A21.1}$$

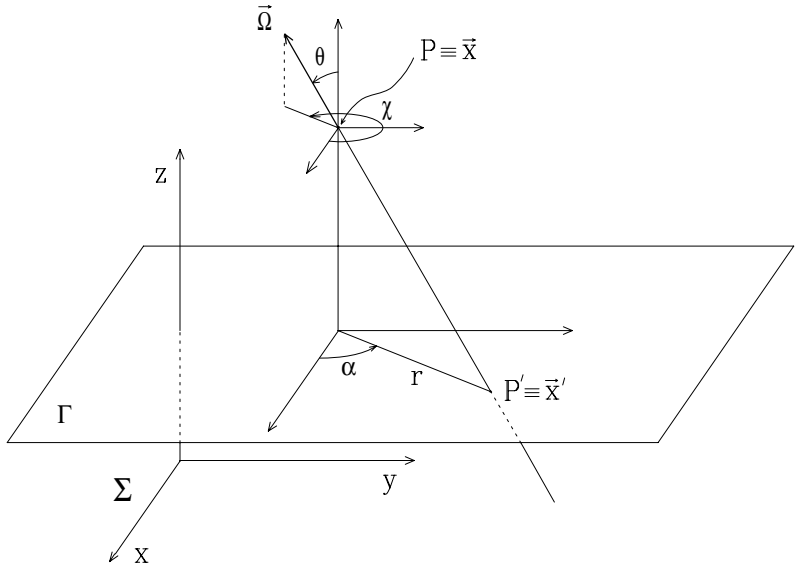

Fig.A21.1. In the reference system Σ we consider a fixed point P located at height z corresponding to line optical depth $t_{\rm L}$. The point P$'$ lies on the plane Γ parallel to the x-y plane; its height is z' corresponding to line optical depth $t'_{\rm L}$. The cylindrical coordinates (r, α) define the position of P$'$ in the plane Γ. The angles θ and χ specify the direction $\vec{\Omega}$.

where $G_{KQ,K'Q'}(\vec{x}, \vec{x}\,')$ is defined in Eq. (14.24), $\Delta\nu_{\rm D}$ is a constant (representing the Doppler broadening of the absorption profile), and the geometry is illustrated in Fig. A21.1 (for the case $t'_{\rm L} > t_{\rm L}$ or $z' < z$). Introducing the cylindrical coordinates r and α of the point P$'$, one has

$$\mathrm{d}x'\,\mathrm{d}y' = r\,\mathrm{d}r\,\mathrm{d}\alpha\ .$$

On the other hand

$$(\vec{x} - \vec{x}\,')^2 = (z - z')^2 + r^2\ ,$$

and

$$r = (z - z')\tan\theta\ , \qquad \mathrm{d}r = \frac{z - z'}{\cos^2\theta}\,\mathrm{d}\theta\ .$$

From these relations we get

$$\frac{\mathrm{d}x'\,\mathrm{d}y'}{(\vec{x} - \vec{x}\,')^2} \;=\; \tan\theta\;\mathrm{d}\theta\,\mathrm{d}\alpha\ ,$$

and since $\chi = \alpha + \pi$, the double integral over x' and y' can be transformed into an integral over the angles θ and χ specifying the direction $\vec{\Omega}$,

$$\mathcal{I} = \frac{\Delta\nu_{\rm D}}{4\pi} \int_0^{2\pi} \mathrm{d}\chi \int_0^{\pi/2} \mathrm{d}\theta\ \ \tan\theta\ G_{KQ,K'Q'}(\vec{\Omega})\ . \tag{A21.2}$$

To make the dependence of $G_{KQ,K'Q'}(\vec{\Omega})$ on θ and χ explicit, we express the optical thickness $\tau_\nu(\vec{x},\vec{x}')$ defined in Eq. (14.17) in terms of the line optical depth of Eq. (14.25)

$$\tau_\nu(\vec{x},\vec{x}') = \frac{\Delta\nu_{\rm D}\ p(\nu_0-\nu)\ (t'_{\rm L}-t_{\rm L})}{\cos\theta}\ , \tag{A21.3}$$

and write the profile $p(\nu_0-\nu)$ in the form (see Eq. (14.6))

$$p(\nu_0-\nu) = \frac{1}{\Delta\nu_{\rm D}}\ \varphi(v)\ , \tag{A21.4}$$

where

$$v = \frac{\nu_0-\nu}{\Delta\nu_{\rm D}}\ , \qquad \varphi(v) = \frac{1}{\sqrt{\pi}}\ \mathrm{e}^{-v^2}\ , \tag{A21.5}$$

with

$$\int\limits_{-\infty}^{\infty} \varphi(v)\ \mathrm{d}v = 1\ .$$

Substitution of Eqs. (A21.3), (A21.4) into Eq. (A21.2) and use of Eq. (A20.2) leads to the expression

$$\mathcal{I} = \frac{1}{4\pi}\int\limits_{-\infty}^{\infty}\mathrm{d}v\ \big[\varphi(v)\big]^2 \int\limits_0^{2\pi}\mathrm{d}\chi \int\limits_0^{\pi/2}\mathrm{d}\theta\ \tan\theta\ \ \mathrm{e}^{-\frac{(t'_{\rm L}-t_{\rm L})\,\varphi(v)}{\cos\theta}} \times\ w^{(K)}_{J_u J_\ell}\ w^{(K')}_{J_u J_\ell}\ \mathit{\Gamma}_{KQ,K'Q'}(\vec{\Omega})\ . \tag{A21.6}$$

Equation (A20.10) shows that the dependence of $\mathit{\Gamma}_{KQ,K'Q'}(\vec{\Omega})$ on the angles θ and χ is contained in the factor

$$\mathcal{D}^{f''}_{0,Q'-Q}(-\gamma-\theta-\chi) = \mathrm{e}^{\,\mathrm{i}\chi(Q'-Q)}\ d^{f''}_{0,Q'-Q}(-\theta)\ ,$$

hence the integration over χ yields 2π for $Q=Q'$ and zero for $Q\neq Q'$. On the other side, Eqs. (A20.11) show that the quantities $\mathit{\Gamma}_{KQ,K'Q}(\vec{\Omega})$ are linear combinations of factors of the form $[\cos\theta]^{2n}$ with $n=0,1,2$,

$$\mathit{\Gamma}_{KQ,K'Q}(\vec{\Omega}) = \sum_{n=0}^{2}\ c_n(K,K',Q)\ [\cos\theta]^{2n}\ . \tag{A21.7}$$

It follows that Eq. (A21.6) can be rewritten as

$$\mathcal{I} = \delta_{QQ'}\ \frac{1}{2}\ w^{(K)}_{J_u J_\ell}\ w^{(K')}_{J_u J_\ell}\ \sum_{n=0}^{2}\ c_n(K,K',Q)\int\limits_{-\infty}^{\infty}\mathrm{d}v\ \big[\varphi(v)\big]^2\ \mathcal{I}_n\big[(t'_{\rm L}-t_{\rm L})\,\varphi(v)\big]\ ,$$

where

$$\mathcal{I}_n\big[(t'_{\rm L}-t_{\rm L})\,\varphi(v)\big] = \int\limits_0^{\pi/2} {\rm e}^{-\frac{(t'_{\rm L}-t_{\rm L})\,\varphi(v)}{\cos\theta}}\ [\cos\theta]^{2n}\ \tan\theta\ {\rm d}\theta\ .$$

Introducing the variable $y = 1/\cos\theta$, it can readily be seen that the last integral is nothing but the exponential-integral function of order $(2n+1)$ – cf. Eq. (12.6)

$$\mathcal{I}_n\big[(t'_{\rm L}-t_{\rm L})\,\varphi(v)\big] = \int\limits_1^{\infty} \frac{{\rm e}^{-(t'_{\rm L}-t_{\rm L})\,\varphi(v)\ y}}{y^{2n+1}}\ {\rm d}y \ \equiv\ E_{2n+1}\big[(t'_{\rm L}-t_{\rm L})\,\varphi(v)\big]\ .$$

In the above calculations we assumed $t'_{\rm L} > t_{\rm L}$. The opposite case can be treated in a strictly similar way. The final result is that, irrespective of the relative height of the points $\vec{x}$ and $\vec{x}\,'$, the integral in Eq. (A21.1) can be written in the form

$$\mathcal{I} = \delta_{QQ'}\ \frac{1}{2}\ w^{(K)}_{J_u J_\ell}\ w^{(K')}_{J_u J_\ell} \times \sum_{n=0}^{2} c_n(K,K',Q) \int\limits_{-\infty}^{\infty} {\rm d}v\ \big[\varphi(v)\big]^2\ E_{2n+1}\big[|t'_{\rm L}-t_{\rm L}|\,\varphi(v)\big]\ , \qquad \text{(A21.8)}$$

with the coefficients $c_n(K,K',Q)$ implicitly defined by Eq. (A21.7).

A22. The Generalization of the $\sqrt{\epsilon}$-Law

One of the few analytical results that can be established in the scalar theory of radiative transfer concerns the integral equation

$$(1+\epsilon)\,S(\tau) = \epsilon\,B_{\rm P} + \int\limits_0^{\infty} K\big(|\tau'-\tau|\big)\,S(\tau')\,{\rm d}\tau'\ , \qquad \text{(A22.1)}$$

that can also be written in the form

$$S(\tau) = \epsilon' B_{\rm P} + (1-\epsilon') \int\limits_0^{\infty} K\big(|\tau'-\tau|\big)\,S(\tau')\,{\rm d}\tau'\ ,$$

with

$$\epsilon' = \frac{\epsilon}{1+\epsilon}\ . \qquad \text{(A22.2)}$$

This equation is encountered in the non-LTE approach to the problem of line formation for a two-level atom in plane-parallel atmospheres, and relates the source function at optical depth τ to the same function at different optical depths. $B_{\rm P}$

is the Planck function at the kinetic temperature of the colliding particles (characterized by a Maxwellian velocity distribution), and ϵ is the ratio of collisional to radiative de-excitation rates for the upper level – a quantity specifying the degree of coupling between atoms and radiation.

Provided ϵ and $B_{\rm P}$ are independent of τ, and the kernel K obeys the integral property

$$\int_0^\infty K(t)\,{\rm d}t = \frac{1}{2}\,, \tag{A22.3}$$

it can be proved that the value of the source function at $\tau = 0$ is given by

$$S(0) = \sqrt{\epsilon'}\; B_{\rm P}\;.$$

This result, generally referred to as the $\sqrt{\epsilon}$ - *law*, is discussed in classical papers and textbooks (Avrett and Hummer, 1965; Jefferies, 1968; Mihalas, 1978). It is already contained in the discrete-ordinate method for coherent scattering developed by Chandrasekhar (1947), but, according to Avrett and Hummer (1965), it is also implicit in the work of a number of earlier scientists. More recent derivations based on different mathematical methods can be found in Ivanov (1973), Frisch and Frisch (1975), Rybicki (1977), and Landi Degl'Innocenti (1979b).

The $\sqrt{\epsilon}$ - law can be generalized to a linear system of $(N+1)$ equations of the form

$$a_i\,S_i(\tau) = b\,\delta_{i0} + \sum_{j=0}^{N}\int_0^\infty K_{ij}\big(|\tau'-\tau|\big)\,S_j(\tau')\,{\rm d}\tau' \qquad (i=0,\ldots,N)\;, \tag{A22.4}$$

where:

- a_i and b are non-vanishing quantities independent of τ, with

$$a_0 > 1\;, \qquad b > 0\;;$$

- the kernels K_{ij} are integrable functions of their argument and satisfy the symmetry property

$$K_{ij}(t) = K_{ji}(t) \qquad (i,j=0,\ldots,N)\;, \tag{A22.5}$$

and the integral property

$$\int_0^\infty K_{0j}(t)\,{\rm d}t = \frac{1}{2}\;\delta_{j0} \qquad (j=0,\ldots,N)\;. \tag{A22.6}$$

Under these hypotheses, it can be proved (Landi Degl'Innocenti and Bommier, 1994) that the surface values of the 'source functions' $S_i(\tau)$ obey the relation

$$\sum_{i=0}^{N} a_i\,\big[S_i(0)\big]^2 = \frac{b^2}{a_0-1}\;. \tag{A22.7}$$

To prove this relation, first we consider the asymptotic value of $S_i(\tau)$ for $\tau \to \infty$. Since the kernels are integrable functions of their argument, the functions $S_i(\tau)$ tend to finite values, $S_i(\infty)$, for $\tau \to \infty$. Such values can be found by solving the system

$$a_i\, S_i(\infty) = b\, \delta_{i0} + \sum_{j=0}^{N} \left\{ \lim_{\tau\to\infty} \left[\int_{\tau}^{\infty} K_{ij}(\tau' - \tau)\, \mathrm{d}\tau' + \int_{0}^{\tau} K_{ij}(\tau - \tau')\, \mathrm{d}\tau' \right] \right\} S_j(\infty)\ ,$$

where $i = 0, \ldots, N$. Performing the substitutions $(\tau' - \tau) = u$ and $(\tau - \tau') = v$ in the first and second integral, respectively, we get

$$a_i\, S_i(\infty) = b\, \delta_{i0} + 2 \sum_{j=0}^{N} A_{ij}\, S_j(\infty) \qquad (i = 0, \ldots, N)\ , \tag{A22.8}$$

where

$$A_{ij} = \int_{0}^{\infty} K_{ij}(t)\, \mathrm{d}t\ . \tag{A22.9}$$

Owing to property (A22.6), the system (A22.8) decouples into

$$\begin{aligned} a_0\, S_0(\infty) &= b + S_0(\infty) \\ a_i\, S_i(\infty) &= 2 \sum_{j=1}^{N} A_{ij}\, S_j(\infty) \qquad (i = 1, \ldots, N)\ , \end{aligned}$$

whose solution is

$$S_i(\infty) = \frac{b}{a_0 - 1}\ \delta_{i0}\ . \tag{A22.10}$$

Next we consider the τ-derivative of Eq. (A22.4),

$$a_i\, \frac{\mathrm{d}S_i(\tau)}{\mathrm{d}\tau} = \sum_{j=0}^{N} \frac{\mathrm{d}}{\mathrm{d}\tau} \left[\int_{0}^{\infty} K_{ij}\big(|\tau' - \tau|\big)\, S_j(\tau')\, \mathrm{d}\tau' \right]\ .$$

The derivative in the right-hand side can be evaluated by splitting the integral in two parts (cf. the derivation of Eq. (A15.3)). One obtains

$$a_i\, \frac{\mathrm{d}S_i(\tau)}{\mathrm{d}\tau} = \sum_{j=0}^{N} K_{ij}(\tau)\, S_j(0) + \sum_{j=0}^{N} \int_{0}^{\infty} K_{ij}\big(|\tau' - \tau|\big)\, \frac{\mathrm{d}S_j(\tau')}{\mathrm{d}\tau'}\, \mathrm{d}\tau'\ .$$

Following a method developed by Frisch and Frisch (1975) to derive the $\sqrt{\epsilon}$-law in the scalar case, we multiply both members by $S_i(\tau)$, integrate in $\mathrm{d}\tau$, and sum over i,

$$\sum_{i=0}^{N} a_i \int_0^\infty S_i(\tau)\,\frac{\mathrm{d}S_i(\tau)}{\mathrm{d}\tau}\,\mathrm{d}\tau = \sum_{i=0}^{N}\sum_{j=0}^{N} S_j(0)\int_0^\infty K_{ij}(\tau)\,S_i(\tau)\,\mathrm{d}\tau$$
$$+\sum_{i=0}^{N}\sum_{j=0}^{N}\int_0^\infty \mathrm{d}\tau\;S_i(\tau)\int_0^\infty \mathrm{d}\tau'\;K_{ij}\big(|\tau'-\tau|\big)\,\frac{\mathrm{d}S_j(\tau')}{\mathrm{d}\tau'}\,. \quad \text{(A22.11)}$$

The term in the left-hand side is immediately evaluated via integration by parts, and gives

$$\frac{1}{2}\sum_{i=0}^{N} a_i\left\{\big[S_i(\infty)\big]^2-\big[S_i(0)\big]^2\right\}.$$

Using Eqs. (A22.5) and (A22.4), the first term in the right-hand side can be cast into the form

$$\sum_{i=0}^{N} a_i\big[S_i(0)\big]^2-\,b\,S_0(0)\,.$$

For the second term in the right-hand side we obtain, by interchanging the integration order and by using again Eqs. (A22.5) and (A22.4)

$$\sum_{i=0}^{N} a_i\int_0^\infty S_i(\tau)\,\frac{\mathrm{d}S_i(\tau)}{\mathrm{d}\tau}\,\mathrm{d}\tau-\,b\int_0^\infty\frac{\mathrm{d}S_0(\tau)}{\mathrm{d}\tau}\,\mathrm{d}\tau\,,$$

or

$$\frac{1}{2}\sum_{i=0}^{N} a_i\left\{\big[S_i(\infty)\big]^2-\big[S_i(0)\big]^2\right\}-\,b\left\{S_0(\infty)-S_0(0)\right\}.$$

Using these expressions, we obtain from Eq. (A22.11)

$$\sum_{i=0}^{N} a_i\big[S_i(0)\big]^2=\,b\,S_0(\infty)\,,$$

which proves – taking into account Eq. (A22.10) – the generalized $\sqrt{\epsilon}$-law of Eq. (A22.7).

In the following we show that the 'classical' $\sqrt{\epsilon}$-law can be recovered as a special case of Eq. (A22.7), and we deduce the explicit expression of the generalized $\sqrt{\epsilon}$-law for some physical situations that are treated in the text.

a) *Scalar case*

Equation (A22.1) is a special case of Eq. (A22.4) corresponding to

$$N=0\,,\quad S_0=S\,,\quad a_0=1+\epsilon\,,\quad b=\epsilon\,B_{\mathrm{P}}\,.$$

Since the quantities ϵ and $B_{\rm P}$ in Eq. (A22.1) are τ-independent and positive, and the kernel K obeys Eq. (A22.3), it is easily seen that all the conditions for the validity of Eq. (A22.7) are met. Performing the above substitutions, we obtain from Eq. (A22.7)

$$(1+\epsilon)\left[S(0)\right]^2 = \epsilon\, B_{\rm P}^2 \ ,$$

or

$$S(0) = \sqrt{\frac{\epsilon}{1+\epsilon}}\ B_{\rm P} = \sqrt{\epsilon'}\, B_{\rm P} \ , \tag{A22.12}$$

where Eq. (A22.2) has been used. Equation (A22.12) is just the 'classical' $\sqrt{\epsilon}$-law.

b) *Non-magnetic atmosphere*

Consider the system of integral equations (14.27) under the assumption that ϵ, $B_{\rm P}$, and $\delta_u^{(K)}$ are independent of $t_{\rm L}$ and that $H_u = 0$: we obtain the system of Eqs. (14.35) with the only difference that the factor in front of $S_0^2(t_{\rm L})$ in the left-hand side of the second equation is $(1+\epsilon+\delta_u^{(2)})$ instead of $(1+\epsilon)$. This system has the form of Eq. (A22.4) with

$$N=1\ , \quad S_0 = S_0^0\ , \quad S_1 = S_0^2\ , \quad a_0 = 1+\epsilon\ , \quad a_1 = 1+\epsilon+\delta_u^{(2)}\ , \quad b = \epsilon\, B_{\rm P}\ ,$$

and because the multipolar kernels $\mathcal{G}_{KQ,K'Q}(x)$ defined in Eq. (14.28) are integrable functions of x satisfying the symmetry properties of Eq. (14.29) and the integral properties of Eqs. (14.32), Eq. (A22.7) can be applied. We get

$$(1+\epsilon)\left[S_0^0(0)\right]^2 + (1+\epsilon+\delta_u^{(2)})\left[S_0^2(0)\right]^2 = \epsilon\, B_{\rm P}^2\ ,$$

or

$$\sqrt{\left[S_0^0(0)\right]^2 + \left[\,1+(1-\epsilon')\ \delta_u^{(2)}\,\right]\left[S_0^2(0)\right]^2} \ = \ \sqrt{\epsilon'}\, B_{\rm P}\ . \tag{A22.13}$$

This is the explicit form of the generalized $\sqrt{\epsilon}$-law for the physical situation considered.

c) *Magnetic atmosphere (Hanle effect regime)*

The system in Eq. (14.39) has the form of Eq. (A22.4) with

$$N=5\ , \quad S_0 = \left[S_0^0\right]_{\rm M}\ , \quad S_i = \left[S_{i-3}^2\right]_{\rm M} \quad (i=1,\ldots,5)\ ,$$
$$a_0 = 1+\epsilon\ , \quad a_i = 1+\epsilon+\delta_u^{(2)} + {\rm i}H_u(i-3) \quad (i=1,\ldots,5)\ , \quad b = \epsilon\, B_{\rm P}\ .$$

Let us assume that ϵ, $B_{\rm P}$, $\delta_u^{(2)}$, and the magnetic field vector are independent of $t_{\rm L}$, and that the x-axis of the 'magnetic frame' lies in the plane containing the magnetic field and the perpendicular to the atmosphere ($R_B = R'_B \equiv (0, -\theta_B, -\chi_B)$ in Eq. (14.40)). Under these assumptions the kernels $\hat{\mathcal{G}}_{KQ,K'Q'}(x)$ obey the properties

of Eqs. (14.41) and (14.42), and the conditions for the validity of Eq. (A22.7) are satisfied. We get

$$\sqrt{\left[S_0^0(0)\right]_{\rm M}^2 + \sum_{Q=-2}^{2} \left[\,1 + (1-\epsilon')\,(\delta_u^{(2)} + {\rm i}H_u Q)\,\right] \left[S_Q^2(0)\right]_{\rm M}^2} \;=\; \sqrt{\epsilon'}\; B_{\rm P}\;. \quad \text{(A22.14)}$$

d) *Magnetic atmosphere (strong field regime)*
The system in Eq. (14.62) has the form of Eq. (A22.4) with

$$N = \frac{1}{2} K_{\max}\;, \quad S_0 = \left[S_0^0\right]_{\rm M}\;, \quad S_i = \left[S_0^{2i}\right]_{\rm M} \quad (i = 1, \ldots, N)\;,$$

$$a_0 = 1 + \epsilon\;, \quad a_i = 1 + \epsilon + \delta_u^{(2i)} \quad (i = 1, \ldots, N)\;, \quad b = \epsilon\, B_{\rm P}\;.$$

The kernels $\tilde{\mathcal{G}}_{K0,K'0}(x)$ obey the properties in Eqs. (14.65) and (14.66). Provided ϵ, $B_{\rm P}$, and $\delta_u^{(K)}$ are independent of $t_{\rm L}$, all the conditions for the validity of Eq. (A22.7) are satisfied, so that

$$\sqrt{\left[S_0^0(0)\right]_{\rm M}^2 + \sum_{K=2,4,\ldots,K_{\max}} \left[\,1 + (1-\epsilon')\;\delta_u^{(K)}\,\right] \left[S_0^K(0)\right]_{\rm M}^2} \;=\; \sqrt{\epsilon'}\; B_{\rm P}\;. \quad \text{(A22.15)}$$

Finally, it should be remarked that a further generalization of the $\sqrt{\epsilon}$-law has been proved by Frisch (1998). This generalization concerns the coupled system of $(N+1)$ integral equations of the form

$$a_i\, S_i(\tau) = b_i \,+ \sum_{j=0}^{N} \int_0^{\infty} K_{ij}\big(|\tau' - \tau|\big)\; S_j(\tau')\; {\rm d}\tau' \qquad (i = 0, \ldots, N)\;,$$

where:
- the coefficients a_i, b_i are independent of τ, with

$$a_0 > 1\;, \qquad b_0 > 0\;;$$

- the kernels K_{ij} have the same properties as the kernels appearing in Eq. (A22.4).
Following a procedure similar to the former, it can be proved that

$$\sum_{i=0}^{N} a_i \left[S_i(0)\right]^2 = \frac{b_0^2}{a_0 - 1} + \sum_{i=1}^{N} \sum_{j=1}^{N} b_i\, (X^{-1})_{ij}\, b_j\;,$$

where the matrix $\boldsymbol{X}$ is defined by

$$X_{ij} = a_i\, \delta_{ij} - 2\, A_{ij} \qquad (i, j = 1, \ldots, N)\;,$$

with A_{ij} given by Eq. (A22.9).

A23. The Generalized Multipole Coupling Coefficients

The generalized multipole coupling coefficients are defined by Eq. (14.60),

$$\tilde{G}_{K0,K'0}(\vec{x},\vec{x}') = \sum_{K''K'''} \int_{-\infty}^{\infty} \mathrm{d}\nu \;\tilde{\Phi}_0^{KK''}(J_\ell, J_u\,;\nu)\,\tilde{\Phi}_0^{K'K'''}(J_\ell, J_u\,;\nu) \times \sum_{i=0}^{3}\sum_{j=0}^{3} \mathcal{T}_0^{K''}(i,\vec{\Omega})\; O_{ij}(\vec{x},\vec{x}';\nu)\; \mathcal{T}_0^{K'''}(j,\vec{\Omega})\;, \qquad \text{(A23.1)}$$

where the profiles $\tilde{\Phi}_0^{KK'}(J_\ell, J_u\,;\nu)$ are given by Eq. (14.48), $O_{ij}(\vec{x},\vec{x}';\nu)$ is the evolution operator defined in Eq. (14.57), $\vec{\Omega}$ is the direction of the vector joining point $\vec{x}'$ with point $\vec{x}$, and the tensors $\mathcal{T}_0^K$ are defined in the reference system of the magnetic field. They are real quantities (because the single factors appearing in the right-hand side are real – see Eqs. (5.158) and (A13.2)),[1] and obey the following properties:

a) *Limitation on indices*
As apparent from Eq. (14.48), the indices K and K' are restricted to the range

$$K, K' = 0, 1, \ldots, 2J_u\;.$$

The number of generalized multipole coupling coefficients is therefore $(2J_u+1)^2$.

b) *Limit for zero magnetic field*
From Eq. (A13.5) we have

$$\lim_{\nu_{\mathrm{L}}\to 0} \tilde{\Phi}_0^{KK'}(J_\ell, J_u\,;\nu) = \delta_{KK'}\; w^{(K)}_{J_u J_\ell}\; p(\nu_0-\nu)\;, \qquad \text{(A23.2)}$$

and from Eq. (A13.13)

$$\lim_{\nu_{\mathrm{L}}\to 0} \tilde{\Psi}_0^{0K}(J_\ell, J_u\,;\nu) = \delta_{K0}\; q(\nu_0-\nu)\;, \qquad \text{(A23.3)}$$

where the profile $q(\nu_0-\nu)$ is given by Eq. (14.53). As a consequence, Eqs. (14.51) and (14.52) yield

$$\lim_{\nu_{\mathrm{L}}\to 0}\; \eta_i^{\mathrm{A}}(\nu,\vec{\Omega}) = k_{\mathrm{L}}^{\mathrm{A}}\; p(\nu_0-\nu)\;\delta_{i0} \qquad (i=0,1,2,3)$$
$$\lim_{\nu_{\mathrm{L}}\to 0}\; \rho_i^{\mathrm{A}}(\nu,\vec{\Omega}) = 0 \qquad (i=1,2,3)\;,$$

[1] Equation (A13.2) refers in fact to the generalized profiles $\Phi_Q^{KK'}$, but it can easily be seen that the same relation holds for $\tilde{\Phi}_Q^{KK'}$. This remark also applies to other properties that will be needed in the following.

so that the matrix $\boldsymbol{H}(\nu,\vec{\Omega})$ defined in Eq. (14.56) becomes diagonal,

$$\lim_{\nu_{\mathrm{L}}\to 0} H_{ij}(\nu,\vec{\Omega}) = p(\nu_0-\nu)\ \delta_{ij}\ .$$

Thus from Eq. (14.57)

$$\lim_{\nu_{\mathrm{L}}\to 0} O_{ij}(\vec{x},\vec{x}';\nu) = \mathrm{e}^{-\tau_\nu(\vec{x},\vec{x}')}\ \delta_{ij}\ , \tag{A23.4}$$

where $\tau_\nu(\vec{x},\vec{x}')$ is given by Eq. (14.17). Substitution of Eqs. (A23.2) and (A23.4) into Eq. (A23.1) yields

$$\lim_{\nu_{\mathrm{L}}\to 0} \tilde{G}_{K0,K'0}(\vec{x},\vec{x}') = \int_{-\infty}^{\infty} \mathrm{d}\nu\ \left[p(\nu_0-\nu)\right]^2\ \mathrm{e}^{-\tau_\nu(\vec{x},\vec{x}')}\ w^{(K)}_{J_u J_\ell}\ w^{(K')}_{J_u J_\ell} \times \sum_{i=0}^{3} \mathcal{T}_0^K(i,\vec{\Omega})\ \mathcal{T}_0^{K'}(i,\vec{\Omega})\ .$$

This expression formally coincides with the definition of $G_{K0,K'0}(\vec{x},\vec{x}')$ given in Eq. (14.24), but one must bear in mind the difference between the reference systems where the two quantities are defined.

c) *Expression in terms of rotation matrices*

Taking into account Eq. (5.159), the generalized multipole coupling coefficients can be expressed in the form

$$\tilde{G}_{K0,K'0}(\vec{x},\vec{x}') = \sum_{K''K'''} \sum_{PP'} \int_{-\infty}^{\infty} \mathrm{d}\nu\ \tilde{\Phi}_0^{KK''}(J_\ell,J_u\,;\nu)\,\tilde{\Phi}_0^{K'K'''}(J_\ell,J_u\,;\nu) \times \left[\sum_{i=0}^{3}\sum_{j=0}^{3} t_P^{K''}(i)\ O_{ij}(\vec{x},\vec{x}';\nu)\ t_{P'}^{K'''}(j)\right] \mathcal{D}_{P0}^{K''}(R)\ \mathcal{D}_{P'0}^{K'''}(R)\ , \tag{A23.5}$$

where R is the rotation carrying the reference system $(\vec{e}_a(\vec{\Omega}),\vec{e}_b(\vec{\Omega}),\vec{\Omega})$ into the system of the magnetic field.

d) *Vanishing values*

$$\tilde{G}_{K0,K'0}(\vec{x},\vec{x}') = (-1)^{K+K'}\,\tilde{G}_{K0,K'0}(\vec{x},\vec{x}')\ , \tag{A23.6}$$

a relation showing that all the generalized multipole coupling coefficients connecting irreducible components of the source function of different parity are identically zero.

To prove this property, we consider two frequencies ν, ν' symmetrical about line center ($\nu'-\nu_0=\nu_0-\nu$). From Eqs. (A13.4) and (A13.12) we have

$$\tilde{\Phi}_0^{0K}(J_\ell,J_u\,;\nu') = (-1)^K\,\tilde{\Phi}_0^{0K}(J_\ell,J_u\,;\nu)$$
$$\tilde{\Psi}_0^{0K}(J_\ell,J_u\,;\nu') = (-1)^{1+K}\,\tilde{\Psi}_0^{0K}(J_\ell,J_u\,;\nu)\ .$$

Using these relations and the expressions of the tensors $\mathcal{T}^K_Q(i,\vec{\Omega})$ – Table 5.6 – it is easily seen from Eqs. (14.51) and (14.52) that the radiative transfer coefficients $\eta^{\rm A}_0$, $\eta^{\rm A}_1$, $\eta^{\rm A}_2$, $\rho^{\rm A}_3$ are symmetrical about line center, while $\eta^{\rm A}_3$, $\rho^{\rm A}_1$, $\rho^{\rm A}_2$ are antisymmetrical. Thus the matrix $\boldsymbol{H}$ of Eq. (14.56) satisfies the symmetry property[1]

$$H_{ij}(\nu') = \xi_i\,\xi_j\,H_{ij}(\nu) \qquad (i,j=0,\ldots,3)\ ,$$

where ξ_i is the formal vector defined in Eqs. (5.161). Since this property remains valid for any arbitrary function of the matrix $\boldsymbol{H}$, it holds also for the evolution operator,

$$O_{ij}(\vec{x},\vec{x}';\nu') = \xi_i\,\xi_j\,O_{ij}(\vec{x},\vec{x}';\nu)\ .$$

Using the first of Eqs. (5.162), it can be shown that the integrand in Eq. (A23.5) has the parity of $(K+K')$, so that Eq. (A23.6) follows after integration.

e) *Symmetry with respect to the indices*

$$\tilde{G}_{K0,K'0}(\vec{x},\vec{x}') = \tilde{G}_{K'0,K0}(\vec{x},\vec{x}')\ . \tag{A23.7}$$

To prove this property, one should bear in mind that the generalized multipole coupling coefficients do not depend, as obvious on general physical grounds, on the reference direction $\vec{e}_a(\vec{\Omega})$ chosen to define the Stokes parameters of the radiation flowing in the direction $\vec{\Omega}$. On the other hand, it can easily be shown that if the reference direction is rotated through an angle α, the components $\mathcal{T}^2_0(1,\vec{\Omega})$ and $\mathcal{T}^2_0(2,\vec{\Omega})$ transform according to the equations

$$\left[\mathcal{T}^2_0(1,\vec{\Omega})\right]_{\rm new} = \cos 2\alpha\left[\mathcal{T}^2_0(1,\vec{\Omega})\right]_{\rm old} + \sin 2\alpha\left[\mathcal{T}^2_0(2,\vec{\Omega})\right]_{\rm old}$$

$$\left[\mathcal{T}^2_0(2,\vec{\Omega})\right]_{\rm new} = -\sin 2\alpha\left[\mathcal{T}^2_0(1,\vec{\Omega})\right]_{\rm old} + \cos 2\alpha\left[\mathcal{T}^2_0(2,\vec{\Omega})\right]_{\rm old}\ .$$

This implies that it is possible to find a reference direction such that $\mathcal{T}^2_0(2,\vec{\Omega})$ vanishes. With this choice, one obtains from Eqs. (14.51) and (14.52) that $\eta^{\rm A}_2(\nu,\vec{\Omega}) = \rho^{\rm A}_2(\nu,\vec{\Omega}) = 0$, so that the matrix $\boldsymbol{K}^{\rm A}$ defined in Eq. (14.50) takes the form

$$\boldsymbol{K}^{\rm A} = \begin{pmatrix} \eta^{\rm A}_0(\nu,\vec{\Omega}) & \eta^{\rm A}_1(\nu,\vec{\Omega}) & 0 & \eta^{\rm A}_3(\nu,\vec{\Omega}) \\ \eta^{\rm A}_1(\nu,\vec{\Omega}) & \eta^{\rm A}_0(\nu,\vec{\Omega}) & \rho^{\rm A}_3(\nu,\vec{\Omega}) & 0 \\ 0 & -\rho^{\rm A}_3(\nu,\vec{\Omega}) & \eta^{\rm A}_0(\nu,\vec{\Omega}) & \rho^{\rm A}_1(\nu,\vec{\Omega}) \\ \eta^{\rm A}_3(\nu,\vec{\Omega}) & 0 & -\rho^{\rm A}_1(\nu,\vec{\Omega}) & \eta^{\rm A}_0(\nu,\vec{\Omega}) \end{pmatrix}\ .$$

[1] This is the well-known property of the absorption matrix deduced in Chap. 9, Eq. (9.51). We recall that in the non-LTE problem considered in Sect. 14.3 the lower level is assumed to be unpolarized.

It follows that the matrix $\boldsymbol{H}$ of Eq. (14.56) obeys the symmetry property

$$H_{ji} = \tau_i \tau_j H_{ij} \qquad (i,j = 0,\ldots,3) ,$$

where τ_i is the formal vector defined in Eqs. (5.161). Since this property holds for any function of the matrix $\boldsymbol{H}$, it is also valid for the evolution operator,

$$O_{ji}(\vec{x},\vec{x}';\nu) = \tau_i \tau_j O_{ij}(\vec{x},\vec{x}';\nu) .$$

On the other hand, being $\mathcal{T}_0^K(2,\vec{\Omega}) = 0$, one also has

$$\tau_i \mathcal{T}_0^K(i,\vec{\Omega}) = \mathcal{T}_0^K(i,\vec{\Omega}) ,$$

so that

$$\mathcal{T}_0^{K''}(i,\vec{\Omega})\, O_{ji}(\vec{x},\vec{x}';\nu)\, \mathcal{T}_0^{K'''}(j,\vec{\Omega}) = \mathcal{T}_0^{K''}(i,\vec{\Omega})\, O_{ij}(\vec{x},\vec{x}';\nu)\, \mathcal{T}_0^{K'''}(j,\vec{\Omega}) .$$

This means that the indices i and j of the evolution operator in Eq. (A23.1) can be interchanged. This is sufficient to prove Eq. (A23.7) by exchange of the dummy summation indices K'' and K''' in Eq. (A23.1).

f) *Symmetry with respect to the arguments*

$$\tilde{G}_{K0,K'0}(\vec{x},\vec{x}') = \tilde{G}_{K0,K'0}(\vec{x}',\vec{x}) . \tag{A23.8}$$

To prove this property, we observe that the interchange of $\vec{x}$ and $\vec{x}'$ implies the interchange of the direction $\vec{\Omega}$ with the opposite direction $-\vec{\Omega}$. Since, as already noticed at point e), the generalized multipole coupling coefficients do not depend on the reference direction, we choose for the direction $-\vec{\Omega}$ a reference direction unit vector $\vec{e}_a(-\vec{\Omega}) = \vec{e}_a(\vec{\Omega})$, as shown in Fig. 5.15. With this choice, one has from Eq. (5.163)

$$\mathcal{T}_0^K(i,-\vec{\Omega}) = \zeta_i \mathcal{T}_0^K(i,\vec{\Omega}) \qquad (i = 0,\ldots,3) , \tag{A23.9}$$

where ζ_i is the formal vector defined in Eqs. (5.161). Substitution of Eq. (A23.9) into Eqs. (14.51) and (14.52) shows that the matrix $\boldsymbol{H}$ of Eq. (14.56) satisfies, at each point of the medium, the property

$$H_{ij}(\nu,-\vec{\Omega}) = \zeta_i \zeta_j H_{ij}(\nu,\vec{\Omega}) ,$$

and because the optical depth $\tau(\vec{x},\vec{x}')$ is obviously invariant under interchange of its arguments, it follows that

$$O_{ij}(\vec{x}',\vec{x};\nu) = \zeta_i \zeta_j O_{ij}(\vec{x},\vec{x}';\nu) . \tag{A23.10}$$

Substituting Eqs. (A23.9) and (A23.10) into Eq. (A23.1), property (A23.8) is easily proved.

A24. Reduced Matrix Elements for Photoionization Cross Sections

We consider a simple case where photoionization involves the absorption of a photon by an optical electron belonging to an open shell ($n\ell_{\rm b}$). The photoionized electron leaves the atom with kinetic energy ϵ, orbital angular momentum ℓ, and total angular momentum (orbital + spin) j. Assuming the atom to be described in the L-S coupling scheme, the reduced matrix element entering the photoionization cross section is of the form (see Eq. (14.83))

$$\mathcal{M} = |\left\langle \beta\, L_0 S_0, n\ell_{\rm b}; LSJ \| \vec{d} \,\| \beta\,(L_0 S_0) J_0, \epsilon\ell j; J' \right\rangle|^2 \,, \tag{A24.1}$$

where, with obvious notations, $(\beta L_0 S_0)$ is the set of quantum numbers describing the parent term of the photoionized level and, at the same time, the term encompassing the level where the atom is left after photoionization (this final level being further described by the quantum number J_0).

Notwithstanding the simplifications introduced, the evaluation of the matrix element is rather complicated because of the different coupling schemes of the 'bra' and 'ket' vectors. A recoupling of the various angular momenta is necessary. With standard techniques one has

$$\begin{aligned} |\beta\, L_0 S_0, n\ell_{\rm b}; LSJ\rangle = \sqrt{(2L+1)(2S+1)} \sum_{J_0'\, j_{\rm b}} \sqrt{(2J_0'+1)(2j_{\rm b}+1)} \\ \times \begin{Bmatrix} L_0 & S_0 & J_0' \\ \ell_{\rm b} & \frac{1}{2} & j_{\rm b} \\ L & S & J \end{Bmatrix} |\beta\,(L_0 S_0) J_0', n\ell_{\rm b} j_{\rm b}; J\rangle \,. \end{aligned} \tag{A24.2}$$

On the other hand, since the operator $\vec{d}$ only acts on the variables of the optical electron, using Eq. (2.109) one has

$$\begin{aligned} &\left\langle \beta\,(L_0 S_0) J_0', n\ell_{\rm b} j_{\rm b}; J \| \vec{d} \,\| \beta\,(L_0 S_0) J_0, \epsilon\ell j; J' \right\rangle = \\ &= (-1)^{J_0+j+J+1} \sqrt{(2J'+1)(2j_{\rm b}+1)} \begin{Bmatrix} j_{\rm b} & j & 1 \\ J' & J & J_0 \end{Bmatrix} \left\langle n\ell_{\rm b} j_{\rm b} \| \vec{d} \,\| \epsilon\ell j \right\rangle \delta_{J_0 J_0'} \,, \end{aligned}$$

and taking into account that $\vec{d}$ only acts on the *orbital* variables of the optical electron, from Eq. (2.108) one obtains

$$\begin{aligned} &\left\langle \beta\,(L_0 S_0) J_0', n\ell_{\rm b} j_{\rm b}; J \| \vec{d} \,\| \beta\,(L_0 S_0) J_0, \epsilon\ell j; J' \right\rangle = \\ &= (-1)^{J_0+J-\ell_{\rm b}-\frac{1}{2}} \sqrt{(2J'+1)(2j_{\rm b}+1)(2j+1)(2\ell_{\rm b}+1)} \\ &\quad \times \begin{Bmatrix} j_{\rm b} & j & 1 \\ J' & J & J_0 \end{Bmatrix} \begin{Bmatrix} \ell_{\rm b} & \ell & 1 \\ j & j_{\rm b} & \frac{1}{2} \end{Bmatrix} \left\langle n\ell_{\rm b} \| \vec{d} \,\| \epsilon\ell \right\rangle \,. \end{aligned} \tag{A24.3}$$

The reduced matrix element $\langle n\ell_{\rm b}\| \vec{d} \,\|\epsilon\ell\rangle$ can be evaluated through standard methods. One has

$$\langle n\ell_{\rm b}\| \vec{d} \,\|\epsilon\ell\rangle = e_0 \, (-1)^{\ell+1} \sqrt{2\ell+1} \begin{pmatrix} \ell_{\rm b} & \ell & 1 \\ 0 & 0 & 0 \end{pmatrix} \mathcal{I}(n\ell_{\rm b}, \epsilon\ell) \, , \tag{A24.4}$$

where $\mathcal{I}(n\ell_{\rm b}, \epsilon\ell)$ is the radial integral defined by

$$\mathcal{I}(n\ell_{\rm b}, \epsilon\ell) = \int_0^\infty P_{n\ell_{\rm b}}(r) \; r \; \chi_{\epsilon\ell}(r) \; {\rm d}r \, , \tag{A24.5}$$

$P_{n\ell_{\rm b}}(r)$ being the reduced radial wavefunction of the bound electron and $\chi_{\epsilon\ell}(r)$ being the same quantity for the free electron with kinetic energy ϵ at infinite distance from the atomic nucleus.

Substituting Eq. (A24.4) into Eq. (A24.3), and taking into account Eq. (A24.2), one obtains from Eq. (A24.1)

$$\begin{aligned} \mathcal{M} = {} & e_0^2 \, (2L+1)(2S+1)(2J_0+1)(2J'+1)(2j+1)(2\ell_{\rm b}+1)(2\ell+1) \\ & \times \sum_{j_{\rm b} \, j'_{\rm b}} (2j_{\rm b}+1)(2j'_{\rm b}+1) \begin{Bmatrix} L_0 & S_0 & J_0 \\ \ell_{\rm b} & \tfrac{1}{2} & j_{\rm b} \\ L & S & J \end{Bmatrix} \begin{Bmatrix} L_0 & S_0 & J_0 \\ \ell_{\rm b} & \tfrac{1}{2} & j'_{\rm b} \\ L & S & J \end{Bmatrix} \\ & \times \begin{Bmatrix} j_{\rm b} & j & 1 \\ J' & J & J_0 \end{Bmatrix} \begin{Bmatrix} j'_{\rm b} & j & 1 \\ J' & J & J_0 \end{Bmatrix} \begin{Bmatrix} \ell_{\rm b} & \ell & 1 \\ j & j_{\rm b} & \tfrac{1}{2} \end{Bmatrix} \begin{Bmatrix} \ell_{\rm b} & \ell & 1 \\ j & j'_{\rm b} & \tfrac{1}{2} \end{Bmatrix} \\ & \times \begin{pmatrix} \ell_{\rm b} & \ell & 1 \\ 0 & 0 & 0 \end{pmatrix}^2 \left[\mathcal{I}(n\ell_{\rm b}, \epsilon\ell)\right]^2 . \end{aligned} \tag{A24.6}$$

Equation (A24.6) can be substituted into Eq. (14.83) to find the dichroism coefficient due to photoionization. The summation over ℓ, j, J' in the denominator of Eq. (14.83) can be evaluated by summing first over J' and then over j. Applying twice Eq. (2.39) one gets

$$\begin{aligned} \sum_{\ell j J'} \mathcal{M} = {} & e_0^2 \, (2L+1)(2S+1)(2J_0+1) \sum_{j_{\rm b}} (2j_{\rm b}+1) \begin{Bmatrix} L_0 & S_0 & J_0 \\ \ell_{\rm b} & \tfrac{1}{2} & j_{\rm b} \\ L & S & J \end{Bmatrix}^2 \\ & \times \sum_{\ell} (2\ell+1) \begin{pmatrix} \ell_{\rm b} & \ell & 1 \\ 0 & 0 & 0 \end{pmatrix}^2 \left[\mathcal{I}(n\ell_{\rm b}, \epsilon\ell)\right]^2 . \end{aligned} \tag{A24.7}$$

For the numerator, recalling the definition of $w_{JJ'}^{(K)}$ (see Eq. (10.11)) and applying twice Eq. (2.41), one gets

$$\sum_{\ell j J'} w_{JJ'}^{(K)}\, \mathcal{M} = e_0^2\, (2L+1)(2S+1)(2J_0+1)(2\ell_{\rm b}+1)\, \sqrt{3(2J+1)}$$
$$\times \sum_{j_{\rm b}\, j'_{\rm b}} (2j_{\rm b}+1)(2j'_{\rm b}+1) \begin{Bmatrix} L_0 & S_0 & J_0 \\ \ell_{\rm b} & \frac{1}{2} & j_{\rm b} \\ L & S & J \end{Bmatrix} \begin{Bmatrix} L_0 & S_0 & J_0 \\ \ell_{\rm b} & \frac{1}{2} & j'_{\rm b} \\ L & S & J \end{Bmatrix}$$
$$\times \begin{Bmatrix} j_{\rm b} & j'_{\rm b} & K \\ \ell_{\rm b} & \ell_{\rm b} & \frac{1}{2} \end{Bmatrix} \begin{Bmatrix} j_{\rm b} & j'_{\rm b} & K \\ J & J & J_0 \end{Bmatrix}$$
$$\times \sum_{\ell} (-1)^{\frac{1}{2}+J+J_0+\ell}\, (2\ell+1) \begin{Bmatrix} 1 & 1 & K \\ \ell_{\rm b} & \ell_{\rm b} & \ell \end{Bmatrix} \begin{pmatrix} \ell_{\rm b} & \ell & 1 \\ 0 & 0 & 0 \end{pmatrix}^2$$
$$\times \left[\mathcal{I}(n\ell_{\rm b}, \epsilon\ell)\right]^2 . \qquad \text{(A24.8)}$$

Equations (A24.7) and (A24.8), when substituted into Eq. (14.83), allow one to express the dichroism coefficients due to photoionization as functions of the radial integrals defined in Eq. (A24.5). Obviously, such integrals can be evaluated only when the wavefunctions of the bound and free electronic states are known. To this aim, one needs to solve the radial Schrödinger equation, which generally requires the use of self-consistent Hartree-Fock methods. An approximate method that can conveniently be used in many cases to express the radial integrals is the so-called *Quantum Defect Method* developed by Seaton (1958) and Burgess and Seaton (1960).

This page intentionally left blank

LIST OF TABLES

This page intentionally left blank

REFERENCES

Abramowitz, M., and Stegun, I.A.: 1965, *Handbook of Mathematical Functions*, Dover Publications, New York.

Achmad, L., de Jager, C., and Nieuwenhuijzen, H.: 1991, *Astron. Astrophys.* **250**, 445.

Akhiezer, A.I., and Berestetskii, V.B.: 1965, *Quantum Electrodynamics*, Wiley Interscience, New York [etc.].

Alder, K.: 1952, *Helv. Phys. Acta* **25**, 235.

Allen, C.W.: 1973, *Astrophysical Quantities*, 3rd ed., Athlone Press, University of London, London.

Aller, L.H.: 1963, *The Atmospheres of the Sun and Stars*, 2nd ed., Ronald Press, New York.

Angel, J.R.P., Borra, E.F., and Landstreet, J.D.: 1981, *Astrophys. J. Suppl.* **45**, 457.

Arena, P., and Landi Degl'Innocenti, E.: 1982, *Astron. Astrophys. Suppl.* **48**, 81.

Arnaud, J.: 1982, *Astron. Astrophys.* **112**, 350.

Arnaud, J., and Newkirk, G.N. Jr.: 1987, *Astron. Astrophys.* **178**, 263.

Athay, R.G., Querfeld, C.W., Smartt, R.N., Landi Degl'Innocenti, E., and Bommier, V.: 1983, *Solar Phys.* **89**, 3.

Auer, L.H.: 1967, *Astrophys. J.* **150**, L53.

Auer, L.H., and Heasley, J.N.: 1978, *Astron. Astrophys.* **64**, 67.

Auer, L.H., Heasley, J.N., and House, L.L.: 1977a, *Astrophys. J.* **216**, 531.

Auer, L.H., Heasley, J.N., and House, L.L.: 1977b, *Solar Phys.* **55**, 47.

Auvergne, M., Frisch, H., Frisch, U., Froeschlé, C., and Pouquet, A.: 1973, *Astron. Astrophys.* **29**, 93.

Avrett, E.H., and Hummer, D.G.: 1965, *Monthly Not. R. A. S.* **130**, 295.

Babcock, H.W.: 1949, *Astrophys. J.* **110**, 126.

Babcock, H.W.: 1953, *Astrophys. J.* **118**, 387.

Back, E., and Landé, A.: 1925, *Zeemaneffekt und Multiplettstruktur der Spektrallinien*, Springer, Berlin.

Bagnulo, S.: 1993, Tesi di Laurea, Università di Firenze.

Baur, T.G., Elmore, D.E., Lee, R.H., Querfeld, C.W., and Rogers, S.R.: 1981, *Solar Phys.* **70**, 395.

Beckers, J.M.: 1969a, *Solar Phys.* **9**, 372.

Beckers, J.M.: 1969b, *A Table of Zeeman Multiplets*, Air Force Cambridge Research Laboratory.

Beckers, J.M., and Milkey, R.W.: 1975, *Solar Phys.* **43**, 289.

Bellot Rubio, L.R., Ruiz Cobo, B., and Collados, M.: 1997, *Astrophys. J.* **478**, L45.

Bethe, H.A., and Salpeter, E.E.: 1957, *Quantum Mechanics of One and Two Electron Atoms*, Springer-Verlag, Berlin [etc.].

Bevington, P.R.: 1969, *Data Reduction and Error Analysis for the Physical Sciences*, McGraw-Hill, New York [etc.].

Biedenharn, L.C.: 1952, Oak Ridge National Laboratory, Report No.1098.
Biedenharn, L.C., Blatt, J.M., and Rose, M.E.: 1952, *Rev. Mod. Phys.* **24**, 249.
Blackwell, D.E., Ibbetson, P.A., Petford, A.D., and Shallis, M.J.: 1979, *Monthly Not. R. A. S.* **186**, 633.
Blum, K.: 1981, *Density Matrix Theory and Applications*, Plenum Press, New York [etc.].
Bommier, V.: 1977, Thèse de 3ème cycle, Université de Paris VI.
Bommier, V.: 1980, *Astron. Astrophys.* **87**, 109.
Bommier, V.: 1997a, *Astron. Astrophys.* **328**, 706.
Bommier, V.: 1997b, *Astron. Astrophys.* **328**, 726.
Bommier, V., and Landi Degl'Innocenti, E.: 1996, *Solar Phys.* **164**, 117.
Bommier, V., and Sahal-Bréchot, S.: 1978, *Astron. Astrophys.* **69**, 57.
Bommier, V., Leroy, J.L., and Sahal-Bréchot, S.: 1981, *Astron. Astrophys.* **100**, 231.
Bommier, V., Leroy, J.L., and Sahal-Bréchot, S.: 1986a, *Astron. Astrophys.* **156**, 79.
Bommier, V., Leroy, J.L., and Sahal-Bréchot, S.: 1986b, *Astron. Astrophys.* **156**, 90.
Bommier, V., Landi Degl'Innocenti, E., and Sahal-Bréchot, S.: 1991, *Astron. Astrophys.* **244**, 383.
Bommier, V., Landi Degl'Innocenti, E., Leroy, J.L., and Sahal-Bréchot, S.: 1994, *Solar Phys.* **154**, 231.
Born, M., and Wolf, E.: 1964, *Principles of Optics*, 2nd ed., Pergamon Press, Oxford.
Boyarchuk, A.A., Efimov, Yu.S., and Stepanov, V.E.: 1961, *Soviet Astron.* **4**, 766.
Brink, D.M., and Satchler, G.R.: 1968, *Angular Momentum*, 2nd ed., Clarendon Press, Oxford.
Brissaud, A., and Frisch, U.: 1971, *J. Quant. Spectrosc. Rad. Transfer* **11**, 1767.
Brix, P., and Kopfermann, H.: 1952, *Hyperfeinstruktur der Atomterme und Atomlinien*, in Landolt-Börnstein, *Zahlenwerte und Funktionen aus Physik, Chemie, Astronomie, Geophysik und Technik*, Sechste Auflage, I Band, 5 Teil, 1, Springer-Verlag, Berlin.
Buckmaster, H.A.: 1964, *Can. J. Phys.* **42**, 386.
Buckmaster, H.A.: 1966, *Can. J. Phys.* **44**, 2525.
Burgess, A., and Seaton, M.J.: 1960, *Monthly Not. R. A. S.* **120**, 121.
Caccin, B., Gomez, M.T., Marmolino, C., and Severino, G.: 1977, *Astron. Astrophys.* **54**, 227.
Calamai, G., and Landi Degl'Innocenti, E.: 1983, *Astron. Astrophys. Suppl.* **53**, 311.
Calamai, G., Landi Degl'Innocenti, E., and Landi Degl'Innocenti, M.: 1975, *Astron. Astrophys.* **45**, 297.
Canfield, R.C., de la Beaujardière, J.F., Fan, Y., Leka, K.D., McClimont, A.N., Metcalf, R.F., Mickey, D.L., Wülser, J.P., and Lites, B.W.: 1993, *Astrophys. J.* **411**, 362.

Cannon, C.J.: 1985, *The Transfer of Spectral Line Radiation*, Cambridge University Press, Cambridge [etc.].
Casini, R., and Judge, P.G.: 1999, *Astrophys. J.* **522**, 524.
Chandrasekhar, S.: 1947, *Astrophys. J.* **106**, 145.
Chandrasekhar, S.: 1950, *Radiative Transfer*, Clarendon Press, Oxford.
Chandrasekhar, S., and Breen, F.H.: 1947, *Astrophys. J.* **105**, 435.
Charvin, P.: 1965, *Ann. Astrophysique* **28**, 877.
Clarke, D.: 1974, *Appl. Opt.* **13**, 222.
Clarke, D., and Grainger, J.F.: 1971, *Polarized Light and Optical Measurement*, Pergamon Press, Oxford [etc.].
Cohen-Tannoudji, C., Diu, B., and Laloë, F.: 1977, *Mécanique Quantique*, Hermann, Paris.
Cohen-Tannoudji, C., Dupont-Roc, J., and Grynberg, G.: 1987, *Photons et Atomes*, InterEditions, Editions du CNRS, Paris.
Cohen-Tannoudji, C., Dupont-Roc, J., and Grynberg, G.: 1988, *Processus d'Interaction entre Photons et Atomes*, InterEditions, Editions du CNRS, Paris.
Colegrove, F.D., Franken, P.A., Lewis, R.R., and Sands, H.R.: 1959, *Phys. Rev. Letters* **3**, 420.
Collatz, L.: 1966, *The Numerical Treatment of Differential Equations*, Springer-Verlag, Berlin [etc.].
Condon, E.U., and Odabaşi, H.: 1980, *Atomic Structure*, Cambridge University Press, Cambridge [etc.].
Condon, E.U., and Shortley, G.H.: 1935, *The Theory of Atomic Spectra*, Cambridge University Press, Cambridge.
Corliss, C., and Sugar, J.: 1982, *J. Phys. Chem. Ref. Data* **11**, No.1, 135.
Cuperman, S., Ofman, L., and Semel, M.: 1990, *Astron. Astrophys.* **227**, 227.
Débarbat, S., Dumont, S., and Pecker, J.C.: 1970, *Astron. Astrophys.* **8**, 231.
Delbouille, L., Neven, L., and Roland, G.: 1973, *Photometric Atlas of the Solar Spectrum from 3000 to 10000 Å*, Institut d'Astrophysique de l'Université de Liège.
Derouich, M., Sahal-Bréchot, S., Barklem, P.S., and O'Mara, B.J.: 2003, *Astron. Astrophys.* **404**, 763.
Dirac, P.A.M.: 1935, *The Principles of Quantum Mechanics*, Clarendon Press, Oxford.
Dolginov, A.Z., and Pavlov, G.G.: 1972, *Soviet Astron.* **16**, 450.
Domke, H.: 1969, *Astrofizika* **5**, 525.
Domke, H.: 1971, *Astrofizika* **7**, 39.
Edmonds, A.R.: 1957, *Angular Momentum in Quantum Mechanics*, Princeton University Press, Princeton, New Jersey.
Elliott, J.P., and Flowers, B.H.: 1955, *Proc. Roy. Soc.* A **229**, 536.
Faddeeva, V.N., and Terent'ev, N.M.: 1961, *Tables of Values of the Function $w(z)$ for Complex Argument*, Pergamon Press, New York.
Falkoff, D.L., Colladay, G.S., and Sells, R.E.: 1952, *Can. J. Phys.* **30**, 253.
Fano, U.: 1949, *J. Opt. Soc. Am.* **39**, 859.
Faulstich, R.: 1980, *J. Quant. Spectrosc. Rad. Transfer* **24**, 229.

Faurobert, M.: 1987, *Astron. Astrophys.* **178**, 269.
Faurobert, M.: 1988, *Astron. Astrophys.* **194**, 268.
Faurobert-Scholl, M.: 1991, *Astron. Astrophys.* **246**, 469.
Faurobert-Scholl, M.: 1992, *Astron. Astrophys.* **258**, 521.
Faurobert-Scholl, M., and Frisch, H.: 1989, *Astron. Astrophys.* **219**, 338.
Feautrier, P.: 1964, *Comptes Rendues Acad. Sci. Paris* **258**, 3189.
Fermi, E.: 1932, *Rev. Mod. Phys.* **4**, 87.
Figger, H., and Walther, H.: 1974, *Z. Phys.* **267**, 1.
Fluri, D.M., and Stenflo, J.O.: 1999, *Astron. Astrophys.* **341**, 902.
Franken, P.A.: 1961, *Phys. Rev.* **121**, 508.
Frazier, E.N., and Stenflo, J.O.: 1972, *Solar Phys.* **27**, 330.
Frisch, H.: 1998, *Astron. Astrophys.* **338**, 683.
Frisch, U., and Frisch, H.: 1975, *Monthly Not. R. A. S.* **173**, 167.
Fuller, G.H., and Cohen, V.W.: 1969, in K. Way (ed.), *Nuclear Data Tables*, Vol. A5, Academic Press, New York, p. 433.
Gail, H.P., Sedlmayr, E., and Traving, G.: 1980, *J. Quant. Spectrosc. Rad. Transfer* **23**, 267.
Gantmacher, F.R.: 1966, *Théorie des Matrices*, Dunod, Paris.
Gingerich, O., Noyes, R.W., Kalkofen, W., and Cuny, Y.: 1971, *Solar Phys.* **18**, 347.
Glauber, R.J.: 1964, in C. de Witt, A. Blandin, and C. Cohen-Tannoudji (eds.), *Quantum Optics and Electronics*, Gordon and Breach, New York, p. 63.
Gradshteyn, I.S., Ryzhik, I.M.: 1965, *Tables of Integrals, Series, and Products*, Academic Press, New York [etc.].
Griem, H.: 1974, *Spectral Line Broadening by Plasmas*, Academic Press, New York [etc].
Grossmann-Doerth, U., Larsson, B., and Solanki, S.K.: 1988a, *Astron. Astrophys.* **204**, 266.
Grossmann-Doerth, U., Schüssler, M., and Solanki, S.K.: 1988b, *Astron. Astrophys.* **206**, L37.
Hagyard, M.J., West, E.A., and Cumings, N.P.: 1977, *Solar Phys.* **53**, 3.
Hagyard, M.J., Cumings, N.P., West, E.A., and Smith, J.E.: 1982, *Solar Phys.* **80**, 33.
Hale, G.E.: 1908, *Astrophys. J.* **28**, 315.
Hamilton, D.R.: 1947, *Astrophys. J.* **106**, 457.
Hanle, W.: 1924, *Z. Phys.* **30**, 93.
Hartmann, W.: 1970, *Z. Phys.* **240**, 323.
Harvey, J.W.: 1969, Ph.D. Thesis, University of Colorado.
Harvey, J.W.: 1973, *Solar Phys.* **28**, 9.
Harvey, J.W., and Livingston, W.: 1969, *Solar Phys.* **10**, 283.
Harvey, J., Livingston, W., and Slaughter, C.: 1972, in *Line Formation in the Presence of Magnetic Fields*, High Altitude Observatory, NCAR, Boulder, Colorado, p. 227.
Hauge, P.S.: 1976, in W.L. Hyde and R.M.A. Azzam (eds.), *Polarized Light*, Proc. Soc. Photo-Opt. Instr. Eng. **88**, p. 3.

Heading, J.: 1958, *Matrix Theory for Physicists*, Longmans, Green and Co., London [etc.].
Heitler, W.: 1954, *The Quantum Theory of Radiation*, 3rd ed., Clarendon Press, Oxford.
Hopf, E.: 1934, *Mathematical Problems of Radiative Equilibrium*, Cambridge Tracts, No.31.
House, L.L.: 1970a, *J. Quant. Spectrosc. Rad. Transfer* **10**, 909.
House, L.L.: 1970b, *J. Quant. Spectrosc. Rad. Transfer* **10**, 1171.
House, L.L.: 1971, *J. Quant. Spectrosc. Rad. Transfer* **11**, 367.
Howard, R., and Stenflo, J.O.: 1972, *Solar Phys.* **22**, 402.
Hui, A.K., Armstrong, B.H., and Wray, A.A.: 1978, *J. Quant. Spectrosc. Rad. Transfer* **19**, 509.
Humlicek, J.: 1982, *J. Quant. Spectrosc. Rad. Transfer* **27**, 437.
Hummer, D.G.: 1962, *Monthly Not. R. A. S.* **125**, 21.
Illing, R.M.E., Landman, D.A., and Mickey, D.L.: 1975, *Astron. Astrophys.* **41**, 183.
Ivanov, V.V.: 1973, *Transfer of Radiation in Spectral Lines*, National Bureau of Standards Spec. Publ. No.385, Govt. Printing Office, Whashington D.C.
Ivanov, V.V.: 1990, *Soviet Astron.* **34**, 621.
Ivanov, V.V., Grachev, S.I., and Loskutov, V.M.: 1997, *Astron. Astrophys.* **321**, 968.
Jackson, J.D.: 1962, *Classical Electrodynamics*, John Wiley & Sons, New York [etc.].
Jahn, H.A., and Hope, J.: 1954, *Phys. Rev.* **93**, 318.
Jefferies, J.T.: 1968, *Spectral Line Formation*, Blaisdell, Waltham, Mass. [etc.].
Jefferies, J.T., Lites, B.W., and Skumanich, A.: 1989, *Astrophys. J.* **343**, 920.
Jones, R.C.: 1941, *J. Opt. Soc. Am.* **31**, 488.
Katz, J.M.: 1971, *Solar Phys.* **20**, 362.
Kawakami, H.: 1983, *Publ. Astron. Soc. Japan* **35**, 459.
Kemp, J.C.: 1969, *J. Opt. Soc. Am.* **59**, 950.
Kemp, J.C.: 1970, *Astrophys. J.* **162**, 169.
Kemp, J.C., Henson, G.D., Barbour, M.S., Kraus, D.J., and Collins II, G.W.: 1983, *Astrophys. J.* **273**, L85.
Kemp, J.C., Macek, J.H., and Nehring, F.W.: 1984, *Astrophys. J.* **278**, 863.
Kerkeni, B.: 2002, *Astron. Astrophys.* **390**, 783.
Kerkeni, B., Spielfiedel, A., and Feautrier, N.: 2003, *Astron. Astrophys.* **402**, 5.
de Kertanguy, A.: 1998, *Astron. Astrophys.* **333**, 1130.
Kjeldseth-Moe, O.: 1968, *Solar Phys.* **4**, 267.
Knölker, M., Schüssler, M., and Weisshaar, E.: 1988, *Astron. Astrophys.* **194**, 257.
Kopfermann, H.: 1958, *Nuclear Moments*, Academic Press, New York.
Kourganoff, V., and Busbridge, I.W.: 1952, *Basic Methods in Transfer Problems*, Clarendon Press, Oxford.
Kponou, A., Hughes, V.W., Johnson, C.E., Lewis, S.A., and Pichanik, F.M.J.: 1971, *Phys. Rev. Letters* **26**, 1613.
Kramers, H.A.: 1924, *Nature* **113**, 783.

Krebs, K., and Winckler, R.: 1960, *Z. Phys.* **160**, 320.
Lamb, F.K., and Sutherland, P.G.: 1974, in C. J. Hansen (ed.), *Physics of Dense Matter*, IAU Symp. 53, Reidel, Dordrecht, p. 265.
Lamb, F.K., and ter Haar, D.: 1971, *Physics Reports* **2**, 253.
Landi Degl'Innocenti, E.: 1975, *Astron. Astrophys.* **45**, 269.
Landi Degl'Innocenti, E.: 1976, *Astron. Astrophys. Suppl.* **25**, 379.
Landi Degl'Innocenti, E.: 1978a, *Astron. Astrophys. Suppl.* **33**, 157.
Landi Degl'Innocenti, E.: 1978b, *Astron. Astrophys.* **66**, 119.
Landi Degl'Innocenti, E.: 1979a, *Solar Phys.* **63**, 237.
Landi Degl'Innocenti, E.: 1979b, *Monthly Not. R. A. S.* **186**, 369.
Landi Degl'Innocenti, E.: 1982a, *Solar Phys.* **77**, 285.
Landi Degl'Innocenti, E.: 1982b, *Solar Phys.* **79**, 291.
Landi Degl'Innocenti, E.: 1983, *Solar Phys.* **85**, 3.
Landi Degl'Innocenti, E.: 1984, *Solar Phys.* **91**, 1.
Landi Degl'Innocenti, E.: 1985a, *Solar Phys.* **99**, 1.
Landi Degl'Innocenti, E.: 1985b, in H.U. Schmidt (ed.), *Theoretical Problems in High-Resolution Solar Physics*, Max-Planck-Institute für Physik und Astrophysik, München, p. 162.
Landi Degl'Innocenti, E.: 1985c, *Solar Phys.* **102**, 1.
Landi Degl'Innocenti, E.: 1987, in W. Kalkofen (ed.), *Numerical Radiative Transfer*, Cambridge University Press, Cambridge, p. 265.
Landi Degl'Innocenti, E.: 1990, in V. Ružđjak and E. Tandberg-Hanssen (eds.), *Dynamics of Quiescent Prominences*, IAU Coll. 117, *Lecture Notes in Physics* **363**, 206.
Landi Degl'Innocenti, E.: 1992, in F. Sánchez, M. Collados, and M. Vázquez (eds.), *Solar Observations: Techniques and Interpretation*, Cambridge University Press, Cambridge, p. 71.
Landi Degl'Innocenti, E.: 1994, in R.J. Rutten and C.J. Schrijver (eds.), *Solar Surface Magnetism*, NATO ASI Ser. C **433**, Kluwer, Dordrecht, p. 29.
Landi Degl'Innocenti, E., and Bommier, V.: 1993, *Astrophys. J.* **413**, L49.
Landi Degl'Innocenti, E., and Bommier, V.: 1994, *Astron. Astrophys.* **284**, 865.
Landi Degl'Innocenti, E., and Calamai, G.: 1982, *Astron. Astrophys. Suppl.* **49**, 677.
Landi Degl'Innocenti, E., and Landi Degl'Innocenti, M.: 1972, *Solar Phys.* **27**, 319 (see *erratum* in *Solar Phys.* **29**, 528).
Landi Degl'Innocenti, E., and Landi Degl'Innocenti, M.: 1973, *Solar Phys.* **31**, 299.
Landi Degl'Innocenti, E., and Landi Degl'Innocenti, M.: 1975, *Il Nuovo Cimento* **27** B, 134.
Landi Degl'Innocenti, E., and Landi Degl'Innocenti, M.: 1977, *Astron. Astrophys.* **56**, 111.
Landi Degl'Innocenti, E., and Landi Degl'Innocenti, M.: 1981, *Il Nuovo Cimento* **62** B, 1.
Landi Degl'Innocenti, E., and Landi Degl'Innocenti, M.: 1985, *Solar Phys.* **97**, 239.

Landi Degl'Innocenti, M., and Landi Degl'Innocenti, E.: 1988, *Astron. Astrophys.* **192**, 374.
Landi Degl'Innocenti, E., and Landolfi, M.: 1983, *Solar Phys.* **87**, 221.
Landi Degl'Innocenti, M., Landolfi, M., and Landi Degl'Innocenti, E.: 1976, *Il Nuovo Cimento* **35** B, 117.
Landi Degl'Innocenti, E., Bommier, V., and Sahal-Bréchot, S.: 1987, *Astron. Astrophys.* **186**, 335.
Landi Degl'Innocenti, E., Landi Degl'Innocenti, M., and Landolfi, M.: 1988, *Astron. Astrophys.* **204**, 133.
Landi Degl'Innocenti, E., Bommier, V., and Sahal-Bréchot, S.: 1990, *Astron. Astrophys.* **235**, 459.
Landi Degl'Innocenti, E., Bommier, V., and Sahal-Bréchot, S.: 1991, *Astron. Astrophys.* **244**, 391.
Landi Degl'Innocenti, E., Landi Degl'Innocenti, M., and Landolfi, M.: 1997, in N. Mein and S. Sahal-Bréchot (eds.), *Forum THEMIS*, Publications de l'Observatoire de Paris, p. 59.
Landolfi, M.: 1987, *Solar Phys.* **109**, 287.
Landolfi, M., and Landi Degl'Innocenti, E.: 1982, *Solar Phys.* **78**, 355.
Landolfi, M., and Landi Degl'Innocenti, E.: 1985, *Solar Phys.* **98**, 53.
Landolfi, M., and Landi Degl'Innocenti, E.: 1986, *Astron. Astrophys.* **167**, 200.
Landolfi, M., and Landi Degl'Innocenti, E.: 1996, *Solar Phys.* **164**, 191.
Landolfi, M., Landi Degl'Innocenti, E., Arena, P.: 1984, *Solar Phys.* **93**, 269.
Lehmann, J.C.: 1964, *J. Physique* **25**, 809.
Lenz, W.: 1933, *Z. Phys.* **80**, 423.
Leroy, J.L.: 1962, *Ann. Astrophysique* **25**, 127.
Leroy, J.L.: 1972, *Astron. Astrophys.* **19**, 287.
Leroy, J.L., Ratier, G., and Bommier, V.: 1977, *Astron. Astrophys.* **54**, 811.
Lin, H., Penn, M.J., and Kuhn, J.R.: 1998, *Astrophys. J.* **493**, 978.
Lin, H., Penn, M.J., and Tomczyk, S.: 2000, *Astrophys. J.* **541**, L83.
Lites, B.W., and Skumanich, A.: 1990, *Astrophys. J.* **348**, 747.
Lites, B.W., Low, B.C., Martínez Pillet, V., Seagraves, P., Skumanich, A., Frank, Z.A., Shine, R.A., and Tsuneta, S.: 1995, *Astrophys. J.* **446**, 887.
Lites, B.W., Leka, K.D., Skumanich, A., Martínez Pillet, V., and Shimizu, T.: 1996, *Astrophys. J.* **460**, 1019.
Lorentz, H.A.: 1915, *The Theory of Electrons*, 2nd ed., Dover Publications, New York.
Loudon, R.: 1983, *The Quantum Theory of Light*, 2nd ed., Clarendon Press, Oxford.
Louisell, W.H.: 1973, *Quantum Statistical Properties of Radiation*, John Wiley & Sons, New York [etc.].
Lyot, B.: 1948, *Comptes Rendues Acad. Sci. Paris* **226**, 25.
Magain, P.: 1986, *Astron. Astrophys.* **163**, 135.
Makita, M.: 1986, *Solar Phys.* **106**, 269.
Manso Sainz, R.: 2002, Ph.D. Thesis, Universidad de La Laguna.

Manso Sainz, R., and Trujillo Bueno, J.: 2001, in M. Sigwarth (ed.), *Advanced Solar Polarimetry. Theory, Observations and Interpretation*, ASP Conf. Ser. **236**, p. 213.
Marquardt, D.W.: 1963, *J. Soc. Ind. Appl. Math.* **11**, No.2, p. 431.
Martin, B.R.: 1971, *Statistics for Physicists*, Academic Press, London [etc.].
Mathys, G., and Stenflo, J.O.: 1987a, *Astron. Astrophys.* **171**, 368.
Mathys, G., and Stenflo, J.O.: 1987b, *Astron. Astrophys. Suppl.* **67**, 557.
Maxwell, J.C.: 1873, *A Treatise on Electricity and Magnetism*, Oxford University Press, Oxford.
Mein, P.: 1971, *Solar Phys.* **20**, 3.
Messiah, A.: 1961, *Quantum Mechanics*, North-Holland, Amsterdam [etc.].
Mickey, D.L.: 1973, *Astrophys. J.* **181**, L19.
Mickey, D.L., and Orrall, F.Q.: 1974, *Astron. Astrophys.* **31**, 179.
Mihalas, D.: 1978, *Stellar Atmospheres*, 2nd ed., W.H. Freeman, San Francisco.
Mitchell, A.C.J., and Zemansky, M.W.: 1934, *Resonance Radiation and Excited Atoms*, Cambridge University Press, Cambridge.
Moore, C.E.: 1949, *Atomic Energy Levels*, Vol. I, National Bureau of Standards.
Moore, C.E.: 1952, *Atomic Energy Levels*, Vol. II, National Bureau of Standards.
Moore, C.E.: 1958, *Atomic Energy Levels*, Vol. III, National Bureau of Standards.
Mueller, H.: 1948, *J. Opt. Soc. Am.* **38**, 661.
Nagendra, K.N.: 1988, *Astrophys. J.* **335**, 269.
Nagendra, K.N.: 1994, *Astrophys. J.* **432**, 274.
Nagendra, K.N., Frisch, H., and Faurobert-Scholl, M.: 1998, *Astron. Astrophys.* **332**, 610.
Öhman, Y.: 1929, *Monthly Not. R. A. S.* **89**, 479.
Omont, A.: 1965, *J. Physique* **26**, 26.
Omont, A.: 1977, *Progr. Quant. Electron.* **5**, 69.
Omont, A., Smith, E.W., Cooper, J.: 1972, *Astrophys. J.* **175**, 185.
Ord-Smith, R.J.: 1954, *Phys. Rev.* **94**, 1227.
Oxenius, J.: 1986, *Kinetic Theory of Particles and Photons*, Springer-Verlag, Berlin [etc].
Pauli, W.: 1927, *Z. Phys.* **43**, 601.
Pavlov, G.G., and Shibanov, Yu.A.: 1978, *Soviet Astron.* **22**, 43.
Pecker, J.C.: 1999, *Solar Phys.* **184**, 1.
Perrin, F.: 1942, *J. Chem. Phys.* **10**, 415.
Pichanik, F.M.J., Swift, R.D., Johnson, C.E., and Hughes, V.W.: 1968, *Phys. Rev.* **169**, 55.
Poincaré, H.: 1892, *Théorie Mathématique de la Lumière*, Gauthiers-Villars, Paris.
Prudnikov, A.P., Brychkov, Yu.A., and Marichev, O.I.: 1986, *Integrals and Series*, Vol. I, Gordon and Breach, New York.
Querfeld, C.W., and Smartt, R.N.: 1984, *Solar Phys.* **91**, 299.
Querfeld, C.W., Smartt, R.N., Bommier, V., Landi Degl'Innocenti, E., and House, L.L.: 1985, *Solar Phys.* **96**, 277.
Racah, G.: 1942, *Phys. Rev.* **62**, 438.
Rachkovsky, D.N.: 1962a, *Izv. Krymsk. Astrofiz. Obs.* **27**, 148.

Rachkovsky, D.N.: 1962b, *Izv. Krymsk. Astrofiz. Obs.* **28**, 259.
Ramsauer, J., Solanki, S.K., and Biémont, E.: 1995, *Astron. Astrophys. Suppl.* **113**, 71.
Rayrole, J.: 1967, *Ann. Astrophysique* **30**, 257.
Reader, J., and Sugar, J.: 1975, *J. Phys. Chem. Ref. Data* **4**, No.2, 353.
Rees, D.E.: 1969, *Solar Phys.* **10**, 268.
Rees, D.E.: 1978, *Publ. Astron. Soc. Japan* **30**, 455.
Rees, D.E.: 1987, in W. Kalkofen (ed.), *Numerical Radiative Transfer*, Cambridge University Press, Cambridge, p. 213.
Rees, D.E., and Murphy, G.A.: 1987, in W. Kalkofen (ed.), *Numerical Radiative Transfer*, Cambridge University Press, Cambridge, p. 241.
Rees, D.E., and Saliba, G.: 1982, *Astron. Astrophys.* **115**, 1.
Rees, D.E., Murphy, G.A., and Durrant, C.J.: 1989, *Astrophys. J.* **339**, 1093.
Reichel, A.: 1968, *J. Quant. Spectrosc. Rad. Transfer* **8**, 1601.
Riordan, J.: 1968, *Combinatorial Identities*, John Wiley & Sons, New York [etc.].
Robinson, R.D. Jr.: 1980, *Astrophys. J.* **239**, 961.
Rotenberg, M., Bivins, R., Metropolis, N., and Wooten, J.K. Jr.: 1959, *The 3-j and 6-j Symbols*, MIT, Cambridge, Mass.
Rüedi, I., Solanki, S.K., Livingston, W., and Harvey, J.: 1995, *Astron. Astrophys. Suppl.* **113**, 91.
Ruiz Cobo, B., and del Toro Iniesta, J.C.: 1992, *Astrophys. J.* **398**, 375.
Ruiz Cobo, B., and del Toro Iniesta, J.C.: 1994, *Astron. Astrophys.* **283**, 129.
Rust, D.M.: 1966, Ph.D. Thesis, University of Colorado.
Rybicki, G.B.: 1977, *Astrophys. J.* **213**, 165.
Sahal-Bréchot, S.: 1974a, *Astron. Astrophys.* **32**, 147.
Sahal-Bréchot, S.: 1974b, *Astron. Astrophys.* **36**, 355.
Sahal-Bréchot, S.: 1977, *Astrophys. J.* **213**, 887.
Sahal-Bréchot, S., Bommier, V., and Feautrier, N.: 1998, *Astron. Astrophys.* **340**, 579.
Saito, R., and Morita, M.: 1955, *Progr. Theor. Phys.* **13**, 540.
Saliba, G.: 1986, Ph.D. Thesis, University of Sidney.
Sánchez Almeida, J.: 1992, *Solar Phys.* **137**, 1.
Sánchez Almeida, J.: 1997, *Astrophys. J.* **491**, 993.
Sánchez Almeida, J., and Lites, B.W.: 1992, *Astrophys. J.* **398**, 359.
Sánchez Almeida, J., and Lites, B.W.: 2000, *Astrophys. J.* **532**, 1215.
Sánchez Almeida, J., and Vela Villahoz, E.: 1993, *Astron. Astrophys.* **280**, 688.
Sánchez Almeida, J., Collados, M., and del Toro Iniesta, J.C.: 1989, *Astron. Astrophys.* **222**, 311.
Sánchez Almeida, J., Landi Degl'Innocenti, E., Martínez Pillet, V., and Lites, B.W.: 1996, *Astrophys. J.* **466**, 537.
Schiff, L.I.: 1949, *Quantum Mechanics*, McGraw-Hill, New York [etc.].
Schmidt, G.D.: 1987, *Mem. S. A. It.* **58**, 77.
Seares, F.H.: 1913, *Astrophys. J.* **38**, 99.
Seaton, M.J.: 1958, *Monthly Not. R. A. S.* **118**, 504.

Segrè, E.: 1976, *Personaggi e Scoperte nella Fisica Contemporanea*, Mondadori, Milano.
Semel, M.: 1967, *Ann. Astrophysique* **30**, 513.
Semel, M., and Skumanich, A.: 1998, *Astron. Astrophys.* **331**, 383.
Sharp, W.T., et al.: 1954, *Tables of Coefficients for Angular Distribution Analysis*, CRT-556, AECL No.97, Atomic Energy of Canada Ltd.
Shenstone, A.G., and Blair, H.A.: 1929, *Phil. Mag.* **8**, 765.
Shu, F.H.: 1991, *The Physics of Astrophysics.* Vol. I:*Radiation*, University Science Books, Mill Valley, California.
Shurcliff, W.A.: 1962, *Polarized Light*, Harvard University Press, Cambridge, Mass.
Šidlichovsky, M.: 1976, *Bull. Astron. Inst. Czech.* **27**, 71.
Simon, A.: 1954, Oak Ridge National Laboratory, Report No.1718.
Simon, A., Vandersluis, V.H., and Biedenharn, L.C.: 1954, Oak Ridge National Laboratory, Report No.1679.
Sistla, G., and Harvey, J.W.: 1970, *Solar Phys.* **12**, 66.
Skumanich, A., and Lites, B.W.: 1987, *Astrophys. J.* **140**, 1120.
Skumanich, A., Lites, B.W., Martínez Pillet, V., and Seagraves, P.: 1997, *Astrophys. J. Suppl.* **110**, 357.
Smith, K.: 1958, *Supplement to a Table of Wigner 9-j Coefficients for Integral and Half-integral Values of the Parameters*, Argonne National Laboratory, Report No.5860 I-II.
Smith, K., and Stevenson, J.W.: 1957, *A Table of Wigner 9-j Coefficients for Integral and Half-integral Values of the Parameters*, Argonne National Laboratory, Report No.5776.
Sobel'man, I.I.: 1972, *An Introduction to the Theory of Atomic Spectra*, Pergamon Press, Oxford.
Socas Navarro, H., and Trujillo Bueno, J.: 1997, *Astrophys. J.* **490**, 383.
Socas Navarro, H., Trujillo Bueno, J., and Ruiz Cobo, B.: 2000, *Astrophys. J.* **530**, 977.
Solanki, S.K.: 1993, *Space Science Rev.* **63**, 1.
Solanki, S.K., and Montavon, C.A.P.: 1993, *Astron. Astrophys.* **275**, 283.
Solanki, S.K., and Pahlke, K.D.: 1988, *Astron. Astrophys.* **201**, 143.
Solanki, S.K., and Stenflo, J.O.: 1985, *Astron. Astrophys.* **148**, 123.
Solanki, S.K., Biémont, E., and Mürset, U.: 1990, *Astron. Astrophys. Suppl.* **83**, 307.
Staude, J.: 1969, *Solar Phys.* **8**, 264.
Stenflo, J.O.: 1971, in R. Howard (ed.), *Solar Magnetic Fields*, IAU Symp. 43, p. 101.
Stenflo, J.O.: 1973, *Solar Phys.* **32**, 41.
Stenflo, J.O.: 1980, *Astron. Astrophys.* **84**, 68.
Stenflo, J.O.: 1994, *Solar Magnetic Fields*, Kluwer, Dordrecht [etc].
Stenflo, J.O., and Lindegren, L.: 1977, *Astron. Astrophys.* **59**, 367.
Stenflo, J.O., and Stenholm, L.: 1976, *Astron. Astrophys.* **46**, 69.

Stenflo, J.O., Twerenbold, D., and Harvey, J.W.: 1983a, *Astron. Astrophys. Suppl.* **52**, 161.
Stenflo, J.O., Twerenbold, D., Harvey, J.W., and Brault, J.W.: 1983b, *Astron. Astrophys. Suppl.* **54**, 505.
Stenflo, J.O., Harvey, J.W., Brault, J.W., and Solanki, S.K.: 1984, *Astron. Astrophys.* **131**, 33.
Stepanov, V.E.: 1958, *Izv. Krymsk. Astrofiz. Obs.* **19**, 20.
Stokes, G.G.: 1852, *Trans. Cambridge Phil. Soc.* **9**, 399.
Tam, A.C.: 1975, *Phys. Rev.* A **12**, 539.
Tandberg-Hanssen, E.: 1995, *The Nature of Solar Prominences*, Kluwer, Dordrecht [etc.].
Ten Bruggencate, P., and von Klüber, H.: 1939, *Z. Astrophys.* **18**, 284.
del Toro Iniesta, J.C., Semel, M., Collados, M., and Sánchez Almeida, J.: 1990, *Astron. Astrophys.* **227**, 591.
Trujillo Bueno, J.: 1990, in F. Sanchez and M. Vazquez (eds.), *New Windows to the Universe*, XI^{th} European Meeting of the IAU, Cambridge University Press, Cambridge, p. 119.
Trujillo Bueno, J.: 1999, in K.N. Nagendra and J.O. Stenflo (eds.), *Solar Polarization*, Kluwer, Dordrecht, p. 73.
Trujillo Bueno, J., and Fabiani Bendicho, P.: 1995, *Astrophys. J.* **455**, 646.
Trujillo Bueno, J., and Landi Degl'Innocenti, E.: 1996, *Solar Phys.* **164**, 135.
Trujillo Bueno, J., and Landi Degl'Innocenti, E.: 1997, *Astrophys. J.* **482**, L183.
Trujillo Bueno, J., and Manso Sainz, R.: 1999, *Astrophys. J.* **516**, 436.
Unno, W.: 1956, *Publ. Astron. Soc. Japan* **8**, 108.
Unsöld, A.: 1955, *Physik der Sternatmosphären*, 2nd ed., Springer, Berlin [etc.].
Van Ballegooijen, A.A.: 1985, in M.J. Hagyard (ed.), *Measurements of Solar Vector Magnetic Fields*, NASA Conf. Publ. 2374, p. 322.
Van Ballegooijen, A.A.: 1987, in W. Kalkofen (ed.), *Numerical Radiative Transfer*, Cambridge University Press, Cambridge, p. 279.
Varshalovich, D.A., Moskalev, A.N., and Khersonskii, V.K.: 1988, *Quantum Theory of Angular Momentum*, World Scientific, Singapore [etc.].
Vernazza, J.E., Avrett, E.H., and Loeser, R.: 1981, *Astrophys. J. Suppl.* **45**, 635.
Walker, M.J.: 1954, *American J. Phys.* **22**, 170.
Warner, B.: 1969, *Observatory* **89**, 11.
Weisskopf, V.F.: 1932, *Z. Phys.* **75**, 296.
Westendorp Plaza, C., del Toro Iniesta, J.C., Ruiz Cobo, B., Martínez Pillet, V., Lites, B.W., and Skumanich, A.: 1997, *Nature* **389**, 47.
Wieder, I., and Lamb, W.E. Jr.: 1957, *Phys. Rev.* **107**, 125.
Wiehr, E.: 1975, *Astron. Astrophys.* **38**, 303.
Wiehr, E.: 1978, *Astron. Astrophys.* **67**, 257.
Wiese, W.L., Smith, M.W., and Glennon, B.M.: 1966, *Atomic Transition Probabilities*, Vol. I (NSRD-NBS4), U.S. Department of Commerce.
Wittmann, A.: 1971, *Solar Phys.* **20**, 365.
Wittmann, A.: 1974, *Solar Phys.* **35**, 11.
Zirin, H., and Severny, A.B.: 1961, *Observatory* **81**, 155.

This page intentionally left blank

AUTHOR INDEX

Italic numbers refer to 'et al.' quotations. Multiple occurrences of an author's name on the same page are not indicated.

SUBJECT INDEX

Astrophysics and Space Science Library

Volume 302:***Stellar Collapse,*** edited by Chris L. Fryer
Hardbound, ISBN 1-4020-1992-0, April 2004

Volume 301: ***Multiwavelength Cosmology***, edited by Manolis Plionis
Hardbound, ISBN 1-4020-1971-8, March 2004

Volume 300:***Scientific Detectors for Astronomy****,* edited by Paola Amico, James W. Beletic, Jenna E. Beletic
Hardbound, ISBN 1-4020-1788-X, February 2004

Volume 299: ***Open Issues in Local Star Fomation,*** edited by Jacques Lépine, Jane Gregorio-Hetem
Hardbound, ISBN 1-4020-1755-3, December 2003

Volume 298: ***Stellar Astrophysics - A Tribute to Helmut A. Abt****,* edited by K.S. Cheng, Kam Ching Leung, T.P. Li
Hardbound, ISBN 1-4020-1683-2, November 2003

Volume 297: ***Radiation Hazard in Space****,* by Leonty I. Miroshnichenko
Hardbound, ISBN 1-4020-1538-0, September 2003

Volume 296: ***Organizations and Strategies in Astronomy, volume 4****,* edited by André Heck
Hardbound, ISBN 1-4020-1526-7, October 2003

Volume 295: ***Integrable Problems of Celestial Mechanics in Spaces of Constant Curvature*****,** by T.G. Vozmischeva
Hardbound, ISBN 1-4020-1521-6, October 2003

Volume 294: ***An Introduction to Plasma Astrophysics and Magnetohydrodynamics****,* by Marcel Goossens
Hardbound, ISBN 1-4020-1429-5, August 2003
Paperback, ISBN 1-4020-1433-3, August 2003

Volume 293: ***Physics of the Solar System****,* by Bruno Bertotti, Paolo Farinella, David Vokrouhlický
Hardbound, ISBN 1-4020-1428-7, August 2003
Paperback, ISBN 1-4020-1509-7, August 2003

Volume 292: ***Whatever Shines Should Be Observed****,* by Susan M.P. McKenna-Lawlor
Hardbound, ISBN 1-4020-1424-4, September 2003

Volume 291: ***Dynamical Systems and Cosmology***, by Alan Coley
Hardbound, ISBN 1-4020-1403-1, November 2003

Volume 290: ***Astronomy Communication,*** edited by André Heck, Claus Madsen
Hardbound, ISBN 1-4020-1345-0, July 2003

Volume 287/8/9: ***The Future of Small Telescopes in the New Millennium,*** edited by Terry D. Oswalt
Hardbound Set only of 3 volumes, ISBN 1-4020-0951-8, July 2003

Volume 286: ***Searching the Heavens and the Earth: The History of Jesuit Observatories,*** by Agustín Udías
Hardbound, ISBN 1-4020-1189-X, October 2003

Volume 285: ***Information Handling in Astronomy - Historical Vistas,*** edited by André Heck
Hardbound, ISBN 1-4020-1178-4, March 2003

Volume 284: ***Light Pollution: The Global View,*** edited by Hugo E. Schwarz
Hardbound, ISBN 1-4020-1174-1, April 2003

Volume 283: ***Mass-Losing Pulsating Stars and Their Circumstellar Matter,*** edited by Y. Nakada, M. Honma, M. Seki
Hardbound, ISBN 1-4020-1162-8, March 2003

Volume 282: ***Radio Recombination Lines,*** by M.A. Gordon, R.L. Sorochenko
Hardbound, ISBN 1-4020-1016-8, November 2002

Volume 281: ***The IGM/Galaxy Connection,*** edited by Jessica L. Rosenberg, Mary E. Putman
Hardbound, ISBN 1-4020-1289-6, April 2003

Volume 280: ***Organizations and Strategies in Astronomy III,*** edited by André Heck
Hardbound, ISBN 1-4020-0812-0, September 2002

Volume 279: ***Plasma Astrophysics , Second Edition,*** by Arnold O. Benz
Hardbound, ISBN 1-4020-0695-0, July 2002

Volume 278: ***Exploring the Secrets of the Aurora,*** by Syun-Ichi Akasofu
Hardbound, ISBN 1-4020-0685-3, August 2002

Volume 277: ***The Sun and Space Weather,*** by Arnold Hanslmeier
Hardbound, ISBN 1-4020-0684-5, July 2002

Volume 276: ***Modern Theoretical and Observational Cosmology,*** edited by Manolis Plionis, Spiros Cotsakis
Hardbound, ISBN 1-4020-0808-2, September 2002

Volume 275: ***History of Oriental Astronomy,*** edited by S.M. Razaullah Ansari
Hardbound, ISBN 1-4020-0657-8, December 2002

Volume 274: ***New Quests in Stellar Astrophysics: The Link Between Stars and Cosmology,*** edited by Miguel Chávez, Alessandro Bressan, Alberto Buzzoni,Divakara Mayya
Hardbound, ISBN 1-4020-0644-6, June 2002

Volume 273: ***Lunar Gravimetry,*** by Rune Floberghagen
Hardbound, ISBN 1-4020-0544-X, May 2002

Volume 272:***Merging Processes in Galaxy Clusters,*** edited by L. Feretti, I.M. Gioia, G. Giovannini
Hardbound, ISBN 1-4020-0531-8, May 2002

Volume 271: ***Astronomy-inspired Atomic and Molecular Physics,*** by A.R.P. Rau
Hardbound, ISBN 1-4020-0467-2, March 2002

Volume 270: ***Dayside and Polar Cap Aurora,*** by Per Even Sandholt, Herbert C. Carlson, Alv Egeland
Hardbound, ISBN 1-4020-0447-8, July 2002

Volume 269: ***Mechanics of Turbulence of Multicomponent Gases,*** by Mikhail Ya. Marov, Aleksander V. Kolesnichenko
Hardbound, ISBN 1-4020-0103-7, December 2001

Volume 268: ***Multielement System Design in Astronomy and Radio Science,*** by Lazarus E. Kopilovich, Leonid G. Sodin
Hardbound, ISBN 1-4020-0069-3, November 2001

Volume 267: ***The Nature of Unidentified Galactic High-Energy Gamma-Ray Sources,*** edited by Alberto Carramiñana, Olaf Reimer, David J. Thompson
Hardbound, ISBN 1-4020-0010-3, October 2001

Volume 266: ***Organizations and Strategies in Astronomy II,*** edited by André Heck
Hardbound, ISBN 0-7923-7172-0, October 2001

Volume 265: ***Post-AGB Objects as a Phase of Stellar Evolution,*** edited by R. Szczerba, S.K. Górny
Hardbound, ISBN 0-7923-7145-3, July 2001

Volume 264: ***The Influence of Binaries on Stellar Population Studies,*** edited by Dany Vanbeveren
Hardbound, ISBN 0-7923-7104-6, July 2001

Volume 262: ***Whistler Phenomena - Short Impulse Propagation,*** by Csaba Ferencz, Orsolya E. Ferencz, Dániel Hamar, János Lichtenberger
Hardbound, ISBN 0-7923-6995-5, June 2001

Volume 261: ***Collisional Processes in the Solar System,*** edited by Mikhail Ya. Marov, Hans Rickman
Hardbound, ISBN 0-7923-6946-7, May 2001

Volume 260: ***Solar Cosmic Rays,*** by Leonty I. Miroshnichenko
Hardbound, ISBN 0-7923-6928-9, May 2001

Volume 259: ***The Dynamic Sun,*** edited by Arnold Hanslmeier, Mauro Messerotti, Astrid Veronig
Hardbound, ISBN 0-7923-6915-7, May 2001

Volume 258: ***Electrohydrodynamics in Dusty and Dirty Plasmas- Gravito-Electrodynamics and EHD,*** by Hiroshi Kikuchi
Hardbound, ISBN 0-7923-6822-3, June 2001

Volume 257: ***Stellar Pulsation - Nonlinear Studies,*** edited by Mine Takeuti, Dimitar D. Sasselov
Hardbound, ISBN 0-7923-6818-5, March 2001

Volume 256: ***Organizations and Strategies in Astronomy,*** edited by André Heck
Hardbound, ISBN 0-7923-6671-9, November 2000

Volume 255: ***The Evolution of the Milky Way- Stars versus Clusters,*** edited by Francesca Matteucci, Franco Giovannelli
Hardbound, ISBN 0-7923-6679-4, January 2001

Volume 254: ***Stellar Astrophysics***, edited by K.S. Cheng, Hoi Fung Chau, Kwing Lam Chan, Kam Ching Leung
Hardbound, ISBN 0-7923-6659-X, November 2000

Volume 253: ***The Chemical Evolution of the Galaxy***, by Francesca Matteucci
Paperback, ISBN 1-4020-1652-2, October 2003
Hardbound, ISBN 0-7923-6552-6, June 2001

Volume 252: ***Optical Detectors for Astronomy II***, edited by Paola Amico, James W. Beletic
Hardbound, ISBN 0-7923-6536-4, December 2000

Volume 251: ***Cosmic Plasma Physics***, by Boris V. Somov
Hardbound, ISBN 0-7923-6512-7, September 2000

Volume 250: ***Information Handling in Astronomy***, edited by André Heck
Hardbound, ISBN 0-7923-6494-5, October 2000

Volume 249: ***The Neutral Upper Atmosphere***, by S.N. Ghosh
Hardbound, ISBN 0-7923-6434-1, July 2002

Volume 247: ***Large Scale Structure Formation***, edited by Reza Mansouri, Robert Brandenberger
Hardbound, ISBN 0-7923-6411-2, August 2000

Volume 246: ***The Legacy of J.C. Kapteyn***, edited by Piet C. van der Kruit, Klaas van Berkel
Paperback, ISBN 1-4020-0374-9, November 2001
Hardbound, ISBN 0-7923-6393-0, August 2000

Volume 245: ***Waves in Dusty Space Plasmas,*** by Frank Verheest
Paperback, ISBN 1-4020-0373-0, November 2001
Hardbound, ISBN 0-7923-6232-2, April 2000

Volume 244: ***The Universe***, edited by Naresh Dadhich, Ajit Kembhavi
Hardbound, ISBN 0-7923-6210-1, August 2000

Volume 243: ***Solar Polarization***, edited by K.N. Nagendra, Jan Olof Stenflo
Hardbound, ISBN 0-7923-5814-7, July 1999

Volume 242: ***Cosmic Perspectives in Space Physics***, by Sukumar Biswas
Hardbound, ISBN 0-7923-5813-9, June 2000

Volume 241: ***Millimeter-Wave Astronomy: Molecular Chemistry & Physics in Space,*** edited by W.F. Wall, Alberto Carramiñana, Luis Carrasco, P.F. Goldsmith
Hardbound, ISBN 0-7923-5581-4, May 1999

Volume 240: ***Numerical Astrophysics,*** edited by Shoken M. Miyama, Kohji Tomisaka,Tomoyuki Hanawa
Hardbound, ISBN 0-7923-5566-0, March 1999

Volume 239: ***Motions in the Solar Atmosphere,*** edited by Arnold Hanslmeier, Mauro Messerotti
Hardbound, ISBN 0-7923-5507-5, February 1999

Volume 238: ***Substorms-4,*** edited by S. Kokubun, Y. Kamide
Hardbound, ISBN 0-7923-5465-6, March 1999

Volume 237: ***Post-Hipparcos Cosmic Candles,*** edited by André Heck, Filippina Caputo
Hardbound, ISBN 0-7923-5348-X, December 1998

Volume 236: ***Laboratory Astrophysics and Space Research,*** edited by P. Ehrenfreund, C. Krafft, H. Kochan, Valerio Pirronello
Hardbound, ISBN 0-7923-5338-2, December 1998

Missing volume numbers have not yet been published.
For further information about this book series we refer you to the following web site:
http://www.wkap.nl/prod/s/ASSL

To contact the Publishing Editor for new book proposals:
Dr. Harry (J.J.) Blom: harry.blom@wkap.nl